NATURE ENVIRONMENT & POLLUTION TECHNOLOGY

A Multidisciplinary, International Journal on Diverse Aspects of Environment

Technoscience Publications
website: www.neptjournal.com

INSTRUCTIONS TO AUTHORS

Scope of the Journal

The Journal publishes original research/review papers covering almost all aspects of environment like monitoring, control and management of air, water, soil and noise pollution; solid waste management; industrial hygiene and occupational health hazards; biomedical aspects of pollution; conservation and management of resources; environmental laws and legal aspects of pollution; toxicology; radiation and recycling etc. Reports of important events, environmental news, environmental highlights and book reviews are also published in the journal.

Format of Manuscript

- The manuscript (mss) should be typed in double space leaving wide margins on both the sides.
- First page of mss should contain only the title of the paper, name(s) of author(s) and name and address of Organization(s) where the work has been carried out along with the affiliation of the authors.

Nature Environment and Pollution Technology
Vol. 22, No. (3), September 2023

CONTENTS

The Journal is Currently Abstracted and Indexed in:

CNKI Scholar (China National Knowledge Infrastructure)

Scopus Cite Score (2022) 0.90	Scopus®, SJR (2022) 0.191

Index Copernicus (2021) = 111.68

Indian Science Abstracts, New Delhi, India

Chemical Abstracts, U.S.A.	Pollution Abstracts, U.S.A.

Elsevier Bibliographic Databases

Paryavaran Abstract, New Delhi, India

Zoological Records	CAB Abstracts, U.K.

Electronic Social and Science Citation Index (ESSCI)

Indian Citation Index (ICI)	CrossRef (DOI)
EBSCO: Environment Index™	ProQuest, U.K.
Google Scholar	DOAJ
Zetoc	J-Gate
Environment Abstract, U.S.A.	Centre for Research Libraries

Elektronische Zeitschriftenbibliothek (EZB)

CSA: Environmental Sciences and Pollution Management

Access to Global Online Research in Agriculture (AGORA)

Present in UGC-CARE List (Group II)

UDL-EDGE (Malaysia) Products like i-Journals, i-Focus and i-Future

WorldCat (OCLC)

British Library

Connect Journals (India)

Indian Science

JournalSeek

Research Bible (Japan)

SHERPA/RoMEO

Directory of Science

AGRIS (UN-FAO)

Ulrich's (Refereed) database

www.neptjournal.com

Nature Environment and Pollution Technology

Negative Effects of the Urban River Pollution on the Environment and Human Health in Bangladesh

Kudrat-E-Khuda (Babu)*†, Md. Riaduzzaman*, Tahmina Akter** and Sumaia Akther*

*Department of Law, Daffodil International University, Dhaka, Bangladesh
**Department of Law, University of Portsmouth, United Kingdom
†Corresponding author: Kudrat-E-Khuda (Babu); kekbabu@gmail.com

ABSTRACT

Based on research findings, Bangladesh's river water, crucial for domestic, agricultural, and industrial use, has long been in a terrible situation. There have been numerous instances of significant contamination in the waterways surrounding Dhaka city, including the Buriganga River, and in Chattogram city, including the Karnaphuli River, over the past 40 years. The existing data demonstrate that other urban rivers, particularly Karatoa, Teesta, Rupsa, Pasur, and Padma, are also in severe condition due to the disposition of huge pollutants. Contaminants flowing with the water have severely polluted the downstream areas of the rivers. High metal concentrations are frequently observed in river water during the dry season. In the Buriganga River and at certain locations in the Turag, Balu, Sitalakhya, and Karnaphuli Rivers, the presence of dissolvable oxygen (DO) is nearly zero. NO_3, NO_2, and PO_4^{-3} pollution has also occurred in many rivers. Most rivers have Cr, Zn, Fe, Pb, Cu, Cd, Mn, As, and Ni concentrations beyond the legal limit for drinking water. In contrast, some rivers have metal concentrations above the legal irrigation water limit. The majority of the rivers, particularly the peri-urban rivers in Dhaka city, Teesta, Korotoa, Rupsha, Karnaphuli, and Meghna Rivers, have significantly higher metal concentrations, according to sediment data. Metal concentrations in sediment are generally higher than USEPA standards in most rivers. Metal concentrations in fish and crops demonstrate metal bioaccumulation. The trend in metal concentration follows the order of water, fish, and sediment. It has been shown that crops irrigated with tainted water contain dangerous metals. The analysis of daily intake data on carcinogenic and noncarcinogenic substances reveals that consuming contaminated food can seriously impact human health.

INTRODUCTION

Without water, a precious natural resource, life on Earth would not be imagined. Other planets don't have water like Earth, making them uninhabitable for living species. The oceans and seas comprise 97% of the planet's water, often salty and worthless (Ranjan 2020). Only 3% of water is considered freshwater, and 2% is frozen in ice and glaciers, both unusable water sources (Ahaduzzaman 2017). The only water supply for human consumption is the final 1%, kept in lakes, canals, and underground reservoirs (Sakamoto & Ahmed 2019). Therefore, appropriate water management and sustainable planning are crucial to maintaining life on Earth.

Before the industrial revolution in the eighteenth century, the concepts of water scarcity and water pollution were unthinkable (Uddin & Jeong 2020). But now, it has become one of the major concerns as millions of people suffer from various health hazards caused by water pollution. Developed nations like the USA, Japan, and South Korea have created numerous effective technologies and national strategies over time to ensure that their citizens have access to safe water (Akindele & Akinpelu 2020). On the other hand, developing and underdeveloped countries are struggling with severe water resource crises as they cannot develop a proper water resource management system. Bangladesh is a developing country with a serious water resource crisis (Islam 2019).

The riverine nation has at least 238 important rivers, the minor tributaries of the Ganges, Brahmaputra, and Meghna, and large transboundary rivers (Gray 2010). Karnafuli, Jomuna, Surma, Kushiyara, Padma, Tista, Atrai, Dudhkumar, Mohananda, Sitalakhya, Rupsa, Pasur, and Dharla are a few of the significant and prominent rivers. Earlier, irrigation completely depended on river water in Bangladesh (Doza et al. 2020). Farmers depend on groundwater for irrigation as the river water is highly contaminated (Sarkar et al. 2020). Moreover, the groundwater level is declining gradually due to intensive continuous exploitation, posing a serious threat

to living species as toxic materials. Arsenic contamination currently affects millions in Bangladesh (Reza & Yousuf 2016). Most industries are set up on the rivers' banks and dump thousands of tonnes of waste into the rivers daily. Although laws and norms govern this, they virtually never adhere to them.

Also, because of high-profit objectives, several industries do not operate effluent treatment plants (ETPs). Consequently, the river water has become hazardous for living species, while the agricultural areas are also badly affected (Sultana et al. 2019). Farmers are irrigating their fields with tainted river water, which allows hazardous substances to enter the food chain and, eventually, the human body. It is extremely dangerous for people from low-income families to use this tainted water for cooking and washing. Rivers surrounding the city areas are getting more contaminated due to increasing industrialization. Sitalakhya, Balu, Turag, and Buriganga are the adjoining rivers of Dhaka, the capital city of Bangladesh, and they are nearly dead due to continuous pollution (Whitehead et al. 2019).

In summer, the water of Buriganga River looks dark black, like burned mobil, and smells bad. On the other hand, the Karnaphuli River in Chittagong, the country's port city, is being severely polluted by waste materials such as hundreds of ship-breaking industries on its bank. Several areas of the lower basin's irrigation system use river water, polluted by toxic chemicals, oils, Mobil, and tonnes of iron elements. Bangladesh has a population of approximately 162.7 million, according to the latest figure from the Bangladesh Bureau of Statistics.

To feed this vast population, only 59.8% of the total agricultural land (14.3 million ha) is accessible (Islam et al. 2018). Farmers use a large amount of inorganic fertilizer, insecticides, herbicides, and pesticides every year, hoping for more yield. Most of these are dissolved in water and move to the lower basins, eventually ending up in the rivers. In most rivers, the concentration of Pb, Cr, Cu, Ni, As, Mn, Zn, Fe, and Cd is over the standard limit for drinking water, while several metals are even beyond the recommended level for irrigation water. Most rivers have much greater metal concentrations, especially the peri-urban rivers in Dhaka, Rupsha, Korotoa, Karnaphuli, Meghna, and Teesta Rivers (Bashar & Fung 2020). Metal concentrations in sediment are generally higher than USEPA (United States Environmental Protection Agency) standards in most rivers.

The metal concentrations in fish and crops indicate metal bioaccumulation. The trend in metal concentration is like the water-fish-sediment sequence. Crops irrigated with contaminated water are found to contain harmful metals. The analysis of daily intake data on carcinogenic and noncarcinogenic substances reveals that consuming contaminated food can seriously impact human health. Sometimes, farmers apply pesticides, which are banned by the government, to their crops for more profit (Alam et al. 2020). Every year, agricultural chemicals worth millions of tonnes enter the country illegally to meet the farmers' demand.

However, the farmers are unaware of the negative effect of these toxic chemicals. Several years back, plenty of fish of many species was available in the neighboring field of agriculture water bodies. There is hardly any fish in fields and water bodies as the water quality has become extremely poisonous due to agricultural fertilizers and pesticides. This study's primary objective is to gather and evaluate existing studies on Bangladesh's rivers' water quality during the previous 40 years.

The source and trend of the pollution will be highlighted here using relevant figures and tables. The risks to human health and the environment posed by river water pollution have been displayed using the metal consumption, toxicity, and ecological risk indexes. Moreover, future challenges have also been discussed based on the current pollution scenario. On top of that, important strategies for sustainable water resource management have also been suggested in this paper.

MATERIALS AND METHODS

Throughout the study, both primary and secondary data were used. The previous paper's data and material were all gathered and utilized from primary and secondary sources. Books, periodicals, national and international legal reports, acts, and other secondary data sources are included. The data was assembled chronologically from various books, journals, booklets, sessions, bulletins, souvenirs, and reports by different institutions and organizations. Elsevier, the Internet, and Bangladesh Today, a news outlet, were used to gather the essential evidence and data. The chosen data shows that there has been serious contamination in the rivers surrounding Dhaka city over the past 40 years (taken from the chosen stations between 2021 and 2022).

It also demonstrates that other urban rivers, particularly Karatoa, Teesta, Rupsa, Pasur, and Padma, are also in severe condition due to the disposition of huge pollutants. Contaminants flowing with the water have severely polluted the downstream areas of the rivers. High metal concentrations are found in the river water during the dry season. In the Buriganga River and at certain locations in the Turag, Balu, Sitalakhya, and Karnaphuli Rivers, the dissolvable oxygen (DO) level is nearly zero. NO_3, NO_2, and PO_4^{-3} pollution have also occurred in many rivers. Research papers, thesis

papers, books, articles, conference papers, and reports from various Govt. organizations, including the DoE (Department of Environment), have all been used to try and compile information about river contamination.

All of that data's conclusions have been included in this report as tables and figures. However, it is difficult to get a clear state of pollution trend due to differences in several factors such as the source points, time and data, process, and parameter selection for data analysis and sample collections. This is why the data in the statistics are not consistent. However, the key figures point out that river contamination is, at present, in a very serious state. The existing data collected from the studies conducted in recent times show an exceptionally low state of pollution in the river water, which could be attributed to these factors or certain effective initiatives taken by the government and public on water management. Therefore, considering these circumstances, an in-depth study is necessary to analyze river pollution thoroughly.

RESULTS AND DISCUSSION

Bangladesh was recently elevated from a low-income country to a lower-middle-income country (LMIC) in the World Bank's classification system (LIC). By 2021, laws are expected to have been upgraded from LDC to LMIC status according to the United Nations categorization. The country's gross domestic product (GDP) increased at its highest-ever rate of 7.86 percent in the 2017–18 fiscal year as per capita income rose to $1,751 from $1,610 in the prior fiscal year (UNCTAD 2021). Agriculture contributed 13.82 percent of GDP in the previous fiscal year, while industry and services contributed 31.18 percent and 57 percent, respectively. Mining and quarrying are included in the broad industry sector, as are manufacturing, power, gas, water delivery, and building activities.

Large and medium-sized businesses manufacture newspapers, cement, paper, chemicals, chemical products, textiles, food, leather, tobacco, pharmaceuticals, medical devices, machinery, and equipment. In the 1950s, Bangladesh started to industrialize, focusing mostly on agro-based industries like sugar, cotton, and jute. After the nation gained independence (in 1971), interest increased, but industrialization didn't get off until the late 1970s, largely due to the ready-made clothing industry (BRMG 2022). Several government initiatives, such as developing industrial estates and EPZ (Export Processing Zones), were also undertaken to stimulate industrial expansion. There were 4,560 registered textile industries in 2016-20, and about 220 tanneries, 2,500 footwear manufacturing units, and 90 big corporations are now running with leather (BRMG 2022).

There are about 257 licensed pharmaceutical companies in Bangladesh, of which about 150 are active, according to the Bangladesh Association of Pharmaceutical Industries (BAPI 2023) and the Directorate General of Drug Administration (DGDA). The Bangladesh Chemical Industries Company (BCIC) owns and operates two DAP (Diammonium Phosphate) factories, one ammonium sulfate plant, and six urea fertilizer facilities. Moreover, the Karnaphuli Fertilizer Company Limited, a joint venture between the government of Bangladesh and foreign businesses, produces urea fertilizer and additional ammonia products for export.

Additionally, Bangladesh is home to a sizable number of other industries. The current industrial growth rate negatively impacts the country's national economy and development. Bangladesh is a riverine country with over 700 rivers, including tributaries (Rakib & Fukunaga 2019). Most of them are transboundary rivers of Asia that enter Bangladesh through India and fall in the Bay of Bengal in the southern part of the country.

Fish and agriculture are mostly sourced from rivers, and canal transportation is important in many country regions. These rivers discharge a significant amount of rich silt every year. In the southern part of the country, rivers dumped over 2.4 billion tonnes of sediment, enhancing the available land for habitation. However, riverbank erosion has become one of the major concerns over the years. Since the river bed is silt, flush floods occur during the monsoon, affecting the lives, infrastructures, and crops badly.

The length of rivers, which includes various streams, canals, lakes, khals, beels, and haors, is around 24140 km (BWDB 2023). The varying temperatures and rainfall throughout the year give them and their tributaries a beautiful appearance. Some of the rivers in Bangladesh are Buriganga, Atrai, Arial Khan, Bhairab, Bangshi, Dhaleshwari, Chitra, Karatoya, Kobadak, Karnaphuli, Rupsha, Purnarbhaba, Tista, and Pasur (Fig. 1). However, the Ganges-Padma, Brahmaputra-Jomuna, Chittagong, and Surma-Meghna river systems, as well as their tributaries and distributaries, are the four principal river systems that encompass most of the country. The amount of environmental pollution created by each industrial sector, which substantially influences both the environment and public health, is one of the fundamental problems with the spread of industrialization. For instance, the tannery industry generates 232 tonnes of solid waste and around 20,000 cubic meters of liquid waste daily.

The DoE (Department of Environment) report reveals that the textile industry was responsible for generating 217 million cubic meters of wastewater in 2016, while the amount of wastewater may rise to 349 m3 in 2021 (DoE 2022). Some
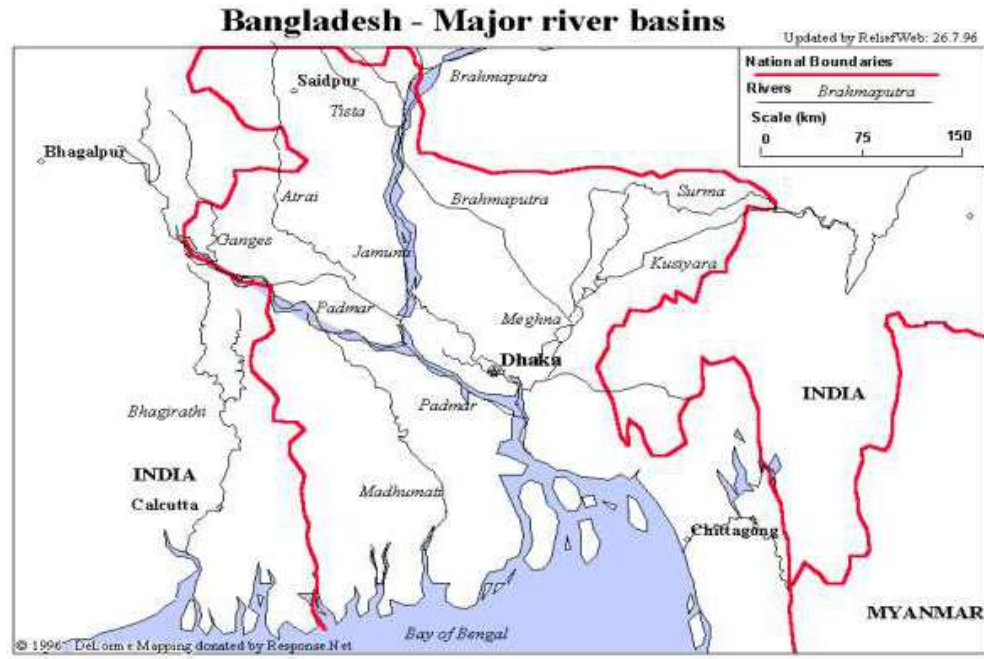
Fig. 1: Major rivers in Bangladesh.

main sources of water pollutants are dying, paper industries, pulp, sugar, and leather. Mineral resource-based enterprises, i.e., hard rock, glass, limestone, various forms of clays, and sands, are examples of non-renewable local resource-based industries, and cement and fertilizer factories are the prime polluters in this category. Metalworking, pharmaceuticals, textiles, petroleum, and plastics are among the industries that primarily rely on imported raw materials, and many of them are proven to be extremely polluting. The prime sources of water contamination in Bangladesh are depicted in Fig. 2.

In Bangladesh, open-field dumping is the main technique for removing solid and liquid trash. The liquid wastes combine with water, travel down drains to the canals, and end up in the river water. Wastes from households,

(Source: ResearchGate)

Fig. 2: Bangladesh's primary sources of water pollution.

hospitals, markets, and industries are dumped into the open field. The aerobic and anaerobic decomposition of wastes is a continuous process. Both insoluble and soluble waste materials get mixed with water during the rainy season and eventually reach the nearby canals and rivers. Most of the farmers in the country lack education, and they often apply a huge amount of agrochemicals to boost productivity.

Most of these substances pollute water, pose health risks, and are swept into surface waters. Detergents, soaps, pharmaceuticals, personal care items, and oils are among the many items dispersed in water and dumped as domestic garbage into rivers. Many hazardous solid and liquid waste is also discharged into rivers, as the country has about 600 hospitals. Hundreds of launches and steamers occur daily from Dhaka city to different destinations while the passengers throw waste materials straight into the river water. These hazardous wastes contaminate the river water and settle in the southern part of Bangladesh after drifting downstream with the river currents. However, adequate data on water pollution by water vehicles is not available yet. Most of the Bazars (rural marketplace) and markets are set up on the bank and rivers, and they produce several tonnes of organic waste straightly discharged into the river.

Due to a lack of supervision and maintenance, water vehicles go bad, and accidents occur, releasing hazardous liquids into the river that pose a serious hazard to the river basin's environment and fauna—the high concentration of Fe and As have also left Bangladesh's surface and groundwater extremely polluted. The decline of groundwater level caused by the excessive extraction for various purposes also facilitates the harmful metals, particularly Fe and As, to accumulate in the groundwater. The air quality of Bangladesh is the worst in the world due to continuous pollution, while its capital, Dhaka, ranks as the second most polluted city

globally. The atmospheric deposition of hazardous metals significantly impacts surface water and agricultural fields.

Due to atmospheric deposition, many metals are added to the urban rivers every year. Newaz et al. (2020) also found a high heavy metal concentration in roadside sediments. Moreover, large quantities of hazardous metals are accumulated in crops planted in the neighborhoods of urban highways. Furthermore, the number of recognized brick fields in Bangladesh is nearly 6000, while many unregistered brick fields are also operating their activities. Since most of the brick fields are set up on the banks of the river, they are significantly contributing to the river pollution in the country. The sand, soil, and silt of the Potenga Sea beach in Chattogram City were also contaminated by geologically formed radioactive elements. Many hazardous substances are also found in the water and sediments deposited in lower basins in Bangladesh's southern coastal areas. The pollution of river water by these contaminants, as well as by local pollutants, has currently become a hot topic.

Chemical materials are now used in more industries due to rapid industrialization. As a result, many organic and inorganic hazardous metals are released from these industries into the soil, water, and air. Though the problems arise in particular places and areas, their escalating incidence, size, and possible consequences make their global issues. These industrial pollutants adversely affect people's lives, either directly through toxic action or indirectly through water quality changes. Industrial, urban, and agricultural waste pollution has reached dangerous levels in several rivers and aquatic bodies in Bangladesh.

Dhaka, the capital of Bangladesh, is among the world's most populous cities, with a population of more than 16 million. On December 31, Dhaka city topped the list of worst cities worldwide regarding air quality as the capital's air
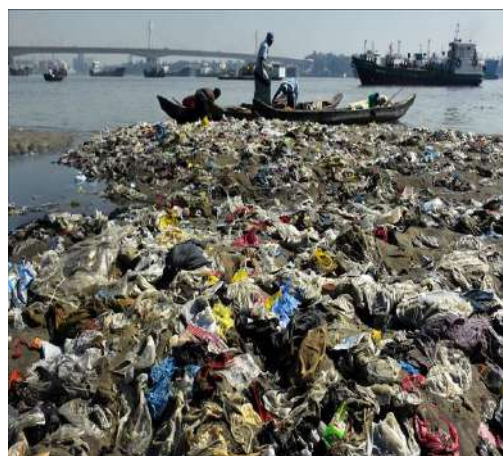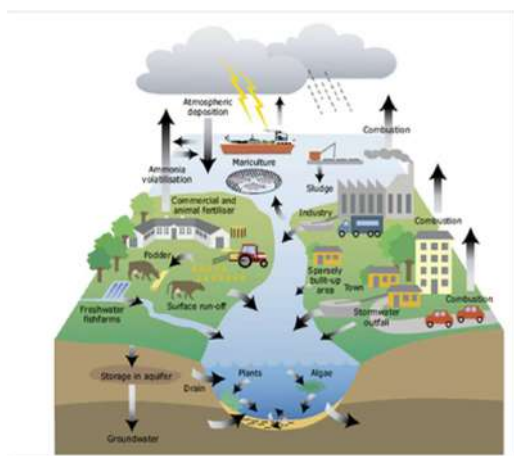
Fig. 3: & Fig. 4: River pollution in Bangladesh.

quality index (AQI) was recorded at 221. The city is situated on the Buriganga River's northern bank, while some other rivers surround it, namely Dhaleshwari, Turag, Sitalakhya, TongiKhal, and Balu.

Most of the city's factories and industries are near or along these rivers' banks (Fig. 3 and Fig. 4). On the banks of the rivers in three important sections of Dhaka city—Hazaribagh, Tejgaon, and Dhaka-Narayanganj-Demra dam—are more than 7,000 industries. A significant amount of hazardous waste from industrial regions and sewage lines and petroleum discharge from ships, launches, cargoes, boats, etc., often poison the rivers surrounding the capital city. About 60,000 cubic meters of hazardous wastes are dumped into the Buriganga and its connected rivers, i.e., the Dhaleshwari, Turag, Sitalakhya, TongiKhal, and Balu Rivers each day, mostly from nine major industrial clusters—Hazaribagh, Tejgaon, Tongi, Tarabo, Savar, Narayangonj, DEPZ, Gharashal, and Gazipur (Rai et al. 2019).

A report of Bangladesh Poribesh Andolon (BAPA 2023) reveals that the Buriganga River absorbs 6,000 tonnes of liquid waste daily, while Hazaribagh tanneries discharge 3,000 tonnes of liquid waste alone. According to the findings of another study, The Hazaribagh tanneries alone produce 88 million tonnes of solid trash and 7.7 million liters of liquid waste daily, compared to about 7000 tonnes of solid waste produced daily in and outside the Dhaka City Corporation region. This huge waste gets to the river water since domestic pipelines are linked to drains directly connected to various khals and canals. Household wastes, such as oils and chemical products used for personal care, thus, enter the river water. Moreover, hundreds of water vehicles ply the river to transport passengers from Dhaka to other destinations and contribute to river water pollution at an alarming rate.

The Buriganga River's water turns dark black and resembles burned engine gasoline during the dry season. The majority of the physicochemical characteristics of the water surpass the water standard fixed by the World Health Organisation (WHO). The dissolved oxygen in the water was 2 milligrams per liter in 2000 but turned zero in 2019, while abrupt changes in TDS, BOD, and COD are also seen. The changes might be due to the differences in various aspects such as procedure, time, and where the sample collections are kept. However, the findings of most research work clearly state that the basin area of the Buriganga River is experiencing severe pollution. The presence of heavy metals, particularly Cr, Cd, and Pb, has made the river water toxic. The research data of the last 40 years depicts that the river water turns out to be extremely poisonous in some particular periods when it becomes hazardous for drinking and irrigation. A high concentration of toxic metals is also

noticed in the sediment samples as a huge amount of organic materials might be settled down in the river water with toxic metals.

Furthermore, a high concentration of toxic metals is also found in the specimens of fish taken from the Buriganga River, according to findings of certain research works. Although most of the data were below the recommended and safe limits of the DoE, they can cause serious health risks if consumed continuously. The current study data lacks essential physical and chemical examinations of the river water, sediment, and fish.

Hence, it is vitally necessary to conduct a complete investigation of organic pollutants, personal care items, pharmaceuticals, etc., to study the natural characteristics of river water, which are crucial for a successful water management system. The Buriganga River is clearly in danger, and if this pollution trend persists, The flora and fauna and people will suffer greatly, according to the research findings. The Buriganga River's water and sediment contain thirteen elements: the accumulation index (Igeo), CF, PERI, PLI, HEI, heavy metal pollution index, and NI. Akbor et al. (2020) analyzed these elements and discovered that the Buriganga River is extremely polluted with heavy metals.

Northwest of the city of Dhaka is where the Turag River is located. As the majority of the clothing industries are located on the river bank, and farmers who use they reside close to the river and use inorganic fertilizers, insecticides, and herbicides in their agricultural areas, untreated industrial wastes, agricultural runoff, and urban garbage from the slum area all have a negative impact on the water quality of this river. All these waste materials are swept with water during the rainy season and eventually end up in the river.

The extensive pollution made the Department of Environment announce the Turag River as an ecologically critical one in 2009. The water quality of the upstream river was very poor due to the extensive industrial activities in the area. Farmers irrigate their lands using the river water to cultivate crops sold in the markets. So, people who regularly eat vegetables, fish, and rice produced in this area are likely to suffer serious health hazards as toxic metals are found in them, according to the research findings. The flora and fauna's bioaccumulation of toxic metals may negatively impact human health. During the dry season, the river water looks black and stinks. According to the source and types of the discharged effluents, the pH level also varies from one point to another in the river. In addition, the dissolved oxygen (DO) in the Turag River's water is also found to be far below the recommended standards set by DoE. Besides, along with the toxic metals, high amounts of BOD, COD, and TDS are also found in the river water. The fish and sediment samples

collected from the river are also found to have concentrations of toxic metals. The toxicity analysis data based on the metal concentration shows that the river water has become toxic and highly poisonous to human health and living animals.

Balu River, mainly a tributary of the Shitalakshya River, goes by through the wetlands of Beel Belai and Dhaka before it merges with the Shitalakshya at the Demerara area of Dhaka city. The river is linked to the Turag River via Tongi Khal in the northern part of the city. The river is also linked to several khals and canals, i.e., Rampura Khal, Norai Khal, and Tongi Khal. The hazardous wastes from industries are dumped into the khals and canals, where they finally find their way into the Balu River. Wastes from the TIZ, textile, pharmaceutical, food, dishwashing soap, metal, and dying industries, among others, harm the river's water.

Besides, the river absorbs wastes from municipal and agricultural fields as well. As a result of continuous extensive pollution, the DoE declared the Balu River as one of the ecologically critical rivers in 2009. The level of dissolved oxygen in the river water is nearly zero, drastically affecting the flora and fauna. The findings of some research also show the presence of excess TDS, BOD COD, and metals in the river water. The existing research data clearly state that the water of the Balu River is being polluted continuously. The research data depict many pollutants flowing to the Balu River via Tongi Khal, Norai Khal, and Tejgoan-Rampura Khal. The concentrations of pollutants in sediments are also several times higher than the recommended standard of USEPA. Farmers in the region largely depend on the water of these canals and the Balu River for irrigation. Consequently, crops are affected by various toxic substances.

Shitalakshya River is a distributary of the Brahmaputra, the source of origin of most rivers in Bangladesh. The river runs east of Dhaka city and merges with the Meghna River at Kolagachi of Munsiganj district. The water of the Balu and Dhaleshwari rivers flows to the Shitalakshya River (the Buriganga River ends in this river). Many industries are established on the bank of this river, especially in the Narayanganj district, where industrial concentration is high. Various watercraft also use the river to travel to Chandpur and Chittagong districts. Narsingdhi district also affects the river in many ways.

The Sitalakhya River is the principal water source for various daily and commercial activities, including washing, bathing, drinking, industrial use, and irrigation. However, the enterprises situated along the riverside, such as those producing textiles, pulp, paper, fertilizer, cement, jute, sugar, etc., significantly negatively impact the river water quality. The water of the Shitalakshya River also becomes more contaminated as pollutants enter the river with water

from Balu and Dhaleshwari Rivers. The Sitalakhya River near Demraghat is also the raw water source for Saidabad's water treatment plant. The findings of the research state that the extensive river pollution poses serious challenges to the drinking water plant and suggest that the existing intake point is unsafe because of the presence of poisonous substances and microbial loads. In the dry season, the dissolved oxygen level is nearly zero at several points of the Sitalakhya River. The concentrations of BOD, COD, and TDS, on the other hand, have not exceeded the standard set by DoE for surface water.

However, the data analysis affirms that the designated river's basin area has also been polluted. A huge amount of pollutants is also accumulated yearly as it is linked with other extensively polluted rivers. The river water also contains a high presence of Cu, Ni, Cr, As, and Fe, exceeding the standard DoE set for surface water. The concentration of heavy metals in sediment is also found to be higher than the safe limit determined by USEPA. Direct consumption of river water is very risky as it can invite severe health problems. Moreover, transmitting poisonous substances into fish and crops (through irrigation) can also pose serious health risks to humans.

Kaliganga and Dhaleswari are the two branches of the Jamuna River, one of the three major rivers in Bangladesh. The northern branch, Dhaleswari, flows to the Shialakhya River in the lower region. The pollutants from the Buriganga River flow to the Dhaleshwari River with water. The latter river carries them down to the lower Sitalakhya River before merging with the Meghna River. In the water of the Sitalakhya River, the presence of Cr exceeds the FAO standard value of irrigation water. The values of Cd, Ni, Pb, Cr, Cu, and sediment samples collected from the Dhaleswari River are higher than those of USEPA standards.

One of the three rivers that make up the Ganges Delta, the world's biggest and most populated delta system, is Meghna, the broadest river in Bangladesh. The river, which originates in the Kishoreganj district and is part of the Surma-Meghna River System, empties into the Bay of Bengal. It absorbs silt and pollutants from Surma, Kushiyara, Padma, and Sitalakhya Rivers at its confluence with these rivers.

The river's water is the primary source for agriculture and fish, while it is also used by many industries set up along the riverbank. However, agricultural and industrial activities largely affect the river water. While Ni, Mn, and Cd concentrations are greater than the acceptable limit for irrigation water, Cd, Mn, Ni, Cr, and fe concentrations are well over the standard threshold set by the WHO for drinking water. The amounts of Ni, Cr, Pb, Zn, and Cd in the silt exceed the USEPA regulatory limit at various locations along

the river. Significant metal concentrations are also present in various riverbank locations.

The study's findings demonstrate how urbanization and industrialization have significantly influenced the Balu, Turag, Sitalakhya, and Buriganga Rivers. Due to continuous extensive contamination, these rivers were declared ecologically critical by DoE in 2009. The trend of concentrations is found in several studies to be surface<sub-surface<sediment after examining the concentrations of several physicochemical variables and metals in soil, surface water, and subsurface water. The accumulation of poisonous substances in fish samples is also a serious concern for human consumption. In Dhaka, groundwater is used for domestic purposes by at least 78% of residents, while surface water meets the remaining 22% of demand. The findings of several studies reveal that the groundwater is also severely impacted by the intense pollution in the adjacent rivers. At the same time, heavy metal concentrations have also been noticed in the water samples of several areas.

Dhaleshwari and Meghna rivers are being polluted as pollutants from upper boundary rivers enter these rivers with water. The water and silt of the duo river are also being affected by anthropogenic activity. The most alarming element is that all the studies done so far only consider a few common parameters, such as TDS, pH, BOD, DO, COD, and some metals. No consideration is given to analyses of microbiological, organic, personal care, pharmaceutical, and other harmful contaminants.

Karnaphuli is the largest and most important river in the Chittagong region. The river, located in the southeastern part of Bangladesh, flows through the port city of Chittagong and the Chittagong Hill Tracts. Exporting and importing products nationally and internationally is a very important getaway. People use the water of this river, which has been severely contaminated recently, for domestic, irrigation, and industrial purposes. Industries that greatly impact river water include tanning, textile, oil refineries, spinning mills, dyeing,

fertilizer, paper, steel, cement, cotton, soap, bitumen, rayon mills, and detergent factories.

Other industries include insect killer production plants, paint manufacturing, merchant ships, naval, and ship recycling. The air in Chittagong ship breaking is also polluted due to the high concentrations of organic pollutants. The values of oil and grease in the sediment collected from the river are high. Geo-accumulation index (Igeo) for Zn, Fe, Ti, Y, Zn, and Rb in silts of the ship-breaking area illustrates that the presence of these elements moderately pollutes the silts. The research data demonstrate that the quality of Karnaphuli River water is very poor as most of the physicochemical properties in the river waterfall are below the standard level recommended by DoE for drinking and surface water. The river's water is becoming dangerous for humans, flora, and fauna due to a gradual decrease in DO concentration and increased BOD and COD values. Severe pollution occurs at specific key points during the selected period.

It is evident from the EC and Cl values that the water of Karnaphuli River is comparatively salty. Therefore, the low presence of metals is found in the Karnaphuli River water (Fig. 5). However, at the locations where khals and canals merge with the rivers, high metal concentration is found, according to some studies, and it is evident that the river is being polluted uninterruptedly. For instance, according to a study by Kibria et al. (2016), the Karnaphuli River and the Bay of Bengal coastal region exhibit significant levels of Cd, Ni, Pb, U, Hg, Cr, and Cu contamination. The study recognizes the 'hotspots' of pollution and the origin of pollutants.

The level of dissolved oxygen is below 4 percent in the water of the Halda River, while the concentrations of Fe and Mn are higher than the stipulated standard set by FAO for irrigation water. Similarly, the concentrations of Cu and Pb exceed the ESEPA standard limit in the sediments of the Bakkhali River. At the same time, a high amount of Ni, Cr, Cu, Zn, and Pb is also traced in the Sangu River's water, originating from neighboring Myanmar.

Fig. 5: Karnaphuli River pollution.

Various metropolis and agricultural activities also affect the Korotoa, Teesta, Atrai, and Padma rivers in northern Bangladesh. The concentrations of Fe, Cr, Pb, As, Ni, and Mn in the Korotoa River water exceed the WHO stipulated standard limit for irrigation water. At the same time, those of Cr and Cd are higher than the FAO-recommended values. The highest concentrations of Pb, Cu, As, Ni, Cr, Pb, and Cd in the sediment of Korotoa River are determined to be 183, 163, 118, 51, 2.9, and 84 mg/kg, correspondingly. According to the analysis of Pollution Load Index (PLI) values of the existing research data, the silts of the river are severely polluted (PLI>1), particularly for the high presence of Cr, Cd, and Pb.

The Contamination Fact (CF) calculation also demonstrates a high amount of As and Cd CF>1). At the same time, the Enrichment factor (EF) analysis confirms that human activities have also affected the river. The possible causes of the pollution are the wastes released by various industries, such as textile, steel, gasoline, and tanning industries, municipal, agrochemicals, and atmospheric deposition. The presence of Zn, Cu, Pb, Cd, As, Cr, and Ni in sediments samples obtained from the Korotoa River is higher than the USEPA recommended standard, which clearly states that the river is polluted.

Islam et al. (2018) have also found heavy metal concentrations in the water and sediment of the Teesta River, which originated in the Pauhunri Mountain of the eastern Himalayas and confluences with the Jamuna River in Bangladesh, flowing through the Indian states of Sikkim and West Bengal. Teesta flows across the country's northern area, including the Ranpur and Bogura districts. Cd in the river's water is higher than the recommended value set by the WHO for drinking water. Besides, the concentrations of Fe and Mn are also found to exceed the FAO recommended standard for irrigation water.

For the first time in Bangladesh, the Positive Matrix Factorization (PMF) receptor model is used by Islam et al. (2018) for the identification of the source of pollutants and the pollution in sediment in Pasur, Teesta, Meghna, Korotoa, Sitalakhya, and Rupsa Rivers. Data obtained from Risk Index and Geo-accumulation Index demonstrates the sediment of the rivers to be severely contaminated by Cd. The findings of the studies reveal that Ni, Fe, and Mn have a significant co-occurrence network with Cr.

The data collected by the PMF receptor model recognized four sources of sediment pollution, and they are – the mixed source (for Cd), industrial (for Ni and Mn), anthropogenic (for Cd), and agricultural (for Cu and As) (for Fe and Cr). The water and sediment quality data analysis demonstrates that severe pollutant consumption has drastically affected the

Teesta River. The findings of several research data also point out the presence of radioactive and toxic metals in Teesta River water that can pose serious health hazards like cancer.

On the banks of the Padma River stands Rajshahi City, the divisional city of the northern districts. This river enters Bangladesh through the Chapainawabganj district from neighboring India and flows through many districts before its confluence with the Meghna River in Chandpur. The Padma River gets many pollutants from the city through various drains, khals, and canals. The Rajshahi region has been facing severe deforestation for a long. The water of the Padma River is being contaminated continuously due to the depositing of garbage on the open field, industrial and household wastes, and direct sewer lines.

Since the region is an agricultural-based area, farmers apply many fertilizers, pesticides, and insecticides, most of which are inorganic, in their fields, and all of these materials eventually enter the river with water. In summer, an excess amount of coliform and Vibrio cholera counts are found in the river's water, according to Haque et al., 2018. The analysis of fish samples collected from the Padma River also reveals high concentrations of Cr, Cu, Cd, Zn, Pb, and Mn, which can pose serious health problems if consumed continuously.

Rapid and unplanned urbanization and industrialization in the southern part of the country largely affect the lower basin of Meghna, Kirthankhola, and Rupsa Rivers, various tributaries, and Distributary Rivers, canals, and khals as almost all of the cities are established on the river banks. Being adjacent to the Bay of Bengal, nearly every southern river contains salty water in most parts. The intrusion of salty water during the rainy season is common in this region. People nowadays complain of more frequent intrusion of salty water. The reason for this frequent intrusion may be the result of climate change. Each year, the coastal areas face natural calamities such as Aila, Sidr, and Fani that cause serious damage to crops, plantations, and households. The most important problem this region faces following any natural catastrophe is that a large area is submerged under salty water. Both the natural hazards and human activities have a severe impact on the ecology of this area.

Barisal City, one of the nation's oldest cities and river ports, is built on the bank of the Kirtankhola River and flows through south-central Bangladesh. Many wastes, including domestic and industrial effluents, used water, sewerage, and organic loads, straightly enter the Kirtankhola River from the city through various canals and khals. Moreover, the city has numerous hospitals and clinics that generate sensory waste daily.

Besides, a significant amount of garbage is also produced daily by the municipal corporation, and these are left in an

open field, namely "Moilakhola," as the city does not have any waste management system to tackle sensorial wastes. Consequently, most of these wastes are washed away into the Kirtankhola River with water during the rainy season. The river water is constantly contaminated by cement, pharmaceutical, food, textile industries, brick kilns, and watercraft. Similar pollution also occurs in Khulna's Rupsha River and Rajshahi's Padma River. Generally, water from upper rivers flows to the lower point and meets large bodies such as the ocean.

Similarly, pollutants enter the rivers and eventually the Bay of Bengal. The research findings on the surface water quality in the Barishal region include high concentrations of suspended solids, turbidity, Nitrate, phosphate, and electrical conductivity in the water of the Kirtankhola River, which are above the permissible levels. Generally, the water of surface water also affects groundwater. The findings of several studies demonstrate that the quality of the upper aquifer is mostly affected by salty water and arsenic. Arsenic in groundwater is one of the long-standing problems that people of the Barisal region have been facing.

However, there is a lack of enough research data on metals and other organic and inorganic pollutants, and it cannot be determined how bad or good the water of the Kirtankhola River is. Pashur, a distributary of the Ganges River, flows in the southwestern region of Bangladesh, while the Rupsha River is the continuation of the first one. The concentrations of Nitrate in the Rupsha River water are also higher than the safe limit recommended by FAO for irrigation. The metal concentrations are also noticed above the permissible limit at several river points.

The research findings reveal a high amount of Fe, Pb, Cr, Mn, and Ni in the river water at several points, and it exceeds the standard values recommended by WHO and FAO for drinking and irrigation water, respectively. The wastes from Khulna City and anthropogenic activities are the primary sources of pollution in that area. In addition, the groundwater of that region contains a high concentration of natural arsenic which forces people to use the surface water for drinking, household activity, and irrigation purposes. Therefore, pollution in surface water adds to the woe of the people in that region. The water of Rupsha River contains higher concentrations of Cd, Ni, As, Pb, and Cr, while eighty-five percent of the samples pose a mild ecological concern. Khulna region is very popular for shrimp farming which may contribute to further pollution there. The sediments collected from the Rupsha River also contain a high amount of Zn, Cu, Pb, Cd, As, Cr, and Ni, higher than the standard level recommended by USEPA, hinting that the river is highly polluted.

Research papers, thesis papers, books, articles, conference papers, and reports from various government organizations, including the Department of Environment, have all been used to try and compile information about river contamination. Tables and figures presenting the results of all those data have been included in this publication. However, it is difficult to get a clear state of pollution trend due to differences in factors such as the source points, time, data, process, and parameter selection for data analysis and sample collections. This is why the data in the statistics are not consistent.

However, the key figures point out that river contamination is, at present, in a very serious state. The existing data collected from the studies conducted in recent times show an exceptionally low state of pollution in the river water, which could be attributed to these factors or certain effective initiatives taken by the government and public on water management. Therefore, considering these circumstances, an in-depth study is necessary to analyze river pollution.

Since Bangladesh is a riverine country, most soils fall within the 'Inception' category, demonstrating that they are formed continuously. During rainy reason, a huge amount of sediment is accumulated in the soils of riparian areas. As silty soil is usually more fertile, farmers prefer this type of soil for cultivating various crops and vegetables. Furthermore, the growers can easily use the river water for irrigation as it is cheap and easily available. Currently, most rivers are polluted with a high concentration of heavy metals, a large portion of which ultimately accumulate in soils and enter the food chain through irrigation.

According to Uddin et al. (2014), the soil samples taken from the Shitalakshya River had values of 86, 36.24, 17.75, and 0.12 mg/kg of Zn, Cu, Pb, and Cd, respectively. For experiment purposes, Kalmi (Ipomoea aquatic), one type of vegetable, was cultivated on a piece of land close to the Sitalakhya River, and the river water was used for irrigation. The concentration of Zn, Cu, Pb, and Cd in the harvested vegetable (growing time: 35 days) was 113.16, 36.69, 14.07, and 0.08 mg/kg, respectively. Some researchers have found high concentrations of toxic metals by analyzing and comparing the soil samples collected from the river basin area with uncontaminated soil samples. A huge amount of heavy metals is also found in the crop cultivated and irrigated in the polluted soil and by river water respectively than the crop is grown in pure soil and with safe water. Most of the researchers found that the soil, water, and crops they took from the farmland next to the contaminated river had a significant level of toxicity. Aside from these few investigations, very little is known about the metal concentrations in the upper soil layer. Significant research is needed to examine the concentration of heavy metals in

the upper soil layer to better understand how heavy metals travel from rivers to agricultural soil and from soil to crops.

The pattern of metal concentration trend in the Buriganga, Turag, Sitalakhya, and Meghna rivers is nearly alike –water from fish and fish from sediment. However, the metal concentrations in the Buriganga River are comparatively higher than the remaining three rivers. While the trend for Cd is similar for the rivers Turag, Buriganga, Sitalakhya, and Meghna, the level of Pb and Cr in fish samples from the Buriganga and Sitalakhya rivers is also found to be high.

When a chemical enters an organism through any exposure channel (water, sediment, soil, air, or diet), the process is known as bioaccumulation and is quantified by a bioaccumulation factor (BAF). According to the existing research data analysis, the BAF trend of all metals is like Turag<Buriganga<Sitalakhya<Meghna. However, the Buriganga River has a significantly greater BAF of Cr. The following are the bioaccumulation sequences in Turag, Buriganga, Sitalakhya, and Meghna: CrPbCd, CdCrPb, CdPbCr, etc.

Sarah et al. (2019) showed that the bio-concentration of metals in fish liver and kidney occurs in the following order: Fe-As-Cd-Zn-Pb and Zn-Fe- As-Cd-Pb, respectively. The existing data have been chosen for this paper through a random selection process (though our target was to collect data on water, silt, and fish from a particular year's research works, it was sometimes troublesome because of the lack of enough available research data). Though metal concentrations in the river water were low, they were higher in fish. The reason for this difference might be the bioaccumulation of metals into fish. In addition, large quantities of toxic metals may be dumped by various pollutant outlets with water, and most of them are stored in sediments. At the same time, the uninterrupted deposition increases their concentrations above the toxic limit. About 90 types of vegetables and 60 types of fruits are grown in Bangladesh, most of which are cultivated during winter.

The existing research data shows that the river water's pollution level is comparatively high this season. In Bangladesh, riverbanks are ideal for growing vegetables since water is simply available for irrigation. Crops cultivated around the riverbank with river water are more prone to high concentrations of toxic metals. Some researchers have also identified the presence of a heavy load of metals in crops cultivated in the polluted area and with the water from the polluted river. The findings of Khan et al. (2014) demonstrated the high presence of specific metals in the crops cultivated in the surrounding areas of the Buriganga River. The vegetables gathered from various markets and bazaars in Dhaka city also have high levels of heavy metals.

According to the research data findings, vegetables cultivated in urban areas accumulate more heavy metals than those in rural areas. A high presence of metals, particularly Pb, is noticed in the vegetables grown in roadside areas. The analysis of geo-accumulation index values reveals that the soils of the Dhaka city area are extensively contaminated. A high amount of Cd, Ni, Pb, Zn, As, and Cr is also identified in the agricultural soils of the city areas in the country.

In this case, the primary source of metal contamination is the massive use of agrochemicals and polluted river water. Ecologically, Bangladesh has been facing arsenic problems in its water, soil, and even crops. Generally, a high accumulation of arsenic is found in crops irrigated with water with a high arsenic level. And crops, including rice and vegetables contaminated by arsenic, are consumed in many areas of the country. Thus, we take the metals in our bodies by consuming the accumulated crops. As a result, routinely consuming contaminated foods will result in a high concentration gradient of hazardous metals in the body, which may lead to both non-cancerous and cancerous health issues.

Along with surface water, groundwater, the most important safe water source, is also affected due to the continuous accumulation of heavy metals. In Bangladesh, about 96% of people rely on groundwater, which meets nearly 86% of Dhaka city's drinking water demand. The Dupi Tilla sand aquifer, which lies under the Modhupur clay layer and has a 10m thickness, is Dhaka's key groundwater reservoir. Generally, the thickness of the aquifer ranges from 100 m to 200 m. The surrounding rivers to which this aquifer is exposed facilitate groundwater recharge to the aquifer.

Due to extensive exploitation and contamination, groundwater is unsafe and cannot be used without proper treatment. The groundwater level dropped by nearly 20 m in the last decade while 70 m since 1990. The deep tube wells installed by the DWASA for extracting groundwater must be repositioned due to river pollution. Groundwater is more likely to be polluted by contaminants moving into groundwater downward from nearby contaminated rivers. The findings of Khan et al. (2014) revealed that harmful metals in river water and soil leach with infiltrating water and mix with groundwater, posing a serious health risk. Metal concentrations in groundwater may rise as a result of excessive groundwater exploitation. These concentrations in the aquifer may also rise if a high amount of metals deposited in riverbed silt get mixed with groundwater flow.

In Dhaka city, approximately 1% of tube well water has a high concentration of Pb than the standard level recommended by WHO for drinking water. As DDT, ammonia, Fe, Ni, Co, Nitrate, Mn, arsenic, and B have been found in groundwater

in significant amounts across the nation, the extensive use of inorganic fertilizers, herbicides, and insecticides has an effect on groundwater. Both surface and groundwater are continuously contaminated due to various natural processes and anthropogenic activities. Pollutants move into the aquifers, the main source of drinking water in Bangladesh, during the recharge process of groundwater between the river water and aquifers.

Water contamination is causing major health problems for people living in developing countries, and surprisingly, most people have little knowledge about the cause of their suffering. Asia has the largest concentrations of dissolved heavy metals among the five continents (these continents are: North America, South America, Europe, Asia, and Africa)- while Europe has the lowest concentrations. Asia saw the greatest decline in cancer risk owing to Cr contamination from 1970 to 2017, followed by Africa and North America. However, the existing research data analysis reveals that Bangladesh is experiencing severe Cr pollution.

People in various parts of the country have long been facing serious health hazards caused by arsenic in both surface and groundwater. Moreover, the researcher has found bioaccumulation of toxic metals in the fish samples collected from rivers. The excessive presence of different harmful metals is also found in the foods cultivated in the surrounding areas of polluted rivers or with the water of contaminated river water. When people consume these foods, these metals enter the human body, causing various toxic effects.

Also, human health is very vulnerable to various diseases due to hazardous microorganisms in surface water. Common diseases caused by consuming contaminated water include cholera, typhoid, diarrhea, fever, dengue, viral hepatitis, and gastroenteritis. Because of the severe surface and groundwater contamination, many people in Bangladesh suffer from waterborne hazards yearly. The hazardous level in heavy metals is often calculated using several variables, including target TR, HI, and THQs, and compared to a predetermined set of values. Human health is very vulnerable to potential diseases when the value of THQ is >1. On the other hand, if TR is > 106, there is a chance of adverse health effects.

Islam et al. (2018) demonstrated the excessive presence of THQ (THQ>1) for Pb in vegetables and As in grains, which can be fatal for human health. In Karatoa River, adjacent to Bogura City, the value of TR is found to be>106 for intake of Pb and As from food, suggesting the risk of serious cancer. Besides, water samples from Teesta, Pashur, Meghna, Sitalakhya, Karatoya, and Rupsa Rivers have also been examined to determine the status of As, Pb, and Cr and their possible threat to public health. According to the analysis of HI value, people, especially children, and adults, are exposed to serious health risks if they consume water from these rivers. Furthermore, the presence of Cr was higher than USEPA's recommended value for drinking water, which can also pose a serious threat to public health.

Ali et al. (2020) assembled six fish samples from the vicinity of Karnaphuli River and examined the concentration
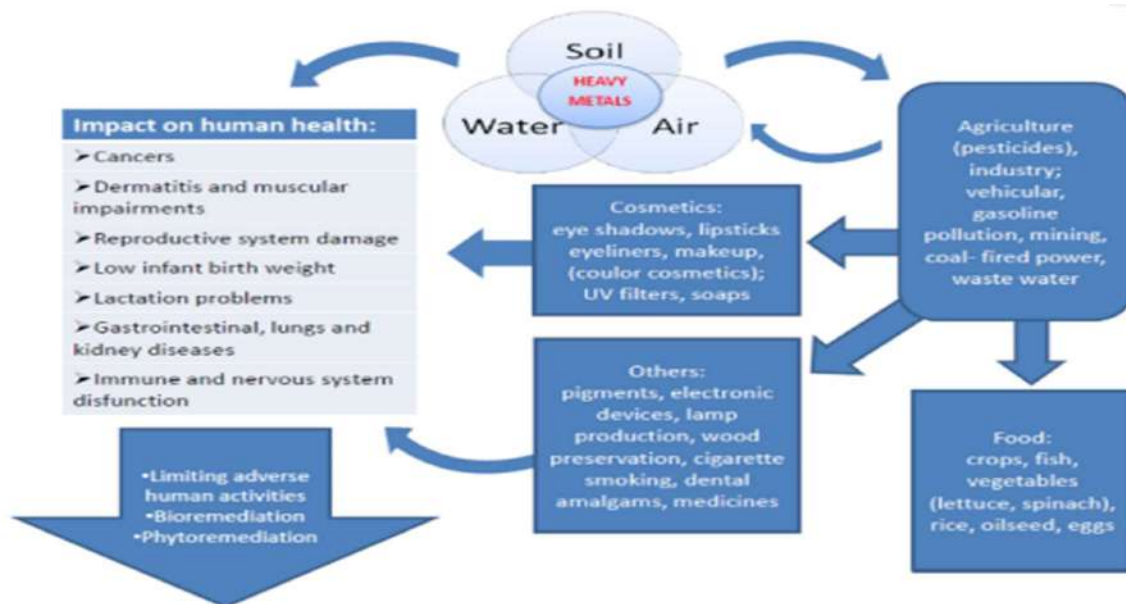
Fig. 6: Heavy metals and human health.

of heavy metals in them. According to the THQs and TR values of the analysis, people consuming these fish are vulnerable to noncarcinogenic and carcinogenic health consequences. People living in the southwestern (Turag-Buriganga- Dhaleshwari) region in Dhaka city are also exposed to severe health risks due to the analyzed HQ and HI values in the groundwater of that area. Besides, people consuming vegetables cultivated in the basin area of the Buriganga River are also vulnerable to deadly cancer problems since the TCR value for Cr, Ni, and Pb in these grains is found to be higher than the USEPA-recommended value. Hasan et al. (2020) also examined the concentrations of ten heavy metals in the fish samples taken from the Dhaleshwari River and found the excessive presence of Ni and Cr.

Humans consuming these contaminated fish are subject to experiencing various carcinogenic (TR>104) health hazards. The presence of Pb, Cd, As, Ni, and Cr in estimated daily intakes (EDIs) is also above the maximum tolerable daily intake (MTDI), indicating food consumption as the possible source of these metals. The value of PHQ (combined hazard quotient) is found to be >1 in fish, vegetables, fruits, and rice samples, which may pose a serious health threat to the city residents (Fig. 6). The findings of Palash et al. (2020), who examined the values of Cr, As, Cu, Cd, Zn, Pb, and As in nine fish samples obtained from the Meghna River, reveal that fish may not, in accordance with the EDI value, pose any toxicity to public health.

Moreover, all metals, with the exception of those that remain in fish bodies in their biological form, have a THQ value of 1. They have concluded that Cd can pose a cancer risk among children and elderly people. Macrobrachium rosenbergii, an economically significant gigantic freshwater shrimp, gathered from various farms, Meghna and Karnaphuli rivers are also analyzed to determine the concentrations of heavy metals. The analysis findings reveal elevated Pb, Cr, Cu, Pb, and Mn concentrations in the collected water and fish. The calculated value is also higher than the acceptable level for Pb and Cr.

Furthermore, the THQ values of Zn, Cu, Cd, and Pb are also found to be less than one, while the TR values for Ni and Pb exceed the standard limit. Researchers have observed that prawn species have greater quantities of hazardous metals that can pose serious health hazards. Two searchers, Saha and Zaman, employed THQ and HI factors to examine vegetable, fruit, and seafood samples obtained from Rajshahi City's major market in 2012. According to the findings of their calculation, vegetable, fruit, and fish samples can seriously harm one's health if consumed regularly. Poisonous metals and detrimental microorganisms can pose serious

health complications to aquatic life, including damaging tissue, DNA, and cellular, and severely cause restlessness, hyperactivity, neurotoxicity, genotoxicity, etc.

It is also found that people consuming fish from the Buriganga River are exposed to severe toxic consequences, including genotoxicity since the Cr concentration in them exceeds the standard value. Besides, fish species are also exposed to severe toxicity due to the presence of an elevated amount of Cr in polluted rivers. Hilsa fish is known worldwide for its unique deliciousness, and over half of the total production of this popular fish occurs in various rivers and the Bay of Bengal in Bangladesh.

However, the interrupted river water contamination and climate changes have badly affected the Hilsa fish production and genotypic alterations of the kind. The largest natural spawning habitat for carp fishes like Cirrhinus cirrhosis, Gibelioncatla, and Labeorohita is the Halda River in Bangladesh's southeast. Analysis of heavy metal concentrations in seven economically significant shellfish and fish species' edible tissue reveals that certain species' amounts of Zn, Ni, and Pb are higher than the dietary limit values.

According to the bioaccumulation factor BAF, dangerous metals have inevitably bioaccumulated in the studied species. According to figures from Fulton's condition factor, some fish species are unhealthy. Even when the CR, THQ, and EWI values appear under the acceptable limit, Monte Carlo simulation data reveals that Pb concentration causes significant carcinogenic and noncarcinogenic health concerns to children.

Islam et al.'s (2018) analysis of the sediment pollution data in 2020 suggested that flora and fauna in Bangladesh's headwater, midstream, and downstream rivers are experiencing frightening conditions. In addition, EF, Igeo, and contamination factor data analysis on metal concentrations in river sediment revealed moderate to high contamination concentrations for Ag, Co, and Hg. According to calculations for probable impact concentration (PEC) and threshold effect concentration, only Cr and Ni concentrations occasionally showed harmful effects on ecosystems (TEC). According to research, Ag, Ni, and Hg originate from several anthropogenic causes.

Bangladesh has passed numerous ordinances, laws, rules, acts, and policies to control environmental pollution. The Bangladesh Environment Policy of 1992, the Environmental Conservation Act of 1995 (as amended in 2000, 2002, and 2010), the Environment Pollution Control Ordinance of 1977, the Environmental Conservation Rules of 1997 (as amended in 2002, 2005, and 2010), the National Water Policy of 1999, the National Policy for Safe Water Supply and Sanitation of

1998, the Bangladesh Environment Court Act of 2000, the National Policy for As Mitigation of 2004, the Environment Court Act of 2010, and the Bangladesh Environment Policy of 1992 are among the laws and regulations currently exist.

To carry out the Environmental Conservation Act of 1995, the government of Bangladesh also formed the Department of Environment (2023), whose top administrative officer is a director, a general-level officer. This division is in charge of monitoring all national environmental pollution activities. Additionally, the Centre for Environmental and Geographic Information Services, often known as CEGIS for short, was founded to support inclusive growth, a healthy environment, and clean water for the nation's benefit. Environmental pollution in Bangladesh must be protected, and appropriate actions must be taken by the Ministry of Water Resources, Ministry of Environment, Forest, and Climate Change.

The Water Supply and Sewerage Authority, a signatory authority, regulates surface water contamination in cities. They have offices in important cities where they supervise the supply and management of water. A joint venture titled "To the Prime Minister: Save Rivers, Save Dhaka" was taken by Channel-I, a popular television channel, and a reputed English daily newspaper, in 2009. They highlighted the critical state of water contamination in the four rivers that encircle Dhaka. Based on it, the concerned officials immediately took certain actions to control pollution. However, sudden news accompanied by sparse data proved inadequate to significantly influence the current pollution rate. In recognition of this and light of the necessity, the High Court announced the rivers as "legal entities" with rights comparable to those of living things on February 3, 2019. It formed a river protection commission to oversee and prevent contamination.

After its measures, the High Court noted that DWASA was in charge of 68 subterranean drainage and sewerage lines that were interruptedly contaminating river water. On December 9 of the same year, the High Court also ordered DWASA to suspend all sewage lines and directed the Department of Environment to take indispensable measures against contamination. The Department of Environment is now working to monitor and regulate river contamination.

The findings of several types of research demonstrate that the current water quality in significant city rivers is not favorable for human health and the environment. High reliance on groundwater and irresponsible surface water treatment is ineffective in saving the Earth from being dearth. As per the United Nations Report 2012 estimation, the demand for water by 2030 will be 40% higher than the amount available. Specific (S), measurable (M), assignable (A), realistic), and time-based (T) are all part of the acronym

SMART. Bangladesh needs SMART water management immediately, considering the extent of river contamination.

According to available research data, the Balu, Turag, Buriganga, Karnaphuli, and Sitalakhya Rivers are the most contaminated. Besides, Rupsha, Teesta, Korotoa, Karnaphuli, and Meghna rivers are also facing contamination, according to the data analysis on water quality. In many areas of the country, groundwater level has already decreased and is affected badly due to ongoing contamination. Both anthropogenic and geological pollutants contribute to the contamination of river water. Bangladesh's population increased to 149.77 million in 2011 from 76.2 million in 1974. The estimated populations for 2030 and 2050 are 186 and 202 million, respectively (Uddin et al. 2014). People now largely depend on groundwater for drinking, irrigation, and industrial purposes, causing gradual depletion in groundwater levels.

River water is, therefore, the most crucial resource for supplying the enormous demand for water. However, the research data analysis reveals that the current quality of river water is unsafe for agriculture and drinking. According to toxicology analysis data, consuming foods and fish cultivated and collected with and from contaminated river water may cause people to develop both cancerous and non-cancerous diseases. Some common health problems people in Bangladesh face include fever, obesity, pain, hypertension, coughing, heart failure, mental disorder, brain stroke, diabetes, tumor, cancer, etc. According to study data on the current ground and surface water status, Bangladesh is already experiencing a safe water crisis, which will become a serious situation shortly.

Natural hazards are common and frequently occur in Bangladesh. The chemistry of the chemical constituents of water is negatively altered by salinity intrusion in rivers and groundwater. According to the analysis of available research data, nearly two crore people living in southern Bangladesh are experiencing safe water deficiency. The research data analysis on climate change demonstrates that the safe water crisis will affect the country's coastal areas adversely in the future. Being Bangladesh, a riverine country, its land is filled with fertility. The lone way to meet the country's huge demand for water in the future is to implement the SMART river water management system. Most parts of Bangladesh are covered by several rivers, which act as natural reservoirs to retain rainfall and rehydrate the groundwater. The environmentally friendly strategy to control water demand and protect human health and the environment is switching from groundwater to river water.

Hence, importance should be given to strengthening laws and monitoring urgently with a proper concentration

on the current situation. Contamination-specific research is required to assess the accumulation and destiny of elements and compounds in human health and the ecosystem. The government ought to make an effort to create awareness among people about the use of surface water and gain public confidence in safe water. Unattended automated water quality measurement stations can be installed along a river's course. A central monitoring system for many rivers can keep the river clean of pollutants. It is possible to use a variety of software and programming models (SCADA-Supervisory control and data acquisition) to monitor and measure river water quality. Data from both public and commercial studies may be shared to get a more accurate and realistic picture of pure water quality management.

CONCLUSION

This paper has collected and compiled the research data of the past 40 years on river pollution in Bangladesh and has attempted to convey river pollution patterns and current conditions using a tabular and graphical representation. According to trends of physicochemical and hazardous metals data, intense contaminations have occurred but are not frequent. Most of the metrics in the Buriganga and Turag River water exhibit a similar surge from 2008 to 2012, and the Sitalakhya River also shows a similar surge from 2011 to 2015.

This may result from severe Turag and Buriganga Rivers contamination, which eventually flows into the Sitalakhya River. Karnaphuli River experienced a high level of contamination between the periods 2012-2015. The analysis of the existing research data reveals that the water and sediment of the Turag, Buriganga, Balu, Sitalakhya, and Dhaleshwari Rivers are polluted with harmful metals, and at certain samplings locations, are higher than the standard values for surface water, irrigation, and drinking. Lower Basin Rivers constantly get these massive amounts of pollution while anthropogenic contamination also goes along the river banks.

In the Karnaphuli River, heavy metals are higher than the standard value for safe drinking water. The concentrations of Cd, Ni, Mn, and Cr also exceed the standard limit for irrigation water. Fe and Mn concentrations in the Teesta River are above irrigation standards, as are the concentrations of Cd and Cr in the Korotoa and Fe, Mn, Zn, and Cr in the water of the Rupsha River. The sediment samples of the rivers also have high concentrations of metals. Metal concentrations in the Old Brahmaputra River are below the USEPA recommended standard limit. Most river silt is contaminated with Cr, Cd, Zn, Fe, Cu, Pb, and Ni at levels above standard values. Accumulation of these metals in

groundwater has the potential to contaminate groundwater. The groundwater in some areas of Dhaka City requires treatment before consumption due to the concentrations of toxic metals. The contaminated river causes heavy metals to bioaccumulate in fish bodies, posing hazardous consequences. Consuming this tainted fish can have serious toxic effects on the human body.

Additionally, grains grown close to the contaminated river contain high metal concentrations. Numerous studies have examined data on TCR, THQ, EDI, TR, and HI and found that long-term consumption of food contaminated with metals may have serious carcinogenic and noncarcinogenic health effects in people. According to research findings, it is evident that all the key urban rivers are receiving pollutants while some of them are experiencing severe contamination.

Furthermore, all the research data that is currently accessible is based on only physicochemical and metals evaluation. It is not common practice to undertake studies on organics, antibiotics, microplastics, personal care products, and other hazardous pollutants in river water. Therefore, it is urgently necessary to stop Bangla'esh's river pollution, and in-depth research, ongoing observation, and strict laws and regulations are needed.

REFERENCES

Ahaduzzaman, P.S. 2017. Overview of Bangladesh's main industries. J. Chem. Eng., 30(1): 51-58.

Akindele, E.O. and Akinpelu, O.T. 2020. Heavy metal toxicity in a degraded tropical stream benthic sediments and water column. Ecotoxicol. Environ. Saf., 190: 110153.

Alam, M., Uddin, M. and Sattar, M. 2020. Water quality and garbage loads in the Buriganga River vary seasonally and are visualized using GIS. Bangladesh. J. Sci. Ind. Res., 55(2): 113-130.

Ali, M. M., Ali, M. L., Proshad, R. and Mamun, A. A. Heavy metal concentrations in commercially valuable fishes with health hazard inference from Karnaphuli river, Bangladesh. Hum. Ecol. Risk. Assess. 26(5). DOI: 10.1080/10807039.2019.1676635.

Bangladesh Association of Pharmaceutical Industries (BAPI). 2023. Competitive edge of Bangladesh Pharma. Retrieved from http://www.bapi-bd.com (accessed date February 7, 2023).

Bangladesh Poribesh Andolon (BAPA) 2023. BAPA Report-2023. Retrieved from https://www.bapa.org.bd (accessed date January 11, 2023).

Bangladesh Ready-Made Garments (BRMG) 2022. Bangladesh Made Clothing. Retrieved from https://www.newclothmarketonline.com

Bangladesh Water Development Board (BWDB) 2023. River Management Improvement Program (RMIP) Environmental Management Framework (E-F) - Ministry of Water Resources of the People's Republic of Bangladesh. Retrieved from https://bwdb.gov.bd/annual-reports (accessed date February 1, 2023).

Bashar, T. and Fung, I. 2020. Water contamination in Dhaka, a megacity with a large population. Water, 12(8): 1-13.

Department of Environment (DoE) 2023. Bangladesh Report: State of the Environment. Retrieved from http://www.doe.gov.bd (accessed date November 30, 2022).

Doza, M.B., Islam, S.M.D. and Rume, T. 2020. Assessment of the quality

of the groundwater and the risks to human health for a secure and long-lasting water supply for Bangladesh's residents of Dhaka City. Groundwater Sustain. Dev., 10: 374.

Gray, N.F. 2010. A Primer for Engineers and Scientists Working in the Environmental Field. CRC Press, London, pp. 152.

Hasan, M. R. Mawa, Z. and Hassan, H. U. 2020. Impact of eco-hydrological factors on growth of the Asian stinging catfish *Heteropneustus fossilis* (Bloch, 1794) in a Wetland Ecosystem. Egypt. J. Aquat. Biol. Fish., 24(5): 77-94.

Islam, G.M.M., Tarafder, S.K. and Hasan, A.B.M.M. 2018. Physical-chemical evaluation of water quality indicators in Bangladesh's Khulna region's Rupsha River. Int. J. Eng. Sci., 7(2): 57-62.

Islam, N. 2019. What Happened to Our Waterways in 2019? Retrieved from https://www.thedailystar.net

Khan, S., Anwar, K., Kalim, K., Saeed, A., Shah, S. Z., Ahmad, Z., Ikram, H. M., Khan, S. and Safirullah 2014. Nutritional evaluation of some top fodder tree leaves and shrubs of district Dir (lower), Pakistan as a quality livestock feed. Int. J. Curr. Microbiol. App. Sci., 3(5): 941-947.

Newaz, K.K., Pal, S. K., Hossain, S. and Karim, A. 2020. Evaluation of heavy metal pollution risk associated with road sediment. Environ. Eng. Res., 26(3): 200239. DOI: https://doi.org/10.4491/EER.2020.239

Palash, M. L., Jahan, I., Rupam, T. H. Harish, S. and Saha, B. B. 2020. Novel technique for improving the water adsorption isotherms of metal-organic frameworks for performance enhancement of adsorption driven chillers. Inorganica Chim. Acta, 501. DOI: https://doi.org/10.1016/j.ica.2019.119313.

Rai, P.K., Lee, S.S. and Kim, K. H. 2019. Risks to human health, destiny, processes, and control of heavy metals in food crops. Environ. Int., 125(1): 365-385.

Rakib, M. A., and Fukunaga, M. 2019. In Bangla'esh's southwest coastal region, where drinking water is severely salinized, and there are

related health risks, migration risk is increased. J. Environ. Manag., 240(1): 238-248.

Ranjan, A. 2020. Bangladesh's water problems: Escalating pollution and poor administration. Asian Aff., 51(2): 328-346.

Reza, A. and Yousuf, T.B. 2016. Trash dumping affects Bangladesh's Buriganga River's water quality and potential solutions. J. Environ., 11(1):35-40.

Sakamoto, M. and Ahmed, T. 2019. Bangladesh's textile industry and water pollution: a result of poor business practices or limited opportunity? Sustainability, 6: 11.

Sarah, R., Tabassum, B., Idrees, N., Hashem, A. and Abdullah, E, F. 2019. Bioaccumulation of heavy metals in *Channa punctatus* (Bloch) in river Ramganga (U.P.), India. Saudi J. Biol. Sci., 26(5): 979-984.

Sarkar, A.M., Rahman, A.K. and Islam J.B. 2020. Bangladesh's surface and groundwater pollution: A review. Asian Rev. Environ. Earth Sci., 6(1):47-69.

Sultana, M.N., Latifa, G. A. and Hossain, M. S. 2019. Evaluation of the Balu River's water quality in Dhaka, Bangladesh. Water Conserv. Manag., 3(2):8-10.

Uddin, M.J. and Jeong, Y.K. 2021. Urban river pollution in Bangladesh over the past 40 years: Potential risks to public health and the environment, existing regulations, and potential future directions for smart water management. Heliyon, 7(2): 1-23.

Uddin, M.J., Mamun, S.A. and Huq, S. I. 2014. Wastewater irrigation's effects on the development and nutrient status of kalmi (Ipomoea aquatica Forssk.). Dhaka Univ. J. Biol. Sci., 23(2): 1-8.

United Nations Conference on Trade and Development (UNCTAD) 2021. Least Developed Countries Ranking. Retrieved from https://unctad.org (accessed date November 10, 2022).

Whitehead, P.G., Bussi, G. and Alabaster, G. 2019. calculating the impact of tannery pollution control on the levels of heavy metals in the Buriganga River System, Dhaka, Bangladesh. Sci. Total Environ., 13: 409.

Polycyclic Aromatic Hydrocarbons in Thai and Myanmar Rice: Concentrations, Distribution and Health Concerns

C. Choochuay*, W. Deelaman**† and S. Pongpiachan***

*Faculty of Environmental Management, Prince of Songkla University, Hat-Yai Campus, Songkhla, 90110, Thailand
**Division of Environmental Science and Technology, Faculty of Science and Technology, Rajamangala University of Technology, Phra Nakhon, Bangkok 10800, Thailand
***NIDA Center for Research & Development of Disaster Prevention and Management, School of Social and Environmental Development, National Institute of Development Administration (NIDA), 118 Moo 3, Sereethai Road, Klong-Chan, Bangkapi, Bangkok, 10240, Thailand
†Corresponding author: W. Deelaman; woranuch.d@rmutp.ac.th

ABSTRACT

In the present study, we studied the concentrations and proportions. We identified the potential sources and health risks of 12 probably carcinogenic polycyclic aromatic hydrocarbons (PAHs) in rice grain from 31 sites in Thailand and Myanmar. The findings showed that PAH concentrations in rice grain samples from Thailand and Myanmar were in the range of 0.09 to 37.15 $ng.g^{-1}$ with an average value of 18.22 ± 11.76 $ng.g^{-1}$ and 0.07 to 150.73 $ng.g^{-1}$ with an average value of 34.70 ± 40.57 $ng.g^{-1}$, respectively. The majority group of PAHs in the rice grain samples from Thailand were the five-ring PAHs (78%), followed by four-rings (12%) and three-ring PAHs (9.5%), respectively, while for Myanmar was the five-ring PAHs were the majority (64.02%), followed by six-rings (15.22%) and four-ring PAHs (13.58%), respectively. The diagnostic ratio analysis suggested that pyrogenic origin is a major source of PAHs, and principal component analysis (PCA) identifies the incomplete combustion of fuel as likely the primary source of emissions source of PAHs contamination in rice grain samples. The total values of incremental lifetime cancer risk (ILCR) of PAH content of rice grain for children and adults were 1.95×10^{-8} and 1.44×10^{-8}, respectively, for Thailand and 1.83×10^{-7} and 1.35×10^{-7} for Myanmar, which showed that the incremental lifetime cancer risk from rice grain was lower than the baseline set is considered to be safe levels.

INTRODUCTION

Polycyclic aromatic hydrocarbons (PAHs) contain two or more benzene rings and are classified as persistent organic pollutants (Deelaman et al.2020a, 2021). It is generally recognized that both natural and anthropogenic combustion plays a major role in the formation of PAHs (Bamforth & Singleton 2005, Ravindra et al. 2008, Zhang & Tao 2009, Abdel-Shafy & Mansour 2016). Since many PAHs have been released into the environment due to swift industrial and economic development, various governments are currently concentrating on controlling PAHs. Some PAHs originate from the incomplete combustion of fuels, such as oil, gas, coal, and wood, for energy supplies, including vehicles and machinery (Maliszewska-Kordybach 1999, Qin et al. 2018, Zhu et al. 2019). Moreover, PAHs are released while manufacturing dyes, plastics, agrochemicals, resins, and pesticides (Abdel-Shafy & Mansour 2016). According to the World Health Organization, around 50% of people in Africa

and 75% in Southeast Asia, India, and China use wood-based fuels for daily cooking. More than 90% of the concentration of PAHs in the environment is estimated to be attributable to combustion sources (Neilson 1998).

PAHs can be found in several components of the environment, such as the atmosphere, soil, water, sediment, vegetables, food, and adipose tissue of living organisms (Bamforth & Singleton 2005, Pongpiachan et al. 2017, ChooChuay et al. 2020, Deelaman et al. 2020b). The International Agency for Research on Cancer under the World Health Organization has designated that 17 types of PAHs are of the greatest concern with adverse health effects on humans, and the US Environmental Protection Agency (USEPA) has identified seven PAHs as probable human carcinogens (IARC 2010, Kim et al. 2013, Abdel-Shafy & Mansour 2016). The main issue with PAHs is that they can reactively metabolize; some can attach to DNA and proteins in cells, resulting in cell damage, tumor formation,

and mutations. High PAH concentrations in the ecosystem can affect living organisms, such as fish, shellfish, and birds (Tudoran & Putz 2012, Inomata et al. 2012). Additionally, PAHs can enter the human body by eating, touching, and inhaling contaminated plants. Plants can absorb PAHs from polluted soil through their roots and transfer them to other parts (bio-accumulate) (Dong et al. 2012, Veltman et al. 2012, Abdel-Shafy & Mansour 2016).

Approximately half of the world's population consumes rice (*Oryza sativa* L.) as a staple food, particularly in Asia. By 2050, the world population is estimated to reach 9.8 billion (United Nations 2017, Liu et al. 2019, Fried et al. 2021). In the following decades, global population expansion is anticipated to increase demand for agricultural products (Foley et al. 2011, Alexandratos & Bruinsma 2012, Martin & Sauerborn 2013, Fried et al. 2021). Southeast Asia has a large agricultural area, accounting for 32% of the total land surface in 2018, with 50 million ha of rice plantation (Fried et al. 2021). In 2019, Thailand was the world's sixth producer of rice after China, India, Indonesia, Bangladesh, and Vietnam, with an estimated harvest of 28 million tons, which accounted for approximately 3.8% of the world's rice output (FAO 2020. Myanmar, which borders Thailand, is the seventh largest rice producer worldwide, harvesting approximately 26 million tons of rice. The consumption behaviors of people in both countries are similar in that they primarily rely on rice for their daily food intake. Over the past decade, numerous studies have examined the PAH contents that contaminate the environment. Several studies have assessed the levels of PAH contamination in food and the effects of pollution sources. Studies on PAH contents in ten major foods (cereals, nuts, fruit, meat, fish and shellfish, beverages, seasoning, pulse crops, vegetables, and eggs) in Korea detected PAHs in seven major food groups: cereals, nuts, fruit, meat, fish, beverages, and seasoning (Lee et al. 2018).

Similarly, phenanthrene, fluoranthene, and pyrene are the PAHs detected in raw fruits and vegetables. Numerous studies have revealed that the PAH concentrations in fruits and vegetables may vary considerably, depending on the area surrounding the plant, aromatic hydrocarbons, or the product itself (Paris et al. 2018). However, studies on PAH contamination in rice, a staple food in many Asian countries, are limited. Therefore, to provide more information on the safety of rice consumption, focusing on and supporting the studies on this major food group are necessary. This study randomly collected rice grain samples from different areas of the two countries (Thailand and Myanmar). Qualitative and quantitative analyses of 12 PAHs in the rice grain samples were carefully conducted to (i) assess the concentrations and proportions of PAHs in the areas of Thailand and Myanmar;

(ii) identify possible sources of PAHs in rice grains using diagnostic binary ratios; (iii) assess the risk of exposure to PAHs using toxicity equivalent concentration (TEQ) equations; moreover, this is the first assessment of health risks associated with farmers and consumers in the areas of 12 dominant PAHs that have been found in rice grain samples in each age range. We also compared the impact of the age range of affected rice grain samples on the risk.

MATERIALS AND METHODS

Sampling Sites

Rice grain samples were randomly collected from 11 sites in Thailand: northern (Phayao, Lamphun, Phichit, and Tak provinces), eastern (Ubon Ratchathani, Yasothon, and Loei provinces), central (Nakhon Sawan and Suphan Buri provinces), and southern (Phatthalung and Nakhon Si Thammarat provinces). Samples were collected from 20 sites in Myanmar, including Nwar Kyoe Aing, Taung Ywar Naung, Patheingyi, Yae Htwet, Amarapura, Pan Chi, Hpa Ye Kyun, and Myauk Kaing. Fig. 1 shows a sampling point with a global positioning system used to accurately locate each point. The sampling duration was from December 2017 to February 2018 ($n = 31$).

Sample Collection and Preparation

All sampling sites were situated in the city of agricultural areas. Rice grain samples were collected from fields grown for four months. All precautions for rice sampling followed the "Crop Sampling Protocols for Micronutrient Analysis" to avoid contamination (Stangoulis & Sison 2008). First, the rice grains were manually threshed and wrapped in pre-cleaned aluminum foil. The samples were stored in labeled plastic bags to avoid the degradation of PAH caused by heat, gas, and ultraviolet radiation when transported to the laboratory. Samples were ground to homogenize, wrapped in pre-cleaned aluminum foil, packed in a plastic bag, and stored at -20 °C in a refrigerator before chemical extraction.

Chemicals and Standards

A concoction of twelve PAHs was formed according to the Norwegian Standard (NS 9815: S-4008-100-T) (phenanthrene [Phe], anthracene [An], fluoranthene [Fluo], pyrene [Pyr], Benz [a]anthracene [B[a]A], chrysene [Chry], benzo[b] fluoranthene [B[b]F], benzo[k]fluoranthene [B[k]F], benzo[a] pyrene [B[a]P], indeno[1,2,3-cd]pyrene [Ind], dibenz[a,h] anthracene [D[a,h]A], and benzo[g, h, i] perylene [B[g, h, i] P]) with each 100 μg.mL^{-1} in toluene (1×1 mL). Additionally, deuterated-perylene [d_{12}-Per] and deuterated-fluorene [d_{10}-Fl] were synthesized as a mixture of recovery standard (IS) PAHs at a concentration of 100 μg.mL^{-1} in xylene. All
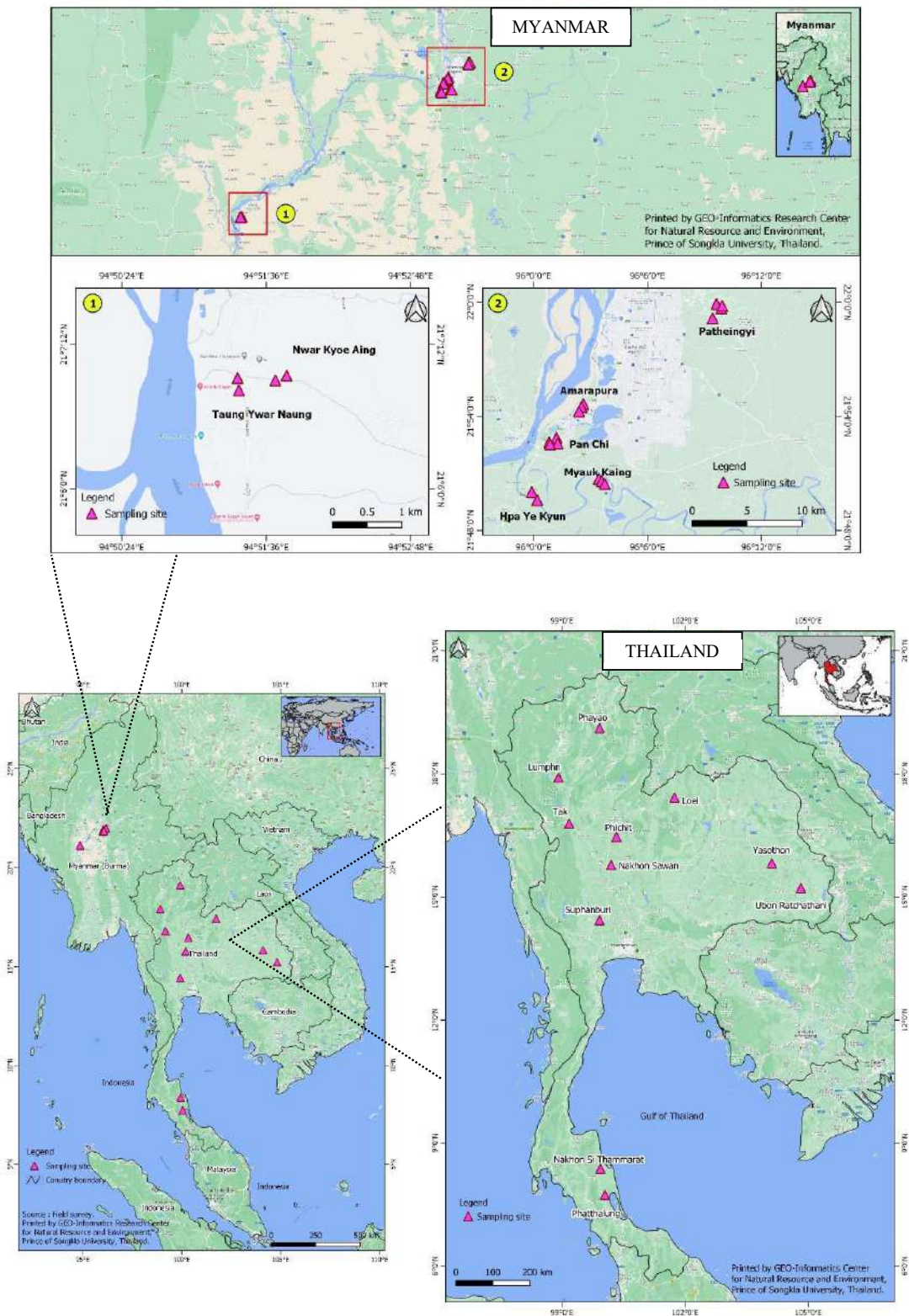
Fig. 1: Rice paddy sampling stations in Thailand and Myanmar.

substances utilized in this work were purchased from Chiron AS (Stiklestadveine 1, N-7041 Trondheim, Norway).

Sample Extraction, Cleanup and Analysis

This investigation used dichloromethane (DCM; Fisher Scientific) of high-performance liquid chromatography grade to chemically extract all rice grain samples, similarly to other organic solvents (e.g., hexane). A Soxhlet extraction thimble (cellulose fiber; size: 30 × 100 mm) was pre-cleaned and filled with around 50 g of the freeze-dried, homogenized rice grain sample. Subsequently, 50 µL was spiked with a known amount of internal reference standard before adding 250 mL of DCM to the sample along with 1 g of copper powder, and extraction was completed using a Soxhlet extractor for 8 h. Fractionation, cleanup, and blow-down were performed following the method described by Gogou et al. (1998). The pre-cleaned silica gel was then oven-dried at 150°C for 3 h, and the extract was transferred to the column. The PAH compound groups were classified by eluting with 15 mL of n-hexane and 5.6:9.4 (v/v) toluene: hexane. Subsequently, the solution was rotary evaporated and purged with a gentle nitrogen stream to almost dryness. The solvent was then changed to cyclohexane, and the volume was reduced with nitrogen again until the final volume was 100 µL; the solution was then quantified using a gas chromatograph/mass spectrometer (GC/MS; Shimadzu GCMS-QP, 2010 Ultra, Japan). Additional details about the GC/MS method can be found in previous studies (Pongpiachan et al. 2012, Deelaman et al. 2020a, b).

Source Identification of PAHs

Some PAHs are regarded as markers for specific environmental PAH-releasing processes. They are tracers, signatures, or origin markers (Ravindra et al. 2008). The relative thermodynamic stability of the various parent PAHs must be understood to use the PAH ratio for sediment attribution, according to Yunker et al. (2002). The relative stability of different PAH isomers and PAHs from different sources and the nature of different PAH sources can be used to determine their origin. The characteristics of the PAH patterns detected in the rice grains were consistent with the emission sources in the surrounding agricultural fields, where the PAH source can be distinguished based on the concentration and type of PAH found in the rice grain. PAHs with molecular weights of 178 and 202 were used to differentiate their sources between combustion and petroleum (Budzinski et al. 1997, Soclo et al. 2000, Yunker et al. 2002, Katsoyiannis & Breivik 2014). Diagnostic binary ratios of PAHs were employed to determine the sources of PAHs found in rice grains, which included six ratios of PAH isomer pairings. The details and PAHs emission rates for the various sources are shown in Table 1.

Table 1: Comparing the values obtained from this investigation with the characteristics of selected diagnostic ratios for petroleum, single-source combustion, and traffic emissions. (Modified from Yunker et al. 2002, Katsoyiannis & Breivik 2014)

Source	An/ (An+Phe)	Flou/ (Flou+Pyr)	B[a]A/ (B[a]A+ Chry)	Ind/ (Ind+ B[g,h,i]P)	B[a]P/ B[g,h,i]P	B[b]F/ B[k]F
Non-traffic emissions	-	-	-	-	< 0.6	
Traffic emissions	-	-	-	-	> 0.6	
Petroleum	< 0.10	< 0.40	< 0.20			
Crude oil (n=9) [a,b,c]	0.07	0.22	-	-	-	
Diesel oil (n=8) [d,e,f,g]	0.09	0.26	-	-	-	
Lubricating oil		0.29	0.10	0.12	-	
Asphalt [l,m]	-	-	0.50	0.52-0.54	-	
Combustion	> 0.10		> 0.35			
Bituminous coal (n=3) [h]	0.33	0.53	-	-	-	
Gasoline (n=2) [i,j]	0.11	0.44	0.33-0.38	0.09-0.22	-	0.73
Road dust	0.18	0.42	0.13	0.51	-	
Used engine oil, gasoline passenger car	0.22	0.30	0.50	0.18	-	
Used engine oil, diesel car, truck, and bus	-	0.37	-	0.29	-	> 0.50
Aluminum smelter emissions						2.50-2.90

[a] Grimmer et al. 1983. [b] Wise et al. 1988. [c] Benner et al. 1990. [d] Westerholm & Li 1994. [e] Wang et al. 1999. [f] Schauer et al. 1999. [g] Westerholm et al. 2001. [h] Oros & Simoneit 2000. [i] Li & Kamens 1993. [j] Rogge et al. 1993.

Toxicity Potential of PAHs Contamination of Rice Grains

Through dietary consumption, skin contact, and the respiratory system, PAHs may be bio-transferable and absorbed into human bodies, where they may lead to cancer. To estimate the risk of exposure to PAHs and the cumulative effects brought on by all potentially human carcinogenic PAHs, "B[a]P equivalents" were calculated using the toxic equivalency factors (TEFs) defined by the USEPA. The toxicity value estimated by B[a]P equivalent concentrations for Phe, Fluo, and Pyr was 0.001; for An, Chry, and B[g,h,i]P was 0.01; for B[a]A, B[b]F, B[k]F and Ind were 0.1, and for B[a]P and D[a,h]A were 1 (Nisbet & Lagoy 1992). The total TEQ can be calculated as follows:

$$TEQs = \sum_{s} C_S \times TEF_s \qquad ...(1)$$

TEQs are the total toxicity equivalency concentrations, C_S are the concentrations of individual PAHs, and TEFs are toxic equivalency factors.

Health Risk Assessment of PAH Contamination Rice Grains

PAHs are generally found in the environment, exhibiting different types and chemical compositions. Each PAHs type has a specific toxicity level. Depending on the unique characteristics of PAHs, the bioaccumulation of PAHs in the adipose tissue of species varies significantly. Vegetables may be contaminated with PAHs by uptake from the soil through the roots and transportation to other parts. Additionally, plants can adsorb PAHs from gas-phase PAH deposition (Lu et al. 2014). The three main ways most people are exposed to PAHs in the environment are cutaneous absorption, inhalation, and ingestion (Ravindra et al. 2008, Deelaman et al. 2021). We calculated the risk of people exposed to PAHs in rice grains using the USEPA evaluation manual (USEPA 1991) by dividing the population into two groups: childhood and adulthood. Incremental lifetime cancer risk (ILCR) was used to evaluate the risks and potential health concerns associated with three different routes: inhalation (ILCR$_{Inhalation}$), dermal contact (ILCR$_{Dermal}$), and direct ingestion (ILCR$_{Ingestion}$). In this study, the rice grain ILCR can be calculated using the following equations 2, 3, 4, and 5, by the full details and variable description used according to Deelaman et al. (2021)

$$ILCR_{Inhalation} = \frac{CS \times \left(CSF_{Inhalation} \times \sqrt[3]{\frac{BW}{70}} \right) \times IR_{inhalation} \times EF \times ED}{BW \times AT \times PEF}$$

$$...(2)$$

$$ILCR_{Dermal} = \frac{CS \times \left(CSF_{Dermal} \times \sqrt[3]{\frac{BW}{70}} \right) \times SA \times AF \times ABS \times EF \times ED}{BW \times AT \times 10^6}$$

$$... (3)$$

$$ILCR_{Ingestion} = \frac{CS \times \left(CSF_{ingestion} \times \sqrt[3]{\frac{BW}{70}} \right) \times IR_{ingestion} \times EF \times ED}{BW \times AT \times 10^6}$$

$$...(4)$$

$$ILCRs = ILCR_{Inhalation} + ILCR_{Dermal} + ILCR_{Ingestion}$$

$$... (5)$$

The total ILCR results were used to determine potential health hazards to Thailand and Myanmar residents exposed to rice grain PAH contamination. Designated ILCR over 10^{-4} is considered a serious concern for potential health problems, such as cancer; and value between 10^{-6} and 10^{-4} ILCR is considered to have a low-risk level, and an ILCR below 10^{-6} is considered safe.

RESULTS AND DISCUSSION

Concentration and Profile of PAHs from Rice Grain

In this study, 31 rice grain samples were collected from the agricultural areas of Thailand and Myanmar. The total concentrations of 12 PAHs ($\sum_{12}$PAHs: sum of Phe, An, Fluo, Pyr, B[a]A, Chry, B[b]F, B[k]F, B[a]P, Ind, D[a,h]A, and B[g,h,i]P) in these samples were qualitatively and quantitatively assessed. The total PAH concentrations of Thailand ($n = 11$) ranged from 0.09 to 37.15 ng.g^{-1}, with an average value of 18.22 ± 11.76 ng.g^{-1}. In this study, the $\sum_{12}$PAHs had the highest value at TH2, followed by TH5, TH10, and TH, with values of 37.15, 37.00, 25.81, and 22.30 ng.g^{-1}, respectively (Table 2, Fig. 2a). The TH2 station is located in the Lamphun Province, northern Thailand. Very few studies have examined PAH content in Lamphun Province in recent years. However, the area of Lamphun Province is adjacent to Chiang Mai Province, where considerable research has been conducted on PAHs. The sample study of ChooChuay et al. (2020) reported that the major sources of PM$_{2.5}$-bound PAHs could be attributed to the incomplete combustion of biomass, petroleum fuels, and coal, particularly vehicular exhaust. Rice grains from Myanmar ($n = 20$) had a total PAH concentration between 0.07 to 150.73 ng.g^{-1}, with an average of 34.70 ± 40.57 ng.g^{-1}. The $\sum_{12}$PAHs exhibited the decreasing trend of MM3, MM1, MM2, and MM20, with values of 150.73, 106.74, 80.54, and 61.60 ng.g^{-1}, respectively. The first three highest concentrations were detected in a similar area in the

Nyaung-U District in the Mandalay Division of Myanmar. Overall, the results showed that Thailand and Myanmar had similar PAH concentrations (Table 2, Fig. 2a, and Fig. 2c). However, when comparing these values with the total concentrations of PAH detected in other plants, the values were generally lower than those found in lettuce grown near the smelter (300-920 ng.g^{-1}; Larsson & Sahlberg 1982), kale grown near the highway (500 ng.g^{-1}; Brorstrom-Lunden & Skarby 1984), sugar maple grown in urban areas of the USA (500–1,100 ng.g^{-1}; Simonich & Hites 1995), and grass grown in urban areas in the UK (153 ± 8 ng g^{-1}; Meharg et al. 1998); however, the values are similar to that of rice grown in Nanjing, Jiangsu Province, China (80.56-195.97 ng.g^{-1}, Lu et al. 2021).

Four groups of PAH molecular structures were identified in this investigation. Three-ring PAHs (i.e., Phe and An) are acutely toxic with low molecular weights (LMW-PAHs). High-molecular-weight PAHs (HMW-PAHs) comprise four-ring PAHs (i.e., Fluo, Pyr, B[a]A, and Chry), five-ring PAHs (i.e., B[b]F, B[k]F, B[a]P, and D[a,h]A), and six-ring PAHs (i.e., Ind and B[g,h, i]P), which are generally considered as genetic toxins (Abdel-Shafy & Mansour 2016, Lu et al. 2021). Additionally, HMW-PAHs are partially stable and difficult to degrade (Duan et al. 2015, Lu et al. 2021). Fig. 2b shows that the five-ring PAHs were the most abundant group in the rice grain samples of Thailand, ranging from 32% to 97% with an average of 78%, followed by four-ring (12%), three-ring (9.5%), and six-ring (0.5%) PAHs. Meanwhile, PAHs detected in the rice grains of Myanmar showed the highest content of the five-ring group, with abundance ranging from 4% to 98%, with an average of 64.02%. The second most abundant PAH group was the six-ring group (15.22%), followed by four-ring (13.58%) and three-ring groups (7.18%) (Fig. 2d). Miguel et al. (1998) suggested that HMW-PAHs are derived from gasoline and light-duty gasoline vehicles, including gasoline and oil burning at high temperatures. These previous studies are consistent with the results of Marr et al. (1999), who found that four-and five-ring PAHs dominate light-duty vehicles. In addition, incineration can release reasonably high levels of pyrene and fluoranthene (Smith & Harrison 1998).

The TEQs of PAHs in rice grains collected from Thailand and Myanmar were computed using the TEQs of 12 PAHs as TEFs (Table 2). TEQs (12 PAHs) in Thailand samples varied from 0.01 ± 0.00 to 3.60 ± 1.00 ng.g^{-1} with an average of 1.67 ± 1.20 ng.g^{-1}, whereas that in Myanmar samples ranged from N.D. to 121.89 ± 33.70 ng.g^{-1} with an average of 16.75 ± 36.83 ng.g^{-1}. Furthermore, the TEQs of 7 PAHs (B[a]A, Chry, B[b]F, B[k]F, B[a]P, Ind, and D[a,h]A) which are important carcinogens, were discovered. The TEQs of

7 PAHs were similar to those of 12 PAHs; however, the results in Thailand revealed that B[k]F had the greatest TEQs, followed by D[a,h]A and B[a]P with values of 1.51 ± 1.19, 0.07 ± 0.07, and 0.05 ± 0.08, respectively. For Myanmar samples, the highest TEQs were detected for D[a,h]A, followed by B[b]F and B[a]P with values 295.85 ± 36.33, 23.63 ± 1.29, and 8.672 ± 0.58, respectively. Very few studies have been conducted on rice-grain-based TEQ. The Canadian soil quality recommendations created by the Council of Canadian Environment Ministers (CCME) for the protection of the environment and human health are most likely the closest standard setting, which specifies an acceptable TEQ threshold of 7 PAHs of 600 ng.g^{-1} (CCME 2007, Zhong et al. 2012, Chen et al. 2018). In this investigation, the TEQ readings of rice grain samples from Thailand and Myanmar were below the recommended levels.

Source Apportionment via Diagnostic PAH Isomer Ratios

The major sources of PAHs in rice grains sampled from Thailand and Myanmar can be classified into petrogenic and pyrolytic processes. Petrogenic processes involve PAHs formed at low temperatures, for example, the slow maturation of organic materials and the environmental effects of crude oil spills (Abdel-Shafy & Mansour 2016). The incomplete combustion of biomass and fossil fuels occurs during pyrolytic reactions. It also naturally occurs during volcanic eruptions, wildfires, and brush fires under conditions of high temperature and limited oxygen. Six diagnostic binary ratios of PAH isomer pairings were employed in this work. They were displayed in Fig. 3, showing the Flou/(Flou+Pyr) ratio versus B[a]A/(B[a]A+ Chry) ratio and An/(An+Phe) ratio versus Ind/(Ind+ B[g,h, i]P. Cross-plots showing the ratios of Flou/(Flou+Pyr) and B[a]A/(B[a]A+ Chry) can be used to determine the possible source of PAH contamination in rice grains. The results showed that most of the PAHs in the grain samples came from incomplete combustion of various sources.

Furthermore, the individual Flou/(Flou+Pyr) ratios reveal that samples collected from stations TH2, TH3, TH5, TH8, TH10, and TH11 in Thailand may be contaminated by incomplete combustion of biomass, fossil fuel, coal, and possibly diesel emissions. The samples TH1, TH7, and TH9 were formed from petrogenic processes. However, TH4 and TH6 from Thailand could not use the diagnostic binary ratios to determine the source due to the absence of some PAHs in the grain samples of these stations. The results in Myanmar showed that the PAHs of almost all the rice grain samples originated from incomplete combustion, similar to those from Thailand, except for the MM1 station, which originated from
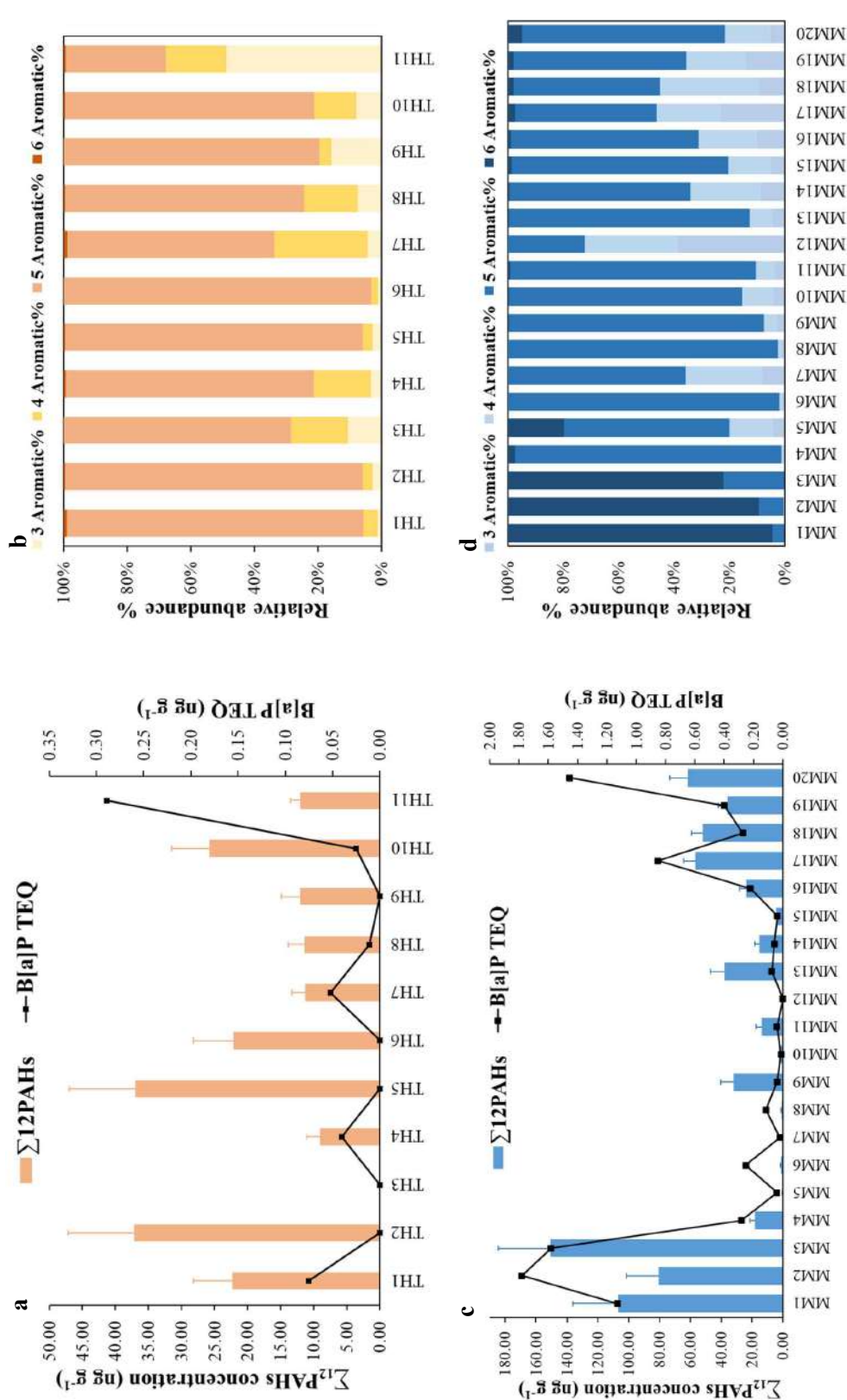
Fig. 2: (a) Total PAH concentrations of 12 PAHs ($\sum_{12}$PAH) and B[a]P toxic equivalence quotient (TEQ) in the rice grain samples of Thailand. (b) Distribution patterns of % contribution and classification of 3–6 ring PAHs in the rice grain samples of Thailand. (c) Total PAH concentrations of 12 PAHs ($\sum_{12}$PAH) and B[a]P TEQ in the rice grain samples of Myanmar and (d) distribution patterns of % contribution and classification of 3–6 ring PAHs in the rice grain samples of Myanmar.

Table 2: The total 12 PAH concentrations and toxic equivalent concentrations.

Sampling sites	$\sum_{12}$PAHs [ng.g^{-1}]	$\sum_{12}$TEQ [ng.g^{-1}]	$\sum_{7}$TEQ [ng.g^{-1}]	Sampling sites	$\sum_{12}$PAHs [ng.g^{-1}]	$\sum_{12}$TEQ [ng.g^{-1}]	$\sum_{7}$TEQ [ng.g^{-1}]
MM1	106.74 ± 29.32	103.43 ± 29.40	103.43 ± 38.45	TH1	22.30 ± 5.89	2.41 ± 0.59	2.41 ± 0.76
MM2	80.54 ± 20.94	75.36 ± 21.03	75.36 ± 27.47	TH2	37.15 ± 9.99	3.60 ± 1.00	3.60 ± 1.31
MM3	150.73 ± 33.68	121.89 ± 33.70	121.89 ± 43.98	TH3	0.09 ± 0.02	0.01 ± 0.00	0.01 ± 0.00
MM4	18.32 ± 3.28	2.22 ± 0.33	2.22 ± 0.38	TH4	9.04 ± 1.96	0.77 ± 0.20	0.77 ± 0.26
MM5	0.36 ± 0.03	0.08 ± 0.01	0.08 ± 0.02	TH5	37.00 ± 9.95	3.58 ± 1.00	3.58 ± 1.30
MM6	1.25 ± 0.24	0.35 ± 0.07	0.35 ± 0.09	TH6	22.13 ± 6.04	2.16 ± 0.61	2.16 ± 0.79
MM7	0.15 ± 0.01	0.03 ± 0.01	0.03 ± 0.01	TH7	11.31 ± 2.00	0.92 ± 0.20	0.92 ± 0.26
MM8	0.80 ± 0.16	0.18 ± 0.04	0.18 ± 0.04	TH8	11.44 ± 2.42	0.95 ± 0.25	0.9 5± 0.32
MM9	31.82 ± 8.37	3.03 ± 0.84	3.03 ± 1.10	TH9	12.09 ± 2.78	0.98 ± 0.28	0.97 ± 0.37
MM10	2.42 ± 0.57	0.22 ± 0.06	0.22 ± 0.08	TH10	25.81 ± 5.66	2.21 ± 0.57	2.20 ± 0.74
MM11	13.93 ± 3.50	1.35 ± 0.35	1.35 ± 0.46	TH11	12.02 ± 1.50	0.75 ± 0.12	0.73 ± 0.15
MM12	0.07 ± 0.01	N.D	N.D				
MM13	37.66 ± 9.30	3.45 ± 0.94	3.45 ± 1.22				
MM14	15.36 ± 2.78	1.17 ± 0.28	1.16 ± 0.37				
MM15	4.32 ± 0.94	0.42 ± 0.09	0.42 ± 0.12				
MM16	23.62 ± 4.33	2.08 ± 0.44	2.06 ± 0.56				
MM17	56.76 ± 7.61	4.76 ± 0.80	4.70 ± 0.97				
MM18	51.81 ± 7.32	4.00 ± 0.75	3.98 ± 0.94				
MM19	35.81 ± 5.92	3.14 ± 0.61	3.11 ± 0.77				
MM20	61.60 ± 11.62	7.75 ± 1.26	7.72 ± 1.52				
Myanmar (n = 20)	34.70 ± 40.57	16.75 ± 36.83	16.74 ± 36.83	Thailand (n = 11)	18.22 ± 11.76	1.67 ± 1.20	1.66 ± 1.20

a petrogenic source. The same is true for the B[a]A/(B[a]A+ Chry) ratio, which separates the origin of PAHs into two major contributors: vehicular combustion and mixed sources. The values > 0.35 indicate combustion sources, which consisted of stations TH1, TH4, TH8, TH9, TH10, and TH11 (samples collected from Thailand) and MM1, MM2, MM4, MM5, MM7, MM15, MM16, MM17, MM18, MM19, and MM20 (samples collected from Myanmar). TH2, TH5, TH7, MM3, MM9, MM10, MM11, MM13, and MM14 stations had values ranging from 0.2 to 0.35, indicating the possibility of a mixed origin from incomplete combustion of multiple sources or petroleum. The ratios of An/(An+Phe) versus Ind/(Ind+ B[g,h, i]P) revealed the origins of the petrogenic and pyrogenic PAHs in the rice grain samples (Fig. 3b). The Ind/(Ind+ B[g,h, i]P) ratio, in particular, showed that the majority of the PAHs were produced during the burning of petroleum. Additionally, the values of B[a]P/B[g,h, i]P > 0.6 indicate that traffic emissions form PAHs. The results confirmed that the source of approximately 81% of the stations capable of measuring PAHs was traffic-originated.

Source Identification Based On Principal Component Analysis (PCA)

In this study, we employed PCA to determine the sources of 12 PAHs in 31 samples from Thailand and Myanmar. PCA is the most extensively used statistical technique in research. PCA makes complex systems easier to understand. The major goal of this study was to save maximum original data as feasible while reducing the number of variables. The varimax rotation technique and Kaiser standardization were employed in PCA to determine the origins of PAHs in Thailand (Table 3). Principal components of four eigenvector elements explain the scaled data, accounting for 85.98% of the total variance. 32.88% of the variance was explained by the first principal component (PC1). This factor was primarily loaded on the four-ring elements Pyr, B[a]A, and Chry, with the exception of B[g,h, i]P. Many sources are associated with pyrolysis and incomplete combustion of fuels, particularly gasoline-powered cars (Duval & Friedlander 1981, Khalili et al. 1995, Ravindra et al. 2008, Deelaman et al.2020). The PCA result was associated with the ratio of B[a]P/B[g,h, i]P, indicating > 80% of the contaminated samples were caused by traffic emissions. The second principal component (PC2), which was primarily loaded on Phe, An, and B[a]P, the three- and five-ring PAHs produced from various sources linked to emissions from heavy-duty vehicles, accounted for 27.51% of the total variation. This is consistent with the studies of Caricchia et al. (1999), Fang et al. (2004), and Ravindra et al.
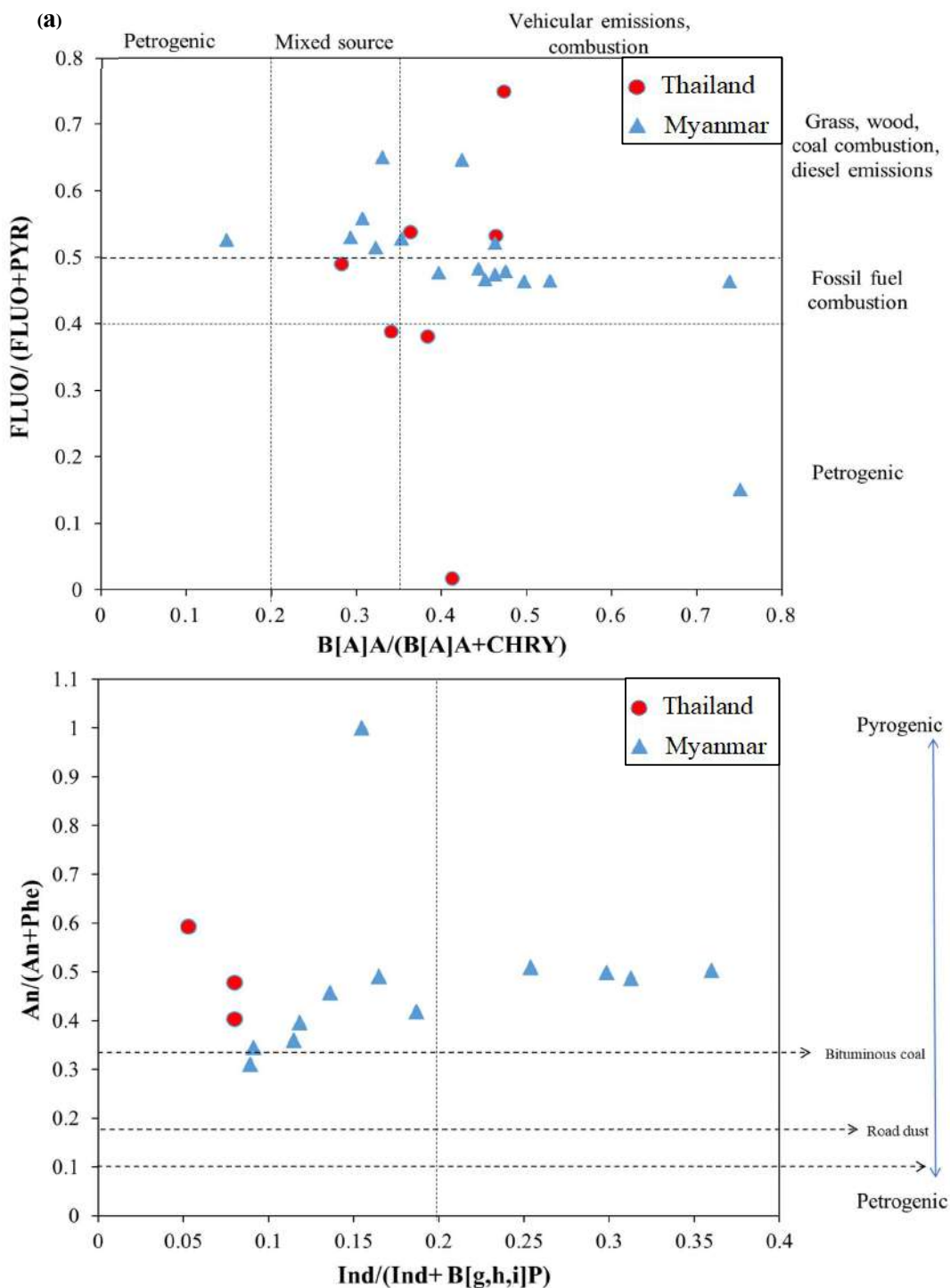
Fig. 3: Cross-plot for the ratios: (a) Flou/(Flou+Pyr) versus B[a]A/(B[a]A+ Chry) and (b)An/(An+Phe) versus Ind/(Ind+ B[g,h, i]P)in the sample from Thailand and Myanmar.

(2008), who reported that phenanthrene and anthracene are high load factors owing to diesel emissions. However, B [a] P originates from fossil fuel-based power plants (Ravindra et al. 2008). The significant loading of B[k]F and D[a,h]A, which are five-ring PAHs, explained 13.37% of the total variance in the third main component (PC3). Therefore,

PC3 is associated with incomplete biomass combustion and is considered a pyrogenic source. Freeman and Cattel (1990) reported that the indicator of biomass combustion (e.g., wood and grass) is D[a,h]A. Burning biomass is a common technique in tropical Asia for clearing land and converting it for other uses (Hyer & Chew 2010, Tsay et al.2016, Punsompong et al.2021). In Thailand, a country with a large agricultural sector in Southeast Asia, most farmers burn agricultural waste to make way for new crop cycles (Pani et al. 2018, Vadrevu et al. 2019, Punsompong et al. 2021). However, Thailand has different land-use patterns, and agricultural burning behavior depends on the region. In the northern and central regions, most biomass is combusted with rice straw and sugar cane leaves. In the south, there is very little burning of agricultural waste (Punsompong et al. 2021). Therefore, PC3 can be considered to indicate biomass combustion. Finally, the fourth principal component (PC4) was strongly connected to B[b]F and accounted for only 12.23% of the total variance. A high factor loading of B[b]F has been suggested for stationary emission sources (Kulkarni & Venkataraman 2000, Ravindra et al.2006). B[b]F has also been associated with moderate oil burns (Harrison et al. 1996, Ravindra et al. 2008). Thus, it could be interpreted that PC4 represents an industrial plant or incinerator. This result matches the current scenario. Thailand is a middle-income country developing into a high-income country using new technology and innovation-based economic engines (Ministry of Industry 2021). Many industries have benefited

from government support resulting in increased consumption of fossil fuels.

Two eigenvector-principal components could account for the source of PAHs found by PCA in Myanmar, controlling 76.38% of the total variance (Table 4). The first principal component (PC1) describes 60.58% of the total variance, which is due to the strong loading of three- to six-ring PAHs, such as Phe, An, Fluo, Pyr, B[a]A, Chry, B[b]F, Ind, and B[g, h, i]P. As the low- to moderate-molecular-weight PAHs (3-4 rings) originated from the use of diesel fuel in vehicles, such as trucks, trains, and ships, we interpret that PC1 may represent incomplete combustion from energy-dense secondary fuel for light-duty vehicles (gasoline) and heavy-duty vehicles (diesel fuel). Diesel emissions have also been reported to have a high load factor for Fluo, Phe, An, and Pyr (Caricchia et al. 1999, Ho et al. 2002, Fang et al.2004, Ravindra et al.2006). In addition, the combustion of gasoline is reportedly associated with high-molecular-weight compounds (5–6 rings), such as B[b]F and Ind (Harrison et al.1996, Ravindra et al. 2006, Deelaman et al. 2020b). Therefore, PC1 may suggest that incomplete fuel combustion is the source of PAH formation. In comparison, 15.80% of the total variation was explained by the second principal component (PC2). Only two compounds, B[a]P and D[a,h]A, two high-molecular-weight PAHs with five rings, comprised most of the factor's weight. The indicator compound in PC2 was D[a,h]A, similar to PC3 in Thailand. PC2 was likely a reasonable representative of biomass burning in Myanmar

Table 3: Principal component analysis results for PAHs in the rice grains sampled from Thailand.

PAH composition	Principle component (PC)			
	1	2	3	4
Phe	-0.050	**0.967**	0.036	-0.031
An	-0.056	**0.974**	-0.114	-0.025
Fluo	0.375	0.457	0.327	0.345
Pyr	**0.923**	0.262	0.049	-0.106
B[a]A	**0.896**	0.059	-0.022	0.332
Chry	**0.968**	0.079	0.061	0.076
B[b]F	0.022	-0.105	0.071	**0.836**
B[k]F	-0.158	-0.294	**0.859**	-0.081
B[a]P	0.148	**0.914**	-0.053	0.032
Ind	0.669	-0.293	0.176	-0.567
D[a,h]A	0.149	0.145	**0.824**	0.129
B[g,h,i]P	**0.830**	-0.304	-0.147	-0.418
Total variance [%]	32.883	27.507	13.367	12.225
Cumulative [%]	32.883	60.390	73.757	85.982
Estimated source	Gasoline-powered vehicles	Heavy-duty vehicles	Biomass burning	Stationary point sources

Extraction method: Principal component analysis.
Rotation method: Varimax with Kaiser normalization.

Table 4: Principal component analysis results for PAHs in the rice grains sampled from Myanmar.

PAH composition	Principle component (PC)	
	1	2
Phe	**0.866**	-0.086
An	**0.833**	-0.037
Fluo	**0.958**	-0.136
Pyr	**0.962**	-0.112
B[a]A	**0.951**	-0.058
Chry	**0.942**	-0.102
B[b]F	**0.800**	0.301
B[k]F	-0.183	-0.014
B[a]P	0.247	**0.946**
Ind	**0.839**	0.201
D[a,h]A	-0.242	**0.884**
B[g,h,i]P	**0.834**	0.187
Total variance (%)	60.576	15.801
Cumulative (%)	60.576	76.377
Estimated source	Incomplete combustion	Biomass burning

Extraction Method: Principal component analysis.
Rotation Method: Varimax with Kaiser normalization.

(Nepstad et al. 1999, Lambin et al. 2003). In Myanmar, forests reportedly account for approximately 48% of the total land area, and most have an agriculture-based economy. In both urban and rural settings, wood is a significant energy source for households and some industries (Khaing 2012, Tun et al. 2019). Over half of Myanmar's entire energy supply in 2012–2013 came from biomass, comparable to 10 million tons of oil (Tun & Juchelková 2019). There have also been reports of biomass burning being associated with the threat of forest clearing for agriculture and infrastructure development. Based on the above reasons, we conclude that PC2 in Myanmar may originate from biomass combustion.

Identifying the sources of PAHs in rice grains revealed that incomplete combustion of petroleum from various activities was the key source of PAHs in Thailand and Myanmar, followed by biomass combustion. The results would aid future agricultural food product control and environmental management planning.

Health Risk Assessment of PAHs in Rice Grains

According to the health risk assessment of PAHs in rice grain samples from Thailand, the mean values for inhalation of $ILCR_{inhalation}$ for children and adults in all grain samples were 33.61×10^{-14} and 4.02×10^{-13}, respectively. The ILCR results were less than the baseline value, indicating that PAHs obtained from rice grain exposure by inhalation are at safe levels. The mean values of $ILCR_{Dermal}$ were 1.08×10^{-8} and 9.21×10^{-9}, respectively, and $ILCR_{Ingestion}$ values were
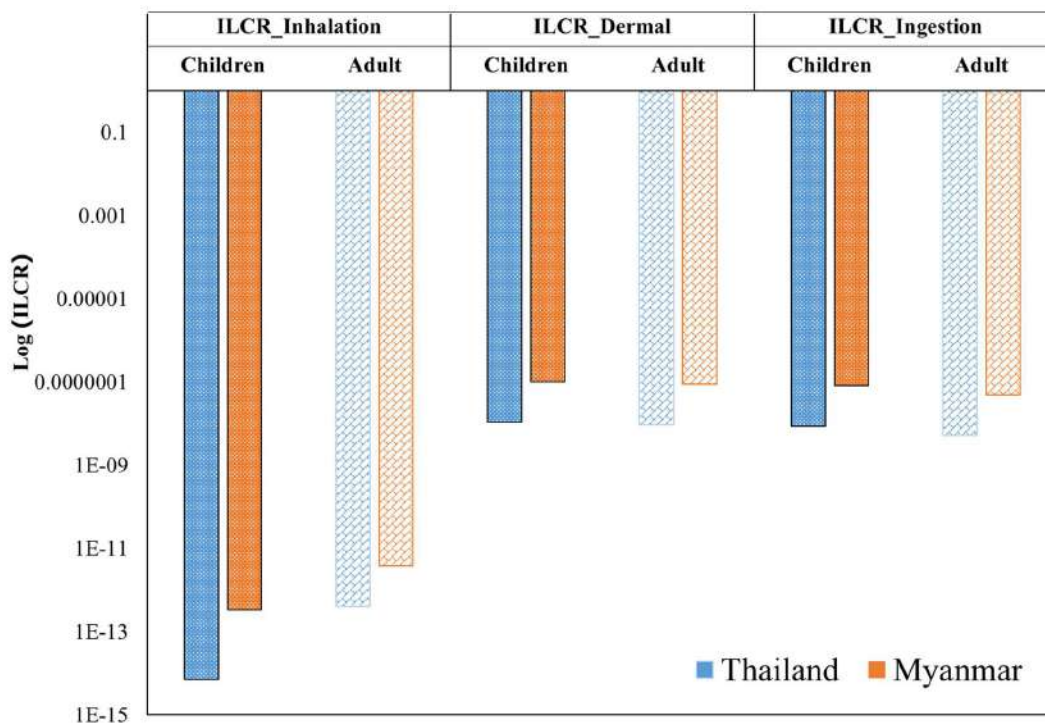
Fig. 4: Logarithmic comparisons of different exposure pathways to the ILCRs between Thailand and Myanmar.

8.68×10^{-9} and 5.18×10^{-9} for children and adults, respectively. However, these results showed that PAH exposure pathways for rice grain samples collected from the Thailand area through dermal contact were at the highest risk, followed by ingestion and inhalation, with the ILCR value higher in children than in adults (Fig. 4). All these results showed that ILCRs values in Thailand were 1.95×10^{-8} for children and 1.44×10^{-8} for adults, which were lower than the standards set and are considered to be safe levels.

All PAHs contributed to the health risk of rice grains in Myanmar, with mean $ILCR_{inhalation}$ values of 3.39×10^{-13} and 3.78×10^{-12} for children and adults, respectively. $ILCR_{Dermal}$ mean values for children and adults were 1.02×10^{-7} and 8.65×10^{-8} respectively, whereas $ILCR_{Ingestion}$ mean values were 8.16×10^{-8} and 4.87×10^{-8}, respectively. In addition, the $ILCR_{inhalation}$ was higher in adults than children; however, the ILCR of ingestion and exposure was higher in children than in adults. The total health risks (ILCRs) from three main pathways (inhalation, dermal contact, and ingestion) showed a mean value of 1.83×10^{-7} and 1.35×10^{-7} for children and adults, respectively. According to these findings, the cumulative lifetime cancer risk from rice grains obtained from Myanmar was lower than the baseline set for safe values.

CONCLUSIONS

This study used multivariate descriptive statistical methods to examine the PAH composition in rice grains. We determined the origin of PAH in rice grains from Thailand and Myanmar using diagnostic ratios and PCA together with its toxicity and health risk assessment. The findings can be summarized as follows: (i) The level of PAHs ($\sum$ 12PAHs) in Thailand varied from 0.09 to 37.15 $ng.g^{-1}$ with an arithmetic mean of 18.22 ± 11.76 $ng.g^{-1}$, whereas that in Myanmar varied from 0.07 to 150.73 $ng.g^{-1}$ with an arithmetic mean of 34.70 ± 40.57 $ng.g^{-1}$, which are relatively low compared to previous studies. (ii) The attribution of PAHs in Thailand and Myanmar rice grains was based on diagnostic ratios and PCA. The results of the diagnostic ratio show that pyrogenic sources were the main sources of PAHs in the rice grain samples from Thailand and Myanmar. In addition, the results indicated that the majority of PAHs in the samples at all sampling sites were formed by incomplete combustion of petroleum products and biomass combustion, consistent with the PCA results of PAHs in both Thailand and Myanmar, indicating that they primarily originated from pyrogenic sources (gasoline-powered vehicles, heavy-duty vehicles, and biomass). (iii) The rice grains of Thailand and Myanmar contaminated with PAH congeners exhibited relatively low toxicity. However, the increased lifetime cancer risk assessment results showed that both adults and

children had low cancer risks that fell under the USEPA allowed range. Although PAHs in rice have a low impact on crops and human health in Thailand and Myanmar, as rice is predominantly consumed in these areas, preventive practices are required to check the PAH content.

ACKNOWLEDGEMENTS

REFERENCES

Abdel-Shafy, H.I. and Mansour, M.S.M. 2016. A review on polycyclic aromatic hydrocarbons: source, environmental impact, effect on human health and remediation. Egypt. J. Petrol., 25: 107–123. https://doi.org/10.1016/j.ejpe.2015.03.011.

Alexandratos, N. and Bruinsma, J. 2012. World Agriculture towards 2030/2050: The 2012 Revision. ESA Working Paper No. 12, Rome, Italy.

Bamforth, S. and Singleton, I. 2005. Bioremediation of polycyclic aromatic hydrocarbons: current knowledge and future directions, J. Chem. Technol. Biotechnol., 80: 23-736.

Benner, B.A., Bryner, N.P., Wise, S.A., Mulholland, G.W., Lao, R.C. and Fingas, M.F. 1990. Polycyclic aromatic hydrocarbon emissions from the combustion of crude oil on water. Environ. Sci. Technol., 24: 1418 -1427.

Brorstrom-Lunden, E. and Skarby, L. 1984. Plants as monitoring samplers of airborne PAH.In: Versino B, Angeletti G, editors. Physico-chemical behavior of atmospheric pollutants. Riedel., 101-110.

Budzinski, H., Jones, I., Bellocq, J., Pie´rard, C. and Garrigues, P. 1997. Evaluation of sediment contamination by polycyclic aromatic hydrocarbons in the Gironde estuary. Mar. Chem., 58: 85-97.

Caricchia, A.M., Chiavarini, S. and Pezza, M. 1999. Polycyclic aromatic hydrocarbons in the urban atmospheric particulate matter in Naples (Italy). Atmos. Environ., 33: 3731- 3738.

Canadian Council of Ministers of the Environment (CCME). 2007. Canadian soil Quality Guidelines for the Protection of Environmental and Human Health: Retrieved from https://support.esdat.net/Environmental%20Standards/canada/soil/rev_soil_summary_tbl_7.0_e.pdf

Chen, F., Lin, Y., Cai, M., Zhang, J., Zhang, Y., Kuang, W., Liu, L., Huang, P. and Ke, H. 2018. Occurrence and Risk Assessment of PAHs in Surface Sediments from Western Arctic and Subarctic Oceans. Int. J. Environ. Res. Public Health, 15(4): 734.

ChooChuay, C., Pongpiachan, S., Tipmanee, D., Deelaman, W., Iadtem, N., Suttinun, O., Wang, Q., Xing, L., Li, G., Han, Y., Hashmi, M.Z., Palakun, J., Poshyachinda, S., Aukkaravittayapun, S., Surapipith, V. and Cao, J. 2020. Effects of agricultural waste burning on $pm_{2.5}$-bound polycyclic aromatic hydrocarbons, carbonaceous compositions, and water-soluble ionic species in the ambient air of Chiangmai, Thailand. Polycycl. Aromat. Compd., 7: 15-22.

Deelaman, W., Pongpiachan, S., Tipmanee, D., Suttinun, O., Choochuay, C., Iadtem, N., Charoenkalunyuta, T.and Promdee, K. 2020a. Source apportionment of polycyclic aromatic hydrocarbons in the terrestrial

soils of King George Island, Antarctica. J.S. Am. Earth Sci.,104: 102832. https://doi.10.1016/j.jsames.2020.102832.

Deelaman, W., Pongpiachan, S., Tipmanee, D., Choochuay, C., Iadtem, N., Suttinun, O., Wang, QY., Xing, L., Li, GH., Han, YM., Hashmi, MZ. and Cao, JJ. 2020b. Source identification of polycyclic aromatic hydrocarbons in terrestrial soils in Chile. J. S. Am. Earth Sci., 99: 102514. https://doi.org/10.1016/j.jsames.2020.102514.

Deelaman, W., Pongpiachan, S., Tipmanee, D., Choochuay, Suttinun, O., Charoenkalunyuta, T.and Promdee, K. 2021. Ecotoxicological risk and health risk characterization of polycyclic. Polar Sci., 29: 100715. https://doi.org/10.1016/j.polar.2021.100715.

Dong, CD., Chen C.F. and Chen, C.W. 2012. Determination of Polycyclic Aromatic Hydrocarbons in Industrial Harbor Sediments by GC-MS. Int. J. Environ. Res. Public Health, 9: 2175-2188.

Duan, L., Naidu, R., Thavamani, P., Meaklim, J. and Megharaj, M. 2015. Managing long-term polycyclic aromatic hydrocarbon contaminated soils: a risk-based approach. Environ. Sci. Pollut. Res., 22: 8927-8941. https://doi.org/10.1007/s11356-013-2270-0.

Duval, M.M.and Friedlander, S.K. 1981. Source resolution of polycyclic aromatic hydrocarbons in Los Angeles atmosphere application of CMB with first-order decay. USEPA Report no EPA-600/2-81-161, USEPA.

Fang, G.C., Wu, Y.S., Chen, M.H., Ho, T.T., Huang, S.H. and Rau, J.Y. 2004. Polycyclic aromatic hydrocarbons study in Taichung, Taiwan, during 2002-2003. Atmos. Environ., 38: 3385 - 3391.

FAO. 2020. Faostat. Retrieved from http://faostat.fao.org/. (accessed 9th May 2021).

Foley, J.A., Ramankutty, N., Brauman, K.A., Cassidy, E.S., Gerber, J.S., Johnston, M., Mueller, N.D., O'Connell, C., Ray, D.K., West, P.C., Balzer, C., Bennett, E.M., Carpenter, S.R., Hill, J., Monfreda, C., Polasky, S., Rockströom, J., Sheehan, J., Siebert, S., Tilman, D. and Zaks, D.P.M. 2011. Solutions for a cultivated planet. Nature, 478: 337-342. https://doi.org/10.1038/nature10452.

Freeman, D.J. and Cattel, C.R. 1990. Wood burning is a source of atmospheric polycyclic aromatic hydrocarbons. Environ. Sci. Technol., 24: 1581-1585.

Fried, O., Westphal, C., Schellenberg, J., Grescho, V., Kühn, I., Sinh, N.V., Settele, J. and Bergmeier, E. 2021. Vascular plant species diversity in Southeast Asian rice ecosystems is determined by climate and soil conditions and the proximity of non-paddy habitats. Agric. Ecosyst. Environ., 314: 107346.

Gogou, I.A., Apostolaki, M. and Stephanou, G.E.1998. Determination of organic molecular markers in marine aerosols and sediments: onx10step flash chromatography compound class fractionation and capillary gas chromatographic analysis. J. Chromatogr., 799 (1-2): 215-231.

Grimmer, G., Jacob, J. and Naujack, K.W. 1983. Profile of the polycyclic aromatic compounds from crude oils. Part 3. Inventory by GCGC/MS PAH in environmental materials. Fresenius Z. Anal. Chem., 314: 29-36.

Harrison, R.M., Smith, D.J.T.and Luhana, L. 1996. Source apportionment of atmospheric polycyclic aromatic hydrocarbons collected from an urban location in Birmingham, UK. Environ. Sci. Technol., 30: 825-832.

Hyer, E.J. and Chew, B.N. 2010. Aerosol transport model evaluation of an extreme smoke episode in Southeast Asia. Atmos. Environ., 44: 1422-1427.

International Agency for Research on Cancer (IARC). 2010. Some non-heterocyclic polycyclic aromatic hydrocarbons and some related exposures. Monogr. Eval. Carcinog. Risks Hum., 92: 765-771.

Inomata, Y., Kajino, M., Sato, K., Ohara, T., Kurokawa, J., Ueda, H., Tang, N., Hayakawa, K., Ohizumi, T.and Akimoto, H. 2012. Emission and atmospheric transport of particulate PAHs in Northeast Asia. Environ Sci Technol., 46: 4941-4949.

Katsoyiannis, A.and Breivik, K. 2014. Model-based evaluation of the use of polycyclic aromatic hydrocarbons molecular diagnostic ratios as a source identification tool. Environmental Pollution., 184: 488-494. https://doi.10.1016/j.envpol.2013.09.028.

Khaing, W. 2012. Myanmar's Future Potentials in Low Carbon Energy. In Proceedings of the Myanmar 2nd Forum, Green Economy Green Growth, MICC, Nay Pyi Taw, Myanmar, 13-15 November.

Khalili, N.R., Scheff, P.A. and Holsen, T.M. 1995. PAH source fingerprints for coke ovens, diesel and gasoline engines, highway tunnels, and wood combustion emissions. Atmos. Environ., 29: 533-542.

Kim, K.H., Jahan, S.A., Kabir, E. and Brown, R.J. 2013. A review of airborne polycyclic aromatic hydrocarbons (PAHs) and their human health effects Brown. Environ Int., 60: 71-80.

Kulkarni, P. and Venkataraman, C. 2000. Atmospheric polycyclic aromatic hydrocarbons in Mumbai, India. Atmos. Environ., 34: 2785-2790.

Lambin, E.F., Geist, H.J. and Lepers, E. 2003. Dynamics of land-use and land-cover change in tropical regions.Annu. Rev. Environ. Resour., 28(1):205-241. https://doi. 10.1146/annurev.energy.28.050302.105459.

Larsson, B. and Sahlberg, G. 1982. Polycyclic aromatic hydrocarbons in lettuce. Influence of a highway and an aluminium smelter. In: Cooke M, Dennis AJ, Fisher GL, editors. Polynuclear aromatic hydrocarbons: physical and biological chemistry. New York: Springer-Verlag. 417-426.

Lee, J., Jeong, J.H., Park, S. and Lee, K.G. 2018. Monitoring and risk assessment of polycyclic aromatic hydrocarbons (PAHs) in processed foods and their raw materials. Food Control, 92: 286- 292.

Liu, Z., Zhang, W., Zhang, Y., Chen, T., Shao, S., Zhou, L., Yuana, Y., Xiee, T. and Rogers, K.M.2019. Using chemometric models to ensure food safety and traceability of polished rice from different production regions in China and Southeast Asia. Food Control., 99: 1-10. https://doi.10.1016/j.foodcont.2018.12.011.

Lu, C., Hong, Y., Odinga, E. S., Liu, J., Tsang, D. C. W. and Gao, Y. 2021. Bacterial community and PAH-degrading genes in paddy soil and rice grain from PAH-contaminated area. Appl. Soil Ecol., 158: 103789. https://doi.10.1016/j.apsoil.2020.103789.

Lu, H., Cai, Q-Y., Jones, KC., Zeng, Q-Y., Katsoyiannis, A.2014. Levels of organic pollutants in vegetables and human exposure through diet: a review. Crit Rev Environ Sci Technol., 44: 1 - 33.

Maliszewska-Kordybach, B.1999. Sources, Concentrations, fate and effects of polycyclic aromatic hydrocarbons (PAHs) in the environment. Part A: PAHs in Air. Pol. J. Environ. Stud., 8(3): 131 - 136.

Martin, K. and Sauerborn, J. 2013. Agroecology. Springer, Dordrecht, Netherlands.

Marr, L.C., Kirchstetter, T.W., Harley, R.A., Miguel, A.H., Hering, S.V. and Hammond, S.K. 1999. Characterization of polycyclic aromatic hydrocarbons in motor vehicles fuels and exhaust emissions. Environ. Sci. Technol., 33: 3091 - 3099.

Meharg, A.A., Wright, J., Dyke, H. and Osborn, D. 1998. Polycyclic aromatic hydrocarbon PAH dispersion and deposition to vegetation and soil following a large-scale chemical fire. Environ. Pollut., 99: 29 - 36.

Miguel, A.H., Kirchstetter, T.W., Harley, R.B. and Hering, R.A. 1998. On-road emissions of particulate polycyclic aromatic hydrocarbons and black carbon from gasoline and diesel vehicles. Environ. Sci. Technol., 32: 450-455.

Ministry of Industry. 2021. Thailand. https://www.industry.go.th/en/home (accessed 14 December 2021).

Neilson, AH. 1998. PAHs and Related Compounds: Handbook of Environmental Chemistry (Ed O Hutzinger). Volume 3 Parts I and J. Springer-Verlag, Berlin.

Nepstad, D.C., Versssimo, A., Alencar, A., Nobre, C., Lima, E., Lefebvre, P., Schlesinger, P., Potter, C., Moutinho, P., Mendoza, E., Cochrane, M.and Brooks, V. 1999. Large scale Amazonian forests by logging and fire. Nature, 398(6727): 505 - 508.

Nisbet, I.C.T. and LaGoy, P.K. 1992. Toxic equivalency factors (TEFs) for polycyclic aromatic hydrocarbons (PAHs). Regul. Toxicol. Pharmacol., 16(3): 290 - 300.

Oros, D.R. and Simoneit, B.R. 2000. Identification and emission rates of molecular tracers in coal smoke particulate matter. Fuel., 79: 515-536.

Pani, S.K., Lin, N.H., Chantara, S., Wang, S.H., Khamkaew, C., Prapamontol, T., Janjai, S. 2018. Radiative response of biomass-burning aerosols over an urban atmosphere in northern peninsular Southeast Asia. Sci. Total Environ., 633: 892 - 911.

Paris, A., Ledauphin, J., Poinot, P. and Gaillard, J.L. 2018. Polycyclic aromatic hydrocarbons in fruits and vegetables: Origin, analysis, and occurrence. Environ. Pollut., 234: 96 - 106.

Pongpiachan, S., Hattayanone, M., Pinyakong, O., Viyakarn, V., Chavanich, S.A., Bo, C., Khumsup, C., Kittikoon, I.and Hirunyatrakul, P. 2017. Quantitative ecological risk assessment of inhabitants exposed to polycyclic aromatic hydrocarbons in terrestrial soils of King George Island, Antarctica. Polar Sci., 11: 19-29.

Pongpiachan, S., Hirunyatrakul, P., Kittikoon, I.and Khumsup, C. 2012. Parameters influencing sensitivities of polycyclic aromatic hydrocarbons measured by Shimadzu GCMS-QP2010 ultra. InTech Open, London.

Punsompong, P., Pani, K.S., Wang, S.H. and Pham, T.T.B. 2021. Assessment of biomass-burning types and transport over Thailand and the associated health risks. Atmos. Environ., 247: 118176.

Qin, L., Xing, F., Zhao, B., Chen, W. and Han, J. 2018. Reducing polycyclic aromatic hydrocarbon and its mechanism by porous alumina bed material during medical waste incineration. Chemosphere, 212: 200-208.

Ravindra, K., Bencs, L., Wauters, E., de Hoog, J., Deutsch, F., Roekens, E., Bleux, N., Bergmans, P. and Van Grieken, R. 2006. Seasonal and site specific variation in vapor and aerosol phase PAHs over Flanders (Belgium) and their relation with anthropogenic activities. Atmos. Environ., 40: 771-785.

Ravindra, K., Sokhi, R. and Grieken, RV. 2008. Atmospheric polycyclic aromatic hydrocarbons: Source attribution, emission factors, and regulation. Atmos Environ., 42: 2895-2921.

Rogge, W.F., Hildemann, L.M., Mazurek, M.A., Cass, G.R. and Simoneit, B.R.T. 1993. Sources of fine organic aerosol. 2. Noncatalyst and catalyst-equipped automobiles and heavy-duty diesel trucks. Environ. Sci. Technol., 27: 636-651.

Schauer, J.J., Kleeman, M.J., Cass, G.R.and Simoneit, B.R. 1999. Measurement of emissions from air pollution sources. 2. C1–through C30 organic compounds from medium-duty diesel trucks. Environ. Sci. Technol., 33: 1578-1587.

Simonich, SL. and Hites, RA. 1995. Organic pollutant accumulation in vegetation. Environ. Sci. Technol., 29: 2905-2914.

Smith, D.J.T. and Harrison, R.M. 1998. Polycyclic aromatic hydrocarbons in atmospheric particles. In: Harrison, R.M., Van Grieken, R. (Eds.), Atmospheric Particles. Wiley.

Soclo, H.H., Garrigues, P.and Ewald, M. 2000. Origin of polycyclic aromatic hydrocarbons (PAHs) in coastal marine sediments: case studies in Cotonou (Benin) and Aquitaine (France) areas. Mar. Pollut. Bull., 40: 387-396.

Stangoulis, J. and Sison, C. 2008. Crop sampling protocols for micronutrient analysis. Harvest Plus Tech. Monogr. Ser., 7: 54.

Tsay, S.C., Maring, H.B., Lin, N.H., Buntoung, S., Chantara, S., Chuang, H.C., Gabriel, P. M., Goodloe, C.S., Holben, B.N., Hsiao, T.C., Hsu, N.C., Janjai, S., Lau, W.K.M., Lee, C.T., Lee, J., Loftus, A.M., Nguyen, A.X., Nguyen, C.M., Pani, S.K., Pantina, P., Sayer, A.M., Tao, W.K., Wang, S.H., Welton, E.J., Wiriya, W. and Yen, M.C. 2016. Satellite-surface perspectives of air quality and aerosol-cloud effects on the environment: An overview of 7-SEAS/BASELInE. Aerosol Air Qual. Res., 16: 2581-2602.

Tudoran, M.A. and Putz, M.V. 2012. Polycyclic Aromatic Hydrocarbons: from in Cerebro to in Silico Eco-Toxicity Fate. Chem. Bull., 57(71): 1.

Tun, M.M. and Juchelková, D. 2019. Biomass Sources and Energy Potential for Energy Sector in Myanmar: An Outlook. Resources., 8(2): 102.

United Nations 2017. World Population Prospects: The 2017 Revision, Key Findings, and Advance Tables: Working Paper No. ESA/P/WP/248. Department of Economic and Social Affairs, Population Division, New York, USA.

USEPA 1991. Risk assessment of guidance for superfund. Volume 1 - Human health evaluation manual (part b, development of risk-based preliminary goals). Washington DC, USA. https://epa-prgs.ornl.gov/radionuclides/HHEMB.pdf (accessed 1 January 2022).

Vadrevu, K.P., Lasko, K., Giglio, L., Schroeder, W., Biswas, S. and Justice, C. 2019. Trends in vegetation fires in South and southeast Asian countries. Sci. Rep., 9: 7422.

Veltman, K., Huijbregts, M.A., Rye, H. And Hertwich, EG. 2012. Including impacts of particulate emissions on marine ecosystems in life cycle assessment: The case of offshore oil and gas production. Integr. Environ. Assess. Manag., 7: 678-686.

Wang, Z., Chen, J., Qiao, X., Yang, P., Tian, F. and Huang, L. 2007. Distribution and sources of polycyclic aromatic hydrocarbons from urban to rural soils: A case study in Dalian, China. Chemosphere., 68(5): 965-971.

Westerholm, R.N., Christensen, A., Tornqvist, M., Ehrenberg, L., Rannug, U., Sjogren, M., Rafter, J., Soontjens, C., Alme´n, J. and Gra¨gg, K. 2001. Comparison of exhaust emissions from Swedish Environmental Classified Diesel Fuel (MK1) and European Program on Emissions, Fuels and Engine Technologies (EPEFE) reference fuel: a chemical and biological characterization, with viewpoints on cancer risk. Environ. Sci. Technol., 35: 1748-1754.

Westerholm, R.N. and Li, H. 1994. A multivariate statistical analysis of fuel-related polycyclic aromatic hydrocarbon emissions from heavy-duty diesel vehicles. Environ. Sci. Technol., 28: 965-972.

Wise, S.A., Hilpert, L.R., Rebbert, R.E., Sander, L.C., Schantz, M.M., Chesler, S.N. and May, W.E.1988. Standard reference materials for the determination of the polycyclic aromatic hydrocarbons. Fresenius J. Anal. Chem., 332: 573-582.

Yunker, M.B., Macdonald, R.W., Vingarzan, R., Mitchell, R.H., Goyette, D. and Sylvestre, S. 2002. PAHs in the Fraser River basin: a critical appraisal of PAH ratios as indicators of PAH source and composition. Org. Geochem., 33: 489-515.

Zhang, Y.and Tao, S. 2009. Global atmospheric emission inventory of polycyclic aromatic hydrocarbons (PAHs) for 2004. Atmos Environ., 812-819.

Zhong, G., Xie, Z., Cai, M., Moller, A., Sturm, R., Tang, J., Zhang, G., He, J. and Ebinghaus, R. 2012. Distribution and Air-Sea Exchange of Current-Use Pesticides (CUPs) from East Asia to the High Arctic Ocean. Environ. Sci. Technol., 46: 259-267.

Zhu, Y., Duan, X., Qin, N., Lv, J., Wu, G. and Wei, F. 2019. Health risk from dietary exposure to polycyclic aromatic hydrocarbons (PAHs) in a typical high cancer incidence area in southwest China. Sci. Total Environ., 649: 731-738.

Petroleum-Based Plastics Versus Bio-Based Plastics: A Review

Shikha Kumari*, Alka Rao*, Manjeet Kaur** and Geeta Dhania*†

*Department of Environmental Science, Maharshi Dayanand University, Rohtak-124001, Haryana, India
**University Institute of Engineering and Technology, Maharshi Dayanand University, Rohtak-124001, Haryana, India
†Corresponding author: Geeta Dhania; geetadhaniaevs@gmail.com

ABSTRACT

Plastic needs have expanded along with population growth, industrialization, and urbanization. Plastic is unrivaled due to its useful properties and is used to prepare numerous important goods daily. This paper encloses the different kinds and applications of petroleum-based plastic and the drawbacks related to their use, i.e., its nonbiodegradability which leads to their stay in the environment for a very long time. Additionally, there are not enough effective disposal techniques for the large volume of plastic waste produced; thus, plastic garbage builds up in the environment and endangers it. Limiting the usage of plastic is necessary to protect the environment. This can be done with the help of bioplastic, which is an excellent substitute for plastic. The different kinds of bioplastic and their biodegradability in different mediums, viz., soil compost and aquatic systems, are addressed in this paper. Along this, the different areas of application of bioplastic have been explored. The present study also addresses the underlying mechanism of plastic polymerization and biodegradation and the current status of bioplastics in the global market.

INTRODUCTION

Synthetic plastic finds vast applications due to its excellent characteristic properties (Luckachan & Pillai 2011). Plastic is widely used from the domestic to the industrial level to produce carry bags, storage containers, water bottles, jugs, glass, water pipes, chairs, tables, and agricultural products. Having excellent properties and being present at a low cost, the importance of plastic cannot be ignored (Sangale et al. 2012). However, the overuse of plastic has given birth to many environmental problems. Over a million tons of plastic waste is generated annually from different sources (Pathak & Navneet 2017). Most plastic debris is non-biodegradable, and its management has become a global challenge. Sea beaches are the depository sites for plastic, as plastic waste is carried to aquatic sources through rivers, canals, etc. (Singh et al. 2016). The accumulation of plastic waste in the ocean affects marine fauna and flora adversely (Laist 2006). Plastic debris also affects terrestrial ecosystems and human health. So there is a need for proper management of plastic waste. The environmental problems caused by plastic waste have triggered the need to develop environmentally friendly materials.

Bio-based plastic is a perfect alternative to synthetic plastic as they are made of renewable and natural sources like corn starch, potato starch, inedible food waste, and lingo-cellulosic crop residue (Saharan & Ankita 2012). The raw material used for bioplastic production greatly impacts bioplastic properties and production expenses. Bioplastics are generally biodegradable or compostable based on their composition. The production and use of such plastic material may help resolve many environmental problems, and their production and consumption are expected to grow soon. Thus, there is a need to evaluate these bioplastics carefully. There are many reviews available on the investigation of bioplastics.

Palaniswamy & Venkatachalam (2020) critically reviewed the different kinds of bioplastic, their advantage, and their disadvantage. The global statistics related to bioplastics were also discussed. Hong et al. (2021) reviewed bioplastic as a material for food packaging. The various characteristic properties of bioplastic for food packaging are discussed. Different kinds of bioplastic used for packing fruits, vegetables, eggs, fish, meats, etc., were also included in the study.

Similarly, most review studies covered only one aspect of either bioplastic or synthetic plastic, and their detailed comparative study was unavailable. Therefore, the current review encloses synthetic plastic and bioplastic aspects. This review focuses on polymerization, the various kinds of plastic materials used in daily life, and the harmful effects of plastic waste. Further, the various kinds of bioplastic and different feedstock used for their production were discussed.

The mechanism of biodegradation, the biodegradability of bioplastic in different mediums, viz., soil, compost, and aquatic system, and the role of microorganisms in biodegradation are included in the present study. The review also highlights the application, global market status, global producers of bioplastic, and limitations of bioplastics.

PETROLEUM-BASED PLASTICS

Plastic, a synthetic polymer, is a petroleum product. Natural gas, coal, and crude oil are the precursors for preparing synthetic plastic. In 1907 Baekeland obtained the first synthetic polymer named Bakelite, which was formed by polycondensation of phenol with formaldehyde. Plastics are lightweight, strong, and cheap to produce polymers with high molecular weight and consist of hundreds to thousands of repeating units of monomers (Kuhn et al. 2007). Production of synthetic plastic begins from distilling crude oil in an oil refinery. This distillation step separates heavy crude oil into its lighter constituents; these more lightweight components are called segments. Each segment consists of a hydrocarbon chain of varying sizes and structures. Naphtha is one such segment required to produce monomers, say ethylene, propylene, and styrene, which act as a precursor for the production of plastic. The conversion of monomers into a polymer through polymerization releases greenhouse gases and other toxic pollutants into the environment. The characteristic properties of plastic play an essential role in deciding its applications. The molecular weight of plastic determines many physical properties and affects the plastic's toughness, tensile strength, adherence, and resistance. The increase in molecular weight increases the tensile and impact strength. Crystallization controls the structural formation process of plastic.

A few important mechanical properties of plastic are tensile strength, flexural and compressive strength, hardness, fatigue resistance, and impact resistance. The tensile strength of plastic material tells about the load or stress the material can bear before permanent deformation (Goswami et al. 2015). The transport properties describe how rapidly any molecule can pass through the plastic material. There are several kinds of plastics, and they are used for various purposes.

Type of Plastics Based on Thermal Properties

Based on the thermal properties, there are only two kinds, namely thermoplastic and thermoset plastic, which are discussed further. Fig. 1 shows the kind of plastic based on thermal properties and their subtypes.

Thermoplastics

This kind of plastic is brittle and glossy in appearance and can be softened and remolded into different kinds of shapes by applying heat and then cooling at room temperature. There is a minimum or no change in the properties after remolding. A few examples of thermoplastic are polyolefin, polyethylene, nylons, Poly-ethers, and Polyvinyl chloride (PVC). This plastic can be a linear or branched chain with an intermolecular force between the elastomers and fiber (O'Neil 2010).

Thermosetting Plastics
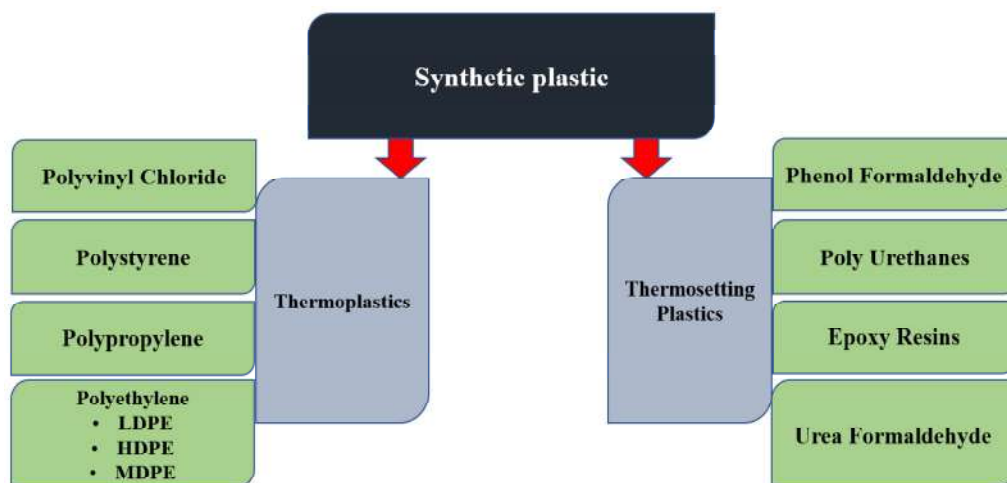
(LDPE: Low-density Polyethylene; HDPE: High-density Polyethylene; MDPE: Medium-density Polyethylene)

Fig. 1: Classification of synthetic plastics based on thermal properties.

This plastic cannot be remolded or reshaped to form a new product. On application of heat, these plastics undergo some chemical reactions, resulting in changes in their properties, and thus cannot be reused. These polymers are generally robust, durable, and resistant to high temperatures. Thermosets are mostly cross-linked polymers. A few examples of thermoset plastic are phenolic, Bakelite, resins, urea, and epoxy resin (O'Neil 2010).

Commonly Used Synthetic Plastics

Polystyrene

Styrene monomer is a predecessor of polystyrene. It is a very hard, lightweight, and mouldable plastic. Styrofoam is formed by heating polystyrene and then blowing air through this mixture. Polystyrene makes furniture, glasses, and utensils (Casado et al. 2013).

Polyvinyl Chloride (PVC)

PVC is obtained by polymerization of vinyl chloride. A plasticizer is added to it to enhance the properties of PVC and make it soft and mouldable. They are cheaper and more durable. PVC is used to prepare pipes and plumbing materials (Chung et al. 2011).

Polytetrafluoroethylene

It was first produced in 1938 by Dupont. When the monomers of tetrafluoroethylene are polymerized, it results in the formation of polytetrafluoroethylene. It is also called teflon and is stable, strong, and resistant to high temperatures. It makes cookware and waterproof coating (Cole et al. 2013).

Polyethylene

It is the most common and widely used plastic material. The polymerization of ethylene monomer obtains it. The first polyethylene was produced in 1934 (Della et al. 2014). Polyethylene is tough, chemically inert, possesses low moisture adsorption, and are bad conductor of electricity. The properties vary according to the type of branching and crystal structure (Huang et al. 2007). They are used in making electric wires and cables, pipes, medical devices, and automotive and space applications (Fang et al. 2005, Zhang et al. 2006, Dey & Tripathi 2010, Manu et al. 2013).

There are three kinds of PE-1) HDPE (High-density polyethylene), 2) LDPE (Low-density polyethylene, and 3) MDPE (Medium-density polyethylene).

LDPE is ductile, flexible, tough, transparent, and has weak intermolecular interactions due to high chain branching. Its long chain irregular packing contributes to low crystallinity. LDPE possesses tensile strength lower than HDPE and finds uses in preparing containers, plastic films, and plastic bags.

HDPE is the most versatile plastic material with the highest crystallinity degree. It is highly stable due to the presence of many short branches. HDPE makes milk jugs, water pipes, and detergent bottles (Pasch & Eselem 2018). HDPE has a higher melting point than LDPE (Della et al. 2014).

MDPE is a combination of LDPE and HDPE. It has drop resistance and better-cracking resistance than HDPE but is softer than HDPE and harder than LDPE. It is used in making carry bags, packaging, gas pipe, and fittings

Polypropylene (PP)

Karl Ziegler and Givlionatta first produced it in 1953. PP is obtained from the combination of propylene monomers. It is the second most used plastic, possesses good mechanical properties, and is highly available at a moderate cost. PP is used in packaging, electronics, household appliance, battery cases, bottle tubes, filaments, and bags (Castro et al. 2009)

There are three kinds of PP.

1) Atactic PP has a low melting point and consists of methyl groups on the main chain in random order.

2) Syntactic PP is semi-crystalline and is more homogenous than atactic PP.

3) Isotactic PP possesses a high degree of crystallinity and is homogenous and highly stable (Maddah 2016).

Process of Making Plastics: Polymerization

The polymerization process involves linking a large number of monomers to form a polymer molecule. Monomers are low molecular units that join with the help of chemical reactions forming large molecules having high molecular weight called polymers.

Different methods of polymerization can be used to produce various kinds of plastic materials, which are as-

A. Condensation Polymerization

It is also called step-growth polymerization. It is a chemical reaction in which a low molecular weight by-product called condensate (NH_3, H_2O, HCL) is released, and the polymer is formed.

B. Addition Polymerization/Chain Polymerization

In this process, two or more monomer molecules combine to form a polymer, and no by-product is formed. This involves a chain reaction linking the monomer molecule (Karana 2012).

C. Ionizing Radiation Polymerization

Ionizing radiations generate free radicals, which initiate the

polymerization process. Both solid and liquid mediums can be used for achieving ionizing radiation polymerization. There is not much influence of temperature in this process. Sometimes the process continues even after moving away from the radiation source, and the phenomenon is called post-polymerization.

D. Non-ionizing Radiation Polymerization

It is a kind of chain-growth polymerization. The absorption of visible or UV light influences the process. In this process, the reactant monomer can absorb light directly and by a photosensitizer, which absorbs light and transfers the energy to the monomer.

Disadvantages of Petroleum-Based Plastics

Plastic is produced from non-renewable energy sources and is non-biodegradable (Anderson, 2006). The Chemical structure of plastic cannot be modified by the microorganism, which leads to their nonbiodegradability (Tokiwa et al. 2009, Babu et al. 2013). High molecular weight, high degree of crystallinity, and high hydrophobicity reduce the degradability of plastic (David et al. 2019). The production and disposal of plastic are increasing every year. As plastic is non-biodegradable, there is no method for its proper disposal (Yadav et al. 2020). Plastic waste has dramatically influenced the environment by causing land, water, and air pollution and contributes to global warming (Khyalia et al. 2022). It also affects human and animal health by causing infectious and chronic diseases. Groundwater movement can be obstructed by a massive amount of plastic waste (Silva 2014). Plastic waste may contain heavy metals, impeding the soil and reaching water sources. Soil fertility is also influenced by plastic. Incineration and open burning of plastic waste produce dioxins and toxic gases. The lack of suitable landfill sites is another issue in waste disposal.

Plastic debris accumulated in marine ecosystem leads to aesthetic concerns and affect tourism. Large amounts of plastic debris also affect fishing activities, as debris is trapped in the fishing net along with fish (Gregory 2009). Ingestion of plastic waste by aquatic animals affects their health adversely. Further, this may affect other animals and human beings because the ingestion of plastic by marine animals leads to their introduction into the food chain, and toxic substances are transferred from one organism to another (Thomson et al. 2009).

Another matter of concern is very small fragments of plastic, commonly called microplastics. They are thread-like in appearance, and their size varies from 0.1 mm to ≤ 5 mm (Yadav et al. 2023). A number of studies evidence the presence of microplastics in plankton, fishes, and human

beings. Phthalates and Bisphenol A (BPA) are added as an additive during the manufacturing of plastic and are very toxic and can bioaccumulate in organisms. Recycling is a good method to reduce plastic waste, but it is not cost-effective because sometimes the expense of the production of new plastic is much lower than that of recycling (Faris et al. 2014, Faure et al. 2015).

BIOPLASTICS

Bioplastics are polymers obtained from natural resources and are entirely or partially biodegradable depending upon the renewable sources and additives used in bioplastic production. Under natural conditions, bioplastic degrades into CO_2, H_2O, and other inorganic compounds, by the action of enzymes of different organisms. No toxic residue is left after the degradation process is completed. In addition, the production and use of bioplastic conserve the petrochemicals used to make conventional plastic, and it lessens environmental damage brought on by improperly discarding plastic garbage. Bioplastic poses a lower carbon footprint than synthetic plastic, helps in the reduction of CO_2 emission, saving fossil fuels, and removes non-biodegradable plastic waste. The selection of raw materials and other additives affects the cost of bioplastic production (Mostafa et al. 2018). These days' bioplastic is used for making plastic films. With technological advancement and research, other high-value products for automobiles and electronics can be produced shortly (Chen 2014).

Types of Bioplastics

Bioplastic can be produced from renewable, edible, and in-edible raw materials like starch, cellulose, proteins, and bacteria like PHA, PHB, PLA, etc. They are mainly divided into starch-based, cellulose-based, and microbes-based. The different kinds of bioplastic and the sources for their production are illustrated in Fig. 2.

Cellulose-based Bioplastics

Cellulose is a natural polymer having molecular formula $(C_6H_{10}O_5)n$ and consists of a linear chain of 100-1000 of $\beta(1{\rightarrow}4)$ linked D-glucose units. It is the most abundant biopolymer made from thousands of monosaccharide units. Cellulose is mainly found in the primary cell wall of green plants and can be obtained from plant biomass with the help of synthetic and natural methods. Cellulose is produced from fibers, and these fibers are not soluble in water and thus are treated at high temperatures with acids and sodium chloride to obtain cellulose.

Cellulose is highly crystalline and hydrophilic, producing brittle packaging material that cannot be used for packaging
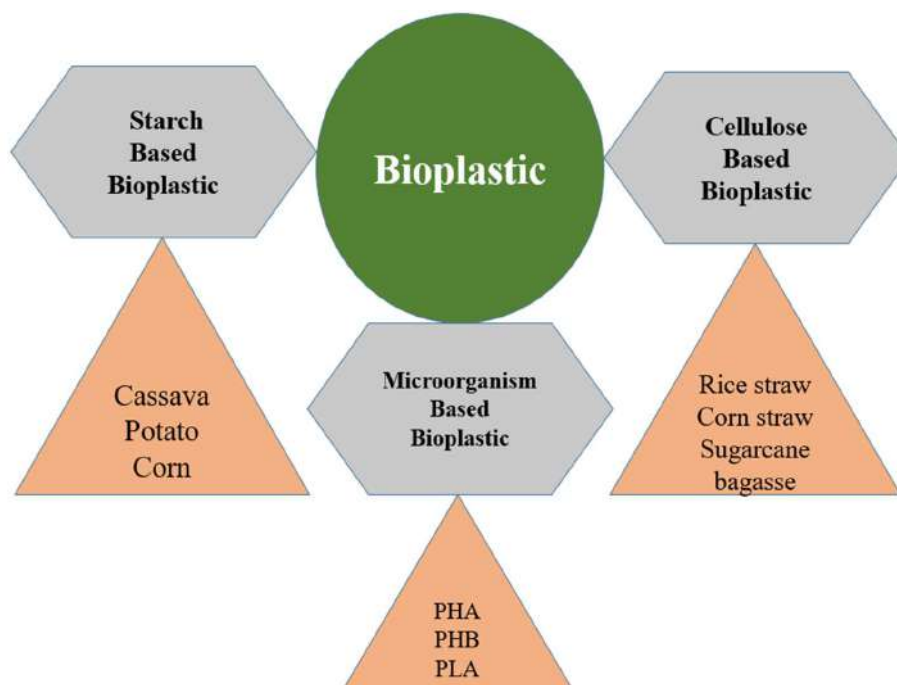
Fig. 2: Different kinds of bioplastics and their sources.

purposes due to poor flexibility and tensile strength. However, cellulose derivatives like hydroxypropyl cellulose, hydroxypropyl methylcellulose, carboxymethylcellulose, and methylcellulose are suitable for packaging applications (Morillon et al. 2002).

Starch-based Bioplastics

Starch comprises monomeric glucose units joined by α-1,4-linkage and has the molecular formula $(C_6H_{10}O_5)_n$. It is a polysaccharide having amylose and amylopectin as its major constituents. It is a granular, tasteless, soft organic chemical, white in appearance. Starch is a biodegradable, inexpensive, abundant, and renewable polymer from green plants. It possesses good polymeric properties and is used to produce bioplastic. Further starch can be blended with non-degradable polymer to enhance the biodegradability process. The mechanical properties of starch can be improved by modifying it into thermoplastic starch by heating it with a plasticizer and other additives (Sun et al. 2014).

The production of bioplastic film from starch involves a wet process and a dry process. The wet process is a laboratory-scale method that includes casting. In contrast, the dry process involves advanced methods like extrusion and molding and can be applied to an industrial scale (Zhong et al. 2018, Liu et al. 2020). Generally, the casting method has two types- solvent casting and tape casting. The solvent casting method includes gelatinizing starch and heating it with some additives to get a filmogenic solution.

Further, the fibrogenic solution is dried onto Teflon sheets or petri plates to get thin plastic films. The tape casting method is different from the solvent casting method in that the drying of the fibrogenic solution is controlled by heat convection. To produce high-quality plastic products, the modified thermoplastic starch can be subjected to advanced methods like thermoforming, compression molding, injection molding, and extrusion (Emin 2017). Starch-based bioplastic is used as a food packaging material and for disposable utensils. About 80% of the total bioplastic production is contributed by starch-based bioplastic.

Microorganisms-based Bioplastics

Polylactic acid (PLA): The monomer precursor for PLA is lactic acid, produced by the chemical synthesis of carbohydrates. The process involved in the production of PLA includes bacterial fermentation and enzymatic hydrolysis of lactide (Lim et al. 2008). Ring-opening polymerization and direct condensation of acid-free in the solution are also used for producing PLA (Mehta et al. 2005, Rasal et al. 2010). PLA is a thermoplastic with high transparency, gloss, stiffness, printability, brittleness, processability, low melting strength, and aroma barrier (Lim et al. 2008). After modification, PLA is used with additives such as plasticizers, starch, and fillers.

Further, the stiffness and tensile strength can be improved by blending PLA with biodegradable polymers. Recently, PLA has been used in food packaging. PLA can be used for

various applications after modification (Mehta et al. 2005, Rasal et al. 2010).

Polyhydroxyalkanoates (PHA): PHA is obtained as a result of bacterial fermentation of lipids and sugars. The fermentation of PHA involves two stages, viz., producing a high-density culture followed by increasing the concentration of PHA. Balanced pH, low stirrer speed, and temperature ranging between 30°C -37°C are conditions for optimal production. Whenever a bacterial cell experience nutrient imbalance, it accumulates PHA as a nutrient reserve (Kawaguchi et al. 2016). It is required to break the bacterial cell to obtain PHA, followed by solubilizing this cellular material (Snell & Peoples 2009). Various prokaryotes, including bacteria and archaes, *Pseudomonas aeruginosa, P. putida,* and *E. coli* are suitable for PHA production. In addition, several kinds of bacterial cultures are capable of PHA production.

Gram-negative, as well as gram-positive bacteria produce PHA. Different kinds of bioplastic are obtained by selecting high PHA-producing bacterial species, altering and managing the process conditions, and using additives (Keenan et al. 2006, Suriyamongakol et al. 2007). A big constraint in PHA production is cost, which could be resolved by selecting appropriate media capable of producing large quantities of PHA. Further, starchy wastewater, corn, whey, rice bran, and industrial waste effluents can be utilized as a cheap source of fermentation. PHA is usually combined with monomers to enhance their properties. They possess characteristic properties similar to synthetic polymers like Polypropylene (PP) and Polyethylene (PE) (Mannina et al. 2019). PHA is brittle, ductile, thermosensitive, and has a high production cost, which limits its applications (Keskin et al. 2017, Vandi et al. 2018, Valentini et al. 2019, Kim et al. 2005). PHA are eco-friendly and biodegradable and are used as packaging material.

Polyhydroxybutyrate (PHB): PHB is transparent, biodegradable, and resembles polypropylene in many characteristic properties. PHB is obtained as a result of the action of the bacteria. The synthesis of PHB includes a complex enzymatic process. Firstly, the condensation of two molecules of acetyl CoA leads to the production of acetocetyl-CoA; β-ketothiolase act as a catalyzer in this process. Further, acetoacetyl CoA reduces itself, producing β-hydroxybutyryl-CoA. Finally, the polymerization of β-hydroxybutyryl-CoA results in the synthesis of PHB. PHB exists as cysts in the cytoplasm of the bacterial cell, and these cells are destroyed to obtain PHB. PHB is produced and accumulated by a wide range of bacteria. About 300 species of bacteria are found to produce PHB, but the amount of PHB capable of producing bioplastic is present in very few species. Although PHB can be utilized for a number of applications, the high production cost is a matter of concern (Singh et al.

Synthetic Plastic
- Based on non renewable source of energy.
- Contains Toxic compounds.
- Not Biodegradable.
- Not Eco-friendly.
- Degradation time- Million of years.
- Threat for flora and fauna.
- About 345 million tons is produced annually.
- Difficult to recycle.
- Conversion of raw plastic into useful material is not easy process.
- Lack of suitable disposal methods.
- Cause harm to abiotic factors.
- Reduce soil fertility.
- Eco-toxic.
- Economic and cost effective.

Bioplastic
- Based on renewable source of energy.
- Doesn't contain toxic compound.
- Biodegradable.
- Eco-friendly.
- Degradation time- 180-300 days.
- Doesn't threaten flora and Fauna.
- Annual global production is 2.4 million tons.
- Easy to recycle.
- Conversion of raw bioplastic into useful material is easy process.
- Suitable disposable (composting, landfilling) methods are available.
- Doesn't harm abiotic environment.
- Improve soil fertility.
- Not Eco-Toxic.
- Not cost effective.

Fig. 3: Comparison of synthetic plastic with bioplastic.

2009). After suitable pre-treatment, agricultural waste and industrial waste effluents may be utilized in the production of PHB to reduce the cost constraints. A few bacterial species capable of producing PHB are *Pseudomonas, Ralstonia eutropha, Staphylococcus,* and *Bacillus*. Fig. 3 shows the general points of comparison between synthetic plastic and bioplastic.

Biodegradation of Bioplastics

Biodegradation of plastic involves specific changes in plastic material's chemical and physical properties by the action of microorganisms like fungi, bacteria, actinomycetes, etc. (Ishigaki et al. 2004). Plastics are degraded both aerobically and anaerobically. Aerobic biodegradation involves the degradation of plastic in the availability of oxygen. The microbes use oxygen as an electron acceptor to break down plastic material into more minor organic compounds, leaning behind CO_2 and water as the by-product. Anaerobic biodegradation is the breakdown of plastic waste in the unavailability of oxygen. Microbes use nitrate, sulfate, and CO_2 as electron acceptors, breaking the organic chemicals into smaller components. In this process, methane is produced as a by-product (Mohe et al. 2008, Priyanka & Archna 2011, Haider et al. 2019).

Mechanism of Biodegradation

The primary mechanism behind plastic biodegradation is microorganisms sticking on the polymer surface's hydrophilic end. After being attached to the polymer surface, the microbes use the latter as a carbon source and obtain nutrition for growth. These microorganisms reduce extracellular enzymes, which act on specific sites in the plastic material (Shah, 2014).

These enzymes work directly on the plastic, transforming the polymer into a shorter chain and low molecular weight fragments like dimers, monomers, and oligomers. The monomer of small size enters the cell to be hydrolyzed by an internal enzyme (Shah et al. 2008, Sivan 2011). The final stage of biodegradation is the assimilation of monomers into a microbe to generate cellular biomass, CO_2 and methane, depending upon oxygen availability. The mechanism behind biodegradation of bioplasic is shown in Fig. 4. Several factors affect the process of degradation. The type of organism, molecular weight and density of the polymer, molecular composition, hardness, physical form of polymer, pH, and moisture content. Fig. 5 shows the various factors that affect the process of biodegradation.

Biodegradability in Compost

Composting involves the microbes-assisted conversion of organic matter into CO_2 and humus. Compostable plastic is considered biodegradable (Kale et al. 2007). Several studies have been conducted on the biodegradability of plastic in compost. Various environmental conditions like temperature, pH, and humidity affect the process of biodegradation of bioplastic in compost (Rudnick et al. 2011). Bioplastic degradation in compost took about 90-110 days, and the degradability rate was 79.9- 85% (Sarasa et al. 2009, Gomez & Michel 2013, Weng et al. 2011). Biodegradability of PLA ranged from 13-84% under different temperatures and
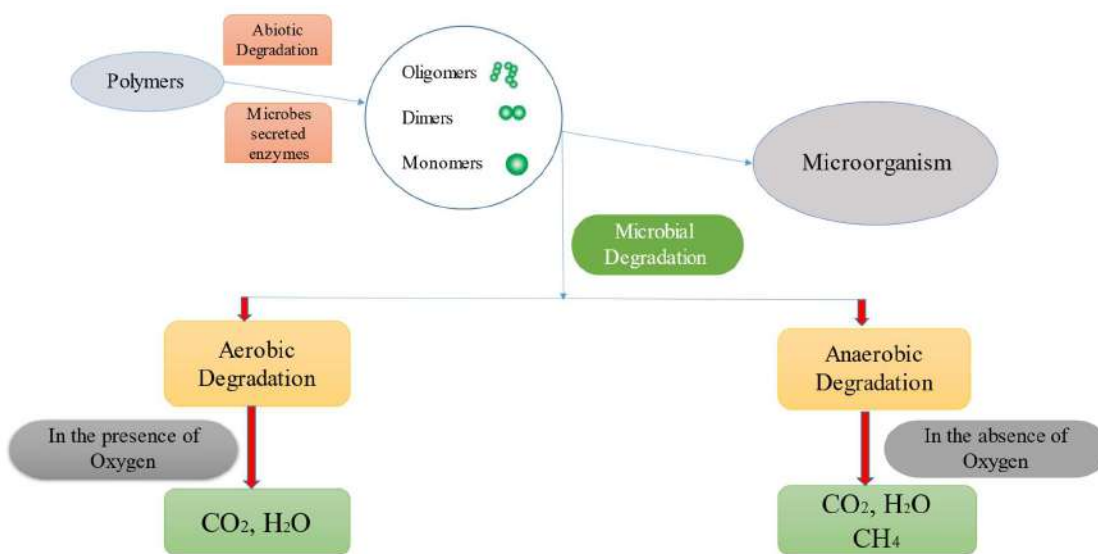
Fig. 4: Mechanism of biodegradation of bioplastics.
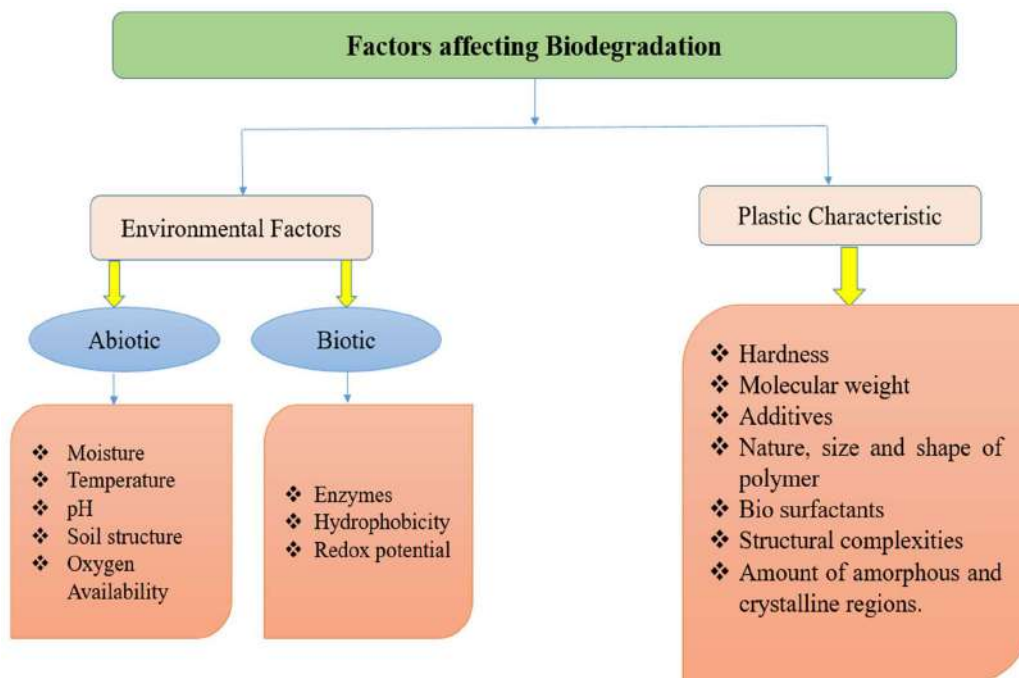
Fig. 5: Factors affecting the process of biodegradation.

humidity conditions in compost (Kale et al. 2007, Ahn et al. 2011, Mihai et al. 2014, Tabasi & Ajji 2015).

Biodegradability in Soil

A huge number of microorganisms are found in the soil environment. The action of this microorganism on the bioplastic accelerates the process of biodegradation. The rate of biodegradation depends on the soil environment and the microorganisms present. The rate of biodegradation ranged from 10-53%, 31.5-98%, 40-48.5%, and 60% for PLA, PHB, PHA, and starch-based bioplastic, respectively (Adhikari et al. 2016, Jain & Tiwari 2015, Jain & Verma 2015, Harmaen et al. 2015, Wu 2014, 2012, Gomez & Michel 2013, Boyandin et al. 2013).

Biodegradability in Aquatic Systems

The degradation rate varied in different kinds of seawater (Sekiguchi et al. 2011). Biodegradation is affected by the shape and type of bioplastic and water temperature (Volova et al. 2007). In their study, Volova et al. 2010 found that the degradation rate of PHA films is faster/higher than PHA pellets. The addition of sediments positively affects biodegradation (Thellen et al. 2008).

Role of Microorganisms in Biodegradability

Different microorganisms, including eukaryotic, aerobic, and anaerobic bacteria, catalyzed and accelerated bioplastic biodegradation (Lee et al. 2005, Kumaravel et al. 2010). Table 1 shows the different kinds of bioplastics and the microorganism responsible for their biodegradation. Both intracellular and extracellular enzymes aid in the enzymatic degradation of bioplastic. Enzymes like depolymerase, lipase, and esterase obtained from different microorganisms are very effective in bioplastic degradation (Tokiwa & Calabia 2004, Chua et al. 2013, Trivedi et al. 2016).

Application of Bioplastics

Bioplastics are used mainly in food packaging and agriculture (Briassoulis et al. 2010). With the advancement in technology and increased interest of researchers in bioplastics, the quality of bioplastics is improved. Thus, it can be used for preparing automobile parts like dashboards. Bioplastic is used in the manufacturing of sanitary products and medical implants. Table 2 shows the different kinds of bioplastic and their applications.

Market Status and Future

Different kinds of bioplastics have been introduced in the global market. The annual global production is about 2.4 million tons, which accounts for 2% of the total plastic production. The production of bioplastic is expected to increase in the future. Bioplastic is widely used for packaging (about 48%) and can be used as single-use plastic. The most commonly used and produced bioplastic is starch-based

Table 1: Different kinds of bioplastics and their degrading microorganisms.

Bioplastic	Degrading Microorganism	Reference
Polyhydroxybutyrate (PHB)	• *Streptomyces* sp. • *Bacillus* sp. • *Mycobacterium* sp. • *Nocardiopsis* sp. • *Streptomyces bangladeshensis* • *Pseudomonas lemoignei* • *Entrobacter* sp. • *Bacillus* sp. • *Gracibacillus* sp.	(Hoang et al. 2007) (Kumaravel et al. 2010) (Volova et al. 2010
Polyhydroxyalkanoates (PHA)	• Pseudomonas putida • *Leptothrix* sp. • *Variovorax* sp. • *Psedomonas aerugusina* • *Bacillus subtilis* • *Psedomonas fluorescens* • *Psedomonas putida* • *Psedomonas* sp.	(Volova et al. 2007) (Bhatt et al. 2008)
Starch-based Bioplastic	• Clostridium acetobutylicum • Laceyella sacchari	(Yoshida et al. 2016)

Table 2: Applications of different kinds of Bioplastics.

Bioplastics	Polyhydroxyalkanoates (PHA)	Starch-based Bioplastics	Cellulose-based bioplastics	Polylactic Acid (PLA)
Application	Tissue Engineering, Pharmaceutical applications, Packaging, Bottles, Pens, Cosmetic containers, Composting bags, Fishing net.	Mulch films, Fruits and vegetable packing tray, Food packaging.	Gardening products, Polymer blend, Agriculture net and films, Disposable gloves, Food packaging.	Agricultural mulches, Food packing films, Medical applications (Implants, nails), Cosmetic packaging, Automobile applications (Dashboard and door treadplates).

(Source: Muniyandi et al. 2020, Zhang et al. 2019, Luchese et al. 2017, Nunes et al. 2020, Mozaffari et al. 2019, Rahman et al. 2019).

(European Bioplastics 2020). There is estimated to be a 25% growth in the global bioplastic market by 2023 (European Bioplastics 2018).

According to the latest report of European Bioplastic in cooperation with nova institute, global bioplastic production is expected to be approx. 7.59 million tons by the year 2026 (Fig. 6). PLA, PHA, and starch-based bioplastic account for more than 64% of bioplastic production capacities. Bioplastic has found many applications in packaging, electronics, automobiles, etc. (European Bioplastic 2021).

There are many global producers and suppliers of bioplastics based on starch, PLA, PHA, and cellulose. Various global producers and suppliers of various kinds of bioplastic are listed in Table 3. Asia has the largest manufacturing capacities of about 50-55% of the bioplastic. The bioplastic market is not much developed in India; the significant bioplastic producers in India are m/s NatureTec, m/s Biotec Bags, m/s Envigreen, Ecolife, Truegreen, and

Plastobag. According to a report of the Central Pollution Control Board (CPCB), India, 120 sellers have been granted licenses for selling compostable and biodegradable products in India. The bioplastic market shall grow considerably in the next few years. Many big companies have also started using biobased products. McDonalds uses bowls made with PLA for serving fresh salad, Mosburger uses cups made with PLA for beverages (Sudesha & Iwata 2008), Walmart uses biobased trays wrapped with cellulose films for packing kiwi, and Boulder Canyon uses metalized cellulose films for packing potato chips.

The commercialization of bioplastic has also become a global challenge because bioplastic production is not sustainable and economic. The cost of production of bioplastic is 2-4 times higher compared to synthetic plastic. The high production cost is a major issue and is mainly contributed to a lack of adequate technologies, slow growth of microbes, and high energy requirements (European

(Source: European Bioplastics, nova-institute 2021.)

Fig. 6: Global production capacities of bioplastic by the year 2026.

Table 3: Global producers and suppliers of various kinds of bioplastics.

Kind of bioplastic	Brand Name	Country
Cellulose-based	Natural flex	UK
	Tenite	USA
	Biograde	Germany
	Sateri	China
Starch-based	Mater-Bi	Italy
	Livan	Canada
	Ever corn	Japan
	Plaststa rch	USA
	Rodenburg biopolymers	Netherlands
	Cardia Bioplastics	Australia
	GreenDot Bioplastics	USA
	GXT Green Products Pvt Ltd	India
	EnviGreen	India
Polylactic Acid (PLA)	Biofoam	Netherland
	Ingeo	USA
	Hisun	China
	Biofront	Japan
	Greengran	Netherlands
	Good Natured Products Inc.	Canada
	Total Corbion PLA	Netherlands
	NatureWorks LLC	US
Polyhydroxyalkanoates (PHA)	Minerv	Italy
	Biogreen	Japan
	Biocycle	Brazil
	Green Bio	China
	Metabolix	USA
Polyamide	Arkema	France
	Evonik	Germany
Polyhydroxybutyrate (PHB)	Kaneka Corp	Japan

(Source: Palaniswamy & Venkatachalam 2020, Goel et al. 2021)

Bioplastic 2020, Hatti-Kaul et al., 2020, Bhatia et al. 2021).

Another issue is using first-generation feedstock like sugarcane, corn, wheat, and cassava for bioplastic production (Okolie et al. 2019). Using renewable and inedible feedstock (crop residue, woody biomass) and multiple fission to increase microbes' growth rate and optimize culture conditions may prove useful (Bhatia et al. 2021, Prasanth et al. 2021).

The technologies used for bioplastic production are relatively new and are used at a small scale. The large-scale production of bioplastic may help in substituting traditional plastic and also in resolving problems related to environmental problems.

Limitations of Bioplastics

The major drawback of bioplastic is its cost of manufacturing, which is much higher than synthetic plastic. Bioplastics get mixed with synthetic plastics and affect the recycling process of synthetic plastic. Thus, segregating them is needed (Arikan & Ozsoy 2015). Bioplastics are made from starch, cellulose, and other feedstocks and have many limitations. They possess poor mechanical strength and thermal instability. Their biodegradability and long-term stability are another matter of concern. These bioplastics give brittleness and poor processability because they are hydrophilic (Palaniswamy & Venkatachalam 2020). Bioplastics are generally regarded as compostable and biodegradable. But not all the bioplastics are compostable. Their biodegradability and compostability vary with their composition. Composting of bioplastic requires treatment at the industrial level. Certain kinds of bioplastics are degradable only under certain temperature ranges and humidity. There is no appropriate legislation regarding the production and applications of bioplastic, and there is a lack of standards for waste management (Arikan & Ozsoy 2015). Many edible food substances, such as corn and potato, extract starch from them for the production of bioplastic, which may affect food safety. And the over-utilization of these raw materials may reduce their reserves for future use. Many unedible food by-products and agro-residues can be used for preparing bioplastic (Lagaron & Lopez-Rubio 2011).

CONCLUSIONS

This review has disclosed the types of plastic material being used, the different methods of polymerization and problems caused by their overuse, and the alternative solution, "bioplastic," their sources, applications, and biodegradability. Bioplastics are biodegradable, made from natural and renewable sources, compostable, and able to be recycled and burned without producing toxins. This is high

time to go for further growth of bioplastics. There is a need to develop standards for bioplastic production and waste management. Based on various studies, it can be concluded that it takes about 3-4 months for the biodegradation of bioplastic. The biodegradability of bioplastic must be popularized, and society must be made aware of the benefits of using bioplastic. The government must deal with the retailer and food industry to enhance the use of bioplastic. Starchy food waste, lignocellulosic agro-residue, starchy wastewater, and industrial waste effluent have been used by many researchers for preparing bioplastic. The production of bioplastic from different kinds of feedstock should be explored. There is a need for environmental awareness and improved methods for manufacturing biomass into plastic. This article studied the global market status of bioplastics. There are many producers and sellers of bioplastic globally, yet the bioplastic market is not much developed. Leading brands and Companies must invest in the production of bioplastic. Currently, these bioplastics find application in filmmaking and food packaging. But with the help of further research and improved technologies, the properties of the bioplastic may be improved.

REFERENCES

Adhikari, D., Mukai, M., Kubota, K., Kai, K., Kaneko, N., Araki, K.S. and Kubo, M. 2016. Degradation of bioplastics in soil and their degradation effects on environmental microorganisms. J. Agri. Chem. Environ., 5: 23-34.

Ahn, H.K., Huda S.M., Smith, M.C., Mulbry, W., Schmidt, F.W. and Reeves, B.J. 2011. Biodegradability of injection molded bioplastic pots containing polylactic acid and poultry feather fiber. Bioresour. Technol., 102(7): 4930-4933.

Andersen, M.E., Clewell, H.J., Tan, Y.M., Butenhoff, J.L. and Olsen, G.W. 2006. Pharmacokinetic modeling of saturable, renal resorption of perfluoroalkyl acids in monkeys—probing the determinants of long plasma half-lives. Toxicology, 227(1-2): 156-164.

Arikan, B.E. and Ozosy, D.H. 2015. A review: investigation of bioplastic. J. Civ. Eng. Arch., 9: 188-192.

Babu, P.R., O'Connor, K. and Seeram, R. 2013. Current progress on bio-based polymers and their future trends. Prog. Biomater., 2(1): 1-16.

Bhatia, S.K., Otari, S.V., Jeon, J.M., Gaurav, R., Choi, Y.K., Bhatia, R.K., Pugazhendhi, A., Kumar, V., Banu, J.R. and Yoon, J.J. 2021. Biowaste-to-bioplastic (polyhydroxyalkanoates): conversion technologies, strategies, challenges, and perspective. Biores. Technol., 326: 124733.

Bhatt, R., Shah, D., Patel, K.C. and Trivedi, U. 2008. PHA–rubber blends: Synthesis, characterization, and biodegradation. Bioresour. Technol., 99(11): 4615-4620.

Boyandin, A.N., Pudnikova, V.S., Karpov, A.V., Ivonin, V.N., Lanh Do, N., Nguyen, T.H., Hiep Le, T.M., Filichev, N.L., Levin, A.L., Filipenko, M.L., Volova, T.G. and Gitelson, I.I. 2013. Microbial degradation of polyhydroxyalkanoates in tropical soils. Int. Biodeter. Biodegrad., 83: 77-84.

Briassoulis, D., Dejean, C. and Picuno, P. 2010. Critical Review of Norms and Standards for Biodegradable Agricultural Plastics Part II: Composting. J. Polym. Environ., 18(3): 364-383.

Casado, M.P., Macken, A. and Byrne, H.J. 2013. Ecotoxicological assessment of silica and polystyrene nanoparticles assessed by a multitrophic test battery. Environ. Int., 51: 97-105.

Chen, Y.J. 2014. Bioplastics and their role in achieving global sustainability. J. Chem. Pharm. Res., 6(1): 226-231.

Chua, T.K., Tseng, M. and Yang, M.K. 2013. Degradation of poly(e-caprolactone) by thermophilic *Streptomyces thermoviolaceus* Subsp. *thermoviolaceus* 76T-2. AMB Express, 3(1):1-8.

Chung, S.Y., Yettella, R.R., Kim, J.S., Kwon, K., Kim, M.C. and Min, D.B. 2011. Effects of grilling and roasting on the levels of polycyclic aromatic hydrocarbons in beef and pork. Food. Chem., 129(4):1420-1426.

Cole, M., Lindeque, P., Fileman, E., Halsband, C., Goodhead, R. and Moger, J. 2013. Microplastic ingestion by zooplankton. Environ. Sci. Technol., 47(12): 6646-6655.

David, A., Thangavel, D.Y. and Sankriti, R. 2019. Recover, recycle and reuse: An efficient way to reduce the waste. Int. J. Mech. Prod. Eng. Res. Dev., 9(3): 31-42.

Della, T.C., Bergami, E., Salvati, A., Faleric, C., Cirino, F., Dawson, K.A. and Corsi, I. 2014. Accumulation and embryotoxicity of polystyrene nanoplastic at a bearly stage of development of sea urchin embryos *Paracentrotus lividus*. Environ. Sci. Technol., 48(20): 12302-12311.

Dey, K.T. and Tripathi, M. 2010. Thermal properties of silicon powder filled High-density Polyethylene composites. Thermochim. Acta., 502(1-2): 35-42.

Emin, M.A. and Schuchmann, H.P. 2017. A mechanistic approach to analyze extrusion processing of biopolymers by numerical, rheological, and optical methods. Trends Food Sci. Technol., 60: 88-95.

European Bioplastics 2018. Bioplastics market data 2018. https://www.european-bioplastics.org/wp-content/uploads/2016/02/Report_Bioplastics-Market-Data_2018.pdf

European Bioplastics 2020. Bioplastics - facts and figures. https://docs.european-bioplastics.org/publications/EUBP_Facts_and_figures.pdf

European Bioplastics 2021. Bioplastics Market Development Update 2021. https://docs.european-bioplastics.org/publications/market_data/Report_Bioplastics_Market_Data_2021_short_version.pdf

Fang, L., Leng, Y. and Gao, P. 2005. Processing of hydroxyapatite-reinforced ultrahigh molecular weight polyethylene for biomedical applications. Biomaterials, 26(17): 3471-3478.

Faris, N.A., Noriman, N.Z. and Sam, S.T. 2014. Current research in biodegradable plastic. Appl. Mech. Mater., 679: 273-280.

Faure, F., Saini, C., Potter, G., Galgani, F., Alencastro, L.F. and Hagmann, P. 2015.An evaluation of surface micro- and mesoplastic pollution in aquatic ecosystems of the Western Mediterranean Sea. Environ. Sci. Pollut. Res., 22(16): 12190-12197.

Goel, V., Luthra. P., Kapur, S.G. and Ramakumar, V.S.S. 2021. Biodegradable/bioplastics: Myths and realities. J. Polym. Environ., 29: 3079-3104.

Gomez, E.F. and Michel, F.C. 2013. Biodegradability of conventional and bio-based plastics and natural fiber composites during composting, anaerobic digestion, and long-term soil incubation. Polym. Degrad. Stab., 98(12): 2583-2591.

Goswami, G., Goswami, M.G. and Purohit, P. 2015. Bioplastics from organic waste. Int. J. Eng. Res. Technol., 3(23): 1-3.

Gregory, M.R. 2009. Environmental implications of plastic debris in marine settings-entanglement, ingestion, smothering, hangers-on, hitch-hiking, and alien invasion. Phil. Trans. R. Soc. B., 364: 2013-2025.

Haider, T.P., Volker, C., Kramm, J., Landfester, K. and Wurm, F.R. 2019. Plastics of the future? The impact of biodegradable polymers on the environment and society. Angew. Chem. Int. Ed., 58(1): 50-62.

Harmaen, A.S., Khalina, A., Azowa, I., Hassan, M.A., Tarmain, A. and Jawaid. M. 2015. Thermal and biodegradation properties of poly(lactic acid)/fertilizer/oil palm fibers blend biocomposites. Polym. Compo., 36 : 576-583.

Hatti-Kaul, R., Nilsson, L.J., Zhang, B., Rehnberg, N. and Lundmark, S. 2020. Review designing biobased recyclable polymers for plastics. Trend. Biotech., 38(1): 50-67.

Hoang, K.C., Tseng, M. and Shu, W.J. 2007. Degradation of polyethylene succinate(PES) by a new thermophilic *Microbispora* strain. Biodegard., 18(3): 333-342.

Hong, G.L., Yuhana, Y.N. and Zawawi, E.Z.E. 2021. Review of bioplastic as food packaging materials. AIMS. Mater. Sci., 8(2): 166-184.

Huang, X., Ke, Q., Kim, C., Zhong, H., Wei, P., Wang, G., Liu, F. and P. Jiang. 2007. Non-isothermal crystallization behavior and nucleation of LDPE/AI nano- and microcomposites. Polym. Eng. Sci., 47(7):1052-1061.

Ishigaki, T., Sugano, W., Nakanishi, A., Tateda, M., Ike, M. and Fujita, M. 2004. The degradability of biodegradable plastics in aerobic and anaerobic waste landfill model reactors. Chemosphere, 54(3): 225-233.

Jain, R. and Tiwari, A. 2015. Biosynthesis of planet-friendly bioplastic using renewable carbon source. J. Environ. Heal. Sci. Eng., 13: 11.

Jain, R. and Verma, V.K. 2015. Synthesis and characterization of cadmium selenide nanoparticles for optoelectronic application. Int. J. Sci. Engine. Technol., 2: 11-16.

Kale, G., Auras, R., Singh, S.P. and Narayan, R. 2007. Biodegradability of polylactide bottles in real and simulated composting conditions. Polym. Test., 26(8): 1049-106.

Karana, E. 2012. Characterization of 'Natural' and 'High-Quality' Materials to Improve Perception of Bioplastics. J. Clean. Prod., 37: 316-325.

Kawaguchi, H., Hasunuma, T., Ogino, C. and Kondo, A. 2016. Bioprocessing of bio-based chemicals produced from lignocellulosic feedstocks. Curr. Opin. Biotechnol., 42: 30-39.

Keenan, T.M., Nakas, J.P. and Tanenbaum, S.W. 2006. Polyhydroxyalkanoate copolymers from forest biomass. J. Ind. Microbiol. Biotechnol., 33(7): 616-626.

Keskin, G., Kızıl, G, Bechelany, M. and Pochat-Bohatier. 2017. Potential of polyhydroxyalkanoate (PHA) polymers family as substitutes for petroleum-based polymers for packaging applications and solutions brought by their composites to form barrier materials. Pure Appl. Chem., 89(12): 1841-1848.

Khyalia, P., Gahlawat, A., Jugiani, H., Kaur, M., Laura, S, J. and Nandal, M. 2022. Review on the use of microalgae biomass for bioplastic synthesis: A sustainable and green approach to control plastic pollution. Pollution, 8(3): 844-859.

Kim, H.S., Yang, H.S., Kim, H.J., Lee, B.J. and Hwang, T.S. 2005. Thermal properties of agro-flour-filled biodegradable polymer bio-composites. J. Therm. Analy. Calorimet., 81(2): 299-306.

Kuhn, P., Semeril, D., Matt, D., Chetcuti, J.M. and Lutz, P. 2007. Structure–reactivity relationships in SHOP-type complexes: tunable catalysts for the oligomerization and polymerization of ethylene. Dalton. Trans., (5): 515-528.

Kumaravel, S., Hema, R. and Lakshmi, R. 2010. Production of polyhydroxybutyrate (bioplastic) and its biodegradation by *Pseudomonas lemoignei* and *Aspergillus niger*. J. Chem., 7(S1): S536-S542.

Lagaron, J.M. and Lopez-Rubio, A. 2011. Nanotechnology for bioplastics: Opportunities, challenges, and strategies. Trend Food. Sci. Tech., 22(11): 611-7.

Laist, D.W. 2006. Overview of the biological effects of lost and discarded plastic debris in the marine environment. Mar. Pollut. Bull., 18(6): 319-326.

Lim, T.L., Auras, R. and Rubino, M. 2008. Processing technologies for poly (lactic acid). Prog. Polym. Sci., 33: 820-852.

Liu, W., Wang, Z., Liu, J., Dai, B., Hu, S., Hong, R., Xie, H., Li, Z., Chen, Y. and Zeng, G. 2020. Preparation, reinforcement, and properties of the thermoplastic starch film by film blowing. Food. Hydrocoll., 108: 106006.

Luchese, C.L., Sperotto, N., Spada, J.C. and Tessaro, I.C. 2017. Effect of blueberry agro-industrial waste addition to corn starch-based films for the production of a pH-indicator film. Int. J. Biol. Macromol., 104: 11-18.

Luckachan, G.E. and Pillai, C.K.S. 2011. Biodegradable polymers- A review of recent trends and emerging perspective. J. Polym. Environ., 19: 637-676.

Maddah, A.H. 2016. Polypropylene as a promising plastic: A review. American J. Polym. Sci., 6(1): 1-11.

Mannina, G., Presti, D., Montiel-jarillo, G. and Suarez-ozeda E. M. 2019. Bioplastic recovery from wastewater: A new protocol for polyhydroxyalkanoates (PHA) extraction from mixed microbial cultures. Bioresour. Technol., 282: 361-369.

Manu, M.T., Soni, S., Murthy, K.R.V. and Sebastian, T.M. 2013. Ba(Zn$_{1/3}$Ta$_{2/3}$)O$_3$ ceramics reinforce high-density polyethylene for microwave applications J. Mater. Sci. Mater. Electron., 24(6): 2098-2105.

Mehta, R., Kumar, V., Bhunia, H. and Upadhyay, S.N. 2005. Synthesis of poly (lactic acid): A review. J. Macro. Sci. C Polym. Rev., 45: 325-349.

Mihai, M., Legros, N. and Alemdar, A. 2014. Formulation-properties versatility of wood fiber biocomposites based on polylactide and polylactide/thermoplastic starch blends. Polym. Eng. Sci., 54(6): 1325-1340.

Mohe, R., Unmar, G.D., Mudhoo, A. and Khadoo, P. 2008. Biodegradability of biodegradable/degradable plastic materials under aerobic and anaerobic conditions. J. Waste Manag., 28(9): 1624-1629.

Morillon, V., Debeaufort, F., Blond, G., Capelle, M. and Voilley, A. 2002. Factors affecting the moisture permeability of lipid-based edible films: A Review. Crit. Rev. Food Sci. Nutr., 42(1): 67-89.

Mostafa, N.A., Farag, A.A., Abo-dief, H.M. and Tayeb, A.M. 2018. Production of biodegradable plastic from agricultural wastes. Arab. J. Chem., 11(4): 546-553.

Muniyandi, K., Punamalai, G., Sachithanatham, P., Chandersekaran, N. and Kamaraj, Y. 2020. The perspective of bioplastic: A review. Int. J. Sci. Technol. Res., 9: 374-381.

Nunes, L.A., Silva, M.L.S., Gerber, J. Z. and Kalid, R.D.A. 2017. Waste green coconut shells: Diagnosis of the disposal and applications for use in other products. J. Clean. Prod., 255: 120169.

O'Neil, C. 2010. So many polymers, so little time. MD+ DI, 32(9): 162-172

Okolie, J.A., Rana, R., Nanda, S., Dalai, A.K. and Kozinski, J.A. 2019. Supercritical water gasification of biomass: a state-of-the-art review of process parameters, reaction mechanisms, and catalysis. Sustain. Energy Fuels., 3: 578-598.

Palaniswamy, R. and Venkatachalam, H. 2020. Bioplastic world: a review. J. Advan. Scient. Res., 11(3): 43-53.

Pasch, H. and Eselem, B.P.S. 2018. Branching and molar mass analysis of low-density polyethylene using the multiple preparative fractionation concept. Polym. Chem., 9: 1116-1131.

Pathak, V.M. and Navneet, R. 2017. Review on the current status of polymer degradation: a microbial approach. Bioresour. Bioprocess., 4(15): 1-31.

Prasanth, S.M., Kumar, P.S., Harish, S., Rishikesh, M., Nanda, S. and Vo, D.V.N. 2021. Application of biomass-derived products in mid-size automotive industries: a review. Chemo., 280: 130723.

Priyanka, N. and Archana, T. 2011. Biodegradability of polythene and plastic by the help of microorganisms: A way for brighter future. J. Anal. Toxicol., 1(4): 1-4.

Rahman, R., Sood, M., Gupta, N., Bandral, D.J., Hameed, F. and Ashraf, S. 2019. Bioplastics for food packaging: A review. Int. J. Curr. Microbiol. Appl. Sci., 8(3): 2319-7706.

Rasal, R.M., Janorkar, A.V. and Hirt, D.E. 2010. Poly (lactic acid) modifications. Prog. Polym. Sci., 35(3): 338-356.

Rudnik, E. and Briassoulis, D. 2011. Degradation behavior of poly (lactic acid) films and fibers in soil under Mediterranean field conditions and laboratory simulations testing. Ind Crops Prod., 33(3): 648-658.

Saharan, B.S. and Ankita, S.D. 2012. Bioplastics-for sustainable development: A review. Int. J. Microb. Resour. Technol., 1(1): 11-23.

Sangale, K.M., Shahnawaz, M. and Ade, B.A. 2012. Review on biodegradation of polythene: The microbial approach. J. Bioremediat. Biodegrad., 3(10): 1-31.

Sarasa, J., Gracia, J.M. and Javierre, C. 2007. Study of the biodisintegration of bioplastic material waste. Bioresour. Technol., 100(15): 3764-3768.

Sekiguchi, T., Saika, A., Nomura, K., Watanabe, T., Fujimoto, Y., Enoki, M., Sato, T., Kato, C. and Kanehiro, H. 2011. Biodegradation of aliphatic polyesters soaked in deep seawaters and isolation of poly(e-caprolactone)-degrading bacteria. Polym. Degrad. Stab., 96(7): 1397-1403.

Shah, A.A., Hasan, F., Hameed, A. and Ahmed, S. 2008. Biological degradation of plastics: A comprehensive review. Biotechnol. Adv., 26(3): 246-265.

Silva, V.R., Brito, D.J. and Dhir, R. 2014. Properties and composition of recycled aggregates from construction and demolition waste suitable for concrete production. Constr. Build. Mater., 65: 201-217.

Singh, M., Patel, S.K.S. and Kalia, V.C. 2009. Bacillus subtilis a potential producer of polyhydroxy alkanoates. Microbial. Cell. Factor., 8: 38-48.

Singh, S., Shankar, S. and Shikha. 2016. Microbial degradation of plastic: A review. Int. J. Sci. Innov. Res., 4(1), 112-119.

Sivan, A. 2011. New perspectives in plastic biodegradation. Curr. Opin. Biotechnol., 22(3): 422– 426.

Snell, K.D. and Peoples, O.P. 2009. PHA bioplastic: A value-added coproduct for biomass biorefineries. Biofuels. Bioprod. Biorefin., 3: 456-467.

Sudesh, K, and Iwata, T. 2008. Sustainability of biobased and biodegradable plastics. Clean: Soil, Air, Water., 36(5-6): 43-442.

Sun, Q., Xi, T., Li, Y. and Xiong, L. 2014. Characterization of corn starch films reinforced with CaCO$_3$ nanoparticles. Plos One, 9(9): e106727.

Suriyamongakol, P., Weselake, R., Narine, S., Moloney, M. and Shah, S. 2007. Biotechnological approaches for the production of polyhydroxyalkanoates in microorganisms and plants e a review. Biotechnol. Adv., 25(2): 148-175

Tabasi, R.Y. and Ajji, A. 2015. Selective degradation of biodegradable blends in simulated laboratory composting. Polym. Degrad. Stab., 120: 435-442.

Thellen, C., Coyne, M., Froio, D., Auerbach, M., Wirsen, C. and Ratto, J.A. 2008. A processing, characterization, and marine biodegradation study of melt-extruded polyhydroxyalkanoate (PHA) films. J. Polym. Environ., 16(1): 1-11.

Thomson, C.R., Moore, J.C., Saal, F.S. and Swan, H.S. 2009. Plastics, the environment and human health: Current consensus and future trends. Phil. Trans. R. Soc. B., 364: 2153-2166.

Tokiwa, Y. and Calabia, B.P. 2004. Degradation of microbial polyesters. Biotechnol. Lett., 26(15): 1181-1189.

Tokiwa, Y., Calabia, P.B., Ugwu, U.C. and Aiba, S. 2009. Biodegradability of plastics, Int. J. Mol. Sci., 10 (9): 3722-3742.

Trivedi, P., Hasan, A., Akhtar, S., Siddiqui, M.H., Sayeed, U. and Khan, M.K.A. 2016. Role of microbes in degradation of synthetic plastics and manufacture of bioplastics. J. Chem. Pharm. Res., 8(3): 211-216.

Valentini, F., Dorigato, A., Rigotti, D. and Pegoretti, A. 2019. Polyhydroxyalkanoates/fibrillated nanocellulose composites for additive manufacturing. J. Polym. Environ., 27(2): 1333-1341.

Vandi, L., Chan, C.M., Werker, A., Richardson, D., Laycock, B. and Pratt, S. 2018. Wood-PHA composites: Mapping opportunities. Polym., 10(7): 1-15.

Volova, T.G., Boyandin, A.N., Vasiliev, A.D., Karpov, V.A., Prudnikova, S.V., Mishukova, O.V., Boyarskikh, U.A., Filipenko, M.L., Rudnev, V.P., Bá Xuân, B., Vit Dung, V. and Gitelson, I.I. 2010. Biodegradation of polyhydroxyalkanoates (PHAs) in tropical coastal waters and identification of PHA-degrading bacteria. Polym. Degrad. Stab., 95(12): 2350-2359.

Volova, T.G., Gladyshev, M.I., Trusova, M.Y. and Zhila, N.O. 2007. Degradation of polyhydroxyalkanoates in eutrophic reservoir. Polym. Degrad. Stab., 92(4): 580-586.

Weng, Y.X., Wang, X.L. and Wang, Y.Z. 2011. Biodegradation behavior of PHAs with different chemical structures under controlled composting conditions. Polym. Test., 30(4): 372-380.

Wu, C.S. 2012. Preparation, characterization, and biodegradability of renewable resource-based composites from recycled

polylactide bioplastic and sisal fibers. J. Appl. Polym. Scien., 123: 347-355.

Wu, C.S. 2014. Preparation and characterization of polyhydroxyalkanoate bioplastic-based green renewable composite from rice husk. J. Polym. Environ., 22: 384-392.

Yadav, A.A., Phadatare, R.S., Kadam, A.P., Patil, S.D. and Pisal, Y.S. 2020. Utilization of plastic waste for making plastic bricks. Int. Res. J. Eng. Technol., 7(2): 152-154.

Yadav, S., Kataria, N., Khyalia, P., Rose, K.P., Mukherjee, S., Sabherwal, H., Chai, S.W., Rajendran, S., Jiang, J. and Khoo, S.K. 2023. Recent analytical techniques and potential eco-toxicological impacts of textile fibrous microplastic (FMPs) and its associated contaminates: A review. Chemo. J., 23: 138495.

Yoshida, S., Hiranga, K., Takehana, T., Taniguchi, I., Yaamji, H., Maeda, Y., Toyohara, K., Miyamoto, K., Kimura, Y. and Oda, K. 2016. A bacterium that degrades and assimilates poly(ethylene terephthalate). Science, 351(6278): 1196-1199.

Zhang, Q., Rastogi, S., Chen, D., Lippits, D. and Lemstra, P.J. 2006. Low percolation threshold in single-walled carbon nanotube/high-density polyethylene composites prepared by Mel processing technique. Carbon, 44(4): 778-785.

Zhang, X., You, S., Tian, Y. and Li, J. 2019. Comparison of plastic film, biodegradable paper, and biobased film mulching for summer tomato production soil properties, plant growth, fruit yield, and fruit quality. Sci. Horticult., 249: 38-48.

Zhong, Y., Li, Y., Liang, W., Liu, L., Li, S., Xue, J. and Guo, D. 2018. Comparison of gelatinization method, starch concentration, and plasticizer on physical properties of high-amylose starch films. J. Food. Process. Eng., 41(2): e12645.

Process for the Reduction of High Water Content from Oily Sludge and Scum by Hot Washing

Le Zhang*†, Longlong Yan, Huan Zhang***, Zhe Shen*, Si Chen*, Tao Yu***(*****)**
and Chengtun Qu**(*****)**

*The Institute of Energy and Architecture, Xi'an Aeronautical University, Xi'an 710077, PR of China
**No.10 Oil Production Plant, Changqing Oilfield Company, Qingyang 745100, PR of China
***College of Chemistry and Material, Weinan Normal University, 714099, PR of China
****College of Chemistry and Chemical Engineering, Xi'an Shiyou University, 710065, PR of China
*****College of Chemistry and Chemical Engineering, Shaanxi Province Key Laboratory of Environmental Pollution Control and Reservoir Protection Technology of Oilfields, Xian Shiyou University, Xi'an 710065, PR China
†Corresponding author: Le Zhang; zl_202106011@163.com

ABSTRACT

The reduction of oily sludge and scum with high water content by hot washing and analysis of the main factors that affect the reduction and oil recovery rate of oily sludge and scum in hot washing were investigated. Best process conditions for the reduction of tank bottom sludge, refining sludge, and oily scum were carried out, which can make the oil recovery rate and reduction rate of tank bottom sludge after reduction reach 96.30% and 93.00%, respectively, the oil recovery rate and reduction rate of refining sludge after reduction reach 95.36% and 92.60% respectively, and the oil recovery rate and reduction rate of oily scum after reduction reach 95.92% and 93.60% respectively. After treatment, the oil content of the residue is reduced to below 5.1%, and the water content is reduced to below 59.0%. Oil content in the separated water is lower than 200 mg.L^{-1}, and the water content in the separated oil is lower than 0.2%, far below the requirement of 0.5% in the oilfield's crude oil gathering and transportation standard.

INTRODUCTION

Oily sludge occurs in oilfield exploitation, gathering, transportation, storage, refining, etc. (Tahhan & Abu-Ateih 2009). According to the specific location, it is mainly composed of four parts. First, oil sludge falls from drilling, operation, and pipeline perforation (Johnson & Affam 2018, Rocha et al. 2010). Second, the bottom mud of oil tanks, settling tanks, sewage tanks, and oil separators in transfer and combined stations (Egazaryants et al. 2015, Inguanzo et al. 2012). When the oil is stored in the tank, the oil sludge at the bottom is formed due to the oil's heavy, oily components deposited at the bottom (Murungi & Sulaimon 2022). Third, oil sludge is removed from oil-bearing water treatment facilities, light hydrocarbon processing plants, and natural gas purification devices in refineries (Chen et al. 2019, Hochberg et al. 2022). Oily sludge is generally a stable suspension emulsion system composed of oil in water (o/w), water in oil (w/o), and suspended solids, with poor dewatering effect (Long et al. 2013). The composition and physical properties of sludge are affected by factors such as sewage quality, treatment process, and dosing agent, which have large differences, high treatment difficulty, and large differences in oil content. Some of them have recycling value, and oily sludge contains PAHs, heavy metals, and other harmful substances, which also cause radioactive pollution to the environment (Puasa et al. 2019). The volume of oily sludge is huge. If it is directly discharged without treatment, it will not only occupy a large amount of cultivated land but also pollute the surrounding soil, water, and air, accompanied by the generation of malodorous gas (Hayhurst 2013, Anna et al. 2015, Ramirez & Collins 2018). Sludge contains a large number of pathogenic bacteria, parasites (eggs), copper, zinc, chromium, mercury, and other heavy metals, salts, polychlorinated biphenyls, dioxins, radionuclides, and other toxic and harmful substances that are difficult to degrade, such as shown in Fig.1 (Crelier & Dweck 2009). The arbitrary landfill will lead to serious pollution of groundwater and the destruction of the original ecology of food crops (Wu et al. 2019).

A large amount of oily sewage is usually produced in oil exploitation and refining. For the treatment of such oily
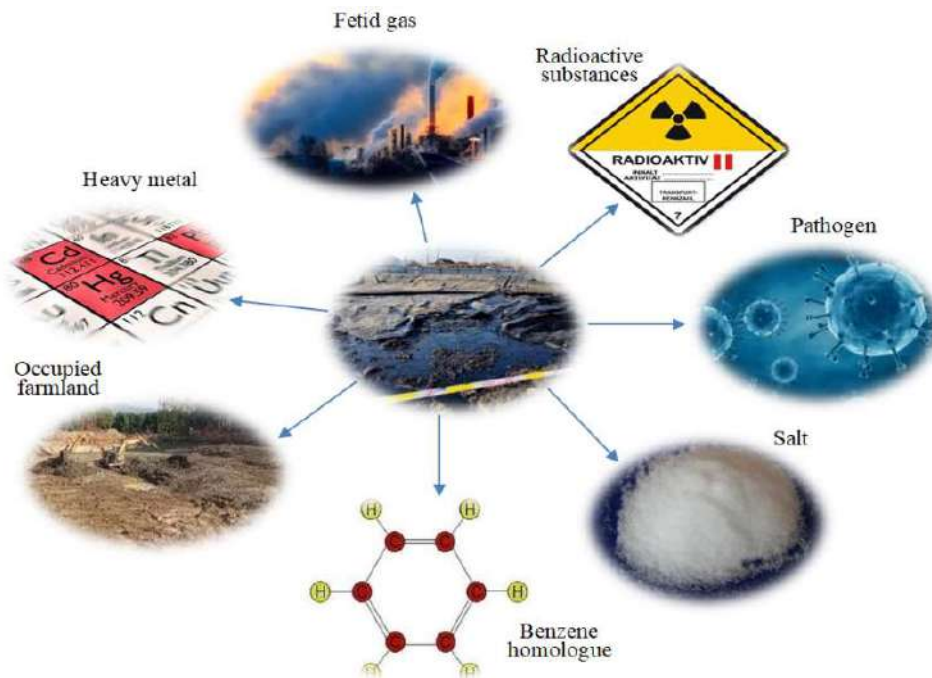
Fig. 1: Hazards of oily sludge.

sewage, the old three processes of "oil separation air flotation biochemical treatment" are generally adopted (Suganthi et al. 2018, Muneeswari et al. 2022). A large amount of oily scum will be produced by removing emulsified oil in the air flotation unit (Motlagh et al. 2019). The composition of oily scum is extremely complex, containing a large amount of aged crude oil, wax, asphaltene, colloid, solid suspension, etc., as well as various chemical agents such as coagulant and corrosion inhibitors added in the production process (Hu et al. 2013, Amudha et al. 2016). Oily sludge and scum have been included in the National Catalogue of Hazardous Wastes in China, and they are hazardous wastes (Wang et al. 2019). The amount of oily sludge and scum is large, and the moisture content is high, so direct refining or incineration will inevitably consume a lot of heat, leading to high energy consumption for enterprises (Skinner et al. 2015). Therefore, oily sludge and scum must be dewatered and reduced before harmless or resourceful disposal (Duan et al. 2018). Many domestic enterprises have adopted the mechanical conditioning three-phase separation process for dehydration treatment (Cheng et al. 2017, Shperber et al. 2011). Although certain results have been achieved, there are still some defects, mainly as follows: it is difficult to separate oil and water from oily sludge and scum, the oil recovery rate is low, the overall reduction rate of sludge is low, and the equipment cannot operate stably for a long period (Liu et al. 2022). Therefore, it is necessary to screen

and analyze all the influencing factors in the process of sludge reduction, determine which are the main influencing factors, and determine the best process parameters to provide technical support for the reduction, recycling, and harmless treatment of oily sludge in the future (Mowla et al. 2013, Barneto et al. 2014, Gourdet et al. 2017).

TREATMENT PROCESS AND APPLICATION STATUS

There are many industrial application processes for the thermal washing reduction treatment of oily sludge and scum at home and abroad, but the principles are basically the same (Mahmoud et al. 2018). They all use pH adjustment, heating, stirring, demulsifier, flocculant, mechanical dehydration, and other means and methods to finally achieve the reduction treatment of oily sludge and scum (Bao et al. 2022). Through a large number of field investigations and actual operations, the author of this paper summarizes the treatment of oily sludge and scum at some oily sludge stations in China, as shown in Table 1. The reduction process of some sludge stations is shown in Fig. 2.

It can be seen from Table 1, and the technical status of development that the sludge reduction rate and oil recovery rate of most technologies and stations are lower than 85%, and the oil content of sludge after final treatment is higher than 6%. Most technologies and processes only reduce the
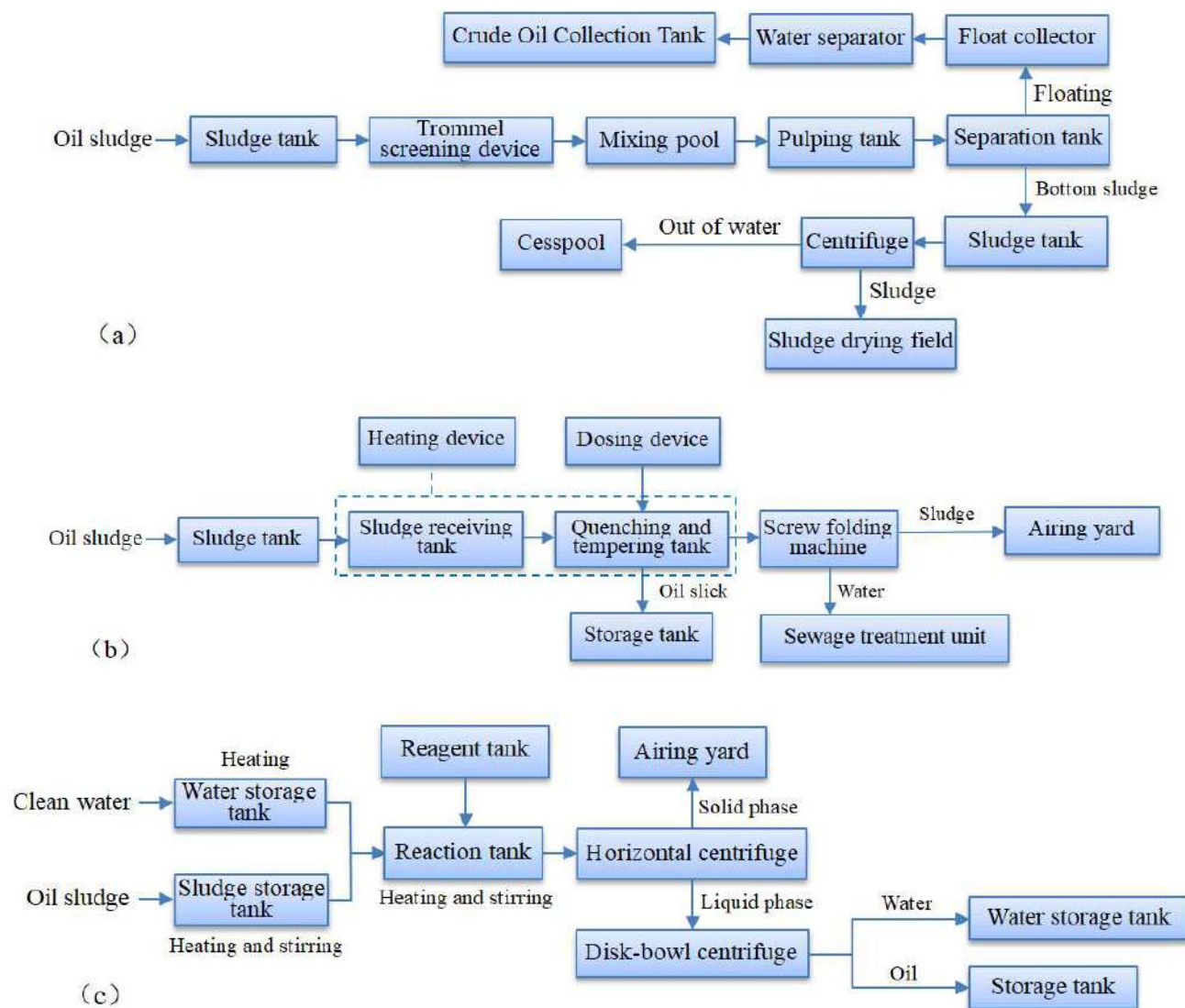
Fig. 2: Sludge reduction treatment process of (a) Oil Sludge Station in Tuha Oilfield; (b) Wuqi Oil Sludge Station in Changqing Oilfield; (c) Yumen Refineryfield.

sludge and do not achieve the best treatment effect. In this paper, the problems of unsatisfactory oily sludge and its reduction treatment effect and high oil content of sludge after treatment are studied in depth, the optimal operating conditions for oily sludge treatment and scum treatment are selected, and the importance of the influencing factors in the oily sludge and scum treatment process is ranked. The key factors affecting the oily sludge treatment are finally obtained.

MATERIALS AND METHODS

Materials

Analytical grade Sodium hydroxide (NaOH), hydrochloric acid (HCl), and demulsifier were used in the experiment. Industrial grade Poly Aluminum Chloride (PAC), poly aluminum sulfate (PAS), Polymerization Ferric Chloride (PFC), Polymeric Ferric Sulfate (PFS), and polyacrylamide (PAM) were used in this experiment.

Oil sludge samples were obtained from Yanchang Oilfield Shimian United Station, Yongping Refinery of Yanchang Oilfield, and Yan'an Petrochemical Plant of Yanchang Oilfield in Shaanxi Province, China. These samples were stored in a refrigerator at 4℃ to minimize biological and chemical reactions as much as possible. The general characteristics of the oil sludge samples from the workplace are shown in Table 2.

Experimental Procedure

Heat the sludge system temperature to the set temperature at the set heating rate. Adjust the pH of the system to the best experimental conditions. Adding a certain amount of demulsifier and adopting the best mixing method to stir for a certain time at a certain rate. After mixing, stand for a certain period of time. After standing, take out the upper clean water and oil to the oil-water separation device, and record the volume of oil and water, respectively. Adding

Table 1: Current situation of sludge reduction treatment in China.

Site name	Major equipment	Process parameters	Treatment effect
Tuha Oilfield Sludge Station	Drum screening device Mixing tank Slurry tank Sludge separation tank Sludge tank Centrifuge	Alternate operation of two pulping tanks Processing capacity: 100 $m^3.d^{-1}$ Add demulsifier and flocculant Heating method: steam-heat transfer oil Heating temperature: 70°C Vertical mixing shaft mixing mode Mixing time: 40 min Standing time: 30 min Rotating speed of centrifuge: 2600 $r.min^{-1}$ Centrifuge time: 30 min	The reduction rate can reach 85% The oil recovery rate can reach 80% The minimum oil content of the reduced sludge can be reduced to 7%
Dongrengou Oil Sludge Station of Yanchang Oilfield	Slag remover Conditioning tank Centrifuge Oil-water separator Heat exchanger Centrifuge	The three conditioning tanks operate alternately Processing capacity: 200 $m^3.d^{-1}$ Add demulsifier and flocculant Heating mode: steam. Vertical mixing shaft mixing mode Heating temperature: 60°C The mixing time: 30 min The standing time: 20 min Rotating speed of centrifuge: 2400 $r.min^{-1}$ Centrifuge time: 20 min	The reduction rate can reach 80%. The oil recovery rate can reach 83%. The minimum oil content of the reduced sludge can be reduced to 10%. The oil content in the treated water is less than 1%.
Yanchang Oilfield Fengchuan Youni Station	Sand setting device Reaction tank Screw stacking machine	Two reaction tanks operate alternately Processing capacity: 120 $m^3.d^{-1}$ Add regulator, demulsifier, and flocculant Heating mode: steam Vertical mixing shaft mixing mode Heating temperature 55°C The mixing time: 20 min The standing time: 40 min Sludge treatment time: 10 min	The reduction rate can reach 75%. The oil recovery rate can reach 81%. The minimum oil content of the reduced sludge can be reduced to 7%.
Changqing Oilfield Wuqi Oil Mud Station	Reaction tank Centrifuge Oil-water separation tank	Two reaction tanks operate alternately Processing capacity: 150 $m^3.d^{-1}$ Add regulator, demulsifier, cleaning agent, and flocculant Heating mode: steam Vertical mixing shaft mixing mode Heating temperature: 60°C The mixing time: 40 min The standing time: 30 min Rotating speed of centrifuge: 2400 $r.min^{-1}$ Centrifuge time: 15 min	The reduction rate can reach 70%. The oil recovery rate can reach 75%. The minimum oil content of the reduced sludge can be reduced to 10%.
Oil-bearing scum treatment workshop of Changqing Petrochemical	Homogenizing tank Reaction tank Centrifuge	Four reaction tanks operate alternately. Processing capacity: 300 $m^3.d^{-1}$. Add demulsifier and flocculant Heating mode: steam Inclined 45 ° mixing mode Heating temperature 50°C The mixing time: 20 min The standing time: 30 min Rotating speed of centrifuge: 2800 $r.min^{-1}$ Centrifuge time: 40 min	The reduction rate can reach 85%. The oil recovery rate can reach 78%. The minimum oil content of the reduced sludge can be reduced to 6%.

Table Cont....

Site name	Major equipment	Process parameters	Treatment effect
Oil sludge workshop of Yumen Refinery	Settling tank Reaction tank Centrifuge	The three reaction tanks operate alternately Processing capacity: 200 m^3.d^{-1} Add demulsifier and flocculant Heating mode: steam - heat transfer oil Vertical mixing shaft mixing mode Heating temperature: 50°C The mixing time: 40 min The standing time: 30 min Rotating speed of centrifuge: 2600 r.min^{-1} Centrifuge time: 25 min	The reduction rate can reach 80%. The oil recovery rate can reach 78%. The minimum oil content of the reduced sludge can be reduced to 6%.
Nanyang Oilfield Sludge Station	Prefabrication tank Reaction tank Centrifuge Oil-water separation tank	The three reaction tanks operate alternately Processing capacity 150 m^3.d^{-1} Add demulsifier and flocculant Heating mode: steam Vertical mixing shaft mixing mode Heating temperature 70°C The mixing time: 30 min The standing time: 50 min Rotating speed of centrifuge: 2400 r.min^{-1} Centrifuge time: 40 min	The reduction rate can reach 84%. The oil recovery rate can reach 83%. The minimum oil content of the reduced sludge can be reduced to 9%.

Table 2: Characteristics of the oil sludge samples.

Sludge type	Oil content [%]	Water content [%]	Solid content [%]
Bottom mud of combined station tank	17.86	80.53	1.61
Refining sludge	24.33	75.32	0.35
Oily scum	9.80	86.75	3.45

PAM of a certain concentration to the bottom sludge after standing before entering the centrifuge and stirring it evenly. Centrifuge it for a certain time at a certain speed in the centrifuge. Take out the centrifuged sludge, then take out the upper clean water and oil to the oil-water separation device, and record the volumes of oil and water, respectively. Take out the centrifuged bottom sludge to measure the water and oil content.

The single-factor experimental method was used to screen the best process. The final experimental effect was based on the overall sludge reduction rate, oil recovery rate, and the bottom sludge's water content and oil content after centrifugation.

Analytical Methods

The initial pH was measured using a pH meter (PHS-3C, Shanghai INESA & Scientific Instrument Co., Ltd.).

The determination method of water content in oil shall be in accordance with the method specified in the Determination of Water Content in Crude Oil Distillation Method (GB/T 8929-2006). Oil content in water shall be determined according to the method specified in Water Quality Determination of Petroleum, Animal, and Vegetable Oils Infrared Spectrophotometry (HJ 637-2012). The oil content of the bottom sludge shall be tested according to the method specified in the Control Limits for Disposal and Utilization of Oily Sludge (DB61/T 1025-2016).

The oil recovery rate was calculated by using the following equation:

$$\text{Oil recovery rate}: \mu = \frac{m}{n} \times 100\%$$

where μ is the oil recovery rate (%), m is the volume of reduced separated oil (mL), and n is the volume of oil in crude mud (mL).

The reduction rate was calculated by using the following equation:

$$\text{Reduction rate}: \rho = \frac{x}{y} \times 100\%$$

where ρ is the reduction rate (%), x is the final residual solid sludge volume after centrifugation (mL), and y is the volume of crude oil sludge (mL).

RESULTS AND DISCUSSION

Many factors affect the reduction process and the effect of oily sludge and scum. For example, the pH value of the system, the type, and dosage of agents can affect the aggregation degree of sludge particles, the temperature can affect the oil recovery rate in the reduction process of oily sludge and scum, and the mixing time, speed and method can affect the size, existing state and particle grading of sludge particles (Zhang et al. 2021, Liang et al. 2017). Therefore,

the effect of operating conditions on the reduction process and oily sludge and scum was investigated.

Effects of Operating Parameters on the Reduction Process and Oily Sludge and Scum

Initial pH

It can be seen from Fig. 3 that when the pH is acidic, the oil recovery rate of the three samples is lower than 70%, and the reduction rate is lower than 80%. When pH becomes alkaline, oil recovery and decrement increase gradually, and when pH=8.5, oil recovery and decrement reach the highest. When the pH exceeds 8.5, the oil recovery and decrement rates decline slightly. The reason for this phenomenon is that when the system's pH is weakly alkaline, it is helpful for the demulsification of oily sludge and scum. It can also react with the colloid and asphaltene in the sludge to generate salts, increase its water solubility, saponify with naphthenic acids, and improve the separation performance of chemical agents on oily sludge and scum. The oil recovery rate and the reduction effect worsen with the continuous pH increase. That is because some chemicals added have higher requirements for pH, and their effects will be weakened when they exceed a certain value.

Through the screening of this group of experiments, the optimal pH value of the three samples in the reduction process is 8.5. At this time, the oil recovery and reduction rates of the tank bottom mud of the combined station are 69.43%, and 71.40%, respectively. The oil recovery and reduction rates of refinery sludge were 75.63% and 73.60%, respectively. The oil recovery and reduction rate of oily scum is 71.43% and 81.20%, respectively.
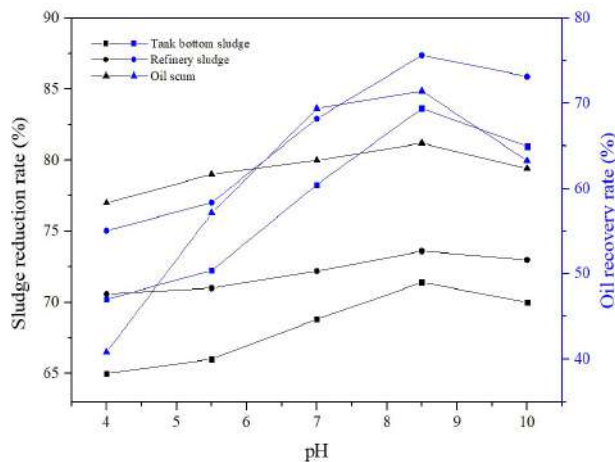
System Temperature

It can be seen from Fig. 4 that when the temperature rises from 40°C to 80°C, the oil recovery and decrement rate of the three samples show a trend of gradual increase. That is because the viscosity of the oil film is closely related to the temperature. The increase in temperature reduces the viscosity and surface tension, and the thermal expansion weakens the adhesion of the oil film, making it easier to separate the oil during the mixing process. However, when the temperature exceeds a certain value, the increasing trend of oil recovery and decrement rate is no longer obvious. This may be because the performance of the system in the system will gradually decline when the temperature exceeds a certain value.

Through the screening of this group of experiments, the optimal temperature for treating tank bottom sludge and refining sludge is 70°C, and the oil recovery rate and sludge reduction rate of tank bottom sludge are 77.27% and 76.60%, respectively. The oil recovery and reduction rates of refinery sludge were 82.20% and 79.40%, respectively. The optimum temperature for the treatment of oily scum is 60°C, and the oil recovery and reduction rates are 77.55% and 84.00%, respectively.

Heating Rate

It can be seen from Fig. 5 that the optimal heating rate in the process of the three samples' reduction is different, but the changing trend of the treatment effect of the three samples is the same. With the acceleration of the heating rate, the effect becomes better first and then worse. The reason may be that the time for the sludge to reach the experimental temperature is too short due to a too-fast heating rate,

Fig. 3: The black line and blue line represent the sludge reduction rate and oil recovery rate at different pH, respectively.

Fig. 4: The black line and blue line represent the sludge reduction rate and oil recovery rate at different temperatures, respectively.

Fig. 5: The black line and blue line represent the sludge reduction rate and oil recovery rate at different heating rates, respectively.

which leads to uneven heating of the sludge, especially for the sludge in contact with the wall of the reaction vessel. The temperature rise of some sludge in the middle of the reactor that increases the temperature by heat transfer will be relatively slow, resulting in a relatively large temperature difference in the sludge system, which cannot completely separate the emulsion to the maximum extent, resulting in a trend of increasing first and then decreasing.

Through this group of experiments, the optimal heating rate of tank bottom sludge and refining sludge during treatment is 3°C. min^{-1}. The oil recovery rate of tank bottom sludge and refining sludge is 79.51% and 84.67%, respectively, and the reduction rate is 79.40% and 80.80%, respectively. The optimum heating rate of oily scum is 4°C. min^{-1}, and the oil recovery and reduction rates are 83.67% and 84.40%, respectively.

Type and an Additional Amount of Demulsifier

It can be seen from Fig. 6 (a) that the best demulsifiers in the reduction process of the three samples are different because different types of sludge have certain differences in properties, and different demulsifiers have different demulsifying capacities for the organic phase, with a certain degree of specificity. The demulsifying performance directly affects the effect of oil-water separation; therefore, it is a key factor in selecting appropriate emulsifiers for this high-emulsified oil cement system. It can be seen from Fig. 6 (b) that the optimum dosage of the three samples in the process of decrement is different. With the dosage increase, the oil recovery and the decrement rates increase first and then decrease. This may be because the demulsifier acts as an emulsion after exceeding a certain amount in the system, decreasing dehydration efficiency.

Through the screening of this group of experiments, the best demulsifier for treating tank bottom mud in the multi-purpose station is 1 # demulsifier. When the dosage is 220 $mg.L^{-1}$, the oil recovery and reduction rates reach 85.11% and 81.00%, respectively. The best demulsifier for refining sludge treatment is a 2 # demulsifier. When the dosage is 200 $mg.L^{-1}$, the oil recovery and reduction rates reach 84.67% and 80.80%, respectively. The best demulsifier for oily scum treatment is a 4 # demulsifier. When the dosage is 200 $mg.L^{-1}$, the oil recovery and reduction rate reach 85.71% and 86.00%, respectively.

Mixing Speed and Mixing Time

It can be seen from Fig. 7 (a) that the reduction treatment effects of the three kinds of sludge show a trend of increasing and then decreasing with the increase of mixing speed. That is because proper mixing intensity can improve the combination of agent and oil sludge, enhance the flocculation of sludge

Fig. 6: (a) Sludge reduction and oil recovery rates at different demulsifiers. (b) Sludge reduction rate and oil recovery rate at different demulsifier dosage.

particles, and accelerate the falling off of surface sand, which is conducive to separating oil sludge water. However, when the mixing speed exceeds a certain value, the emulsification of oily sludge and scum will become more serious, so the oil recovery and reduction rates will decline. It can be seen from Fig. 7 (b) that the reduction treatment effects of the three kinds of sludge show a trend of first increasing and then stabilizing with the extension of mixing time. Because with the extension of the mixing time, the oil sludge and the agent will be mixed more fully, and the temperature of the oil sludge will be more uniform. However, when the mixing time exceeds a certain value, the oil sludge and the agent will be fully mixed, and the oil sludge will be heated uniformly, so the overall treatment effect will not change too much.

Through this group of experiments, when the mixing speed is 200 r.min^{-1} and the mixing time is 30 min, the oil recovery and reduction rate can reach 89.58% and 82.00%, respectively. When the stirring speed is 180 r.min^{-1} and the stirring time is 30min, the oil recovery and reduction rates can

reach 87.96% and 81.20%, respectively. When the stirring speed is 160 r.min^{-1} and the stirring time is 30min, the oil recovery and reduction rate can reach 89.79% and 86.60%, respectively.

Type of Flocculant

It can be seen from Fig. 8 that PAM has the best effect on reducing three kinds of sludge. The oil recovery and tank bottom sludge reduction rates are 90.71% and 82.60%, respectively. The oil recovery and reduction rates of refinery sludge were 90.42% and 81.00%, respectively. The oil recovery and reduction rate of oily scum is 91.84% and 86.80%, respectively. For five agents, the trend of treatment effect is the same when treating three types of sludge, and the order of effect from good to bad is PAM>PAS>PFS>PAC>PFC.

Molecular Weight and Dosage of PAM

It can be seen from Fig. 9 (a) that the influence of PAM molecular weight on the three kinds of sludge during the
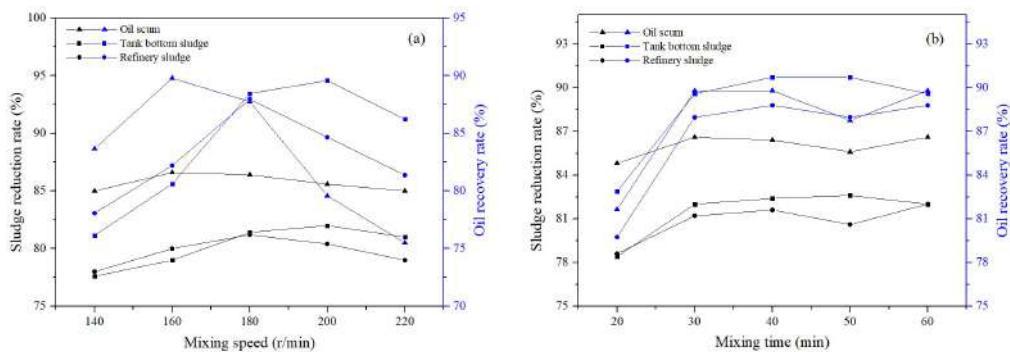
Fig. 7: (a) Sludge reduction and oil recovery rates at different mixing speeds. (b) Sludge reduction rate and oil recovery rate at different mixing times.
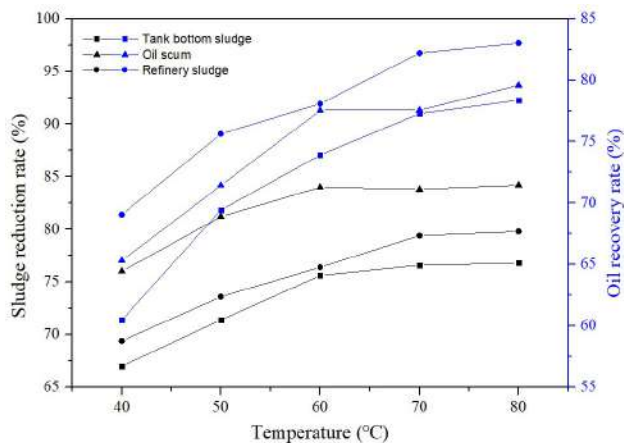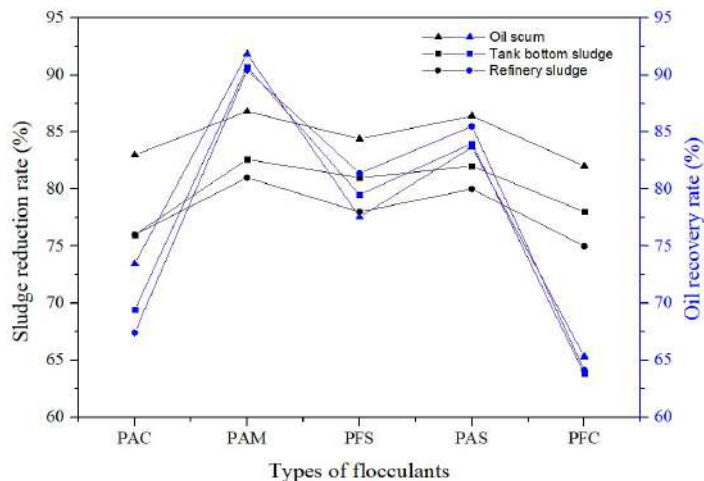

Fig. 8: The black line and blue line represent the sludge reduction rate and oil recovery rate at different types of flocculants, respectively.
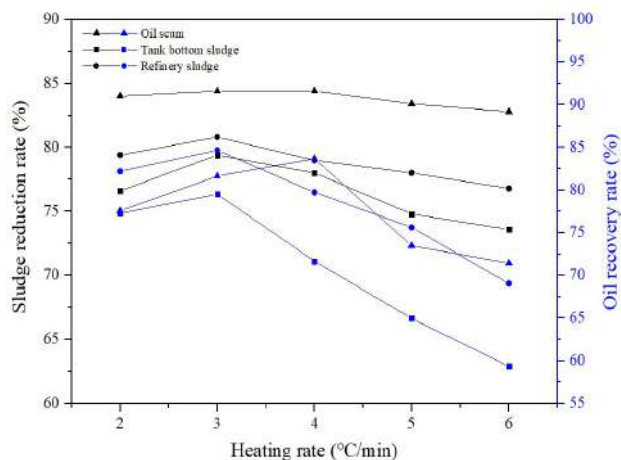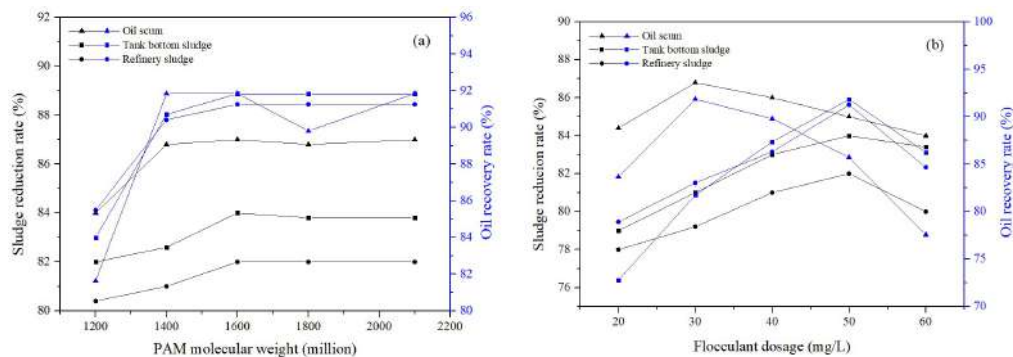
Fig. 9: (a) Sludge reduction and oil recovery rates at different PAM molecular weights. (b) Sludge reduction rate and oil recovery rate at different flocculant dosage.

reduction treatment process is the same. With the gradual increase of molecular weight, the oil recovery rate and the reduction rate show a gradual increase trend because, with the increase of molecular weight, the chain of PAM is longer, the more impurities or suspended solids can be attached, and the larger the flocs are formed, the better the dehydration effect will be. However, when the molecular weight reaches a certain level, the treatment effect will no longer be significantly improved, or even partially decreased, because in the same experimental time, the higher the molecular weight of PAM is, the worse its solubility will be, and the treatment effect will become worse. It can be seen from Fig. 9 (b) that with the gradual increase of flocculant dosage, the oil recovery rate and reduction rate show an upward trend because flocculant is a strong electrolyte with charge, which is added to the sludge to break the imbalance of an original colloid or emulsion, to achieve sludge destabilization. The treatment effect becomes better with the increase of flocculant dosage. It shows that the added flocculation dose is insufficient to make the system's positive and negative charges reach equilibrium. However, when the amount of flocculant continues to increase, and the positive and negative charges in the system reach the equivalent state, the sludge treatment effect is the best at this time. If the amount of flocculant continues to increase, the excess negative charges will repel each other in the sludge, leading to a decline in the treatment effect.

Through this group of experiments, the PAM with a molecular weight of 16 million is better when treating tank bottom sludge and refining sludge. When the dosage is 50 mg.L^{-1}, the oil recovery rate can reach 91.83% and 91.25%, respectively, and the sludge reduction rate can reach 84.00% and 82.00%, respectively. When treating oily scum, the PAM with 14 million molecular weight is better. When the dosage is 30 mg.L^{-1}, the oil recovery and sludge reduction rates reach 91.84% and 86.80%, respectively.

Centrifuge Speed and Centrifuge Time

It can be seen from Fig. 10 (a) that the influence trend of different centrifuge speeds on the three kinds of sludge in the process of reduction treatment is the same. With the increase in centrifuge speed, the oil recovery and reduction rates are also increasing. That is because the higher the speed is, the greater the centrifugal force is, and the easier the solid and liquid phases are separated. However, when the rotating speed of the centrifuge exceeds a certain value, the centrifugal effect will no longer change significantly because the best separation state of the centrifuge has been reached. This experiment's rotating speed has not increased because the best separation state has been reached. However, if the rotating speed increases, the centrifugal force and the mechanical force on the gauze in the centrifuge increase. When the rotating speed exceeds a certain value, the gauze will be damaged, the density of the gauze will become smaller, so some small particles of sludge will flow out with the water phase, resulting in a decline in the effect. It can be seen from Fig.10 (b) that with the increase of centrifuge speed, the oil recovery rate and decrement rate also increase because the longer the centrifugation time is, the longer the solid-liquid phase has enough time to separate, making the separation more thorough. However, when the centrifuge time reaches a certain value, the centrifuge effect will no longer change significantly because the best separation state of the centrifuge has been reached. It can be seen from the comparison between the oil recovery rate and the decrement rate that, with the increase of centrifugation time, the decrement rate is still rising when the oil recovery rate is no longer changing within the same time. Therefore, the optimal centrifugation time under this phenomenon should be the time corresponding to the maximum decrement rate.

Through this group of experiments, when the rotating speed of the centrifuge for treating tank bottom sludge is 2800 r.min^{-1} and the centrifuge time is 15 min, the oil recovery rate and sludge reduction rate can reach 96.30% and
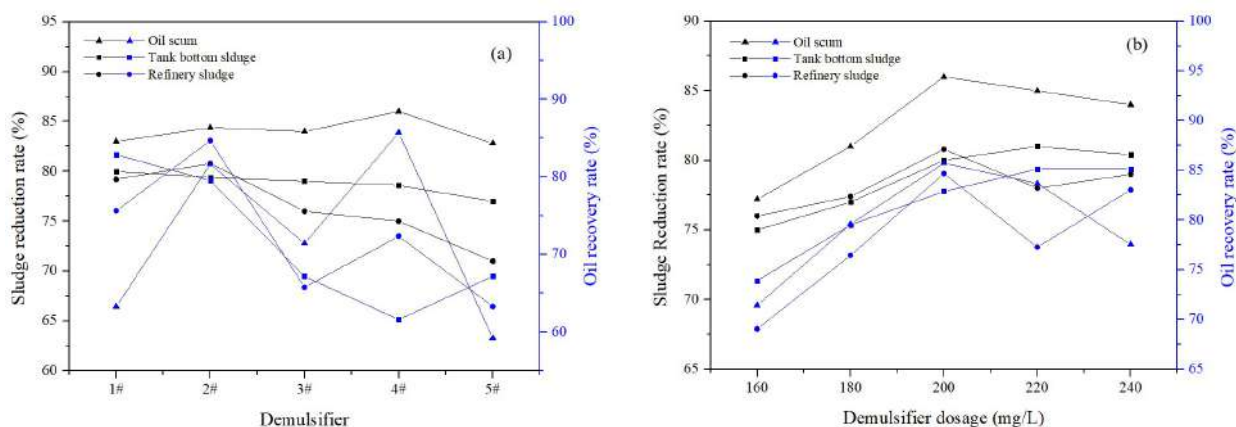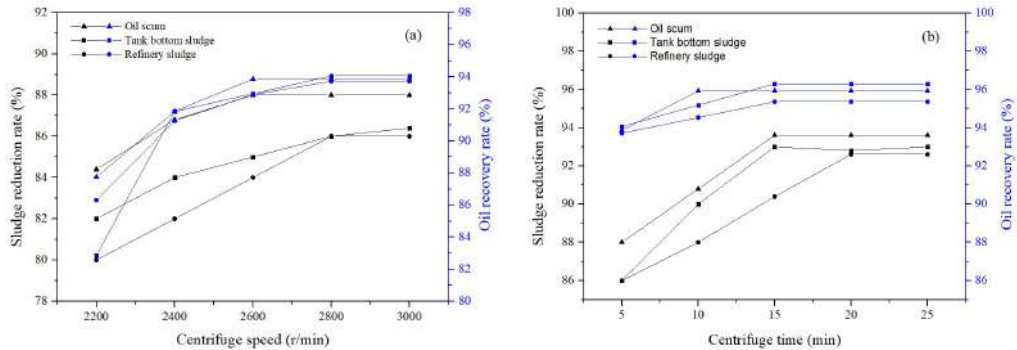
Fig.10: (a) Sludge reduction and oil recovery rates at different centrifuge speeds. (b) Sludge reduction rate and oil recovery rate at different centrifuge time.

93.00%, respectively. When treating refinery sludge, when the rotating speed of the centrifuge is 2800 r.min^{-1} and the centrifuge time is 20 min, the oil recovery rate and sludge reduction rate can reach 95.36% and 92.60%, respectively. When dealing with oily scum, the oil recovery rate and sludge reduction rate can reach 95.92% and 93.60%, respectively, when the rotating speed of the centrifuge is 2600 r.min^{-1} and the centrifugation time is 15 min.

Process Optimization

All the above experimental conditions are summarized,

and the best process for each of the three kinds of sludge is shown in Table 3.

Determine the oil content, water content, and solid content of the residues of the three kinds of sludge after treatment according to the best process, the oil content of the separated water, and the water content of the separated oil. The test results are shown in Table 4.

It can be seen from Table 4 that the determination results of the three kinds of sludge after being treated by the best process show that the oil content of the residue can be reduced to below 5.1%. The water content can be reduced

Table 3: The best process for reducing different types of sludge.

Sludge type	Optimum process conditions
Tank bottom sludge	The pH value of the system is 8.5. Temperature 70°C. The heating rate is 3°C.min^{-1}. Add 220 mg.L^{-1} 1 # demulsifier. Mixing speed 200 r.min^{-1}. The mixing time is 30 min. Before centrifugation, add 50 mg.L^{-1} PAM with a molecular weight of 16 million into the sludge and stir it evenly. Centrifuge at 2800 r.min^{-1} for 15 min in a centrifuge. Under the above experimental conditions, the oil recovery rate and reduction rate of tank bottom sludge in the process of reduction treatment can reach 96.30% and 93.00%, respectively.
Refining sludge	The pH value of the system is 8.5. Temperature 70°C. The heating rate is 3°C.min^{-1}. Add 200 mg.L^{-1} of 2 # demulsifier. Mixing speed 180 r.min^{-1}. The mixing time is 30 min. Before centrifugation, add 50 mg.L^{-1} PAM with a molecular weight of 16 million into the sludge and stir it evenly. Centrifuge in a centrifuge at 2800 r.min^{-1} for 20 min. Under the above experimental conditions, the oil recovery rate and reduction rate of refinery sludge in the process of reduction treatment can reach 95.36% and 92.60%, respectively.
Oily sludge	The pH value of the system is 8.5. Temperature 60°C. The heating rate is 4°C.min^{-1}. Add 200 mg.L^{-1} of 4 # demulsifier. Mixing speed 160 r.min^{-1}. The mixing time is 30 min. Before centrifugation, add 30 mg.L^{-1} PAM with a molecular weight of 14 million into the sludge and stir it evenly. Centrifuge at 2600 r.min^{-1} for 15 min in a centrifuge. Under the above experimental conditions, the oil recovery and reduction rate of oily scum in the process of reduction treatment can reach 95.92% and 93.60%, respectively.

Table 4: Analysis of residue, water, and oil after sludge reduction.

After sludge reduction treatment		Processing results		
		Tank bottom sludge	Refinery sludge	Oil scum
Residue after sludge reduction	Oil content [%]	4.5~5.0	4.3~5.1	3.5~4.5
	Water content [%]	53.2~55.7	52.4~56.5	55.5~59.0
	Solid content [%]	39.3~42.3	38.4~43.3	36.5~41.0
Oil content in water after sludge centrifugation [mg.L^{-1}]		175~190	180~200	150~180
Water content in oil after sludge centrifugation [%]		≤0.2	≤0.2	≤0.15

to below 59.0%, and the treatment effect has exceeded the technical level at home and abroad. The oil content of the separated water is less than 200 mg.L^{-1}, which can be directly sent to the sewage treatment system of the oilfield combined station for advanced treatment. The water content of the separated oil is lower than 0.2%, which is lower than the requirement of 0.5% in the oilfield's crude oil gathering and transportation standard.

Morphological Changes of Oily Sludge and Scum Before and After Treatment

To more intuitively explain the effect of oily sludge reduction, the morphology of oily sludge and scum before and after treatment was analyzed and studied by scanning electron microscope, as shown in Fig. 11.

It can be seen from Fig. 11 that the oily sludge and scum present a certain spatial network structure before treatment, with a certain cross-linking structure. The volume of the oily sludge and scum is swollen and wrapped with oil droplets, which leads to the enhanced stability of the oily sludge and scum, and the oil is wrapped and difficult to remove. After the reduction treatment, the oily sludge and scum have obvious differences in structure, which split into small pieces of blocky material. The spatial network structure is broken, and
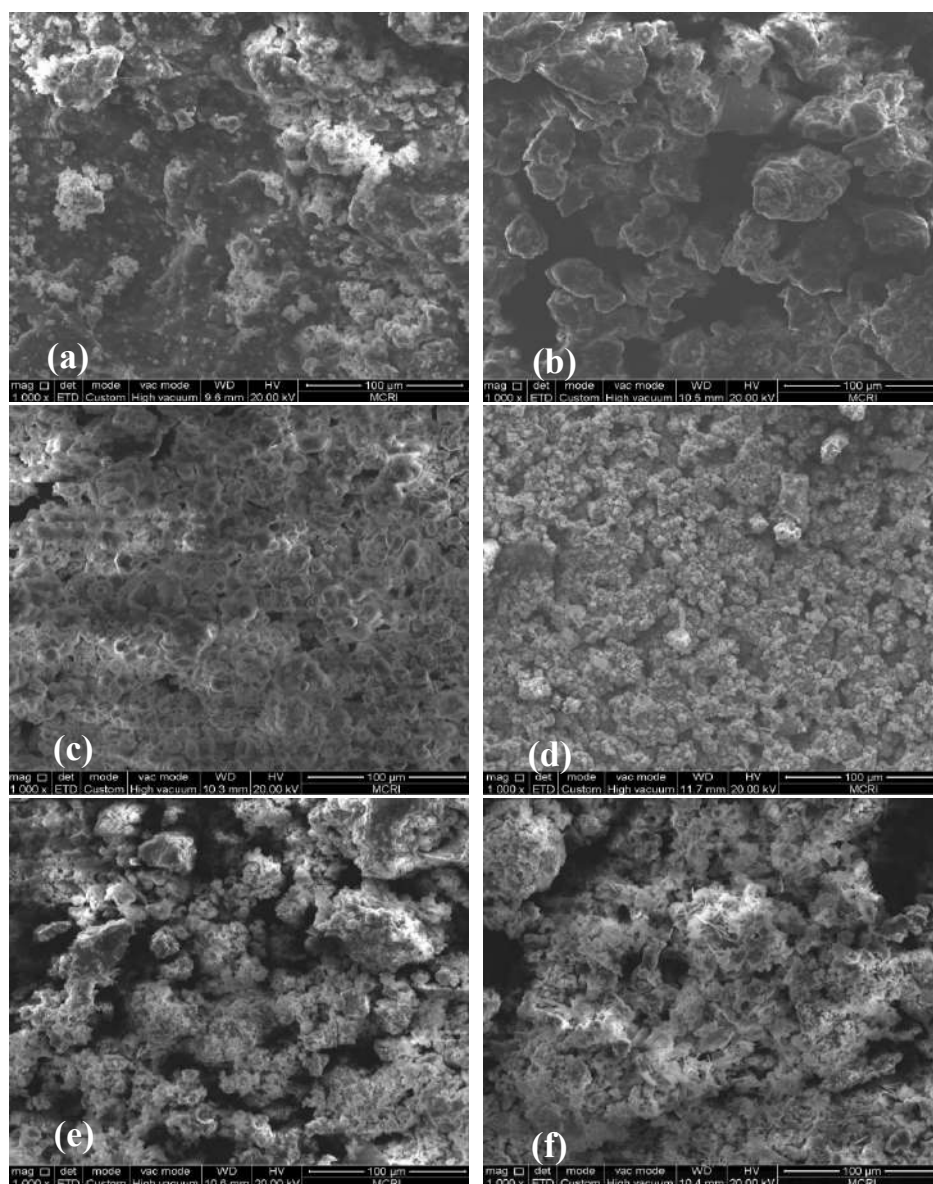
Fig. 11: Morphological comparison of (a,b) tank bottom mud (c,d) refinery sludge (e,f) oily scum before and after treatment.

the oil droplets wrapped in them can be released to remove the oil in the oily sludge and scum.

CONCLUSION

(1) Under the conditions of the best experimental parameters, the oil recovery rate and reduction rate of the tank bottom sludge after the reduction could reach 96.30% and 93.00%, respectively, and the oil recovery rate and reduction rate of the refining sludge after the reduction treatment could reach 95.36% and 92.60% respectively, the oil recovery rate and reduction rate of oily scum after reduction treatment reached 95.92% and 93.60% respectively.

(2) Oil content of the residue can be as low as 5.1% and the water content as low as 59% after three types of sludge are treated under the best process conditions.

(3) Oil content in the water separated from the three types of sludge is less than 200 mg.L^{-1}, which can be directly sent to the sewage treatment system of the oilfield combined station for advanced treatment. The water content in the separated oil is lower than 0.2%, far lower than the requirement of 0.5% in the oilfield's crude oil gathering and transportation standard.

(4) Based on the morphology of sludge, oily sludge, and scum had obvious differences in structure. They split into small pieces of blocky material, the spatial network structure was broken, and the oil droplets wrapped in them could be released so that the oil in the oily sludge and scum could be removed.

ACKNOWLEDGEMENT

REFERENCES

Amudha, V., Kavitha, S., Fernandez, C., Adishkumar, S. and Banu, J.R. 2016. Effect of deflocculation on the efficiency of sludge reduction by the Fenton process. Environ. Sci. Pollut. Res., 23(19): 19281-19291.

Anna, Z., Payryk, O., Barbara, C., Jadwiga, S.Z. and Sylwia, P.P. 2015. Effect of sewage sludge properties on the biochar characteristic. J. Anal. Appl. Pyrol., 112: 201-213.

Bao, Q., Huang, L., Xiu, J., Yi, L., Zhang, Y. and Wu, B. 2022. Study the thermal washing of oily sludge used by rhamnolipid/sophorolipid binary mixed bio-surfactant systems. Ecotoxicol Environ. Saf., 240: 113696.

Barneto, A.G., Moltó, J., Ariza, J. and Conesa, J.A. 2014. Thermogravimetric monitoring of oil refinery sludge. J. Anal. Appl. Pyrol., 105: 8-13.

Chen, G., Cheng, C., Zhang, J., Sun, Y., Hu, Q., Qu, C. and Dong, S. 2019.

Synergistic effect of surfactant and alkali on the treatment of oil sludge. J. Petrol. Sci. Eng., 183: 106420.

Cheng, S., Wang, Y., Fumitake, T., Kouji, T., Li, A. and Kunio, Y. 2017. Effect of steam and oil sludge ash additive on the products of oil sludge pyrolysis. Appl. Energy, 185: 146-157.

Crelier, M. and Dweck, J. 2009. Water content of a Brazilian refinery oil sludge and its influence on pyrolysis enthalpy by thermal analysis. J. Thermal Anal. Calor., 97(2): 551-557.

Duan, M., Wang, X., Fang, S., Zhao, B., Li, C. and Xiong, Y. 2018. Treatment of Daqing oily sludge by the thermochemical cleaning method. Coll. Surf. A Physicochemi. Eng. Aspects, 554: 272-278.

Egazaryants, S.V., Vinokurov, V.A., Vutolkina, A.V., Talanova, M., Yu, F.V.I. and Karakhanov, E.A. 2015. Oil sludge treatment processes. Chem. Technol. Fuels Oils, 51: 506-515.

Gourdet, C., Girault, R., Berthault, S., Richard, M., Tosoni, J. and Pradel, M. 2017. In quest of environmental hotspots of sewage sludge treatment combining anaerobic digestion and mechanical dewatering: A life cycle assessment approach. J. Clean. Prod., 143: 1123-1136.

Hayhurst, A.N. 2013. The kinetics of the pyrolysis or devolatilisation of sewage sludge and other solid fuels. Comb. Flame, 160: 138-144.

Hochberg, S.Y., Tansel, B. and Laha, S. 2022. Materials and energy recovery from oily sludges removed from crude oil storage tanks (tank bottoms): A review of technologies. J. Environ. Manag., 305: 114428.

Hu, G., Li, J. and Zeng, G. 2013. Recent development in the treatment of oily sludge from petroleum industry: A review. J. Hazard. Mater., 261: 470-490.

Inguanzo, M., Dominguez, A., Menendez, J.A., Blanco, C.G. and Pis, J.J. 2012. On the pyrolysis of sewage sludge: the influence of pyrolysis conditions on solid, liquid and gas fractions. Adv. Mater. Res., 89: 3412-3420.

Johnson, O.A. and Affam, A.C. 2018. Petroleum sludge treatment and disposal: A review. Environ. Eng. Res., 24: 191-201.

Liang, J., Zhao, L. and Hou, W. 2017. Solid effect in chemical cleaning treatment of oily sludge. Coll. Surf. A Physicochem. Eng. Aspects, 522: 38-42.

Liu, B., Teng, Y., Song, W. and Wu, H. 2022 Novel conditioner for efficient dewater ability and modification of oily sludge with high water content. Environ. Sci. Pollut. Res., 29: 25417-25424.

Long, X., Zhang, G., Han, L. and Meng, Q. 2013. Dewatering of floated oily sludge by treatment with rhamnolipid. Water Res., 47(13): 4303-4311.

Mahmoud, A., Hoadley, A.F.A., Citeau, M., Sorbet, J.M., Olivier, G., Vaxelaire, J. and Olivier, J. 2018. A comparative study of electro-dewatering process performance for activated and digested wastewater sludge. Water Res., 129: 66-82.

Motlagh, A.H., Klyuev, S., Suendar, A., Ibatova, A.Z. and Maseleno, A. 2019. Steam gasification of oil sludge with calcined olivine. Petrol. Sci. Technol., 37: 19-24.

Mowla, D., Tran, H.N. and Allen, D.G. 2013. A review of the properties of biosludge and its relevance to enhanced dewatering processes. Biomass Bioenergy, 58: 365-378.

Muneeswari, R., Iyappan, S., Swathi, K.V., Vinu, R., Ramani, K. and Sekaran, G. 2022. Biocatalytic lipoprotein bioamphiphile induced treatment of recalcitrant hydrocarbons in petroleum refinery oil sludge through transposon technology. J. Hazard. Mater., 5: 431.

Murungi, P.I. and Sulaimon, A.A. 2022. Petroleum sludge treatment and disposal techniques: A review. Environ. Sci. Pollut. Res., 29: 40358-40372.

Puasa, S.W., Ismail, K.N., Musman, M.Z.A. and Sulong, N.A. 2019. Enhanced oily sludge dewatering using plant-based surfactant technology. Mat. Today Proceed., 19: 1159-1165.

Ramirez, D. and Collins, C.D. 2018. Maximisation of oil recovery from an oil-water separator sludge: Influence of type, concentration, and application ratio of surfactants. Waste Manag., 82: 100-110.

Rocha, O., Dantas, R.F., Duarte, M., Duarte, M. and Silva, V. 2010.

Oil sludge treatment by photocatalysis applying black and white light. Chem. Eng. J., 157: 80-85.

Shperber, E.R., Bokovikova, T.N. and Shperber, D.R. 2011. Sources of formation and methods of utilization of oil sludges. Chem. Technol. Fuels Oils, 47(2): 160-164.

Skinner, S.J., Studer, L.J., Dixon, D.R., Hillis, P., Rees, C.A., Wall, R.C., Cavalida, R.G., Usher, S.P., Stickland, A.D. and Scales, P.J. 2015. Quantification of wastewater sludge dewatering. Water Res., 82: 2-13.

Suganthi, S.H., Murshid, S., Sriram, S. and Ramani, K. 2018. Enhanced biodegradation of hydrocarbons in petroleum tank bottom oil sludge and characterization of biocatalysts and biosurfactants. J. Environ. Manag., 220: 87.

Tahhan, R.A. and Abu-Ateih, R.Y. 2009. Biodegradation of petroleum industry oily-sludge using Jordanian oil refinery contaminated soil. Int. Biodegrad., 63: 1054-1060.

Wang, S., Ma, C., Zhu, Y., Yang, Y., Du, G. and Li, J. 2019. Deep dewatering process of sludge by chemical conditioning and its potential influence on wastewater treatment plants. Environ. Sci. Pollut. Res., 26(33): 33838-33846.

Wu, X., Qin, H., Zheng, Y., Zhang, Y., Chen, W., Zuo, J.Y., Sun, C. and Chen, G. 2019. A novel method for recovering oil from oily sludge via water-enhanced CO_2 extraction. J. CO_2 Utiliz., 33: 513-520.

Zhang, Q., Jiang, Q., Bai, Y., Li, H., Xue, J., Gao, Y. and Cheng, D. 2021. Optimization and mechanism of oily sludge treatment by a novel combined surfactant with an activated-persulfate method. Sci. Tot. Environ., 800: 149525.

Original Research Paper   https://doi.org/10.46488/NEPT.2023.v22i03.005   **Open Access Journal**

Assessment of Noise Pollution and Health Impacts of the Exposed Population in an Urban Area of Chhattisgarh, India

Vishal Kumar*†, Ajay Vikram Ahirwar* and A. D. Prasad*

*Department of Civil Engineering, National Institute of Technology, Raipur, Chhattisgarh, India

†Corresponding author: Vishal Kumar; rprvishal@gmail.com

ABSTRACT

The present study aimed to evaluate the possible impact of noise pollution. This study was conducted in Raipur, the capital of Chhattisgarh state, India, to analyze the relationship between noise pollution and health complaints. A total of 18 locations were selected for monitoring noise pollution levels in the morning (9:00-10:30 AM) and evening (7:00-8:30 PM). Noise maps were prepared for both the time interval, and it was found that the highest equivalent noise level (L_{eq}) of 81.31 dBA was observed at location L3 whereas the lowest L_{eq} of 63.25 dBA was observed at L16 in the morning and in the evening 77.33 dBA at L3 and 60.14 dBA at L16 were observed. A questionnaire survey was performed on the population (n = 400) exposed to noise and analyzed through a variance-based partial least square (PLS) structural equation model (SEM). From the survey, it was found that most of the respondents are exposed to higher noise levels and are facing health issues of "pain in the ear," "rise in blood pressure," "loss of sleep," "whistling and buzzing" in their ear, "headache," "heaviness" and "efficiency problem." A total of 109 hypotheses were proposed and analyzed through bootstrapping with a subsample size of 5000 in SmartPLS software. 18 hypotheses were found to be significant in the proposed model. SEM analysis revealed an interrelation between noise pollution and health effects. It is recommended that strict regulation in nearby sensitive areas must be imposed and an awareness drive on a large scale shall be conducted to enlighten the city's population regarding noise effects as well as various measures for controlling.

INTRODUCTION

One of the invisible pollutants present in our environment is noise. Any disturbing or unwanted sound that affects the wellbeing and health of a human or any other organism is defined as noise pollution. Air and noise pollution are mainly generated by road traffic, which both affect human health (Stansfeld & Clark 2015). For the community noise, the main source is road traffic. It is well known to everyone that, mainly in larger cities, noise pollution is continuously affecting the exposed population (Wu et al. 2019). Major factors contributing to the higher environmental noise levels are increased rail, road, and air traffic, economic growth, and urbanization (de Souza et al. 2019, Ramanathan & Renuka 2008). The increase in noise levels on roads is mainly due to an increase in the number of vehicles, vehicles type and conditions, road quality, the density of vehicles, and weather conditions (Farooqi et al. 2019, Tabraiz et al. 2015, Gilani & Mir 2021, Hunashal & Patil 2011) Apart from this, festivals also contribute to higher noise levels in India. The Diwali festival is one of the major factors contributing to air and noise pollution throughout the country (Garg et al. 2017).

A large number of railway helps improve public transport but cause different harmful effects on the nearby population (Sarikavak & Boxall 2019). Noise from locomotives during idling or operation, bunching, and stretching wagons during braking or acceleration, and noise from the flanging of wheels on the curve is typical noise generated from the railways (Jiang et al. 2015). Electrified rail line causes less air pollution, but at the other end reduction in noise pollution is not observed. Noise from the tire can dominate other sources at 70km.h^{-1} speed of vehicles. Hence noise on the road can be mitigated by limiting the speed in streets in densely populated areas. If the road gradient is reduced by 5%, then 1.5dB of noise can also be reduced by plantations of trees can help in mitigating higher levels of noise. Similarly, reducing 10dB of noise construction of barriers along the road is recommended (Farooqi et al. 2019).

People with higher noise levels in surroundings significantly have higher noise annoyance and stress levels. Continuous exposure to higher noise levels causes permanent or temporary hearing loss. It can induce physiological effects (anxiety, depression), which can be permanent or temporary

(de Souza et al. 2019, Al-Mutairi et al. 2011, Juang et al. 2010, Chakraborty & Banerjee 2007). It can also cause high blood pressure, irregular heartbeat, sleep disturbance, and lack of concentration and efficiency (Farooqi et al. 2020, Terry et al. 2021, Hahad et al. 2021). In the middle-aged group, self-reported hypertension and higher noise levels from road traffic are interconnected (Bodin et al. 2009). Noise also affects adversely to children by causing premature birth and low birth weight (Stansfeld &Clark 2015). According to the World Bank Population Report of 2019, India is the second largest country in terms of population worldwide (World Bank 2019). As per the Department of Economic Division (2019) United Nations, India will overtake China by 2027 in terms of population (UN 2019). As of 31st March 2019, India also has 296 million registered vehicles, and an annual growth rate of 9.9 percent during the last ten years (2009 to 2019) was recorded (MORTH 2019). In Raipur, the total number of registered vehicles is 1.5 million, among which 1.4 million are non-transport vehicles and 0.13 million

are transport vehicles as of 31st March 2019. The number of registered vehicles in the city has increased by a very large number. The total number of vehicles registered in Raipur City from 2010 to 2019 is shown in Fig. 1, and the percentage of different classes of vehicles as of 31st March 2019 is shown in Fig. 2.

People living near noisy streets and residential areas near highways and railways are most vulnerable to noise pollution. The exposed people mostly face difficulty in sleeping and get awakened at night, as a result of which they feel tired and have work efficiency problems mostly. Also, these populations have short and long-term effects due to higher noise levels (Ristovska & Lekaviciute 2013, Gholami et al. 2012). This study was designed to determine the impacts of noise pollution on the selected target population. Raipur City, the capital of Chhattisgarh state of India, is selected as the study site in the current investigation. To find the relationship between the demographic, physiological, and psychological factors of the exposed population in the study variance-
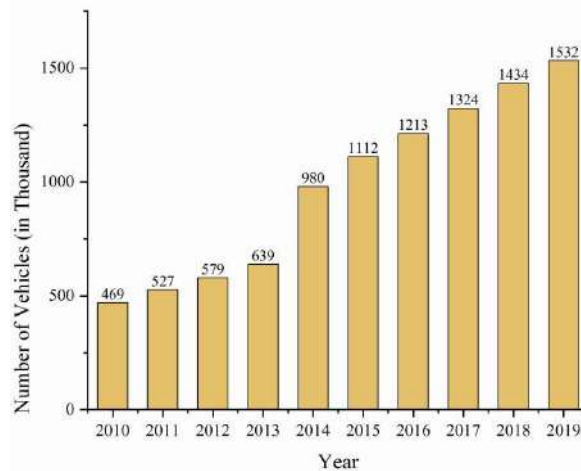
Fig. 1: Total number of registered vehicles.
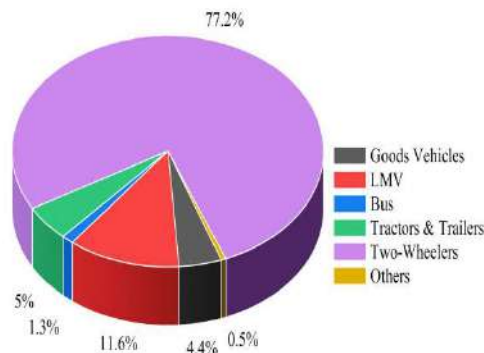
Fig. 2: Different classes of vehicles in Raipur.

based structural equation model (SEM) method is used. This work using SEM is conducted for the first time in the selected study area, which makes it new and different. The previous study by Fhyri and Aasvang (2010) incorporated SEM to find the relationship between traffic noise and heart problems. Also, SEM was used by Fyhri and Klaeboe (2009) to explore the relation between noise from traffic, self-reported health issues, annoyance, and sensitivity. Their study suggested a strong relationship exists between sensitivity to noise and health complaints. Variance-based Partial Least Square (PLS) SEM is mostly preferred over covariance-based (CB-SEM) by most researchers because of its different advantages (Ooi et al. 2018). PLS-SEM performance on a different scale is good, and like other multivariate analysis techniques, it thoroughly evaluates the results, makings it reliable in studying hypothetical theory (Hair et al. 2011. 2012).

MATERIALS AND METHODS

Description of the Study Area

The acoustic study was conducted in Raipur City of Chhattisgarh, India (1st August to 15th September 2022). The City is situated in the East Central part of the state at the latitude of 21°16'N, longitude 81°36'E with an altitude of 289.5m above mean sea level. Raipur is the capital of Chhattisgarh, with the highest population density among other state cities. As per the census 2011 of India, the total population in Raipur is 1,010,433, of which 518,611 are male, and 491,822 are female, respectively. The density of the city is 328 people per km^2. The city's climate is sub-humid, with an annual average rainfall of 1489mm, of which 1348mm is received during the monsoon season. Historically it has been found that wind speed in September was 6.8mph. Raipur is well connected to other cities of the state, and it has a wide road network. The city's road network and sampling locations are shown in Fig. 3.

Study Design

This study measured equivalent noise levels (L$_{eq}$) at major city squares and a questionnaire survey. Random sampling was used for the survey work. The sample size was determined using the formula 4pq.L^{-2}(Sahu et al. 2020). "p" was taken as 50% with a permissible error of 5%. A 95% confidence limit sample size was determined as 396, rounded to 400. Measurement of L$_{eq}$ was done both in the morning and evening. Noise maps were prepared using the inverse distance weighting (IDW) interpolation method in ArcGIS software. A survey was carried out on the determined sample size, and data were analyzed using PLS-SEM. The detailed methodology of the study is shown in Fig. 4.
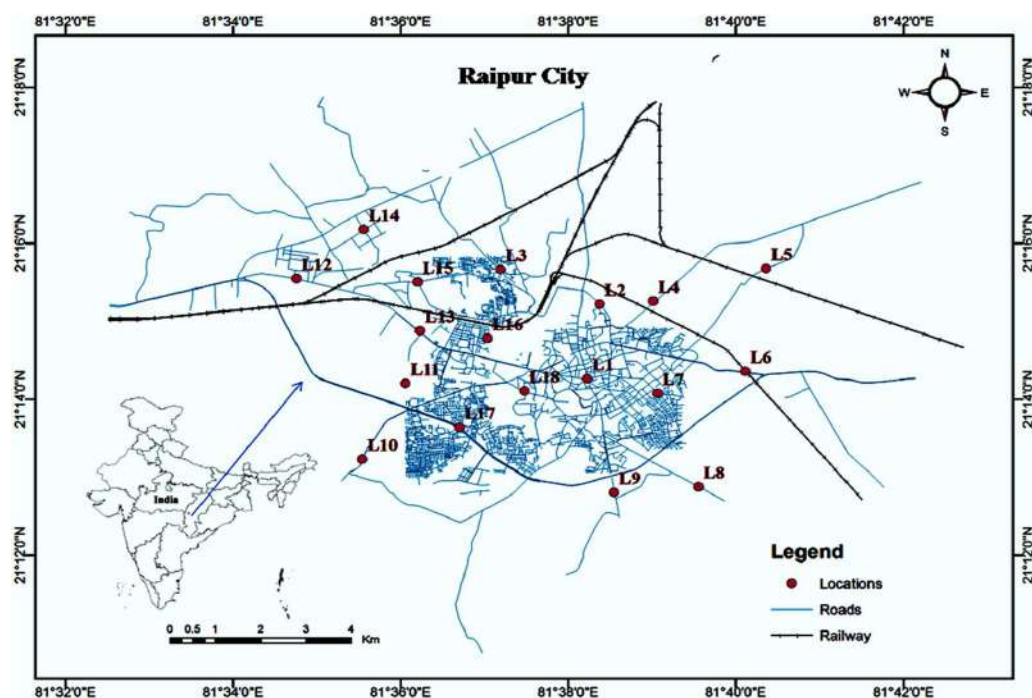
Fig. 3: Study area map.
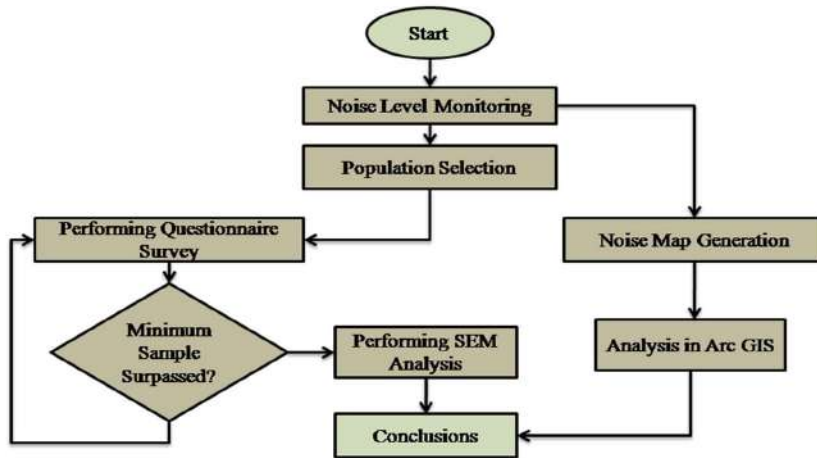
Fig. 4: Methodology of the study.

Noise Measurement and Mapping

Noise levels were observed at 18 locations in the study area using Extech (Model: SL-400) sound level meter (SLM) during the morning (9:00-10:30 AM) and evening (7:00-8:30 PM). The instrument was mounted on a tripod and elevated to 1.5 m above the ground level. ISO 1996-1:2016 standard method was used for measuring noise at different locations (ISO 1996-1 2016). SLM was placed on the side of the road 2m from reflecting objects. L_{eq} was recorded at each location, and an average value was obtained using statistical analysis. The latitude and longitude of each location were recorded and inserted in ArcGIS software to prepare the map. The average L_{eq} of each location was used to perform IDW interpolation in GIS, and noise maps were prepared for each morning and evening, respectively.

Table 1: Framed question for the survey

Noise Exposure Questionnaire	
You are: __Male __ Female Your Age: ___ Occupation:_____	
Q1	Do you feel that there is noise in your area of work and home that is disturbing you?
Q2	Do you feel that this noise is affecting you?
Q3	Can you say that the high level of noise affects your health?
Q4	How often are you exposed to high noise in your daily routine?
Q5	Due to noise, do you feel pain in your ears after/while listening to music?
Q6	Is there whistling and buzzing in your ears when exposed to higher noise levels?
Q7	Due to noise, do you feel Interference with speech?
Q8	Due to noise, do you feel Annoyance?
Q9	Due to noise, do you feel that you have Efficiency Problems?
Q10	Due to noise, do you feel Loss of sleep/insomnia?
Q11	Due to noise, do you feel Visual Disturbances?
Q12	Due to the noise, do you feel Giddiness?
Q13	Due to noise, do you feel Raise in Blood Pressure?
Q14	Due to noise, do you feel Headache and heaviness?
Q15	Due to noise, do you feel an Increased heart rate and breathing?
Q16	Due to noise, do you feel an Increase in sweating?
Q17	Do your friends say that you are a habitual debater?
6 Point Scale used: 1 - Rarely 2 - Sometimes 3 - Often 4 - Usually 5 - Never 6 - Always	

Table 2: Proposed hypothesis for the study

Hypothesis	There is relation between	Hypothesis	There is relation between
HP1	Age and gender	HP55	Q1 and Q3
HP2	Age and occupation	HP56	Q1 and Q4
HP3	Age and Q1	HP57	Q1 and Q5
HP4	Age and Q2	HP58	Q1 and Q6
HP5	Age and Q3	HP59	Q1 and Q7
HP6	Age and Q4	HP60	Q1 and Q8
HP7	Age and Q5	HP61	Q1 and Q9
HP8	Age and Q6	HP62	Q1 and Q10
HP9	Age and Q7	HP63	Q1 and Q11
HP10	Age and Q8	HP64	Q1 and Q12
HP11	Age and Q9	HP65	Q1 and Q13
HP12	Age and Q10	HP66	Q1 and Q14
HP13	Age and Q11	HP67	Q1 and Q15
HP14	Age and Q12	HP68	Q1 and Q16
HP15	Age and Q13	HP69	Q1 and Q17
HP16	Age and Q14	HP70	Q2 and Q5
HP17	Age and Q15	HP71	Q2 and Q6
HP18	Age and Q16	HP72	Q2 and Q7
HP19	Age and Q17	HP73	Q2 and Q8
HP20	Gender and occupation	HP74	Q2 and Q9
HP21	Gender and Q1	HP75	Q2 and Q10
HP22	Gender and Q2	HP76	Q2 and Q11
HP23	Gender and Q3	HP77	Q2 and Q12
HP24	Gender and Q4	HP78	Q2 and Q13
HP25	Gender and Q5	HP79	Q2 and Q14
HP26	Gender and Q6	HP80	Q2 and Q15
HP27	Gender and Q7	HP81	Q2 and Q16
HP28	Gender and Q8	HP82	Q2 and Q17
HP29	Gender and Q9	HP83	Q3 and Q5
HP30	Gender and Q10	HP84	Q3 and Q6
HP31	Gender and Q11	HP85	Q3 and Q7
HP32	Gender and Q12	HP86	Q3 and Q8
HP33	Gender and Q13	HP87	Q3 and Q9
HP34	Gender and Q14	HP88	Q3 and Q10
HP35	Gender and Q15	HP89	Q3 and Q11
HP36	Gender and Q16	HP90	Q3 and Q12
HP37	Gender and Q17	HP91	Q3 and Q13
HP38	Occupation and Q1	HP92	Q3 and Q14
HP39	Occupation and Q2	HP93	Q3 and Q15
HP40	Occupation and Q3	HP94	Q3 and Q16
HP41	Occupation and Q4	HP95	Q3 and Q17
HP42	Occupation and Q5	HP96	Q4 and Q3
HP43	Occupation and Q6	HP97	Q4 and Q5
HP44	Occupation and Q7	HP98	Q4 and Q6
HP45	Occupation and Q8	HP99	Q4 and Q7
HP46	Occupation and Q9	HP100	Q4 and Q8
HP47	Occupation and Q10	HP101	Q4 and Q9
HP48	Occupation and Q11	HP102	Q4 and Q10
HP49	Occupation and Q12	HP103	Q4 and Q11
HP50	Occupation and Q13	HP104	Q4 and Q12
HP51	Occupation and Q14	HP105	Q4 and Q13
HP52	Occupation and Q15	HP106	Q4 and Q14
HP53	Occupation and Q16	HP107	Q4 and Q15
HP54	Occupation and Q17	HP108	Q4 and Q16
		HP109	Q4 and Q17

Questionnaire Survey

Questionnaire surveys were conducted on the population (n = 400) exposed to high noise levels. The questionnaire was divided into different sections containing demographic information of the respondents, such as their age, gender, occupation, and duration of the exposed high noise levels. 6 point scale was used to get the response from the exposed population. "Rarely = 1", "Sometimes = 2", "Often = 3","Usually = 4","Never = 5," and "Always = 6" were the anchors to the questionnaire. Respondents were asked to fill out the survey form based on their thinking over the last 12 months regarding noise pollution. Questions (Q1- Q17) to assess problems like sleeping, headache, pain in the ear, blood pressure, visualization, sweating, etc., were asked from the respondents. Based on the response received, statistical analysis was carried out to find the impact of noise on the exposed population of the study area. The questions that the respondents were asked are shown in Table 1.

PLS-SEM Hypothesis Development

To investigate the relationship between noise pollution and its effect on the following human hypothesis (HP) was proposed which is shown in Table 2.

Analysis of Data Through PLS-SEM

SEM path analysis is used in this study using Smart-PLS 3.0 software. SEM is expressed as a path model that estimates direct and indirect effects. SEM and path models are more advantageous and powerful than multiple regression models (Davvetas et al. 2020). A total of 109 hypotheses have been developed and examined. The hypothesis has been made by connecting demographical, physiological, and psychological factors. Bootstrap of the developed model was done, and results were obtained by taking 5000 subsamples. The developed model is shown in Fig. 5.

RESULTS AND DISCUSSION

Noise Pollution Monitoring and Mapping

This study included 18 locations for monitoring noise pollution in the morning and evening. Fig. 6 & 7 depict the noise map of the study area, respectively. Table 3 depicts the locations' detail and the observed average L_{eq} for both intervals. A better understanding can be developed by noise map compared to tabular form. The above-mentioned figure reveals that all the locations have a higher level of noise in the environment. A road network with high traffic volume
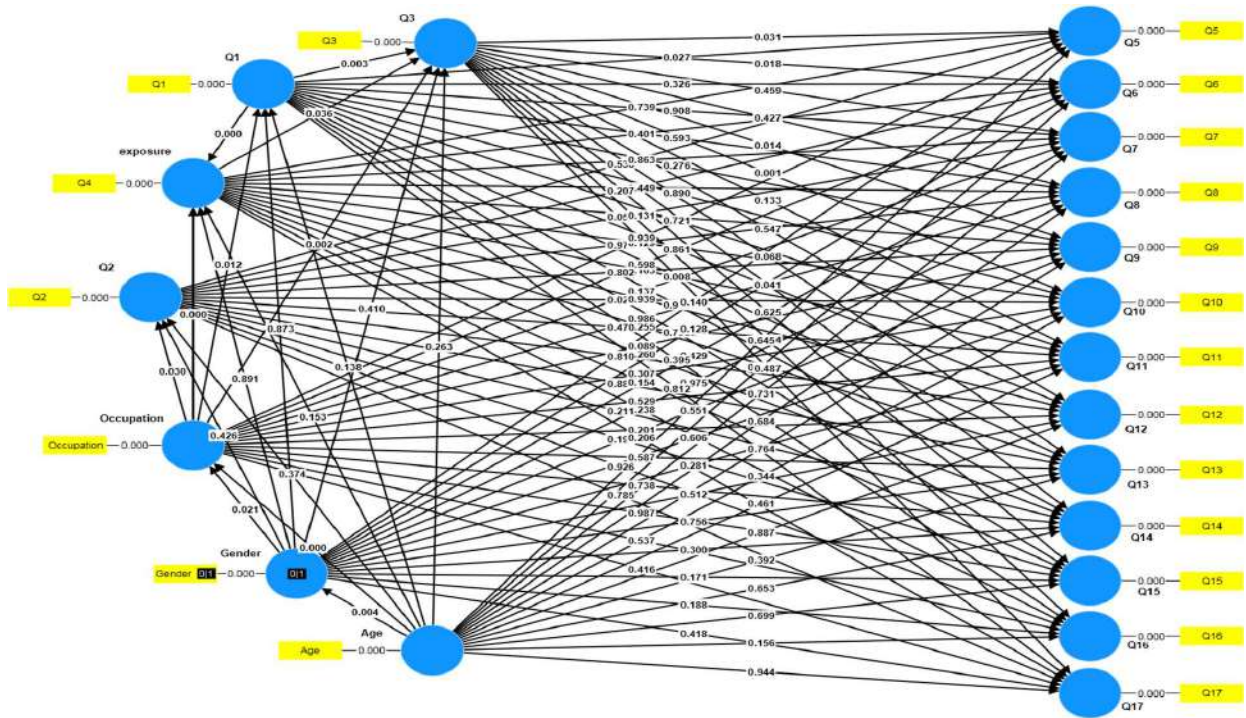
Fig. 5: Developed SEM model in Smart-PLS 3.0.

surrounds all the locations. The Highest L_{eq} of 81.31 dBA was observed at location L3, whereas the lowest L_{eq} of 63.25 dBA was observed at L16 in the morning.

Consequently,77.33 dBA at L3 and 60.14 dBA at L16 were observed in the evening. All the locations breached the ambient standard noise level prescribed by the Central Pollution Control Board (CPCB), New Delhi. While studying, it was found that in the morning, 0% of the locations had noise levels less than 50 dBA, 44.46% fell between 60 to 70 dBA, 33.34% between 70 to 75 dBA, and 22.23% above 75 dBA.

Similarly, in the evening, 0 % below 50dBA, 27.78% between 60 to 70 dBA, 38.8% between 70 to 75 dBA, and 33.34% above 75 dBA, respectively. The noise levels' results are close to those obtained in Delhi City by Mishra et al. (2021). In his study, the morning noise levels varied between 68.5 to 80.4 dBA, whereas evening varied between 71.9 to 83.7 dBA. Pathak et al. (2008) studied Varanasi city of India and found a maximum noise level of 75.3 dBA in their study location. Similar to other studies in India, our results reveal that Raipur is also facing the problem of noise pollution, and exposed people are affected by it.

Questionnaire Analysis

This study included 400 respondents in the questionnaire survey. 73.84% of the respondents were male, whereas 26.16% were female. The average age of the respondents is 30.7 ± 10.69 years. The response analysis was carried out in two phases, one for overall response and the other for a response based on age group. Fig.8 depicts the overall response, whereas Fig. 9 depicts the response in the age group. The questionnaire revealed that respondents suffer from disturbing noise in their workplace or residence. 31.28% of respondents considered "sometimes" they are exposed to a high level of noise, followed by 24.10% "usually," 20.14% "often," 13.34% "always," 9.74% "rarely," and 1.53% "never." Respondents also considered high noise affected their health and caused different physiological and psychological effects. 32.30% of considered pain in the ear "sometimes," followed by 21.53% "never" and 18.97% "often." Consequently, 22.05% reported whistling and buzzing, and 28.71% had interference with the speech in the ear "often." As per the survey report, 34.35%, 28.71%, and 33.34% of the respondents "sometimes" suffer from annoyance, efficiency problems, and sleep loss, respectively. However, 60.51%, 51.79%, and 40.10% "never" suffered from visual disturbance, giddiness, and a rise in blood pressure due to higher noise levels but 12.30%, 19.48%, and 28.20% "sometimes" suffered. 21.5% "often" felt headaches and heaviness due to noise, while 25.12% agreed that their friends say they are habitual debaters. A similar study by Swain & Goswami (2013) in Baripada, India found that due to noise, 41 % of respondents were annoyed, 11% had a loss
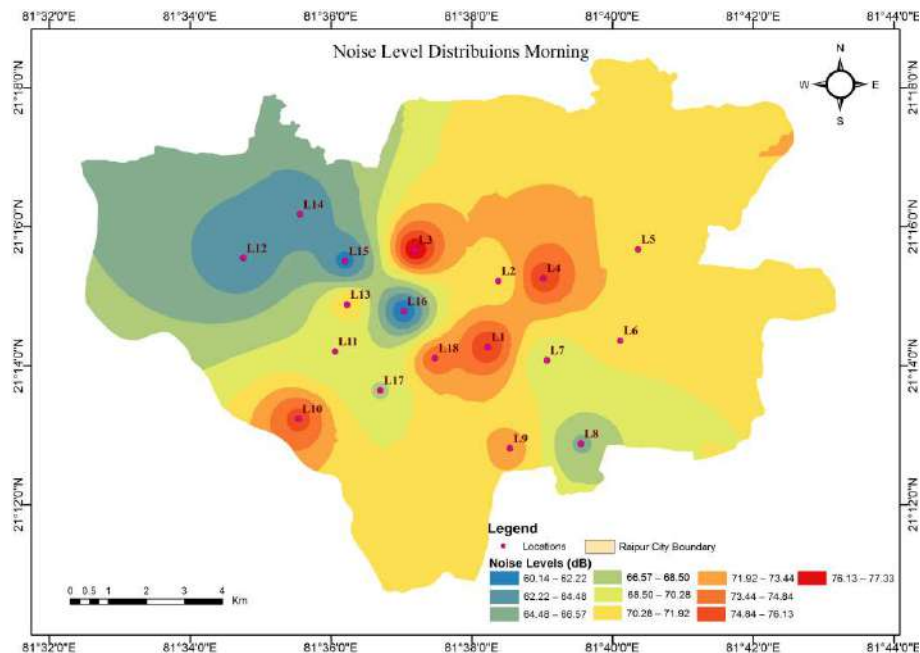
Fig. 6: Noise map of morning noise levels.
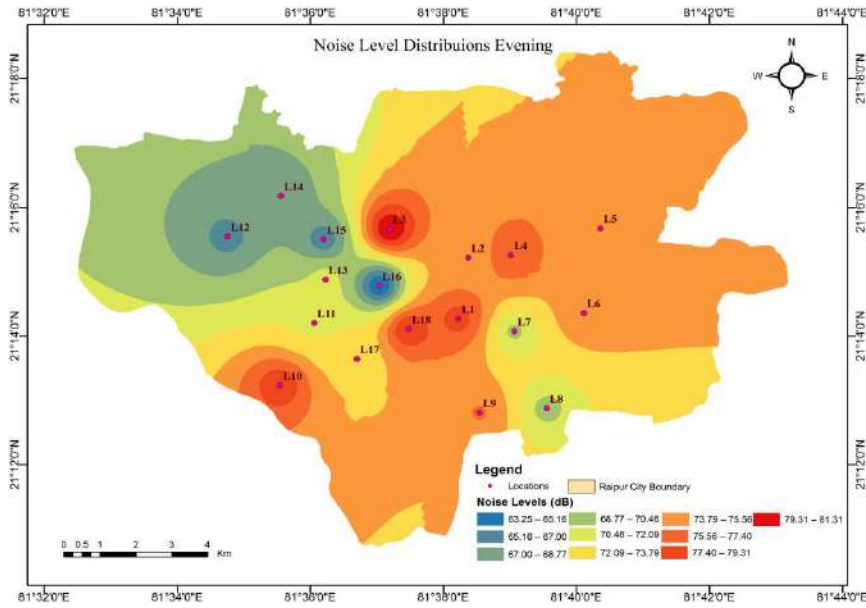
Fig. 7: Noise map of evening noise levels.

Table 3: Observed noise levels during the study

Location	Symbol	Latitude	Longitude	L_{eq} Morning	L_{eq} Evening
City Kotwali	L1	21.23781	81.63712	78.31	76.25
Mekahara	L2	21.25363	81.63961	73.75	70.54
Gudhyari	L3	21.26107	81.6199	81.31	77.33
Pandri	L4	21.25434	81.65025	77.18	75.86
Sankar Nagar	L5	21.26125	81.6727	74.19	71.15
Avanti Vihar	L6	21.23934	81.66855	74.93	70.37
Tagor Nagar	L7	21.23458	81.65112	70.11	68.42
Lalpur	L8	21.21461	81.65923	69.96	66.28
Santoshi Nagar	L9	21.21347	81.64244	75.68	72.53
Raipura	L10	21.22057	81.59239	78.73	75.39
Goal Chowk	L11	21.23674	81.60099	71.95	68.61
AIIMS Raipur	L12	21.25916	81.57929	66.45	62.25
NIT Gate	L13	21.24794	81.60383	70.99	72.24
Kabir Nagar	L14	21.26965	81.59269	67.38	62.83
Kota	L15	21.2584	81.6034	65.95	61.38
Samta Colony	L16	21.24637	81.61728	63.25	60.14
Kushalpur Chowk	L17	21.22737	81.61174	72.25	68.29
Purani Basti	L18	21.23513	81.62466	79.35	74.57

of sleep, and 34 % identified headache as a major problem. A similar response was found in a study by Pathak et al. (2008) and Murthy et al. (2007).

The survey result is analyzed based on age group. It is found that 53.84 % of the respondents below 20 years accept that "sometimes" noise pollution is present in their environment, and 76.92 % feel that noise is affecting their health. Problem-related sleep loss ranges from 30-37 % in the age groups<20, 21-30, and 31-40. This might be because this age group mostly moves around for work, study, and other activities and gets exposed to a higher level of noise. Visual disturbance and sweating have been reported very less

by this age group. The rise in blood pressure due to noise in the age group 41-50 is 47.36% "sometimes." All the other

effects of noise in the age group are shown graphically. The response of the respondents is shown in Table 4.
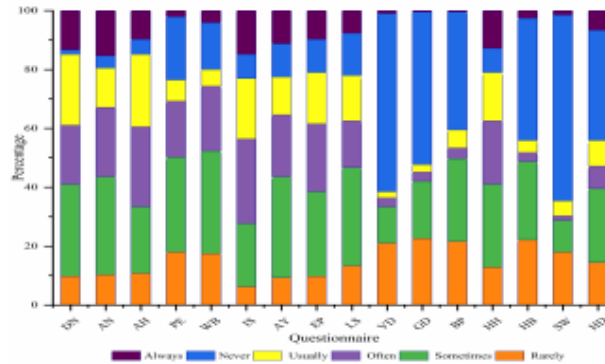
Fig. 8: Self-reported health complaints by the overall exposed population (in Percentage).
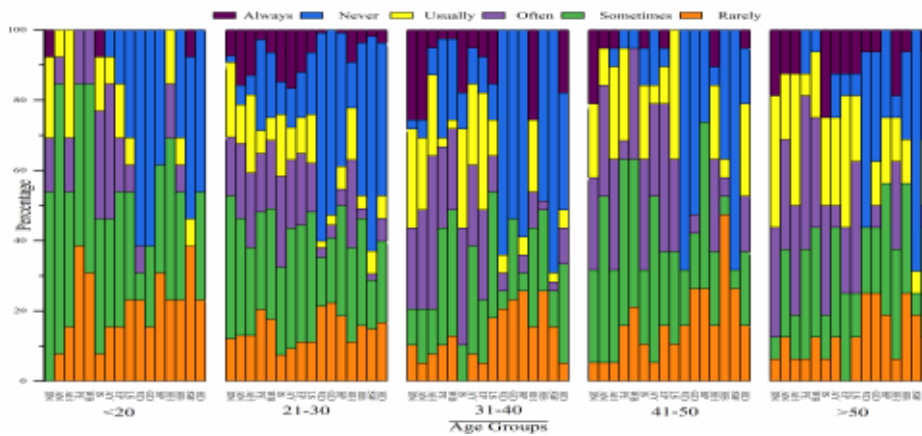
Fig. 9: Self-reported health complaint by age group population (in Percentage).

Table 4: Response of the participated population (in Percentage)

	Symbol	Rarely	Sometimes	Often	Usually	Never	Always
Disturbing Noise	DN	9.74	31.28	20.14	24.10	1.53	13.34
Affecting Noise	AN	10.25	33.34	25.58	13.34	4.10	15.38
Affecting Health	AH	10.76	22.56	27.17	24.61	5.12	9.74
Pain in Ear	PE	17.94	32.30	18.97	7.17	21.53	2.65
Whistling and buzzing	WB	17.43	34.87	22.05	5.64	15.89	4.10
Interference with speech	IS	6.15	21.53	28.71	20.51	8.20	14.87
Annoyance	AY	9.23	34.35	21.02	12.82	11.28	11.28
Efficiency Problems	EP	9.74	28.71	23.07	17.43	11.28	9.74
Loss of sleep	LS	13.34	33.34	15.89	15.38	14.35	7.69
Visual Disturbances	VD	21.02	12.30	3.07	2.05	60.51	1.02
Giddiness	GD	22.56	19.48	3.07	2.56	51.79	0.51
Rise in Blood Pressure	BP	21.53	28.20	3.5	6.15	40.10	0.51
Headache and heaviness	HH	12.82	28.20	21.5	16.41	8.20	12.82
Increase in heart rate and breathing	HB	22.05	26.66	3.07	4.10	41.53	2.56
Sweating	SW	17.94	10.76	1.5	5.12	63.07	1.53
Habitual debater	HD	14.35	25.12	7.69	8.71	37.43	6.67

Table 5: Correlation between responses to the survey.

	Age	Gender	Occupation	Q1	Q2	Q3	Q4	Q5	Q6	Q7	Q8	Q9	Q10	Q11	Q12	Q13	Q14	Q15	Q16	Q17
Age	1.000	-0.170	-0.218	-0.074	-0.083	0.065	-0.118	0.128	0.123	0.022	0.013	0.026	0.057	0.070	0.080	-0.010	0.053	-0.082	-0.081	0.054
Gender	-0.170	1.000	**0.494**	0.210	0.033	0.052	**0.318**	-0.026	-0.046	0.035	-0.042	0.078	0.002	0.019	-0.074	-0.046	0.089	-0.056	0.067	-0.008
Occupation	-0.218	**0.494**	1.000	0.263	0.165	-0.088	**0.456**	-0.081	-0.042	0.128	-0.041	0.100	-0.110	0.000	-0.140	-0.002	0.084	-0.045	-0.049	0.020
Q1	-0.074	0.210	0.263	1.000	**0.427**	**0.236**	0.343	-0.129	-0.018	0.121	0.036	0.153	0.068	-0.109	-0.019	-0.147	0.135	-0.017	-0.068	-0.044
Q2	-0.083	0.033	0.165	0.427	1.000	**0.312**	**0.273**	0.012	0.118	**0.214**	0.021	0.114	0.199	-0.142	-0.022	-0.005	0.184	0.077	-0.032	-0.025
Q3	0.065	0.052	-0.088	**0.236**	**0.312**	1.000	0.154	0.147	0.204	0.110	0.067	**0.206**	**0.280**	-0.164	0.059	0.093	**0.214**	0.035	0.067	-0.072
Q4	-0.118	**0.318**	**0.456**	**0.343**	**0.273**	0.154	1.000	-0.055	-0.039	0.093	-0.051	0.009	-0.058	-0.147	-0.052	0.050	0.169	-0.097	-0.083	-0.090
Q5	0.128	-0.026	-0.081	-0.129	0.012	0.147	-0.055	1.000	**0.412**	0.212	0.139	0.103	0.168	0.098	0.228	**0.389**	0.122	**0.237**	0.143	0.184
Q6	0.123	-0.046	-0.042	-0.018	0.118	0.204	-0.039	**0.412**	1.000	**0.218**	0.185	0.108	0.087	0.050	**0.240**	**0.264**	0.153	0.198	0.148	0.185
Q7	0.022	0.035	0.128	0.121	**0.214**	0.110	0.093	0.212	**0.218**	1.000	**0.254**	0.178	**0.361**	0.129	0.129	0.063	0.147	0.156	0.062	0.172
Q8	0.013	-0.042	-0.041	0.036	0.021	0.067	-0.051	0.139	0.185	**0.254**	1.000	**0.221**	0.143	0.033	0.018	0.012	0.117	0.104	0.009	0.055
Q9	0.026	0.078	0.100	0.153	0.114	**0.206**	0.009	0.103	0.108	0.178	**0.221**	1.000	**0.202**	0.095	-0.015	0.136	0.185	-0.058	-0.016	0.117
Q10	0.057	0.002	-0.110	0.068	0.199	**0.280**	-0.058	0.168	0.087	**0.361**	0.143	**0.202**	1.000	0.055	0.083	0.072	**0.246**	0.096	0.077	0.098
Q11	0.070	0.019	0.000	-0.109	-0.142	-0.164	-0.147	0.098	0.050	0.129	0.033	0.095	0.055	1.000	**0.259**	**0.247**	-0.049	0.096	0.102	**0.220**
Q12	0.080	-0.074	-0.140	-0.019	-0.022	0.059	-0.052	0.228	**0.240**	0.129	0.018	-0.015	0.083	**0.259**	1.000	**0.262**	0.040	**0.300**	**0.292**	**0.290**
Q13	-0.010	-0.046	-0.002	-0.147	-0.005	0.093	0.050	**0.389**	**0.264**	0.063	0.012	0.136	0.072	**0.247**	**0.262**	1.000	0.042	**0.306**	0.167	0.145
Q14	0.053	0.089	0.084	0.135	0.184	**0.214**	0.169	0.122	0.153	0.147	0.117	0.185	**0.246**	-0.049	0.040	0.042	1.000	0.059	-0.013	0.167
Q15	-0.082	-0.056	-0.045	-0.017	0.077	0.035	-0.097	**0.237**	0.198	0.156	0.104	-0.058	0.096	0.300	**0.300**	**0.306**	0.059	1.000	0.180	0.253
Q16	-0.081	0.067	-0.049	-0.068	-0.032	0.067	-0.083	0.143	0.148	0.062	0.009	-0.016	0.077	0.102	**0.292**	0.167	-0.013	0.180	1.000	0.021
Q17	0.054	-0.008	0.020	-0.044	-0.025	-0.072	-0.090	0.184	0.185	0.172	0.055	0.117	0.098	**0.220**	**0.290**	0.145	0.167	**0.253**	0.021	1.000

Furthermore, Pearson correlation was measured between the responses received to study their strength of association. Table 5 depicts the correlation result among the survey responses. 12 coefficients were found in a range of 0.30 to 0.49, which states that moderate relation is found between them. Consequently,6 coefficient values were found nearly to 0.5, revealing a strong correlation.

Response Analysis Through PLS-SEM

Based on the result of the questionnaire SEM model was prepared to find the path coefficient and study the relation between the different effects of the noise on the exposed population. The prepared model using Smart PLS software is shown in **Fig. 5**. After bootstrapping, the result shows that

18 hypotheses are supported. The t statistics value greater than 1.96 is taken as supporting, whereas less than that value is rejected. The result of the SEM analysis is shown in Table 6**.** The HP1, HP2, HP20, HP38, HP39, HP40, HP41, HP55, HP56, HP57, HP65, HP75, HP83, HP84, HP87, HP88, HP92 and HP96 are found to be significant. From the significant hypothesis, respondents who agreed that noise pollution in their area are facing health issues like pain in the ear, rise in blood pressure, loss of sleep, whistling and buzzing in their ear, headache, heaviness, and efficiency problem. Also, an association between exposure time and noise affecting health is found to be significant in this study. Seidler et al. (2017) found that exposure to traffic noise results in depression. A similar study on the health effect of noise was carried out by

Table 6: Result of path analysis

Hypothesis		T statistics	P values	Confidence interval		Supported
				2.50%	97.50%	
HP1	**Age > Gender**	**2.871**	**0.004**	**-0.118**	**-0.022**	**Yes**
HP2	**Age > Occupation**	**8.199**	**0**	**0.361**	**0.584**	**Yes**
HP3	Age > Q1	1.484	0.138	-0.037	0.237	No
HP4	Age > Q2	0.889	0.374	-0.215	0.087	No
HP5	Age > Q3	1.118	0.263	-0.063	0.243	No
HP6	Age > Q4	1.431	0.153	-0.039	0.229	No
HP7	Age > Q5	0.461	0.645	-0.101	0.175	No
HP8	Age > Q6	0.36	0.719	-0.149	0.111	No
HP9	Age > Q7	0.343	0.731	-0.19	0.14	No
HP10	Age > Q8	0.408	0.684	-0.198	0.126	No
HP11	Age > Q9	0.301	0.764	-0.126	0.175	No
HP12	Age > Q10	0.946	0.344	-0.076	0.232	No
HP13	Age > Q11	0.737	0.461	-0.094	0.234	No
HP14	Age > Q12	0.142	0.887	-0.169	0.144	No
HP15	Age > Q13	0.857	0.392	-0.217	0.088	No
HP16	Age > Q14	0.45	0.653	-0.153	0.224	No
HP17	Age > Q15	0.387	0.699	-0.205	0.129	No
HP18	Age > Q16	1.42	0.156	-0.051	0.277	No
HP19	Age > Q17	0.071	0.944	-0.171	0.163	No
HP20	**Gender > Occupation**	**2.314**	**0.021**	**-0.615**	**-0.053**	**Yes**
HP21	Gender > Q1	0.16	0.873	-0.321	0.297	No
HP22	Gender > Q2	0.796	0.426	-0.445	0.197	No
HP23	Gender > Q3	0.824	0.41	-0.202	0.5	No
HP24	Gender > Q4	0.137	0.891	-0.324	0.282	No
HP25	Gender > Q5	1.475	0.14	-0.08	0.612	No
HP26	Gender > Q6	1.523	0.128	-0.067	0.606	No
HP27	Gender > Q7	0.791	0.429	-0.203	0.46	No

Table Cont....

Hypothesis		T statistics	P values	Confidence interval		Supported
				2.50%	97.50%	
HP28	Gender > Q8	0.031	0.975	-0.343	0.348	No
HP29	Gender > Q9	0.596	0.551	-0.232	0.443	No
HP30	Gender > Q10	0.516	0.606	-0.226	0.4	No
HP31	Gender > Q11	1.079	0.281	-0.16	0.524	No
HP32	Gender > Q12	0.656	0.512	-0.245	0.462	No
HP33	Gender > Q13	0.31	0.756	-0.399	0.279	No
HP34	Gender > Q14	1.037	0.3	-0.166	0.538	No
HP35	Gender > Q15	1.369	0.171	-0.579	0.106	No
HP36	Gender > Q16	1.315	0.188	-0.584	0.106	No
HP37	Gender > Q17	0.81	0.418	-0.205	0.513	No
HP38	**Occupation > Q1**	**2.509**	**0.012**	**0.047**	**0.376**	**Yes**
HP39	**Occupation > Q2**	**2.165**	**0.03**	**0.02**	**0.36**	**Yes**
HP40	**Occupation > Q3**	**3.169**	**0.002**	**-0.407**	**-0.091**	**Yes**
HP41	**Occupation > Q4**	**5.082**	**0**	**0.212**	**0.478**	**Yes**
HP42	Occupation > Q5	0.077	0.939	-0.191	0.174	No
HP43	Occupation > Q6	0.527	0.598	-0.139	0.229	No
HP44	Occupation > Q7	1.486	0.137	-0.043	0.314	No
HP45	Occupation > Q8	0.017	0.986	-0.188	0.183	No
HP46	Occupation > Q9	1.703	0.089	-0.03	0.312	No
HP47	Occupation > Q10	1.022	0.307	-0.268	0.089	No
HP48	Occupation > Q11	0.63	0.529	-0.119	0.233	No
HP49	Occupation > Q12	1.278	0.201	-0.309	0.066	No
HP50	Occupation > Q13	0.544	0.587	-0.133	0.227	No
HP51	Occupation > Q14	0.335	0.738	-0.152	0.214	No
HP52	Occupation > Q15	0.016	0.987	-0.184	0.187	No
HP53	Occupation > Q16	0.618	0.537	-0.234	0.123	No
HP54	Occupation > Q17	0.814	0.416	-0.105	0.269	No
HP55	**Q1 > Q3**	**2.999**	**0.003**	**0.078**	**0.38**	**Yes**
HP56	**Q1 > Q4**	**3.656**	**0**	**0.108**	**0.35**	**Yes**
HP57	**Q1 > Q5**	**2.218**	**0.027**	**-0.328**	**-0.017**	**Yes**
HP58	Q1 > Q6	0.982	0.326	-0.267	0.091	No
HP59	Q1 > Q7	0.116	0.908	-0.169	0.183	No
HP60	Q1 > Q8	0.534	0.593	-0.143	0.239	No
HP61	Q1 > Q9	1.091	0.276	-0.079	0.281	No
HP62	Q1 > Q10	0.139	0.89	-0.179	0.155	No
HP63	Q1 > Q11	0.357	0.721	-0.198	0.124	No
HP64	Q1 > Q12	0.175	0.861	-0.144	0.166	No
HP65	**Q1 > Q13**	**2.663**	**0.008**	**-0.377**	**-0.055**	**Yes**
HP66	Q1 > Q14	0.108	0.914	-0.158	0.182	No
HP67	Q1 > Q15	0.335	0.738	-0.198	0.136	No
HP68	Q1 > Q16	0.85	0.395	-0.238	0.095	No
HP69	Q1 > Q17	0.238	0.812	-0.186	0.146	No

Hypothesis		T statistics	P values	Confidence interval		Supported
				2.50%	97.50%	
HP70	Q2 > Q5	0.616	0.538	-0.112	0.221	No
HP71	Q2 > Q6	1.262	0.207	-0.069	0.292	No
HP72	Q2 > Q7	1.917	0.055	-0.011	0.354	No
HP73	Q2 > Q8	0.032	0.974	-0.181	0.176	No
HP74	Q2 > Q9	0.25	0.802	-0.144	0.195	No
HP75	**Q2 > Q10**	**2.177**	**0.029**	**0.014**	**0.338**	**Yes**
HP76	Q2 > Q11	0.723	0.47	-0.218	0.101	No
HP77	Q2 > Q12	0.241	0.81	-0.181	0.145	No
HP78	Q2 > Q13	0.144	0.886	-0.154	0.172	No
HP79	Q2 > Q14	1.252	0.211	-0.061	0.261	No
HP80	Q2 > Q15	1.3	0.194	-0.055	0.262	No
HP81	Q2 > Q16	0.093	0.926	-0.186	0.161	No
HP82	Q2 > Q17	0.272	0.785	-0.147	0.192	No
HP83	**Q3 > Q5**	**2.164**	**0.031**	**0.016**	**0.323**	**Yes**
HP84	**Q3 > Q6**	**2.358**	**0.018**	**0.029**	**0.359**	**Yes**
HP85	Q3 > Q7	0.741	0.459	-0.103	0.238	No
HP86	Q3 > Q8	0.795	0.427	-0.1	0.233	No
HP87	**Q3 > Q9**	**2.456**	**0.014**	**0.035**	**0.364**	**Yes**
HP88	**Q3 > Q10**	**3.33**	**0.001**	**0.097**	**0.364**	**Yes**
HP89	Q3 > Q11	1.502	0.133	-0.279	0.034	No
HP90	Q3 > Q12	0.602	0.547	-0.108	0.2	No
HP91	Q3 > Q13	1.823	0.068	-0.011	0.282	No
HP92	**Q3 > Q14**	**2.043**	**0.041**	**0.008**	**0.312**	**Yes**
HP93	Q3 > Q15	0.489	0.625	-0.106	0.179	No
HP94	Q3 > Q16	1.361	0.174	-0.043	0.234	No
HP95	Q3 > Q17	0.696	0.487	-0.21	0.099	No
HP96	**Q4 > Q3**	**2.095**	**0.036**	**0.007**	**0.323**	**Yes**
HP97	Q4 > Q5	0.334	0.739	-0.197	0.139	No
HP98	Q4 > Q6	0.84	0.401	-0.24	0.095	No
HP99	Q4 > Q7	0.172	0.863	-0.188	0.154	No
HP100	Q4 > Q8	0.757	0.449	-0.242	0.106	No
HP101	Q4 > Q9	1.511	0.131	-0.299	0.04	No
HP102	Q4 > Q10	1.517	0.129	-0.257	0.039	No
HP103	Q4 > Q11	1.631	0.103	-0.302	0.029	No
HP104	Q4 > Q12	0.077	0.939	-0.155	0.167	No
HP105	Q4 > Q13	1.139	0.255	-0.07	0.264	No
HP106	Q4 > Q14	1.127	0.26	-0.069	0.258	No
HP107	Q4 > Q15	1.425	0.154	-0.289	0.047	No
HP108	Q4 > Q16	1.179	0.238	-0.249	0.06	No
HP109	Q4 > Q17	1.263	0.206	-0.28	0.067	No

Martin et al. (2006), and Kjellberg et al. (1998) found that headache and fatigue are the two most commonly reported health issues by the respondents. According to Ismaila & Odusote (2014), multiple articles have reported health issues related to traffic noise exposure and blood pressure. Higher-paid people are less exposed to noise pollution

than the lower-paid (Kjellberg et al. 1996); hence strong significance is found in our study between "occupation and 4 other questions". Thus this study reveals that the population of Raipur City faces the above-mentioned health issues due to high noise levels. The population exposed to traffic noise is mostly affected by noise and faces the health issues mentioned above.

CONCLUSIONS

Noise pollution monitoring and mapping in the current study revealed that all 18 locations recorded higher noise levels and breached the ambient noise standard of CPCB. Hence the governing bodies must implement mitigating approaches for controlling it as higher levels cause different health problems among the exposed population of the city. From the survey study, it is found that most of the respondents are exposed to higher noise levels and are facing health issues of "pain in the ear," "rise in blood pressure," "loss of sleep," "whistling and buzzing" in their ear, "headache," "heaviness" and "efficiency problem." It can be concluded that the exposed population of the city is highly affected by noise pollution. SEM analysis reveals an interrelation between noise pollution and health effects. The association between exposure time and noise affecting health is significant in this study. The study gives ample evidence that higher noise levels in the study area are present and the population is highly affected; hence study supports the importance of making guidelines in context to mitigating approaches. The study recommends making strict regulations near the most sensitive areas like hospitals, schools, and residential areas to ensure a good and healthy environment in the city. Environment and health agencies must conduct awareness drives on a large scale and keep enlightening the city's population regarding noise effects and various measures for controlling the higher noise levels in the ambient environment.

REFERENCES

Al-Mutairi, N.Z., Al-Attar, M.A. and Al-Rukaibi, F.S. 2011. Traffic-generated noise pollution: exposure of road users and populations in Metropolitan Kuwait. Environ. Monit. Assess., 183(1): 65-75.

Bodin, T., Albin, M., Ardö, J., Stroh, E., Östergren, P.O. and Björk, J. 2009. Road traffic noise and hypertension: results from a cross-sectional public health survey in southern Sweden. Environ. Health, 8(1): 1-10.

Chakraborty, S.K. and Banerjee, D. 2007. A study of transport related noise pollution in Asansol town, West Bengal using modeling techniques. Nat. Environ. Pollut. Technol., 6(4):.601.

Davvetas, V., Diamantopoulos, A., Zaefarian, G. and Sichtmann, C. 2020. Ten basic questions about structural equations modeling you should know the answers to–But perhaps you don't. Industrial Market. Manag., 90: 252-263.

De Souza, T.B., Alberto, K.C. and Barbosa, S.A. 2020. Evaluation of noise pollution related to human perception in a university campus in Brazil. Appl. Acous., 157: 107023.

Farooqi, Z.U.R., Ahmad, I., Zeeshan, N., Ilić, P., Imran, M. and Saeed, M.F. 2021. Urban noise assessment and its nonauditory health effects on Chiniot and Jhang, Punjab, Pakistan residents. Environ. Sci. Pollut. Res., 28(39): 54909-54921.

Farooqi, Z.U.R., Sabir, M., Latif, J., Aslam, Z., Ahmad, H.R., Ahmad, I., Imran, M. and Ilić, P. 2020. Assessment of noise pollution and its effects on human health in the industrial hub of Pakistan. Environ. Sci. Pollut. Res., 27(3): 2819-2828.

Fyhri, A. and Aasvang, G.M. 2010. Noise, sleep, and poor health: Modeling the relationship between traffic noise and cardiovascular problems. Sci. Tot. Environ., 408(21): 4935-4942.

Fyhri, A. and Klæboe, R. 2009. Road traffic noise, sensitivity, annoyance and self-reported health—A structural equation model exercise. Environ.t Int., 35(1): 91-97.

Garg, N., Sinha, A.K., Gandhi, V., Bhardwaj, R.M. and Akolkar, A.B. 2017. Impact of Diwali celebrations on environmental noise pollution in India. Acoust. Aust., 45(1): 101-117.

Gholami, A., Nasiri, P., Monazzam, M., Gharagozlou, A., Monavvari, S.M. and Afrous, A. 2012. Evaluation of traffic noise pollution in a central area of Tehran through noise mapping in GIS. Adv. Environ. Biol., 6(8): 2365-2371.

Gilani, T.A. and Mir, M.S. 2021. A study on assessing traffic noise-induced annoyance and awareness levels about the potential health effects among residents living around a noise-sensitive area. Environ. Sci. Pollut. Res., 28(44): 63045-63064.

Hahad, O., Wild, P.S., Prochaska, J.H., Schulz, A., Lackner, K.J., Pfeiffer, N., Schmidtmann, I., Michal, M., Beutel, M., Daiber, A. and Münzel, T. 2021. Midregional pro atrial natriuretic peptide: A novel important biomarker for noise annoyance-induced cardiovascular morbidity and mortality? Clin. Res. Cardiol., 110(1): 29-39.

Hair, J.F., Ringle, CM, Sarstedt, M. 2011 PLS-SEM: Indeed a silver bullet. J. Mark. Theory Pract., 19: 139–152. https://doi.org/10.2753/MTP1069-6679190202.

Hair, J.F., Sarstedt, M., Ringle, C.M. and Mena, J.A. 2012. An assessment of partial least squares structural equation modeling in marketing research. J. Acad. Market. Sci., 40(3): 414-433.

Hunashal, R.B. and Patil, Y.B. 2011. Environmental noise pollution in Kolhapur City, Maharashtra, India. Nat. environ. Pollut. Technol., 10(1): 39-44.

Ismaila, S.O. and Odusote, A. 2014. Noise exposure is a factor in the increase of blood pressure of workers in the sack manufacturing industry. Beni-Suef University Journal of Basic and Applied Sciences, 3(2): 116-121.

ISO/1996-1. Acoustics Description, measurement, and Assessment of environmental noise - Part 1: Basic quantities and assessment procedures. Acoustique, 3: 2–7

Jiang, J., Hanson, D. and Dowdell, B. 2015. At-source control of freight rail noise: A case study. Acoust, Aust., 43(3): 233-243.

Juang, D.F., Lee, C.H., Yang, T. and Chang, M.C. 2010. Noise pollution and its effects on medical care workers and patients in hospitals. Int. J. Environ. Sci. Technol., 7(4): 705-716.

Kjellberg, A., Landström, U.L.F., Tesarz, M., Söderberg, L. and Akerlund, E. 1996. The effects of nonphysical noise characteristics, ongoing tasks and noise sensitivity on annoyance and distraction due to noise at work. J. Environ. Psychol., 16(2): 123-136.

Kjellberg, A., Muhr, P. and Skoldstrom, B. 1998. Fatigue after work in noise-an epidemiological survey study and three quasi-experimental field studies. Noise Health, 1(1): 47.

Martin, P.R., Reece, J. and Forsyth, M. 2006. Noise as a trigger for headaches: Relationship between exposure and sensitivity. Headache: The Journal of Head and Face Pain, 46(6): 962-972.

Mishra, R.K., Nair, K., Kumar, K. and Shukla, A. 2021. Dynamic noise mapping of road traffic in an urban city. Arab. J. Geosci., 14(2): 1-11.

MORTH. Road Transport Year Book 2017-18 & 2018-19. Ministry of Road Transport Highway, 2019.

Murthy, V.K., Majumder, A.K., Khanal, S.N. and Subedi, D.P. 2007. Assessment of traffic noise pollution in Banepa, a semi-urban town of Nepal. Kathmandu Univ. J. Sci. Eng. Technol., 3(2): 12-20.

Ooi, K.B., Lee, V.H., Tan, G.W.H., Hew, T.S. and Hew, J.J. 2018. Cloud computing in manufacturing: The next industrial revolution in Malaysia? Exp. Sys. Appl., 93: 376-394.

Pathak, V., Tripathi, B.D. and Kumar Mishra, V. 2008. Evaluation of traffic noise pollution and attitudes of exposed individuals in working place. Atmos. Environ., 42(16): 3892-3898.

Ramanathan, R. and Renuka, R. 2008. Status and implications of noise pollution in temples of Tamil Nadu-Srirangam temple. Nat. Environ. Pollut. Technol., 7(1): 101.

Ristovska, G. and Lekaviciute, J. 2013. Environmental noise and sleep disturbance: Research in central, eastern and south-eastern Europe and newly independent states. Noise Health, 15(62): 6.

Sahu, P., Galhotra, A., Raj, U. and Ranjan, R.V. 2020. A study of self-reported health problems of the people living near railway tracks in Raipur city. J. Med. Primary Care, 9(2): 740.

Sarikavak, Y. and Boxall, A. 2019. The impacts of pollution for new high-speed railways: the case of noise in Turkey. Acoust. Aust., 47(2): 141-151.

Seidler, A., Hegewald, J., Seidler, A.L., Schubert, M., Wagner, M., Dröge, P., Haufe, E., Schmitt, J., Swart, E. and Zeeb, H. 2017. Association between aircraft, road, and railway traffic noise and depression in a large case-control study based on secondary data. Environ. Res., 152: 263-271.

Stansfeld, S. and Clark, C. 2015. Health effects of noise exposure in children. Curr. Environ. Health Rep., 2(2): 171-178.

Swain, B.K. and Goswami, S. 2013. Integration and comparison of assessment and modeling of road traffic noise in Baripada town, India. Int. J. Energy Environ., 4(2): 303-310.

Tabraiz, S., Ahmad, S., Shehzadi, I. and Asif, M.B. 2015. Study of physio-psychological effects on traffic wardens due to traffic noise pollution; exposure-effect relation. J. Environ. Health. Sci. Eng., 13(1): 1-8.

Terry, C., Rothendler, M., Zipf, L., Dietze, M.C. and Primack, R.B. 2021. Effects of the COVID-19 pandemic on noise pollution in three protected areas in metropolitan Boston (USA). Biol. Consev., 256: 109039.

UN 2019. United Nations, World population prospects 2019. https://population.un.org/wpp/publications/files/wpp2019_highlights.pdf

World Bank. Population 2019 -2020. https://doi.org/https://databank.worldbank.org/data/download/POP.pdf.

Wu, J., Zou, C., He, S., Sun, X., Wang, X. and Yan, Q. 2019. Traffic noise exposure of high-rise residential buildings in urban areas. Environ. Sci. Pollut. Res., 26(9): 8502-8515.

Environmental Toxicity, Human Hazards and Bacterial Degradation of Polyethylene

N. Yoezer*† iD, D. B. Gurung* and K. Wangchuk

*Department of Forest Science, College of Natural Resources, Royal University of Bhutan, Punakha, Bhutan
**Department of Food Science and Technology, College of Natural Resources, Royal University of Bhutan, Punakha, Bhutan
†Corresponding author: N. Yoezer; yoezernima12@gmail.com

ABSTRACT

Plastics are the most rapidly growing materials in terms of production and consumption. The durability, inertness, light weight, flexibility, and low cost are the key characteristics that make plastic suitable for application in various fields, including the construction, automotive, electronics, and packaging industries. Due to widespread usage in daily life and many industrial processes and operations, more than 300 million tons of plastic waste are produced globally annually. Indiscriminate use of plastics such as polyethylene causes environmental pollution and impacts human health due to irreversible changes in the ecological cycle. Due to its low biodegradability, polyethylene accumulation has recently emerged as a momentous environmental concern. The conventional methods, such as recycling or disposing of polyethylene, are exorbitant, and incineration results in the emission of toxic chemical compounds. Therefore, the most recent research progressively focused on the biodegradation of polyethylene with the application of bacteria as novel approaches to counteract plastic waste. This review summarizes the type of polyethylene and the environmental issues. It also briefly discussed the genes and enzymes of bacteria involved in the degradation of polyethylene. In addition, it attempts to address factors influencing degradation and techniques used for monitoring degradation.

INTRODUCTION

The etymology of plastic is derived from the Greek word "plastikós," which defines materials as being able to be molded into different desired shapes and sizes due to their chemical composition of carbon, chlorine, hydrogen, nitrogen, oxygen, and silicon. Plastics are polymer macromolecules with long chains, and other compounds are added to alter properties such as stability and processability (Bardají et al. 2020). The introduction of plastics into archaeological and geologic history may serve as the defining characteristic of anthropogenic pollution, and the twentieth century is referred to as the "Plastic Age" (Mytum & Meek 2021). Plastics have generally substituted paper and packaging materials due to superior tensile properties, lightweight nature, and low susceptibility to microbial degradation (Muhonja et al. 2018).

Around 80% of all plastics used globally are petrochemical plastics, including polyethylene (PE), polypropylene (PP),

polyvinyl chloride (PVC), polystyrene (PS), and polyethylene terephthalate esters (PET) (Urbanek et al. 2018). Although plastic materials are indispensable to the world economy, serious complications associated with their widespread use must not be omitted (Chu et al. 2023). The everyday use of plastic has increased global plastic production exponentially, reaching 367 metric tons in 2020 (Plastics Europe 2021), and the amount is significantly increasing annually due to extremely efficient applications. It is estimated that approximately 710 million metric tons of plastic will be accumulated in the environment or landfills by 2040 if the current management practices, use, and production endure (Lau et al. 2020). Hefty amounts of plastic waste are produced primarily due to the short product lifecycle. In 40% of cases, the lifespan of thermoplastic plastic products is anticipated to be less than one month (Hahladakis et al. 2018). Furthermore, plastic waste management has lagged significant manufacturing output, resulting in environmental pollution (Geyer et al. 2017).

Polyethylene is the most significant consumer plastic, primarily used to manufacture plastic bags, bottles, and

containers (Mercy et al. 2023). With 86.08 metric tons, PE accounts for 22% of all plastic produced globally. In comparison to low-density polyethylene (LDPE) and linear low-density polyethylene (LLDPE), which make up 12%, high-density polyethylene (HDPE) comprises 10% of global plastic (Šišková et al. 2021). However, PE's resistance to degradation due to high molecular weight, antioxidants, and stabilizers, promotes environmental pollution after a short period of use. The resistance to biodegradation of PE through enzymatic cleavage via oxidative reaction is also due to the carbon-carbon (C–C) backbone and semi-crystal structure (Andler et al. 2022).

The plastic waste entering freshwater and terrestrial environments results in the formation of mesoplastics (0.5–5 cm), microplastics (MP; 1 μm–5 mm), and nanoplastics (NP; < 1μm) due to mechanical abrasion and degradation of larger plastic debris (Bianco & Passananti 2020). Plastic debris such as MPs has ecotoxicological effects on chemical and physical properties, nutrient cycling, and flora and fauna of terrestrial soil (Ya et al. 2021). The presence of LDPE–MPs can affect terrestrial ecosystems. Several alterations were demonstrated in the kidney, liver, pancreas, muscles, gills, spinal cord, notochord, and intestine of *Oreochromis niloticus* (tilapia), affecting survival due to MPs (Hamed et al. 2021). The NPs have a considerable impact compared to other plastic particles due to their capacity to enter cells and tissues and cause molecular impairment besides the toxicity of the polymers. Thus, decreasing the surface of PE increases damage to fish tissue (Hamed et al. 2022). The toxic effects of PE are an emerging concern for aquatic environments. People are exposed to various polymers, including PE, through dermal contact, ingestion, and inhalation due to their occurrence in foods, water, air, and consumer products (Rahman et al. 2021).

Furthermore, toxic chemical compounds such as Bisphenol A (BPA), phthalates, antiminitroxide, flame retardants, and polyfluorinated compounds are also found in plastics. These substances pose environmental and public health risks (Proshad et al. 2018). Hence, it is necessary to reduce plastic pollution through environmentally friendly methods. Conventional methods such as recycling, dumping, and incineration are not feasible and generates toxic substances as a by-product (Venkatesan et al. 2022).

Actinomycetes, bacteria, and fungi are among the microorganisms capable of degrading PE (Dang et al. 2018, Saritha et al. 2021). Bacteria degrading PE include *Phormidium lucidum, Oscillatoria subbrevis* (Sarmah & Rout 2018), *Bacillus wudalianchiensis*, and *Pseudomonas aeruginosa* (Bakht et al. 2020). Those potential microorganisms are isolated from different soil types, including landfill soil (Montazer et al. 2018), to water bodies (Dhanraj et al. 2022). This indicates that the bacteria exist in most places and in sufficient numbers to cause PE biodegradation.

Biodegradation is defined as the capability of microbes to degrade plastic materials into simpler molecules with the help of enzymes by altering the chemical structures of the plastics into an easily degradable property (Gaur et al. 2022). Temperature, crystallinity, hydrophobicity, structure, and enzymes influence the mechanism of PE's biodegradation. Therefore, this review focuses on the toxicity, bacterial degradation, and factors affecting the degradation mechanism of PE. Moreover, it summarizes the technique used to investigate the biodegradation and bacterial enzymes responsible for the degradation of PE and suggests future research scopes.

GLOBAL PLASTIC AND POLYETHYLENE PRODUCTION

Every year, the world witnesses an unprecedented production of plastics. 335 million tons of plastic were produced worldwide in 2016 and 367 million tons in 2020. Europe produced 55 million tons of plastics in 2020 (Plastics Europe 2021). It was estimated that Asia produced 49% of the global plastics, with China as the leading manufacturer (28%). Furthermore, Europe and North America contributed approximately 19% of global plastics production in 2015, while the rest of the country contributed negligible production, but not necessarily of plastic usage (Worm et al. 2017). According to Hahladakis et al. (2018), European nations primarily used plastic for wrapping (38%), infrastructure tools (21%), motorized (7%), electrical applications (6%), as well as other segments (28%). In India, PE had the highest demand (33%) in 2020, followed by PP (32%), and worldwide consumption of PE was growing at a rate of 12% per year (Venkatesan et al. 2022). Bhutan generates over 170 metric tons of waste daily, encompassing various types. Plastics, including HDPE, soft plastics, and PET bottles, contribute to approximately 17% of this overall waste production (Namgay 2020).

CLASSIFICATION OF POLYETHYLENE

The polymerization of ethylene monomers yields polyethylene, also known as polyethylene, a thermoplastic polymer. The chemical formula for ethylene is C_2H_4, while PE has the formula $(C_2H_4)_n$. The Ziegler-Natta and metallocene catalysts are used for the polymerization of polyethylene. Polyethylene is a polyolefin resin family that is the most commonly used plastic worldwide for various
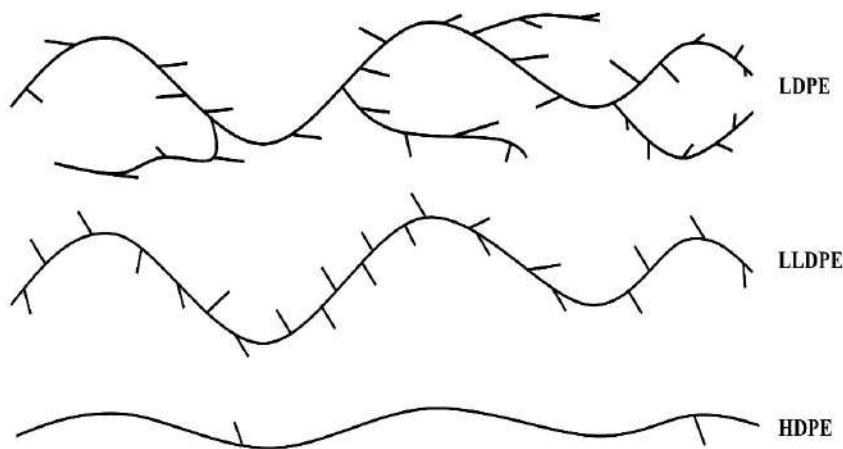
Fig. 1: Polyethylene structures.

purposes, such as wrapping, films, packaging, and nursery bags. There are mainly three types of PE: LDPE, LLDPE, and HDPE (Fig. 1). The fundamental distinction between HDPE, LDPE, and LLDPE is the branching degree at the microstructural level. High-density polyethylene has the lowest or no branching, LLDPE incorporates a high degree of short chain, and LDPE contains an irregular distribution of short and long branches (Rani et al. 2020, Varyan et al. 2022).

THE EFFECT OF PE POLLUTION

The effect of polyethylene on aquatic, terrestrial, and human health are illustrated in Fig. 2.

THE EFFECT OF PE ON AQUATIC LIFE

The main source of plastics in the water is anticipated to be from the terrestrial environment. Microplastics are diluted as transport from the deposition hotspot downstream. Therefore, ineffective waste management practices lead to environmental contamination. Several plastic materials, encompassing PP, PVC, PE, PET, and nylon, as well as particle shapes such as fragments, sheets, and threads, have been found in the *Megaptera novaeangliae* (humpback whales) intestinal tract (Guzzetti et al. 2018). Microplastic accumulation in the hindguts of Lysianassoidea amphipod populations is found at depths ranging from 7,000 m to 10,890 m in the Pacific Ocean (Cózar et al. 2017). This suggests that MP contamination can occur in the ocean beds as well.

Histological fluctuations were detected in the intestine and liver of *Dicentrarchus labrax* (European sea bass) exposed to PE-MPs. Polyethylene microplastics suppress immunity and antioxidant enzyme activity, signifying the oxidative response/stress, and longer exposure resulted in irreversible damage to fish health (Espinosa et al. 2019). Antioxidants, biochemistry, cholinesterase activity, erythron profile, hematological, histological, and immune parameters were altered in young *Cyprinus carpio* (common carps), divulging to PE particles (Hamed et al. 2022).

Polyethylene microplastic ingestion alters morphology, erythrocyte mutagenicity, and cytotoxicity in *Physalaemus cuvieri* tadpoles, affecting their development and health (da Costa Araújo et al. 2020). The gut examination of *Phalaropus fulicarius* carcasses in Canada found that most commonly ingested plastics such as PE and PP likely contributed to mortality (Teboul et al. 2021). Polyethylene microplastics induce oxidative damage and alter the functioning of antioxidant enzymes in *Mytilus galloprovincialis* (mussels) at environmentally relevant concentrations (Abidli et al. 2021). Apart from disruption of metabolic activity in an organism, plastic waste in the rivers also contributes to the spatial distribution of invasive species leading to competition with native species (Hasnat & Rahman 2018). Thus, through ingestion, PE-MPs and NPs can enter organisms' bodies and continue to be transferred along food chains.

POLYETHYLENE IMPACT ON THE TERRESTRIAL ENVIRONMENT

Plastic mulching and shading materials protect crops from pests, and harsh weather suppresses weeds (Maraveas 2020). However, plastic mulch significantly impacts soil properties such as pH, electrical conductivity, infiltration, nutrient exchange, and microbial community (Sintim et al. 2019). Polyethylene microplastics escalate the movement of pollutants while decreasing the retention capacities of the soil. For instance, the holding capacity of cadmium was reduced in MP-contained soil, thereby increasing the possibilities of lethal heavy metal accumulation in agriculture

products and groundwater and bestowing additional risks on the environment (Zhang et al. 2020). Plants exposed to PE particles had lower biomass, slow photosynthetic rates, and abnormal mineral nutrient metabolism. This indicates that various PE particles with different molecular weights could adversely affect the soil-plant physiology (Fu et al. 2022).

Low-density polyethylene fragments affect the microarthropod and nematode but slightly influence the biomass and soil microorganism (Lamichhane et al. 2022). Polymers such as LDPE and HDPE have been found in terrestrial species *Armadillo, Porcellio, Lumbricus terrestris, Scolopendra, Eobania vermiculata,* and *Rumina decollata* causing adverse effects on metabolic function and survival (Al Malki et al. 2021). Low-density polyethylene microplastics affect manure worms' nervous system, morphology, and oxidative response. The result illustrates that the MPs may have adverse biochemical effects on earthworms (Chen et al. 2020). The intestinal tract of terrestrial birds also contains cellulose, PE, and PET-MPs (Carlin et al. 2020). This indicates the abundance and variety of plastics on terrestrial land.

EFFECT OF PE ON HUMAN HEALTH

Microplastics and NPs enter humans through ingestion, inhalation, and dermal contact with water, air, food, and consumer products containing plastics (Karami et al. 2018). Moreover, humans consume plastic directly through table salts (Renzi & Blašković 2018), seafood (De-la-Torre 2020), and canned sardines and sprats (Karami et al. 2018). The most common plastic materials in foodstuffs are PP, PE, PET, polyether (PES), PVC, PS, PA, and nylon (Karbalaei et al. 2018). The various MPs of polycarbonate (PC), polyoxymethylene (POM), polyurethane (PUR), PA, PE, PET, PS, PP, and PVC were found in human stool. Among the nine plastic types, PP (62.8%), PET (17.0%), PS (11.2%), and PE (4.8%) were the most abundant (Schwabl et al. 2019). The inhalation and ingestion of high concentrations of PE-MPs with their rough structures increases the risk of cytotoxicity in epithelial cells and triggers the release of pro-inflammatory cytokines. Polyethylene microplastics also cause the production of reactive oxygen species and nitric oxide in cells (Choi et al. 2021, Gautam et al. 2022). Depending on the hydrophilic nature, dimensions, and surface energy, inhaled airborne MPs can enter the bloodstream with increased epithelial or endothelial diffusion. Most MP particles (PE) measured in abdominal lymph nodes were 1–50 μm (Zarus et al. 2021).

The presence of MPs and NPs causes disruption of molecular and cellular function in humans. Ingestion of such plastic causes various types of cancer, particularly in industrial workers, because of exposure to high intensities of air pollutants (Wang et al. 2020). Human dopaminergic neurons and neurospheres in culture can absorb PE-NPs, which modifies gene expression and elevates malondialdehyde levels, signaling the initiation of
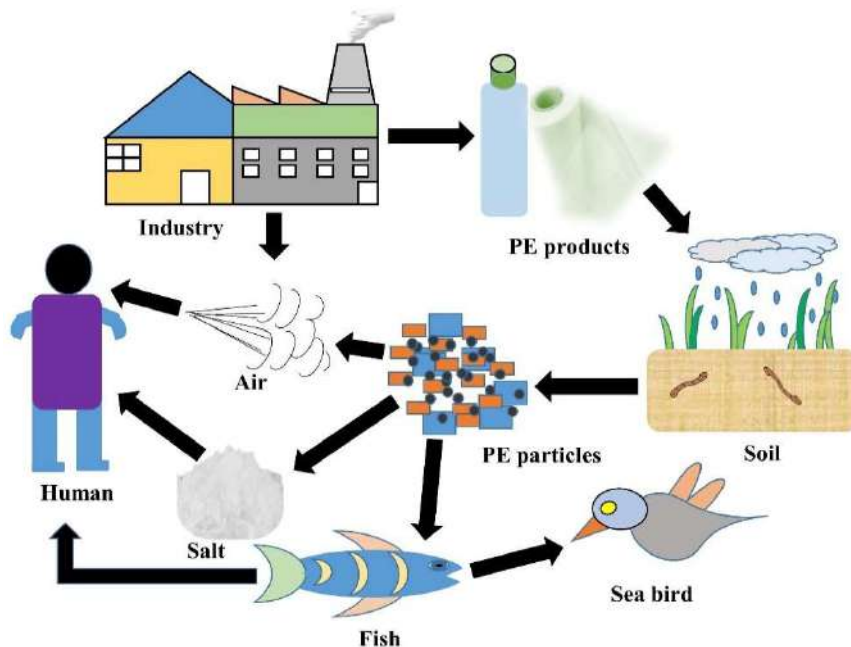
Fig. 2: Effect of plastic particles in aquatic, terrestrial, and human.

oxidative metabolism (Windheim et al. 2022). In addition to potentially endangering the pulmonary and digestive systems, researchers have proposed NPs can significantly increase levels of DNA damage that causes mutagenic processes (Rubio et al. 2020). All that evidence suggests that PE, especially micro and nano, may be prevalent in human foodstuffs, ultimately creating health problems.

MICROBIAL POLYMER DEGRADATION MECHANISM

The mechanism of PE degradation occurs in four stages, as shown in Fig. 3.

Biodeterioration: This process encompasses biotic and abiotic factors that cause erosion of the polymer surface, altering the chemical, mechanical, and physical characteristics. The LDPE exposure to different physicochemical treatments and biotic conditions increases biodeterioration as treatment changes hydrophobicity and surface roughness. Chemical alteration, such as generating polar groups and crosslink formation, also occurs (Gómez-Méndez et al. 2018). The biofilm that develops on the plastic enlarges the aperture dimension and accentuates cracks, compromising the polymer's physical properties (physical deterioration) or releasing chemicals that alter the pH inside the hole to cause structural changes known as chemical deterioration (Jacquin et al. 2019).

Biofragmentation: The lytic phenomenon crucial for reducing large molecules into subunits. The microorganisms cleave polymers using a variety of mechanisms, comprising secretion of particular extracellular enzymes such as oxidoreductases (monooxygenases and dioxygenases), hydrolases (cellulases, amylases, and cutinases), and free radicals (Ali et al. 2021). Enzymes cleave polymer carbon chains or bonds, producing low molecular weight, such as monomers, oligomers, and dimers (Kalidas et al. 2021). Due to low molecular weight, the cell can assimilate. Therefore, biofragmentation of the process involves enzymatic activities to reduce low molecular weight and oxidize the polymer. Depolymerization is another name for this process.

Bioassimilation: The low molecular weight polymer formed through the biofragmentation is absorbed into the cytoplasm of the microbes. The fragmented products are assimilated into cells through the cell membrane using specific membrane carriers. While unassimilated oligomers, dimers, and monomers have to undergo biotransformation reactions to be absorbed by microbial cells with the help of intracellular enzymes (Danso et al. 2019).

Mineralization: It is the final phase in the biodegradation of polymers. The term "mineralization" denotes the complete degradation of molecules with the production of oxidized metabolites. Microorganisms can either aerobically or anaerobically mineralize monomers, dimmers, and oligomers. Water, carbon dioxide, and biomass are produced as end products during aerobic degradation. Under anaerobic biodegradation conditions, by-products are water, carbon dioxide, and methane (Tamoor et al. 2021).

FACTORS INFLUENCING THE BACTERIAL DEGRADATION OF PE

The several factors that affect the bacterial degradation of PE depend on polymer properties and exposure conditions (Fig. 4). Polymer properties include additives, crystallinity, functional groups, hydrophobicity, molecular weight, shape, and size. The exposure conditions include biosurfactants,
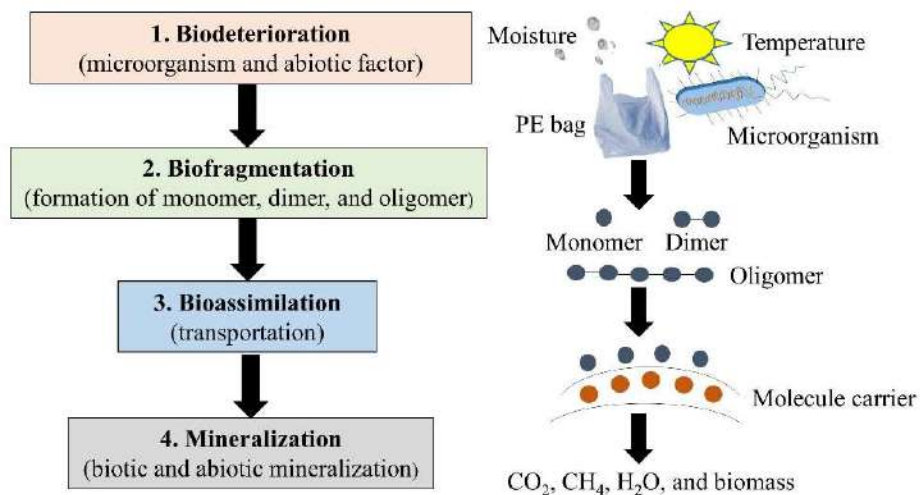
Fig. 3: Mechanism of PE degradation.

enzymes, and microorganisms as biotic factors and moisture, pH, and temperature as abiotic factors.

Exposure Conditions

The moisture provides favorable conditions for respiration, increasing the population of microbes. Furthermore, the chain scission of the polymers takes place in the presence of moisture (Mistretta et al. 2020). In the modification of the PE chemical bond, *Streptomyces* sp. performed better at pH 8, and *Arthrobacter* sp. was more effective at pH 6 with incubation in Czapek–Dox medium and liquid carbon-free basal medium containing PE (Han et al. 2020). Thermophile microorganisms can grow at high temperatures ranging from 45 to 122°C, while psychrophilic microorganisms need temperatures between −20 and 20°C, and temperatures lower than 15°C are considered optimal growth and produce numerous enzymes (Atanasova et al. 2021). However, denaturation of enzymes may occur in psychrophilic bacteria due to high temperature, decreasing the enzymatic degradation of PE (Chamas et al. 2020). The biosurfactant in biofilm growth significantly decreased hydrophobicity and increased hydrophilic functional groups, devising PE sensitive to microbial attack (Tu et al. 2020).

Polymer Properties

The prooxidant additives present in polymer weaken the microstructure, leading to dissociation and allowing microorganism consumption that produces humus, carbon dioxide, and water (Al-Salem et al. 2019). Furthermore, weight loss and structural change with the formation of the new functional group of polymer can occur due to additives (Zhang et al. 2022). Thus, additives and impurities are required to remove before the investigation of biodegradation. High molecular weight polymers are stable and less susceptible to degradation than low molecular weight (Priya et al. 2022). Semi-crystalline polymers (PP, PE, and PET) display greater toughness, strength, and resistance compared to amorphous (Issac & Kandasubramanian 2021), making them less susceptible to enzymatic degradation. The PE backbone consists of linear alkyl chains, and the absence of polar characteristics or hydrolyzable functional groups renders it inactive to degradation. The biotic and abiotic treatments increase PE's hydrophilicity, microbial colonization, and degradation rapidity (Taghavi et al. 2021). The increase in surface area, water, and microorganism availability promotes biodegradation as the high surface area provides space for the growth of organisms.

Role of Bacterial Gene and Emzyme in Biodegradation of PE

The specialized bacteria and their genes and enzymes are imperative to PE biodegradation. It was found that the alkane hydroxylase (alkB) genes in the *Pseudomonas* sp. The E4 strain degraded 28.6% of organic carbon in 80 days. The ability of the alkB gene was verified by selecting the *Escherichia coli* BL21 strain as a host for gene expression
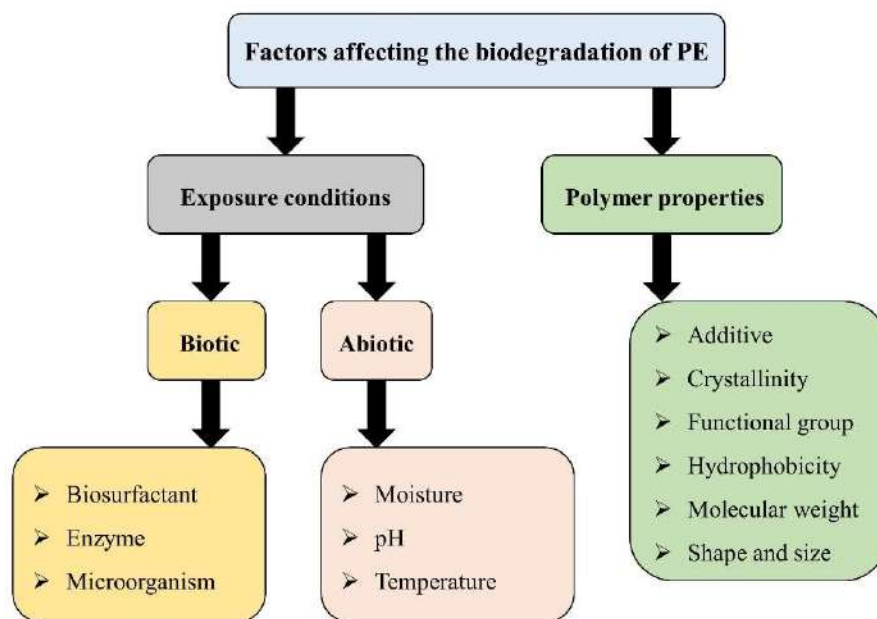
Fig. 4: Factors affecting PE biodegradation.

and achieving a degradation potential of 19.3% for the PE's organic carbon (Priya et al. 2022). Similarly, three putative PE degrading enzymes (esterase, hydrolase, and hydrolase) were expressed in an *E. coli* cell, and their effects on PE films showed significant degradation (Gao & Sun 2021). It was also found that *P. aeruginosa* E7 isolated from an oil-contaminated area possesses alkane hydroxylase. The rubredoxin and rubredoxin reductase transport electrons, and the alkB gene participate in the mineralization of low molecular weight PE (Chen et al. 2020).

Moreover, *Pseudomonas knackmussii* N1-2 and *P. aeruginosa* RD1-3 have 26 and 20 genes, respectively, in their genomes that encode monooxygenases, dioxygenases, and hydroxylases (Hou et al. 2022). Similarly, the genome of *Streptomyces albogriseolus* LBX-2 also embraces 53 oxygenase genes, including monooxygenases and dioxygenases. Thus, *S. albogriseolus* LBX-2 utilized unprocessed PE films as an exclusive carbon source, causing surface deterioration and indicating enzyme-assisted degradation (Shao et al. 2019). The genome of *Alcanivorax* sp. revealed enzymes such as esterases, peroxidases, and laccase that could play an imperative role in biodegradation (Zadjelovic et al. 2020). There are potential genes in Brevibacillus borstelensis AK1 responsible for the breakdown of PE and hydrocarbons. The genes encode enzymes involved in plastic degradation, including cutinase, laccases, hydroxylases, lipases, proteases, and polyphenol oxidase (Khalil et al. 2018). The ligninolytic and hydrolyzing enzymes degrade different plastics, including PE, at 37°C after two days of incubation. Furthermore, the activities of laccase increase by 13 times with 20 µm of copper treatment (Jaiswal et al. 2020).

MATERIALS AND METHODS

Analytical Tools for Determination of Polythene Degradation

Various analytical techniques are applied to determine the biodegradation of PE (Table 1). Fourier transform infrared spectroscopy (FTIR) is used to identify the occurrence of new functional groups. The changes in peak values and functional groups, which typically vary in the double bond and carbonyl group formation, supported the conformational change of the polymer surface (Montazer et al. 2018). Scanning electron microscopy (SEM) assessed the alteration of physical structure on the surface of polyethylene films due to the microorganism's degradative activities through biofilm development (Soleimani et al. 2021). Higher resolution analysis of surface modification can be obtained using Atomic Force Microscopy (AFM), although SEM

provides evidence of the polymers' biodeterioration. Atomic Force Microscopy makes it possible to map the topography of a polymer surface (Sullivan et al. 2018). Gel permeation chromatography (GPC) analysis determines the number average molecular weight (Mn), and weight average molecular weight (Mw), and molecular weight distribution (MWD). These parameters are the primary indicator of modification, depolymerization, and polymer degradation (Peng et al. 2020). The major method for assessing polymer degradation is weight loss as microorganism growth and their activities cause the polymer to reduce weight (Waqas et al. 2021). Additional techniques for assessing PE biodegradation include Raman spectroscopy, Nuclear Magnetic Resonance spectroscopy (NMR), Thermogravimetric Analysis (TGA), Electrospray Ionization Mass Spectrometry Analysis (ESI-MS), Different Scanning Calorimetry Analysis (DSC), Carbon, Hydrogen, and Nitrogen (CHN) Analyzer, and Universal Testing Machine (UTM), Sturm test, and Bacterial Adherence to Hydrocarbons (BATH) assay.

RESULTS AND DISCUSSION

Bacterial Biodegradation

The degradation rate of polythene was observed in various microorganisms (Table 1). The six *Bacillus* sp. isolated from landfills and dumping sites were identified as LDPE-degrading bacteria. The degradation potential rates in mineral agar and mineral broth were found that *B. carboniphilus* (34.55% and 25%), *B. sporothermodurans* (36.54% and 21%), *B. coagulans* (18.37% and 16%), *B. neidei* (36.07% and 14%), *B. smithii* (16.40% and 8%), and *B. megaterium* (34.48% and 21%), respectively. Those bacteria were incubated for two months at 30°C (Shrestha et al. 2019). Pretreated LLDPE particles were incubated with the marine bacteria *Microbulbifer hydrolyticus* IRE-3 for up to 30 days. SEM images revealed the creation of cracks at various locations on the polymer surface, which was also confirmed using FTIR analysis with the formation of hydroxyl and carbonyl functional groups (Li et al. 2020). A consortium of *Enterobacter* and *Pseudomonas* reduced 64.25% of PE (Skariyachan et al. 2021), indicating the mixture has a higher degradation rate. The weight of LDPE and HDPE with consortia of *Lysinibacillus* sp. and *Salinibacterium* sp. decreased to higher than 20% after 60 days and 11.1% at 6 months, respectively (Syranidou et al. 2017). The bacterial consortia of *Enterobacter* sp. (IS2), *Enterobacter* sp. (IS3), and *Pantoea* sp. (IS5) degrade 38% and 81% of LDPE pellets and strips, respectively, after 120 days. Further, consortia of *P. putida* (MTCC1), *P. stutzeri* (MTCC2), and *B. subtilis* (MTCC3) 20% LDPE pellets and 49% for LDPE strips after 120 days of incubation respectively

Table 1: Bacteria species reported for biodegradation of PE.

Sl. No.	Bacteria strains	Sources	Substrates	Incubation period (days)	Techniques used to assess degradation	Main experimental outcomes	References
1.	*Bacillus weihenstephanensis*	Garbage soil	LDPE and HDPE	180	Weight loss and FTIR	7.02%, 7.08%, and formation of new functional carbonyl.	(Ingavale & Raut 2018)
2.	*Brevibacillus borstelensis*	Coastal region	HDPE	20	FTIR and SEM	Formation of acids, ester groups, aldehydes, ketones, and surface erosion.	(Mohanrasu et al. 2018)
3.	*Bacillus amyloliquefaciens*	Composting plant	Treated LLDE	60	Weight loss, FTIR, GPC, DSC, TGA, and ESI-MS	3.20%, decrease of the carbonyl band and flattening, decrease in Mn and Mw, decrease of crystallinity, improved thermal stability, and disappearance of LLDPE oligomers.	(Novotný et al. 2018)
4.	Alcanivorax borkumensis	Sea water	LDPE	80	Weight loss, SEM, and ATR-FTIR	3.50%, chemical modifications, and appearance of holes, and cracks.	(Delacuvellerie et al. 2019)
5.	*Pseudomonas aeruginosa* strain SKN1	Waste disposal	LDPE	60	Weight loss, FTIR, and SEM	10.32%, changes in the C–C and C–H bands, and surface degradation.	(Nourollahi et al. 2019)
6.	*Nostoc carneum*	Domestic sewage water	LDPE	42	SEM, FTIR, CHN analysis, TGA-DSC, UTM, and NMR	Surface damage, occurrence of a new C–H stretching band, utilization of about 3% carbon, reduction in melting point, and appearance of new organic substances.	(Sarmah & Rout 2019)
7.	*Bacillus paramycoides*	Biomedical plastic disposal site	Treated LDPE and HDPE	70	Weight loss	36.30% and 31.11%.	(Fibriarti et al. 2021)
8.	*Lysinibacillus* sp. JJY0216	Soil grove	LDPE	26	SEM and GC-MS	9%, increase in rough surface, and detected various carboxylic acids of the hydrocarbon family.	(Jeon et al. 2021)
9.	*Serratia* sp., *Stenotrophomonas* sp. and *Pseudomonas* sp.	Solid waste-dumping sites	LDPE	150	Loss in weight and FTIR	40%, 32%, 21%, and change in functional group.	(Nadeem et al. 2021)
10.	*Alcaligens faecalis*	Sea water	LDPE	70	FTIR, SEM, XRD, and AFM	Reduction of the carbonyl index, formation of bacterial biofilm, and reduction in crystallinity.	(Nag et al. 2021)
11.	*Micrococcus luteus* CGK112	Cow dung	HDPE	90	Weight loss, BATH test, FE-SEM, EDX, and FTIR	3.85%, increase hydrophobicity, biofilm formation, surface modification, reduction of carbon content, alternation of functional groups, and an increase in the carbonyl index.	(Gupta et al. 2022)

Table Cont....

Sl. No.	Bacteria strains	Sources	Substrates	Incubation period (days)	Techniques used to assess degradation	Main experimental outcomes	References
12.	*Bacillus cereus, Citrobacter koseri,* and *Pseudomonas tuomurensis*	Municipal landfill	HDPE	30	Weight loss and GC-MS	1.78%, 1.31%, and 0.34% and detected degradation products.	(Kopecká et al. 2022)
13.	*Exiguobacterium* sp. strain LM-IK2	Plastic dumped soil	Pretreated LDPE	90	FE-SEM, FTIR, and XRD	5.70%, surface erosion, production of carbonyl peaks, decrease in carbonyl index, and increase in percent crystallinity.	(Maroof et al. 2022)
14.	*Alcaligenes faecalis* MK517568	Municipal dumpsites	LLDPE, HDPE	40	Weight loss, Sturm test, FTIR, SEM, AFM, and BATH assay	3.50%, 5.80%, CO_2 produced, changes in the infrared spectra, the formation of rough surfaces, scions, and high hydrophobicity.	(Tareen et al. 2022)
15.	*Methylobacterium radiotolerans* MN525302, *Methylobacterium fujisawaense* KT720189, and *Lysinibacillus fusiformis*	Solid waste disposal area	LDPE	60	Weight loss, FTIR, and SEM	42.87%, 37.20%, 23.87%, generation of new functional groups, and deformation of the LDPE film.	(Nademo et al. 2023)

(Skariyachan et al. 2016). However, pure or consortia of bacteria degradation also depends on the polymer and incubation period.

CONCLUSIONS

The massive accretion of plastic has emerged as a main concern across the world. PE's toxicity to the environment and human health is obvious, but research is still in its infancy. It is significant to have sustainable and robust technologies to combat plastic pollution and its impacts. Microbial degradation of PE is an environmentally friendly technique to reduce plastic waste. The biodeterioration and biofragmentation mechanisms are explicitly illustrated, but few reports on the bioassimilation or mineralization of PE exist. Thus, most investigation in the field of microbial degradation of PE is superficial rather than intrinsic. The biotic and abiotic factors, as well as the PE properties, substantially influence biodegradation. Therefore, it is critical to thoroughly consider the role of various factors when evaluating PE biodegradation.

The study found that most potential polyethylene-degrading bacteria are conducted in pure culture. This clearly illustrates that the high diversity of bacteria in various habitats has not been fully utilized. Moreover, bacteria consortiums have superior proficiency in plastic degradation due to synergism between the bacteria and enzymes involved. The enzymes responsible for PE degradation have been identified in bacteria; however, enzyme properties have not been thoroughly investigated for enzyme engineering. Therefore,

a deep understanding of the mechanism of enzyme action is valuable for improving degradation efficiency. Further research into the mechanism of enzymatic degradation will lead to the discovery of efficient, biodegradable plastic.

Since the bacteria constantly adapt to their surroundings, viable PE-degrading bacteria are also expected to be acquired and developed commercially. In many studies, a variety of techniques are used to evaluate biodegradation. However, the lack of a standard protocol creates discrepancies in assessing biodegradation. Therefore, it is fundamental to establish a standardized protocol to acquire reliable and consistent outcomes. It is also indispensable to eliminate the additives and impurities and examine the pretreatment for a better result in the biodegradation of PE.

REFERENCES

Abidli, S., Pinheiro, M., Lahbib, Y., Neuparth, T., Santos, M.M. and Trigui El Menif, N. 2021. Effects of environmentally relevant levels of polyethylene microplastic on *Mytilus galloprovincialis* (Mollusca: Bivalvia): filtration rate and oxidative stress. Environ. Sci. Pollut. Res., 28(21): 26643-26652. https://doi.org/10.1007/s11356-021-12506-8.

Afrin, S., Uddin, M.K. and Rahman, M.M. 2020. Microplastic contamination in the soil from the urban landfill site, Dhaka, Bangladesh. Heliyon, 6(11): e05572. https://doi.org/10.1016/j.heliyon.2020.e05572

Al Malki, J.S., Hussien, N.A., Tantawy, E.M., Khattab, Y. and Mohammadein, A. 2021. Terrestrial biota as bioindicators for microplastics and potentially toxic elements. Miner. Nutr. Livest., 11(10): 1152. https://doi.org/10.1079/9781845934729.0489.

Ali, S.S., Elsamahy, T., Koutra, E., Kornaros, M., El-Sheekh, M., Abdelkarim, E. A., Zhu, D. and Sun, J. 2021. Degradation of conventional plastic wastes in the environment: A review on current status of knowledge and future perspectives of disposal. Sci. Total Environ., 771: 144719. https://doi.org/10.1016/j.scitotenv.2020.144719.

Al-Salem, S.M., Al-Hazza'a, A., Karam, H.J., Al-Wadi, M.H., Al-Dhafeeri, A.T. and Al-Rowaih, A.A. 2019. Insights into the evaluation of the abiotic and biotic degradation rate of commercial pro-oxidant-filled polyethylene (PE) thin films. J. Environ. Manage., 250: 109475. https://doi.org/10.1016/j.jenvman.2019.109475.

Andler, R., Tiso, T., Blank, L., Andreeßen, C., Zampolli, J., D'Afonseca, V., Guajardo, C. and Díaz-Barrera, A. 2022. Current progress on the biodegradation of synthetic plastics: From fundamentals to biotechnological applications. Rev. Environ. Sci. Biotechnol., 21(4): 829-850. https://doi.org/10.1007/s11157-022-09631-2.

Atanasova, N., Stoitsova, S., Paunova-krasteva, T. and Kambourova, M. 2021. Plastic degradation by extremophilic bacteria. Int. J. Mol. Sci., 22(11): 5610. https://doi.org/doi.org/10.3390/ijms22115610

Bakht, A., Rasool, N. and Iftikhar, S. 2020. Characterization of plastic degrading bacteria isolated from landfill sites. Int. J. Clin. Microbiol. Biochem. Technol., 3(1): 030–035. https://doi.org/10.29328/journal.ijcmbt.1001013.

Balzani, P., Galeotti, G., Scheggi, S., Masoni, A., Santini, G. and Baracchi, D. 2022. Acute and chronic ingestion of polyethylene (PE) microplastics has mild effects on honey bee health and cognition. Environ. Pollut., 305: 119318. https://doi.org/10.1016/j.envpol.2022.119318.

Bardají, D.K.R., Moretto, J.A.S., Furlan, J.P.R. and Stehling, E.G. 2020. A mini-review: current advances in polyethylene biodegradation. World J. Microbiol. Biotechnol., 36(2): 32. https://doi.org/10.1007/s11274-020-2808-5.

Beltrán-Sanahuja, A., Benito-Kaesbach, A., Sánchez-García, N. and Sanz-Lázaro, C. 2021. Degradation of conventional and biobased plastics in soil under contrasting environmental conditions. Sci. Total Environ., 787: 147678. https://doi.org/10.1016/j.scitotenv.2021.147678.

Bianco, A. and Passananti, M. 2020. Atmospheric micro and nanoplastics: An enormous microscopic problem. Sustainability, 12(18): 7327. https://doi.org/10.3390/SU12187327.

Budhiraja, V., Urh, A., Horvat, P. and Krzan, A. 2022. Synergistic adsorption of organic pollutants on weathered polyethylene microplastics. Polymers, 14(13): 2674. https://doi.org/10.3390/polym14132674.

Carlin, J., Craig, C., Little, S., Donnelly, M., Fox, D., Zhai, L. and Walters, L. 2020. Microplastic accumulation in the gastrointestinal tracts in birds of prey in central Florida, USA. Environ. Pollut., 264: 114633. https://doi.org/10.1016/j.envpol.2020.114633.

Chamas, A., Moon, H., Zheng, J., Qiu, Y., Tabassum, T., Jang, J.H., Abu-Omar, M., Scott, S.L. and Suh, S. 2020. Degradation rates of plastics in the environment. ACS Sustain. Chem. Eng., 8(9): 3494-3511. https://doi.org/10.1021/acssuschemeng.9b06635.

Chen, C.C., Dai, L., Ma, L. and Guo, R.T. 2020. Enzymatic degradation of plant biomass and synthetic polymers. Nat. Rev. Chem., 4(3): 114-126. https://doi.org/10.1038/s41570-020-0163-6.

Chen, Y., Liu, X., Leng, Y. and Wang, J. 2020. Defense responses in earthworms (Eisenia fetida) exposed to low-density polyethylene microplastics in soils. Ecotoxicol. Environ. Saf., 187: 109788. https://doi.org/10.1016/j.ecoenv.2019.109788.

Choi, D., Hwang, J., Bang, J., Han, S., Kim, T., Oh, Y., Hwang, Y., Choi, J. and Hong, J. 2021. In vitro toxicity from a physical perspective of polyethylene microplastics based on statistical curvature change analysis. Sci. Total Environ., 752: 142242. https://doi.org/10.1016/j.scitotenv.2020.142242.

Chu, J., Zhou, Y., Cai, Y., Wang, X., Li, C. and Liu, Q. 2023. Flows and waste reduction strategies of PE, PP, and PET plastics under plastic limit order in China. Resour. Conserv. Recycl., 188:106668. https://doi.org/10.1016/j.resconrec.2022.106668.

Cózar, A., Martí, E., Duarte, C. M., García-de-Lomas, J., Van Sebille, E., Ballatore, T. J., Eguíluz, V. M., Ignacio González-Gordillo, J., Pedrotti, M. L., Echevarría, F., Troublè, R. and Irigoien, X. 2017. The Arctic Ocean as a dead end for floating plastics in the North Atlantic branch of the Thermohaline Circulation. Sci. Adv., 3(4): e1600582. https://doi.org/10.1126/sciadv.1600582.

da Costa Araújo, A. P., de Melo, N. F. S., de Oliveira Junior, A. G., Rodrigues, F. P., Fernandes, T., de Andrade Vieira, J. E., Rocha, T. L. and Malafaia, G. 2020. How much are microplastics harmful to the health of amphibians? A study with pristine polyethylene microplastics and Physalaemus cuvieri. J. Hazard. Mater., 382: 121066. https://doi.org/10.1016/j.jhazmat.2019.121066.

Dang, T.C.H., Nguyen, D.T., Thai, H., Nguyen, T.C., Hien Tran, T.T., Le, V.H., Nguyen, V.H., Tran, X B., Thao Pham, T.P., Nguyen, T.G. and Nguyen, Q.T. 2018. Plastic degradation by thermophilic Bacillus sp. BCBT21 isolated from composting agricultural residual in Vietnam. Adv. Nat. Sci. Nanosci. Nanotechnol., 9(1): 015014. https://doi.org/10.1088/2043-6254/aaabaf.

Danso, D., Chow, J. and Streita, W.R. 2019. Plastics: Environmental and biotechnological perspectives on microbial degradation. Appl. Environ. Microbiol., 85(19): e01095-19. https://doi.org/10.1128/AEM.01095-19.

de Assis, G.C., de Jesus, R.A., da Silva, W.T.A., Ferreira, L.F.R, Figueiredo, R.T. and de Oliveira, R.J. 2021. Conversion of plastic waste into supports for nanostructured heterogeneous catalysts: Application in environmental remediation. Surfaces, 5(1): 35-66. https://doi.org/10.3390/surfaces5010002.

Delacuvellerie, A., Cyriaque, V., Gobert, S., Benali, S. and Wattiez, R. 2019. The plastisphere in the marine ecosystem hosts potential specific microbial degraders, including Alcanivorax borkumensis, as a key player in the low-density polyethylene degradation. J. Hazard. Mater., 380: 120899. https://doi.org/10.1016/j.jhazmat.2019.120899.

De-la-Torre, G.E. 2020. Microplastics: An emerging threat to food security and human health. J. Food Sci. Technol., 57(5): 1601-1608. https://doi.org/10.1007/s13197-019-04138-1.

Dhanraj, N.D., Hatha, A.A.M. and Jisha, M. S. 2022. Biodegradation of petroleum-based and bio-based plastics: approaches to increase the rate of biodegradation. Arch. Microbiol., 204(5): 258. https://doi.org/10.1007/s00203-022-02883-0.

Espinosa, C., Esteban, M.Á. and Cuesta, A. 2019. Dietary administration of PVC and PE microplastics produces histological damage, oxidative stress, and immunoregulation in European sea bass (Dicentrarchus labrax L.). Fish Shellfish Immunol., 95: 574-583. https://doi.org/10.1016/j.fsi.2019.10.072.

Fibriarti, B.L., Feliatra, A.B. and Darwis, B. 2021. Biodegradation of LDPE plastic by the local strain of bacillus sp. Isolated from dump soil of Pekanbaru, Indonesia. Biodiversitas, 22(12): 5484-5490. https://doi.org/10.13057/biodiv/d221232.

Fu, Q., Lai, J.L., Ji, X.H., Luo, Z.X., Wu, G. and Luo, X.G. 2022. Alterations of the rhizosphere soil microbial community composition and metabolite profiles of Zea mays by polyethylene-particles of different molecular weights. J. Hazard. Mater., 423(Pt A): 127062. https://doi.org/10.1016/j.jhazmat.2021.127062.

Gao, R. and Sun, C. 2021. A marine bacterial community capable of degrading poly(ethylene terephthalate) and polyethylene. J. Hazard. Mater., 416: 125928. https://doi.org/10.1016/j.jhazmat.2021.125928.

Gaur, V. K., Gupta, S., Sharma, P., Gupta, P., Varjani, S., Srivastava, J. K., Chang, J. S. and Bui, X. T. 2022. Metabolic cascade for remediation of plastic waste: A case study on microplastic degradation. Curr. Pollut. Reports, 8(1): 30-50. https://doi.org/10.1007/s40726-021-00210-7.

Gautam, R., Jo, J. H., Acharya, M., Maharjan, A., Lee, D. E., Pramod, P. B., Kim, C. Y., Kim, K. S., Kim, H. A. and Heo, Y. 2022. Evaluation of potential toxicity of polyethylene microplastics on human-derived cell lines. Sci. Total Environ., 838: 156089. https://doi.org/10.1016/j.scitotenv.2022.156089.

Geyer, R., Jambeck, J.R. and Law, K.L. 2017. Production, use, and fate of all plastics ever made. Sci. Adv., 3(7): 25-29. https://doi.org/10.1126/sciadv.1700782.

Gómez-Méndez, L. D., Moreno-Bayona, D. A., Poutou-Piñales, R.A., Salcedo-Reyes, J.C., Pedroza-Rodríguez, A.M., Vargas, A. and Bogoya, J.M. 2018. Biodeterioration of plasma pretreated LDPE sheets by *Pleurotus ostreatus*. PLoS One, 13(9): e0203786. https://doi.org/10.1371/journal.pone.0203786.

Gupta, K.K., Sharma, K.K. and Chandra, H. 2022. *Micrococcus luteus* strain CGK112 isolated from cow dung demonstrated efficient biofilm-forming ability and degradation potential toward high-density polyethylene (HDPE). Arch. Microbiol., 204(7): 1-13. https://doi.org/10.1007/s00203-022-03023-4.

Guzzetti, E., Sureda, A., Tejada, S. and Faggio, C. 2018. Microplastic in marine organism: Environmental and toxicological effects. Environ. Toxicol. Pharmacol., 64: 164-171. https://doi.org/10.1016/j.etap.2018.10.009.

Hahladakis, J.N., Velis, C.A., Weber, R., Iacovidou, E. and Purnell, P. 2018. An overview of chemical additives present in plastics: Migration, release, fate and environmental impact during their use, disposal, and recycling. J. Hazard. Mater., 344: 179-199. https://doi.org/10.1016/j.jhazmat.2017.10.014.

Hamed, M., Monteiro, C. E. and Sayed, A. E. D. H. 2022. Investigation of the impact caused by different sizes of polyethylene plastics (nano, micro, and macro) in common carp juveniles, *Cyprinus carpio* L., using multi-biomarkers. Sci. Total Environ., 803: 149921. https://doi.org/10.1016/j.scitotenv.2021.149921.

Hamed, M., Soliman, H.A.M., Badrey, A.E.A. and Osman, A.G.M. 2021. Microplastics induced histopathological lesions in some tissues of tilapia (*Oreochromis niloticus*) early juveniles. Tissue Cell, 71: 101512. https://doi.org/10.1016/j.tice.2021.101512.

Han, Y.N., Wei, M., Han, F., Fang, C., Wang, D., Zhong, Y.J., Guo, C.L., Shi, X.Y., Xie, Z.K. and Li, F.M. 2020. Greater biofilm formation and increased biodegradation of polyethylene film by a microbial consortium of *Arthrobacter* sp. and *Streptomyces* sp. Microorganisms, 8(12): 1979. https://doi.org/10.3390/microorganisms8121979.

Hasnat, A. and Rahman, M.A. 2018. A review paper on the hazardous effect of plastic debris on marine biodiversity with some possible remedies. Asian J. Med. Biol. Res., 4(3): 233-241. https://doi.org/10.3329/ajmbr.v4i3.38461.

Hou, L., Xi, J., Liu, J., Wang, P., Xu, T., Liu, T., Qu, W. and Lin, Y.B. 2022. Biodegradability of polyethylene mulching film by two *Pseudomonas* bacteria and their potential degradation mechanism. Chemosphere, 286(3): 131758. https://doi.org/10.1016/j.chemosphere.2021.131758.

Ingavale, RR. and Raut, P.D. 2018. Comparative biodegradation studies of LDPE and HDPE using *Bacillus weihenstephanensis* isolated from garbage soil. Nat. Environ. Pollut. Technol., 17(2): 649-655.

Issac, M.N. and Kandasubramanian, B. 2021. Effect of microplastics in water and aquatic systems. Environ. Sci. Pollut. Res., 28(16): 19544-19562. https://doi.org/10.1007/s11356-021-13184-2.

Jacquin, J., Cheng, J., Odobel, C., Pandin, C., Conan, P., Pujo-Pay, M., Barbe, V., Meistertzheim, A.L. and Ghiglione, J.F. 2019. Microbial ecotoxicology of marine plastic debris: A review on colonization and biodegradation by the "plastisphere". Front. Microbiol., 10: 865. https://doi.org/10.3389/fmicb.2019.00865.

Jaiswal, S., Sharma, B. and Shukla, P. 2020. Integrated approaches in microbial degradation of plastics. Environ. Technol. Innov., 17: 100567. https://doi.org/10.1016/j.eti.2019.100567.

Jeon, J.M., Park, S.J., Choi, T.R., Park, J.H., Yang, Y.H. and Yoon, J.J. 2021. Biodegradation of polyethylene and polypropylene by *Lysinibacillus* species JJY0216 isolated from soil grove. Polym. Degrad. Stab., 191: 109662. https://doi.org/10.1016/j.polymdegradstab.2021.109662.

Kalidas, V.K., Pavendhan, R., Sudhakar, K., Sumanth, T.P., Sharvesh, R.A., Santhosh, K.S. and Yeswanth, K.K. 2021. Study of synthesis and analysis of bio-inspired polymers-review. Mater. Today Proc., 44(5): 3856-3860. https://doi.org/10.1016/j.matpr.2020.12.831.

Karami, A., Golieskardi, A., Choo, C.K., Larat, V., Karbalaei, S. and Salamatinia, B. 2018. Microplastic and mesoplastic contamination in canned sardines and sprats. Sci. Total Environ., 612: 1380-1386. https://doi.org/10.1016/j.scitotenv.2017.09.005.

Karbalaei, S., Hanachi, P., Walker, T.R. and Cole, M. 2018. Occurrence, sources, human health impacts and mitigation of microplastic pollution. Environ. Sci. Pollut. Res., 25(36): 36046-36063. https://doi.org/10.1007/s11356-018-3508-7.

Khalil, A.B., Sivakumar, N., Arslan, M., Saleem, H. and Qarawi, S. 2018. Insights into *Brevibacillus borstelensis* AK1 through whole genome sequencing: A *Thermophilic* Bacterium isolated from a hot spring in Saudi Arabia. Biomed. Res. Int., 2018: 5862437. https://doi.org/10.1155/2018/5862437.

Kopecká, R., Kubínová, I., Sovová, K., Mravcová, L., Vítěz, T. and Vítězová, M. 2022. Microbial degradation of virgin polyethylene by bacteria isolated from a landfill site. SN Appl. Sci., 4(11): 1-12. https://doi.org/10.1007/s42452-022-05182-x.

Lamichhane, G., Acharya, A., Marahatha, R., Modi, B., Paudel, R., Adhikari, A., Raut, B.K., Aryal, S. and Parajuli, N. 2022. Microplastics in environment: global concern, challenges, and controlling measures. Int. J. Environ. Sci. Technol., 20: 4673-4694.. https://doi.org/10.1007/s13762-022-04261-1.

Lau, W.W.Y., Shiran, Y., Bailey, R.M., Cook, E., Stuchtey, M.R., Koskella, J., Velis, C.A., Godfrey, L., Boucher, J., Murphy, M.B., Thompson, R.C., Jankowska, E., Castillo, A.C., Pilditch, T.D., Dixon, B., Koerselman, L., Kosior, E., Favoino, E., Gutberlet, J.and Palardy, J.E. 2020. Evaluating scenarios toward zero plastic pollution. Science, 369(6509): 1455-1461. https://doi.org/10.1126/SCIENCE.ABA9475.

Li, Z., Wei, R., Gao, M., Ren, Y., Yu, B., Nie, K., Xu, H. and Liu, L. 2020. Biodegradation of low-density polyethylene by *Microbulbifer hydrolyticus* IRE-31. J. Environ. Manage., 263: 110402. https://doi.org/10.1016/j.jenvman.2020.110402.

Maraveas, C. 2020. Environmental sustainability of plastic in agriculture. Agriculture, 10(8): 310. https://doi.org/10.3390/agriculture10080310.

Maroof, L., Khan, I., Hassan, H., Azam, S. and Khan, W. 2022. Microbial degradation of low-density polyethylene by Exiguobacterium sp. strains LM-IK2 isolated from plastic dumped soil. World J. Microbiol. Biotechnol., 38(11): 1-9. https://doi.org/10.1007/s11274-022-03389-z.

Mercy, F.T., Alam, A.K.M.R. and Akbor, M.A. 2023. Abundance and characteristics of microplastics in major urban wetlands of Dhaka, Bangladesh. Heliyon, 9(4): e14587. https://doi.org/10.1016/j.heliyon.2023.e14587.

Mistretta, M. C., Mantia, F. P. La, Titone, V., Botta, L., Pedeferri, M. and Morreale, M. 2020. Effect of ultraviolet and moisture action on biodegradable polymers and their blend. J. Appl. Biomater. Funct. Mater., 18: 1-8. https://doi.org/10.1177/2280800020926653.

Mohanrasu, K., Premnath, N., Prakash, G.S., Sudhakar, M., Boobalan, T. and Arun, A. 2018. Exploring multi potential uses of marine bacteria; an integrated approach for PHB production, PAHs and polyethylene biodegradation. J. Photochem. Photobiol. B: Biol., 185: 55-65. https://doi.org/10.1016/j.jphotobiol.2018.05.014.

Montazer, Z., Habibi-Najafi, M.B., Mohebbi, M. and Oromiehei, A. 2018. Microbial degradation of UV-pretreated low-density polyethylene films by novel polyethylene-degrading bacteria isolated from plastic-dump soil. J. Polym. Environ., 26(9): 3613-3625. https://doi.org/10.1007/s10924-018-1245-0.

Muhonja, C.N., Makonde, H., Magoma, G. and Imbuga, M. 2018. Biodegradability of polyethylene by bacteria and fungi from Dandora dumpsite Nairobi- Kenya. PLoS One, 13(7): 1-17. https://doi.org/10.1371/journal.pone.0198446.

Mytum, H. and Meek, J. 2021. The iron age in the plastic age: Anthropocene signatures at Castell Henllys. Antiquity, 95(379): 198-214. https://doi.org/10.15184/aqy.2020.237

Nadeem, H., Alia, KB., Muneer, F., Rasul, I., Siddique, M.H., Azeem, F. and Zubair, M. 2021. Isolation and identification of low-density

polyethylene degrading novel bacterial strains. Arch. Microbiol., 203(9): 5417-5423. https://doi.org/10.1007/s00203-021-02521-1.

Nademo, Z.M., Shibeshi, N.T. and Gemeda, M.T. 2023. Isolation and screening of low-density polyethylene (LDPE) bags degrading bacteria from Addis Ababa municipal solid waste disposal site "Koshe." Ann. Microbiol., 73(1): 1-11. https://doi.org/10.1186/s13213-023-01711-0.

Nag, M., Lahiri, D., Dutta, B., Jadav, G. and Ray, R. R. 2021. Biodegradation of used polyethylene bags by a new marine strain of Alcaligenes faecalis LNDR-1. Environ. Sci. Pollut. Res., 28(30): 41365-41379. https://doi.org/10.1007/s11356-021-13704-0.

Namgay, T. 2020. Nation's waste on the scale: The first Bhutan waste inventory report. Stat. J. IAOS, 36(4): 915-924. https://doi.org/10.3233/SJI-200742.

Nourollahi, A., Sedighi-Khavidak, S., Mokhtari, M., Eslami, G. and Shiranian, M. 2019. Isolation and identification of low-density polyethylene (LDPE) biodegrading bacteria from waste landfill in Yazd. Int. J. Environ. Stud., 76(2): 236-250. https://doi.org/10.1080/00207233.2018.1551986.

Novotný, Č., Malachová, K., Adamus, G., Kwiecień, M., Lotti, N., Soccio, M., Verney, V. and Fava, F. 2018. Deterioration of irradiation/high-temperature pretreated, linear low-density polyethylene (LLDPE) by Bacillus amyloliquefaciens. Int. Biodeterior. Biodegrad., 132: 259-267. https://doi.org/10.1016/j.ibiod.2018.04.014.

Peng, B. Y., Li, Y., Fan, R., Chen, Z., Chen, J., Brandon, A. M., Criddle, C. S., Zhang, Y. and Wu, W. M. 2020. Biodegradation of low-density polyethylene and polystyrene in superworms, larvae of Zophobas atratus (Coleoptera: Tenebrionidae): Broad and limited extent depolymerization. Environ. Pollut., 266: 115206. https://doi.org/10.1016/j.envpol.2020.115206.

Plastics Europe. 2021. Plastics the Fact 2021. An analysis of European plastics production, demand and waste data. https://plasticseurope.org/.

Priya, A., Dutta, K. and Daverey, A. 2022. A comprehensive biotechnological and molecular insight into plastic degradation by microbial community. J. Chem. Technol. Biotechnol., 97(2): 381-390. https://doi.org/10.1002/jctb.6675.

Proshad, R., Kormoker, T., Islam, M.S., Haque, M.A., Rahman, M.M. and Mithu, M.M.R. 2018. Toxic effects of plastic on human health and environment : Consequences of health risk assessment in Bangladesh. Int. J. Health, 6(1): 1-5. https://doi.org/10.14419/ijh.v6i1.8655.

Rahman, A., Sarkar, A., Yadav, O.P., Achari, G. and Slobodnik, J. 2021. Potential human health risks due to environmental exposure to nano- and microplastics and knowledge gaps: A scoping review. Sci. Total Environ., 757: 143872. https://doi.org/10.1016/j.scitotenv.2020.143872.

Rani, A., Singh, P. and Kumar, R. 2020. Microbial deterioration of high-density polyethylene by selected microorganisms. J. Appl. Biol. Biotechnol., 8(6): 64-66. https://doi.org/10.7324/JABB.2020.80611.

Renzi, M. and Blašković, A. 2018. Litter and microplastics features in table salts from marine origin: Italian versus Croatian brands. Mar. Pollut. Bull., 135: 62-68. https://doi.org/10.1016/j.marpolbul.2018.06.065.

Rubio, L., Marcos, R. and Hernández, A. 2020. Potential adverse health effects of ingested micro- and nanoplastics on humans. Lessons learned from in vivo and in vitro mammalian models. J. Toxicol. Environ. Health - Part B Crit. Rev., 23(2): 51-68. https://doi.org/10.1080/10937404.2019.1700598.

Saritha, B., Sindgi, S.A. and Remadevi, O.K. 2021. Plastic degrading microbes: A Review. Microbiol. Res. J. Int., 22: 28. https://doi.org/10.9734/mrji/2021/v31i630324.

Sarmah, P. and Rout, J. 2018. Efficient biodegradation of low-density polyethylene by cyanobacteria isolated from submerged polyethylene surface in domestic sewage water. Environ. Sci. Pollut. Res., 25(33): 33508-33520. https://doi.org/10.1007/s11356-018-3079-7.

Sarmah, P. and Rout, J. 2019. Cyanobacterial degradation of low-density polyethylene (LDPE) by Nostoc carneum isolated from submerged

polyethylene surface in domestic sewage water. Energy Ecol. Environ., 4(5): 240-252. https://doi.org/10.1007/s40974-019-00133-6.

Schwabl, P., Koppel, S., Konigshofer, P., Bucsics, T., Trauner, M., Reiberger, T. and Liebmann, B. 2019. Detection of various microplastics in human stool: A prospective case series. Ann. Intern. Med., 171(7): 453-457. https://doi.org/10.7326/M19-0618.

Shao, H., Chen, M., Fei, X., Zhang, R., Zhong, Y., Ni, W., Tao, X., He, X., Zhang, E., Yong, B. and Tan, X. 2019. Complete genome sequence and characterization of a polyethylene biodegradation strain, Streptomyces albogriseolus LBX-2. Microorganisms, 7(10): 379. https://doi.org/10.3390/microorganisms7100379.

Shrestha, J.K., Joshi, D.R., Regmi, P. and Badahit, G. 2019. Isolation and identification of low-density polyethylene (LDPE) degrading Bacillus spp. from a soil of landfill site. Acta Sci. Microbiol., 2(4): 30-34. https://www.researchgate.net/publication/331702789.

Sintim, H.Y., Bandopadhyay, S., English, M.E., Bary, A.I., Debruyn, J.M., Schaeffer, S.M., Miles, C.A., Reganold, J.P., and Flury, M. 2019. Agriculture, ecosystems and environment impacts of biodegradable plastic mulches on soil health. Agric. Ecosyst. Environ., 273: 36-49. https://doi.org/10.1016/j.agee.2018.12.002.

Šišková, A. O., Peer, P., Andicsová, A. E., Jordanov, I. and Rychter, P. 2021. Circulatory management of polymer waste: Recycling into fine fibers and their applications. Materials, 14(16): 4694. https://doi.org/10.3390/ma14164694.

Skariyachan, S., Manjunatha, V., Sultana, S., Jois, C., Bai, V. and Vasist, K.S. 2016. Novel bacterial consortia isolated from plastic garbage processing areas demonstrated enhanced degradation for low density polyethylene. Environ. Sci. Pollut. Res., 23(18): 18307-18319. https://doi.org/10.1007/s11356-016-7000-y.

Soleimani, Z., Gharavi, S., Soudi, M. and Moosavi-Nejad, Z. 2021. A survey of intact low-density polyethylene film biodegradation by terrestrial Actinobacterial species. Int. Microbiol., 24(1): 65-73. https://doi.org/10.1007/s10123-020-00142-0.

Souza, P.M.S., Coelho, F.M., Sommaggio, L.R.D., Marin-Morales, M. A. and Morales, A.R. 2019. Disintegration and biodegradation in soil of pbat mulch films: Influence of the stabilization systems based on carbon black/hindered amine light stabilizer and carbon black/vitamin E. J. Polym. Environ., 27(7): 1584-1594. https://doi.org/10.1007/s10924-019-01455-6.

Sullivan, C., Thomas, P., Stuart, B., Sullivan, C., Thomas, P. and Stuart, B. 2018. An atomic force microscopy investigation of plastic wrapping materials of forensic relevance buried in soil environments. Aust. J. Forensic Sci., 51(5): 596-605. https://doi.org/10.1080/00450618.2018.1450893.

Syranidou, E., Karkanorachaki, K., Amorotti, F., Repouskou, E., Kroll, K., Kolvenbach, B., Corvini, P.F.X., Fava, F. and Kalogerakis, N. 2017. Development of tailored indigenous marine consortia for the degradation of naturally weathered polyethylene films. PLoS One, 12(8): e0183984. https://doi.org/10.1371/journal.pone.0183984.

Szlachetka, O., Witkowska-Dobrev, J., Baryła, A. and Dohojda, M. 2021. Low-density polyethylene (LDPE) building films – tensile properties and surface morphology. J. Build. Eng., 44: 103386. https://doi.org/10.1016/j.jobe.2021.103386.

Taghavi, N., Udugama, I.A., Zhuang, W.Q. and Baroutian, S. 2021. Challenges in biodegradation of non-degradable thermoplastic waste: From environmental impact to operational readiness. Biotechnol. Adv., 49: 107731. https://doi.org/10.1016/j.biotechadv.2021.107731.

Tamoor, M., Samak, N. A., Jia, Y., Mushtaq, M. U., Sher, H., Bibi, M. and Xing, J. 2021. Potential use of microbial enzymes for the conversion of plastic waste into value-added products: A viable solution. Front. Microbiol., 12: 777727. https://doi.org/10.3389/fmicb.2021.777727.

Tareen, A., Saeed, S., Iqbal, A., Batool, R. and Jamil, N. 2022. Biodeterioration of microplastics: A promising step towards plastics waste management. Polymers, 14(11): 2275. https://doi.org/10.3390/polym14112275.

Teboul, E., Orihel, D.M., Provencher, J.F., Drever, M.C., Wilson, L. and Harrison, A.L. 2021. Chemical identification of microplastics ingested by red phalaropes (*Phalaropus fulicarius*) using Fourier transform infrared spectroscopy. Mar. Pollut. Bull., 171: 112640. https://doi.org/10.1016/j.marpolbul.2021.112640.

Tharayil, A., Banerjee, S. and Kar, K. K. 2019. Dynamic mechanical properties of zinc oxide reinforced linear low-density polyethylene composites. Mater. Res. Express, 6(5): 2-30. https://doi.org/https://doi.org/10.1088/2053-1591/aaff8b.

Tu, C., Chen, T., Zhou, Q., Liu, Y., Wei, J., Waniek, J. J. and Luo, Y. 2020. Biofilm formation and its influences on the properties of microplastics as affected by exposure time and depth in the seawater. Sci. Total Environ., 734: 139237. https://doi.org/10.1016/j.scitotenv.2020.139237.

Urbanek, A.K., Rymowicz, W. and Miro, A.M. 2018. Degradation of plastics and plastic-degrading bacteria in cold marine habitats. Appl. Microbiol. Biotechnol., 102(18): 7669-7678. https://doi.org/10.1007/s00253-018-9195-y.

Varyan, I., Tyubaeva, P., Kolesnikova, N. and Popov, A. 2022. Biodegradable polymer materials based on polyethylene and natural rubber: Acquiring, investigation, properties. Polymers, 14(12): 2457. https://doi.org/10.3390/polym14122457.

Venkatesan, R., Santhamoorthy, M., Alagumalai, K., Haldhar, R., Raorane, C. J., Raj, V. and Kim, S. C. 2022. Novel approach in biodegradation of synthetic thermoplastic polymers: An overview. Polymers, 14(20): 4271. https://doi.org/10.3390/polym14204271.

Wang, Y., Lee, Y., Chiu, I. and Lin, Y. 2020. Potent impact of plastic nanomaterials and micromaterials on the food chain and human health. Int. J. Mol. Sci., 21(5): 1757. https://doi.org/10.3390/ijms21051727.

Waqas, M., Haris, M., Asim, N., Islam, H., Abdullah, A., Khan, A., Khattak, H., Waqas, M. and Ali, S. 2021. Biodegradable potential of *Bacillus amyloliquefaciens* and *Bacillus safensis* using low density polyethylene thermoplastic (LDPE) substrate. Eur. J. Environ. Public Health, 5(2): em0069. https://doi.org/10.21601/ejeph/9370.

Windheim, J., Colombo, L., Battajni, N.C., Russo, L., Cagnotto, A., Diomede, L., Bigini, P., Vismara, E., Fiumara, F., Gabbrielli, S., Gautieri, A., Mazzuoli-Weber, G., Salmona, M. and Colnaghi, L. 2022. Micro- and nanoplastics' effects on protein folding and amyloidosis. Int. J. Mol. Sci., 23(18): 10329. https://doi.org/10.3390/ijms231810329.

Worm, B., Lotze, H. K., Jubinville, I., Wilcox, C. and Jambeck, J. 2017. Plastic as a persistent marine pollutant. Annu. Rev. Environ. Resour., 42: 1-26. https://doi.org/10.1146/annurev-environ-102016-060700

Ya, H., Jiang, B., Xing, Y., Zhang, T., Lv, M. and Wang, X. 2021. Recent advances on ecological effects of microplastics on soil environment. Sci. Total Environ., 798: 149338. https://doi.org/10.1016/j.scitotenv.2021.149338.

Zadjelovic, V., Gibson, M.I., Dorador, C. and Christie-Oleza, J.A. 2020. Genome of *Alcanivorax* sp. 24: A hydrocarbon degrading bacterium isolated from marine plastic debris. Mar. Genomics, 49: 0–1. https://doi.org/10.1016/j.margen.2019.05.001.

Zarus, G.M., Muianga, C., Hunter, C.M. and Pappas, R.S. 2021. A review of data for quantifying human exposures to micro and nanoplastics and potential health risks. Sci. Total Environ., 756: 144010. https://doi.org/10.1016/j.scitotenv.2020.144010.

Zhang, S., Han, B., Sun, Y. and Wang, F. 2020. Microplastics influence the adsorption and desorption characteristics of Cd in an agricultural soil. J. Hazard. Mater., 388: 121775. https://doi.org/10.1016/j.jhazmat.2019.121775.

Zhang, Y., Pedersen, J.N., Eser, B.E. and Guo, Z. 2022. Biodegradation of polyethylene and polystyrene: From microbial deterioration to enzyme discovery. Biotechnol. Adv., 60: 107991. https://doi.org/10.1016/j.biotechadv.2022.107991.

Zhao, S., Pei, L., Li, H., Zhang, X., Hu, W., Zhao, G. and Wang, Z. 2020. Enhanced comprehensive properties of polybenzoxazine via tailored hydrogen bonds. Polymer, 201: 122647. https://doi.org/10.1016/j.polymer.2020.122647.

Recycling Practices of E-Waste and Associated Challenges: A Research Trends Analysis

Jit Das* and Arpita Ghosh**† iD

*Department of Biotechnology, National Institute of Technology Durgapur, Durgapur-713209, India
**Indian Institute of Management Sirmaur, Paonta Sahib, Punjab India
†Corresponding author: Arpita Ghosh; arpita.ghosh@iimsirmaur.ac.in

ABSTRACT

In this fast-moving world, we use many electronic items daily to fulfill our daily work. Also, in the fast-growing economy, electronic items play key roles. India's e-waste is projected to be around 18 lakh metric tons. According to industry sources, electronic trash will climb to almost 50 lakh metric tons in the next three years. According to government sources, only ten percent of electronic waste is gathered. These electronic items and batteries contain many heavy metals that are hazardous to humanity's and the environment's health. These heavy metals should be retrieved from the disposed of e-waste, so the resource can be reused or recycled, rather than continuously extracting heavy metals from the earth's crust. In 2015, The "Initiative on Environmental Threats of Electronic Waste" was introduced by the Ministry of Electronics and Information Technology (MeitY). This project is part of the Indian government's 'Digital India' strategy. There is an immediate need to implement green supply chain management and resource recovery from electronics waste so that circular material management (SDG 12) & sustainability can be achieved. This article demonstrates the problems and presents E-Waste recycling procedures, Life cycle assessment of E-waste, and EPR practices, along with potential areas for improvement. The bibliometric analysis was performed using R-studio biblioshiny tools for the last 53 years and 1243 published articles to understand the research trends.

INTRODUCTION

Large volumes of e-waste have caused worldwide issues, including degradation of the environment and food chains, mineral shortages, and a significant risk to human health. Metal and metalloid buildup in people can cause bodily harm: copper can harm the liver, and lead can affect a person's behavior and ability to learn. Lung cancer and kidney damage risk are increased by cadmium exposure (Gao et al. 2019). Because Guiyu is China's e-waste recycling town, statistical analysis revealed that children living there had considerably increased blood mercury levels compared to Chendian residents (p < 0.01) (Huo et al. 2007). The early findings show that in soil from a Guiyu printing rolling waste dump, the overall amount of polycyclic aromatic hydrocarbons (PAHs) was 595 g.kg^{-1} dry weight (dry wt.) and 514 g.kg^{-1} in silt from a crane lake (dry wt.) of Guiyu. The number of polychlorinated biphenyls (743 g.kg^{-1}) in drainage from the Lianjiang River was discovered to be close to three times

the 277 g.kg^{-1} Canadian Environmental Quality Guidelines likely impact guideline (Leung et al. 2006).

Electronic waste makes the biggest universal waste problem. According to United Nations worldwide, approximately 53.6 metric tons of electronic waste are produced (Forti et al. 2020). Approx. 25% of e-waste is recycled formally in centers located in Asia & Africa (Perkins et al. 2014). Most of the waste disposal is either unknown or done at home. This leads to adverse health effects for residents in developing countries like India, China, Bangladesh, Pakistan, Ghana, and Kenya. There are 13 types of e-waste, cell phones being the largest. The others include washing machines, refrigerators, computers, televisions, and air conditioners. The market would increase due to emerging products like Fitbits, Bluetooth gadgets, and technological advancements.

Valuable metals recuperation is mindboggling to companies due to their endless mechanical applications in different industries, huge market costs, and the constrained resource of these metals. E-waste and used converters have various hazardous elements in addition to precious metals (e.g.,

toxic metals, smokeless materials, and organic compounds). These hazardous substances might contaminate the earth and groundwater and affect people's health; with the increment in environmental awareness, the disposal of unsafe waste has become a significant concern for industries and governments. Recouping and reusing a few industrial wastes containing metals (Au, Ag, Pt, Pd, Rh, etc.) is assessed as a financial and environmental security opportunity (Castro & Bassin 2022).

The amazing physical and chemical characteristics of precious metals (PMs), such as their capacity for catalysis, exceptional electrical conductivity, and corrosion resistance, have led to a wide range of applications. Electronics (e-waste) and the catalyst business, which utilize more than 90% of precious metals, are the two key sectors needed. Electronic garbage, or "e-waste," has been produced in enormous quantities in recent years due to device obsolescence. In the electronics industry, contacts, bonding wires, and switches are made of gold, silver, and palladium, while hard disc drives are made of this metal. 2015 experienced 254 tons, 12,816 tons, and 40.18 tons, respectively, increased demand for gold, silver, and palladium in electronics worldwide. By 2016, there has been an approximate global e-waste production of 44.7 million tons (Mt) (Ilankoon et al. 2018). In sum, only around 20% of the e-waste was adequately processed; 71 tons of gold, 3275 tons of silver, and 15 tons of palladium were recycled in 2016. (Onete et al. 2018).

Fig. 1 shows generated electronic garbage globally from 2010 to 2019 (in a million metric tons). It is rapidly increasing; in 2019, the e-waste was 53.6 million metric tons (Statista 2020).

Valuable metals are often used as dynamic components in the catalyst industry. Most catalysts are employed in refining oil, fine chemicals, medicines, and automotive exhaust. Additionally, the net PGM (elements gather in platinum) utilizations are even now quite expensive because of the booming car and other catalytic industries. Catalytic converters used over 66% of palladium (182.64 tons), 44% of platinum (98 tons), and 84% of rhodium (25.7 tons) (Onete et al. 2018). Many analysts have been investigating replacement materials to reduce the need for expensive metals in products. Different catalysts were used, and the number of valuable metals changed from 200 ppm to 100%. Catalysts also have a variety of carrier materials, which complicate attempts to reuse them.

However, valuable metal concentrations in Troposphere are negligible, with the majority below 0.01 ppm. Over 30% PGMs were recovered for used catalysts, specifically 35 tons of Pt, 60 tons of Pd, and 7 tons of Rh (USGS 2017). It was shown that potentials processed the majority of e-waste before being placed in landfills or basic recycling systems. A scarcity of professional recyclers, problems with the dependability of remanufactured devices, and harmful impacts on the climate and people's life are also associated with illegal e-waste management (Chi et al. 2011). E-waste can be harmful, is not recyclable, and builds up in the land, air, water, and other living things in the environment. In recovering precious items from electronic components, open-air burning and acid baths are two methods that emit harmful substances into the atmosphere and adversely affect people's health. These effects include cancer, miscarriages,
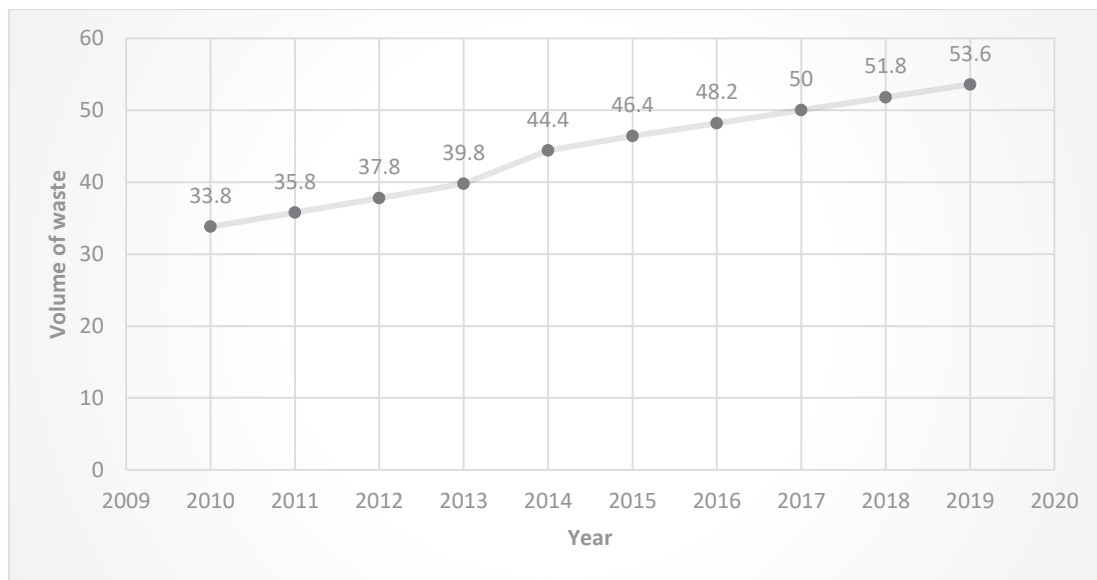

Fig. 1: Produced electronic garbage globally from 2010 to 2019 (in a million metric tons) (Statista 2020).

neurological damage, and lowered IQs. It is important to take into account how technological products affect climate change. Every piece of machinery created has a carbon output, leading to human-caused global climate change. Most CO_2 emitted over a device's lifetime happens during manufacturing before a client buys a product. Reducing carbon production techniques and inputs—such as using recycled raw materials and product lifespans—are key factors in determining the total environmental effect. According to Brianna (2022), between 2014 and 2020, the release of greenhouse gases from electronic gadgets and the trash they produce rose by 53%. According to the experts, this involves 580 metric tons of carbon dioxide in 2020. They predict that by 2030, e-waste sources will be responsible for the yearly emission of around 852 million metric tons of CO_2 compounds if there is no legislation or legal framework to extend the usable life of information and communication technology (ICT) equipment (Brianna 2022).

This article discusses the current practices of recycling E-Waste and challenges along with the improvement scopes. A bibliometric analysis was conducted in the current study to reveal the underlying trends in research publications concerning e-waste. An analysis of the top nations, journals, authors, academic institutions, and keyword co-occurrences is presented using the Scopus database.

MATERIALS AND METHODS

A bibliometric analysis was conducted for the current study to reveal the underlying trends in research publications on e-waste. An analysis of the top nations, journals, authors, academic institutions, and co-occurrences of keywords is presented using data from the famous research database Scopus.' With the keywords "Electronic waste" in the article title, a total of 1853 documents were found in the Scopus database. Further, filtering criteria were used, like only articles and the year 2023 was excluded from the search. The search was performed on 29th November 2022. The bibliometric analysis was performed using the R-studio software Biblioshiny module. A total of 1243 articles were found with these filtering criteria from 1969 to 2022 (last 53 years), 518 publication sources, and 3709 authors with an annual growth rate of 9.55% (Fig. 2). Fig. 3 shows the publication rate annually in the 'Electronic waste' domain. Fig. 4 shows the most relevant journal sources in the 'Electronic waste domain. Waste Management (81 articles) has been shown as a prominent journal in this domain focusing on E-waste management.

Fig. 5 shows the most relevant authors in the 'Electronic waste' domain. Wang, J, Xu, X, Zhang, and Y are the most influential authors in the field. Each of them has published 20

research articles. Fig. 6 shows the most relevant affiliations in the 'Electronic waste' domain. Guangzhou Institute of Geochemistry (90 published articles) is the most prominent affiliation in the research area of e-waste.

Table 1 shows the most influential published articles in this domain, along with the influential authors' names, their countries, citations per year, and journal names. In the Electronic waste research domain, most citations were received from the article Strategies to managing electronic waste: An summary written by Kiddee et al. (2013) from the University of South Australia, Australia.

Fig. 7 shows the most cited countries in the 'Electronic waste' domain. China is more focused in this area than other countries. Hence other countries need to come forward for more collaborative research work to enhance the handling of e-waste. Fig. 8 shows the most occurred words in the 'Electronic trash' domain. E-waste, Recycling, waste management, electronic machinery, China, and waste disposal are mostly co-occurring words in this research domain.

RESULTS AND DISCUSSION

E-waste has become increasingly significant as precious metals supplier. The most significant use of precious metals in the economy is in the electronics and catalysts sectors, which account for almost 90% of total consumption. Recycling valuable metals from alternative resources is crucial because of disputes over finite natural resources, rising demand, and the importance of valuable metals to the economy. In recent years, electronic devices that have outlived their usefulness have generated enormous amounts of electronic trash (also known as e-waste). The total volume of electronic garbage produced worldwide in 2016 was 44.8 million tons (Mt) (Baldé et al. 2017). An estimated 30% of the world's mining output during the past ten years was from recycled precious metals. Research into creating efficient recycling methods for valuable metals, notably from e-waste and used catalytic systems, has increased during the past ten years. Environment-friendly precious metal recycling technologies have steadily emerged. Several methodologies have been developed to manage e-waste, particularly in industrialized nations. These include Life Cycle Assessment (LCA), Material Flow Analysis (MFA), Multi-Criteria Analysis (MCA), and Extended Producer Responsibility (EPR) (Kiddee et al. 2013).

Based on current technology, numerous methods for recycling precious metals have been considerably enhanced. Precious metal losses should be kept to a minimum because they have the highest value in the recycling of e-waste. However, in e-waste industrial processing, valuable metals

Table 1: The most influential published articles in the electronic waste domain.

Title	First Author	Affiliation	Country	Total Citations	TC per Year	Journal name	Year
Challenges, facilitators, and governmental considerations in the use of circular economy ideas in the electrical and electronic equipment (EEE) area	Vasileios Rizos Rizos and Bryhn (2022)	Centre for European Policy Studies (CEPS)	Belgium	17	17	Journal of Cleaner Production	2022
Study on medical waste tracking: Historical development, contemporary issues, and ideas on the transformation to a circular economy	Meisam Ranjbari Ranjbari et al. (2022)	Henan Agricultural University	China	41	41	Journal of Hazardous Materials	2022
To use the grey-theory and DEMATEL paradigm to evaluate the e-waste reduction solutions	Chandra Prakash Garg Garg (2021)	Indian Institute of Management Rohtak	India	57	28.5	Journal of Cleaner Production	2021
An assessment focusing on the treatment of electronic trash in the EU regarding behavior interventions for the circular economy	Keshav Parajuly Parajuly et al. (2020)	United Nations University	Germany	75	25	Resources, Conservation & Recycling	2020
Strategies to managing disposal: A summary	Peeranart Kiddee Kidee et al. (2013)	University of South Australia	Australia	466	46.6	Waste management	2013
Kids in Guiyu, a Chinese town that recycles disposal, had higher serum levels	Xia Huo Huo et al. (2007)	Shantou University Medical College	China	423	26.44	Environmental Health Perspectives	2007
Analysis of U.S. Facilities and technological solutions for reusing electronic trash	Hai-Yong Kang Kang and Schoenung (2005)	University of California	USA	397	22.06	Resources, Conservation, and Recycling	2005

are disseminated throughout each resulting process. With no mechanical processing, almost all precious metals and other significant metals can be recovered through direct smelting. Fume treatment needs to receive a lot of attention because this process may produce dangerous gases (such as dioxins and bromide). When working with used catalysts, metallic stage concentrations of valuable metals might minimize the reagents required for the subsequent dissolving and purifying processes. Hydrometallurgical, economic, and creative approaches have been devised to significantly lessen the

Main Information

Fig. 2: Main information of the Scopus (.csv) file used for bibliometric analysis.

Annual Scientific Production
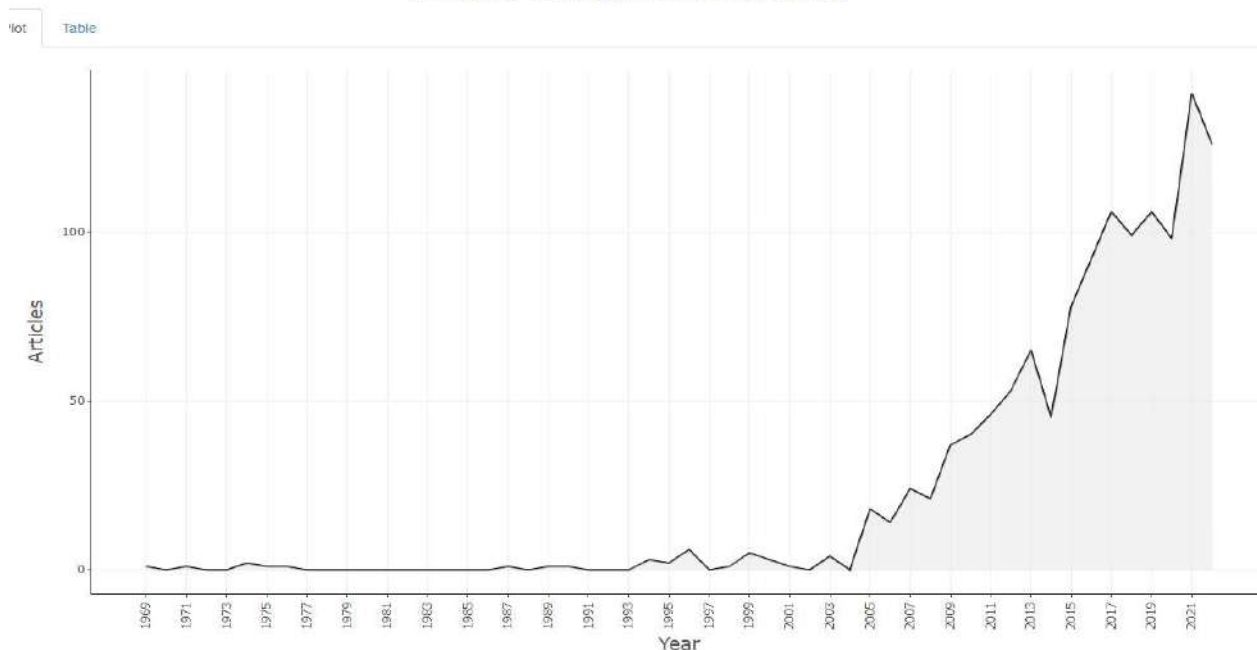
Fig. 3: Publication rate annually in the 'Electronic waste' domain.
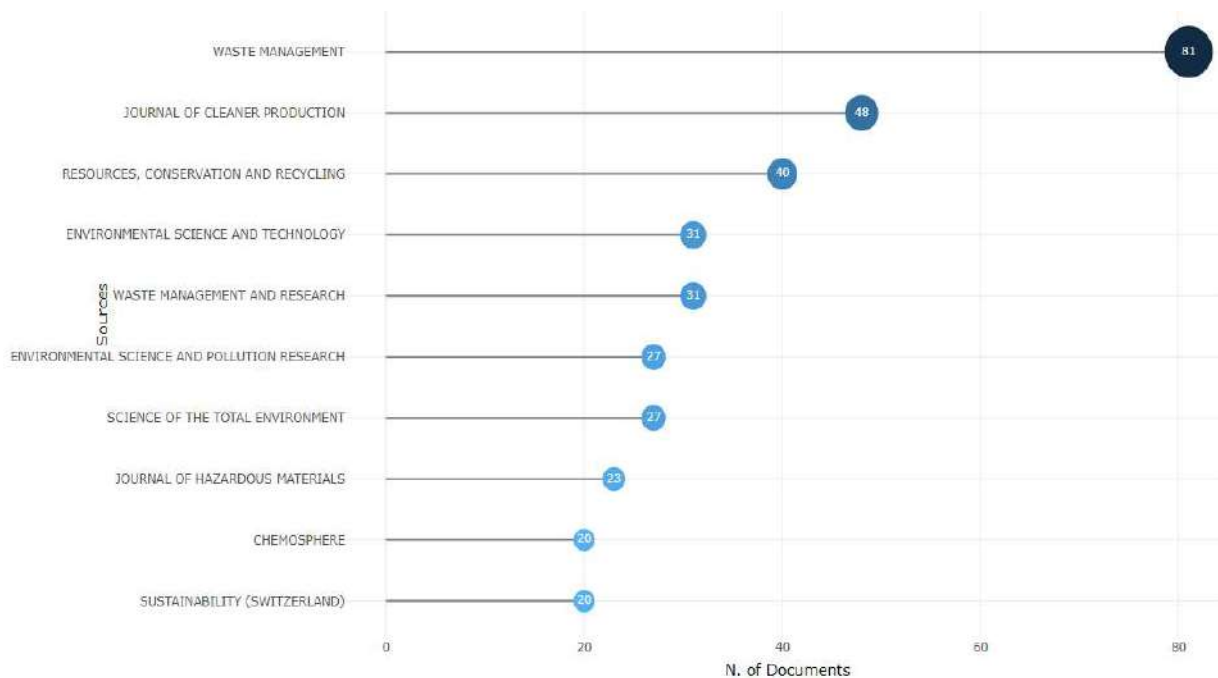
Fig. 4: Most relevant journal sources in the 'Electronic waste' domain.
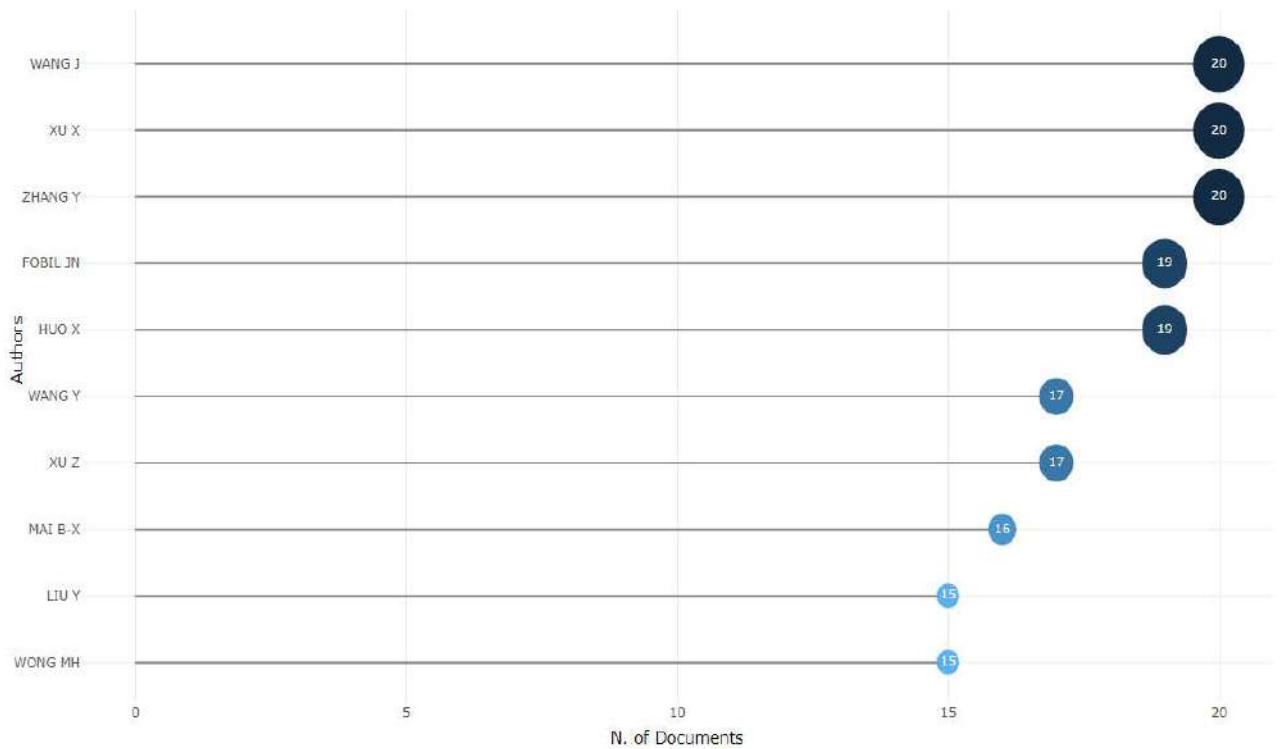
Fig. 5: Most relevant authors in the 'Electronic waste' domain.

Fig. 6: Most relevant affiliations in the 'Electronic waste' domain.
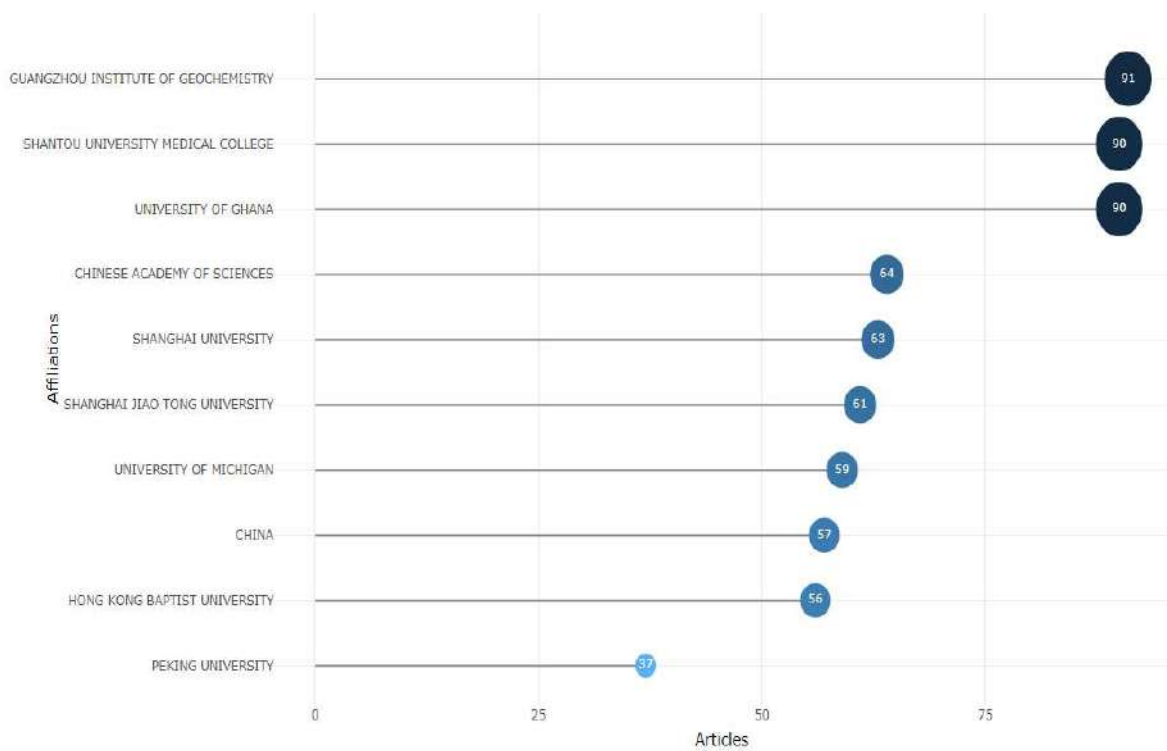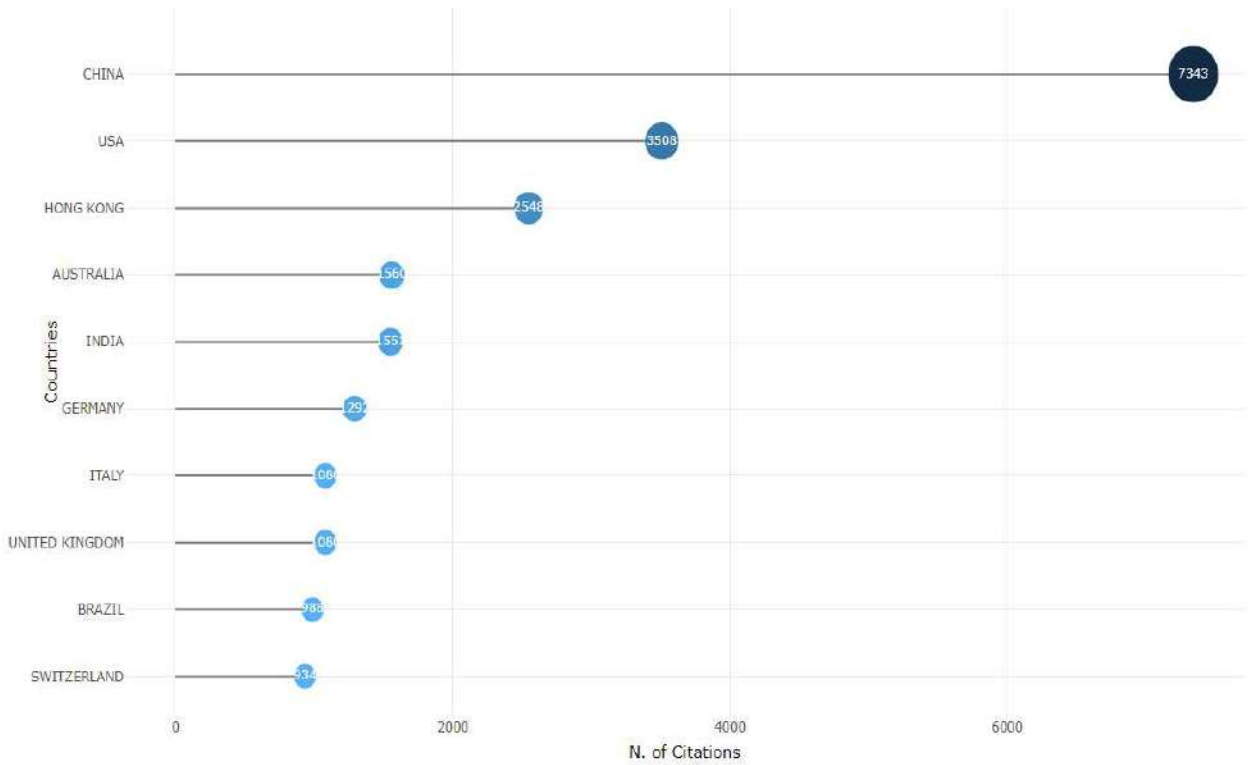
Fig. 7: Most cited countries in the 'Electronic waste' domain.
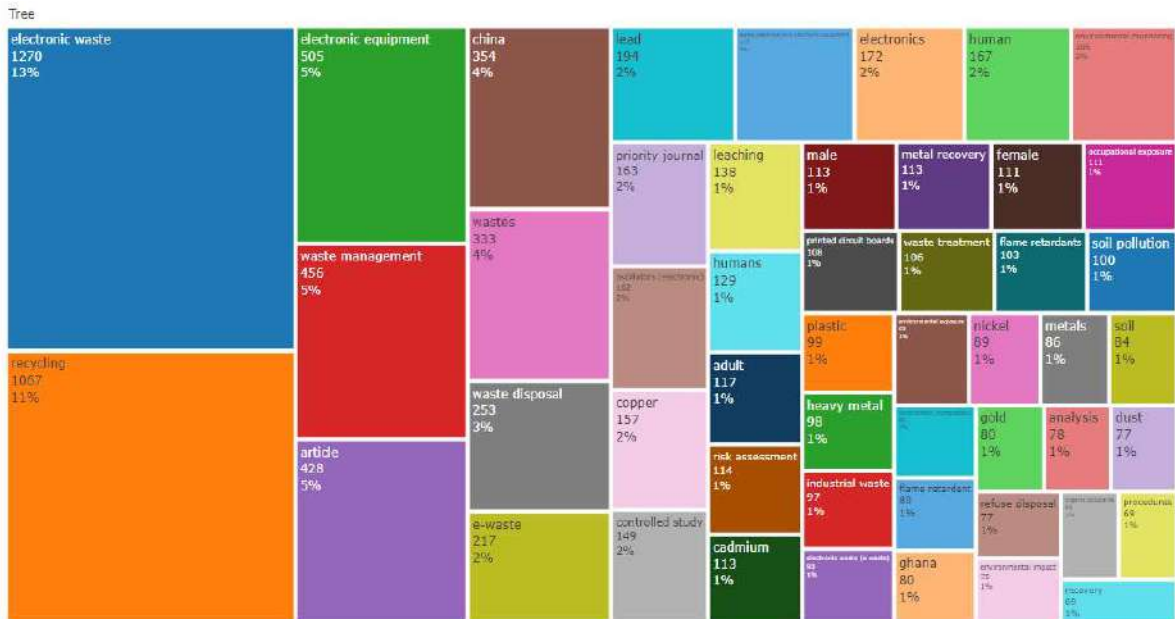
Fig. 8: Most occurred words in the 'Electronic waste' domain.

influence on the environment. Some cyanide-free lixiviants that have shown the ability to leach precious metals include S_2O_3, CH_4N_2S, chlorination, iodine-iodide, and HCl in the influence of an oxidizing agent (Ding et al. 2019).

E-waste importation and recycling have increased manifold in a decade in China, so their government has passed regulations to ensure imported e-waste is reduced and disappears by 2023. Per head, the estimated yearly generated e-waste is 5 kg per Chinese whereas 29.5 kg per US citizen (Li & Achal 2020). Guiyu, a town in China, is famous for the informal disassembling and recycling of e-waste, which supports the livelihood of locals. It gives rise to other problems like increasing social gaps. The e-waste contributes to a large Chinese GNP, leading to the involvement of Chinese children in informal e-waste disposal at home by dumping and burning in the backyard. Due to this, the Chinese government has wisely stepped in to streamline and regulate the e-waste disposal sector by bringing in more awareness, regulations, and funds from governments and NGOs. China launched plants in 29 provinces over a decade for formal e-waste disposal. Workers directly involved with e-waste disposal without proper protection have serious health risks. However, informal recycling leads to regaining valuable materials, which can be greedy for workers. This informal disposal also leads to the release of more air pollutants which enter the water and soil, too, thus indirectly entering the human body and affecting aquatic life. The plastics used in gadgets are complicated to process, and studies indicate that heavy metals enter the food chain through vegetables and aquatic life and can increase in the body.

Additionally, burning and disposal leads to releasing POPS, PCBs, PAHs, and dioxins in the surroundings and migrating through the food chain by living inside them. China abandoned areas where the PCB concentration was more than twice the tolerable threshold. Capacitors also release PCB when dismantled by hand (Li & Achal 2020).

One study showed 2510 e-waste studies were done between 2009 and 2018, making up 89.65% of all research taken into account (Gao et al. 2019). With 40.93% of the papers covered, China authored the most research, followed by the United States (345 publications, 12.32 percent), India (190 publications,6.79 percent), the United Kingdom (147 publications, 5.25 percent), and Japan (135 publications, 4.82 percent). There were 9282 keywords, but only 18 had a frequency greater than 120. A co-occurrence frequency analysis found that the most prevalent keywords were e-waste, polybrominated, diphenyl ethers, China, brominated flame retardants, management, recycling, recovery, printed-circuit boards, and heavy metals. The top 10 scientists are all Chinese, showing that Chinese researchers are engaged in this subject and have produced a large number of research findings (Gao et al. 2019). The Chinese government should deploy proper and sustainable methods for metal recycling from e-waste (Li & Achal 2020).

Treatment Methods

Table 2 summarizes different studies on electronic waste treatment methods. Micro-factories are a new type of technology that can turn polymers from e-waste into high-value goods (BBC 2016). Micro-factory technologies stand out because they convert and repurpose electronic waste polymers into new and more expensive items instead of making them into plastic again. In traditional manufacturing industries like steel production, power storage, rising metals, copolymers, and many others, the systems in this class are designed to benefit from various characteristics of plastic trash, including its carbon content, binding properties, chain organization, engineering, thermodynamic properties, etc. Micro-factories might represent the fifth type of polymer recycling, absorbing the growing volume of plastic waste while working with current technologies. Although micro-factories may handle waste from ceramics, glass, and metals, this evaluation focuses mostly on the plastics sector (Sahajwalla & Gaikwad 2018). Decentralized manufacturing, which allows lean, agile, and customizable technology, lies at the micro-factories' heart.

Table 3 shows the electronic waste usage in value-added product making. The "Waste to wealth" strategies are important to reduce e-waste. To stop the degradation of gold materials, guarantee a steady supply of precious metal sources, and lessen the environmental effect of harmful metals, a method to precisely extract and purify gold from additional resources is necessary. 95% of gold is recycled using the TCLP test from e-waste (Panda et al. 2020). For application in the recycling of gold in total e-waste, Magnetic core spinning poles with excellent selectivity and redox activity (MCSR-ATU) were created. The MCSR-ATU demonstrates improved adsorption capability and kinetics attributable to the rotating magnetic field, achieving the maximum adsorption capacity for Au(III) after 30 minutes at pH 3.0 and 313 K (Li et al. 2022).

Machine learning can be applied in e-waste management. Firstly, the MEPH (Magnetic separation, Eddy current, Pyrometallurgical, and Hydrometallurgical) method handles metal removal, filtration, and segregation. In the second section, the cleaned metal is photographed using a camera. The acquired picture is then processed to remove noise before being sent to a CNN classifier. There are two techniques to classify information; the first involves accepting input and classifying output. Secondly, determining the degree of resemblance to the specific class (Senthilselvi et al. 2020). Fig. 9 shows recycling different techniques of e-waste.

Life Cycle Assessment (LCA) Analysis of E-Waste

A useful method for evaluating the environmental effects of e-waste from "cradle to grave" is life cycle assessment

Table 2: Different treatment techniques for electronic waste.

AIM	Composition of Waste	Methods of Treatment	Findings	References
To know the existing and emerging technologies of e-trash plastic recycling	Plastics	Micro-factory; Waste to energy process	The annual growth rate of e-waste is 3-4%; 15% of e-waste recycled	Sahajwalla & Gaikwad (2018)
To evaluate the toxicity of E-trash plastics	Plastics; huge metals; brominated flame retardants (BFRs)	Electronic trash is utilized as raw materials in closed-loop regeneration.	44.7 MT E-waste produced in the US in 2016	Singh et al. (2020)
To investigate the production of E-waste and various management practices	Heavy metals, i.e., Fe, Al, Cu, Cd, Ag, Au, Pd	Sustainable E-waste recycling management	4100 t E-waste produced in Chandigarh annually	Ravindra and Mor (2019)
To describe behavioral reasoning theory perspectives on E-waste recycling and management	Electrical and electronic waste materials		41.8 MMt e-waste generated in 2018 and 50 MMt generated in 2018 worldwide	Dhir et al. (2020)
To recycling of WEEE (Waste from Electronic and Electric Equipment)	LCD notebooks, LED notebooks, TVs, CRT monitors, Cell phones, Smartphones, PV panels, tablets	Collection of materials; pre-treatment; recovery of valuable materials and disposed of nonrecyclable ones	30-50 million tons of WEEE disposed of per year	Cucchiella et al. (2015)
To study the determinants of an individual's E-waste recycling decision	Waste from electronic and electric equipment	Economic E-waste recycling	In the European Union, 10960799 tons of E-waste generated in 2020	Delcea et al. (2020)
To recycle copper and gold from E-waste	Circuit boards of mobile phones containing gold and copper	Two stages leaching process and solvent extraction process	30% of E-waste is recycled using these processes	Rao et al. (2021)
To enhance the accuracy of the mobile phone reprocessing method	Mobile phones waste	Using Machine learning method; MEPH (Magnetic separation, Eddy current, Pyrometallurgical, and Hydrometallurgical)	140 million cell phones landfilled per year	Senthilsevi et al. (2020)
To know policies on E-waste in the emerging economics	Waste from electronic and electrical equipment	Recycling of E-waste supply chain	1975 kt of E-waste produced in India in 2016; South Africa produced 321 kt in 2016	Borthakur (2019)
To recycling of gold from electronic devices waste	Electronic devices	TCLP test	95% of gold recycled using this process	Panda et al. (2020)

(LCA). Regarding all phases of the system boundaries, LCA may concurrently, methodically, and successfully analyze and identify environmental survey, effect, critical variables, choices, and development prospects. Numerous studies have used life cycle assessments (LCAs) to examine the environmental effects of treating e-waste (Song et al. 2012, Niu et al. 2012). Since the system boundaries include steps for collecting, pre-processing, and processing tiny WEEE (electronic toys). Solé et al. (2012) utilized LCA to enhance the process of gathering and recycling. Disposable cell phones are the most frequently used and are thought to have the poorest lifespan of all WEEE (waste electrical and electronic equipment).

Consequently, smartphones will be a key study topic for LCA studies as a specialized tiny electronic and electrical item. The LCA findings suggest a 70%

Table 3: Micro-factory waste inputs and value-added products (Sahajwalla & Gaikwad 2018).

Waste input	Waste resources	Value added items
Plasma LCD TVs. Smart Phone screen.	Waste electrical and electronic equipment	Metals manufacturing
Computer, Laptop, and smartphone circuit board. E-waste plastics.		Construction and built environment and automotive industry.

possibility that recycling used smartphones would have no emissions or negative emissions. Throughout the entire life cycle of treatment, the metal electronic secondary treatment will have the largest environmental implications (He et al. 2021).

Extraction of PMs from Electronic Waste

Electronic applications' average lifespan is shortened, and their revamp is accelerated by technological innovation and market need. As a consequence, e-waste has emerged as one of the fastest-production trash sources. Numerous literary works have described the repurposing of precious metals from e-waste. Over the past 20 years, various reusable innovations have been developed, many of which have already been applied commercially. Smelting in the furnace, Alkali smelting, Traditional Leaching, Non-Cyanide Leaching, Chlorination Leaching, and Iodination Leaching are a few techniques for recovering PMs from e-waste (Cui & Zhang 2008). PMs are recovered from used catalysts.

In contrast to mine generation, recovering valuable metals from wasted catalysts has advantages such as minimal preparatory requirements, quick production cycles, low levels of speculation, and minimal environmental impact. Furthermore, other catalyst transporters are also applied in various applications, and between 100 ppm to 100% of utilized converters contain PMs. Many analysts have worked to reuse valuable metals from used catalysts.

Some ways to recuperate PMs from spent catalysts are the pyrometallurgical process, Cyanide (weight) leaching, HCl+Cl$_2$/NaClO$_3$/NaClO HCl+H$_2$O$_2$, Supercritical liquids extraction, Microwave-assisted leaching. The most useful recycling processes are those that concentrate valuable metals by pyrometallurgy or through selective leaching. Recently, efforts have been undertaken to advance the recovery rate and reduce the natural contamination of important metals from e-waste and used converters. Through purifying and refining, pyrometallurgy may reuse expensive and base metals (such as Cu, Pb, Sn, etc.) with high virtue for e-waste (Islam et al. 2020). A few projects in industrialized countries have been linked to cutting-edge refining advances. The majority of purifying plants in poor nations still are unable to meet the emission requirements, although these pyrometallurgical plants have completed the criterion of tight contamination outflow. However, more than 80% of electronic garbage is dumped in developing nations. Despite the advancements and improvements in smelting technologies in developing countries, contamination problems are still unavoidable. The transmission of gaseous fuel and sludges needs to be carefully considered. Considering the production and emission of particulate matter (PM) 2.5 and carcinogens is important. Devices for treating smoke are necessary for moving dangerous gases and burning residue. Due to the high operating temperature, the release of dangerous gases, and PM 2.5, word-related security is essential. It is not reasonable for small and medium-sized projects because they are large and the supplies are expensive. Perspective and conclusion The business world relies heavily on valuable metals in many sectors. Reusing important metals from secondary assets is crucial due to the conflicts between constrained characteristic
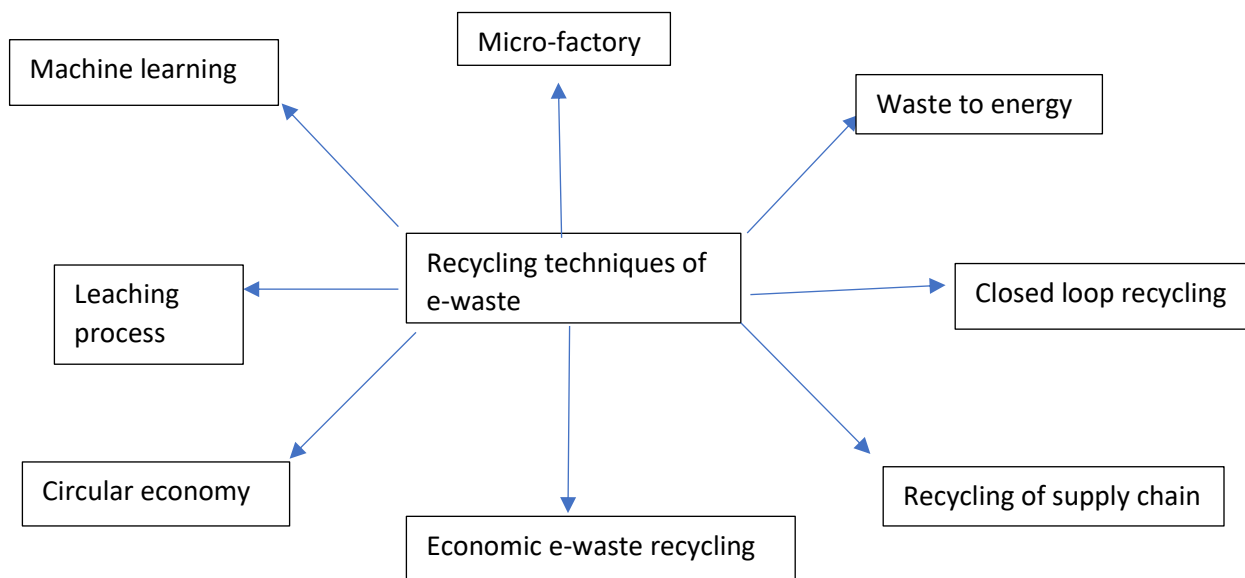
Fig. 9: Some recycling techniques of e-waste.

assets and growing needs and their financial value. Over the last ten years, it has been estimated that the total amount of recycled important metals accounts for 30% of global mining production. In the past ten years, interest has risen in projects that aim to develop effective reuse techniques for valuable metals, particularly e-waste and used catalysts. Environmentally friendly developments for refining priceless metals have evolved throughout time. Different strategies have been developed due to the usual advancements for refining valuable metals, which at the time commanded the highest regard for reusing e-waste.

In underdeveloped countries and regions, pyrometallurgical innovations are less commonly used than hydrometallurgical forms. Although technologies for recovering important metals have undergone self-evident alterations, certain obstacles remain to future promotion. Several considerations have been made to accomplish the economically viable and environmentally responsible refining of valuable metals with a large recovery speed. First, it is important to develop sophisticated advancements from a commercialization perspective in terms of cost and speculation. Second, reusing passageways should be modified and planned in accordance with the physical and chemical characteristics of various materials. Third, a few assisted techniques or pre-treatments are crucial due to increased leaching effectiveness and less contamination. Future advancements for recycling valuable metals can be more effective and have a less natural influence, lower fetched, and greater recuperation rate with over-inquiry direction.

Advantages of Recycling E-waste with Respect to the Circular Economy

Self-reliance, or Atmanirbhar Bharat, becomes increasingly important as India recovers from the effects of COVID-19, particularly on society and the economy, to solve these issues and rebuild through stable economic models. The policies for India's economic recovery must foster sustainable circumstances for people, the environment, and the economy to reconstruct. Achieving long-term affluence for humanity and a sustainable planet might require increasing investment in knowledge, industries, products, business models, procedures, digitalization, and technology.

Because of the increasing usage and quick dumping of electronic devices as well as a lack of infrastructure for proper disposal, electronic trash is an issue that exists everywhere. India is no exception. A staggering 53.6 Mt of electronic garbage, or 7.3 kg per person on average, was produced worldwide in 2019, the Worldwide E-Waste Report 2020 claims. E-waste is on the rise due to the increased use of electrical and electronic equipment (EEE), shorter product life spans, rapid technological advancement, and fewer options for repair. India now generates more than 3.23 million tons of e-waste yearly, ranking third behind China and the United States, as reported in the Worldwide E-Waste Report 2020 (Sengupta et al. 2022). Only 10% of the expected amount of electronic garbage created in India in 2018–19 was recovered (CPCB report). To make resource efficiency successful in India, the gap between e-waste creation and collection for recycling needs to be evaluated. According to the FICCI Circular Economy Report (2017), there is a \$0.7 to \$1 billion market capacity to extract gold from e-waste.

Moreover, a ton of ore has an extractable gold resource of roughly 1.4 g, but a ton of mobile phone PCBs may yield about 1.5 kg. The Worldwide E-Waste Report 2020 claims just 17.4% of electronic trash was collected and recycled in 2019, resulting in the loss of almost \$47 billion in recyclable materials, including gold, silver, copper, platinum, and other high-value materials. The importance of natural sources in the e-waste must be used to construct the remanufacturing supply chain, and developed economic devices must be used to make it economically feasible. A circular economy (CE) strategy for managing e-waste will be crucial for resource utilization, reducing waste, increased product life, restoration of rare and valuable materials, reduction of occupational and health risks, and the development of the recycling sector, which will result in formalization and employment opportunities. At every stage of the material's life span, the CE process in the EEE sector has the potential to generate employment. The CE strategy can promote domestic resource security, leading to increased production and the creation of skilled employment in the industry (MeitY 2021).

Indian Policies, EPR and Regulations Related to the Handling of E-waste

Extended producer responsibility (EPR) stresses companies that come after the consumption phase of products regarding waste treatment (Chung & Murakami-Suzuki 2008). India's importance in the world is anticipated to increase in the next years as a member of the BRICS group, especially from an economic standpoint (Shen et al. 2017). India has significant environmental difficulties as it advances in economic development and prosperity. In contrast, India faces a substantial E-waste challenge due to high production and insufficient management techniques. India has developed and implemented regulations during the past ten years to address the e-waste produced in the nation. The "Guidelines for Environmentally Sound Handling of E-waste" are guidelines for managing e-waste in India that was announced by the Ministry of Environment and Forest (MoEF) in 2008 (Borthakur 2020). Under the March 22,

2018, G.S.R. 261(E) notice, the E-Waste Management Regulations 2016 have been revised (Vikaspedia 2016). The laws have been changed to formalize the e-waste recycling industry by directing the electronic garbage produced in the nation toward approved recyclers and reconstructors. The updated e-waste recovery objectives under EPR will take effect on October 1, 2017. The sequence collection goals for e-waste in weight during 2017–18 must be 10% of the waste-generating amount as mentioned in the EPR Plan, with a 10% rise each year until 2023. The objective has been set at 70% of the waste generated, as stated in the EPR Plan after 2023 (PIB 2018). The guidelines for managing e-waste were issued by the environment ministry in draught form in 2022 for public comment. In accordance with it, manufacturers of consumer goods and electronics must make sure that by 2023, a minimum of 60 percent of their electronic trash will be gathered and reused, with goals to raise those percentages to 70% and 80% in 2024 and 2025, respectively (MeitY 2021). The regulations establish a system of certificate trading that will let businesses temporarily fill gaps. This system is like the trade of carbon credits. According to a draught notification, companies must pay environmental compensation for failed objectives. The CPCB monitors the entire procedure.

Issues and Recommendations

Rigid regulatory frameworks are necessary without conflicting waste management goals, such as collecting home e-waste, to help advance waste disposal in poor countries. These regulations and adjusted EPR plans that consider the local economy might offer readily deployable waste management solutions that would benefit all parties as much as possible. It would significantly reduce negative environmental effects, promoting the Sustainable Development Goals (SDGs), including life below the ocean, balanced urban and rural areas, clean water and sanitation, and ethical ingestion and manufacturing. All manufacturers of EEE specified by the 2016 E-Waste (Governance) Regulations, including manufacturers, e-retailers, online sellers, eBay, etc., must receive an EPR authorization. A manufacturer can execute its EPR by establishing hubs, a take-back program, or both to direct e-waste and end-of-life items to licensed junkyards and recycling plants.

A fundamental change is required to focus on transformation as a reform program for the electronics and electrical industry to enable a circular economy in e-waste. Although precious metals recovery technologies have progressed noticeably, there are still some obstacles to overcome in terms of future promotion. Several considerations for environmentally friendly and sustainable precious metals recycling with a high recovery rate have been offered. New technologies should be developed with the goal of commercialization in mind, both in terms of investment and cost. Recycling technologies should be changed and combined depending on the physicochemical properties of various materials. Various aided procedures or pretreatments should be used to improve leaching efficiency and deduct pollution.

The livelihood and the local economy of provinces like Guiyu depends on e-waste recycling. Thus, formal banning is not an option. Several provinces' environment – soil, water, air – has been completely contaminated and carcinogenic, thus making it irreversible for human life to sustain on the hazardous lands. High technological advancements, high demand for recycled electronics, and a considerable GNP of China depending on the informal e-waste disposal sector make it extremely hard to ban it completely. Recommendations: Since informal recycling contaminates the environment and neonatal and human health, there should be government intervention to reduce the difference in e-waste recycling between regular and irregular, not simply trying to ban it since the livelihood of many depends on the income from it. Pyrometallurgy is still the most conventional and widely-used treatment, and hydrometallurgy is the primary metal separation and recovery method. With the rapid development of numerous hydrometallurgical procedures, such as bioleaching, hydrometallurgy has recently advanced and gained popularity. Pyrometallurgy comprises burning, smelting in plasma arc or coke ovens, roasting, melting, and gas-phase processes at extreme heat. It is the most conventional and widely used metal separation and recovery method. Hydrometallurgy is easier to regulate than pyrometallurgy, more precise, reliable, and ecologically beneficial. To separate and gather the metals from the extractable mixtures and condense them., electroplating techniques typically include a series of acid or corrosive dissolves of e-waste. These leaches are then followed by purification methods like adhesion, solvent evaporation, electro-dialysis, and adsorption using activated carbon. Polymers and flame-retardant plastics comprise most non-metallic fractions (NMF) in Printed circuit boards (PCBs). Polymers and plastics may be transformed into premium fuel; therefore, many physical and chemical methods have been studied in the NMF that are separated and recovered from used PCBs.

a) Management system should supervise to prevent risk from the origin of e-waste.

b) Government – state & central - and NGOs involved in environmental protection should provide ample funds to deploy the best recycling and disposal technologies.

Policymakers in advanced and emerging economies have concentrated a large portion of their legislative and policy efforts since the Worldwide E-waste Report 2017 on establishing funding and advertising programs to encourage greater engagement from business entities and private citizens. Here, the goal is to ensure improved recycling and recovery rates as well as to provide the money needed to cover treatment expenses. Most legislative measures encourage resource recovery through recycling and protection against the negative effects of human health and environmental contamination at the end of a product's life. E-waste volume reduction and significant repair and reuse of EEE have thus far been confined. This is consistent with worldwide legislative initiatives to advance the recycling industry.

CONCLUSION

The recycling trend is significant from the standpoint of maximizing precious metals recovery and minimizing environmental damage. Noble metal separation can potentially be an economic engine for sustainable growth. Historically, pyro-metallurgy has been applied to retrieve valuable metals from e-waste. This research on e-waste has improved our knowledge of the amount of e-trash produced by the fast-improving world. The huge amount of e-trash has caused degradation of the environment and food chains, shortage of minerals and nutrients, and impact on human health. The process emits harmful dioxin fumes that negatively affect the ecosystem. The general rise of electronic gadget users and the global economy has increased the amount of electronic garbage worldwide during the previous few decades.

However, e-waste and its continued use in the present and future can not be ignored. But all e-waste cannot be ignored. This study also reveals some recycling techniques for e-waste. But all e-waste cannot be composted or recycled, and some waste will be landfilled. That landfilled e-waste can be used in energy generation.

If the growing amount and flow of electronic garbage are not handled soon, it will undoubtedly negatively affect the environment and people. The supply of easily extractable materials, notably metals, declines as more PCBs are disposed of in landfills, disrupting the entire material cycle. Reprocessing of e-trash is still motivated by the high economic worth and presence of a base and precious metals in PCB. There is an immediate need for new, ecologically acceptable methods to recycle and recover energy elements from waste PCBs since PCBs' current manufacturing and handling are not sustainable. As shown by the thorough assessments of the alternative treatments, the processing

and recycling of PCB is a complex problem. Engineers, politicians, and other sectors must collaborate to close the loopholes and create a more cost-effective and ecologically pleasant recycling process.

Waste control progressively shifts from a "reduction of waste" focus to a "sustainable materials policy" objective that views certain wastes as resources. The literature review highlights environmental circumstances, governance structures, and policy perspectives, advancing waste management toward the ecological agenda's emphasis on resource and material systems theory. Each time, the trash unit was combined with an environmental agency, demonstrating the advantages of incorporating trash management into a larger viability initiative. The value may be obtained from considering the instances as synergistic garbage and materials administration improvements, feasible at various levels of governance instead of examining them in opposition to one another. San Francisco's Zero Waste project illustrates building a superior recycling approach through landfill reduction (Silva et al. 2017). The e-waste dump should be considered a significant source of additional raw resources related to the circular economy. The need to enhance secondary asset mining and lessen the demand for virgin materials has arisen due to problems with primary mining, market rate changes, material shortage, affordability, and accessibility. Countries might reduce their material consumption safely and sustainably by recycling their electronic trash.

There has been a great deal of e-waste research recently due to nations and academics' rising concern for environmental protection. Due to a strong positive correlation between the series of studies and the year of publication, we may expect e-waste research to expand in the next few years.

REFERENCES

Baldé, C.P., Forti, V., Gray, V., Kuehr, R. and Stegmann, P. 2017. The Global E-Waste Monitor 2017: Quantities, Flows, And Resources. United Nations University, International Telecommunication Union, and International Solid Waste Association.

BBC 2016. The rise of miniature 'microfactories'. https://www.bbc.com/future/article/20161117-the-rise-of-miniature-microfactories

Borthakur, A. 2020. Policy approaches on e-waste in the emerging economies: A review of the existing governance with special reference to India and South Africa. J. Clean. Prod., 252: 119885.

Brianna, Aldrich 2022. Emissions from e-waste spiked 53% in 6 years. https://www.gcn.com/emerging-tech/2022/10/emissions-e-waste-spiked-53-6-years/379043/

Castro, F.D. and Bassin, J.P. 2022. Electronic waste: Environmental risks and opportunities. Hazard. Waste Manag., 11: 421-458.

Chi, X., Streicher-Porte, M., Wang, M.Y. and Reuter, M.A. 2011. Informal electronic waste recycling: A sector review with special focus on China. Waste Manag., 31(4): 731-742.

Chung, S.W. and Murakami-Suzuki, R. 2008. A comparative study of e-waste recycling systems in Japan, South Korea, and Taiwan from

the EPR perspective: implications for developing countries. Kojima. Chiba, 21: 11-23.

Cucchiella, F., D'Adamo, I., Koh, S.L. and Rosa, P. 2015. Recycling of WEEEs: An economic assessment of present and future e-waste streams. Renew. Sustain. Energy Rev., 51: 263-272.

Cui, J. and Zhang, L. 2008. Metallurgical recovery of metals from electronic waste: A review. J. Hazard. Mater., 158(2-3): 228-256.

Delcea, C., Crăciun, L., Ioanăl, C., Ferruzzi, G. and Cotfas, L.A. 2020. Determinants of Individuals' E-Waste Recycling Decision: A Case Study from Romania. Sustainability, 12(7): 2753.

Dhir, A., Koshta, N., Goyal, R.K., Sakashita, M. and Almotairi, M. 2021. Behavioral reasoning theory (BRT) perspectives on E-waste recycling and management. J. Clean. Prod., 280: 124269.

Ding, Y., Zhang, S., Liu, B., Zheng, H., Chang, C. C. and Ekberg, C. 2019. Recovery of precious metals from electronic waste and spent catalysts: A review. Resources, conservation and recycling, 141: 284-298.

FICCI Circular Economy Report, 2017. Accelerating India's Circular Economy. https://ficci.in/spdocument/22977/FICCI-Circular-Economy.pdf

Forti, V., Baldé, C.P., Kuehr, R. and Bel, G. 2020. The global e-waste monitor 2020. Quantities, flows, and the circular economy potential, UN. Bonn, Geneva, pp. 1-119.

Gao, Y., Ge, L., Shi, S., Sun, Y., Liu, M., Wang, B. and Tian, J. 2019. Global trends and future prospects of e-waste research: a bibliometric analysis. Environ. Sci. Pollut. Res., 26(17): 17809-17820.

Garg, C. P. 2021. Modeling the e-waste mitigation strategies using Grey-theory and DEMATEL framework. J. Clean Prod., 281: 124035.

He, P., Feng, H., Chhipi-Shrestha, G., Hewage, K. and Sadiq, R. 2022. Life Cycle Assessment of e-Waste–Waste Cellphone Recycling. In Holuszko, M.E., Kumar, A. and Espinosa, D.C.R. (eds), Electronic Waste: Recycling and Reprocessing for a Sustainable Future, Wiley, NY, pp. 231-253.

Huo, X., Peng, L., Xu, X., Zheng, L., Qiu, B., Qi, Z. and Piao, Z. 2007. Elevated blood lead levels of children in Guiyu, an electronic waste recycling town in China. Environ. Health Persp., 115(7): 1113-1117.

Ilankoon, I.M.S.K., Ghorbani, Y., Chong, M.N., Herath, G., Moyo, T. and Petersen, J. 2018. E-waste in the international context: A review of trade flows, regulations, hazards, waste management strategies and technologies for value recovery. Waste Manag., 82: 258-275.

Islam, A., Ahmed, T., Awual, M.R., Rahman, A., Sultana, M., Abd Aziz, A. and Hasan, M. 2020. Advances in sustainable approaches to recover metals from e-waste-A review. J. Clean. Prod., 244: 118815.

Kang, H.Y. and Schoenung, J. M. 2005. Electronic waste recycling: A review of US infrastructure and technology options. Resour. Conserv. Recycl., 45(4): 368-400.

Kiddee, P., Naidu, R. and Wong, M.H. 2013. Electronic waste management approaches: An overview. Waste Manag., 33(5): 1237-1250.

Leung, A., Cai, Z.W. and Wong, M.H. 2006. Environmental contamination from electronic waste recycling at Guiyu, southeast China. J. Mater Cycl. Waste Manag., 8(1): 21-33.

Li, H., Pan, Y., Wu, F., Zhou, Y. and Pan, J. 2022. Turning waste into wealth: efficient and rapid capture of gold from electronic waste with thiourea functionalized magnetic core stirring rod adsorbent and its application for heterogeneous catalysis. Green Chem., 24(19): 7592-7601.

Li, W. and Achal, V. 2020. Environmental and health impacts due to e-waste disposal in China–A review. Sci. Total Environ., 737: 139745.

MeitY 2021. Circular Economy In Electronics And Electrical Sector. https://www.meity.gov.in/writereaddata/files/Circular_Economy_EEE-MeitY-May2021-ver7.pdf

Niu, R., Wang, Z., Song, Q. and Li, J. 2012. LCA of scrap CRT display at various scenarios of treatment. Proced. Environ. Sci., 16: 576-584.

Onete, C. B., Albăstroiu, I. and Dina, R. 2018. Reuse of electronic equipment and software installed on them–an exploratory analysis in the context of circular economy. Amfiteatru Economic, 20(48): 325-339.

Panda, R., Jadhao, P.R., Pant, K.K., Naik, S.N. and Bhaskar, T. 2020. Eco-friendly recovery of metals from waste mobile printed circuit boards using low-temperature roasting. J. Hazard. Mater., 395: 122642.

Parajuly, K., Fitzpatrick, C., Muldoon, O. and Kuehr, R. 2020. Behavioral change for the circular economy: A review with a focus on electronic waste management in the EU. Resourc. Conserv. Recycl., 6: 100035.

Perkins, D.N., Drisse, M.N.B., Nxele, T. and Sly, P.D. 2014. E-waste: a global hazard. Annals Glob. Health, 80(4): 286-295.

PIB 2018. E-Waste Management Rules amended for effective management of E-Waste in the country: Union Environment Minister. https://pib.gov.in/newsite/PrintRelease.aspx?relid=177949

Ranjbari, M., Esfandabadi, Z.S., Shevchenko, T., Chassagnon-Haned, N., Peng, W., Tabatabaei, M. and Aghbashlo, M. 2022. Mapping healthcare waste management research: Past evolution, current challenges, and future perspectives towards a circular economy transition. J. Hazard. Mater., 422: 126724.

Rao, M.D., Singh, K.K., Morrison, C.A. and Love, J.B. 2021. Recycling copper and gold from e-waste by a two-stage leaching and solvent extraction process. Sep. Purif. Technol., 263: 118400.

Ravindra, K. and Mor, S. 2019. E-waste generation and management practices in Chandigarh, India and economic evaluation for sustainable recycling. J. Clean. Prod., 221: 286-294.

Rizos, V. and Bryhn, J. 2022. Implementation of circular economy approaches in the electrical and electronic equipment (EEE) sector: Barriers, enablers, and policy insights. J. Clean. Prod., 338: 130617.

Sahajwalla, V. and Gaikwad, V. 2018. The present and future of e-waste plastics recycling. Curr. Opinion Green Sustain. Chem., 13: 102-107.

Sengupta, D., Ilankoon, I.M.S.K., Kang, K.D. and Chong, M.N. 2022. Circular economy and household e-waste management in India: Integration of formal and informal sectors. Minerals Eng., 184: 107661.

Senthilselvi, A., Sellam, V., Alahmari, S.A. and Rajeyyagari, S. 2020. Accuracy enhancement in mobile phone recycling process using machine learning technique and MEPH process. Environ. Technol. Innov., 20: 101137.

Shen, L., Shuai, C., Jiao, L., Tan, Y. and Song, X. 2017. Dynamic sustainability performance during the urbanization process between BRICS countries. Habitat Int., 60: 19-33.

Silva, A., Rosano, M., Stocker, L. and Gorissen, L. 2017. From waste to sustainable materials management: Three case studies of the transition journey. Waste Manag., 61: 547-557.

Singh, N., Duan, H. and Tang, Y. 2020. Toxicity evaluation of E-waste plastics and potential repercussions for human health. Environ. Int., 137: 105559.

Solé, M., Watson, J., Puig, R. and Fullana-i-Palmer, P. 2012. Proposal of a new model to improve the collection of small WEEE: A pilot project for the recovery and recycling of toys. Waste Manag. Res., 30: 1208-1212.

Song, Q., Wang, Z. and Li, J. 2013. Sustainability evaluation of e-waste treatment based on emergy analysis and the LCA method: a case study of a trial project in Macau. Ecol. Indic., 30: 138-147.

Statista 2020. Electronic waste generated worldwide from 2010 to 2019 (in million metric tons). https://www.statista.com/statistics/499891/projection-ewaste-generation-worldwide/

USGS 2017. Mineral commodity summaries 2017: U.S. Geological Survey, 202 p., https://doi.org/10.3133/70180197.

Vikaspedia 2016. E-Waste Management Rules, 2016. https://vikaspedia.in/energy/environment/waste-management/e-waste-management/e-waste-management-rules-2016

Original Research Paper   **Open Access Journal**

Spatial Model of Post-Earthquake Spring Performance in the Watershed Areas

Akhbar Akhbar* (iD)**, Naharuddin Naharuddin*†** (iD)**, Adam Malik*** (iD)**, Rahmat Kurniadi Akhbar*** (iD)
and Sudirman Daeng Massiri* (iD)

*Department of Forestry, Faculty of Forestry, Tadulako University, Palu, Central Sulawesi 94118, Indonesia
†Corresponding author: Naharuddin Naharuddin; nahar.pailing@gmail.com

ABSTRACT

The 7.4 Mw of tectonic earthquake caused liquefaction in Pasigala on September 28, 2018, happened due to the fault movement of Palu-Koro. It affected the water availability every spring. The research aim is to determine the spatial model of water production every spring after the natural tectonic disaster, especially in Palu and Poboya watersheds-a model built based on the integration between the spatial data overlaying and the statistical regression correlation. The sites are purposively selected at six springs spots and divided into four clusters (Poboya, Uemanje, Ranjuri Beka, Mantikole). The model assessment was generated based on the springs' performance from x variables (catchment area, land cover, aquifer, free-ground water depth, fault, number of springs users) and the y variable (water discharge). The result shows that Poboya's performance is bad-disturbed, while Uemanje, Ranjuri, Beka, and the performance of Mantikole are disturbed. The bad performance of springs requires conserving watershed areas through forest and land conservation, tree enrichment planting, wise land management, and good water use.

INTRODUCTION

Issues related to natural disasters have become a central issue in every country in the world (Albris et al. 2020, Galata et al. 2020). It has an impact on the economy, humans, and the environment (Botzen et al. 2019, Ali et al. 2020), especially in Asian countries that are prone to earthquakes, tsunamis, and liquefaction (De Goyet 2007, Wekke et al. 2019).

A natural disaster of the tectonic earthquake on September 28, 2018, followed by tsunamis and liquefaction, hit Palu, Sigi, and Donggala (Pasigala) in Central Sulawesi. It negatively impacted the infrastructures, causing severe land surface destruction and property loss. It cost billions of rupiahs or even human life lost. According to Nugroho (2018), the disaster on October 25, 2018, hitched 2,065 deaths in Pasigala, 15 deaths in Parigi Moutong, and 1 person death in Pasangkayu (West Sulawesi). Further, 4,438 were severely injured, 8,130 were injured, 1,309 were lost, 214,925 were refuged, and 21,321 had evacuated.

The earthquake caused by the Palu-Koro fault movement hit Pasigala with 7.4 Mw. Palu-Koro fault is an active

ORCID details of the authors:

Akhbar Akhbar : https://orcid.org/0000-0001-7859-6121
Naharuddin Naharuddin : https://orcid.org/0000-0001-8889-0463
Adam Malik : https://orcid.org/0000-0002-0184-0058
Rahmat Kurniadi Akhbar : https://orcid.org/0000-0001-7600-8939
Sudirman Daeng Massiri : https://orcid.org/0000-0003-3974-7761

segment of the Tumbu-Talise-Bora and Gumbasa-Kulawali segments). These cross to the western coastal area of Donggala Regency, Palu's Bay, and the South Kulawi district of Sigi Regency. The earthquake ground spot is in Tompe village, a part of the Sirenja district of Donggala Regency. This earth movement then predicted impacts the water resource availability of each spring, whether in a water basin (WB) or a non-water basin. Several water basins are spread across the Palu, Sigi and Donggala, such as the WB of Palu, Bobo, Tawaeli, Oti, Tompe, Labea, and Palado.

The earthquakes can cause hydrological responses, such as groundwater availability in and above the ground (Wang et al. 2004, Liao et al. 2015). Stockpiling a reservoir risks an earthquake (Xuan-Nam et al. 2020) and can cause landslides and soil erosion (Tunas et al. 2020, Naharuddin et al. 2021). Each of Palu's watershed and Poboya's watershed are equipped with springs. Both were affected by the Palu-Koro movement when the earthquake event occurred. The ground movement then predicts the impact of the Poboya Springs, Ranjuri Springs in Beka village, Mantiloke Springs in Mantiloke village, and Uemanje Springs in Uemanje village. Those springs are generally located in the tectonic fault pathway. The tectonic fault structure controls the emergence of water sources and water channels under the surface. The tectonic fault structure affects the emerging water sources (Santosa 2006).

Research on the impact of the earthquake, tsunamis, and liquefaction in Palu and Donggala concerning water sources' performance has not been conducted. The research was carried out only on the focus on assessing the level of erosion hazard in some land uses after earthquakes and liquefaction (Naharuddin et al. 2020), mapping of post-disaster damage and liquefaction (Syifa et al. 2019), landslide study in the East Palu Valley after the earthquake (Mason et al. 2021). Earthquakes can cause hydrological responses, such as groundwater availability in and above the ground. This statement is in line with King et al. (2006) statement that there is a temporal change in underground water hydrology due to the earthquake. This knowledge is very important for watershed management planning and modeling of springs (Wilkerson 2008, Reghunath et al. 2009, Jakubis & Jakubisová 2019). The research on the water production in Palu's watershed and Poboya's watershed is interested in assessing water's present condition and availability at the ground and surface pathway. The research aims to determine the spatial model of springs' performance on water production post-impact of the earthquake at these sites. The research would provide spatial data and information on springs' performance. At the same time, the guideline of water resource recovery and the science and spatial technology of watershed management is also arranged as the basis for post-earthquake management planning.

MATERIALS AND METHODS

Study Area

This study was collaborative research involving the Palu Poso Watershed Management Center and the Forestry Faculty of Tadulako University. It will be conducted for two years, from May to October 2019, for data collecting and June to December 2020, for spatial model arrangement.

Technically, sites were divided into four clusters. The watershed in Palu consisted of 3 clusters: Ranjuri-springs, Mantiloke-springs, and Uemanje-springs. Furthermore, the last cluster chose Poboya-springs as a part of the Poboya watershed. Geographically the location is at the coordinate point, according to Table 1. The study sites are shown in Fig. 1.

Tool and Study Material

Data were divided into primary data collected by the collaborative team, including primary data on the field condition of each spring taken from May to October 2019, and secondary data types consisting of the map. These maps were collected from a particular center or agency. National Mapping Centre (NMC) provides spatial data with a scale of 1:50,000 – 1:100,000 consisting of digital maps such as Indonesian land cover, route map, river flow, and settlement area. Other data were prepared by the Palu Poso watersheds management center, such as the catchment area, land and geological map, rain intensity zonation map, and topographical and water resources.

While fault maps, water basin maps, and spatial planning maps are collected from the provincial planning agency with a scale of 1:100,000 – 1,250,000. Palu's regional forestry mapping agency provides land cover data and forest area. This kind of map is available for scale 1:100,000 – 1,250,000. Furthermore, those particular satellite images have been collected from the national space agency for SPOT6/7.

Research Methodology

A spatial analytical method has been implemented for this research, combined with overlaying spatial data and made a score through statistical analysis (regression-correlation). The spatial analysis, through overlying a basic map, thematic map, and SPOT image, tries to build parameter attributes and count the indicator values (Wahyuningrum & Putra 2018).

The spatial elements studied include the distribution of the fault path on September 28, 2018, geomorphological (river flow, tectonic surface pattern) and the river basin, aquifer, free land water depth, land texture, climate (the intensity of rain), topographic, land cover (vegetated or non-vegetated), water quality (discharge), catchment area

Table 1: Research locations.

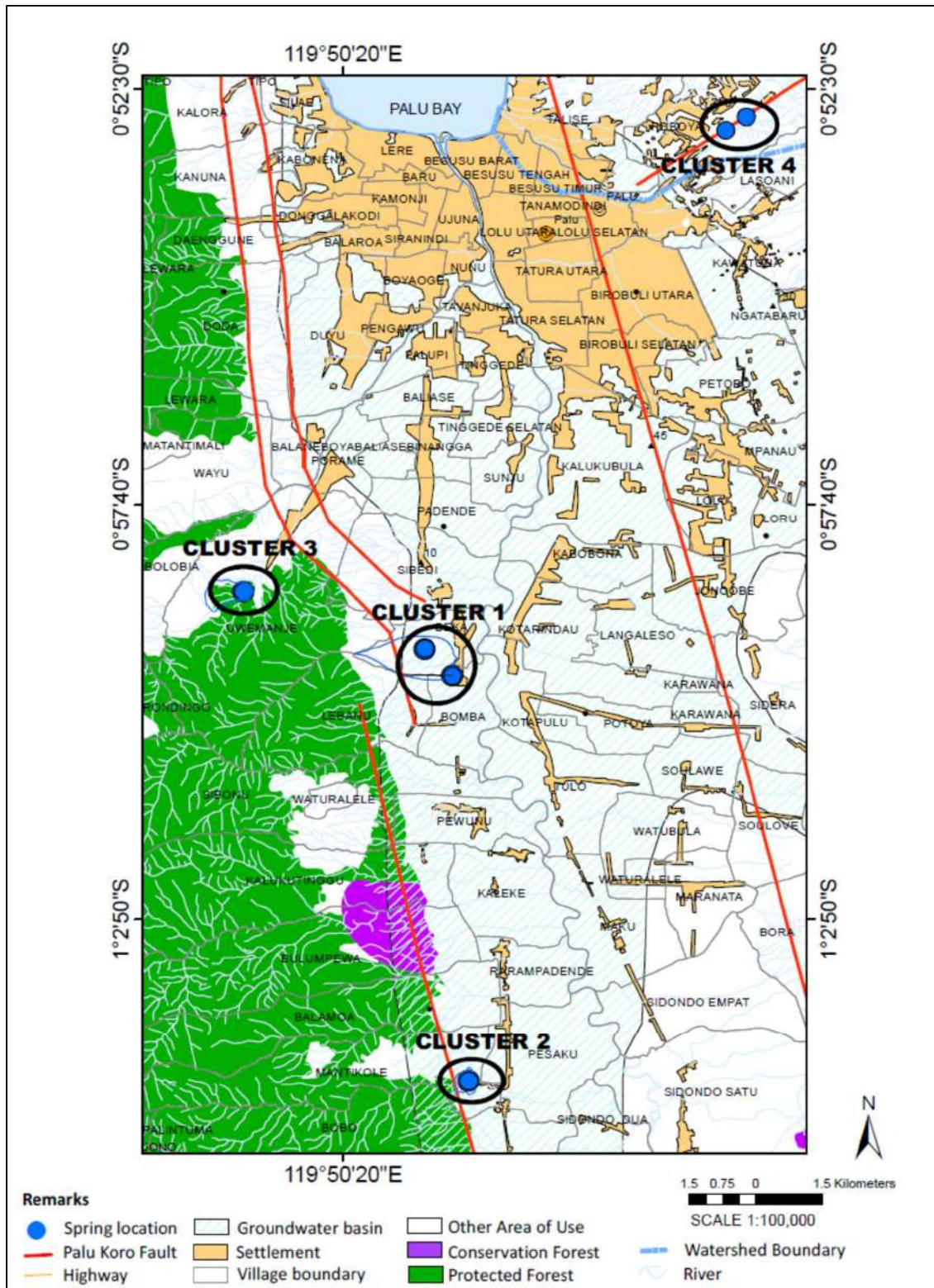| Cluster		Geographical coordinate		Site/Area
Number	Code	East longitude (E)	South latitude (S)	
1	SP1	119°51'20.82"	0°59'28.20"	Ranjuri
	SP2	119°51'40.18"	0°59'48.25"	Ranjuri
2	SP	119°51'52.08"	0°04'51.60"	Mantiloke
3	SP	119°49'07.50"	0°58'45.42"	Uemanje
4	SP1	119°55'00.48"	0°53'00.72"	Poboya
	SP2	119°55'15.48"	0°52'50.76"	Poboya

Fig. 1: Research location of Palu and Poboya watersheds.

and the various utilization of water by the local community. Besides, supplement data support the research, i.e., springs typology, geological, land texture, elevation, kind of land cover, land uses, land status, watershed area, accessibility, infrastructure, and community profile (number of residents).

The selection of springs locations that were examined for their spatial performance was done purposively as presented in Fig. 1 with the following considerations: (a) Poboya springs are located close to the tectonic fault lines, tectonic plains, non-forest areas, non-water basin area, typology of springs 'contact', type of land use in settlement area/ mining areas, owned land status; (b) the Uemanje springs is located a distance from the cesarean line, tectonic mountains, protected forest, non-water basin area, springs 'contact' typology, land use types in forest areas, state-owned land status; (c) Ranjuri springs is located near the cesarean line, river flow path, outside the forest state area, at the water basin area, 'depressive' springs type, residential areas land use type, land owned by the community/village property; (d) Mantikole springs is located near cesarean lines, hot springs, river flow paths, located in outside of state forest areas, in a water basin, 'depressed' springs type, agricultural land use type/ tourist areas, owned by the community/local government property. The springs' location selection is a catchment area typical of land cover, soil texture, water quantity (discharge), water quality, annual rainfall, and potential groundwater in aquifers.

The process of the research describes as follows:

1. The analysis process is based on inventory and identification data of springs.

   Overlaying and delineated boundary research areas (spatial and tabular): The boundaries of the Palu and Poboya watersheds, regencies/cities, districts, villages, and forest area boundaries (status/function of the area). Spatial tabulation and analysis based on the inventory and field identification of six springs locations into the four clusters) in the Palu and Poboya watersheds.

2. Spatial modeling of springs performance.

Springs performance modeling with a spatial data overlaying approach and regression-correlation analysis was made to determine the relationships and trends among variables. The water quantity/water discharge ($L.s^{-1}$) variable was analyzed with the cesarean moving path (kilometers), soil texture (related to infiltration/permeability), catchment area (ha), geomorphology (watershed /non-watershed in river flow paths, tectonic mountains, rainfall ($mm.y^{-1}$), aquifer productivity, free groundwater depth, slope (% slope), vegetated land cover (% of the coverage area), number of springs users (households, worship, offices, education, health, tourism, agriculture, etc.). The results of

the regression-correlation analysis become a reference for the scoring and variable scores selection. Range correlation value (R) $\geq$ 0.50 were selected as modelers in the spatial analysis system of springs performance. The size of each chosen variable's scoring is determined based on the coefficient determination (the level of accuracy of the regeneration model) with a value of R2 $\geq$ 0.25.

The springs spatial performance criteria are as follows:

- Poor performance springs category: The springs' condition regarding water production has connected to a bio-geophysical and socioeconomic variable with a total weighting value of 20-46. Springs area recovery is recommended.

- Disturbed performance springs category: The springs' condition regarding water production has connected to a bio-geophysical and socioeconomic variable with a total weighting value of 47-73. Countermeasures action is recommended.

- Good performance springs category: The springs' condition regarded water production has connected to a bio-geophysical and socioeconomic variable with a total weighting value of 74-100. Prevention is recommended (The Ministry of Environment and Forestry 2017), (modified according to the research needs).

RESULTS AND DISCUSSION

The Springs Condition

Characteristics observation of groundwater has been conducted on the spot that naturally springs. The springs indicated groundwater comes out as surface runoff. The springs condition in Palu and Poboya watersheds in four clusters are shown in Table 2.

Spatial Model of Springs Performance

The spatial model of springs performance begins with regression analysis and correlation among the determining variables of the performance of springs concerning each spring's ability to produce water (discharge) in liters/second. There are ten variables: (a) The proximity of springs from the movable tectonic fault; (b) Soil texture related to the level of infiltration; (c) water catchment areas; (d) geomorphology of river flow paths, plains/hills/tectonic mountains in the water basin/ non-water basin areas; (e) rain intensity; (f) Aquifer productivity; (g) vegetated land cover; (h) topography class; (i) Number of springs users; (j) Depth of free groundwater. The results of regression and correlation are as in Table 3.

The regression correlation analysis in Table 3 used the transformed data from Table 2. The transformation for data

Table 2: Water discharge conditions, biogeophysical, and socioeconomic location of the springs.

Variable	Name of Springs					
	Cluster 4 Poboya		Cluster 3 Uemanje (SP)	Cluster 1 Ranjuri Beka		Cluster 2 Mantikole (SP)
	Springs$_1$ (SP1)	Springs$_2$ (SP2)		Springs$_1$ (SP1)	Springs$_2$ (SP2)	
Watershed area	Poboya	Poboya	Palu	Palu	Palu	Palu
Regency/city	Palu	Palu	Sigi	Sigi	Sigi	Sigi
Forest area	non-forest area		Protected forest	non-forest area		non-forest area
Land status	Community		Government	Community		Local government
Springs typology	Contact		Contact	Depressive		Depressive
Water catchment area [ha]	8.05	20.30	51.61	64.04	68.77	22.82
Water discharge [L.s^{-1}]	1.18	5.09	0.51	0.70	0.18	1.04
Tectonic fault distance from the springs [km]	0.02	0.03	17.04	12.75	12.17	11.19
Geomorphology	Non-water basin - tectonic land surface		Non-water basin - tectonic mountains	Ground water basin-river flow path		Ground water basin-river flow path
Aquifer productivity	Moderate		High	High		High
Ground-free water depth [m]	0.85	0.85	0.50	0.48	0.48	0.48
Elevation (meters above sea level)	175-200	150-200	550-650	75-125	25-125	75-200
Slope class [%]	25.06	23.05	43.20	12.75	11.05	50.28
Geology type and formations	QTms (molasa celebes sarasin and sarasin)/ Sediment)		Kls (latimojong); gr (intrusive rocks)/ Metamorphic)	Qa (AluviumCoastal sediment/ Alluvium)		QTms (molasa celebes sarasin and sarasin)/Alluvium)
Soil type	Red-yellow podzolic, litosol			Alluvial, Glei humus		Brown forest soil, alluvial
Soil texture	Clay	Clay	Sandy clay	Clay	Dusty clay	Dusty clay
Climate/Rain intensity [mm.y^{-1}]	D/ 800-1.000		D/ 1.200-1.400	D/ 800-1.000		D/ 1.200-1.400
Land use	Forests, mixed gardens, settlements, shrubs, grass, fields, open land		Forests, shrubs, open land	Shrubs, open land	Forests, Coconut groves, scrub, settlement	Coconut stand, shrubs, open land, tourist areas.
Vegetated land cover [ha]	7.46	17.01	42.98	60.25	61.03	20.23
Type of plant	Timber, coconut, banana, corn		Candlenut, tamarind, sugar palm, bamboo	Acacia, Jatropha	Manggo, coconuc, banana, timbers.	Timber, Lamtoro, Coconut, Banana, Guava, Mango
The Accessibility/ Infrastructure	Village Road		Village Road	Village Road		Village Road
Number of the population) (soul/head of household)	1.716/ 643		1.234/ 305	2.649/ 609		1.208/ 281
Population density [souls.km^{-2}]	27		74	1.172		96
Livelihood	Gold miners, farmers, gov. employee		Farmers	Farmers		Farmers
Community needs for springs (l/day / person/head of household)	50		50	50		50
Springs utilization (head of household)	643		305	609		281
Springs user	Household, agriculture)	Household, house of worship	House holds, baths, houses of worship, schools	Household, Agriculture	Household, houses of worship, and schools.	Household, Tourism, Agriculture

Source: Results of the 2019 springs inventory/identification; a result of the SPOT image analysis and maps; a result of socioeconomic data analysis (Central Statistical Agency Sigi Regency 2018 and Central Statistical Agency Palu City 2018).

consists of null with SQRT=$\sqrt{xi}$+0,5, and other than null, has transformed with SQRT=$\sqrt{xi}$. The qualitative data such as geomorphology, aquifer productivity, and soil texture are quantified by scores 1,2,3 according to the level. The high aquifer productivity received a score of 3, while the medium and low productivity levels received scores of 2 and 1, respectively. The same treatment is also done for the soil texture, scoring 3 for fine texture, 2 for fine soil texture, and 1 for rough texture. The geomorphological water basin path and tectonic land received a score of 3. The non-water basin received 2 and 1 for tectonic hills.

Table 3 shows the results of the regression analysis and the correlation between the response variable (Y) water discharge with explanatory variables (X1-X10), which are generally weak-moderate negative correlations due to the fewer water discharges (1.45 L.s^{-1}). SP2 Poboya became the only site supported by an adequate water discharge from those six springs locations, which is 5,09 L.s^{-1}. In contrast, the SP1 Poboya and SP Mantikole (hot springs) are supported by lower discharge, 1.18 L.s^{-1} and 04 L.s^{-1}, respectively. Each SP1 Ranjuri, SP2 Ranjuri, and SP Uemanje supported the water flow of 0.70 L.s^{-1}, 0.18 L.s^{-1}, and 0.51 L.s^{-1}. The potential quantitative level of free groundwater (small-medium) and small potential (<1.0 L.s^{-1}) occupied the eastern part of the river basin in East Palu District, South Palu, Dolo. Medium potential (1.0-5.0 L.s^{-1}) covers the entire western part of the water basin and only 40% in Sigi Biromaru and Gumbasa Districts.

The fault movement may cause less water discharge in SP Ranjuri Beka and SP Mantikole. Somehow, cesarean has led to landslides upstream of the Beka Village, disrupting the existing water flow as springs. Generally, the pattern of springs is caused by groundwater level cross topography, so the springs seem depressed and associated with the presence of fault (Santosa 2006). The topography in Mantikole was impacted by water discharge. Steep topography with alluvium rocky type (Molas Celebes Sarasin and Sarasin) and the existence of fault movement affect the rock structure disruption (Fig. 2). Santosa (2006) suggested that hot springs appear due to non-gravitational power are located in the fracture of the long earth's crust, and very deep. The water source mostly comes from rainwater that falls around it, and only a small portion comes from inside the earth (magmatic). The falling rain infiltrates the ground and is heated by magma underneath, forming a large convection current that pushes to the ground's surface.

Poboya springs cluster outside the water basin area in tectonic plains and contain two springs with different discharges, namely springs (SP) Poboya with small water discharge and SP2 Poboya with moderate water flow. Both of these SP locations are very close to the tectonic fault movement, steep topography, rock type sediment (molasa Celebes Sarasin and Sarasin) (Fig. 3). Further, SP Ranjuri Beka and Uemanje have a small water discharge located outside of the water basin area and far from the fault movement (Fig. 4). The movement disrupted the rock structure so which affects water flow. Rock cracks could decrease slope stability. The landslide may occur the rainwater seeps into the crack or when the slope is shaken. The appearance of springs is mostly influenced by the tectonic fault structure, other than the rock's constituent condition. The tectonic fault

Table 3: The correlation regression analysis of water discharge with biogeophysical variables and springs users at six locations in four springs clusters.

The simple regression analysis variables		Regression model $\bar{Y} = a + bX$	Determi-nant coeffi-cient (R2)	Correlation (R)	(Test) F	
					F_{count}	$F_{tab.}(\alpha_{0.05,1,4})$
Explanatory variable X		Response variable Y Water discharge				
X1	Catchment area	$\bar{Y} = 0.17 - 2.06X$	0.35	-0.59	6.15 [nr]	7.71
X2	Geomorphology	$\bar{Y} = 0.33 - 1.55X$	0.02	-0.15	4.09 [nr]	7.71
X3	Distance Fault moves from the springs (The distance of tectonic fault from springs	$\bar{Y} = 0.26 - 1.70X$	0.56	-0.75	9.14 [r]	7.71
X4	Aquifer Productivity	$\bar{Y} = 2.75 - 5.80X$	0.47	-0.69	7.59 [nr]	7.71
X5	Depth of Free Groundwater	$\bar{Y} = 4.07+2.09-X$	0.56	0.75	9.14 [r]	7.71
X6	Slope class	$\bar{Y} = 0.04 +0.83X$	0.01	0.11	4.05 [nr]	7.71
X7	Soils texture	$\bar{Y} =-0.28 + 0.99X$	0.07	0.26	4.30 [nr]	7.71
X8	Rain intensity	$\bar{Y} = 0.05 - 2.73X$	0.05	-0.23	4.23 [nr]	7.71
X9	Vegetation Cover	$\bar{Y} = 0.18 - 2.07X$	0.36	-0.60	6.29 [nr]	7.71
X10	Springs users	$\bar{Y} = 1.39 - 3.31X$	0.29	-0.54	5.61 [nr]	7.71

Remarks: nr: not different; r: real

structure controls the appearance of springs and subsurface waterways (Rahayu et al. 2009, Santosa 2006).

The analysis of free groundwater depth (X5) shows a strong positive correlation (0.75) with water discharge and significantly affects spring supply. The level of free groundwater depth at the site was 0.61 m (<1.0 m). Therefore, the regression model explained that the shallower free groundwater from SP would better the supply of water sources. This is in line with research conducted by Zeffitni (2012), phreatic face level fluctuations in Palu's water basin are generally low (<1.0 m), lowest in the western basin in Dolo Barat District (0.48 m), highest in the eastern basin in Sigi Biromaru District (0.85 m).

The proximity analysis of the cesarean movement on September 28, 2018, shows a strong negative correlation (-0.75) with water discharge and significantly affects the water supply to the springs. The distance of the cesarean movement at the study site is an average of 8.87 km (somewhat close), so according to the obtained regression model explains that the closer the cesarean movement distance from the SP will, the greater disturbance to the water availability at the SP. According to the Meteorological, Climatological, and Geophysical Agency, the earthquake on

28 September 2018 was located at 119.85° E: 0.18° S about 80 km north of Palu City at 10 km depth. The earthquake occurred along the Palu-Koro on the eastern side along ± 160 km in three segments, two active fault segments on the tram-Talise-Bora ± 130 km long, and one segment of the active Gumbasa-Kulawi fault ± 30 km long (Soehaimi et al. 2018, Supartoyo et al. 2018).

The occurrence of a negative-moderate 'correlation between water discharge and Water Catchment Area (WCA), vegetated land, aquifer productivity, and springs users caused by less water discharge. Ideally, WCA and extensive vegetated area, high aquifer productivity, and many springs users, water discharge must also be larger to have a 'positive, strong correlation. The discrepancy between the response variable (Y) and the explanatory variable (X) in the four SP clusters in the Palu and Poboya watersheds can occur due to the fault earthquake on 28 September 2018. Each landform has characteristics of rock structure as a container aquifer groundwater (Sumartoyo 2010).

The determinant coefficient value (R2) in Table 3 shows the level of accuracy of the regression model, ranging from good (0.56) to very bad (0.01). The regression suggested that only those R2 with moderate to good category (0.29 − 0.56)

Table 4: Criteria and spatial modeling techniques for springs performance.

Criteria	Parameter	Indicator	Weight	Value	Total Value
Water quantity	Water discharge	Great): >10 l/s	50	5	250
		Moderate: 5-10 l/s		3	150
		Few: <5 l/s		1	50
Water catchment area	Large area	>50 ha	7	5	35
		10-50 ha		3	31
		<10 ha		1	7
Vegetation cover	Area of vegetation cover	> 50%	8	5	40
		25 -50%		3	24
		< 25%		1	8
Aquifer	Potential groundwater capacity	High productivity	9	5	45
		Medium productivity		3	27
		Low Productivity		1	9
Groundwater	Depth of free groundwater level	<1 m	10	5	50
		1-5 m		3	30
		>5 m		1	10
Faulting	The proximity of the fault moves with the location of the springs	>10 km	10	5	50
		5-10 km		3	30
		<5 km		1	10
Use of springs	Number of springs users	<2 users	6	5	30
		2-3 users		3	18
		>3 users		1	6

are suitable to build a performance model. Thus, the variable of free groundwater depth (X5), fault movement distance from springs (X3), aquifer productivity (X4), vegetated land (X9), catchment area (X1), and springs users (X10) as modelers' performance conditions in evaluation. Spatial modeling of SP performance conditions is approached by the weighting of variables X and Y. This was confirmed by Gunawan et al. (2016); weighting each parameter (factor) should be based on a correlation matrix between parameters.

Table 4 shows the X and Y variables formulated as a spatial model in evaluating SP performance conditions. The model explains the water catchment area (WCA) as a reservoir for rain, as a place for vegetation to grow, and various types of land use, soil type, and groundwater potential are also included. This aligns with Gunawan et al. (2016), who stated that catchment area condition depends on several factors, including land use, slope (topography), rainfall, soil type, and groundwater potential.

Formula: $$TVS = \sum_{n=1}^{\infty}(weight \; x \; value / \max value)$$
$$\dots (1)$$

Where:

TVS = Total Value of Springs;

Value = springs value of each criterion (springs value of each criterion);

The maximum value = each criterion 5 (criterion each of 5); maximum total value of 100 (maximum total value of 100.). (Ministry of Environment and Forestry 2017).

The results of spatial model performance for six springs locations in the four clusters are given in Table 5.

Table 5 shows 'bad' performance in one site, and the other five are disturbed. The correlation regression analysis between variables Y and X with negative regression coefficient values and moderate-strong negative correlations were analyzed as the factor of springs 'bad-disturbed' water production performance. The only variable X with a great positive regression-correlation coefficient value is the level of free groundwater that averages <1 meter so that the springs can still produce water throughout the year, even with small discharge. The catchment areas have a high ability to absorb rain to fill up the aquifers as a source of water. The catchment area depends on land use, slope, rainfall, soil type, and groundwater potential (Ministry of Environment and Forestry 2017, Gunawan et al. 2016).

A spatial model shows the exceed of water utilization. Several factors are identified, such as fault movement, shrinking water catchment coverage area (8.05-68.77 ha), shrubs and grasses dominated land cover or loss of trees.

The texture and depth of plant roots determine groundwater storage capacity. The deeper the roots are, the more water is stored in the soil (Sari & Prijono 2019). The soil's adequate depth determines the groundwater storage capacity in a land-use system, the distribution of soil micro-pore spaces, and the balanced soil particle size between clay and sand particles. Groundwater content values and soil physical properties influence groundwater reserves. Solum thickness affects water storage capacity (Rahayu et al. 2009, Sari & Prijono 2019).

Based on the bad-disturbed performance value of modeling, thus, could be analyzed that performance

Table 5: The performance of the spatial model of springs.

Variables	Total value					
	Cluster 4 Poboya		Cluster 3 Uemanje	Cluster 1 Ranjuri Beka		Cluster 2 Mantikole
	Springs1 SP1)	Springs2 (SP2)	Springs (SP)	Springs1 (SP1)	Springs2 (SP2)	Springs (SP)
Water discharge	50	150	50	50	50	50
Water catchment area	7	21	35	35	35	21
Vegetation cover	40	40	40	40	40	40
Aquifer	27	27	45	45	45	45
Free groundwater	50	50	50	50	50	50
A fault movement distance from the springs)	10	10	50	50	50	50
Use of springs	18	18	6	18	18	18
Total score	202	316	276	288	288	274
Springs performance value	40	63	55	58	58	55
Springs performance	bad	Disturbed	disturbed	disturbed	disturbed	Disturbed

Remarks: SP = springs

Fig. 2: Map of the spatial model of the post-earthquake springs performance conditions 28 September 2018 in the Mantikole Cluster 2 (Scale 1:50,000).

improvement and mitigation are needed through forest and land conservation, enrichment planting of trees, wise land management, and proper water utilization. Soil permeability in the secondary forest is faster than in mixed upland, monocultures, and paddy fields. Soil permeability in monocultures is higher than in mixed upland. The ability of forest areas to absorb water is faster than the rice field or even a mixed upland area. This finding is supported by Lopes et al. (2019), that the forest is a groundwater reservoir and provides a wide range of ecosystem services. It fasts in permeability and relatively fast on mixed land, has medium permeability on dry land and yard, and is slower on degraded land. Forest area consists of numerous trees and diverse upland areas provided by the better ability on water permeability. It makes
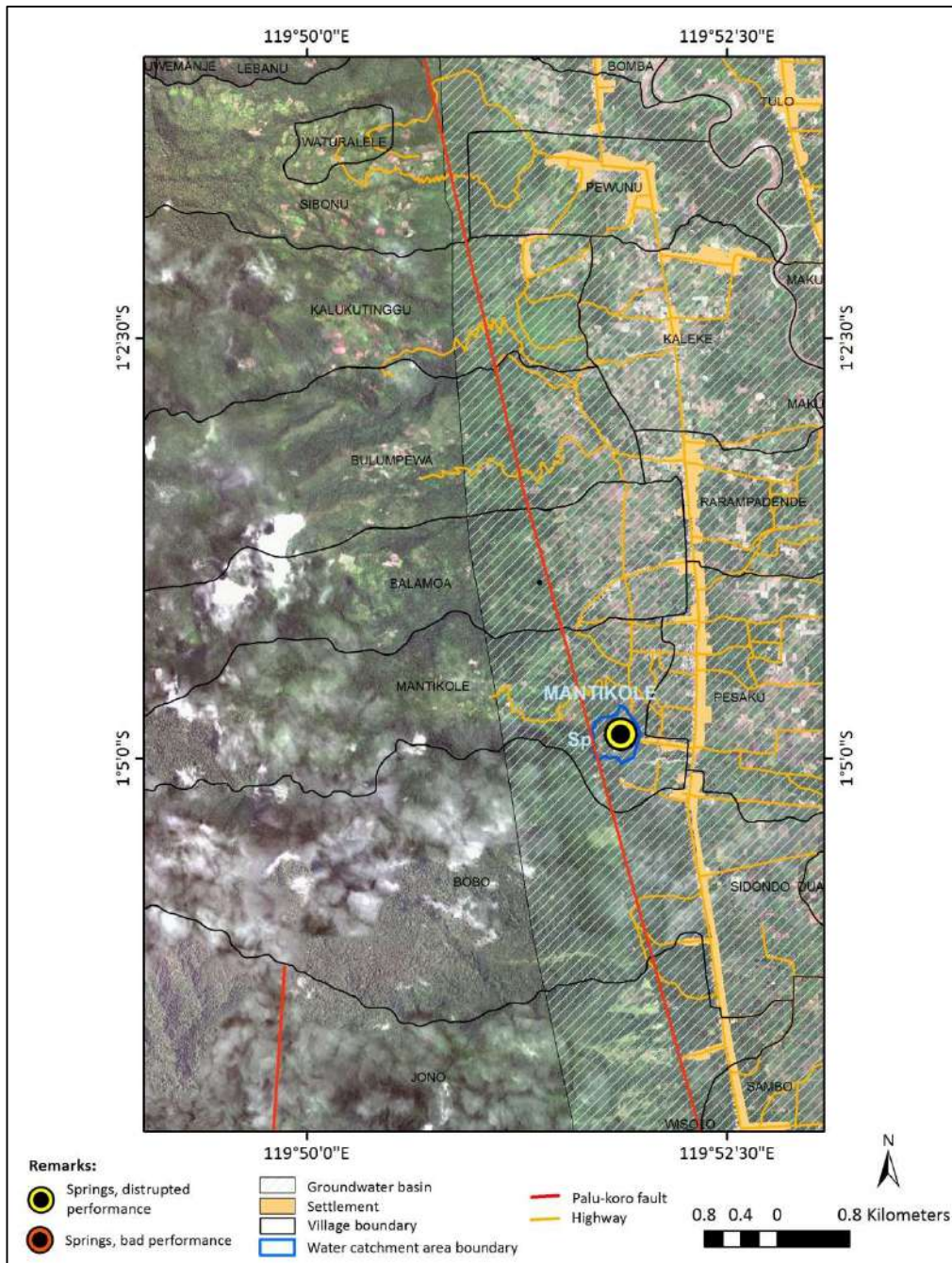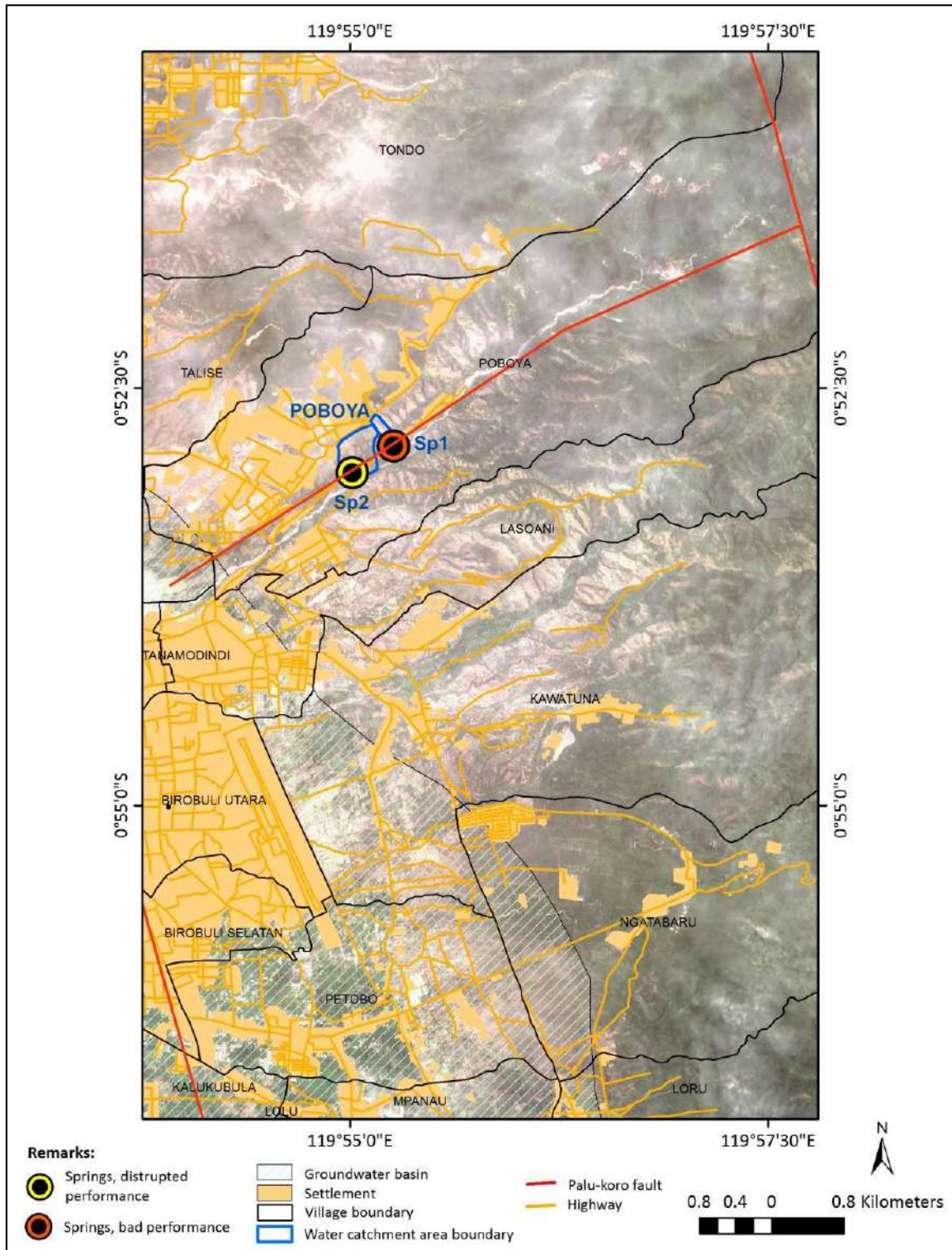
Fig. 3: Map of the spatial model of the post-earthquake springs performance conditions 28 September 2018 in the Poboya Cluster 4 (Scale 1:50,000).
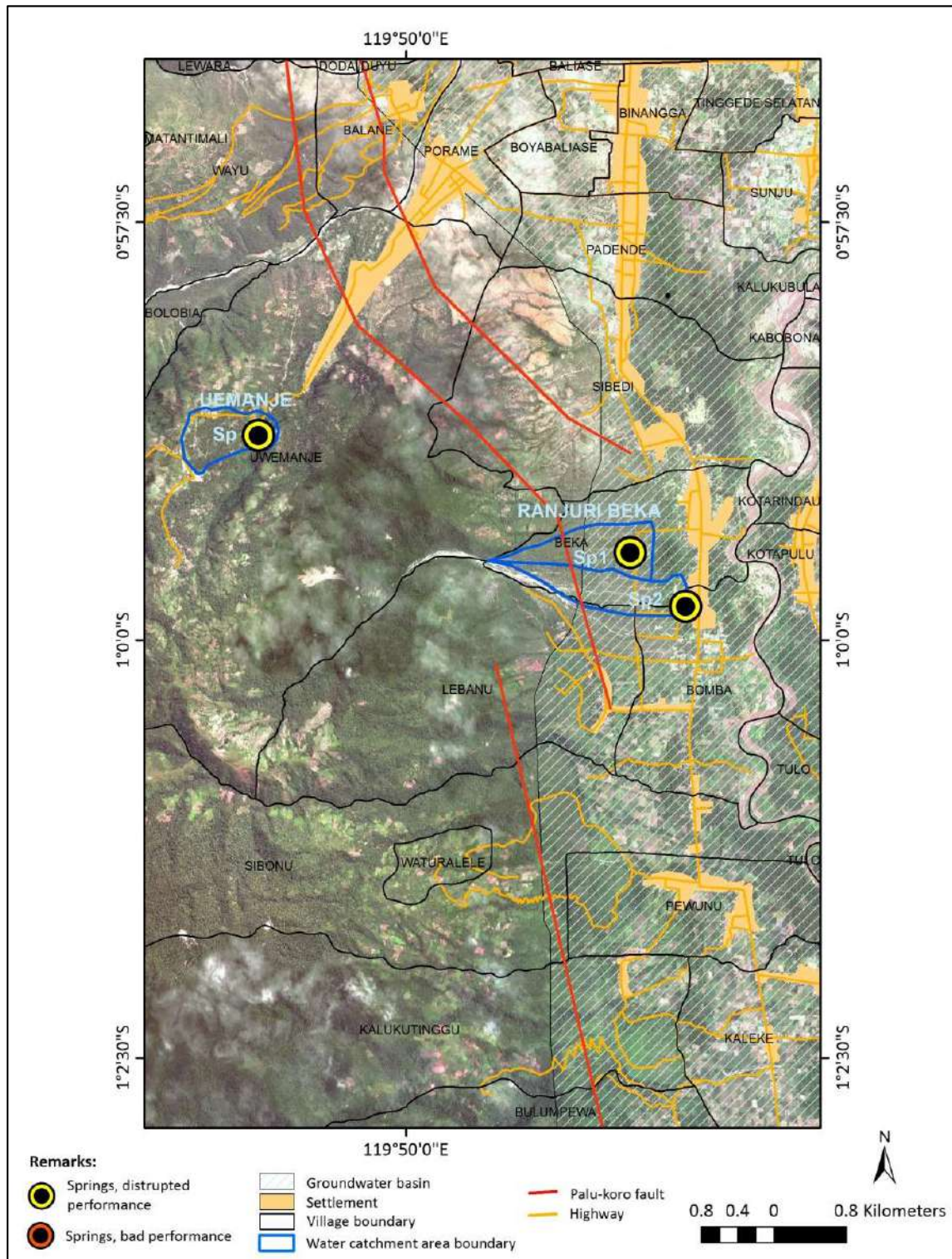
Fig. 4: Map of the spatial model of the post-earthquake springs performance conditions 28 September 2018 in the Ranjuri Beka Cluster 1 and Uwemanje Cluster 3 (Scale 1:50,000).

CONCLUSION

From the results of spatial-statistical modeling, it is known that the condition of the springs in producing water after the tectonic earthquake in the Palu and Poboya watersheds has a "poor-disturbed" performance. This performance was caused by the use of water sources at each location of the springs that had exceeded its water production capacity, the movement of faults/faults, the water catchment area was not wide (8.05 - 68.77 ha), vegetation cover dominated by shrubs and grasses and a few forest trees. Considering these conditions, it is necessary to increase the recharge area and improve evapotranspiration through the enrichment of forest and annual plants, as well as protection around springs within a radius of 200 m from various land clearing activities. To maintain the performance of springs in areas prone to tectonic earthquakes with low-moderate aquifer productivity and the presence of deep-free groundwater, it is important to conduct scientific research related to the hydrogeological aspects of the area, which is integrated with trials of developing plant species that have high water storage capacity.

ACKNOWLEDGMENTS

REFERENCES

Albris, K., Lauta, K. C. and Raju, E. 2020. Disaster knowledge gaps: Exploring the interface between science and policy for disaster risk reduction in Europe. Int. J. Dis. Risk Sci., 11(1): 1-12.

Ali, R., Kuriqi, A. and Kisi, O. 2020. Human–environment natural disasters interconnection in China: A review. Climate, 8(4): 48.

Botzen, W.W., Deschenes, O. and Sanders, M. 2019. The economic impacts of natural disasters: A review of models and empirical studies. Rev. Environ. Econ. Policy, 13(2): 167-188.

De Goyet, C.D.V. 2007. Health lessons learned from the recent earthquakes and tsunami in Asia. Prehosp. Disas. Med., 22(1): 15-21.

Galata, A., Tullu, K. and Guder, A. 2020. Evaluating Watershed Hydrological Responses to Climate Changes at Hangar Watershed, Ethiopia. Authorea Preprints, Hoboken, NJ.

Gunawan, S.A., Prasetyo, Y. and Amarrohman, F.J.. 2016. Reforestation of wilis circles: an effort to maintain the water permeating area in Tulungagung District East Java. J. Geodesi UNDIP, 5(2): 125-135.

Jakubis, M. and Jakubisová, M. 2019. The impact of hydrologic characteristics of mountain watersheds on geometric and hydraulic parameters of natural torrent beds. J. Ecol. Eng., 20(3): 1016.

King, C.Y., Zhang, W. and Zhang, Z. 2006. Earthquake-induced groundwater and gas changes. Pure Appl. Geophys., 163(4): 633-645.

Liao, X., Wang, C.Y. and Liu, C.P. 2015. Disruption of groundwater systems by earthquakes. Geophys. Res. Lett., 42(22): 9758-9763.

Lisnawati, Y. and Wibowo, A. 2010. Analysis of water discharge fluctuation due to land use change in Puncak Area, Bogor District. Plant. Forest. Res., 7(4): 221-226

Lopes, A.F., Macdonald, J.L., Quinteiro, P., Arroja, L., Carvalho-Santos, C., Cunha-e-Sá, M. A. and Dias, A.C. 2019. Surface vs. groundwater: The effect of forest cover on the costs of drinking water. Water Resour. Econ., 28: 100123.

Mason, H.B., Montgomery, J., Gallant, A.P., Hutabarat, D., Reed, A.N., Wartman, J. and Yasin, W. 2021. East Palu Valley flow slides induced by the 2018 MW 7.5 Palu-Donggala earthquake. Geomorphology, 373: 107482.

Ministry of Environment and Forestry. 2017. Guidelines for Inventorying and Identifying Damage to Springs in Watershed Areas (DAS). Directorate of Land Water Damage Management, Directorate General of Watershed Control and Protected Forests, Jakarta.

Naharuddin, N., Malik, A. and Ahyauddin, A. 2021. Soil loss estimation for conservation planning in the Dolago Watershed Central Sulawesi, Indonesia. J. Ecol. Eng., 22(7): 242-251.

Naharuddin, N., Malik, A., Rachman, I., Muis, H., Hamzari, H. and Wahid, A. 2020. Land use planning for post-disaster soil liquefaction area based on erosion hazard index. Int. Inform. Eng. Technol. Assoc., 15: 573-578. http://iieta. org/journals/ijdne, 15(4), 573-578.

Naharuddin, N., Wahid, A., Rukmi, A. and Sustri, M. 2019. Erosion hazard assessment in forest and land rehabilitation for managing the Tambun watershed in Sulawesi, Indonesia. J. Chin. Soil Water Conserv., 50 (3): 124-130.

Naharuddin, N., Wulandari, R. and Paloloang, A.K. 2018. Surface runoff and erosion from agroforestry land use types. J. Animal Plant Sci., 28(3): 875-882.

Nugroho, S.P. 2018. Disaster Management M 7.4 Earthquake and Tsunami in Central Sulawesi. Center for Data, Information, and Public Relations of the National Disaster Management Agency, Jakarta

Rahayu, S., Widodo, R.H., van Noordwijk, M., Suryadi, I. and Verbist, B. 2009. Monitoring of Water in Watersheds. Bogor, Indonesia. World Agroforestry Centre - Southeast Asia Regional Office, Nairobi, Kenya, pp. 10-19

Reghunath, R., Sekhar, S.B., Nithin, R. and Kumar, R.B. 2009. Demarcation of groundwater prospective zones in a degraded region of Western Ghats: A GIS-based approach. Nature Environ. Pollut. Technol., 8(2): 347-350.

Santosa, L.W. 2006. Hydrogeomorphological study of springs on the western slopes of Mount Lawu. Forum Geografi., 20(1): 68-85

Sari, I.L. and Prijono, S. 2019. Infiltration and water storage in different types of shade in coffee fields in Amadanom village, Dampit District, Malang Regency. J. Land Resour., 6(1): 1183-1192. http://doi: 10.21776/ub.jtsl.2019.006.1.17

Soehaimi, S., Yopyan, Y. and Sulistyawan, I.H. 2018. Earthquake Genetics: Behind the Enchantment of the Palu Disaster Affects Organizing Geology. Geological Agency, Bandung, pp. 33-40.

Sumartoyo, I. 2010. Landform typological approach to estimate groundwater potency in Bogor Regency, West Java Province. Globë, 12(1): 57-67.

Supartoyo, C.A., Omang, A. and Hidayati, S. 2018. Impact of the Surface of the Palu-Donggala-Sigi Earthquake. National Center for Earthquake Studies, Research, and Development Center for Housing and Settlements of the PUPR, Jakarta, pp. 57-73.

Syifa, M., Kadavi, P.R. and Lee, C.W. 2019. An artificial intelligence application for post-earthquake damage mapping in Palu, Central Sulawesi, Indonesia. Sensors, 19(3): 542.

Tunas, I.G., Tanga, A. and Oktavia, S.R. 2020. Impact of landslides induced by the 2018 Palu earthquake on flash flood in Bangga river basin, Sulawesi, Indonesia. J. Ecol. Eng., 21(2): 190-200. DOI: https://doi.org/10.12911/22998993/116325

Wahyuningrum, N. and Putra, P.B. 2018. Land evaluation to assess the performance of the Rawakawuk subwatershed). J. Watershed Manag. Res., 1(2): 16 https://doi.org/10.20886/jppdas.2018.2.1.1-16

Wang, C.Y., Wang, C.H. and Manga, M. 2004. Coseismic release of water from mountains: Evidence from the 1999 (Mw=7.5) Chi-Chi, Taiwan, earthquake. Geology, 32(9): 769-772.

Wekke, I.S., Sabara, Z., Samad, M.A., Yani, A., Abbas, T. and Umam, R. 2019. Earthquake, tsunami, and society cooperation: Early findings in Palu of Indonesia post-disaster. Geoscience, 10: 322.

Wilkerson, G.V. 2008. Improved bank full discharge prediction using 2-year recurrence-period discharge 1. JAWRA J. Am. Water Resour. Assoc., 44(1): 243-257.

Xuan-Nam, B., Dinh, C.T., Quoc, N.L., Xuan, M.B., Le Hung, T., Ropesh, G. and Nam, P. H. 2020. Assessment on the maximum magnitude of a natural and triggered earthquake when water is impounded in the mining pit: A case study in Nui Nho quarry, Vietnam, based on gravity and magnetic data. Russ. J. Earth Sci., 20(1): 1-10.

Zeffitni Z. 2012. Spatial ecological distribution of groundwater potency to domestic availability at Palu Groundwater Basin Central Sulawesi Province. J. Hum. Environ., 19(2): 105-117.

Chemical Pretreatment of Rice and Wheat Straws to Reduce the Recalcitrant Structure: Comparative and Kinetic Studies with Different Chemicals for Biogas Production

Nikita Kanaujia,* Shalu Rawat* and Jiwan Singh*† iD

*Department of Environmental Science, Babasaheb Bhimrao Ambedkar University, Lucknow-226025, India
†Corresponding author: Jiwan Singh; jiwansingh95@gmail.com

ABSTRACT

In this study, a comprehensive comparison of two different chemical pretreatments of wheat straw (WS) and rice straw (RS) was made. The pretreatment was performed using piranha solution and *p*-toluenesulfonic acid (PTSA) to dissolve the biomass's complex lignin and hemicellulose matrix to enhance its methane production. Energy dispersive spectroscopy (EDS), Fourier transform infrared spectroscopy (FTIR), scanning electron microscopes (SEM), and X-ray diffraction (XRD) analysis, were used to analyze the characteristics of untreated and pretreated feedstock. WS and RS treated with piranha solution showed maximum methane yield (1234 mL and 1196 mL, respectively). The piranha pretreatment increased the methane yield of wheat straw by 2.37 folds and rice straws by 2.31 folds. The maximum VFA concentration was observed in WS on the 14th day in the piranha-treated sample, 1553.33 ± 2.8 mg.L^{-1}, while in RS on the 21st day in the untreated sample, 676 ± 5.77 mg.L^{-1}. SEM analysis of piranha-treated WS indicated a reduction in recalcitrant structure. Deformation of C-O, C=C, C-C-O, and C-H bonds in cellulose, hemicellulosic, and lignin as a result of chemical pretreatment in WS and RS was also indicated by FTIR analysis. The modified Gompertz model (MGM) and logistic function model (LFM) appropriately defined the degradation process and explained cumulative biogas' kinetic. Pretreatment with piranha solution reduces the complexity of WS and RS, thus increasing methane production by reducing the retention time.

INTRODUCTION

In a time of rapid fossil fuel depletion, air pollution, and increased waste generation, it is vital to encourage the production of a sustainable, reliable, and affordable energy source. Production of clean energy has now become necessary since the power demand is ever-increasing (Owusu et al. 2016, Karuppiah & Azariah 2019, Korys et al. 2019). The fuel shortage could adversely affect economic activity; therefore, the dependency on fossil fuels must be reduced by opting for renewable energy. The utilization of agricultural residue in the energy sector is growing continuously as it is generated in huge quantities and is inexhaustible. The biomass is being replenished continuously with an increase in agricultural activities. Unscientific burning of agricultural waste produces a significant amount of hazardous gases, most notably nitrogen dioxide, sulfur dioxide, nitrous oxide, carbon monoxide, methane, polycyclic aromatic hydrocarbons,

particulate matter, and volatile organic compounds (Dar et al. 2016, Singh et al. 2020). Sustainable agricultural waste management through anaerobic digestion can efficiently resolve some energy crises. According to a report from the Food and Agriculture Organization (FAO RMM 2018), rice comes in the third position after maize and wheat among the most cultivated crops, producing a significant amount of lignocellulosic trash (Singh & Kumar 2019, Kainthola et al. 2019a). The three primary components of any lignocellulosic biomass are lignin, hemicellulose, and cellulose, along with some portion of soluble and insoluble materials like pectin, protein, and minerals (Maldonado-Bustamante et al. 2022). Different biomass has different ratios of these constituents according to crop variety, environmental condition, and soil quality (Kumar et al. 2021). Both amorphous and crystalline forms of cellulose are present in rice straw and wheat straw. Amorphous cellulose degrades effortlessly, while crystalline cellulose is hard to degrade due to microfibril binding. Hemicellulose is linear and highly branched heteropolymer with C-5 and C-6 sugars as its main components. It is

susceptible to hydrolysis during anaerobic digestion owing to low molecular weight and low degree of polymerization (Ahmad et al. 2018). Lignin is a hard, hydrophobic, and complicated biopolymer that provides structural strength by producing a barrier that prevents the digestion of WS and RS (Kumar et al. 2021). Cellulose is a linear polymer of D-glucose units linked together by -1,4 bonds and closely maintained by inter and intra-chain hydrogen bonding to form microfiber, which protects the plant cell wall and provides mechanical strength to them (Ma et al. 2019). According to Halac & Ragauskas (2011), RS has more polymerization degree than WS. Hemicellulose is interconnected to lignin by covalent bonds, while hemicellulose and cellulose are linked by hydrogen bonding. Lignin comprises propyl phenol units, namely coniferyl alcohol, sinapyl alcohol, and some amount of p-coumaryl alcohol. These are connected by various ether and carbon-carbon linkages, such as β-O-4, 4-O-5, β-β, β-1, and β-5, to produce phenylpropanoid units like guaiacyl (G), ayringyl (S), and p-hydroxyphenyls (H). The β-O4-linkage is the leading ether bond (60%-40) in the lignin of RS (Sheng et al. 2021). Lignin is difficult to remove because of its attachment with carbohydrates through benzyl esters, benzyl ethers, and phenyl glycosides which provide a robust structure to RS (Satlewal et al. 2018). Pretreatment of WS and RS is necessary as various interlinked bonds mentioned above are hard to digest (Zoghlami & Paes 2019). High silica content in RS and WS also inhibits enzymatic hydrolysis; hence the removal of silica content is required to improve enzymatic accessibility (Athira et al. 2019). Anaerobic digestion of lignocellulosic biomass without pretreatment is un-remunerative. There are numerous pretreatment methods to reduce the recalcitrant nature, such as physical, chemical, and biological among them, chemical pretreatment has become the most approachable and promising method. Chemical pretreatment effectively increases cellulose biodegradability by reducing the complexity of lignin and hemicelluloses (Mancini et al., 2018). Chemical pretreatment techniques include oxidative, ozonolysis, organosolv, acidic, alkaline, and ionic liquid pretreatment. According to the current studies reported in the literature, acidic pretreatment is perhaps the best among these chemical pretreatments if lignocellulose is pretreated with a diluted acid at a high temperature (Mahmood et al. 2019). Oxidative pretreatment of lignocellulose by oxidant is referred to as an effective process. However, it has been studied rarely (Chen et al. 2017). Chemicals varying from oxidizing agents, alkali, acids, and salts are capable of degrading lignin, cellulose, and hemicellulose from lignocellulosic biomass; moreover, organic (formic, acetic, and propionic) inorganic (Sulfuric, nitric, hydrochloric and phosphoric) acids are also used to break the internal bond of lignin and hemicellulose

(Behera et al. 2014). Chiranjeevi et al. (2018) reported that a novel assisted dilute acid pretreatment with boric acid (1% w/v) + H_2SO_4 (0.75%v/v) + glycerol (0.5% v/v) at 150 C for 20 min significantly enhanced the delignification of RS and consequently glucan-to-glucose conversion. An extensive study was performed by Pellera et al. (2018) in which they assessed how chemical pretreatment affected the solubilization of agro-industrial waste. The study selected different wastes such as wineries, cotton gins, olive pomace, and the juice industry. For the pretreatment, eight reagents were used: NaOH, NaHCO₃, NaCl, H₃Cit, AcOH, H_2O_2, Me_2CO, and EtOH. Among all the reagents, H3Cit, H_2O_2, and EtOH were effective as they altered the substrate's structure and broke the bond between cellulose hemicellulose and lignin. Wet oxidation comprises oxidizing agents such as oxygen, ozone, and hydrogen peroxide. The wet oxidation process affects all three components of lignocellulosic biomass. Hemicellulose is enormously broken into monomeric sugars and reduced into organic acids, the crystallinity of cellulose reduces, and the lignin breaks and oxidizes (Den et al. 2018). Wet oxidation is quite effective on maize straw (Chen et al. 2017). It is analyzed that p-toluene sulfonic acid has tremendous potential for the delignification of biomass (Wang et al. 2020). Therefore, the current study compares the piranha solution with p-toluene sulfonic acid pretreatment on WS and RS. As piranha solutions are strong oxidizing agents, p-toluene sulfonic acid is strong. At the same time, no study has been conducted on the pretreatment of WS and RS with piranha solution. In this study, a comprehensive comparison of novel chemical pretreatment on RS and WS was performed also tries to understand the significance of silica reduction as much literature is present on the reduction of lignin from agricultural residue. However, the reduction of silica was neglected.

MATERIALS AND METHODS

Chemicals and Reagents

All experiments were conducted with analytical-grade chemicals bought from Fisher Scientific India. To prepare concentrated piranha solution, 3 parts of concentrated sulfuric acids and 1 part of 30 % hydrogen peroxide solution were mixed, as Shrivash et al. (2017) reported. In addition, Para toluene sulfonic acid ($CH_3C_6H_4SO_3$), phosphate buffer, iron chloride ($FeCl_3.7H_2O$), magnesium sulfate ($MgSO_4.7H_2O$), calcium chloride ($CaCl_2.2H_2O$), cobalt nitrate ($Co(NO_3)_2.6H_2O$), nickel chloride ($NiCl_2.2H_2O$), sodium hydroxide (NaOH), ferrous ammonium sulfate ($Fe(NH_4)_2(SO_4)_2.6H_2O$), potassium dichromate ($K_2Cr_2O_7$), silver sulfate (Ag_2SO_4) and ferroin indicator were also used in this study. All the reagents used in this study were prepared using double distilled water.

Collection and Analysis of WS, RS and Inoculum

WS and RS were collected from Mohanlalganj (Lucknow, Uttar Pradesh, India). Both the biomasses were kept in an oven for one week separately at 45°C to dry them, afterward crushed using a grinder and kept in air-tight plastic bags at room temperature, cow dung (CD) was collected from a nearby dairy in Rajnikhand (Lucknow, Uttar Pradesh, India). The physicochemical characteristics of WS, RS, and CD were analyzed and individually shown in Table 1. Moisture content (MC), volatile solids (VS), and soluble chemical oxygen demand (sCOD) were determined with the help of methods mentioned in the American public health association (APHA). The direct titration method measured volatile fatty acids (VFA) (DiLallo & Albertson, 1961), and pH values were measured by water analyzer 371 (Systronics, India)

Pretreatment of WS and RS

For pretreatment, 50 g of WS was taken in two 250 mL conical flasks (a and b), then in the flask (a), 150 mL of 10% piranha solution, and in flask (b), 150 mL of PTSA solution was added separately. Then these flasks were kept for shaking for 24 h at a magnetic stirrer. A similar procedure was also done for RS for pretreatment. Afterward, the pretreated biomass was filtered and dried for further use.

Each experiment was performed in triplicates in this work. The untreated WS and RS were denoted as WSU and RSU, respectively, and WS and RS treated with piranha solution were denoted as WSP and RSP. And WS and RS treated with PTSA were denoted as WSPT and RSPT, respectively.

Batch Study for Anaerobic Digestion of WS and RS

The influence of chemical pretreatment of WS and RS on methane production was analyzed through the daily water displacement technique for 35 days. Borosil glass bottles of 1000 mL capacity were used as reactors in the batch study. For the anaerobic digestion of WS, 20.9 g of WSU, WSP, and WSPT were added to the reactor bottles separately. A 50 g of CD was mixed in each reactor, and the volume of the reaction mixture was maintained at 700 mL using double distilled water. Macronutrients (phosphate buffer of 7 pH) and micronutrients $MgSO_4$ (400 mg.L^{-1}), $CaCl_2$ (50 mg.L^{-1}), $FeCl_3$ (40 mg.L^{-1}), $CoCl_2$ (10 mg.L^{-1}), $ZnCl_2$ (0.5 mg.L^{-1}) and $NiCl_2$ (0.5 mg.L^{-1}) were added in reactor along with feedstock and inoculum. A similar setup was also maintained for the anaerobic digestion of RS using 23.6 g of RSU, RSP, and RSPT. Anaerobic digestion of WSU and RSU were set as control experiments. The amount of WS and RS (20.9 and 23.6 g, respectively) was selected per food-to-microbe ratio (F/M) 2. The selection of this F/M ratio was
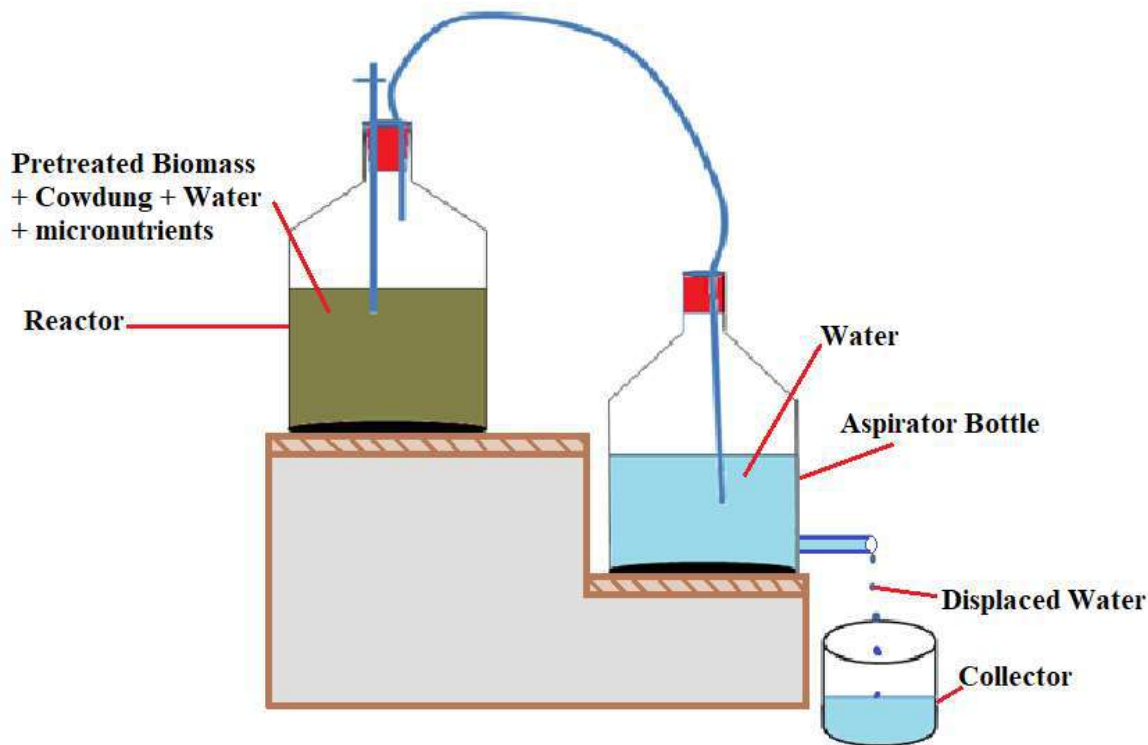
Fig. 1: Set up for anaerobic digestion study.

made based on previous literature, which reported it best for anaerobic digestion (Kainthola et al. 2019b, Saha et al. 2018, Veluchamy et al. 2017). The reactor bottles were connected with 1000 mL aspirator bottles through a pipe filled with distilled water. The water of the aspirator bottle displaced on the methane generation was collected in a collector placed at the end. A rubber cork was fitted on the reactor to sustain the anaerobic condition inside the glass bottles (Fig. 1). All the experiments were performed in triplicate.

Instrumental Analysis

SEM and EDS analysis for the morphological and elemental analysis of WSP, WSPT, WSM, WSU and RSP, RSPT, RSM, and RSU were done by JSM 4490 (JEOL, Japan). Surface functional group analysis was done using an FTIR model NICOLET6700 (Thermo Fisher Scientific, U.S.A). XRD was used to determine the degree of crystallinity in untreated and pretreated feedstock using D8 Advance Eco (Bruker, Germany); moreover, the crystallinity index (CI) was determined as the following equation (Kumar et al. 2016).

$$Crystallinity\ index(\%) =$$
$$\frac{Area\ of\ all\ the\ crystalline\ peaks}{Area\ of\ all\ the\ crystalline\ and\ amorphous\ peaks} \times 100$$
$$...(1)$$

Analysis of Data through Kinetic Models

MGM and LFM were used to model the kinetics of methane generation. To calculate the methane production and the kinetic parameters for the current investigation, IBM SPSS statistics were employed. The following equations and nonlinear regression analysis used the experimental cumulative methane yield data to determine the bio-kinetic parameters.

$$y(t) = P * Exp\left(-Exp\left(\frac{R*Exp}{P}\right)(L-1)+1\right)$$
$$...(2)$$

$$y(t) = \frac{P}{1+exp\{\frac{4R(L-1)}{P}+2\}}$$
$$...(3)$$

Where y (t) is cumulative methane potential (mL), P represents the maximum yield of biogas (mL), R denotes the highest production rate of biogas (mL), L is the lag phase constant (day), and the value of the constant e is 2.7183. The parameters P, R, and L were calculated by curve fitting IBM SPSS 20. Regression analysis was done to estimate the coefficient of correlation R^2.

RESULTS AND DISCUSSION

Effect of Pretreatment on the Degree of Solubilization

Piranha solution and PTSA can break down the interunit of lignocellulosic biomass. The high oxidative properties and generation of singlet oxygen radicals are responsible for the degradation of feedstock. The chemical pretreatment effect on the solubilization of WS and RS was measured by the change in VFA, sCOD, VS, and pH alterations of the digestate as shown in Fig. 2 and Fig. 3. The large molecule partially degraded while pretreatment and consecutively converted into VFA during the digestion process.

At the initial stage of anaerobic digestion, the concentration of VFA varied from 233.33 ± 28.86 mg.L^{-1} to 986.66 ± 2.88 mg.L^{-1}. Minimum VFA was observed in RSU, while maximum VFA was detected in WSP. The VFA concentration rapidly increased with digestion time in all the reactors (Fig. 2c and 2d). As the VFA increased, the pH decreased (Fig. 2a and 2b), indicating the formation of acidic conditions in the reactors. VFA is produced in the acidogenesis phase and contains acetic acid, propionic acid, butyric acid, and valeric acid, which causes a drop in pH. At last, they get converted into methane. VFA is utilized as a substrate in anaerobic digestion for methane production as it preserves all chemical energy of the substrate (Valentino et

Table 1: Initial physicochemical characteristics of WS, RS and CD.

Parameters	WS	RS	CD
pH	7.48 ± 0.5	7.79 ± 0.5	7.31
Moisture content [%]	8.1 ± 0.33	5.94 ± 1.5	81.235 ± 0.6
Volatile solids [% Total solid]	92.53 ± 0.613	80 ± 0.7	82.39 ± 0.09
Ash content [% Total solid]	14.47 ± 0.99	20 ± 0.56	17.61 ± 1.25
TS [%]	90 ± 0.25	94.09 ± 0.76	18.27 ± 0.07
Lignin [%]	18.52 ± 0.55	14.76 ± 0.87	NA
Hemicellulose [%]	25 ± 1.99	29.09 ± 0.45	NA
Cellulose [%]	39 ± 1.25	37.98 ± 0.56	NA

*NA - Not Analyzed

al. 2021). The maximum concentration of VFA was achieved on the 14th day, and WSP showed a maximum concentration of VFA (1553.33 ± 2.8 mg.L^{-1}) followed by WSPT (1414.66 ± 25 mg/L), RSP (1333.33 ± 28.86 mg.L^{-1}), RSPT (1269.33 ± 19 mg.L^{-1}) while in WSU and RSU maximum VFA found on 21st day that is 752.33 ± 4.04 mg.L^{-1} and 676 ± 5.77 mg.L^{-1} respectively. Subsequently, an abrupt decrease was observed in all the reactors due to the commencing of the methanogenic phase. WSP has 1.09 fold higher VFA than WSPT, and RSP has 1.05 fold higher VFA than RSPT. A higher concentration of VFA in piranha-treated biomasses may be due to fast hydrolysis caused by piranha solution, which potentially breaks the lignocellulosic matrix because of its strong oxidative nature. Compared to the inhibitory concentration, i.e., 8000 mg.L^{-1}, the VFA concentration was lower during the digesting time in all eight reactors, demonstrating favorable conditions for the growth of acid-producing bacteria.

sCOD indicates the degree of substrate solubilization attained by microbes to generate methane (Kavitha et al.

2014). As WS and RS are anaerobically digested, the change in an sCOD is depicted in Fig. 3a and 3d, respectively. The initial sCOD for WS ranged from 6612 ± 97 mg.L^{-1} to 6166.6 ± 57 mg.L^{-1}, and that of RS ranged from 5157.3 ± 136 mg.L^{-1} to 7844 ± 135 mg.L^{-1}. In all the reactors, sCOD increased with digestion time and achieved the maximum value on the 14th day in all chemically pretreated substrates, while the maximum sCOD in WSU and RSU was found on the 21st day. Afterward, sCOD gradually decreased in all the reactors. Cellulose is hydrolyzed to produce fermentable reducing sugars, which help to raise sCOD levels (Panigrahi et al. 2020). Among all the pretreated substrates highest sCOD was found in WSP, i.e., 16333.33 ± 144.33 mg.L^{-1}. The sCOD of piranha-treated WS and RS was 1.05 times and 1.04 times higher than PTSA treatment, respectively. The lowest sCOD was found in WSU and RSU due to their recalcitrant nature, which made them difficult to solubilize.

The initial VS of WSP, WSPT, and WSU was $87.3 \pm 2\%$, $89.3 \pm 0.57\%$, and $91.6 \pm 2\%$, respectively, and the initial
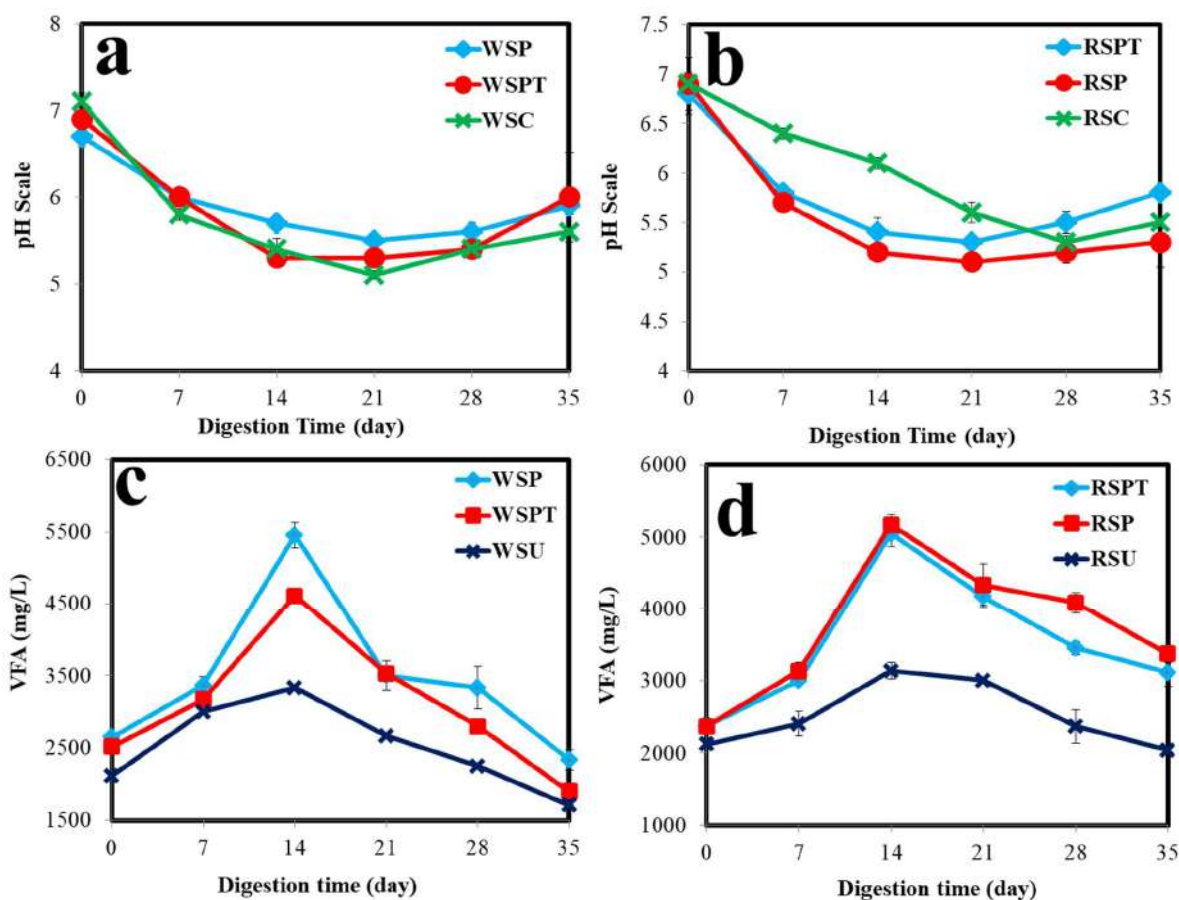
Fig. 2: Effect of Pretreatment on (a) and (b) pH change and (c) and (d) VFA of WS and RS.

VS of RSP, RSPT and RSU were 82.66 ± 1.5%, 85.33 ± 1%, and 89 ± 1%, respectively. VS content of piranha-treated biomasses was lower initially may be due to the removal of non-structural components present in WS and RS during pretreatment. The VS content in anaerobic digestion of WS decreased up to 43.6 ± 1% (WSP), 55.33 ± 0.57% (WSPT), and 61.3 ± 1.5% (WSU), and in RS, the VS was decreased up to 55.66% (RSP), 56.33% (RSPT) 65.66% (RSU). The VS content decreased by increasing digestion time (Fig. 3c and 3d). The reduction in VS is directly proportional to the conversion of organic matter and methane production (Miah et al. 2016). During the delignification process, the β-O-4 linkage is cleaved and converted into a stable C-C bond which makes the enzyme more accessible to the cellulose and consequently degrades it to produce methane (Li et al. 2020, Esposito et al. 2012).

In WSPT VS, the reduction was less (56 ± 2%), probably due to PTSA being inconsiderable to degrade lignin in WS; hence microbes were unable to degrade WSPT, while in WSP VS, the reduction is (43.6 ± 1%) because piranha solution efficiently reduces the rigid structure of WS and RS subsequently it digests effortlessly.

Effect of Pretreatment on Methane Yield

The chemical pretreatment had a consequential impact on methane yield from the initial days. In the pretreated samples, the lag phase ranges from 2 to 4 days; in untreated samples, the lag phase was between 5 to 6 days. Pretreatment improved the lag phase as organic content was solubilized during pretreatment and was easily converted into methane by microbes. The value of the highest daily methane yield in WSP (95 mL.d^{-1}) and WSPT (90 mL.d^{-1}) was observed on the 17th and 18th day, respectively, and in RSP (81 mL.d^{-1}) and RSPT (74 mL.d^{-1}) was observed on the 16th day and 13th day, respectively (Fig. 4a and 4b). Whereas, in untreated samples, the highest value of daily methane production was 23 mL.d^{-1} (WSU) and 27 mL.d^{-1} (RSU) obtained on the 35th day. Compared to the treated samples, the untreated samples produced a very low amount of methane over a comparatively longer time. The cumulative methane yield acquired in this study was 1234 mL, 1208 mL, 1120 mL, 992 mL, 520 mL, and 483 mL for WSP, WSPT, RSP, RSPT, WSU, and RSU, respectively. As shown in Fig. 4c and 4d, the maximum cumulative methane yield for WS was obtained in WSP. Compared with WSU, the cumulative
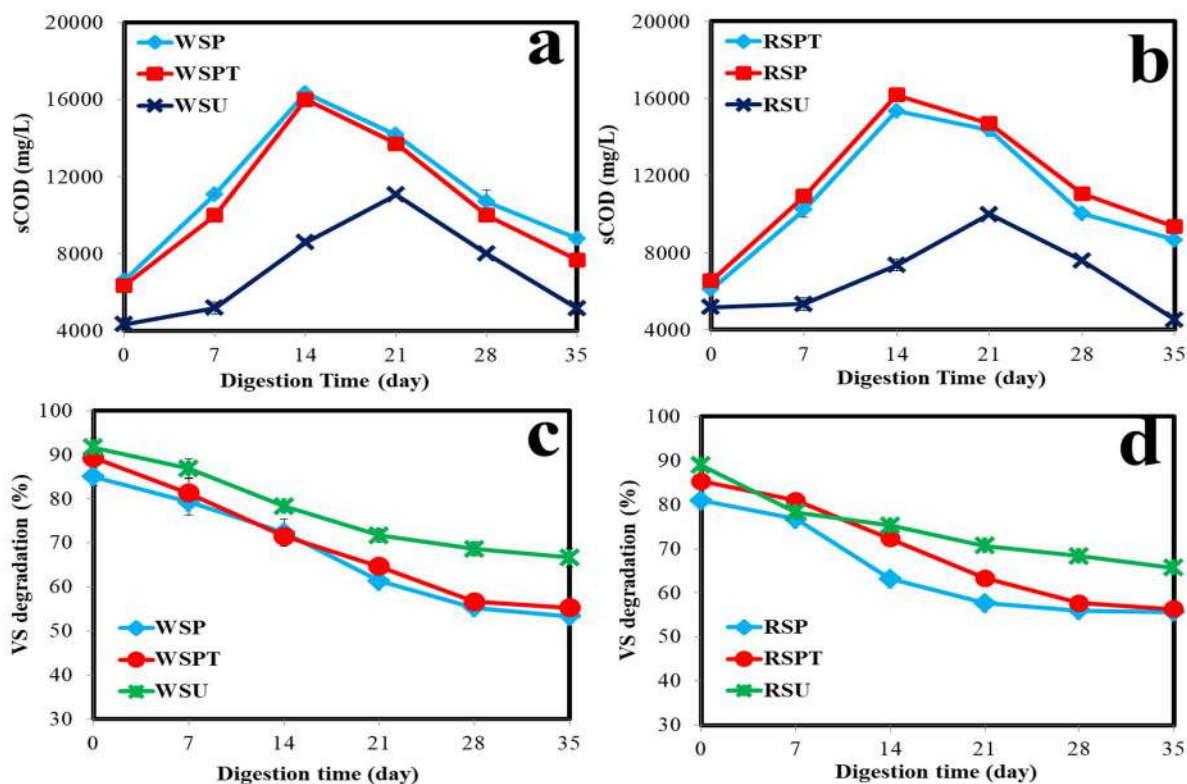
Fig. 3: Effect of pretreatment on (a) and (b) sCOD and (c) and (d) VS degradation of WS and RS.

methane yield was 2.37 folds higher in WSP and 2.32-fold higher in WSPT.

Similarly, the maximum cumulative methane was observed in RSP at 2.31 times higher for RS, followed by RSPT with 2.05 times higher methane production than RSU. As compared to WSPT, WSP showed 1.02-fold increased cumulative methane. Piranha-treated biomasses showed the best yield, probably because the piranha solution effectively breaks the ether linkage. WSP showed the best result compared to RSP may be due to cellular degradation, and microfibrils are disrupted during pretreatment. Moreover, it successfully reduced the recalcitrant nature of RS. Cellulose is the significant structural constituent of cell walls in plants, comprised of a linear polymer of D-glucose subunits connected by β- 1,4 linkage the long chain of cellulose is connected by hydrogen bond and van der Waals bond makes cellulose packed into microfibrils (Perez et al. 2002). After the pretreatment of biomasses,

the fermentable D-glucose is produced from cellulose by breaking a β-1,4 glycosidic bond.

Analysis of Untreated and Pretreated WS and RS

SEM and EDS Analysis

Morphological alterations of biomasses were observed through SEM analysis. As the SEM analysis (Fig. 5a to 5c and 6a to 6c) shows, WSU had a smooth and closed-packed surface with fiber arranged in the bundle due to the occurrence of a strong bond between lignin, hemicellulose and cellulose which is a hard-to-digest. The surface of pretreated WS and RS was very loose, scattered, and rough due to chemical pretreatment, possibly due to the dissolution or removal of complex lignin structure from the surface. Piranha solution effectively damaged WS and RS's surface since it is a strong oxidizing agent. PTSA in RS caused minimal alteration on the surface structure, as shown in Fig. 6c. Untreated RS had a very ordered structure that got disordered after
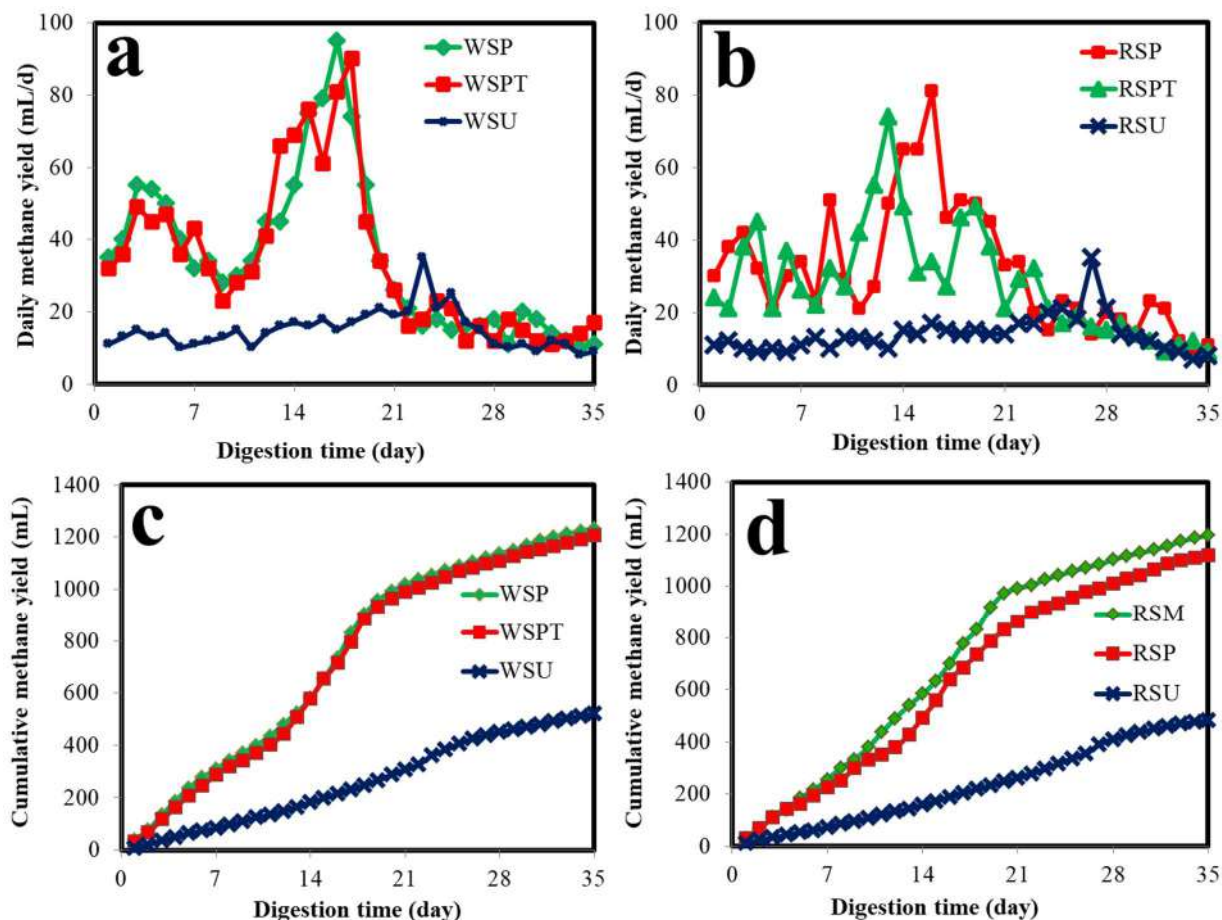
Fig. 4: (a) and (b) Daily methane yield and (c) and (d) cumulative methane yield of WS and RS.
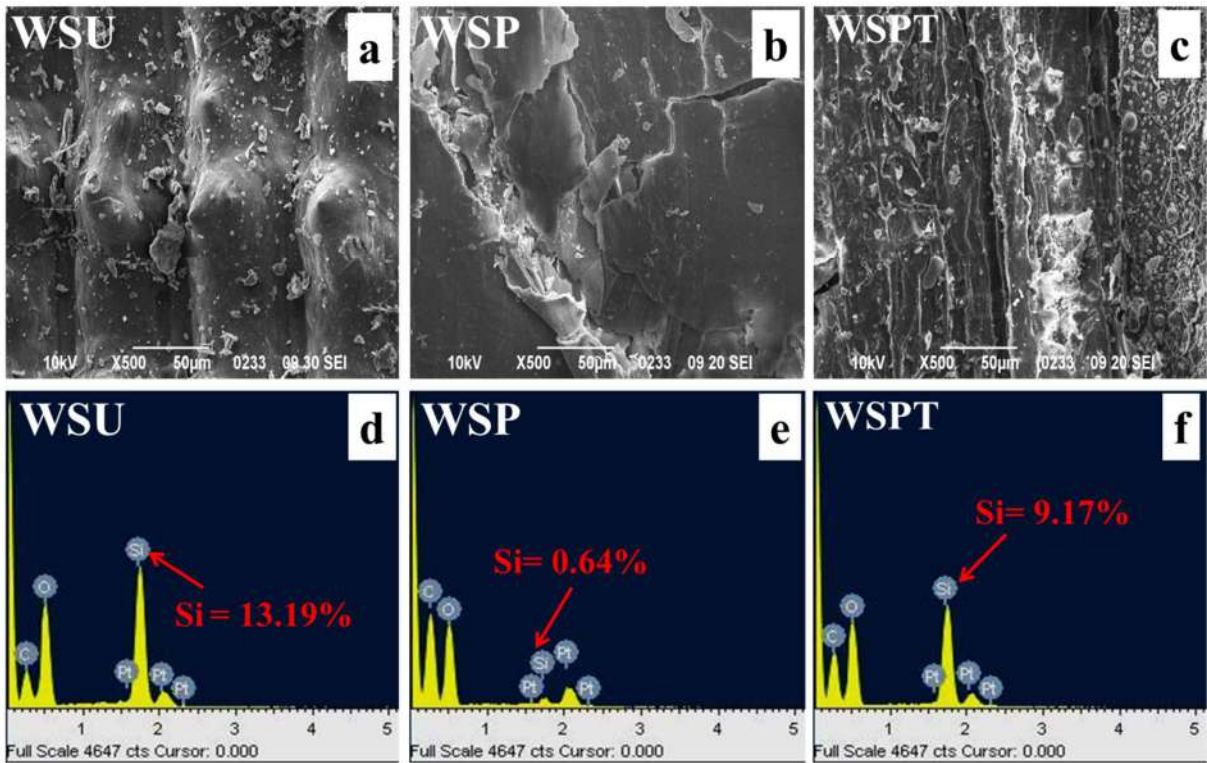
Fig. 5: Morphological and elemental analysis of untreated and pretreated WS.
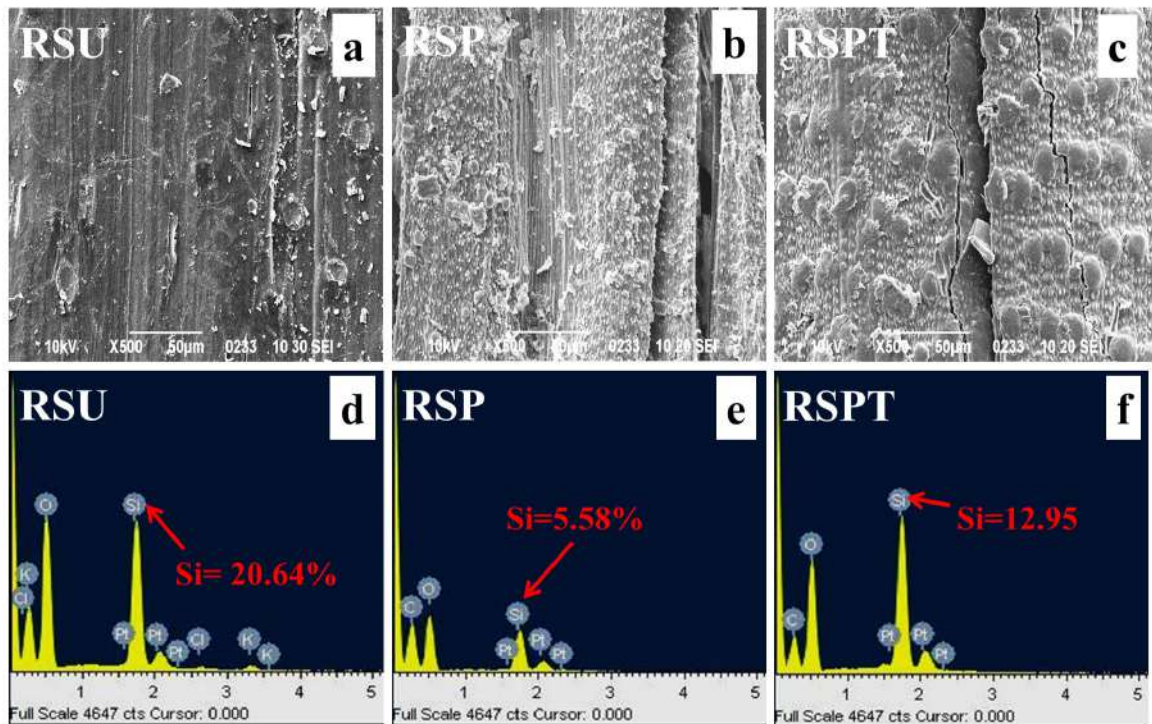
Fig. 6: Morphological and elemental analysis of untreated and pretreated RS.

pretreatment with piranha solution, PTSA. It is clearly shown in Fig. 6b RSP had a high degree of roughness. As shown in the EDS analysis (Fig. 5d to 5f), the peak of silica is reduced significantly in WSP by 95.07%. However, in WSPT, it was reduced to 30.47% silica. RS pretreatment also showed a reduced silica content of 72.1% in RSP and 37.25% in RSPT (Fig. 6d to 6f). The reduced peaks of silica in EDS analysis show its possible solubilization after pretreatment. Reduction in silica also enhances methane production as a high silica concentration restricts the fermentation process; therefore, it needs to reduce the concentration for effortless digestion (Satlewal et al. 2018).

Change in the Chemical bond of Untreated and Pretreated WS and RS

FTIR was used to examine the functional group alterations between untreated and pretreated WS and RS. The peaks of WSU, WSP, WSPT, RSU, RSP, and RSPT are shown in Fig. 7a. The peaks emerged at 3377 cm^{-1}, 2920 cm^{-1}, 1645 cm^{-1}, 1242 cm^{-1}, and 1067 cm^{-1} in FTIR spectra indicate the cellulose and hemicellulose content. The spectra of WSP, WSPT, RSP, and RSPT were different from WSU and RSU, indicating their different surface structure due to pretreatment. The absorption band at 3413 cm^{-1} was assigned to -OH stretching and 2926 cm^{-1} to C-H stretching in CH_3 and CH_2 groups showing the presence of polysaccharides in biomass (Kumar et al. 2011). Comparing the pretreated and untreated WS, in pretreated, it is observed that the intensity of the -OH group decreased, indicating the dehydration reaction takes place (Rajput et al. 2018). A decrease in peak intensity at 1242 cm^{-1} in all the pretreated WS and RS suggested breaking the -C=O hemicellulose-linked lignin stretch. The band range of 1770 -500 cm^{-1} in WS and RS is considered the lignin region. The absorbance peak at 1645cm^{-1} assigned to aromatic C=C stretching from lignin and aliphatic C-H stretching in methyl and phenol, -OH, and syringyl units of lignin (Tian et al. 2020, Rambo et al. 2015) the decrease in peak at 1645 cm^{-1} pretreated WS and RS were due to the
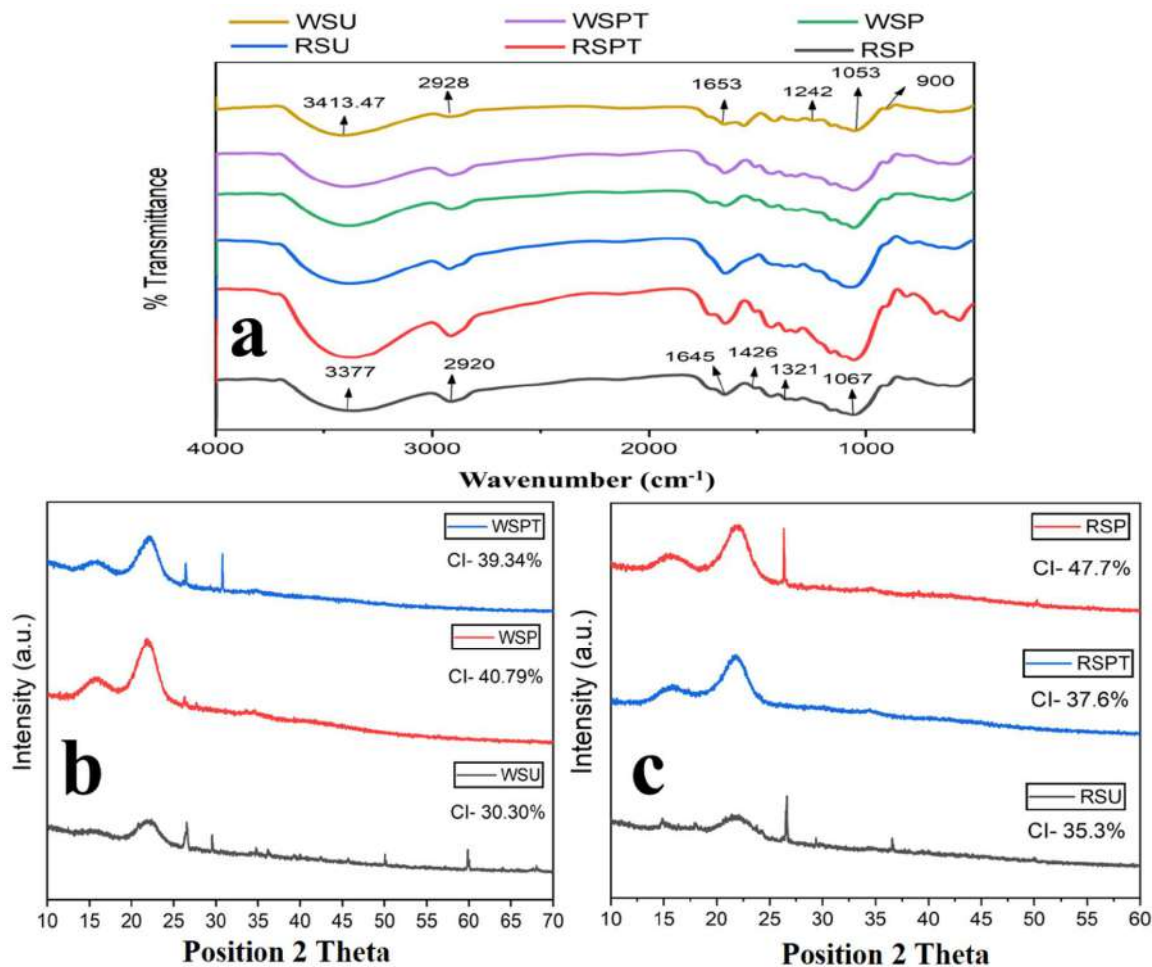
Fig. 7: (a) FTIR analysis (b) and (c) XRD analysis of WS and RS.

removal of lignin which is attributed to the polymerization of polysaccharide after chemical pretreatment. A notable drop of band intensity detected at 1067 cm^{-1} and 1321 cm^{-1} indicates the C-O, C=C, C-C-O, and C-H deformation in cellulose, hemicellulose, and lignin due to chemical pretreatment (Barua & Kalamdhad 2017).

X-ray Diffraction of Untreated and Pretreated WS and RS

The crystallinity of lignocellulosic biomass was assessed by XRD analysis. WS and RS mainly consist of cellulose, lignin, and hemicellulose, although cellulose exhibits crystalline nature, whereas lignin and hemicellulose are amorphous. The crystallinity of lignocellulosic biomass significantly affects the hydrolysis process of anaerobic digestion; therefore, it is vital to determine the degree of crystallinity. XRD analysis of untreated and pretreated WS and RS is shown in Fig. 7b and 7c, respectively. The pretreated samples show a notable change in peak intensities and broadening of the peaks. The characteristics of crystalline peaks for cellulose were identified at 2Θ =26.2°-26.5°, 13.5°, and 18.6° in untreated and pretreated samples (Sharma et al. 2020). It is evident from XRD analysis that the crystallinity of WS and RS increases after pretreatment. The crystallinity value of WS was decreasing in the order of WSP>WSPT>WSU. The CI of WSU was calculated to be 30.3%, while the CI of WSP was 40.79%, and WSPT was 39.34%. In the RS sample also, the CI of RSP (47.70%) was higher compared to RSPT (37.60%) and was lowest in RSU (35.3%). Hemicellulose, lignin, and the amorphous component of cellulose all degraded, which led to an increase in crystallinity in pretreated samples.

Kinetic Study

In the current work, MGM and LFM were applied to estimate the methane production of rice and WS that had undergone chemical pretreatment. The experimental cumulative methane yield was used to estimate the kinetic parameters using nonlinear regression. Table 2 outlines the obtained bio-kinetic parameters (P, R, and L) and statistical measure (R2) values for the studied kinetic model. The maximum predicted value of P (mL) was obtained in WSP (1234 mL) for MGM, which is 7.64% higher than the experimental value, while in LFM value of P is -0.12 % lower than the experimental value. The maximum percentage difference between the experimental and the predicted value was found in RSU (64.52%) for MGM, followed by WSU (28.44%) for LMF. The lag phase constant, L, describes how long bacteria can adapt to their new environment. In this study, the value of L ranges from 5.94 to 1.65 days. Lower L suggested a shorter degradation rate. It is observed from the table that pretreated WS requires the lowest time for acclimatization. Among the pretreated WS and RS, the shortest lag phase was seen in WSP, followed by RSP, WSPT, RSPT, WSU, and RSU. Maximum reduction in lag phase in piranha-treated biomasses was probably due to its higher potential for the removal and destruction of the recalcitrant structure of biomass and prior solubilization of large particles. The kinetic analysis using MGM and LFM in this investigation was able to fit the expected outcomes. The simulated kinetic values are presented in Table 2. It is evident from Fig. 8 that experimental cumulative methane yield fits with the predicted methane yield in both models. The projected values were plotted against the experimental data to assess the model's viability, and it was found that the value of R^2 varies between 0.987-0.998 of the model. For RSPT, RSU MGM fits best for WSP, WSPT, WSU, and RSP LFM fit best.

CONCLUSION

The effects of two different types of chemical pretreatments

Table 2: Generated kinetic parameters from the evaluated model.

Sample	Model used	P[mL]	R[mL]	L[d]	Exp. data [mL]	Δ [%]	R^2	MSE
WSP	MGM	1328.38	55.72	2.22	1234	7.64	0.991	31.29
	LFM	1232.44	59.30	3.30		-0.12	0.994	26.47
WSPT	MGM	1284.39	56.39	2.78	1208	5.94	0.992	28.99
	LFM	1195.21	60.23	3.87		-1.05	0.995	23.23
WSU	MGM	714.84	19.08	4.39	520	37.46	0.997	8.36
	LFM	573.32	21.13	5.9		10.25	0.997	6.69
RSP	MGM	1226.28	48.88	3.06	1120	8.66	0.995	17.27
	LFM	1119.12	52.57	4.22		-0.07	0.997	17.27
RSPT	MGM	1095.68	44.81	2.80	992	10.45	0.998	12.65
	LFM	1011.43	47.19	3.76		1.95	0.997	12.65
RSU	MGM	807.52	17.35	5.33	483	67.08	0.997	6.59
	LFM	581.24	18.93	6.72		20.33	0.996	7.83
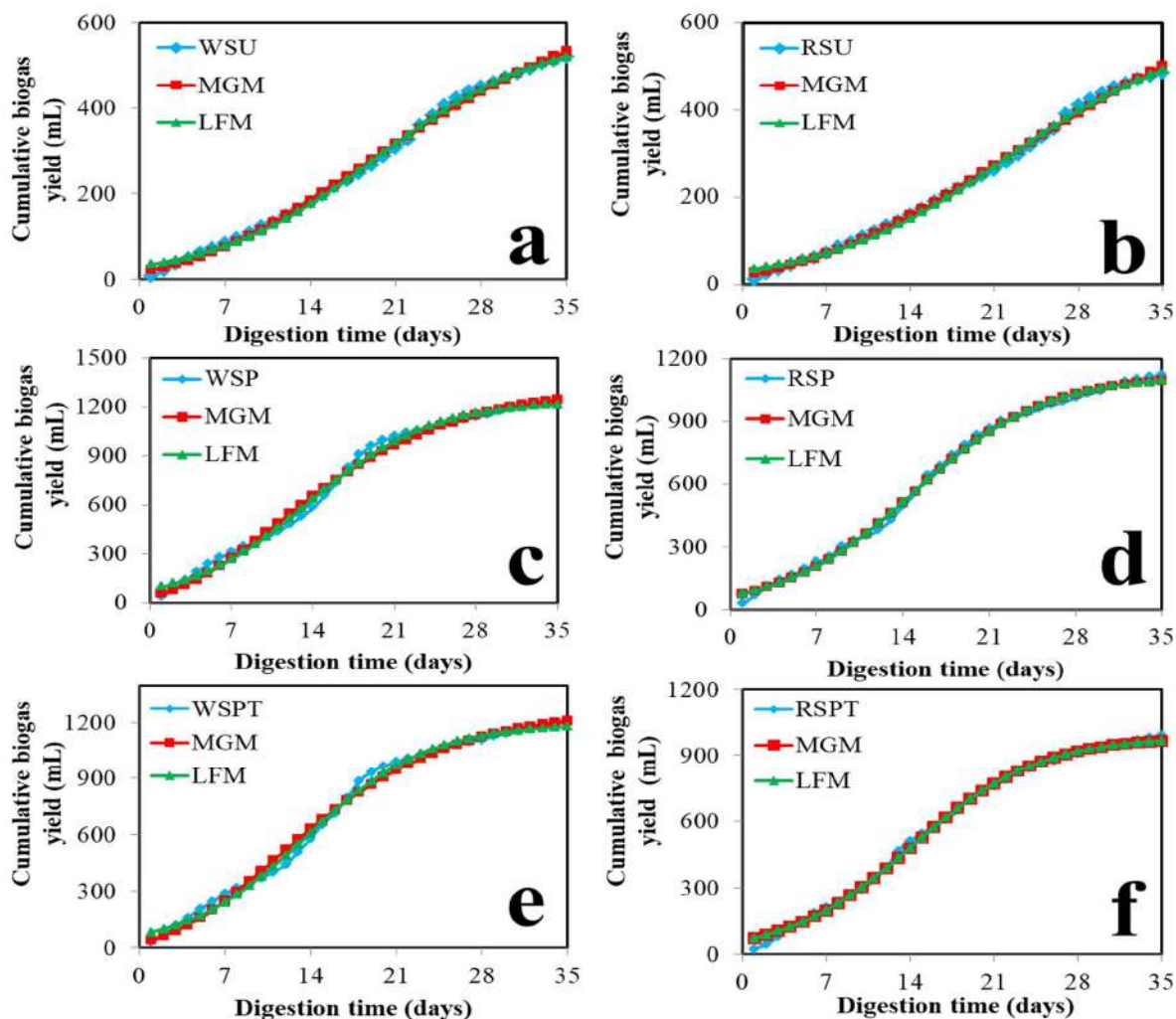
Fig. 8: MGM and LFM fitting for methane yield data of WS and RS.

(piranha and PTSA treatment) to reduce the recalcitrant nature of WS and RS for the production of enhanced methane were compared in this study. The chemical pretreatments were found successful in the enhancement of methane production of both biomasses. The present study suggests that pretreatment boosts enzymatic activity by reducing the recalcitrant structure of WS and RS. Methane production was maximum after piranha treatment 1234 mL, and 1120 mL in WSP and RSP, respectively, followed by PTSA treatment 1208 mL (WSPT) and 992 mL (RSPT), and minimum methane was produced in untreated samples 520 mL (WSU) and 483 mL (RSU). In comparison with RS, the methane production in WS was higher. Enhancement in methane production resulted from the solubilization of organic matter. Pretreatment with piranha solution was the best technique, as it effectively reduced the recalcitrant nature

of RS and WS and increased methane production. SEM, EDS, FTIR, and XRD analysis also supported the positive effect of chemical pretreatment. MGM and LFM accomplished the kinetic model of methane production. The outcome of the experiments was compared with the predicted value obtained from these two models. The statistical analysis shows that LFM fitted best with the experimental results than MGM. This was verified by analyzing the root means square error and regression.

ACKNOWLEDGEMENT

REFERENCES

Ahmad, F., Silva Edson, L., Varesche, M. and Bernadete, A. 2018. Hydrothermal processing of biomass for anaerobic digestion – A review. Renew. Sustain. Energy Rev., 98: 108-124. doi:10.1016/j.rser.2018.09.008

Athira, G., Bahurudeen, A. and Appari, S. 2019. Sustainable alternatives to carbon-intensive paddy field burning in India: A framework for cleaner production in agriculture, energy, and construction industries. J. Clean. Prod., 236: 117598.

Barua, V.B. and Kalamdhad, A.S. 2017. Effect of various types of thermal pretreatment techniques on the hydrolysis, compositional analysis, and characterization of water hyacinth. Bioresour. Technol., 227: 147-154.

Behera, S., Arora, R., Nandhagopal, N. and Kumar, S. 2014. Importance of chemical pretreatment for bioconversion of lignocellulosic biomass. Renew. Sustain. Energy. Rev., 36: 91-106.

Chen, H., Liu, J., Chang, X., Chen, D., Xue, Y., Liu, P., Lin, H. and Han, S. 2017. A review on the pretreatment of lignocellulose for high-value chemicals. Fuel Process.Technol., 160: 196-206.

Chiranjeevi, T., Mattam, A.J., Vishwakarma, K.K., Uma, A., Peddy, V.R., Gandham, S. and Ravindra Velankar, H. 2018. Assisted single-step acid pretreatment process for enhanced delignification of RS for bioethanol production. ACS Sustain. Chem.Eng., 6: 8762-8774.

Dar, R.A., Parmar, M., Dar, E.A., Sani, R.K. and Phutela, U.G. 2021. Biomethanation of agricultural residues: Potential, limitations and possible solutions. Renew. Sustain. Energy. Rev., 135: 110217.

Den, W., Sharma, V.K., Lee, M., Nadadur, G. and Varma, R.S. 2018. Lignocellulosic biomass transformations via greener oxidative pretreatment processes: access to energy and value-added chemicals. Front. Chem., 6: 141.

DiLallo, R. and Albertson, O.E. 1961. Volatile acids by direct titration. J. Water Pollut. Control Fed., 33: 356-365

Esposito, G., Frunzo, L., Liotta, F., Panico, A. and Pirozzi, F. 2012. Bio-methane potential tests to measure the biogas production from the digestion and co-digestion of complex organic substrates. The Open Environmental Engineering Journal, 5(1).

FAO RMM, 2018. Food and Agriculture organization of the united nations, 2018 Rice Market Monitor (FAO, RMM) XXI (1). April 2018.

Hallac, B.B. and Ragauskas, A.J. 2011. Analyzing cellulose degree of polymerization and its relevancy to cellulosic ethanol. Biofuel Bioprod. Biorefin., 5: 215-225.

Kainthola, J., Kalamdhad, A.S. and Goud, V.V. 2019a. A review on enhanced biogas production from anaerobic digestion of lignocellulosic biomass by different enhancement techniques. Process Biochem., 84: 81-90.

Kainthola, J., Shariq, M., Kalamdhad, A.S. and Goud, V.V. 2019b. Electrohydrolysis pretreatment methods to enhance the methane production from anaerobic digestion of RS using graphite electrode. Renew. Energy, 142: 1-10.

Karuppiah, T. and Azariah, V.E. 2019. Biomass pretreatment for enhancement of biogas production. IntechOpen, 150: 111509.

Kavitha, S., Jayashree, C., Kumar, S.A., Yeom, I.T. and Banu, J.R. 2014. The enhancement of anaerobic biodegradability of waste-activated sludge by surfactant-mediated biological pretreatment. Bioresour. Technol., 168: 159-166.

Koryś, K.A., Latawiec, A.E., Grotkiewicz, K. and Kuboń, M. 2019. The review of biomass potential for agricultural biogas production in Poland. Sustainability, 11(22): 6515.

Kumar, A.K., Parikh, B.S. and Pravakar, M. 2016. Natural deep eutectic solvent-mediated pretreatment of RS: bioanalytical characterization of lignin extract and enzymatic hydrolysis of pretreated biomass residue. Environ. Sci. Pollut. Res., 23: 9265–9275. https://doi.org/10.1007/s11356-015-4780-4

Kumar, S., D'Silva, T.C., Chandra, R., Malik, A., Vijay, V.K. and Misra, A. 2021. Strategies for boosting biomethane production from RS: A systematic review. Bioresour. Technol. Rep., 100813.

Kumar, S., Kothari, U., Kong, L., Lee, Y.Y. and Gupta, R.B. 2011. Hydrothermal pretreatment of switchgrass and corn stover for production of ethanol and carbon microspheres. Biomass Bioenerg., 35(2): 956-968.

Li, P., Ji, H., Shan, L., Dong, Y., Long, Z., Zou, Z. and Pang, Z. 2020. Insights into delignification behavior using aqueous p-toluenesulfonic acid treatment: comparison with different biomass species. Cellulose, 27: 10345-10358

Ma, S., Wang, H., Li, J., Fu, Y. and Zhu, W. 2019. Methane production performances of different compositions in lignocellulosic biomass through anaerobic digestion. Energy, 189: 116190.

Mahmood, H., Moniruzzaman, M., Iqbal, T. and Khan, M.J. 2019. Recent advances in the pretreatment of lignocellulosic biomass for biofuels and value-added products. Curr. Opin. Green Sustain. Chem., 20:18-24.

Maldonado-Bustamante, S.R., Mondaca-Fernández, I., Gortares-Moroyoqui, P., Berg, A., Balderas-Cortés, J.J., Meza-Montenegro, M.M., Brown-Bojórquez, F. and Arvayo-Enríquez, H. 2022. The effectiveness of the organosolv process in WS delignification optimizing temperature and time reaction. Cellulose, 29: 7151–7161. https://doi.org/10.1007/s10570-022-04708-1

Mancini, G., Papirio, S., Lens, P.N. and Esposito, G. 2018. Increased biogas production from WS by chemical pretreatments. Renew. Energy, 119: 608-614.

Miah, M.R., Rahman, A.K.M.L., Akanda, M.R., Pulak, A. and Rouf, M.A. 2016. Production of biogas from poultry litter mixed with the co-substrate cow dung. J. Taibah Univ. Sci. 10: 497-504.

Owusu, P.A. and Asumadu-Sarkodie, S. 2016. A review of renewable energy sources, sustainability issues, and climate change mitigation. Cogent Eng., 3:1167990.

Panigrahi, S., Sharma, H.B. and Dubey, B.K. 2020. Anaerobic co-digestion of food waste with pretreated yard waste: A comparative study of methane production, kinetic modeling, and energy balance. J. Clean. Prod., 243: 118480.

Pellera, F.M. and Gidarakos, E. 2018. Chemical pretreatment of lignocellulosic agro-industrial waste for methane production. Waste Manage., 71: 689-703.

Perez, J., Munoz-Dorado, J., De la Rubia, T.D.L.R. and Martinez, J. 2002. Biodegradation and biological treatments of cellulose, hemicellulose, and lignin: An overview. Int. J. Microbiol., 5(2): 53-63.

Rajput, A.A. and Visvanathan, C. 2018. Effect of thermal pretreatment on chemical composition, physical structure, and biogas production kinetics of WS. J. Environ. Manage., 221: 45-52.

Rambo, M.K.D., Schmidt, F.L. and Ferreira, M.M.C. 2017. Analysis of the lignocellulosic components of biomass residues for biorefinery opportunities. Talanta, 144(2015): 696–703.

Saha, B., Sathyan, A., Mazumder, P., Choudhury, S.P., Kalamdhad, A.S., Khwairakpam, M. and Mishra, U. 2018. Biochemical methane potential (BMP) test for Ageratum conyzoides to optimize ideal food-to-microorganism (F/M) ratio. J. Environ. Chem. Eng., 6(4): 5135-5140.

Satlewal, A., Agrawal, R., Bhagia, S., Das, P. and Ragauskas, A.J. 2018. RS as a feedstock for biofuels: Availability, recalcitrance, and chemical properties. Biofuel Bioprod. Biorefin., 12: 83-107.

Sharma, H.B., Panigrahi, S., Sarmah, A.K. and Dubey, B.K. 2020. Downstream augmentation of hydrothermal carbonization with anaerobic digestion for integrated biogas and hydrochar production from the organic fraction of municipal solid waste: A circular economy concept. Sci. Total Environ., 706: 135907.

Sheng, Y., Lam, S.S., Wu, Y., Ge, S., Wu, J., Cai, L., Huang, Z., Le, Q.V., Sonne, C. and Xia, C. 2021. Enzymatic conversion of pretreated

lignocellulosic biomass: A review on the influence of structural changes of lignin. Bioresour. Technol., 324: 124631.

Shrivash, M.K., Adeppa, K., Singh, R., Pandey, J. and Misra, K. 2017. A novel, efficient, multigram scale synthesis of s-alkyl thiocarbamates via Newman Kwart rearrangement. Proc. Natl. Acad. Sci. India Phys. Sci., 87(2): 189-193. https://doi.org/10.1007/s40010-017-0345-x.

Singh, B., Szamosi, Z., Siménfalvi, Z. and Rosas-Casals, M. 2020. Decentralized biomass for biogas production. Evaluation and potential assessment in Punjab (India). Energy Rep., 6: 1702-1714.

Singh, R. and Kumar, S. 2019. A review on biomethane potential of paddy straw and diverse prospects to enhance its biodigestibility. J. Clean. Prod., 217: 295-307.

Tian, W., Chen, Y., Shen, Y., Zhong, C., Gao, M., Shi, D., He, Q. and Gu, L. 2020. Effects of hydrothermal pretreatment on the mono-and co-digestion of waste-activated sludge and WS. Sci. Total Environ., 732: 139312.

Valentino, F., Munarin, G., Biasiolo, M., Cavinato, C., Bolzonella, D. and Pavan, P. 2021. Enhancing volatile fatty acids (VFA) production from food waste in a two-phase pilot-scale anaerobic digestion process. J. Environ. Chem. Eng., 9: 106062.

Veluchamy, C. and Kalamdhad, A.S. 2017. Biochemical methane potential test for pulp and paper mill sludge with different food/microorganisms ratios and its kinetics. IBBS, 117: 197-204.

Wang, B., Shen, P., Zhu, W., Pang, Z. and Dong, C. 2020. Effect of ground wood particle size on biomass fractionation using p-toluenesulfonic acid treatment. Cellulose, 27: 4043-4052.

Zoghlami, A. and Paës, G. 2019. Lignocellulosic biomass: understanding recalcitrance and predicting hydrolysis. Front. Chem., 7: 874.

Landslide Potential Analysis Using Unmanned Aerial Vehicle in South Leato Village, Gorontalo City, Indonesia

S. S. Eraku*† iD **, A. P. Permana*** iD **and M. N. Baruadi*** iD

*Department of Earth Science and Technology, Universitas Negeri Gorontalo, Indonesia
†Corresponding author: S. S. Eraku; sunarty.eraku@ung.ac.id

ABSTRACT

Spatial data technology using unmanned aerial vehicle (UAV) is one of the aerial imaging technologies used to produce detailed data. However, its utilization for mapping, especially disaster mapping needs an in-depth study. The research site is located within 00-"00′29° 51′31°00" N and 12327′5°-123"00′3°" E that covers an area of 2,531 Ha, which consists of 1,745 Ha land and 786 Ha water areas. Administratively, the research site is in South Leato Village of Dumbo Raya sub-district of Gorontalo city with a total area of 41,9 Ha. This study is aimed at assessing the landslide by creating a landslide zonation map and finding out the landslide potential area by using the UAV. This research employs field surveys by using drones and Geographic Information System (GIS) analysis. It is found that the parameters that influence landslides are lithology, rainfall, slope inclination, lineament density, and land use. The landslide vulnerability analysis reveals three levels of vulnerability in this site; low, medium, and high vulnerability, in which, 19 Ha is classified as low vulnerability area, 9.5 Ha is classified as medium vulnerable, and 13.5 Ha is classified as highly vulnerable area.

INTRODUCTION

Gorontalo province is prone to landslides through various types and mechanisms. Several studies were carried out to identify landslides using various methods. These research results serve as a reference to determine landslides' disaster mitigation steps (Asiki et al. 2019, Eraku & Permana 2020, Naryanto et al. 2019, Usman et al. 2022). Specific to Gorontalo province, there are a few studies on landslides. The latest research on landslides showed that within landslides there are rotation slides, planar slides, flow slides, and stone block slides. Landslide is usually influenced by the slope and shape of the slope surface (Patuti et al. 2017, Lihawa et al. 2021).

Since Gorontalo City has been established as the capital of the province, various issues, including rapid population growth, have become more evident. The population growth for the last five years has been showing an uptrend. This creates a high demand for land and an increase in the fulfillment of services and city facilities, which may have an impact on the decrease in environmental quality, such as environmental degradation and natural disasters. One of

the most common problems in this city is natural disasters, especially floods, and landslides (Doda 2013, Wunarlan 2019).

A landslide is a natural disaster that can be predicted due to the high level of rainfall in a region. Other factors like lithology, geological structure, types of soil, slope inclination, and land use also add to the severity of the landslide. Landslides often cause large casualties, both materials and humans. Landslide-prone areas needed to be minimized to minimize their destruction. Efficient and time-effective mapping of landslide-vulnerable areas can employ GIS (Kumoro & Yunarto 2010, Yunianto 2011, Naryanto et al. 2019, Silalahi et al. 2019).

Remote sensing is one of the methods used in various industries. It offers many benefits and can analyze different information. Remote sensing technology for land use rapidly develops with unmanned aerial vehicles (UAV).

THEORETICAL REVIEW

Landslides and mass soil movement are similarly defined as slides, and both need distinction. Soil movement is defined as the process of vertical, horizontal, or oblique displacement of soil or stone masses. Based on this definition, the landslide is part of soil movement. When following the vertical soil metabolism, bending happens due to the collapse of the

soil foundation during the vertical movement, and then it is classified as a type of soil (Shanmugam 2013, Shanmugam & Wang 2015, Naryanto et al. 2019, Yanrong & Mo 2019). Gorontalo geological structure is influenced by three plates, micro-plates of Banggai-Sula from the south, Sangihe plates from the east, and Sulawesi Sea plates from the north (Hall 2002, 2012, Hall & Spakman 2015, Watkinson et al. 2011, Purmana et al. 2020).

Soil or rock debris materials were first moved to the bottom part, for the slope to be able to penetrate the rock pores through water penetration. Such conditions can increase the load of the material on the surface of the slope and put pressure on the materials like rocks. When this pressure is unstable due to natural phenomena or due to human intervention, it could cause disaster, which further causes casualty of both materials and injuries, destruction of public facilities, and disturbance of people's lives and livelihoods (Bogaard & Greco 2016, Asikin et al. 2019, Naryanto et al. 2019, Lucas et al. 2020).

The Regional Disaster Management Agency (BPBD) of Bone Bolango Regency recorded a soil movement disaster in April 2019 in Suwawa Selatan sub-district. This incident destroyed one house in Bondawuna village. In 2016, the Social Protection Agency of Gorontalo province established the Suwawa Selatan sub-district as a Disaster Prepared Village due to its assessment that revealed this sub-district is prone to land movement disasters due to its geographical condition (Djakun et al. 2020).

On the other hand, drone technology, also called unmanned aerial vehicle (UAV) has become more and more popular among society. It is one of the alternative means for aerial imaging. Researchers and foreign practitioners have been using this technology in various mapping applications. UAV is an affordable remote sensing technology (Rokhmana 2015). Further, the scoring method is a method to determine the score of each parameter. The scoring is adjusted to the assessment criteria. The higher the influence of a parameter on landslides, the higher the score (Rokhmana 2015).
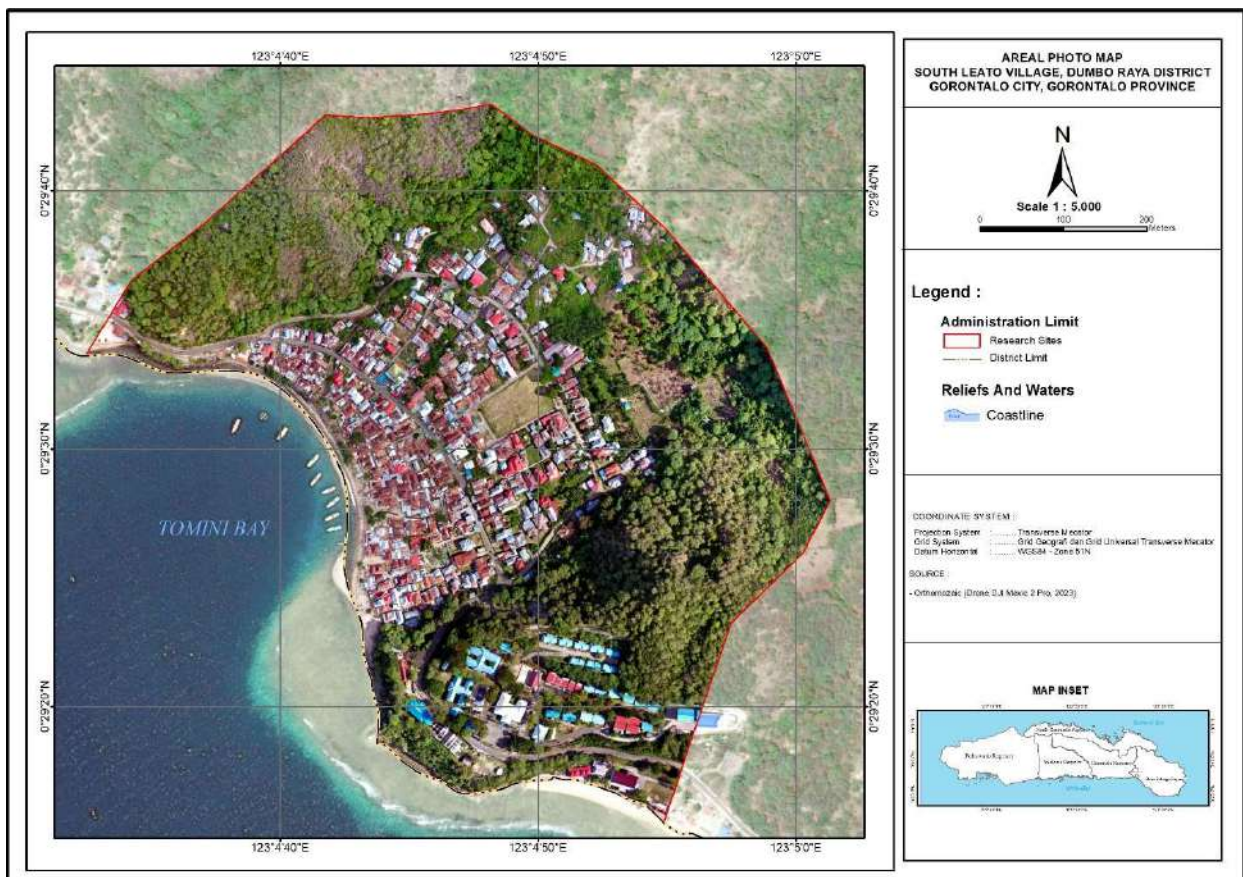
Fig. 1: Research site in South Leato Village of Gorontalo City.

MATERIALS AND METHODS

The research site is located between 0051'31°-00°00'29°'' N and 12327'5°-123°00'3°'' E, which covers an area of 2,531 ha that comprises 1,745 ha of land and 786 ha of water area. Administratively, the research site is located in South Leato village of Dumbo Raya sub-district, Gorontalo city. The research focus in this village covers an area of 41.9 ha. The research site can be reached in about ± 17 minutes by motored vehicle from the capital city, and the total distance from the capital city is ± 8.9 km (Fig. 1).

The research started with planning the aerial imaging using the DJI Mavic 2 Pro UAV, remote sensing for mapping. Once the flying track map was planned, aerial photos were taken at the research site. The photos were then processed into orthophotos data and Digital Elevation Model as the basis for mapping. Following this, a field survey and GIS analysis were performed. The field survey was implemented to collect field data such as geological data, geomorphology, structure, region's stratigraphy and field validation on the level of landslide vulnerability of the research site. Landslide vulnerability analysis utilized scoring and valuation on the factors that influenced landslide namely: lithology, rainfall, slope inclination, soil type, land use and the lineament density. Further, these parameters are overlaid to obtain the level of landslide vulnerability. This process produced a zonation map of the landslide vulnerability level of the

Table 1: Landslide vulnerability classification.

Vulnerability class	Score
low	Minimum value – (class interval + minimum value)
medium	>low vulnerability score – (low vulnerability score + class interval)
high	> medium vulnerability score – maximum value

research site. The level of vulnerability analysis is performed using the landslide predictability model (BBSDLP 2009, Dewi et al. 2017, Asikin et al. 2019).

Total score = (20% * slope inclination) + (20% * lineament density) + (10% * rainfall) + (25% * Lithology) + (25% * land use)   ….(1)

Further, a calculation is made to obtain class intervals for each level of landslide vulnerability by using the equation (BBSDLP 2009, Dewi et al. 2017, Asikin et al. 2019).

$$I = \frac{R}{K} \qquad ….(2)$$

In which:

I = class interval;

R = *range* (largest data – smallest data) from the total score; and

K = number of landslide classes.

Table 2: Characteristics of parameters of landslide-prone determination.

No.	Variable	Criteria	Weights	Score
1.	Lithology	Alluvial and Coastal Deposits	25%	1
		Limestone		3
		Pyroclastic Breccia		5
2.	Rainfall	< 1000	10%	1
		1000-1200		2
		1200-1500		3
		> 1500		4
3.	Slope	< 13	20%	1
		14-20		2
		21-55		3
		>55		4
4.	Land Use	Sea water	25%	1
		Plantation/Garden		3
		Settlements and Places of Activity		3
		Shrubs/Reeds		5
5.	Lineament Density	Low	20%	1
		Currently		3
		Tall		5

Next, vulnerability levels are created based on the obtained interval. Thus, the landslide vulnerability classification is obtained as shown in Table 1 (Yunianto 2011).

The determination of landslide-prone areas used GIS tools with the Storie Index method to obtain a total score. This scoring range was converted at several levels according to requirement, landslide-prone levels were classified into five classes or levels, which were: High, Medium and Low, using the natural break method in Table 2 (Thoha et al. 2020).

RESULTS AND DISCUSSION

Aerial Photo Imaging

Small-format aerial photos are the initial data used as spatial basic data for mapping. Before aerial photo imaging using the UAV with DJI Mavic 2 Pro drone, aerial photo acquisition planning is needed. A photo shooting plan is made to describe the flight pathway in as much detail as possible using Pix4Dcapture software with two missions.

The photos were taken between 08.00-10.00 am, where each flight took 12-19 minutes in ideal conditions. The cruising height was 300 meters above the ground level expected to produce ± 11.9 cm pixel photos. This pixel photo is theoretically expected to produce maps with the scale of 1:5.000 and 1:10.000. End lap and side lap setting of the drone is planned using the small drone which can safely move, as such a small UAV can easily deviate and be disturbed by the wind. An aerial photo shoot using UAV was carried out on the 18th of February 2023. The shooting site was a coastal area with a high tendency for high-speed wind that influences the durability of the UAV battery. This was due to the faster moving rotation of the UAV motor to be able to penetrate wind obstacles. The observation of the battery condition and vehicle is carried out through Pix4Dcapture software on Ground Sampling Distance (GSD).

Aerial Photo Processing into DSM data, Orthophoto Mosaic and DTM

Aerial photo processing is the selection of photos obtained from the first phase through the unification of contras of each
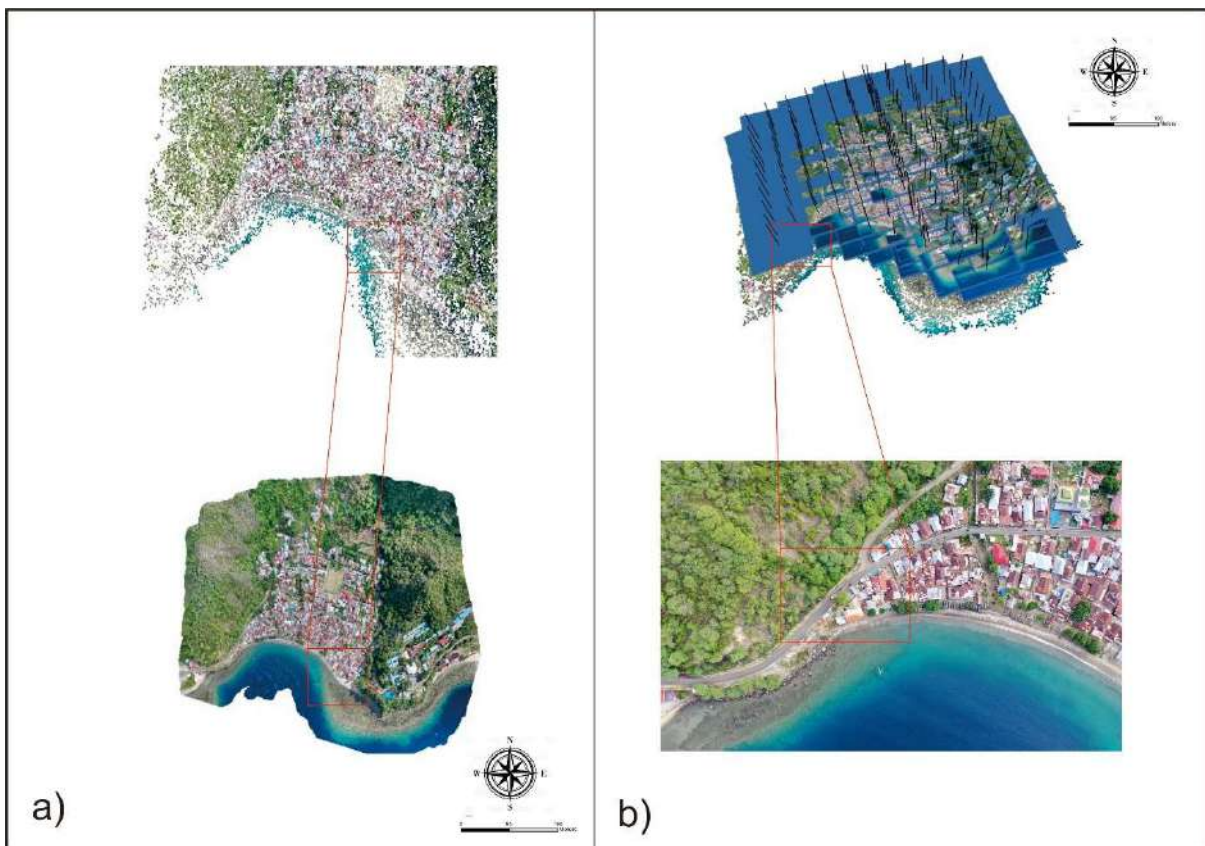
Fig. 2: Photo aligning process at agisoft photo scan, a) Collection of point clouds, b) camera position during exposure.

photo. This unification of contras (enhancement) is needed to detect point clouds on the software. This point cloud is used in recognizing the sequence and photo angle. Photos with high contrast and high levels of brightness that are different from other photos would not be able to be identified and would make it difficult to be converted into orthophoto mosaic and further processing into DSM would similarly be difficult. The total photos obtained from 15 flight photo shooting missions that could be used for processing were 2001/2005 aligned photos.

The processing using Agisoft software was started with photo aligning. Photo aligning consisted of the process to detect similar objects between photos as a point cloud using workflow for all photos. The result is that these pinto clouds, which formerly had pixel coordinates (model) were turned into actual coordinates at the field. Reconstruction of a photo sequence and camera position during the shooting was also performed in this stage. The collection of point clouds and camera position detected during the photo aligning is presented in Fig. 2.

Digital Surface Model (DSM) and Digital Terrain Model (DTM) Development

The initial function of DSM was to create a DSM orthophoto mosaic to eliminate relief errors from the produced aerial photos, thus, they had orthogonal projections and had similar scales in all areas of photos. DSM was created using the Agisoft photo scan software during the densification of point clouds. This point cloud densification was followed by an interpolation process to convert DSM into raster data.

Digital Terrain Model (DTM) is a DSM derivative data, where DTM is the earth surface level without any vegetation object or manmade features like buildings. Converting DSM data to DTM data was initiated by determining the earth level height points, selecting them, and removing other height objects that were not earth-level height. The removed area is then interpolated with earth's surface height data around it (Meiarti et al. 2019). When there was a point above the earth's surface that is hard to recognize, DTM data extraction will be difficult.

On the other hand, this research site is composed of pyroclastic hills geomorphology. Pyroclastic hills with dense vegetation will not produce optimum DTM data. This supports (Meiarti et al. 2019) who noted that mountain objects with dense forest canopy would be hard to be extracted into DTM data. To overcome this, a semi-automatic
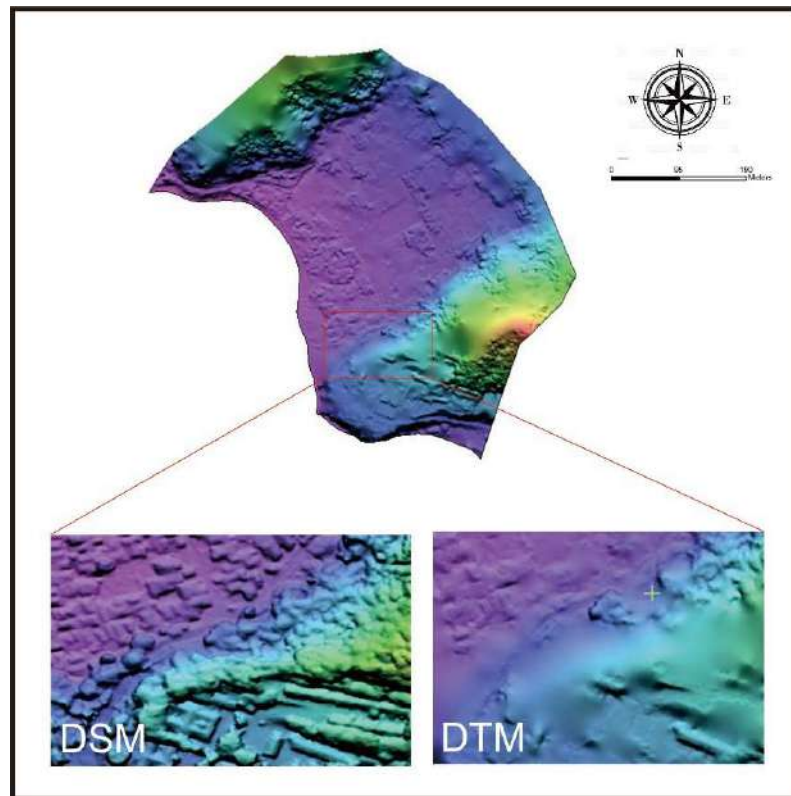
Fig. 3: (a) DTM from DSM processing using PCI Geomatica and after manual editing, (b) example of snippet comparison between DSM and DTM.

method using PCI Geomatica 2016 is employed. Manmade feature objects or vegetation trees are manually eliminated. This resulted in the elimination of most non-earth surface objects. DTM from PCI Geomatica software was manually edited to produce the best result (Fig. 3).

Development of Orthophoto Mosaic

The final stage in this aerial photo processing is combining each orthophoto into an orthophoto mosaic. This process uses DSM input (in TIN form) and aerial photos. TIN is used in correcting object displacement relief of the aerial photo. Thus, the photo has an orthogonal projection and a more accurate coordinate position. When all photos within the blocks have been orthorectified, the next process is the blending process among photos. Thus, photos are connected seamlessly. Photos' brightness and contrast are even in all areas. The produced orthophoto mosaic size is ± 11.6 cm (GSD). This backs up (Rohmana 2015), who noted that GSD produced from UAV technology would be within the range of 5-30 cm/pixel on photos taken from 300 meters above the earth's surface. This GSD size is considered more detailed compared to other remote sensing such as satellite images available to date. Orthophoto mosaic is used as the spatial primary data for disaster mapping. The result of the orthophoto mosaic is presented in Fig. 4 below.

Geometric Correction of Drone Image

Geometric correction is performed by transforming the
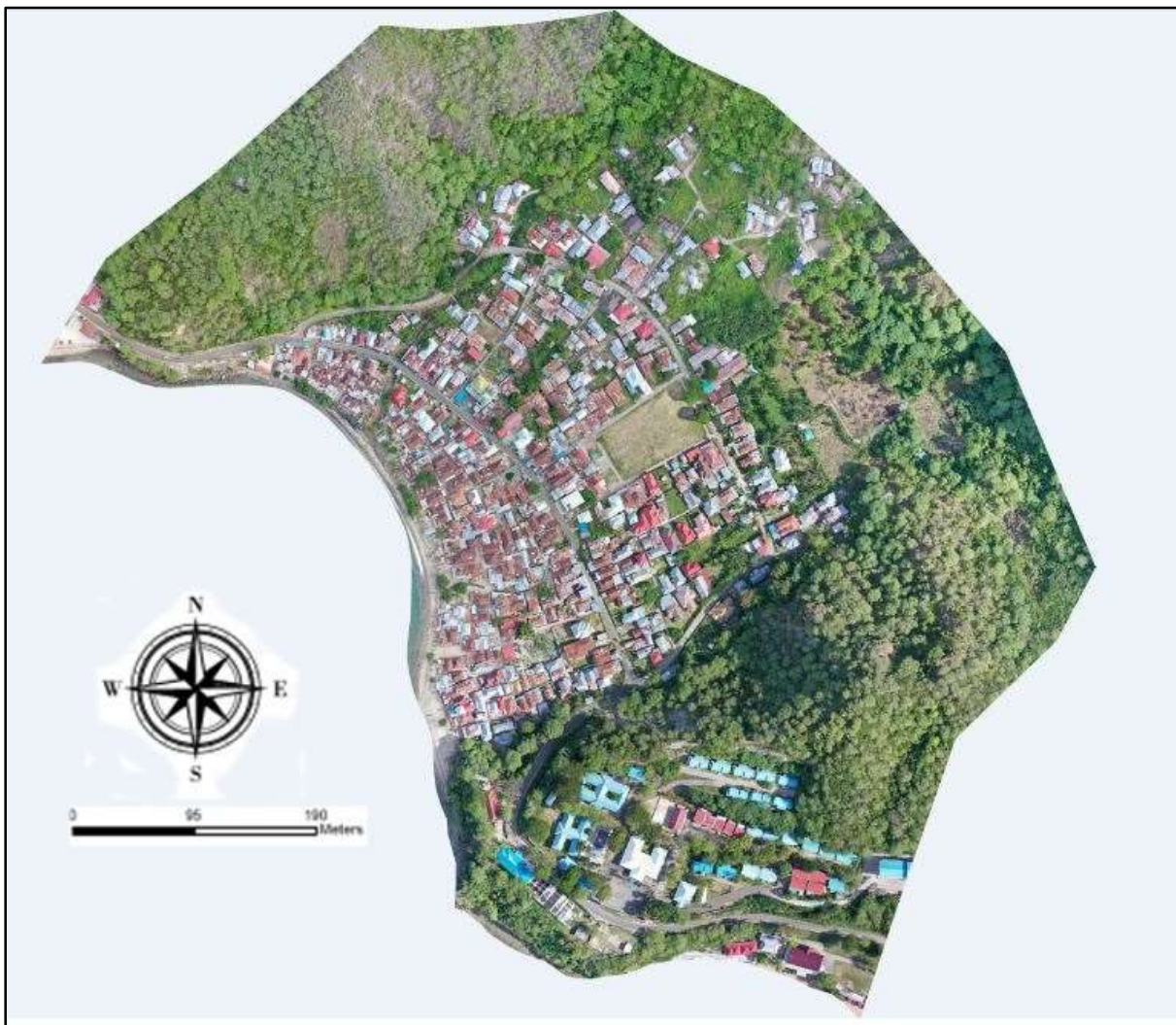
Fig. 4: Orthophoto mosaic of the research site produced from the DJI Mavic 2 Pro drone.

Table 3: Type of lithology (Dewi et al. 2017).

No.	Lithology	Area (ha)	Score
1.	Alluvial and Coastal Deposits	20.24	1
2.	Limestone	7.01	3
3.	Pyroclastic Breccia	14.62	5

Table 4: South Leato Village rainfall rate.

No.	Rainfall	Score
1.	< 1000	1
2.	1000-1200	2
3.	1200-1500	3
4.	> 1500	4

position of each pixel within the image toward each similar object position within the earth's surface using the ground control point (GCP). The common location for CGP is an area that usually has the most striking color, road intersection, road corner, railway intersection with road and buildings that can be easily identified or recognized. During the rectification stage, the total RMS error was 0.173795 with five binding points distributed on the drone image points that would be corrected. This value of RMS error on the corrected geometric drone image has met the tolerance level, in which, the RMSE value is below one. Townshend et al. (1992) wrote that the accuracy in binding the coordinate system is usually stated by RMSE with several control points. The range value of 0.5 to 1.0 pixels is sufficient to achieve 10% or less error in the position when the two overlayed images (map) are within the tolerance level.

Lithology

Based on the geological map of the Southern Leato the

study area is composed of three lithologies namely breccia, limestone, and alluvial (Table 3). Each rock type is given a score according to its level of sensitivity to landslides. The higher the score given, the higher the influence on the occurrence of landslides. An overview of the distribution of rock types in the study area can be seen in Fig. 5.

Rainfall

The rainfall data used in the study were taken from only one rainfall observation, namely the BPP Kabila Bone Post Office. Rainfall data is in areas that have an average rainfall of <1000 to >1500 mm.year^{-1}. The described rainfall data can be seen in Table 4.

From the rainfall data above, rainfall modeling is then made using interpolation. So that the rainfall data for the South Leato Village area is obtained as shown in Fig. 6.
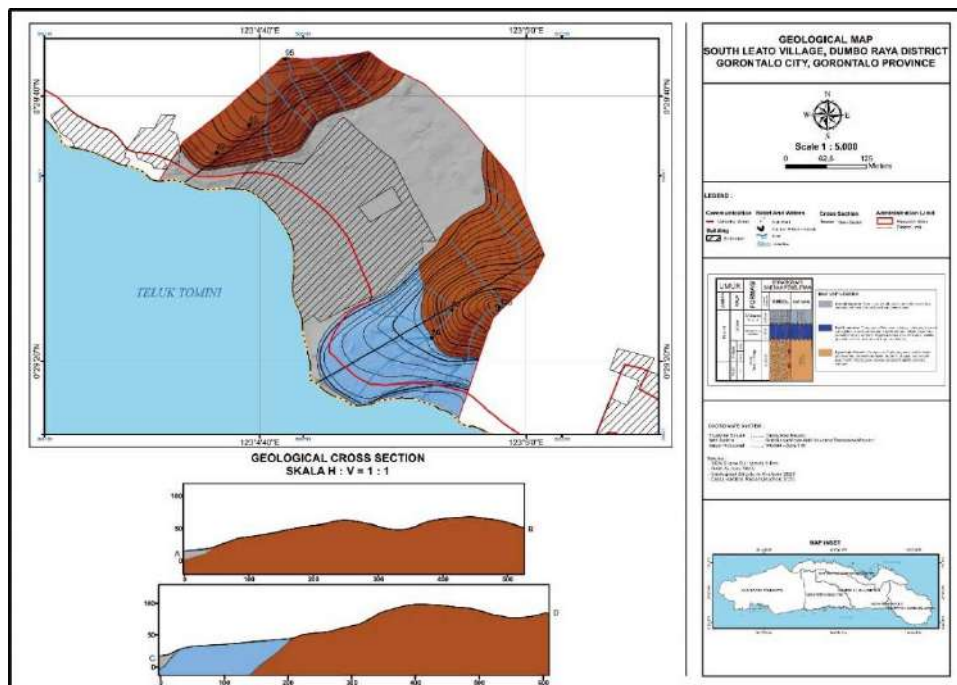
Fig. 5: Geological map of study area.
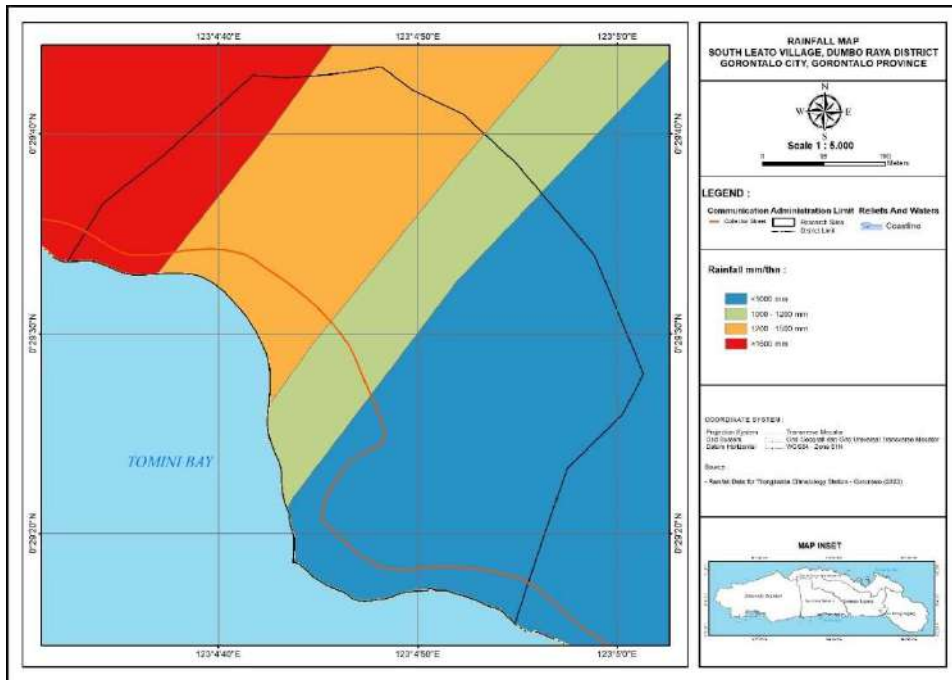
Fig. 6: South Leato Village rainfall map.

Table 5: Slope inclination (Van Zuidam 1983).

No.	Slope	Area (ha)	Score
1.	<13	12.7	1
2.	14-20	7.8	2
3.	21-55	13.5	3
4.	>55	7.9	4

Slope

The slope of the slope is the most influential factor in the occurrence of landslides. South Leato Village is an area that has different slopes. The slope of <13% with an area of 12.7 ha is used as a residential area. While on a slope of 14-20% with an area of 7.8 ha used as plantation land, the area surrounded by hills has a slope of 21-55% with a total
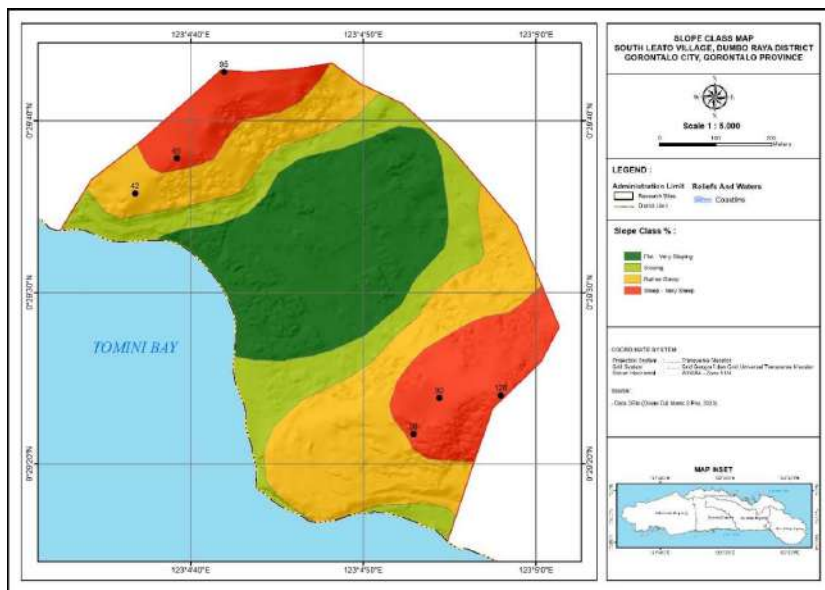
Fig. 7: South Leato Village slope map.

Table 6: Land use.

No.	Land use	Area (ha)	Score
1.	Seawater	1.1	1
2.	Plantation/Garden	1.1	3
3.	Settlements and Places of Activity	18.2	3
4.	Shrubs/Reeds	21.5	5

area of 59.31 ha which is used as a naval base. Complete data can be seen in Table 5 and Fig. 6. In general, areas with higher slopes will have a higher potential for landslides to occur. Sumiyatinah & Yohanes (2020) said that landslides can occur in areas with slopes. The higher the slope of an area, the higher the potential for landslides in that area.

Land Use

Land use is one of the factors causing landslides. Land use affects land stability, control of water saturation, and the strength of soil particle bonds. Land covered by forests or plantations will be more able to maintain land stability because of the deep root system that will maintain the cohesiveness between soil particles and between soil particles and bedrock. In addition, land covered by forests or plantations can regulate runoff and water absorption when it rains so that soil erosion can be avoided. Meanwhile, dry fields, paddy fields, and shrubs have a shallow and inundated root system that is unable to maintain soil stability and compactness of soil particles. Wahyunto (Anwar 2012) said land use such as rice fields, as well as dry fields and shrubs, especially in areas with steep slopes, landslides are common. Based on the results of the DJI Mavic 2 Pro drone orthophoto mosaic analysis, land use in the study area is shown in Table 6 and Fig. 7.

Lineament Density

Alignment is a straight stream and valley, a straight surface, changes in soil tones, alignment of vegetation areas, changes from differences in vegetation types and heights, or striking topographical differences. All of these phenomena may be the result of structural phenomena that occur such as faults (faults), joints, folds, and fractures (Adama & Sukartono 2017). In lineament density analysis, the lineament identified
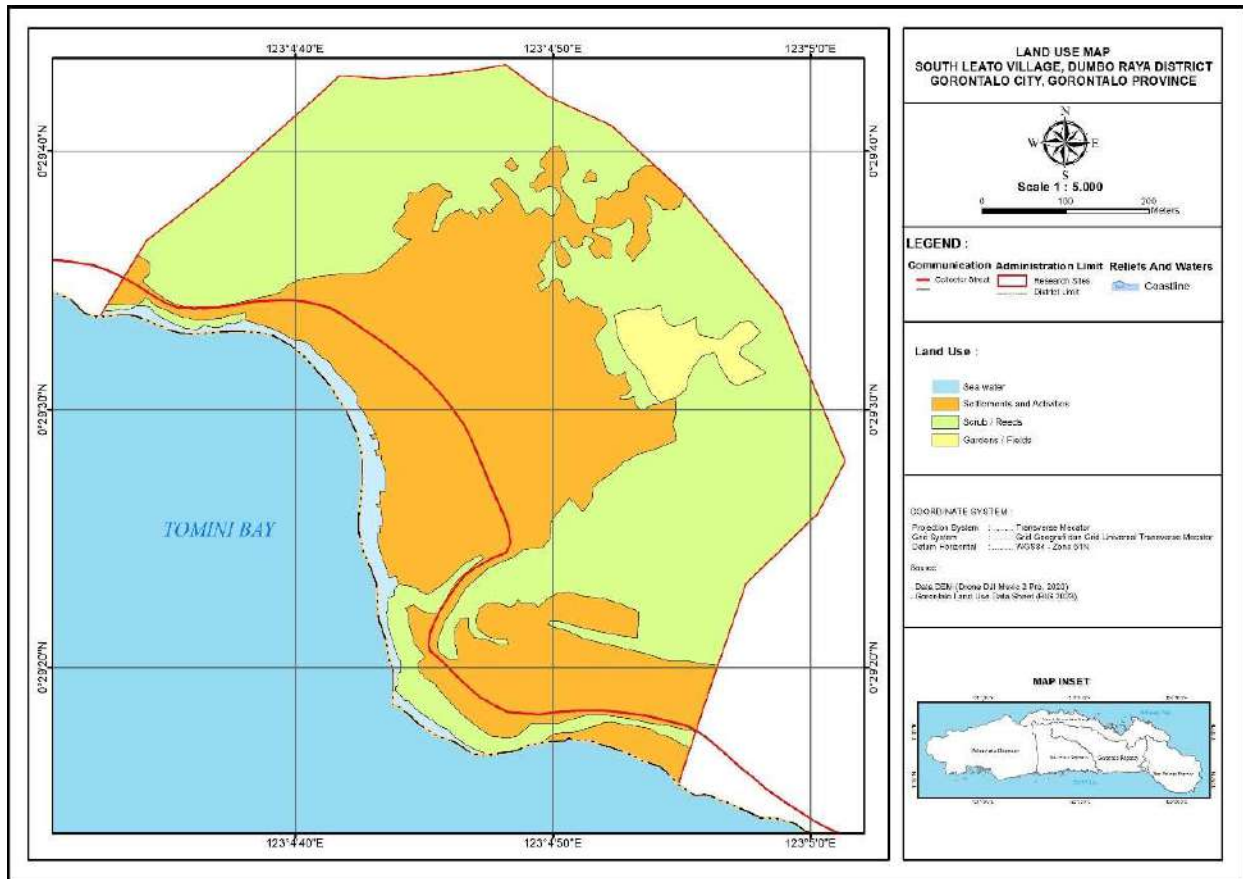
Fig. 8: South Leato village land use map.

Table 7: Lineament density (Adama & Sukartono 2017).

No.	Lineament Density	Density Value m/m^2	Score
1.	Low	1-3.7	1
2.	Currently	3.7-7.4	3
3.	Tall	7.4-11.14	5

Table 8: Classification of landslide vulnerability level.

Vulnerability level	Class interval
Low	1.1-2.3
Medium	>2.3-3.5
High	>3.5-4.7

is a straight line pattern of a river or escarpment produced by fault activity (Chemong & Chenrai 2013, Saputra 2016).

Linearity studies can help uncover generalizations that can assist in understanding the causes of landslides (Ramli et al. 2010, Bera et al. 2019). The landslides were widely observed to have severe impacts, the lineament density of the study area was analyzed using the line density analyzer extension from ArcView GIS and classified into three density classes (Fig. 8). The alignment pattern of South Leato village shows relatively the same trend as the slope pattern in the area (Table 7).

The results of the analysis are: This study shows that most of the landslides are located in high lineament density classes (1.33–1.67 m.m^{-2}).

Landslide Vulnerability Level and Landslide Potential Analysis

The landslide vulnerability prediction model in this study is modeled after (Dewi et al. 2017, Asikin et al. 2019) based on the model developed by Balai Besar Sumberdaya Lahan Pertanian (BBSDLP)/Agricultural Land Resources Agency. This model used lithology, slope inclination, rainfall, lineament density, and land use as its parameters. All these parameters are classified based on their scores and given values based on each of its contribution toward the landslide incidence. Following this, all parameters are overlayed to create a zonation map of the landslide vulnerability level. The landslide vulnerability level is presented in Table 8.
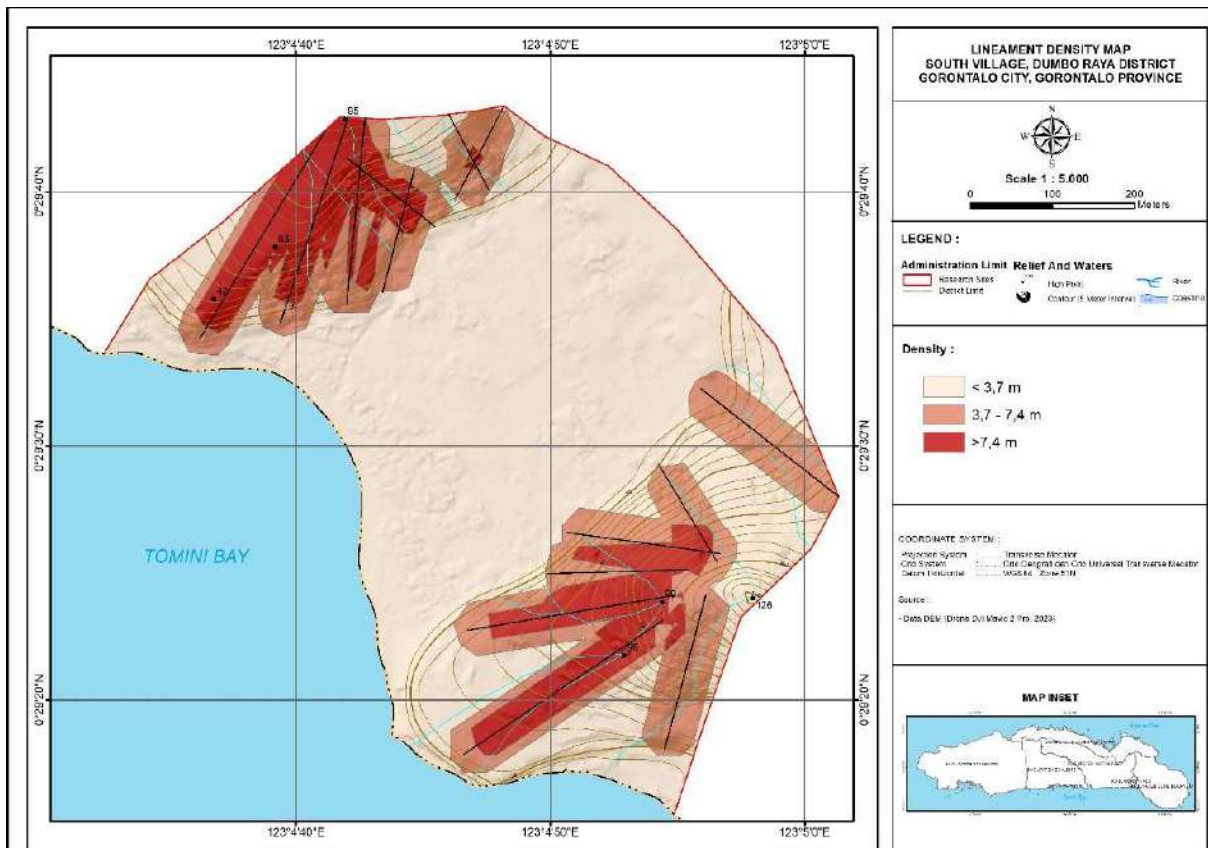
Fig. 9: South Leato village lineament density map.
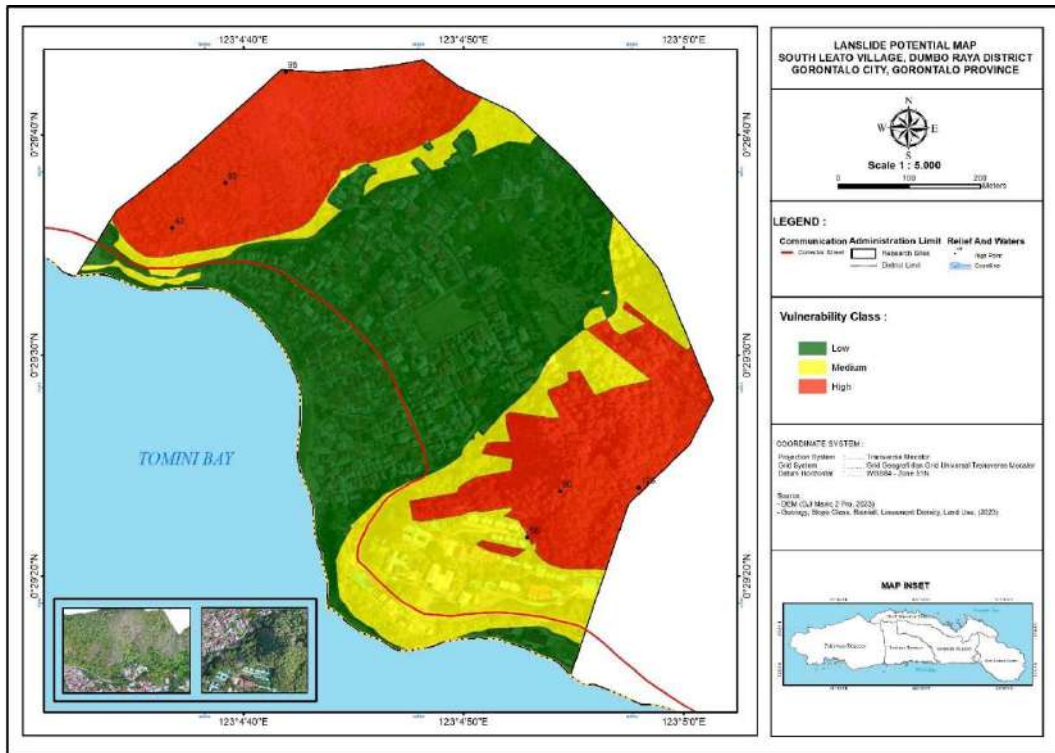
Fig. 10: Landslide potential map for South Leato Village of Gorontalo City.

The analysis revealed that South Leato village has all three levels of vulnerability. Those three levels are described as follows:

a. **Low vulnerability level:** This area is an area that is not prone to landslides. There are 19 ha of land that is considered as area with a low vulnerability level for landslides. This class dominated the residence area in the Leato Selatan village.

b. **Medium vulnerability level:** A medium vulnerability level is an area where a landslide either large or small might happen on this area, especially in areas such as road-cutting cliffs, ridges, and disturbed slopes. This medium-level vulnerability stretches in an area of 19.5 ha. It includes the Marine headquarters that is located within the Tran Sulawesi Road. The landslide has happened once in this area of medium susceptibility level on the part of Trans Sulawesi Road, which has breccia and reef limestone lithology. Thus, the sensitivity of landslides to these lithologies will increase at any time.

c. **High vulnerability level:** A high landslide susceptibility level is an area that is highly prone to landslides. This area often experiences landslides of different magnitudes. There is 13.5 ha of land in this area that is classified as highly susceptible to landslides. It is dis-

tributed in the mountainous area of South Leato village and is characterized by breccia lithology that is highly vulnerable to landslides.

In the past, a landslide happened in KM 6 of the Naval base. In an area characterized by breccia and limestone lithology. The landslide destroyed local residences. The landslide happened suddenly due to continuous rain. The locals had to be evacuated and local people together with the Navy troops had to work together to clean the debris of the landslide from the road. This research has revealed some landslide-prone spots; hence, the South Leato village is classified as a disaster prone zone (Fig. 9).

CONCLUSION

The landslide analysis scoring produced three classes of landslide vulnerability. There was 19 ha of areas within the site classified as low-level vulnerability, 9.5 ha was classified as medium-level vulnerability, and 13.5 ha of land classified to have a high vulnerability level. This highly vulnerable area is on a highly inclined slope.

This method could calculate the extent of landslide volume. However, landslide incidents may further escalate. Considering the strategic location of the current research site, which was located along the *Trans Sulawesi* Road, the

impact of landslide would be unimaginable for not only the population near the site but also these road users and the economic activities that depend on the existence of this road. Thus, mitigating landslide potentials in this area is required.

REFERENCES

Adama, O. V. and Sukartono. 2017. Alignment Density Analysis to Know the Developing Structural Patterns in the Kebutuhduwur and Surrounding Areas, Pagedongan District, Banjarnegara Regency, Central Java Province. Prosiding Seminar Nasional XII "Rekayasa Teknologi Industri dan I formasi" STTNAS Yogyakarta.

Anwar, A. 2012. Mapping of Landslide-Prone Areas in Agricultural Land in West Sinjai District, Sinjai Regency/Pemetaan Daerah Rawan Longsor di Lahan Pertanian Kecamatan Sinjai Barat Kabupaten Sinjai. Skripsi. Makassar: Universitas Hasanuddin.

Asiki, M. I., Maryati, S. and Akase, N. 2019. Analysis of landslide susceptibility in the delta of Bone River Gorontalo City/ Analisis tingkat kerentanan longsor daerah muara Sungai Bone Kota Gorontalo. Jambura Geoscience Review, 1(2): 87-101. https://doi.org/10.34312/jgeosrev.v1i2.2474

Balai Besar Litbang Sumberdaya Lahan Pertanian (BBSDLP). 2009. Identification and characterization of landslide and erosion prone areas in the highland to support sustainable management of agricultural land/ Identifikasi dan karakterisasi lahan rawan longsor dan rawan erosi di dataran tinggi untuk mendukung keberlanjutan pengelolaan sumberdaya lahan pertanian. Laporan Tengah Tahun, DIPA 2009. Bogor: Balai Besar Litbang Sumberdaya Lahan Pertanian.

Bera, A., Mukhopadhyay, B. P. and Das, D. 2019. Landslide hazard zonation mapping using multi-criteria analysis with the help of GIS techniques: A case study from Eastern Himalayas, Namchi, South Sikkim. Natural Hazards, 96: 935-959. https://link.springer.com/article/10.1007/s11069-019-03580-w

Bogaard, T.A. and Greco, R. 2016. Landslide hydrology: from hydrology to pore pressure. WIREs Water, 3: 439-459. https://doi.org/10.1002/wat2.1126

Chemong, C.A. and Chenrai, P. 2013. Fracture Density Analysis in the Sai Yol Fault, Western Thailand and Its Implications for Hydrological Exploration. Research Journal of Applied Sciences, 8(2): 125-130.

Dewi, T.S. Sari, B.K. and Heru, S.P. 2017. Landslide susceptible zonation using the GIS analysis: Case study in Semono and its surrounding areas of Bagelen sub-district, Purworejo regency/ Zonasi rawan bencana tanah longsor dengan metode analisis GIS: studi kasus Daerah Semono dan sekitarnya, Kecamatan Bagelen, Kabupaten Purworejo, Jawa Tengah. Jurnal Mineral, Energi, dan Lingkungan., 1(1): 50-59. https://doi.org/10.31315/jmel.v1i1.1773

Djakun, J. Maryati, S. and Kasim, M. 2020. Identification of vulnerability area of landslide using storie method in Bone Bolango Regency, Gorontalo Province. Geographica: Science & Education Journal., 1(2): 90-98. https://doi.org/10.31327/gsej.v1i2.1268

Doda, N. 2013. GIS approach in analyzing Flood susceptible area in Gorontalo city/ Analisis daerah rawan banjir Kota Gorontalo berbasis sistem informasi geografis (SIG). RADIAL-Jurnal Peradaban Sains, Rekayasa dan Teknologi., 1(2): 112-125. https://doi.org/10.37971/radial.v1i2.33

Eraku, S.S. and Permana, A.P., 2020. Erosion hazard analysis in The Limboto Lake catchment area, Gorontalo Province, Indonesia. News of the National Academy of Sciences of the Republic of Kazakhstan. Series of Geology and Technical Sciences., 3(441): 110-116. DOI: https://doi.org/10.32014/2020.2518-170X.61

Hall, R. 2002. Cenozoic geological and plate tectonic evolution of SE Asia and the SW Pacific: computer-based reconstructions, model and animations. Journal of Asian Earth Sciences, 20: 353-431.

Hall, R. 2012. Late Jurassic–Cenozoic reconstructions of the Indonesian region and the Indian Ocean. Tectonophysics, 570-571: 1-41. http://dx.doi.org/10.1016/j.tecto.2012.04.021

Hall, R. and Spakman, W. 2015. Mantle structure and tectonic history of SE Asia, Tectonophysics, 658: 14-45. http://dx.doi.org/10.1016/j.tecto.2015.07.003

Kumoro, Y. and Yunarto 2010. Microzonation of potential land movement areas based on remote sensing and geographic information systems in the southern part of Cianjur, West Java / Mikrozonasi daerah potensi gerakan tanah berbasis penginderaan jauh dan sistem informasi geografis di wilayah Cianjur Bagian Selatan, Jawa Barat. PROSIDING Pemaparan Hasil Penelitian Puslit Geoteknologi, 251-262.

Lihawa, F., Zainuri, A. Indriati, M., Permana, A. and Pradana, I.G.N.Y. 2021. The analysis of sliding surface in Alo Watershed, Gorontalo District, Indonesia. News of the National Academy of Sciences of the Republic of Kazakhstan Series of Geology and Technical Sciences., 3(447): 53-58. https://doi.org/10.32014/2021.2518-170X.62

Lucas, D., Fankhauser, K., Maurer, H., McArdell, B., Grob, R., Herzog, R., Bleiker, E. and Springman, S.M. 2020. Slope Stability of a Scree Slope Based on Integrated Characterization and Monitoring. Water, 12(2): 447. https://doi.org/10.3390/w12020447

Meiarti, R. Seto, T. and Sartohadi, J. 2019. Accuracy testo of unmanned aerial vehicle in coastal disaster mapping application/ Uji akurasi hasil teknologi pesawat udara tanpa awak (unmanned aerial vehicle) dalam aplikasi pemetaan kebencanaan kepesisiran. Jurnal Geografi, Edukasi dan Lingkungan (JGEL)., 3(1): 1-17. https://journal.uhamka.ac.id/index.php/jgel/article/view/2987

Naryanto, H.S. Suwandita, H. Ganesha, D. Prawiradisastra, F. and Kristijono, A. 2019. Incident Analysis and evaluation of landslide disaster in Banaran Village of Pulung Sub-district, Ponorogo Regency of East Java/ Analisis penyebab kejadian dan evaluasi bencana tanah longsor di Desa Banaran, Kecamatan Pulung, Kabupaten Ponorogo, Provinsi Jawa Timur Tanggal 1 April 2017. Jurnal Ilmu Lingkungan., 17(2): 272-282, doi:10.14710/jil.17.2.272-282

Patuti, I.M., Rifa'i, A. and Suryolelono, K. B. 2017. Mechanism and characteristics of the landslides in Bone Bolango Regency, Gorontalo Province. GEOMATE Journal, 12(29): 1-8. Retrieved from https://geomatejournal.com/geomate/article/view/720

Purmana, S., Suparka, E., Abdullah, C. I. and Sucipta, I. E. 2020. Characteristic of the Mount Colo Volcano, Una-Una Island, Central Sulawesi Province: Tectonic Evolution and Disaster Mitigation. IOP Conf. Ser.: Earth Environ. Sci. 589 012005 DOI -1755/10.1088 012005/1/589/1315

Ramli, M.F., Yusof, N., Yusoff, M.K., Juahir, H. and Shafri, H.Z.M. 2010. Lineament mapping and its application in landslide hazard assessment: a review. Bull. Eng. Geol. Environ., 69: 215-233. https ://doi.org/10.1007/s1006 4-009-0255-5

Rokhmana, C.A. 2015. The potential of UAV-based remote sensing for supporting precision agriculture in Indonesia. Procedia Environmental Sciences, 24: 245-253. https://doi.org/10.1016/j.proenv.2015.03.032

Saputra, I. 2016. Fault Fracture Density Method for Potential Ground Movement in Kendari City, Southeast Sulawesi Province/ Metode Fault Fracture Density untuk Potensi Gerakan Tanah di Kota Kendari Provinsi Sulawesi Tenggara. ReTII.

Shanmugam, G. 2013. Slides, slumps, debris flows, and turbidity currents. In: Elias, S. A. (ed), Reference Module in Earth Systems and Environmental Science. Elsevier Online.

Shanmugam, G. and Wang, Y. 2015. The landslide problem. Journal of Palaeogeography, 4(2): 109-166. https://doi.org/10.3724/SP.J.1261.2015.00071.

Silalahi, F.E.S., Pamela, Arifianti, Y. and Hidayat, F. 2019. Landslide susceptibility assessment using frequency ratio model in Bogor, West Java, Indonesia. Geosci. Lett., 6: 10. https://doi.org/10.1186/s40562-019-0140-4

Sumiyatinah and Yohanes 2000. GIS modeling to determine erosion-prone areas due to landslides in West Java Province/ Pemodelan SIG untuk menentukan daerah rawan erosi akibat longosran di Propinsi Jawa Barat. Prosiding Forum Ilmiah Tahunan Ikatan Surveyor Indonesia. Ikatan Surveyor Indonesia. Bandung.

Thoha, A. S., Sundari, D., Patana, P. and Sulistiyono, N. 2020. Spatial distribution of landslide vulnerability level in Dairi District, North Sumatera Province, Indonesia. Journal of Physics: Conference Series, 1542(1): 012011. IOP Publishing. https://doi.org/10.1088/1742-6596/1542/1/012011

Townshend, J.R.G. Justice, C.O. Gurney, C. and McManus 1992. The impact of misregistration on change detection. IEEE Transactions on Geoscience and Remote Sensing, 30(5): 1054-1060. https://doi.org/10.1109/36.175340

Usman, F.T. Arifin, Y.I. Hutagalung, R. and Permana, A.P. 2022. Analysis of landslide types in Pohe area of Gorontalo city based on geological structure orientation/ Analisis tipe longsor Daerah Pohe Kota Gorontalo berdasarkan orientasi struktur geologi. Journal of Applied Geoscience and Engineering, 1(1): 37-48. doi:https://doi.org/10.34312 jage.v1i1.15517

Van Zuidam, R.A. 1983. Guide to Geomorphologic Aerial Photographic Interpretation and Mapping. Netherlands: International Institute for Aerial Survey and Earth Sciences (ITC). 325 p.

Watkinson, I., Hall, R. and Ferdian, F. 2011. Tectonic re-interpretation of the Banggai-Sula-Molucca Sea margin, Indonesia. Geological Society of London Special Publications, 355: 203-224. 10.1144/SP355.10.

Wunarlan, I. 2013. Local people's adaptation on flood disaster in Gorontalo city/ Adaptasi penduduk terhadap bencana banjir di Kota Gorontalo. Seminar Nasional Infrastruktur Berkelanjutan 2019 Era Revolusi Industri 4.0 Fakultas Teknik Sipil dan Perencanaan, 1-7.

Yanrong, L. and Mo, P. 2019. A unified landslide classification system for loess slopes: A critical review. Geomorphology, 340: 67-83. https://doi.org/10.1016/j.geomorph.2019.04.020.

Yunianto, A.C. 2011. Landslide susceptibility with GIS and remote sensing in Bogor Regency/ Analisis kerawanan tanah longsor dengan aplikasi sistem informasi geografis (SIG) dan penginderaan jauh di Kabupaten Bogor. Skripsi. Bogor: Institut Pertanian Bogor.

Effect of Elevated Ozone on Soybean (*Glycine max* L.) Cultivar: Role of Orange Juice and Synthetic Ascorbic Acid

Indra Jeet Chaudhary iD **, Bhavna Nigam** iD **and Dheeraj Rathore†** iD

School of Environment and Sustainable Development, Central University of Gujarat, Gandhinagar, Gujarat, India
†Corresponding author: Dheeraj Rathore; dheeraj.rathore@cug.ac.in

ABSTRACT

Ozone is a hazardous gas for the environment and negatively affects plant and human health. These days, phytoextracts are commonly used as a source of bioactive compounds for reducing the detrimental environmental effects on plants. In the presented study, soybean cultivar JS-335 was used to assess the protective role of synthetic ascorbic acid (SAA) and orange juice (25% orange juice, enriched ascorbic acid) under ozone stress conditions. The results showed that under ozone stress, soybean cultivar JS-335 reduced growth and biomass and negatively affected the biochemical properties of plants due to these changes, finally causing yield losses. Foliar-applied OJ >and SAA improved plant growth and development and increased crop yield. It was discovered that a 25% OJ coupled with ascorbic acid and other essential nutrients and biomolecules was almost as effective as a 100 ppm SAA in reducing the harmful effects of ozone stress on soybean plants. As a result, it was determined that OJ, a less expensive source of ascorbic acid, can improve ozone resistance in plants in ozone-prone areas.

INTRODUCTION

Anthropogenic activity causes environmental pollution, including air, water, and soil environment. Environmental pollutants, including gaseous and suspended particulate matter, cause injurious effects on plant growth and biomass (Chaudhary & Rathore 2018a, b, 2019). Ozone is a secondary pollutant that negatively affects plant and human health (Rathore & Chaudhary 2019, 2021c, Soni et al. 2021). The tropospheric ozone (O_3) is presently raised in widespread areas of the Northern Hemisphere (Feng et al. 2015, Sicard et al. 2017) and is possibly phytotoxic to ozone-sensitive vegetation (Saitanis et al. 2015). When plants uptake higher doses of ozone, they experience a chain of physiological and biological alterations alternating from a single cell to a whole plant (Jolivet et al. 2016). When exposed to higher oxygen levels, vegetation threatens food sources and affects ecosystem stability and biosphere survival (Lu et al. 2015, Wang et al. 2016).

The vegetation protection against destructive ozone effects is thus a significant problem. Several potential

agrochemicals available in the market are tested as a protector of plants against ozone phytotoxicity (Saitanis et al. 2015, Chaudhary & Rathore 2022). A recent study by Chaudhary & Rathore 2020 states that the exogenous application of EDU, PU, and ascorbic acid protects against ozone stress. Exogenous application of ascorbic acid is considered to mitigate the extreme stress circumstances on the whole plants (Khalil et al. 2010). Exogenous ascorbic acid has been used to investigate the influence of exogenous ascorbic acid on many morphological, physiological, and biochemical processes in plants under stress, including wheat (Singh & Bhardwaj 2016), soybean (Amira & Qados 2014) and groundnut (Chaudhary & Rathore 2020).

Many plants are identified that naturally contain huge quantities of ascorbic acid in their fruit or other parts. The sweet orange (*Citrus sinensis* L.) is a common fruit (Etebu & Nwauzoma 2014) that is high in ascorbic acid (Galaverna & Dall'Asta 2014). It also contains trace amounts of minerals such as calcium, magnesium, potassium, polyphenols, niacin, thiamin, and folate (Yahia 2017, Chanson-Rolle et al. 2016). The Exogenous application of orange juice on soybean plants under ozone stress was not yet conducted. Therefore, these applications maybe develop a better tool for plants to survive against ozone stress and shield against agricultural loss.

ORCID details of the authors:

Indra Jeet Chaudhary: https://orcid.org/0000-0002-2735-5632
Bhavna Nigam: https://orcid.org/0000-0001-6627-6614
Dheeraj Rathore: https://orcid.org/0000-0002-6608-0926

Soybean can grow as a substitute crop in areas where abiotic stresses, such as ozone stress, are a major constraint to agricultural production (Fita et al. 2015, Bazile et al. 2016). Thus, the exogenous application of organic substances containing ascorbic acid, which effectively improves the hostile effects of abiotic and biotic stress on plant species, can boost soybean plant tolerance under such conditions. Numerous studies have stated in the literature that ascorbic acid is a powerful mitigating feature against ozone and other abiotic stresses. However, evidence on the impact of foliar ascorbic acid treatment on the harmful effects of ozone stress in soybean plants is currently unavailable. As a result, this study aimed to compare the effects of pure synthetic ascorbic acid and OJ rich in ascorbic acid on soybean plants under ozone stress.

MATERIALS AND METHODS

Experimental Design and Protectants Application

Pots experiment was conducted with three replicates of soybean (Glycine max L) cultivar at the Central University of Gujarat Campus in 2018. Under OTC (Open top chamber) 75 ppb ozone was applied for 4 hours every day till harvesting and foliar spray of synthetic ascorbic acid and sweet orange phytoextract was applied. Four treatments were applied, such as Treatment T1 (Control), T2 (ozone fumigation 75 ppb), T3 (ozone fumigation + SAA), and T4 (ozone fumigation + OJ). Seeds of a soybean (variety JS-335) were obtained from the groundnut research station Junagadh. The pots were filled with 30.0 kg of sandy loam soil with a pH of 8.1 and a composition of 65% sand, 27.5% silt, and 7.5% clay. Twenty seeds were sown in equal size of each pot, and after two weeks of seed germination, thinning was performed. In addition to the control distilled water (DW) foliar spray, 100 ppm synthetic ascorbic acid (SAA) and 25% OJ rich in ascorbic acid (25 percent OJ) were applied 10 days interval after plant germination till maturity. Fresh sweet oranges (Citrus sinensis L.) were purchased from a nearby fruit market, and after extracting the peel, the pulp was used to remove juice using an electric juicer. The juice was then processed at 4 degrees Celsius for one day before use.

Before use, the content of ascorbic acid in 25 % OJ was estimated to be 20.7 mg/L using Keller & Schwager's (1977). In addition to ascorbic acid, the OJ produces a mixture of inorganic and organic nutrients (Chanson-Rolle et al. 2016). In distilled water, various solutions were prepared, including 25% OJ and 100 ppm synthetic ascorbic acid. The sample was collected for growth & physiology analysis after 25 DAS and 50 DAS, and final harvesting was done at 120 DAS.

Growth and Biomass

The growth and biomass of the plant part were estimated separately. A triplicate of each plant per pot was taken and washed with purified water before being used to assess growth and biomass. Although other plants were refrigerated, the following biochemical parameters were determined: Graphical methods were used for leaf area measurement, and a regular meter scale measured root and shoot length. The mass of plants, such as the fresh and dry weight of plant parts, was determined by electric balance. Plants' parts were dried in a hot air electric oven at 80 degrees centigrade till a constant weight was achieved.

Photosynthetic and Non-Photosynthetic Pigments

Method Arnon (1949) was used to check for photosynthetic pigments (chlorophyll a, b, carotenoid, and total chlorophyll). A 0.25 g leaf sample was mixed with 5 mL of an 80 percent acetone solution for chlorophyll analysis. The sample was crushed with the help of pestle mortar and kept overnight at 4°C, and their optical density was taken at 663 nm and 645 nm with the help of a spectrophotometer.

The amount of anthocyanin in soybean leaves was calculated using Beggs and Wellmann's process (1985). A 100 mg leaf sample was blended with 100 mL propanol, hydrochloric acid, and water (18:1:81 v/v) in a mixture of 100 mL propanol, hydrochloric acid, and water. The following formula was used to measure the total sum of anthocyanin:

Anthocyanin (mg.g^{-1} fresh leaf) = A535 - 2.2 A650/W ×V

Where V = mL volume of extract, W = g fresh weight of leaf

Estimation of Oxidative Stress

Hydrogen peroxide activity was analyzed by Velikova et al. (2000). The extraction solution makes with the help of 5 mL of 0.1% TCA (ice cold). In a pestle mortar takes, 0.25 g of fresh leaf and 5 mL of TCA were added, and the sample was crushed. After centrifuging the homogenate, 500 liters of supernatant is combined with 500 liters of 10 mM potassium phosphate buffer (7.0 pH). After mixing the solution with 1 mL of 1 M potassium iodide (KI) and leaving it at room temperature for 20 minutes, the OD was measured at 390 nm.

MDA content was measured using Heath & Packer's (1968) method. MDA was determined using 5% TCA and 0.5 percent TBA. In a pestle mortar, 0.25 g fresh leaf was mixed with 5 mL of 5% TCA solution, and the homogenate was centrifuged after crushing. After centrifugation, mix 500 mL of the supernatant with 2 mL of 0.5 percent thiobarbituric acid (TBA). The solution mixtures were then kept in a water bath at 95°C for 50 minutes before being cooled in

an ice bath. The solution's OD was estimated at 600nm and 532nm.

Membrane permeability was determined by the described method by Blum and Ebercon (1981). An electrical conductivity meter was used to calculate ion leakage from fresh leaves in deionized water (Eutech Instruments). A punching machine carved the leaf samples into 1 cm diskettes. After cutting 20 diskettes from each sample, 10 mL of deionized water was applied to a glass beaker. The conductivity of the solution was calculated after the beakers had been held at room temperature for 3 hours.

Estimation of Antioxidants

Non-enzymatic Antioxidants

Flavonoids: Cameron et al. (1943) proposed a method for estimating flavonoid material. A 0.1 g fresh leaf sample was put in 100 mL ethanol and acetic acid mixture (99:1, v/v) and boiled for 2 minutes. After cooling to room temperature, the solution was centrifuged for 10 to 15 minutes at 8000xg. The solution's absorbance was estimated at different wavelengths from 250 to 350 nm and represented as flavonoid absorbance (A mg^{-1} fresh wt).

Ascorbic acid: For the determination of ascorbic acid in a leaf sample of soybean, used method of Keller & Schwager (1977). Ascorbic acid contents were estimated with the help of extracting solution (extracting solution: Dissolved 5 g oxalic acid and 0.75 g EDTA in one liter of distilled water). In an ice bath, a 500 mg fresh leaf sample was homogenized with 20 mL of extracting solution, and the homogenate was centrifuged at 6000xg for 15 min. After centrifuging the sample, 1 mL of the supernatant was taken, and added 5 mL of 2, 6-dichlorophenol-indophenol solution in pink color developed. After constant shaking, the O.D. of the solution was taken (Es) at 520 nm wavelength. Then one drop of ascorbic acid 1% solution was added to bleach the pink color and obtain the OD of turbid solution (Et) at the same wavelength.

For blank (Eo), 1 mL of extracting solution and 5 mL of DCPIP solution were mixed, and O.D. was measured as mentioned above.

A 1% aqueous ascorbic acid solution was used for the calibration curve, which was diluted to obtain varying concentrations. The total amount of ascorbic acid was calculated by using the following formula.

Ascorbic acid (mg g^{-1} fresh leaf) = [{Eo − (Es − Et)} × V] / (v × W × 1000)

Where W = weight of leaf taken (g); V = total volume of the mixture (mL); v = supernatant taken for analysis (mL). The standard curve estimates the value of {Eo-(Es − Et)}.

Total phenols: The amount of total phenols was estimated by Mallick and Singh (1980) using 70% acetone. For phenol determination, a 100 mg fresh leaf sample was crushed with 10 mL of 70% acetone, and the suspension was centrifuged at 6000xg for 10 minutes. Then, 1 mL of supernatant was taken in a test tube, 1 mL of folin-ciocalteu reagent was added, 2 mL of Na_2CO_3 (20% w/v) solution, and the final volume was made up of 10 mL with distilled water. This mixture was heated in a water bath for one minute and then cooled at room temperature. The blue color developed in a solution and the solution's OD was measured at 650 nm wavelength. A standard curve was prepared with known amounts of quinine for the phenol contents.

Enzymatic Antioxidants

For estimating antioxidative enzyme activity, fresh leaves sample (250 mg) was crushed in 5 mL (50 nM) of cool potassium phosphate buffer (7.8 pH). The homogenate was centrifuged for 20 min at 4°C at 12,000 xg. The supernatant was kept at -200°C to estimate the following antioxidative enzymes.

Catalase activity: Catalase activity was estimated by Chance & Maehly 1955, using 100 μL supernatant in 1.9 mL potassium phosphate buffer (50 mM, pH 7.8). 1 mL of 5.9mM H2O2 was also added to the mixture, and the OD was measured at 240 nm after every 20 seconds for two minutes.

SOD activity: For estimating SOD activity, 50μL supernatant was added with 400 μL distilled water, 250 μL (50 mM) potassium phosphate buffer (pH 7.8), 100μL L-methionine, 100 μLtritron-X, 50 μL nitro blue tetrazolium (NBT) and 50 μL riboflavin. The solution's optical density (OD) was recorded at 560 nm (Van Rossum et al. 1997).

POD activity: For estimating peroxidase activity, 100μL supernatant was added with 1.8 mL potassium phosphate buffer (50 mM, 7.8 pH), 100 μL guaiacol (20 mM), and 100 μL H_2O_2 (40 mM), and the OD of the solution was calculated at 470 nm after every 20 seconds for 3 min as defined in Chance & Maehly (1955).

APX activity: For the APX activity, 100 μL supernatant was mixed with a 3 mL solution containing 100 mM phosphate (pH 7), 0.1 mM EDTA-Na2, 0.3 mM ascorbic acid, and 0.06 mM H_2O_2. The OD was read at 290 nm for 30-second intervals until the ascorbic acid oxidized. One unit of APX forms 1 μ M of ascorbate oxidized per minute in assay conditions (Nakano & Asada 1981).

Primary Metabolites

Total soluble sugars, reducing sugars: Foliar sugar contents were estimated using the method described by Somogyi (1952). The leaf sample (50 mg) was crushed in

5 mL of 80% ethanol and centrifuged for 15 min at 3500xg. Pellets obtained were washed four-time using 80% ethanol and distilled water. The mixture was centrifuged at every washing. 1 mL of aliquot was mixed with 1 mL of copper reagent and boiled in the hot water bath for 10 minutes. After boiling, the solution was kept cooled to room temperature straightway, and 1 mL of arsenomolybdate was added. The solution was left for 30 minutes to complete the reaction before taking OD at 500 nm to estimate soluble sugars. For reducing sugar, 0.5 mL of diluted aliquot was mixed with 1 mL of 5% phenol reagent and left for 10 minutes to uphold room temperature. This solution was mixed in 5 mL of H_2SO_4. The solution was shacked well and left in a water bath for 10 minutes before measuring the OD at 480 nm. A standard curve obtained using purified glucose estimated total soluble sugar and total reducing sugar. The remaining pellet samples were washed twice with 52% perchloric acid and distilled water and then centrifuged to estimate starch content. The volume of supernatant was made to 50 mL with distilled water. 1 mL aliquot of pooled supernatant was taken to estimate the starch content.

Amino acids and proteins: The amino acid was determined using Hamilton et al. (1943) method. 1 mL of the sample (used for antioxidants) was added with an equal amount of 10% pyridine and acidic ninhydrin in test tubes. The mixture was heated for 30 min at 100°C, cooled at room temperature, and upraised volume to 7.5 mL using distilled water. The OD was recorded at 570 nm. Protein was estimated by using the method of Lowry et al. (1951).

Yield Characteristics

Yield characteristics were calculated using the number of capsules plant^{-1}, number of seed plant^{-1}, and weight of seed and pod plant^{-1}.

Statistical Analysis

The study involved a fully randomized two-factor ozone stress and exogenous ascorbic acid treatment. Using the HPSS software, the data collected for each parameter were subjected to Duncan's Multiple Range Test analysis. The least significant difference was estimated at the 0.05 percent likelihood stage to estimate the significant differences among the mean values. Using Origin Pro software, PCA was used to describe the homogeneous characteristics of a soybean cultivar and the association between each vector tested under different treatments at two sampling dates (2019).

RESULTS

Growth and Biomass

Leaf area and plant height: The leaf area and plant height of ozone-treated plants was highly affected compared to a control plant. At the same time, the application of natural ascorbic acid played a protective role against ozone stress than synthetic ascorbic acid as compared to control plants. The maximum increase in leaf area was found in treatment T4 (14.86%) at 25 DAS and plant height in the same treatment (28.17%) at 50 DAS (Fig. 1). The treatment-wise difference in leaf area and plant height was noted as maximum in treatments T4 > T3 > T1 > T2 (Fig. 1).

Total biomass and root shoot ratio: Plant biomass and root shoot ratio show variable treatment and age factors results. Total plant biomass was reduced by the ozone stress of the experimental crop (Fig. 1). However, exogenous application of SAA and OJ-treated plants neutralized the ozone effect. It enhanced the weight of dry leaf mass and total plant biomass of the experimental cultivar. A maximum increase in dry leaf weight was found at 70.13% under treatment T4 at 25 DAS, and a higher increment of total plant biomass (117.57%) was noted under the same treatment on the same day after the sowing of plants. The root-shoot ratio of the plant showed a negative percentage reduction in an enhanced ozone-treated plant at 25 DAS compared to control plants. In comparison, exogenous applied AA showed a positive value of percentage increments at 25 DAS and a negative value at 50 DAS.

Oxidative Stress

Hydrogen peroxide and MDA contents: Enhance ozone increases the production of hydrogen peroxide and MDA contents in plants. Higher production was found at 16.56% at 50 DAS in treatment T2. Application of natural and synthetic ascorbic acid reduced the production of Hydrogen peroxide in soybean cultivar (Fig. 2). Treatment-wise, hydrogen peroxide production was noted as T2 > T1 > T3 > and T4. Accumulation of MDA in ozone-stressed seedlings was higher than in control, whereas, in the presence of exogenous application of SAA and OJ, MDA contents were reduced significantly (Fig. 1). The maximum increase of MDA was observed in treatment T2 (25.35%) at 25 DAS (Fig. 2).

Membrane permeability: Membrane permeability showed a significant increase in ozone stress. The higher membrane injury was recorded under ozone stress. The maximum increase of membrane permeability was found under treatment T2 (12.53%) at 50 DAS (Fig. 2), and the lowest percentage of membrane permeability was found in treatment T4 (-20.22%) at 20 DAS as compared to control plants. Membrane stability shows reverse trends as membrane permeability.

Photosynthetic and Non-Photosynthetic Pigments

Total chlorophyll and carotenoids: Ozone-treated plants
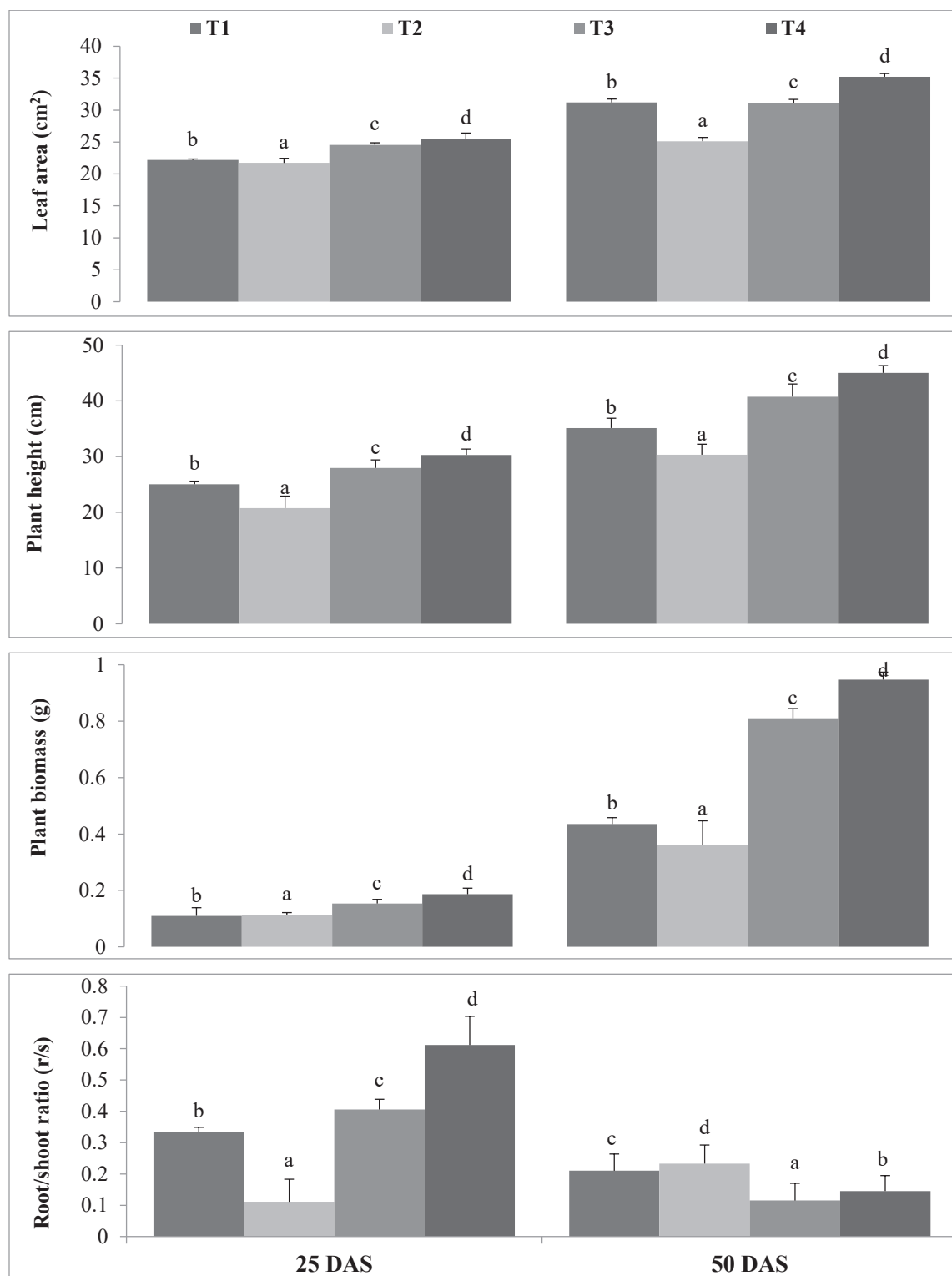
Fig. 1. Role of natural and synthetic ascorbic acid on leaf area (cm^2), plant height (cm), total plant biomass (g), root shoot ratio (R/S) of soybean cultivar (Mean ± standard deviation of three replicates presented by thin vertical bars, Value within each column followed by the same letter are not significantly different (p< 0.05) using Duncan's Multiple Range Test).
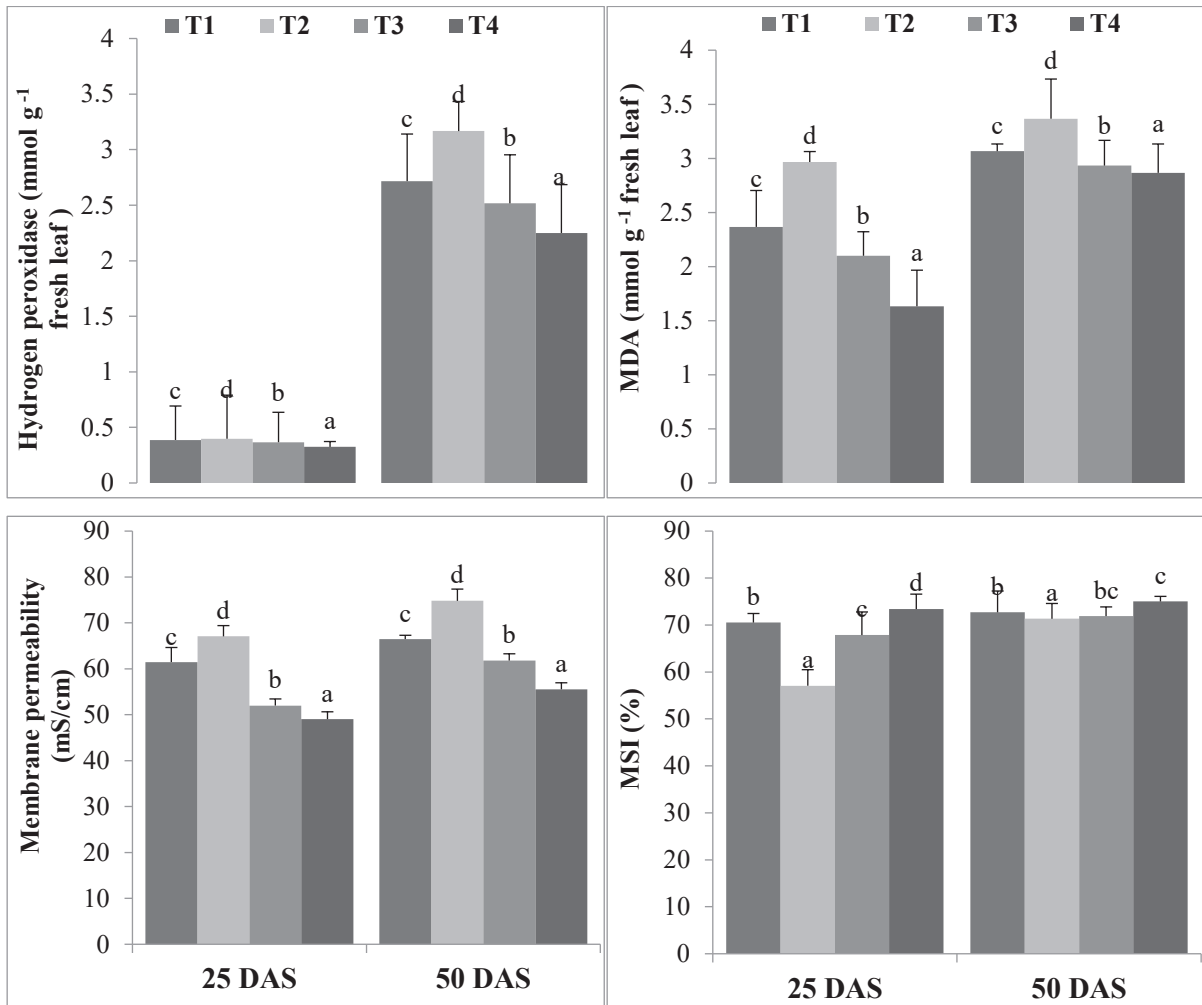
Fig. 2. Role of natural and synthetic ascorbic acid on hydrogen peroxide (mmol.g^{-1} fresh leaf), MDA contents (mmol.g^{-1} fresh leaf), membrane permeability (mS.cm^{-1}), and membrane stability (%) of soybean cultivar (Mean ± standard deviation of three replicates presented by thin vertical bars, Value within each column followed by the same letter are not significantly different ($p < 0.05$) using Duncan's Multiple Range Test).

caused a significant decrease in chlorophyll a, b and total chlorophyll content compared to the control (Fig. 3). While application of SAA and OJ precipitated significant increases in chlorophyll a, b and total chlorophyll content in stressed plants. The maximum increase of total chlorophyll was noted under treatment T4 (35.84%) at 50 DAS and a minimum in treatment T2 (-33.38%) at 25 DAS compared to control plants. Increasing chlorophyll trends in treatments were T4>T3>T1>and T2. Carotenoid and anthocyanin contents were also reduced under ozone stress. The maximum carotenoid increase was found in treatment T4 (29.81%) at 50 DAS and a minimum in treatment T2 (-18.83%) at 25 DAS.

Anthocyanin: Ozone stress also negatively affects the anthocyanin of plants. While the application of OJ and SAA increased the anthocyanin concentration in plants. Anthocyanin of plant leaf also follows the same trends as carotenoids content and maximum values were noted in treatment T4 (19.12%) at 25 DAS as compared to control plants (Fig. 3). Treatment-wise, increasing trends of anthocyanin in plants were noted T4>T3>T1> and T2.

Antioxidants Activity

Flavonoids, Phenol and Ascorbic Acid

According to the data, the production of flavonoids decreases remarkably under ozone stress (Fig. 3). The flavonoid content maximum increased (97.96%) at 50 DAS under treatment T4. Ozone increased total phenolic compounds significantly (Fig. 2). The maximum increase of phenolic contents was 101.40% at 50 DAS under the T3 treatment. Ozone caused
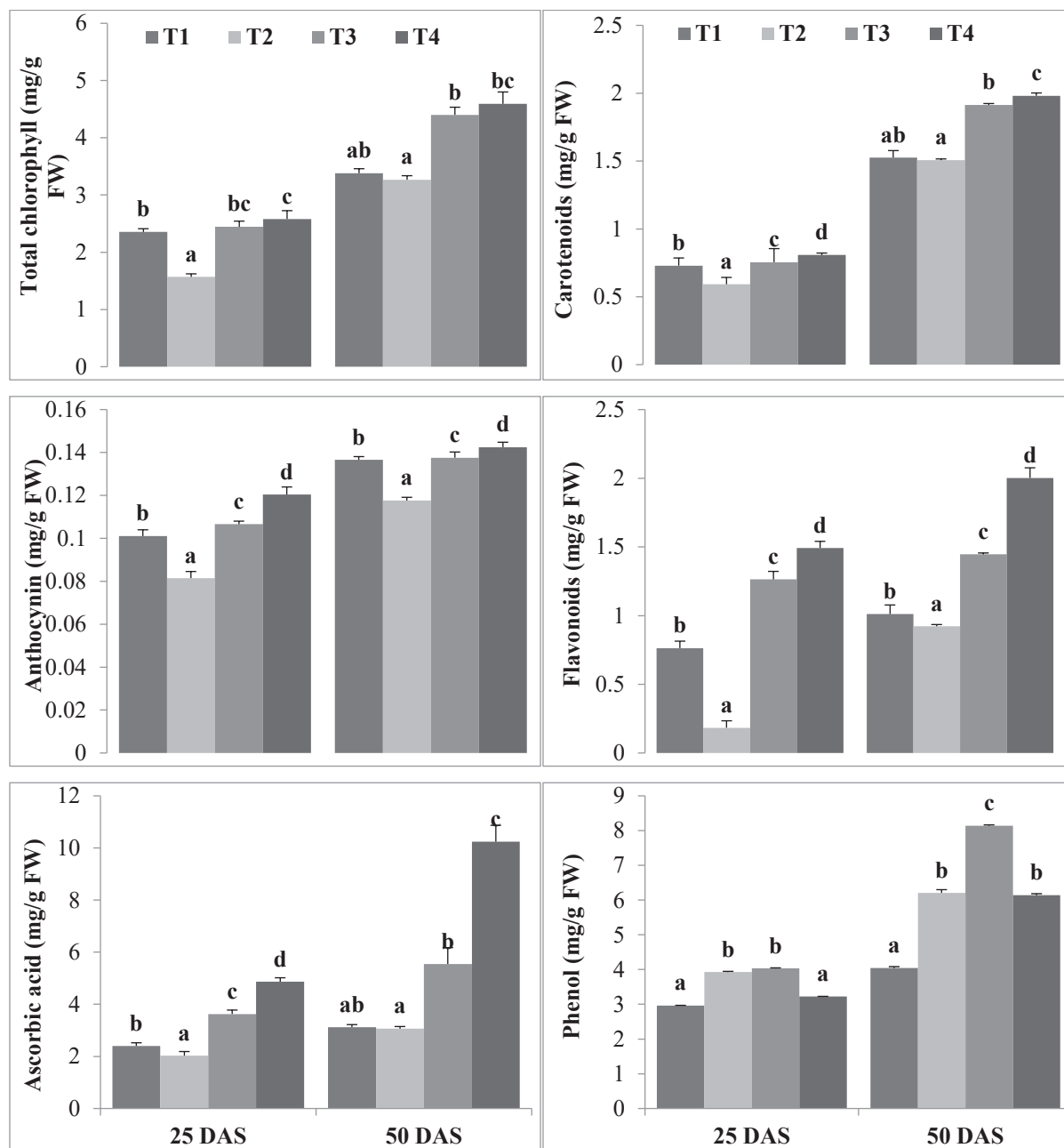
Fig. 3. Role of natural and synthetic ascorbic acid on total chlorophyll (mg.g^{-1} fresh wt.), carotenoids (mg.g^{-1} fresh wt.), anthocyanin (mg.g^{-1} fresh wt.), flavonoids (mg.g^{-1} fresh wt.), ascorbic acid (mg.g^{-1} fresh wt.) and phenol (mg.g^{-1} fresh wt.) of soybean cultivar (Mean ± standard deviation of three replicates presented by thin vertical bars, Value within each column followed by the same letter are not significantly different ($p< 0.05$) using Duncan's Multiple Range Test).

a negative effect on ascorbic acid content in selected crops. A maximum increase in ascorbic acid (228.20%) was found under T4 treatment at 50 DAS and a minimum in treatment T2 (-15.55%) at 25 DAS (Fig. 3).

Enzymatic Antioxidants

CAT, POD, SOD, and APX: The antioxidant enzymes CAT showed deviation in their activities under ozone stress. A maximum increment of CAT (0.74%) was found under T2 treatment at 50 DAS and a minimum in treatment T4 at 25 DAS. POD (430.38%) under T2 treatment at 50 DAS. The maximum increase of SOD (143.77%) was noted at 50
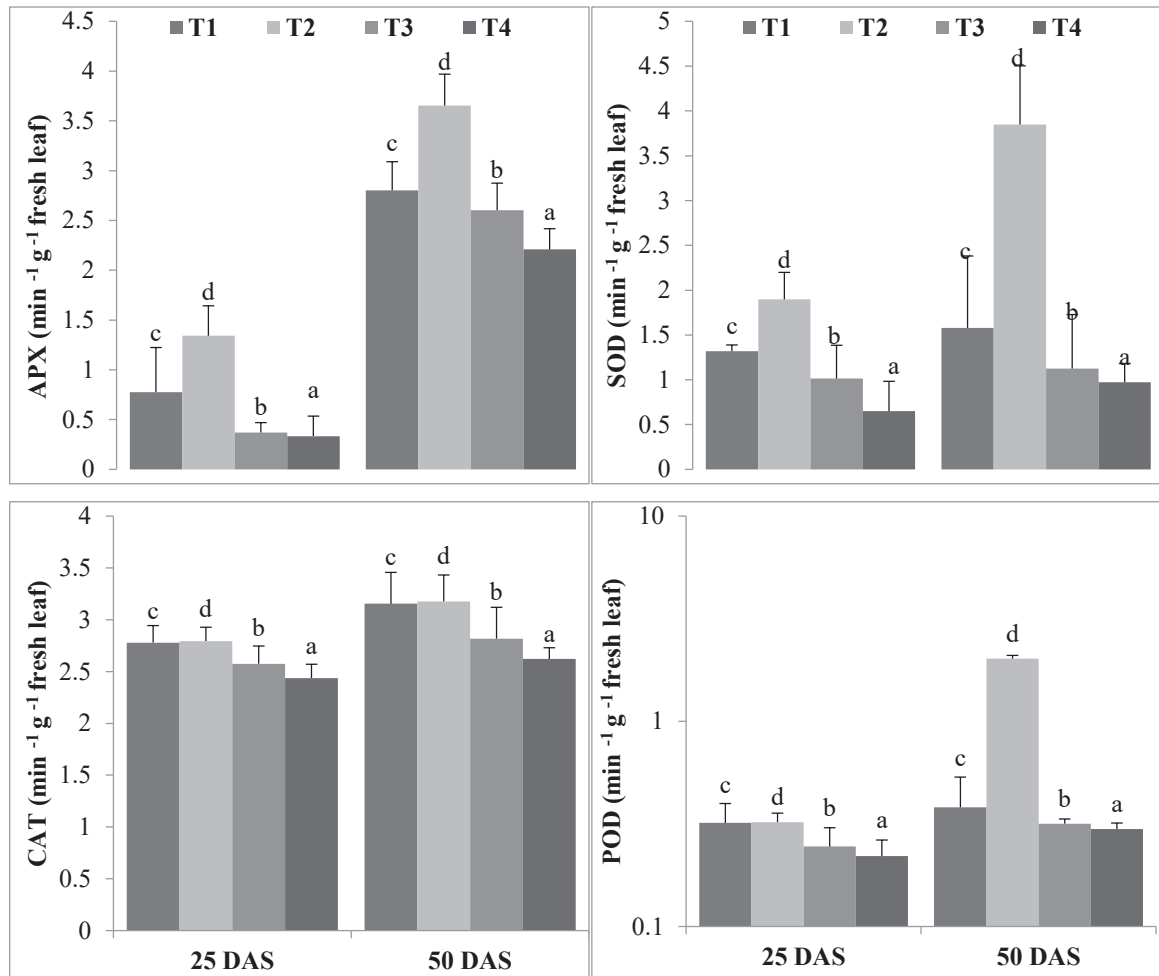
Fig. 4. Role of natural and synthetic ascorbic acid on CAT (min^{-1} .g^{-1} fresh leaf.), POD (min^{-1} .g^{-1} fresh leaf), SOD (min^{-1} g^{-1} fresh leaf), and APX (min^{-1} .g^{-1} fresh leaf) of soybean cultivar (Mean ± standard deviation of three replicates presented by thin vertical bars, Value within each column followed by the same letter are not significantly different (p< 0.05) using Duncan's Multiple Range Test).

DAS under T2 treatment, and APX (72.90%) was noted at 25 DAS under T2 treatment (Fig. 4). Activity of POD was also increased due to the application of elevated ozone. At the same time, protectants applied to plants reduced POD activity at both sampling periods. Higher activity of POD was noted at 25 DAS of plants than at 50 DAS of plants. Maximum values of POD activity were found in treatment T2 at 50 DAS of plants compared to control plants. Ozone pollution increased the SOD activity in soybean plants, and higher values was observed at 50 DAS of plants. Treatment-wise trends of SOD activity were noted higher in T2 > T1 > T3 > and T4. Higher values of APX were also found in ozone-treated plants than in control and SAA > and OJ. The age-wise higher value of APX was estimated 50 days after the plant sowing in all selected treatments.

Primary Metabolites

Total soluble and reducing sugar: The quantitative profile of total soluble sugar and reducing sugar varied significantly within the plants under ozone stresses (Fig. 5). Maximum increase of total soluble sugar and reducing sugar content (24.91% and 46.90%, respectively) was noted at 50 DAS under T4 treatment. The maximum increase of reducing sugar (18.05%) was found at 25 DAS under the T4 treatment. The trends of increasing concentration of TSS and TRS were found in treatment T4 than T3> T1 > and T2.

Total soluble proteins and free amino acids: Total soluble proteins and free amino acids decreased significantly under ozone stress conditions. A major difference was found in protein and amino acids under ozone stress conditions. At the same time, exogenous applied SAA and OJ increased
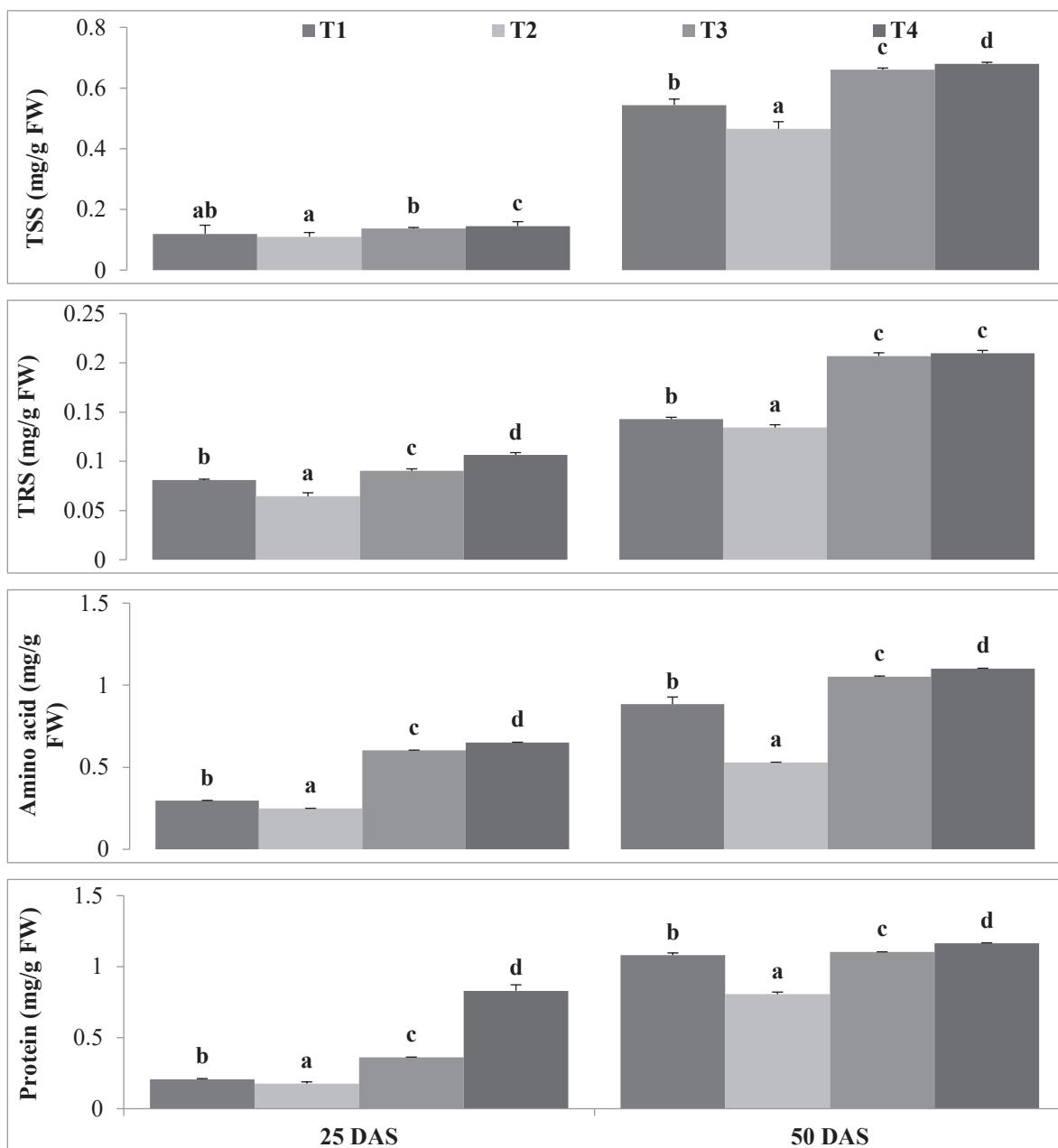
Fig. 5. Role of natural and synthetic ascorbic acid on TSS (mg/g fresh wt.), TRS (mg/g fresh wt.), amino acid (min^{-1} .g^{-1}fresh wt.) and protein (min^{-1} .g^{-1} fresh wt.) of soybean cultivar (Mean ± standard deviation of three replicates presented by thin vertical bars, Value within each column followed by the same letter are not significantly different (p< 0.05) using Duncan's Multiple Range Test).

these content in plants (Fig. 5). Maximum increase of total soluble protein was found in T4 treatment (301.71%) at 25 DAS and while a maximum increment of amino acid was also noted in same treatment (119.14%), at same DAS.

Yield Characteristics

Yield characteristics of soybean cultivars, such as the number of pods, number of seeds, seed weight, and total yield, are also affected by the application of elevated ozone. While the application of the protectant increased the yield of plants. Total yield reduction was observed under the T2 treatment (-19.16%). The maximum yield increase (19.46%) was noted under T4 treatment as compared to control plants (Fig. 6). While the application of SAA
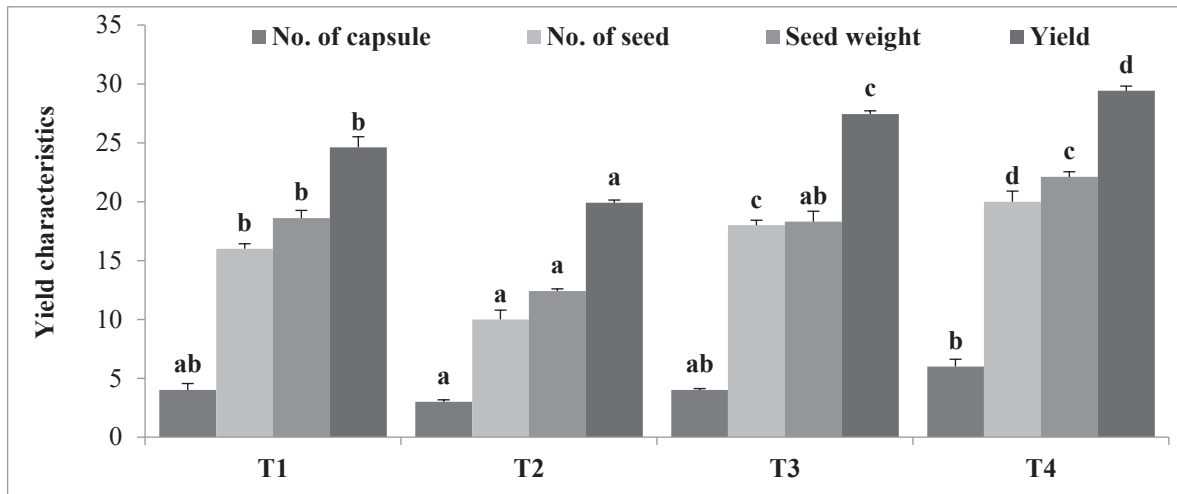
Fig. 6. Role of natural and synthetic ascorbic acid on no. of the capsule (plant^{-1}), number of seeds (plant^{-1}), seed weight (g.plant^{-1}), and total yield (g.plant^{-1}) of soybean cultivar (Mean ± standard deviation of three replicates presented by thin vertical bars, Value within each column followed by the same letter are not significantly different (p< 0.05) using Duncan's Multiple Range Test).
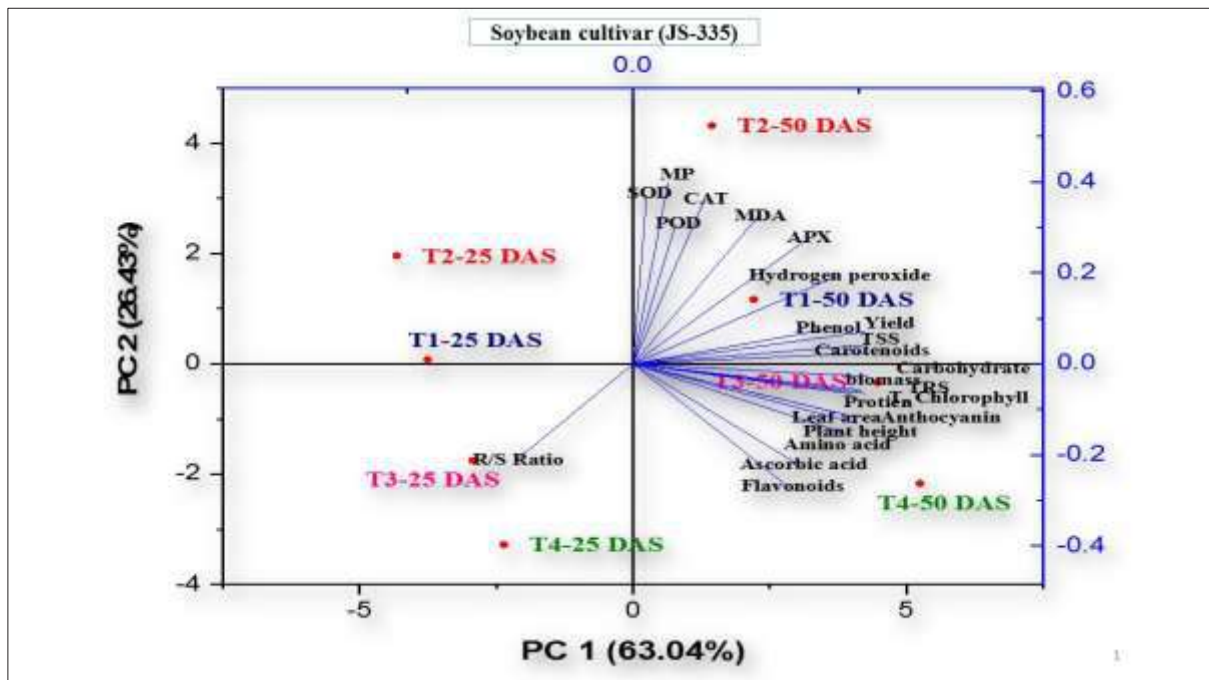
Fig. 7. Principle component analysis (PCA) correlation bi-plot of growth, biomass, and biochemical responses to ozone stress. Symbols represent the standardized scores on PC1 (x-axis) and PC2 (y-axis) for the ozone stress and ascorbic acid protectants on soybean cultivars (cv. JS-335). Vector coordinates represent the correlations between standardized variables and principal components (PCs).

shows a moderate increment in the yield of soybean plants.

Principle Component Analysis

PCAs analysis shows that the protectant application positively correlated with each parameter (Fig.7). The total percent-age variance of cultivar JS-335 was found to be 63.04% and 26.43% at PC1 and PC2 with Eigenvalue 14.49 and 6.04. Percentage variation at PC3 was noted at 5.43% and eigenvalue 1.24. Leaf area, plant height, and protein content were highly correlated, while plant biomass, total chlorophyll, and TRS also showed strong relationships among the parameters.

All selected treatments showed a negative value 25 days after the sowing of the plant, while 50 days after the sowing of the plant represented a positive value at PC1. Treatment, wise highest positive score value of the cultivar was noted in T4 (5.52) than in T3 (4.47) >T1 (2.21) > and T2 (1.47). Antioxidant defense, such as non-enzymatic and enzymatic antioxidants, showed positive values at both PCs. Therefore, PCA analysis data confirmed that OJ is more effective than SAA compared to control plants, and elevated ozone caused a negative effect on soybean cultivar JS-335.

DISCUSSION

For plant growth and development, ozone is a toxic pollutant. A higher concentration of ozone caused agricultural losses and created food crises worldwide. Therefore a current study was carried out to improve plants' growth and yield using phytoextract enriched with ascorbic acid. The presented study showed that 100 ppm SAA and 25% OJ (enriched with ascorbic acid) could improve the ozone resistance of soybean plants. A study also reported that the ambient level (13.89 to 22.42 ppb day^{-1}) of ozone caused a negative effect on groundnut cultivars while applying synthetic ascorbic acid improved plant growth and yield (Chaudhary & Rathore 2020). In the present work, leaf area, plant height, and total plant biomass of soybean were reduced under ozone stress. While the application of exogenous OJ >and SAA increases the plant's leaf area and the plant's height and total biomass of the plant, its means that natural ascorbic acid is a more effective protectant against ozone stress. Various studies also reported that the elevated ozone caused a negative impact on leaf area and plant height and reduced plant biomass (Agathokleous et al. 2018, Rathore & Chaudhary 2019, 2021). However, exogenous application of ascorbic acid is attributed to ozone resistance by oxidative resistance organization, photosynthesis, and Osmo protection metabolism. The photosynthetic rate of chlorophyll a,b, and carotenoids was reduced under ozone stress, either due to reduced synthesis of key chlorophyll complexes (Agathokleous et al. 2018) or due to the destruction of pigment and protein molecules (Amira & Qados 2014). Ozone stress significantly reduced the contents of photosynthetic pigments such as chlorophyll a, b, and carotenoids in the current study. Foliar-applied 100 ppm OJ >and SAA improved soybean plants' chlorophyll and carotenoid contents.

Ozone enters through stomata and generates ROS in plants. It is a natural process, but due to elevated ozone, the production of H_2O_2 was higher and also increased lipid peroxidation and finally caused leaf membrane damage (Chaudhary & Rathore 2019, Rathore & Chaudhary 2019, 2021). In this study, H_2O_2 production, MDA, and membrane damage were higher in elevated ozone. The application of OJ >and SSA controlled the production rate of H_2O_2 and membrane damage in soybean plants. Malondialdehyde (MDA) is a signaling molecule that reflects oxidative stress-induced membrane damage (Shafiq et al. 2015). Moreover, exogenous application of protectants such as ethylene diurea, ascorbic acid, and phenyl urea controlled the leaf membrane injury (Chaudhary & Rathore 2020, Rathore & Chaudhary 2021).

Antioxidant defense systems, including enzymatic (SOD, POD, APX, and CAT) and non-enzymatic (phenolics, carotenoids, ascorbic acid, and flavonoids) antioxidant defense systems, protect cells from oxidative stress (Akram et al. 2017, Chaudhary & Rathore 2018a, 2019, Rathore & Chaudhary 2021). When exposed to ozone, CAT, SOD, APX, and POD behaviors were enhanced in soybean plants. Although the foliar application of natural ascorbic acid > and synthetic ascorbic acid has reduced the activities of CAT, SOD, POD, and APX in plants, the increasing incidence was higher in elevated ozone as compared to control plants. Rathore & Chaudhary (2021c) reported that ozone pollution increased the activity of these enzymes. Darvishan et al. (2013) also reported one more study under a water shortage regime of corn plants.

Non-enzymic antioxidants also played a vital role in defense, contrary to stress. Non-enzymatic antioxidant ascorbic acid (AA) plays a key function in stress safety by enzymatically detoxifying hydrogen peroxide and directly scavenging reactive oxygen species (ROS) (Hemavathi et al. 2011, Ye et al. 2012). Under ozone stress, the content of endogenous ascorbic acid in Soybean plants decreased in the current research. However, when applied 100 ppm SAA or NAA was under ozone conditions, internal ascorbic acid content improved in soybean plants. Previous reports show that oxidative stress reduced ascorbic acid contents in plants (Chaudhary & Rathore 2018d, 2019, 2020), and foliar application of ascorbic acid effectively improved the inherent ascorbic acid content under drought and ozone stress (Singh & Bharadwaj 2016, Chaudhary & Rathore 2020).

The synthesis of flavonoids is more under ozone stress conditions. The elevated ozone gradually reduced flavonoid contents while plants' phenolic content increased. Phenolic groups consume plants' flavonoids and protein formation (Rathore & Chaudhary 2021). According to some research, flavonoid synthesis is thought to increase in most plants when water-stressed (Ma et al. 2014, Nichols et al. 2015). Compared to our observations, total flavonoids decreased in soybean plants under ozone stress, while foliar application of 100 ppm synthetic ascorbic acid and 25% OJ enhanced with ascorbic acid increased flavonoid content in soybean

plants under ozone stress. Phenol contents of soybean plants were increased due to elevated ozone, and applied natural and synthetic ascorbic acid reduced the production of phenol in plant leaves.

Primary metabolites such as sugars, carbohydrates, and proteins were also affected due to ozone pollution. Sugars are important in increasing plant tolerance to abiotic stresses like ozone because higher sugar levels can reduce water loss, sustain turgor, and reduce membrane destruction, improving plant growth (Rodziewicz et al. 2014). Total soluble sugars and declining sugars in soybean plants exposed to ozone stress decreased dramatically in this research. Earlier reports also revealed that the ozone reduced the sugar content in cotton and groundnut cultivars (Chaudhary & Rathore 2021b, Rathore & Chaudhary 2021). The content of total soluble sugars and reducing sugars in soybean plants was increased by foliar application of ascorbic acid. Amira & Qados (2014) reported that ascorbic acid increased the sugar content in okra and soybean plants under water stress conditions, which is close to our findings. The reduction of total carbohydrates in plants was also higher in elevated ozone-treated plants than in control plants. Applying OJ> and SAA increased the total carbohydrate in plants.

Amino acid and protein contents were also decreased under the elevated ozone of the plant. Applied exogenous protectants increased the amino acid and protein contents in plant leaves. Enzymes that catalyze the hydrolysis of protein increasing the concentration of the phenolic compound in plants due to ozone stress may increase the synthesis of amino acids and proteins, resulting in reduced protein content in plants (Ambasht & Agrawal 2003, Chaudhary & Rathore 2020). Water stress affects amino acid metabolism, and their content usually rises, potentially causing protein synthesis (Zonouri et al. 2014). Ozone stress decreased the content of free amino acids and total proteins in soybean plants in this study. Furthermore, when foliar OJ and SAA were implemented under ozone stress, both sources of ascorbic acid increased the content of amino acids and total proteins in soybean plants. Similar findings have recently been reported in a variety of plants, including corn (Dolatabadian et al. 2010), wheat (Malik et al. 2015), and grapes (Zonouri et al. 2014), with the authors claiming that an increase in amino acid and protein content is positively associated with stress tolerance mechanisms in plants.

Overall, under ozone stress conditions, plants increased the production of H_2O_2 and MDA contents, damaging the leaves membrane (Chaudhary & Rathore, 2021a,b,c). The over-production of H_2O_2 in plant cells negatively affects plant growth, photosynthetic pigments, protein content, and, finally caused, yield loss. While increasing activities of antioxidants such as enzymatic (CAT, SOD, APX, and POD) and non-enzymatic (carotenoids, flavonoids, phenol, ascorbic acid) properties play a defensive role against ozone stress. In soybean plants, 25 percent OJ was more effective than 100 ppm SAA. OJ's effectiveness can be expected because it contains a variety of biomolecules and nutrients other than AA that could help plants grow and perform key metabolic functions. As a response, growth promotion by OJ may have been possible due to all nutrients in OJ rather than only AA. The foliar application of OJ (25 percent OJ) could increase soybean plant ozone resistance.

Agricultural productivity is a major part of the economy of the world's developed and developing countries. In the present investigation, ozone pollution caused a negative impact on the yield of soybean plants. A recent study also reported that ozone pollution reduced the growth and yield of castor beans and groundnut (Rathore & Chaudhary 2019, Chaudhary & Rathore 2021a). While the application of exogenous protectants such as OJ >and SAA improves the plant growth and yield of soybean cultivars. Higher effectiveness was found in natural ascorbic acid than in synthetic ascorbic acid. This means that 25% of orange juice enriched with AA will have a useful tool for agricultural sustainability against ozone stress. PCAs analyzed data, and the application of OJ and SAA showed strong relation with yield and plant physiological characteristics. This means OJ applications are a potent tool for agricultural productivity in ozone-prone areas.

CONCLUSION

Ozone is a burning problem for the agriculture of developed and developing countries. Overall, ozone enters through stomata in plant cells and causes negative effects in membrane damage, loss of relative water contents, and reduced plant growth and yield. However, to protect plants from oxidative stress, the exogenous application of protectants will be an enormous tool for agricultural loss. In the present study, foliar-applied synthetic or natural ascorbic acid improved plant growth, physiology, and yield of soybean cultivars. It was observed that 25% of OJ-enriched ascorbic acid was more effective than 100 ppm SAA in soybean plants subjected to ozone stress. Since OJ comprises several biomolecules and nutrients other than AA that could help promote plant growth and main metabolic activities, growth promotion by OJ may have been possible due to all nutrients found in OJ rather than by AA working slowly. Thus, foliar application of 100 ppm SAA and OJ (25 percent orange juice enriched) could increase soybean plant ozone resistance.

ACKNOWLEDGMENT

REFERENCES

Agathokleous, E. 2018. Environmental hormesis is a fundamental non-monotonic biological phenomenon with implications in ecotoxicology and environmental safety. Ecotoxicol. Environ. Safety, 148: 1042-1053.

Akram, N.A., Shafiq, F. and Ashraf, M. 2017. Ascorbic acid- a potential oxidant scavenger and its role in plant development and abiotic stress tolerance. Front. Plant Sci., 8: 613.

Ambasht, N.K. and Agrawal, M. 2003. Interactive effects of O_3 and UV-B singly and in combination on physiological and biochemical characteristics of soybean. J. Plan. Biol., 30: 37-45.

Amira, M.S. and Qados, A. 2014. Effect of ascorbic acid antioxidant on soybean (Glycine max L.) plants grown under water stress conditions. Int. J. Adv. Res. Biol. Sci., 1: 189-205.

Arnon, D.T. 1949. Copper enzyme in isolated chloroplasts polyphenol oxidase in Beta vulgaris. Plant Physiol., 24: 1-15.

Bazile, D., Jacobsen, S.E. and Vernaiu, A. 2016. The global expansion of quinoa: Trends and limits. Front. Plant Sci., 7: 622.

Beggs, C.J. and Wellmann, E. 1985. Analysis of light-controlled anthocyanin formation in coleoptiles of Zea mays L: the role of UV-B, blue, red, and far red light. Photochem. Photobiol., 41: 481486.

Blum, A. and Ebercon, A. 1981. Cell membrane stability as a measure of drought and heat tolerance in wheat. Crop Sci., 21: 43-47.

Cameron, G.R. Milton, R.F. and Allen, J.W. 1943. Measurement of flavonoids in plant samples. Lancet, 11: 179.

Chance, B. and Maehly, A. 1955. Assay of catalase and peroxidase. Meth. Enzymol., 2: 764-817.

Chanson-Rolle, A. Braesco, V. Chupin, J. and Bouillot, L. 2016. Nutritional composition of orange juice: A comparative study between French commercial and home-made juices. Food Nutrit. Sci., 7: 252-261. http://dx.doi.org/10.4236/fns.2016.74027

Chaudhary, I.J. and Rathore, D. 2018d. Suspended particulate matter deposition and its impact on urban trees. Atmos. Pollut. Res., 9: 1072-1082.

Chaudhary, I.J. and Rathore, D. 2019. Dust pollution: Its removal and effect on foliage physiology of urban trees. Sustain. Cities Soc., 51: 101696. https://doi.org/10.1016/j.scs.2019.101696.

Chaudhary, I.J. and Rathore, D. 2020. Relative effectiveness of ethylenediurea, phenyl urea, ascorbic acid, and urea in preventing groundnut (Arachis hypogaea L.) crop from ground level ozone. Environ. Technol. Innov., 19: 100963. https://doi.org/10.1016/j.eti.2020.100963.

Chaudhary, I.J. and Rathore, D. 2021a. Micro-morphological and anatomical response of groundnut (Arachis hypogaea L.) cultivars to ground-level ozone. J. Appl. Biol. Biotech., 9 (04):137-150. DOI: 10.7324/JABB.2021.9419.

Chaudhary, I.J. and Rathore, D. 2021b. Assessment of ozone toxicity on cotton (Gossypium hirsutum L.) cultivars: Its defensive system and intraspecific sensitivity. Plant Physiol. Biochem., 166: 912-927. https://doi.org/10.1016/j.plaphy.2021.06.054.

Chaudhary, I.J. and Rathore, D. 2021d. Assessment of dose–the response relationship between ozone dose and groundnut (Arachis hypogaea L) cultivars using Open Top Chamber (OTC) and ethylenediurea (EDU). Environmental Technology & Innovation, 101494. https://doi.org/10.1016/j.eti.2021.101494.

Chaudhary, I.J. and Soni, S. 2020. Crop Residue Burning and Its Effects on the Environment and Microbial Communities. In Singh, C., Tiwari, S., Singh, J.S. and Yadav, A.N. (eds), Microbes in Agriculture and Environmental Development. CRC Press, Boca Raton, Florida, pp. 87-106

Chaudhary, IJ. and Rathore, D. 2018c. Phytomonitoring of dust load and its effect on foliar micro morphological characteristics of urban trees. Journal of Plant Science, 2:(3): 170-179, ISSN: 2456 – 9259.

Darvishan, M., Tohidi-Moghadam, H.R. and Zahedi, H. 2013. The effect of foliar application of ascorbic acid (vitamin C) on physiological and biochemical changes of corn (Zea mays L.) under irrigation withholding in different growth stages. Maydica, 58: 195-200.

Dolatabadian, A., Sanavy, S.A.M.M. and Asilan, K.S. 2010. Effect of ascorbic acid foliar application on yield, yield component and several morphological traits of grain corn under water deficit stress conditions. Not. Sci. Biol., 2: 45-50.

Ebrahimian, E. and Bybordi, A. 2012. Influence of ascorbic 582 acids foliar application on chlorophyll, flavonoids, anthocyanin, and soluble sugar contents of sunflower under water deficit stress conditions. J. Food Agric. Environ., 10: 1026-1030.

Etebu, E.N. and Nwauzoma, A.B. 2014. A review of sweet orange (C. Sinensis), health disease and management. Am. J. Res. Commun., 2: 343-70.

Feng, Z., Hu, E., Wang, X., Jiang, L. and Liu, X. 2015. Ground-level O3 pollution and its impacts on food crops in China: A review. Environ. Pollut., 199: 42-48. doi:10.1016/j.envpol.2015.01.016.

Fita, A., Rodríguez-Burruezo, A., Boscaiu, M., Prohens, J. and Vicente, O. 2015. Breeding and domesticating crops adapted to drought and salinity: A new paradigm for increasing food production. Front. Plant Sci., 6: 978.

Galaverna, G. and Dall'Asta, C. 2014. Production processes of orange juice and effects on antioxidant components. In Preedy, V. (ed), Processing and Impact on Antioxidants in Beverages Elsevier, London, UK, pp. 203-214.

Hamilton, P.B. and Van Slyke, D.D. 1943. The gaso-metric determination of free amino acids in blood filtrates by the ninhydrin-carbon dioxide method. J. Biol. Chem., 150: 231-250.

Heath, R. and Packer, L. 1968. Photoperoxidation in isolated chloroplast I. Kinetics and stoichiometry of fatty acid peroxidation. Arch. Biochem. Biophys., 125: 189-198.

Jolivet, Y., Bagard, M., Cabané, M., Vaultier, M.N., Gandin, A., Afif, D., Dizengremel, P. and Le Thiec, D. 2016. Deciphering the ozone-induced changes in cellular processes: a prerequisite for ozone risk assessment at the tree and forest levels. Annals of Forest Sci., 73: 923-943. doi:10.1007/s13595-016-0580-3.

Keller, T. and Schwager, H. 1977. Air pollution and ascorbic acid. Europ. J. Forest Pathol., 7: 338-350.

Khalil, S.E., Nahed, G., Aziz, A. and Bedour, L.A.H. 2010. Effect of water stress and ascorbic acid on some morphological and biochemical composition of Ocimum basilicum plant. J. Am. Sci., 6: 33-46.

Lowry, O.H., Rosebrough, N.J., Farr, A.L. and Randall, R.J. 1951. Protein measurement with the foliar phenol reagent. J. Biol. Chem., 193: 265-275.

Lu, Y., Jenkins, A., Ferrier, R.C. Bailey, M., Gordon, I.J., Song, S., Huang, J., Jia, S., Zhang, F., Liu, X., Feng, Z. and Zhang, Z. 2015. Addressing China's grand challenge of achieving food security while ensuring environmental sustainability. Sci. Adv., 1417: e1400039. doi:10.1126/sciadv.1400039.

Ma, D., Sun, D., Wang, C., Li, Y. and Guo, T. 2014. Expression of flavonoid

biosynthesis genes and accumulation of flavonoids in wheat leaves in response to drought stress. Plant Physiol. Biochem., 80: 60-66.

Malik, C.P. and Singh, M.B. 1980. Plant Enzymology and Histoenzymology. Kalyani Publishers, New Delhi, p. 53.

Malik, S., Ashraf, M., Arshad, M. and Malik, T.A. 2015. Effect of ascorbic acid application on the physiology of wheat under drought stress. Pak. J. Agri. Sci., 52: 209-217.

Nakano, Y. and Asada, K. 1981. Hydrogen peroxide is scavenged by ascorbate-specific peroxidase in spinach chloroplasts. Plant Cell Physiol., 22: 867-880.

Nichols, S.N., Hofmann, R.W. and Williams, W.M. 2015. Physiological drought resistance and accumulation of leaf phenolics in white clover interspecific hybrids. Environ. Exp. Bot., 119: 40-47.

Rathore, D. and Chaudhary, I.J. 2019. Ozone risk assessment of castor (*Ricinus communis* L.) cultivars using open-top chamber and ethylene urea (EDU). Environ. Pollut., 244: 257-269.

Rathore, D. and Chaudhary, I.J. 2021. Effects of tropospheric ozone on groundnut (Arachis hypogea L.) cultivars: Role of plant age and antioxidative potential. Atmos. Pollut. Res., 21: 63-79. 10.1016/j.apr.2021.01.005.

Rodziewicz, P., Swarcewicz, B., Chmielewska, K., Wojakowska, A. and Stobiecki, M. 2014. Influence of abiotic stresses on plant proteome and metabolome changes. Acta Physiol. Plant, 1: 36.

Sadiq, M., Akram, N.A., Ashraf, M. and Ali, S. 2017. Tocopherol confers water stress tolerance: Sugar and osmoprotectant metabolism in mung bean [*Vigna radiata* (L.) Wilczek]. Agrochimica, 61: 28-42.

Saitanis, C.J., Lekkas, D.V., Agathokleous, E. and Flouri, F. 2015. Screening agrochemicals as potential protectants of plants against ozone phytotoxicity. Environ. Pollut., 197: 247-255. Doi:10.1016/j.envpol.2014.11.013.

Shafiq, S., Akram, N.A. and Ashraf, M. 2015. Does exogenously-applied trehalose alter the oxidative defense system in the edible part of radish (*Raphanus sativus* L.) under water-deficit conditions? Sci. Hort., 185: 68-75.

Sicard, P., Anav, A., De Marco A. and Paoletti, E. 2017. Projected global tropospheric ozone impacts on vegetation under different emission and climate scenarios. Atmos. Chem. Phys. Disc., 17: 12177-12196.

Singh, N. and Bhardwaj, R.D. 2016. Ascorbic acid alleviates water deficit-induced growth inhibition in wheat seedlings by modulating endogenous antioxidants. Biologia, 71: 402-413.

Somogyi, M.J. 1952. Notes on sugar determination. J. Biol. Chem., 195: 19-23.

Van Rossum, M.W.P.C., Alberda, M. and Van der Plas, L.H.W. 1997. Role of oxidative damage in tulip bulb scale micropropagation. Plant Sci., 130: 207-216.

Velikova, V., Yordanov, I. and Edreva, A. 2000. Oxidative stress and some antioxidant systems in acid rain-treated bean plants: Protective roles of exogenous polyamines. Plant Sci., 151: 59.

Wang, X., Agathokleous, E., Qu, L., Watanabe, M. and Koike, T. 2016. Effects of CO_2 and O_3 on the interaction between the root of woody plants and ectomycorrhizae. J. Agric. Meteorol., 72: 95-105. doi:10.2480/agrmet.D-14-00045.

Yahia, E.M. 2017. Citrus. Fruit and Vegetable Phytochemicals: Chemistry and Human Health 2, John Wiley & Sons.

Yazdanpanah, S., Baghizadeh, A. and Abbassi, F. 2011. The interaction between drought stress and salicylic and ascorbic acids on some biochemical characteristics of Satureja hortensis. Afric. J. Agric. Res., 6: 798-807.

Zonouri, M., Javadi, T., Ghaderi, N. and Saba, M.K. 2014. Effect of foliar spraying of ascorbic acid on chlorophyll a, chlorophyll b, total chlorophyll, carotenoids, hydrogen peroxide, leaf temperature and relative water content under drought stress in grapes. Bull. Environ. Pharmacol. Life Sci., 3: 178-184.

Original Research Paper

Open Access Journal

Analysis of Solid Waste in Hospitals of Lahan and Rajbiraj Municipalities, Madhesh Province, Nepal

R. S. Mehta*†, R. C. Adhikari* and B. B. Bist**

*Department of Zoology, Tribhuvan University, Degree Campus, Biratnagar, Nepal
**Nepal Government, Nagarjun Secondary School, Sharmali, Baitadi, Nepal
†Corresponding author: Ram Chandra Adhikari (R.C.Adhikari): ram.adhikari@pgc.tu.edu.np

ABSTRACT

Hospital waste is a burning issue that severely impacts public health. This study in three big hospitals in Lahan and Rajbiraj, Nepal, for one year (2019 March-2020 February) aims to analyze some parameters that directly help waste management properly. Field study, questionnaire, and interview methods were followed. The average moisture content of wastes of all three hospitals was 55.79%. There was no variance in the three hospitals' moisture content values of wastes (F = 1.89 P-value = 0.165 F crit = 3.284917651). The average temperature of dumped waste was 23.23°C, and the temperature of all three hospitals was closely associated (F = 0.998, P-value 0.379, Fcrit = 3.28). The average pH value of wastes from the three hospitals was 4.44, and it from all three sites was strongly associated (F = 0.0668, P-value 0.935, Fcrit = 3.284). There was no relation between income and types of waste production (χ^2 = 0.8, df = 4, significance level = 0.05), but there was a high association between the level of income and amount of waste production. There was a high association between the nature of hospitals and types and the amount of waste (χ^2 = 77.09, df = 4, Significance level = 0.05). In Sagarmatha Choudhary eye hospital Lahan, there was no significant correlation between the number of patients and the amount of waste (Correlation = -0.187889 at 0.05% significance level). Unique Hospital Rajbiraj showed a correlation between the number of patients and the amount of waste (correlation = 0.1183 at 0.05% significance level). In Gajendra Narayan Singh Hospital, there was a correlation between the number of patients and the amount of waste (Correlation = 0.3453, at 0.05% significance level). There was no association between the qualification of respondents and their responsibilities regarding the services provided by hospitals (χ^2 = 1.43, df = 6, Significance level = 0.05). It is recommended for better management and installment of modern technologies for waste management.

INTRODUCTION

Solid waste is the undesired or pointless waste produced by a region's combined commercial, industrial, and residential activity (Sharma et al. 2014). The process of gathering, handling, and getting rid of solid waste abandoned because it has fulfilled its function or is no longer usable is known as solid waste management (Jerry 2020).

In many areas of Nepal, environmental deterioration, including contaminated water, declining groundwater levels, unhealthy soils, and dirty air, have been affected by waste materials. The resources required to lessen the negative effects of a damaged environmental situation are limited, but their destruction continues (Pathak 2016).

Different types of healthcare wastes, such as sharp, pathological, or other potentially infectious, pharmaceutical, biological, and hazardous wastes, need specific consideration and are typically referred to together as hazardous or special Health care waste (Johannessen et al. 2000). The Health Care Wastes (HCW) cover all wastes produced by medical institutions, research centers and labs (WHO 1999). According to (WHO 2004a), the waste from Health Care Facilities (HCF) falls into the following categories; non-risk and special care required wastes like infectious and high infectious waste and other hazardous and radioactive waste. Approximately 20% of HCF wastes are hazardous, and 80% are general. Managing healthcare waste (HCWM) was regarded as one of the key elements of effective infection prevention methods (WHO 1999).

According to one research, Nepal's healthcare waste equals 0.533 kg.bed^{-1}.day^{-1}. There was 0.256 kg.bed^{-1}.day^{-1} of general, hazardous, and non-biodegradable waste, 0.147 kg.bed^{-1}.day^{-1} of biodegradable waste, and 0.120 kg.bed^{-1}.day^{-1} of infectious waste, including sharps, and 0.009

kg.bed^{-1}.day^{-1} of hazardous chemical and pharmaceutical waste (UNEP 2012).

Numerous institutions discard or dump rubbish near ponds, open fields, ditches, rivers, and in the backyards of hospitals and other buildings. Utilizing a container for municipal waste is the third possibility. In various sections of the nation, large hospitals use municipal waste in around

60% of cases (Bhatta 2013).

Nepal's government prioritizes offering all citizens high-quality healthcare services as per the concept 'Health for all' of the World Health Assembly. Government and non-government groups are using various initiatives to address the many diseases and problems the nation is now experiencing. So, the appropriate management of HCW is
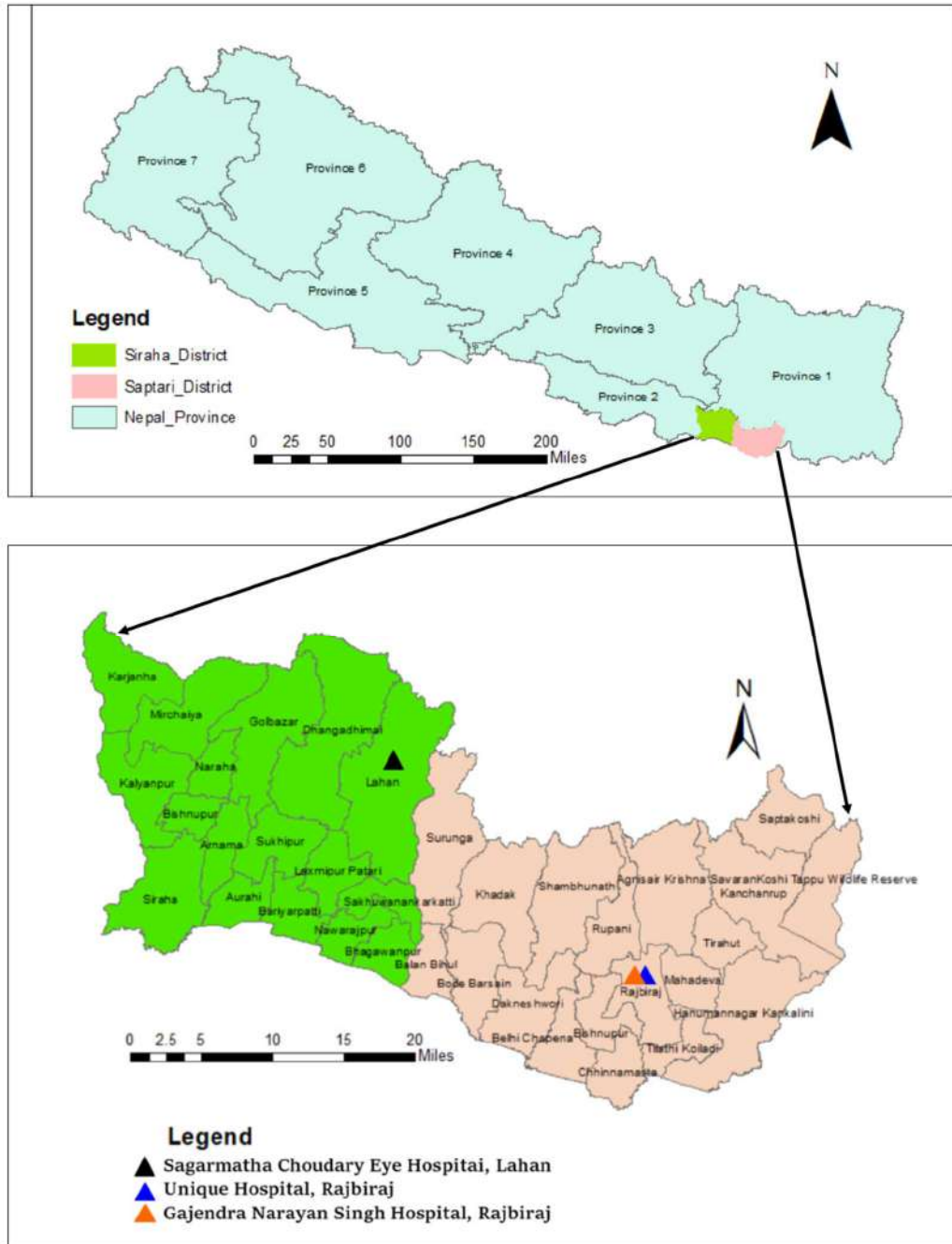
Fig. 1: Map of SCEH, Unique and GNS Hospital Rajbiraj.

one of the biggest issues the nation is now facing. The high risk of infection and the environmental population is caused by poor HCW management. Medical care waste affects the waste handlers, the general environment, and the waste creators. On the other hand, people have the right to survive in a neat and clean environment. Every person in Nepal has a right to a clean environment and basic medical treatment, according to the constitution of 2072.

Some surveys and works have been carried out in hospitals related to solid waste management in Nepal. But we did a different. We selected three big hospitals having over 100 beds in the Saptari and Sirha districts of Madhes province, Nepal. The complete work regarding sources, types, amounts, temperatures, pH, moisture content, and legal measures for healthcare waste has not been carried out in these hospitals. We aimed to analyze the types, parameters, and management practices of solid waste generated from Sagarmatha Choudhary Eye Hospital of Lahan, Unique Hospital, and Gajendra Narayan Singh Hospital of Rajbiraj municipality. We hope this study supports reducing hospital waste and properly managing it.

MATERIALS AND METHODS

Description of the Study Area

Sagarmatha Choudhary Eye Hospital Lahan: Sagarmatha Choudhary Eye Hospital (SCEH) Lahan is non- profitable eye hospital for residents of Eastern Nepal and neighboring districts of India. That was established in 1983 with more than 100 beds. The present services are general OPD, paying OPD, and fast-track OPD. The hospital can handle more than 250 patients in a day. The study   area (Lahan) lies in 26.4230 °N, 86.2930°E (Fig. 1).

Unique Hospital: Unique Medical College and Teaching Hospital Pvt. Ltd is a private hospital that was established in January 2001. It is situated in Rajbiraj municipality, with its wing at Raipur. It has more than 100 beds and can handle more than 300 patients. The study area lies in 26.599195°N and 86.722810°E (Fig. 1).

Gajendra Narayan Singh Hospital Rajbiraj: The Gajendra Narayan Singh (GNS)/ Sagarmatha Zonal Hospital in the Saptari district of southern Nepal was established in 1996. It has more than 100 beds and can handle more than

500 patients. The study area Rajbiraj lies in 26.5420°N, 86.7567°E (Fig. 1).

METHODS

Site selection: Three hospitals were selected, one from Sirha and two from Saptari district. The selected hospitals of sites are given in Table 1.

Sample collection: Three color-coded buckets were managed in each hospital ward. The blue bucket was for general waste, the red color bucket was for hazardous waste, and the green color bucket was for sharp waste. The collected waste was bought on-site and transported from the point of generation to assembly storage by wheeled trolleys, containers, or carts with the bits of help of hospital waste management staff from each ward of the hospitals in the evening, daily. In the morning, such collected samples were poured into plastic bags to take their exact weight. It was accordingly (WHO 2004b).

Types of wastes: According to (WHO 1999), the waste from hospitals was divided into three types which were general, hazardous, and sharp. A brief description of them is described below.

- *General waste:* Those disposed of at landfill sites are called general waste. Examples are paper, plastic, polythene, metal, carton, food, vegetable waste, dust matter, glass, cardboard, and others.

- *Hazardous wastes:* Those wastes with the potential to cause hazards to the health and life of humans are hazardous wastes. Examples of hazardous wastes are cotton, gloves, pus, blood container, gauze-soiled bandage, the cotton used for dressing, blood bags, etc.

- *Sharp wastes:* Those wastes used to puncture or lacerate the skin are known as sharp waste. Sharp wastes are infected needles, syringes, scalpels, blades, glass, infusion sets, saws, knives, broken glass, etc.

Total production of wastes: To calculate the weight of general, hazardous, and sharp wastes, the weight from each ward was taken individually. These products (general, hazardous, and sharp) from each ward were summed to find the total weight of sharp, hazardous, and general wastes. The average total waste production per day and every ten days of each month were estimated. Then the average percentage

Table 1: Sampling sites in hospitals.

S.N	Hospitals	Site A	Site B	Site C	Site D	Site E
1.	SCEH Lahan	Refraction ward	Vision ward	Minor OT	Cornea and glaucoma	Retina ward
2.	Unique Hospital	Gynae ward	Pediatric ward	General ward	Emergency ward	Surgery ward
3.	Gajendra N.S Hospital	Gynae ward	Pediatric Ward	General ward	Emergency ward	Surgery ward

of sharp waste was calculated. Finally, the weight from each ward is summed to find out the total weight. This way, the total solid waste produced per day and month was calculated.

Measurement of moisture content: A sample of 100 g was taken in a Petridis. The Petridis was placed into a hot air oven for 48 h at 105°C in the Department of Zoology, Degree Campus Biratnagar laboratory. The calculation was done based on the formula given by (Nancy Trautmann 1996), which was calculated below.

Percentage of moisture content = $(X_1-X_2) \times 100/X_1$

　　Where X_1 = wt. of the wet sample

　　X_2 = wt. of dry sample

Measurement of temperature: To measure the temperature of the solid waste, (Daniel 1987) was followed. According to this, the temperature of the collected sample from the selected sites was measured by dipping a thermometer into the sample up to 10-15 cm depth. At the same time, its average was also calculated.

Measurement of pH: The pH was tested by using an electric pH meter. It was also checked with pH paper at the site. One gram sample was mixed into 20 mL of waste in the grinder of the mixture, and it was ground well. The pH meter was washed with distilled water, and the pH was adjusted to 7 by dipping into a buffer solution, and the pH meter was dipped into the sample solution hence giving the pH value of the sample. The above calculation was done based on the formula by Pathak (2016).

$$pH = -\log[H+]$$

Statistical analysis: From the software Microsoft (MS) Excel 2007, The Pearson correlation of the number of patients and the amount of waste in SCEH, Unique Hospital, and GNS Hospital was calculated by the formula

$$r = \frac{n\sum x_i y_i - \sum x_i \times \sum y_i}{\sqrt{n\sum x_i^2 - \left(\sum x_i\right)^2}\sqrt{n\sum y_i^2 - \left(\sum y_i\right)^2}} \quad \ldots(1)$$

Chi-Square was calculated. It was calculated for Economic value versus waste production. The chi-square of three hospitals with three different types of waste was calculated. Similarly, the Chi-square of the education level of respondents and their response to waste management was also calculated by formula.

$$\chi^2 = \Sigma(O-E)^2/E \quad \ldots(2)$$

Where, χ^2 = Chi square, O = Observed value, E = Expected value. Analysis of Variance (ANOVA) was also calculated using Statistical Package for Social Science (SPSS).

Management practices: To study the management practice by direct observation, a questionnaire, focal group discussion, and interview methods were used.

RESULTS

Moisture Content

The moisture content of solid waste of Sagarmatha Choudhary Eye Hospital Lahan varied from 50% to 65.5% from month to month. The moisture content was highest in November. The average moisture content of Sagarmatha Choudhary Eye Hospital Lahan collection was 55.65% (mean value 58.27, standard deviation 4.72, and standard error 1.36)

The moisture content of hospital solid waste of Unique Hospital varied from 52% to 65.5%. The average moisture content of the Unique Hospital was recorded at 50.98%. The moisture content was highest in January (mean value 59.58, standard deviation 5.28, and standard error 1.52).

The moisture content of hospital solid waste of Gajendra Narayan Hospital varied from 50% to 73%. The moisture content was highest in June, and the average was 60.74% (mean value 62.42, standard deviation 5.53, and standard error 1.71). There was a high association between the moisture content of solid wastes in three different hospitals. Hence null hypothesis was accepted, stating there was no difference in the variance of the moisture content value of the wastes of the three hospitals. (F = 1.898 P-value = 0.165 F crit = 3.284917651)

Temperature

In Sagarmatha Choudhary Eye Hospital, the temperature of the waste varied from a minimum of 9.5°C to a maximum of 37.5°C from February to July (The mean value was 55.59, with a standard deviation of 8.85 and a standard error of 2.55). In Unique Hospital, the temperature of the waste varied from a minimum of 9.5°C to a maximum of 36.5^{0}c from January to August (The mean value was 30.08, the standard deviation was 6.99, and the standard error 3.02). In Gajendra Narayan Hospital, the temperature of the waste varied from a minimum of 9.5°C to 37°C in January and September, respectively. The mean value was 29.27, the standard deviation was 8.87, and the standard error was 2.27. The temperature of dumped wastes in all three hospitals was closely associated. Hence null hypothesis was accepted, stating there was no difference in the variance of the temperature of wastes of the three hospitals. (F = 0.998, P-value 0.379, Fcrit = 3.28). The average temperature of the waste was recorded as 23.23°C.

pH

It was found that the wastes from the Sagarmatha Chaoudhary

Table 2: Economic level versus waste production (weight in kg).

Annual income (NRS)	General waste	Hazardous waste	Sharp waste	Total Waste Production in Hospital
0-5 lakhs	5	3.0	1.5	9.5
5-10 lakhs	10	3.5	2.0	15.5
10-above	15	4.0	2.5	21.5
Total	30	10.5	6	46.5

Eye Hospital Lahan had the highest pH value, which was 6.9 in July, and the lowest was 3.7 in April. The mean value was 4.96, the Standard deviation was 1.29, and the standard error was 0.37.

On the wastes of the unique hospital, the pH value was 6.7, which was highest in July, and the lowest pH value is 3.6 in March. The mean value was 4.98, the Standard deviation was 1.22, and the standard error was 0.35.

The pH value of Gajendra Narayan Hospital was highest (pH 7) in August, whereas the lowest pH value was 3.6 in March. The mean value was 4.82, the Standard deviation was 1.10, and the standard error was 0.32.

The pH value of all three sites was strongly associated (F= 0.0668, P-value 0.935, Fcrit = 3.284). Hence null hypothesis was accepted, stating there was no difference in the variance of pH value of wastes of the three hospitals.

The average pH value of the three hospitals' entire sampling site was 4.44.

Economic Level and Waste Production

From Table 2, as a whole, we can say that as the economic level increases, the production of waste increases and vice versa. Hence there was no relation between income and types of waste production ($x^2 = 0.8$, df = 4 at a significance level of 0.05). But from Table 2, it can be stated that there is a high association between the level of income and the amount of waste production.

Hospitals and Amount of Waste

Hence it showed high association production of the waste from different hospitals ($x^2 = 77.09$, df = 4, Significance level = 0.05) (Table 3).

Number of Patients and Amount of Waste Production

In Sagarmatha Choudhary eye hospital Lahan, there was no significantly correlated between the number of patients and the amount of waste. The calculated correlation (at 0.05% significance level) was 0.187889.

In Unique Hospital Rajbiraj, it showed a correlation between the number of patients and the amount of waste— the calculated correlation (at 0.05% significance level), i.e., 0.118375.

In Gajendra Narayan Singh Hospital, there was a correlation between no. of patients and the amount of waste. The correlation (at 0.05% significance level) was calculated, i.e., 0.3453.

Public Response in Solid Waste Management

The Chi-square value was 1.463, at 6 degrees of freedom, a 5% level of significance which was less than the tabulated value (12.592) (Table 4). It can be described that there was no association between the qualification of respondents and their responsibilities regarding the services from hospitals.

Existing Management Practices

a. Collection of wastes: Three color-coded buckets were managed for different types of wastes.

Table 3: Hospitals and type and amount of waste production.

S.N	Hospitals	General waste	Hazardous waste	Sharp waste	Total waste
1.	SCEH Lahan	12.05	5.39	4.71	22.15
2.	Unique Hospital	16.59	6.28	7.05	29.92
3.	G.N.Singh Hospital	18.6	8.41	9.82	36.83
	Total	47.24	20.08	21.58	88.9

Table 4: Public Response to existing solid waste management.

Education	Good	Worse	Bad	Total
Under SLC	**7**	4	5	16
+2 Level	8	6	4	18
Bachelor	6	5	7	18
Above	7	6	5	18
Total	28	21	21	70

b. Segregation of waste: Collection and segregation of wastes were done, but we found the mixing of all wastes in most cases.

c. Proper sharps management system: Sagarmatha Choudhary Eye Hospital Lahan uses puncture-resistant and sharp leakproof containers, whereas the other two hospitals usually use a needle destroyer to collect sharp waste.

d. Transportation: Different methods transported waste to dumping sites from all hospitals.

e. Safety measures: Only the use of masks, gloves, and shoes for the workers were managed, but no other modern and guaranteed safety measures were applied.

f. Treatment and Disposal: Treatment and disposal of the collected wastes were seen to be defective in these hospitals. They do not have any on-site treatment facilities. Sagarmatha Choudhary Hospital Lahan has an incinerator, but it remains unused.

g. Education training: All three hospitals had a monitoring and evaluation of the waste management works and a reviewing process for the regulation. Unique and Sagarmatha Chaoudhary Eye Hospital Lahan had a sufficient budget allocated for waste management, but Gajendra Narayan Singh Hospital often faces a scarcity of budget.

h. Policy and planning practices: They organized frequent refresher training programs, usually once a year.

DISCUSSION

The problem of healthcare waste (HCW) management problem was growing rapidly with increasing urbanization, modernization, a revolution in medical science, and hospitalization. The waste greatly affects the environment as well as human health.

The quantities and waste generation amount per day/per week/per month vary widely. Health care wastes generated from different hospitals constitute a variety of wastes categorized mainly as general, hazardous, and sharp waste.

During the study period, the waste types were recorded as bottles, glass, metal, paper, plastic, carton, cotton gauze, gloves, bandages, broken glass needles, syringes, etc. They were produced from different sites such as the refraction ward, vision ward, minor OT, Retina ward, gynecology ward, pediatric ward, general ward, emergency ward, and surgery ward of hospitals.

UNCHS (1990) Studied wastes from hospitals and listed medical wastes, radioactive wastes, industries waste as hazardous wastes, organic wastes, and animal wastes as common sources of waste in the hospital.

The next study showed that medical centers and regional hospitals were major sources of healthcare waste. That study suggested that large hospitals were the major source of medical waste in Taiwan (Cheng et al. 2009).

Shrestha et al. (2014) studied wastes from the market and listed them as the major sources of solid waste production, with 66% of solid waste in Kathmandu. Starovoytova (2018) Studied wastes from industries, hospitals, institutes, municipalities, construction, residence, etc., and concluded that debris and agriculture were the main types of sources of waste.

Medical waste was a source of generation of hazardous biomedical waste. Medical centers, mainly hospitals, clinics, and diagnostic places, were the major places where large amounts of healthcare waste could be produced and might put people at risk of infectious diseases (Padmanabhan & Barik 2019).

This research collected data from different hospitals in Lahan and Rajbiraj over twelve months. The waste was categorized into general, sharp, and hazardous. It was found that out of the total waste generated, 52.21% of waste was general, 25.51% of waste was hazardous, and 22.27% of waste was sharp.

According to the Ministry of Health (MoH), 26% of the waste produced by HCF was hazardous, while 74% was general. According to (WHO 2004), of the entire quantity of HCW produced, 80% was general HCW, 15% was hazardous, 1% was chemical or pharmaceutical waste, and less than 1% was specific waste such as radioactive or cytotoxic waste.

The HCW$_s$ produced at several hospitals in Pokhara city demonstrate that ed, 22% of the HCWs were hazard out of the total trash produced, and the remaining 78% of the garbage was an un-harmful general waste (Enayetullah et al. 2011).

According to CSH 2011, only 25% of the garbage produced by the Civil service hospital in Minbhaban, Kathmandu, was hazardous, with the remaining 75% being general waste.

The above bove scenario showed that the hazardous waste produced from the different hospitals of Lahan and Rajbiraj was improper and non-scientific management of HCWs in the HCFs due to a lack of effective training courses about hospital waste management and their associated hazards then.

WHO (1999) reported that unsafe injection practices (reusing syringes and needles without sterilization) and HCW

transmission result in about 20 million cases of hepatitis B, C, and HIV yearly. These viruses are typically spread by wounds caused by syringes, needles, or other objects contaminated with human blood.

The moisture content was higher in November at 65.5%, whereas the lowest was in April in the Sagarmatha Choudhary Eye Hospital Lahan. Among the sampling, Unique Hospital showed that the highest moisture content was 66.6% in January, and the lowest was 52% in September. The moisture content of Gajendra Narayan Hospital Rajbiraj was higher by 73% in June, and the lower moisture content was 50% in September. The average moisture content was 55.65% in Sagarmatha Choudhary Eye Hospital Lahan, 50.98 in the Unique Hospital collection, and 60.74 in Gajendra Narayan Singh Hospital Rajbiraj.

The type and nature of waste determine the amount of moisture content Garbage comprising of meat, fruits, vegetable, etc., have a moisture content of about 70%. In contrast, the moisture content of rubbish (paper, wood, leather, metals, glass) is about 25% (Rajbhandari 1997). The higher the moisture, the greater the chances of microorganisms' growth. The average moisture content of the wastes of Biratnagar was found to be 64.47%.

Some researchers reported that the higher moisture content results in stronger leachate production. This would help particularly at the onset of the biodegradation process. Hence they boldly described the effects of moisture contents on the leachate treatment facilities (El-Fadel et al. 2002). Gawande et al. (2003) found that present moisture content measurement techniques suffer several drawbacks in Orlando. A moisture sensor recorded 72% of garbage materials. Adhikari (2005) suggested any waste containing greater than 80% moisture content will create problems unless the addition of a suitable absorbent takes special care. Nyoung & Vrisheid (2008) reviewed landfill solid waste's physiochemical and biological characteristics. He also described the moisture content of wastes in Japan and suggested higher moisture content higher will be the rate of decomposition. Some authors in Pakistan launched the next work relating to the moisture content with a special research design, and they found the moisture percentage decreased from 50% with the increase in an interval of time. Their results highlighted that the compost was mature in a good way to be used as organic manure or biofertilizer (Ameen et al. 2016).

Sagarmatha Choudhary Eye Hospital, the temperature of the waste varied from a minimum of 9.5°C to a maximum of 37.5°C from February to July. In Unique Hospital, the temperature of the waste varied from a minimum of 9.5°C to a maximum36.5°C from January to August. In Gajendra

Narayan Hospital, the temperature of the waste increased from a minimum of 9.5°C to 37°C in January and September. During January and February, the temperature of the solid waste was recorded as the minimum due to the low production, whose land coverage area at the landfill site was less, due to which the recorded temperature was less compared to July when the production of the waste was higher than the average resulting in the accumulation of the waste in the landfill site as bulky so temperature noted down was maximum.

The average denoted soil temperature of the waste was recorded as 23.23°C. Gawande et al. (2003) recorded the maximum average temperature of 28°C and the minimum average temperature of 10.5°C in Orlando. The temperature of waste varied from a minimum of 10.5°C to a maximum of 37°C. The average denoted temperature of the waste was recorded at 23.5°C. Yesiller & Hanson (2003) found the annual average high temperature was 15.1°C, and the annual average low temperature was 5.5°C in the USA. Since the beginning of the study, the warmest month on record, July, was 23.5°C. The coldest month on record was December or January, and the temperature was 3.3°C. Liu et al. (2016) found that the temperature of solid waste in China ranged from 22°C to 45°C. During the study, three kinds of controlled temperatures were performed: the variation of weight, leachate, and biogas production.

It was found that the wastes from Sagarmatha Choudhary Eye hospitals have the highest pH value, 7, and the lowest, 3.7, in August and April, respectively. Among the sampling sites, Unique hospitals showed the highest pH value of 6.9 in the month of 3.6 and the lowest value of August in March. The pH value of the wastes from Gajendra Narayan Hospital showed the highest pH value on July 7, whereas the lowest value was 3.6 in December. The average pH value of all of the sampling sites of the hospitals was recorded as 4.66.

Ying et al. (2002) found the pH from the trace metals and 4-8 from heavy metals in China. Some researchers reported that the pH affects the decaying rate of solid wastes. Acidity or alkalinity changes the basic environment of solid wastes accelerating and retarding microbial activity (El-Fadel et al. 2002). Ahmad & Hazi (2016) found alkaline nature (pH 7 -8) of municipal waste in Lahore, Pakistan. The alkalinity was due to the few short-chain organic acids, mainly lactic and acetic acids.

The output of Hospitals and the amount of waste (between the nature of the hospital and the types and amount of waste) were high association between hospitals and types and amount of waste because the calculated value was higher than the tabulated value. Hence it shows that there was high association production of the waste from different hospitals ($\chi^2 = 77.09$, df = 4 and significant level = 0.05).

The output of solid trash and people's income levels are closely related. According to the study, the amount of garbage produced by households was positively correlated with household size, monthly household income, and other factors. Alternatively, there is a negative link between home trash production and the household head's education level. Poor economic conditions may cause developing nations to create less solid trash, yet poorly managed garbage has been causing several environmental and health issues. Due to urbanization, economic activity, and quality of life, around 145 emerging nations experience comparable issues with solid waste. Issues have worsened as garbage production and population increase have increased (Kumar et al. 2019).

In the next regard, the author reviewed the literature and found that waste production varies according to income level. It was recorded from 0.25 kg to 1.38 kg per capita per day in developing countries. In South South America, it was reported that 1.07 kg per capita per day, and in Asian countries, 0.4 to 1.62 kg per capita per day. And in the African region, it was estimated as 0.49 kg per capita per day of waste production. It was concluded the amount of waste production is directly proportional to the amount of income (Adhikari 2022).

The correlation between the number of patients and the amount of waste produced in Sagarmatha Choudhary Eye Hospital Lahan is no connection between income and the many forms of waste output. (x^2 = -0.8, df = 4, 0.05 level of significance). In particular hospitals, it was discovered that families with higher income levels produced significantly more solid waste than those with lower income levels. Unique Hospital Rajbiraj demonstrates a strong correlation between waste generation from various situations (df = 4, significance level = 0.05, x^2 = 179.98. However, there was a link between the quantity of trash produced and the number of patients at Unique Hospital (correlation = - 0.118375). Similarly, from the Gajendra Narayan Singh Hospital (correlation = 0.34). It could be described that there was no association between the qualification of respondents and their responsibilities regarding the services from hospitals (x^2 = 1.463, df = 6, at significant level = 00.05).

A non-significant negative association was found between polyethylene waste and total monthly income (r = -0.064, p> 0.05). It implies that the production of polyethylene trash declines as household wealth rises (Duminda & Prasansa 2005). The recycling of polyethylene waste was the major cause of the negative connection. In the research region, about 40% of residents recycle polyethylene waste. By doing this, they produce less polyethylene waste at home. The creation of metal was shown to have a significant positive connection (r = 0.308, p 0.05), increased wealth results

in more consumption of commodities, which may have contributed to an increase in the production of metal waste.

Present research work clearly showed that in the hospitals of Lahan and Rajbiraj, there were no waste minimization policies to reduce the waste. Only some materials, including glass, plastic, aluminum cans, paper, cardboard, and iron, are recycled without sterilization. But plastic, syringe, and waste are contaminated with radioactive substances and not recycled or reused.

The HCW_s are segregated at the site of generation into color-coded containers, but information for proper handling is not displayed properly. The wastes are collected by trolley and wheel card to store at the storage area before being transported to the off-site treatment facility. The collected wastes are stored for 24 hours. This area is not marked with warning signs but is located away from patient rooms, laboratories hospital functions. The municipal vehicles collected HCW and disposed at the landfill site without pre-treatment.

All individuals who create, collect, receive, store, transport, treat, dispose of, or otherwise handle bio-medical waste in any way should be subjected to the bio-medical waste (management and handling) laws of 1998. Additionally, it provides rules for different bio-medical waste types, color-coding of containers, transportation, and processing using autoclaves, microwaves, and incinerators.

Segregation, mutilation, disinfection, storage, transportation, and final disposal are essential to safely and effectively manage bio-medical waste at any facility (Acharya & Singh 2000).

According to research (CEPHED 2012), just 6.45% of hospitals have any source separation procedures, and 90.32% do not use any environmentally sound waste treatment system. The criteria for establishing the supplied facts are not entirely clear. Still, among them, 67.42% of hospitals have extremely inadequate transportation, and 80.65% do not implement suitable and separate garbage collection.

According to the MoHP research (MoHP 2012), supported by WHO and done at hospitals throughout Nepal, the waste management system was subpar, and only 38.7% of institutions have implemented proper HCW segregation. The rubbish, including medical waste, was by municipal vehicles in Kathmandu and dumped in the Okharpauwa dumping site without pre-treatment. In and near hospitals and disposal sites, most rag pickers may frequently be observed gathering plastic bags, plastic bottles, syringes, needles, and iron materials. These widespread practices increase the danger of illness and harm to rag pickers and the local people.

Research done in western Nepal (DoHS 2013) found that 63% of non-clinical employees and 70% of clinical staff reported a needle stick injury (NSI) or other sharp injuries at some time.

A study by (Bhatt 2013) revealed that almost all of the studies that covered HCF$_s$ focused only on solid waste management, mostly by incineration. 70% of the incinerators were not working as planned due to the lack of skilled manpower, spare parts, high fuel consumption, cultural and public objection, and lack of management commitment. Many institutions dumped or throw waste in the back yard, ditches, rivers, open fields, corners of the hospital building, nearby ponds, or anywhere around the premises. About 60% of the big hospitals in different parts of the country followed municipal waste disposal systems for the final disposal of the HCW.

A cross-sectional study conducted at the Gandaki Medical College Teaching Hospital revealed that 70.79% of healthcare professionals had experienced Needle Stick Injuries (NSI); of these, 52.5% had occurred while using unused needles, and 47.5% had used needles. Of those who had experienced NSI from used needles, 68.42%had reported the incident (Gurung et al. 2010).

In the context of Nepal, it can be actively encouraged for the commercial sector, CBO$_s$, and NGO$_s$ to get involved in collection and transport. Many hospitals in Nepal were found to be in accordance with the Local Self Governance Act -1999. Lahan and Rajbiraj Municipality were deemed to be adhering to the Solid Waste Management Acts to handle solid waste- 2011. Nepal government has formulated dozens of acts, rules, and regulations for the protection of the environment and biodiversity, including waste management acts (Adhikari 2020, 2022).

One research showed that the hospital in Nepal had no healthcare waste management committee. They did not formulate a policy or standard operating procedure for the waste. Especially in the medical waste management system, there was no color coding system for waste segregation and collection of wastes. That investigation also did not find an implementation of particular acts and rules for transportation and storage. No specific well-trained waste handlers were working in the field (Sapkota et al. 2014).

CONCLUSION

This study analyzed the waste physically and categorized wastes into general waste, Hazardous waste, and sharp waste. The research showed that the general waste was higher than the sharp and hazardous waste. Maximum general waste occupied 52.21%, minimum sharp waste occupied 22.7%,

whereas the hazardous waste was occupied between the two, i.e., 25.5%.

The moisture content of the solid waste of Gajendra Narayan ranged from 50.08% to 73.0% from month to month. The moisture content was highest in June. Unique Hospital's solid waste's moisture content ranges from 50.98% to 70.0%. Similarly, the Gajendra Narayan Hospital's moisture content of Solid waste ranged from 50.65% to 65.5%. The average moisture of the collection was 50.98% and 55.65%, and the average moisture content was 60.74%. It could be concluded that since the waste had higher moisture content, it could be easily disposable. There was a high association between the moisture content of solid wastes in three different hospitals; hence null hypothesis was accepted, stating there was no difference in the variance of moisture content value of wastes of the three hospitals.

The temperature of the waste varied from a minimum of 10.5°C to a maximum of 37°C. During January, the temperature of solid waste was recorded as minimum due to low production of solid waste whose land coverage area at the landfill site was less due to which the recorded temperature was less as compared to June when the production of the waste was higher than the average resulting in the accumulation of the waste in landfill site as bulky. Hence, the temperature noted down was maximum. The temperature record showed the decaying rate might be slow. The temperature of dumped wastes in all three hospitals was closely associated. Hence null hypothesis was accepted, stating there was no difference in the variance of the temperature of wastes of the three hospitals.

It was found that the wastes from the eye hospital of Lahan had the highest pH value of 7 and the lowest of 3.7 in August and April, respectively. Among the sampling sites considered, the unique hospital showed the highest pH value of 6.6% in August and the lowest value of 3.6 in March. The pH value of the wastes from Gajendra Narayan Hospital was 7 highest pH value in July, whereas the lowest value of 3.6 in March. It could be concluded that the waste was more acidic and harmful to the environment. The pH value of all three sites was strongly associated; hence null hypothesis was accepted, stating there was no difference in the variance of pH value of wastes of the three hospitals.

There was no relation between income and types of waste production. ($\chi^2 = 0.8$, df = 4 at the significance level of 0.05). It was found that families with higher economic levels comparatively produced higher amounts of solid waste in unique hospitals than that in lower ones. Hence it shows that there is high association production of the waste from different hospitals $\chi^2= 179.98$. df = 4, Significance level= 0.05). The finding showed no positive relationship

between the number of patients and the amount of waste production (correlation = - 0.1878) in SCEH. But there was a positive relation (correlation = 0.118375) between the number of patients and the amount of waste produced in Unique Hospital; the same finding was in Gajendra Narayan Hospital (correlation = 0.34). It could be described that there was no association between the qualification of respondents and their responses regarding the services from hospitals ($\chi2 = 1.463$, df = 6 at significance level= 0.05).

Partly the legal measure was implemented, but it could strongly recommend formulating and implementing more legal provisions. Since wastes contain a high quantity of hazardous (infectious) waste, it is recommended that at hospitals of Lahan and Rajbiraj, judicious reduction, segregation, storage, processing, and disposal of HCWs is essential to reduce the risk to public health. And it is also recommended to install advanced technology for hospital waste management.

ACKNOWLEDGMENT

REFERENCES

Acharya, D.B. and Ineeta, S. 2000. Hospital Waste Management. Minerva Press, New Delhi. pp.15- 47.

Adhikari, R.C. 2005. Study of Solid Waste and Its Management in Biratnagar Sub-Metropolitan City. M.Sc Thesis. Department of Zoology, Post Graduate Campus, T.U. Biratnagar, Nepal.

Adhikari, R.C. 2020. Legal Protection of Biodiversity in Nepal. Nepal Biological Society, Biratnagar, Nepal.

Adhikari, R.C. 2022. Investigation on solid waste management in developing countries. J. Res. Dev., 5(1): 42-52. https://doi.org/10.3126/jrdn.v5i1.50095

Ahmad, J. and Hazi, H. 2016. Factors influencing solid waste. Int. J. Sci. Res. Publ., 6: 2250- 2553.

Ameen, A., Ahmad, J. and Raza, S. 2016. Effect of pH and moisture content on composting of municipal solid waste. Int. J. Sci. Res. Publ., 6(5): 35-37.

Bhatta, J. 2013. Situation of Healthcare Waste Management and an Effort for Improvement at Resource-Poor Setting. Retrieved from www.hjulmandweb.dk\HCRW-CD (accessed on 20th December 2022).

CEPHED. 2012. Environment Health Condition of Hospitals in Nepal. Retrieved from https:\\www.Scribed.com>CE (accessed on 20th December 2022).

Cheng, Y.W., Sung, F.C. Yang, Y. Lo, Y.H. Chung, Y.T. and Li, K.C. 2009. Medical waste production at hospitals and associated factors. Waste Manag., 29(1): 440-444.

Civil Service Hospital (CSH) 2011. Health Care Waste Management Policy at Civil Service Hospital. Report. Minbhawan, Kathmandu.

Daniel, D.E. 1987. Earthern liners for land disposal facilities. Geotech. Facil. Waste Disp., 87: 24-39.

DoHS 2013. Presentation During the Health professional training on Health Care Waste Management at Manang, Hotel Kathmandu, 2-4 June 2013. Report. Ministry of Health of Population, Nepal.

Duminda, K. and Prasansa, K. 2005. The problem of solid waste: A case study of the Maharagama local authority. J. Nat. Sci. Found., 33(1): 51-53.

El-Fadel, M., Bou-Zeid, E. Chahine, W. and Alayli, B.J.W.M. 2002. Temporal variation of leachate quality from pre-sorted and baled municipal solid waste with high organic and moisture content. Waste Manag., 22(3): 269-282.

Enayetullah, I., Sinha, A.H. Kabir, A.M. Rahman, S.M. and Yesmin, M.M. 2011. Feasibility Study for the Establishment and Operation of a Common/central Treatment Facility (CTF) for a Hospital in Pokhara City under PPP Arrangement. Waste Concern Consultants, Dhaka, Bangladesh.

Gawande, A., Debra, R., Philip, A. and Thomas, T. 2003. Municipal solid waste in in-situ moisture content measurement using an electrical resistance sensor. J. Energy Conserv., 23(7): 667-74.

Gurung, N.S., Paudel, K. and Pun, C.B. 2010. Needle Stick Injuries among health care workers in a tertiary care teaching hospital, Pokhara. J. Gandaki Med. College, 3: 47 -50.

Jerry, A. 2020. Solid Waste Management. Encyclopedia Britannica, p.10.

Johannessen, L.M., Dijkman, K., Bartone, C., Hanrahan, D. and Boyer, M.G. 2000. Note on waste management in the healthcare industry. Discussion Paper on Health, Nutrition, and Population (HNP). Bank for International Settlements, The World Bank's Reconstruction and Development Program, Geneva.

Kumar, R., Bhattarai, D. and Neupane, S. 2019. Designing solid waste collection strategy in small municipalities of developing countries using choice experiments. J. Urb. Manag., 8: 386-395.

Liu, R., Zhao, X. and Chen, L. 2016. The effect of temperature on the biodegradation properties of municipal solid wastes in China. J. Sustain. Circ. Econo. Waste Manag., Res., 34(3): 265- 74.

Ministry of Health and Population (MoHP) 2012. Study overview and baseline injection safety assessment in Nepal preliminary main finding and Recommendations. Report. Ministry of Health and Population, Nepal.

Nyoung, M. and Vrisheid, M. 2008. Health effect of residence near hazardous waste landfill sites. Rev. Epidemiol. Lit. Health Persp., 108(1): 1:101-12.

Padmanabhan, K.K. and Barik, D. 2019. Health hazards of medical waste and its disposal. Woodhead Publishing, London.

Pathak, D.R. 2016. Study on the municipal waste of 60 new municipalities of Nepal. Pulchowk, Lalitpur, Nepal.

Rajbhandari, B. 1997. Study on solid waste management of Lalitpur Municipality. Master Thesis. Central Department of Zoology, T.U. Kirtipur, Kathmandu.

Sapkota, B., Gupta, G. K. and Mainali, D. 2014. Impact of intervention on healthcare waste management practices in a tertiary care governmental hospital of Nepal. BMC Pub. Health, 14(1): 1-8.

Sharma, P., Dhanwantri, K. and Mehta, S. 2014. Municipal Solid Waste Generation, Composition And Management in India. Amity School of Architecture and Planning, Hariyana Gurgaon India.

Shrestha, R.S. 2014. Solid waste management in Kathmandu city, Nepal. Solid Waste Manag. Res., 49(2): 55-69.

Starovoytova, D. 2018. Prospective of roof rain water harvesting (RRWH) in Kesses constituency, Uasin Gishu County, Kenya. J. Environ. Earth Sci., e(7): 111-129.

Trautmann, N. 1996. Waste processing System. Waste Management Institute Cornell University, Ithaca, New York.

United Nations Center for Human Settlement (UNCHS). 1990. Community Participation- Solid Waste Management in Low-Income Housing Project: The Scope for Community Participation. United Nations Center for Human Settlement (Habitat), Nairobi, p54.

United Nations Environment Programme (UNEP). 2012. Compendium of Technologies for Treatment and Destruction of Health Care Wastes. Retrieved from http://www.unep.org\ietc\portal \136\publicatens\wastes%20 (asccessed 19th November 2021).

World Health Organization (WHO) 1999. Safe management of wastes from health care activities. World Health Organization, Geneva.

World Health Organization (WHO) 2004a. Preparation of National Health Care Waste Management Plans in Sub – Saharan Countries: Guidance Manual Secretariat of the Basel Convention. World Health Organization, Geneva.

World Health Organization (WHO). 2004b. Management of Solid Health Care Waste at Primary Health Care Centers: A Decision-Making Guide. World Health Organization, Geneva.

Yesiller, N. and Hanson, J.L. 2003. Analysis of Temperature At A Municipal Solid Waste Landfill, Sardinia 2003. 9th International Waste Management and Landfill Symposium. CISA, Italy, pp. 1- 10.

Ying, L., Guang, P., Xue, Y. and Fen, X. 2002. National Bureau of Standards. Standard Reference Material Catalog, 1986-87, p. 260.

Land Use Land Cover (LULC) Dynamics by CA-ANN and CA-Markov Model Approaches: A Case Study of Ranipet Town, India

Malathy Jayabaskaran and Bhaskar Das†

School of Civil Engineering (SCE), VIT, Vellore, Tamil Nadu, India

†Corresponding author: Bhaskar Das; bhaskar.ju@gmail.com

ABSTRACT

The present study analyzed the spatio-temporal variations in the Land Use Land Cover types within Ranipet Municipal town in Ranipet District, Tamil Nadu State, India, using two different platforms (QGIS and IDRISI Selva v.17.0). The possible parameters driven the net changes in the Land Use Land Cover (LULC) types were also incorporated for the analysis. Results revealed the positive net changes in the built-up area are about 26.8%, and combined other classes like vegetation, barren land, and water bodies have net negative changes during 1997-2019. Particularly barren land was found to have a reduction of 17.4% due to the massive industrialization in the study area. Further, the LULC maps were used for future prediction (2029) using the dynamic models of CA-ANN (Cellular Automata and Artificial Neural Network) and CA-Markov. Predicted maps yielded a kappa index of 81.6% and 82.6% for CA-ANN and CA-Markov, representing their respective accuracy levels. The CA-Markov model is extended for determining the probable long-term changes for 2080 in LULC with a kappa index of 76.2%. Compared to the CA-ANN model using the QGIS platform, CA-Markov provided better analysis, particularly from one cell to the other. According to the survey and the ground truth in the locality, industrialization and occupational shift were the most influential drivers of LULC dynamics. Moreover, the results of this study assist the stakeholders in the decision-making process for future sustainable land use management.

INTRODUCTION

Land Use Land Cover (LULC) provides substantial ecosystem services and greatly impacts landscape patterns and long-term ecological sustainability (Muyibul et al. 2018). The LULC dynamics delineates the transformations from one land use class to another for two different periods due to the human activities on the earth's surface (Lambin et al. 2001). Alteration of LULC results in landscape homogenization and fragmentation of natural habitats (Muyibul et al. 2018) and destabilize the pattern of ecosystem services (Sutton et al. 2016). Encroachment on natural habits is a very common issue in rapid urbanization due to industrialization or other developmental motives, which leads to land degradation through deforestation, soil compaction, water and soil salinity, disposal of untreated waste on land, etc., on the local and global scale (Geist & Lambin et al. 2004, Reynolds & Smith 2002, Romm 2011, Bucx et al. 2010). Hence LULC dynamics become an essential component of monitoring and quantifying climate change, biodiversity, hydrology, and air pollution (Sellers et al. 1995, Bonan 2008, Butchart et al. 2010, Schröter et al. 2010) to minimize the effects of human activities on the environment (Tripathy & Kumar 2019, Norman et al. 2009).

Recent advancements in remote sensing (RS) and Geographical Information Systems (GIS) have proven to be effective tools for studying LULC dynamics by acquiring, analyzing, and quantifying data rapidly and regularly at lower cost and time than traditional ground survey methods (Mishra & Rai 2016). The suitability of RS and GIS in LULC dynamics has led to the evolution of several geospatial models to simulate and predict future spatial-temporal patterns and act as decision-support tools (Wang & Maduako 2018). Most of these models work based on a probability approach simulating and predicting the land use changes for any location (Verburg et al. 2004), and their outcomes have been proven to be effective tools for future planning and land use management and also in evaluating the land use policies (Turner et al. 2007). Based on the recent literature, some of the most popular models are CA (Berberoğlu et al. 2016, Jat et al. 2017, Mustafa et al. 2017), ANN model (Mozumder & Tripathi 2014, Maithani 2015), regression models (Nong & Du 2011), Markov chain (Arsanjani et al. 2011, Al-Sharif & Pradhan 2014), CA-logistic regression models (Arsanjani 2012, Mustafa et al. 2018), CA-Markov models (Arsanjani et al. 2013, Mondal et al. 2016) and CA-ANN Model (Rahman et al. 2017, Gantumur et al. 2020), etc. Many kinds of literature

have also discussed individual models' limitations (Araya & Cabral 2010, Balzter 2000, Triantakonstantis & Mountrakis 2012). Among the existing models, CA is the simplest and most popular open structure model capable of intercepting the spatio-temporal dynamics of LULC. This model is flexible, can be integrated with multiple techniques, and is best suited at the micro level (Aburas et al. 2017, Tripathy & Kumar 2019)). Markov Chain is a stochastic modeling approach that also can be used conveniently to study and simulate LULC trends in short-term projections. One limitation of this model is that it does not intercept and simulate spatial trends in LULC (Rahman et al. 2017, Mishra & Rai 2016). Combining CA with Markov techniques can efficiently be applied for a large area with spatial-temporal interpretation, thus overcoming their limitations (Gantumur et al. 2020, Keshtkar et al. 2015, Rimal et al. 2017). The artificial neural networks (ANN) system model is vaguely inspired by biological neural networks, which effectively simulate multiple land-used changes in complex non-linear environments (Saputra & Lee 2019, Mishra & Rai 2016, Pijanowski et al. 2002). The details of methodologies adopted in these models are mentioned in the Material and Methods section.

The present study aims to understand and simulate the changes in LULC of a Ranipet Municipal town in the Raipet district of Tamil Nadu state. The municipality includes the Ranipet industrial area, one of India's biggest exporting centers of tanned leather. The total number of tannery industrial units in and around this town is 240, besides industrial hubs like Bharat Heavy Electrical Limited (BHEL) and State Industries Promotion Corporation of Tamil Nadu Limited (SIPCOT) of other industries like ceramic, refractory, boiler auxiliary plant, and chromium chemicals. This is also the place of TCCL (Tamil Nadu Chromate and Chemicals Limited), which operated from 1975 to 1995, mainly producing chromium bichromate, and basic chromium sulfate, reagents required for the chemical processing of leather. After its closure in 1995, it was reported to have 2.27 Lakh tons of chromium-bearing solid waste got accumulated and dumped at the premise (TNPCB 2010). Ranipet industrial town was considered one of the world's worst polluted places by the New York-based Blacksmith Institute (BI) in 2007 (http://www.blacksmithinstitute.org/). The history of pollution in Ranipet is more than two decades older, raising Public Interest Litigation (PIL) by Vellore Citizens' Welfare Forum vs. Union of India (1996). The petition was filed against the discharge of untreated effluent sewages, which consist of 170 types of chemicals, by more than 900 tanneries in Vellore. The large-scale land and water degradation had been reported to have affected 35,000 hectares of land (Vellore Citizens' Welfare Forum 1996). There is a limited number of reports

concerned about the extreme heavy metal like Cr, Pb, Ni, Zn, and Cd contamination in groundwater and lake water (Srinivasa Gowd & Govil 2008, Rao et al. 2013), problems associated with the partially treated solid and liquid waste (Rao et al. 2011, Mandal et al. 2011) and bioaccumulation of heavy metals in indigenous plant species (Vidya et al. 2010) from the study area. But there is no available study on the spatio-temporal dynamics of LULC due to unplanned human interventions in this vulnerable town. Rapid industrialization has triggered the change in LULC, eventually leading to land and water degradation in the study area. Hence, the study of LULC dynamics will bridge the gap of available scientific data required to accurately assess the pollution trend and plan for a holistic mitigation approach. Based on the above discussion, the present study's scope is (i) to analyze the spatial-temporal variations in the Land Use Land Cover of Ranipet Municipality, Ranipet district, Tamil Nadu state for two decades. (ii) to simulate and predict the future changes in LULC for the year 2029 using the CA-ANN model (iii) to predict the LULC changes for 2029 & 2080 using IDRISI Selva v.17.0 and comparing the results with the CA-ANN model (iii) to explain the impacts of LULC in Ranipet and the drivers influenced for the change with due consideration to socio-economic factors.

MATERIALS AND METHODS

Study Area

Ranipet is a Municipality in Ranipet district (formed by trifurcating erstwhile Vellore district in 2019) which lies in the North Latitude of 12°55'0" to 12°58'0" and East Longitude of 79°17'30" to 79°17'30" and falls in the survey of India Toposheet No. 57-P/5 (Fig. 1). This bustling industrial hub is situated 116 km from Chennai, the capital city of Tamil Nadu state, and 43 km before the Chittor district of Andhra Pradesh. It is sited in Plot 25 of SIPCOT Industrial Estate along the NH- 4 Ranipet, TN. The study area is surrounded by hillocks on the northern and western sides. The southern side of the location is a Pedi plain. The major source of drinking water is the Palar River, which runs from west to east and is located 4.5 km downstream of the side. The area falls under the moderate to high rainfall zone, receiving 1000mm rainfall annually from South-West and North-East monsoons. The rapidly growing large and small-scale industries like leather and leather-based industries, pharmaceuticals, and other chemical factories and their pollution levels, groundwater, and soil contamination are the primary reasons for choosing Ranipet as the study area.

Data and Pre-Processing

The required images for the study of land use land cover
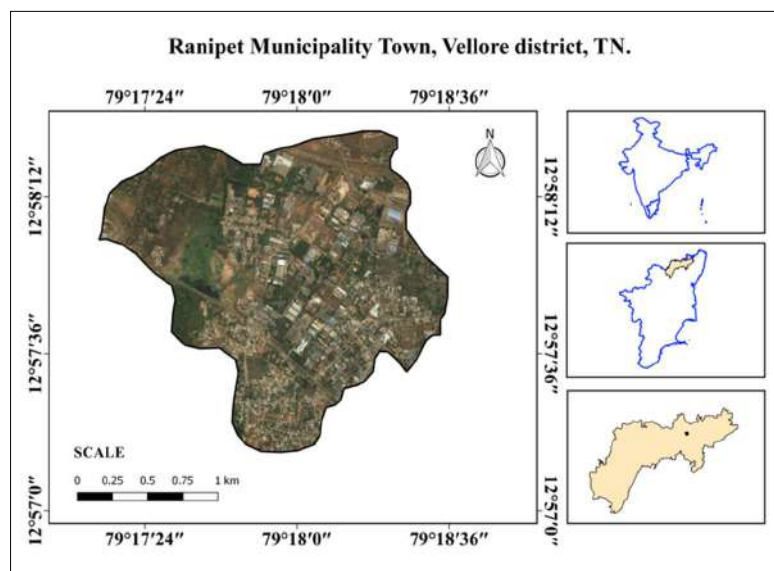
Fig. 1: Ranipet – Study area of the given study.

changes of the location were obtained and downloaded from the official USGS website (https://earthexplorer.usgs.gov/). Landsat Thematic Mapper (TM) remote sensing images were used as the basic data, and relatively the images are free from the cloud cover (Vasconcelos et al. 2015). The satellite image details used in the study are shown in Table 1. The Landsat images were geometrically corrected to UTM (Universal Transverse Mercator), Zone 44 North, and WGS 84 (World Geodetic system 84) datum, with a spatial resolution of 30m. Images were classified by visual interpretation.

The initial land use land cover (LULC) types were classified into four basic and primary types: settlements, vegetation, barren land, and water bodies. The details are shown in Table 2. Data regarding the population and GDP

were taken from the census 2001-2011 handbooks. These parameters were used to determine the driving forces of the land use land cover in the study area (Pan et al. 2012). Fig. 2 shows the methodology adopted for carrying out the entire study. It clearly explains the two methods, CA-ANN and CA-Markov are the models used to predict the LULC for 2029 and 2080. QGIS open source Platform is used to study the land use and land cover of the study area since it has less processing time and better rendering capabilities. Here in the current study, the QGIS platform has been used to follow the CA-ANN model. To adopt CA-Markov for future prediction, IDRISI Selva v.17.0 interface has been effectively utilized for ease. The Land Change Modeller (LCM) in the IDRISI interface uses machine learning procedures to analyze historical land cover data to model the future. LCM uses Markov Chain analysis to project the expected quantity of

Table 1: Satellite data specifications.

Sensor	Path	Row	Spatial resolution (m)	Acquisition Year
Landsat 4/5 Thematic Mapper (TM)	143	51	30	1997
Landsat 4/5 Thematic Mapper (TM)	143	51	30	2009
Sentinel 2	-	-		2019

Table 2: Classification of Land Use Land cover.

LULC class	Description
Settlements/Built up area	Residential, commercial, and industrial services, transportation networks, socio-economic infrastructure, and urban and rural settlements.
Vegetation/Cultivated land	Agricultural area, crop fields, cultivated area, and vegetable lands.
Barren land/Uncultivated land	Exposed soils, open fields, landfills, and sand fill areas.
Water-bodies	Rivers, lakes, ponds, perennial water bodies, and reservoirs

change and a competitive land allocation model to determine scenarios for a specified future date.

Cellular Automata – Artificial Neural Network (CA-ANN) Model

Some of the earliest approaches of CA models to simulate and predict LULC dynamics are developed by Couclelis (1985), Batty & Xie (1994) and White & Engelen (1994). Later, many utilized it for modeling and predicting present and future spatial and geographical changes (Mishra & Rai 2016, Halmy et al. 2015, Arsanjani et al. 2013).

The principle behind the model is that the change in the land use of any cell could be defined by the present state and the changes in the adjacent neighboring cells (Koomen & Borsboom-van Beurden 2011). With this cellular Automata (CA) model, when ANN was integrated, there would be sound improvement in the simulation and future predictions (Li et al. 2001, Pijanowski et al. 2002). In this work, the extensively used CA-ANN model is used to predict the future (2029) land use land cover changes using multiple satellite images of 1997, 2009, and 2019 as input parameters.
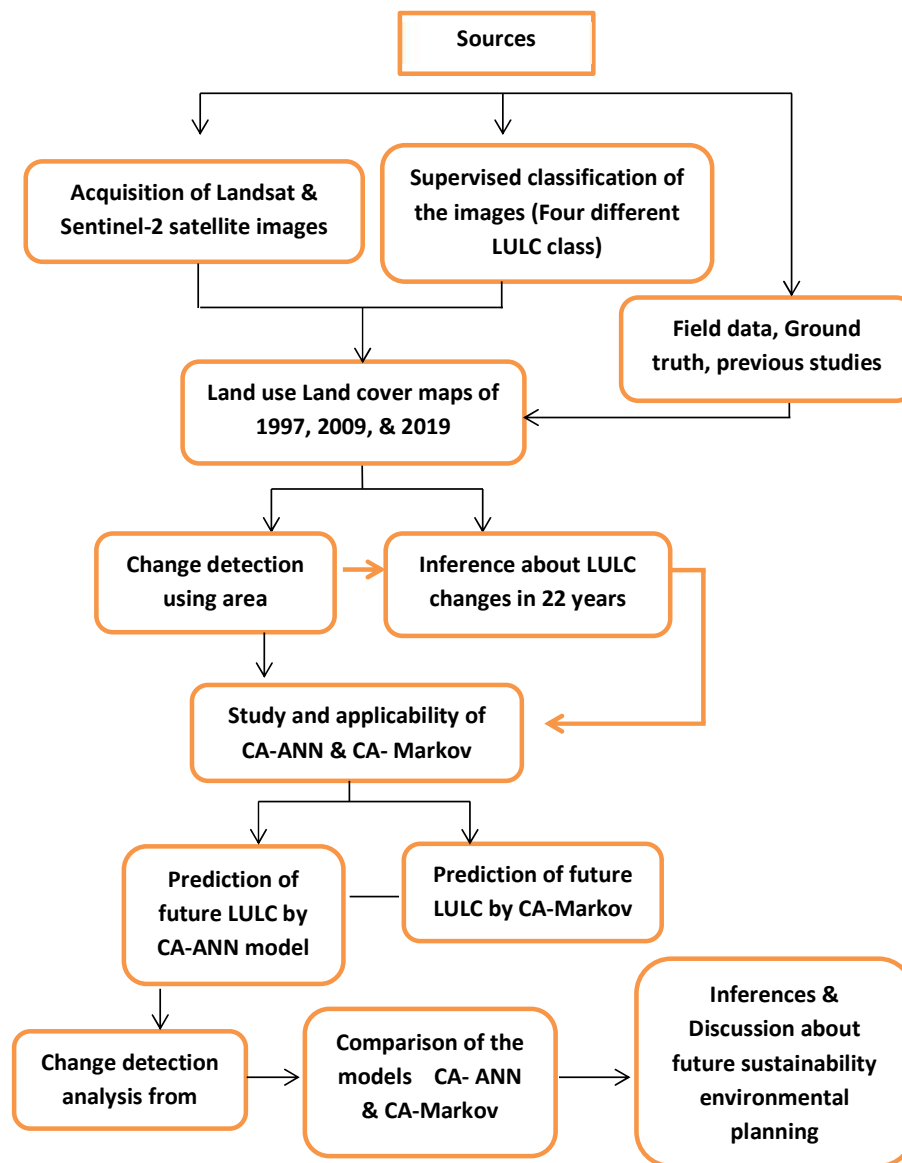
Fig. 2: Flow chart for the current study.

The Markov Model

To model and predict the changes in land use and to understand the future land development in any area, Markov models are widely used (Parsa et al. 2016, Subedi et al. 2013). Also, it is used in ecological modeling and other land-based simulations. The mathematical equation (eq. 1) helps calculate the required future land use changes.

$$L(t, t+1) = P_{ij} * L(t) \qquad ...(1)$$

Where L(t) and L(t+1) represents the corresponding land use status at time t and t+1 respectively, P_{ij} represents the transition probability matrix in a given state.

$$P_{ij} = \begin{bmatrix} P_{11} & P_{12} & ... & P_{1n} \\ P_{21} & P_{22} & ... & P_{2n} \\ ... & ... & ... & ... \\ P_{m1} & P_{m2} & ... & P_{mn} \end{bmatrix} \qquad ...(2)$$

$$(0 \le P_{ij} \le 1)$$

Where 'i' is the current state and 'j' represents the next state (one period to the other). The cells in the transition matrix range from zero to one. A higher value close to one indicates a high transition probability, and a lower value close to zero predicts a lower transition probability. Two LULC images are processed to determine transition probability and area matrices through the Markovian chain (Mishra & Rai 2016). These models are effectively used when the socioeconomic factors influencing the change are difficult to represent (Turner et al. 1989).

Cellular Automata – Markov Chain model

To simulate and predict the changes in the LULC, the CA-Markov model was more advantageous since it integrated both the cellular automata and Markov chain (Singh et al. 2015, Parsa et al. 2016). The transition probability matrix can be found by cross-tabulating two satellite images for two periods (Singh et al. 2015). CA-Markov model is a strong and powerful method in LULC dynamic modeling where any spatial characters also could be incorporated into the model (Singh et al. 2011, Wang & Maduako 2001). This model helps simulate the two-way transitions between classes for several periods (Poutius et al. 2005, Ye et al. 2008). Remember, Cellular Automata (CA) is a common dynamic model which is been used for several years to determine the spatio-temporal changes for any location. Every cell value in the matrix will represent the land area and its growth actions since they are dynamic (Brown et al. 2004). The prime advantage of the model (CA) is that it clearly explains the dynamics of the classes despite the dependency on the

neighboring cell values. The expression of the CA model is as follows (Subedi et al. 2013, Sang et al. 2011).

$$L(t, t+1) = f(L(t), P) \qquad ...(3)$$

Here L(t, t+1) represents the class status at time (t, t+1),

$$Contiguity\ filter\ 5x5 = \begin{bmatrix} 0 & 0 & 1 & 0 & 0 \\ 0 & 1 & 1 & 1 & 0 \\ 1 & 1 & 1 & 1 & 1 \\ 0 & 1 & 1 & 1 & 0 \\ 0 & 0 & 1 & 0 & 0 \end{bmatrix} \qquad ...(4)$$

To state the neighborhood of each cell on a suitability image, a contiguity filter of size 5 × 5 pixels is used. This standard filter has a cellular space which helps gain a class to occur near where the class already existed. Furthermore, it helps to eliminate the unknown changes that might occur in land use land cover (Ahmed & Ahmed 2012).

RESULTS AND DISCUSSION

Landscape Dynamics

A supervised classification was performed using raw satellite images to know the study area's land use and land cover dynamics. Two different platforms, say QGIS platform and IDRISI Selva v.17.0, were used to identify the spatio-temporal dynamics to obtain accurate changes. Likewise, a detailed analysis was carried out to identify the key variations and drivers influencing the LULC changes. The Land Use Land Cover (LULC) classified images for 1999, 2009 and 2019 are shown in Fig. 3, representing four major settlement classes: barren land, water bodies, and vegetation cover. The corresponding percentage area changes for 1997, 2009 & 2019 are represented in Fig. 4. A detailed discussion of the change in the four major classes is in the subsequent sections.

Change in the Barren Land

Barren land refers to exposed soils, unoccupied land, uncultivated area, open fields, landfills & sand fill areas. In this study area, overall barren land covered up to 37.8% in 1997. This may be due to the initial evolution period of industries like leather and leather-based, chemical, pharmaceutical, and ceramic factories. Noticeably, in the next ten years (1997-2009), there was a steep decline in the percentage of open fields from 37.8% to 21.7%. This date gives a clear picture of the sudden growth of large and medium-scale industries in Ranipet municipality, which reduced the percentage of open fields and made the other LULC type (settlement) grow. It is also important to know that the Small industries promotion corporation of Tamil Nadu (SIPCOT) and Small Industries Development Corporation of Tamil Nadu (SIDCO) Industrial complexes were established

(a) **(d)**

(b) **(e)**

(c) **(f)**
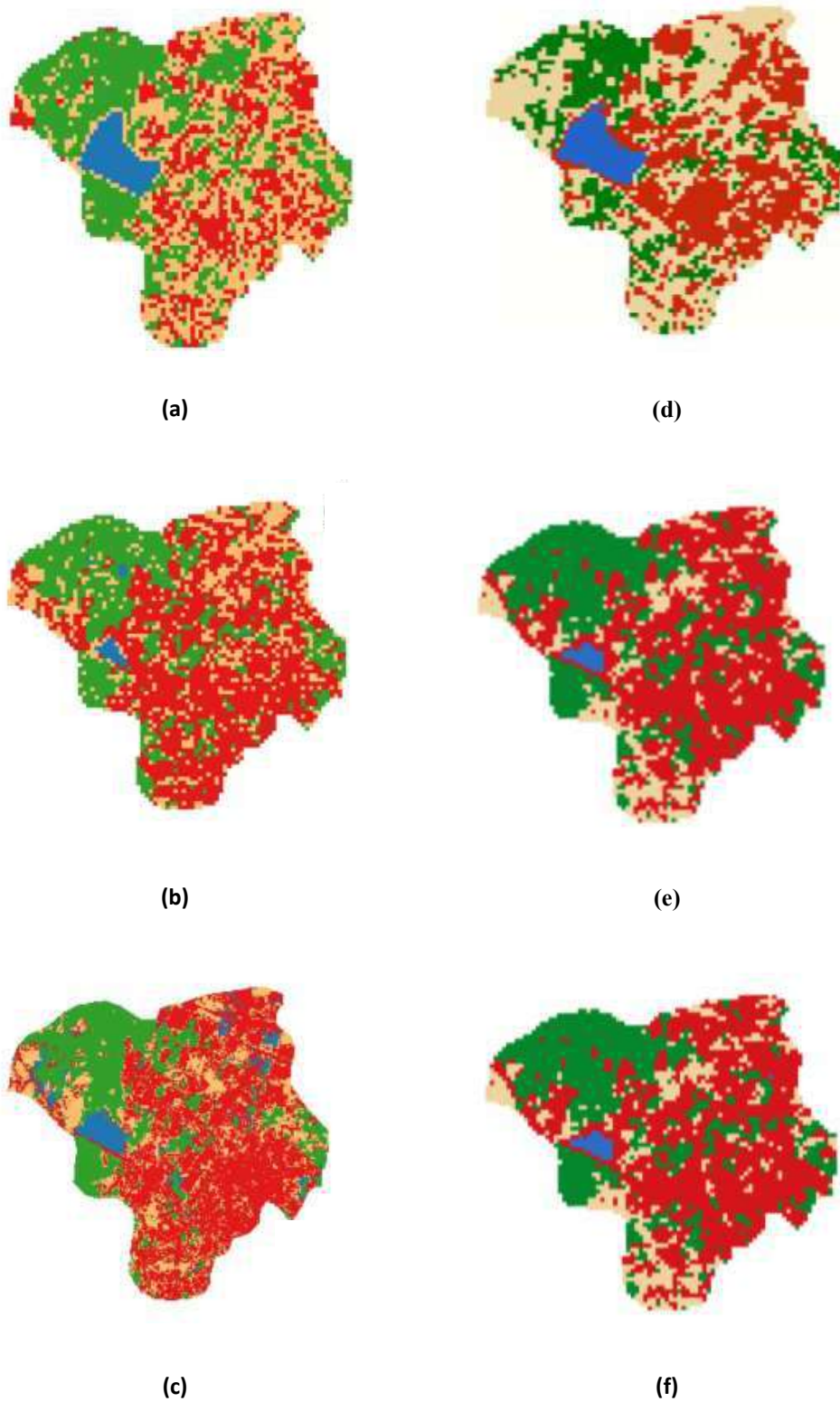
Fig. 3: Land use/Land cover classification of the study area for 1997, 2009 and 2019 using CA-ANN and CA-Markov models.

in Ranipet in the 18th century by the government of Tamil Nadu for the massive economic development of the state.

This may be one of the reasons behind the drastic reduction in the year 1997-2009. Further reductions say 1.22% of the total area in the barren land, were observed for the next consequential decade, 2009-2019. But there is no significant reduction as it happened in the earlier decade. We must consider the growing number of small-scale industries during the 19th century. The minor change in the barren land in the 19th century did not affect the economic development of the municipal town. Instead, it increased. The immense difference in the 18th century made drastic industrialization and settlements in the study area. Ministry of Micro, Small and Medium Enterprises (MSME: 2015-16) reports that the shift from barren lands to settlements made Ranipet town the top 10 contributors to the state's GDP.

Change in Settlements/Built Area

Built-up areas or settlements refer to residential, commercial, and industrial services, transportation networks, socio-economic infrastructure, and urban and rural settlements. The LULC analysis on the QGIS platform revealed a sharp increase in the settlement class from 1997-2009. The settlement covers about 23.28% in 1997 and 48.74% in 2009. The percentage change in this decade is 25.456% which is very drastic within 10 years. This helps us understand the growth of the second-grade municipality to a first-grade municipal town, Ranipet. The increasing trend in the settlement is due to the local employment opportunity available in the area because of the massive industrialization in the 19th century. Also, the road and railway network was fully established (NH-4: Chennai-Bangalore Highway in the early 19th century) for transporting men, goods, and other easy movements of essential commodities to the industries. Settlement cover in 2009 and 2019 is about 48.74% and 50.1%. There is no profound change in the settlement cover in the latter decade, but only a smaller gradient of change,

i.e. 1.257 %, is observed. It also can be seen in the LULC change map in 2019 that the area between the road and railway network has increased in the past 20 years.

Change in the Vegetation Cover

Vegetation cover refers to agricultural, crop fields, and cultivated areas. The land use land cover analysis revealed a reduction in the agricultural area from 33.05% to 27.59% during 1997-2009. Trivial alterations could be tallied with respect to the pre and post-monsoon conditions since the satellite images were collected between January 1997 and August 2009. The decreasing trend during this decade may also be due to the establishment of Phase I and Phase II industrial complexes of SIPCOT, Ranipet, by the Government of Tamil Nadu. Further, the trend is declining up to 2.7% in the next decade (2009-2019), which gives a real picture of the industrial clustering in the study area. Visible agricultural cover can be seen on the southern and eastern sides of the location in the land use land cover maps.

Change in the Water Bodies

Water bodies refer to perennial rivers, lakes, ponds, and reservoirs. It can be seen from the land use land cover map of Ranipet in 1997 that there are so many visible water bodies that contributed 4.84% of the total area, but in 2009, it was observed that there is a steep declining trend in the water bodies, about 1%. Almost a decrease of 2.7% is observed from the LULC data. This may be due to (i) over-exploitation of the surface water bodies by the nearby large and medium scale industries for leather processing and finishing, (ii) Satellite maps of 1997 and 2009 are collected from two dissimilar periods, say January and August. It should also be understood that rainfall plays an important role in the change in the percentage area of the water bodies. Likewise, increased settlement area in the earlier decade (1997-2009) may contribute to the change of water bodies.

Table 3: Transitional probability matrix of LULC change.

Transition period	LULC types				
	To	Barren land	Settlements	Vegetation	Water bodies
1997-2009	Barren land	0.2533	0.5647	0.1791	0.0028
	Settlements	0.1932	0.7397	0.0659	0.0011
	Vegetation	0.2106	0.2570	0.5252	0.0072
	Water bodies	0.1257	0.3443	0.3989	0.1311
2009-2019	Barren land	0.2901	0.4848	0.1678	0.0572
	Settlements	0.2059	0.6869	0.0716	0.0355
	Vegetation	0.1386	0.1967	0.6262	0.0384
	Water bodies	0.1370	0.3136	0.1963	0.3531

The latter decade (2009-2019) does not show a decreasing trend, instead, there is an increasing gradient from 1% to 4.77%. Fluctuations in the surface bodies may also have other environmental reasons.

LULC Change Pattern in 22 Years (1997-2019)

The spatial maps were developed and studied thoroughly to understand the overall land use and land cover change from 1997-2019 (22 years). The analysis revealed the major shift in the [1]9th century concerning the classification types like barren land and settlement cover. The primary reason behind the major changes from barren lands to settlements may be the growing industrialization and the economic development of the Ranipet municipality. Within ten years, from 1997-2009, the change in the settlement cover is observed as 26.8% of the total area. The major reason behind the massive industrialization in Ranipet municipality is its proximity to the Palar River, a major perennial river in Tamil Nadu state. No predominant change was noticed in the water bodies from 1997 to 2019. But there is a noticeable decline in the vegetation cover from 1997-2019. The shift might be either from vegetation cover to settlement/Barren land. The area's economic development and industrialization lifted the employment opportunities, which attracted the local people to work for the industries.

The transition matrix in Table 3 properly explains the trend in the LULC change. The values in the matrix reveal the chances or likelihood of getting transformed from one LULC change to the other. The transition probability values are for 1997-2009 and 2009-2019. The LULC classifies images for 1997, 2009 & 2019 used in the QGIS platform (MOLUSCE plugin). The value in the cell reveals that the probability is very high in the case of settlements compared with any other classes. In both consecutive decades, the probability of getting transformed into settlements is high. About 26.8% of the total area has transformed into settlements from 1997-2019. No other classification type has witnessed this drastic transformation except settlement.   Changes in the LULC from 1997-2019 in Ranipet Municipal Town are critically influenced by many drivers such as population, number of industries, local workers' occupational dependency, agriculture & livelihood, and economy. The detailed discussions on the major drivers for the LULC change are in the following sections.

Perceived Drivers of LULC Change

Industrialization

As per reports, Ranipet town is a protracted polluted area, one of the biggest exporting centers of tanned leather (NGRI studies). The state government selected this town to establish SIPCOT and SIDCO industrial complexes in 1973 since it is 3.5 km from the River Palar and NH-4 (Chennai-Bangalore Highway). The numbers of tannery industrial units in and around the town are almost 300, besides other industries like Chromium chemicals, petrochemicals, pharmaceuticals, drugs, foundry, boilers, refractories, auxiliary plants, and Heavy engineering. As per Tamil Nadu Pollution Control Board (TNPCB) reports in 2010, 123 leather-based industries, including chemical, galvanizing, paint, and rubber, fall under the category (Highly Polluting and hazardous). Besides this, 167 industries, like dry tannery processing, light engineering, plastic products, leather boards, pulverizing, etc., fall under the orange and green category in Ranipet town. Industries like Tamil Nadu Chromate Chemicals Ltd (TCCL), Thirumalai Chemicals Ltd (25B), Malladi Drugs & Pharmaceuticals Ltd. (I & III, 7C), and SVIS Labs were categorized as highly polluting industries by TNPCB in 2010. The SIPCOT industrial complexes (phase I & II) are surrounded by four villages such as Agraharam (North), Vanapadi (East), Karai (South) & Puliyankannu (West). The respective population in these villages as per Census: 2001 are 10628, 3971, 5344, and 4777, respectively. The population increase since 2001 is 7.45%, and the number of large and medium-scale industries in Ranipet town has increased from 143 to 240. Apart from this, 158 footwear-based industries and 27 leather goods-based industries were also identified. The local people found employment in the above-mentioned industries, and the total number of workers in each category was 2700, 1986, & 18249, respectively (Statistical Handbook, Vellore district, 2016-17). Small-scale industries based on leather-related products were 392 (registered) and 372 nos' in chemicals and chemical products. People dependent on these industries are 14018 & 2050, respectively, in 2016-17. Due to the greater economic lift and massive industrialization from 1980 to 2019 in Ranipet, the district became one of the ten top contributors to the GDP of the state (MMSME, 2015-16 survey). There is an occupational shift from the agricultural sector to the industrial sector solely because of the increased income. The massive shift from barren land to settlement also confirms the industrialization in the past 20 years.

Agriculture and Livelihood

In the 1960s, the main occupation in Ranipet was agriculture. Later in the 1970s, the establishment of the industrial complexes of SIPCOT and SIDCO took place by the state government. Still, few are involved in agricultural -work in the town. Major crops like paddy, sugarcane, maize, groundnuts, and other pulses are cultivated in the area. Palar River is the major water source running from West to East, and Pulianthangal, Karai, Vanapadi, Thandalam, and Puliyankannu are the major surface water bodies within the

location. The local people in surrounding villages depend on these water bodies for agriculture and other domestic purposes. Industries in the town are liquidating their effluents on the open land and in the major water bodies (Srinivasan Gowd & Govil 2008). Since Ranipet is located on the River Palar, the effluents/leachate, as a runoff, move downstream and worsen the soil and water quality. LULC maps reveal a reduction in the agricultural area from 1997-2019. The drivers behind the reduction of 8.33% of the total area may be due to (i) the adverse industrial pollution in the town, (ii) increased income, and the occupational shift from agriculture to industrial employment. The cultivators and the agricultural laborers are 9.10% and 15.20%, whereas the main industrial workers are found to be 56.17% (Statistical Handbook, Vellore district, 2016-17).

Prediction and Comparison of LULC Change Using CA-ANN and CA-Markov for 2029

One of the major objectives of the work is to predict and understand the future LULC (2029) changes in the Ranipet town using CA-ANN in the QGIS Platform and CA-Markov model in IDRISI Selva v.17.0, respectively. The Cellular Automata – Artificial Neural Network (CA-ANN) and Cellular Automata – Markov models are different models implemented to simulate and predict the Land Use Land Cover Change (LULCC) pattern. Also, the above-mentioned models could be used to produce the probable transition of a cell from one period to the other (1997-2029). The models use the projected recent classified images (1997/2009/2019) to predict the future of 2029. Furthermore, the models analyzed and predicted the spatial changes from 1997-2029, and the corresponding percent area transformations can be observed in Table 4.

Distances from the nearby main roads (NH-4) are the primary variable in predicting the LULC for 2029. The observed value from the transition matrix specifies the probable increase or decrease in the land use classes for 2029.

From Table 4, the CA-Markov and CA-ANN values could be compared for further analysis, and the effectiveness of the models could be understood. The transition values from class BL – BL in CA-Markov and CA-ANN are observed to be 0.0420 & 0.9804. The probable transition chances for a class BL in the near future (say 2029) would reduce, particularly for an industrialized town like Ranipet. In this transition, CA-ANN shows a higher value than the other model.

Moreover, the transition value from the class BL – SET are 0.2752 & 0.0196, respectively, for the two models. It is implicit that the settlement should increase substantially with respect to the increase in time. But here, in this prediction, the CA-ANN model gives an underestimated value of 0.0196. The model's effectiveness could finally be agreed upon from the other two classes' transition values of the foresaid models. The transition values from the class BL-VEG, BL-WB, SET-SET, VEG – sets are 0.2468, 0.4360, 0.3749 and 0.2392 for CA-Markov and 0, 0, 0.9956 & 0.0081 for CA-ANN respectively. The predicted values using CA-ANN showed no significant changes in land use classes. Average changes in settlement, vegetation, and barren land are recorded to be 0.01 sq. km only. There is no change in the class water bodies in 2029 using CA-ANN. However, the analysis and prediction performed using CA-Markov showed significant changes compared to the former model. The overall kappa accuracy of the model was found to be 81.58%. The predicted spatial map and the comparison of the predicted land use changes are shown in Fig. 5. The prediction might be more accurate if more spatial variables are incorporated, like rainfall, mean surface temperature, and socio-economic factors in both models.

Prediction and Comparison of LULC Change using CA-Markov for 2080

The CA-Markov model predicts the future LULC change easily and more accurately than the CA-ANN model. But as mentioned earlier, considering and giving equal weightage

Table. 4: Transition probability matrix of LULC from 1997-2029 using CA-ANN and CA-Markov.

Transition period	LULC types				
	To	Barren land	Settlements	Vegetation	Water bodies
1997-2029 (CA-Markov)	Barren land	0.0420	0.2752	0.2468	0.4360
	Settlements	0.0003	0.3749	0.2181	0.4067
	Vegetation	0.0002	0.2392	0.3584	0.4022
	Water bodies	0.0002	0.3046	0.2421	0.4531
1997-2029 (CA-ANN)	Barren land	0.9804	0.01958	0.0000	0.0000
	Settlements	0.0011	0.9956	0.003117	0.0000
	Vegetation	0.0000	0.0081	0.9871	0.00487
	Water bodies	0.0000	0.0000	0.0000	1.0000

Malathy Jayabaskaran and Bhaskar Das

LULC from 1997-2019 using QGIS
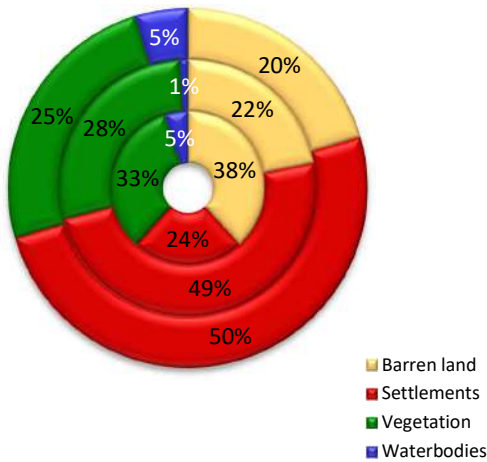
LULC from 1997-2019 using IDRISI Selva v.17.0

(a)
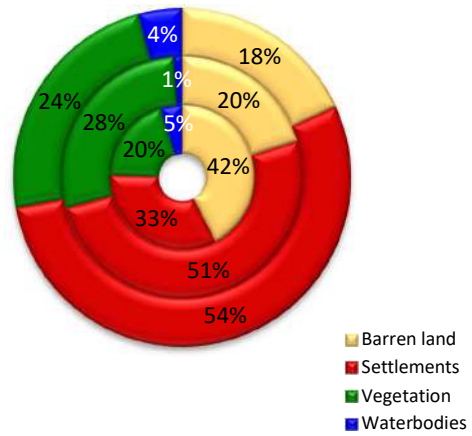
(b)

Fig. 4: Percentage contribution of LULC types for 1997, 2009 and 2019 - (a) Using CA ANN (b) CA-Markov model.
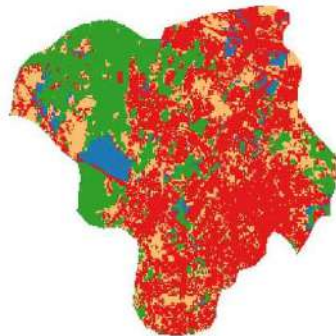
(a)
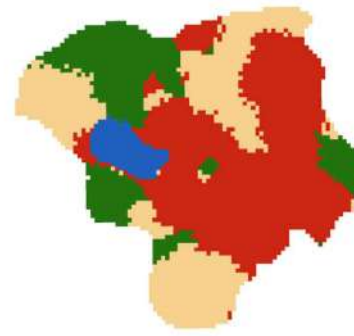
(b)

Comparison of Predicted LULC (2029) using CA-ANN (a) & CA-Markov (b)
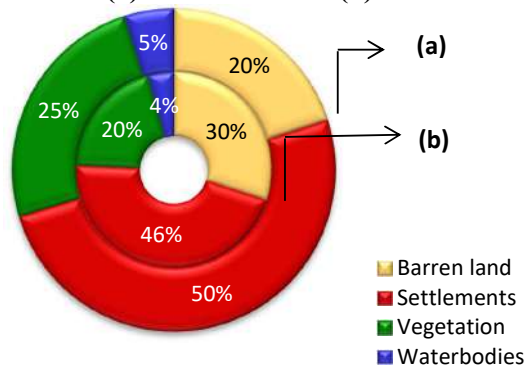
(c)

Fig. 5: Predicted LULC map of Ranipet area for the year 2029 using (a) CA-ANN (b) CA-MARKOV (c) Comparison of the two models for 2029.

Table. 5: Percentage change in the area from the year 1997-2080 using CA-Markov.

Land Use Type	Change in percentage				
	Present state			Predicted future	
	1997-2009	2009-2019	1997-2019	20019-2029	2019-2080
Barren land	-22.28	-1.98	-24.26	-12.40	-8.04
Settlements	17.65	3.19	20.84	12.58	13.65
Vegetation cover	8.42	-4.30	4.11	0.42	-5.35
Water bodies	-3.78	3.10	-0.69	-0.60	-0.26

Table 6: Transition probability matrix of LULC from 1997-2080.

Transition period	LULC types				
	To	Barren land	Settlements	Vegetation	Water bodies
1997-2080 (CA-Markov)	Barren land	0.2171	0.3021	0.4712	0.0096
	Settlements	0.1718	0.4037	0.4190	0.0055
	Vegetation	0.2005	0.3391	0.4522	0.0081
	Water bodies	0.1889	0.3647	0.4394	0.0069

to the factors influencing the dynamics would produce more accurate results. In this study, the future LULC for the year 2029 is predicted and extended to 2080 by the CA-Markov model. The overall kappa indices of the CA-Markov model are found to be 76.2%. The extension of the work is based on the area changes and transitional probability matrices of the earlier classified images.

Table 5 shows the percentage change in the area from 1997-2080 using the CA-Markov model. It could be observed from the table that there will be an 8% reduction in the class BL and an almost 4% increase in the class SET in the locality from 2019-2080. Only a minor reduction could be seen in the class VEG and almost negligible changes are observed in class WB for the same period. This could be clearly understood from the transition probability matrix shown in Table 6. The predicted images and the percent land changes can be seen in Fig. 6.

The cubic spatial trend in the transformation of land use class to the other using IDRISI Selva.17.0 could be observed in Fig. 7. The values close to one represent the growth, and

2080

14% 34% 47%

■ Barren land
■ Settlements
■ Vegetation
■ Waterbodies

(a)   **(b)**
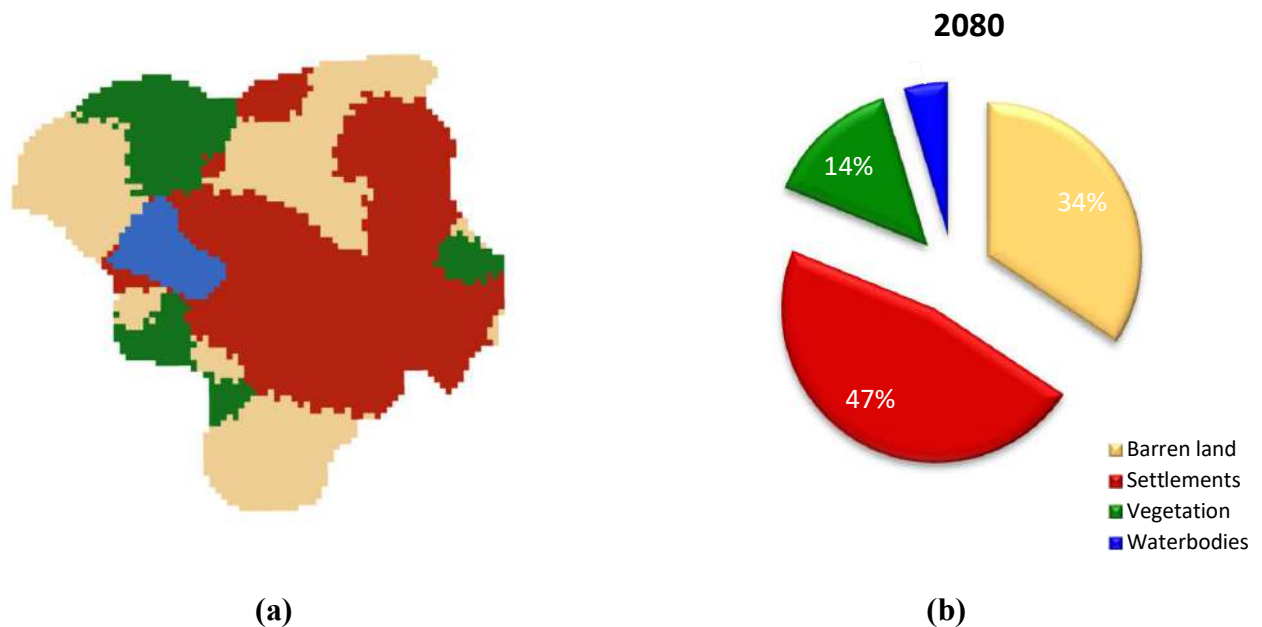
Fig. 6: (a) Predicted LULC map of Ranipet area for the year 2080 using CA-Markov (b) Percentage area changes with respect to the LULC types.

(a)

(b)

(c)

(d)
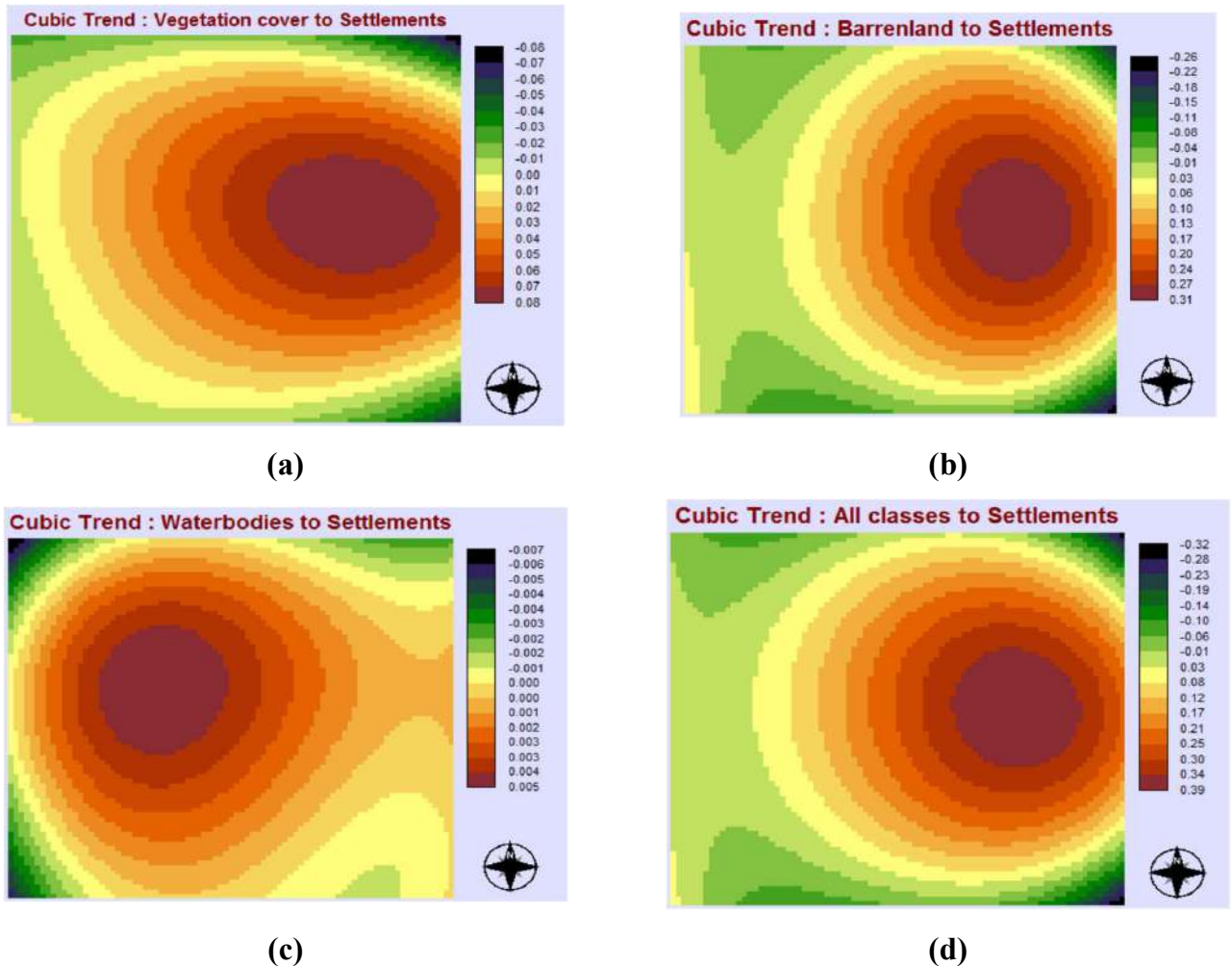
Fig. 7: Cubical trend in transformation of one LULC type to the other using IDRISI
(a) Vegetation to Settlement   (b) Barren land to Settlement
(c) Water bodies to settlement   (d) All the classes to settlement.

the one close to zero represents the reduction of one class to the other. Fig. 8 describes the spatial distribution of the gains and losses between the years 1997 to 2080 for each land use class. In this study area, the persistence of the existing land use is included for a better understanding of the gains and losses. It is evident from Fig. 8 (a) that the area in and around the existing settlement increases in the predicted spatial map of 2080. Since temperature and annual rainfall are not been considered in this analysis, which influences the area changes in water bodies, there could not be any significant changes observed in Fig. 8 (c).

CONCLUSION

Using land use maps for the years 1997, 2009, and 2019, the future LULC maps were predicted by the CA-Markov model

and the CA-ANN technique using two different platforms efficaciously. Although these models are commonly used in predicting the future LULC transformations for a bigger area, this study successfully employed the models in a smaller area and attained satisfactory kappa indices. The rapid shift in industrialization indicated the economic development of the Ranipet district, and the prediction of future 2029 maps revealed that the growth would continue in the future as well. Changes in water bodies are almost near zero, possibly due to the monsoonal variations, mean rainfall, temperature, and groundwater fluctuations in the locality. The study gives an understanding and effectiveness of the CA-Markov and CA-ANN models. But from, the results show that the CA-Markov model predicts the future LULC change easily and more accurately than the CA-ANN model.
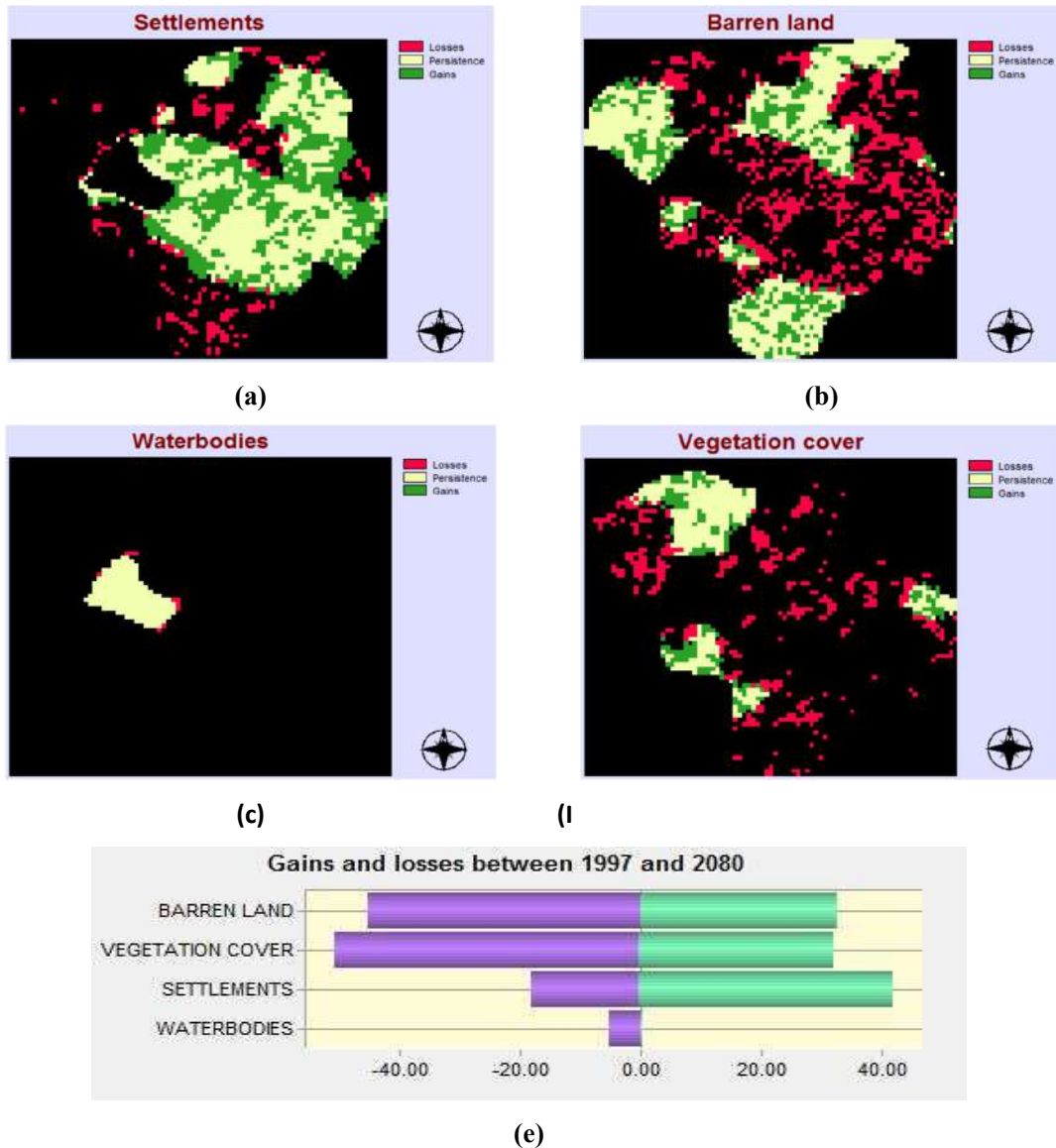
Fig. 8: Spatial distribution of gains and losses in each LULC classification type using IDRISI (a) settlement (b) barren land (c) water bodies (d) vegetation (e) percent change.

Furthermore, Land Change Modeler (LCM) in the IDRISI interface shows a widespread application in addressing the spatial and temporal dynamics and imparts knowledge about the parameters and drivers influencing land dynamics. Though the results derived have promoted the 'district's economy, the most important human demands in such areas should also be prioritized for agricultural development and the protection of the ecosystems and environment. Raising the standard of living and safeguarding the existing ecosystems are a mandate, according to 'India's statutory domestic Environmental laws. A strong, striking balance and harmony should be maintained between the imperatives of development and ecology. The Vellore case illustrates the Supreme Court's activist approach towards the implementation of 'Precaution' and 'Polluter pays,' which does little to end the prevailing problems of environmental degradation (Gupta 2018). Likewise, due consideration should be given to the land's sensitivity toward the topography and economic variables. The study also points out that land degradation cannot be addressed only by Land Use Land Cover Change maps, but it is one of the effective tools for managing and regulating land use policies in the future.

A long-term evaluation and analysis should be conducted for detailed and accurate future planning. Furthermore, it would be beneficial to the stakeholders in the decision-making process. Moreover, CA-ANN and CA-Markov models were extremely advantageous in predicting future land use changes, which would assist in a comprehensive study of land use management and planning.

ACKNOWLEDGEMENTS

REFERENCES

Ahmed, B. and Ahmed, R. 2012. Modeling urban land cover growth dynamics using multi-temporal satellite images: A case study of Dhaka, Bangladesh. ISPRS Int. J. Geo-Inform., 1: 3-31.

Al-Sharif, A.A. and Pradhan, B. 2014. Monitoring and predicting land use change in Tripolimetropolitan city using an integrated Markov chain and cellular automata models in GIS. Arab. J. Geosci., 7: 4291-4301.

Arsanjani, J.J., Kainz, W. and Mousivand, A.J. 2011. Tracking dynamic land-use change using spatially explicit Markov Chain based on cellular automata: The case of Tehran. Int. J. Image Data Fusion, 2(4): 329-345.

Arsanjani, J.J. 2012. Dynamic Land Use/Cover Change Simulation: Geosimulation and Multi Agent Based Modelling. Springer-Verlag, Berlin Heidelberg.

Arsanjani, J.J., Helbich, M., Kainz, W. and Boloorani, A.D. 2013. Integration of logistic regression, Markov chain and cellular automata models to simulate urban expansion. Int. J. Appl. Earth Observ. Geoinform., 21: 265-275.

Araya, Y.H. and Cabral, P. 2010. Analysis and modeling of urban land cover change in Setúbal and Sesimbra, Portugal. Remote Sensing., 2: 1549-1563.

Balzter, H. 2000. Markov chain models for vegetation dynamics. Ecol. Model., 126: 139-154.

Batty, M. and Xie, Y. 1994. Modeling inside GIS: Part 1. Model structures, exploratory spatial data analysis, and aggregation. Int. J. Geogr. Inform. Sys., 8(3): 291-307.

Berberoğlu,, S., Akın, A. and Clarke, K.C. 2016. Cellular automata modeling approaches to forecast urban growth for Adana, Turkey: A comparative approach. Landsc. Urban Plan., 153: 11-27.

Brown, D.G., Pijanowski, B.C. and Duh, J.D. 2000. Modeling the relationship between land use and land cover on private lands in the Upper Midwest, USA. J. Environ. Manag., 59: 247-263.

Bucx, T., Marchand, M., Makaske, B. and van de Guchte, C. (Eds.) 2010. Comparative assessment of the vulnerability and resilience of 10 deltas, synthesis report. Delta Alliance Report; No. nr. 1, Deltares. https://edepot.wur.nl/188269

Butchart, S.H.M., Walpole, M., Collen, B., Van Strien, A., Scharlemann, J.P.M., Almond, R.E.A and. Oldfield, T.E.E. 2010. Global biodiversity: Indicators of recent declines. Science, 328: 1164-1168.

Cabral, A.I.R., Vasconcelos, M.J., Oom, D. and Sardinha, R. 2010. Spatial dynamics and quantification of deforestation in the central-plateau woodlands of Angola (1990-2009). Appl. Geogr., 31: 1185-1193.

Coucelis, H. 1985. Cellular worlds: a framework for modeling micro-macrodynamics. Environ. Plan., 17(5): 585-596.

Gantumur, B., Wu, F., Vandansambuu, B., Tsegmid, B., Dalaibaatar, E. and Zhao, Y. Spatiotemporal dynamics of urban expansion and its simulation using CA-ANN model in Ulaanbaatar, Mongolia. Geocarto Int., 17: 237. DOI: 10.1080/10106049.2020.1723714.

Geist, H.J. and Lambin, E.F. 2004. Dynamic causal patterns of desertification. Bioscience, 54: 817-829.

Halmy, M.W.A., Gessler, P.E., Hicke, J.A. and Salem, B.B. 2015. Land use/land cover change detection and prediction in the north-western coastal desert of Egypt using Markov-CA. Appl. Geogr., 63: 101-112.

Jat, M.K., Choudhary, M. and Saxena, A. 2017. Application of geo-spatial techniques and cellular automata for modelling urban growth of a heterogeneous urban fringe. Egypt. J. Remote Sens. Space Sci., 20(2): 223-241.

Kaliraj, S., Chandrasekar, N., Ramachandran, K.K., Srinivas, Y. and Saravanan, S. 2017. Coastal land use and land cover change and transformations of Kanyakumari coast, India using remote sensing and GIS. Egypt. J. Remote Sens. Space Sci., 16: 454

Keshtkar, H. and Voigt, W. 2015. A spatiotemporal analysis of landscape change using an integrated Markov chain and cellular automata models. Model Earth Syst. Environ., 2(1): 10.

Koomen, E. Borsboom-van Beurden, J. 2011. Land-use Modelling in Planning Practice. Springer, XVI-214.

Lambin, E.F. Turner, B.L. Geist, H.J. Agbola, S.B. Angelsen, A. Bruce, J.W. Coomes, O.T. Dirzo, R. Fischer, G. Folke, C. George, P.S. Homewood, K. Imbernon, J. Leemans, R. Li, XB. Moran, EF. Mortimore, M. Ramakrishnan, P.S. Richards, JF. Skanes, H. Steffen, W. Stone, GD. Svedin, U. Veldkamp, TA. Vogel, C. Xu, JC. 2001. The causes of land-use and land-cover change: moving beyond the myths. Global Environmental Change: Human and Policy Dimensions,11: 261–269.

Lambin, E.F. 1997. Modeling and monitoring land-cover change processes in tropical regions. Progress in Physical Geography, 21: 375-383.

Li, T. and Li, W. 2015. Multiple land use change simulation with Monte Carlo approach and CA-ANN model, a case study in Shenzhen, China. Environmental Systems Research, 4(1).

Li, S.H., Jin, B.X., Wei, X.Y., Jiang, Y.Y. and Wang, J.L. 2015. Using CA-Markov model to model the spatiotemporal change of land/ cover in Fuxian lake for decision support. ISPRS Annals Photogram. Remote Sens. Spatial Inform. Sci., 42: 163-168.

Maithani, S. 2015. Neural networks-based simulation of land cover scenarios in Doon Valley, India. Geocarto Int., 30: 163-185.

Mendoza, M.E., Granados, E.L., Geneletti, D., Pérez-Salicrup, D.R. and Salinas, V. 2011. Analyzing land cover and land use change processes at watershed level: a multitemporal study in the Lake Cuitzeo Watershed, Mexico (1975-2003). Appl. Geogr., 31: 237-50.

Mishra, V.N. and Rai, P.K. 2016. A remote sensing aided multi-layer perceptron Markov chain analysis for land use and land cover change prediction in Patna district (Bihar), India. Arabian Journal of Geosciences, 9(4): 1-18.

Mondal, M.S., Sharma, N., Garg, P.K. and Kappas, M. 2016. Statistical independence test and validation of CA Markov land use land cover (LULC) prediction results. Egypt. J. Remote Sens. Space Science, 19(2): 259-272.

Mozumder, C. and Tripathi, N.K. 2014. Geospatial scenario based modelling of urban and agricultural intrusions in Ramsar wetland Deepor Beel in Northeast India using a multi-layer perceptron neural network. Int. J. Appl. Earth Observ. Geoinform., 32: 92-104.

Mustafa, A., Cools, M., Saadi, I. and Teller, J. 2017. Coupling agent-based, cellular automata and logistic regression into a hybrid urban expansion model (HUEM). Land Use Policy, 69: 529-540.

Mustafa, A. Heppenstall, A. Omrani, H. Saadi, I. Cools, M. and Teller, J. 2018. Modeling built-up expansion and densification with

multinomial logistic regression, cellular automata and genetic algorithm. Comp. Enviro. Urban Syst., 67: 147-156.

Muyibula, Z., Jianxina, X., Muhtara, P., Qingdongc, S. and Rund, Z. 2018. Spatiotemporal changes of land use/cover from 1995 to 2015 in an oasis in the middle reaches of the Keriya River, southern Tarim Basin, Northwest China. Catena, 171: 416-425.

Nong, Y. and Du, Q. 2011. Urban growth pattern modeling using logistic regression. Geo-Spatial Inform. Sci., 14(1): 62-67.

Norman, L., Feller, M. and Guertin, D.P. 2009. Forecasting urban growth across the united states–Mexico border. Comp. Environ. Urban Syst., 33: 150-159.

Pan, J.H., Su, Y.C., Huang, Y.S. and Liu, X. 2012. Land use & landscape pattern change and its driving forces in Yumen city. Geogr. Res., 31(9): 1631-1639.

Parsa, V.A., Yavari, A. and Nejadi, A. 2016. Spatio-temporal analysis of land use/land covers pattern changes in Arasbaran Biosphere Reserve: Iran. Model. Earth Syst. Environ., 2(4): 178.

Pijanowski, B.C., Brown, D.G. and Manik, G. 2002. Using neural nets and GIS to forecast land use changes: a land transformation model. Comp. Environ. Urban Sys., 26(6): 553-575.

Rahman, M.T.U., Tabassum, F., Rasheduzzaman, M., Saba, H., Sarkar, L., Ferdous, J., Uddin, SZ. and Islam, AZ. 2017. Temporal dynamics of land use/land cover change and its prediction using CA-ANN model for south western coastal Bangladesh. Environ. Monit. Assess., 56: 189: 565.

Reynolds, J.F. and Smith, S.M. 2002. Global Desertification: Do Humans Cause Deserts? Dahlem University Press, Berlin.

Rimal, B., Zhang, L.F., Keshtkar, H., Wang, N. and Lin, Y. 2017. Monitoring and modeling of spatiotemporal urban expansion and land-use/land-cover change using integrated Markov chain cellular automata model. Int. J. Geogr. Inform., 6(9): 288.

Gupta, R. 2018. Vellore Citizen's Welfare Forum v. Union of Indian and Others: A critique of Precautionary and Polluter Pays Principle.

Romm, J. 2011. Desertification: the next dust bowl. Nature, 478: 450-451.

Sang, L., Zhang, C., Yang, J., Zhu, D. and Yun, W. 2011. Simulation of land use spatial pattern of towns and villages based on CA-Markov model. Math. Comp. Model, 54: 938-943.

Saputra, M.H. and Lee, HS. 2019. Prediction of land use and land cover changes for north Sumatra, Indonesia, using an artificial-neural-network-based cellular automaton. Sustainability, 11: 3024.

Schröter, D., Cramer, W. and Leemans, R. 2010. Ecosystem service supply and vulnerability to global change in Europe. Science, 310: 1333-1337.

Sellers, P.J., Meeson, B.W., Hall, F.G., Asrar, G., Murphy, R.E., Schiffer, R.A., Bretherton, F.P., Dickinson, R.E., Ellingson, R.G., Field, C.B., Huemmric, K.F., Justice, C.O., Melack, J.M., Roulet, N.T., Schime, D.S. and Try, P.D. 1995. Remote sensing of the land surface for studies of global change: models, algorithms and experiments. Remote Sens. Environ., 51(1): 3-26.

Singh, S.K., Srivastava, P.K., Gupta, M., Thakur, J.K. and Mukherjee, S. 2014. Appraisal of land use/land cover of mangrove forest ecosystem using support vector machine. Environm. Earth Sci., 71: 2245-2255.

Srinivasa Gowd, S. and Govil, P.K. 2008. Distribution of heavy metals in surface water of Ranipet industrial area in Tamil Nadu, India. Environ. Monit. Assess., 136: 197-207.

Subedi, P., Subedi, K. and Thapa, B. 2013. Application of a hybrid cellular automaton Markov (CA-Markov) Model in land-use change prediction: a case study of saddle creek drainage Basin, Florida. Appl. Ecol. Environ. Sci., 1(6): 126-132.

Sutton, P.C., Anderson, S.J., Costanza, R. and Kubiszewski, T. 2016. The ecological economics of land degradation: Impacts on ecosystem service values. Ecol. Econ., 129: 182-192.

Tamil Nadu Pollution Control Board (TNPCB) 2010. Revised Action Plan for critically polluted Area – Ranipet, 2010. https://www.tnpcb.gov.in/pdf/Action_plan_Ranipet070916.pdf

Tripathy, P. and Kumar, A. 2019. Monitoring and modelling spatio-temporal urban growth of Delhi using cellular automata and geoinformatics. Cities, 90, 52-63.

Triantakonstantis, D. and Mountrakis, G. 2012. Urban growth prediction: A review of computational models and human perceptions. J. Geogr. Inform. Syst., 4: 555-587.

Turner, B.L., Lambin, E.F. and Reenberg, A. 2007. The emergence of land change science for global environmental change and sustainability. Proceed. Nat. Acad. Sci., 104(52): 20666-20671.

Vasconcelos, M.J., Cabral, A.I.R., Melo, J.B., Pearson, T.R.H., Pereira, H.A. and Cassam, V. 2015. Can blue carbon contribute to clean development in West Africa? The case of Guine-Bissau. Mitig. Adap. Strat. Glob. Change, 20: 1361-1383.

Verburg, P.H., Eck, J.R.V., Hijs, T.C.D. and Dijst, M.J.S. 2004. Determination of land use change patterns in the Netherlands. Environ. Plan. B Urban Anal. City Sci., 31(1): 125-150.

Wang, J. and Maduako, I.N. 2018. Spatio-temporal urban growth dynamics of Lagos Metropolitan Region of Nigeria based on Hybrid methods for LULC modeling and prediction. Europ. J. Remote Sens., 51: 251-265.

White, R. and Engelen, G. 1994. Cellular dynamics and GIS: Modeling spatial complexity. Geogr. Sys., 1(3): 237-253.

Characteristics of Nickel Laterite Mine Waste in Caraga Region, Philippines and Its Potential Utilization

Abigael Balbin*(**)†, Jobelle Capilitan*(**), Evelyn Taboada* and Ian Dominic Tabañag*(***)

*School of Engineering, University of San Carlos, Talamban, Cebu City, Philippines
**College of Engineering and Geosciences, Caraga State University, Ampayon, Butuan City, 8600, Philippines
***Philippine Council for Industry, Energy, and Emerging Technology Research and Development, Department of Science and Technology (DOST-PCIEERD), Bicutan, Taguig City, 1631, Philippines
†Corresponding author: Abigael Balbin: albalbin@carsu.edu.ph

ABSTRACT

Nickel laterite mining is one of the sources of nickel-iron material used for producing steel and various materials. This mining activity leaves waste in the mine, including rocks, overburden, silt, and dust. Characterization is an important primary step in understanding waste for proper management, utilization, and disposal. The pH, organic matter, and elemental composition are analyzed in this study. The pH of nickel laterite mine waste is neutral to moderately alkaline, which makes it unlikely to cause acid mine drainage, which is one of the most prevailing environmental problems of mines. The organic matter content also showed favorable results for plant growth. However, the macronutrients necessary for the plant are too high, making it less favorable for agricultural utilization. Elemental composition shows the presence of nickel and other elements lower than the economically acceptable level. However, processing the lower grade can be the best option when all higher-grade resources are exhausted. The nickel laterite mine waste can be reused to further extract the metals when sources of higher grades are depleted, repurposed such as in the production of bricks and ceramics, or mined-out mines can be repurposed for renewable energy sources such as solar and wind farms.

INTRODUCTION

In the next several years, humanity will face extreme challenges as sources of fresh raw mineral materials become depleted and scarce (Lottermoser 2010, Sahajwalla 2018). While this may cause global concern, this can also be an opportunity for scientists and engineers to develop technology and apply concepts and results of numerous research to cope with the demand of the times. Economists, scientists, and researchers have presented different concepts like circular economy, industrial symbiosis, life cycle assessment, and sustainable development, which have one common goal: to optimize the use of the limited resources today and provide for the future. Therefore, researching cost-effective processes that can turn waste materials into valuable resources is necessary (Lottermoser 2011, Sahajwalla 2018).

Mining is extracting materials from the earth to recover one or more valuable minerals. Along with this process is producing solid, liquid, or gaseous unwanted by-products of no current economic value called mine wastes. Additionally, any mineral-containing unexploited material on-site may be considered waste (Lebre et al. 2017). Mine wastes can be classified into mining, processing, and metallurgical wastes (Lottermoser 2010). Mining wastes, which is the focus of this study, are everything left in the mine after extracting the valuable material. Mine waste may include waste rocks, overburden, spoils, mining water, atmospheric emissions, acid mine water, dust, and silt.

Nickel laterite is one of the sources of nickel, along with the less complex ore of nickel sulfide. Laterite constitutes about 70% of the worldwide nickel resource, but sulfide contributes to about 60% of the world's nickel production (Elias 2013). This is due to the complexity of laterite ore, making it more difficult and costly to process than sulfide ore. With the increasing demand for nickel and improved processing economics for nickel laterite, nickel production has increased. But due to its complexity, nickel laterite mining is known to produce more waste than nickel sulfide.

The Philippines is the 2nd largest nickel ore producer, next to Indonesia in 2020 (Garside 2021). The country has 24 nickel laterite mines, of which 16 are found in the Caraga Region, the southern part of the Philippines (MGB13 2021). The extraction of nickel in the country is using an open cast

or strip mining method, which involves the removal of 1 to 2 meters of topsoil or the overburden to remove the limonite and saprolite deposits that occupy the soil from 3 to 25 meters below the ground (Tabios III 2020). Most nickel and iron ores in the Philippines are exported to countries like China to extract and refine nickel, iron, chromium, cobalt, and even some highly valued metals such as platinum, vanadium, and titanium (Tabios III 2020).

In general, mining has substantially improved the Philippines' economic status, specifically in the Caraga Region, creating more than 23,000 jobs in a 2020 report from Mines and Geosciences Bureau (MGB). However, despite the economic contribution of mining, the industry is still controversial because of environmental issues, inherent to the destructive nature of mining activity. About 2-12 tons of overburden material is removed as waste for every ton of metal produced (Mohanty et al. 2010). Active and abandoned mines significantly contribute to metal contamination worldwide (Schaider et al. 2007). Uncontrolled disposal of nickel mine wastes, for example, increases turbidity in receiving waters. Turbidity is visually evident in the red-orange bay area along causeways, stockpiles, and siltation ponds (Tabios III 2020). The Total Suspended Solid (TSS) reaches as high as 1000mg/L during heavy runoff (Apodaca et al. 2018). Moreover, mining generates enormous amounts of waste (Lebre et al. 2017) and is among the world's most significant prevailing waste concerns (Bian et al. 2012, Ceniceros-Gómez et al. 2018).

This study determines the characteristic of the nickel laterite mine waste in a nickel laterite mine project in Caraga, Philippines. Mineralogical characterization in mine waste helps improve risk assessment, guide proper mine planning, and optimize pollution control design (Jamieson et al. 2015). The chemical composition and geotechnical properties determine the most appropriate uses and whether reuse is economically feasible (Bian et al. 2012). Understanding the waste's physical, chemical, and mineralogical content is vital in developing appropriate and effective waste management protocols. Information on the characteristics of mine wastes is also required to select the most reliable and cost-effective treatments that will lead to successful site reclamation and restoration (Amacher & Brown 1999). Understanding the waste's physicochemical and mineralogical characteristics can predict the potential for acidic drainage, metal leaching, and reactivity (Anderson et al. 1999, Van der Ent et al. 2013). Characterization, therefore, is an integral part of properly managing waste (Chileshe et al. 2020). In particular, the pH, organic matter, and elemental composition of a nickel laterite mine waste are analyzed.

Further, some published research and reports are reviewed to provide information on the potential utilization of the waste and the mined-out area after all valuable minerals are exhausted. The industry can reference these studies to give them options other than the usual mine rehabilitation by revegetation.

MATERIALS AND METHODS

Samples and Study Area

A nickel laterite mine in the Caraga region, Philippines, was chosen for this particular study. The laterite profile of this mine consists of ferruginous laterite, limonite, and saprolite (Gifford 2013). This mining project ended in 2022, and the area is under rehabilitation. Soil samples were taken randomly from each of the eight mine settling ponds and stockpiles of waste rocks and analyzed for pH, organic matter, and elemental composition. Settling ponds are usually located at a lower elevation in the mine and contain silt, eroded soil from the upper stockpile of waste rocks, overburden, and other waste, such as degraded plants.

pH

The pH is measured using a 1:1 mine waste/ deionized water suspension method using a pH meter (Amacher & Brown 2000, Thomas 1996). 20g of mine waste sample is added with 20 mL of deionized water, and stirred for 5 minutes at 240 rpm. The sample was allowed to rest for 30 minutes, and the pH was measured using an APERA PH800 pH meter. The probe is swirled around the sample without touching the bottom part.

Organic Matter

The loss-on-ignition method estimates the soil organic matter based on gravimetric weight change associated with high-temperature oxidation of organic matter (Amacher & Brown 2000). Mine waste samples were placed in previously dried and weighed crucibles. Samples in the crucible were then dried in an oven at 105°C for 16 h, cooled in a desiccator, and weighed. The samples were ignited in a muffle furnace at 450°C for 16 h, cooled in a desiccator, and weighed again. The loss-on-ignition (LOI) organic matter is then calculated using the equation:

$$\text{LOI Organic Matter (\%)} = \frac{oven\ dried\ weigth - ignited\ weight}{oven\ dried\ weight} \times 100 \quad \cdots(1)$$

Elemental Composition

The elemental composition was analyzed using X-Ray Fluorescence (XRF), the most widely used method to analyze nickel laterite elemental content in Philippine mines. The

samples were analyzed at the mine laboratory, where the samples were taken.

RESULTS AND DISCUSSION

Besides giving information on the acidity or basicity of the sample, pH can be used to estimate the available nutrients and toxicity of the elements present in the sample using its relationship with pH (Thomas 1996). The pH analysis results in Table 1 showed that the pH in mine 5 is neutral, mines 2, 3, 4, and 9 are slightly alkaline, mine 7 is moderately alkaline, and mine 1 is strongly alkaline. The pH range also indicates that this type of waste will likely not cause acid mine drainage problems to the surrounding water bodies. Normally soil at 7.6-8.3 pH is calcareous and most likely controlled by calcium carbonate, which usually does not need further treatment (Thomas 1996). The pH of 8.57 at mine 1 could mean the presence of sodium carbonate controlling the soil system rather than calcium carbonate, which could indicate future soil degradation (Thomas 1996). A little amendment to lower the pH may be necessary.

The loss-on-ignition analysis revealed 1.77%-7.95% organic matter, which can be considered a good percentage for OM for plant growth. The highest OM percentage is at mine 5 (7.95%) and the lowest at mine 1 (1.77%). Organic matter is an important characteristic of soil to be considered when considering the rehabilitation of mine waste by revegetation or growing plants. The OM contains all essential plant nutrients and serves as a storehouse for the nutrients necessary for plant growth. It can be easily reinforced with organic fertilizers. OM also influences the soil to form a stable structure. In mines, the higher organic matter content of the soil is more favorable since it lowers soil erodibility and the risk of soil erosion (Kadlec et al. 2012).

The elemental composition in Table 2 show that the average nickel content of the sample ranges from 0.50 to 1.10% by weight, confirming that it is low-grade and currently of no economic value. The lowest economic grade for a nickel at this particular mine is 1.2%. Iron (Fe) content ranges from 9-46%, a typical characteristic of lateritic soil. A lateritic soil profile is divided into two, which are limonite with 25% or higher iron content and saprolite with less than 25% iron. Other elements like cobalt, aluminum, magnesium, potassium, chromium, and tin were also found. Though the elemental composition of the mine waste is already below the minimum economic grade, the metal concentration is still too high for plant growth. Discharge of these elements caused by soil erosion or water runoff during heavy rainfall can contaminate neighboring agricultural land and water bodies. Most micro and macronutrients like iron, nickel, potassium, zinc, and others are found in too high concentrations for farming applications. Vegetables can absorb elements at high concentrations, which can harm humans in the long term.

Utilization of Nickel Laterite Mine Waste

Given that the nickel concentration of the mine waste is below 1.2%, the researchers reviewed some of the studies using low-grade nickel laterite. The industry can further explore these studies to utilize the mining waste. The low-grade nickel laterite mine waste can be reused or repurposed based on the information gathered. Reuse means using the waste to extract the remaining metals using new or old technology, which allows profitable extraction in the future. Reuse can be further categorized into metallurgical processing, biomining, or using bacteria or fungi to concentrate the metal, and phytomining, which uses plants to harvest the metals. On the other hand, repurposing can be divided into two; repurposing the mine waste and the mined-out area. To repurpose the mine waste is to use it for other purposes such as in brick making, ceramic, and as an additive to construction materials. Repurposing the mined-out area means converting the mined-out area into tourism sites (Aysan et al. 2019), solar farms (Pouran 2018, Murphy 2022), or other renewable energy-generating industries.

Reuse by Metallurgical Process

In Table 3 are some studies proposed to improve the current widely used high-pressure acid leaching (HPAL), caron process, and smelting to recover the nickel-iron and by-products like cobalt. Guo et al. (2021a) studied the effects of the different dosages of red mud (RM) from China and low-grade laterite ore in co-reduction with laterite. The recorded iron and nickel recoveries are 94.71 wt%, and 95.98 wt%, respectively. Guo et al. (2021b) did a related study on using straw charcoal as a reductant on the co-reduction of RM and laterite. Recovery of nickel is 97.21 wt%, and iron is 98.87% using 15wt.% of straw charcoal and roasted for 80 min. at 1250°C. Xiao et al. (2020) tried selective roasting garnierite

Table 1: pH and Organic Matter content of nickel laterite mine waste in Caraga, Philippines.

Characteristic	Mine 1	Mine 2	Mine 3	Mine 4	Mine 5	Mine 7	Mine 9	Final Discharge
	Average of 4 samples (Standard Deviation)							
pH	8.57(0.14)	7.82(0.12)	7.69(0.07)	7.47(0.11)	7.17(0.16)	7.91(0.15)	7.72(0.08)	8.24(0.06)
Organic matter (%)	1.77(0.91)	4.87(1.04)	3.93(0.62)	6.52(2.86)	7.95(1.28)	3.24(1.58)	2.84(1.46)	3.84(0.78)

Table 2: Elemental Analysis results using XRF of nickel laterite mine waste in Caraga, Philippines.

Ave. Element % (n = 4)	Mine 1	Mine 2	Mine 3	Mine 4	Mine 5	Mine 7	Mine 9	Final Discharge
Ni	0.84	0.96	1.10	1.04	0.91	0.94	0.83	0.50
Fe	9.53	24.53	17.71	28.04	46.38	19.63	19.08	15.38
Co	0.04	0.06	0.06	0.06	0.11	0.06	0.05	0.05
Al	0.47	2.55	0.98	1.75	2.55	1.07	1.01	3.00
Mg	16.80	9.57	12.11	11.54	4.11	13.55	13.72	9.43
P	LDL	0.01	LDL	0.01	0.01	LDL	LDL	0.01
Si	18.18	12.59	17.03	12.60	5.48	15.10	15.26	16.39
Ca	0.82	0.18	0.17	0.14	0.05	0.13	0.15	1.47
Cr	0.41	1.31	0.79	1.02	1.64	0.81	0.83	0.62
K	0.03	0.01	0.01	0.01	0.01	LDL	LDL	0.27
Mn	0.20	0.44	0.32	0.51	0.85	0.37	0.36	0.33
Na	0.02	0.02	0.02	0.03	0.05	0.02	0.02	0.03
Ti	0.03	0.08	0.04	0.06	0.07	0.04	0.04	0.10
NiO	1.06	1.22	1.40	1.33	1.17	1.20	1.06	0.64
Fe_2O_3	13.62	35.07	25.34	40.09	66.31	28.07	27.28	21.98
CoO	0.05	0.07	0.07	0.08	0.14	0.07	0.06	0.06
Al_2O_3	0.89	4.81	1.85	3.31	4.81	2.02	1.90	5.66
MgO	27.86	15.88	20.08	19.13	6.80	22.46	22.76	15.64
P_2O_5	LDL	0.03	0.01	0.01	0.03	0.01	0.01	0.03
SiO_2	38.90	26.94	36.42	26.96	11.73	32.30	32.63	35.07
CaO	1.15	0.24	0.24	0.19	0.07	0.18	0.21	2.05
Cr_2O_3	0.59	1.91	1.16	1.49	2.40	1.18	1.22	0.90
K_2O	0.04	0.01	0.01	0.01	0.01	LDL	LDL	0.32
MnO	0.26	0.57	0.41	0.66	1.10	0.48	0.46	0.43
Na_2O	0.03	0.03	0.03	0.04	0.07	0.03	0.03	0.04
TiO_2	0.04	0.13	0.06	0.09	0.12	0.07	0.07	0.16

LDL – lower than detectable limit

laterite (0.72% Ni) ore to form ferronickel. The ferronickel produced is at 16.16% Ni and 73.67% Fe or 90.33% Ni recovery. Xue et al. (2020) modified the traditional sintering process in nickel extraction by introducing pressurized densification sintering. An external mechanical pressure field is added by weight adjustment at the top of the sinter bed after ignition. As a result, productivity and tumble index increased by 18.6% and 19.2%, respectively. The solid fuel rate is decreased by 10.3%, making it more economical than the traditional process. A related study on CO_2 reduction with this new sintering method was also made by Zhu et al. (2020). In the study of Komnitsas et al. (2019), low-grade Ni (0.97%) and the effect of adding sodium sulfite (Na_2SO_3) in the leaching medium (sulfuric acid, H_2SO_4) were investigated. After 25 days at 147 g/L of H_2SO_4 and 20 g.L^{-1} of Na_2SO_3, the extraction was 72.5% and 47.4%

for Ni and Co, respectively. The group also investigated the possibility of using the leaching residue as an inorganic polymer (IP). The residue was mixed with alkali activators NaOH and Na_2SiO_3 and added with metakaolin. The IP exhibited high compressive strength at 40 MPa, which is suitable for various applications in construction. Zhu et al. (2019) proposed improving nickel laterite processing by a selective reduction-wet magnetic separation process. The proposal was to use silica and calcium sulfate. The nickel content of the laterite used is 0.97% by wt. from Indonesia. The laterite, the reductant (graphite), and additives (silica and calcium sulfate) were mixed and roasted at 900-1300°C for a pre-determined time for the reduction process. After reduction, the roasted samples were crushed and grounded to 90 wt% passing 0.043 mm for magnetic separation using magnetic field strength of 1800 G. The highest Ni recovery

is 95.6%, and Fe is 42.8% at a reduction temperature of 1250°C for 60 min, 3% calcium sulfate and 8% silica. Li et al. (2018a) studied the solid-state deoxidation of low-grade nickel laterite (0.82% Ni) with methane at various reduction temperatures, times, and concentrations. The nickel laterite, of particles size <0.25mm, was made into pellets for reduction. CH_4 and N_2 gases were used in the reduction process using a fixed bed apparatus. The volumetric gas rate used was 30 mL.min^{-1} at a reduction time of 30-90 minutes. The best condition identified was at a temperature of 700°C, 60 min., and 20vol% % methane reduction time. The metallization at this condition was 91.17% and 23.67% for Ni and Fe, respectively. Li et al. (2018b) proposed a new method to improve atmospheric acid leaching. Atmospheric phosphoric acid leaching was used to select Ni and Co. The laterite ore (Ni at 1.043%) was first calcined and treated with different concentrations of acid (1M, 2M, 3M, and 4M) at different temperatures (20°C, 40°C, 60°C, 80°C, and 90°C). Based on

the results, the best condition was at 3M phosphoric acid, at 90°C and 180 min leaching temperature and time, respectively. Ni's leaching efficiency is 98.7 %, and Co's is 89.8%. The result was higher than previous studies, indicating about 40-60% of Ni recovery by atmospheric leaching using sulfuric acid (Coto et al. 2008, Luo et al. 2015). Luo et al. (2015) used an alternative processing method for HPAL by using sulfuric acid in the presence of sodium sulfite at atmospheric pressure. The influence of temperature and agitation rate on atmospheric acid leaching (AL) was studied by MacCarthy et al. (2016). They believe that nickel laterite processing will be greatly improved through greater knowledge of the factors that influence atmospheric AL. Results showed that leaching greatly improved at a higher temperature of 95°C than at 70°C (from %9 to %67 for Ni). Agitation, on the other hand, had no noticeable impact on AL. The sintering behavior of low-grade nickel laterite (1.2% Ni) was studied by Guo et al. (2014) to provide technical information on ferronickel production.

Table 3: Research using nickel laterite mine waste with < 1.2% Ni by the metallurgical process.

No	Process	Ni (*wt%)	Fe (*wt%)	Method/ Description	Reference
Metallurgical Processing					
1.	Co-reduction – Roasting	0.98	37.57	Recovery of nickel and iron from low-grade laterite using the co-reduction roasting technique	(Guo et al. 2021a)
2.	Roasting-Leaching	1.2	41.9	Selective recovery of scandium from nickel laterite ore by acid roasting–water leaching	(Anawati et al. 2020)
3.	Roasting-Separation	0.72	8.65	Extraction of nickel from garnierite with iron concentrate using roasting and magnetic separation	(Xiao et al. 2020)
4.	Sintering	0.15-0.34	31.59-40.36	Improved limonitic laterite sintering using a pressurized densification process	(Xue et al. 2020, Zhu et al. 2020)
5.	Leaching	0.97	21.79 Fe_2O_3	Column leaching using sulfuric acid and sodium sulfite. Valorization of leaching residues as inorganic polymer	(Komnitsas et al. 2019)
6.	reduction-separation	0.97	40.09	selective reduction-wet magnetic separation process using silica and calcium sulfate	(Zhu et al. 2019)
7.	Reduction-Deoxidization	0.82	9.67	Reduction of nickel and Iron from low-grade nickel laterite via a solid-state deoxidization method using methane	(Li et al. 2018a)
8.	Leaching	1.03	43.95	Leaching of calcined laterite using phosphoric acid	(Li et al. 2018b)
9.	Atmospheric Acid Leaching	0.93	22.01	Effect of temperature and agitation rate on atmospheric acid leaching	(MacCarthy et al. 2016)
10.	Sintering	1.2	46.26	Ferronickel production via sintering blast furnace route	(Guo et al. 2014)
11.	Direct extraction	0.62-1.1	35.70-44.30	Direct extraction of nickel from laterite ore by carbonyl method	(Terekhov & Emmanuel 2013)
12.	Reduction-Deoxidization	1.09	9.12	Reduction of nickel from low-grade nickel laterite via a solid-state deoxidization method using CO_2-CO gas mixture	(Li et al. 2011a)
13.	Leaching	1.03	43.95	Selective leaching of cobalt by acidic thiosulfate solution	(Li et al. 2011b)
14.	Leaching	0.98 NiO	15.80 Fe_2O_3	Green process technology for recovering nickel	(Zhai et al. 2010, Liu et al. 2012)
15.	Reduction	0.38 NiO	50.88	Reduction of laterite by CO- CO_2	(Purwanto et al. 2001)
16.	Digestion – Neutralization-Calcination	0.93 NiO	34.41 Fe_2O_3	Chromite overburden as a source of nickel. Low-grade nickel is enriched through the digestion – neutralization-calcination process.	(Bhattacharjee et al. 2000)

The study showed that the yield increased with basicity from 1.1 to 1.7 and decreased with a further increase in basicity. Terekhov & Emmanuel 2013 evaluated the use of carbonyl in the direct extraction of Ni and iron from nickel laterite (0.62%). The reduction process was carried out using carbon monoxide in a high-pressure thermogravimetric analyzer. The carbonyl + metal in gaseous form (at 60 bar, 180°C) was then passed through a heat exchanger and condensed in storage tanks. Fractional distillation separated Ni and Fe, which is the process in a pilot unit. But in this study, the Ni recovery is calculated by mass balance using the weight loss of the sample. The limonite sample with the lowest Ni grade (0.62wt%) yielded a 0.02 percent Ni residue, equivalent to an estimated Ni yield of 98.9% and 86.5 percent Fe. Li et al. (2011) also studied the solid-state deoxidation of low-grade nickel laterite (1.09% Ni) with CO_2-CO gas mixture as the gaseous reductant and anthracite as the solid reductant. Based on the study, the conversion of total nickel to metallic nickel generally increases with the increase in reaction temperature until not more than 850°C. Overall results showed that 90% of metallic nickel could be obtained using CO_2-CO gas and 80% anthracite. Bhattacharjee et al. 2000 proposed a process to enrich nickel concentration in chromite overburden, a low-grade laterite. The process includes digestion with acid or a combination of HCl, HNO_3, and H_2SO_4, neutralization with alkali (Na_2CO_3, NaOH), and calcination at 900°C. The final product was found to have 2.54% NiO from an initial concentration of 0.93% or increased by 173%. Iron and nickel extraction from chromite overburden is also studied by Boi et al. (2011). Their study used reduction roasting, magnetic separation, and smelting processes to recover iron and nickel.

Most of the studies on low-grade nickel laterite are alternative processing routes. The recovery of metals like cobalt (Li et al. 2011) and scandium (Anawati et al. 2020) was also studied. Anawati et al. (2020) tried to extract scandium, an expensive rare earth metal, from low-grade nickel laterite. They used a two-stage process of acid roasting and water leaching. The ore was mixed with sulfuric acid and roasted at 600°C. Water-leaching at ambient temperature followed. The highest extraction of scandium is at 80%, with less than 15% co-extraction of the iron. In the study of Li et al. (2011), sodium thiosulfate and sulfuric acid were used as leaching agents. The thiosulfate selectively recovered 91% of the cobalt in the sample.

Reuse by Biomining

Biomining describes systems that utilize microorganisms to extract and recover metals from ores and other materials (Johnson 2014, Johnson et al. 2013). This process finds its earlier application with copper in the 1960s (Barrie 2018) and nickel as early as the 1980s. A summary of the studies on the biomining of nickel laterite is in Table 4. Oliveira et al. (2021) applied a new method in processing low-grade nickel by reduction with hydrogen gas followed by bioleaching with *Acidithiobacillus ferooxidants*. After the reduction process at 900°C and H_2 gas (99.9990%), the Ni content increased from 1.2% to 1.46%.

Bioleaching at 32°C with 35g of sulfuric acid/ kg of ore resulted in the overall extraction of nickel and cobalt at 92% and 35%, respectively. Newsome et al. (2020) also proposed a new bioprocessing strategy for cobalt extraction from lateritic soil. Organic substrates (acetate or glucose)

Table 4: Research on biomining to extract nickel and other metals from nickel laterite.

No	Process	Ni (*wt%)	Fe (*wt%)	Method/ Description	Reference
1.	Reduction of roasting/ bioleaching	1.2	44.9	Reduction with hydrogen gas followed by bioleaching using *Acidithiobacillus ferooxidants*	(Oliveira et al. 2021)
2.	Bioprocess	< 0.30	13.4-44.6	Manganese and cobalt enrichment through biogeochemically enhanced process	(Newsome et al. 2020)
3.	Bioprocessing (leaching)	0.91	44.51	Enhanced bioleaching with the use of *Acidithiobacillus (At.) thiooxidans*	(Marrero et al. 2017)
4.	Bioprocessing (leaching)	1.2	49.8 Fe_2O_3	biological leaching of nickel by indigenous fungi (Indonesia) isolated from Indonesian limonite	(Handayani & Suratman 2017)
5.	Bioprocess	0.99	48.88	Anoxic microbial reduction of nickel from lateritic soil (chromite overburden)	(Behera et al. 2012)
6.	Bioprocessing	0.4	7.0	Four species of iron-reducing acidophilic bacteria were evaluated in their ability to make nickel soluble.	(Hallberg et al. 2011)
7.	Bioprocess (leaching)	8.5 ppm	2014 ppm	Bio-extraction of different metals by *Penicillium chrysogenum*	(Ahmad et al. 2011)
8.	Bioleaching and bioprecipitation	0.92 NiO	19.36 Fe_2O_3	Leaching of nickel laterite with heterotrophic organisms	(Alibhai et al. 1993)

generated metal-reducing conditions and separated cobalt by washing it with acetic acid. Their study mobilized minimal iron oxide, which may generate less waste. The Marrero group tried to compare the reductive capability of *Acidithiobacillus (At.) thioxidants* in aerobic conditions and using *At. Ferrooxidants* in anaerobic conditions. Nickel laterite overburden from Cuba was used in the study. Based on the results using *At. thioxidants* in aerobic condition was more efficient than the ferrooxidants. The sample treated with the oxidants achieved the highest solubilization (Co 85%, Mn 74%, Ni 16%) after seven days at pH 0.8, while the ferrrooxidants sample achieved the same values after 28 days increased pH of 1.8. Handayani and Suratman (2017) studied the feasibility of using fungi as a new technique in nickel metal recovery. Two types of fungi were used, the *Aspergillus sp* and *Penicillium sp*. The experiment used low-grade nickel laterite (1.66% NiO) from Pomalaa, Southeast Sulawesi. *Aspergillus* sp. showed better nickel recovery of 57% at 5% pulp density after 20 days than 48% using *Penicillium* sp. Using fungi is a potential technique in nickel recovery; however, the primary concern is the long fermentation period of about 8-14 days of the fungi. Behera et al. (2012) investigated the microbial extraction of nickel from lateritic soil of chromite overburden. *A. ferroxidans* was used, and the experiment showed a promising result for anoxic microbial processing without energy-intensive pre-processing activities. The maximum nickel extraction was at 41% from 0.99% Ni. Hallberg et al. (2011) proposed bio-processing as an alternative for the energy and reagent extensive processing (i.e., smelting, HPAL, etc.) of nickel laterite. Low-grade nickel (0.4%) from a mine in Western Australia was used in the study. Four acidophilic bacteria were used, namely; (i) *ferrooxidans* a mesophilic iron- and sulfur-oxidizing chemolithotroph; (ii) *Sulfobacillus benefaciens*, a thermotolerant iron- and sulfur-oxidizing mixotroph; (iii) *Acidicaldus organivorans*, a moderately thermophilic, sulfur-oxidizing heterotroph; (iv) *Acidiphilium SJH*, a mesophilic heterotroph. Based on the findings, an acidophilic sulfur-oxidizing bacterium could be utilized for nickel separation from laterite. Ahmad et al. (2011) studied the use of *Penicillium chrysogenum* in extracting various metal ions from laterite ore. The incubation period was 24 days, and they extracted 57.31% of the nickel, which employed some flask shaking compared to 46.53% recovery without shaking. Iron extraction was at 97.78%, aluminum (86.78%), manganese (77.61%), and chromium (34.32%).

Reuse by Phytomining

In phytomining, hyperaccumulator plants are used to grow and concentrate metals by burning, which can be a potential source of heat for energy generation. In the 1990s, Anderson et al. (1999) used *Alyssum bertolonii* from Italy and *Berkheya coddii* from South Africa to recover nickel, thallium, and gold. In Indonesia, the world's largest producer of nickel laterite, a phytomining viability study was conducted from 2004 to 2007. Identification of hyperaccumulator plants was also conducted in Malaysia for its potential in phytomining. There are over 400 identified hyperaccumulator plants for nickel (Laubie et al. 2021), and numerous studies have been conducted in different mining countries. As part of a long-term rehabilitation plan, phytomining allows for revegetation and ensures good erosion control while generating revenue from the extracted nickel (Van der Ent et al. 2013).

Both, biomining and phytomining have the advantage of being environmentally friendly and less energy intensive. Still, the drawback of these processes is the longer processing time to extract the valuable mineral in the ore, which can take months or years (Johnson 2014).

Repurpose for Other Products

There are also some studies on the use of nickel laterite for other purposes (Table 5), such as the use of waste for indirect carbon sequestration (Eusebio et al. 2020), as geopolymer precursor (Longos et al. 2020), ceramic tiles (Bernardo-Arugay et al. 2022) and bricks (Shanmukha et al. 2017). Eusebio et al. (2020) evaluated waste rock from a nickel laterite mine in Southeastern Philippines for its potential utilization in indirect carbon sequestration. Hydrochloric acid was used in the acid-leaching process. The group concluded that nickel laterite waste rock could be a feedstock. However, further study is necessary on cost and energy requirements

Table 5: Repurpose nickel laterite mine waste for other products.

No.	Type of Waste	Description	Reference
1.	Waste Rock	Use of nickel laterite waste rock as feedstock for carbonation in indirect carbon sequestration	(Eusebio et al. 2020, Razote et al. 2021)
2.	Silt	The potential of nickel laterite mine waste as geopolymer precursor by mechanical and thermal activation	(Longos et al. 2020, Tiguea et al. 2021)
3.	Silt	Production of ceramic tiles from nickel laterite mine waste through the ceramic casting method	(Bernardo-Arugay et al. 2022)
4.	Laterite soil	Production of stabilized and compressed lateritic soil bricks	(Shanmukha et al. 2017)

and the effect of reducing agents to yield to prove applicability. Longos et al. (2020) investigated the possibility of producing geopolymer cement using nickel laterite silt or nickel mine waste (NMW). The silt was mixed with coal fly ash (CFA) and sodium hydroxide with sodium silicate (SH-SS) as activators. Different NMW, CFA, and SH-SS ratios were prepared and tested for compressive strength. The results show that the 50%NMW-50%CFA- 0.5 SH-SS attained the highest unconfined compressive strength of 22.10 $\pm$ 5.40MP after 28 days of curing. Bernardo-Arugay et al. (2022) used slip casting to make ceramic tiles from nickel laterite mine waste. They found NMW a suitable raw material for producing ceramic wall and floor tiles. Lastly, Shanmukha et al. (2017) prepared different proportions of laterite, cement, and sand to produce stabilized blocks or bricks. The mix was compacted with a hydraulic press instead of burning to save energy, which is an energy-intensive process. The group found out that the required compressive strength was achievable after 28 days of curing time, and compressive strength is higher than red clay bricks produced by firing.

Processing the NMW for bricks, ceramic, and other products shows great potential to reduce waste in the mined-out areas. However, once the laterite is formed into these products, the metals contained in the material, which is a potential resource in the future, will be contained in the products. The use of the lowest-grade waste rocks and silt should be considered. It is also important to consider the cost of producing such products, especially the energy requirement, to confirm viability.

Repurpose of Mined-Out Area

In a report by the Intergovernmental Forum (IGF) for Mining, Minerals, Metals and Sustainable Development, two case studies were presented on the successful use of mined-out areas in the production of renewable energy resources, the solar energy field in Sullivan Mine, British Columbia and the wind energy park in Ruhr coal mine in Germany (IGF Case Study 2022). In addition, there is the floating solar farm conversion from a collapsed coal mine in China (Pouran 2018). Conversion of the mined-out area to energy farms and tourism sites is a very good option as the final utilization of the area. But much consideration should be taken on the soil stability since mined-out areas are usually filled with loose soil from the overburden and waste rocks previously removed to access the valuable materials. Also, the same as repurposing for other products, it must be considered that there is a potential that the mine waste will become a resource in the future. This must be considered before putting any structure for solar or wind farms. The industry may consider one or a combination of alternative utilization. The mine may allocate a portion of the mined-out area to store the low-grade material and repurpose some areas for solar or wind energy farms. Using hyperaccumulator plants with high heating value to revegetate the temporary storage areas is also a good alternative for phytomining and biomass-to-energy conversion. Studies to recover nickel and other metals in the low-grade nickel laterite are already available. However, applying these studies on an industrial scale has a long way to go. Usually, processing low mineral concentrations increases the amount of the material that must be processed and requires capital-intensive processing technologies (Turcheniuk et al. 2021). Processing waste is often expensive and requires a lot of energy (Mauthoor 2017, Neves et al. 2019). Hence, economics is vital in conducting and presenting research on the reuse of waste. It is not enough to consider only the environmental benefit since it is always the profit that drives the industrial-scale application of these processes.

CONCLUSIONS

The pH of nickel laterite mine waste in this area is neutral to moderately alkaline; hence, the threat of acid mine drainage is unlikely to be a problem. The organic matter is acceptable for plant growth whenever revegetation is considered for mine rehabilitation. Moreover, the laterite mine waste still contains metals that are too low to process for profit but too high for plants and animals if discharged into water and agricultural soil. The plants can absorb high metal content, making them unfit for agricultural products for human consumption.

Considering that nickel laterite is a limited resource, the fate of lower-grade nickel laterite regarded as waste today may change when the higher grade is fully exhausted. Therefore, the best option is to consider further extraction of metals by metallurgical processing when technology and economics allow or use environmentally friendly processes like biomining or phytomining. With this, mines should consider strategic mine rehabilitation, which may include planned positioning and mapping of the waste based on its grade to provide easier access to the waste, which can be a potential resource in the future. Using the lowest grade material for other purposes, such as in brick or ceramic production and additive to construction materials, is also a good option. The, conversion of the mined-out area to renewable energy farms and tourism sites is best for final land use when all extractable materials are exhausted. Finally, it is advisable to take into account the combined application of the various utilization possibilities

ACKNOWLEDGMENT

the administration of Agata Mining Ventures Incorporated for allowing us to conduct this study.

REFERENCES

Ahmad, B., Bhatti, H.N. and Ilyas, S. 2011. Bio-extraction of metal ions from laterite ore by Penicillium chrysogenum. Afr. J. Biotechnol., 10(54): 11196-11205. https://doi.org/10.5897/AJB11.1296

Alibhai, K.A.K., Dudeney, A.W.L., Leak, D.J., Agatzini, S. and Tzeferis, P. 1993. Bioleaching and bioprecipitation of nickel and iron from laterites. FEMS Microbiol. Rev., 11(1-3): 87-95. https://doi.org/10.1111/j.1574-6976.1993.tb00271.x

Amacher, M.C. and Brown, R.W. 1999. D. Barcel6 sample handling and trace analysis of pollutants: Techniques, applications and quality assurance. Mine Waste Character., 6: 585-622.

Amacher, M.C. and Brown, R.W. 2000. Mine waste characterization. Techniq. Instrument. Anal. Chem., 21(C): 585-622. https://doi.org/10.1016/S0167-9244(00)80019-0

Anawati, J., Yuan, R., Kim, J. and Azimi, G. 2020. Selective recovery of scandium from nickel laterite ore by acid roasting–water leaching. Rare Metal Technol., 20: 77-90.

Anderson, C.W.N., Brooks, R.R., Chiarucci, A., Lacoste, C.J., Leblanc, M., Robinson, B.H., Simcock, R. and Stewart, R.B. 1999. Phytomining for nickel, thallium, and gold. J. Geochem. Explor., 67(1-3): 407-415. https://doi.org/10.1016/S0375-6742(99)00055-2

Apodaca, D.C., Domingo, J.P.T., David, C.P.C. and David, S. D. 2018. Siltation load contribution of nickel laterite mining on the coastal water quality of Hinadkaban Bay, Surigao Provinces, Philippines. IOP Conf. Ser. Earth Environ. Sci., 191(1): 1755. https://doi.org/10.1088/1755-1315/191/1/012048

Aysan, G., Gyuer, O.F. and Sangu, E. 2019. Compound geotourism and mine tourism potentiality of Soma region, Turkey. Arab. J. Geosci., 17: 492. https://doi.org/https://doi.org/10.1007/s12517-019-4927-6

Behera, S.K., Panda, S.K., Pradhan, N., Sukla, L. B. and Mishra, B.K. 2012. Extraction of nickel by microbial reduction of lateritic chromite overburden of Sukinda, India. Bioresour. Technol., 125: 17-22. https://doi.org/10.1016/J.BIORTECH.2012.08.076

Bernardo-Arugay, I.C., Fel Jane, A., Echavez, R.H., Aquiatan, L., Carlito, B., Tabelin, R.V. R.V. and Resabal, V.J.T. 2022. Development of ceramic tiles from Philippine nickel laterite mine waste by ceramic casting method. Minerals, 6: 56-69.

Bhattacharjee, S., Dasgupta, P., Kar, D., Bhattacharjee, R. N., Ghosal, S. and Paul, A. R. (2000). A new process for the enrichment of nickel in Sukinda chromite overburden ore. Processing of Fines (2). https://eprints.nmlindia.org/2927/1/307-316.PDF

Bian, Z., Miao, X., Lei, S., Chen, S. E., Wang, W. and Struthers, S. 2012. The challenges of reusing mining and mineral-processing wastes. Science, 337(6095): 702-703. https://doi.org/10.1126/science.1224757

Ceniceros-Gómez, A.E., Macías-Macías, K.Y., de la Cruz-Moreno, J.E., Gutiérrez-Ruiz, M. E. and Martínez-Jardines, L.G. 2018. Characterization of mining tailings in México for the possible recovery of strategic elements. J. South Am. Earth Sci., 88: 72-79. https://doi.org/10.1016/j.jsames.2018.08.013

Chileshe, M.N., Syampungani, S., Festin, E.S., Tigabu, M., Daneshvar, A. and Odén, P.C. 2020. Physico-chemical characteristics and heavy metal concentrations of copper mine wastes in Zambia: Implications for pollution risk and restoration. J. Forest. Res., 31(4): 1283-1293. https://doi.org/10.1007/s11676-019-00921-0

Coto, O., Galizia, F., Hernández, I., Marrero, J. and Donati, E. 2008. Cobalt and nickel recoveries from laterite tailings by organic and inorganic bio-acids. Hydrometallurgy, 94(1-4): 18-22. https://doi.org/10.1016/j.hydromet.2008.05.017

Barrie, J.D. 2018. The evolution, current status, and future prospects of using biotechnologies in the mineral extraction and metal recovery sectors. Minerals, 5: 343.

IGF Case Study. 2022. Achieving a Successful Post-Mining Transition with Renewable Energy. https://www.iisd.org/system/files/2022-01/igf-case-study-post-mining-transition-renewable-energy.pdf

Elias, M. 2013. Nickel Laterites in SE Asia: Geology, Technology, and Economics; Finding the Balance. https://www.csaglobal.com/wp-content/uploads/2015/03/Bali-2013-Elias.pdf

Eusebio, R.C.P., Razote, B.J.B., Del Pilar, H.J.T., Alorro, R.D., Beltran, A.B. and Orbecido, A. H. 2020. Evaluation of the leaching characteristics of low-grade nickel laterite waste rock for indirect carbon sequestration application. Geosyst. Eng., 23(4): 205-215. https://doi.org/10.1080/12269328.2020.1745694

Garside, M. 2022. Distribution of mine production of nickel worldwide in 2020, by country. https://www.statista.com/statistics/603621/global-distribution-of-nickel-mine-production-by-select-country/

Gifford, M. G. 2013. Independent Report on the Nickel Laterite Resource, Agata North, Philippines. April.

Guo, E., Liu, M., Pan, C., Yuan, Q. and Lv, X. 2014. Sintering Process for Limonitic Nickel Laterite. Proceedings of the Extraction and Processing Division Symposium on Pyrometallurgy in Honor of David G.c. Robertson, pp. 623-630.

Guo, X., Li, Z., Jicai Han, Yang, D. and Sun, T. 2021a. Study of straw charcoal as reductant in co-reduction roasting of laterite ore and red mud to prepare powdered ferronickel. Mining Metall. Explor., 16: 466. https://doi.org/10.1007/s42461-021-00466-z

Guo, X., Xu, C., Wang, Y., Xiaohui Li, T. and Sun, T. 2021b. Recovery of nickel and iron from low–grade laterite ore and red mud using co–reduction roasting: Industrial-scale test. Physicochem. Prob. Min. Process., 57(3): 61-72. https://doi.org/10.37190/ppmp/135436

Hallberg, K. B., Grail, B. M., Plessis, C. A. D. and Johnson, D. B. 2011. Reductive dissolution of ferric iron minerals: A new approach for bio-processing nickel laterites. Minerals Engineering, 24(7): 620-624. https://doi.org/10.1016/j.mineng.2010.09.005

Handayani, S. and Suratman, S. 2017. Bioleaching of low grade nickel ore using indigenous fungi. Indonesian Mining Journal, 19(3): 143-152. https://doi.org/10.30556/imj.vol19.no3.2016.540

Jamieson, H. E., Walker, S. R. and Parsons, M. B. 2015. Mineralogical characterization of mine waste. Applied Geochemistry, 57: 85-105. https://doi.org/10.1016/j.apgeochem.2014.12.014

Johnson, D.B. 2014. Biomining-biotechnologies for extracting and recovering metals from ores and waste materials. Curr. Opin. Biotechnol., 30: 24-31. https://doi.org/10.1016/j.copbio.2014.04.008

Johnson, D.B., Grail, B.M. and Hallberg, K.B. 2013. A new direction for biomining: Extraction of metals by reductive dissolution of oxidized ores. Minerals, 3(1): 49-58. https://doi.org/10.3390/min3010049

Kadlec, V., Holubik, O., Prochazkova, E. and Urbanova, J. and Tippl, M. 2012. Soil organic carbon dynamics and its influence on the soil erodibility factor. Soil Water Res., 7: 97-108.

Kaya, S. and Topkaya, Y.A. 2015. Extraction behavior of scandium from a refractory nickel laterite ore during the pressure acid leaching process. Technol., Econ., Environ. Impl., 15: 651. https://doi.org/10.1016/B978-0-12-802328-0.00011-5

Komnitsas, K., Petrakis, E., Bartzas, G. and Karmali, V. 2019. Column leaching of low-grade saprolitic laterites and valorization of leaching residues. Sci. Total Environ., 665: 347-357. https://doi.org/10.1016/j.scitotenv.2019.01.381

Laubie, B., Vaughan, J. and Simonnot, M.O. 2021. Processing of hyperaccumulator plants to nickel products. Metals, 16: 545. https://doi.org/https://doi.org/10.1007/978-3-030-58904-2_3

Lebre, E., Corder, G. and Golev, A. 2017a. The Role of the Mining Industry in Circular Economy. Wiley, NY.

Lèbre, É., Corder, G. D. and Golev, A. 2017b. Sustainable practices in the management of mining waste: A focus on the mineral resource. Minerals Eng., 107: 34-42. https://doi.org/10.1016/j.mineng.2016.12.004

Li, B., Ding, Z., Wei, Y., Zhou, S. and Wang, H. 2018a. Reduction of

nickel and iron from low-grade nickel laterite ore via a solid-state deoxidization method using methane. Mater. Trans., 59(7): 1180-1185. https://doi.org/10.2320/matertrans.M2017351

Li, B., Wang, H. and Wei, Y. 2011a. The reduction of nickel from low-grade nickel laterite ore using a solid-state deoxidization method. Min. Eng., 24(14): 1556-1562. https://doi.org/10.1016/J.MINENG.2011.08.006

Li, G., Rao, M., Jiang, T., Huang, Q. and Peng, Z. 2011. Leaching of limonitic laterite ore by acidic thiosulfate solution. Min. Eng., 24(8): 859-863. https://doi.org/10.1016/j.mineng.2011.03.010

Li, G., Zhou, Q., Zhu, Z., Luo, J., Rao, M., Peng, Z. and Jiang, T. 2018. Selective leaching of nickel and cobalt from limonitic laterite using phosphoric acid: An alternative for value-added processing of laterite. J. Clean. Prod., 189: 620-626. https://doi.org/10.1016/j.jclepro.2018.04.083

Liu, Y., Tian, Y. W. and Zhai, Y. C. 2012. A comprehensive utilization of laterite nickel ore. Adv. Mater. Res., 415-417: 934-937. https://doi.org/10.4028/www.scientific.net/AMR.415-417.934

Longos, A., Tigue, A.A., Dollente, I. J., Malenab, R.A., Bernardo-Arugay, I., Hinode, H., Kurniawan, W. and Promentilla, M.A. 2020. Optimization of the mix formulation of geopolymer using nickel-laterite mine waste and coal fly ash. Minerals, 16: 36-59.

Longos, A., Tigue, A.A., Malenab, R.A., Dollente, I.J. and Promentilla, M.A. 2020. Mechanical and thermal activation of nickel-laterite mine waste as a precursor for geopolymer synthesis. Engineering, 7(6): 100148. https://doi.org/10.1016/j.rineng.2020.100148

Lottermoser, B.G. 2010. Mine Wastes Characterization, Treatment, and Environmental Impacts. Springer-Verlag, Berlin.

Lottermoser, B.G. 2011. Recycling, reuse, and rehabilitation of mine wastes. Elements, 7(6): 405-410. https://doi.org/10.2113/gselements.7.6.405

Luo, J., Li, G., Rao, M., Peng, Z., Zhang, Y. and Jiang, T. 2015. Atmospheric leaching characteristics of nickel and iron in limonitic laterite with sulfuric acid in the presence of sodium sulfite. Minerals Eng., 78: 38-44. https://doi.org/10.1016/j.mineng.2015.03.030

MacCarthy, J., Nosrati, A., Skinner, W. and Addai-Mensah, J. 2016. Atmospheric acid leaching mechanisms, kinetics, and rheological studies of a low-grade saprolitic nickel laterite ore. Hydrometallurgy, 160: 26-37. https://doi.org/10.1016/J.HYDROMET.2015.11.004

Marrero, J., Coto, O. and Schippers, A. 2017. Anaerobic and aerobic reductive dissolutions of iron-rich nickel laterite overburden by Acidithiobacillus. Hydrometallurgy, 168: 49-55. https://doi.org/10.1016/j.hydromet.2016.08.012

Mauthoor, S. 2017. Uncovering industrial symbiosis potentials in a small island developing state: The case study of Mauritius. J. Clean. Prod., 147: 506-513. https://doi.org/10.1016/j.jclepro.2017.01.138

MGB13. 2021. Caraga Region Mineral Profile. Philippines Mines and Geosciences Bureau Region 13. Retrieved from https://www.mgbr13.ph/wp-content/uploads/2021/04/Caraga-Regional-Mineral-Profile-Quickfacts-2020-Infographics.pdf

Mohanty, M., Dhal, N., Patra, P., Das, B. and Reddy, P. (2010). Phytoremediation: a Novel Approach for Utilization of Iron-Ore Wastes. Reviews of Environmental Contamination and Toxicology.

Murphy, Z. 2022. Virginia, Abandoned Coal Mines Are Transformed into Solar Farms. The Washington Post. Retrieved from https://www.washingtonpost.com/climate-solutions/2022/03/03/coal-mines-solar-farms-climate-change-video/

Neves, A., Godina, R., Azevedo, S.G., Pimentel, C. and Matias, J.C.O. 2019. The potential of industrial symbiosis: case analysis and main drivers and barriers to its implementation. Sustainability (Switzerland), 11(24): 1-68. https://doi.org/10.3390/su11247095

Newsome, L., Solano Arguedas, A., Coker, V.S., Boothman, C. and Lloyd, J.R. 2020. Manganese and cobalt redox cycling in laterites; Biogeochemical and bioprocessing implications. Chemical Geol., 531: 119330. https://doi.org/10.1016/J.CHEMGEO.2019.119330

Oliveira, V.D.A., Rodrigues, M.L.M. and Leão, V.A. 2021. Reduction roasting and bioleaching of limonite ore. Hydrometallurgy, 200: 105554. https://doi.org/10.1016/J.HYDROMET.2021.105554

Pouran, H.M. 2018. From collapsed coal mines to floating solar farms, why China's new power stations matter. Energy Policy, 123: 414-420. https://doi.org/10.1016/J.ENPOL.2018.09.010

Purwanto, H., Shimada, T., Takahashi, R. and YagiJun-ichiro. 2001. Reduction rate of cement bonded laterite briquette with CO-CO2 gas. ISIJ Int., 41: S31-S35. https://doi.org/https://doi.org/10.2355/isijinternational.41.Suppl_S31

Razote, B.J., Cerna, K.M. Dela, P.M.J., Ramon Eusebio, C., Alorro, R., Beltran, A. and Orbecido, A. 2021. Leaching characteristics of an iron-rich siltation pond waste and its viability in indirect carbon sequestration. Int. J. Mining, Reclam. Environ., 10: 212. https://doi.org/0.1080/17480930.2021.1876819

Sahajwalla, V. 2018. Green processes: Transforming waste into valuable resources. Engineering, 4(3): 309-310. https://doi.org/10.1016/j.eng.2018.05.011

Schaider, L.A., Senn, D.B., Brabander, D., Mccarthy, K.D. and Shine, J.P. 2007. Characterization of zinc, lead, and cadmium in mine waste: Implications for transport, exposure, and bioavailability. Environ. Sci. Technol., 41(11): 4164-4171. https://doi.org/10.1021/es0626943

Shanmukha, K., Manjunath, K. and Prahallada, M. 2017. Stabilized and compressed laterite soil bricks. J. Civ. Eng., 7(3): 35-40.

Tabios III, G.Q. 2020. Impacts of Laterite Mining of Nickel and Iron Ores on Watersheds. National Academy of Science and Technology, Philippines.

Terekhov, D.S. and Emmanuel, N.V. 2013. Direct extraction of nickel and iron from laterite ores using the carbonyl Process. Minerals Engineering, 54: 124-130. https://doi.org/10.1016/j.mineng.2013.07.008

Thomas, G.W. 1996. Methods of Soil Analysis. Soil Science Society of America and American Society of Agronomy, Madison, WI.

Tiguea, A A.S., Longos Jr., A.L., Malenab, R.A.J., Dollentea, I.J.R. and Promentilla, M.A.B. 2021. Compressive strength and leaching characteristic of geopolymer composite from coal fly ash and nickel laterite mine spoils. Chem. Eng. Trans., 88: https://doi.org/10.3303/CET2188194

Turcheniuk, K., Bondarev, D., Amatucci, G.G. and Yushin, G. 2021. Battery materials for low-cost electric transportation. Mater. Tod., 42: 57-72. https://doi.org/10.1016/J.MATTOD.2020.09.027

Van der Ent, A., Baker, A.J.M., van Balgooy, M. M.J. and Tjoa, A. 2013. Ultramafic nickel laterites in Indonesia (Sulawesi, Halmahera): Mining, nickel hyperaccumulators and opportunities for phytomining. J. Geochem. Explor., 128: 72-79. https://doi.org/10.1016/J.GEXPLO.2013.01.009

Xiao, J., Ding, W., Peng, Y., Chen, T., Zou, K. and Wang, Z. 2020. Extraction of nickel from garnierite laterite ore using roasting and magnetic separation with calcium chloride and iron concentrate. Minerals, 10(4): 1-13. https://doi.org/10.3390/min10040352

Xue, Y., Zhu, D., Pan, J., Guo, Z., Yang, C., Tian, H., Duan, X., Huang, Q., Liaoting, P. and Huang, X. 2020. Effective utilization of limonitic nickel laterite via pressurized densification process and its relevant mechanism. Minerals, 1: 21-36.

Zhai, Y.C., Mu, W.N., Liu, Y. and Xu, Q. 2010. A green process for recovering nickel from nickeliferous laterite ores. Trans. Nonferr. Metals Soc. China, 20(1): s65-s70. https://doi.org/10.1016/S1003-6326(10)60014-3

Zhu, D., Pan, L., Guo, Z., Pan, J. and Zhang, F. 2019. Utilization of limonitic nickel laterite to produce ferronickel concentrate by the selective reduction-magnetic separation process. Adv. Powder Technol., 30(2): 451-460. https://doi.org/10.1016/j.apt.2018.11.024

Zhu, D., Xue, Y., Pan, J., Yang, C., Guo, Z., Tian, H., Wang, X., Huang, Q., Pan, L. and Huang, X. 2020. Co-benefits of CO_2 emission reduction and sintering performance improvement of limonitic laterite via hot exhaust-gas recirculation sintering. Powder Technol., 373: 727-740. https://doi.org/10.1016/J.POWTEC.2020.07.018

An Attempt to Reduce the Electrocoagulation Costs and to Ensure the Reuse of Treated Aqueous Dye Solution

D. Jovitha Jane*, M. S. Asath Murphy*, Riju S Robin*, S Sahaya Leenus*, Jegathambal Palanichamy** and Parameswari Kalivel†

*Department of Applied Chemistry, Karunya Institute of Technology and Sciences, Coimbatore-641114, Tamil Nadu, India

**Water Institute, Karunya Institute of Technology and Sciences, Coimbatore-641114, Tamil Nadu, India

†Corresponding author: Parameswari Kalivel; parameswari@karunya.edu

ABSTRACT

In most of the research works, similar metal electrodes were used, resulting in high operating costs, and the reuse of the treated water was not explored. The major goal of this research is to lower the cost of the electrocoagulation (EC) process by employing electrodes made of different metals and to investigate whether it is possible to reuse the water that has been treated by doing so. It was done to optimize the operational parameters such as pH, voltage, time, electrolyte, and dye concentrations. The energy and electrode consumption was calculated as 0.29 kWh.m^{-3} and 3.5×10^{-2} kg.m^{-3}, respectively. The HPLC and LC-MS studies shows the degradation of dye and the formation of intermediary compounds, which were less toxic. The sludge obtained from the EC process was subjected to EDX and XPS analysis to know the composition of metals and the formation of metal hydroxide coagulants. The phytotoxicity of the treated water after EC was examined using *Trigonella foenum-graecum* seeds. The results showed an utmost color removal efficiency (CRE%) and COD removal of 99.78% and 92.86% with an operating cost of US$ 0.028, which is comparatively 98.12% lower than the other conventional electrodes. The treated toxicity test of water was comparable to the toxicity test of tap water.

INTRODUCTION

All living things primarily depend on water. Nowadays, as the water bodies which are the sources for drinking water and agricultural purposes are getting polluted at a high rate due to the release of contaminants from industries, the scarcity of water has emerged as one of the biggest issues in the world. The wastewater can come from textiles (Kim et al. 2002), food (Sengil & Ozacar 2006), poultry slaughterhouses (Bayramoglu et al. 2006), cosmetic and pharmaceutical (Boroski et al. 2009), paper (Katal & Pahlavanzadeh 2011), paint (Akyol 2012) and various other industries too. But the textile dyeing industry greatly contributes to water pollution (Sharma & Uma 2011). This is because these industries ingest high volumes of water in their fabricating process, such as dyeing and finishing. In the dyeing stage, innumerable dyes are used, eventually giving out a wide range of colors so that the effluent's attributes vary greatly (Gurses et al. 2002).

The most widely used dye in the dyeing units, azo dyes, makes up more than 50% of the commercially available dyes. The next widely used group is the anthraquinone dyes (Holkar et al. 2016). Around 10,000 commercially available dyes are produced annually, and 7×105 tonnes of dye-related materials (Rai et al. 2005). Coraline Rubine GFL, an azo dye, has an annual fabrication rate of about 70%. And 370 thousand metric tons of dyes and pigments are being produced globally (Tony et al. 2009). A mixture of acids, pesticides, salts, pigments, and heavy metals constitutes textile wastewater (Pensupa et al. 2017). Most synthetic dyes and their intermediary compounds may be poisonous, mutagenic, carcinogenic, or teratogenic to the environmental species (Wang et al. 2019, Maron & Ames 1983).

Due to their disorganization, an extensive quantity of dyestuff has been sent out from the industries during the dyeing process. These dyes may easily be distinguished because of their capacity to absorb light in the visible region, even at very low concentrations of around 1 ppm (Holkar et al. 2016). These dye particles avert the sunlight's permeation into the water, constricting the photosynthetic activity of the aquatic plants and decreasing the dissolved oxygen in the water bodies, possibly affecting the marine animals. This is because the dyes easily absorb and reflect

the light (Solis et al. 2012, Mansour et al. 2011). As these dyestuffs undergo biodegradation, many aromatic amines are formed, responsible for the momentous lethal effect on living organisms. Most aromatic amines are found to be suspect cancer factors (Chung 2016). Even before cleaving into aromatic amines, certain azo dyes seem carcinogenic. But this carcinogenicity is due to the other cleaved product known as benzidine, which is a causative agent for plenty of tumors. P-phenylenediamine (p-PDA), another dye constituent, is a contact allergen (Graca et al. 2001). Reports on the negative impact of anthraquinone and triphenylmethane dyes are also seen in the literature (Cui et al. 2016, Sharma et al. 2004, Cheriaa et al. 2012).

Therefore, an urgent need arises to treat these wastewaters by conventional technique. The common methods adopted for the treatment are biological (Wu et al. 2019), chemical oxidation (Azbar et al. 2004), electrocoagulation (EC), electroflotation (Rajeshwar et al. 1994), activated charcoal adsorption, chemical coagulation (Slokar & Le Marechal 1998), photocatalytic degradation (Behera et al. 2008), membrane separation (Van der Bruggen et al. 2001, Joshi et al. 2001), Fenton process (Pan et al. 2020), electrodialysis (Shahi et al. 2001), ultrafiltration and ozonation (Lin & Chen 1997) and aerobic or anaerobic digestion (An et al. 1996). Even though all these methods have been known, each has its drawbacks when treating real-time effluent. When the biological treatment method is used, the microorganisms employed in the treatment process get deceased due to a high amount of dye particles (Vlyssides et al. 1999). Secondary water pollution will occur as other chemicals are added to chemical coagulation and oxidation (Azbar et al. 2004). Adsorption with activated carbon (AC) often removes the dye from an aqueous solution. Still, AC regeneration and efficiency are confined to its equilibrium (Low & Lee 1997, McKay 1984). In the photocatalytic process, a pre-treatment is required to prevent the deterioration of the active sites and the detrimental interference of the catalyst used (Ochiai & Fujishima 2012). In the Fenton process, the pH range has to be controlled greatly (Giroto et al. 2006). Other processes like reverse osmosis, ultrafiltration, and other membrane separation techniques have their limitations of high cost and low output (Marcucci et al. 2001, Sridhar et al. 2002, Voigt et al. 2001).

Even though the electrocoagulation process has merits and demerits, it almost suits the processing of textile dyeing effluents compared to other techniques. The equipment used in the EC process is easy to handle, and there is less need for adding chemicals throughout the process (Kobya et al. 2017). Some of their demerits include high electrical energy consumption, restoration of the sacrificial anodes at regular intervals, and passivation could occur due to the development of oxide film on the negative electrode. Sludge is generated when dye contaminants are removed, but less sludge is created in the EC than during flocculation or chemical coagulation procedures (Barrera-Diaz et al. 2011, Moussa et al. 2017).

The primary goal of this work is to remove the dye particles from the simulated Coralene Rubine GFL 200% dye solution using different metal electrodes to lower the overall process' operational costs. Studies have been done on operating parameter optimization, COD removal, operating cost, and color removal efficiency (CRE%). Through the phytotoxicity investigations, attention has also been paid to the treatment dye solution's toxicity assessment and potential for reuse.

MATERIALS AND METHODS

Experiment

The experimentations were done using the simulated dye solutions of Coralene Rubine GFL 200% dye. The characteristics and structure of the dye are specified in Table 1 and Fig. 1.

Table 1: Characteristics of the dye.

C. I name	Disperse Red 73, Allilon Rubine FL, Chemilene Rubine SE-GFL
Empirical formula	$C_{18}H_{16}N_6O_2$
Molecular weight	348.36
IUPAC name	2-[[4-[(2-cyanoethyl)ethylamino]phenyl]azo]-5-nitro benzonitrile
Melting point	149-150°C
Boiling point	614.2 ± 55°C
Density	1.22 ± 0.1 g.cm^{-3}
Absorption maximum	618 nm
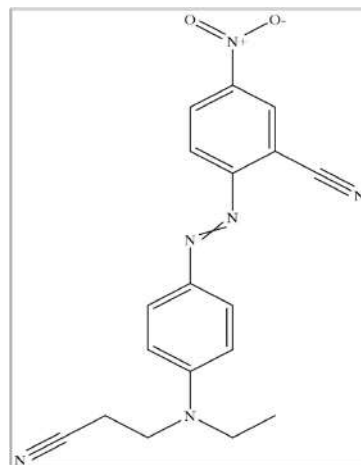
Fig. 1: Structure of the dye.

The aqueous solution of the dye was made with a 110 mg.L^{-1} dye, which required dissolving 0.022 g of dye in 200 mL of double-distilled water.1 g.L^{-1} (0.2 g) of sodium chloride was added to the simulated dye solution, which acts as an electrolyte and facilitates the movement of ions and formation of flocs. 0.1 N hydrochloric acid was used to make the solution acidic, and to make it alkaline, 0.1 N sodium hydroxide was used. For electrocoagulation, aluminum and copper plates with a length of 9 cm, width of 3.5 cm, and thickness of 0.5 mm were used as an anode and cathode, respectively. The interelectrode distance was kept at about 4 cm. Every experiment was conducted at room temperature using a magnetic stirrer to speed up the movement of ions, and an external DC power supply was used. The area submerged in the solution is about 5.1 cm. Fig. 2 shows the EC setup and simulated dye solution before and after the EC process. The experiments involved changing the pH. (4, 5, 6, 7, 8, 9, 10), voltage (4, 6, 8, 10, 12, 15), reaction time (5, 10, 15, 20, 25, 30 min), initial dye concentration (70 mg.L^{-1} to 130 mg.L^{-1}), and the concentration of electrolyte (0.1, 0.15, 0.2, 0.25, 0.3, 0.35 g) and the color removal efficiency (CRE%) was calculated. After each reaction, the treated dye solution was filtered, and the sludge was air-dried and given for further analysis. The COD digester (HACH DRB 200 Digital Reactor) was used to calculate the COD. The other apparatus required were the COD vials, burette, and 250 mL conical flask. 2.5 mL of the treated dye solution was taken in the COD vial. 0.25 N of standard potassium dichromate ($K_2Cr_2O_7$) solution was added to the sample. Then, the vials added a pinch of mercuric sulfate ($HgSO_4$) and 3.5 mL of concentrated sulphuric acid (conc. H_2SO_4). It was then tightly closed and kept at the COD digester at 150°C for 2 h. It was then allowed to cool down to room temperature and transferred into the conical flask. The burette was then filled with 0.1 N standard ferrous

ammonium sulfate (FAS) [Fe(SO_4)(NH_4)$_2$], and 2 drops of ferroin indicator were added to the sample. It was titrated against the FAS solution. The final point was marked by a color change from green to reddish brown, and the COD was determined.

Analytical Methods

UV-Visible Spectrophotometer

The absorption maximum of the dye was measured using a UV-Visible spectrophotometer [JASCO V-650]. From the absorbance values, the color removal efficiency was calculated by the formula,

$$CRE\% = \frac{C_0 - C}{C_0} \times 100 \qquad …(1)$$

where,

C_0 is the initial absorbance of the dye

C is the final absorbance of the treated dye solution

Chemical Oxygen Demand (COD)

The COD was calculated for the simulated dye solution and the treated sample with maximum CRE% obtained. It is then compared with the blank, i.e., the double distilled water, and calculated using the formula,

$$COD = \frac{(a-b) \times N \times 8 \times 1000}{Volume\ of\ sample} \qquad …(2)$$

where,

a is the volume of FAS consumed for the titration of blank (mL)

b is the volume of FAS consumed for the titration of the sample (mL)

N is the normality of titrant (FAS)

8×1000 is the milli equivalent weight of oxygen (mL.L^{-1})

Fig. 2: (a) EC set up, simulated dye solution (b) before EC (c) after EC.

X-Ray Photoelectron Spectroscopy (XPS)
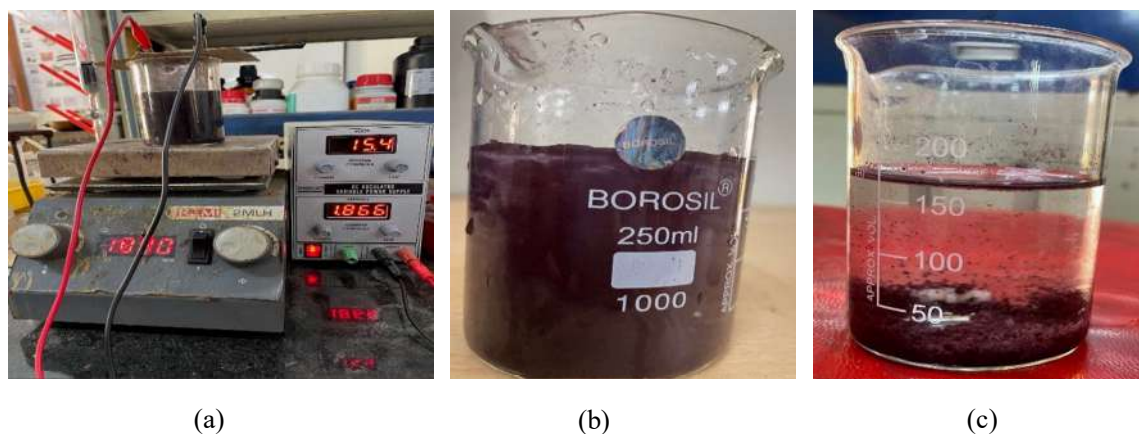
The sludge of the treated dye solution with the highest CRE% of 99.78 (at pH 7, contact time of 15 min, at 4 V, initial dye concentration of 110 mg.L^{-1} and 1 g.L^{-1} of electrolyte concentration) was secluded, air-dried, and investigated for the hydroxides formed during the EC process using X-ray Photoelectron Spectroscopy (XPS). The spectrum was obtained using Al monochromatic light as the source and energy of 1486.6 eV in the Scienta Omicron Nanotechnology by Oxford Instrument.

High-Performance Liquid Chromatography (HPLC)

The HPLC analysis was carried out to determine the number of dye components present in the dye solution before the EC process and the treated sample following the EC process. The Shimadzu SPD-M20A generated the HPLC chromatogram with acetonitrile as the filtrate's solvent.

Liquid Chromatography-Mass Spectrometry (LC-MS)

The plausible degradation of the dye can be studied through the intermediate product peaks formed when the samples are subjected to LC-MS. The simulated and treated dye solutions were analyzed through LC-MS, and the mass spectrum was captured from Shimadzu Japan 2020.

Energy Dispersive X-Ray Analysis (EDX)

During electrocoagulation, the metals used as electrodes may undergo dissolution, and the metal ions may combine with the sludge particles. Therefore, to know the percentage of the elemental composition of the metals in the sludge, the sludge obtained from the EC process was subjected to EDX analysis.

Phytotoxicity Studies

Even a meager concentration of the dyestuffs in the treated water can exhibit a major effect on plant growth and drastically affect the photosynthesis process (Kalivel et al. 2021). In the electrocoagulation process, the dyes are not completely removed. Instead, they form many transitional compounds. These compounds should be less toxic for the plant to attain its normal growth (Kalivel et al. 2020). Therefore, to check the feasibility of reusing the treated dye solution, phytotoxicity studies were carried out with *Trigonella foenum-graecum* seeds. 50 seeds were taken in three different pots.

Fenugreek is an annual plant cultivated worldwide, and India is its largest producer. It can flourish in almost every climatic environment and booms well in places with moderate showers and temperatures. Even though fertile soil is the epitome for its growth, it can also sustain in acidic to neutral soil. Therefore, these seeds were chosen for the studies. An equal volume of tap water (control), simulated dye solution, and treated dye solution with Al/Cu electrodes were taken and watered for about 10 days. The shoot and root length and the germination percentage were calculated for the dye and treated dye solution and was compared with the control. The formula calculated the germination percentage.

$$Germination\ percentage = \frac{number\ of\ seeds\ germinated}{total\ number\ of\ seeds\ sown} \times 100 \qquad …(3)$$

RESULTS AND DISCUSSION

Influence of Operational Parameters on CRE %

The color removal efficiency is largely altered by many operational parameters such as pH, voltage, contact time, electrolyte concentration, initial dye concentration, interelectrode distance, and electrode surface area dipped in the solution. The simulated dye solution was taken, and a few parameters were varied. The maximum CRE% from the optimized results was determined; the findings are in Fig. 2.

Influence of pH

In the electrocoagulation process, one of the key criteria is the preliminary pH of the dye solution (Hutcherson 2015). The pH of the solution affects the electrical conductivity. Therefore, pH, either lower or higher than the optimal range, alters the color removal efficiency of the solution (Canizares et al. 2009). The pH was optimized by varying from acidic to alkaline medium, i.e., 4 to 10. The dye concentration, electrolyte concentration, and voltage were kept constant at 110 mg.L^{-1}, 1 g.L^{-1}, and 15 V, respectively. Fig. 3(a) shows the graph for each pH (4, 5, 6, 7, 8, 9, 10) varying the time (5, 10, 15, 20, 25, 30 min). For pH 4, the CRE% was 97.24 at 5 min; as the time escalated, the CRE% also escalated to 98.95% at 30 min. The same increment in the CRE% was observed for the pH 5, 6, 7, 8, 9, and 10. At pH 5 and 6, the CRE% was 98.72 and 98.25, respectively, at 5 min, and it raised to 99.44% and 99.36% at 30 min. At a neutral pH, the CRE% was 99.62 at 5 min, constantly increasing as the time increased to 30 min. At pH 8, 9, and 10, the same elevation in CRE% was seen. By comparing the CRE% of all the pH at different times, the CRE% was high in acidic and alkaline mediums. But, when the optimal pH is taken as acidic or alkaline, the usage of chemicals to alter the pH will be required. Therefore, the EC process becomes more effective when a neutral medium is taken as an optimal range. For pH 7, the CRE% obtained for time 5, 10, 15, 20, 25, and 30 min are 99.62, 99.68, 99.87, 99.87, 99.87, and 99.89, respectively. The CRE% remains constant for 15 min to 25 min, so the minimal time of 15 min with a CRE% of 99.87 is taken as the best optimum time for the abstraction

of dye from the aqueous solution of the dye.

Influence of Voltage

The time was varied for different voltages to ascertain the optimal voltage for the abstraction of the dye particles from the aqueous dye solution. The experiments were carried out at optimized pH 7 at a time of 15 min and constant initial dye concentration of 110 mg.L^{-1}, and electrolyte concentration at 1 g.L^{-1}. The amount of current given through the DC power supply greatly influences the CRE%. Therefore, the voltage is changed and taken as the varying parameter to achieve a specific electric current. As the voltage was tuned, the corresponding current was also noted. When the electric current increases, the dissolution of the anode also increases, thereby producing a high operational cost. If the electric current is lowered or raised from the optimal value, the CRE% also fluctuates (Yadav et al. 2012, Shankar et al. 2014). The experiments were performed by varying voltage from 4 V to 15 V (4, 6, 8, 10, 12, and 15 V), shown in Fig. 3(b). At 4 V for 5 min, the CRE% was 99.33 and gradually increased to 99.79% at 30 min. The same pattern of change was observed for 6, 8, 10, 12, and 15 V. At the optimized time of 15 min. The CRE% was 99.78, 99.78,

99.78, 99.85, 99.86, and 99.87 for 4, 6, 8, 10, 12, and 15 V, respectively. When the voltage was increased at 15 min, there was no significant difference in the CRE%, so the optimal value was 4 V with the CRE% of 99.78. This shows that, even at a very low voltage, the color removal efficiency was high, yielding a low energy consumption and electrode dissolution.

Influence of Initial Dye Concentration

Given that the coloring chemicals' concentration in the textile industry varies widely, the initial dye concentration also significantly affects the electrocoagulation process (Golder et al. 2006). The experimentations were done by varying the dye concentration from 70 mg.L^{-1} to 130 mg.L^{-1} at constant pH of 7, time 15 min, and 4 V, and the graph is shown in Fig. 3(c). The CRE% decreased as the dye concentration increased. At 70 mg.L^{-1}, the CRE% was 99.84 and decreased to 99.42% at 130 mg.L^{-1}. The CRE% at 110 mg.L^{-1} is 99.78, which showed a slight elevation to the other lower concentrations. So, the optimum initial dye concentration was taken as 110 mg.L^{-1}. This decreasing pattern may be due to the development of intermediary compounds, which may reduce the performance of the electrodes by blocking their active sites (Modirshahla et al. 2007).
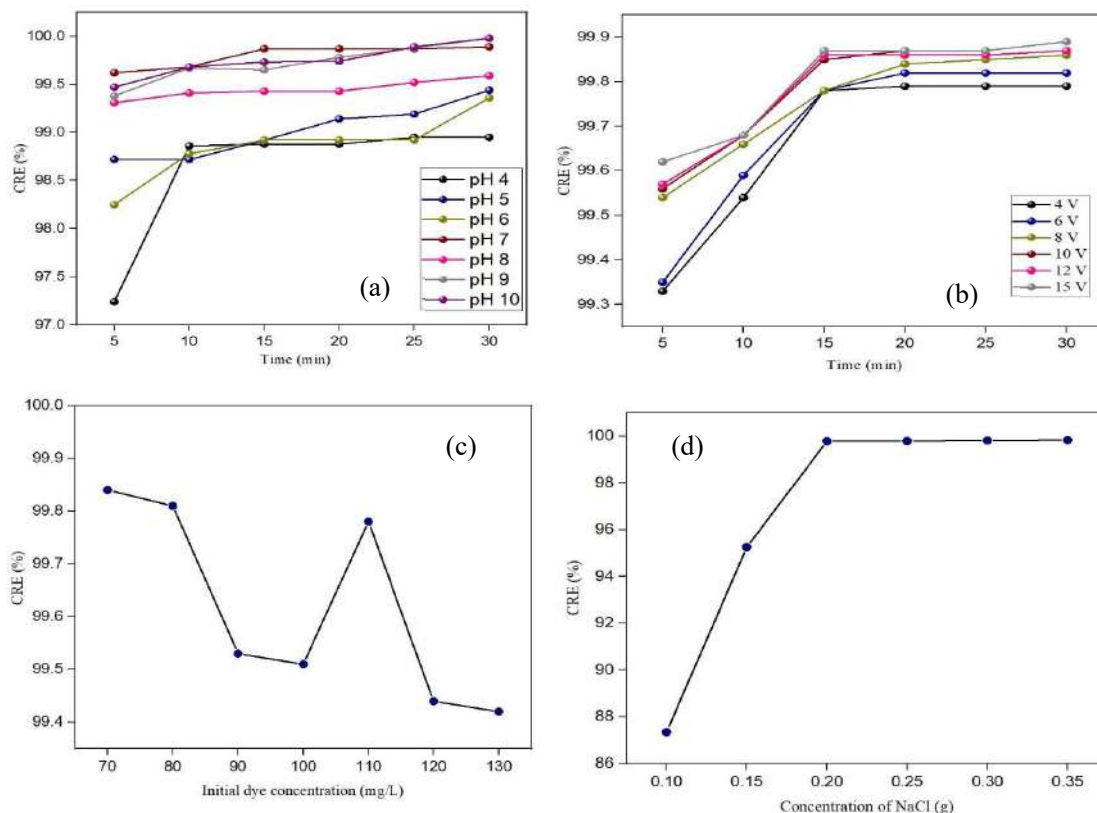

Fig. 3: Effect of CRE% on (a) pH vs. time, (b) voltage vs. time, (c) initial dye concentration, (d) electrolyte concentration.

Influence of Concentration of the Electrolyte

The electrolyte is added to the EC process to facilitate the conductivity and the movement of ions in the solution. The higher the electrolyte concentration, the greater its conductivity and current density. When the strength of the electrolyte is high, the conductivity may increase with the same cell voltage applied (Sengil & Ozacar 2006, Mollah et al. 2001). The experiments were performed using NaCl as an electrolyte by varying its concentration at 0.5, 0.75, 1, 1.25, 1.5, and 1.75 g.L^{-1} (i.e., 0.1, 0.15, 0.2, 0.25, 0.3, 0.35 g) under the optimized conditions of pH 7, 15 min, 4 V and 110 mg.L^{-1} and the graph is shown in Fig. 3(d). The CRE% increased as the concentration of the electrolyte increased. At 0.5 g.L^{-1}, CRE% was 87.33, increasing to 99.83% at 1.75 g.L^{-1}. There were minute differences in the CRE% from 1 g.L^{-1} to 1.75 g.L^{-1}, so the minimum concentration of 1 g.L^{-1} was optimal for the dye removal process.

Economical Parameters

Consumption of Energy and Electrode

The energy and electrode consumption is plotted against different voltages, and the graph is given in Fig. 4(a) and (b), respectively. The plots indicate that the amount of energy and electrode consumed for the EC process increases when the voltage increases. At 4 V for 15 min, the energy consumption and electrode were 0.29 kWh.m^{-3} and 0.035 kg.m^{-3}. When the voltage was tuned constantly (6, 8, 10, 12, 14, 16, 18, and 20 V), an elevation was observed, giving 9.28 kWh.m^{-3} and 0.253 kg.m^{-3} of consumption of energy and electrode, respectively, at 20 V. Therefore, with a very low voltage, a maximum CRE% (99.78) was obtained.

Operating Cost

The operational cost analysis is one of the major economical parameters in electrocoagulation. The cost analysis includes the cost of electrodes, the cost of energy used during the EC process, the cost of the equipment, and other fixed costs. As the equipment used in the EC process is very cost-effective and easy to maintain, the operating cost mainly depends on the other two categories (Daneshvar et al. 2006). The operating cost was calculated using the formula,

$$\text{Operational cost, } C_{op} = a\, C_{energy} + b\, C_{electrode} \qquad \ldots(4)$$

where,

C_{energy} and $C_{electrode}$ are energy and electrode consumption

a is the cost of current per unit (US$ 0.077)

b is the cost of a single plate of the electrode (US$ 0.13)

The operating cost analysis was done after the optimization of the operational parameters. The cost calculated was around 0.028 US$/$m^3$. As in the literature, when aluminum and iron electrodes were used, the operating cost was 1.5 US$/m (Bener et al. 2019). Similarly, when aluminum was used as an anode and cathode, the operating cost analysis was reported as 0.7 US$/$m^3$ (Villalobos-Lara et al. 2021). While using copper sheets as electrodes, the cost reported was 0.803-3.03 US$/$m^3$ (Shaker et al. 2021). The above data proves that, while using dissimilar electrodes of Al/Cu, the cost is much lower than other conventional electrodes.

EDX Studies

From the EDX analysis of the sludge, it is clear that the metal ion from the anode has been released, which is the main source for the formation of the metal hydroxide coagulants

Fig. 4: Voltage vs. (a), (b) Energy, Electrode consumption.
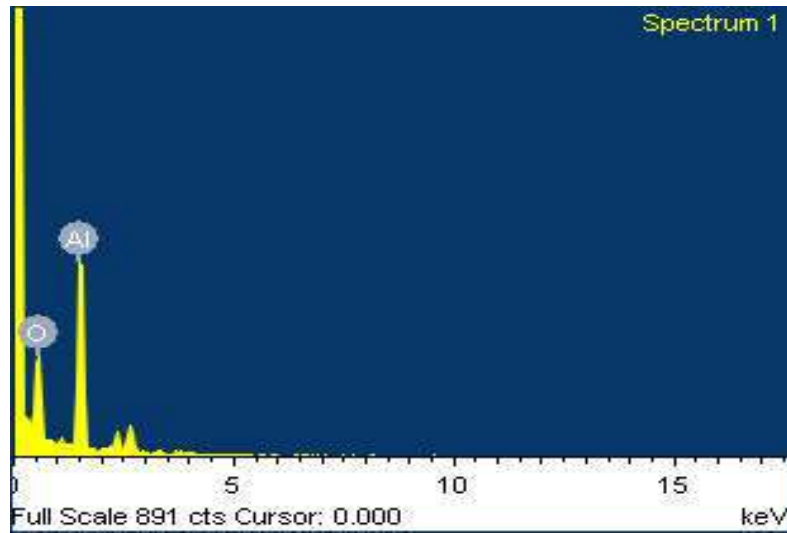
Fig. 5: EDX spectrum of the sludge obtained.

having high adsorbing capacity, which then acts as the floc and binds with the dye components from the simulated dye solution thus producing a clear solution (Chen 2004). From the Fig. 5 EDX graph, 31.38 atomic percentages of aluminum and 68.62 atomic percentages of oxygen are present in the sludge obtained after filtration of the treated dye solution.
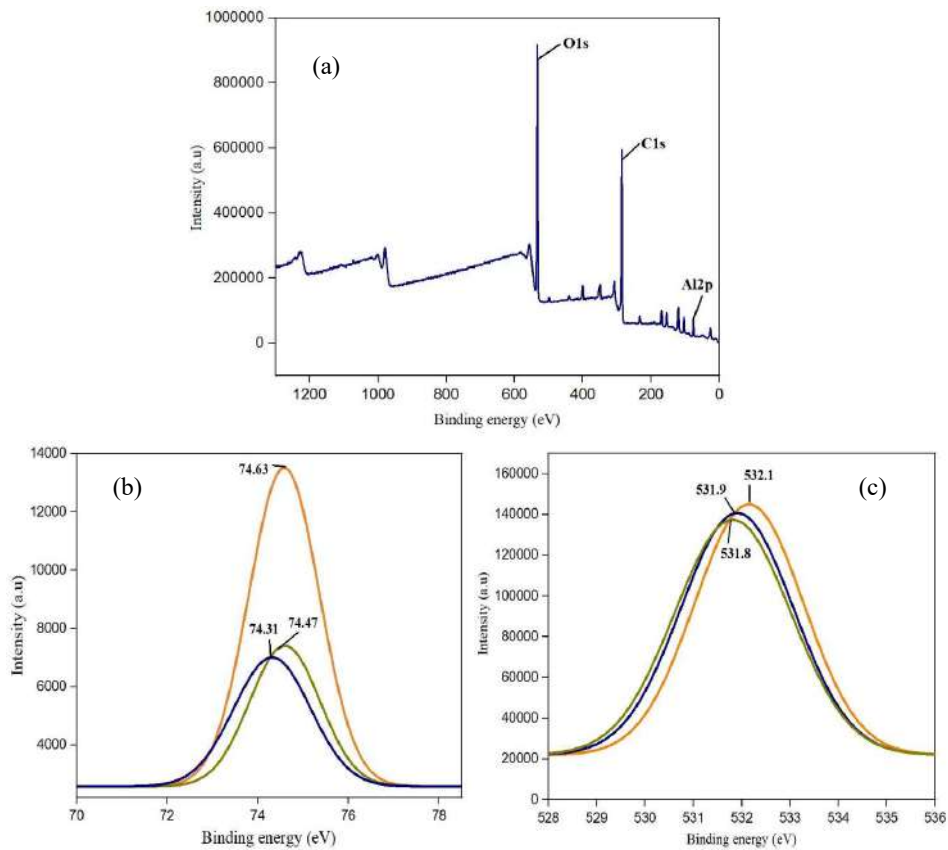
Fig. 6: XPS spectra of sludge (a) core line spectra of Al (b) Al 2p (c) O 1s.

XPS Analysis of Sludge

In electrocoagulation, the metal hydroxide flocs are responsible for the dye removal. More metal hydroxides, if formed, will facilitate high color removal efficiency. The formation of the metal hydroxides can be confirmed from the XPS data of the sludge obtained from the treatment of dye solution using Al/Cu electrodes. Fig. 6 shows the XPS core line spectra. From Fig. 6(b), the formation of Bayerite $Al(OH)_3$ at a binding energy of 74.31 eV, Gibbsite at 74.63 eV, and Boehmite at 74.47 eV were confirmed (Sherwood 1998). From Fig. 6(c), the O1s transitions for the Gibbsite were observed at 531.8 eV, Bayerite at 531.9 eV, and Boehmite at 532.1 eV (Kloprogge et al. 2006). This showed the O-H binding energy, thus substantiating the formation of aluminum hydroxides, enhancing the electrocoagulation process.

HPLC Analysis

The untreated and treated dye solution was subjected to HPLC analysis at the wavelength of about 254 nm from the UV detector. The HPLC chromatograms are shown in Fig. 7. In the chromatogram of the dye solution, three major compounds were formed at a retention time of 1.849, 3.002, and 7.476 min with the percentage area of about 31.685, 37.42, and 25.884 respectively, as shown in Fig. 7(a). After the process of electrocoagulation, the HPLC chromatogram, as in Fig. 7(b), compared with that of the dye, and it was found that the eluted peaks of the dye with a large percentage area decreased drastically from 31.685 to 27.89 at RT 1.849, 37.42 to 5.482 at RT 3.002 and 25.884 to 2.284 at RT 7.476. The other peaks that were eluted at the wavelength of 254 nm in the HPLC chromatogram of the treated dye solution with Al/Cu electrodes were at the retention time of 2.073, 2.24, 2.429, 2.755, 3.374, 4.659, and 5.8 min with percentage area of 24.026, 8.579, 9.502, 1.639, 1.856 and 3.471 respectively. These peaks indicate the bonds were cleaved, and the chromophoric groups present in the dye responsible for its color had been removed and converted into smaller colorless molecules, thus giving a high CRE% of 99.78.
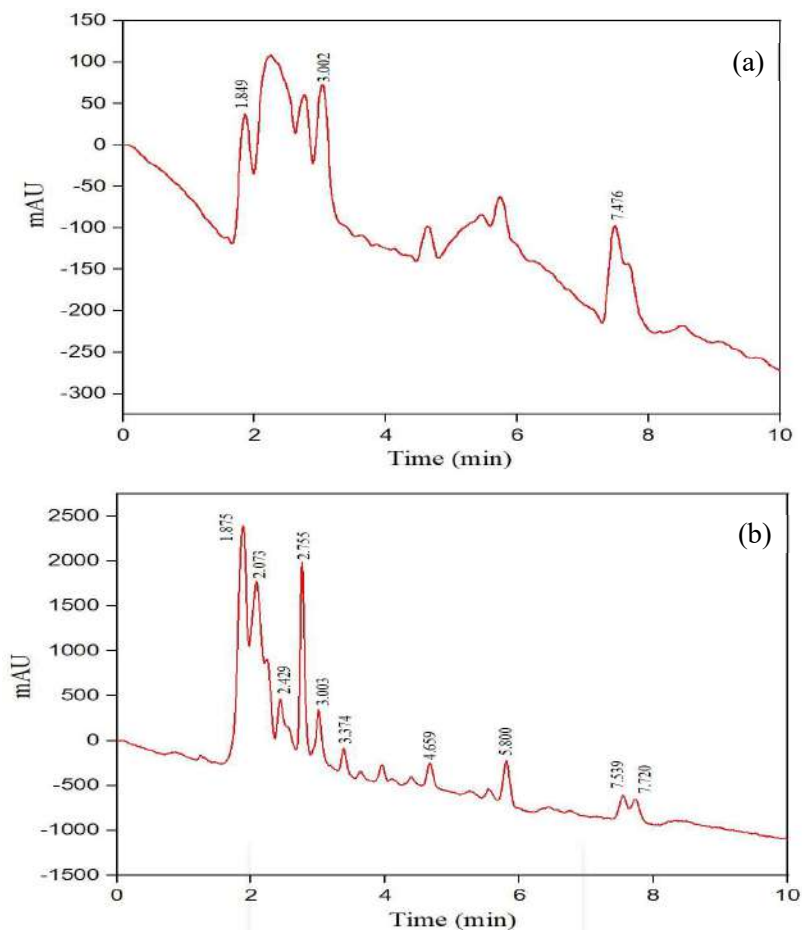
Fig. 7: HPLC chromatogram (a) Dye solution (b) Treated dye solution.

Mass Studies

The mass spectrum of the treated Coralene Rubine GFL was 200% compared to the mass spectrum of the raw dye. Fig. 8(a) shows the mass spectra of the dye, in which it is obvious that the peak that appeared at 347.2 is associated with the actual molecular weight of the dye. The base peak here is the peak that appeared at 726.05, which may be due to the dimer formation of the dye components. The other molecular ion peaks formed at 446.55, 537, 695.3, and 752.25 are due to various organic components responsible for the dye's color. When this is compared with the mass spectrum of the
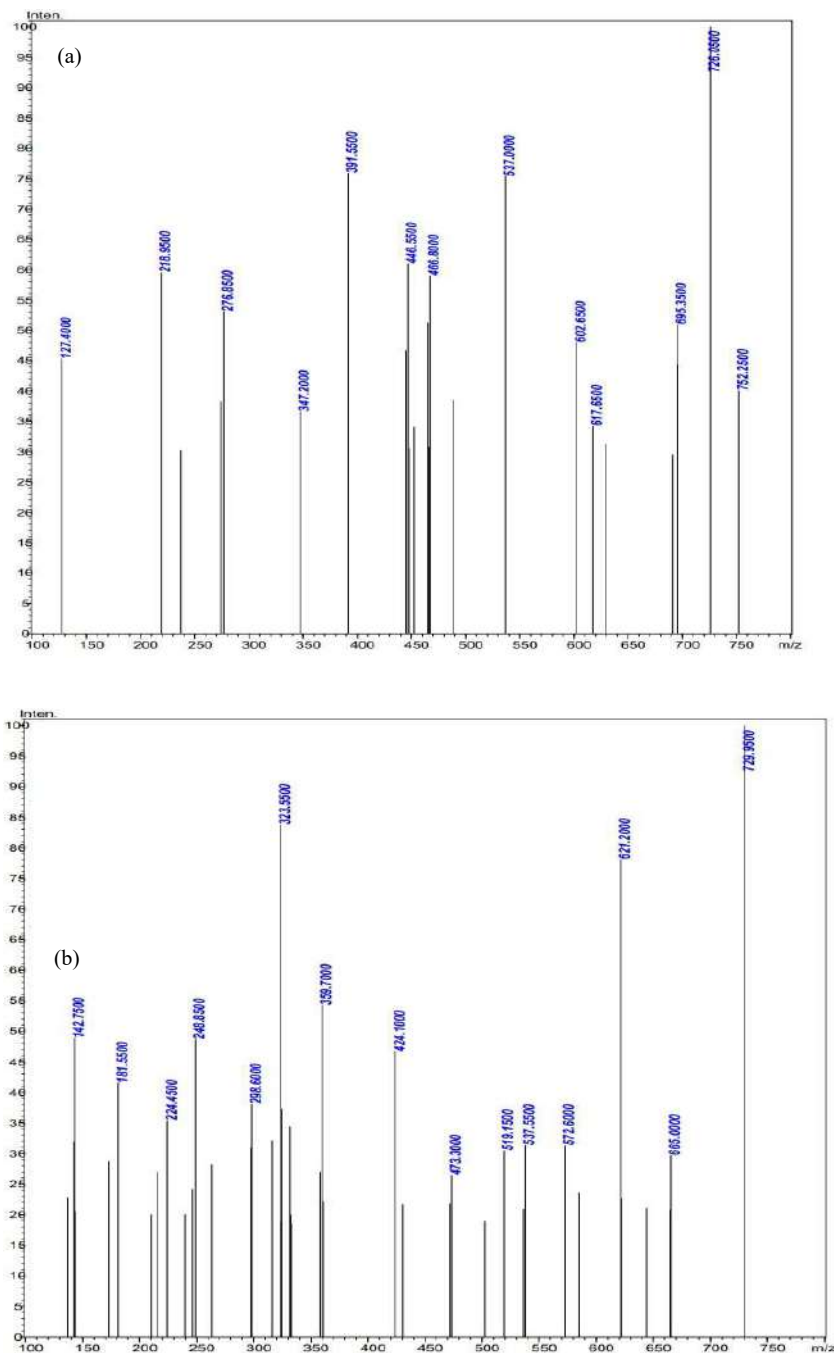
Fig. 8: Mass spectrum (a) Dye solution (b) Treated dye solution.

treated dye solution with Al/Cu electrodes that are shown in Fig. 8(b), it is evident that the peak at 347.2 has disappeared, indicating the cleavage of the bonds in the dye, thus giving other molecular ion peaks. Further, the peaks at 323.55 and 298.6 show the elimination of the cyanide group in the dye, eventually leading to the harmless nature of the treated water. The HPLC analysis also coincides with the fact that the major peaks present before the EC process were decomposed into colorless small molecular weight compounds.

Phytotoxicity Studies

The simulated dye solution was treated by electrocoagulation to remove the dye components. During this process, many intermediary compounds may be formed, which may or may not be toxic. Therefore, to evaluate the toxic levels in the dye solution treated using Al/Cu electrodes and the untreated Coralene Rubine GFL solution, *Trigonella foenum-graecum* was taken for the studies. These were compared with the control, i.e., tap water. Fig. 9 shows the phytotoxicity images. The length of the root and shoot in the control and treated dye solution was almost similar, as shown in Fig. 9(a) and (b). The length of the root for the control and treated dye solution was found to be 10.5 cm and 9 cm, respectively.

Similarly, the shoot length for the control and treated dye solution was 16.2 cm and 15.8 cm. Fig. 9(c) shows the image of the plant in the dye solution, with the root and shoot

length of 4 cm and 9.4 cm, respectively. The germination percentage was calculated for control, untreated, and treated dye solutions, which were found to be 99%, 50%, and 96%, respectively. Table 2 shows the parameters such as germination percentage, root length, and *Trigonella foenum-graecum* shoot. From these studies, it is conspicuous that the length of the root and shoot of the control and treated dye solution with Al/Cu electrodes is very similar compared to the dye solution, thus indicating that the intermediary compounds are non-toxic to the environment.

CONCLUSION

The present work analyzes the efficacy of the EC process for eliminating dye components from the simulated dye solution using Al/Cu electrodes. Under the optimized pH 7, 15 min, and 4 V, the maximum CRE% of 99.78 and COD removal of 92.86% were obtained. The EDX analysis proved the anodization of the electrode, which paved the way for forming metal hydroxide flocs. The HPLC analysis indicates the degradation of the dye, thus forming intermediary products which are not lethal. The mass analysis shows the cyanide removal, which approves the removal of toxic nature in the treated water. XPS studies using the sludge established the formation of aluminum hydroxide coagulants making the EC process effective. The phytotoxicity and ecotoxicity studies affirm that the treated water is not noxious and thus can be reused. Compared with the literature, the cost

Table 2: Parameters of *Trigonella foenum-graecum*.

Parameters	Control	Untreated Coralene Rubine GFL solution	Treated Coralene Rubine GFL solution with Al/Cu
Germination percentage [%]	99	50	96
Length of the shoot [cm]	16.2	9.4	15.8
Length of the root [cm]	10.5	4	9

(a)   (b)   (c)
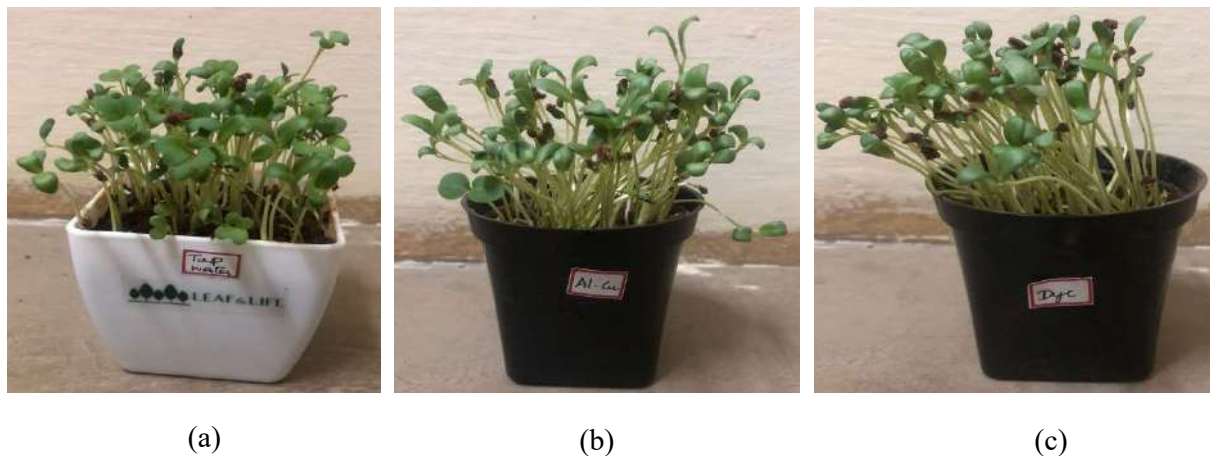
Fig. 9: Growth of *Trigonella foenum-graecum* in (a) Tap water, (b) treated dye solution, (c) untreated dye solution.

of electrocoagulation using Al/Cu electrodes was 98.12% lower, indicating this process's cost-effectiveness. Therefore, this method may remediate dye effluents in small dying textile operations.

ACKNOWLEDGEMENTS

REFERENCES

An, H., Qian, Y., Gu, X. and Tang, W.Z. 1996. Biological treatment of dye wastewaters using an anaerobic-oxic system. Chemosphere, 33(12): 2533-2542.

Akyol, A. 2012. Treatment of paint manufacturing wastewater by electrocoagulation. Desalination, 285: 91-99.

Azbar, N., Yonar, T. and Kestioglu, K. 2004. Comparison of various advanced oxidation processes and chemical treatment methods for COD and color removal from a polyester and acetate fiber dyeing effluent. Chemosphere, 55(1): 35-43.

Barrera-Diaz, C., Bilyeu, B., Roa, G. and Bernal-Martinez, L. 2011. Physicochemical aspects of electrocoagulation. Sep. Purif. Rev., 40(1): 1-24.

Bayramoglu, M., Kobya, M., Eyvaz, M. and Senturk, E. 2006. Technical and economic analysis of electrocoagulation for the treatment of poultry slaughterhouse wastewater. Sep. Purif. Technol., 51(3): 404-408.

Behera, S.K., Kim, J.H., Guo, X. and Park, H.S. 2008. Adsorption equilibrium and kinetics of polyvinyl alcohol from aqueous solution on powdered activated carbon. J. Hazard. Mater., 153(3): 1207-1214.

Bener, S., Bulca, O., Palas, B., Tekin, G., Atalay, S. and Erzoz, G. 2019. Electrocoagulation process of the treatment of real textile wastewater: Effect of operative conditions on the organic carbon removal and kinetic study. Process Saf. Environ. Prot., 129: 47-54.

Boroski, M., Rodrigues, A.C., Garcia, J.C., Sampaio, L.C., Nozaki, J. and Hioka, N. 2009. Combined electrocoagulation and TiO$_2$ photoassisted treatment applied to wastewater effluents from pharmaceutical and cosmetic industries. J. Hazard. Mater., 162(1): 448-454.

Canizares, P., Jimenez, C., Martinez, F., Rodrigo, M.A. and Saez, C. 2009. The pH is a key parameter in the choice between coagulation and electrocoagulation for the treatment of wastewater. J. Hazard. Mater., 163(1): 158-164.

Chen, G. 2004. Electrochemical technologies in wastewater treatment. Sep. Purif. Technol., 38(1): 11-41.

Cheriaa, J., Khaireddine, M., Rouabhia, M. and Bakhrouf, A. 2012. Removal of triphenylmethane dyes by bacterial consortium. Sci. World J., 512454.

Chung, K.T. 2016. Azo dyes and human health: A review. J. Environ. Sci. Health C Environ. Carcinog. Ecotoxicol. Rev., 34(4): 233-261.

Cui, D., Zhang, H., He, R. and Zhao, M. 2016. The comparative study on the rapid decolorization of azo, anthraquinone, and triphenylmethane dyes by anaerobic sludge. Int. J. Environ. Res. Public Health., 13(11): 1053.

Daneshvar, N., Oladegaragoze, A. and Djafarzadeh, N. 2006. Decolorization of basic dye solutions by electrocoagulation: an investigation of the effect of operational parameters. J. Hazard. Mater., 129(1-3): 116-122.

Giroto, J.A., Guardani, R., Teixeira, A.C.S.C. and Nascimento, C.A.O. 2006. Study on the photo-Fenton degradation of polyvinyl alcohol in aqueous solution. Chem. Eng. Process.: Process Intensif., 45(7): 523-532.

Golder, A.K., Samanta, A.N. and Ray, S. 2006. Anionic reactive dye removal from aqueous solution using a new adsorbent-sludge generated

in the removal of heavy metal by electrocoagulation. Chem. Eng. J., 122(1-2): 107-115.

Graca, M.B.S., Maria, C.F. and de Amorim, M.T.P. 2001. Decolorization of an anthraquinone-type dye using a laccase formulation. Bioresour. Technol., 79(2): 171-177.

Gurses, A., Yalcin, M. and Dogar, C. 2002. Electrocoagulation of some reactive dyes: a statistical investigation of some electrochemical variables. Waste Manag., 22(5): 491-499.

Holkar, C.R., Jadhav, A.J., Pinjari, D.V., Mahamuni, N.M. and Pandit, A.B. 2016. A critical review on textile wastewater treatments: possible approaches. J. Environ. Manag., 182: 351-366.

Hutcherson, J.R. 2015. A Comparison of Electrocoagulation and Chemical Coagulation Treatment Effectiveness on Frac Flowback and Produced Water. Doctoral Thesis. Colorado State University, Colorado, US.

Joshi, M., Mukherjee, A.K. and Thakur, B.D. 2001. Development of a new styrene copolymer membrane for recycling polyester fiber dyeing effluent. J. Membr. Sci., 189(1): 23-40.

Kalivel, P., Singh, R.P., Kavitha, S., Padmanabhan, D., Krishnan, S.K. and Palanichamy, J. 2020. Elucidation of electrocoagulation mechanism in the removal of Blue SI dye from aqueous solution using Al-Al, Cu-Cu electrodes-A comparative study. Ecotoxicol. Environ. Saf., 201: 110858.

Kalivel, P., Jisson, J.C., Kavitha, S., Padmanabhan, D., Bhagavathsingh, J., Palanichamy, J., Stephen, A.M.M. and David, J.J. 2021. Efficiency assessment of Cu and Al electrodes in removing anthraquinone based disperse dye aqueous solution in electrocoagulation-an analytical approach. Int. J. Environ. Anal. Chem., 15: 65-78.

Katal, R. and Pahlavanzadeh, H. 2011. Influence of different combinations of aluminum and iron electrode on electrocoagulation efficiency: Application to the treatment of paper mill wastewater. Desalination, 265(1-3): 199-205.

Kim, T.H., Park, C., Shin, EB. and Kim, S. 2002. Decolorization of disperse and reactive dyes by continuous electrocoagulation process. Desalination., 150(2): 165-175.

Kloprogge, J.T., Duong, L.V., Wood, B.J. and Frost, R.L. 2006. XPS study of the major minerals in bauxite: Gibbsite, bayerite, and (pseudo-) boehmite. J. Colloid Interface Sci., 296: 572-576.

Kobya, M., Demirbas, E., Ozyonar, F., Sirtbas, G. and Gengec, E. 2017. Treatments of alkaline non-cyanide, alkaline cyanide, and acidic zinc electroplating wastewaters by electrocoagulation. Process Saf. Environ. Protect., 105: 373-385.

Lin, S.H. and Chen, M.L. 1997. Treatment of textile wastewater by chemical methods for reuse. Water Res., 31(4): 868-876.

Low, K.S. and Lee, C.K. 1997. Quaternized rice husk as sorbent for reactive dyes. Bioresour. Technol., 61(2): 121-125.

Mansour, H.B., Boughzala, U., Dridi, D., Barillier, D., Chekir-Ghedira, L. and Mosrati, R. 2011. Textile dyes as a source of wastewater contamination: screening of the toxicity and treatment methods. Journal of Water Sciences., 24(3): 209-238.

Marcucci, M., Nosenzo, G., Capannelli, G., Ciabatti, I., Corrieri, D. and Ciardelli, G. 2001. Treatment and reuse of textile effluents based on new ultrafiltration and other membrane technologies. Desalination, 138(1-3): 75-82.

Maron, D.M. and Ames, B.N. 1983. Revised methods for the Salmonella mutagenicity test. Mutat. Res., 113(3-4): 173-215.

McKay, G. 1984. The adsorption of dyestuffs from aqueous solutions using the activated carbon adsorption model to determine breakthrough curves. Chem. Eng. J., 28(2): 95-104.

Modirshahla, N., Behnajady, M.A. and Kooshaiian, S. 2007. Investigation of the effect of different electrode connections on the removal efficiency of tartrazine from aqueous solutions by electrocoagulation. Dyes Pigm., 74(2): 249-257.

Mollah, M.Y.A., Schennach, R., Parga, J. and Cocke, D.L. 2001. Electrocoagulation (EC)-science and applications. J. Hazard. Mater., 84(1): 29-41.

Moussa, D.T., El-Naas, M.H., Nasser, M. and Al-Marri, M.J. 2017. A comprehensive review of electrocoagulation for water treatment: Potentials and challenges. J. Environ. Manage., 186(1): 24-41.

Ochiai, T. and Fujishima, A. 2012. Photoelectrochemical properties of TiO_2 photocatalyst and its applications for environmental purification. J. Photochem. Photobiol. C: Photochem. Rev., 13(4): 247-262.

Pan, Y., Liu, Y., Wu, D., Shen, C., Ma, C., Li, F., Zhang, Y. and Ma, H. 2020. Application of fenton pre-oxidation, Ca-induced coagulation, and sludge reclamation for enhanced treatment of ultra-high concentration poly (vinyl alcohol) wastewater. J. Hazard. Mater., 389: 121866.

Pensupa, N., Leu, S.Y., Hu, Y., Du, C., Liu, H., Jing, H., Wang, H. and Lin, C.S.K. 2017. Recent trends in sustainable textile waste recycling methods: Current situation and future prospects. Top. Curr. Chem., 375(5): 76.

Rai, H.S., Bhattacharyya, M.S., Singh, J., Bansal, T.K., Vats, P. and Banerjee, U.C. 2005. Removal of dyes from the effluent of textile and dyestuff manufacturing industry: a review of emerging techniques with reference to biological treatment. Crit. Rev. Environ. Sci. Technol., 35(3): 219-238.

Rajeshwar, K., Ibanez, J.G. and Swain, G.M. 1994. Electrochemistry and the environment. J. Appl. Electrochem., 24: 1077-1091.

Sengil, I.A. and Ozacar, M. 2006. Treatment of dairy wastewaters by electrocoagulation using mild steel electrodes. J. Hazard. Mater., 137(2): 1197-1205.

Shahi, V.K., Thampy, S.K. and Rangarajan, R. 2001. The effect of conducting spacers on transport properties of ion exchange membranes in electrodriven separation. Desalination., 133(3): 245-258.

Shaker, O.A., Matta, M.E. and Safwat, S.M. 2021. Nickel and chromium removal by electrocoagulation using copper electrodes. Desalin. Water Treat., 213: 371-380.

Shankar, R., Singh, L., Mondal, P. and Chand, S. 2014. Removal of COD, TOC, and color from pulp and paper industry wastewater through electrocoagulation. Desalin. Water Treat., 52(40-42): 7711-7722.

Sharma, D.K., Saini, H.S., Singh, M., Chimni, SS. and Chadha, BS. 2004. Biological treatment of textile dye Acid Violet 17 by a bacterial consortium in an up-flow immobilized cell bioreactor. Lett. Appl. Microbiol., 38(5): 345-350.

Sharma, Y.C. and Uma, S.N.U. 2011. An economically viable removal of methylene blue by adsorption on activated carbon prepared from rice husk. Can. J. Chem. Eng., 89(2): 377-383.

Sherwood, P.M.A. 1998. Introduction to studies of aluminium and its compounds by XPS. Surf. Sci. Spectra., 5: 1.

Slokar, Y.M. and Le Marechal, A.M. 1998. Methods of decoloration of textile wastewaters. Dyes Pigm., 37(4): 335-356.

Solis, M., Solis, A., Perez, H.I., Manjarrez, N. and Flores, M. 2012. Microbial decolouration of azo dyes: a review. Process Biochem., 47(12): 1723-1748.

Sridhar, S., Kale, A. and Khan, A.A. 2002. Reverse osmosis of edible vegetable oil industry effluent. J. Membr. Sci., 205(1-2): 83-90.

Tony, B.D., Goyal, D. and Khanna, S. 2009. Decolorization of textile azo dyes by aerobic bacterial consortium. Int. Biodeterior. Biodegrad., 63(4): 462-469.

Van der Bruggen, B., Daems, B., Wilms, D. and Vandecasteele, C. 2001. Mechanisms of retention and flux decline for the nanofiltration of dye baths from the textile industry. Sep. Purif. Technol., 22-23: 519-528.

Villalobos-Lara, A.D., Alvarez, F., Gamino-Arroyo, Z., Navarro, R., Peralta-Hernandez, J.M., Fuentes, R. and Perez, T. 2021. Electrocoagulation treatment of industrial tannery wastewater employing a modified rotating cylinder electrode reactor. Chemosphere, 264(2): 128491.

Vlyssides, A.G., Loizidou, M., Karlis, PK., Zorpas, AA. and Papaioannou, D. 1999. Electrochemical oxidation of a textile dye wastewater using a Pt/Ti electrode. J. Hazard. Mater., 70(1-2): 41-52.

Voigt, I., Stahn, M., Wohner, S., Junghans, A., Rost, J. and Voigt, W. 2001. Integrated cleaning of coloured waste water by ceramic NF membranes. Sep. Purif. Technol., 25(1-3): 509-512.

Wang, H., Zhong, Y., Yu, H., Aprea, P. and Hao, S. 2019. High-efficiency adsorption for acid dyes over $CeO_2 \cdot xH_2O$ synthesized by a facile method. J. Alloys Compd., 776: 96-104.

Wu, H.F., Yue, L.Z., Jiang, S.L., Lu, Y.Q., Wu, Y.X. and Wan, Z.Y. 2019. Biodegradation of polyvinyl alcohol by different dominant degrading bacterial strains in a baffled anaerobic bioreactor. Water Sci. Technol., 79(10): 2005-2012.

Yadav, A.K., Singh, L., Mohanty, A., Satya, S. and Sreekrishnan, T.R. 2012. Removal of various pollutants from wastewater by electrocoagulation using iron and aluminum electrode. Desalin. Water Treat., 46(1-3): 352-358.

Occurrence of Heavy Metals in Soil and Selected Edible Plants in the Vicinity of Major Lead-Zinc Mining Sites in Ebonyi State, Nigeria

E.B. Ogbuene*†, O.G. Aloh, C.T. Eze***, O.O. Eze****, T.E. Ugochukwu*****, A.M. Oroke*,**
C.E. Izueke-Okolo*, A.V. Ozorme*, C.J. Ibekwe* and C.A. Eze*

*Centre for Environmental Management and Control (CEMAC), University of Nigeria, Enugu Campus, Nigeria
**Department of Geography and Meteorology, Enugu State University of Science Technology (ESUT), Enugu State, Nigeria
***Department of Biochemistry, Federal University Oye-Ekiti, Ekiti State, Nigeria
****Department of Biochemistry, University of Nigeria Nsukka, Enugu State, Nigeria
*****Department of Civil Engineering, Federal University Oye-Ekiti, Ekiti State, Nigeria
†Corresponding author: E.B. Ogbuene; ogbuene.emeka@unn.edu.ng

ABSTRACT

The occurrence of heavy metals in soil and selected edible plants (*Manihot esculenta, Dioscorea rotundata, Ipomoea batatas, Telfairia occidentalis,* and *Chromolaena odorata*) in the vicinity of major Lead-Zinc mining sites in Ebonyi State, Nigeria was investigated. The concentrations of the detected heavy metals in soil from the study sites ranged from 0.38-77830.99 (mg.kg^{-1}). The limit values for all detected metals in soil from the mining sites were exceeded in most instances. The results showed that the plant species accumulated heavy metals near the mining sites to varying levels in their shoots and roots. The limit values for all detected heavy metals in the edible plants were not exceeded except in a few instances. The plant species demonstrated varying effectiveness for phytoextraction, indicating their appropriateness in the phytoremediation of heavy metal-contaminated soil. Therefore, examining the environmental consequences of uncontrolled mining activity in the vicinity of the mining sites with a scientific approach has helped to increase our knowledge of the pollution problem in the mining sites, reveal the ferocity of the situation, and contribute to the techniques presently in use for monitoring chemical pollution in a mining-impacted ecosystem.

INTRODUCTION

Mining is an important economic activity that plays an indispensable role in the evolution and growth of a nation (Mohsin et al. 2021). Uncontrolled mining methods are often employed in most developing nations, such as Nigeria (Elom et al. 2018). When not adequately controlled, mining activities could lead to environmental pollution and social problems (Rajasekaran 2007, Štofejová et al. 2021). Environmental pollution by heavy metals from mining activities could negatively affect the health of the local residents and biota (Rajasekaran 2007, Roba et al. 2016, Nawab et al. 2016, Wang et al. 2017, Nuapia et al. 2018). The occurrence of toxic metals such as lead (Pb), cadmium (Cd), arsenic (As), and chromium (VI) (Cr^{+6}), among others, in the vicinity of mining sites could constitute serious health risks to the ecosystem (Sharma & Dubey, 2005, Lamare & Singh 2017). Heavy metals are toxic chemicals that could create

scores of upset in a plant due to their bioaccumulation in plant tissues and concomitant interference with several metabolic processes (Mahdavian & Somashekar 2009, Gomes et al. 2014). As most heavy metals are not essential elements, most plants lack mechanisms for their uptake. Therefore, these metals bind to specific functional groups (carboxylic groups) of plant secretion (mucilage uronic acids) on root surfaces (Sharma & Dubey 2005). However, it is still unknown how these metals, especially Pb, are absorbed into the root tissue.

Although some plants tolerate toxic metals through specific chemical interactions, other species could experience toxicity, as toxic metals could hamper several plant metabolic pathways (Wierzbicka 1999). In a few plant species, higher levels of toxic metals such as Pb inhibit the germination of seeds, growth of plants, and synthesis of chlorophyll, among other effects (Peralta-Videa et al. 2009). Generally, heavy metals reduce the uptake and transport of vital nutrients in plants by obstructing the attachment of ions to ion carriers,

making them inaccessible from plant roots (Xiong 1997). Heavy metals could form strong bonds in interaction with active chemical groups and adversely affect metabolism in plants (Taub 2004). Under normal circumstances, these bonds should produce vital linkages that maintain molecules in their true configuration.

Mining and industrial processing of natural resources remain a primary source of the increased toxic metals in the environment (Davis 1995, Rajasekaran 2007, Sherene 2009). Lead-Zinc (Pb-Zn) mining in Ebonyi State dates back to 1925 (Chrysanthus 1995) and has progressed enormously in an unregulated manner (Elom et al. 2018). In Nigeria, Lead-zinc mining is not strictly monitored (Elom et al. 2018) and hence could serve as a great source of metal contamination in the vicinity of the mining sites (Abrahams 2002). Toxic metals are usually released into the surrounding environment during mining activities (Roba et al. 2016, Nawab et al. 2016, Wang et al. 2017, Nuapia et al. 2018, Štofejová et al. 2021), and this could pose a serious threat to various life forms in the mining zones (Soucek et al. 2000). The occurrence of toxic metals in the environment portends significant health risks to the ecosystem and public health (Elom et al. 2018, Eze et al. 2019, 2020). In developing nations, little attention is often paid to the environmental consequences of unregulated mining (Mohsin et al. 2021). Reports of heavy metal levels in soil from the vicinity of major Pb-Zn mining sites in Ebonyi State exceed soil guideline values (SGVs) (Elom et al. 2018, Okeke & Ifemeje 2021). Since farming is a major source of income in the area, the quality of farm produce, such as edible plants near the mining sites, is likely to be affected. Therefore, the occurrence of heavy metals in soil and selected edible plant species (*Manihot esculenta* (Cassava), *Dioscorea rotundata* (White yam), *Ipomoea batatas* (Sweet potatoes), *Telfairia occidentalis* (Fluted pumpkin) and *Chromolaena odorata* (Siam weed)) in the vicinity of major lead-zinc mining sites in Ebonyi State, Nigeria was investigated. Determining the exposure pathway to toxic chemicals is vital in health risk assessment to properly establish adequate monitoring plans and risk management strategies (Bierkens et al. 2009).

MATERIALS AND METHODS

Study Area

Ebonyi State is located on latitude 6° 15' N and 6° 20'N and longitude 8° 05' E and 8° 10'E, in the eastern part of Nigeria and shares a border with Benue State in the North, Cross River State by East, Enugu State by the West, and Abia, and Imo states by South (Odoh et al. 2012). The state has 13 Local Government Areas and occupies a surface area of about (5,923 sq.km) representing 2% of Nigeria's total surface Area

(Odoh et al. 2012). It has a population of about 2,176,947 million (NPC 2010). The lead-zinc mine communities in Ebonyi State are situated in three local government areas generally referred to as the Abakaliki lead-zinc mine area (Fig. 1). The Abakaliki lead-zinc area is primarily made up of three lodes: Enyigba, Ameri, and Ameka in the lower Benue trough located in Ebonyi State (Agumanu 1989). The Enyigba, Ameri, and Ameka communities are situated in the south of Abakaliki (Okeke & Ifemeje 2021) and are notable lead-zinc mining zones in Nigeria (Eze et al. 2021) that have experienced significant mining activities (Okeke & Ifemeje 2021). The area experiences a warm, humid tropical climate. The relative humidity is high, usually over 90% in the early morning but falls between 6 and 80 % in the afternoon; it is highest between May and October and ranges between 57.6 % in the dry season to 82.1% in the wet season. The temperature range is between 23°C and 26 °C for the dry season and 26°C and 28°C for the wet season. Rainfall in the area is heaviest during July and September and relatively low between November and March. About 80% of the total rainfall occurs between June and September, while only about 12% of the annual total fall between November and February (Odoh et al. 2012). The cultivated crops in the area include rice, cassava, leafy vegetables, and yam of different species (Okeke & Ifemeje 2021). The most prevalent tree species found in the study area are the agricultural tree crops, particularly oil palm, and kolanut. Many timber species of economic importance still exist in the area. The soil parent material is primarily shale and fine-grained sandstones of the Asu River formation (Agumanu 1989). The texture varied from loamy clay on the surface (0-15 cm) to clay at the subsurface layers (below 15 cm). The soil has a good potential to support tree crops and arable crops. However, there have been reports of heavy metal pollution resulting from uncontrolled mining activity (Eze et al. 2021).

Sample Collection

Top (0-30cm) and sub (30-45 cm) soil samples were collected randomly from the vicinity of Enyigba, Ameri, and Ameka Pb-Zn mining sites. Control soil (top and sub) was also collected from a remote location with no lead-zinc mining activity (about 25km from the Abakaliki area) to serve as reference soil. The soil samples were collected during September 2021 using a soil auger, geo-referenced, homogenized accordingly to form representative soil from each site, and transported to the laboratory in a black polythene bag. Each representative soil was air dried, ground using mortar and pestle into powder, sieved using a 2mm mesh, and stored in polythene bags before analysis. A total of hundred (100) plant samples were used for this study. Five (5) of each of the plant samples (*Manihot esculenta*

(Cassava), *Dioscorea rotundata* (White yam), *Ipomoea batatas* (Sweet potatoes), *Telfairia occidentalis* (Fluted pumpkin), and *Chromolaena odorata* (Siam weed)) were randomly collected from the vicinity of the mining sites.

Furthermore, five (5) of each plant species were also collected from the control site to serve as reference plant species. The underground and aerial parts of the plant species were collected in September 2021, placed accordingly in a labeled polyethylene bag, and transported to the laboratory. The plant samples were cleaned of residual materials, dried, homogenized accordingly, and divided into parts (root and shoot) for metal analysis. All samples were collected, putting into consideration the pollution dynamics of the mining sites.

Heavy Metal and Physicochemical Analysis

The representative soil, as well as root and shoot of the selected plant species, were analyzed for the presence and varying concentrations of lead (Pb), copper (Cu), zinc (Zn), cadmium (Cd), manganese (Mn), chromium (VI), iron (II) (Fe) and nickel (Ni) using the spectrometric method as described by Štofejová et al. (2021). The physicochemical analysis of soil was done using standard methods described by American Public Health Association (APHA) (2005). The obtained values were compared with data from a reference site and limit values for toxic metals as set by USEPA (1986). The quality control and assessment measures adopted in this investigation included field blanks, field duplicates, reference sites, lab replicates, and calibration blanks and standards.

Determination of Phytoextraction Quotient

The translocation factor (T/F), defined as the ratio of heavy metals in a plant's shoot to that of the root ([metals]$_{Shoot}$/[metals]$_{Root}$), was used in the determination of the phytoextraction quotient as described by Cui et al. (2007).

Statistical Analysis

The data generated were presented as mean ± Standard deviation (SD) of three replicates. One-way Analysis of variance (One-way ANOVA) performed with SPSS version 9.2 (Inc. Chicago, USA) was used to analyze data while significant differences were determined at $P \leq 0.05$.

RESULTS AND DISCUSSION

The result of the soil physicochemical and heavy metal analyses is shown in Table 1 and 2 respectively, while the result of the occurrence of heavy metals in the shoot and root of the plant species (*Manihot esculenta* (Cassava), *Dioscorea rotundata* (White yam), *Ipomoea batatas* (Sweet potatoes), *Telfairia occidentalis* (Fluted pumpkin) and *Chromolaena odorata* (Siam weed)) from the vicinity of Ameka, Ameri, Enyigba and control sites are presented in Tables 3 to 6
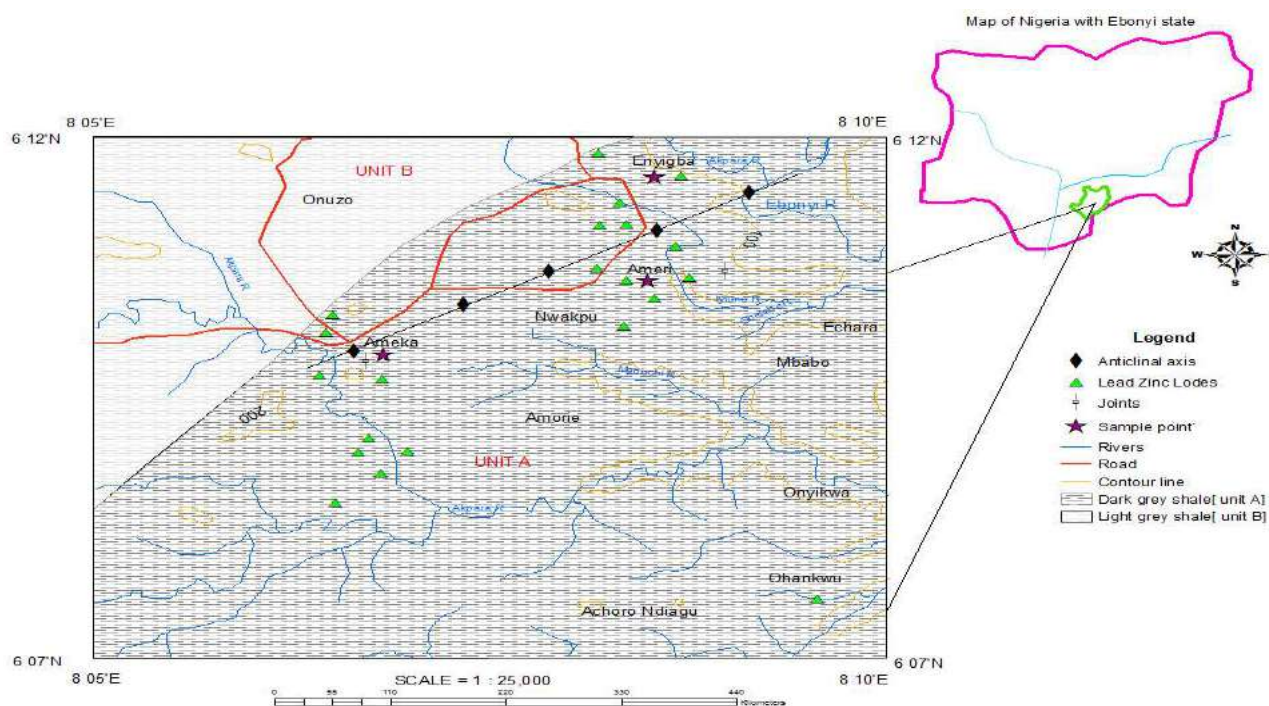

Fig. 1: Map of Abakaliki lead-zinc mining zone showing sample locations.

respectively. The limit values for all detected metals in soil from the mining sites were exceeded in most instances. The obtained soil pH value ranged from 6.36 ± 0.07 - 6.81 ± 0.05, EC ranged from 1.12 ± 1.05 - 4.87 ± 1.61 (mS.m^{-1}), CEC ranged from 19.37 ± 0.74 - 59.12 ± 1.31 (Cmol.kg^{-1}), TOC ranged from 0.90 ± 0.50 - 2.35 ± 0.21 (%), TOM ranged from 1.55 ± 0.85 - 4.05 ± 0.72 (%), Clay ranged from 0.92 ± 0.31 - 8.44 ± 0.35 (%), Silt ranged from 0.28 ± 0.40 - 4.20 ± 0.50 (%) and Sand (%) 87.36 ± 0.28 - 98.80 ± 0.53 (%) (Table 1). The topsoil from the Ameka mining site showed the highest pH value, while sub soil from the Ameri mining site showed the lowest (Table 1). The highest level of EC, CEC, TOC, TOM, Clay, Silt, and Sand was detected in topsoil from Enyigba, subsoil from Ameri, topsoil from Ameri, topsoil from Ameri, subsoil from Ameka, subsoil from Ameka and subsoil from the control site respectively (Table 1). The concentrations of the detected heavy metals in soil from the study sites ranged from 0.38 ± 0.33 - 77830.99 ± 5.12 (mg.kg^{-1}), with Fe showing the highest concentration in topsoil from Ameri and Cd showing the lowest concentration

in subsoil from the control site (Table 2). The determined physicochemical parameters and heavy metals in soil from the mining sites differ significantly (P ≤ 0.05) from the control site. The obtained soil pH values suggest that soil from the study sites is slightly acidic and might have influenced the distribution of heavy metals in soil in the vicinity of the study sites (Sherene 2009, Štofejová et al. 2021, Kashyap et al. 2016).

The limit values for all detected metals in the shoots and roots of plants from the Ameka mining site were not exceeded except for Cd and Fe in the shoot of *Telfairia occidentalis* (Table 3). The highest average concentration of Pb (2.56 mg.kg^{-1}) in plants from Ameka mining site was detected in the root of *Telfairia occidentalis,* Zn (2.76 mg.kg^{-1}) in the shoot of *Chromolaena odorata*, Fe (990.5 mg.kg^{-1}) in the shoot of *Telfairia occidentalis*, Cu (1.05 mg.kg^{-1}) and Cd (1.48 mg.kg^{-1}) in the root of *Telfairia occidentalis*, Mn (0.31mg.kg^{-1}) in the shoot of *Chromolaena odorata*, Ni (0.90 mg.kg^{-1}) in the shoot of *Dioscorea rotundata* and Cr (0.99 mg.kg^{-1}) in roots of *Ipomoea batatas* and *Telfairia*

Table 1: Physicochemical parameters of soil from the study sites.

Parameters	AMEKA Topsoil	AMEKA Subsoil	AMERI Topsoil	AMERI Subsoil	ENYIGBA Topsoil	ENYIGBA Subsoil	CONTROL Topsoil	CONTROL Subsoil
pH	6.81 ± 0.05	6.47 ± 0.18	6.57 ± 0.03	6.36 ± 0.07	6.55 ± 0.15	6.41 ± 0.05	6.57 ± 0.05	6.74 ± 0.13
EC [mS.m^{-1}]	1.17 ± 0.62	1.74 ± 0.65	3.95 ± 1.13	4.46 ± 0.33	4.87 ± 1.61	4.04 ± 1.19	1.12 ± 1.05	1.79 ± 0.73
CEC [Cmol. kg^{-1}]	40.55 ± 1.12	56.31 ± 0.63	53.58 ± 0.56	59.12 ± 1.31	53.92 ± 1.04	58.49 ± 0.27	20.42 ± 0.42	19.37 ± 0.74
TOC [%]	1.45 ± 0.37	1.02 ± 0.93	2.35 ± 0.21	1.54 ± 0.28	1.93 ± 0.34	0.90 ± 0.50	1.55 ± 0.25	1.47 ± 0.41
TOM [%]	2.50 ± 0.19	1.76 ± 0.11	4.05 ± 0.72	2.65 ± 0.36	3.33 ± 0.27	1.55 ± 0.85	2.67 ± 0.54	2.53 ± 0.15
Clay [%]	6.21 ± 0.27	8.44 ± 0.35	8.00 ± 0.40	7.96 ± 0.15	8.02 ± 0.26	7.57 ± 0.22	1.40 ± 0.14	0.92 ± 0.31
Silt [%]	2.26 ± 0.16	4.20 ± 0.50	2.49 ± 0.53	2.15 ± 0.15	2.67 ± 0.32	2.96 ± 0.23	0.35 ± 0.25	0.28 ± 0.40
Sand [%]	91.53 ± 0.87	87.36 ± 0.28	89.51 ± 0.45	89.89 ± 0.93	89.31 ± 0.29	89.47 ± 0.71	98.25 ± 0.47	98.80 ± 0.53

EC = Electrical conductivity, **CEC** = Cation exchange capacity, **TOC** = Total organic carbon, **TOM** = Total organic matter.

Table 2: Heavy metal contents [mg.kg^{-1}] of soil from the study sites.

Metals [mg.kg^{-1}]	USEPA [mg.kg^{-1}]	AMEKA Topsoil	AMEKA Subsoil	AMERI Topsoil	AMERI Subsoil	ENYIGBA Topsoil	ENYIGBA Subsoil	CONTROL Topsoil	CONTROL Subsoil
Pb	300	1953.59 ± 1.78	1946.24 ± 0.83	154.88 ± 0.96	1154.05 ± 0.26	214.67 ± 1.12	212.33 ± 0.41	30.03 ± 0.34	29.95 ± 0.15
Zn	200	141.06 ± 2.38	1140.75 ± 0.52	1197.23 ± 0.74	1193.13 ± 1.11	1182.82 ± 1.05	1179.04 ± 0.63	8.88 ± 0.68	8.77 ± 0.45
Fe	1000	44595.70 ± 3.17	44619.28 ± 2.11	77830.99 ± 5.12	77545.80 ± 1.58	7903.73 ± 2.74	77525.58 ± 0.93	70.17 ± 0.17	70.12 ± 0.31
Cu	250	141.69 ± 0.32	139.53 ± 0.41	35.54 ± 0.18	33.99 ± 0.33	34.40 ± 0.56	29.83 ± 0.12	18.02 ± 0.35	12.65 ± 0.64
Cd	3.0	4.53 ± 0.44	3.46 ± 0.72	5.37 ± 0.55	5.04 ± 0.23	5.65 ± 22	4.67 ± 0.34	0.39 ± 0.31	0.38 ± 0.33
Mn	80	2211.0 9 ± 2.11	2283.70 ± 1.78	1238.11 ± 1.37	1238.28 ± 2.13	1219.21 ± 0.96	1224.15 ± 1.64	5.96 ± 0.52	6.91 ± 0.75
Ni	150	38.96 ± 0.33	38.75 ± 0.12	72.28 ± 0.24	72.17 ± 0.93	64.61 ± 0.19	61.76 ± 0.35	2.60 ± 0.51	2.50 ± 0.20
Co	NA	55.81 ± 0.42	47.52 ± 0.30	33.07 ± 0.38	32.44 ± 0.45	56.22 ± 0.51	56.06 ± 0.36	0.8.03 ± 0.29	1.02 ± 0.81
Cr	750	1176.05 ± 0.40	1194.63 ± 0.73	1127.57 ± 0.47	1121.80 ± 0.85	196.70 ± 0.50	144.37 ± 0.23	1.40 ± 0.26	1.58 ± 0.33

Table 3: Occurrence [mg.kg⁻¹] of heavy metals in plant species from the Ameka mining site.

Metals	USEPA [mg.kg⁻¹]	Manihot esculenta		Dioscorea rotundata		Ipomoea batatas		Telfairia occidentalis		Chromolaena odorata	
		Shoot	Root	Shoot	Root	Shoot	Root	Shoot	Root	Shoot	Root
Pb	5.0	1.69 ± 1.11	1.72 ± 0.08	0.98 ± 0.33	1.12 ± 0.09	0.89 ± 0.22	0.11 ± 0.55	1.550 ± 0.05	2.560 ± 0.05	0.90 ± 0.03	1.250 ± 0.02
Zn	100.0	1.05 ± 0.13	1.10 ± 0.03	1.07 ± 0.06	1.11 ± 0.44	1.08 ± 0.51	1.17 ± 0.33	2.200 ± 0.05	1.05 ± 0.03	2.760 ± 0.04	1.27 ± 0.05
Fe	250	230.85 ± 0.21	120.5 ± 0.23	90.45 ± 0.09	130.92 ± 1.02	100.22 ± 0.37	130.14 ± 1.07	990.50 ± 0.05	166.21 ± 0.13	60.00 ± 0.03	60.05 ± 0.05
Cu	40.0	0.36 ± 0.09	0.75 ± 0.15	0.64 ± 0.03	0.94 ± 0.75	0.66 ± 0.82	0.91 ± 0.62	0.92 ± 0.04	1.05 ± 0.11	0.92 ± 0.02	0.99 ± 0.03
Cd	0.10	0.37 ± 0.23	0.95 ± 0.05	0.54 ± 0.07	0.98 ± 0.34	0.25 ± 0.09	0.53 ± 0.34	0.980 ± 0.02	1.48 ± 0.02	1.26 ± 0.02	1.035 ± 0.03
Mn	1.0	0.195 ± 0.17	0.245 ± 0.22	0.145 ± 0.11	0.210 ± 0.35	0.170 ± 0.42	0.225 ± 0.08	0.19 ± 0.01	0.11 ± 0.01	0.310 ± 0.05	0.20 ± 0.11
Ni	10-100	0.75 ± 0.04	0.170 ± 0.67	0.90 ± 0.05	0.75 ± 0.11	0.85 ± 0.50	0.70 ± 0.22	0.060 ± 0.02	0.10 ± 0.02	0.180 ± 0.02	0.186 ± 0.02
Cr	2.0	0.21 ± 0.03	0.52 ± 0.32	0.32 ± 0.05	0.55 ± 0.31	0.59 ± 0.12	0.99 ± 0.13	0.530 ± 0.05	0.991 ± 0.02	0.195 ± 0.02	0.720 ± 0.04

Data are presented as mean ± SD of three replicates. Statistical significance was determined at $P \leq 0.05$.

Table 4: Occurrence [mg.kg⁻¹] of heavy metals in plant species from Ameri mining site.

Metals	USEPA [mg.kg⁻¹]	Manihot esculenta		Dioscorea rotundata		Ipomoea Batatas		Telfairia occidentalis		Chromolaena odorata	
		Shoot	Root	Shoot	Root	Shoot	Root	Shoot	Root	Root	Shoot
Pb	5.0	0.78 ± 0.21	0.90 ± .11	0.92 ± 0.44	0.98 ± 0.97	1.21 ± 0.12	0.84 ± 0.05	0.08 ± 0.08	1.10 ± 0.02	0.19 ± 0.04	0.19 ± 0.02
Zn	100.0	0.209 ± 0.34	0.150 ± .09	0.64 ± 0.11	0.86 ± 0.22	1.42 ± 0.02	0.86 ± 0.22	0.14 ± 0.02	1.58 ± 0.04	2.050.05	0.145 ± 0.03
Fe	250	56.390 ± 1.77	55.850 ± 1.09	23.980 ± 0.84	14.125 ± 1.50	44.76 ± 0.17	31.04 ± 0.06	6.92 ± 0.12	118.75 ± 0.11	58.32 ± 0.17	48.44 ± 0.12
Cu	40.0	0.131 ± 0.41	0.088 ± 0.11	0.42 ± 0.43	0.74 ± 0.11	1.31 ± 0.11	0.88 ± 0.02	0.99 ± 0.11	1.10 ± 0.02	0.92 ± 0.05	0.76 ± 0.04
Cd	0.10	0.127 ± 0.33	0.102 ± 0.23	0.041 ± 0.52	0.132 ± 0.34	0.31 ± 0.03	0.98 ± 0.02	0.98 ± 0.02	0.99 ± 0.05	0.52 ± 0.04	0.95 ± 0.05
Mn	1.0	0.278 ± 0.07	0.295 ± 0.44	0.125 ± 0.38	0.200 ± 0.52	0.31 ± 0.01	0.24 ± 0.03	0.66 ± 0.04	0.50 ± 0.04	0.26 ± 0.07	0.28 ± 0.02
Ni	10-100	0.094 ± 0.18	0.075 ± 0.52	0.085 ± 0.21	0.078 ± 0.35	0.11 ± 0.01	0.08 ± 0.01	0.06 ± 0.01	0.09 ± 0.01	0.10 ± 0.02	0.07 ± 0.01
Cr	2.0	0.046 ± 0.22	0.099 ± 0.12	0.031 ± 0.33	0.102 ± 0.17	0.82 ± 0.02	0.57 ± 0.02	0.45 ± 0.02	0.64 ± 0.02	0.18 ± 0.03	0.34 ± 0.03

Data is presented as mean ± SD of three replicates. Statistical significance was determined at $P \leq 0.05$.

Table 5: Occurrence [mg.kg⁻¹] of heavy metals in plant species from the Enyigba mining site.

Metals	USEPA [mg.kg⁻¹]	Manihot esculenta		Dioscorea rotundata		Ipomoea Batatas		Telfairia occidentalis		Chromolaena odorata	
		Shoot	Root	shoot	Root	Shoot	Root	Shoot	Root	Shoot	Root
Pb	5.0	0.089 ± 0.12	0.201 ± 0.43	0.099 ± 0.52	0.315 ± 0.44	0.79 ± 0.05	0.42 ± 0.02	0.16 ± 0.07	0.11 ± 0.02	0.120 ± 0.11	0.21 ± 0.01
Zn	100.0	0.068 ± 034	0.199 ± 0.11	0.054 ± 0.28	0.260 ± 0.23	1.09 ± 0.13	0.87 ± 0.03	0.86±0.02	0.54 ± 0.02	0.95 ± 0.03	0.50 ±0.04
Fe	250	24.150 ±.17	56.010 ± 0.45	24.070 ± 25	78.110 ± 1.04	38.11 ± 1.13	25.54 ± 1.15	18.12 ± 0.15	26.02 ± 0.08	28.44 ± 0.16	76.15 ± 0.21
Cu	40.0	0.110 ± 0.22	0.275 ± 0.51	0.048 ± 0.33	0.099 ± 0.24	0.75 ± 0.05	0.56 ± 0.05	0.55±0.04	0.82 ± 0.04	0.84 ± 0.02	0.95 ± 0.07
Cd	0.10	0.055 ± 0.31	0.102 ± 0.22	0.032 ± 0.45	0.154 ± 0.19	0.76 ± 0.02	0.26 ± 0.01	0.450.04	0.26 ± 0.01	0.18 ± 0.01	0.10 ± 0.03
Mn	1.0	0.495 ± 0.06	0.700 ± 0.37	0.505 ± 0.53	0.702 ± 0.13	0.51 ± 0.03	0.39 ± 0.02	0.20±0.02	0.11 ± 0.02	0.28 ± 0.04	0.30 ± 0.02
Ni	10-100	0.087 ± 0.81	0.090 ± 0.44	0.089 ± 0.13	0.091 ± 0.54	0.07 ± 0.03	0.04 ± 0.02	0.03±0.01	0.06 ± 0.02	0.03 ± 0.01	0.05 ± 0.01
Cr	2.0	0.025 ± 0.23	0.099 ± 0.17	0.020 ± 0.34	0.120 ± 0.35	0.48 ± 0.02	0.31 ± 0.01	0.15±0.03	0.23 ± 0.03	0.13 ± 0.02	0.24 ± 0.02

Data are presented as mean ± SD of three replicates. Statistical significance was determined at P ≤ 0.05.

Table 6: Occurrence [mg.kg⁻¹] of heavy metals in plant species from the Reference site.

Metals	USEPA [mg.kg⁻¹]	Manihot esculenta		Dioscorea rotundata		Ipomoea batatas		Telfairia occidentalis		Chromolaena odoranta	
		Shoot	Root	Shoot	Root	Shoot	Root	Shoot	Root	Shoot	Root
Pb	5.0	0.03 ± 0.01	0.02 ± 0.01	0.01 ± 0.03	0.03 ± 0.02	0.03 ± 0.02	0.09 ± 0.03	0.10 ± 0.01	0.09 ± 0.01	0.02 ± 0.01	0.01 ± 0.01
Zn	100.0	0.45 ± 0.03	0.10 ± 0.05	0.44 ± 0.02	0.92 ± 0.05	0.80 ± 0.05	0.89 ± 0.09	0.18 ± 0.09	0.13 ± 0.01	0.32 ± 0.01	0.42 ± 0.02
Fe	250	2.85 ± 0.05	2.40 ± 0.02	3.51 ± 0.03	3.66 ± 0.05	2.18 ± 0.03	2.99 ± 0.09	12.18 ±0.03	13.17 ± 0.04	12.08 ± 0.06	10.20 ± 0.10
Cu	40.0	0.21 ± 0.04	0.03 ± 0.05	0.03 ± 0.05	0.06 ± 0.02	0.26 ± 0.02	0.02 ± 0.01	0.09 ± 0.05	0.05 ± 0.02	0.13 ± 0.03	0.12 ± 0.03
Cd	0.10	0.42 ± 0.02	0.13 ± 0.01	0.28 ± 0.02	0.62 ± 0.02	0.15 ± 0.01	0.26 ±0.02	0.70 ± 0.02	0.97 ± 0.07	0.99 ± 0.03	0.81 ± 0.03
Mn	1.0	0.13 ± 0.01	0.11 ± 0.03	0.21 ± 0.05	0.45 ± 0.03	0.23 ± 0.03	0.44 ± 0.02	0.42 ± 0.02	0.27 ± 0.02	0.47 ± 0.05	0.41 ± 0.05
Ni	10-100	0.09 ± 0.01	0.02 ± 0.01	0.05 ± 0.03	0.07 ± 0.02	0.04 ± 0.02	0.05 ± 0.01	0.01 ± .01	0.02 ± 0.01	0.06 ± 0.01	0.08 ± 0.02
Cr	2.0	0.11 ± 0.02	0.09 ± 0.01	0.08 ± 0.02	0.09 ± 0.01	0.01 ± 0.01	0.05 ± 0.01	0.06 ± 0.01	0.11 ± 0.01	0.04 ±0.01	0.07 ± 0.01

Data are presented as mean ± SD of three replicates. Statistical significance was determined at P ≤ 0.05.

occidentalis (Table 3). The limit values for all detected metals in the shoots and roots of plants from the Ameri mining site were not exceeded except for Cd in the shoot of *Manihot esculenta*, the root of *Dioscorea rotundata*, and shoots and roots of *Ipomoea batatas, Telfairia occidentalis, and Chromolaena odorata* (Table 4). The highest average concentration of Pb (1.21 mg.kg^{-1}) in plants from the Ameri mining site was detected in the shoot of *Ipomoea batatas,* Zn (2.05 mg.kg^{-1}) in the root of *Chromolaena odorata*, Fe (118.75 mg.kg^{-1}) in the root of *Telfairia occidentalis*, Cu (1.31 mg.kg^{-1}) in the shoot of *Ipomoea batatas*, Cd (0.99 mg.kg^{-1}) and Mn (0.66 mg.kg^{-1}) in the root and shoot of *Telfairia occidentalis respectively* and Ni (0.11 mg.kg^{-1}) as well as Cr (0.82 mg.kg^{-1}) in the shoot of *Ipomoea batatas* (Table 4). The limit values for all detected metals in the shoots and roots of plants from the Enyigba mining site were not exceeded except for Fe in the shoot of *Telfairia occidentalis* and Cd in the root of *Dioscorea rotundata*, shoots, and roots of *Ipomoea batatas* and *Telfairia occidentalis* as well as the shoot of *Chromolaena odorata* (Table 5). The highest average concentration of Pb (0.79 mg.kg^{-1}) and Zn (1.09 mg.kg^{-1}) in plants from Enyigba mining site was detected in the shoot of *Ipomoea batatas*, Fe (78.1 mg.kg^{-1}) in the root of *Dioscorea rotundata*, Cu (0.95 mg.kg^{-1}) in the root of *Chromolaena odorata*, Cd (0.45 mg.kg^{-1}) in the shoot of *Telfairia occidentalis*, Mn (0.7 mg.kg^{-1}) and Ni (0.09 mg.kg^{-1}) in the roots of *Manihot esculenta* and *Dioscorea rotundata* and Cr (0.48 mg.kg^{-1}) in the shoot of *Ipomoea batatas* (Table 5). The limit values for all detected metals in the shoots and roots of plants from the reference site were not exceeded except for Cd (Table 6). The highest average concentration of Pb (0.1 mg.kg^{-1}) in plants from the reference site was detected in the shoot of *Telfairia occidentalis*, Zn (0.92 mg.kg^{-1}) in the root of *Dioscorea rotundata*, Fe (13.17 mg.kg^{-1}) in the root of *Telfairia occidentalis*, Cu (0.26 mg.kg^{-1}) in the shoot of *Ipomoea batatas*, Cd (0.99 mg.kg^{-1}) and Mn (0.47 mg.kg^{-1}) in the shoot of *Chromolaena odorata,* Ni (0.09 mg.kg^{-1}) in the shoot of *Manihot esculenta* and Cr (0.11 mg.kg^{-1}) in the shoot and root of *Manihot esculenta* and *Telfairia occidentalis* respectively (Table 6). The plant species accumulated heavy metals to varying levels in their shoots and roots. However, higher average concentrations of the detected metals occurred in the shoot compared to the root (Tables 3 - 6). Although the limit values for all detected metals in shoots and roots of the plants from the mining sites were not exceeded except in a few instances, accumulation of these metals over time could result in accumulation and have deleterious consequences on biota in the impacted area. In general, the average concentration of Fe was highest in both soil and plants compared to other detected metals detected in this study (Tables 3 - 6). This

aligns with the study report by Okeke and Ifemeje (2021). The highest average concentration of Pb (2.56 mg.kg^{-1}), Zn (2.76 mg.kg^{-1}), Fe (990.5 mg.kg^{-1}), Cd (1.48 mg.kg^{-1}), Ni (0.90 mg.kg^{-1}) and Cr (0.99 mg.kg^{-1}) recorded in this study occurred in plants from Ameka mining site. In comparison, the highest average concentration of Cu (1.31 mg.kg^{-1}) and Mn (0.7 mg.kg^{-1}) occurred in plants from Ameri and Enyigba mining sites, respectively (Tables 3 - 6). Significantly ($P \leq 0.05$), higher concentrations of the detected metals were determined in the mining sites than in plants from the reference site. The obtained results suggest that the degree of heavy metal pollution of the mining sites could range in the following order: Ameka > Ameri > Enyigba.

Plants' accumulation of toxic metals and uptake of essential elements varies greatly among plant species due to variations in plant metabolic activities (Nasim & Dhir 2010, Cai et al. 2020). According to Obasi et al. (2012), accumulation of Pb could inhibit the activity of enzymes, give rise to water imbalance, trigger hormonal changes and alter membrane structure in plants. These series of changes disrupt metabolic activities in a plant and, at high concentrations, may lead to the death of plant cells (Seregin et al. 2004, Soucek et al. 2000). The phytotoxic characteristics of Pb may include blackening of the roots, chlorosis, and stunted growth (Sharma & Dubey 2005). The plant species used for this study exhibited observable characteristics such as stunted growth and chlorosis, which may have resulted from the accumulation of toxic metals near the mining sites. In non-tolerant plants, higher levels of Zn could cause chlorosis and inhibit root elongation (Sharma & Dubey 2005). The elevated levels of the detected Fe call for serious concern since the plants are edible. Accumulation of Fe over time could result in severe health conditions for consumers (Khan et al. 2009). Cu is a vital element necessary for plant growth; however, it could be potentially toxic at higher levels (Yruela 2005, Prasad & Strzalka 1999). At concentrations above 40mg.kg-^{1}, Cu could be phytotoxic (Prasad & Strzalka 1999). In some plants, accumulated Ni protects against fungi and bacteria pathogens (Prasad et al. 2005) and, as such, may confer such an advantage to plants in the study sites. Cr could disrupt metabolic activities and inhibit plant growth (Shanker et al. 2005).

The results of the translocation factor (Phytoextraction quotient) of heavy metals in the selected plants are shown in Fig. 2 (a-e). The results showed that the translocation factor of *Manihot esculenta* was greater than one (TF > 1) for Zn at Ameka site, greater than one (TF > 1) for all the detected metals with the exception of Cu, Mn, Zn and Cd at Ameri site and less than one (TF < 1) for all the detected metals at Enyigba (Fig. 2a). The *Dioscorea rotundata* had translocation
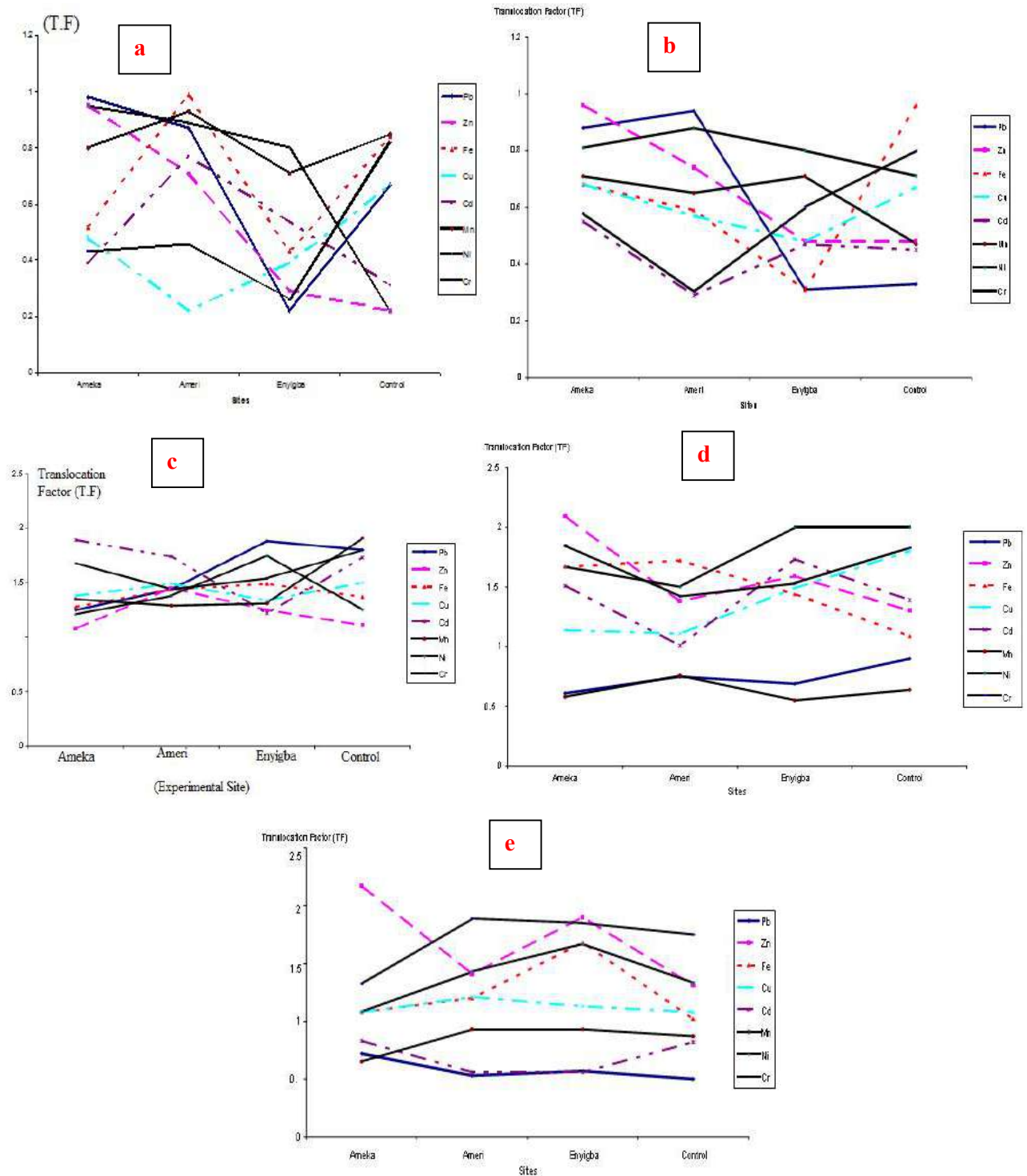
Fig. 2: Translocation Factor (TF) of (a) *Manihot esculenta*, (b) *Dioscorea rotundata*, (c) *Ipomoea batatas*, (d) *Telfairia occidentalis* and (e) *Chromolaena odorata* for all the detected Metals.

factor less than one (TF < 1) for all the detected metals at the study sites with the exception of Ni which had translocation factor greater than one (TF > 1) at Ameka and Ameri sites and Zn which had translocation factor greater than one (TF > 1)

at Ameri site (Fig. 2b). The translocation factor for *Ipomoea batatas* was greater than one (TF > 1) for all tested heavy metals at the study sites (Fig. 2c). The same observation was noted for *Telfairia occidentalis*, except for Ni and Cr that has TF < 1 in all the sites (Fig. 2d). The *Chromolaena odorata* exhibited TF greater than one (TF > 1) for all tested heavy metals in all the sites, except for Cd and Cr.

CONCLUSION

The study revealed the occurrence of heavy metals in some selected plant species (*Manihot esculenta* (Cassava), *Dioscorea rotundata* (White yam), *Ipomoea batatas* (Sweet potatoes), *Telfairia occidentalis* (Fluted pumpkin) and *Chromolaena odorata* (Siam weed)) from the vicinity of major Lead-Zinc mining sites in Ebonyi State, Nigeria. The results showed that plant species in the mining sites accumulated varying metals in their shoots and roots. The plant species have demonstrated varying effectiveness for phytoextraction, indicating their appositeness in the phytoremediation of heavy metal-contaminated soil. However, the limit values for all detected metals in the shoots and roots of the plant species were not exceeded except in a few instances. The results obtained in our study suggest that the Ameka mining site could be more polluted than Ameri and Enyigba mining sites. Therefore, examining the environmental consequences of uncontrolled Pb-Zn mining activity in the vicinity of the mining sites with a scientific approach has helped to increase our knowledge of the pollution problem in the mining sites, reveal the ferocity of the situation, and contributed to the techniques presently in use for monitoring of chemical pollution in a mining-impacted ecosystem.

REFERENCES

Abrahams, P.W. 2002. Soils: Their implications to human health. Sci. Tot. Environ., 291: 1-32.

Agumanu, A.E. 1989. The Abakaliki and the Ebonyi Formations: Sub-divisions of the Albian Asu River Group in the southern Benue trough, Nigeria. J. Afr. Earth Sci., 207-195 :(1)9.

APHA 2005. Standard Methods for the Examination of Water and Wastewater, Washington DC: American Public Health Association.

Bierkens, J., Holderbeke, M.V and Cornelis C. 2009. Parameterisation of Exposure Pathways for Children. Full-Chain and Uncertainty Approaches for Assessing Health Risks in Future Environmental Scenarios. FP6 Project-2005-Global-4, Integrated Project.

Cai, X., Yu, X., Lei, L., Xuan, B., Wang J., Zhang, L. and Zhao, S. 2020. Comparison of lead tolerance and accumulation characteristics of fourteen. Nat. Environ. Pollut. Technol., 19(4): 1547-1555. https://doi.org/10.46488/NEPT.2020.v19i04.021.

Chrysanthus, C.S. 1995. Evaluating baseline data for copper, manganese, nickel and zinc in rice, yam, cassava, and guinea grass from cultivated soils in Nigeria. Agric. Ecosyst. Environ., 53: 47-61.

Davis, B.E. 1995. Lead and Other Heavy Metals in Urban Areas and Consequences for the Health of Their Inhabitants. In Majumdar, S.K.,

Miller, E.W. and Brenner, F.S. (eds) Environmental Contaminants, Ecosystem, and Human Health, The Pennsylvania Academy of Science, Easton PA, USA, pp. 287-307.

Elom, N.I., Udeh, D.G., Anyigor, C.M. and Okpani, N. A. 2018. Lead (Pb) mining in Ebonyi State, Nigeria: Implications for environmental and human health risk. International Journal of Environment and Pollution Research, 6(1): 24-32

Eze, C.T, Michelangeli, F and Otitoloju, A.A. 2019. In vitro cytotoxic assessment of heavy metals and their binary mixtures on mast cell-like, rat basophilic leukemia (RBL-2H3) Cells. Chemosphere, 223: 686 -693. https://doi.org/10.1016/j.chemosphere.2019.02.0350045-6535/© 2019.

Eze, C.T, Michelangeli, F., Otitoloju, A.A., Eze, O.O, Omodele, I., Ogbuene, E.B and Ogunwole, G.A. 2020. Occurrence of chemical pollutants in major e-waste sites in West Africa and usefulness of cytotoxicity and induction of ethoxy resorufin-O-demethylase (EROD) in determining the effects of some detected brominated flame retardants and e-waste soil-derived extracts. Environ. Sci. Pollut. Res., 28(9): 10832-10846. DOI:10.1007/s11356-020-11155-7.

Eze, V.C., Ndife, C.T. and Muogbo, M.O. 2021. Carcinogenic and non-carcinogenic health risk assessment of heavy metals in Njaba River, Imo State, Nigeria. Brazil. J. Anal. Chem., 17: 521. https://doi.org/10.30744/brjac.2179-3425.AR-05-2021.

Gomes, M.P., Smedbol, E., Chalifour, A., Hénault-Ethier, L., Labrecque, M., Lepage, L. Lucotte, M. and Juneau, P. 2014. Alteration of plant physiology by glyphosate and its by-product aminomethylphosphonic acid: an overview. J. Exp. Bot., 65(17): 4691-4703.

Kashyap, R., Verma, K.S., Thakur, M., Verma, Y. and Handa, S. 2016. Phytoextraction and bioconcentration of heavy metals by Spinacia oleracea grown in paper mill effluent irrigated soil. Nat. Environ. Pollut. Technol., 15(3): 817-824.

Khan, S., Ahmad, I., Shah, M.T., Rehman, S. and Khaliq, A. 2009. Use of constructed wetlands for the removal of heavy metals from industrial wastewater. J. Environ. Manag., 90(11): 3451-3457.

Lamare, E.R. and Singh, O.P. 2017. Changes in soil quality in the limestone mining area of Meghalaya, India. Nat. Environ. Pollut. Technol., 16(2): 545-550.

Mahdavian, S.E. and Somashekar, R.K. 2009. Heavy metal contamination of vegetables and fruits from Bangalore City. Nature Environ. Pollut. Technpl., 8(4): 829-834.

Mohsin, M., Zhu, Q., Naseem, S., Sarfraz, M. and Ivascu, L. 2021. Mining industry impact on environmental sustainability, economic growth, social interaction, and public health: An application of the semi-quantitative mathematical approach. Processes, 9(6): 972.

Nasim, S.A. and Dhir, B. 2010. Heavy metals alter the potency of medicinal plants. Rev. Environ. Contamin. Toxicol., 17: 139-149.

National Population Commission (NPC) 2010. Population and housing census of the Federal Republic of Nigeria, 2006.

Nawab, J., Li, G., Khan, S., Sher, H., Aamir, M., Shamshad, I. and Khan, M.A. 2016. Health risk assessment from contaminated foodstuffs: a field study in chromite mining-affected areas northern Pakistan. Environ. Sci. Pollut. Res., 23(12): 12227-12236.

Nuapia, Y., Chimuka, L. and Cukrowska, E. 2018. Assessment of heavy metals in raw food samples from open markets in two African cities. Chemosphere, 196: 339-346.

Obasi, N.A., Akubugwo, E.I., Ugbogu, O.C. and Otuchristian, G. 2012. Assessment of physico-chemical properties and heavy metals bioavailability in dumpsites along Enugu-port Harcourt Expressways, South-east, Nigeria. Asian J. Appl. Sci., 5(6): 342-356.

Odoh, B.I., Utom, A.U., Ezeh, H.N. and Egboka, B.C. 2012. Hydrogeochemical properties of groundwater in parts of Abakaliki City, southeastern Nigeria. Environ. Geosci., 19(2): 53-61.

Okeke, D.O and Ifemeje, J.C. 2021. Levels of heavy metals in soils and food crops cultivated within selected mining sites in Ebonyi State, Nigeria. Health Environ., 2(1): 84-95. https://doi.org/10.25082/HE.2021.01.003

Peralta-Videa, J.R., Lopez, M.L., Narayan, M., Saupe, G. and Gardea-Torresdey, J. 2009. The biochemistry of environmental heavy metal uptake by plants: Implications for the food chain. Int. J. Biochem. Cell Biol., 4(9): 1665-1677.

Prasad, M.N.V and Strzałka, K. 1999. Impact of Heavy Metals on Photosynthesis. Springer, Berlin, Heidelberg.

Prasad, S.M., Dwivedi, R. and Zeeshan, M. 2005. Growth, photosynthetic electron transport, and antioxidant responses of young soybean seedlings to simultaneous exposure of nickel and UV-B stress. Photosynthetica, 43(2): 177-185.

Rajasekaran, D. 2007. Environmental pollution by gold mining: A case study of Robertsonpet (K.G.F.) urban agglomeration, Karnataka. Nature Environ. Pollut. Technol., 6(4): 589-594.

Roba, C., Roşu, C., Piştea, I., Ozunu, A. and Baciu, C. 2016. Heavy metal content in vegetables and fruits cultivated in Baia Mare mining area (Romania) and health risk assessment. Environ. Sci. Pollut. Res., 23(7): 6062-6073.

Seregin, I.V., Shpigun, L.K and Ivanov, V.B. 2004. Distribution and toxic effects of cadmium and lead on maize roots. Russ. J. Plant Physiol., 4)51): 525-533.

Shanker, A.K., Cervantes, C., Loza-Tavera, H. and Avudainayagam, S. 2005. Chromium toxicity in plants. Environ. Int., 31(5): 739-753.

Sharma, P. and Dubey, R.S. 2005. Lead toxicity in plants. Brazil. J. Plant Physiol., 17: 35-52.

Sherene T. 2009. Heavy metal status of soils in industrial belts of Coimbatore District, Tamil Nadu. Nature Environ. Pollut. Technol., 8(3): 613-618.

Soucek, D.J., Cherry, D.S., Currie, R.J., Latimer, H.A and Trent, G.C. 2000. Laboratory to field validation in an integrative assessment of an acid mine drainage–impacted watershed. Environ. Toxicol. Chem. Int. J., 19(4): 1036-1043.

Štofejová, L., Fazekaš, J. and Fazekašová, D. 2021. Analysis of heavy metal content in soil and plants in the dumping ground of magnesite mining factory Jelšava-Lubeník (Slovakia). Sustainability, 13: 4508. https://doi.org/ 10.3390/su13084508.

Taub, F.B. 2004. Biological Impacts of Pollutants on Aquatics Organisms. University of Washington College of Ocean and Fishery Sciences, Seattle.

USEPA, S. 1986. Test methods for evaluating solid waste: physical/chemical methods. http://www. epa. gov/epaoswer/hazwaste/test/7_series.

Wang, Y., Wang, R., Fan, L., Chen, T., Bai, Y., Yu, Q. and Liu, Y. 2017. Assessment of multiple exposures to chemical elements and health risks among residents near Huodehong lead-zinc mining area in Yunnan, Southwest China. Chemosphere, 174: 613-627.

Wierzbicka, M. 1999. Comparison of lead tolerance in Allium cepa with other plant species. Environ. Pollut., 104(1): 41-52.

Xiong, Z.T. 1997. Bioaccumulation and physiological effects of excess lead in a roadside pioneer species Sonchus oleraceus L. Environ. Pollut., 279-275 :(3)97.

Yruela, I. 2005. Copper in plants. Brazil. J. Plant Physiol., 17: 145-156.

Role of Eco-Enzymes in Sustainable Development

B. Varshini and V. Gayathri†

Department of Microbiology, Ethiraj College for Women, Chennai, India

†Corresponding author: V. Gayathri; gayathri16@ethirajcollege.edu.in

ABSTRACT

Globally organic wastes are generated from fruits, vegetables, and their peels. It is mostly decomposed in landfills or by composting methods. Food processing industries, vegetable markets, and restaurants produce a huge amount of organic waste daily, generally disposed of in the environment or composted. Producing an eco-enzyme from organic kitchen waste was an innovative solution for domestic waste pollution. It is an enzyme solution obtained from an organic waste substance that contains organic acids, enzymes, and mineral salts. It is produced by performing a simple batch fermentation that involves a mixture of brown sugar, fruit or vegetable waste, and water in the ratio of 1:3:10. Two types of the eco-enzyme were produced by a fermentation process using vegetable and fruit peels for about 90 days involving *Saccharomyces cerevisiae*. The ultimate liquid or enzyme obtained was brown. Eco-enzyme 1 from (Cucurbita maxima) contained hydrolytic enzymes like amylase and lipase. The microbial diversity was observed, and bacteria like *Yersinia sp., Bacillus sp.*, and fungi like *Trichoderma sp.* and *Penicillium sp.* No enzymes and microorganisms were observed in Eco-enzyme 2 (Citron). Eco-enzyme 1 with 50% dilution effectively reduced various parameters like BOD, COD, TDS, Nitrate, Nitrite, and Ammonium in the effluent. Also, it promoted plant growth within 10 days compared to the control. Therefore, the present study outlines how the eco-enzyme could be used to treat industrial effluent cost-effectively and environmentally friendly.

INTRODUCTION

Fruits and vegetables, as well as their peels, are organic wastes that are generated worldwide. The majority of it decomposes in landfills or through composting methods. Food processing industries, vegetable markets, and restaurants generate massive amounts of organic waste daily, typically disposed of in the environment or composted.

Pollution is caused by waste fruit and vegetable peels being disposed into the environment. To avoid such issues, they must be properly disposed of. Even though organic waste is decomposed, greenhouse gas emissions are possible during decomposition (Geetha et al. 2017). This method of producing an enzyme from organic kitchen waste was more novel than the usual method of involving them in composting (Sarabhai et al. 2019).

The result was an enzyme, after fermentation of waste fruits and vegetable peels which was named "Garbage enzyme" or "Eco-enzyme." This innovative development of producing eco-enzyme was the best alternative method for productively processing household organic waste; additionally, it leads to a zero-waste framework by reducing, reusing, and recycling organic household waste materials.

Industrial Effluent

Different industries' industrial effluents contain chemicals that should not be released into the environment. Many methods exist for treating industrial effluent. Many industries struggle with reducing organic content in wastewater and only succeed after many processing stages. The use of eco-enzymes to treat industrial effluent was a cost-effective alternative.

The leather industry is a centuries-old manufacturing sector that produces a wide range of goods, such as leather footwear, bags, and garments. The leather industry's raw material is from food waste, specifically meat processing. Humans use leather products every day. Any leather processing industry's primary raw material comes from slaughterhouses and meat industry waste. This raw material is processed and converted into usable leather in tanneries. As a result, the tanning industry is regarded as one of the industry's most important leather processing units. Fig. 1 shows various chemicals employed in the processes of tanning. The leather industrial effluent contains many chemicals and acids, as the tanning process involves many chemicals. Chemicals in leather industry effluent include

ammonium salts, calcium salts, phenol, chromium, nitrogen, sulfides, solvents, surfactants, acids, and metallo-organic dyes; natural or synthetic tanning agents; sulfonated oils, and salts. Pre-tanning and tanning operations account for roughly 90% of total leather industry pollution (Sivaram & Barik 2019). The pre-tanning operation causes pH differences, which raises the chemical oxygen demand (COD), total dissolved solids (TDS), chlorides, and sulfates in tannery wastewater. Heavy chromium is widely used in the leather, electroplating, and metallurgical industries (Nur-E-Alam et al. 2020). Leather industries struggle to treat their effluent, which contains many harmful chemicals. They use many technologies to reduce the net harmful contents as much as possible. Leather industries also recycle some of their waste into value-added products for waste management. However, solid waste from leather industries isn't recycled for any purpose (CPCB 2019).

The industrial sludge also contains a large number of hazardous chemicals that pose a risk, out of which Chromium in the effluent of the leather industry poses a serious threat to soil and plant, so it cannot be reused for any purpose without proper treatment (Liknaw et al. 2017). Industries use various techniques to treat effluent, including biological, chemical, and oxidation. Waste management in tannery effluent is even more difficult due to numerous chemicals such as chromium, aluminum salts, and chloride (CBCP 2019). Bioremediation is one of the most recent technological advances for treating heavy metals-containing industrial wastes. (CPCB 2019). It primarily employs microorganisms such as bacteria, algae, and fungi to biodegrade toxic components (Biswas et al. 2015). Bioremediation process using microbes like bacteria (*Bacillus* spp., *Staphylococcus* spp.), yeast (*Candida* spp., *Saccharomyces* spp.,) fungi (*Paecilomyces* spp., *Aspergillus* spp., *Penicillium* spp., *Rhizopus* spp.,) and algae were carried out. (Nur-E-Alam et al. 2020, Santhosh et al. 2020). Waste treatment with bacteria entails stabilizing waste by decomposing it into harmless inorganic solids via an aerobic or anaerobic process. The aerobic process decomposes faster than the anaerobic process and produces no unpleasant odors, whereas the anaerobic process requires a longer retention period and produces unpleasant odors. In effluent treatment, microbes were used to facilitate the process to avoid these laborious methods. The eco-enzyme was an innovative method in the industrial effluent treatment process. Eco-
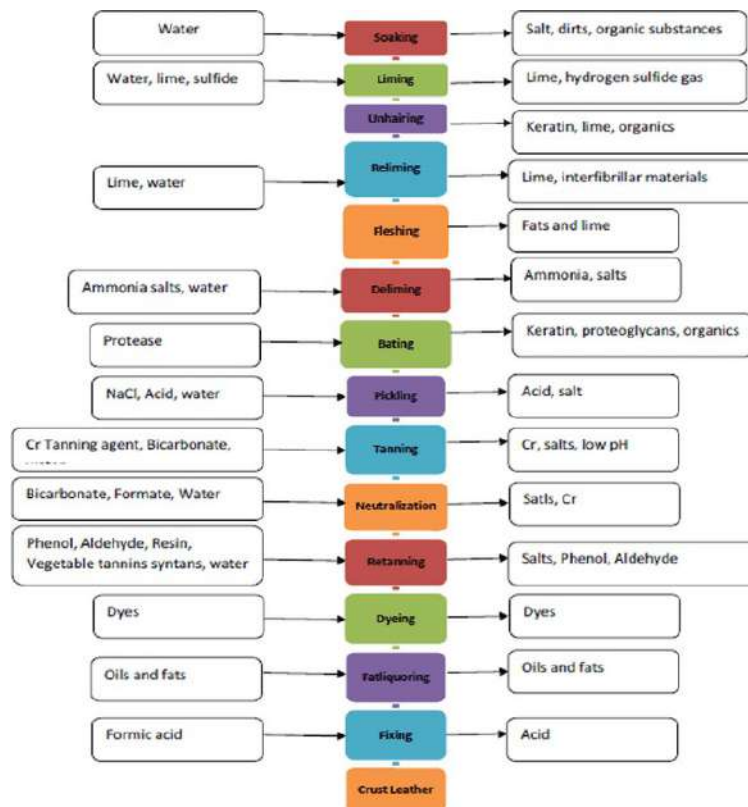

Fig. 1: Processes in the leather industry.

enzyme use in industrial effluent treatment could be a useful, nonhazardous, and time-saving method.

Eco-enzyme

An Eco-enzyme is an enzyme solution obtained from organic waste that contains organic acids, enzymes, and mineral salts. It is a simple Batch Fermentation that uses a 1:3:10 ratio of sugar, fruit or vegetable waste, and water (Neupane & Khadka 2019). The fermentation process takes place up to 60-90 days. As a result of fermentation, the final liquid or enzyme obtained was brown and contained various Organic acids, Carbon dioxide, and Ethanol. Fermentation is a chemical process in which microorganisms (non-pathogenic bacteria and yeast) break down large complex molecules into smaller ones, resulting in carbon dioxide, ethanol, and various acidic end products. The bacteria found naturally in vegetables, fruits, and their peels help convert carbohydrates into simple ones that yeast can use (Chakraborty 2020). *Saccharomyces cerevisiae* is the most commonly used yeast, producing ethanol and other acidic end products. Depending on our needs and alcoholic content, the ethanol produced in this manner can be used as a biofuel and a disinfectant. The eco-enzyme has many applications like treating domestic wastewater, contaminated ponds, lakes, and many more (Teo et al. 2021, Application of Eco-Enzyme for Domestic Waste Water Treatment 2020, Effect of Bio-Enzyme in the Treatment of Fresh Water Bodies 2019).

The eco-enzyme was mostly made using citrus and papaya peels or fruit as it showed greater antimicrobial activity (Saleem & Saeed 2020). Various fruits and vegetables produce the garbage enzyme depending on availability, flavor, etc. (Arora Amar et al. n.d., Narender et al. 2018). Composting organic household waste was the most efficient and cost-effective method of disposing of and biologically managing household waste materials (Nengah Muliarta & Darmawan 2021). The traditional Eco-enzyme manufacturing process varies depending on the alcoholic content and pH. The eco-enzyme has a variety of applications, and their use varies depending on their content. This research focuses on producing eco-enzymes using various fruits and vegetable peels as a substrate and their application in treating industrial effluent.

MATERIALS AND METHODS

Sample Collection

The research was carried out between 2021 and 2022. In the study, tannery effluent was collected simultaneously in two stages in the tannery industry. The following effluents were collected: i) post-tanning process and ii) final effluent.

Preparation of Samples

Because there were no larger particles in the effluent, the collected samples were used directly for analyzing physicochemical parameters.

Tanning Effluent Characteristics

BOD, COD, TDS, nitrate, nitrite, and ammonium levels were measured before and after treatment.

Biochemical Oxygen Consumption

The biological oxygen demand is the amount of oxygen organisms require over a given period to break down organic materials. The standard BOD level in industrial effluent is 30 mg.L^{-1} (CETP 1986)

The biological oxygen demand was calculated by preparing all of the necessary reagents. The initial dissolved oxygen content of the effluent sample was determined first. The sample is filled to half the neck of the BOD bottle. After adding the reagents, the bottle was checked for any air bubbles. The bottles are then sealed and incubated at 20°C for 5 days.

The dissolved oxygen content of a bottle incubated at 20°C for 5 days was measured. The formula was used to calculate the BOD.

Chemical Oxygen Demand

Chemical oxygen demand measures the oxygen equivalent of organic matter content in a sample oxidizable by a strong chemical oxidant.

Potassium dichromate can almost completely oxidize a wide range of organic substances to Water and Carbon dioxide. To oxidize organic matter completely. The solution must be strongly acidic and at an elevated temperature. Standard potassium dichromate, sulphuric acid, ferrous ammonium, and mercuric sulfate were prepared as reagents.

Total Dissolved Solid Content (TDS)

The mass of residue left after a measured volume of filtered water is evaporated is used to calculate the total dissolved solid content. TDS levels were also measured before and after treatment.

Nitrate Content

Titration and UV-spectrometry methods can estimate the nitrate content present in the sample. This study employs the spectrometry method for determining nitrate in the sample. The nitrite and ammonia content were also analyzed.

Eco-enzyme Production

Two types of eco-enzyme were created using vegetable and fruit peels. Cucurbita maxima and Citron (Citrus medica) peels were collected to make eco-enzymes. It was important to avoid spoiled peel waste. The samples are air-dried before being processed to create Eco-enzyme. An airtight container was filled with 200 g of brown sugar, 600 g of peels, and 2 L of water. Optionally, yeast (Saccharomyces cerevisiae) was added to speed up the fermentation process. The container's lid was tightly closed to prevent any air exchange. Fermentation was allowed to take place for a minimum of three months. The container's lid was opened intermittently during the first and second weeks to release the gases that formed inside, preventing the contents from explosion. After three months of fermentation, the fruits and vegetable peels settle to the bottom, leaving a clear liquid on top that appeared to be a brown liquid containing organic acids, ethanol, and carbon dioxide. The eco-enzyme was then collected after being filtered to remove residues. Fig. 2 shows the fermentation process of eco-enzyme.

Characteristics of Eco-enzymes

After 3 months of fermentation, the characteristics of the purified eco-enzymes were examined. The pH, enzyme activity, and physicochemical properties of the enzyme extract, such as color, and odor, were measured.

pH

The pH meter was used to determine the PH of the eco-enzyme. The meter was first calibrated using a buffer solution to pH 4, 7, and 9. The electrode was then gently dipped in the eco-enzyme sample. The pH of the eco-enzyme was displayed and recorded in the digital reader.

Enzyme Assay

The enzyme assay was carried out using qualitative analysis - A method of Agar diffusion

Activity of amylase: The activity of amylase in the medium was tested using starch as the substrate. The starch agar was prepared and sterilized by autoclaving it for 15 minutes at 121ºC. After cooling to 55ºC, the agar was poured onto sterile petri plates. After that, the plates were left alone to solidify.

10 µL of the eco-enzyme sample was inoculated in the plates. The plates were then incubated for 24 h at 37°C. The plates were flooded with iodine, and a clearance zone was determined. The presence of amylase was indicated by the clearance zone, which was compared to control plates.

Lipase activity: The eco-enzyme's lipase activity was discovered using tributyrin as a substrate in the agar medium. After incubation, the zone of clearance is observed.

Protease activity: The presence of protease activity in the agar medium is determined by using casein 1 percent as a
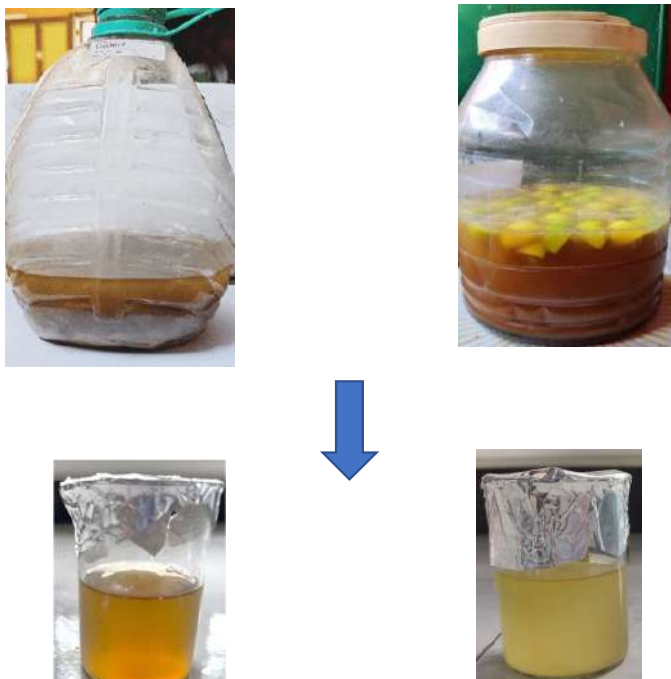

Fig. 2: Fermentation process of Eco-enzyme.

substrate (1.5 percent). After inoculating the plates with the sample, they were incubated at 37°C for 24 h. The clearance zone is observed and recorded

Gas Chromatography-Mass Spectrometry

Gas chromatography-mass spectrometry was used to detect enzymes both qualitatively and quantitatively. Gas chromatography-mass spectrometry (GC-MS) is a technique for identifying various substances in a test sample that combines the advantages of gas chromatography and mass spectrometry.

Microbial Diversity

The spread plate method was used to examine the microbial diversity present in the eco-enzyme. Gram staining and LPCB staining were used to identify bacteria and fungi. 0.1mL of the eco-enzyme sample was spread on the Nutrient agar and SDA mediums using a glass L- rod. The plates had been incubated. SDA plates were incubated at room temperature for 48-72 h, while nutrient agar plates were incubated at 37°C for 24 h (Sarabhai et al. 2019).

Treatment of Effluent Using Eco-enzyme

The treatment was carried out for approximately 30 days in two dilutions of the eco-enzyme (25 percent and 50%). The parameters were analyzed before the treatment process to compare the results after treatment with the eco-enzyme.

Dilution by 25%: The industrial effluent was placed in a conical flask (375 mL), to which the eco-enzyme sample (125 mL) was added. The flask was then sealed with aluminum foil. The same setup was used for both eco-enzyme samples. For a month, the flask was left alone. After 30 days of treatment, the color change and parameter reduction were tested.

50 percent dilution: 250 mL of effluent was mixed with 250 mL of eco-enzyme sample. The flask was sealed with aluminum foil. Fig. 3 shows the treatment of effluent using Eco-enzyme in 2 dilutions.

Sludge Treatment

The dry leather industrial sludge was collected. The sludge was mixed in a 1:1 ratio with eco-enzyme and left for 2-3 days. Before treating with sludge, the eco-enzyme was diluted to about 1:500. After about 2-3 days, the sludge was mixed in a 1:1 ratio with the sand. It was then used to control plant growth. (Nabila et al. 2021)

Four pots were selected as controls: soil alone, raw sludge without enzyme treatment, sludge treated with eco-enzyme 1, and sludge treated with eco-enzyme 2. Each pot was labeled and filled with Indian mustard, *Brassica juncea*. The pots were watered regularly, and the plant growth was monitored. The heights of the plant shoots were measured.

RESULTS AND DISCUSSION

Production of Eco-enzyme

The batch fermentation process produced two eco-enzymes. After fermentation, the enzyme extract was obtained by filtration method. Centrifugation was done at 5000 rpm for 5 mins to obtain the same enzyme extract. Fig. 4

Fig. 3: Treatment of effluent using Eco-enzyme in 2 dilutions.
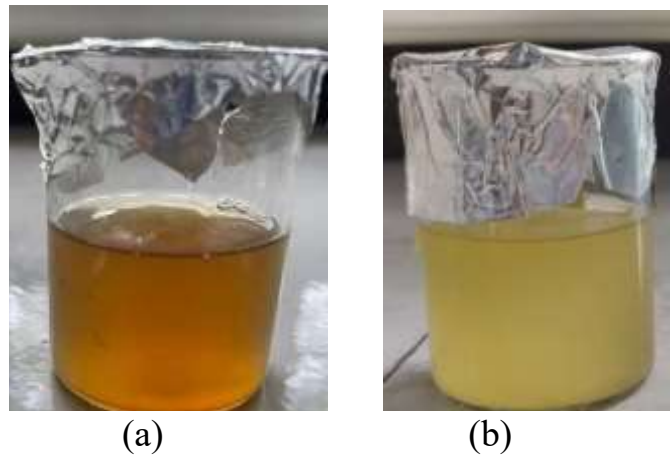
Fig. 4: Eco-enzyme 1. Eco-enzyme 2.

shows the enzyme obtained after the batch fermentation process.

Examination of Microbial Diversity in Eco-enzyme

Microscopic examination revealed Gram-negative bacilli and Gram-positive bacilli observed, and other biochemical tests were performed. It was found that there was the presence of *Bacillus* sp., *Yersinia* sp. Figs. 5 and 6 show the preliminary tests (Gram staining and biochemical tests performed). Fig. 7 shows the LPCB staining and growth on the SDA plate.

The eco-enzyme was inoculated in SDA plates and incubated for 48-72 h. Upon further staining using LPCB, fungi like Trichoderma viride, Saccharomyces cerevisiae, and Penicillium sp. were present in both the
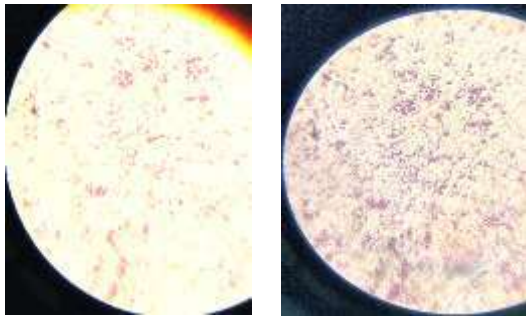
Fig. 5: Gram staining (a) Gram negative bacilli (b) Gram positive bacilli.

Fig. 6: Biochemical test.
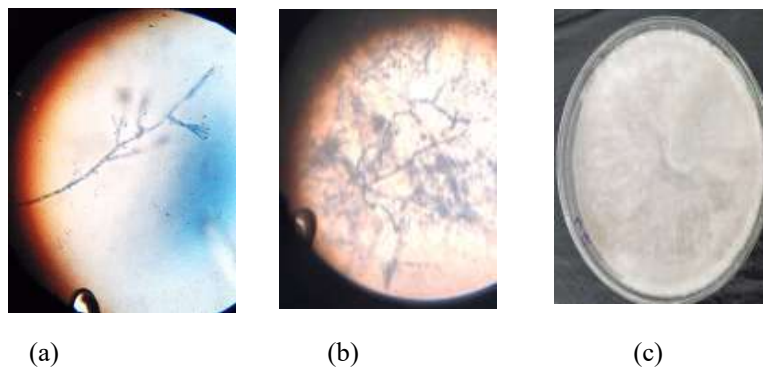
Fig. 7: LPCB staining (a)- *Penicillium* sp. (b)- *Trichoderma* sp., (c) – SDA plate with growth.

Table 1: Characteristics of the Eco-enzyme.

Physical characteristics	Eco-enzyme -1	Eco-enzyme -2
Color	Brown colored liquid	Pale yellow colored liquid
pH	4.10	3.83
Turbidity	Clear liquid, non-viscous	Clear liquid, non-viscous
Odor	Pungent	Sweet sour

Table 2: Biochemical test done for Eco-enzyme 1.

PRELIMINARY TEST	RESULT
Gram staining	Gram positive bacilli and Gram-negative bacilli
BIOCHEMICAL TEST	**RESULT**
Indole	Negative
Methyl red	Negative
Voges Proskauer	Positive
Citrate	Negative
Triple sugar ion	Yellow slant and yellow butt, no gas production
Urease	Negative
Nitrate	Positive

eco-enzyme samples. Table 1 shows the characteristics of eco-enzyme.

Table 2 shows the biochemical tests performed for Eco-enzyme 1 as there was growth in the Nutrient agar and SDA plates. Eco-enzyme 1 was found to contain Gram positive and negative bacilli.ss There was no growth observed in the eco-enzyme 2 solution.

Enzyme Assay

There was a zone of clearance after adding iodine in starch ag, indicating the presence of amylase activity in both the eco-enzymes produced. Figs. 8, 9 and 10 show the amylase, protease, and lipase activities respectively. There was no protease activity seen in the eco-enzymes. There was a small zone of clearance in case of lipase activity in both the eco-enzymes.

Gas Chromatography-Mass Spectrophotometry

Gas Chromatography-Mass Spectrophotometry was performed for both the eco-enzyme samples after batch fermentation. It was found that Eco-enzyme 1 consists of active ingredients like alcohol, and acids. Fig. 11 a and b show the graphical peaks of various compounds present in the eco-enzyme sample.
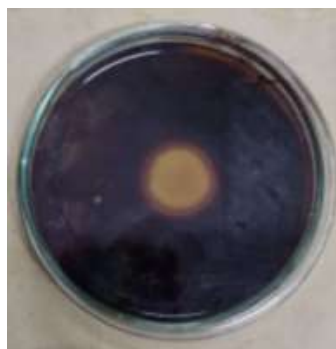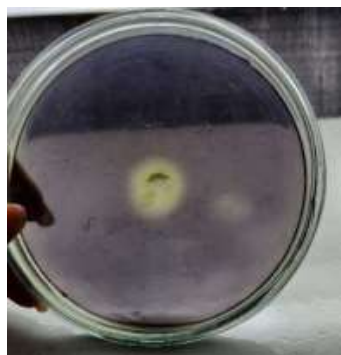
Fig. 8: Amylase activity of eco enzyme 1 and eco enzyme 2.
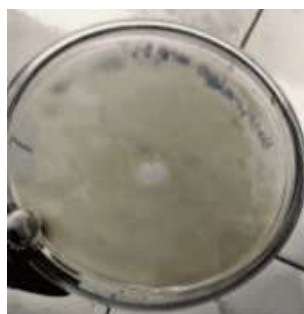
Fig. 9: Protease activity -Nil in both eco enzyme 1 and eco enzyme 2.
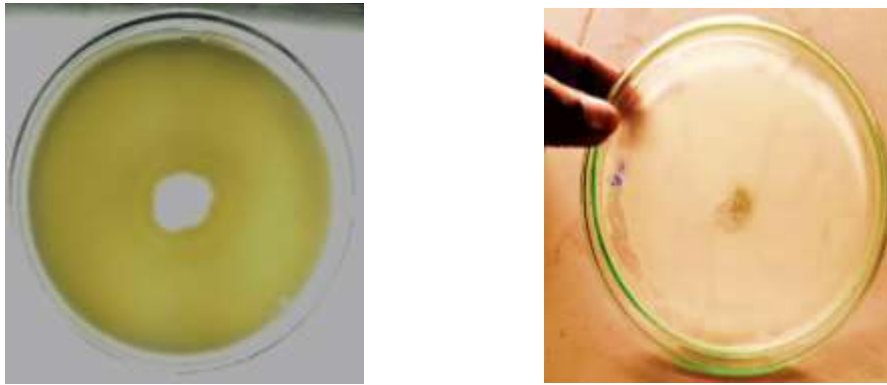
Fig. 10: Lipase activity - positive for Eco enzyme 1 and nil for Eco enzyme 2.
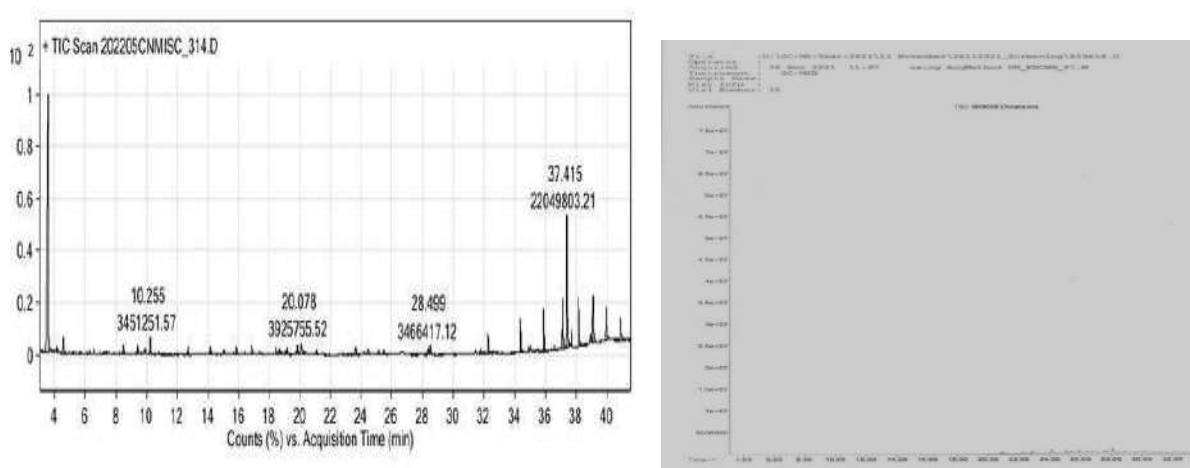
Fig. 11: (a) GC- MS of Eco-enzyme 1 (b) GC- MS of Eco-enzyme 2.

Characterization of Industrial Effluent

The characteristics of industrial effluent were studied before treatment. Both the effluent was found to be acidic and black in color. Table 3 shows the characteristics of industrial effluent used in this study.

Effluent Treatment

Table 4 shows the results of parameters tested before and after treatment of the effluent. It was found that Eco-enzyme

diluted to 50% which was found to be effective in the treatment of leather industrial effluent.

Fig. 12 shows the process of effluent treatment after 30 days. There was a considerable amount of reduction in parameters and color as well. Eco-enzyme 1 was found to be effective when used in the dilution of 50%.

Sludge Treatment

The sludge without eco-enzyme treatment showed no plant growth, indicating that it cannot be used to grow plants directly. Plant growth was aided when the sludge was treated with the eco-enzyme. The conversion of ammonium in the sludge into nitrogen, which the plant readily utilizes for growth, could cause plant growth. The seeds were planted in each pot, and the pots were watered daily. Plant growth was monitored, and shoot heights were measured. When compared to the control, sludge treated with eco-enzyme

Table 3: Characteristics of industrial effluent.

Parameters	Raw effluent	Tannery effluent
P^H	3.42	2.76
Color	Black	Black
Odor	Unpleasant foul odor	Repulsive, offensive chemical smell

Table 4: Treatment of Industrial effluent using Eco-enzyme.

Parameters	Before Treatment	After Treatment			
		Raw Effluent		Tannery Effluent	
		25%	50%	25%	50%
BOD	1080	344 mg.L^{-1}	297 mg.L^{-1}	372 mg.L^{-1}	324 mg.L^{-1}
COD	4250	678 mg.L^{-1}	606 mg.L^{-1}	730 mg.L^{-1}	576 mg.L^{-1}
TDS	5096	1560 mg.L^{-1}	1420 mg.L^{-1}	2510 mg.L^{-1}	1680 mg.L^{-1}
Nitrate	0.90	0.30 mg.L^{-1}	0.17 mg.L^{-1}	0.32 mg.L^{-1}	0.11 mg.L^{-1}
Nitrite	0.73	0.21 mg.L^{-1}	0.18 mg.L^{-1}	0.26 mg.L^{-1}	0.12 mg.L^{-1}
Ammonia	0.36	0.11 mg.L^{-1}	0.09 mg.L^{-1}	0.13 mg.L^{-1}	0.06 mg.L^{-1}

Raw effluent   Tannery effluent

After 30 days

Raw effluent (25% and 50% dilution)   Tannery effluent (25%and 50%

Fig. 12: Effluent treatment process.

showed greater plant growth. Fig. 13 a and b shows the sludge taken from the industry and (c) shows the growth of plants when sludge was treated with eco-enzyme.

Table 5 shows the plant shoot height measured after 10 days. These results show that Eco-enzyme 1 was found to be effective in the treatment of industrial sludge when compared with the control (sludge alone). Further, the active component present in eco-enzyme which makes it a better solution for treating the effluent and sludge should be studied in detail.

Fig. 13: Sludge treatment (a) (b) Sludge mixed with eco-enzyme and sand (c) Plant growth after 10 days.

Table 5: Plant shoot height measurement after 10 days.

Treatment	Plant Height (in cm)
Control – Soil +Sludge	1.0
Control- Soil	3.5
Soil + Sludge treated with the Eco-enzyme 1	5.7
Soil + Sludge treated with the Eco-enzyme 2	4.2

DISCUSSION

The production of the eco-enzyme from organic waste is a novel method that replaces the traditional method of composting waste. Numerous studies have been conducted to test various applications of the eco-enzyme. These eco-enzymes effectively treated water bodies such as ponds and lakes. Similar to the study conducted, the antimicrobial activity of the eco-enzyme was found to be effective against a wide range of microorganisms (Arun & Sivashanmugam 2015). According to (Made Rai Rahayu et al. 2021), the eco-enzyme contains hydrolytic enzymes such as amylase and lipase.

Leather industrial effluent contains several chemicals introduced at various stages of the leather manufacturing process. Both humans and the environment are endangered by the chemicals used. Proper treatment and waste management methods must be implemented in industries to ensure the safety of humans and the environment. Waste management in industries has traditionally been a time-consuming process. Many industries use enzyme technologies and microorganisms to treat effluent (Choudhary et al. 2004, Pandey et al. 2017). Microbial isolates like *Saccharomyces cerevisiae* and *Torulaspora delbrueckii* from watermelon were used to treat raw tannery effluent. They were found to degrade the physicochemical parameters and could be used to treat tannery effluent biologically (Okoduwa et al. 2017). The concept of using eco-enzymes to treat industrial effluent is novel. The hydrolytic enzymes were discovered in eco-enzyme 1, made from vegetable peel waste.

These enzymes are involved in the breakdown of compounds found in effluent. In about 50% dilution of the eco-enzyme, there was a significant reduction in major

parameters such as BOD, COD, and TDS. Similarly, Rasit and Chee Kuan (2018) used eco-enzymes to treat Palm oil mill effluent. There was a decrease in oil and grease content observed. The eco-enzyme was also used to treat metal-based effluents, which were observed by Hemalatha and Visantini (2020)

Similarly, Teo et al. (2021) discovered decreased nitrate content in wastewater samples. In contrast to the previous study, there was a significant reduction in nitrate content in the effluent sample in the current study.

Similarly, a study found that the yeast Saccharomyces cerevisiae reduced various parameters in tanneries. Galintin et al. (2021) conducted a study similar to the current one. To treat aquaculture sludge, they used eco-enzymes. It was discovered that 10% dilution was effective in lowering various parameters. The study used tannery sludge that had been collected in dry form. Compared to the control, sludge treated with eco-enzymes 1 and 2 promoted plant growth. This was similar to the research by Hemalatha and Visantini (2020). The beneficial effect of the eco-enzyme on plants was investigated by Nabila et al. (2021)

The plant growth of Turi (*Sesbania grandiflora*) increased in the study. In a study conducted by discharging leather industrial effluent into the soil, there was an increase in soil microbiota and enzyme activity (Reddi & Narasimha 2012). Plant growth could be attributed to the organic acids found in the eco-enzyme. Production and usage of the eco-enzyme effectively treated leather industry effluent and paved the way to sustainable development. The current study used eco-enzyme production as an innovative approach. Using eco-enzymes to treat effluent would be a promising method and the best alternative to the chemicals commonly used in industry. It protects both humans and the environment. It is also less expensive and saves time. Enzyme stabilization would be a better way to increase their efficacy.

CONCLUSION

Organic and agricultural waste is being used in a variety of fields. They are becoming more popular as value-added products, and many industrial firms use them as raw materials. Fruit and vegetable peels contain a variety of bioactive components. When organic waste is disposed of in trash or landfills, its components and nutrients are lost. Eco-enzyme production is a new and innovative method of reducing and reusing waste as a value-added product.

Eco-enzymes are being developed, and it has been discovered that they can be used in various fields. It also replaces the traditional composting method of disposing of organic waste. The Eco-enzyme is a collection of enzymes

that reduce organic compounds in industrial effluent. Agar diffusion and GC-MS methods revealed that Eco-enzyme 1 contained enzymes such as amylase and lipase. The eco-enzyme 2, made from citrus peels, contained no hydrolytic enzymes.

Hydrolytic enzymes were discovered to cause a decrease in parameters such as BOD, COD, TDS, nitrate, nitrite, and ammonium. Eco-enzyme diluted to 50% was effective in treating leather industrial effluent. The eco-enzyme contained a diverse group of microbes. Bacteria such as *Yersinia sp.* and *Bacillus sp.* were present, as well as fungi such as *Trichoderma* sp. and *Penicillium* sp., More research is needed to test the microorganism species found in the eco-enzyme. Dry sludge collected from the industry was also used in the sludge treatment. Within 10 days, plant growth was observed. The increased shoot heights suggest that the eco-enzyme aids plant growth. The challenging approach in producing Eco-enzyme is that there is no standard protocol for production. Because it takes longer to produce an Eco-enzyme, it is still not used in industries. There has been no research on the mechanism of action of eco-enzymes in component reduction, which should be looked into further.

REFERENCES

Arora Amar, M., Baba, S., Singh, A., Singh, J., Arora, M. and Kaur, P. (n.d.). Antimicrobial & antioxidant activity of orange pulp and peel. Int. J. Sci. Res., 11: 414-426. https://www.researchgate.net/publication/319036539

Arun, C. and Sivashanmugam, P. 2015. Investigation of the biocatalytic potential of garbage enzyme and its influence on stabilization of industrial waste-activated sludge. Process Safety Environ. Protect., 94(C): 471-478. https://doi.org/10.1016/j.psep.2014.10.008

Biswas, S.K., Lisa, L.A., Banu, N.A., Islam, A. and Roy, A.K. 2015. Review paper microbial treatment of tannery effluents : A review. Plant Environ. Dev., 4(2): 13-20.

CBCP 2019. Guidelines for Environmental Improvement in Leather Tannery Sector. Central Pollution Control Board. March, 1–28. https://cpcb.nic.in/openpdffile.php?id=TmV3c0ZpbGVzLzcyXzE1NTQ0NTY2NDhfbWVkaWFfaG90bzIyMTYwLnBkZg==

CETP 1986. Standards laid by the Ministry of Environment and Forests, Government of India for common effluent treatment plants as per Environment Protection Rules, 1986. https://www.mpcb.gov.in/sites/default/files/common-effluent-treatment-plant/guidelines/CETP%20Standards.pdf

Chakraborty, D. 2020. Ethanol Production from Kitchen Waste by Wild Type Yeast Isolated from Natural Sources. Elseiver, Netherlands, pp. 46-71

Choudhary, R.B., Jana, A.K. and Jha, M.K. 2004. Enzyme technology applications in leather processing. Indian J. Chem. Technol., 11(5): 659-671.

Galintin, O., Rasit, N. and Hamzah, S. 2021. Production and characterization of eco-enzyme produced from fruit and vegetable wastes and its influence on the aquaculture sludge. Biointerf. Res. Appl. Chem., 11(3): 10205-10214. https://doi.org/10.33263/BRIAC113.1020510214

Geetha, S., Kaparapu, J. and Saramanda, G. 2017. Antimicrobial activity of fermented citrus fruit peel extract distribution of microalgae in ponds and reservoirs. J. Eng. Res. Appl., 7: 25-28. https://doi.org/10.9790/9622-0711072528

Hemalatha, M. and Visantini, P. 2020. Potential use of eco-enzyme for the treatment of metal-based effluent. IOP Conf. Ser. Mater. Sci. Eng., 716(1): 012016. https://doi.org/10.1088/1757-899X/716/1/012016

Janarthanan, M., Mani, K. and Raja, S.R.S. 2020. Purification of contaminated water using eco-enzyme. IOP Conf. Ser. Mater. Sci. Eng., 955(1): 012098. https://doi.org/10.1088/1757-899X/955/1/012098

Liknaw, G., Tekalign, T. and Guya, K. 2017. Impacts of tannery effluent on environments and human health. J. Environ. Earth Sci., 7(3): 88-97.

Nabila, G., Nurzainah, G., Sayed, U. and Simon, G. 2021. Effect of eco-enzymes dilution on the growth of Turi plant (Sesbania grandiflora). Peter. Integr., 9(1): 29-35.

Narender, B.R., Rajakumari, M., Sukanya, B. and Harish, S. 2018. Antimicrobial activity on peels of different fruits and vegetables. J. Pharma. Res., 7(1):1-7. https://doi.org/10.5281/zenodo.1133694

Nengah Muliarta, I. and Darmawan, K. 2021. Processing household organic waste into eco-enzyme as an effort to realize zero waste. Agric. J., 1(1): 7-12.

Neupane, K. and Khadka, R. 2019. Production of garbage enzyme from different fruit and vegetable wastes and evaluation of its enzymatic and antimicrobial efficacy. Tribhuvan Univ. J. Microbiol., 6: 113-118. https://doi.org/10.3126/tujm.v6i0.26594

Nur-E-Alam, M., Mia, M.A.S., Ahmad, F. and Rahman, M.M. 2020. An overview of chromium removal techniques from tannery effluent. Appl. Water Sci., 10(9): 1-22. https://doi.org/10.1007/s13201-020-01286-0

Okoduwa, S.I.R., Igiri, B., Udeh, C.B., Edenta, C. and Gauje, B. 2017. Tannery effluent treatment by yeast species isolates from watermelon. Toxins, 5(1): 1006. https://doi.org/10.3390/toxics5010006

Pandey, K., Singh, B., Pandey, A.K., Badruddin, I.J., Pandey, S., Mishra, V.K. and Jain, P.A. (2017). Application of Microbial Enzymes in Industrial Waste Water Treatment. Int. J. Curr. Microbiol. Appl. Sci., 6(8): 1243-1254. https://doi.org/10.20546/ijcmas.2017.608.151

Rahayu. M.R., Nengah, M. and Yohanes, P.S. 2021. Acceleration of production of natural disinfectants from the combination of eco-enzyme domestic organic waste and Frangipani Flowers (Plumeria alba). Sustain. Environ. Agric. Sci., 5(1): 15-21. https://doi.org/10.22225/seas.5.1.3165.15-21

Rasit, N. and Chee Kuan, O. 2018. Investigation on the influence of bio-catalytic enzyme produced from fruit and vegetable waste on palm oil mill effluent. IOP Conf. Ser. Earth Environ.Sci., 140(1): 1744. https://doi.org/10.1088/1755-1315/140/1/012015

Reddi. P.M. and Narasimha, G. 2012. Effect of leather industry effluents on soil microbial and protease activity. J. Environ. Biol., 33(1); 39-42.

Saleem, M. and Saeed, M.T. 2020. Potential application of waste fruit peels (orange, yellow lemon, and banana) as a wide range natural antimicrobial agent. J. King Saud Univ. Sci., 32(1): 805-810. https://doi.org/10.1016/j.jksus.2019.02.013

Santhosh, S., Rajalakshmi, A.M., Navaneethakrishnan, M., Jenny Angel, S. and Dhandapani, R. 2020. Lab-scale degradation of leather industry effluent and its reduction by Chlorella sp. SRD3 and Oscillatoria sp. SRD2: A bioremediation approach. Appl. Water Sci., 10(5): 1-11. https://doi.org/10.1007/s13201-020-01197-0

Sarabhai, S., Arya, A. and Arti Arya, C. 2019. Garbage enzyme: A study on compositional analysis of kitchen waste ferments. Pharma Innov. J., 8(4): 1193-1197. www.thepharmajournal.com

Sivaram, N.M. and Barik, D. 2019. Energy From Toxic Organic Waste for Heat And Power Generation, Elsevier, Netherlands, pp. 55-67.

Teo, S., Wen, L.W. and Ling, R.L.Z. 2021. Effective microorganisms in producing eco-enzyme from food waste for wastewater treatment. Appl. Microbiol. Theory Technol., 11: 28-36. https://doi.org/10.37256/amtt.212021726

Original Research Paper

https://doi.org/10.46488/NEPT.2023.v22i03.018

Open Access Journal

Preparation and Characterization of Slow-Release Zinc and Iron Fertilizer Encapsulated by Palm Stearin

Maizatiey Farizza Mohd Nasir*, Md. Kamal Uddin*(†), Mohd Salleh Kamarudin*, Muhammad Fadhil Syukri Ismail*, Arina Shairah Bt Abdul Sukor* and A. Abubakar**

*Faculty of Agriculture, Universiti Putra Malaysia, 43400 Serdang, Selangor, Malaysia
**Faculty of Forestry and Environment, Universiti Putra Malaysia, 43400 Serdang, Selangor, Malaysia
†Correspondance: Md. Kamal Uddin; mkuddin@upm.edu.my

ABSTRACT

Using granular form application in the picsiponic system, this study investigates the effects of supplementation in the piscipionic system on plant growth performance. This study was conducted at the Aquaculture Experimental Station in Puchong, Selangor. The experiment was set up in a greenhouse with a plastic liner at the bottom. The coated fertilizers were immersed in 500 mL of distilled water in the beakers. The immersion times were analyzed for each 3, 6, 12, 18, 24, 30, 36, 42, 48, 54, 60, 66, and 72 hours. Insoluble solids and water were then filtered using filter paper and dried in the oven, followed by the drying process to obtain a constant weight before being put in the desiccators. During the release test, the distilled water was taken at every 48-hour interval, and the concentration of nutrients was determined from the atomic absorption spectrometer. The findings indicate that the weights of release fertilizers, specifically Zn and Fe, significantly decreased over time. At the lowest concentration, the coated zinc and iron weights decreased as time increased. Referring to the curve results, the Zn fertilizer started drastically decreasing its weight at hour 24, which decreased approximately to 0.002 for every subsequent hour. Meanwhile, Fe fertilizer decreased drastically at hour 66, where the weight dropped from 0.10467 to 0.039. However, the final weights for both fertilizers at hour 72 were about the same.

INTRODUCTION

Over the past few years, Malaysian aquaculture production has grown, and its value has also increased (Mustafa et al. 2018). Aquaponics and hydroponics together are called pisciponics, where enriched nutrients are recirculated from fish tanks to grow plants (Goddek et al. 2015). Nonetheless, the world must be concerned about how future generations will be able to produce more food sustainably in the future.

The pisciponics system relies on nutrients to support plant growth and efficiently recycle nutrients (Okomoda et al. 2022). The system provides essential nutrients to the plants. The Pisciponics system is an environment-friendly and sustainable food production (Okomoda et al. 2022). Malaysia has adopted the pisciponics system to feed the ever-increasing human population and for food security (Rafiee & Saad 2008). The world is facing global population growth, and it is exceeding 7.2 billion. It is projected to be 9.7 billion by 2050, with over 85 percent living in urban areas compared with 1990, with 5 billion people only (Alexandratos & Bruinsma 2012). The world population is projected to grow exponentially (Maucieri et al. 2018).

The growing number of people moving to urban areas will likely increase malnutrition, urban poverty, and hunger (United Nations Department of Economic and Social Affairs Population Division 2017).

Fertilizers are chemical substances added to soil to increase crop yield, which is crucial for plant healthy growth (Alam et al. 2013). The production and demand for food have become more dependent on various agricultural techniques (Tilman et al. 2011). The characteristics needed include increasing the productivity of fertilizers and minimizing the cost (Qureshi et al. 2018). Research is needed to develop fertilizers that maximize crop yields, enhance nutrient efficiency and reduce pollution. However, efficient production is crucial since the essential elements of nutrition or fertilization can affect the physiological processes of plants (Ahl & Mahmoud 2010). Plants need macronutrients and micronutrients, which are vital for their growth. In many cases, deficiency diseases are caused by insufficient plant micronutrient supply (Shete et al. 2015).

However, organic farming methods are not the only example of sustainable nutrient management. The leaching

of nutrients can be managed by an appropriate amount of fertilizers and slow-release fertilizers in the pisciponic system to avoid leaching into the environment and causing water eutrophication (Rahman 2015). A good amount of fish combined with insufficient nutrients will result in low nutrient absorption and affect crop production in pisciponics systems. Other than that, it is also reported that pisciponic systems that rely exclusively on fish waste to provide plant nutrients have low levels of micronutrients (Ru et al. 2017). However, there is a paucity of information and a limited number of research investigations on the effects of supplementation of zinc chelate and iron chelate in granular form to absorb in water and effectively alleviate nutrient insufficient in crop plants (Roosta & Hamidpour 2013).

The present work attempt to develop new slow-release zinc and iron fertilizer by palm stearin. The effects of selected micronutrient mineral composition on crop plants in the pisciponic system using granular form were investigated. Then a slow-release process using stearin as a coat for Zinc and Iron was evaluated.

MATERIALS AND METHODS

Location of Experiment

Slow-release fertilizers were processed in the Nutrition Laboratory in Block A, UPM, and the pisciponic recirculating system was conducted in a greenhouse at UPM's Aquaculture Experimental Station in Puchong, Selangor.

Synthesis of Coated Slow-Release Fertilizer

The temperature was set at 60°C in a water bath to melt seven grams of palm stearin in a beaker. After the whole palm stearin was fluxed, it was left to cool until the temperature extended to 30°C. Subsequently, 100 g of zinc chelate and iron fertilizer were added to the beaker of palm stearin and mixed using a spatula. Lastly, the zinc- and iron-coated fertilizers were kept in a desiccator for 48 hours before being dried in an air-tight container for further analysis and investigations.

Total Coating Analysis

Therefore, 10 g of coated zinc and iron micronutrients were flattened and mixed with water to increase the selected micronutrients' dissolution rate. Consequently, the solution was filtered, and the remaining insolvable solid material was dried in the oven until fully preserved. Subsequently, the zinc- and iron-coated fertilizers were dissolved in deionized water. The other steps were conducted similarly in this study. The following formula was used to calculate the coating percentage (Rahman 2016):

$$(\%) \text{ coating} = \text{wt. of residual (g)}/10 \times 100 \qquad …(1)$$

Crushing Strength Analysis

The crushing strength test is essential to ensure the product can resist physical control over the supply chain. 30 granules were randomly selected from the major part population based on the sieve with a capacity of 200 lb (100kg, 1000N). At the same time, 12.7-317.5 mm.min^{-1} speed was used for computation by applying a compressive force on a single granule by using a hardness tester (capacity: 100kg, 1000 N; speed: 12.7–317.5 mm.min^{-1}).

Scanning Electron Microscopy Analysis

To investigate the surface morphology and thickness of the coating material, the samples of coated and uncoated zinc and iron fertilizers were cut in half using a blade. The sample cross-section was placed on the slide and coated using gold. The samples were then viewed using SEM, Model Hitachi TM3030 (Rahman 2016).

Dissolution Rate of Slow-Release Fertilizer

An Erlenmeyer flask was filled with 500 mL of distilled water and sealed before 100 g of coated fertilizers were added. Next, the Erlenmeyer flask was placed in an incubator shaker for 5 h (Zheng et al. 2010). This analysis studies the coated granules' rate of coated fertilizer release when submerged in water. The 16 samples were subjected to a dissolution test, and their dissolution rates were evaluated based on the efficiency equation (Irfan et al. 2018). A relatively long-term process (72 h) was developed to access nutrient release generated by natural-release mechanisms in a laboratory setting. The method was slightly changed in terms of fertilizer usage in the pisciponic system by sponge-soaking at a constant temperature of 27.01 through the system and a flow rate of 10 L.min^{-1}. Uncoated and coated fertilizers using dissolution rates. We sealed 9 samples in a beaker with 500 mL distilled water. The released coated fertilizer solution was measured using a refractometer to the known refractive index of water, and the reading was taken for 0, 3, 6, 12, 18, 24, 30, 36, 42, 48, 54, 60, 66, and 72 h (Rahman 2016).

RESULTS AND DISCUSSION

Morphology Characteristic of Coated Slow-Release Fertilizer

Based on Table 1, mass strength in g/granular was regulated before and after coating. The crushing strength will differ depending on the particle size, which is the force vital to press the particle (Ibrahim et al. 2014). In collating the crushing strength data, a comparison is essential to have

Table 1: The morphology characteristics of coated slow-release fertilizer.

Treatment	Coating [%]	Thickness [mm]	Diameter [mm]	Crushing strength [N]
Zinc-coated	7.67	2.77[a]±0.1	3.72[a]±0.1	56.81[a]±0.2
Iron-coated	7.67	2.95[a]±0.1	4.20[a]±0.1	60.13[a]±0.2
Uncoated Zinc	0.0	2.92[a]±0.2	3.45[a]±0.1	20.12[b]±0.1
Uncoated Iron	0.0	2.83[b]±0.1	3.40[a]±0.1	25.73[b]±0.1

Table 2: The weights of coated zinc and iron using stearin of micronutrients with substrate dissolution rates.

Weight of fertilizer (g)	Time (h)												
	3	6	12	18	24	30	36	42	48	54	60	66	72
Zinc	0.3±0.2	0.28±0.1	0.27±0.1	0.25±0.1	0.22±0.1	0.17±0.1	0.13±0.1	0.11±0.2	0.09±0.2	0.08±0.1	0.07±0.2	0.06±0.1	0.03±0.1
Iron	0.3±0.1	0.28±0.2	0.28±0.1	0.26±0.1	0.24±0.1	0.24±0.1	0.21±0.2	0.18±0.1	0.17±0.2	0.16±0.1	0.13±0.2	0.10±0.1	0.03±0.2
Uncoated Zinc	0.3±0.1	0.2±0.1	0.1±0.2	0	0	0	0	0	0	0	0	0	0
Uncoated Iron	0.3±0.1	0	0	0	0	0	0	0	0	0	0	0	0

abundant mechanical strengths in coated zinc and iron to compare standardized granules because the crushing strength rises significantly with the rise in coated fertilizers to have the mechanical strength to resist the normal handling and storage without rupture. Besides, mechanical strength could influence the granule's porosity, shape, surface crystal, and moisture content. This is in line with the findings of Affendi et al. (2020), in which the coated urea with palm stearin enhances the stability of urea.

Scanning Electron Microscopy Analysis

Fig. 1: SEM of nano-sub nanocomposites: a) present the iron surface coated with stearin; b) without stearin; c) present the zinc surface coated with stearin, and d) without coated with stearin

Dissolution Rate of Slow-Release Fertilizer

Fig. 1 shows the Scanning Electron Microscopy Analysis (SEM) on the fertilizers for coated and non-coated using
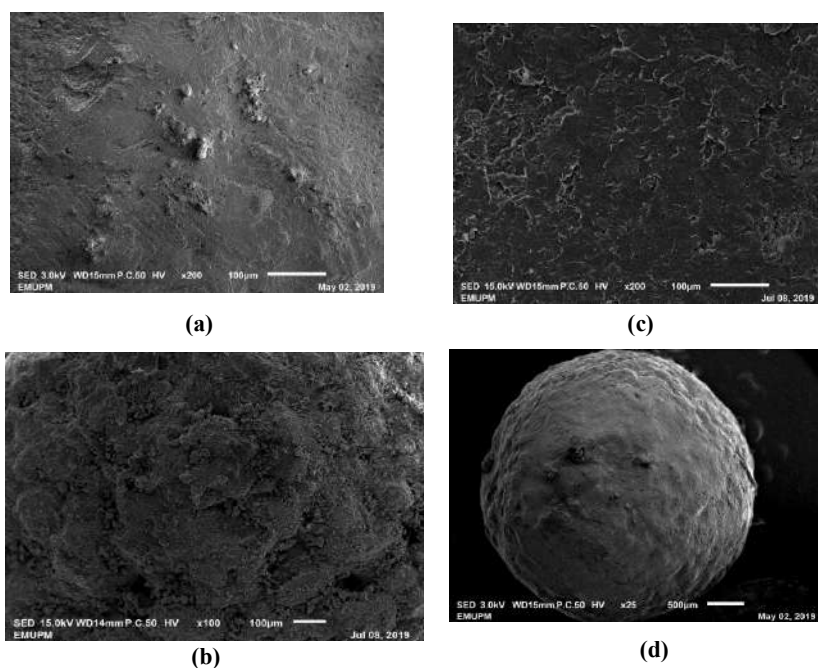

(a)

(c)

(b)

(d)

Fig. 1: SEM of nano-sub nanocomposites: a) present the iron surface coated with stearin; b) without stearin; c) present the zinc surface coated with stearin, and d) without coated with stearin.

Table 3: The nutrient concentrations of coated zinc and iron using stearin of micronutrients with time.

Concentr-ation (g)	Time (h)												
	3	6	12	18	24	30	36	42	48	54	60	66	72
Zinc	0.3±0.1	0.28±0.2	0.27±0.2	0.25±0.1	0.22±0.1	0.17±0.2	0.13±0.1	0.11±0.1	0.09±0.2	0.08±0.1	0.07±0.1	0.06±0.2	0.03±0.1
Iron	0.3±0.1	0.28±0.1	0.28±0.2	0.26±0.1	0.24±0.1	0.24±0.1	0.21±0.2	0.18±0.1	0.17±0.2	0.16±0.1	0.13±0.1	0.10±0.2	0.03±0.1

the stearin. There are significant differences between coated fertilizers and uncoated fertilizers. The concentrations of coated and uncoated fertilizers were measured using the dissolution rates in water. According to Meng et al. (2019), palm stearin is a moisture barrier containing saturated fatty acids. The palm stearin material also led to high hydrophobicity (Aliyu 2017).

Coated zinc, iron, and uncoated fertilizers released nutrients at hour 3. However, Table 2 and 3 shows that iron releases a higher concentration of nutrients than coated zinc. Meanwhile, the uncoated fertilizers were uniformly dissolved in the water until 24 h. In addition, there was a significant difference between coated fertilizers and those not coated. However, these results align with the finding reported by Bley et al. (2017) in nutrient release and potassium leaching from polymer-coated fertilizers. Other results were also in line with studies on the release characteristics of a new controlled-release fertilizer showing the same patterns (Zheng et al. 2010).

In this study, significant differences in the diameters and lengths of pak choi showed the lowest in the graph regarding the highest treatment. The leaf chlorophyll contents in pak choi were higher in Treatment 1 compared to other treatments, and the leaf chlorophyll contents significantly

(p<0.05) correlated with Fe concentration (Fig. 2 a,b). This result is in line with a past study by Kaya et al. (2001) on Fe application and tomato leaf chlorophyll contents in which Fe deficiencies can be corrected with Fe fertilizers, chelating agents or decreased pH in growth media. Adding Fe in Treatment 1 for plant growth significantly increased the leaf chlorophyll contents, lengths, diameters, and heights in the plants (Fig. 2b). As for the production pak choi, the averaged crop cycle, the Soil Plant Analysis Development (SPAD), and plant height showed average values between 15 and 40 (Fig. 3a). However, Treatment 1 showed higher values than other treatments due to the additional iron-coated application. Besides, based on Fig. 3a, the plant height in Treatment 1 for both crops was also increased. Fe deficiency is a major nutritional disorder that causes a decrease in vegetative growth, marked yield, and quality losses. The results showed that Fe deficiency (0 mg Fe-1) and Fe excess could also stunt plant growth and reduce radicle development.

Furthermore, excess Fe can cause plants to lose weight and defoliate earlier (Hembrom & Singh 2015; Sultana et al. 2018). The highest growth and yield observed in Treatment 1 might be due to the addition of iron fertilizers to the system. The results of this study are similar to those found by Rakshit et al. (2016) for pisciponic plants in terms of growth, yield, quality, and nutrition.

(a)   **(b)**

Fig. 2: Chlorophyll and diameter of pak choi in the rearing tank trough outlet in which lemon fin barb hybrids were cultured in the pisciponic system (a) Chlorophyll content of leaves of pak choi; (b) diameter of leaves of pak choi.

(a)   **(b)**

Fig. 3: Height and number of leaves of pak choi in the rearing tank trough outlet in which lemon fin barb hybrids were cultured in the pisciponic system (a) height of pak choi (cm); (b) the number of leaves of pak choi.

In this study, higher chlorophyll contents were recorded in Treatment 2 for pak choi; however, they recorded the lowest mean value in the control treatment. Based on the literature, a few species' depletion of leaf area leads to increased zinc contents that can affect photosynthesis activity. Treatments with a higher amount of zinc and without zinc could record the lowest mean values in length and height. As previously described, Kasozi et al. (2019) found that higher zinc concentrations reduced barley stems and leaves.

Fig. 5 shows the number and height of leaves of pak choi in the rearing tank trough outlet in which lemon fin barb hybrids were cultured in the pisciponic system. In terms of

the heights of pak choi in this study, significant differences were observed in the treatments. The highest mean value was recorded in T0 and followed by T1. However, Treatment 3 recorded the lowest height for pak choi. This indicates that a high zinc concentration does not promote plant growth. This finding aligns with Saeid et al. (2013), who found that gladiolus height was significantly positively correlated with growth. Hembrom & Singh (2015) also made a similar observation when they carried out an experiment on gladiolus pertaining to the foliar application of Zn at a 0.4% dose with the improved length and width of the longest leaf. The number of leaves in Fig. 4 shows the effects of zinc-coated
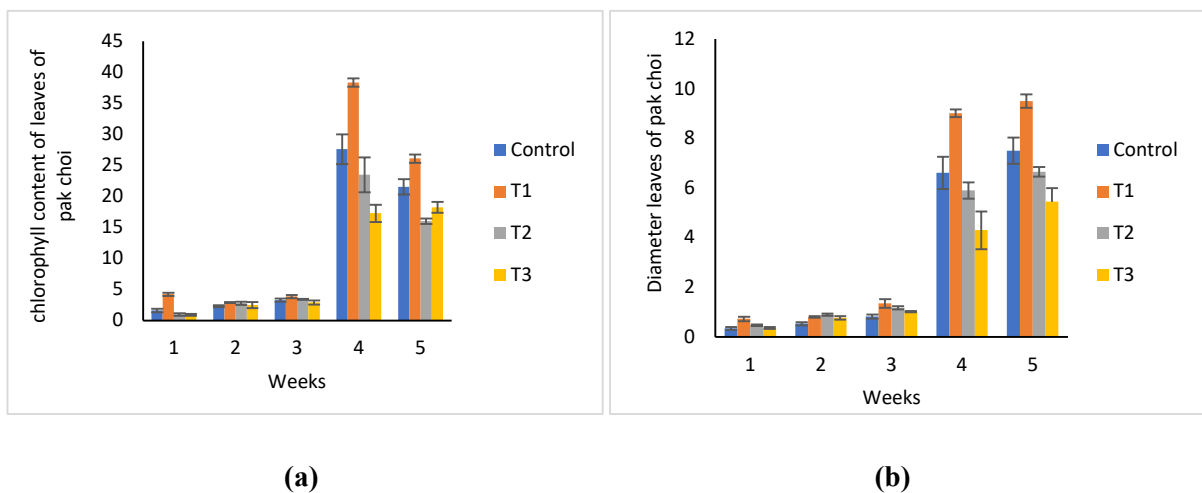

(a)   **(b)**

Fig. 4: Chlorophyll and diameter of pak choi in the rearing tank trough outlet in which lemon fin barb hybrids were cultured in the pisciponic system (a) chlorophyll content of pak choi leaves; (b) diameter of pak choi (cm).
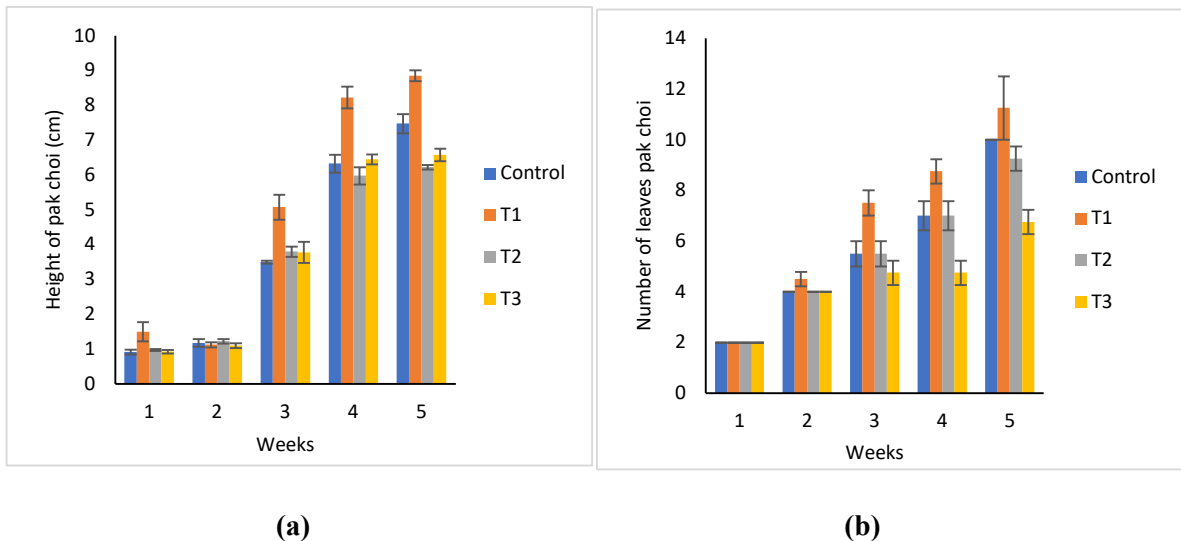
(a)

(b)

Fig. 5: Number and height of leaves of pak choi in the rearing tank trough outlet in which lemon fin barb hybrids were cultured in the pisciponic system.

fertilizers with significant differences in the number of leaves. The highest mean value was recorded in Treatment 1. According to Monnet et al. (2001), a higher concentration of Zn at 3 ppm can reduce the photosynthesis activity, while 1.5 ppm or less shows a good result in increasing the photosynthesis rate.

Higher chlorophyll contents of pak choi were observed in Treatment 2, with the highest value (Fig. 6a). These results align with the findings of Roosta and Hamidpour (2013), which stated that the application of fertilizers had positively affected the leaf concentrations. Besides, the results also

showed a significant gain in terms of plants' length, weight, and chlorophyll contents. These results agree with the findings reported by Yang & Kim (2019) that the combination of zinc yielded a better result than the application of zinc alone. In addition, in Treatment 1, the combination of zinc and iron showed the highest yield. According to Mousavi et al. (2012), the lack of zinc can lead to iron (Fe) deficiency and cause Fe failure from the shoot to root due to zinc shortage. Besides, zinc utilization has a negative effect on Fe concentration in plant tissues if the amount is too much or too little, which may be due to the physiological factors of plants. Overall, on average,
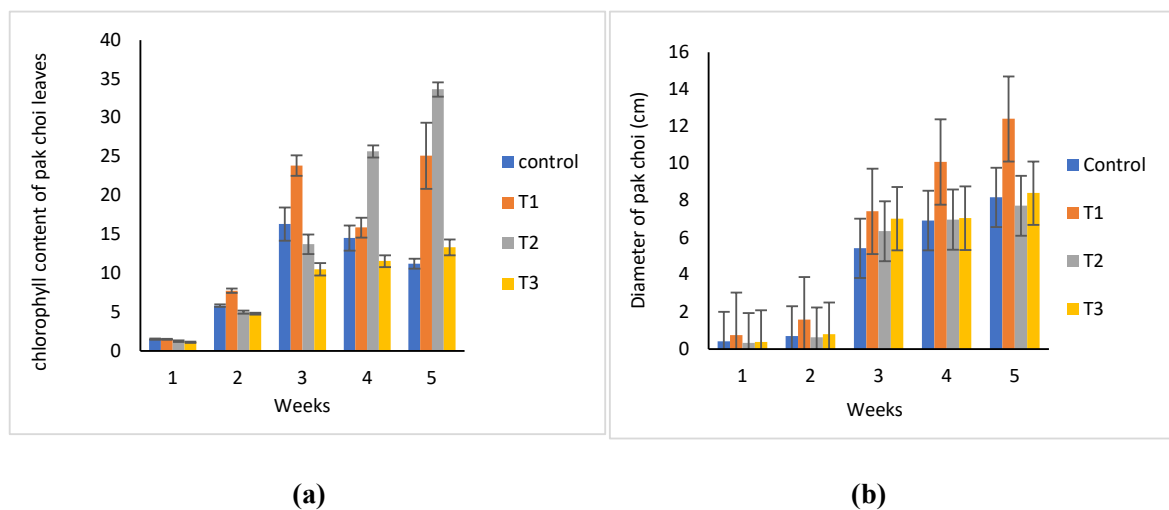

(a)

(b)

Fig. 6: Chlorophyll and height of pak choi in the rearing tank trough outlet in which lemon fin barb hybrids were cultured in the pisciponic system (a) chlorophyll content of pak choi; (b) height of pak choi (cm).

(a)   **(b)**
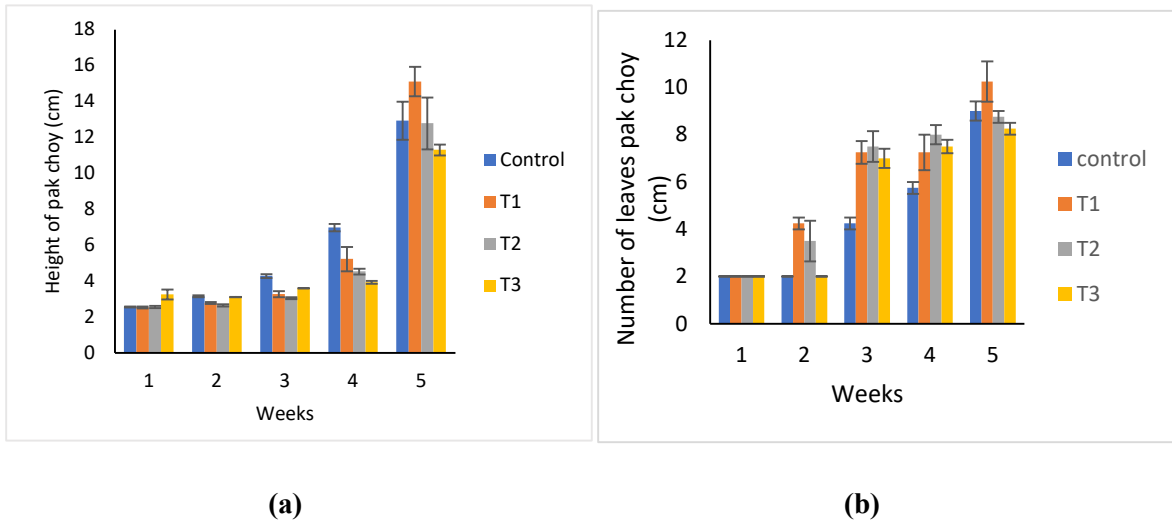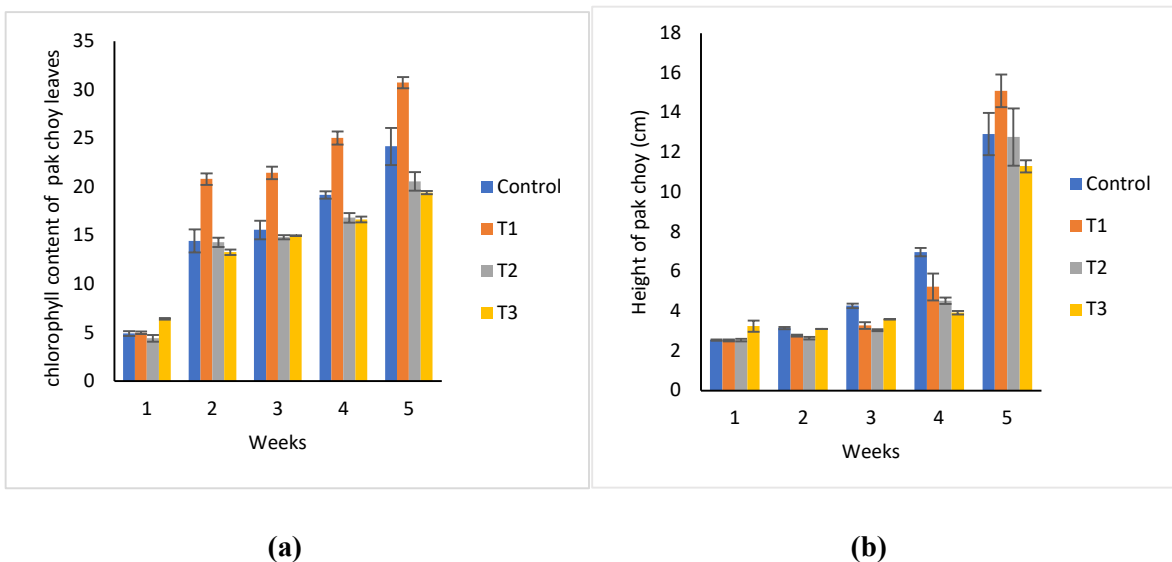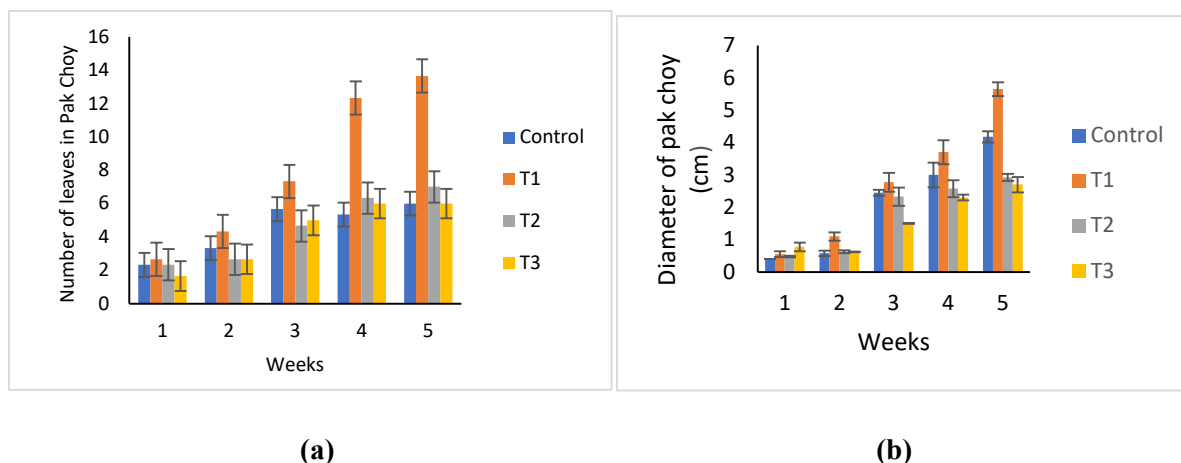
Fig. 7: Number and diameter of leaves of pak choi in the rearing tank trough outlet in which lemon fin barb hybrids were cultured in the pisciponic system (a) number of leaves in pak choi; (b) diameter of pak choi.

the highest height in pak choi was recorded in Treatment 1 at 16 cm (Fig. 6b). Additionally, the plants treated with a mixture of zinc and iron fertilizers in Treatment 1 showed good results.

The number and diameter of leaves of pak choi were observed for the growth performance (Fig 7). Coated zinc and iron and its combination showed significant zinc and iron accumulation in pak choi leaves. The diameters of pak choi showed the highest mean value recorded in T1 (5.07 cm), followed by T0 and T2. The coated zinc and iron did not affect the diameter of the leaves, as the control treatment recorded the highest mean value. In contrast, Treatment 1 affected the diameters of pak choi with a highly significant difference in all treatments, despite the possibility that this was due to the slow release of coated zinc and iron fertilizers over a long exposure. This finding is in line with Sheykhbaglou et al. (2010) study in which nano iron oxide at the concentration of $0.75g^{-1}$ increased the leaf and pod dry weight, as well as Rono et al. (2018) study using 30 Fe kg^{-1} treatment where the iron amino acid chelate supplementation reported better growth in terms of height, the number of leaves, diameter, and dry weight compared to the use of too much and too little fertilizers. In the current study, both treatments recorded the highest number of leaves, while Treatment 3 recorded the lowest number.

The analysis of variance (ANOVA) results showed that the application of coated iron and zinc fertilizers had a significant ($P \leq 0.05$) effect on these parameters. The effects of different iron- and zinc-coated treatments on leaf chlorophyll were significant in pak choi for all treatments. The highest mean value was recorded in Treatment 2 (33.65), and the lowest was in the control treatment (11.22). As for the diameters of pak choi, a significant difference was observed in all treatments. The highest mean value was recorded

in Treatment 3 (28.40), whereas the lowest was recorded in Treatment 2 (7.73). Regarding the heights of pak choi, significant differences were observed in the treatments. The highest mean value was recorded in the control treatment (10.90), and the lowest was in Treatment 3 (5.90). As for the number of pak choi leaves, there were significant differences in the control treatment, Treatment 2, and Treatment 3. Treatment 1 (10.25) recorded the highest mean value, and Treatment 3 (8.25) recorded the lowest.

CONCLUSION

The application of Zn and Fe fertilizers is essential for plant growth performance. It has been observed that coated and uncoated fertilizers behave differently in terms of the release of nutrients at different time intervals. The analysis of variance for plant height revealed highly significant results for treatment 1, combining zinc and iron. Applying micronutrient coated increases the diameters of pak choi showed the highest mean value recorded in T1, followed by T0 and T2, respectively. It is indicated that all treatment levels were significantly different from each other. Besides that, it increases the number of leaves per plant compared to control. Statistical analysis for length per plant has reflected highly significant results. Therefore, plants that received no fertilization of micronutrients show less length of branches per plant. There is a need for further research on the impact of palm stearin-coated fertilizers and their impact on plant growth performance and the rate of nutrient release.

ACKNOWLEDGMENT

REFERENCES

Affendi, N.M.N., Mansor, N. and Mathialagan, R. 2020. Development and characterization of allicin using palm stearin as a binder on urea granules. Journal of Plant Nutrition, 43(5): 621-628. https://doi.org/10.1080/01904167.2019.1701021

Ahl, H.A.H. and Mahmoud, A.A. 2010. Effect of zinc and/or iron foliar application on growth and essential oil of sweet basil (*Ocimum basilicum* L.) under salt stress. Ozean J. Appl. Sci., 3(1): 97-111.

Alam, M.M., Siwar, C., Jaafar, A.H., Talib, B. and Salleh, K.O. 2013. Climate change adaptability of farmers: Malaysian case study. Int. J. Plant Animal Env. Sci., 3(3): 130-135.

Alexandratos, N. and Bruinsma, J. 2012. World Agriculture towards 2030/2050: The 2012 Revision. ESA Working Paper No. 12-03. Rome, FAO.

Aliyu, S. M. 2017. Dietary carbohydrate requirement of lemon fin barb hybrid (Barbonymus gonionotus Bleeker 1849 X *Hypsibarbus wetmorei* Smith 1931) Fingerlings, August 25.

Bley, H., Gianello, C., Santos, L.D.S. and Selau, L.P.R. 2017. Nutrient release, plant nutrition, and potassium leaching from polymer-coated fertilizer. Revista Brasileira de Ciência do Solo, 41. https://doi.org/10.1590/18069657rbcs20160142

Goddek, S., Delaide, B., Mankasingh, U., Ragnarsdottir, K. V., Jijakli, H. and Thorarinsdottir, R. 2015. Challenges of sustainable and commercial aquaponics. Sustainability, 7(4): 4199-4224.

Hembrom, R. and Singh, A.K. 2015. Effect of iron and zinc on growth, flowering and bulb yield in lilium. International Journal of Agriculture, Environment and Biotechnology, 8(1): 61-64.

Ibrahim, K.R.M., Babadi, F.E. and Yunus, R. 2014. Comparative performance of different urea coating materials for slow release. Particuology, 17: 165-172. https://doi.org/10.1016/j.partic.2014.03.009

Irfan, M., Khan Niazi, M.B., Hussain, A., Farooq, W. and Zia, M.H. 2018. Synthesis and characterization of zinc-coated urea fertilizer. Journal of Plant Nutrition, 41(13): 1625-1635. https://doi.org/10.1080/01904167.2018.1454957

Kasozi, N., Tandlich, R., Fick, M., Kaiser, H. and Wilhelmi, B. 2019. Iron supplementation and management in aquaponic systems: A review. Aquaculture Reports, 15: 100221. https://doi.org/10.1016/j.aqrep.2019.100221

Kaya, C., Kirnak, H. and Higgs, D. 2001. Enhancement of growth and normal growth parameters by foliar application of potassium and phosphorous in tomato cultivars grown at high (NaCl) salinity. J. Plant Nutr., 24: 357-367.

Maucieri, C., Forcino, A., Nicoletto, C., Junge, R., Pastres, R., Samno, P. and Borin, M. 2018. Life cycle assessment of micro aquaponic system for educational purposes built using recovered material. J. Clean. Prod., 172: 3119-3127.

Meng, L.P., Li, S., Yang, W.D., Simons, R.Y., Yu, L., Liu, H.S. and Chen, L. 2019. Improvement of interfacial interaction between hydrophilic starch film and hydrophobic biodegradable coating. ACS Sustain. Chem. Eng., 7: 9506-9514. https://doi.org/10.1021/acssuschemeng.9b00909.

Monnet, F., Vaillant, N., Vernay, P., Coudret, A., Sallanon, H. and Hitmi, A. 2001. Relationship between PSII activity, CO2 fixation, and Zn, Mn and Mg contents of Lolium perenne under zinc stress. Journal of Plant Physiology, 158(9): 1137-1144. https://doi.org/10.1078/s0176-1617(04)70140-6

Mustafa, S., Estim, A., Shaleh, S.R.M. and Shapawi, R. 2018. Positioning of aquaculture in blue growth and sustainable development goals through new knowledge, ecological perspectives and analytical solutions. Aqua. Indon., 19(1): 1-9.

Okomoda, V.T., Oladimeji, S.A., Solomon, S.G., Olufeagba, S.O., Ogah, S.I. and Ikhwanuddin, M. 2022. Aquaponics production system: A review of historical perspective, opportunities, and challenges of its adoption. Food Sci. Nutri., 16: 881-893.

Qureshi, A., Singh, D.K. and Dwivedi, S. 2018. Nano-fertilizers: a novel way for enhancing nutrient use efficiency and crop productivity. Int. J. Curr. Microbiol. App. Sci., 7(2): 3325-3335.

Rafiee, G.R. and Saad, C.R. 2008. Roles of natural zeolite (clinoptiolite) as a bed medium on growth and body composition of red tilapia (Oreochromis sp.) and lettuce (Lactuca sativa var longifolia) seedlings in a pisc

iponic system. Iran. J. Fish. Sci., 7(1): 47-58.

Rahman, M.M. 2015. Role of common carp (*Cyprinus carpio*) in aquaculture production systems. Frontiers in Life Science, 8(4): 399-410. https://doi.org/10.1080/21553769.2015.1045629

Rahman, S. 2016. Remediation of nutrients runoff from feedlot by hydroponic treatment. Agricultural Engineering International: CIGR Journal, 18(1): 1-18.

Rakshit, R., Patra, A.K., Purakayastha, T.J., Singh, R.D., Pathak, H. and Dhar, S. 2016. Super-optimal NPK along with foliar iron application influences bioavailability of iron and zinc of wheat. Proceedings of the National Academy of Sciences, India Section B: Biological Sciences, 86: 159-164. https://doi.org/10.1007/s40011-014-0428-2

Rono, K., Manyala, J.O., Lusega, D., Sabwa, J.A., Yongo, E., Ngugi, C., Fitzsimmons, K. and Egna, H., 2018. Growth performance of spinach (Spinacia oleracea) on diets supplemented with iron-amino acid complex in an aquaponic system in Kenya. International Journal of Research Science and Management, 5(7): 117-127. https://doi.org/10.5281/zenodo.1320099

Roosta, H.R. and Hamidpour, M. 2013. Mineral nutrient content of tomato plants in aquaponic and hydroponic systems: Effect of foliar application of some macro-and micro-nutrients. J. Plant Nutri., 36(13): 2070-2083.

Ru, D., Liu, J., Hu, Z., Zou, Y., Jiang, L., Cheng, X. and Lv, Z. 2017. Improvement of aquaponic performance through micro-and macro-nutrient addition. Environmental Science and Pollution Research, 24: 16328-16335. https://doi.org/10.1007/s11356-017-9273-1

Saeid, J.M., Mohamed, A.B. and Baddy, M.A. 2013. Effect of garlic powder (Allium sativum) and black seed (Nigella sativa) on broiler growth performance and intestinal morphology. Iranian Journal of Applied Animal Science, 3(1): 185-188.

Sheykhbaglou, R., Sedghi, M., Shishevan, M.T. and Sharifi, R.S. 2010. Effects of nano-iron oxide particles on agronomic traits of soybean. Notulae Scientia Biologicae, 2(2): 112-113.

Sultana, S., Naser, H.M., Quddus, M.A., Shill, N.C. and Hossain, M.A. 2018. Effect of foliar application of iron and zinc on nutrient uptake and grain yield of wheat under different irrigation regimes. Bangladesh Journal of Agricultural Research, 43(3): 395-406.

Tilman, D., Balzer, C., Hill, J. and Befort, B.L. 2011. Global food demand and the sustainable intensification of agriculture. Proceed. Nat. Acad. Sci., 108(50): 20260-20264.

United Nations, Department of Economic and Social Affairs, Population Division. World Population Prospects: The 2017 Revision, Key Findings and Advance Tables. Working Paper No. ESA/P/WP/248. Available at: https://esa.un.org/unpd/wpp/publications/files/wpp2017keyfindings.pdf

Yang, T. and Kim, H.J. 2019. Nutrient management regime affects water quality, crop growth, and nitrogen use efficiency of aquaponic systems. Scientia Horticulturae, 256: 108619. https://doi.org/10.1016/j.scienta.2019.108619

Zheng, Y., Liu, Z. and Xie, L. 2010. Growing related words from seed via user behaviors: A re-ranking based approach. In: Proceedings of the ACL 2010 Student Research Workshop, pp. 49-54.

Evaluation of Lipase from an Indigenous Isolated *Bacillus* Strain for Biodiesel Production

Neha, Nisha Sethi, Sangita Yadav, Subhash Chander, Sweta Kumari, Ankur and Asha Gupta†

Department of Environmental Science and Engineering, Guru Jambheshwar University of Science and Technology, Hisar, Haryana 125001, India

†Corresponding author: Asha Gupta; guptaasha.phd@gmail.com

ABSTRACT

Lipases are utilized in biodiesel production utilizing various types of substrates. The use of lipase in bioenergy production aims to reduce energy crises and environmental pollution. Lipase-producing indigenous bacteria *Bacillus licheniformis* (Accession no. OP56979) and *Bacillus rugosus* (Accession no. OP56980) were isolated from various oil-contaminated sites. The isolated potential lipolytic bacteria were screened for maximum lipase production. Then, the bacteria showing the highest lipolytic activity were subjected to identification using the 16s rRNA technique while other isolated were identified biochemically. Lipase [LipBL-WII(c)] from *Bacillus licheniformis* having the highest lipolytic activity expressed various characteristics. Characterization of crude LipBL-WII(c) expressed that it showed stability in a wide range of pH (4 to 10) with optimum lipolytic activity observed at pH 8. It was then found to be active at a temperature range from 20°C to 80°C with optimal at 50°C. Lipase activity was also stimulated in metal ions such as Ca^{+1}, Mg^{2+}, and Zn^{2+} the most. Furthermore, LipBL-WII(c) retained lipolytic activity in the presence of various organic solvents and surfactants. The kinetic parameters (Km and Vmax) for LipBL-WII(c) were ascertained using Lineweaver- Burk plot. LipBL-WII(c) showed a potential for biodiesel production using olive oil as a source. Lipase gave 84% yield of biodiesel production from olive oil. Thus, it could be employed as a potential candidate for green biodiesel production using oil sources.

INTRODUCTION

Lipases exist widely in nature while being available greatly. Having low production cost lipases from microbial sources are more favorable. The most common sources of lipases are bacteria and fungi, and the lipases produced by them are generally extracellular (Sarmah et al. 2018). Based on the total sales volume, lipases are considered the third biggest group of enzymes, followed by proteases and amylases. Lipase production is a business of billions of dollars due to its extensive range of applications (Zhao et al. 2021). Over the decade, various bacterial lipase has been stated from different species, including *Pseudomonas* spp., *Burkholderia* sp., *Bacillus* spp., *Streptococcus* sp., and *Staphylococcus* sp. (Bharathi & Rajalakshmi 2019, Priyanka et al. 2019, Rmili et al. 2019).

Industries showcase significant commercial applications performed by Lipases (E.C. 3.1.1.3). Hydrolysis of triacyl-glycerols into free fatty acid, and glycerol was stimulated by Lipases (Javed et al. 2018). Various applications of lipase include fat and oil hydrolysis, flavor enhancement in food processing, analysis of chemicals, racemic mixture resolution,

fat modification, and synthesis of organic materials (Bento et al. 2017, Rios et al. 2018). Various habitats, like wastes from industries, dairies, oil-contaminated soil, etc., were found to be inhabited by lipase-producing microorganisms. Innovative technologies have been utilized on the microbial lipase for degrading and detoxifying the oil effluents (Gururaj et al. 2016).

Recently the interest of researchers has increased in enzymatic transesterification using lipase for biodiesel production. The capability of the lipase (EC 3.1.1.3, triacylglycerol hydrolases) to maintain notable catalytic activity in non-aqueous media made its usage possible in biodiesel production (Sarmah et al. 2018). In biodiesel production, compared to chemical catalysis, lipase uses various advantages like; easy separation of product, easy recovery of glycerol, minimal wastewater treatment requirements, and the absence of side reactions. Due to maintaining a high-temperature environment for alkaline catalysis, hydrolysis of triglycerides produces many free fatty acids (FFAs) in waste cooking oil, leading to various problems in alkaline catalytic biodiesel production (Tripathi et al. 2014). On the contrary, lipase can produce biodiesel

using high FFA feedstocks as it can convert triglycerides and FFAs into FAAEs.

The present work aimed at Isolating, and screening lipase-producing bacteria from various samples, identification of the isolates utilizing both biochemical and molecular methods (16s rRNA sequencing), characterization of the biochemical properties of the crude lipase along with the determination of kinetic parameters for crude lipase and the biodiesel producing potential of the crude lipase.

MATERIALS AND METHODS

Isolation of Bacterial Strains

Samples of wastewater, soil, and sludge rich in lipid sources were collected from different sites near Hisar district, Haryana, India were used after removing debris as listed in Table 1. 1mL or 1g of the samples were dissolved in 10 mL sterilized saline solution and were shacked evenly. Then, they were serially diluted from 10^{-1} to 10^{-6} in the saline solution. 1.0% suspension from all the dilutions was then used as an inoculum to be grown on the NA plates using the spread plate method for obtaining the bacterial colonies after the plates were subjected to 24 h of incubation at 37°C. The bacterial colonies appearing after 24 h of incubation were restreaked several times on the nutrient agar plates to obtain pure bacterial cultures.

Primary Screening for Lipase Production

The primary screening for lipolytic bacteria was done by streaking the pure bacterial cultures on TBA (Tributyrin Agar) plates. The TBA media comprised: 0.5% Peptone, 0.3% Beef extract, and 2.0% Agar supplemented with 1.0%

Table 1: Sample collection for bacterial strain isolation.

S.No.	Sample code	Source
1.	W(I)	Wastewater from Stainless Steel Industry, Hisar
2.	W(II)	Waste Water from Paper Mill, Panipat
3.	W(III)	Sweet Shop Drainage, Hisar
4.	W(IV)	Restaurant Drainage, Hisar
5.	W(V)	Restaurant Drainage, Hansi
6.	W(VI)	Wastewater from STP, Gangua
7.	W(VII)	Sewage discharge from random house, Hisar
8.	W(VIII)	Sewage water from GJU, Hisar
9.	S(A)	Sludge from local sewer hole, Sector-15, Hisar
10.	S(B)	Soil from a Local auto workshop, Hisar
11.	S(C)	Soil from Automarket, Hisar

Tributyrin as a carbon source at 7.5 pH. The media plates were kept at 37°C for 48 h of incubation. The bacterial cultures depicting visible hydrolysis zone around the colonies on the media were then further analyzed for the quantitative determination of lipase activity using agar well diffusion assay (cup well method). Solid media comprising different carbon sources like olive oil, Tween- 20, and Tween- 80 were assessed for lipolytic activity. The detection of enzymatic activity was done by observing visually and measuring the clear zones on the surface of the agar.

Secondary Screening of Lipolytic Bacterial Strains Using Various Media

Phenol red agar: Phenol red agar media comprising: 1.0% Peptone, 0.5% NaCl, 0.01% $CaCl_2$, 0.01% Phenol red, 2.0% Agar and 1.0% Olive oil was prepared, and pH was set at 7.0. The bacterial cultures showing clear zones on TBA were fed into the sterile NB (nutrient broth) media and then incubated at 37°C for 24 h. 50 μL of the obtained new cultures supernatant was poured into the bored wells on plates prepared from phenol red agar media. Then incubation was done at a temperature of 37°C for 48 h. The sterile nutrient broth was employed as a control. The color change from red to yellow around the wells indicated lipase activity. All the experiments were performed in triplicates.

Tween- 20 agar: Tween-20 agar media comprising: 1.0% Peptone, 0.5% NaCl, 0.01% $CaCl_2$, 2.0% Agar and 1.0% Tween-20 was synthesized. 50 μL supernatant of the new bacterial cultures was added in the wells bored on plates prepared from agar media containing Tween- 20 and then subjected to incubation at a temperature of 37°C for incubation of 48 h. The control was used in the form of sterile nutrient broth. Noticeable precipitation around the wells indicated the existence of the activity of lipase. Experiments were performed in triplicates.

Identifying the Lipolytic Bacterial Strains

Physical and Biochemical Characterization

Physical characterization: Morphological and colony characteristics were studied from cultures grown on nutrient agar plates. The shape of the bacterial cells was seen by using Gram's staining method.

16srRNA sequencing: The Chromosomal DNA of the bacterial strain was hauled out by employing a spin column kit (HiMedia) (Clarridge 2004) and was amplified using PCR using a thermal cycler and Exo-SAP (Exonuclease I -Shrimp Alkaline Phosphatase) was utilized for the process of purification (Darby et al. 2005). The purified amplicons were sequenced using the Automated Sanger Sequencing method (ABI 3500xL genetic analyzer, USA). BLAST

was employed for scrutinizing the resulting sequences with flanking culture sequences recovered from the NCBI database that discovers the similarity regions locally amongst the sequences (Altschul et al. 1990). The program then relates the retrieved nucleotide sequences to sequence databases to calculate the match's statistical significance (Gertz 2005). The BLAST algorithms were employed to infer the relationships related to evolutionary and functional parameters amongst the sequences to find members of the gene families. BLASTN program was then primarily used to discover the potentially closely related strains (Altschul et al. 1990). The multiple sequence alignment tool, CLUSTAL W, was employed to align the sequences. MEGA (Molecular Evolutionary Genetics Analysis Version 6.0) was employed for the phylogenetic tree construction (Karlin & Altschul 1990).

Growth Kinetics and Lipase Production

The isolates showing significant zones on the above-mentioned media were inoculated in 15 ml of inoculums media comprising: 2.0% Glucose, 1.0% Yeast extract, 1.0% Peptone, 1.0% $CH_3COONa.3H_2O$, 0.009% $MgSO_4$, 0.003% $MnSO_4$, 0.15% $CuSO_4.5H_2O$, 0.05% KCl, 0.5% olive oil with 7.5 pH. The flasks of inoculums were then subjected to incubation at a temperature of 37°C overnight at 120 rpm. Then the submerged cultures were mixed with 100 ml of lipase production media: 0.2% Peptone, 0.25% NaCl, 0.04% $CaCl_2.2H_2O$, 0.1% $NH_4H_2PO_4$, 0.04% $MgSO_4.7H_2O$, and 2.0% Olive oil. The flasks were then further incubated at 37°C at 120 rpm for 120 h. 1.0M NaCl and 1.0M HCl were used to maintain the medium pH and adjusted to 7.2. The samples were drawn at 12-hour intervals from the production media to determine bacterial growth and lipase activity. The optical density at 600 nm was measured using a UV-Vis spectrophotometer to determine the cultures' bacterial growth. To determine the lipase activity of the samples, a refrigerated high-speed centrifuge was used at 10,000 rpm for 10 min at 4°C. The lipolytic activity of the crude enzyme was then assayed. The lipase activity was analyzed using a Colorimetric assay as distinct by Winkler & Stuckmann (1979).

Lipase Assay

The hydrolysis activity of lipase towards p-nitrophenyl palmitate (NPP) was recorded according to the colorimetric method with minor modifications (Gricajeva et al. 2019). The stock solution of the substrate pNPP (p-nitrophenyl palmitate, 20 mM) was prepared using isopropanol. The final reaction mixture was prepared by mixing 75 µL of pNPP of stock solution in 3 mL of Tris buffer (0.05 M, pH-8.0) and then subjected to incubation at 70°C inside a water

bath for 10 minutes. After that, 25 µL of the crude enzyme was supplemented into the reaction mixture, followed by incubation at 35°C in a water bath for 30 minutes. After 30 min, adding 1 mL of stopping reagent (chilled acetone-ethanol (1:1)) halted the enzymatic reaction. In the control (blank) set, the addition of the crude enzyme step was skipped. The liberation of the yellow-colored compound (p-nitrophenol) in the reaction mixture was measured at the wavelength of 410nm alongside a reagent blank about the p- nitrophenol standard curve (2 to 20 µg.mL^{-1} in 0.05M Tris HCl buffer (pH-8.0). The same assay was carried out in triplicates leading to the presentation of the mean values. One unit (U) of enzyme activity is defined as a micromole (µM) of the liberated p-nitrophenol by the p- nitrophenyl ester breakdown by 1.0 ml of the soluble enzyme every minute at a temperature of 35°C beneath the standard assay conditions.

The enzyme activity (U mL^{-1} min^{-1}) was calculated using equation 1.

$$\text{Lipase activity (Units mL}^{-1}\text{min}^{-1}) = \frac{\mu \text{ moles of p}-\text{nitrophenol liberated}}{Volume\ of\ enzyme\ (0.025mL)*Incubation\ time\ (30)} \quad \ldots(1)$$

Specific activity is the enzyme activity per mg of the total protein (expressed in µ mol min^{-1} mg^{-1}) using equation 2.

$$\text{Specific enzyme activity (Umg}^{-1}) = \frac{\text{Enzyme activity (U/mL)}}{\text{Total protein content (mg/mL)}} \quad \ldots(2)$$

Determination of Protein content: protein content

The protein concentration was estimated using Bradford's method, in which BSA (Bovine Serum Albumin) is a standard protein (Bradford 1976).

Characterization of Crude Lipase

Effect of Temperature: The optima of temperature for crude lipase has been estimated by incubating crude enzyme aliquots at various temperatures ranging from 20-80°C for 24 h at 200 rpm, maintaining pH at 8 using Tris-HCl buffer. The maximum activity was considered 100% at the beginning of incubation.

Effect of pH: The optima of pH for crude lipase was estimated after the incubation of LipBL-WII(c) in various buffers (50mM): pH- 2 (glycine- HCl), pH 3-5 (acetate-acetic acid), pH 6-7 (phosphate), pH 8- 9 (Tris-HCl), pH 10.0 (glycine- NaOH), pH 11.0 (phosphate- NaOH) and pH 12 (KCl- NaOH). The maximum LipBL-WII(c) activity was established as 100% relative lipolytic activity.

Effect of organic solvents: For determining the impact of organic solvents (ethanol, isopropanol, hexane, chloroform, and methanol) on the enzyme activity, LipBL-WII(c) was

incubated with different organic solvents at a concentration of 50% (v/v) for 6 h at 37°C at 150rpm. The lipolytic activity of control (in the absence of organic solvent) was considered 100.0%.

Effect of metal ions: Crude lipase, LipBL-WII(c) was incubated with metal ions (Mg^{2+}, Mn^{2+}, Ca^{2+}, Fe^{2+}, and Zn^{2+}) of 1mM concentration at 37°C temperature with 150 rpm for 6 h to assess the impact of metal ions on enzyme activity. Control was devoid of the metal ion solution. The change in the lipase activity compared to the control's activity was referred to as the relative activity.

Effect of surfactants: Lipase was incubated in the occurrence of various surfactants (Tween- 20, 80, SDS, and Triton X-100) at a concentration of 1.0% for 6 h at 37°C temperature with 150 rpm to assess their effect on the enzyme activity of lipase. No surfactant was used in the sample solution used as a control. The change in the lipase activity compared to the control's activity was referred to as the relative activity.

Kinetic Parameters of Crude Lipase

The velocity of reaction for crude lipase was studied utilizing p- NPP (p-nitrophenyl palmitate) as a substrate at a variable concentration of (0.1-10mM) in buffer Tris- HCl (50 mM, pH 8.0). The Michaelis constant (Km) and maximum velocity (Vmax) were estimated utilizing the Lineweaver-Burk plot.

Biodiesel Producing Potential of Crude Lipase

Biodiesel production was planned to refer to (Yang et al. 2009) with fewer modifications. A 7.89 ml of Olive oil was mixed with 0.99 mL of methanol and kept in glass tubes with screw caps, then added 2.6 mL of crude lipase and incubated at 40°C temperature along with shaking at 220 rpm for 48 h. After the incubation period, 200 μL of the sample was withdrawn from the reaction's mixture and then diluted using 1.0 mL of n-hexane for 2min. Afterward, the centrifugation of samples was done at 10000 rpm for 15 min, and 10 μL of the upper layer was subjected to a Thin Layer Chromatography (TLC) plate. Methyl oleate was utilized as a reference for biodiesel in TLC. After the development of the plate in 90:10:1 (n-hexane/ ethyl acetate/ acetic acid), then iodine vapor was used for visualizing the spots for a short period of time. The yield of the biodiesel production was calculated using Equation 3.

$$\text{Yield} = \frac{Volume\ of\ Biodiesel\ produced}{Volume\ of\ oil} \times 100 \quad …(3)$$

RESULTS AND DISCUSSION

Isolation, Screening and Identification

Lipid-rich wastewater, soil, and sludge samples were collected from sites near Hisar district, Haryana, India. The sites were chosen rationally to offer a good atmosphere for the lipolytic bacteria to thrive. 36 isolates of bacteria were isolated on NA (nutrient agar) medium. The purified isolated bacterial strain is shown in Fig. 1. All 36 strains were screened for lipase activity by streaking them onto a Tributyrin agar medium (TBA). Out of 36 bacterial isolates, only 17 exhibited clear zones around the colonies on the Tributyrin agar (TBA) medium. The clear zones around

Fig. 1: Purified isolated WII(c).

Table 2: Zone production by lipase-producing bacterial isolates.

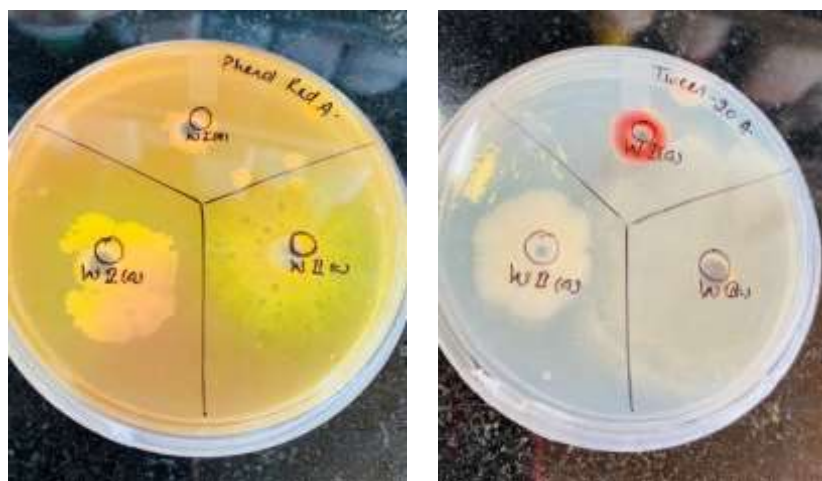| S.No.	Isolate No.	Zone Diameter (in mm)	
		Phenol Red Agar	Tween-20 Agar
1.	SA(b)	20	26
2.	SA(c)	18	26
3.	SA(d)	20	24
4.	SB(a)	14	26
5.	SB(d)	18	32
6.	SB(e)	12	14
7.	SC(d)	14	16
8.	WI(a)	20	22
9.	WII(a)	14	30
10.	WII(c)	30	66
11.	WIII(a)	18	24
12.	WIV(a)	14	32
13.	WIV(c)	18	34
14.	WV(a)	14	24
15.	WVI(a)	14	16
16.	WVII(a)	24	20
17.	WVIII(a)	24	16

Fig. 2: Zone of hydrolysis around the wells by various isolated strains.

the bacterial colonies depicted the degradation of tributyrin into butyric acid by the lipolytic activity of the bacteria. As shown in Table 2, all 17 strains of bacteria were then monitored for the quantitative analysis of enzyme production employing solid media like phenol red and Tween- 20 agar media. In phenol, red, and tween-20 agar media, strain WII(c) exhibited the highest lipase production. At first, the strains were screened using a chromogenic approach by using the dye phenol red as an indicator and olive oil as an inducer substrate. The pH indicator was Phenol red, with a pH of 7.3-7.4 as the endpoint. The lipolytic reaction of olive oil ends in releasing fatty acids. In turn, the dye pH decreases, exhibiting yellow color zones around the wells indicating the lipase activity of the tested strain of bacteria (Patel & Desai 2018).

Further, Tween- 20 agar media consisted of tween- 20 being an inducer substrate. The lipolytic activity of the strains was depicted by the development of a big visible zone of precipitates of calcium salt surrounding the well, resulting from the reduction of tween-20 into fatty acids. Promoting ideal interaction between the enzyme or cells and substrates makes tween- 20 the commonly used substrate for detecting the lipolytic activity of bacteria. Fig. 2 shows the hydrolysis zone depicted by various isolated strains on different media.

Identification

The bacterial strain was initially identified by morphological characterization like Gram staining, which showed maximum lipolytic activity. Studies on the physiological characteristics of all the isolates were performed. The biochemical characteristics (Catalase, Oxidase, Indole, Methyl red, Voges- Proskauer, Nitrate reduction, Citrate utilization, Hydrogen sulfide production, gelatin hydrolysis) and tests

of sugar fermentation were also carried out using standard reference biochemical tests for identification of bacteria genus as per Bergey's manual of systematic bacteriology as described in Table 3. Two strains, WII(c) and SA(c) were selected for further identification using 16SrRNA sequencing due to their exhibition of top-most lipolytic activity amongst all the other strains. BLAST search analysis of the strain WII(c) revealed that it exhibited close homology (99%) with *Bacillus licheniformis*, and SA (c) exhibited closed homology (99.92%) with *Bacillus rugosus* and multiple species. The study impacted the strain WII(c) as B. licheniformis and SA(c) as *Bacillus rugosus*. The 16S rRNA gene sequence was deposited in Gene Bank and obtained accession no. for *Bacillus licheniformis* (Accession no. OP56979) and *Bacillus rugosus* (Accession no. OP56980). Fig. 3 illustrates the constructed tree of phylogeny showing the evolutionary relationships of the strain WII(c) and SA(c) to other lipolytic *Bacillus sp*. The strains WII(c) and SA(c) came from the same genus. Hence, the strain with the maximum lipolytic activity, i.e., WII(c), was used for further study.

Growth Kinetics and Lipase Production

B. licheniformis WII(c) was grown using the basal medium for 120 h to determine the true growth phase, depicting the highest extracellular lipase production. Lipase production and bacterial growth were assayed on samples taken at every 12 h interval. A parallel relationship between lipolytic activity and cell growth was recorded, depicting lipase production as growth linked. The early log phase recorded the initiation of lipase production, and the optimum was reached throughout the late exponential growth phase. Maximum production of lipase ($50 \ U^{-1}.mL^{-1}.min^{-1}$) was detailed at 72 h of the incubation period (Fig. 4). This was

Table 3: Biochemical characterization of isolated lipolytic strains.

Isolate No.	Shape	Gram's Character	Indole	MR	VP	Citrate	H₂S production	Nitrate Red.	Catalase	Oxidase	Urease	Glucose	Lactose	Fructose	Xylose	Probable identity
SA(b)	Rod-shaped	-	-	-	-	+	-	-	+	+	+	+	+		+	*Pseudomonas* sp.
SA(c)	Bacillus	+	-	-/+	-/+	-	-	+	+	-	-	+	+	+	-	*Bacillus* sp.
SA(d)	Coccus	+	-	+	+	-	-	+	+	-	+	+	+	+	-	*Staphylococcus* sp.
SB(a)	Coccus	+	-	-	+	-	+	+	+	-	+	+	+	+	-	*Staphylococcus* sp.
SB(d)	Bacillus	+	-	-/+	-/+	-	-	+	+	-	-	+	+	+	-	*Bacillus* sp.
SB(e)	Coccus	+	-	-	-	+	-	-	+	-	-	-	+	+	-	*Staphylococcus* sp.
SC(d)	Coccus	+	-	-	+	-	-	+	+	-	+	+	+	+	-	*Enterococcus* sp.
WI(a)	Coccus	+	-	-	-	+	-	-	+	-	-	+	+	+	-	*Micrococcus* sp.
WII(a)	Coccus	+	-	-	-	+	-	-	+	-	+	-	+	+	+	*Staphylococcus* sp.
WII(c)	Bacillus	+	-	-/+	+	+	-	+	+	-	+	+	-	+	-	*Bacillus* sp.
WIII(a)	Coccus	+	-	-	-	-	-	-	+	-	-	+	+	+	+	*Micrococcus* sp.
WIV(a)	Coccus	+	-	-	+	-	-	+	+	-	-	-	+	+	-	*Staphylococcus* sp.
WIV(c)	Coccus	+	-	-	-	+	-	-	+	-	-	+	+	+	-	*Staphylococcus* sp.
WV(a)	Coccus	+	-	-	+	+	-	-	-	-	-	+	+	+	-	*Enterococcus* sp.
WVI(a)	Coccus	+	-	-	+	-	-	+	+	-	+	-	+	+	-	*Staphylococcus* sp.
WVII(a)	Bacillus	+	-	-	-/+	+	-	+	+	-	-	+	-	+	-	*Bacillus* sp.
WVIII(a)	Bacillus	+	-	-	+	-	-	-/+	+	-	-	+	+	+	-	*Bacillus* sp.
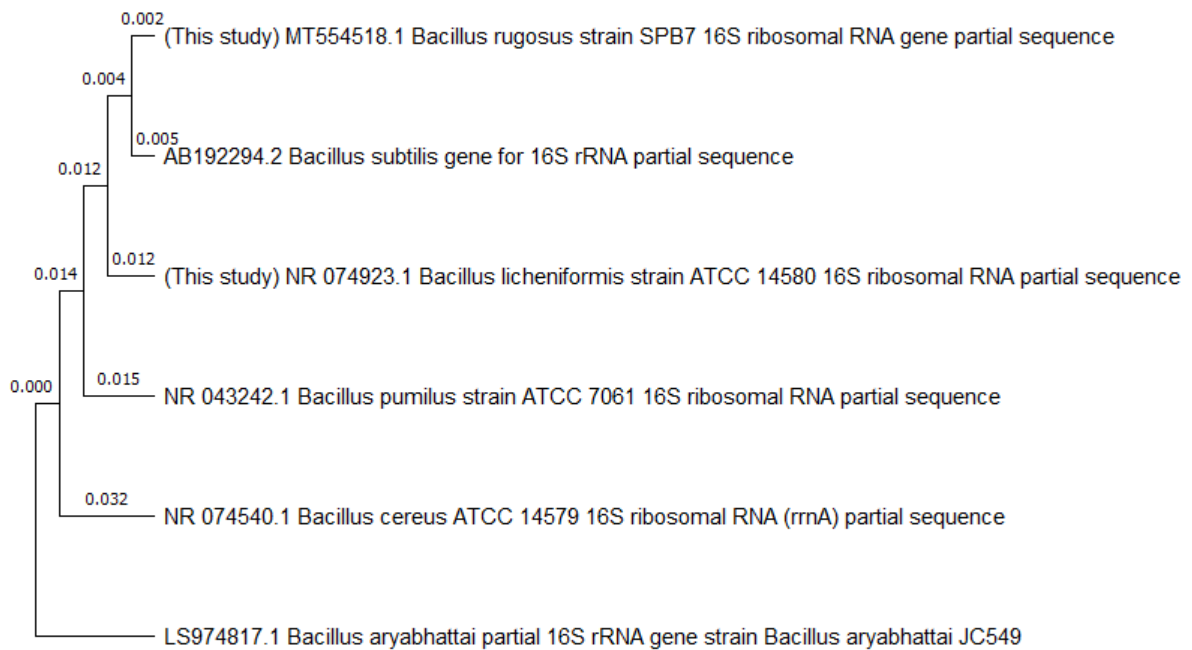
Fig. 3: Phylogenetic tree based on 16S rRNA gene sequences of WII(c) and SA(c) showing their similarity to other lipolytic *Bacillus* sp. strains.
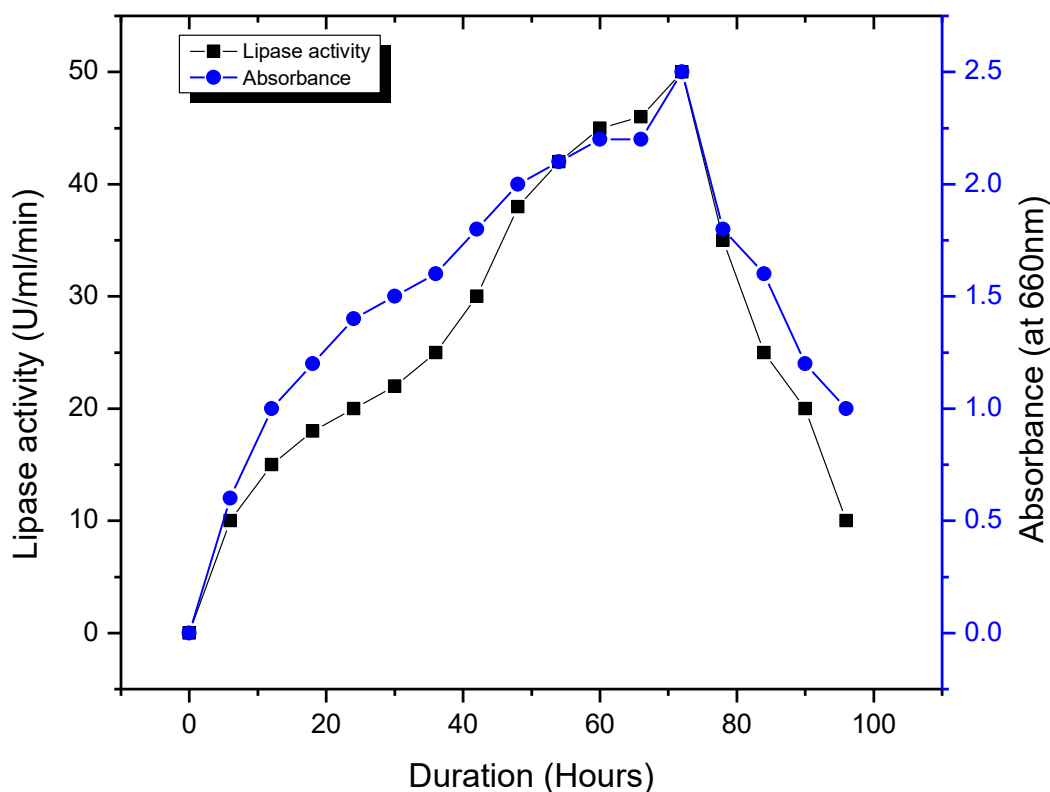
Fig. 4: Growth curve (■) and Lipase production curve (●) by *Bacillus licheniformis* WII(c).

comparable to the conclusions of Tripathi et al. (2014) and Zhao et al. (2021) showing the optimum production of lipase by a *micro bacterium* and *Staphylococcus caprae* through the late exponential phase of growth. The lipolytic activity was reduced after 72 h of incubation, possibly due to proteases in the fermentation media.

Characteristics of LipBL-WII(c)

Effect of temperature: The optimal temperature for LipBL-WII(c), a crude lipase from *Bacillus licheniformis*, was 55°C (Fig. 5 (a)). On increasing the temperature beyond 50°C, lipase activity decreased, indicating thermal destruction of the tertiary enzyme structure. The optimal activity of the lipase from *Anoxybacillus flavithermus* was at the temperature of 50°C and was detected to be firm from 25°C to 50°C for incubation of 24 h (Bakir & Metin 2016). The optimal temperature for the enzyme activity was 40°C with decent stability at 10-30°C for the lipase produced by the bacteria identified as *Acinetobacter haemolyticus* (Sarac & Ugur 2015). Saraswat et al. 2017 reported the alkaline and thermotolerant lipase (BSK-L) production from the strain *Bacillus subtilis*. Lipase has optimum activity at 37°C and exhibits active activity of lipase at the temperature range of 30°C to 60°C.

Effect of pH: The optimal pH of LipBL-WII(c) was estimated to be 8 and exhibited stability in pH from 4 to 10 (Fig. 5 (b)). Lipase from *Cohnella sp*. A01 showed optimum activity at pH 8.5 and was ideally stable at pH 8.5–10 for the incubation of 180 minutes (Golaki et al. 2015). The pH optima for the purified lipase produced by *Bacillus subtilis* was pH 8 (Mazhar et al. 2016). Rmili et al. (2019) reported that lipase SCL produced by *Staphylococcus capitis* retained greater than 60% of its initial activity over extensive pH values ranging from 5 to 11 at room temperature. Sarac and Ugur (2015) reported that the lipase produced by *Acinetobacter haemolyticus* showed the pH optima at 9 with good stability at pH ranging between 5.0- 11.0.

Effect of organic solvents: LipBL-WII(c) from *B. licheniformis* WII(c) was incubated in the presence of 50% (v/v) organic solvents for 6 h and observed notable retaining of relative activity with hexane, ethanol, methanol, and isopropanol while moderately tolerant to chloroform as shown in (Fig. 5 (c)) stating that this lipase unveiled decent stability with the utmost of the organic solvents. Similarly, *Bacillus sp*. was tolerant to methanol, ethanol, and acetonitrile, making the strain produce a solvent-tolerant lipase enzyme, rendering it a likely nominee of the solvent-tolerant lipase for a variety of industrial applications
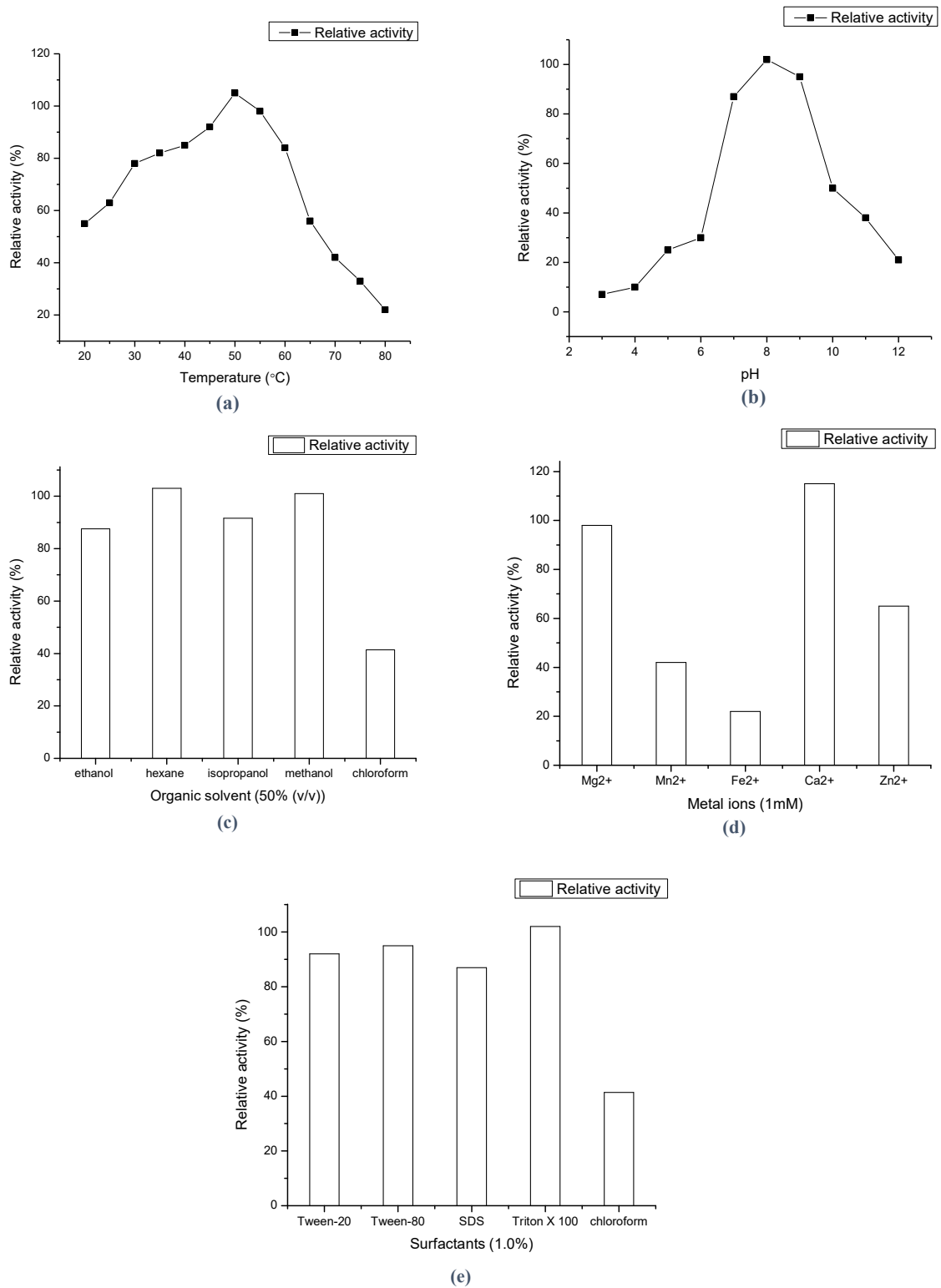
Fig. 5: Effect of various characteristics on the lipolytic activity of LipBL-WII(c). (a) Temperature (b) pH (c) organic solvents (d) metal ions (e) surfactants.

(Jaiganesh & Janganathan 2016). Lipases tolerant to organic solvents are crucial for the production of biopolymeric, fine chemicals, and biodiesel material production (Javed et al. 2018). The lipase produced by *Aureobasidium pullulans* exhibited outstanding stability in some 30% (v/v) organic solutions, including hexane, DMSO (dimethyl sulfoxide), n-propanol, and isopropanol (Li et al. 2019).

Effect of metal ions: LipBL-WII(c) was incubated with 1mM molarity of metal ions for six h and perceived a decent tolerance in the occurrence of Ca^{+1}, Mg^{2+}, and Zn^{2+} (Fig. 5(d)). Likewise, augmentation of the lipolytic activity in the presence of K^+ and Ca^{2+} ions was conveyed by (Wang et al. 2012). A decrease in the lipase activity on treatment with EDTA (a metal ion chelator) along with Ca^{2+} (71.5%) and Mn^{2+} (62.8%), as metal ions assist in the structural and functional maintenance of the enzyme was described by Golaki et al. (2015). While lipase activity of the extracellular lipase from *Azospirillum sp*. was decreased by adding Mg^{2+}, Zn^{2+}, Co^{2+}, and Cu^{2+} metal ions (Lestari et al. 2016). Li et al. (2019) showed that Ca2+ heightened the lipase catalytic activity produced from Aureobasidium pullulans and was marginally inhibited by Zn^{2+} and Mn^{2+} at a concentration of 10 $mmol.L^{-1}$.

Effect of surfactants: The effect of different surfactants on the LipBL-WII(c) was examined by incubating the lipase with various surfactants for six h. The relative activity was upgraded by adding Triton X-100 while it was retained by Tween 20, Tween 80, and SDS (Fig. 5(e)). On the other hand, Golaki et al. (2015) stated that the bio-catalytic activity of the enzyme was considerably reduced to 16.2% by the surfactant SDS. Non-ionic detergents cause disintegration by decreasing the hydrophobic interactions amongst the lipase enzyme, stabilizing the enzyme activity. At the same time, SDS affects the enzyme's denaturation by destroying the disulfide linkages (Sajna et al. 2013). Kaur et al. (2016) reported that the enzyme produced by *Bacillus licheniformis* could preserve its activity in the occurrence of different detergents (Tween- 20, 40, SDS and Triton X-100). Li et al. (2019) described that the lipase from *Aureobasidium pullulans* was stimulated by the non-ionic surfactants (Tween- 80, Triton X- 100, and Tween 20) and the anionic surfactant SDS. Still, it was severely repressed by the cationic surfactant CTAB.

Kinetic Parameters of Lipase

Lineweaver-Burk plot was used to determine the kinetic parameters (Km and Vmax) of the enzyme lipase. The values of Km and Vmax for lipase by utilizing pNPP (p-nitrophenyl palmitate) as a substrate were determined to be 2.05 mM and 6.02 $mmoles^{-1}min^{-1}mg^{-1}$, respectively (Fig. 6). A
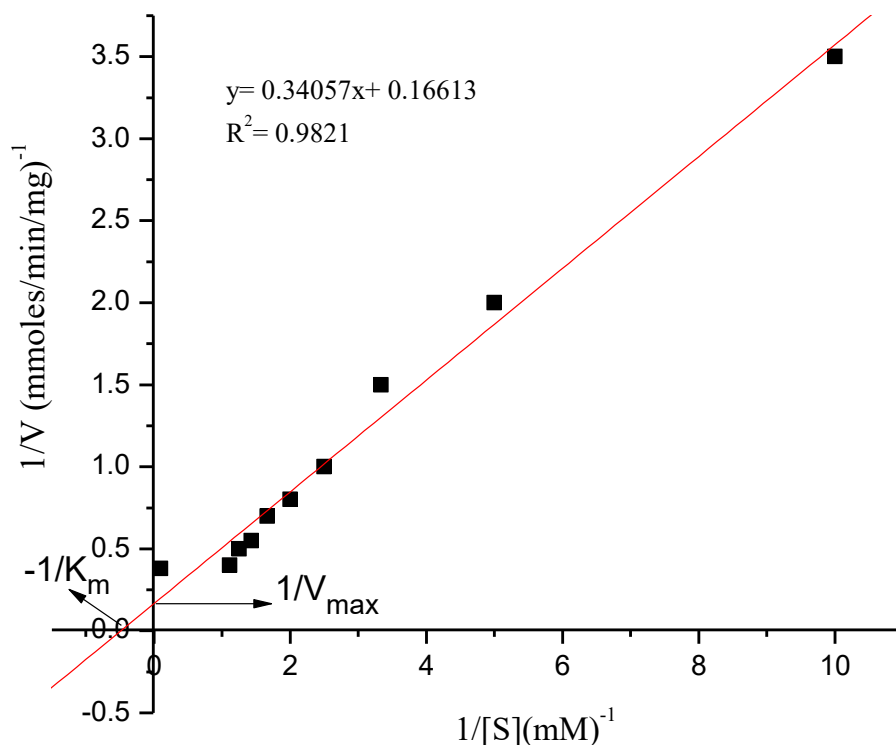

Fig. 6: Line weaver-Burk plot of LipBL-WII(c) from *Bacillus licheniformis*.

low value of Km implies a greater affinity of the enzyme towards its substrate. In comparison, a high Km implies less affinity. Tripathi et al. (2014) stated the values of Km and Vmax being 3.2 mM and 0.005 mmoles^{-1}min^{-1}mg^{-1} for lipase from *Microbacterium sp*. while which depicted the interaction of enzymes toward its substrates. Sarac and Ugur (2015) described the lipase production from *Acinetobacter haemolyticus* depicting lipase's Km and Vmax as 0.8 mM and 3.833 mmoles^{-1}min^{-1}mg^{-1}, respectively. Km and Vmax values of the lipase production by the native *B. subtilis* strain Kakrayal_1 (BSK-L) were perceived to be 2.2 mM and 6.67 mmoles^{-1}min^{-1}mg^{-1}, respectively (Saraswat et al. 2018). Sharma and Kanwar (2015) verified the Vmax and Km of the purified lipase of *Bacillus licheniformis* SCD11501 were to be 2.27 and 0.43 mM^{-1}mmol^{-1}ml^{-1}min^{-1}, respectively, for the breakdown of p-NPP. The values of Vmax and Km of purified lipase for isolates G14, B10, and OI were 17.6, 24.4, and 135 mmoles^{-1}min^{-1}mg^{-1} and 1.3, 1.6, and 0.681 mM, respectively (Shart & Elkhalil 2020).

Biodiesel Production Potential of Crude Lipase

LipBL-WII(c) catalyzed biodiesel production in the occurrence of olive oil and methanol. The production of biodiesel was confirmed by the TLC plate assay (Fig. 7). The separation of compounds in TLC is based on the competition of solute and mobile phase for the binding place on the stationary phase. As the biodiesel sample being separated was colorless, iodine vapors were used as a general non-specific color reagent. The biodiesel sample separated at the same retention factor (R$_f$ of 0.8) as the standard used (methyl oleate). The yield of the biodiesel produced using olive oil was 84%. LipBL-WII(c)'s characteristics, properties, and stability amongst organic solvents make them useful for the trans-esterification process for biodiesel production as a bio-catalyst. Lipase-mediated biodiesel production depicts various merits like; the requirement of low energy and water for isolation of product, moderate reaction conditions, and less alcohol required during the reaction. The essential reaction time for different lipases is 5–72 h (Ugur et al. 2014).

CONCLUSION

In the stated investigation, 17 indigenous lipase-producing strains were isolated and biochemically identified, out of which 2 were identified using the 16srRNA sequencing method. The two strains were: *Bacillus licheniformis* and *Bacillus rugosus*. Lipase produced from WII(c) had the highest lipolytic activity; hence, it was characterized and evaluated for biodiesel production efficiency. Microbes growing indigenously are found to be economical, better adapted to biotic and abiotic stress, and stable. Characterization of crude LipBL-WII(c) divulged that it showed stability in a wide pH range of (4 to 10) with optimum
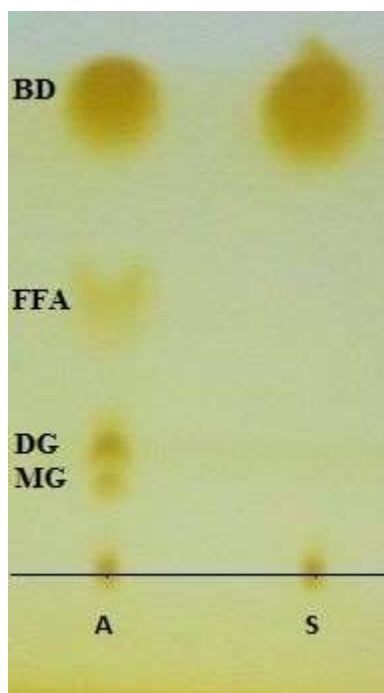

Fig. 7: LipBL-WII(c) catalyzed biodiesel production, TLC plate. S: standard (methyl oleate), A: sample. BD: biodiesel, DG: diglyceride, FFA: free fatty acid, MG: monoglyceride.

lipolytic activity observed at pH 8. LipBL-WII(c) was then found to be lipolytic at a temperature range from 20°C to 80°C, having 50°C as optima. Lipase activity was also stimulated in metal ions like Ca^{+1}, Mg^{2+}, and Zn^{2+} the most.

Furthermore, LipBL-WII(c) retained its lipolytic activity in various organic solvents and surfactants. The kinetic parameters (Km and Vmax) for LipBL-WII(c) were ascertained using Lineweaver- Burk plot. LipBL-WII(c) showed a potential for biodiesel production using olive oil as a source. Thus, it can be employed as a potential candidate for green biodiesel production using oil sources. However, further work is required to optimize lipase production, its purification, and the characterization of purified LipBL-WII(c) for more efficient biodiesel production using oil sources.

ACKNOWLEDGMENT

REFERENCES

Altschul, S.F., Gish, W., Miller, W., Myers, E.W. and Lipman, D.J. 1990. Basic local alignment search tool. J. Mol. Biol., 215(3): 403-410.

Bakir, Z.B. and Metin, K. 2016. Purification and characterization of an alkali-thermostable lipase from thermophilic *Anoxybacillus flavithermus* HBB 134. J. Microbiol. Biotechnol., 26(6): 1087-1097.

Bento, H.B.S., De Castro, H.F., De Oliveira, P.C. and Freitas, L. 2017. Magnetized poly (STY-co-DVB) as a matrix for immobilizing microbial lipase to be used in biotransformation. J. Magn. Magn. Mater., 426: 95-101.

Bharathi, D. and Rajalakshmi, G. 2019. Microbial lipases: An overview of screening, production, and purification. Biocatal. Agri. Biotechnol., 22: 101-368.

Bradford, M.M. 1976. A rapid and sensitive method for the quantitation of microgram quantities of protein utilizing the principle of protein-dye binding. Anal. Biochem., 72(1-2): 248-254.

Clarridge, J.E. 2004. Impact of 16S rRNA gene sequence analysis for identification of bacteria on clinical microbiology and infectious diseases. Clin. Microbiol. Rev., 17(4): 840-862.

Darby, S., Hill, D., Auvinen, A., Barros-Dios, J.M., Baysson, H., Bochicchio, F. and Doll, R. 2005. Radon in homes and risk of lung cancer: collaborative analysis of individual data from 13 European case-control studies. Brit. Med. J., 330(7485): 223.

Gertz, M.A., Comenzo, R., Falk, R.H., Fermand, J.P., Hazenberg, B.P., Hawkins, P.N. and Grateau, G. 2005. Definition of organ1 involvement and treatment response in immunoglobulin light chain amyloidosis (AL): A consensus opinion from the 10th International Symposium on Amyloid and Amyloidosis. Am. J. Hematol., 79(4): 319-328.

Golaki B.P., Aminzadeh S., Karkhane A.A., Yakhchali, B., Farrokh, P., Khaleghinejad, S.H. and Mehrpooyan, S. 2015. Cloning, expression, purification, and characterization of lipase 3646 from thermophilic indigenous *Cohnella* sp. A01. Protein Expr. Purif., 109: 120-126.

Gricajeva A., Bikute I. and Kalediene L. 2019. Atypical organic-solvent tolerant bacterial hormone sensitive lipase-like homologue estag1 from *Staphylococcus saprophyticus* ag1: Synthesis and characterization. Int. J. Biol. Macromol., 130: 253-65.

Gururaj, P., Ramalingam, S., Devi, G.N. and Gautam, P. 2016. Process

optimization for production and purification of a thermostable, organic solvent-tolerant lipase from *Acinetobacter* sp. AU07. Braz. J. Microbiol., 47: 647-657.

Jaiganesh, R. and Jaganathan, M.K. 2018. Isolation, purification, and characterization of lipase from *Bacillus* sp. from kitchen grease. Asian J. Pharm. Clin. Res., 11(6): 224-227.

Javed, S., Azeem, F., Hussain, S., Rasul, I., Siddique, M.H., Riaz, M. and Nadeem, H. 2018. Bacterial lipases: A review on purification and characterization. Prog. Biophys. Mol. Biol., 132: 23-34.

Karlin, S. and Altschul, S.F. 1990. Methods for assessing the statistical significance of molecular sequence features by using general scoring schemes. Proc. Natl. Acad. Sci. Amer., 87(6): 2264-2268.

Kaur, G., Singh, A., Sharma, R., Sharma, V., Verma, S. and Sharma, P.K. 2016. Cloning, expression, purification, and characterization of lipase from *Bacillus licheniformis*, isolated from hot spring of Himachal Pradesh, India. 3 Biotech, 6(1): 1-10.

Lestari, P., Raharjo, T.J., Matsjeh, S. and Haryadi, W. 2016. Partial purification and biochemical characterization of extracellular lipase from *Azospirillum* sp. JG3 bacteria. AIP Conf. Proceed., 1755: 080003.

Li, Y., Liu, T.J., Zhao, M.J., Zhang, H. and Feng, F.Q. 2019. Screening, purification, and characterization of an extracellular lipase from *Aureobasidium pullulans* isolated from stuffed buns steamers. J. Zhejiang Univ.Sci. B, 20(4): 332-342.

Mazhar, H., Abbas, N., Hussain, Z., Sohail, A. and Ali, S.S. 2016. Extracellular lipase production from *Bacillus subtilis* using agro-industrial waste and fruit peels. Punjab Univ. J. Zool, 31(2): 261-267.

Patel, P. and Desai, P. 2018. Isolation, identification, and production of lipase producing bacteria from oil-contaminated soil. BMR Microbiol., 4(1): 1-7.

Priyanka, P., Kinsella, G., Henehan, G.T. and Ryan, B.J. 2019. Isolation, purification, and characterization of a novel solvent stable lipase from *Pseudomonas reinekei*. Prot. Expr. Purif., 153: 121-130.

Rmili, F., Achouri, N., Smichi, N., Krayem, N., Bayoudh, A., Gargouri, Y. and Fendri, A. 2019. Purification and biochemical characterization of an organic solvent-tolerant and detergent-stable lipase from *Staphylococcus capitis*. Biotechnol. Progr., 35(4): e2833.

Rios, N.S., Pinheiro, B.B., Pinheiro, M.P., Bezerra, R.M., dos Santos, J.C.S. and Gonçalves, L.R. B. 2018. Biotechnological potential of lipases from *Pseudomonas*: Sources, properties, and applications. Process. Biochem., 75: 99-120.

Sajna, K.V., Sukumaran, R.K., Jayamurthy, H., Reddy, K. K., Kanjilal, S., Prasad, R. B. and Pandey, A. (2013). Studies on biosurfactants from *Pseudozyma* sp. NII 08165 and their potential application as laundry detergent additives. Biochem. Eng. J., 78: 85-92.

Saraç, N. and Ugur, A. 2016. A green alternative for oily wastewater treatment: lipase from *Acinetobacter haemolyticus* NS02-30. Desal. Water Treat., 57(42): 19750-19759.

Saraswat, R., Verma, V., Sistla, S. and Bhushan, I. 2017. Evaluation of alkali and thermotolerant lipase from an indigenous isolated *Bacillus* strain for detergent formulation. Elec. J. Biotechnol., 30: 33-38.

Saraswat, R., Bhushan, I., Gupta, P., Kumar, V. and Verma, V. 2018. Production and purification of an alkaline lipase from *Bacillus* sp. for enantioselective resolution of (±)-Ketoprofen butyl ester. 3 Biotech, 8(12): 1-12.

Sarmah, N., Revathi, D., Sheelu, G., Yamuna Rani, K., Sridhar, S., Mehtab, V. and Sumana, C. 2018. Recent advances on sources and industrial applications of lipases. Biotechnol. Progress, 34(1): 5-28.

Sharma, S. and Kanwar, S.S. 2017. Purification and bio-chemical characterization of a solvent-tolerant and highly thermostable lipase of *Bacillus licheniformis* strain SCD11501. Proceed. Nat. Acad. Sci. India Sec. B Biol. Sci., 87(2): 411-419.

Shart, A.O. and Elkhalil, E.A. 2020. Biochemical Characterization of Lipase Produced by *Bacillus* spp. Isolated from Soil and Oil Effluent. Adv. Enzyme Res., 8(04): 39.

Tripathi, R., Singh, J., Kumar Bharti, R. and Thakur, I.S. 2014. Isolation, purification, and characterization of lipase from *Microbacterium* sp. and its application in biodiesel production. Energy Procedia, 54: 518-529.

Ugur, A., Sarac, N., Boran, R., Ayaz, B., Ceylan, O. and Okmen, G. 2014. New lipase for biodiesel production: partial purification and characterization of LipSB 25-4. Int. Sch. Res. Notices, 2014.

Wang, H., Zhong, S., Ma, H., Zhang, J. and Qi, W. 2012. Screening and characterization of a novel alkaline lipase from *Acinetobacter calcoaceticus* 1-7 isolated from Bohai Bay in China for detergent formulation. Braz. J. Microbiol., 43: 148-156.

Winkler, U.K. and Stuckmann, M. 1979. Glycogen, hyaluronate, and some other polysaccharides greatly enhance the formation of exolipase by *Serratia marcescens*. J. Bacteriol., 138(3): 663-670.

Yang, K.S., Sohn, J.H. and Kim, H.K. 2009. Catalytic properties of a lipase from *Photobacterium lipolyticum* for biodiesel production containing a high methanol concentration. J. Biosci. and Bioeng., 107(6): 599-604.

Zhao, J., Ma, M., Zeng, Z., Yu, P., Gong, D. and Deng, S. 2021. Production, purification, and biochemical characterization of a novel lipase from a newly identified lipolytic bacterium *Staphylococcus caprae* NCU S6. J. Enzyme Inhib. Med. Chem., 36(1): 248-256.

Efficacy of Tree Leaves as Bioindicator to Assess Air Pollution Based on Using Composite Proxy Measure

J. S. Berame*, J. E. Josue*†, M. L. Bulay*, J. J. Delizo**, M. L. A. Acantilado**, J. B. Arradaza*** and D. W. M. G. Dohinog****

*Caraga State University, Butuan City, Philippines
**Bancasi Integrated School, Butuan City, Philippines
***West Integrated School, Butuan City, Philippines
****Ampayon National High School, Butuan City, Philippines
†Corresponding author: Jacob E. Josue, Jr; jacob.josuejr@gmail.com

ABSTRACT

Air pollution has become a major issue in cities due to urbanization, population growth, industrial development, and increasing number of vehicles. The study used *Gmelina arborea* tree leaves as a bioindicator to determine the Air Pollution Tolerance Index (APTI) as a simple and effective compositional index of environmental health in three cities in the Caraga Region, Philippines. To calculate the APTI, four biochemical parameters of tree leaves were calculated: relative water content, total chlorophyll content, leaf-extract pH, and ascorbic acid content. In terms of the APTI category, results showed that all *G. arborea* species collected in all sample sites are classified as sensitive to air pollution, with the sample collected in Bayugan City being the most sensitive, with an APTI value of 7.66, and the samples collected in Butuan and Cabadbaran City being the least sensitive, with APTI values of 9.54 and 9.11, respectively. A Kruskal-Wallis test revealed a significant difference between the APTI values of *G. arborea* trees in the three sampling areas in the Caraga region. Based on the APTI computed values of the tree leaves determined in all sites, it is concluded that *G. arborea* species can be used as a bioindicator of air pollution, classified as sensitive.

INTRODUCTION

Urbanization, industrialization, population development, and an increase in the number of cars are all contributing to an ever-increasing problem of air pollution in cities. Plants have the potential to significantly reduce air pollution in metropolitan settings (Irshad et al. 2020, Leghari et al. 2019). Air pollution is one of the most serious issues affecting people's health. The problem is especially significant in the Philippines' urban areas. Air pollution represents a major concern that has far-reaching implications for the health and environment of a region (Alpy & Sanjay 2016). Various physical and chemical technologies have been developed and deployed in the past to help improve air quality. Still, the high costs of establishing and maintaining these systems remain a worry (Xie et al. 2017). Biological solutions such as cultivating green plants in and around Metro Manila's urban areas are a viable alternative to employing physical and chemical ways to mitigate air pollution (Su et al. 2018).

Plants have been a tried-and-true solution to various air-related issues (Swami & Chouhan 2015, Achakzai et al.

2017). The content, concentration, and interaction of primary and secondary pollutants in the atmosphere change as the population, urbanization, motorization, and industrialization increase (Sahu et al. 2020). The leaves of plants are the major receptors of air pollution. Because the leaves have a vast surface area for absorption and accumulation, they serve as a sink for pollutants (Liu et al. 2008, Kim et al. 2015). Pollution's impacts are most visible on leaves, which have a direct negative impact on them (Lohe et al. 2015). Because roadside plants' leaves come into close contact with pollutants, they may act as pollutants' stressors (Ogboru et al. 2021). Conveniently, plant leaves have been recommended for testing to determine their ability to absorb and/or adsorb pollutants (Escobedo et al. 2008). Tolerant plants are so effective at absorbing toxins that they can create pockets of clean air (Brilli et al. 2018). Thus, such tolerant trees can help to improve air quality by exchanging gasses and acting as a sink for air pollutants, decreasing pollutant concentrations in the air and contributing to air pollution mitigation. Monitoring for injurious levels of air pollutants by plants is a standard technique to diagnose air pollution injury in

plants (Ram et al. 2015). Recently, there has been a greater emphasis on using plants to detect air quality.

Biomonitoring is increasingly used as a cost-effective alternative to instrumental methods for studying local air pollution in the terrestrial environment (Yousaf et al., 2020, Nakazato et al. 2018). Lichens and mosses have already been used as biomonitors. However, dissimilar bioaccumulation dynamics were observed due to differences in morphology, ecophysiology, and habitat (Drava et al. 2019, Al-Khashman et al. 2011, Simon et al. 2014, Gonze & Sy 2016, Margitai et al. 2017). Due to their continual exposure and low-cost sampling, trees provide an alternative means of monitoring urban air quality (Lei et al. 2018, Selmi et al. 2016).

The Air Pollution Tolerance Index can be used to determine how plants react to pollution. APTI is the bio-indicator species' biological monitoring and assessment index. It's a method for determining how plants respond biochemically and physically (Gulliermo & Mallapre 2016.). Plants that are sensitive to pollution help to detect it, whereas those that are tolerant help to reduce pollution by acting as sinks in polluted areas (Lakshmi et al. 2009). The air pollution tolerance index (APTI) is a plant's innate ability to withstand air pollution stress, a major concern in industrial and non-industrial locations (Rai et al. 2013). The suitability of tree species as bioindicators/biomonitors are decided by their tolerance and sensitivity to air pollution, which is frequently tested using the air pollution tolerance index (Ogunkunle et al. 2014). Plants in urban locations are continually exposed to pollutants, resulting in pollutant buildup and integration into their systems, affecting the leaf's character, tolerance, and sensitivity. This sensitivity is assessed using a variety of biochemical measures, followed by an APTI (Tak & Kakde 2017). Among all the trees investigated along Metro Manila's key roadside corridors, *Gmelina arborea* Roxb. had the highest APTI value (Glenn et al. 2018). The study was conducted to determine the Air Pollution Tolerance Indicator (APTI) as a simple and effective compositional index of environmental health by using *G. arborea* tree leaves as a bioindicator in three cities in Caraga Region in the Philippines.

The study aimed to assess the efficacy of biomonitoring methods using *G. arborea* tree species as a bioindicator in investigating the level of tolerance to air pollutants, especially in high-traffic areas of the three cities in Caraga Region on the susceptibility level of *G. arborea* tree to air pollutants in terms of the following biochemical parameters for air pollution tolerance index, namely: relative leaf water content, total chlorophyll content, leaf-extract pH, and ascorbic acid content.

MATERIALS AND METHODS

This chapter discussed the methods and measures undertaken to conduct the study, such as choosing the research design, selecting the locale of the study, sampling technique, data gathering procedure, instrumentation, and the statistical treatment used in data analysis.

Research Design

This study used a quantitative experimental research design with a test configuration performed in a laboratory. Before, during, and after the test experiments, comparative assessments, study guides, and related articles were considered to ensure that there is clear and cut evidence to provide adequate results that could be based on by future researchers who would follow suit in the same or related research. The collected data were analyzed using correlation measures to determine trees' air pollution tolerance index in various sampling areas.

Research Locale

The study sites were conducted in three cities in the Caraga region, particularly on the roadsides of Butuan City, Cabadbaran City, and Bayugan City. *G. arborea* tree species were found and selected on purpose by the researchers in each city, respectively, at Capitol Drive, Butuan City, Ilban Street, Cabadbaran City, and Narra Avenue, Bayugan City. These sampling areas were considered polluted due to the large volume of vehicles on each city's roadsides. Fig. 1 below presents the map of the Caraga Region, Philippines, where three sampling areas were located.

Sampling Technique Used

During the dry season in the morning, fresh leaves of *G. arborea* trees were accumulated from the conveyance congested areas of the three sampling sites, along the road of Capitol Drive, Butuan City, Ilba Street, Cabadbaran City, and Narra Avenue, Bayugan City. Plenarily grown leaves of *G. arborea* were taken from above 3 m height in each of the three sampling areas and were brought to the laboratory. The loose dust particles amassed on the leaf surface were removed with a fine brush before the fresh weight of the leaves was recorded. For the turgid weight, the leaves were marinated for 24 h in distilled water before acquiring the weight. The leaves' dry weight was taken in an oven at 105°C for 2 h. The pH of the leaf extract was measured with an EZDO PH-5011 pH meter. To determine the remaining city samples' total chlorophyll and ascorbic acid content, 1-gram *G. arborea* leaf samples were brought to the Mindanao State University-IIT Chemistry Department Laboratory.
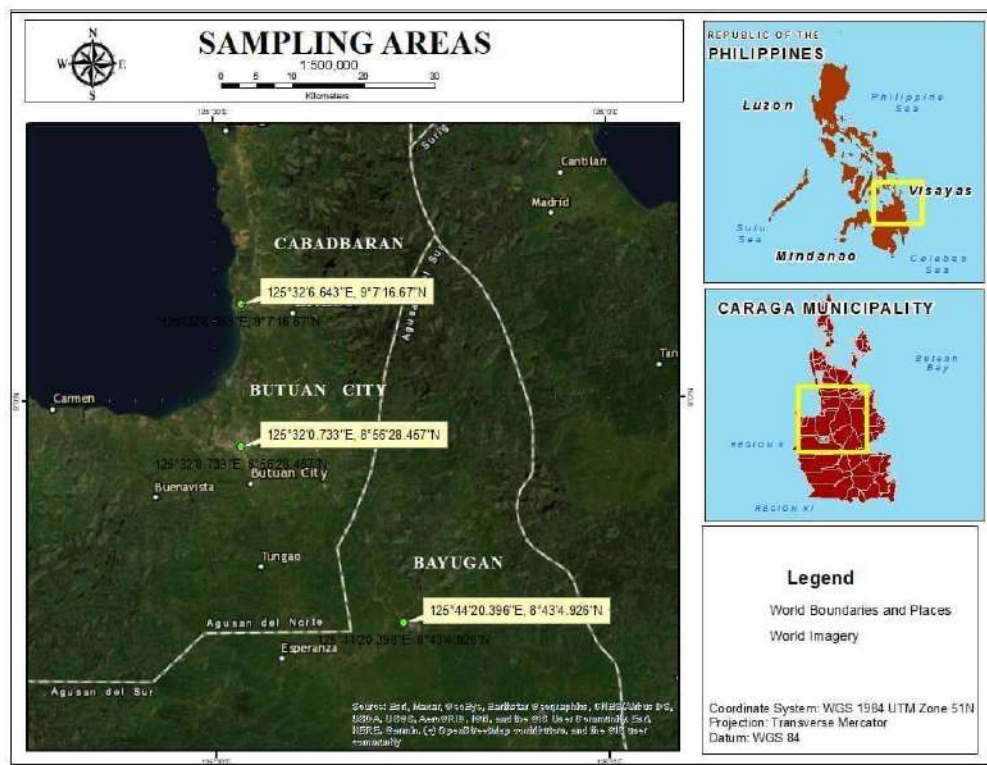
Fig. 1: Map of the study area in Caraga Region, Philippines.

Data Gathering Procedure

The researchers requested permission to conduct an Air Pollution Tolerance Index of *G. arborea* tree species in each city via email to the City Environment and Natural Resources office. Experiments for relative leaf water content and leaf-extract pH were carried out in the laboratory of Ampayon National High School. Due to a lack of equipment in Ampayon National High School and Caraga State University laboratories, the sample leaves' total chlorophyll and ascorbic acid content in three sampling areas were determined at Mindanao State University-IIT. The results of the four biochemical parameters were then used to obtain the Air Pollution Tolerance Index of *G. arborea* leaves in each sampling area. Comparison between the APTI values between each sampling site in Caraga, Philippines, were obtained using the Kruskal-Wallis statistical test.

Samples were handled as follows to obtain four parameters in the APTI (Air Pollution Tolerance Index formula:

Relative Leaf Water Content (RWC): Turner's (1981) formula for calculating RWC was used. Fresh leaves were collected, weighed using a triple beam balance, and recorded. After that, the leaves were soaked in distilled water overnight and weighed to determine the turgid weight (Dash & Dash 2017). The leaves were then dried for 2 h at 105°C in an oven before being reweighed to get the dry weight. The relative water content of leaves was calculated using the formula:

Relative water content (%) = $\{(F-D)/(T-D)\} \times 100$

F = Fresh weight of leaves (g)

D = Dry weight of leaves (g)

T = Turgid weight of leaves (g)

Total Chlorophyll Content (TCC): The sample leaves of each sampling area were brought to the laboratory of the Chemistry Department at Mindanao State University-IIT to determine the total chlorophyll content of *G. arborea* leaves. The chemist used the DMSO method (Ter et al. 2020). The extraction process was carried out using the amphiphilic DMSO solvent. Pepper tissue was sliced into smaller pieces and placed in test tubes with 10 mL of solvent. For an hour, test tubes were incubated in a water bath at 60-65°C. Based on preliminary research (Caabay 2020, Banerjee et al. 2018), this period was deemed adequate for complete tissue decolorization. Cooling at room temperature for 30 minutes was followed by filtration and absorbance measurements at 665 and 648 nm. DMSO was used for the

blank determination. The absorption was measured using a HITACHI Spectrophotometer U-2000.

Chlorophyll concentrations were estimated using the methods below and represented as mg/g fresh weight (Barnes et al. 1992).

Chlorophyll a (mg.g^{-1} F.W) = (14.85 A$_{665}$ -5.14 A$_{648}$)

Chlorophyll b (mg.g^{-1} F.W) = (25.48 A$_{665}$ − 7.36 A$_{648}$)

Total chlorophyll (mg.g^{-1} F.W) = (7.49 A$_{665}$ + 20.34 A$_{648}$)

where: A$_{665}$ = absorption value at 665 nm, A$_{648}$= absorption value at 648 nm.

Leaf Extract pH: The pH of the leaf extract was calculated using the Datta and Sinha (2018) method. A 5 g of fresh leaves were rinsed in distilled water before being crushed and homogenized in a mortar and pestle with 25 mL of distilled water. A pH meter was used to determine the pH of the leaf extract filtrate (Pandey et al. 2016).

Ascorbic Acid Content (AAC): The concentration of ascorbic acid or Vitamin C content (mg.100 g^{-1}) in the leaf of each sample leaf was determined through a laboratory test at the Chemistry Department at Mindanao State University-IIT. The chemist Singh & Chauhan (2014) spectrophotometric approach to determine ascorbic acid concentration. Fresh leaf samples (1g) were placed in a test tube, followed by 4 mL oxalic acid-EDTA, 1 mL orthophosphoric acid, 1 mL sulfuric acid, 2 mL ammonium molybdate solution, and 2 mL distilled water. After allowing the solution to rest for about 15 minutes, the clear solution from the tube was tested using a Spectrophotometer for absorbance at 760 nm (Model No. 31). The concentration of ascorbic acid in the leaf was determined using a standard graph that included absorbance and ascorbic acid concentrations and was created using the same method.

Air Pollution Tolerance Index (APTI)

Plant APTI values were obtained using the Datta and Sinha (1995) equation.

$$APTI = A (T + P) + R/10$$

Where A =Ascorbic Acid Content of the leaf (mg.g^{-1})

P = pH of leaf extract

R = Relative Water Content of leaf (%)

T = Total Chlorophyll level of leaf extract (mg/g)

The APTI category described by Lakshmi et al. (2009) is shown in Table 1. The APTI values were calculated using each sampling area's four biochemical parameters. The plant species' Air Pollution Tolerance Index (APTI) was then compared to the standard values in the table below to determine how the *G. arborea* tree species responded to air pollution.

Table 1: APTI category described by Lakshmi et al. (2009).

Species	APTI computed values
Tolerant species	30-100
Intermediate tolerant species	17-20
Sensitive species	1-16
Very sensitive species	< 1

Statistical Treatment of Data

With a significance level of $p = 0.05$, the Kruskal-Wallis test was used to determine whether there are significant differences in the APTI values of *G. arborea* trees collected within all three study locations in the Caraga Region, Philippines.

RESULTS AND DISCUSSION

This section discusses the susceptibility level of *G. arborea* tree to air pollutants in terms of the following biochemical parameters for the air pollution tolerance index

Relative Water Content

The study of Gonzalez et al. (2001) defined relative water content as the amount of water in a leaf at the time of sampling in relation to the maximum amount of water a leaf can hold. They also stated that it is an important parameter in air pollution tolerance index relation studies (Jitin 2014) that have evaluated the osmotic potential at full turgor within the leaf to determine the plant's current health. When pollution and transpiration rates stress plants are high, this characteristic also refers to the water present in the plant, which helps it maintain its physiological equilibrium, and plants with higher water content are more drought resistant (Rai et al. 2013). Gholami et al. (2016) noted that in the occurrence of contaminated air in the area, the transpiration rates of plants are typically high, which can contribute to desiccation. Pigment analysis in *G. arborea* can be used as a physiological indicator of plant responses to water scarcity because they provide information about the stress event and because there is an inverse relationship between chlorophyll and carotenoid levels as water stress increases (Rojas et al. 2012).

Table 2 shows the relative water content (RWC) in each sampling area, which includes the fresh, dry, and turgid weights of the leaf samples based on related studies that also conduct tolerance indices with plants (Kaur & Nagpal 2017, Roy et al. 2020, Wolf et al. 2022). As cited by Roy et al. (2020), the location of a tree species' growth could significantly affect the relative weight of its leaves, with a nearby canopy covering inhibiting a greater loss of water

Table 2: Relative water content in *G. arborea* leaf samples.

Sampling areas	Fresh Weight [g]	Dry Weight [g]	Turgid Weight [g]	FW-DW	TW-DW	RWC [%]
Butuan	8.63	1.5	9	7.13	7.50	95.07
Cabadbaran	7.30	1.4	7.9	5.90	6.50	90.77
Bayugan	5.05	1	6.3	4.05	5.30	76.42

content within the leaves. This corresponds with the fact that the Butuan City sample has the highest fresh weight of the three sampling sites, at 8.63g, dwarfing the samples collected from Cabadbaran City (7.30 g) and Bayugan City (5.05 g), because it is located near a building that has the potential to shade it from sunlight at certain times of the day, rather than being within the sidewalk of the main road with little to no cover from the sun. Navarrete et al. 2017 found that the relative water content and subsequent water absorption rate rise as pollution levels rise. They explained why the samples gathered in Bayugan City gained the most weight (1.5 g) after 24 h of soaking in distilled water, then the samples gathered from Cabadbaran (0.6 g) and Butuan (0.37 g), due to its location that is found near a garbage bin. After drying in an oven for 2 h at 105°C, Butuan lost approximately 8.5 g with a dry weight of 1g, whereas Bayugan lost only 5.3g with a dry weight of 1g, and Cabadbaran lost 6.5 g with a dry weight of 1.4 g. For the RWC, the *Gmelina arborea* leaf sample in Butuan had the highest average relative water content (95.07%), Cabadbaran (90.77%), while the area around Bayugan had the lowest (76.42%). RWC in the *G. arborea* tree leaf sample is lower in the Bayugan area. This could be due to some factors, such as the condition of the sample species, which is located near burning garbage, and the tree's age (Shafiq & Iqbal 2012).

The findings of this test complement the study done by Mahecha et al. (2013), where they stated that a plant's high-water content could help it maintain its physiological balance under stress conditions such as air pollution, where transpiration rates are often high. According to Dash and Dash (2017), transpiration rates are relatively high, and a greater volume of water is required to maintain physiological equilibrium in a plant body against contaminants. They also stated that meteorological conditions, humidity, and the availability of moisture content in soil influence relative water content. A decrease in RWC reduces stomatal conductance, and therefore, according to Amulya (2015), CO_2 assimilation Net CO_2 exchange, CO_2 assimilation, and photosynthetic potential all reach zero at very low RWC (around 40%), indicating that the plant species are sensitive to a sudden change in air quality within its area. Plant transpiration rates may increase under stressful conditions, such as exposure to air pollution. Plants with a higher RWC are more resistant to air pollution.

Total Chlorophyll Content

Giri et al. (2013) explained that the amount of chlorophyll in the leaf determines the spectral variation in visible bands during the photosynthetic process. Chauhan (2010) extrapolated its significance because a decrease in the leaf chlorophyll content reduces the amount of solar radiation that can be absorbed, limiting the efficiency of corresponding photosynthetic processes and thus lowering primary photosynthetic production. As a result, an accurate estimation of the plant leaf chlorophyll content is a critical foundation in assessing the plant's tolerance to air pollution.

In accordance with Rai (2019), Roy et al. (2020), and Kousar (2014), stated that high amounts of air pollutants in the urban environment could degrade chlorophyll molecules into pheophytin by replacing Mg++ ions with two hydrogen atoms and increasing the activity of the chlorophyllase enzyme. These findings provide the reason why Table 3 shows that the Cabadbaran City sample has the highest chlorophyll a and b content. Still, the Butuan City sample got the highest total chlorophyll content. Similarly, Notman et al. 2006 explained that a tendency of low chlorophyll content in urban roadside plant leaves could result from constant exposure to the waste, which can be observed in the Bayugan City sample, which has the lowest levels of chlorophyll a, b, and total chlorophyll. These findings reveal a significantly low level of chlorophyll content in the leaf sample collected from Bayugan City compared to those

Table 3: Total chlorophyll content of *G. arborea* leaf samples.

Sampling areas	Chlorophyll content (mg.g^{-1} of fresh leaves)		
	Chlorophyll a	Chlorophyll b	Total Chlorophyll
Butuan City	0.637 ± 0.003	1.15 ± 0.01	1.29 ± 0.01
Cabadbaran City	0.643 ± 0.003	1.29 ± 0.01	1.16 ± 0.01
Bayugan City	0.408 ± 0.001	0.740 ± 0.002	0.863 ± 0.001

collected within Butuan City and Cabadbaran City. The result could be due to the exposure of the Bayugan *G. arborea* tree to the pollutants within its vicinity. This is supported by related studies, which stated that higher chlorophyll content plants are more pollution-resistant (Salimi & Aghdash 2019). Moreover, the decline in chlorophyll concentration appears to be linked to rising pollution levels (Gharge & Menon 2012).

However, all tree samples in all sites are not within the range with standard controlled *G. arborea* tree species found in other research (Dash & Dash 2017) but are higher than those found within heavily polluted sites (Glenn et al. 2018). According to one study, drought stressors significantly negatively influenced physiological parameters and total chlorophyll content, significantly reducing selected growth features. In contrast, proline content was elevated (Sachan et al. 2019, Nikolaeva et al. 2010).

Leaf-Extract pH

As illustrated in Fig. 3 below, there is a substantial difference in pH levels of *G. arborea* leaf samples across the three sites, with the leaf sample from Butuan City having the lowest pH level of 5.95, indicating acidity, and the leaf sample from Bayugan having the highest pH level of 6.51, indicating close to neutral. The acidic leaf extract pH of 6.80 indicates that the leaf extract is more susceptible to air contaminants (Kuddus et al. 2011). High pH has been shown to increase plant tolerance to pollution (Akande et al. 2021).

Stomatal sensitivity is affected by pH, and leaves with a low pH are more susceptible to pollution, while those with a neutral pH are more tolerant (Krishnaveni 2013).

According to Uka and Chukwuka (2014), the pH of the leaf filtrates in the sites indicates the presence of gaseous air pollutants, specifically SO_2 and NO_2. However, Ter et al. (2020) found that in all plant species, the pH value of leaf extract in contaminated sites was lower than in control sites. Additionally, the researchers observed that the high pH of leaf extract at the control site and the low pH at the polluted site could be due to the high pollution levels at the polluted sites.

The graph also illustrates that even if the leaf sample from the Butuan site is more acidic than the Cabadbaran and Bayugan sites, the test showed that the Butuan site has the highest total chlorophyll content ascorbic acid content out of the 3. Thus, it is expected that compared to the other species studied (Glenn 2018), the total chlorophyll content and ascorbic acid content should be relatively lower.

Ascorbic Acid Content

Ascorbic acid is a significant redox buffer that also serves as a cofactor for enzymes that regulate photosynthesis, hormone production, and the regeneration of other antioxidants (Gallie 2012). In this study, Fig. 4 displayed a significant difference between the ascorbic acid levels of *G. arborea* leaf samples in Butuan and Cabadbaran from the sample collected in Bayugan. It shows a 0.0179mg/g difference between the ascorbic acid content from Butuan and Bayugan. Cabadbaran has a closer ascorbic acid to Butuan, which has only a 0.0007mg/g difference. The study found that ascorbic acid levels in plant leaves fell considerably in polluted areas with visible rubbish near the Bayugan sample site compared to
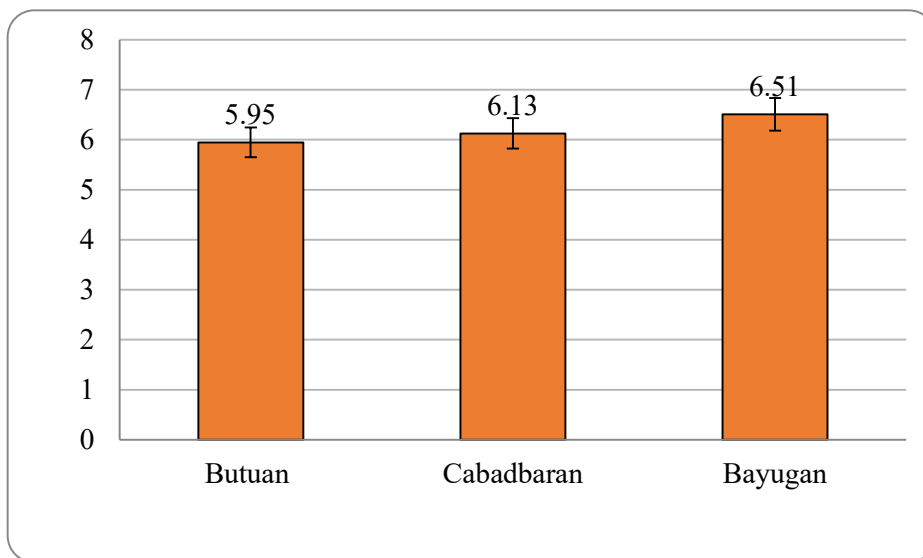

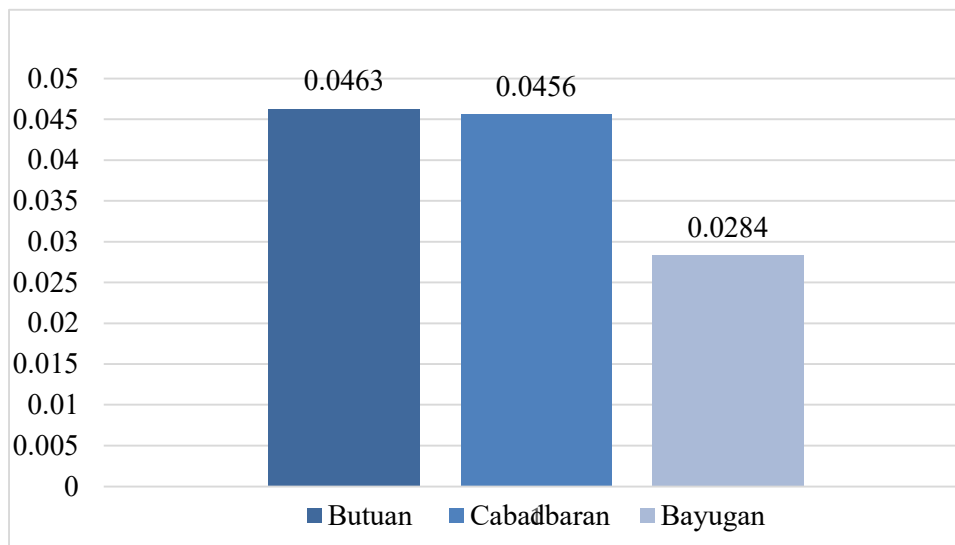Fig. 2: The relative pH level graph of *G. arborea* leaf samples.

Fig. 3. Ascorbic Acid Content of *G. arborea* leaf samples.

Cabadbaran and Butuan sample sites. Consistently, the study of Falusi et al. (2015) reported that pollution of dumpsite habitats is linked to the release of various air pollutants, including acidic gases like SO_2, NO_x, and H_2S. As a result, the drop in ascorbic acid concentration found in *C. odorata* and *M. lucida* gathered from the four dumpsites compared to the control site could be related to acidic gas deposition on the surface of their leaves.

The researchers also discovered that the overall tree health in Cabadbaran and Butuan was better than in Bayugan, although the sample in Butuan is more exposed to vehicular emissions. This discovery is consistent with Conklin's (2001) and Aguiar-Silva et al. (2016) findings that increased ascorbic acid concentration in plants implies resilience to air pollution. *G. arborea* species in the experimental site had the highest ascorbic acid levels (Ogboru et al. 2021). Because its reducing power is related to its concentration, plants that retain a high ascorbic acid content even under polluted environments are thought to be tolerant of air pollutants (Ogunrotimi et al. 2017). Various biochemical parameters acted differently in the tested plant species, but the ascorbic acid level was discovered to be the most important element in providing plants with air pollution resistance (Bharti et al. 2017).

According to Rahul & Jain (2014), the air pollution tolerance index (APTI) describes plants' inherent ability to tolerate air pollution. It is among the most important factors when choosing traffic barrier plant species. Plant APTI has been described using four biochemical parameters: total chlorophyll, relative water content (RWC), ascorbic acid, and leaf extract pH (Nadgórska–Socha et al. 2017). Pollution-induced changes in a single parameter may not provide a complete picture. As a result, four biochemical parameters are considered to obtain an empirical value representing plant APTI.

Table 4 shows the results of the Air Pollution Tolerance Index (APTI) of *G. arborea* trees identified in three cities, as well as biochemical characteristics such as relative water content (RWC), total chlorophyll content (TCC), leaf-extract pH, and ascorbic acid concentration (AA), all of which are required for multiple studies to successfully determine APTI values of any plant species. One sample revealed a significant difference when comparing the APTI values of the three Caraga Region sites. It was discovered that Bayugan samples have a lower APTI value than Butuan and Cabadbaran samples. The reason for the Bayugan City sample *G. arborea*'s low APTI value in the Bayugan City sample may have a low pH value because a higher pH value

Table 4: APTI values of *G. arborea* tree leaves in the 3 cities.

Sampling areas	RWC (%)	TCC (mg/g)	pH	AA (mg/100g)	APTI
Butuan	95.07	1.29 ± 0.01	5.95	4.63 ± 0.07	9.54
Cabadbaran	90.77	1.16 ± 0.01	6.13	4.56 ± 0.07	9.11
Bayugan	76.42	0.86 ± 0.001	6.51	2.84 ± 0.00	7.66

Table 5: The Kruskal-Wallis test between the three sites within the Caraga Region

Factor	Statistics	df	p-value*	Remark
Caraga Region Cities	6.489	2	0.039	Reject H_0

* Tested on 0.05 significant difference

increases plant tolerance to air pollution (Ninave et al. 2001). Despite the wide range of APTI values, the final assessment of labeling all of the trees is sensitive (Nadgórska–Socha et al. 2017, Gulia et al. 2015, Li et al. 2018). Guillermo and Mallarpe (2016) found that the mean APTI value of the *G. arborea* individuals studied was 11.45, putting them in the sensitive category. Furthermore, Viradia et al. (2020) reported that *G. arborea* is a sensitive species, with APTI values of 3.079 and 7.192, respectively, on their sites 1 and 2.

The findings of this study are highly consistent with those of Molnar et al. (2020) and Pandey et al. (2015), who discovered that plant species with lower APTI values are particularly valuable as bioindicators of air pollution and proxies for urban health. Furthermore, APTI determination is a reliable method for screening many plants for their response to air contaminants (Deepalakshmi et al. 2013). However, *G. arborea* species were classified as tolerant in the study of Carillo and Ocampo (2016). Ogunrotimi & Adereti (2017) conducted an earlier study in which *G. arborea* had APTI values, indicating it was an intermediately tolerant species within their respective areas for sample collection. This may lead to the initial assumption that G. arborea species found within the sites are tolerant as the samples tested in previous research (Wang et al. 2011, Ugulu et al. 2015, Liu et al. 2012). As a result, APTI values can be used to select pollution-tolerant plants for urban greening or green belt development (Mondal et al. 2011).

Table 5 shows the Kruskal-Wallis Test in JASP v.0.16.2.0 which is used to answer the hypotheses if significant differences exist between the Air Pollution Tolerance Indices (APTI) of each study site within the Caraga region, which is tested on 0.05 significant difference. The results indicate a significant difference between the APTI values of trees within the 3 cities in the Caraga Region (*p*=0.039). This indicates at least 1 significant difference within all study sites in Caraga Region. It is supported in the study by Dash and Dash and Dash (2017) that low APTI levels were susceptible to air contaminants in general and vice versa. Sensitive plants can serve as indicators, while tolerant plants can serve as a barrier for pollutants in the air (Gholami et al. 2018). Tolerant species are bio accumulators, can be efficient roadside vegetation, and can help with the absorption and screening of air pollution (Kunwar et al. 2016). According to Berame et al. (2021), significant progress has been made due to

biomonitoring efforts relating to industrial, agricultural, and domestic pollution affecting ecosystems in the Philippines. Therefore, plants with high APTI values have the potential to grow under air pollution conditions, while low APTI valued (sensitive) plants can be utilized to detect the current state of pollution indices are recommended to satisfy the concept of the green-belt development program (Dash & Dash 2017).

CONCLUSION

Based on the APTI computed values of the tree leaves determined in all sites, it is concluded that *G. arborea* species can be used as a bioindicator of air pollution classified as sensitive. This could be attributed to the high concentrations of air contaminants at each study site. The large disparity in APTI values obtained across all three sites is attributable to the significant difference in APTI values measured between Bayugan City and Butuan City. Even though the study indicates that all samples are sensitive to air pollution, there is still a disparity between the samples. Thus, rejecting the null hypothesis means that there is a significant difference in the APTI values of the *G. arborea* tree leaves within the three cities in the Caraga Region. Further studies about *G. arborea* as a bioindicator in other areas in the Philippines should be done since it is a sensitive species suitable for identifying the air pollution tolerance of trees. Multiple tree species found in polluted-ridden areas, not specifically about air pollution but also land and water pollution, must be gathered throughout all study sites to ensure a more robust outcome. It is suggested to use various tree species that are tolerant to air pollution as they serve as bioaccumulators of air pollution. Thus, they could be planted along national highways as part of the greening development in the Philippines. Time intervals between collecting samples should be done in comparison to the pollution levels throughout the day.

ACKNOWLEDGEMENT

REFERENCES

Achakzai, K., Khalid, S., Adrees, M., Bibi, A., Ali, S., Nawaz, R. and Rizwan, R. 2017. Air pollution tolerance index of plants around Brick

Kilns in Rawalpindi, Pakistan. J. Environ. Manag., 190: 252-258. https://doi.org/10.1016/j.jenvman. 2016.12.072

Aguiar-Silva, C., Brandao, S.E., Domingos, M. and Bulbovas, P. 2016. Antioxidant responses of Atlantic forest native tree species as indicators of increasing tolerance to oxidative stress when they are exposed to air pollutants and seasonal tropical climate. Eco. Indic., 63: 154-164. https://doi.org/10.1016/j.ecolind.2015.11.060

Akande, A., Dada, E., Olusola J. and Adeyemi, M. 2021. Biochemical and physiochemical assessment of air pollution tolerance index of selected plant species at Ikpoba Okha gas flaring site, Edo State, Nigeria. Pollut, 7(4): 889. DOI: 10.22059/POLL.2021.324224.1098

Al-Khashman, O.A., Al-Muhtaseb, A.H. and Ibrahim, K.A. 2011. Date palm *(Phoenix dactylifera L.)* leaves as biomonitors of atmospheric metal pollution in arid and semi-arid environments. Environ. Pollut., 159(6): 1635-1640. https://doi.org/10.1016/j.envpol.2011.02.045

Alpy, S. and Sanjay K.U. 2016. Heavy metal accumulation in *Pyrrosia flocculosa* ching growing in sites located along a vehicular disturbance gradient. Environ. Monit Assess., 188(10): 547. https://doi.org/10.1007/s10661-016-5561-3

Banerjee, S., Banerjee, A., Palit, D. and Roy, P. 2018. Assessment of vegetation under air pollution stress in urban industrial area for green-belt development. Inter. J. Environ. Sci. Tech., doi:10.1007/s13762-018-1963-9

Barnes, D. L. and Dempsey, C. P. 1992. Influence of period of deferment before stocking spring-burnt sour veld on sheep performance and veld productivity. J. Grassl. Soc. South. Afr., 9 (4): 149-157. https://doi.org/10.1080/02566702.1992.9648316

Berame, J.S., Hojilla M. B., Trinidad E., Lawsin N. L., Orozco J. A., Arevalo I. J. and Alam Z. F. 2021. Strategies and approaches towards environmental biomonitoring of freshwater ecosystems in the Philippines. Nat. Environ. Pollut. Technol., 20(4): 1545-1553. doi:10.46488/NEPT. 2021.v20i04.016

Bharti, K. M., Trivedi, A. and Kumar, N. 2017. Air pollution tolerance index of plants growing near an industrial site. Urban Climate, 8: 007. DOI:10.1016/j.uclim.2017.10.007

Brilli, F., Fares, S., Ghirardo, A., de Visser, P., Calatayud, V., Muñoz, A. and Menghini, F. 2018. Plants for sustainable improvement of indoor air quality. Trends Plant Sci., 23(6): 507-512. https://doi.org/10.1016/j.tplants.2018.03.004

Caabay, S. 2020. Air pollution tolerance index (APTI) selected plant species in Puerto Princesa City for strategic urban forest planning. Inter. J. of Sci. and Mgnt. Stud., 3(1): 2581-5946.

Carillo, N.V. and Ocampo, J.P. 2016. Air pollution tolerance index of selected trees in different parks of Metro Manila. Space Reposit., 27: 4.

Chauhan, S.S. 2010. Mining, development and environment: A case study of Bijo- lia Mining Area in Rajasthan, India. Journal of Human Ecology, 31: 65-72. https://doi.org/10.1080/09709274.2010.11906299

Conklin, P.L. 2001. Recent advances in the role and biosynthesis of ascorbic acid in plants. Plant Cell Environ., 24: 383-394. https://doi.org/10.1046/j.1365-3040.2001.00686.x

Dash, S.K. and Dash, A.K. 2017. Air pollution tolerance index to assess the pollution tolerance level of plant species in industrial areas. Asian J. Chem., 30(1): 991 https://doi.org/10. 14233/ajchem.2018.20991

Datta, J. and Sinha, Ray 1995. Responses of some crops to air pollution by using air pollution tolerance index. Nepal Journals Online. DOI: https://doi.org/10.3126/arj.v1i1.32449

Deepalakshmi, A.P., Ramakrishnaiah, H., Ramachandra, Y.L. and Radhika, R.N. 2013. Roadside plants as bio-indicators of urban air pollution. J. Environ. Sci. Toxicol. Food Technol., 3(3): 14. https://asset-pdf.scinapse.io/prod/2348600621/2348600621.pdf

Drava, G., Comara, L., Giordani, P. and Minganti, V. 2019. Trace elements in *plantago lanceolate L.,* a plant used for herbal and food preparations: new data and literature review. Envr. Sci. and Pollut. Res., 26: 2305-2313. DOI:10.1007/s11356-018-3740-1

Escobedo, F.J., Wanger, J.E. and Nowak, D.J. 2008. Analyzing the cost-effectiveness of Santiago, Chile's policy of using urban forests to improve air quality. J. Envr. Mngt., 86(1): 148-157. DOI: 10.1016/j.jenvman.2006.11.029

Falusi, B.A., Odedokun, O.A., Abubakar, A. and Agoh, A. 2015. Effects of dumpsites air pollution on medicinal plants' ascorbic acid and chlorophyll contents. Cogent Environ. Sci., 2: 10. http://dx.doi.org/10.1080/23311843.2016.1170585

Gallie, D.R. 2012. L-Ascorbic acid: A multifunctional molecule supporting plant growth and development. Hindawi Pub. Corp. Sci., 4: 964. http://dx.doi.org/10.1155/2013/795964

Gharge, S. and Menon, G.S. 2012. Air pollution tolerance index (APTI) of certain herbs from the site around Ambernath MIDC. Asian J. Exp. Biol. Sci., 3(3): 544.

Gholami, A., Mojiri, A. and Amini, H. 2016. Investigation of air pollution tolerance index using some plant species in the Ahvaz Region. The J. of Anml & Plnt Sci., 26(2): 476.

Giri, S., Shrivastava, D., Deshmukh, K., Dubey, P. 2013. Effect of air pollution on chlorophyll content of leaves. Current Agriculture Research Journal, 1(2): 93-98. DOI : http://dx.doi.org/10.12944/CARJ.1.2.04

Glenn, L., Su, S., Solomon, N. and Elena R. 2018. Air pollution tolerance index of selected trees in Major roadsides of Metro Manila, Philippines. Inter. Qtrly. Sci. J., 17(3): 1005-1009. https://doi.org/10.21275/v4i11.nov151452

Gonzalez, L., Gonzalez, V.M. and Reigosa, M.J. 2001. Determination of relative water content. In: Handbook of Plant Ecophysiology Techniques, Kluwer Academic Publishers, Dordrecht, The Netherlands. pp .207-212.

Gonze, M.A. and Sy, M.M. 2016. Interception of wet deposited atmospheric pollutants by herbaceous vegetation: Data review and modeling. Sci. Total Environ., 565: 49-67. doi: 10.1016/j.scitotenv.2016.04.0

Gulia, S., Shiva Nagendra, S. M., Khare, M. and Khanna, I. 2015. Urban air quality management: A review. Atmos. Pollut. Res., 6(2): 286-304. doi:10.5094/apr.2015.033

Gulliermo, M.L. and Mallapre, W.O. 2016. Comparison of air pollution tolerance indices (APTI) of selected plants in three areas in Metro Manila. DSpace Repo., 18: 31.

Irshad, M. I., Nawaz, R., Ahmad, S., Arshad, M., Rizwan, Ahmad, N., Nizami, M. and Ahmed, T. 2020. Evaluation of anticipated performance index of tree species for air pollution mitigation in Islamabad, Pakistan. J. of Envr. Sci. and Mgnt., 23(1): 50.

Kaur, M. and Nagpal, A.K. 2017. Evaluation of air pollution tolerance index and anticipated performance index of plants and their application in the development of green space along the urban areas. Environ. Sci. Poll. Res., 24(23): 18881-18895. doi:10.1007/s11356-017-9500-9

Kim, B.M., Park, J.S., Kim, S.W., Kim, H., Jeon, H., Cho, C. and Yoon, S.C. 2015. Source apportionment of PM10 mass and particulate carbon in the Kathmandu Valley, Nepal. Atmos. Envr., 123: 190-199. doi: 10.1016/j.atmosenv.2015.10.08

Krishnaveni, M. 2013. Biochemical changes in plants indicate air pollution. Inter. J. of Pharm. Pharmaceutical Sci., 5(3): 1.

Kuddus, M., Kumari, R. and Ramteke, P. W. 2011. Studies on air pollution tolerance of selected plants in Allahabad city, India. Journal of Environmental Research and Management, 2: 042-046.

Kunwar, K., Dhamala, M.K. and Rejina Maskey-Byanju, R.M. 2016. Air pollution tolerance index: An approach towards the effective green belt around Kathmandu metropolitan city, Nepal. Nepal J. Environ. Sci., 4: 28. DOI:10.3126/njes. v4i0.22721

Lakshmi, P.S., Sravanti, K.L. and Srinivas, N. 2009. Air pollution tolerance index of various plant species growing in industrial areas. Int. Biannua J. Environ. Sci., 2: 203-206.

Leghari, S.K., Akbar, A., Quasim. S., Ullah, S., Asari M., Rohali, H., Ahmed, S., Mehmood, K. and Ali, I. 2019. Estimating anticipated

performance index and air pollution tolerance index of some trees and ornamental plant species for the construction of Green Belts. Pol. J. Environ. Stud., 28(3): 1-11. DOI: https://doi.org/10.15244/pjoes/89587

Lei, Y., Duan, Y., He, D., Zhang, X., Chen, L., Li, Y., Gao, G., Tian, G. and Zheng, J. 2018. Effects of urban greenspace patterns on particulate matter pollution in Metropolitan Zhengzhou in Henan, China. Atmos. Air Qual., 9: 199. https://doi.org/10.3390/atmos9050199

Li, Y., He, N., Hou, J., Xu, L., Liu, C., Zhang, J. and Wu, X. 2018. Factors influencing leaf chlorophyll content in natural forests at the biome scale. Front. Ecol. Evol., 6: 64. doi:10.33 89/fevo.2018.00064

Liu, L., Guan, D. and Peart, M.R. 2012. The morphological structure of leaves and the dust-retaining capability of afforested plants in urban Guangzhou, South China. Environ. Sci. Pollut. Res., 19(8): 3440-3449. doi:10.1007/s11356-012-0876-2

Lohe, R.N., Tyagi, B., Singh, V., Tyagi, P.K., Khanna, D.R. and Bhutiani, R. 2015. A comparative study for air pollution tolerance index of some terrestrial plant species. Glob. J. Environ. Sci. and Manag., 1(4): 315-324.

Mahecha, G.S., Bamniya, B.R., Nair, N. and Saini, N. 2013. Air pollution tolerance index of certain plant species-A study of Madri industrial area, Udaipur (Raj.), India. Inter. J. Innov. Res. Sci. Engr. Tech., 2 (12): 7928.

Margitai, Z., Simon, E., Fábián, I. and Braun, M. 2016. Inorganic chemical composition of dust deposited on oleander (Nerium oleander L.) leaves. Air Qlty. Atmos. Health, 10(3): 339-347. doi:10.1007/s11869-016-0416-1

Molnar, V.E., Tozser, D., Szabo, S., Tothmeresz, B. and Simon, E. 2020. Use leaves as a bioindicator to assess air pollution based on composite proxy measure, dust amount, and elemental concentration of metals. Plants, 9: 9. doi:10.3390/plants9121743

Mondal, D., Gupta, S. and Datta, J.K. 2011. Anticipated performance index of some tree species considered for green belt development in an urban area. Inter. Res. J. Plant Sci., 2(4): 99-106. http://www.interesjournals.org/IRJPS

Nadgórska-Socha, A., Kandziora-Ciupa, M., Trzęsicki, M. and Barczyk, G. 2017. Air pollution tolerance index and heavy metal bioaccumulation in selected plant species from urban biotopes. Chemosphere, 183: 471-482. doi: 10.1016/j.chemosphere.2017.05.128

Nakazato, R.K., Rinaldi, M.S. and Domingos, M. 2016. Tropical trees: are they good alternatives for monitoring the atmospheric level of potentially toxic elements near the Brazilian Atlantic rainforest? Ecotox. Environ. Safety, 134(1): 72-79. https://doi.org/10.1016/j.ecoenv.2016.08.013

Navarrete, I.A., Gabiana, C.C., Dumo, J.A., Salmo III, S.G., Guzman, M.G., Valera, N.S. and Espiritu, E.Q. 2017. Heavy metal concentrations in soils and vegetation in urban areas of Quezon City, Philippines. Environ. Monit. Assess., 189: 145. DOI 10.1007/s10661-017-5849-y

Nikolaeva, M.K., Maevskaya, S.N., Shugaev, A.G. and Bukhov, N.G. 2010. Effect of drought on chlorophyll content and antioxidant enzyme activities in leaves of three wheat cultivars varying in productivity. USSR J. Plant Physiol., 57(1): 87-95. doi:10.1134/s1021443710010127

Ninave, S. Y., Chaudhari, P. R., Gajghate, D. G. and Tarar, J. T. 2001. Foliar. biochemical features of plants as indicators of air pollution. Bulletin of Environmental Contamination and Toxicology, 67: 133-140 (2001).

Notman, R., Noro, M., O'Malley, B. and Anwar, J. 2006. Molecular basis for dimethylsulfoxide action on lipid membranes. J. Amer. Chem. Soc., 128(43): 13982-13983. doi:10.1021/ja063363t

Ogboru, R.O., Bobadoye, A.O., Ishola, B.F. and Oke, R.A. 2021. Biomonitoring of air pollution for selected plant species along Ondo-IFE Road and Oluwa forest reserve. J. Forest. Res., 18(4): 50-59. https://www.researchgate.net/publication/357476943

Ogunkunle, C.O., Suleiman, L.B., Oyedeji, S., Awotoye, O. and Fatoba, P.O. 2014. Assessing The Air Pollution Tolerance Index and Anticipated Performance Index of Some Tree Species for Biomonitoring Environmental Health. Springer Science+Business Media, NY. DOI 10.1007/s10457-014-9781-7

Ogunrotimi, D.G., Adereti, F.K., Eludoyin, E.O. and Awotoye, O. 2017. Urban air pollution control: selection of trees for ecological monitoring using anticipated performance indices in a medium-sized urban area in Southwest Nigeria. Interdiscip. Environ. Rev., 18(1): 449. DOI:10.1504/IER.2017.10005053

Pandey, A.K., Pandey, M. and Tripathi, B.D. 2015. Air pollution tolerance index of climber plant species to develop vertical greenery systems in a polluted tropical city. Landsc. Urban Plan., 144: 119-127. doi: 10.1016/j.landurbplan.2015.08.014

Pandey, A.K., Pandey, M. and Tripathi, B.D. 2016. Assess some plants' air pollution tolerance index to develop vertical gardens near street canyons of a polluted tropical city. Ecotox. Environ. Sfty., 134: 358-364. doi: 10.1016/j.ecoenv.2015.08.028

Rahul, J. and Jain, M.K. 2014. An investigation into the impact of particulate matter on vegetation along the national highway: Review. Res. J. Environ. Sci., 8(7): 356-372. DOI: 10.3923/rjes.2014.356.372

Rai, P.K., Panda, L.S., Chutia, B.M. and Singh, M.M. 2013. Comparative assessment of air pollution tolerance index (APTI) in the industrial (Rourkela) and non-industrial area (Aizawl) of India: An ecomanagement approach. Afr. J. Environ. Sci. Tech., 7(10): 944-945. DOI: 10.5897/AJEST2013.1532

Ram, S., Majumder, S., Chaudhuri, P., Chanda, S., Santra, S.C., Chakraborty, A. and Sudarshan, M. 2015. A review on air pollution monitoring and management using plants with special reference to foliar dust adsorption and physiological stress responses. Crit. Rev. Environ. Sci. Tech., 11: 125. DOI:10.1080/10643389.2015.1046775

Rojas, A., Moreno, L., Melgarejo, L.M. and Rodriguez, M.A. 2012. Physiological response of gmelina (Gmelina arborea Roxb.) to hydric conditions of the Colombian Caribbean. Agron. Colomb., 30(1): 58. http://www.scielo.org.co/pdf/agc/v30n1/v30n1a08.pdf

Roy, A., Bhattacharya, T. and Kumari, M. 2020. Air pollution tolerance, metal accumulation, and dust capturing capacity of common tropical trees in commercial and industrial sites. Sci. Total Environ., 13: 622. doi: 10.1016/j.scitotenv.2020.137622

Sachan, S., Verma, S., Kumar, S. and Kumar, A. 2019. Morphological, physiological, and biochemical performance of Tectona grandis and Gmelina arborea under drought stress conditions. Inter. J. Chem. Stud., 8(1): 1313. DOI: https://doi.org/10.22271/chemi.2020.v8.i1r.8437

Sahu, C., Basti, S. and Sahu, S.K. 2020. Air pollution tolerance index (APTI) and expected performance index (EPI) of trees in Sambalpur Town of India. SN Appl. Sci., 6: 51. https://doi.org/10.1007/s42452-020-3120-6

Salimi, A. and Aghdash, H.D. 2019. Air pollution tolerance index (APTI) of three tree species of Morus alba L., Ailanthus altissima (Mill.) Swingle, and Salix babylonica L. in different areas of Tehran City. J. Environ. Stud., 45(3): 5. DOI:10.22059/JES.2019.259 202.1007685

Selmi, W., Weber, C., Rivière, E., Blond, N., Mehdi, L. and Nowak, D. 2016. Air pollution removal by trees in public green spaces in Strasbourg City, France. Urban Forest Urban Green, 17: 192-201. https://doi.org/10.1016/j.ufug.2016.04.010

Shafiq, M. and Iqbal, M. 2012. Effect of auto exhaust emission on germination and seedling growth of an important arid tree Cassia Siamea Lamk. Emirates J. of Food Agri., 24: 234-242. https://www.ejfa.me/index.php/journal/article/view/865

Simon, E., Baranyai, E., Braun, M., Cserháti, C., Fábián, I. and Tóthmérész, B. 2014. Elemental concentrations in deposited dust on leaves along an urbanization gradient. Sci. Total Environ. 490: 514-520. https://doi.org/10.1016/j.scitotenv.2014.05.028

Singh, V and Chauhan, D. 2014. Phytochemical evaluation of aqueous and ethanolic extract of neem leaves (Azadirachta indica); Indo American J. of Pharm. Res., 4: 5943-5948.

Su, G.S., Francis, N., Solomon, R. and Ragragio, E.M. 2018. Air pollution tolerance index of selected trees in major roadsides of Metro Manila, Philippines. Nat. Environ. and Pollut. Tech., 17(3): 1005.

Swami, A. and Chauhan, D. 2015. Impact of air pollution induced by automobile exhaust pollution on air pollution tolerance index (APTI) on few species of plants. Inter. J. Sci. Res., 4: 342-343. DOI:10.15373/22778179#sthash.vF0KMdSC.dpuf

Tak, A. and Kakde, U. 2017. Assessment of air pollution tolerance index of plants: A comparative study. Inter. J. of Pharmaceutical Sc., 8(7): 84. DOI:10.22159/ijpps.2017v9i7.18447

Ter, S., Chettri, M.K. and Shakya, K. 2020. Air pollution tolerance index of some tree species of Pashupati and Budhanilkantha Area, Kathmandu. Amrit Res. J., 1(1): 21-22. DOI: https://doi.org/10.3126/arj.v1i1.32449

Turner, N. 1981. Techniques and experimental approaches for the measurement of plant water status. Plant and Soil. University of Western Australia. DOI: 10.1007/BF02180062

Ugulu, I., Durkan, N., and Dogan, Y. 2015. Heavy metal contents of Malva Sylvestris are sold as edible greens in the local markets of Izmir. Ekoloji, 24(96): 13-25. doi:10.5053/ekoloji.2015.01

Uka, U.N. and Chukwuka, K.S. 2014. Assessment of pollution tolerance index of selected plant species in Abakaliki Metropolis, South Eastern, Nigeria. Environ. Sci. Indian J., 9(3): 96.

Viradia, S., Misan, V. and Kaneria, M. 2020. Comparative assessment of air pollution tolerance index (APTI) of selected plants from two different industrial sites of Rajkot. Proceed. Conf. Innov. Biol. Sci., 16: 112. http://dx.doi.org/10.2139/ssrn.3559975

Wang, H., Shi, H. and Li, Y. 2011. Leaf dust capturing capacity of urban greening plant species in relation to leaf micromorphology. Inter. Symp. on Wtr. Resour. Environ. Protect., 7: 589. doi:10.1109/iswrep.2011.5893701

Wolf, M.J., Emerson, J.., Esty, D.C., de Sherbinin, A. and Wendling, Z.A. 2022. Environmental Performance Index. Yale Center for Environment Law & Policy, New Haven, CT.

Xie, X., Semanjski, I., Gautama, S., Tsiligianni, E., Deligiannis, N., Rajan, R.T. and Pasveer, F., Philips, W. 2017. A review of urban air pollution monitoring and exposure assessment methods. Inter. J. of Geo-Infor., 6: 389. doi:10.3390/ijgi6120389

Yousaf, M., Mandiwana, K.L., Baig, K.S. and Lu, J. 2020. Evaluation of Acer Rubrum Tree bark as a bioindicator of atmospheric heavy metal pollution in Toronto, Canada. Wtr. Air Soil Pollut., 231: 382. https://doi.org/10.1007/s11270-020-04758-w

Original Research Paper   https://doi.org/10.46488/NEPT.2023.v22i03.021   **Open Access Journal**

Plant Growth Promoting Efficacy of Endophytic Fungi Isolated from the Terrestrial Plants of North India

Urvasha Patyal* (iD)**, Vikas Kumar*†** (iD)**, Manoj Singh* and Kulbir Singh****

*Department of Bio-Sciences and Technology, MMEC, Maharishi Markandeshwar (Deemed to be University), Mullana (Ambala), 133207, Haryana, India
**Department of Civil Engineering, MMEC, Maharishi Markandeshwar (Deemed to be University), Mullana (Ambala), 133207, Haryana, India
†Corresponding author: Vikas Kumar; vmeashi@gmail.com

ABSTRACT

Enhanced crop health, which is crucial for sustainable agriculture, is facilitated by a unique endophyte or endophytic community that is frequently linked to a variety of crops. Plant growth-promoting (PGP) characteristics of endophytes can directly or indirectly boost crop growth. Endophytic fungi have been proven to create a high percentage of new compounds, making them a particularly potential source of physiologically active chemicals. In this study, we have isolated two endophytic isolates, *i.e., Paecilomyces* sp. (Isolate AT1) and *Aspergillus flavus* (Isolate AT3), from different host plants, namely *Melaleuca citrine* and *Carica papaya*. These endophytes have shown significant plant growth-promoting potential toward different assays such as IAA production, phosphate solubilization, amylase production, cellulose-degrading assay, and ammonia production. These endophytic fungi also exhibit visible antimicrobial action towards selected crop pathogenic fungi (*Aspergillus* sp. and *Penicillium* sp.). Additionally, these fungal strains are reported for the first time from these plants, as we have found no reports in the literature. The research aims to explore the growth-promoting efficacy of endophytic fungi to boost plant growth.

INTRODUCTION

Endophytes that promote plant growth are symbiotic organisms (fungi and bacteria) that the host plant uses to protect itself from herbivores in a secretive manner. These are common microsporic ascomycetes that live inside the healthy tissues of living plants for the duration of their lives and are found below the layer of epidermal cells in those tissues (Mengistu 2020). It offers the plant several advantages, including the ability to absorb vital nutrients and defense against predatory insects, birds, and animals. Endophytes are ubiquitous and distinct from all categories of plant species in an environment, from huge trees to seagrasses. An estimated 300,000 host plant species were naturally distributed among the endophytic fungi in the temperate region and tropical rainforest (Strobel & Daisy 2003). The endophytic fungus can create a large range of novel bioactive secondary metabolites, which are employed in industries to manufacture a variety of natural goods (Sharma et al. 2016).

Endophytes are a good source of bioactive substances that improve the nutritional value of the host plant and increase resistance to pests, diseases, and physical stress (Gouda et al. 2016). These substances (alkaloids, flavonoids, terpenoids, steroids, phenols, phenolic acids, tannins, and peptides), which act as enzymes and exhibit antimicrobial and anti-malarial activities, can be used in the food, agricultural, and pharmaceutical industries (Tungmunnithum et al. 2018). *Taxomyces andrenae*, an endophytic fungus that belongs to the family of hyphomycetes, produces the anticancer drug taxol (Stierle et al. 1993). Plant tissues get inhabited by PGPE (plant growth-promoting endophytes) and exhibit an intimate connection within plant tissues, which improves the activities of enzymes and the flow of nutrients, but this much-appropriate hormone distribution encourages plant development (Hassan 2017). Endophytes have the dynamic ability to activate insoluble phosphate and also feed their host plant with the right amount of nitrogen (Mehta et al. 2019).

In this work, we have selected nine terrestrial plants of the north Indian regions for the isolation of endophytic fungi. We have isolated several different fungal strains from

ORCID details of the authors:

Urvasha Patyal: https://orcid.org/0000-0001-5249-0601
Vikas Kumar: https://orcid.org/0000-0002-6044-3239

these plants. These strains were restricted to the host plants' healthy tissues and did not produce any disease symptoms. When checked for their plant growth-promoting potential, two out of the nine strains exhibited positive results in different assays. The fungal morphology and molecular identification were determined. For molecular characterization, the DNA of these strains was isolated using the CTAB method and then subjected to 18S rRNA sequencing by the Sanger dideoxy method. The obtained sequence was analyzed, and a consensus sequence was prepared, which was then subjected to BLAST analysis and phylogenetic studies (Kumar et al. 2014, Kumar et al. 2017). The consensus sequence was submitted to the National Center for Biotechnology Information (NCBI). The selected isolates were tested against plant pathogens. In this assay, some of them showed a positive antimicrobial response. Also, these two isolates were further checked for their potential to promote plant growth in two different beans, i.e., *Vigna radiata* and *Vigna mungo*. Various growth parameters were checked for these selected beans using the seed germination assay. It is evident from the results that fungal isolates have promoted plant growth in both selected beans.

MATERIALS AND METHODS

To evaluate the plant growth promotion potential of the endophytic fungal isolates, various assays were performed to select the potent isolates. The selected fungal isolates were further identified by microscopic characterization as well as molecular techniques.

Collection of plant parts and isolation technique of endophytic fungi: The fresh, healthy, or disease-free plant parts were collected from *Melaleuca citrina, Phyllanthus emblica, Terminalia arjuna, Eucalyptus globulus, Psidium guajava, Azadirachta indica, Acacia nilotica, Tagetes erecta*, and *Carica papaya*. These plant parts were carefully excised with a sterile scalpel, kept inside sterile poly bags, and brought to the laboratory for storage at 4°C. All plant parts were cut into small pieces (0.5–1.0 cm) and thoroughly washed before processing under running tap water. After surface sterilization, potato dextrose agar medium supplemented with streptomycin was used to culture the fungal isolate and incubated properly at 28±2°C to complete their growth cycle (Kumar et al. 2016).

In-vitro **testing for plant growth promotion by endophytic isolates:** The isolated endophytes were subjected to different plant growth promoting parameters.

Phosphate solubilizing assay: To check the phosphate solubilizing capacity, each isolated fungal culture was inoculated on the Pikovskayas agar medium plates separately and incubated at 25-28°C for 48-72 hours (Talukdar &Tayung 2019).

Indole-3-acetic acid (IAA) synthesis test: Fungal cultures were dipped into LB broth conical flasks and incubated at 25°C in a BOD shaker for 48 hours. Add 1-2 mL of Salkowski's reagent to the supernatant of the fungal culture and keep it in the dark at room temperature for 30 minutes (Bric et al. 1991). A change in the color of the media indicates positive results.

Amylase activity: Fungal cultures were cut into small discs utilizing a sterilized cork borer and placed over the medium plates (Glucose- 0.5g, Yeast extract- 0.05g, peptone- 0.25g, agar- 8g, and pH-6) supplemented with 1% soluble starch, and incubated at 25–28°C for 5 days. After incubation, cultured plates were flooded with 1% iodine and 2% potassium iodide (Hankin & Anagnostakis 1975). A change in the color of the medium from yellow to pink indicates positive results.

Cellulose degrading assay: To select a fungus for cellulolytic activity, fungal isolates were grown in a carboxymethylcellulose (CMC) agar medium. A disc of 8 mm fungal culture was used to inoculate the plates. The test plates were incubated at 25°C for 5–7 days. To visualize the hydrolysis zones, the plates were flooded with an aqueous solution of 0.1% Congo-red (1 mg/mL) for 15 min and washed with 1 M NaCl. Cellulolytic organisms produced a clear zone around the colonies because of the digestion of carboxymethylcellulose (CMC) (Dar et al. 2013).

Ammonia production activity: Peptone medium (broth) was inoculated with different fungal culture discs separately and incubated at 27°C for 48–72 hours. After incubation, 0.5 mL of Nessler's reagent was added individually over the fungal growth in each conical flask (Szilagyi-Zecchinet al. 2014). The change from brown to yellow colour was a positive test for ammonia production.

Identification of Endophytic Fungi

Morphological Identification of Fungi: Morphological identification of all isolated fungal cultures was done by culturing each culture on PDA medium plates (without streptomycin) for seven days and continuously observing the growth appearance on both sides of the culture plates (top and bottom). Based on the standard taxonomic key, we were able to identify each culture according to its color, the diameter of the fungal colony, texture, morphology, and dimensions of conidia and hypha (Barnett & Hunter 1998).

Microscopic identification: By using the tease-mount method, microscopic slides of each isolated fungal culture were prepared using lactophenol cotton blue reagent for tentative recognition, and each slide was observed under a compound microscope. According to the characteristics of culture, the formation of mycelium and spores helps us

identify all unknown isolated endophytic fungi (Aggarwal & Hasija 1986).

Molecular Identification: Using the 18S rRNA gene sequencing method, endophytic fungi were molecularly identified. The DNA extraction was carried out by employing the cetyl trimethyl ammonium bromide (CTAB) method (O'Donnell et al. 1997). The pure DNA extracted was amplified by PCR using universal and degenerate primers. The PCR product was then subjected to gel electrophoresis to check the purity of the DNA, followed by analysis using Sanger's dideoxy method to obtain a DNA sequence (Cubero 1999). The forward and reverse DNA sequences of every sample were subjected to the National Centre for Biotechnology Information Basic Local Alignment Search Tool (NCBI BLAST) algorithm for identification, and the phylogenetic tree was also constructed using NCBI BLAST online (https://blast.ncbi.nlm.nih.gov/Blast.cgi). All the identified 18S rRNA sequences were submitted to GenBank in fast-all format, and accession numbers for the same were obtained. The identification was confirmed by observing the morphological characteristics through microscopic studies of the spores, hyphae, and colony.

Evaluation for Antagonistic Activity of Isolated Endophytic Strains Against Crop Diseases Causing Fungi

To check the antimicrobial activity of each fungal isolate, test organisms (*Penicillium* sp. and *Aspergillus* sp.) were taken from the fresh plate and strewn around the fungal culture discs in PDA plates and incubated at 25°C for 24-48 hours (Huang et al. 2000). Antagonism between both the isolated endophytic fungi and the fungal pathogen was assessed on an individual basis. The testing was carried out in Petri dishes using PDA medium. To remove excess water from the agar surface, 20 mL of melted medium (40–45°C) was placed into sterile Petri plates, cooled, and the plates were left inverted for 24 hours. A mycelial disc of 8 mm in diameter from the actively growing edges of a 4-5 day old culture of a plant pathogen was brought adjacent to the media of the Petri plate to test resistance. An identical 8 mm-diameter mycelial disc from an actively developing culture of isolated strains (to be evaluated for antibacterial activity) was placed next to the pathogenic fungus after a 24-hour interval. At 25°C, the cultures were incubated. Every 24 hours, observations were taken to investigate the antimicrobial activity.

Preparation of the Formulation from Potent Strains and Evaluation of Plant Growth Promoting Efficacy

To confirm the efficacy of seed coating with endophytic fungi to boost the emergence and plant growth of two pulse crops, *Vigna radiata* and *Vigna mungo*, the experiment was first carried out in a growth chamber. Healthy, disease-free seeds were selected and sterilized (Khatun et al. 2008). By covering the culture with sterile saline containing 0.01% (v/v) Tween (BDH) and spreading the spores with a sterile glass spreader, it is possible to collect spores from lawn cultures of the organism on potato dextrose agar media. The spore solution was then filtered through sterile absorbent cotton wool plugs in a row to get rid of any hyphal fragments that might have been present (Jaber & Enkerli 2016). The spore suspension was then transferred into spray bottles. The sterile filter paper was transferred to autoclaved Petri plates, and seeds of two different samples of crop plants were put in the plates in triplicate. The seeds were sprayed with the fungus suspension, and growth conditions of a 12-hour light cycle with corresponding 22°C light/ 18°C darkness and 65% moisture content were provided. The seeds were watered daily, and root and shoot growth were routinely analyzed.

RESULTS

Isolation and Identification of Endophytic Fungi

Various parts were used to isolate fungus strains (stem, root, leaf, bud) of various terrestrial plants (*Melaleuca citrina*, *Phyllanthus emblica*, *Terminalia arjuna*, *Eucalyptus globulus*, *Psidium guajava*, *Azadirachta indica*, *Acacia nilotica*, *Tagetes erecta*, *Carica Papaya*) (Fig. 1). Nine endophytic strains were isolated from all the selected plants.

Identification of Endophytic Fungi

Morphological and microscopic identification: According to the standard protocol of (Barnett & Hunter 1998), fungal strains were characterized based on their microscopical and cultural properties (Fig. 2). The fungal strains which were tested positive for different plant growth-promoting activities were subjected to molecular identification.

Paecilomyces sp. Isolate AT1 was characterized as endophyte *Paecilomyces* sp. isolated from the host plant *Melaleuca citrina*. The cultural characteristics include fast growth, powdery, gold, green-gold, yellow-brown, tan colored growth. Phialides are bulbous at their bottoms and have penicillate crowns. They eventually taper into a long, slender neck. In basipetal continuation from the phialides, long, dry chains of single-celled, hyaline to black, smooth or rough, round to fusid conidia are formed.

Aspergillus flavus Isolate AT3 was characterized as endophyte *Aspergillus flavus* isolated from the host plant *Carica papaya*. The macroscopic characteristics include the white colony changing to greenish, and the central region showing dark greenish growth. The microscopic
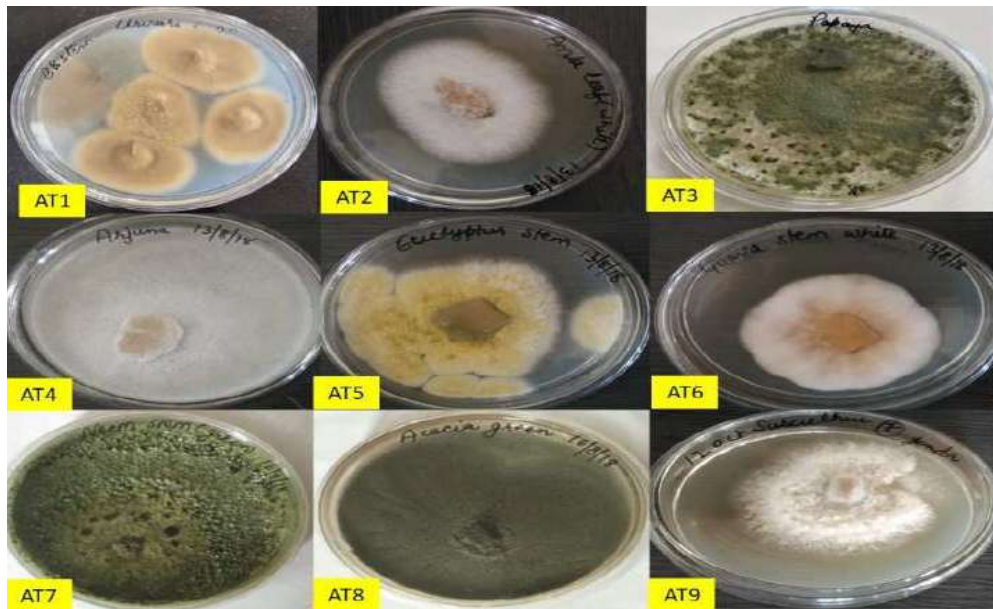
Fig. 1: Endophytic strains isolated from different terrestrial plants.

Fig. 2: Morphology (B, E) (colony appearance) and Microcopy (C, F) (conidia, hypha) view of isolated endophytic strains from different host plants (A- *Melaleuca citrina*, D- *Carica papaya*).

characteristics include a short and columnar conidial head, smooth and brown-colored stripes, biseriatephialides, and globose, smooth conidia.

Molecular Identification

Using the 18S rRNA gene sequencing approach, endophytic fungi were molecularly identified. *Paecilomyces* sp. (Isolate AT1) and *Aspergillus flavus* (Isolate AT3), two endophytic fungi, were amplified and sequenced using universal primers for the 18S rRNA gene. Using BLAST to analyze the sequence similarity of the resulting sequencing products,

it was determined that the isolates were *Paecilomyces* sp. (513 bp) and *Aspergillus flavus* (549 bp). The following accession numbers represent the fungal pathogens' gene sequences that have been submitted to NCBI (Table 1). The phylogenetic trees were constructed to represent the evolutionary relationship of isolated organisms with different biological organisms (Fig. 3).

Screening of Endophytic Fungi for Plant Growth Promoting Activities (PGPA)

Isolated endophytic fungal cultures were screened to

Table 1: Detail about the fungal isolates with their accession number and GenBank submission name.

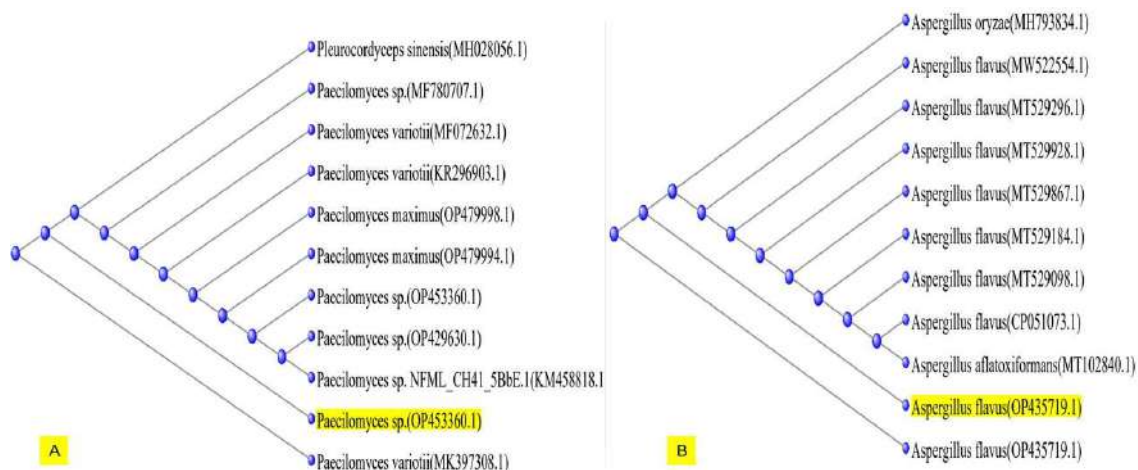| S. No.	Fungal Fugus	Host plant	Plant Part	Accession number	GenBank submission name
1.	*Paecilomyces* sp. (Isolate UP1)	*Melaleuca citrina*	Stem	OP453360	*Paecilomyces* sp. Isolate AT1
2.	*Aspergillus flavus* (Isolate UP3)	*Carica papaya*	Leaf	OP435719	*Aspergillus flavus* Isolate AT3

Fig. 3: Phylogenetic analysis of endophytic isolates (A) *Melaleuca citrine* (B) *Carica papaya* with related genera.

determine the various plant growth-promoting activities (Phosphate solubilizing activity, IAA synthesis test, amylase production activity, cellulolytic activity, HCN production activity, ammonia production activity) and the results are depicted in Table 2. *Melaleuca citrine* (Isolate AT1) and *Carica papaya* (AT3) showed highly positive results in different plant growth-promoting assays (Fig. 4).

Screening of Isolated Fungal Cultures for Antagonistic Activity

Two fungal endophytes (Isolates AT1 and AT3) were selected which showed highly positive plant growth-promoting activities and were then subjected to antimicrobial assessment against various test organisms (fungal plant pathogens) (Fig. 5). As a result, isolates AT1 and AT3

exhibited positive antagonistic response against *Aspergillus* sp. and regarding the other test organism, i.e. *Penicillium* sp, isolate AT3 was somewhere seen inhibiting its growth (Fig. 6).

Preparation of the Formulation from Potent Strains and Evaluation of Plant Growth Promoting Efficacy

The selected endophytes were screened for their ability to colonize two preferred host plant species, namely Mung bean (*Vigna radiata*) and Urad bean (*Vigna Mungo*) through seed inoculation. The fungal elicitors namely Isolate AT1 and AT3 showed a positive growth induction in plants in terms of the radicle length and plumule length elongation along with an increased biomass rate in both cases when compared to the control culture. The growth rates were compared with the

Table 2: Comparison of PGP assay of different endophytic strains.

Isolate	Phosphate solubilizing activity	IAA production	Amylase production activity	Cellulolytic activity	Ammonia production
AT1	positive	positive	positive	positive	negative
AT2	negative	positive	negative	negative	negative
AT3	positive	positive	positive	positive	positive
AT4	negative	positive	negative	negative	positive
AT5	negative	positive	negative	positive	positive
AT6	negative	negative	negative	positive	negative
AT7	positive	positive	negative	negative	negative
AT8	positive	negative	negative	negative	positive
AT9	positive	negative	negative	negative	positive
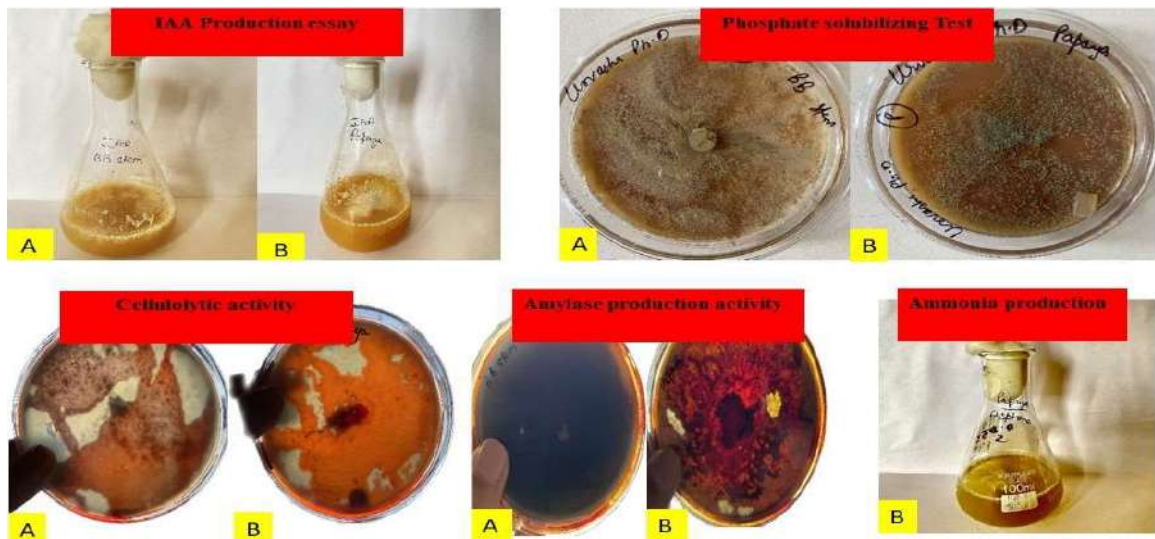
Fig. 4: Positive Plant Growth promoting activities by Endophytes isolated from (A) *Melaleuca citrine;* (B) *Carica papaya*.

Fig. 5: Plant pathogens (A- *Aspergillus* sp., B-*Penicillium* sp.).
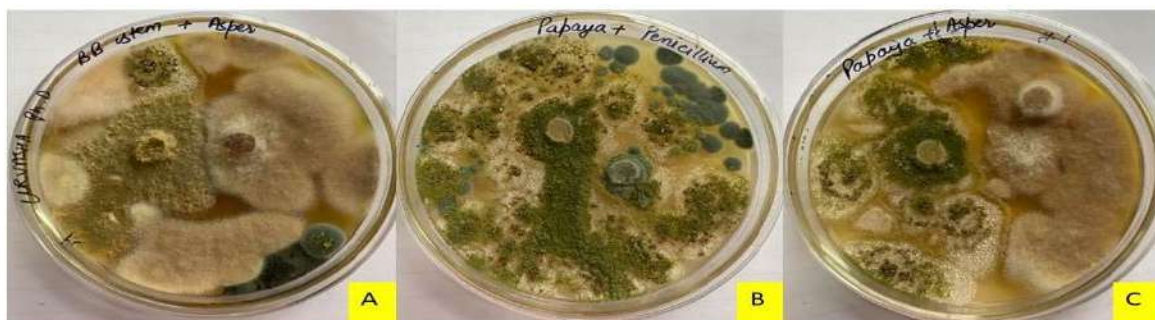
Fig. 6: Endophytes showing antimicrobial activity against test organisms.

help of different graphs. Another component to determine the seed quality was testified by calculating the seed vigor index.

Effect of Culture Supernatant on Mung Bean and Urad Bean Germination

A seed germination essay was carried out and seeds germinated each day were recorded for up to 5 days. The experiment was performed in triplicates. The seeds of *Vigna Radiata* and *Vigna mungo* exhibited a high germination rate when treated with endophytic isolates AT1 and AT3 as compared to the control sample which was treated with water (Fig. 7).

Effect of Culture Supernatant on Growth of Mung Bean (*Vigna radiata*) Plants

Growth promotion was studied using a 15-day plant growth
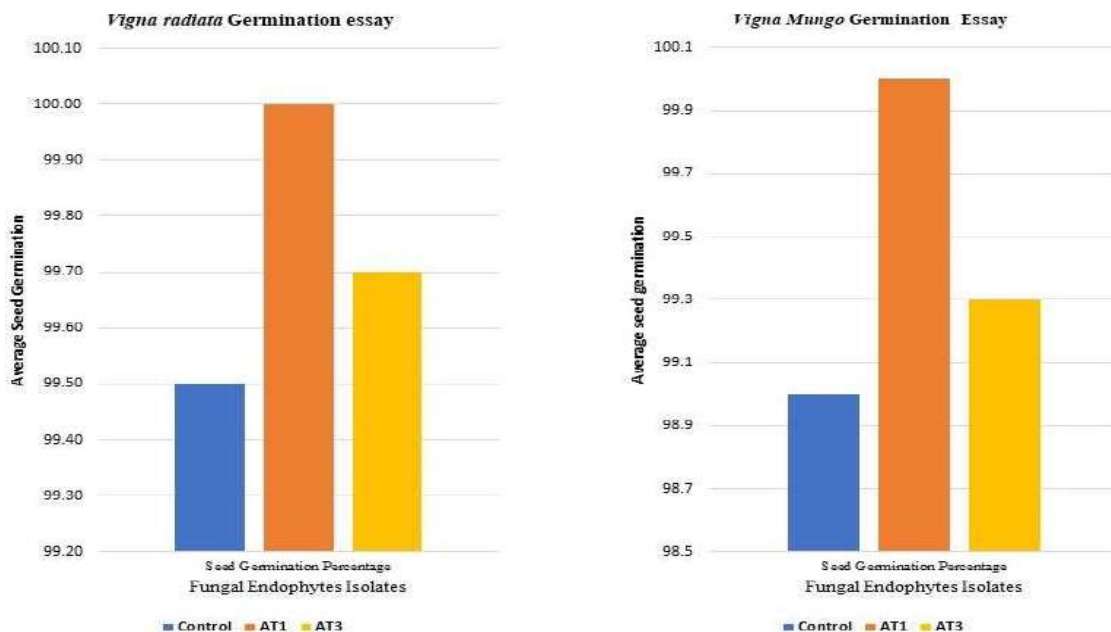
Fig. 7: Seed Germination percentage essay of *Vigna radiata* and *Vigna mungo*.

assay. The average fresh weight of the seedlings was calculated as 3.612 g for Control C, 5.213 g for Isolate AT1, and 4.055 g for Isolate AT3. The average dry weight of the seedlings was calculated as 0.198 g for Control C, 0.213 g for Isolate AT1, and 0.215 g for Isolate AT3. The seed vigor index was calculated to be 1582.05 for Control C, 1840 for isolate AT1, and 2811.54 for isolate AT3. Root and shoot lengths, along with the average seedling length of treated plants, were recorded and are depicted in Fig. 8. The inoculation of *Vigna radiate* seeds with endophytes showed

a variable change in the lengths of the plumule and radicle as compared to the control sample C.

Effect of Culture Supernatant on Growth of Urad Bean (*Vigna mungo*) Plants

Growth promotion was studied using a 15-day plant growth assay. The average fresh weight of the seedlings was calculated as 3.883 g for Control C, 7.210 g for Isolate AT1, and 6.148 g for Isolate AT3. The average dry weight of the seedlings was calculated as 0.197 g for Control C,
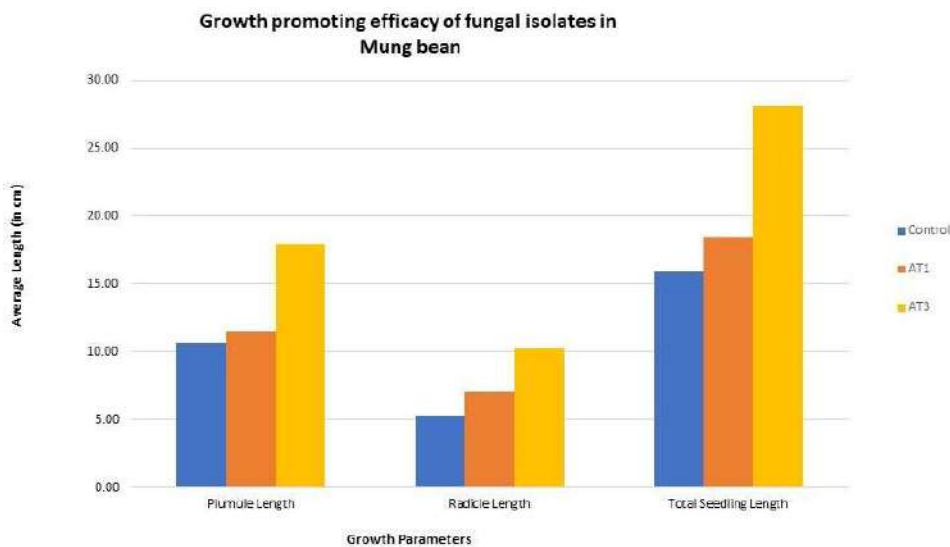
Fig. 8: Effect of Supernatent on Root and shoot lengths of *Vigna Radiata*.

0.208 g for Isolate AT1, and 0.291 g for Isolate AT3. The seed vigor index was calculated to be 1732.5 for Control C, 2340 for isolate AT1, and 2392.13 for Isolate AT3. Root and shoot lengths, along with the average seedling length of treated plants, were recorded and are depicted in Fig. 9. The inoculation of *Vigna mungo* seeds with endophytes showed a variable change in the lengths of the plumule and radicle as compared to control sample C.

Upon seed inoculation with fungal elicitors, in comparison to control it was found that isolates AT1 and AT3 boosted plant growth by initiating root and shoot length and can be noticed visibly (Fig. 10).

DISCUSSION

In this study, according to our research, the isolated fungal isolates *Paecilomyces* sp. and *Aspergillus flavus* have not previously been reported in the host plants *Melaleuca citrina* and *Carica papaya*. The plant growth-promoting assays of fungal endophytes isolated from host plants *Melaleuca citrina* and *Carica papaya* were analyzed to compare

Fig. 9: Effect of the supernatant on root and shoot lengths of *Vigna mungo*.

Fig. 10: Comparison of growth shown by crop beans A (*Vigna radiata*), B (*Vigna mungo*) when inoculated with Control (C) and endophytic fungi (isolates AT1 and AT3).

and evaluate their effects on root and shoot growth. The isolates' indirect plant-promoting actions, such as phosphate mobilization, were also investigated. Out of the nine strains, it is important to emphasize that two strains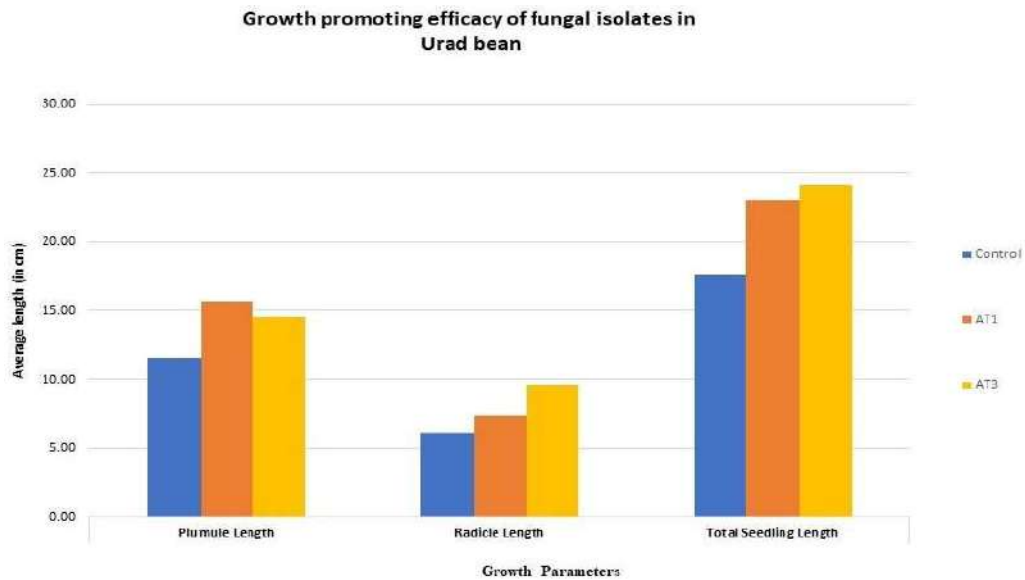 were found to show positive results in other plant growth-promoting assays, *i.e.*, the Indole-3-Acetic Acid production assay, the cellulose degradation essay, and the ammonia and amylase production essays. The strains were found in various plant parts, such as stems (Isolate AT1) and leaves (Isolate AT3). To further confirm the efficiency of these isolates, they were subjected to an antimicrobial essay against various test organisms (*Aspergillus* sp. and *Penicillium* sp.) and surprisingly showed positive results by suppressing the growth. Also, in preparing the formulation of these endophytes, seeds of *Vigna radiata* and *Vigna mungo* were inoculated with the preparation, and it was confirmed by the results that these endophytes have an important role in visibly enhancing the growth of plants. Isolates AT1 and AT3 boosted plant growth remarkably as compared to controlled culture conditions.

Our research added new knowledge to the area and helped researchers better grasp how fungal endophytes influence plant growth. However, because of how complicated these parameters' effects are, it is necessary to further examine them using a variety of methods, particularly if field applications are to be taken into account.

CONCLUSION

According to the current study, various putative fungal endophytes can find an ecological niche in bottle brush and papaya plants. These microorganisms' activities that encourage plant growth help the host plant adapt to stressful situations. The results of this study encourage us to carry out more research on the chosen fungal endophytes.

REFERENCES

Aggarwal, G.P. and Hasija, S.K. 1986. Microorganisms in the laboratory: a laboratory guide of Mycology, Microbiology and Plant Pathology. Print House, Lucknow, Uttar Pradesh, India.

Barnett, H.L. and Hunter, B.B. 1998. Illustrated Genera of Imperfect Fungi. APS press. St. Paul Minnesota, USA.

Bric, J.M., Bostock, R.M. and Silverstone, S.E. 1991. RapidIn Situassay for indole acetic acid production by bacteria immobilized on a nitrocellulose membrane. Appl. Environ. Microbiol., 57(2): 535-538.

Cubero, O.F., Crespo, A., Fatehi, J. and Bridge, P.D. 1999. DNA extraction and PCR amplification methods suitable for fresh, herbarium-stored, lichenized and other fungi. Pl. Syst. Evol., 216: 243-249. https://doi.org/10.1007/BF01084401

Dar, R.A., Shahnawaz, M., Sangale, M.K., Ade, A.B., Rather, S.A. and Qazi, P.H. 2013. Isolation, purification and characterization of carboxymethyl cellulase (CMCase) from endophytic *Fusarium oxysporum* producing podophyllotoxin. Adv. Enzym. Res., 1(4): 91-96.

Gouda, S., Das, G., Sen, S.K., Shin, H.S. and Patra, J.K. 2016. Endophytes: a treasure house of bioactive compounds of medicinal importance. Front. Microbiol., 7: 1538. doi: 10.3389/fmicb.2016.01538

Hankin, L. and Anagnostakis, S.L. 1975. The use of solid media for detection of enzyme production by fungi. Mycologia, 67(3): 597-607.

Hassan, S.E.D. 2017. Plant growth-promoting activities for bacterial and fungal endophytes isolated from medicinal plant of *Teucrium polium* L. J. Advanced Res., 8(6): 687-695.

Huang, X., Xie, W. and Gong, Z. 2000. Characteristics and antifungal activity of a chitin binding protein from Ginkgo biloba. FEBS Letters, 478(1-2): 123-126.

Jaber, L. R. and Enkerli, J. 2016. Effect of seed treatment duration on growth and colonization of *Vicia faba* by endophytic *Beauveria bassiana* and *Metarhizium brunneum*. Biological Control, 103: 187-195.

Khatun, M.K., Haque, M.S., Islam, S. and Nasiruddin, K.M. 2008. In vitro regeneration of mungbean (*Vigna radiata* L.) from different explants. Progressive Agriculture, 19(2): 13-19.

Kumar, V., Aneja, K.R., Aggarwal, N. and Kaur, M. 2014. First report of *Cochliobolus spicifer* causing leaf spot disease of *Trianthema portulacastrum*. J. Pl. Pathol., 96(4, Supplement), S4: 122.

Kumar, V., Kumar, N. and Aneja, K.R. 2017. Three fungal pathogens associated with horse purslane (*Trianthema portulacastrum*) in North India. Ind. J. Weed Sci., 49(4): 411-413.

Kumar, V., Kumar, N., Aneja, K.R. and Kaur, M. 2016. *Gibbago trianthemae*, phaeodictyoconidial genus, causes leaf spot disease of *Trianthema portulacastrum*. Archives of Phytopathology and Plant Protection, 49(1-4): 48-58.

Mehta, P., Sharma, R., Putatunda, C. and Walia, A. 2019. Endophytic fungi: role in phosphate solubilization. In: Singh, B. (eds) Advances in Endophytic Fungal Research. Fungal Biology. Springer, Cham. pp. 183-209. https://doi.org/10.1007/978-3-030-03589-1_9.

Mengistu, A.A. 2020. Endophytes: colonization, behaviour, and their role in defense mechanism. Int. J. Microbiol., 2020: 1-8.Article ID: 6927219 https://doi.org/10.1155/2020/6927219

O'Donnell, K., Cigelnik, E., Weber, N.S. and Trappe, J.M. 1997. Phylogenetic relationships among ascomycetous truffles and the true and false morels inferred from 18S and 28S ribosomal DNA sequence analysis. Mycologia, 89(1): 48-65.

Sharma, D., Pramanik, A. and Agrawal, P.K. 2016. Evaluation of bioactive secondary metabolites from endophytic fungus *Pestalotiopsis neglecta* BAB-5510 isolated from leaves of *Cupressus torulosa* D. 3 Biotech, 6(2): 210.

Stierle, A., Strobel, G. and Stierle, D. 1993. Taxol and taxane production by *Taxomyces andreanae*, an endophytic fungi of Pacific Yew. Sci., 260(5105): 214-216.

Strobel, G. and Daisy, B. 2003. Bioprospecting for microbial endophytes and their natural products. Microbiol. Molecul. Biol. Reviews, 67(4): 491-502.

Szilagyi-Zecchin, V.J., Ikeda, A.C., Hungria, M., Adamoski, D., Kava-Cordeiro, V., Glienke, C. and Galli-Terasawa, L.V. 2014. Identification and characterization of endophytic bacteria from corn (*Zea mays* L.) roots with biotechnological potential in agriculture. AMB Express. 7(4):26. doi: 10.1186/s13568-014-0026-y. PMID: 24949261; PMCID: PMC4052694.

Talukdar, R. and Tayung, K. 2019. Antimicrobial activity of endophytic fungi isolated from *Eryngium foetidum*, an ethnomedicinal plant of Assam. In. J. Pharmaceut. Sci. Drug Res., 11(6): 370-375.

Tungmunnithum, D., Thongboonyou, A., Pholboon, A. and Yangsabai, A. 2018. Flavonoids and other phenolic compounds from medicinal plants for pharmaceutical and medical aspects: an overview. Medicines (Basel). 5(3):93. doi: 10.3390/medicines5030093. PMID: 30149600; PMCID: PMC6165118.

New Frontiers in the Bio-inspired Green Synthesis of NiO NPs and Their Applications: An Overview

Waseem Ahmad*† iD **and Ankita Rawat****

*Department of Chemistry, Graphic Era (Deemed to be University), Dehradun 248001, India

**Department of Chemistry, Uttaranchal University, Dehradun, India

†Corresponding author: Waseem Ahmad, waseemahmad8@gmail.com

ABSTRACT

Nanoparticles are an important tool for new updations and advancements in diverse sectors. The inorganic metal and metal oxide nanoparticles have enormous research interest because of their great relevance in medicine, wastewater treatment, catalysis, biotechnology, and in the formation of energy storage devices. The NiO NPs can be synthesized using different physical and chemical methods and exploring all their possible applications. Green synthesis is the easy, safe, and effective nanoparticle synthesis route. Green metal and metal oxide nanoparticle syntheses provide the most affordable, convenient, and biocompatible approach for fabricating NiO NPs. This way is a good alternative to the conventional methods of synthesis. Green synthesis, being more constructive, is widely used in research and gives promising outcomes. This review highlighted the unique feature of the NiO nanoparticles. This paper brings forth the usage of green synthesis for synthesizing NiO nanoparticles. It also provides readers with a collective review of the recent development in the green synthesis of NiO NPs and their potential application in different fields.

INTRODUCTION

Nanoparticles are one of the important explorations that are remarkably contributing to bringing advancements in the field of science and technology. This area is drawing recognition because of several advantages of nanoparticles over their macro counterparts. Due to their benefits and wide applications, it has become a renowned area of research in recent times.

The term 'Nanoparticles' consists of two words, 'nano'+ 'particle,' which means extremely small fragments usually in the 1-100 nm range. Depending on the shape of nanoparticles, they can be categorized into 0D, 1D, 2D, or 3D (Ayyub et al. 2001). This field drew attention when researchers found that size can influence the physiochemical properties of a substance. A substance in nanoform behaves differently than its bulk part owing to its changed optical, thermal, and electrical properties and larger surface-to-volume ratio, making them more chemically reactive (Khan et al. 2019). These properties of the nanoparticles are responsible for their use in different fields like electronics, textiles, cosmetics, medicines, and many more.

Some of the important contributions of nanoparticles in different industries are:

- In cosmetic industries, TiO_2 nanoparticles are used in sunscreens to block the dangerous UVB and UVA light.

- In PET (Polyethylene Terephthalate) bottles, SiO_2 nanosheets act as an oxygen barrier, thus preventing the beverage in the bottle from deteriorating.

- In the textile industry, Nanosilver with antimicrobial properties, TiO_2 with water-repellent, and SiO_2 with dirt-repellent attributes are used in textiles.

- The nanoscale additives in polymer composite materials are used in tennis rackets and motorcycle helmets, making them lightweight and durable.

- Nano TiO_2 is also used in coatings to form self-cleaning surfaces. A sealed film of water dissolves the dirt making the surface clean.

SYNTHESIS OF NANOPARTICLES

The importance of nanoparticles was well known, so different methods to synthesize these were searched. The top-down and bottom-up approaches were traditionally used to synthesize nanoparticles. The top-down approach includes reducing the size of the bulk material into nanosized
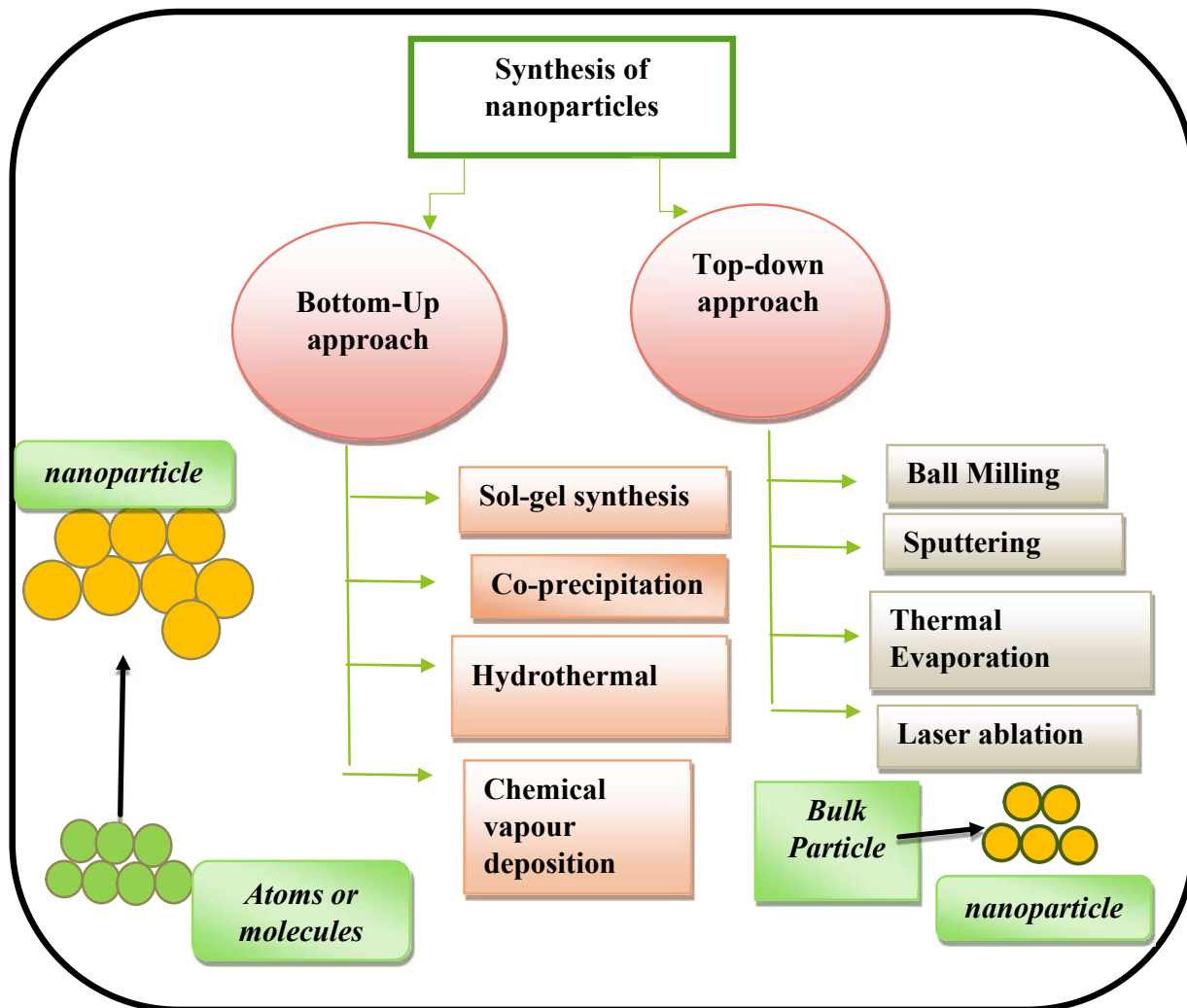
Fig. 1: Flowchart showing conventional methods for nanoparticle synthesis.

particles. Some methods involved in this approach are grinding, cutting, ball milling, Sputtering, and laser ablation (Tiwari et al. 2012). Though these methods are simpler, they have major drawbacks and are unsuitable for nanoparticle synthesis. They require large installations, so they are quite expensive. Besides this, these methods are unsuitable for the soft samples because the mechanical devices used for grinding are stiff and hard (Fig. 1).

The bottom-up approach includes small units like atoms or molecules that combine to form a nanoscopic dimension particle. This approach is based on the principle of molecular recognition. The problem with this method is that various undesired atoms and molecules may be present in the deposited material, and the cost of the chemicals is high. Moreover, these chemicals are toxic, and various poisonous by-products are obtained.

The physical and chemical methods for nanoparticle synthesis, along with their advantages and disadvantages, have been discussed by Namra Abid and the team (Abid et al. 2022). Though these methods possess some advantages, we utilize a different route for nanoparticle synthesis due to their major drawbacks.

GREEN SYNTHESIS

The difficulties faced with the classical approach emphasized the need for an alternative pathway for nanoparticle synthesis. This drove our attention towards herbs due to the availability of effective phytochemicals in various plant extracts, which can potentially reduce metal salts into metal nanoparticles. In today's era of rapid industrialization, urbanization, and population explosion, methods are absolutely necessary to

minimize toxic chemicals: green synthesis is an effective tool to serve this purpose. Green synthesis paves the way for using plants and their extracts to synthesize nanoparticles. Thus, green synthesis uses environment-friendly procedures and focuses on minimizing the usage of hazardous chemicals. It comprises parts of plants such as leaves and fruit peels for nanoparticle synthesis because these contain phytochemicals that act as good reducing, capping, and stabilizing agents for metal nanoparticle synthesis. The advantages of green synthesis are that it is an easier, cost-effective, biologically safe, environment-friendly, and reliable method (Fig. 2).

This bioinspired route gives productive outcomes: therefore, it is being adopted by many for nanoparticle synthesis. Among various nanoparticles, metal oxide nanoparticles are especially drawing recognition due to their vast applications in different fields. Green synthesis is adopted for their synthesis because of their usage as antifungal agents, antibacterial agents, semiconductors, catalysts, nano-medicines (Hussain et al. 2023), and more (Fig. 3).

This biological way provides another important benefit of contributing to keeping the environment clean (Singh et al. 2018) describe that the bio-inspired green synthesis of metal and their oxide nanoparticles are a remedial approach to keeping the environment clean. Many nanoparticles have been synthesized through this eco-friendly route like Ag (using *Tectona grandis*) (Rautela et al. 2019), ZnO (using *Coriandrum sativum*, Varada V (Ukidave & Ingale 2022), NiO (using *Aegle marmelos*) (Angel Ezhilarasi et al. 2018) and more.

The plant-mediated green synthesis plant acts as chemical factories that act as reducing agents. Different phytochemicals are present in the plant extract, which probably act as reducing stabilizing agents and prevent the accumulation of developed nanoparticles. The plant-mediated nanoparticles also show low toxicity as the extract is an adsorbent to absorb the toxicity associated with the plant. Further, the other one of the most important advantages of the plant-mediated green synthesis of the nanoparticles is the rate at which the synthesis occurs (Angel Ezhilarasi et al. 2020). The
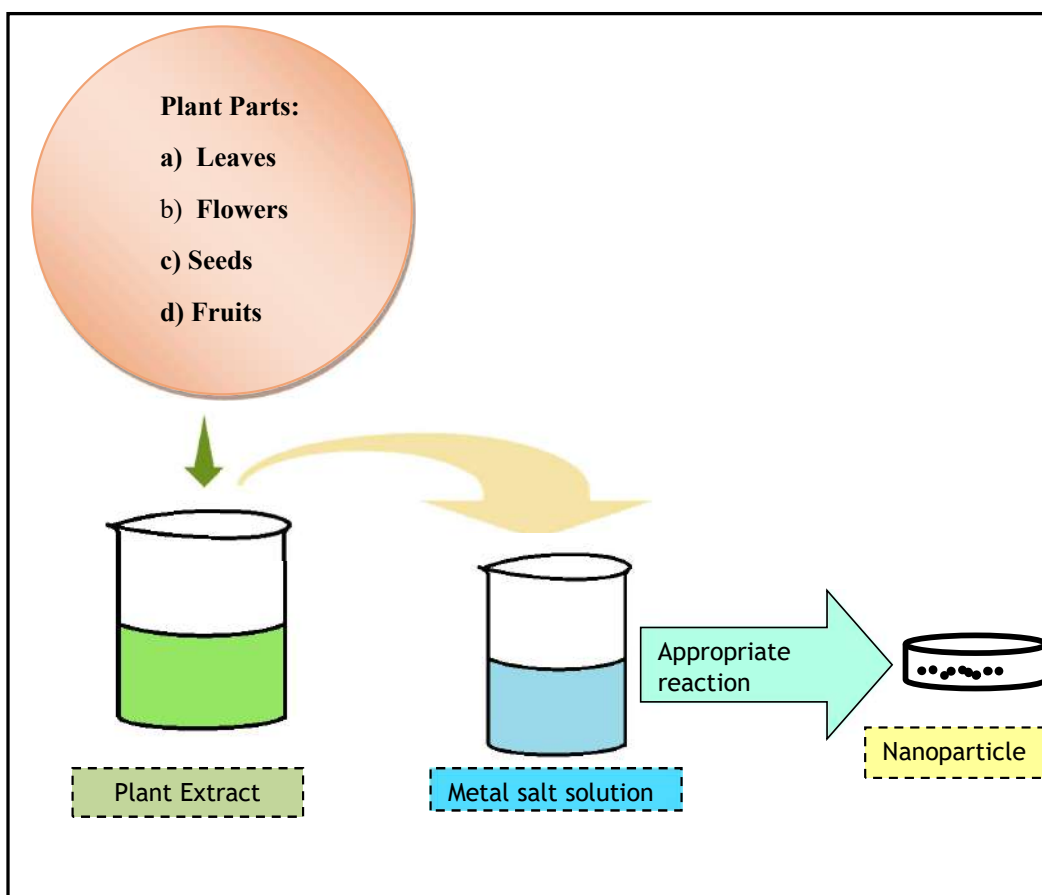

Fig. 2: Diagrammatic overview of the procedure involved in green synthesis.
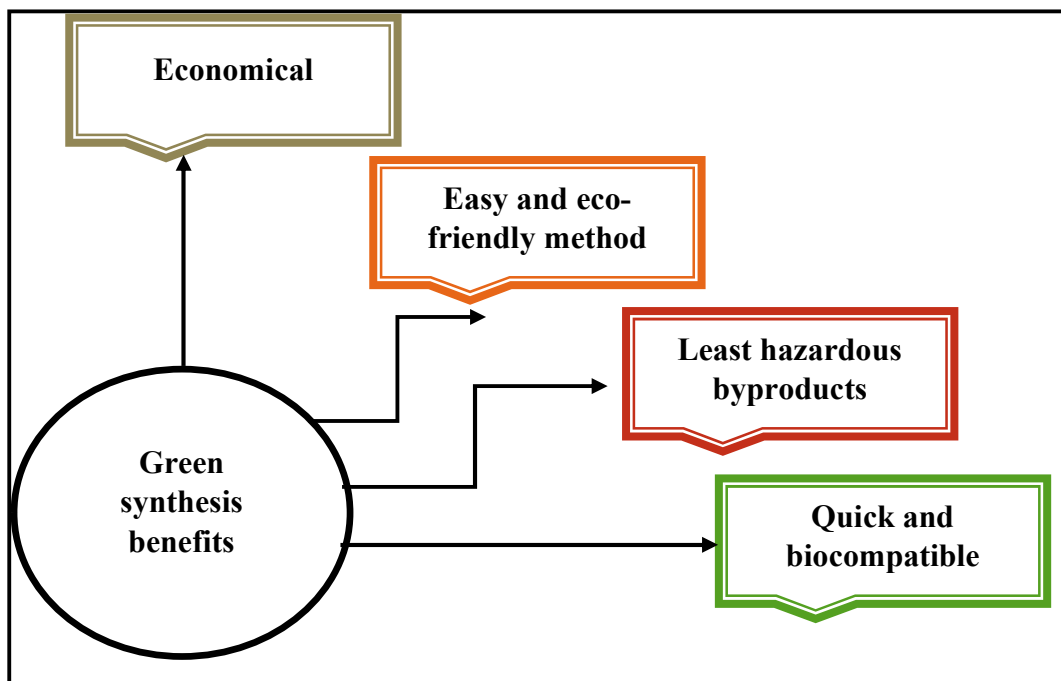
Fig. 3: Some advantages of green synthesis.

plant-mediated synthesis of the nanoparticles occurs much faster than the physical and chemical methods. In the plant-mediated green synthesis of nanoparticles, the leaf, fruit, bark root, and steam play prominent roles in the green synthesis of nanoparticles.

METAL-OXIDE NANOPARTICLES

Scientists are paying more heed to metal oxide nanoparticles because of their easy mode of formation and multidisciplinary implementations. Metal oxide nanoparticles can tackle some major issues owing to their unique properties. They possess antibacterial activity and are useful in wastewater treatment (Naseem & Durrani 2021). They serve as therapeutic agents and are used in paints, cosmetics, and ion batteries. The different useful applications of metal oxide nanoparticles in nanotechnology have been discussed by Murthy & Chavali (2019).

The transition elements have properties like high charge density, catalytic behavior, and the ability to form coordination compounds, so their metal oxides are important. Iron oxide nanoparticles possess unique features such as nontoxicity and biocompatibility and are successfully used in drug delivery systems, electrochemical sensing, hyperthermia, photothermal therapy, nanozymes, and MRI (Vallabani et al. 2018). Zinc oxide nanoparticles are used in drug-delivery systems, cosmetics, biomedical, agriculture,

biosensors, and gas sensors (Bedi & Kaur 2015). Tin oxide nanoparticles are electrochemical/chemo-resistive sensors (Sharma et al. 2021). Ahmad et al. (2021) states various methods for synthesizing tin oxide nanoparticle and their properties and highlights their various biological and physio-chemical applications. Copper oxide nanoparticles have catalytic, anti-cancer, and anti-bacterial applications (Akintelu et al. 2020). TiO_2 nanoparticles have promising uses in drug-delivery systems. Their property to act as photo-sensitizing agents against malignant tumors and their effectiveness in photo-dynamic inactivation of antibiotic-resistant bacteria have been discussed by Ziental et al. (2020). The recent achievement in the field of metal oxide nanoparticles includes the development of nanostructured oxides with two or more metallic components. Different uses of these metal oxide nanoparticles have made these fascinating for researchers, and explorations in this field are continuing for the betterment of existing technologies. NiO nanoparticles are one of many useful metal oxide nanoparticles synthesized via green synthesis. These possess distinctive features like low porosity, high photo absorption, and a larger surface-to-volume ratio, making them convenient to use in different fields. NiO nanoparticles possess superior ferromagnetic properties, chemical stability, and high coercive forces (Ahmad et al. 2022a), contributing to their role in various day-day technologies.

APPLICATIONS OF NIO NANOPARTICLES

Photocatalytic Applications

(i) Wastewater Treatment by Degradation of Toxic Dyes

In the world of rapid development and industrialization, one of the major issues we face is the effective treatment of thousands of liters of wastewater daily for sustainability. Wastewater contains many impurities like sulfates, nitrates, and phosphates and may even contain synthetic dyes and other toxic pollutants. Synthetic dyes are non-biodegradable, toxic, and potentially even carcinogenic, so their removal is paramount. Adsorption is a productive and cost-efficient way to remove these impurities, thereby reducing contaminants in wastewater. Due to their high surface area, photocatalytic activity, and other chemical properties, NiO nanoparticles are used as adsorbents in purifying water. Hamidian and team carried out the bio-inspired synthesis of NiO nanoparticles using Biebersteiniamultifida extract to examine their photocatalytic activity against acid orange 7 (AO7) dye and found these particles to exhibit excellent adsorption as well as photocatalytic behavior (90.2%) (Hamidian et al. 2021). NiO nanoparticles synthesized using Allium cepa peels aqueous extract were used against the Congo red direct dye by Rafique et al. (2021) reported that decolorization of the dye was up to 90% at optimized conditions (Rafique et al. 2021). Nateghi et al. (2021) investigated the decolorization of synthetic wastewater containing mono azo orange II dye at the laboratory scale. They reported that 0.6 g.L^{-1} was the optimum amount of the adsorbent required for the complete decolorization of synthetic wastewater under the condition of 50 mg.L^{-1} initial dye, PH 3, and agitator speed 100 rpm for 30 minutes (Nateghiet al. 2021). Adinaveen et al. (2019) studied the photocatalytic properties of NiO nanoparticles and found these to exhibit high degradation activity against Rhodamine b (92.3%) under UV light illumination (Fig. 4).

Motahari and their team members synthesized NiO nanoparticles through the hydrothermal process in the presence of H2acacen ligand and found them productively work to remove Rhodamine B (Motahari et al. 2015). NiO nanopowder is also useful for removing heavy metals in wastewater treatment. Its application as a productive adsorbent for the heavy metals Zn and Pb in an aqueous solution is discussed in Abdl El Fatah & Ossman (2014).

(ii) Photodegradation

NiO nanoparticles also exhibit photocatalytic activity in the degradation of polyethylene films. Olajire & Mohammed (2020) carried out the biological synthesis of NiO nanoparticles using *Ananas comosus* extract. They suggested that using synthesized nanoparticles in the polymer matrix of LDPE can enhance its photodegradation (Olajire & Mohammed 2020). Wang et al. (2005) reported that the catalytic activity of NiO nanoparticles lowers the decomposition temperature for the thermal decomposition of ammonium perchlorate by 93°C compared to that of the bulk NiO particle. It also increases the heat of decomposition for the same. NiO nanoparticles are important in degrading pharmaceutical products like paracetamol (Ahmad et al. 2022b). The catalytic role of the NiO nanoparticles is also important as they have applications in synthesizing substituted Imidazole (Mahadevaiah et al. 2018).

Medical Applications

(i) Anti-Cancer Activity

NiO nanoparticles are useful in the medical field. (AlSalhi et al. 20202) Worked on the cytotoxicity of NiO nanoparticles towards HeLa cancer cells and reported these to exhibit good response at a concentration of 180 µg.mL^{-1}. NiO nanoparticles also have an inhibitory role against Hep-G2, MCF-7, and HT-29 cancer cell lines responsible for liver, breast, and colon cancer, respectively (Kouhbanani et al. 2021). Angel Ezhilarasi et al. (2016) synthesized NiO nanoparticles and explored their cytotoxicity effect against HT-29 cancer cells. They found that green synthesized nanoparticles showed better cytotoxicity. In Zhang et al. (2021), NiO nanoparticles were examined against the carcinoma cell lines of FLO-1, ESO26, 0E33, and KYSE-207, and it was reported that the nanoparticles showed significant cytotoxicity against all these cell lines. Sabouri et al. (2021) conducted a bio-synthesis of NiO nanoparticles using Arabic gum and reported their cytotoxic effects on normal CNs cell lines and cancer U87MG cell lines Sabouri et al. (2021). Betageri et al. (2021) analyzed the cytotoxic effects of green synthesized NiO nanoparticles against A549 cancer cell lines and demonstrated that the synthesized nanoparticles exhibited significant anticancer activity.

Anti-Bacterial Activity

NiO nanoparticles also possess antibacterial properties. Therefore, these serve as remarkable antibacterial agents. These nanoparticles resist the growth of gram-positive and gram-negative bacteria. Ilbeigi and the team worked on the antibiotic activity of NiO nanoparticles against some bacterial strains. They reported the effectiveness of these nanoparticles even for those bacteria which had developed resistance to antibiotics like rifampicin, cefazolin, penicillin, ampicillin, erythromycin, and streptomycin (Ilbeigi et al. 2019). Khashan et al. (2016), in their study, indicated that NiO nanoparticles could potentially cause growth inhibitions of bacterial strains because, on their application, the bacterial

cell wall showed increased permeability, so amoxicillin accumulations occur in them. Khan et al. (2021) conducted a comparative study of green synthesized NiO nanoparticles and chemically synthesized nanoparticles for antibacterial, anticancer, and antioxidant activities. They reported the effectiveness of biologically synthesized nanoparticles against the bacteria *E. coli, B. bronchiseptica, B. subtilis* and *S. aureus*.

Anti-diabetic, Anti-pseudomonal, and Anti-oxidant activity

NiO nanoparticles also have significant antidiabetic effects because they exert a hypoglycemic effect, as discussed in Betageri et al. (2021). These also exhibit antimicrobial and antioxidant properties (Haq et al. 2021). Khan et al. (2021) reported that phytomolecules-coated NiO nanoparticles showed excellent antioxidant activity. Irum et al. (2021) carried out the chemical synthesis of NiO nanoparticles. They worked on the antipseudomonal activity of Al-doped NiO nanoparticles and reported the resistance of these nanoparticles against pathogens, especially *Pseudomonas aeruginosa* (Irum et al. 2021). Zhang et al. (2021) worked on the anti-oxidant properties of NiO nanoparticles and reported in their result the effectiveness of these nanoparticles as an anti-oxidant through DPPH assay. Srihasam et al. (2020) evaluated NiO nanoparticles' anti-oxidant and anti-microbial

activity. They reported that the nanoparticles were found efficient against fungi *A. niger* and *A. fumigatus*, and they also exhibited strong anti-oxidant properties shown through DPPH reduction assay. Uddin et al. (2021), synthesized NiO nanoparticles from *Berberis balochistanica* stem and reported the nanoparticles to exhibit total antioxidant capacity (64.77%) and for 2,2- diphenyl-1-picrylhydrazyl (71.48%).

Agricultural Applications

Uddin et al. (2021) also reported that the nanoparticles could have stimulatory efficacy in enhancing the rates of seed germination and seedling growth rates. Singh et al. (2022) carried out the biosynthesis of NiO nanoparticles using Spirogyra sp. cell-free extract. They reported that the nanoparticles showed stimulatory and inhibitory effects on Mung bean seed germination and seedlings at varying concentrations.

Electronic Devices

NiO nanoparticles also exhibit a vital part in enhancing the structural properties of other nanoparticles: TiO_2 has limitations because of the rapid recombination rates of electron/hole pair and the wide band gap, so NiO nanoparticles were used productively in enhancing the structural properties of TiO_2 (Mannaa et al. 2021). NiO
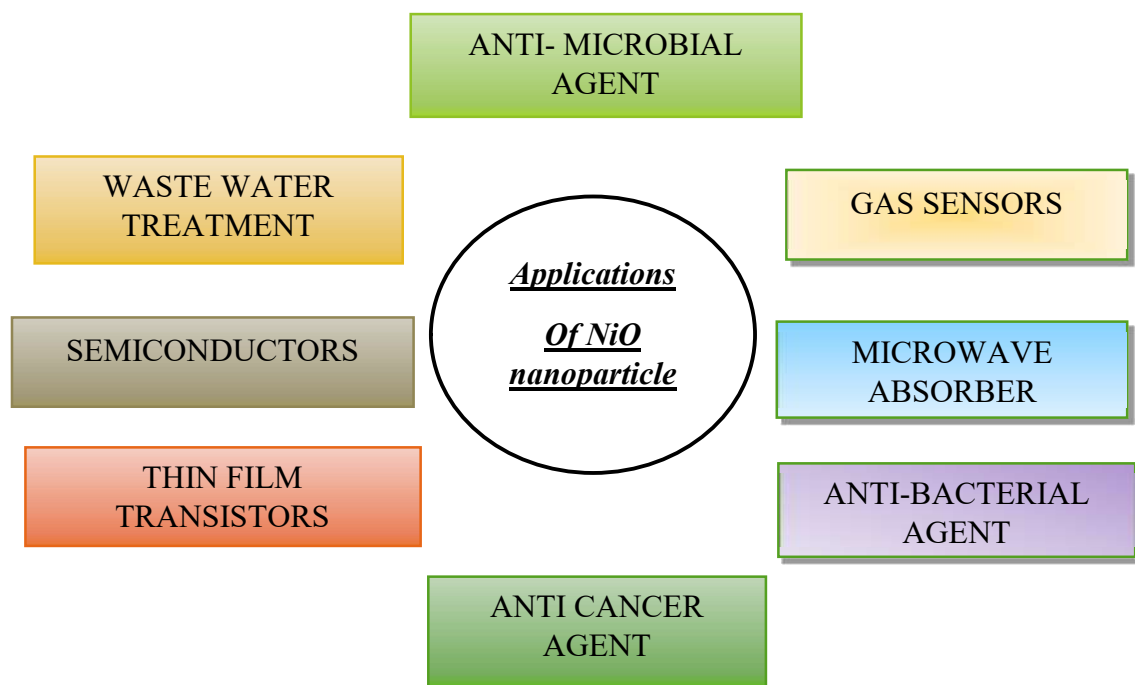

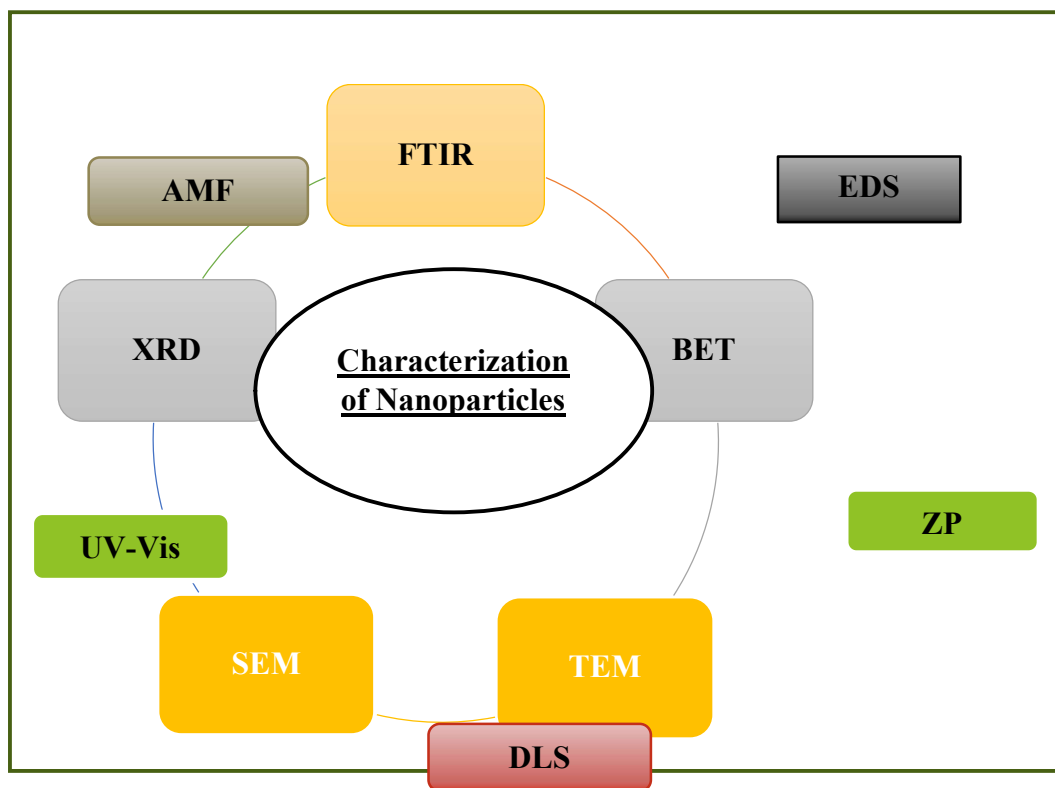Fig. 4: Different applications of NiO nanoparticles.

Fig. 5: Different characterization techniques of NiO NPs.

nanoparticles are also used in carbon-based perovskite solar cells to increase the device performance by reducing charge recombination (Cai et al. 2019).

Niu et al. (2019) synthesized NiO-decorated tetragonal rutile SnO_2 nanosheet-based sensors and found these to have improved sensitivity and excellent selectivity for ethanol gas (Niu et al. 2019). NiO nanoparticles also exhibit electrochromic properties (Obaida et al. 2022). Arif et al. 2018: prepared a chlorine gas sensor based on the NiO nanoparticles (Hamidian et al. 2021).

CHARACTERIZATION OF NANOPARTICLES

Nanoparticles can be synthesized differently, leading to their different sizes and shapes, ultimately affecting their properties. It is, therefore, necessary to know the size, shape, crystal structure, and other properties of the synthesized nanoparticle for its efficient usage. Nanoparticle characterization hence plays a major role. Characterization of nanoparticles is done to know the size, distribution, crystal structure, surface charge, and other properties of the nanoparticles. Various techniques are used for the characterization, such as UV-Visible spectroscopy, Fourier Transform Infrared Spectroscopy (FT-IR), Zeta Potential (ZP), transmission electron microscopy (TEM), Scanning Electron Spectroscopy (SEM), Atomic Force Microscopy (AMF), Dynamic Light Scattering (DLS), Brunauer-Emmett-Teller (BET), X-ray Diffraction (XRD), Nuclear Magnetic Resonance (NMR), Thermogravimetric Analysis (TGA), Diffuse Optical Spectroscopy (DCS) and many more (Fig.5). Different techniques derive different information for a particular sample to be analyzed. For example, XRD gives information about the crystal structure, BET tells us about the surface area and the pore size of nanoparticles, FTIR gives an idea about the surface composition of ligand bindings and the analysis of the functional groups present on the surface of the green synthesized nanoparticles. For this analysis, the developed nanoparticles were generally scanned in the 400-4000 cm^{-1}. With the help of FTIR analysis, the binding capping and stabilizing agents were identified. AFM gives knowledge about nanoparticle size and shapes in 3D mode (Table 1). The scanning electron microscope uses a beam of electrons to capture the image of the fabricated nanoparticles. With the help of SEM images, the particle size, surface morphology, and distribution of the particles were estimated.

Table 1: Summary of the synthesis, characterization and applications of NiO NPs.

S. No	Name of the plant	Size	Morphology	Characterization Techniques	Applications	Reference
1	*Biebersteinia multifida*	54-58 nm	Cubic structure	SEM, EDX, PXRD, UV-Vis, Raman analysis	Photocatalytic degradation of acid orange 7 dye under visible light	Hamidian et al. (2021)
2	*Aegle marmelos*	8-10 nm	Single crystalline with fcc phase	XRD, HR-TEM, HR-SEM, FT-IR	Antibacterial activity Cytotoxicity towards A549 cell culture Photocatalytic degradation of 4- chlorophenol(4-CP)	Angel Ezhilarasi et al. (2018)
3	*Andrographis paniculata*	24 nm	Cubic structure	XRD, FTIR, SEM, HRTEM, UV-Vis	Photocatalytic and anti-cancer activity	Karthik et al. (2019)
4	*Berberis balochistanica*	31.44 nm	Rhombohedral agglomerated shape	FTIR, XRD, UV-Vis, SEM	Antioxidant activity, stimulatory effect to fasten the rates of seed germination and seedling growth	Uddin et al. (2021)
5	*Ananas comosus*	0.63-5.75 nm	fcc crystalline structure	UV-Vis, XRD, HRTEM, FTIR, EDX	Photocatalytic activity	Olajire et al. (2020)
6	*Salvia hispanica* L.	30 nm	Spherical	TGA, FTIR, UV-Vis, XRD, EDAX	Cytotoxicity and photocatalytic activity	Sabouri et al. (2021)
7	*Stevia*	20-50 nm	Spherical, and a few are agglomerated	XRD,FTIR, FE-SEM, TEM, UV-Vis	in -vitro oxidant and antimicrobial activity against multi-drug resistant microbes	Srihasam et al. (2020).
8	*Ageratum conyzoides* L.	11.5 nm	Cubic structure	XRD, FTIR, TEM	Catalytic activity	Wardani et al. (2019)
9	*Rhamnus virgata*	34 nm	-	FTIR, XRD, SEM,TEM, DLS	Antibacterial activity, anti-fungal activity, alpha-amylase inhibition, antioxidant activity, antileishmanial activity	Iqbal et al. (2019)
11	*Stevia*	2-16 nm	Spherical	-	Antibacterial activity against S. mutans	Moghadam et al. (2022)
12	*Abutilon indicum*	-	-	XRD, SEM, EDX, DLS, FTIR, UV-Vis.	Antioxidant, Antibacterial, and Anticancer activities	Khan et al.:2021
13	*Allium cepa*	-	-	SEM, FTIR, UV-Vis	Photocatalytic Activity-Degradation of Congo red direct dye	Rafique et al. (2021)
14	*Calendula officinalis*	60.39 nm	Spherical	TEM, SEM, EDS, FTIR, XRD, UV- Vis.	Antioxidant activity, Cytotoxicity, Anti-esophageal Carcinoma activity	Zhang et al. (2021)
15	*Areca catechu*	5.46 nm	Hexagonal shaped	XRD, SEM, TEM, UV- Vis.	Anti-diabetic and Cytotoxicity Effects.	Shwetha et al. (2021)

CONCLUSION

A vital and budding research field that has the potential to bring advancements in the world and provide solutions to many existing problems is nanoparticles. The nano-sized particles do not limit their usage to one field. Rather, they have multidisciplinary implementations. The major targeted areas are cancer treatment, gene therapy, and drug delivery system. Owing to their importance, synthesizing them also draws our attention.

The synthesized NiO nanoparticles have their role in various areas such as water treatment, pharmaceutical and medical sector, electronic devices, photodegradation and catalysis, and many other fields. The principle is that various phytochemicals in the plant extracts can remarkably reduce the metal salts into corresponding nanoparticles, thus synthesizing desired nanoparticles. This route helps keep the environment clean and less toxic by minimizing the usage of hazardous chemicals. The overview of the diverse benefits of NiO nanoparticles reflects that we should focus more on

them and other nano-dimensional particles and explore more of this area to bring forth new innovative solutions for the welfare of mankind.

ACKNOWLEDGMENTS

REFERENCES

Abd El fatah, M. and Ossman, M.E. 2014. Removal of Heavy Metal by Nickel Oxide Nano Powder. Int. J. Environ., 8: 741-750.

Abid, N., Khan, A.M., Shujait, S., Chaudhary, K., Imran, M., Haider, J., Khan, M., Khan, Q. and Maqbool, M. 2022. Synthesis of nanomaterials using various top-down and bottom-up approaches, influencing factors, advantages, and disadvantages: A review. Adv Coll. Interf. Sci., 300: 102597.

Adinaveen, T., Karnan, T. and Selvakumar, S.A.S. 2019. Photocatalytic and optical properties of NiO added *Nephelium lappaceum L.* peel extract: An attempt to convert waste to a valuable product. Heliyon, 5: 5-65.

Ahmad, W., Bhatt, S. C., Verma, M., Kumar, V. and Kim, H. 2022a. A review of current trends in the green synthesis of nickel oxide nanoparticles, characterizations, and their applications. Environ. Nanotechnol. Monit. Manag., 18: 5-6.

Ahmad, W., Pandey, A. Rajput, V., Kumar, V., Verma, M. and Kim, H. 2021. Plant extract mediated cost-effective tin oxide nanoparticles: A review on synthesis, properties, and potential applications. Curr. Res. Green Sustain. Chem., 4: 2-3.

Ahmad. W., Kaur, N. and Joshi, H.C. 2022b. Photocatalytic behavior of NiO nanoparticles towards photocatalytic degradation of paracetamol. Mater. Today Proceed., 6: 54

Akintelu, S.A., Folorunso A.S., Folorunso, F.A. and Oyebamiji, A.K. 2020. Green synthesis of copper oxide nanoparticles for biomedical applications and environmental remediation. Heliyon, 6: I7-23

AlSalhi, M.S., Hammad Aziz, M., Atif, M., Fatima, M., Shaheen, F., S. Devanesan, W.A Farooq. 2020. Synthesis of NiO nanoparticles and their evaluation for photodynamic therapy against HeLa cancer cells. J. King Saud Univ. Sci., 32: 1395-1402.

Angel Ezhilarasi, A., Judith Vijaya J., Kaviyarasu, K., John Kennedy, L., Ramalingam, R.J. and Al-LohedanH A. 2018. Green synthesis of NiO nanoparticles using *Aegle marmelos* leaf extract for the evaluation of in-vitro cytotoxicity, antibacterial and photocatalytic properties. J. Photochem. Photobiol. B Biol., 180: 39-50.

Angel Ezhilarasi, A., Judith Vijaya, J., Kaviyarasu, K., Maaza, M., Ayeshamariam, A. and John Kennedy, L. 2016. Green synthesis of NiO nanoparticles using *Moringa oleifera* extract and their biomedical applications: Cytotoxicity effect of nanoparticle against HT- 29 cancer cells. J. Photochem. B Biol., 164: 352-360.

Angel Ezhilarasi, A., Judith Vijaya, J., Kaviyarasu, K., Zhang, X. and John Kennedy, L. 2020. Green synthesis of nickel oxide nanoparticles using *Solanum trilobatum* extract for cytotoxicity, antibacterial and photocatalytic studies. Surf. Interf., 20: 100553

Arif, M., Sanger, A. and Singh, A. 2018. Highly sensitive NiO nanoparticle-based chlorine gas sensor. J. Electr. Mater., 7: 3451-3458.

Ayyub, P., Chandra, R., Taneja, P., Sharma, A. K. and Pinto, R. 2001. Synthesis of nanocrystalline material by sputtering and laser ablation at low temperatures. Appl. Phys. A., 73: 67-73.

Bedi, P.S. and Kaur, A. 2015. An overview on uses of zinc oxide nanoparticles. World Journal. Pharm. Pharm. Sci., 4: 12.

Betageri K., Veerapur L., Lamraoui G., Al-Kheraif A.A., Elgorban A.M, Syed A., Shivamallu, C. and Prasad Kollur, S. 2021. Biogenic synthesis

of NiO nanoparticles using *Areca catechu* leaf extract and their antidiabetic and cytotoxic effects. Molecules, 26: 2448.

Cai, C., Zhou, K., Guo, H., Pei, Y., Hu, Z., Zhang, J. and Zhu. Y. 2019. Enhanced hole extraction by nio nanoparticles in carbon-based perovskite solar cells. Electrochim. Acta, 312: 100-108.

Haider, A., Ijaz, M., Ali, S., Haider, J., Imran., M., Majeed, H., Shahzadi, I., Ali, M.M., Khan, J.A. and Ikram, M. 2020. Green synthesized phytochemically (*Zingiber officinale* and *Allium sativum*) reduced nickel oxide nanoparticles confirmed bactericidal and catalytic potential. Nanosc. Res. Lett., 15: 50

Hamidian, K., Rigi, A.H., Najafidoust, A M. Sarani and Miri. A. 2021. Study of photocatalytic activity of green synthesized nickel oxide nanoparticles in the degradation of acid orange dye under visible light. Bioprocess Biosyst. Eng., 44: 2667-2678.

Haq, S., Dildar, S., Ali, M.B, Mezni, A., Hedfi, A., Shahzad, M.I., Shahzad, N. and Shah, A. 2021. Antimicrobial and antioxidant properties of biosynthesized NiO nanoparticles using *Raphanus sativus* (*R. sativus*) extract. Mater. Res. Xpress, 8: 55-60.

Hussain, S., Muazzam, M. A., Ahmed, M., Ahmad, M., Mustafa, Z., Murtaza, S., Ali, J., Ibrar, M., Shahid, M. and Imran, M. 2023.Green synthesis of nickel oxide nanoparticles using *Acacia nilotica* leaf extracts and investigating their electrochemical and biological properties. J. Taibah Univ. Sci., 17: 1, DOI: 10.1080/16583655.2023.2170162

Ilbeigi, G., Kriminik, A. and Moshafi, M.H. 2019. The antibacterial activities of NiO Nanoparticles against some gram-positive and gram-negative bacterial strains. Int. J. Basic Sci. Med., 4(2): 69-74.

Iqbal, J., Abbasi, B.A, Mahmood, T., Hameed, S., Munir., A. and Kanwal, S. 2019. Green synthesis and characterizations of Nickel oxide nanoparticles using leaf extract of *Rhamnus virgata* and their potential biological applications. Appl. Organomet. Chem., 33: 8-10.

Irum, S., Andleeb, S., Sardar, S., Mustafa, Z., Ghaffar, G., Mumtaz, M., Arslan, M. and Abbas, M. 2021. Chemical synthesis and antipseudomonal activity of al-doped NiO nanoparticles. Front. Mater., 8: 673458.

Karthik, K., Shashank, M., Revathi, V. and Tararchuk, T. 2019. Facile microwave-assisted green synthesis of NiO nanoparticles from *Andographis paniculate* leaf extract and evaluation of their photocatalytic and anti-cancer activities. Mol. Cryst. Liq. Cryst., 673: 70-80.

Khan S A, Shahid S, Ayaz A, Alkahtani, J., Elshikh, M.S and Riaz, T. 2021. Phytomolecules- coated NiO nanoparticles synthesis using *Abutilon indicum* leaf extract: Antioxidant, antibacterial, and anticancer activities. Int. J. Nanomed., 1773-1757 :2.

Khan, I., Saeed, K. and Khan, I. 2019. Nanoparticles: Properties, applications, and toxicities. Arab. J. Chem., 12: 908-931.

Khan, S.A., Shahid, S., Ayaz, A., Alkahtani, J., Elshikh, M.S. and Riaz. T. 2021. Phytomo antioxidant, antibacterial, and anticancer activities. Int. J. Nanomed., 16: 1757-1773.

Khashan, K.S, Sulaiman, G.M., Abdul Ameer, F.A. and Napolitano, G. 2016. Synthesis, characterization, and antibacterial activity of colloidal NiO nanoparticles. Pak. J. Pharm. Sci., 29: 34-39

Kouhbanani, M A J., Sadeghipour, Y., Sarani, M., Sefidgar, E., Ilkhani, S., Amani, A A. and Beheshtkhoo, N. 2021. The inhibitory role of synthesized Nickel oxide nanoparticles against Hep-G2, MCF-7, and HT-29 cell lines. Green Chem. Lett. Rev., 454-444 :14.

Mahadevaiah, R., Vinay, S.P., Shankraiah, L.H. 2018. Nano NiO catalyst: synthesis, characterization, and their applications for the synthesis of substituted imidazoles. Tumbe Group Int. J., 1: 1-18

Mannaa, M.A., Qasim, K.F., Alshorifi, F.T., El- Bahy, S.M. and Salama, R.S. 2021. Role of NiO nanoparticles in enhancing structure properties of TiO$_2$ and its applied photodegradation hydrogen evolution. ACS Omega., 6: 30386-30400.

Moghadam, N. C. Z., Jasim, S.A., Ameen, F., Alotaibi, D.H., Nobre, M. A. L., Sellami, H. and Khatami, M. 2022. Nickel oxide nanoparticles

synthesis using plant extract and evaluating their antibacterial effects on *Streptococcus mutans*. Bioprocess Biosyst. Eng., 45: 1201-1210.

Motahari, F., Mozdianfard, M.R. and Niasari, M.S. 2015. Synthesis and adsorption studies of NiO nanoparticles in the presence of H_2acacen ligand for removing Rhodamine B in wastewater treatment. Process Saf. Environ. Protect., 93: 282-292.

Murthy, S. and Chavali, P. 2019. Metal oxide nanoparticles and their applications in nanotechnology. SN Appl. Sci., 1: 607.

Naseem, T. and Durrani, T. 2021. The role of some important metal oxide nanoparticles for wastewater treatment and antibacterial applications: A review. Environ. Chem. Ecotoxicol., 3: 59-75.

Nateghi, R., Bonyadinejad, G.R., Amin, M.M. and Mohammadi, H. 2021. Decolorization of synthetic wastewaters by nickel oxide nanoparticles. Int. J. Environ. Health Eng., 2: 25.

Niu. G., Zhao, C., Gong, H., Yang, Z., Leng, X. and Wang, F. 2019. NiO nanoparticles-decorated SnO_2 nanosheets for ethanol sensing with enhanced moisture resistance. Microsyst. Nanoeng., 5: 21.

Obaida, M., Fathi, A M., Moussa, I. and Afify, H H. 2022. Characterization and electrochromic properties of NiO thin films prepared using a green aqueous solution by pulsed spray pyrolysis technique. J. Mater. Res., 37: 2282-2292.

Olajire, A.A. and Mohammed, A.A. 2020. Green synthesis of nickel oxide nanoparticles and studies of their photocatalytic activity in degradation of polyethylene films. Adv. Powder Technol., 31: 211-218.

Rafique, M. A., Kiran, S., Javed, S., Ahmad, I., Yousaf, S., Iqbal, N., Afzal, G. and Rani, F. 2021. Green synthesis of nickel oxide nanoparticles using *Allium cepa* peels for Congo red direct dye degradation: an environmental remedial approach. Water Sci. Technol., 84: 2793-2804.

Rautela, A., Rani, J. and Debnath M. 2019. Green synthesis of silve*Tectona grandis* seeds extracts: characterization and mechanism of antimicrobial action on different microorganisms. J. Anal. Sci. Technol., 10: 5.

Sabouri, Z., Akbari, A., Hosseini, H.A., Khatami, M. and Darroudi, M. 2021. Green-based bio-synthesis of nickel oxide nanoparticles in Arabic gum and examination of their cytotoxicity, photocatalytic and antibacterial effects. Green Chem. Lett. Rev., 14: 404-414.

Sharma, A., Ahmed, A., Singh, A., Oruganti, S.K, Khosla, A. and Arya, S. 2021. Review: Recent advances in tin oxide nanomaterials as elecrochemical/chemiresistive sensors. J. Electrochem. Soc., 168: 2.

Shwetha, U.R., Latha, M.S., Kumar, C.R., Kiran, M.S., Onkarappa, H.S. and Betageri, V.S. 2021. Potential antidiabetic and anticancer activity of copper oxide nanoparticles synthesised using *Areca catechu* leaf extract. Advances in Natural Sciences: Nanoscience and Nanotechnology, 12(2): 025008.

Singh, J., Dutta, T., Kim, K.H., Rawat, M., Samddar, P. and Kumar, P. 2018. 'Green' synthesis of metals and their oxide nanoparticles: Applications for environmental remediation. J. Nanotechnol., 16: 84.

Singh, Y., Sodhi, R.S., Singh, P.P. and Kaushal, S. 2022. Biosynthesis of NiO nanoparticles using Spirogyra sp. cell-free extract and their potential biological applications. Mater. Adv., 3: 4991-5000.

Srihasam, S., Thyagarajan, K., Korivi, M., Lebaka, V.R. and Reddy Mallem, S.P. 2020. Phytogenic generation of NiO nanoparticles using stevia leaf extract and evaluation of their in-vitro antioxidant and antimicrobial properties. Biomolecules. 10(1): 89-93.

Tiwari, J.N., Tiwari, R.N. and Kim, K.S. 2012. Zero-dimensional, one-dimensional, two-dimensional, and three-dimensional nanostructured materials for advanced electrochemical energy devices. Prog. Mater. Sci., 57: 724-803.

Uddin, S., Safdar, L.B. Anwar. S., Iqbal, J., Laila, S., Abbasi, B.A., Saif, M.S., Ali, M., Rehman, A. and Basit, A. 2021. Green Synthesis of Nickel Oxide Nanoparticles from *Berberis balochistanica* Stem for Investigating Bioactivities. Molecules, 26: 1548.

Ukidave, V.V. and Ingale, L.T. 2022. Green synthesis of zinc oxide nanoparticles from *Coriandrum sativum* and their use as fertilizer on Bengal gram, Turkish gram, and green gram plant growth. Int. J. Agron., 8: 14.

Vallabani, N.V.S. and Singh, S. 2018. Recent advances and future prospects of iron oxide nanoparticles in biomedicine and diagnostics. 3 Biotech, 8: 279.

Wang, Y., Zhu, J., Yang, X., Lude, Lu. and Wang, X. 2005. Preparation of NiO nanoparticles and their catalytic activity in the thermal decomposition of ammonium perchlorate. Thermochim. Acta, 437: 106-109.

Wardani, M., Yulizar, Y., Abdullah, I. and Apriandanu, D.O.B. 2019. Synthesis of NiO nanoparticles via green route using *Ageratum conyzoides* L. leaf extract and their catalytic activity. IOP Conf. Ser. Mater. Sci. Eng., 509: 012077.

Zhang, Y., Mahdavi, B., Mohammadhosseini, M., Rezaei-Seresht, E., Paydarfard, S., Qorbani, M., Karimian, M., Abbasi, N., Ghaneialvar., H. and Karimi, E. 2021. Green synthesis of NiO nanoparticles using *Calendula officinalis* extract: Chemical characterization, antioxidant, cytotoxicity, and anti-esophageal carcinoma properties. Arab. J. Chem., 14: 103105.

Ziental, D., Czarczynska- Goslinska, B., Mlynarczyk, D. T. Glowacka-Sobotta., A. Stanisz, B., Goslinski., T. and Sobotta, L. 2020. Titanium dioxide nanoparticles: Prospects and applications in medicine. Nanomaterials, 10: 387.

Radiation Tolerant Life Forms and Methods Used to Remediate Radioactive Wastes from Soil

Richa Verma† iD and Anamika Shrivastava iD

Amity Institute of Environmental Sciences (AIES), Amity University, 201313, Noida, Uttar Pradesh, India
†Corresponding author: Richa Verma; vermarich1997@gmail.com

ABSTRACT

The expanding nuclear industry has led to increasing radioactive waste in the environment. Exposure to these wastes causes considerable irreversible damage to the organisms, some of them being even lethal. Conventional methods like incineration, wet oxidation, and acid digestion have been used for radwaste treatment to control this. Apart from them, other organic methods like bioremediation are being widely applied by scientists. Many bacteria, fungi, algae, and plants are observed to possess remediating properties. Hence, these are now used on a large scale to treat the radioactive matter as quickly and effectively as possible. Techniques like bioaccumulation, enzymatic reduction, bioprecipitation, or phytoremediation methods such as phytoextraction and phytostabilization involving such organisms with remedial abilities have successfully removed the radioactive matter to an extent from the contaminated site. Further research is needed to increase the efficiency of the techniques and help remove radionuclides in an environment-friendly manner.

INTRODUCTION

Nuclear energy was used in the 1940s by many military troops and organizations as a new energy source. Seeing the success, it was used widely for military and research purposes such as testing nuclear weaponry, installing weapons for military use, producing nuclear energy, setting up nuclear energy facilities, and mining other radioactive elements. These activities generated huge amounts of waste, almost 90 million gallons (Uzair et al. 2019), including accidental radiation leakages and improper disposal of radioactive wastes. This caused radioactive pollution, exposure to radiation, and other radioactive matter, which had degenerating and lethal effects. To prevent and minimize it, physical methods like barrier construction, solidification, and tilling of fields for radio waste transfer (Ostoich et al. 2022); chemical methods like chemical removal; physical-chemical methods like electrokinetic application, and soil washing have been employed (Yan et al. 2021). Although the above-mentioned techniques have been successful in remediation and are used from time to time, they had limitations such as the high cost of specialized machinery, complex procedures, inefficient for low concentration radio waste removal, risk of perfusion of chemicals used for remediation into the groundwater, permanent biological and physiochemical changes to the soil, causing secondary pollution (Singh et al. 2022). To tackle these limitations, a technique called bioremediation was introduced.

Bioremediation is the method that uses living entities to remove hazardous substances under specified conditions (Dubchak & Bondar 2019) through the organisms' metabolic processes.

In layman's terms, bioremediation is a process to help clean the environment by involving living organisms like plants (called phytoremediation), fungi (mycoremediation), algae (phycoremediation), or enzymes to transform and detoxify the pollutants into less toxic forms (Kumar et al. 2018).

The remediation can be done with different methods, like mycoremediation (Bosco & Mollea 2019), microbe-aided phytoremediation (Dotaniya et al. 2018), nano bioremediation (Cecchin et al. 2017) through omics (Chandran et al. 2020), system biology (Malla et al. 2018) or a combination of inorganic and organic method like electrokinetic bioremediation (Gill et al. 2014).

ORCID details of the authors:

Richa Verma: https://orcid.org/0000-0003-1034-0052
Anamika Shrivastava: https://orcid.org/0000-0003-1201-1885

Bioremediation is advantageous and is preferred over other conventional methods owing to its low cost, low maintenance (Roh et al. 2015), feasibility, and usage of living entities which reduce the involvement and impact of artificially produced substances on the soil, hence cleaner method (Natarajan et al. 2020). The technique has a lot of potential to be used to remove different types of contaminants, including radwaste, much more efficiently. Intensive research on this technique can help to tap into its potential and develop it further.

EFFECT OF RADIOACTIVE WASTES ON ENVIRONMENT AND LIFE FORMS

Exposure to radionuclides can severely affect the life forms' surroundings and bring detrimental changes to them. Alterations in DNA and lesions formation may occur, eventually leading to DNA degradation by direct and indirect mechanisms (Shukla et al. 2017).

Radwaste bioaccumulating in the plants can enter the food chain and can damage the food chain seriously (Dubchak et al. 2019). Longer-living, larger plant species of an area gradually switch to short-living, smaller plants. All this ultimately leads to losing plant species diversity (Geras'kin 2016).

In the ocean, radioactive wastes stored at great depths can still spread in the water due to high radiation exposure of radwaste or leakage by defective sealing (Natarajan et al. 2020). Exposure to nearby organisms or consumption of such water by the organism can cause grave damage to the health of those organisms. Both terrestrial and aquatic biotas are unsuitable for dumping radioactive wastes.

In humans, low-intensity exposures cause mild skin irritation, but if the exposure continues for a longer time, it can cause hair loss, nausea, dizziness, vomiting, diarrhea, etc. Continuous exposure can lead the person to experience weakness, fatigue, fever, disorientation, low blood pressure, blood in stool, and eventually death (Kaushik et al. 2021).

High-intensity radiation exposure for long durations can cause leucopenia, leukemia, and kidney damage. Skin, lung, and thyroid cancers are some of the diseases also caused by radiation (Kautsky et al. 2013). It also causes irreversible damage like DNA mutations which can pass to future generations. Fetuses are especially susceptible to radiation since contact with radionuclides can cause organ malfunction like poorly formed eyes, smaller brain size or head, mental retardation and abnormal growth, solid childhood cancer, and other congenital disorders (Tang et al. 2018).

The most significant examples are the cases of atomic bomb survivors of Hiroshima and Nagasaki, where nearly 70,000 pregnancies were affected. Some lead to stillborn infants dying within the first 2 weeks or are born deformed with chromosomal aberrations (Brent 2015). The effect can be seen even after 65 years.

RADIONUCLIDES WHEN PRESENT IN SOIL

Radioactive wastes are usually present in minute concentrations in the soil. Depending upon the amount of radwastes, the method and organism are chosen for treatment. For soil with concentrations ranging from 10 μCi of $^{137}Csg^{-1}$ to 20 μCi of $^{137}Csg^{-1}$, microbes like *Rhodococcus*, *Nocardia*, or *Deinococcus radiodurans* are used, whereas concentrations greater than 20 μCi of $^{137}Csg^{-1}$, *Pseudomonas putida*, *Shewanella putrefaciencs* or *Deinococcus radiodurans* are preferred (Shukla et al. 2017). Naturally, radionuclides occur in various forms at different locations around the world. For example, ^{232}Th occurs as monazite rock deposits in Guarapari, Brazil, and Kerela, India, whereas ^{222}Rn is present in the hot springs of Ramsar, Iran (Ostoich et al. 2022).

In India, few regions are exposed to different radionuclides. For example, in South Konkan village, the occurrence of ^{238}U, ^{232}Th, and ^4K has caused the soil's radiation level to be $68.08 * 10^{-9}$ Svh^{-1}. In Gujarat, the presence of U and Th in the groundwater of Thar Desert and Th and Ca from Naredi Cliff has been observed (Sahay et al. 2015). In the soils of Jodhpur and Nagaur regions of Rajasthan, natural radionuclides such as ^{226}Ra, ^{232}Th, and ^{40}K are present (Rani et al. 2015).

In Jharkhand, mining and milling from the Jaduguda uranium mine into the Bay of Bengal has accounted for emitting alpha particles affecting indigenous microbial populations (Patnaik et al. 2018).

TECHNIQUES OF BIOREMEDIATION

In the case of microbial remediation, the metabolic activity of a microorganism determines the degree to which toxic waste is degraded (Natarajan et al. 2020). Effective bioremediation depends on physical, chemical, and biological interaction (Roh et al. 2015, Sengupta et al. 2021). Environmental factors favorable to microbial and plant growth also influence the process, and proper conditions can lead to the remediation process much faster (Dubchak & Bondar 2019). Different methods are performed considering all the above criteria and the organisms engaged. Some of them are discussed below.

Direct and indirect enzymatic reduction: Selecting either method depends on the site's radionuclide presence and soil conditions (Francis & Nancharaiah 2015).

In the direct method, bacteria reduce the organic compounds (substrate) to release electrons which are used to transform oxidized, soluble, and mobile forms of radionuclides (for example, U, Cr, or Tc) into reduced, insoluble, and their respective immobile forms (Shukla et al. 2017). In vitro, Uranium precipitation is exhibited in *Shewanella putrefaciens* on its surface and with hydrogenase combination (as electron donor) in the case of *Desulfovibrio vulgaris* (Jabbar & Wallner 2015). This technique is also applied for reduction of Pu(VI) and Pu(V) to Pu(IV) by *S. putrefaciens*, *G. metallireducens* and *B. subtilis* (Natarajan et al. 2020).

In the Indirect Method, mostly lithotrophic-type bacteria reduce the substance, leading to the reduction of radionuclides. Indirect reduction of soluble contaminants is triggered in belowground and sedimentary environments by sulfate-reducing or metal-reducing microorganisms. An example of a microbe is *Microbacterium flavescens*, used for remediating U-, Th-, and Pu-contaminated soils (Jabbar & Wallner 2015).

Bioaccumulation: Bioaccumulation is the deposition of the radionuclides within the organism (Francis & Nancharaiah 2015) and comprises the phenomenon of bioconcentration and biomagnification (Shukla et al. 2017). It relies on the property of adsorption of radioactive matter on the cell surface of the microbe owing to prevailing electrostatic forces of attraction between the metal cations of radionuclides and the negatively charged cell surface, leading to their binding (Ayansina et al. 2017). This makes removing radionuclides easier and thus prevents leakage (Natarajan et al. 2020). The process can be either active or passive. Active bioaccumulation needs more energy and takes much time. Passive bioaccumulation consumes lesser energy and is relatively faster (Ding et al. 2019). It is best for areas with nutrient limitations. The process was reported for radionuclides like plutonium, cesium-137, americium, strontium-85, radium, Thorium, and cobalt-60. Some of the Gram-positive bacteria, like *Bacillus* sp. (Zhao 2016) And Cyanobacteria like *Arthrospira* (*Spirulina*) *platensis* (Zinicovscaia et al. 2020) indicated the potential for bioremediation by this method. Uranium bioaccumulation in *Pseudomonas* has also been observed (Mahadevan et al. 2017).

Biosorption: The phenomenon of biosorption is described as "The sequestration of positively charged metal ions to the negatively charged cell membranes and polysaccharides secreted on the outer surfaces of bacteria" (Shukla et al. 2017). It immobilizes the radionuclide present and can occur either directly, by nuclide cation interaction with functional groups which have anionic cell walls, or indirectly with EPS, S-layer, or capsule (Chauhan et al. 2021). It is a passive uptake process (Dey et al. 2021). Pu, Np, U, and Th are some radionuclides that can bind onto the cell surface with the help of ligands like amine, carboxyl, phosphate, hydroxyl, and sulfhydryl (Mahadevan et al. 2017). The process is species-specific, i.e., depends on the ligands attached, and is affected by factors such as temperature, aeration, pH, the growth phase of cells, presence of organic or inorganic content and metabolites, secretion or production of exopolymers (Ding et al. 2019). Other factors include the chemical interaction of extracellular biopolymers, functional groups, metal ions, and electrostatic attraction (Dobrowolski et al. 2017). *Pseudomonas* strain is one example that can biosorp U and Th ions through intracellular sequestration (Natarajan et al. 2020). Few bacteria and algal cultures were reported to retain strontium through biosorption (Francis & Nancharaiah 2015). These are shown in Table 1.

Biotransformation/Bioreduction: Biotransformation occurs through various mechanisms: metal oxidation-reduction, changes in pH, solubilization and leaching, volatilization, immobilization, remobilization, or alteration of metal-radionuclide complexes (Francis & Nancharaiah 2015). Bacterial transformations occur through basic chemical processes which direct the formation of co-precipitates, oxides, and organic, inorganic, and ionic complexes of radionuclides (Ding et al. 2019). Different types of bacteria, aerobic or anaerobic (that are actively growing), retain the ability to transform through redox reactions. In most cases, nuclides that are non-sorptive are transformed non-enzymatically or enzymatically (Shukla et al. 2017). It was observed that triheme periplasmic cytochrome type-c has a key role in biotransformation (Jabbar et al. 2015). For U (VI) bioremediation, bacterial groups like acid-tolerant, fermentative, and sulfate-reducing bacteria can act as alternative electron acceptors (Mahadevan et al. 2017). Ecological conditions, electron donors and acceptors, and supplements can affect microbial activity during biotransformation (Uzair et al. 2019).

Some known examples are *Geobacter sulfurreducens* (Vogel et al. 2018) strain PCA, *Shewanella putrefaciencs* strain CN-32, and *Anaeromyxobacter dehalogenans* strain K.

Bioleaching: Also called biomining or bio solubilization involves leaching out of radionuclides from their compact matrices (Qiu et al. 2019). It is not a direct solubilization method, and the energy here is obtained in autotrophic bacteria from reduced Fe or S compounds while simultaneously solubilizing the metals and nuclides. It needs components like moisture, acidic pH, and oxygen to oxidize Fe or S and filter out metals in sulfide form (Shukla et al. 2017). These bacterial types are acidophilic and mesophilic in nature (Srichandan et al. 2019). Scientists have reported

Table 1: Radionuclide-microorganism interaction of certain radioactive elements.

Radionuclide	Microorganism	Type of Interaction	Reference
Hydrogen Uranyl Phosphate (HUP)	*Serratia* sp.	Precipitation via the activity of a high radio-stable phosphatase enzyme.	Lopez-Fernandez et al. (2021)
Strontium ^{90}Sr	*Bacillus* sp	Accumulation into biogenic carbonate minerals.	
	Cyanobacteria	Accumulation into calcium carbonates.	
Technetium ^{99}Tc	*Geobacter sulfurreducens* and *Shewanella oneidensis*	Bacterial accumulation.	
Thorium ^{232}Th	*Streptomyces sporoverrucosus*	pH and ionic strength-dependent biosorption in living and dead cells of the organism.	
Neptunium ^{237}Np	*Shewanella* sp.	Biosorption by whole cells, the cell wall, and extracellular polymeric substances of algae.	
Uranium ^{238}U ^{235}U	*Pseudomonas aeruginosa*, *Staphylococcus aureus*, *Gallionella*, *Bacillus* and *Sphingomonas*	Biomineralization by passive sorption on cell wall extracellular polymers and secretion of phosphate groups.	
	Stenotrophomonas sp.	Immobilization using phosphatase enzymes under changing environmental conditions.	
Plutonium ^{239}Pu	*Pseudomonas* sp.	Influencing the redox cycling and mobility of Pu in the environment as a reductant and sorbent.	
	Saccharomyces cerevisiae	Sorption from aqueous radionuclide solutions at pH 1-2 by immobilized algae.	
Americium ^{241}Am	*Saccharomyces cerevisiae*		
Cerium ^{140}Ce	*Saccharomyces cerevisiae*		
Curium ^{242}Cm	*Rhodotorula mucilaginosa*	Reversible and pH-dependent biosorption.	

Acidithiobacillus ferrooxidans (Mao et al. 2015), *Sulfolobus* (Reitz et al. 2015), and *Acetobacter* sp. (Qu et al. 2019) as microbes that can solubilize metals. The process is affected by microbial activity, physical factors like pH surrounding the bacteria, moisture, oxidation state of the nuclide, and inorganic content as substrate needed for the bacteria (Kaksonen et al. 2017). A vital bacterial metabolite, the presence of citrate also enhances the solubility of nuclides.

Bioprecipitation: This occurs after converting a nuclide from soluble to insoluble (Sahinkaya et al. 2017). It is achieved by carrying out oxidative and reductive reactions leading to precipitation. Precipitation of radionuclides and metals happens largely in carbonates or hydroxides form (Shukla et al. 2017). The site where precipitation occurs in a microbial cell is the 'nucleation site,' and the precipitation process in it depends on the ligand concentration produced by the cell (Shukla et al. 2017). Microbial ligand production, biogenic mineral formation (Jabbar & Wallner 2015), valence, and oxidation state of the radionuclide are important factors of bio precipitation. Secretions from bacteria and metabolism can cause changes in pH in its immediate surroundings, hence, changing the pH of the area adjoining the metal in the process. Co-precipitation is a phenomenon related to

it where elements amalgamate in minerals of metal oxide during precipitation. The method has been investigated for removing Strontium (Francis & Nancharaiah 2015), Uranium (Xu 2018). *Shewanella putrefaciens* is known for successful U(VI) bioprecipitation (Huang et al. 2017).

Biomineralization: The method uses living organisms like fungi, microalgae, bacteria, protozoa, or cyanobacteria to form minerals (Ding et al. 2019). It can be of two types: biologically controlled biomineralization (BCM) or biologically induced biomineralization (BIM) (Singh et al. 2021). This depends on temperature, pH, ions, enzyme activity, and humic substances (Jiang et al. 2020). It often leads to stiffening and hardening of the mineralized contaminants, which are later removed separately, so it lessens soil contamination. In the case of fungi, many microbial biomineralization formations are supplemented by sorptive interactions and fungal mycelium branching for a strong metal removal system (Gadd & Pan 2016). The method is attempted to remove toxic radioisotopes like Tc by flow through biostimulated sediment column bioreactors at even minute concentrations (Thorpe et al. 2016). Biomineralization for U(VI) is possible with the help of *Kocuria* sp. (Wang et al. 2019) and *Saccharomyces*

cerevisiae (Zheng et al. 2017). *Serratia* sp. relies on the synthesis of crystalline hydroxyapatite to be used later to recover Eu and Sr (Gangappa et al. 2016).

Genetically modified organisms: Recombinant DNA technology and genetic engineering are employed to generate tailor-made organisms, which increase their biodegradation potential and therefore help in the successful remediation of radwaste (Kumar et al. 2018). This method generates different protein constructs with genes with desired traits and properties for remediation. These genes of interest are then combined in a single bacterial cell with improved metal binding properties and high adsorption capacity (Omran 2021). Finally, they accumulate metal ions by sorption. One example is *Deinococcus radiodurans*, a microorganism observed to tolerate ionizing radiations up to $10*10^3$ Sv (Shukla et al. 2017) and is currently known as the most radiation-tolerant organism. It is an extremophilic bacterium that can thrive under high temperatures, low nutrients, and high radiation exposure (Manobala et al. 2019) by producing several copies of its genome and performing DNA repair mechanisms when required (Natarajan et al. 2020). This microbe is genetically engineered and then used for remediation purposes. It converts volatile and highly toxic metals into less mobile and toxic forms. It remediates the radionuclides through biofilm formation (Shukla et al. 2017). Genetically engineered *Pseudomonas aeruginosa* (Tapadar et al. 2021) and *E. coli* strain with genes from *Serratia marcescens* and *Helicobacter pylori* (Uzair et al. 2019) have also been experimented with to successfully remove uranium through precipitation and sorption, respectively.

Omics-Implemented bioremediation: It takes into account the genomic structure of the remediating organisms. Data regarding catabolic genes, enzymes, or proteins with bioremediating capabilities are taken from proteomics, metabolomics, transcriptomics, metagenomics, and functional genomics (Upadhyay et al. 2019). These are then identified and isolated for further bioremediation processes. Metagenomics is the study of genetic matter taken from the environment, which has the potential for bioremediation (Sengupta et al. 2021). Proteomics is the study of proteins through biochemical means (Dey et al. 2021). The combination of the above studies helps to obtain efficient strains of microbes and increase the metabolism of the contaminants (Malla et al. 2018). Many microorganisms' genome sequencing and profiling have been conducted. For example, transcriptional profiling of *Shewanella oneidensis* (known to contain co-metabolic pathways) was performed during U(VI) reduction (Wang et al. 2017a, 2017b). A biomarker of *G. sulfurreducens* activity was also developed through proteogenomic analysis for Uranium bioremediation (Marques 2018).

With improving technology, more progress can be made in this direction. Next-generation sequencing allows enhanced expression of desirable genes and proteins (Fonti et al. 2015). Genome-wide transcriptome methods lead to better analysis of metabolic pathways and physiology of the microbes (Lourenço et al. 2019). Integrating all the information gathered related to the properties and functions of microbes helps in their improved selection during the bioremediation process.

PROCESSES SIMILAR TO BIOREMEDIATION

Biostimulation: Here environmental conditions are optimized to encourage the growth of existing bioremediating microbial populations. It is done by adding rate-limiting nutrients or electron acceptors like oxygen, nitrogen, carbon, or phosphorous (Tribedi et al. 2018), modifying physical factors like pH, temperature, aeration, etc. (Mallavarapu et al. 2020) to stimulate the growth of present microscopic assemblage for degradation of radionuclides. These micro-organisms then help in bioremediation of toxicants. A biostimulation experiment by UMTRA, Colorado, confirmed the precipitation of U(IV) by adding acetate as an electron donor (Roh et al. 2015). Since the method accelerates the development of indigenous or non-indigenous microbes for bioremediation purposes, it comes under 'enhanced bioremediation' (Kumar et al. 2018). The method is advantageous for low-cost and native microbial population exploitation without adding allochthonous species (Bosco & Mollea 2019). Care must be taken when adding nutrients since they should be evenly distributed and readily available to the subsurface microbes. Also, the surface should be permeable with no cracks or fractures (Jayaprakash et al. 2019). *Arthrobacter ilicis* and *Geobacter* have been identified to remove radionuclides like U(VI), Pu(IV), Tc(VII), and Np(V) through biostimulation (Shukla et al. 2017).

Bioaugmentation: The method is executed when the native microbial population present at the contamination site is unable to degrade the pollutants (Mallavarapu et al. 2020). In this method, microorganisms are added to enhance and speed up the degradation process of pollutants (Xu 2018). Microbes with high catabolic potential are generally added (Agnello et al. 2016). This is done by (i) adding pre-modified bacteria, (ii) adding pre-modified consortium, (iii) adding relevant genes in microbes for biodegradation (iv) introducing genetically modified bacteria (Upadhyay et al. 2019). The microbes introduced should retain genetic stability and viability during storage, withstand harsh conditions, and adapt to a foreign environment. Nutrient content, moisture, aeration, pH, and soil type can affect the

efficiency of bioaugmentation (Jayaprakash et al. 2019). It is applied with biostimulation and comes under 'enhanced bioremediation' (Kumar et al. 2018).

Through the above processes of crystallization and precipitation of immobile and insoluble compounds by micro (or macro) organisms, metal biorecovery is possible.

Phytoremediation: Bioremediation done by plants is phytoremediation. It is a subcategory that includes plants, accompanied by rhizospheric and endophytic microbes, to remove the contamination in soil, sediments, sludge, and ground or surface water and clean the environment (Kumar et al. 2018). It considers plants' natural ability to uptake or absorb radioactive contaminants through roots and translocation to the upper part of the plant (Sharma et al. 2015). It thus uses this as an advantage to reduce its toxicity. These plants range from hyperaccumulators (e.g., *Helianthus*) to bio-accumulators (Dubchak & Bondar 2019).

It is a cost-effective practice since the expenditure is less than that of conventional methods, and it is environmentally friendly, as it preserves the environment in its natural state. The recovery and reusability rate of valuable metals is higher. Also, the plants can be easily monitored, and the progress can be tracked down (Eskander & Saleh 2017). Its extensive use was started in the 1990s by researchers and US Environment Protection Agency (Shmaefsky 2020). Since then, it has been employed in the sites contaminated by U, Th, and Ra (Natarajan et al. 2020).

Phytoextraction: Also called Phytosequestration, Phytoaccumulation, or Phyto absorption, this technique utilizes the plant's ability to pick up contaminants from the soil and transfer them to the harvestable parts of the plant (Natarajan et al. 2020), which can be obtained later by harvesting the incinerating or composting the particular plant (Kumar et al. 2018). It removes the toxins from the soil by not disturbing the soil structure and impacting little on soil fertility. For this method, fast growing plants are used that (i) can produce large quantities of plant biomass (ii) have capacity to tolerate and extract radionuclides at high concentrations (iii) are able to translocate the radionuclides to the plant biomass (Sheoran & Sheoran 2017). These plants are called hyperaccumulators and are known to accumulate toxicants at a concentration 100 times greater than what a normal plant would accumulate (Sheoran et al. 2016). The contaminants extracted are much smaller than the initial quantity in the soil or sediment. Hence, it is best suitable for areas of low-level contamination (Dubchak & Bondar 2019). The efficiency of the process also depends upon the bioavailability of the radioactive pollutants present (Khan et al. 2020). It is popularly employed for ^{137}Cs, ^{90}Sr, and $^{235,238}U$ (Dijoo et al. 2020). Research has been done on Catharanthus

(for ^{137}Cs), Cannabis (for ^{90}Sr), Festuca, and Zea (for ^{222}Rn and ^{226}Ra) (Filippis 2015).

Rhizofiltration: It is specified for wastewater where the roots of plants are used to concentrate and precipitate radionuclides from that wastewater (Kumar et al. 2018). This can be done ex-situ or in situ, where plants (preferably hydrophytes) are grown hydroponically and, after their growth, relocated to a polluted water stream (Sharma et al. 2015) or grown straight into the water body polluted by radioactive effluent. For this technique, plants with rapidly growing root systems are chosen (Natarajan et al. 2020). Scientists thought of using several ponds in the sequence where the water flow rate is set to be slow to clean water contaminated by radionuclides (Dubchak & Bondar 2019). This permits relatively cheaper procedures with low capital costs. Water, sludge, and plant samples were taken regularly from all the parts of that system created to calculate the complete mass balance of radioactivity. It was later calculated that such a system removed 99.3% of the radioactivity. This approach was used for ^{90}Sr and ^{137}Cs and U removal from water (Filippis 2015) and is most effective in U removal. Nowadays, seedlings (blastofiltration) or excised plant shoots (caulofiltration) are used to remove contaminants from streams (Rezania et al. 2020). *Helianthus annuus L.* is a suitable plant that can remove 80% of the U within 24 hours from the contaminated water (Tonelli et al. 2020). *Phragmites australis* (Wang & Dudel and *Phleum pratense* (Mikheev et al. 2017) are also known for U and Cs remediation, respectively. One limitation of this process is that it can't extract the contaminant below the rooting depth. Also, proper care and maintenance are required since the plants can become a potential radiation source while extracting the contaminants from the soil.

Phytovolatilization: The method uses the plants to convert the toxicants into volatile forms to be discharged into the atmosphere (Kumar et al. 2018). It can be direct (through stems and leaves) or indirect (through roots) (Limmer & Burken 2016). It is used for ^3H, i.e., Tritium remediation, which is a radioactive isotope of Hydrogen with a half-life of 12 years approx., decaying into stable helium. Experiments conducted showed that reduction in radioactive Tritium (up to 40%) could be accomplished by releasing the titrated water into the atmosphere in water vapor form since it gets easily isolated by air and emits almost no exposure externally instead of flowing it in surface water streams near the sites (Dubchak & Bondar 2019). Commonly phreatophytes that are deep-rooted and have high transpiration capacity are deployed for this type of remediation (Khan et al. 2020), providing a system with enhanced evapo – transpiration and hydraulic control. *Typha latifolia* is one of the few plants apt for Selenium decontamination (Tonelli et al. 2020). The

plant enzymes convert the inorganic Se to different volatile forms, like dimethyl selenide and dimethyl selenone (Sharma et al. 2015).

Phytostabilization: It focuses on the stabilization and storage of radionuclides for longer durations. It is based on radionuclides sequestration in the soil near the area of roots (Tonelli et al. 2020) but not in the tissues of the plants. Since the contaminants are stored in the root area, they become less available to livestock, wildlife, and humans, and the exposure is greatly reduced (Natarajan et al. 2020). Additionally, the phytostabilizing plants can reduce soil water and wind erosion and thus prevent radwaste's dispersal into dust particles, runoff, or leachate (Filippis 2015). The technique requires a dense root system to stabilize the soil and minimize water percolation, preventing soil erosion and radionuclide leaching (Dubchak & Bondar 2019). Green plants which are deep-rooted and fast-growing (e.g., *Cyprus*) are preferred since they reduce the stabilization process to large amounts (Sharma et al. 2015). This method has been used to stabilize U mine tailings (Wetle et al. 2020). *Cannabis sativa* L. and *Vetiveria (Chrysopogon) zizanioides* are a few plants used at mine tailings for phytostabilization of U and Cs, respectively (Khan 2020). Some of the plants known for phytoremediation of certain radionuclides are listed in Table 2.

Mycoremediation: Remediation by fungi is known as mycoremediation. It was first observed in Chernobyl Nuclear Power Station, where few fungi could generate spores. It was degrading and feeding on the soil contaminated by high Co, Pu, and C concentrations. Many species of fungi are observed to be able to remediate radionuclides from soil. These were later called radiotrophic fungi (Júnior et al. 2020).

The fungi remediate in the form of arbuscular mycorrhizae by forming associations like ectomycorrhizae or in any other way to immobilize the radionuclides, which are then taken up by plants (Sharma et al. 2015). The physicochemical properties of fungal cell walls play a key factor in radionuclide immobilization (Dighton 2019). Other factors include temperature, moisture, assembly, and activity of the microbial population, soil conditions like type, organic matter amount, and water availability (Kapahi & Sachdeva 2017). The cost-effectiveness, low maintenance, and ubiquitous nature of most fungi species allow their widespread use for bioremediation (Jain et al. 2017). *Aspergillus niger* and *Rhizopus arrhizus* can remove Thorium through mycoremediation (Francis & Nancharaiah 2015). Oyster mushrooms are also known to be bioremediated Plutonium-239 and Americium-241 (Dubchak

Table 2: Higher plant species and algal species-appropriate in phyto/phycoremediation of radionuclide contaminated sites.

Algae/Higher plants	Species Name	Radionuclide	References
Algae	*Oedogonium* sp.	^{90}Sr	Iwamoto and Minoda (2018)
	Ophiocytium sp.	^{125}I	Iwamoto and Minoda (2018)
	Vacuoliviride crystalliferum, *Galdieria sulphuraria*	^{137}Cs	Iwamoto and Minoda (2018)
	Cladophora, Oedogonium, Rhizoclonium	^{238}U	Kumar and Kundu (2020)
Higher plants	*Egeria densa, Euphorbia macroclada, Astragalus gummifer, Verbascum cheiranthifolium, Phaseolus acutifolius*	^{90}Sr	Iwamoto and Minoda (2018)
	Pinus radiata, Pinus ponderosa	^{90}Sr	Dighton et al. 2019
	Amaranthus retroflexus, Beta vulgaris, Brassica napus, Chenopodium quinoa	^{137}Cs	Iwamoto and Minoda (2018)

Table 3: List of certain fungal species known to remediate radionuclides from contaminated sites.

Fungi species	Radionuclides	References
Penicillium sp.	^{90}Sr, ^{238}U, ^{232}Th	Lopez-Fernandez et al. 2021
Pleurotus eringii	^{34}Cs, ^{137}Cs, ^{85}Sr	
Hebeloma cylindrocarpon	^{90}Sr	
Cortinaraiacea sp.	^{137}Cs	
Serratia sp.	^{137}Cs, ^{90}Sr, ^{60}Co	
Boletus, Paxillus, Tylopilus, Lactarius rufus, Leccinum, Amanita, Cortinarius, Suillus variagatus	^{137}Cs	
Aspergillus niger and *Paecilomyces javanicus*	^{238}U	
Rhizopus sp.	^{241}Am, ^{144}Ce, ^{147}Pm, $^{152+154}$Eu, ^{233}U, ^{230}Pu	

& Bondar 2019). A few of the fungal species known for mycoremediation are given in Table 3.

LIMITATIONS OF BIOREMEDIATION AND PHYTOREMEDIATION

Although the above-discussed methods show many prospects for their uses, they still face some challenges. Bioremediation has high specificity, i.e., we can't use every plant for any given remediation method (Dubchak & Bondar 2019). These are based on the properties and compatibility of both organisms and toxicants. Since naturally occurring life forms are involved, the procedure will take comparatively longer (Butnariu & Butu 2020). Also, no method can 100% remediate the soil; some minute amount of radwaste can still be left in the soil (Kumar et al. 2018).

In the case of phytoremediation, the area and depth covered by the roots of the plant pose a limitation to the remediation process (Khan et al. 2020). Again, due to less biomass and slower growth of plants, more time will be taken (Sheoran & Sheoran 2017). The remediation can continue as long as the plant survives in the soil, i.e., proper maintenance and cultivation of plants are essential (Filippis 2015). Successful lab phytoremediation experiments do not guarantee the same success rate at the practical field level (Yadav et al. 2018). Extreme caution is required to handle and dispose of contaminated plants (Farraji et al. 2016).

FUTURE PROSPECTS

Many aspects of bioremediation are explored by the continuous efforts of researchers and scientists, such as electrokinetic remediation (Cameselle 2015), algal remediation (Iwamoto & Minoda 2018), etc. These methods will be used for bioremediation purposes in the future. Numerous organisms with potential bioremediating properties are now discovered, which will be applied to the process in the coming days. These would be either used naturally or may be genetically transformed (called transgenic plants) into better radio-tolerant forms which can perform the procedure effectively. Various branches of science are participating to improve the chances of bioremediation. Geophysics is one of them, which uses geophysical monitoring to supervise the contaminated soils and analyze the changes occurring so. This is started for in situ bioremediation projects for consistent data collection which helps in real-time monitoring (Nivorlis 2019). Within the next few years, it can become essential for bioremediation monitoring.

CONCLUSION

Bioremediation and Phytoremediation methods are fast-

growing and popularly used for radioactive waste removal or treatment. Being organic methods, which does not produce any side effect while performing the process and are cost-effective simultaneously, gives them an advantage. Hence their popularity is increasing. With advancing time, scientists are searching for more organisms (microbes, fungi, or plants) that can be used naturally or by genetic modifications. They can successfully remediate radioactive wastes by any means. The existing biotechnological methods are also enhanced with improving technology for better remediation results. In phytoremediation, plants native to the contaminated area are looked for as they will have the least external input. After remediation, they should be removed, or they might decompose into the contaminated soil. The most used way is to incinerate the ground and use ashes for disposal. Microbial remediation has enormous potential to control the activity and solubility of radioactive matter. New tolerant microbes are discovered that can withstand the wastes of extreme radioactive toxicity. These microbes can be employed in the future, boosting the remediation process and radioactive waste removal rate. Research on this field should be more to find out more ways of effective remediation. New and improvised techniques will be developed only when different science disciplines collaborate and work together.

REFERENCES

Adams, G.O., Fufeyin, P.T., Okoro, S.E. and Ehinomen, I. 2015. Bioremediation, biostimulation, and bioaugmentation: a review. Int. J. Environ. Bioremed. Biodegrad., 3(1): 28-39.

Agnello, A.C., Bagard, M., van Hullebusch, E.D., Esposito, G. and Huguenot, D. 2016. Comparative bioremediation of heavy metals and petroleum hydrocarbons co-contaminated soil by natural attenuation, phytoremediation, bioaugmentation, and bioaugmentation-assisted phytoremediation. Sci. Total Environ., 563-564: 693-703. https://doi.org/10.1016/j.scitotenv.2015.10.061

Ayangbenro, A.S. and Babalola, O.O. 2017. A new strategy for heavy metal polluted environments: a review of microbial biosorbents. Int. J. Environ. Res. Public Health, 14(1): 94. https://doi.org/10.3390/ijerph14010094

Azubuike, C.C., Chikere, C.B. and Okpokwasili, G.C. 2016. Bioremediation techniques–classification based on site of application: principles, advantages, limitations, and prospects. World J. Microbiol. Biotechnol., 32(11): 1-18. https://doi.org/10.1007/s11274-016-2137-x

Bosco, F. and Mollea, C. 2019. Mycoremediation in soil. Environ. Chem. Recent Pollut. Control. 8: 477. http://dx.doi.org/10.5772/intechopen.84777

Brent, R.L. 2015. Protection of the gametes embryo/fetus from prenatal radiation exposure. Health Phys., 108(2): 242-274.

Shmaefsky, B.R. 2020. Principles of Phytoremediation: Phytoremediation, Concepts, and Strategies in Plant Sciences. Springer, Cham, pp. 1-19. https://doi.org/10.1007/978-3-030-00099-8_1

Butnariu, M. and Butu A. 2020. Viability of in Situ and Ex Situ Bioremediation Approaches for Degradation of Noxious Substances in Stressed Environs. In Bhat, R.A. and Hakeem. K.R. (eds.), Bioremediation and Biotechnology, vol 4, Springer, Singapore, pp. 167-223. https://doi.org/10.1007/978-3-030-48690-7_8

Cameselle, C. 2015. Electrokinetic remediation and other physico-chemical remediation techniques for in situ treatment of soil from contaminated nuclear and NORM sites. In Environmental remediation and restoration of contaminated nuclear and NORM sites (pp. 161-184). Woodhead Publishing. https://doi.org/10.1016/B978-1-78242-231-0.00008-9

Cecchin, I., Reddy, K.R., Thomé, A., Tessaro, E.F. and Schnaid, F. 2017. Nanobioremediation: Integration of nanoparticles and bioremediation for sustainable remediation of chlorinated organic contaminants in soils. Int. Biodeter. Biodegrad., 119: 419-428. https://doi.org/10.1016/j.ibiod.2016.09.027

Chandran, H., Meena, M. and Sharma, K. 2020. Microbial biodiversity and bioremediation assessment through omics approaches. Front. Environ. Chem., 1: 9. https://doi.org/10.3389/fenvc.2020.570326

Chauhan, R., Patel, H. and Rawat, S. 2021. Biosorption of Carcinogenic Heavy Metals by Bacteria: Role and Mechanism. In Removal of Emerging Contaminants through Microbial Processes. Springer, Singapore, pp. 237-263. https://doi.org/10.1007/978-981-15-5901-3_12

Dey, P., Gola, D., Chauhan, N., Bharti, R.K. and Malik, A. 2021. Mechanistic Insight to Bioremediation of Hazardous Metals and Pesticides from Water Bodies by Microbes. In Shah, M.P. (ed), Removal of Emerging Contaminants through Microbial Processes, Springer, Singapore, pp. 467-487. https://doi.org/10.1007/978-981-15-5901-3_23

Dighton, J. 2019. Fungi and remediation of radionuclide pollution. In Campocosio, A.T. and Santiesteban, H.H.L. (eds), Fungal Bioremediation: Fundamentals and Applications, CRC Press, Boca Raton, Florida, pp. 84-110. https://doi.org/10.1201/9781315205984

Dijoo Z.K., Ali R. and Hameed M. 2020. 'Role of Free-Floating Aquatic Macrophytes in Abatement of the Disturbed Environs. Bhat, R.A. and Hakeem, K.R. (eds.), Bioremediation and Biotechnology, Springer, Cham, pp. 259-268. http://dx.doi.org/10.1007/978-3-030-48690-7_12

Ding, C., Cheng, W. and Nie, X. 2019. Microorganisms and radionuclides. Interface Sci. Technol., 29: 107-139. https://doi.org/10.1016/B978-0-08-102727-1.00003-0

Dobrowolski, R., Szczes, A., Czemierska, M. and Jarosz-Wikołazka, A. 2017. Studies of cadmium (II), lead (II), nickel (II), cobalt (II), and chromium (VI) sorption on extracellular polymeric substances produced by Rhodococcus opacus and Rhodococcus rhodochrous. Bioresour. Technol., 225: 113-120. https://doi.org/10.1016/j.biortech.2016.11.040

Dotaniya, M.L., Rajendiran, S., Dotaniya, C.K., Solanki, P., Meena, V.D., Saha, J.K. and Patra, A.K. 2018. Microbial-assisted phytoremediation for heavy metal contaminated soils. In Kumar, V., Kumar, M. and Prasad, R. (eds), Phytobiont and Ecosystem Restitution. Springer, Singapore, pp. 295-317. http://dx.doi.org/10.1007/978-981-13-1187-1_16

Dubchak, S. and Bondar, O. 2019. Bioremediation and Phytoremediation: Best Approach for Rehabilitation of Soils for Future Use. In Gupta, D.K.G. and Voronina, A. (eds), Remediation Measures For Radioactively Contaminated Areas. Springer, Cham, pp. 201-221. https://doi.org/10.1007/978-3-319-73398-2_9

Eskander, S. and Saleh, H. 2017. Phytoremediation: An overview. Environ. Sci. Eng. Soil Pollut. Phytoreme., 11:s 124-161.

Farraji, H., Zaman, N.Q., Tajuddin, R. and Faraji, H. 2016. Advantages and disadvantages of phytoremediation: A concise review. Int. J. Env. Tech. Sci., 2: 69-75.

Filippis, M. 2020. Role of Phytoremediation in Radioactive Waste Treatment. In Hakeem, K., Sabir, M., Ozturk, M. and Mermut, A.R. (eds), Soil Remediation and Plants: Prospects and Challenges, Elsevier, The Netherlands, pp. 207-254. http://dx.doi.org/10.1016/B978-0-12-799937-1.00008-5

Fonti, V., Beolchini, F., Rocchetti, L. and Dell'Anno, A. 2015. Bioremediation of contaminated marine sediments can enhance metal mobility due to changes in bacterial diversity. Water Res., 68: 637-650. https://doi.org/10.1016/j.watres.2014.10.035

Francis, A.J. and Nancharaiah, Y.V. 2015. In Situ And Ex Situ Bioremediation Of Radionuclide-Contaminated Soils at Nuclear and NORM Sites. In Leo Van, V. (ed.), Environmental Remediation and Restoration of Contaminated Nuclear and Norm Sites, Springer, Cham., pp. 185-235. https://doi.org/10.1016/B978-1-78242-231-0.00009-0

Gadd, G.M. and Pan, X. 2016. Biomineralization, bioremediation, and biorecovery of toxic metals and radionuclides. https://doi.org/10.1080/01490451.2015.1087603

Gangappa, R., Yong, P., Singh, S., Mikheenko, I., Murray, A.J. and Macaskie, L.E. 2016. Hydroxyapatite biosynthesis by a Serratia sp. and application of nanoscale bio-HA in the recovery of strontium and europium. Geomicrobiology Journal, 33(3-4): 267-273. https://doi.org/10.1080/01490451.2015.1067657

Geras'kin, S. A. (2016). Ecological effects of exposure to enhanced levels of ionizing radiation. Journal of Environmental Radioactivity, 162: 347-357. https://doi.org/10.1016/j.jenvrad.2016.06.012

Gill, R.T., Harbottle, M.J., Smith, J.W.N. and Thornton, S.F. 2014. Electrokinetic-enhanced bioremediation of organic contaminants: A review of processes and environmental applications. Chemosphere, 107: 31-42. https://doi.org/10.1016/j.chemosphere.2014.03.019

Holmes, D.E., Giloteaux, L., Chaurasia, A.K., Williams, K.H., Luef, B., Wilkins, M.J., Wrighton, K.C., Thompson, C.A., Comolli, L.R. and Lovley, D.R. 2015. Evidence of Geobacter-associated phage in a uranium-contaminated aquifer. ISME J., 9(2): 333-346. https://doi.org/10.1038/ismej.2014.128

Huang, W., Nie, X., Dong, F., Ding, C., Huang, R., Qin, Y., Liu, M. and Sun, S. 2017. Kinetics and pH-dependent uranium bioprecipitation by Shewanella putrefaciens under aerobic conditions. J. Radioanal. Nucl. Chem., 3)312): 531-541. https://doi.org/10.1007/s10967-017-5261-7

Iwamoto, K. and Minoda, A. 2018. Bioremediation of biophilic radionuclides by algae. Algae. IntechOpen, 1: 62. http://dx.doi.org/10.5772/intechopen.81492

Jabbar, T. and Wallner, G. 2015. Biotransformation of radionuclides: Trends and Challenges. Springer, Cham, pp. 169-184. https://doi.org/10.1007/978-3-319-22171-7_10

Jain, A., Yadav, S., Nigam, V. K. and Sharma, S.R. 2017. Fungal-mediated solid waste management: a review. Mycoremedi. Environ. Sustain., 9: 153-170. https://doi.org/10.1007/978-3-319-68957-9_9

Jayaprakash, K., Govarthanan, M., Mythili, R., Selvankumar, T. and Chang, Y.C. 2019. Bioaugmentation and Biostimulation Remediation Technologies for Heavy Metal Lead Contaminant. Microbial Biodegrad. Xenobio. Comp., 24: 22151. https://doi.org/10.1201/b22151

Jiang, L., Liu, X., Yin, H., Liang, Y., Liu, H., Miao, B., Peng, Q., Meng, D., Wang, S., Yang, J. and Guo, Z., 2020. The utilization of biomineralization technique based on microbially induced phosphate precipitation in remediation of potentially toxic ions contaminated soil: A mini-review. Ecotoxicol. Environ. Safety, 191: 110009. https://doi.org/10.1016/j.ecoenv.2019.110009

Júnior, D.P.L., da Costa, G.L., de Oliveira Dantas, E.S., Nascimento, D.C., Moreira, D., Pereira, R.S., Ramos, R.T.B., Bonci, M.M., da Silva Maia, M.L., Gandra, R.F. and Auler, M.E., 2020. The rise of fungi: evidence on the global scale: Old known silences or mysterious threats to the planet. Microbiol. Res. J. Int., 2: 18-49. https://doi.org/10.9734/mrji/2020/v30i1030272

Kaksonen, A.H., Boxall, N.J., Usher, K.M., Ucar, D. and Sahinkaya, E., 2017. Biosolubilisation of metals and metalloids. Sustain. Heavy Met., 121: 233-283. https://doi.org/10.1007/978-3-319-58622-9_8

Kapahi, M. and Sachdeva, S. 2017. Mycoremediation potential of Pleurotus species for heavy metals: a review. Bioresour. Bioprocess., 1)4): 1-9. https://doi.org/10.1186/s40643-017-0162-8

Kaushik, S., Alatawi, A., Djiwanti, S.R., Pande, A., Skotti, E. and Soni, V. 2021. The Potential of Extremophiles for Bioremediation. In Panpatte, D.G. and Jhala, Y.K. (eds), Microbial Rejuvenation of Polluted Environment, Springer, Singapore, pp. 293-328. https://doi.org/10.1007/978-981-15-7447-4_12

Kautsky, U., Lindborg, T. and Valentin, J. 2013. Humans and ecosystem over the coming millennia: A biosphere assessment of radioactive waste disposal. AMBIO J. Hum. Environ., 42: 383–392.

Khan, A.G. 2020. Promises and potential of in situ nano-phytoremediation strategy to mycorrhizo-remediate heavy metal contaminated soils using non-food bioenergy crops (*Vetiver zizinoides* & *Cannabis sativa*). Int. J. Phytoremed., 9)22): 900-915. https://doi.org/10.1080/15226514.2020.1774504

Kumar, V., Shahi, S.K. and Singh, S. 2018. Bioremediation: An Eco-sustainable Approach for Restoration of Contaminated Sites. Singh, J. (ed), Microbial Bioprospecting for Sustainable Development, Springer, Cham, pp. 115-136. https://doi.org/10.1007/978-981-13-0053-0_6

Kumar, N.M., Muthukumaran, C., Sharmila, G. and Gurunathan, B. 2018. Genetically modified organisms and their impact on the enhancement of bioremediation. In Varjani, S.J., Agarwal, A.K., Gnansounou, E. and Gurnathan, B. (eds), Bioremediation: Applications for Environmental Protection and Management. Springer, Singapore, pp. 53-76. https://doi.org/10.1007/978-981-10-7485-1_4

Kumar, R. and Kundu, S. 2020. Microbial bioremediation and biodegradation of hydrocarbons, heavy metals, and radioactive wastes in solids and wastewaters. Microbial Bioremed. Biodegrad., 6: 95-112. http://dx.doi.org/10.1007/978-981-15-1812-6_4

Limmer, M. and Burken, J. 2016. Phytovolatilization of organic contaminants. Environ. Sci. Technol., 50(13): 6632-6643. https://doi.org/10.1021/acs.est.5b04113

Lopez-Fernandez, M., Jroundi, F., Ruiz-Fresneda, M.A. and Merroun, M.L. 2021. Microbial interaction with and tolerance of radionuclides: Underlying mechanisms and biotechnological applications. Microbial Biotechnol., 14(3): 810-828. https://doi.org/10.1111/1751-7915.13718

Lourenço, J., Mendo, S. and Pereira, R. 2019. Rehabilitation of Radioactively Contaminated Soil: Use of Bioremediation/Phytoremediation Techniques. In: Gupta, K.D. and Voronina, A. (eds), Remediation Measures for Radioactively Contaminated Areas, Springer, Cham., pp. 28-50. https://doi.org/10.1007/978-3-319-73398-2_8

Khan, M.I., Cheema, S., Anum, N.K., Niazi, M., Azam, S., Bashir, I. and Qadri, R. 2020. Phytoremediation of Agricultural Pollutants. In Shmaefsky, B.R. (ed.), Phytoremediation, Concepts and Strategies in Plant Sciences, Elsevier, The Netherlands, pp. 27-64. https://doi.org/10.1007/978-3-030-00099-8_2

Khan, M.I., Yi, L., Cheng, Z., Samrana, Z., Shuijin, S., Shaheen, M.J., Khan, S., Ali, M., Rizwan, M.D., Khan, M., Azam, M., Afzal, G. and Irum, M. 2020. In Situ Phytoremediation of Metals. In Shmaefsky, B.R (ed), Phytoremediation, Concepts and Strategies in Plant Sciences, Springer, Cham, pp. 103-121. https://doi.org/10.1007/978-3-030-00099-8_4

Mahadevan, G.D. and Zhao, F. 2017. A concise review on microbial remediation cells (MRCs) in soil and groundwater radionuclides remediation. J. Radioanal. Nucl. Chem., 314(3): 1477-1485. https://doi.org/10.1007/s10967-017-5612-4

Malla, M.A., Dubey, A., Yadav, S., Kumar, A., Hashem, A. and Abd_Allah, E.F. 2018. Understanding and designing the strategies for the microbe-mediated remediation of environmental contaminants using omics approaches. Front. Microbiol., 9: 1132. https://doi.org/10.3389/fmicb.2018.01132

Mallavarapu, M. and Lee, Y.B. 2020. Biostimulation and bioaugmentation: Modern strategies for the successful bioremediation of contaminated environments. Environ. Remed., 61: 299. https://doi.org/10.1039/9781788016261-00299

Manobala, T., Shukla, S. K., Rao, T. S. and Kumar, M. D. 2019. A new uranium bioremediation approach using radio-tolerant Deinococcus radiodurans biofilm. J. Biosci., 44(5): 1-9. https://doi.org/10.1007/s12038-019-9942-y

Mao, X.L., Ding, Z.X. and Yuan, S.B. 2015. Dissolution of 238U from low-level contaminated soil by acidithiobacillus ferrooxidans. Appl. Mech. Mater., 700: 225-229. https://doi.org/10.4028/www.scientific.net/AMM.700.225

Marques, C.R. 2018. Extremophilic microfactories: Applications in metal and radionuclide bioremediation. Front. Microbiol., 9: 1191. https://doi.org/10.3389/fmicb.2018.01191

Mikheev, A.N., Lapan, O.V. and Madzhd, S.M. 2017. Experimental foundations of a new method for rhizofiltration treatment of aqueous ecosystems from 137Cs. J. Water Chem. Technol., 39(4): 245-249. https://doi.org/10.3103/S1063455X17040117

Natarajan, V., Karunanidhi, M. and Raja, B. 2020. A critical review of radioactive waste management through biological techniques. Environ. Sci. Pollut. Res., 5: 1-12. https://doi.org/10.1007/s11356-020-08404-0

Newsome, L., Morris, K. and Lloyd, J.R. 2015. Uranium biominerals precipitated by an environmental isolate of Serratia under anaerobic conditions. PloS One, 10(7): e0132392. https://doi.org/10.1371/journal.pone.0132392

Nivorlis, A., Dahlin, T. and Rossi, M. 2019. Geophysical monitoring of initiated in-situ bioremediation of chlorinated solvent contamination. Environ. Eng. Geophys., 1: 1-5. https://doi.org/10.3997/2214-4609.201902386

Omran, B.A. 2021. Facing Lethal Impacts of Industrialization via Green and Sustainable Microbial Removal of Hazardous Pollutants and Nanobioremediation. Removal of Emerging Contaminants Through Microbial Processes, 133-160. https://doi.org/10.1007/978-981-15-5901-3_7

Ostoich, P., Beltcheva, M., Rojas, J.A.H. and Metcheva, R. 2022. Radionuclide contamination as a risk factor in terrestrial ecosystems: Occurrence, biological risk, and strategies for remediation and detoxification. Environ. Pollut., 10: 446. https://doi.org/10.5772/intechopen.104468

Patnaik, R.L. 2018. "Mobile Radiological mapping around the Jaduguda area of Jharkhand, India." Proceedings of the thirty-third IARP international conference on developments towards the improvement of radiological surveillance at nuclear facilities and environment: book of abstracts. 2018.

Prakash, D., Gabani, P., Chandel, A.K., Ronen, Z. and Singh, O.V. 2013. Bioremediation: a genuine technology to remediate radionuclides from the environment. Microbial Biotechnol., 4)6): 349-360. https://doi.org/10.1111/1751-7915.12059

Qiu, L., Feng, J., Dai, Y. and Chang, S. 2019. Mechanisms of strontium's adsorption by Saccharomyces cerevisiae: Contribution of surface and intracellular uptakes. Chemosphere, 215: 15-24. https://doi.org/10.1016/j.chemosphere.2018.09.168

Qu, Y., Li, H., Wang, X., Tian, W., Shi, B., Yao, M. and Zhang, Y. 2019. Bioleaching of major, rare earth, and radioactive elements from red mud using indigenous chemoheterotrophic bacterium Acetobacter sp. Minerals, 9(2): 67. https://doi.org/10.3390/min9020067

Rani, A., Mittal, S., Mehra, R. and Ramola, R.C. 2015. Assessment of natural radionuclides in the soil samples from the Marwar region of Rajasthan, India. Appl. Radiat. Isotopes, 101: 122-126. https://doi.org/10.1016/j.apradiso.2015.04.003

Reitz, T., Rossberg, A., Barkleit, A., Steudtner, R., Selenska-Pobell, S. and Merroun, M.L. 2015. Spectroscopic study on uranyl carboxylate complexes formed at the surface layer of *Sulfolobus acidocaldarius*. Dalton Trans., 44(6): 2684-2692. https://doi.org/10.1039/C4DT02555E

Rezania, S., Taib, S.M., Din, M.F.M., Dahalan, F.A. and Kamyab, H. 2016. A comprehensive review on phytotechnology: heavy metals removal by diverse aquatic plant species from wastewater. J. Hazard. Mater., 318: 587-599. https://doi.org/10.1016/j.jhazmat.2016.07.053

Roh, C., Kang, C. and Lloyd, J.R. 2015. Microbial bioremediation processes for radioactive waste. Korean J. Chem. Eng., 32(9): 1720-1726. https://doi.org/10.1007/s11814-015-0128-5

Sahay, V.K., Mude, S.N. and Samant, B. 2015. The early Eocene Naredi cliff section, Kutch Basin, Gujarat, India: Evidence of a condensed stratigraphic section. Int. Res. J. Earth Sci., 6)3): 12-15.

Sahinkaya, E., Uçar, D. and Kaksonen, A.H. 2017. Bioprecipitation of metals and metalloids. In Rene, E.R., Sahinkaya, E., Lewis, A. and Lens, P.N.L. (eds), Sustainable Heavy Metal Remediation, Springer, Cham, pp. 199-231. https://doi.org/10.1007/978-3-319-58622-9_7

Sardrood, B.P., Goltapeh, E.M. and Varma, A. 2013. An Introduction to Bioremediation. In Goltapeh, E., Danesh, Y. and Varma, A. (eds), Fungi as Bioremediators: Soil Biology, vol 32. Springer, Berlin, Heidelberg, pp. 3-17. https://doi.org/10.1007/978-3-642-33811-3_1

Sengupta, S., Roy, U., Chowdhary, S. and Das, P. 2021. New Bioremediation Technologies to Remove Heavy Metals and Radionuclides. In Shah, M.P. (ed), Removal of Emerging Contaminants Through Microbial Processes. Springer, Singapore, pp. 23-45. https://doi.org/10.1007/978-981-15-5901-3_2

Sharma, B., Singh, V.K. and Manchanda, K. 2015. Phytoremediation: Role of terrestrial plants and aquatic macrophytes in the remediation of radionuclides and heavy metal contaminated soil and water. Environ. Sci. Pollut. Res., 22: 946–962. https://doi.org/10.1007/s11356-014-3635-8

Sheoran, V., Sheoran, A.S. and Poonia, P. 2016. Factors affecting phytoextraction: A review. Pedosphere, 26(2): 148–166. https://doi.org/10.1016/S1002-0160(15)60032-7

Sheoran, A. and Sheoran, S. 2017. Phytoremediation of heavy metals contaminated soils. J. Plant Dev. Sci., 9: 905-915.

Shukla, A., Parmar, P. and Saraf, M. 2017. Radiation, radionuclides, and bacteria: An in-perspective review. J. Environ. Radioact., 180: 27-35. https://doi.org/10.1016/j.jenvrad.2017.09.013

Shukla, A., Parmar, P. and Saraf, M. 2019. Isolation and screening of bacteria from radionuclide-containing soil for bioremediation of contaminated sites. Environmental Sustainability, 2: 255-264. https://doi.org/10.1007/s42398-019-00068-y

Shukla, S.K. and Rao, T.S. 2017. The first recorded incidence of Deinococcus radiodurans R1 biofilm formation and its implications in heavy metals bioremediation. bioRxiv, 23: 4781. https://doi.org/10.1101/234781

Singh, B.M., Singh, D. and Dhal, N.K. 2022. Enhanced phytoremediation strategy for sustainable management of heavy metals and radionuclides. Case Stud. Chem. Environ. Eng., 5: 100176. https://doi.org/10.1016/j.cscee.2021.100176

Singh, S., Jha, P. and Jobby, R. 2021. Fungi: A Promising Tool for Bioremediation of Toxic Heavy Metals. In Saxena, G., Kumar, V. and Shah, M.P. (eds), Bioremediation for Environmental Sustainability. Elsevier, The Netherlands, pp. 123-144. https://doi.org/10.1016/B978-0-12-820524-2.00006-7

Srichandan, H., Mohapatra, R.K., Parhi, P.K. and Mishra, S. 2019. Bioleaching: A bioremediation process to treat hazardous wastes. Soil Microenviron. Bioremed. Polym. Prod., 67: 115-129. https://doi.org/10.1002/9781119592129.ch7

Tang, M., Feng, R. and Konstantin, L. 2018. Low dose or low dose rate ionizing radiation-induced health effects in the human. J. Environ. Radioact., 192: 32-47. https://doi.org/10.1016/j.jenvrad.2018.05.018

Tapadar, S., Tripathi, D., Pandey, S., Goswami, K., Bhattacharjee, A., Das, K., Palwan, E., Rani, M. and Kumar, A. 2021. Role of Extremophiles and Extremophilic Proteins in Industrial Waste Treatment. In Removal of Emerging Contaminants Through Microbial Processes, pp. 235-217. Springer, Singapore. https://doi.org/10.1007/978-981-15-5901-3_11

Thorpe, C.L., Lloyd, J.R., Law, G.T.W., Williams, H.A., Atherton, N., Cruickshank, J.H. and Morris K. 2016. Retention of 99mTc at ultra-trace levels in flowing column experiments – Insights into bioreduction and biomineralization for remediation at nuclear facilities. Geomicrobiol. J., 67: 656. https://doi.org/10.1080/01490451.2015.1067656

Tonelli, F.M.P., Tonelli, F.C.P., de Melo Nunes, N.A. and Lemos, M.S. 2020. Mechanisms and Importance of Phytoremediation. In Hakim, K.R., Bhat, R.A. and Qadri, h. (eds), Bioremediation and Biotechnology, Vol 4, Springer, Cham, pp. 125-141. https://doi.org/10.1007/978-3-030-48690-7_6

Tribedi, P., Goswami, M., Chakraborty, P., Mukherjee, K., Mitra, G., Bhattacharyya, P. and Dey, S. 2018. Bioaugmentation and biostimulation: A potential strategy for environmental remediation. J. Microbiol. Exp., 6: 223-231. https://doi.org/10.15406/jmen.2018.06.00219

Upadhyay, A.K., Mojumdar, A., Raina, V. and Ray, L. 2019. Eco-friendly and economical method for detoxification of pesticides by microbes. Soil Microenviron. Bioremed. Polym. Prod., 95-113. https://doi.org/10.1002/9781119592129.ch6

Uzair, B., Shaukat, A., Fasim, F. and Maqbool, S. 2019. Conjugate magnetic nanoparticles and microbial remediation, a genuine technology to remediate radioactive waste. Soil Microenviron. Bioremed. Polym. Prod., 97-211: 9129. https://doi.org/10.1002/9781119592129.ch11

Vogel, M., Fischer, S., Maffert, A., Hübner, R., Scheinost, A. C., Franzen, C. and Steudtner, R. 2018. Biotransformation and detoxification of selenite by microbial biogenesis of selenium-sulfur nanoparticles. Journal of hazardous materials, 344: 749-757. https://doi.org/10.1016/j.jhazmat.2017.10.034

Wang, W. and Dudel, E.G. 2017 Fe plaque-related aquatic uranium retention via rhizofiltration along a redox-state gradient in a natural *Phragmites australis* Trin ex Steud. Wetland. Environ. Sci. Pollut. Res. Int., 24(13): 12185-12194. https://doi.org/10.1007/s11356-017-8889-5

Wang, C., Zhou, Z., Liu, H., Li, J., Wang, Y. and Xu, H. 2017a. Application of acclimated sewage sludge as a bio-augmentation/bio-stimulation strategy for remediating chlorpyrifos contamination in soil with/without cadmium. Science of the Total Environ., 579: 657-666. https://doi.org/10.1016/j.scitotenv.2016.11.044

Wang, G., Zhang, B., Li, S., Yang, M. and Yin, C. 2017b. Simultaneous microbial reduction of vanadium (V) and chromium (VI) by *Shewanella loihica* PV-4. Bioresour. Technol., 227: 353-358. https://doi.org/10.1016/j.biortech.2016.12.070

Wang, Y., Nie, X., Cheng, W., Dong, F., Zhang, Y., Ding, C., Liu, M., Asiri, A.M. and Marwani, H.M., 2019. A synergistic biosorption and biomineralization strategy for *Kocuria* sp. to immobilizing U (VI) from aqueous solution. J. Mol. Liq., 275: pp.215-220. https://doi.org/10.1016/j.molliq.2018.11.079

Wetle, R., Tarsitano B.B., Johnson, K., Sweat K.G. and Cahill T. 2020. Uptake of uranium into desert plants in an abandoned uranium mine and its implications for phytostabilization strategies. J. Environ. Radioact., 220–221: 106293. https://doi.org/10.1016/j.jenvrad.2020.106293

Xu, R. 2018. Co-expression of YieF and PhoN in *Deinococcus radiodurans* R1 improves uranium bioprecipitation by reducing chromium interference. Chemosphere, 211: 1156-1165. https://doi.org/10.1016/j.chemosphere.2018.08.061

Yadav, K.K., Gupta, N., Kumar, A., Reece, L.M., Singh, N., Rezania, S. and Khan, S.A. 2018. Mechanistic understanding and holistic approach of phytoremediation: A review on application and future prospects. Ecol. Eng., 120: 274-298. https://doi.org/10.1016/j.ecoleng.2018.05.039

Yan, L., Van Le, Q., Sonne, C., Yang, Y., Yang, H., Gu, H., Ma, N.L., Lam, S.S. and Peng, W. 2021. Phytoremediation of radionuclides in soil, sediments, and water. Journal of Hazardous Materials, 407: 124771. https://doi.org/10.1016/j.jhazmat.2020.124771

Zhao, C. 2016. Biosorption and bioaccumulation behavior of uranium on *Bacillus* sp.: Investigation by box-Behenken design method. J. Mol. Liq. 221: 156-165. https://doi.org/10.1016/j.molliq.2016.05.085

Zheng, X.Y., Wang, X.Y., Shen, Y.H., Lu, X. and Wang, T.S. 2017. Biosorption and biomineralization of uranium (VI) by *Saccharomyces cerevisiae*-Crystal formation of chernikovite. Chemosphere, 175: 161-169. https://doi.org/10.1016/j.chemosphere.2018.03.165

Zinicovscaia, I., Safonov, A., Zelenina, D., Ershova, Y. and Boldyrev, K. 2020. Evaluation of biosorption and bioaccumulation capacity of cyanobacteria *Arthrospira* (*Spirulina*) *platensis* for radionuclides. Algal Res., 51: 102075. https://doi.org/10.1016/j.algal.2020.102075

Process Intensification in Gas-Liquid Mass Transfer by the Introduction of Additives: A Review

Huan Zhang*†, Bo Zheng*, Ping Chang**, Tao Yu*** and Chengtun Qu***(****)
*College of Chemistry and Material, Weinan Normal University, Weinan 714099, PR China
**Karamay Linghao Technology Co. Ltd., Karamay 834000, PR China
***College of Chemistry and Chemical Engineering, Shaanxi Province Key Laboratory of Environmental Pollution Control and Reservoir Protection Technology of Oilfields, Xi'an Shiyou University, Xi'an 710065, PR China
****State Key Laboratory of Petroleum Pollution Control, CNPC Research Institute of Safety and Environmental Technology, Beijing, PR China
†Corresponding author: Huan Zhang; zh_228611@163.com

ABSTRACT

To overcome the challenges of the increasing global energy and to solve the global energy & environment problems, process intensification is one way to develop new efficient production pathways for the chemical industry. Process intensification plays an important role in the gas-liquid mass transfer processes. This review provides an overview of the developments in gas-liquid mass transfer enhancement. A major enhancement method, namely introducing additives (including nanoparticles, oil, electrolyte, and surfactant) summarized and discussed here, includes the most recent accomplishments in gas-liquid mass transfer engineering. This review is expected to inspire new research for future developments and potential applications in scientific research and industry regarding gas-liquid mass transfer engineering. Finally, it presents conclusions and perspectives on enhancing gas-liquid mass transfer.

INTRODUCTION

The rapid development of the chemical and energy industries leads to an increase in the emissions of greenhouse gas, then resulting in global warming. It is well-known that global warming is a critical challenge for the international community. Greenhouse gases, including carbon dioxide (CO_2), methane (CH_4), and nitrogen oxides (NO_x), are believed to be the source of global warming (Abeydeera et al. 2019). H_2-liquid mass transfer limits the rate of bio-methanation reactions due to the low distribution of H_2 in solution, limiting its solubility and thus its availability to methanogens. Besides, methane is the main component of natural and shale gas, accounting for 90% of the total abundance (Radler 2011, Kuuskraa et al. 2013). Thus, methane is considered the next generation of carbon feedstock as one of the earth's most widely used high-energy resources.

Nevertheless, methane is a non-polar gas, and its low solubility in solution hinders efficient mass transfer. Oxygen is widely used in microbial growth and product synthesis as a low-cost green oxidant (Garcia-Ochoa et al. 2010). However, oxygen is less soluble in aqueous solution. Ozonation is one of the most widely used AOP technologies, which has been applied to treat various types of organic wastewater. However, ozone's equilibrium concentration and mass transfer efficiency in water are limited, leading to poor ozone utilization (Gome & Upadhyay 2012). As deduced in the above finding, new approaches are needed to address these limitations.

Process reinforcement is important in various chemical science and engineering aspects (Ramshaw 1983). It allows for resource maximization and does more with less (Luo 2013). As shown in Table 1, the more and the less are summarized (Li et al. 2019). The mass transfer between gas and liquid is widely used in chemical engineering. The rate and efficiency of mass transfer determine the cost and potential profit of gas-liquid mass transfer equipment. Therefore, process reinforcement in the gas-liquid mass transfer has been advocated worldwide (Garcia et al. 2017). Fundamentally, process reinforcement of gas-liquid mass transfer is always related to the total driving force, mass transfer coefficient, and gas-liquid interface area (Fig. 1) (Jensen et al. 2021)

Table 1: The interpretation of process reinforcement. Adapted from ref. (Li et al. 2019).

| Types of process reinforcement	"More"	"Less"	Examples
Structural intensification	Production or quality	Size of plants	Microreactor
Energetic intensification	Energy efficiency	Energy consumption	Rotating packed bed
Temporal intensification	Productive rate	Time	Microwave heating
Functional intensification	Functionality	Number of unit operations	Reactive distillation
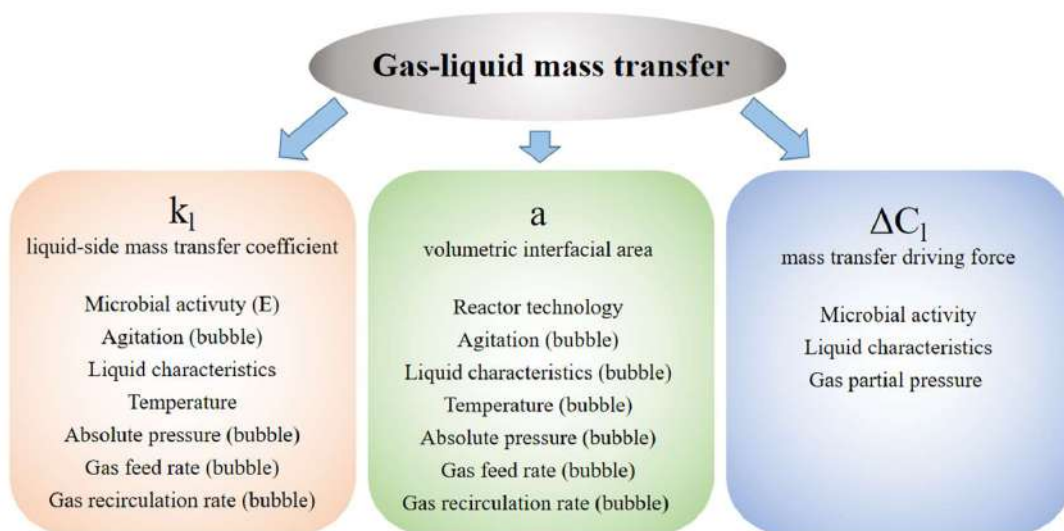
Fig. 1: Overview of the relation between the discussed process parameters and gas-liquid mass transfer. E denotes mass transfer enhancement (Jensen et al. 2021).

This paper summarizes effective reinforcement approaches in the gas-liquid mass transfer process. This technology includes introducing additives such as nanoparticles, oil, electrolyte, and surfactant. It is investigated the recent progress of this technology for enhancing gas-liquid mass transfer performance. More importantly, the mechanisms of different additives are summarized. Finally, the potentials and challenges of this technology of improving gas-liquid mass transfer performance are prospected.

INTRODUCTION OF ADDITIVES

Nanoparticles

When small particles are added to a system, a number of possible reactions, such as predation effects, hydrodynamic effects, or inhibition of bubble coalescence, can occur (Fig. 2) (Beenackers & Swaaij 1993, Zhang et al. 2022). This method increases the gas-liquid interface area a and affects the gas-liquid mass transfer coefficient k_L, which is greatly affected by the particle size, hydrophobicity, hydrophilicity, and other surface characteristics. Additives are not consumed in the reactors and can be reused by appropriate methods, such as filtering or centrifuge.

Mehdipour et al. (2021) studied CO_2 absorption enhancement by SiO_2 and ZnO nanoparticles in the rotating liquid sheet contactor. The effect of the tube rotation rate, nanoparticles concentration, gas flow rate, and CO_2 concentration on the absorption performance was investigated. Also, the adsorption flux increased with an increase in gas flow rate, and increased first and then decreased with an increase in CO_2 inlet concentration. CO_2 absorption measurements confirmed that nanoparticles significantly enhanced the separation effect. In this work, ZnO nanofluids were more efficient than SiO_2 nanofluids. Lee et al. (2021) used SiO_2 to increase CO_2 absorption performance. In this study, to analyze the enhancement of CO_2 absorption performance by a nanofluid, the visualization experiment of CO_2 diffusion was carried out using the shadowgraph method. They observed that the absorption performance of the nanofluid enhanced up to 23.05% by adding 0.05 vol% nanoparticles. The visualization results showed that the hydrodynamic effect was the main factor in improving the mass transfer of nanofluids.

Lakhdissi et al. (2020) examined the influence of inert nonporous hydrophilic glass beads on the volumetric gas-liquid mass transfer coefficient $k_l a_l$. Under constant particle
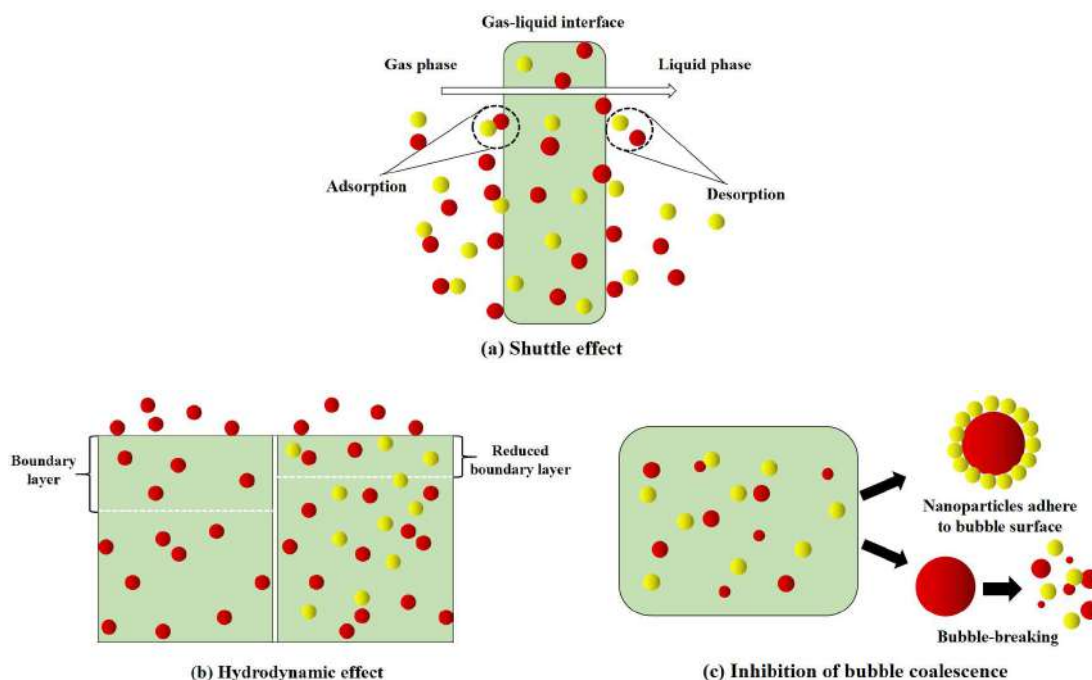
Fig. 2: Shuttle effect (a), hydrodynamic effect (b), and inhibition of bubble coalescence (c). (Beenackers & Swaaij 1993, Zhang et al. 2022).

size, the increase of solid concentration from 1% (v/v) to 5% (v/v) did not affect $k_l a_l$. In addition, increasing particle size in the micron range had little effect on $k_l a_l$ at a constant concentration. In this work, with the increase of solid concentration, the bubble coalescence enhanced, resulting in the increase of bubble size and the decrease of oxygen-liquid interface area a_l. Secondly, the other particles moved towards the bubble surface due to the collision phenomenon, resulting in local turbulence and increased the liquid side mass transfer coefficient k_l. And finally, it was concluded that the two-phase approach does not predict the low variability of the experimental three phases $k_l a_l$ very well. Esmaeili-Faraj et al. (2016) studied H_2S and CO_2 absorption enhancement by exfoliated graphene oxide (EGO) water and synthesized silica (SS). Based on the adsorption of H_2S by these functions in EGO and SS nanoparticles, the mass transfer coefficients were 5- and 2-fold for the base fluid, respectively. They concluded that the grazing effect increased mass transfer coefficients in nanofluids (adsorption of gas molecules on the surface of nanoparticles).

Oil

This part introduces the effect of the addition of the second dispersive liquid phase on the enhancement of gas-liquid mass transfer. Physical properties of the liquid mixture, such as density, viscosity, gas solubility, and gas diffusivity, and the gas-liquid properties, such as droplet distribution

in the boundary layer, possible mass transfer pathways, mass transfer coefficient, and gas-liquid interface area, were changed depending on the interface properties of the dispersed liquid (Dumont & Delmas 2003). In the process of mass transfer, there were two possible path ways in the boundary layer (Dumont & Delmas 2003):

Mass transfer in series: there was a gas→liquid mass transfer, and direct gas→oil contact is impossible (Fig. 3(a-b)).

Mass transfer in parallel: gas→oil contact was possible, and the gas→water mass transfer and the gas→oil mass transfer took place (Fig. 3c).

To examine the effect of the non-aqueous phase on the mass transfer of styrene vapor, Parnian et al. (2016) used silicone oil and experimentally analyzed the parameters that could affect the mass transfer process. Mass transfer of styrene was very sensitive to ϕ when $\phi < 10\%$; however, at $\phi > 10\%$, the introduction of silicone oil was insensitive to the process. It was concluded that the mass transfer mechanism is changed to the gas→water→oil pathway by increasing φ value from 2% to 20%. Thus, the $K_L a$ increased obviously. Ultimately, the $K_L a$ stayed unchanged regardless of the volume fraction of silicone oil because of the dominance of the gas-water distribution coefficient. This was in agreement with the results of other researchers (Dumont et al. 2014), who showed that the decrease in $K_L a$
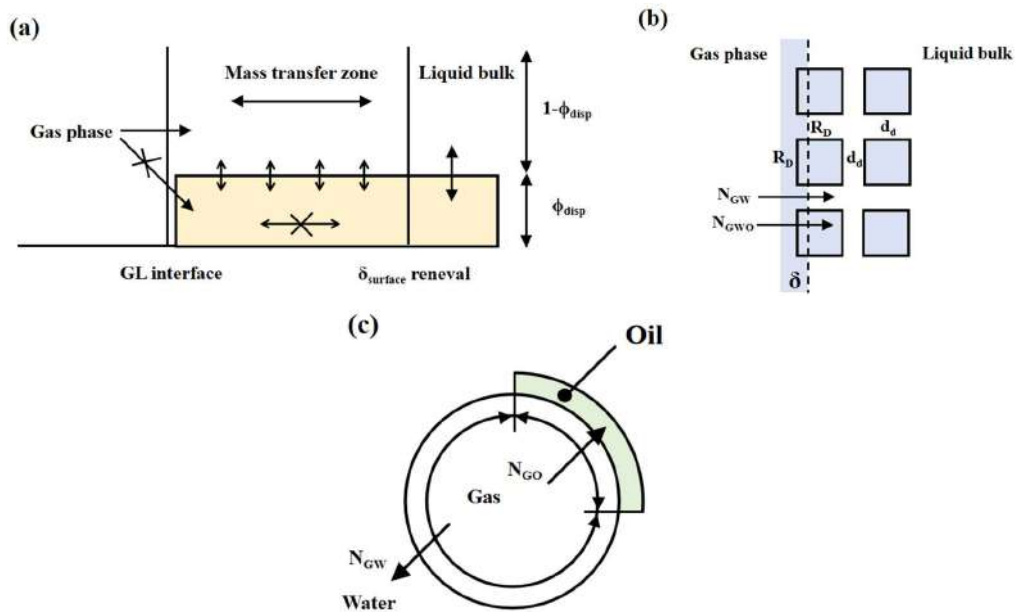
Fig. 3: Mass transfer pathway in series: (a) example of pseudo-homogeneous model representation (no direct gas→oil contact (Brilman et al. 2000); (b) example of heterogeneous model representation (combination of flux to gas→water and gas→water→oil (Zamir et al. 2015)), and (c) mass transfer pathway in parallel (Dumont & Delmas 2003).

value might be related to the change in the distribution coefficient ratio. In addition, Dumont et al. (2014) pointed out that adding silicone oil slightly retarded the mass transfer rate of styrene compared to the air/water system, and K_La decreased. Li et al. (2010) explained the CO_2 mass transfer enhancement mechanism by choosing CO_2-benzene or octane/water as a gas/liquid absorption system. The experimental results indicated that increased energy input increased the mass transfer enhancement factor. Small droplets from the dispersed phase enhanced the gas-liquid mass transfer. Small droplets of oil acted like catalysts in chemical reactions. They analyzed the shuttle mechanism and summarized the essence of enhancement of gas-liquid mass transfer was that the dispersed liquid phase increased the components concentration gradient of solute near the gas-liquid interface by absorption. Rols et al. (1990) proposed that the main mechanism of oxygen transfer enhancement was forming a thin film at the gas-liquid interface. This mechanism required gas bubble-oil droplet coalescence followed by oil droplet-oil film coalescence. When bubbles are submerged in the emulsion, the organic liquid covers the surface of the bubbles, and the film formed is loaded with oxygen as long as the bubbles do not explode. Sauid et al. (2013) found that adding palm oil as the organic phase increased the volumetric mass transfer coefficient (kLa). The effect of palm oil on the viscosity and rheology, k_La, and gas holdup in the xanthan solution was investigated.

The results showed that introducing palm oil up to 10% vol increased k_La by 1.5 to 3 folds, and the maximum k_La value was 84.44 h^{-1} (Fig. 4). High oxygen transfer was obtained without providing additional energy. The increase was due to increased liquid turbulence caused by rigid organic phase droplets (Rols et al. 1990). The spreading coefficient played a significant role in changing the oxygen transfer capability in the system (Yoshida et al. 1970). When the diffusion coefficient was positive, the organic encounter on the water surface propagated like a surfactant to reduce the surface tension, thereby increasing the interface area and eventually increasing (Yoshida et al. 1970). This favorable effect promoted the formation of small bubbles due to the properties of palm oil.

However, other researchers have drawn different conclusions. Boltes et al. (2008) have examined the effect of airflow rate and organic fractions of dodecane on the gas-liquid mass transfer in oil-water emulsions. For the same organic fraction, the airflow rate enhancement has witnessed an increase in the K_La. In agreement with the previous result, it was confirmed that the K_La values obtained for the organic liquids were higher than the corresponding values for water (Mehrnia et al. 2005, Shariati et al. 2007). For the same airflow, the K_La value decreased with an increase in the organic fraction, and then with a further increase in the organic fraction, the K_La value was increased. Shariati et al. (2007) also concluded that the mass transfer decreases
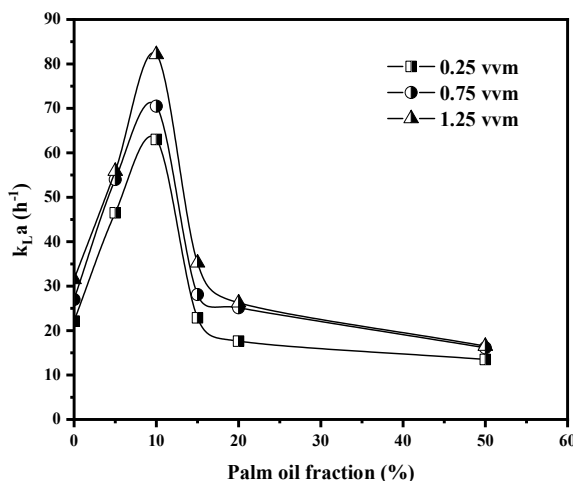
Fig. 4: Influence of palm oil on kLa. (Sauid et al. 2013).

with an increased water-to-oil phase volume ratio. Kundu et al. (2002) have investigated the gas-liquid mass transfer enhancement by adding different second immiscible organic phases (toluene, 2-ethyl-1-hexanol, decyl alcohol, anisole, dodecane, n-decane, and n-heptane). The results showed that adding 1% of n-decane, dodecane, and n-heptane in liquid increased the mass transfer. However, adding toluene, anisole, and 2-ethyl-1-hexanol limited the mass transfer. Non-linear variations of the enhancement factor were to be noticed. This may be due to the formation of an oil-water complex (several small droplets trapped in a large oil droplet as multiple droplets by Sajjadi et al. (2002)) that occurs at a higher concentration of dispersed phase and lower gas velocity. In addition, the main effect of adding oil appears to be a change in bubble size. Larger bubble diameters and lower gas fractions mean lower surface area and, thus,

reduced mass transfer. However, these results cannot be explained by the modest change in the properties of the gas-oil saturated water interface due to oil addiction.

Electrolyte

Kim et al. (2016) employed various electrolytes such as $MgSO_4$, Na_2SO_4, K_2SO_4, $MgCl_2$, NaCl, KCl, $MgBr_2$, NaBr, KBr, $Mg(NO_3)_2$, $NaNO_3$, and KNO_3 to investigate the effect of the electrolytes on methane-water volumetric mass transfer coefficient ($k_L a$). In this work, an increase in electrolyte concentration could enhance the $k_L a$. Anions had a greater effect on $k_L a$ enhancement than that of cations (Fig. 5). For electrolytes with the same cations, the $k_L a$ value of sulfates, chlorides, bromides, and nitrates were 613-711, 381-488, 141-290, and 233-266 h^{-1}, respectively. For electrolytes with the same anions, magnesium-containing electrolytes

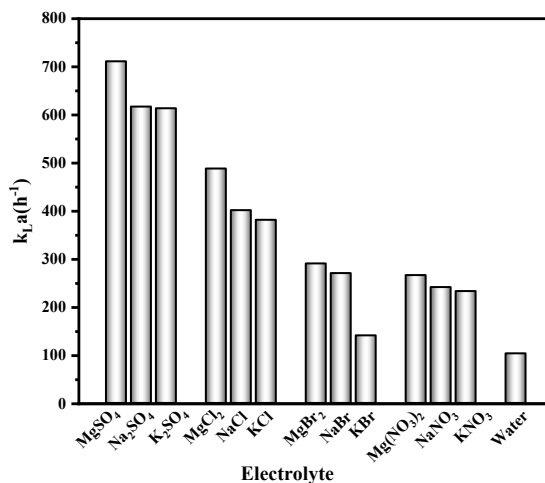
Fig. 5: Methane water volumetric mass transfer coefficient for various electrolytes at 5 wt% concentration. (Kim et al. 2016).

exhibited larger k_La values than those containing sodium and potassium. Magnesium sulfate had the greatest strengthening effect on k_La at the concentration of 5 wt%, up to 711 h^{-1}. This was the highest k_La value of methane water reported in the published literature. Inhibition of bubble coalescence in electrolyte solution favored the increase of the k_La value of methane water. The enhanced effect of electrolytes on methane water mass transfer could be attributed to increased methane water interfacial area. Anions have a stronger effect on k_La enhancement than cations. For all electrolytes, ions with high charge density greatly enhanced methane water's kLa value.

Góngora García et al. (2021) studied the combined effects of mixed electrolyte species (KH_2PO_4, K_2HPO_4, $(NH_4)_2SO_4$, and $MgSO_4 \cdot 7H_2O$) on the oxygen transfer in a bubble column. Electrolytes containing ions are prone to solute interactions or crystallization. Volume mass transfer coefficient (k_La) and specific interface area (a) are enhanced due to the inhibition of bubble coalescence as the electrolyte concentration increases to a critical value. In saline solution, the k_La tended to increase (between 58 and 72%) as the nominal ionic strength increased from 0 to 0.085. The electrolyte inhibits bubble coalescence (resulting in smaller bubbles forming), thus maintaining a higher interface area. In addition, the small bubble and the low slip velocity appeared due to the low oxygen diffusion rate in the salt solution. Thus, the local mass transfer decreased (Taweel et al. 2013, Baz-Rodríguez et al. 2014). Overall, the influence on a seems to control the k_La value. Jang et al. (2018) employed various electrolytes such as $CaCl_2$, K_2HPO_4, $MgSO_4$, NaCl, and NH_4Cl to investigate the effects of the electrolytes on the enhancement of CO mass transfer in hollow fiber membrane bioreactor. The lowest value of k_La for CO achieved in water was 137.2 h^{-1}. However, k_La values of CO increased to 568.8 h^{-1} (5% NH_4Cl), 340.2 h^{-1} (5% $MgSO_4$), 279.4 h^{-1} (3% NaCl), 410.0 h^{-1} (5% $CaCl_2$), and 465.8 h^{-1} (5% K_2HPO_4). Electrolytes inhibited CO bubble coalescence, enhancing

the maximum k_La by a factor of 4.14. Dense electrical layers that formed near the gas bubbles inhibited bubble coalescence (Fig. 6) (Craig et al. 1993),thus increasing the mass transfer area.

Various electrolytes, including $NaNO_3$, NaCl, Na_2CO_3, Na_2SO_4, KCl, LiCl, CsCl, $BaCl_2$, and $MgCl_2$, were employed by Kazakov et al. (2014) to investigate the influence on the O_2 mass transfer in the presence of quartz particles in a poly (vinyl chloride) shell (SiO_2/PVC). Positive hydrating ions significantly reduced the O2 mass transfer enhancement factor and increased by negative hydrating ions. In electrolytes containing different cations with the same anion (KCl, LiCl, CsCl, $BaCl_2$, and $MgCl_2$), the dependences of the O_2 mass transfer enhancement factor E on the salt concentration were various. For KCl, LiCl, CsCl, $BaCl_2$, and E, it was increased with an increase in electrolyte concentration. The introduction of these salts into the aqueous phase strengthened O_2 mass transfer. However, the addition of $MgCl_2$ seemed to not affect E. For electrolytes containing different anions with the same cations ($NaNO_3$, NaCl, Na_2CO_3, and Na_2SO_4), the dependences of the coefficient E on the salt concentration strongly vary between electrolytes. For salts containing singly charged anions ($NaNO_3$ and NaCl), E increased with electrolyte concentrations reaching 2.5-2.6. Nevertheless, the concentrations of salts with doubly charged anions increased, and the E decreased to 0.6-0.7. It was concluded that introducing these electrolytes was detrimental to the O_2 absorption rate. Baz-Rodríguez et al. (2014) have examined the effect of inorganic electrolytes (NaCl, $MgCl_2$, $CaCl_2$) on oxygen-liquid mass transfer in a bubble column. The volumetric mass transfer coefficient (k_La), mass transfer coefficients (k_L), and specific interfacial area (a) were determined. Using a dimensionless concentration ($c_r = c/c_{tc}$) as the independent variable, the k_La value was the same regardless of the kind of electrolytes at constant superficial gas velocities (v_{sg}); the same happened for k_L.

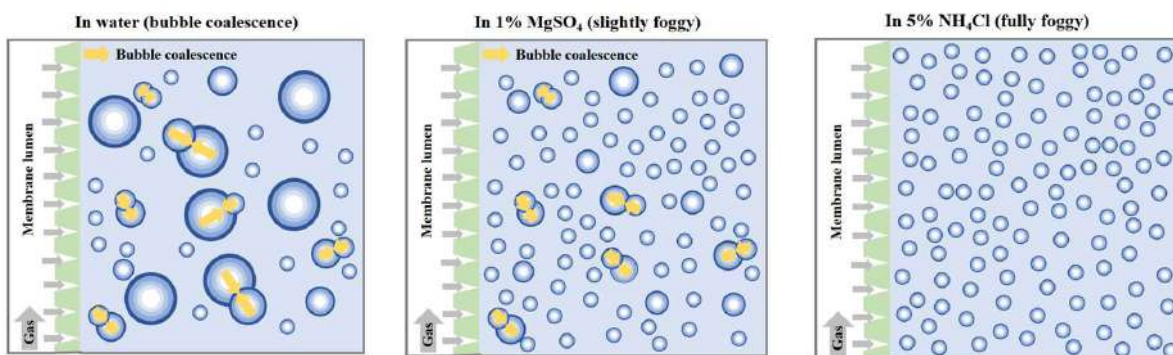
Fig. 6: Comparisons of the gas bubbling in water and electrolyte solutions. (Craig et al. 1993).

The critical concentrations for bubble coalescence (c_{tc}) were the key to characterizing the hydrodynamic behavior (Ribeiro & Mewes 2007, Syeda & Reza 2011). The presence of electrolytes strongly changed the hydrodynamics and gas-liquid mass transfer, mainly due to the decrease of bubble size and the corresponding increase a. The bubble coalescence inhibition played an important role in changing the hydrodynamic behavior. As the slip velocity decreased with the increase of c_r, k_L decreased. The presence of electrolytes reduced the k_L, their effect on a large enough to lead to a net increase in $k_L a$. A 40-50% increase in $k_L a$ compared with air-pure water. Nevertheless, k_L was reduced by about 60% compared to air-pure water. In agreement with the results reported previously, it was confirmed that k_L decreased in the presence of electrolytes (Taweel et al. 2013).

Surfactant

Surfactants are compounds that reduce the surface tension (or interfacial tension) between multiphase. The different types of surfactants are displayed in Fig. 7. (Bakthavatchalam et al. 2020). Adding surfactants in the gas and liquid phases to adjust the surface tension can affect the gas-liquid mass transfer process. We know that surfactants are amphiphilic organic compounds containing hydrophobic and hydrophilic groups. This property makes them accumulate at the gas-liquid interface, which may positively or negatively affect gas-liquid mass transfer. Hence, it's worth studying the influence of surfactants on the mass transfer process.

Pichetwanit et al. (2021) investigated the influence of nonionic surfactants with a small hydrophilic (Tergitol TMN-6, Triton X-100, Tergitol 15-S-9 and Tween-80) and cationic surfactants with a short linear chain (dodecyl trimethyl ammonium bromide (DTAB) and cetyl trimethyl ammonium bromide (CTAB)) on the mass transfer of carbon dioxide (CO_2) from the gas phase to monoethanolamine (MEA) solution. The addition of surfactant reduced the surface tension of the MEA and increased the contact area for the absorption of CO_2. Generally, mass transfer interfacial area increased with the addition of surfactant (Chaumat et al. 2007, Hebrard et al. 2009, García-Abuín et al. 2012, Mcclure et al. 2015). The results showed that the CO_2 equilibrium loading with nonionic and cationic surfactants slightly increased with surfactant concentration. Excluding tween-80 and Triton X-100, other surfactants improved the absorption rate of CO_2 in MEA solution. These results indicated that the initial CO_2 absorption rate of MEA was improved by using a small hydrophilic head non-ionic surfactant or a short linear chain cationic surfactant, such as Tergitol TMN-6 or DTAB. In addition, an increase in the longer hydrocarbon chain in nonionic or cationic surfactants did not significantly promote the absorption rate of CO_2 in the MEA solution. It was worth noting that the surfactant had no significant effect on the MEA solution's kinematic viscosity but slightly increased amine viscosity. Dang et al. (2022) conducted experiments with surfactants (Tween 80 with different surface tensions) to study possible enhancement in oxygen transfer. It had been observed that with increased surfactant concentration, the gas-liquid mass transfer performance first deteriorated and then improved. The addition of surfactant changed the surface tension. Surfactants work in two ways: (1) The addition of surfactant reduced the surface tension of bubbles, resulting in the decrease of bubbles coalescence, fine and uniform dispersion, and increased gas-liquid interface area. (2) Surfactant molecules attached themselves to the gas-liquid interface and formed a single-molecule film with certain mechanical strength, which hindered gas-liquid mass
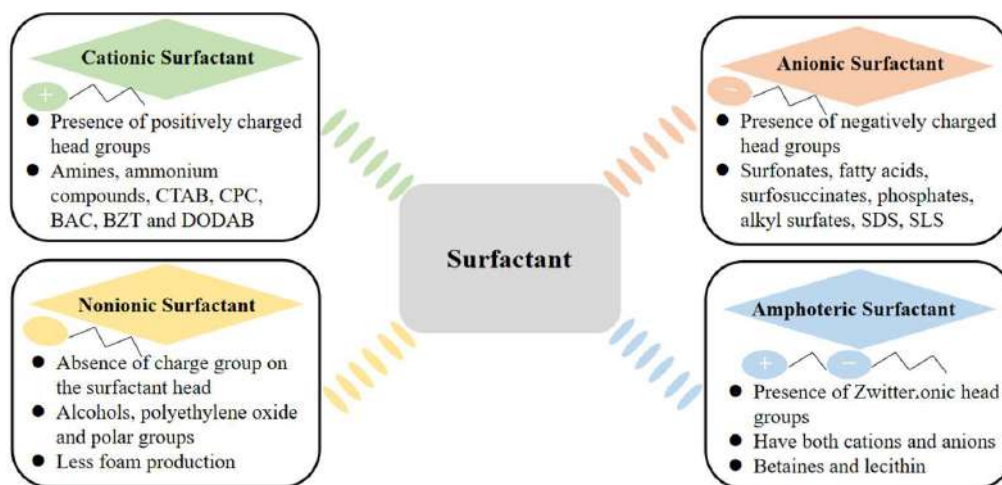

Fig. 7: Types of surfactants. Reproduced from ref. (Bakthavatchalam et al. 2020).
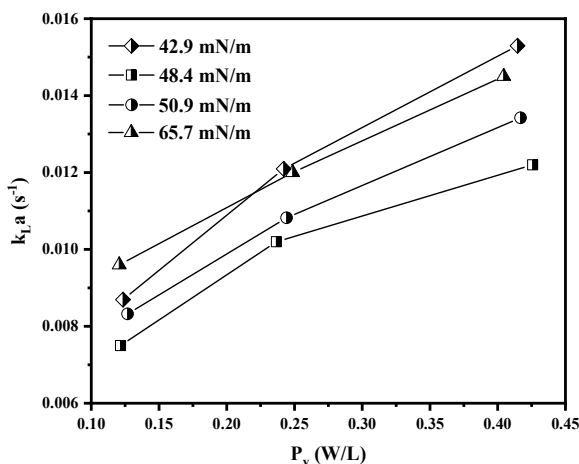
Fig. 8: Effect of surface tension on the gas-liquid mass transfer coefficient $k_L a$ (Dang et al. 2022).

transfer. As could be seen from Fig. 8, with a decrease in the surface tension from 65.7 mN·m^{-1} to 48.4 mN·m^{-1}, the single-molecule film formed by surfactant molecules at the gas-liquid interface had inhibitory oxygen mass transfer than promotion. An increase in surfactant concentration was expected to correspond with an increase in the inhibitory effect. It was observed that the enhancement in gas-liquid mass transfer gradually increased with a decrease in surface tension. At low speeds, however, the smaller mass transfer coefficient of 42.9 mN·m^{-1} than that of 65.7 mN·m^{-1}.

Yang et al. (2020) studied the influence of surfactant (oleic acid) on the nitrogen-liquid mass transfer. When the oleic acid concentration was increased, the mass transfer coefficient decreased, or the interface resistance increased. It was observed that oleic acid decreased the gas-liquid mass transfer by a factor of 4. This indicated that the excess surface concentration of oleic acid at the gas-liquid interface increased with the aqueous phase concentration until the aqueous phase concentration reached the critical micelle concentration. Since the solubility of nitrogen in pure oleic

acid was very small, the presence of oleic acid molecules at the interface increased the possibility that nitrogen transport across the interface would be impeded (Fig. 9). However, when oleic acid concentration was 2 mg L^{-1}, the interface resistance was about four times that for pure water (Birgand et al. 2007). In addition, the low concentration of oleic acid had a litter effect on the diffusion coefficient of nitrogen in water

Lebrun et al. (2022) investigated the effect of the surfactants' nature on oxygen mass transfer. The mass transfer coefficient of oxygen (k_L) values were determined for each of the aqueous solutions with the presence of three cationic surfactants with different hydrophobic chain lengths (including hexade-cyltrimethyl ammonium chloride, dodecyltrimethyl ammonium chloride trimethyl octyl ammonium chloride), and four nonionic surfactants with different hydrophilic chain lengths (including Triton X-100, Triton X-102, Triton X-165, Triton X-305). It could be seen that with an increase in the bulk concentration of surfactant, the liquid-side mass transfer coefficient decreased, ranging
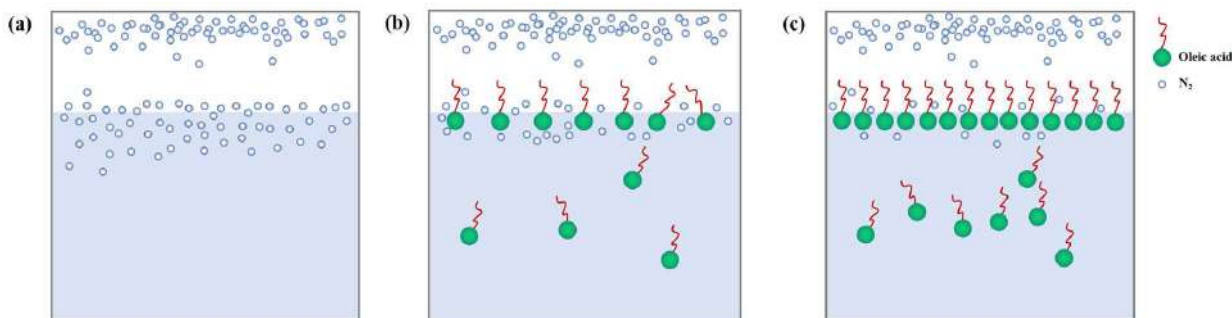

Fig. 9: Schematic of nitrogen transferring into aqueous solution with resistance at the interface due to accumulation of oleic acid: (a) control (no oleic acid); (b) small surface concentration of oleic acid; and (c) large surface concentration of oleic acid (Yang et al. 2020).
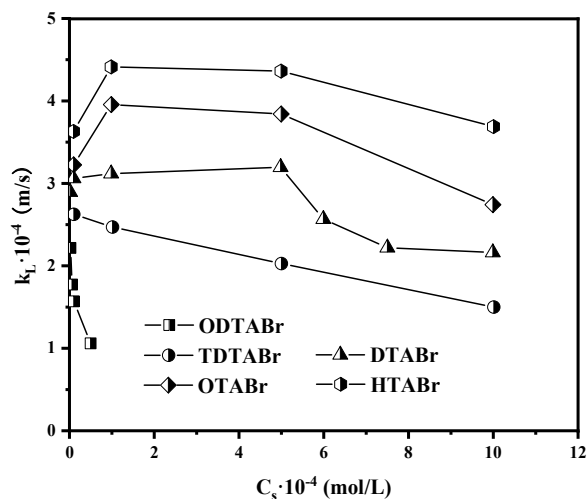
Fig. 10: Influence of different concentrations for several surfactants on the mass transfer coefficient (Gómez-Díaz et al. 2009, García-Abuín et al. 2010).

from 5.6×10^{-4} to 0.4×10^{-4} m.s^{-1}. However, increasing the length of the hydrophilic chain of nonionic surfactants does not affect the oxygen mass transfer, even though it changes the interface density. Increasing the hydrophobic chain length of cationic surfactants led to a decrease in the mass transfer coefficient of oxygen. And finally, the Sherwood number was calculated in each medium and classical correlations for gas-liquid mass transfer prediction.

The effect of the hydrocarbonate chain length of surfactant on the gas-liquid mass transfer process was investigated by García-Abuín et al. (2010). The surfactants with the long hydrocarbonate chain (hexyl-(HTABr)), surfactants with the short hydrocarbonate chain (octyl-(OTABr), decyltrimethylammonium bromide (DTABr)) and surfactants with an intermediate hydrocarbonate chain (tetradecyl-(TDABr), octadecyl-trimethyl ammonium bromide (ODTABr)) were used in this work. When the hydrocarbon chain length of the surface agent was increased, the carbon dioxide (CO_2) absorption rate decreased. At low concentrations of surfactant (HTABr, OTABr, and DTABr), gas-liquid mass transfer enhancement was observed. However, for surfactants TDTABr and ODTABr, the enhancement was not observed due to the reduction in the driving force (Fig. 10). In addition, the effect of various surfactants on the interface area depends on the surfactant with different bicarbonate chain lengths. Generally, mass transfer interfacial area increased with the addition of surfactant (Chaumat et al. 2007, Hebrard et al. 2009, García-Abuín et al. 2012, Mcclure et al. 2015). However, surfactants with a long chain length did not affect the interfacial area, obtaining values for the gas-liquid interfacial area similar to pure water.

CONCLUSION

In this paper, many studies on gas-liquid mass transfer enhancement are reviewed. Gas-liquid mass transfer can be enhanced by increasing one or more of the overall driving force, mass transfer coefficient, and interface area. Research on the intensification of gas-liquid mass transfer by introducing additives must be further strengthened. For further research directions, the following observations are provided.

(1) Study the effect of additives on the overall system performance and downstream processing, including separation and recovery/reuse of additives before the practical application of various mass transfer enhancement systems, which support their application's economic feasibility before additives application becomes a reality.

(2) Please select a suitable liquid solvent and/or gas carrier and study the effect of physical properties of the phase, such as viscosity, interfacial tension, etc., on process design, which help us achieve better process designs.

(3) Mass transfer research should not be limited to determining macroscopic properties; it encourages researchers to explore the underlying mechanisms.

ACKNOWLEDGMENT

REFERENCES

Abeydeera, U., Jayantha, W.M. and Samarasinghalage, T. 2019. Global research on carbon emissions: A scientometric review. Sustainability, 11: 3972.

Bakthavatchalam, B., Habib, K., Saidur, R., Saha, B.B. and Irshad, K. 2020. A comprehensive study on nanofluid and ionanofluid for heat transfer enhancement: A review on current and future perspective. J. Mol. Liq., 305: 112787.

Baz-Rodríguez, S.A., Botello-Alvarez, J.E., Estrada-Baltazar, A., Vilchiz-Bravo, L.E., Padilla-Medina, J.A. and Miranda-López, R. 2014. Effect of electrolytes in aqueous solutions on oxygen transfer in gas-liquid bubble columns. Chem. Eng. Res. Des., 92: 2352-2360.

Beenackers, A.A.C.M. and Swaaij, W.P.M.V. 1993. Mass transfer in gas-liquid slurry reactors. Chem. Eng. Sci., 48: 3109-3139.

Birgand, F., Skaggs, R.W., Chescheir, G.M. and Gilliam, J.W. 2007. Nitrogen removal in streams of agricultural catchments: A literature review. Crit. Rev. Env. Sci. Technol., 37: 381-487.

Boltes, K., Caro, A., Leton, P., Rodriguez, A. and Garcia-Calvo, E. 2008. Gas-liquid mass transfer in oil-water emulsions with an airlift bio-reactor. Chem. Eng. Process. Process Intensif., 47: 2408-2412.

Brilman, D.W.F., Goldschmidt, M.J.V., Versteeg, G.F. and Swaaij, W.P.M.V. 2000. Heterogeneous mass transfer models for gas absorption in multiphase systems. Chem. Eng. Sci., 55: 2793-2812.

Chaumat, H., Billet, A.M. and Delmas, H. 2007. Hydrodynamics and mass transfer in bubble column: Influence of liquid phase surface tension. Chem. Eng. Sci., 62: 7378-7390.

Craig, V.S.J., Ninham, B.W. and Pashley, R.M. 1993. The effect of electrolytes on bubble coalescence in water. Journal of Physical Chemistry, 97: 10192-10197.

Dang, X.H., Guo, J.H., Yang, L., Xue, S., Ai, B.Y., Li, X.N., Chen, L.Y., Li, W., Qin, H.Y. and Zhang, J.L. 2022. Effects of blade structures on the dissolution and gas-liquid mass transfer performance of cup-shaped blade mixers. J. Taiwan Inst. Chem. E, 131: 104149.

Dumont, E., Andrès, Y. and Cloirec, P.L. 2014. Mass transfer coefficients of styrene into water/silicone oil mixtures: New interpretation using the "equivalent absorption capacity" concept. Chem. Eng. J., 237: 236-241.

Dumont, E. and Delmas, H. 2003. Mass transfer enhancement of gas absorption in oil-in-water systems: A review. Chem. Eng. Process. Process Intensif., 42: 419-438.

Esmaeili-Faraj, S.H. and Esfahany, M.N. 2016. Absorption of hydrogen sulfide and carbon dioxide in water-based nanofluids. Ind. Eng. Chem. Res., 55: 4682-4690.

Garcia, G.E.C., Schaaf, J.V.D. and Kiss, A.A. 2017. A review on process intensification in HiGee distillation. J. Chem. Technol. Biot., 92: 1136-1156.

García-Abuín, A., Gómez-Díaz, D., Losada, M. and Navaza, J.M. 2012. Bubble column gas-liquid interfacial area in a polymer+surfactant+water system. Chem. Eng. Sci., 75: 334-341.

García-Abuín, A., Gómez-Díaz, D., Navaza, J.M. and Sanjurjo, B. 2010. Effect of surfactant nature upon absorption in a bubble column. Chem. Eng. Sci., 65: 4484-4490.

Garcia-Ochoa, F., Gomez, E., Santos, V.E. and Merchuk, J.C. 2010. Oxygen uptake rate in microbial processes: An overview. Biochem. Eng. J., 49: 289-307.

Gome, A. and Upadhyay, K. 2012. Chemical kinetics of ozonation and other processes used for the treatment of wastewater containing pharmaceuticals: A review. Int. J. Curr. Res. Rev., 4: 157-168.

Gómez-Díaz, D., Navaza, J.M. and Sanjurjo, B. 2009. Mass-transfer enhancement or reduction by surfactant presence at a gas-liquid interface. Ind. Eng. Chem. Res., 48: 2671-2677.

Góngora-García, O.R., Aca-Aca, G. and Baz-Rodríguez, S.A. 2021. Mass transfer in aerated culture media combining mixed electrolytes and glucose. Bioprocess Biosyst. Eng., 44: 81-92.

Hebrard, G., Zeng, J. and Loubiere, K. 2009. Effect of surfactants on liquid side mass transfer coefficients: A new insight. Chem. Eng. J. Lausanne, 148: 132-138.

Jang, N., Yasin, M., Kang, H., Lee, Y., Park, G.W., Park, S. and Chang, I.S. 2018. Bubble coalescence suppression driven carbon monoxide (CO)-water mass transfer increase by electrolyte addition in a hollow fiber membrane bioreactor (HFMBR) for microbial CO conversion to ethanol. Bioresour. Technol., 263: 375-384.

Jensen, M.B., Ottosen, L.D.M. and Kofoed, M.V.W. 2021. H2 gas-liquid mass transfer: A key element in biological Power-to-Gas methanation. Renew. Sustain. Energy Rev., 147: 111209.

Kazakov, D.A., Vol Khin, V.V., Borovkova, I.S. and Popova, N.P. 2014. Kinetics of oxygen absorption by aqueous electrolyte solutions in the presence of microencapsulated quartz particles activating the mass transfer in the liquid phase. Russ. J. Appl. Chem., 87: 88-94.

Kim, K., Lee, J., Seo, K., Kim, M.G., Ha, K.S. and Kim, C. 2016. Enhancement of methane-water volumetric mass transfer coefficient by inhibiting bubble coalescence with electrolyte. J. Ind. Eng. Chem., 33: 326-329.

Kundu, A., Dumont, E., Duquenne, A.M. and Delmas, H. 2002. Mass transfer characteristics in gas-liquid system. Canad. J. Chem. Eng., 81: 640-646.

Kuuskraa, V., Stevens, S.H. and Moodhe, K.D. 2013. Technically Recoverable Shale Oil and Shale Gas Resources: An Assessment of 137 Shale Formations in 41 Countries Outside the United States. US Energy Information Administration, US Department of Energy, US, pp. 1-730.

Lakhdissi, E.M., Fallahi, A., Guy, C. and Chaouki, J. 2020. Effect of solid particles on the volumetric gas-liquid mass transfer coefficient in slurry bubble column reactors. Chem. Eng. Sci., 227: 115912.

Lebrun, G., Benaissa, S., Men, C.L., Pimienta, V., Hébrard, G. and Dietrich, N. 2022. Effect of surfactant lengths on gas-liquid oxygen mass transfer from a single rising bubble. Chem. Eng. Sci., 247: 117102.

Lee, W., Xu, R.H., Kim, S., Park, J.H. and Kang, Y.T. 2021. Nanofluid and nanoemulsion absorbents for the enhancement of CO_2 absorption performance. J. Clean. Prod., 291: 125848.

Li, H., Wu, C.H., Hao, Z.Q., Li, X.G. and Gao, X. 2019. Process intensification in vapor-liquid mass transfer: The state-of-the-art. Chin. J. Chem. Eng., 27: 1236-1246.

Li, W.X., Peng, H., Zhang, Z.G. and Chen, K. 2010. Gas-liquid mass transfer in oil-water emulsions in a stirrer. Chem. Eng., 11: 5-9.

Luo, L.G. 2013. Heat And Mass Transfer Intensification and Shape Optimization: A Multi-Scale Approach. Springer Science & Business Media, London.

Mcclure, D.D., Lee, A.C., Kavanagh, J.M., Fletcher, D.F. and Barton, G.W. 2015. Impact of surfactant addition on oxygen mass transfer in a bubble column. Chem. Eng. Technol., 38: 44-52.

Mehdipour, M., Keshavarz, P. and Rahimpour, M.R. 2021. Rotating liquid sheet contactor: A new gas-liquid contactor system in CO_2 absorption by nanofluids. Chem. Eng. Process., 165: 108447.

Mehrnia, M.R., Towfighi, J., Bonakdarpour, B. and Akbarnejad, M.M. 2005. Gas hold-up and oxygen transfer in a draft-tube airlift bioreactor with petroleum-based liquids. Biochem. Eng. J., 22: 105-110.

Parnian, P., Zamir, S.M. and Shojaosadati, S.A. 2016. Styrene vapor mass transfer in a biotrickling filter: Effects of silicone oil volume fraction, gas-to-liquid flow ratio, and operating temperature. Chem. Eng. J., 284: 926-933.

Pichetwanit, P., Kungsanant, S. and Supap, T. 2021. Effects of surfactant type and structure on properties of amines for carbon dioxide capture. Coll. Surf. A Physicochem. Eng. Asp., 622: 126602.

Radler, M. 2011. Worldwide oil production steady in 2011: Reported reserves grow. Oil Gas J., 109: 26-27.

Ramshaw, C. 1983. Higee distillation-An example of process intensification. Chem. Eng., 1: 13-14.

Ribeiro, C.P. and Mewes, D. 2007. The influence of electrolytes on gas

hold-up and regime transition in bubble columns. Chem. Eng. Sci., 62: 4501-4509.

Rols, J.L., Condoret, J.S., Fonade, C. and Goma, G. 1990. Mechanism of enhanced oxygen transfer in fermentation using emulsified oxygen-vectors. Biotechnol. Bioeng., 35: 427-435.

Sajjadi, S., Zerfa, M. and Brooks, B.W. 2002. Dynamic behavior of drops in oil/water/oil dispersions. Chem. Eng. Sci., 57: 663-675.

Sauid, S.M., Krishnan, J., Ling, T.H. and Veluri, M.V.P.S. 2013. Enhancement of oxygen mass transfer and gas holdup using palm oil in stirred tank bioreactors with xanthan solutions as simulated viscous fermentation broths. Biomed. Res. Int., 13: 409675.

Shariati, F.P., Bonakdarpour, B. and Mehrnia, M.R. 2007. Hydrodynamics and oxygen transfer behavior of water in diesel microemulsions in a draft tube airlift bioreactor. Chem. Eng. Process. Intensif., 46: 334-342.

Syeda, S.R. and Reza, M.J. 2011. Effect of surface tension gradient on gas hold-up enhancement in aqueous solutions of electrolytes. Chem. Eng. Res. Des., 89: 2552-2559.

Taweel, A.M.A., Idhbeaa, A.O. and Ghanem, A. 2013. Effect of electrolytes on interphase mass transfer in microbubble-sparged airlift reactors. Chem. Eng. Sci., 100: 474-485.

Yang, Z.H., Telmadarreie, A., Dong, M.Z. and Bryant, S. 2020. A pressure-decay method to determine the influence of a surface-active agent on the interface and internal resistances to gas-liquid mass transfer. Chem. Eng. J., 387: 124108.

Yoshida, F., Yamane, T. and Miyamoto, Y. 1970. Oxygen absorption into oil-in-water emulsions. A study on hydrocarbon fermentors. Ind. Eng. Chem. Process Des. Dev., 9: 570-577.

Zamir, S.M., Babatabar, S. and Shojaosadati, S.A.,2015. Styrene vapor biodegradation in single- and two-liquid phase biotrickling filters using *Ralstonia eutropha*. Chem. Eng. J., 268: 21-27.

Zhang, H., Wang, B., Xiong, M.Y., Gao, C.Y., Ren, H.Y. and Ma, L. 2022. Process intensification in gas-liquid mass transfer by nanofluids: Mechanism and current status. J. Mol. Liq., 346: 118268.

Computer Vision Based Machine Learning and Deep Learning Approaches for Identification of Nutrient Deficiency in Crops: A Survey

M. Sudhakar* [iD] **and R. M. Swarna Priya*†** [iD]

*School of Information Technology and Engineering, Vellore Institute of Technology, Vellore, Tamilnadu, India
†Corresponding author: R. M. Swarna Priya; swarnapriya.rm@vit.ac.in

ABSTRACT

Agriculture is a significant industry that plays a major role in a country's sustainable environment and economic development. The global population demands increased food production with minimal losses. Nutrient deficiency is one of the major and crucial factors influencing crop production significantly. Common techniques for determining crop nutrition status are the diagnosis of plant morphology, Enzymology, chemical effects, fertilization, etc. However, the above techniques are invasive and time-consuming or infeasible while considering varied production practices in different locations, environments and climatic conditions. Computer Vision is an area of Computer Science that deals with creating Artificial Intelligence based vision systems that can use image data, process, and analyze as humans perform. Early Detection of Crop Nutrient deficiencies favors the farmers to monitor the affected crops and plan for the manure or fertilizer application, which supports to regain of the crop's efficiency for attaining its maximum yield. Modern computer vision systems rely on Machine Learning (ML), Remote sensing, Satellite imagery, unmanned aerial vehicles (UAVs), Internet of things (IoT) based sensor devices, and Deep Learning (DL) models that use algorithms to extract required features from data. The objective of this work is to provide an overview of recent research and identify the scope of computer vision-based technologies used for identifying crop nutrient content and deficiency, find research challenges in predicting nutrient imbalance in comparison with plant diseases that show certain similar characteristics, thereby to improve crop health and production.

INTRODUCTION

The agriculture sector has witnessed numerous changes for improving crop production. Several standards have been set to promote agricultural businesses, helping farmers improve their operational efficiency, reduce cost, provide quality food, and ensure their food hygiene and safety. Soil productivity closely depends on the available nutrients that result in a good yield of crops. The availability of nutrients in the soil is monitored using a specific system to determine the fertility of that specific area. An analysis is done to decide on fertilizer recommendations to strengthen it. Due to the adoption of synthetic or chemical-based fertilizers by most farmers in the twentieth century, there had been a 50% increase in the overall yield from the field. Still, it has led to the major issue of Soil infertility or unavailability of major natural elements (Kilic et al. 2020). The climatic effects and environmental conditions should not degrade

the yield. Farmers require data-driven or service-based techniques to enhance crop yield with the available field and other resources to meet all these needs. In this regard, precision agriculture has evolved with several tools and techniques that are being formulated, including automated harvesters, robot-weeders, Smartphone-based monitoring, UAVs, computer vision, pervasive computing, wireless ad-hoc sensor networks, Radio Frequency Identifier (RFID), cloud computing based data storage, ML models, IoT based devices combined with DL, satellite monitoring, remote sensing, context-aware computing, etc., which are becoming increasingly popular and beneficial to the farmers for monitoring the crop stress which limits the output. With regard to precision agriculture, many areas of scope or use case models shall be explored. They are as follows:

- Crop health monitoring for deficiencies and diseases
- Soil Nutrient management
- Monitoring of climate conditions
- Farm land monitoring and mapping for predictive analytics

ORCID details of the authors:

M. Sudhakar: https://orcid.org/0000-0001-9208-2565
R. M. Swarna Priya: https://orcid.org/0000-0002-8287-9690

- Greenhouse automation
- Automated irrigation scheduling and optimization
- Production and yield management
- Livestock monitoring
- Farm Inventory management systems
- Crop security

Motivation

In the current scenario, there are four major challenges in agriculture. (I) The availability of groundwater, which cannot be produced artificially, is scarce. (II) Limited agricultural lands as the world population grows. (III) The soil became infertile to produce enough food. (IV) The agriculture production or the output is inefficient. Farmers apply manures and fertilizers to their crops to boost their production. However, over usage or under usage of these applications may harm the crop, soil, humans, and animals. It is important to consider the nutritional values and food quality by understanding the crop's nature during growth, the reasons for low quality and yield, and identifying the crop inefficiencies. Common techniques for determining crop nutrition status are the diagnosis of plant morphology, Enzymology, chemical effects, fertilization, etc. Computer Vision Technologies play a major role in identifying and monitoring crop deficiencies that prevent the prescribed output. It is concerned with building artificial systems or models that make sense out of images through training and processing at a pixel level in the image for extracting application-specific information. These intelligent systems retrieve the visual data and interpret the results using designed software or applications. This domain is widely used in the medical field, industrial manufacturing process, military applications, agriculture or field robots, phenotyping, grading and sorting, livestock monitoring, identification of diseases, and nutrition deficiency in plants/crops.

Significance of Nutrients for Crops

Plant growth requires various minerals and nutrients to grow and complete their life cycles. The application of appropriate nutrients is required to attain maximum sustainable yield. Deficiency of these nutrients results in different symptoms like stunted growth, poor yield, and the poor quality of food output from crops. The Nutrient deficiency should be identified at the earlier growth stage, and necessary actions are to be taken to regain and improve yield. Primary nutrients or macronutrients are required in larger amounts, including nitrogen, phosphorus, and potassium (Espiritu 2017, Haifa Group 2020, CGIAR Platform 2020). The secondary nutrients or micronutrients such as Sulphur, Magnesium, and Calcium are needed in certain quantities depending upon the plant species for its germination, resistance to pathogenic disease, and reproduction that ensures the healthy growth of plants. Calcium provides vital structural support for the plant cell. Magnesium is required for photosynthesis as it activates the enzymes required for plant growth. Sulfur is also required in moderate quantities that help the plants develop chlorophyll and protein synthesis. Feeding the crops with optimum levels of nutrients under experimental conditions becomes very difficult. The absorption of nutrients by plants is not assured by the mere availability of nutrients in the soil due to various factors such as moisture content and temperature of the soil, water pH level, toxic elements, and low salts. Hence, adequate levels of diagnosis are an important process to detect abnormalities and find effective solutions to improve the productivity of crops.

Fig. 1 depicts the identification of crop health using various dimensions of leaf symptoms.

Fig. 1: Examples of Various Dimensions of crop health.

Paper Organization

This survey article enables the readers to get an overview of Computer vision-based advancements in the identification and classification of crop nutrient deficiency, understand the existing shortcomings, and improve the technology by means of further research. The article is framed by studying various articles related to computer vision technologies for predicting crop nutrient deficiencies from 2010. However, most of the papers range between 2018-2022. About 60 articles related to agriculture and crop nutrients were studied, among which 30 papers were selected for this survey as a perspective on computer vision and nutrient deficiency. The study focused on the evolution of computer vision, such as from Image processing to ML or DL, and a combination of recent models or advancements. The subsequent content of this survey paper is structured as follows. The second section explores the factors related to crop stress causing nutrient deficiency and its associated specific works for detection. The third section constitutes various sources and data collection methodologies for stress prediction. The fourth section identifies the outcomes, potential challenges, and future scope. Finally, section five concludes this survey paper.

Factors of Crop Stress Causing Nutrient Deficiency

Nutrient deficiency is visible through different specific symptoms of crop health, which may be visual or internal characteristics. For example, the leaf shape is deformed due to calcium deficiency. Nitrogen deficiency causes the change of color in leaves to light green and yellow at the top and bottom of the plant, respectively. Manganese deficiency causes holes, whereas copper deficiency causes pale pink between the leaves' veins (Karthika et al. 2018). In view of smart agriculture, different robotic machines are developed to improve crop yields, such as the popular FarmBot and Agribots, to determine various crop-dependent factors such as soil depth for effective seeding processes, soil salinity, soil organic carbon (SOC), etc. The major reasons for crop stress are (1) Soil Quality and Nutrient Supply Imbalance (Electric Conductivity and Mobility of Nutrients), (2) Fertilizers, (3) weather conditions, (4) pests, (5) irrigation and pH levels.

Soil Quality and Nutrient Supply Imbalance

In general, soil analysis is performed to measure the nutrient content in the soil. The influence of biological, chemical, and physical processes in the soil plays a major role in plant growth and development. A variety of tools and technologies have been implemented through research findings in terms of monitoring and predicting the soil nutrient distribution, including conditions of moisture, temperature, pH value, level of water holding, and humidity of the air, such as the Geographic Information Systems (GIS), Global Positioning Systems (GPS), Variable Rate Technology (VRT), thereby estimating the present level of nutrients and recommend the required quantity of fertilizers or manures across the field. (Raza et al. 2014) Proposed an automatic Gaussian process classifier with support vector machine algorithm for determining the soil-moisture stress using visible and thermal images of spinach canopies captured remotely, in which the efficiency of using combinational methods was explored. Lavanya et al. (2020) designed an IoT-based NPK sensor system that includes LDR and LED. The colorimetric principle was used for monitoring and analysis of the soil nutrients. The sensed data of NPK sensors from various fields are uploaded to the Google Cloud database to quickly retrieve information, and the fuzzy logic concept was applied to data. Yu et al. (2021) compared the usage of UAV multi-spectral imagery and Planet Scope satellite imagery to predict the nitrogen weight of wheat fields using plant height, leaf area index, soil moisture, and field topographic metrics. Here, Random Forest and support vector machine-based regression models were applied to predict nitrogen weight.

Fertilizers

Fertilization in crops is location-specific and depends upon soil nutrient concentration level, including soil absorption, fertility rate, crop size, and other associated factors. Overusing fertilizers causes unpredictable negative impacts on soil, crops, the atmosphere, and human health. Leaf nitrogen content is an indicator of nitrogen status based on which the required nutrient for crops at regular intervals or during unexpected environmental effects are identified. Appropriate fertilization measures are taken through strategies in smart agriculture. But, parameters such as leaf area index, chlorophyll, amount of protein content, and biomass value are not proportionate to the amount of nitrogen content. The normalized vegetation index (NDVI) is computed to predict the vegetative health status of the soil. Chen et al. (2010) used the NDVI index to determine the nitrogen content of rice crops at the jointing stage. They constructed a nitrogen top dressing regulation model that estimated the accurate level of required fertilizer (Agarwal et al. 2018). The leaf chlorophyll content of spinach seedlings was assessed to distinguish between the healthy and stressed using multivariate data analysis tools. Haider et al. (2021) Devised a computer vision algorithm that extracts the similarity feature and pattern from the leaf image while comparing it with the given reference. The green color value (GCV) index was computed to identify nitrogen content. It could be further used for distinguishing other deficiencies with the diseases.

Weather Conditions

Smart sensors placed across the farm acquire data from the surrounding environment regarding parameters such as humidity, temperature, moisture, precipitation, and dew detection and send them for analyzing or processing through various application-specific tools. Jangam et al. (2018) stated that the sensor data could be used to map the climatic conditions or patterns for selecting appropriate precise methods to improve specific crop productivity. Moreover, the results of accurate measurement and analysis of agro-meteorological factors provide a tool for farmers to predict or enhance crop yield. It also assists in the selection of pesticides and fertilizers. Diedrichs et al. (2018) designed an IoT-based frost prediction system using ML algorithms evaluated by training classification and regression models. The Random Forest algorithms outperform other models in terms of sensitivity, precision, and F1 score. Many smart decision-support User Interface systems have been developed through research to inform farmers about crop management activities. Nabi et al. (2022) quoted that these smart farming techniques also helped the farmers by lowering the investment cost and getting higher yields from their farms. The Global Positioning System coordinates acquired using IoT play a vital role in the event of spatial object topographic analysis by providing low-cost solutions to various areas like field traversal, including ground truth values, recording of weather parameters, and observations. Also, besides providing better accuracy and high consistency using rapid communication protocols, smartphones can provide diverse adaptability to run high-end applications.

Pest Control in Crops

Crop production is severely affected by the occurrence of pests and development of diseases. The pests hide behind the leaves to avoid the thermal heat during the day and start appearing in the evening or at night. Hence, it creates a major issue of observing the pests physically during the daytime, leaving the crops with bacterial infections resulting in large-scale diseases. Wang et al. (2013) created an environmental monitoring system for recording the status of apple orchards using many sensors with YOLO v3 Dense models, which was effective for identifying anthrax and anthracnose on the surface of apples. Chandy (2019) developed a drone-based pest identification system embedded with NVIDIA Tegra System on Chip (SoC), which captures the images in coconut farms and processes using DL algorithms for determining pest-affected or unhealthy trees. The algorithm developed was also suited for unstructured images, and the information being transferred to the farmer's smartphone helped for early pest identification or unhealthy trees. Gladence et al.

(2020) highlighted the application of human-robot interaction by combining sensed environmental data with DL tools or algorithms, which helped farmers to prevent pests and monitor crops, particularly at earlier growth stages. Chen et al. (2020) designed a smart pest identification system using a drone-based YOLO V3 DL model. The designed system provided better control over Tessaratoma papillosa (insect), improving crop yield and quality. Some drawbacks were discussed, such as leaf occlusions, drone stabilization between the trees, Illumination conditions, and improving pest recognition performance using various angles. It tends to be the future scope of research. Image pattern recognition technology is a non-invasive strategy for identifying pest damage and thus helps improve crop production. The recent advances of YOLO v4 DL models are used to monitor pests and crop environmental conditions.

Irrigation and pH

Irrigation in agriculture has evolved with various smart techniques to manage crop loss due to water scarcity. These irrigation systems help estimate water requirements for a specific crop, soil type, moisture, and climate. A precise soil moisture control system using wireless sensor networks and many other advanced tools developed, such as an IoT-based framework measuring crop water stress index, could be used to optimize irrigation to improve crop health and productivity. The pH level below the soil plays a key role in optimizing various factors responsible for nutrient cycling and soil remediation, as it affects the entire crop's interaction with the environmental system. But the pH requirement and sustainability differ from crop to crop. Certain crops, such as lime, can tolerate the soil's acidity, but very few survive in moderately alkaline soils due to the limited mobility of nutrients. Soil with high organic matter has a pH level of 5.0 to 5.5. Liu et al. (2020) created a comprehensive interactive model for dynamic tracking of alfalfa growth by regulating water and fertilizer. The model is added with a simulation platform that closely monitors crop growth by measuring the physical environments parameters such as leaf area and soil water level. Wu (2021) proposed an LSTM-based smart agricultural system using IoT sensors and devices that monitors environmental conditions like soil moisture, sunlight, temperature, and weather forecast information. Depending upon the data collected with respect to the factors considered, the irrigation is done to balance the soil's pH level, hence enriching the yield. Boursianis et al. (2021) explore a smart irrigation system, AREThOU5A, which includes ML algorithms and an IoT platform with inbuilt sensors for sensing the relative surrounding physical environment. Depending on the parametric values, precise irrigation is performed. The system has 5G network capabilities.

MATERIALS AND METHODS

Prediction of Stress

As technology advances, crop stress prediction is performed using various methods and combinations of tools to improve performance factors like accuracy and quality. Agricultural field data monitoring and collection involves the communication of different devices between each other, sensors that provide information about soil, crop health conditions, and other associated factors. This enables us to determine the specific crop variety concerning its location. Several algorithms and models are developed to determine crop efficiency by means of matching crop vegetative index parameters with a particular color: green means no stress, yellow for medium stress, orange with high stress, and red means it has very high stress. Table 1 summarizes the specific works using computer vision with ML, and Table 2 summarizes the specific works using DL to detect nutrient deficiency. This section summarizes some specific works related to data collection methodologies involved with Computer Vision based identification of Nutrient deficiencies using Remote Sensing, ML, DL, and IoT-based UAV Monitoring. The following figure (Fig. 2) depicts the workflow of a typical computer vision model.

Computer Vision-Based Remote Sensing

Remote sensing is utilized for crop nutrient control and enhancing productivity by developing various advanced tools in decision-making systems. A set of IoT-based sensors placed along agricultural fields continuously monitors the environmental conditions. The collected data is transferred to an analytical tool, after which the farmers can track the field and crops through the user interface dashboard. Necessary actions for crops are taken based on the data insights. Remote sensing could be deployed in many agriculture-related applications such as soil versus yield monitoring, stress management of soil to crops, schedule irrigation, crop disease detection, residue estimation, and crop maturity. Liu et al. (2017) proposed a multi-spectral remote sensing technology based on the UAV application of LNC. Diagnosis of other deficiencies other than nitrogen is rarely reported using Remote sensing. Zhang et al. (2018) used a UAV equipped with a digital camera to monitor the nutrition of the maize canopy during summer in terms of nitrogen. By analyzing the dynamic normalized color coefficient values, the diagnosis is performed efficiently and quickly compared to the conventional methods of obtaining those management parameters. With the development of Hyperspectral remote sensing, the spectral information of crops is obtained, and
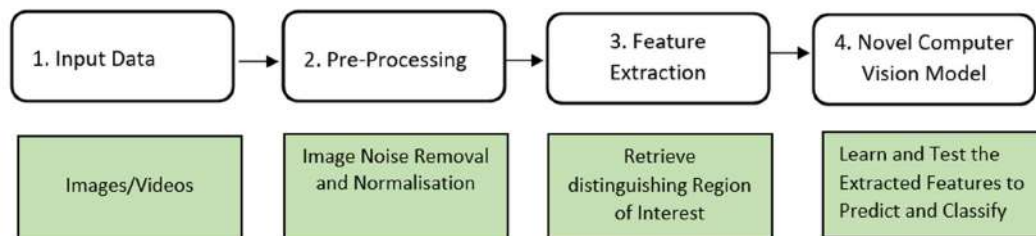

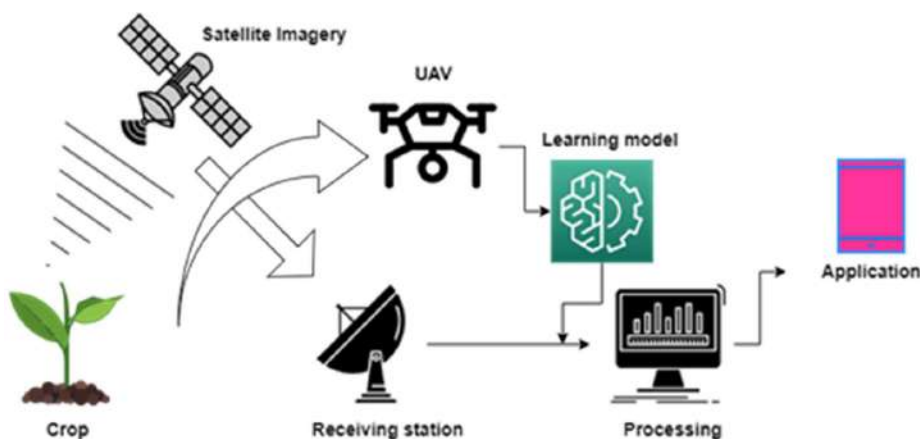Fig. 2: Workflow of a Typical Computer Vision Model.

Fig. 3: Remote Sensing and UAV in Agriculture.

the nutrition diagnosis is made using a computer (Feng et al. 2020). Shendryk et al. (2020) compared the performance parameters of prediction models based on multi-spectral predictors or LiDAR. A benchmark evaluation for the Vegetative Index standard on varied geographical areas is challenging. The Figure (Fig. 3) overviews computer vision-based remote sensing and UAV. Future research could focus on ensembling multi-spectral imaging with LiDAR predictors.

Computer Vision-Based Drones and IOT-Based Crop Monitoring

In recent years, drone technology has become very popular with its built-in camera and autonomous flying capabilities enabling it to be used for various applications. Depending on the flight requirement and application, ground or aerial-based drones are used in agriculture. The drones help assess crop health information using the overall aerial view of agricultural land and geo-sensing data. Computer vision models, in combination with IoT-based devices and DL tools, are trained using captured images by the camera and other sensors being mounted on UAV to know the soil conditions, segment crops, classify crops, identify vegetation, detect disease and weeds, and monitor crop nutrient content. Drones can be remotely controlled or by using specially designed software in synchronization with sensors and GPS, thus creating an Embedded system-based flight. Therefore, UAVs are suitable for various activities ranging from counting and yield prediction enabling smart farm monitoring. As agriculture is related to highly variable environmental conditions and factors, an automated real-time monitoring system is in need. IoT applications in agriculture aim to solve the above issues and equalize the population's food demands with reduced loss (Jesus 2019). Torres-Sanchez et al. (2015) proposed a ground-breaking method for measuring and mapping. The result provided a relation between the factors related to field geometry, its resources, and tree growth. The following Table 1 lists some important activities in agriculture that involves IoT technology.

Table 1: Major activities in agriculture involving IoT technology.

Tasks	Sub Activities
Crop Monitoring	Environmental sensing, Detect crop stress, Pests, weeds, Ripening
Crop Practices	Smart farming, Automation, and precision mapping activities
Services	Education, Crop Models, Financial Management, Information Systems, Accountability, Paying agency (PA), Resource usage
Market operations	Quality and certification, Traceability, Seeds, machinery, Labor

Szewczyk et al. (2018) established a crop monitoring system using UAVs for assessing the impact of fertilizer elements on crop health with the help of captured spectral properties. Niu et al. (2019) found that the height of a UAV flight can affect the detection accuracy of different image spectral bands for irrigation systems of Onion crops using neural networks. The author showed that the RGB combined with the near-infrared (NIR) image band gave the best accuracy. The following are some features of UAVs mentioned in their article. The Agdrone could cover 600 to 800 acres in one hour at an altitude of 400 ft. The DJI Matric100 has a double battery that facilitates an extra 40 minutes of flight time and is an added feature of the GPS system. The advanced Agras MG-1-DJI had a unique feature to carry 10 KG of liquid and spray over an area of 4000 to 6000 sq. meters in about 10 minutes, comparatively 70 times faster than manual spray. The DJI T600 captures the environment with 4K video resolution. The EBEE SQ drone is used for monitoring crop growth at various stages. The Lancaster, 5 precision Hawk, was used to collect atmospheric temperature and the environment's humidity level surrounding the agricultural area. The SOLO AGCO drone with advanced cameras mounted had high resolution and accurate image recording capabilities.

Computer Vision Related to Machine Learning and Deep Learning

Modern Computer vision development models focus on tools based on ML or DL, sensors, and devices that support real-time monitoring of agricultural fields, such as UAV, IoT sensing devices, satellite imagery, etc. (Stokes 2019, Eastern Peak Technology Consulting 2020, Scnsoft 2022, Crop In 2022). The Learning Models and algorithms are pattern recognition based that find the patterns and label the objects on those images. A typical ML architecture consists of feature extraction and classification modules. Watchareeruetai et al. (2018) proposed a Novel method for identifying and analyzing plant nutrient deficiencies using Image segmentation and CNN. The results are validated with a real-time nutrient-controlled environment. Shah et al. (2018) proposed an automated system for nutrient deficiency analysis. A digital camera dataset was created for color feature extraction, edge detection, texture detection, etc. The detection of exact nutrient-deficient and healthy plants was performed using supervised ML algorithms, and necessary care was taken to improve the yield. Ghosal et al. (2018) Implemented a deep convolutional neural network for identifying soybean stress from RGB leaf images. With regard to the plant stress identification model or phenotyping, four stages, namely identification, classification, quantification, and prediction, termed ICQP, were evaluated. This approach

provided a relatively quantitative measure for each modeling stage, such as identifying stress type, classification of stress levels, and severity of stress. The below figure (Fig. 4) gives an architecture of a classification model that differentiates the characteristics between specific crop nutrient deficiency and crop disease.

Learning models with more than 25,000 images classify several biotic and abiotic stress. This methodology allows for accurate stress management in real-world situations providing high reliability and adaptability to certain illumination levels. Wulandhari et al. (2019) developed

a deep convolutional neural network to manage health conditions using crop images. Here, a hybrid network with a transfer learning approach, namely Inception-Resnet architecture, was trained using the ImageNet dataset. It was then experimented with fine tuning of hyperparameters such as learning rate and number of epochs. The authors achieved 96% and 86% accuracy during training and testing, respectively. A comparative graph depicting the number of authors who worked to identify a nutrient deficiency in crops using machine learning and deep learning is shown in Fig. 5 & Fig. 6, respectively.
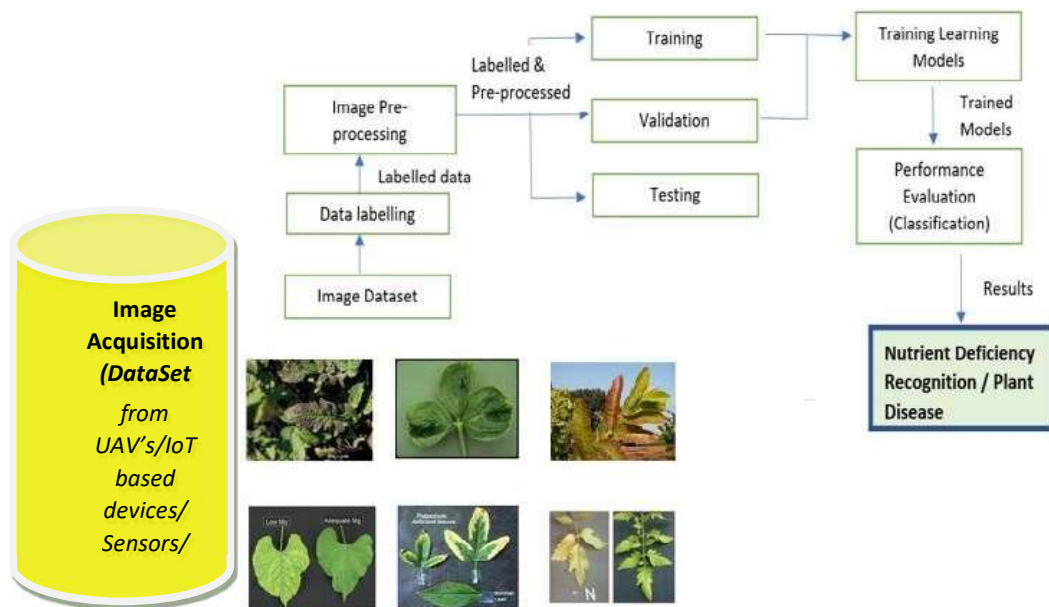

Fig. 4: Architecture of a typical classification model that differentiates the characteristics between specific crop nutrient deficiency and crop disease.
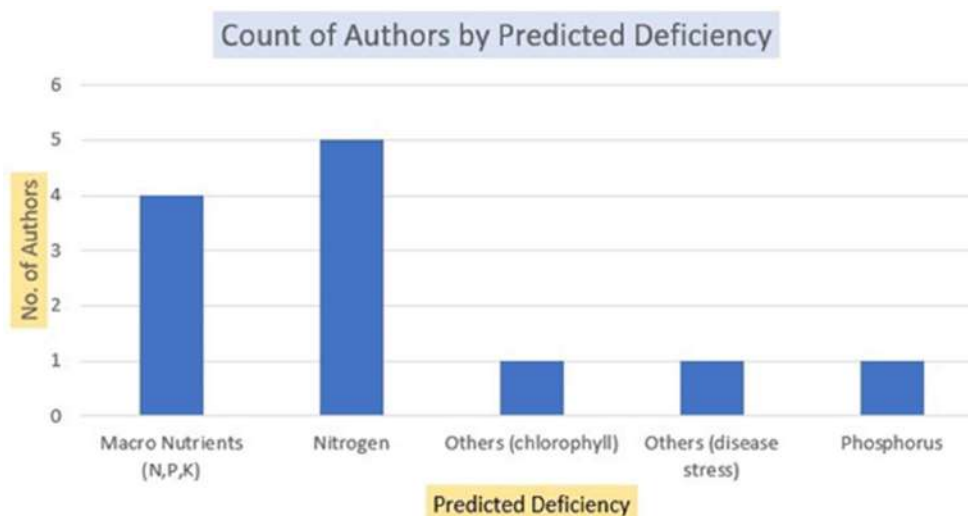

Fig. 5: Machine learning-based prediction of nutrient deficiencies.

Xu et al. (2020) used deep convolution networks (DCNN) to recognize the symptoms of nutrient deficiencies in rice crops using their leaf color and shape. Among the different DCNNs, the DenseNet121 outperformed with the best validation and test accuracy of 98.62 ± 0.57% and 97.44 ±0.57%, respectively. Anami et al. (2020) designed a Deep CNN-based framework that classifies about 12 classes of Biotic and Abiotic stress of the Paddy field using VGG-16. The authors collected about 30,000 images of five different paddy varieties during their growth and compared them with BPCNN (Backpropagation) models. The proposed framework had better classification performance. Sethy et al. (2020) compared Six DL models such as AlexNet, VGG-16, GoogleNet, ResNet-18, ResNet-50, and VGG-19, combining SVM learning to predict nitrogen deficiency using leaf images. Among these architectures, ResNet-50 with SVM outperformed. A Classification Model for handling increased datasets could be upgraded with an updated Leaf color chart (LCC). Sathyavani et al. (2021) designed a DL-based classification model, DenseNet-BC, which utilizes IoT devices for data acquisition. The simulation results of the proposed model showed an improved classification accuracy and F-measure value compared to other models. Karthickmanoj et al. (2021) implemented a stress modeling system that detects the health status of the crop by using leaf images. The captured features in the crop images are sent from the field to an agricultural consultant through the cloud. The classification uses an SVM classifier to determine unhealthy and healthy leaves.

Joshi et al. (2022) proposed a DL-based handheld device, RiceBioS, for detecting the biotic stress in rice crops. The device acts like an Edge-as-a-Service (EaaS) for classifying images into healthy and stressed. The inferences from this work are that the quantification and classification could be improvised with respect to specific crops. Sharma. et al. (2022) designed an ensembled learning framework that uses a transfer learning approach to address rice plant nutrient deficiencies. The authors used two public datasets from Mendeley and Kaggle. The results from Inception ResNet V2 were 90% and Xception of 95.83%. The future scope of this work shall be to design a complete deficiency diagnosis support system for farmers by means of IoT-enabled systems. It may be concentrated on specific conditions affecting yield potential versus yield stress.
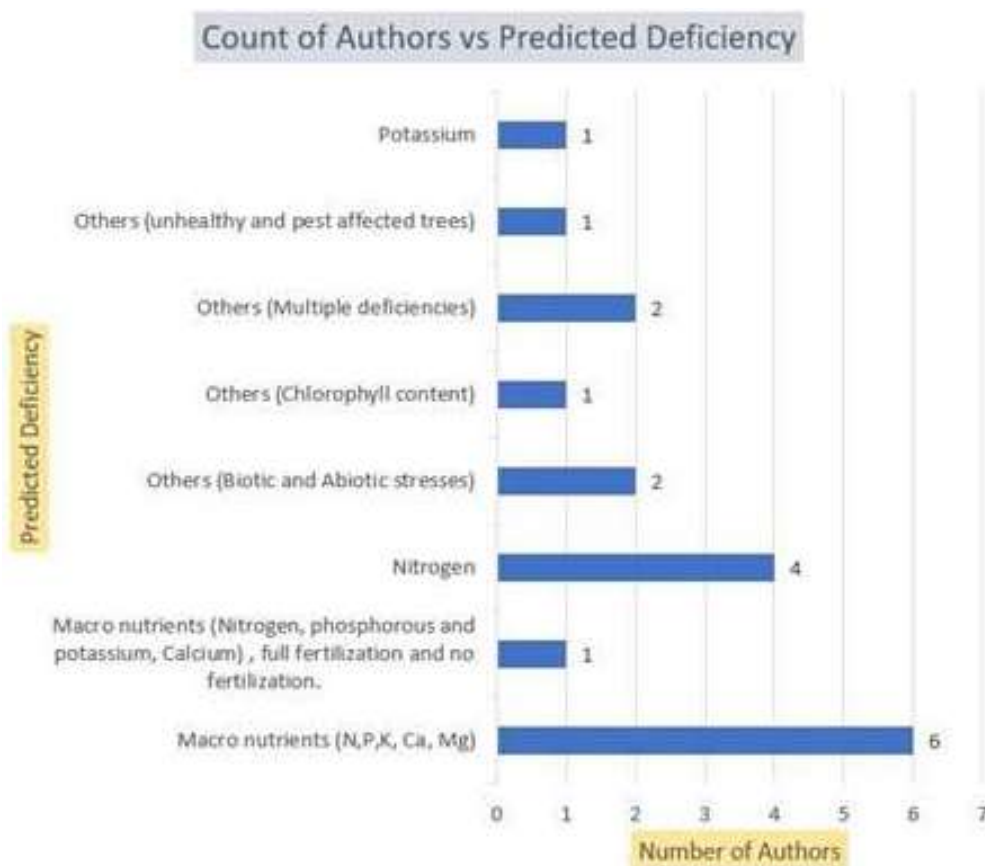

Fig. 6: Deep learning-based prediction of nutrient deficiencies.

Moreover, the severity of crop stress should be identified by designing more efficient models with minimized errors. Also, the nutrient deficiency symptoms differ from crop to crop and within a particular variety of crops. Hence, appropriate models should be developed and integrated to identify diversified stress. The related works for identifying Crop Nutrient deficiencies using Machine Learning and Deep Learning are depicted in Tables 2 and 3, respectively.

RESULTS AND DISCUSSION

This survey article shows that most research uses ML and DL for crop stress management. Such approaches have been modeled for analyzing plant stress from identification, classification, prediction, and quantification perspectives. The AI techniques for modeling plant stress responses, such as the Random Forest, Support Vector Machine, Artificial Neural Networks, and Convolutional Neural Networks, were predominantly used for classifying nutrient deficiencies and other stress symptoms from the image datasets.

Research Gaps Contributing to Future Research Scope

Current challenges include food demand satisfying the growing population using limited agricultural lands, identification of specific factors like limited manpower, changes in environmental conditions, identification of crop deficiencies in different illuminations and geographic locations, weed differentiation, leaf occlusions, etc., causing total yield loss. The future scope with regard to the development of computer vision classification models is related to the above-mentioned research challenges and other specific factors such as the following:

- Limited Datasets specific to secondary and micro nutrients
- Predictive analysis and smart monitoring for improving classification accuracy of deficiencies
- Nutrition imbalance quantification
- Stress due to residues of pesticide application and pest damage or other external factors
- Micro-nutrients identification

Table 2: Summary of Computer Vision works related to Machine learning.

Author& year	Methodology/Equipment Used	Crop	Dataset	Predicted Deficiency
Yu et al. (2021)	Machine Learning - LAI2200C Plant Canopy Analyzer, Da-Jiang Innovations UAV, and DJI Phantom 4 RTK UAV	Wheat	UAVand satellite-Based imagery	nitrogen weight
Agarwal et al. 2018	Machine Vision - PCA and AHCA/SPAD-502Plus chlorophyll meter	Spinach seedlings	Own dataset	High and low chlorophyll content
Haider. et al. (2021)	Machine Vision – GCV index	Spinach	Smartphone camera images	Nitrogen content
Shendryk et. al. (2020)	UAV Light Detection and Ranging (LiDAR) and multi-spectral imaging	Sugarcane	Raw images from UAV and sensors	Nitrogen
Shah et al. (2018)	Machin Vision-RGB color feature extraction	Neem	Own dataset	Nitrogen, Phosphorous and Potassium
Sharif et al. (2018)	Machine Learning – Multi class-SVM – optimized weighted segmentation and feature selection methods.	Citrus plants	Plant Village and own Citrus Images Database	Classification of diseases
Leena & Saju (2019)	Artificial Neural Networks (ANN) and Multiclass Support Vector Machines (SVM) - MATLAB 2015	Maize	Own dataset of 100 sample leaf images	Macronutrients-Nitrogen, Phosphorous, and Potassium
Shidnal et al. (2019)	Machine Learning Algorithms and Google Tensor Flow Library	Paddy	Random Images simulating cropland	Nitrogen, Potassium, Phosphorous
Marin et al. (2021)	Machine Learning – Random Forest	Coffee	Raw images from Remote Piloted Aircraft (RPA)	Spatial variability of Nitrogen content
Zermas et al. (2021)	Machine vision- UAV-assisted RGB sensor and Deep Learning for Training data	Maize, Corn	Field data images	Nitrogen deficiencies
Costa et al. (2021)	Unmanned aerial vehicle (UAV) multi-spectral imagery and AI	Citrus orchards	Raw images from UAV and sensors	Macronutrients (N, P, K, magnesium, calcium and sulfur
Shi et al. (2021)	Hyperspectral Imaging and classification models	Cucumber	Own dataset	Phosphorus

Table 3: Summary of Computer Vision works related to Deep learning.

Author & year	Methodology/Equipment Used	Crop	Dataset	Predicted Deficiency
Chandy (2019)	Deep Learning - Drone interfaced with NVIDIA Tegra System	Coconut	Own dataset	unhealthy and pest-affected trees
Watcha- reeruetai et al. (2018)	Image Segmentation and CNN	Black gram	Own dataset	Ca, Fe, K, Mg, and N deficiencies
Ghosal et al. (2018)	Deep CNN Model framework	Soybean	Own dataset	Multiple stress, herbicide injury, and potassium deficiency
Wulandhari et al. (2019)	Deep CNN- Inception ResNet architecture with Transfer Learning	Okra	Imagenet dataset	Macronutrients (N, P, K, Ca, Fe, Mg)
Sethy et al. (2020)	CNN, pre-eminent classifier -SVM	Rice	Own dataset	Nitrogen
Sathyavani et al. (2021)	IoT-based Nutrient Sensor, CNN Model	Black gram, coriander, pepper, chili, Tomato	Own dataset	Macronutrients (nitrogen, phosphorus, potassium, magnesium, calcium, and sulfur
Joshi et al. (2022)	CNN and using Edge as a service	Rice	Own dataset	Biotic stress
Sharma et al. (2022)	Computer vision, Ensembling of various Transfer Learning (TL) architectures	Rice	public datasets from Mendeley and Kaggle	Multiple deficiencies
Anami et al. 2020	Deep CNN with pre-trained VGG 16	Paddy	Own dataset	Various classes of Biotic and Abiotic stress
Manoharan et al. (2020)	CNN, RCNN	Guava, Groundnut and citrus plant	Own dataset	Nitrogen, phosphorous, and potassium,
Yi et al. (2020)	CNN using RGB images	Sugar beet	(DND-SB) Dataset	N,P,K, Calcium and fertilization status
Song et al. (2020)	BP-ANN and K-nearest neighbors (KNN) - stepwise-based ridge regression (SBRR)	Wheat	Own dataset	Chlorophyll content
Azimi et al. (2021)	Multilayered Deep Learning	Sorghum Plant	Public Dataset -Donald Danforth Plant Science Centre	Nitrogen
Kusanur and Chakravarthi (2021)	Pre-trained deep learning model	Tomato	Own dataset	Calcium and Magnesium
Ahsan et al. (2021)	Deep Learning architectures	Hydroponically Grown Lettuce Cultivars	Own dataset	Nitrogen
Ponce et al. (2021)	CNN based classifier + Artificial Hydrocarbon Network (AHN)	Tomato	Github Repository Dataset (ccevallo/ Monitoreo Jitomate)	nitrogen, phosphorus, potassium
Chang et al. (2021)	Deep Learning Models – CNN, BPNN, DCNN, LSTM	Muskmelon	Own dataset of greenhouse-grown plants	Nitrogen
Sathyavani et al. (2021)	CNN- Densenet-BC, IoT for data acquisition	Rice	Plant village dataset	Multiple deficiencies

- Optimizing the performance parameters in a neural network model for best fit
- Identification of a computer vision model for automated monitoring of crop nutrient cycle
- Most research is based on Static Image Models and pattern recognition

The developed model using IoT devices like sensors for determining the unavailable nutrients and recommendation system is another area that could be focused to get better real-time monitoring datasets for validation. The agricultural industry would evolve as a highly progressive sector when these kinds of systems and tools or techniques are

used for various management strategies, such as sowing to yield forecasting. The other advanced management strategies and approaches needed to be concentrated are the implementations of greenhouses, hydroponics, aquaponics, and vertical farming.

CONCLUSION

This survey provides an overview of the crop stress, and related works performed using Remote sensing, ML, and DL to identify crop nutrient deficiency and the data collection methods. The use of different technological aspects in agriculture enlightens the role of connected farming, particularly computer vision combined with advanced DL models and IoT-based sensing devices, to meet future expectations. This survey would be useful for researchers in this area to discover the advances of computer vision of Crop Stress Identification and establish the research towards fine-tuning the performance hyper-parameters. The integrated system architecture will constitute several agricultural equipment, robots, UAVs, computer vision-based DL models, and IoT enabling various real-time agricultural process management from soil preparation to harvesting. By adopting these smart and precise approaches, farmers will be able to understand the problems that limit production, thereby improving their agricultural resources in terms of yield and quality, leading to sustainable agriculture.

REFERENCES

Agarwal, A., Dutta, M. and Gupta, S. 2018. Assessment of spinach seedling health status and chlorophyll content by multivariate data analysis and multiple linear regression of leaf image features. Comp. Electr. Agric., 152: 281-289. https://doi.org/10.1016/j.compag.2018.06.048

Ahsan, M., Eshkabilov, S., Cemek, B., Kuçuktopcu, E., Lee, C.W. and Simsek, H. 2021. Deep learning models to determine the nutrient concentration in hydroponically grown lettuce cultivars (Lactuca sativa L.). Sustainability, 14(1): 416. https://doi.org/10.3390/su14010416

Anami, B.S., Malvade, N.N. and Palaiah, S. 2020. Deep learning approach for recognition and classification of yield affecting paddy crop stresses using field images. Artificial Intell. Agric., 4: 12-20. https://doi.org/10.1016/j.aiia.2020.03.001

Azimi, S., Kaur, T. and Gandhi, T.K. 2021. A deep learning approach to measure stress levels in plants due to Nitrogen deficiency. Measurement, 173: 108650. https://doi.org/10.1016/j.measurement.2020.108650

Boursianis, A.D., Papadopoulou, M.S., Gotsis, A., Wan, S., Sarigiannidis, P., Nikolaidis, S. and Goudos, S.K. 2021. Smart irrigation system for precision agriculture: The arethou5a IoT platform. IEEE Sens. J., 21(16): 17539-17547. https://doi.org/10.1109/JSEN.20 20.3033526

CGIAR Platform. 2020. N-allyzer: From Nitrogen to all Other Nutrients. Retrieved from https://bigdata.cgiar.org/inspire/inspire-challenge-2020/n-allyzer-from-nitrogen-to-all-other-nutrients/ (Accessed December 3, 2022)

Chandy, A. 2019. Pest infestation identification in coconut trees using deep learning. Journal of Artificial Intelligence and Capsule Networks, 01(01): 10-18. https://doi.org/10.36548/jaicn.2019.1.002

Chang, L., Li, D., Hameed, M.K., Yin, Y., Huang, D. and Niu, Q. 2021. Using a hybrid neural network model dcnn–lstm for image-based nitrogen nutrition diagnosis in muskmelon. Horticulturae, 7(11): 489. https://doi.org/10.3390/horticulturae7110489

Chen, C.J., Huang, Y.Y., Li, Y.S., Chang, C.Y. and Huang, Y.M. 2020. An IoT-based smart agricultural system for pest detection. IEEE Access, 8: 180750-180761. https://doi.org/10.1109/ACCESS.2020.3024891

Chen, Z., Luo, X., Hu, R., Wu, M., Wu, J. and Wei, W. 2010. Impact of long-term fertilization on the composition of denitrifier communities based on nitrite reductase analyses in paddy soil. Microb. Ecol., 60(4): 850-861. https://doi.org/10.1007/s00248-010-9700-z

Costa, L., Kunwar, S., Ampatzidis, Y. and Albrecht, U. 2022. Determining leaf nutrient concentrations in citrus trees using UAV imagery and machine learning. Prec. Agric., 23(3): 854-875. https://doi.org/10.1007/s11119-021-09864-1

Crop In 2022. IoT in agriculture: For real-time farm monitoring. Retrieved from https://www.cropin.com/iot-in-agriculture (Accessed December 3, 2022).

Diedrichs, A. L., Bromberg, F., Dujovne, D., Brun-Laguna, K. and Watteyne, T. 2018. Prediction of frost events using machine learning and IoT sensing devices. IEEE Internet of Things Journal, 5(6): 4589-4597. https://doi.org/10.1109/JIOT.2018.2867333

Eastern Peak Technology Consulting & Development Company. 2020. https://easternpeak.com/blog/iot-in-agriculture-technology-use-cases-for-smart-farming-and-challenges-to-consider/

Espiritu, K. 2017. Plant Nutrients Explained: Everything You Ever Need to Know. Retrieved from https://www.epicgardening.com/plant-nutrients/ (Accessed 18 June 2022)

Feng, D., Xu, W., He, Z., Zhao, W. and Yang, M. 2020. Advances in plant nutrition diagnosis based on remote sensing and computer application. Neural Comp. Appl., 32(22): 16833-16842. https://doi.org/10.1007/s00521-018-3932-0

Ghosal, S., Blystone, D., Singh, A.K., Ganapathysubramanian, B., Singh, A. and Sarkar, S. 2018. An explainable deep machine vision framework for plant stress phenotyping. Proceedings of the National Acad. Sci., 115(18): 4613-4618. https://doi.org/10.1073/pnas.1716999115

Gladence, L.M., Anu, V.M., Rathna, R. and Brumancia, E. 2020. Recommender system for home automation using IoT and artificial intelligence. J. Ambient Intell. Hum. Comp., 65: 00201 https://doi.org/10.1007/s12652-020-01968-2

Haider, T., Farid, M.S., Mahmood, R., Ilyas, A., Khan, M.H., Haider, S.T.A., Chaudhry, M.H. and Gul, M. 2021. A computer-vision-based approach for nitrogen content estimation in plant leaves. Agriculture, 11(8): 766. https://doi.org/10.3390/agriculture11080766

Haifa Group. 2020. How to Identify and Handle Plant Nutrient Deficiencies: Part 1. Retrieved from https://www.haifa-group.com/articles/how-identify-and-handle-plant-nutrient-deficiencies-part-1 (Accessed June 18, 20222)

Jangam, A.R., Kale, K.V., Gaikwad, S. and Vibhute, A.D. 2018. Design and development of IoT-based system for retrieval of agrometeorological parameters. 2018 International Conference on Recent Innovations in Electrical, Electronics & Communication Engineering (ICRIEECE), 27-28 July 2018, Bhubaneshwar, India, IEEE, Piscataway, pp. 804-809. https://doi.org/10.1109/ICRIEECE44171.2018.9008636

Jesus, A.D. 2019. Drones for agriculture-Current applications. Emerj Artificial Intelligence Research. Retrieved December 3, 2022, from https://emerj.com/ai-sector-overviews/drones-for-agriculture-current-applications/

Joshi, P., Das, D., Udutalapally, V., Pradhan, M. K. and Misra, S. 2022. Ricebios: Identification of biotic stress in rice crops using edge-as-a-service. IEEE Sens. J., 22(5): 4616-4624. https://doi.org/10.1109/JSEN.2022.3143950

Karthickmanoj, R., Sasilatha, T. and Padmapriya, J. 2021. Automated machine learning-based plant stress detection system. Mater. Today Proceed., 47: 1887-1891. https://doi.org/10.1016/j.matpr.2021.03.651

Karthika, K.S., Rashmi, I. and Parvathi, M.S. 2018. Biological Functions, Uptake, And Transport of Essential Nutrients in Relation to Plant Growth. In Hasanuzzaman, M., Fujita, H., Oku, K. Nahar, B and Hawrylak-Nowak, M. (eds.), Plant Nutrients and Abiotic Stress Tolerance. Springer, Singapore, pp. 1-49. https://doi.org/10.1007/978-981-10-9044-8_1

Kilic, O., Boz, I. and Eryilmaz, G.A. 2020. Comparison of conventional and good agricultural practices farms: A socio-economic and technical perspective. J. Clean Prod., 258: 120666. https://doi.org/10.1016/j.jclepro.2020.120666

Kusanur, V. and Chakravarthi, V.S. 2021. Using transfer learning for nutrient deficiency prediction and classification in tomato plants. International Journal of Adv. Comp. Sci. Appl., 12(10): 121087. https://doi.org/10.14569/IJACSA.2021.0121087

Lavanya, G., Rani, C., Ganeshkumar, P. 2020. An automated, low-cost IoT-based fertilizer intimation system for smart agriculture. Sustainable Computing: Informatics and Systems, 28: 100300. https://doi.org/10.1016/j.suscom.2019.01.002

Leena, N. and Saju, K.K. 2019. Classification of macronutrient deficiencies in maize plants using optimized multi-class support vector machines. Eng. Agric. Environ. Food, 12(1): 126-139. https://doi.org/10.1016/j.eaef.2018.11.002

Ling, Z., Xin-Ping, C. and Liang-Liang, J. I. A. 2018. Parameter research using UAV-based visible spectral analysis technology in the dynamical diagnosis of nitrogen status of summer maize. J. Plant Nutri. Fert., 24(1): 261-269. https://doi.org/10.11674/zwyf.17193

Liu, H., Zhu, H. and Wang, P. 2017. Quantitative modeling for leaf nitrogen content of winter wheat using UAV-based hyperspectral data. International J. Remote Sens., 38(8-10): 2117-2134. https://doi.org/10.1080/01431161.2016.1253899

Liu, R., Zhang, Y., Ge, Y., Hu, W. and Sha, B. 2020. Precision regulation model of water and fertilizer for alfalfa based on agriculture cyber-physical system. IEEE Access, 8: 38501-38516. https://doi.org/10.1109/ACCESS.2020.2975672

Manoharan, S., Sariffodeen, B., Ramasinghe, K.T., Rajaratne, L.H., Kasthurirathna, D. and Wijekoon, J.L. 2020. Smart plant disorder identification using computer vision technology. 2020 11th IEEE Annual Information Technology, Electronics and Mobile Communication Conference (IEMCON), 4-7 November 2020, Virtual Conference, IEEE, Piscataway, pp. 0445-0451. https://doi.org/10.1109/IEMCON51383.2020.9284919

Marin, D.B., Ferraz, G.A., Guimarães, P.H.S., Schwerz, F., Santana, L.S., Barbosa, B.D.S., Barata, R.A.P., Faria, R., Dias, J.E.L., Conti, L. and Rossi, G. 2021. Remotely piloted aircraft and random forest in evaluating the spatial variability of foliar nitrogen in coffee crops. Remote Sens., 13(8): 1471. https://doi.org/10.3390/rs13081471

Nabi, F., Jamwal, S. and Padmanbh, K. 2022. Wireless sensor network in precision farming for forecasting and monitoring apple disease: A survey. Int. J. Inform. Technol., 14(2): 769-780. https://doi.org/10.1007/s41870-020-00418-8

Niu, H., Zhao, T., Wang, D. and Chen, Y. 2019. A uav resolution and waveband aware path planning for onion irrigation treatments inference. 2019 International Conference on Unmanned Aircraft Systems (ICUAS), 808-812. https://doi.org/10.1109/ICUAS.2019.8798188

Ponce, H., Cevallos, C., Espinosa, R. and Guti´errez, S. 2021. Estimation of low nutrients in tomato crops through the analysis of leaf images using machine learning. J. Artificial Intell. Technol., 1(2): 68. https://doi.org/10.37965/jait.2021.0006

Raza, S.A., Smith, H.K., Clarkson, G.J.J., Taylor, G., Thompson, A.J., Clarkson, J. and Rajpoot, N.M. 2014. Automatic detection of regions in spinach canopies responding to soil moisture deficit using combined visible and thermal imagery. PLoS One, 9(6): e97612. https://doi.org/10.1371/journal.pone.0097612

Sathyavani, R., JaganMohan, K. and Kalaavathi, B. 2021. Detection of plant leaf nutrients using convolutional neural network-based Internet of Things data acquisition. Int. J. Nonlinear Anal. Appl., 12(2): 519. https://doi.org/10.22075/ijnaa.2021.5194

Sathyavani, R., JaganMohan, K. and Kalaavathi, B. 2022. Classification of nutrient deficiencies in rice crop using denseNet-BC. Mater. Today Proceed., 56: 1783-1789. https://doi.org/10.1016/j.matpr.2021.10.466

SCNSoft. 2022. IoT architecture explained: Building blocks and how they work. (n.d.). Retrieved from https://www.scnsoft.com/blog/iot-architecture-in-a-nutshell-and-how-it-works (Accessed December 3, 2022)

Sethy, P.K., Barpanda, N.K., Rath, A.K. and Behera, S.K. 2020. Nitrogen deficiency prediction of rice crop based on convolutional neural network. J. Ambient Intell. Hum. Comp., 11(11): 5703-5711. https://doi.org/10.1007/s12652-020-01938-8

Shah, A., Gupta, P. and Ajgar, Y.M. 2018. Macro-nutrient Deficiency Identification in Plants Using Image Processing and Machine Learning. 2018 3rd International Conference for Convergence in Technology (I2CT), 1–4, 6-7 April 2018, Pune, India, IEEE, Piscataway, pp. 789-793. https://doi.org/10.1109/I2CT.2018.8529789

Sharif, M., Khan, M.A., Iqbal, Z., Azam, M. F., Lali, M.I.U. and Javed, M.Y. 2018. Detection and classification of citrus diseases in agriculture based on optimized weighted segmentation and feature selection. Comp. Electr. Agric., 150: 220-234. https://doi.org/10.1016/j.compag.2018.04.023

Sharma, M., Nath, K., Sharma, R.K., Kumar, C.J. and Chaudhary, A. 2022. Ensemble averaging of transfer learning models for identification of nutritional deficiency in rice plants. Electronics, 11(1): 148. https://doi.org/10.3390/electronics11010148

Shendryk, Y., Sofonia, J., Garrard, R., Rist, Y., Skocaj, D. and Thorburn, P. 2020. Fine-scale prediction of biomass and leaf nitrogen content in sugarcane using UAV LiDAR and multi-spectral imaging. Int. J. Appl. Earth Observ. Geoinform., 92: 102177. https://doi.org/10.1016/j.jag.2020.102177

Shi, J., Wang, Y., Li, Z., Huang, X., Shen, T. and Zou, X. 2022. Characterization of invisible symptoms caused by early phosphorus deficiency in cucumber plants using near-infrared hyperspectral imaging technology. Spectrochim. Acta Part A Mol. Biomol. Spectrosc., 267: 120540. https://doi.org/10.1016/j.saa.2021.120540

Shidnal, S., Latte, M.V. and Kapoor, A. 2021. Crop yield prediction: Two-tiered machine learning model approach. Int. J. Inform. Technol., 13(5): 1983-1991. https://doi.org/10.1007/s41870-019-00375-x

Song, Y., Teng, G., Yuan, Y., Liu, T. and Sun, Z. 2021. Assessment of wheat chlorophyll content by the multiple linear regression of leaf image features. Inform. Process. Agric., 8(2): 232-243. https://doi.org/10.1016/j.inpa.2020.05.002

Stokes, P. 2019. The stages of IoT architecture are explained in simple words. Retrieved from https://medium.datadriveninvestor.com/4-stages-of-iot-architecture-explained-in-simple-words-b2ea8b4f777f (Accessed 3 December 2022)

Szewczyk, R., Zielinski, C. and Kaliczynska, M. (Eds.). 2018. Automation. Springer International Publishing, Singapore. https://doi.org/10.1007/978-3-319-77179-3

Torres-Sanchez, J., Lopez-Granados, F., Serrano, N., Arquero, O. and Pena, J.M. 2015. High-throughput 3-d monitoring of agricultural-tree plantations with unmanned aerial vehicle (Uav) technology. PLOS ONE, 10(6): e0130479. https://doi.org/10.1371/journal.pone.0130479

Wang, K., Zhang, S., Wang, Z., Liu, Z. and Yang, F. 2013. Mobile smart device-based vegetable disease and insect pest recognition method. Intell. Autom. Soft Comp., 19(3): 263-273. https://doi.org/10.1080/10798587.2013.823783

Watchareeruetai, U., Noinongyao, P., Wattanapaiboonsuk, C., Khantiviriya, P. and Duangsrisai, S. 2018. Identification of plant nutrient deficiencies

using convolutional neural networks. Int. Electr. Eng. Cong., 16: 1-4. https://doi.org/10.1109/IEECON.2018.8712217

Wu, H.T. 2021. Developing an intelligent agricultural system based on long short-term memory. Mobile Networks Appl., 26(3): 1397-1406. https://doi.org/10.1007/s11036-021-01750-4

Wulandhari, L.A., Gunawan, A.A., Qurania, A., Harsani, P., Triastinurmiatiningsih, T.F. and Hermawan, R.F. 2019. Plant nutrient deficiency detection using deep convolutional neural network. ICIC Int., 97: 148. https://doi.org/10.24507/icicel.13.10.971

Xu, Z., Guo, X., Zhu, A., He, X., Zhao, X., Han, Y. and Subedi, R. 2020. Using deep convolutional neural networks for image-based diagnosis of nutrient deficiencies in rice. Comp. Intell. Neurosci., 20: 1-12. https://doi.org/10.1155/2020/7307252

Yi, J., Krusenbaum, L., Unger, P., Huging, H., Seidel, S.J., Schaaf, G. and Gall, J. 2020. Deep learning for non-invasive diagnosis of nutrient deficiencies in sugar beet using rgb images. Sensors, 20(20): 5893. https://doi.org/10.3390/s20205893

Yu, J., Wang, J., Leblon, B. and Song, Y. 2021. Nitrogen estimation for wheat using UAV-based and satellite multi-spectral imagery, topographic metrics, leaf area index, plant height, soil moisture, and machine learning methods. Nitrogen, 3(1): 1-25. https://doi.org/10.3390/nitrogen3010001

Zermas, D., Nelson, H.J., Stanitsas, P., Morellas, V., Mulla, D.J. and Papanikolopoulos, N. 2021. A methodology for the detection of nitrogen deficiency in corn fields using high-resolution RGB imagery. IEEE Trans. Autom. Sci Eng., 18(4): 1879-1891. https://doi.org/10.1109/TASE.2020.3022868

The Principles of International Environmental Protection and Global Obligations: An Analysis Based on the Legal Context

Kudrat-E-Khuda Babu*†, Akanda Muhammad Jahid**, Nazia Afroz Ananna*, Arghyadeep Chakraborty*** and Moriom Akter Mou*

*Daffodil International University, Department of Law, Dhaka, Bangladesh
**The Daily Star, Dhaka, Bangladesh
***Department of Law, Sister Nivedita University, Kolkata, India
†Corresponding author: Kudrat-E-Khuda Babu; kekbabu@gmail.com

ABSTRACT

There is now a worldwide collective obligation, a reality, to acknowledge environmental challenges. The paper discusses and analyses the principles of international environmental laws and how those are applied in international conventions and treaties, and the effectiveness and weaknesses of those laws. This discussion mainly focuses on the principles' backdrop, what they mean, and how they have been adopted in international environmental law. Furthermore, the paper focuses on the outcomes of formulating the principles and enforcement of the legal framework. It analyses their prospect to strengthen the legal framework to achieve the objective of these principles. Besides, some recommendations have been made to strengthen these legal frameworks. It shows why it is essential to form efficient environmental platforms in present climate issues and how all nations can be brought under a common platform where they can take decisions regarding the safeguard amid the evolving environmental situations.

INTRODUCTION

Now environmental rights issues are getting more important and have appeared as a significant part of the laws related to human rights law and international environmental law. There are two types of environmental rights — substantive and procedural (Sands 1995). 'Substantive' rights ensure a healthier environment, and 'procedural' rights safeguard the environment and ensure access to justice. However, the principles followed internationally are different from the rules. Principles usually guide a certain course of action.

On the other hand, rules can impose responsibilities and are inherently binding (Bodansky et al. 2007). The principals refer to a broader set of moral norms than commitments. The principles never specify any particular actions, but all activities are done in light of the principles, even when formulating laws or rules. Though many local and international organizations deal with environmental issues, no unique institution will implement the policies as a responsible authority. The United Nations Environment Programme (UNEP) sets environment-related regulations and policies. Environmental laws have undergone various changes, and at present, those are very different from the traditional conception. It is also important in other areas, such as human rights, economic

rights, environmental preservation, and state actions and political interests (Bodansky et al. 2007). The United Nations Environment Programme (UNEP) has been trying to improve international collaboration by implementing environmental regulations and formulating required recommendations. Besides, the organization takes steps to formulate a permanent mechanism for the necessary emergency action to protect the environment. At the same time, it provides the necessary directions in light of UN policy. It also instructed the member states to speed up the procedure to formulate related laws. It insisted they adopt the resolutions of other environmental institutions, including the United Nations Environment Programme and the Commission of Sustainable Development (CSD). Due to increasing industrialization, the ecology and environment are in a major global crisis. International Environmental Law (IEL) works to strengthen the efforts to reduce pollution and natural resources within the framework of sustainable development (Rolston 1988). The member states have created a set of laws to deal with the problems raised in the states or between states. The law addresses the issues regarding population, biodiversity, and climate change. It also deals with many other issues, including air, land, sea, transboundary water pollution, ozone depletion and pollution related to toxic and hazardous

substances, conservation of marine resources, desertification, and nuclear damages (Jardins 2001). Some principles guide this law. Those are the precautionary principle, prevention principle, sustainable development, polluter pay principle, integration principle, and public participation principle.

MATERIALS AND METHODS

During the study, both primary and secondary data were used in this paper. All the relevant data and information from the existing paper were collected and used from primary and secondary sources. The secondary data sources include books, articles, different national and international law reports, Acts, etc. The information from books, journals, booklets, proceedings, newsletters, souvenirs, and consultancy reports available in Daffodil International University, Bangladesh libraries were compiled chronologically to complete successfully. The necessary supports and figures were taken from the *Daily Star*, Forbes, and the Law Column. The selected data (collected from the selected stations between 2020 and September 2021) reveals that there is now a worldwide collective obligation, a reality, to acknowledge environmental challenges. And that is why it is essential to form efficient environmental platforms in the present climates related issues.

Moreover, right now, all nations should be brought under a common platform where they can take decisions jointly regarding safeguarding amid the evolving environmental situations. The codes of international environmental laws and how those are applied in international conventions and treaties. This paper has also focused on the effectiveness and weaknesses of those laws.

RESULTS AND DISCUSSION

Precautionary Principle

The precautionary principles of international environmental laws aim to prevent environmental issues before the inception of any new crisis. It focuses on preventing harm rather than managing it after it happens. Here is a moral word that prevention is better than cure. The precautionary principles have been formulated from this perspective. So the precautionary principles always analyze the future necessities, possible harms, and threats that can lead to an environmental crisis and suggest taking preventive measures to stop the crisis. The precautionary principle supports initiating prior steps before complete scientific proof of a risk. The action should not be delayed simply because of lacking full scientific information. Environmentalists and policymakers have started to rethink their approach to addressing uncertainties following DDT

(dichlorodiphenyltrichloroethane) in the 1960s (Alam et al. 2013). Thanks to the event, environmentalists and policymakers started formulating precautionary principles as a reaction to the limitations of policies based on a notion of "Assimilative Capacity" during the 1970s. *i.e.*, humans and the environment can tolerate a certain amount of contamination or disturbance, which can be calculated and controlled".

In the 1970s, the United States also relegalized the emergence of the principle. However, the term has not been used. The essence of the precautionary principle can be found in several laws, such as the US Federal Food, Drug, and Cosmetic Act of 1958 (Section 409), which outlawed any food additive found to induce cancer regardless of the dose taken (David 1990). The concept of the precautionary principle has been considered for international law and policy following a proposal from environmentalists and the governments of European countries. The 1982 United Nations World Charter for Nature stated that when "potential adverse effects of an activity are not fully understood, it should not proceed" In the Convention for the Protection of the Ozone Layer (Vienna Convention on March 25, 1985) 20 countries. The European Commission adopted a charter on protecting the ozone layer, the first multilateral treaty to explicitly reference precaution. The convention's success was due largely to its precautionary nature, as there was still no scientific certainty on the causes and impacts of ozone depletion at the beginning. Later, the Vienna Convention protocol was adopted in Montreal in 1987. In 1992, the representatives of nations came up with Agenda 21 during the Earth Summit in Rio de Janeiro, Brazil. Chapter 17 thereof refers to the preventive concept, *viz*:

> *"A preventive and anticipatory rather than a reactive approach is necessary to prevent marine environment degradation. This requires, among other things, the adoption of precautionary measures, environmental impact assessments, clean production techniques, recycling, wastes audits and minimization, construction, and improvement of sewage treatment facilities, quality management criteria for handling hazardous substances, and a comprehensive approach to damaging impact from air, land, and water"* (Agenda 21, Chap. 17).

Chapter 17 is not only a clear endorsement of the precautionary principle but also relates the concept of prevention to several specific measures concerning the environment of oceans, seas, and marine. Due to adopting the Rio Declaration at the United Nations Conference on Environment and Development (UNCED) in 1992, "the precautionary concept has become essential to international

environmental policy." Principle, 15 of the Rio Declaration provides hence:

> *"To protect the environment, the precautionary approach shall be widely applied by States according to their capabilities. Where there are threats of serious or irreversible damage, lack of full scientific certainty shall not be used to postpone cost-effective measures to prevent environmental degradation."* (Rio Declaration on Environment and Development 1992)

Besides, the Convention on Biological Diversity also provided for the precautionary concept. It was later adopted at the Earth Summit in 1992. The Earth Summit also opened the opportunity to form international law by converging the precautionary principle and the climate change issue (Gillespie 1997). The precautionary principle has been acknowledged at the international level law after it was adopted in the United Nations Framework Convention on Climate Change (UNFCCC) under Article 3 at the summit in Rio de Janeiro. In the Preamble of the Kyoto Protocol in 1997, an article reference was quoted as "Being guided by Article 3 of the Convention". The stakeholders also endorsed the precautionary principle in the UNFCCC.

Firstly, the decision to endorse the precautionary principle was fruitful and worked flawlessly for the ozone conventions and CBD; but it could not impact the climate change legal frameworks. A few factors in the results will be discussed later by comparing the ozone and climate change conventions (Nanda & Pring 2003). The major difference between the ozone conventions and Kyoto Protocol is that most nations have ratified the first. Still, top greenhouse emission nations, including the United States, did not rat the latter. And Canada also later withdraw from the protocol. This is evidence that all nations have agreed to tackle the ozone problem, but some do not agree with the climate change convention. The biggest greenhouse emission nations are not making any commitment or effort to resolve the issues causing climate change and its impact.

Secondly, stakeholders agree to respond quickly to new scientific information in the Montreal Protocol and expedite the necessary chemical reduction. After such coordination, this protocol automatically applies to all countries approved.

On the other hand, to reduce admission by a certain period, the Kyoto Protocol does not discourage non-compliance by its parties. Through the comparison, it is evident that the ozone conventions are more successful when the parties try to reduce ozone depletion as per the limit of their level. However, in the Kyoto Protocol, the initiative was taken against the non-compliance parties.

Thirdly, the Montreal Protocol settles any dispute through the Non-Compliance procedure, which creates a multilateral

mechanism to build confidence through non-confrontation discussion instead of adjudication. It helps parties pursue an amicable solution to the problem. Meanwhile, there is a lack of enforcement or cooperation between parties to settle any dispute under the climate change conventions. Here we can mention a couple of examples of such incidents. The United Kingdom and Argentina have a long dispute over territories, and there was an application with the Kyoto Protocol.

Meanwhile, regarding the territorial dispute between Hong Kong and Macao, China said they do not want to involve in the protocol. The next issues are monetary advancement. As there are substitutions to CFC, the matter is evidence that ozone conventions are much more successful. Now industries are producing alternatives to CFCs. As a result, the economy is boosting. Mass production for CFC replacement increases the industry's income, essential for a nation's economic growth.

On the other hand, implementing the Kyoto Protocol is comparatively much more expensive. Implementing the Kyoto Protocol requires reducing the main energy sources, such as coal and petroleum, to reduce greenhouse gas emissions. Former US President Donald Trump did not even acknowledge the existence of the greenhouse gas effect and had greatly supported the energy industries. Finally, the application of precautionary measures to international legal instruments is now widely seen, and the Climate Change Convention is losing its usefulness due to the massive success of the Ozone Convention. The reasons for this have already been discussed. Still, recognizing the issue in international environmental law and applying this principle in resolving any new problem is crucial.

Polluter Pays Principle

Polluter Pays policy has dual liability. It includes provisions to compensate those affected by pollution and guidelines for restoring environmental damage. Liability and compensation for pollution are the main sources behind the formulation of this policy. As a result, this policy has been established as sustainable development and precautionary policy, as well as gaining the status of traditional international law. The "polluter pay" principles were first incorporated into policies 21 and 22 of the Stockholm Declaration 1973. Following that, various requirements for implementing the European Charter on Environment and Health (1989) and the Single European Act 1986 were made (Wolf & Neil 2003). The principles of "polluter pay --Principle 16 -- have been envisaged in the United Nations Conference on the Environment and Development, 1992. 1992 Rio Declaration Principle 16 states: "National authorities should endeavor to promote the internalization of environmental costs and the use of economic instruments, taking into account the approach

that the polluter should, in principle, bear the cost of pollution, with due regard to the public interest and without distorting international trade and investment."

Under the "Pollution Control Policy," The polluter must be responsible for limiting, controlling, and cleaning up the pollution's effects. And forces them to bear the cost of pollution. The main purpose of this policy is to allocate costs and internalize those costs. Due to the

Accountability liability under this policy, this policy has acquired prominence in national and international environmental policies, and it has been referred to as the legislation of several countries (Caldwell 1990). The Organization for Economic Cooperation and Development (OECD) established the "polluter pays" principle to avoid public authorities from subsidizing private enterprises' pollution control expenditures (Reid 1997). Giving utmost importance to the "polluter pays principle," This idea should be adopted to determine the cost of pollution as a measure to avoid and regulate pollution, according to the OECD Council (Bullard & Jonson 2000). As per the principle, the product producer who pollutes the environment will be responsible for preventing pollution. These costs are included directly in the property. The government and other agencies introduced the policy to introduce policies and procedures for environmental protection. Initially, the "Pollution Policy" was not part of the law in India. This policy was later adopted as an element of law in the light of the directive of the "Indian Council for Enviro-Legal Action v. Union of India." In that instruction, the court said that the polluting industries were "fully responsible for the damage caused to them by the villagers, soil, and groundwater in the affected area and therefore they are obliged to take all necessary measures to remove silt and other pollutants lying in the affected area." Another case, "Vellore Citizens Welfare Forum v. Union of India," found that "Pollution Policy" plays an important role in sustainable and environmental development. In light of this policy, the court, in this case, stated that the polluter must not only compensate the victims of pollution but also bear full responsibility for the recovery of environmental damage (Sadleer 2002). At present, this policy is considered part of the traditional international law. It has become an important part of the law in India, which plays an important role in protecting the environment for sustainable development.

Prevention Principle

The prevention principle directs action at an early stage to protect the environment. The essence of this principle is that prevention is better than cure. If something is damaged, restoring it to its original form is impossible. This principle has been considered since that position. So,

there is no question of repairing the damage after it has occurred. Not even to prevent such losses. The Prevention Policy recommends early action to protect the environment. Although this principle is similar to the precautionary principle, there are several differences between them. Its main difference with precautionary principles is that precautionary principle primarily identifies the causes of environmental damage through physical analysis and deals with causes for which evidence has not yet been found. Still, the prevention principle directly takes the action of being responsible for the destruction of the environment. In 1967, 120,000 tons of oil spilled from a large oil tanker into the English Channel, which led to the environmental catastrophe known as the "Torre Canyon" catastrophe. The incident was highlighted in the context of the importance of this policy, which draws the international community's attention to stress the need for legal instruments on the prevention principle. The principle of prevention in the context of the

The environment was introduced in principle 21 of the Stockholm Declaration on the Human Environment in 1972, which stated:

> States have . . . the sovereign right to exploit their resources . . . and the responsibility to ensure that activities within their jurisdiction or control do not cause damage to the environment of other States or areas beyond the limits of national jurisdiction (Faruque 2017).

The International Convention for the Prevention of Pollution from Ships in 1973 (MARPOL) was formed on 10 1973 after 154 state parties signed the convention on February 17, 1973 (Mitsuo et al. 2006). It came into effect on October 2, 1983. Since its formation, MARPOL has appeared as the most comprehensive and operative international legal framework for preventing pollution caused by oil or other harmful substances from the vessel and minimizing the accidental discharge of such substances. MARPOL empowers the states to deal with jurisdiction, enforcement, and inspection to prevent pollution by ships. As per Article 4 of MARPOL, any violation is punishable. The punishment might be either under the law of that Party or the existing law of the concerned state.

Article 5 refers to the inspection of ships and special rules regarding the inspection of ships to ensure that no contamination occurs through any vessel. At the same time, Article 5 empowers the relevant state and port authorities to inspect, detain and prosecute ships concerned with environmental pollution. It also empowered the authorities concerned to demand the certificates, and in case of failing to produce the certificates, they can withhold or suspend the permission of the respective vessel. Under the requirements

of MARPOL, a valid certificate is mandatory for the ship. However, the flag States and port States could not delay their process unnecessarily. If they make any delay without logical reasons and if the goods of the vessels are damaged, then the state parties will have to compensate for the loss of the vessel authorities under articles 4, 5, or 6. The MARPOL always contains the movement of cargo oil and its residues, and any member state can inspect the vessel at any time. Apart from that, six Annexes under MARPOL lay out the technical regulation for operational pollution.

Of them, Annexes I prevent pollution caused by oil spilled from the vessel and prescribe the operational measures to prevent accidental discharge by requiring ships whether they have the capacity and equipment and plans to check the oil spills. Annexes II empowers the regulator to control pollution by the liquid substance of the ships. Annex III prescribes to prevent pollution by harmful substances in package form. However, Annex IV prevents pollution by sewage from the shop as discharging substances is prohibited if any vessel has no permitted sewage treatment plan. Annexe V prescribes to prevent pollution by garbage produced by ships. And lastly, Annex IV empowers the regulatory authority to prevent air pollution from ships by curbing nitrogen and sulfur oxide emissions. The provisions of MARPOL have been formulated in line with the prevention principles. It introduces inspection and enforcement mechanisms that can also be applied to the ships of a non-member state.

Another relevant convention that applies the prevention principle is "*The Basel Convention on the control of the transboundary movement of hazardous wastes*" (Basel Convention). At first, 116 countries adopted the Convention on 22 March 1989, which came into effect on 5 May 1992 (Brine & Boyle 2002). Right now, 186 parties are a member of the convention. The US is the only developed country that has not ratified it yet. The main objectives of the Convention are:

(i) Containing transboundary movement of hazardous waste to a minimum level for ensuring sound environmental management

(ii) Treating hazardous wastes and other wastes which would be the possible nearest place from their source in an environmentally sound manner

(iii) Minimizing the generation of hazardous waste and other waste

The Convention regulates the transboundary movement of ships carrying hazardous and other wastes through the "Prior Informed Consent" procedure (shipments made without consent are illegal). Unless there is no special agreement, the shipment between non-parties is illegal. As per the Convention, the parties must properly manage and dispose of hazardous and other wastes. We can explain the "prior informed consent" method in a much easier way:

i. The exporting state must notify about the transit and information about importing state and waste.

ii. Information on the impact of the ship's underlying waste on human health and the environment must be clearly stated.

iii. Based on that information, the importer state may consent, reject the application, or ask for more information.

iv. The importing state may take steps to ban shipping without prior written permission.

v. Transboundary movement of hazardous waste without consent is illegal and punishable under the convention.

vi. In the event of any breach of the Convention, the determination shall be made following the national law of the Contracting State.

Meanwhile, to deal with liability caused by damages of the transboundary movement of hazardous waste, the Basel Protocol on Liability and Compensation (the Basel Protocol) was adopted on December 10, 1999. Under Article 5 of the protocol, the responsible state or the authorities of the vessel would be fined for damages. Currently, there are only 13 signatories and 11 parties to the protocol. The wastes that the Basel Convention generally works to control are- biomedical and healthcare waste, used oil, used lead-acid batteries, lithium batteries, nickel-cadmium batteries, persistent organic pollutant wastes, chemicals, and pesticides in the environment. Waste, etc. It is important to see the outcome of both conventions, including the policy of prevention, whether their existence and implementation reach the purpose, and the policy of prevention in general. Statistics show that the amount of oil entering the sea from other seas has decreased for MARPOL. The annual number of spills in the 1970s was 24.5, which reduced to 1.7 per year from 2010 to 2016 (Faruque 2017). Even 20 years later, toxic waste colonialism is still problematic for the Basel Conference because of the growing hazardous waste and severe economic pressures. Although both Marpol and Basel Conventions apply a policy of resistance, Marpol is still considered more successful than the Basel Convention regarding effectiveness and usefulness. However, the Basel Convention cannot be called a complete failure, as technological advances and human demand have increased the amount of hazardous waste, especially in developing countries always looking for convenient and inexpensive ways to dispose of their waste. Several steps can be taken to make Marpole more effective and the Basel Convention more timely and robust.

First, persuading the United States to ratify the Basel Convention is crucial. Because the United States is one of

the top producers of hazardous waste and the United States has the largest fleet in the world. Considering these aspects, U.S. involvement can encourage compliance with the Convention. And monitoring the transboundary movement of hazardous wastes in the open international sea could be further strengthened.

Second, there is a need for developing countries to develop technology, implement teams, and provide financial assistance in accordance with the principles of cooperation described in the implementation of both conventions. No developing country on the African continent, for example, is receiving the assistance it deserves to stop the dumping of hazardous waste in its territory by foreign ships, even though they are both members of the conference. In this case, developed countries must come forward to assist. In this case, active action by the United Nations is very important. Countries not abiding by these conventions should be barred from various UN benefits as punishment. We must lobby for heavier approvals, such as economic sanctions, against countries responsible for spreading toxic oil. If the United Nations can impose such sanctions on Iran for its nuclear program, the same action should be taken against environmentalist terrorists.

Finally, the "Prevention Policy" should be adopted and implemented in both conventions to prevent environmental disasters. Although both conventions have positive and negative consequences, the existence and application of both conventions and the special work under both conventions have served as the most important international legal instrument to prevent environmental catastrophes.

Principle of Preventive Action

The duty to protect the environment and the idea of pollution prevention are not the same thing (Thornton & Beckwith 2004). This law empowers the state to take steps against pollution within its jurisdiction. To avoid substantial or irreversible damage to the environment and even the ecosystem, all dangerous compounds must be disposed of in quantities that exceed the capacity for environmental deterioration. Steps need to be taken at an early stage to reduce the rate of contamination rather than waiting for the subsequent recovery of contaminated areas. Out of such necessity, the States have developed and approved this policy to acquire information to conduct 'impact assessments' on the environment.

The preventative principles allow the government to act effectively to reduce waste. The government can create the required plans and policies to educate the general public and promote pollution avoidance practices. This principle restricts the entry of pollutants, including treaties, into international environmental law (Joyner 1986).

Resistance to the environment is considered a 'golden rule' for both environmental and economic reasons. Once an environmental injury occurs, it cannot be cured. Extinction of any animal or plant, erosion issues, dumping, or pollutant dumping in the river can all result in irreversible situations that cannot be reversed. Even in such a situation, measures should be taken to protect the environment as much as possible and to minimize the risk as much as possible. Steps must be taken to curb rising costs, increase fines, and civic liability to curb pollution.

Principle of Common but Differentiated Responsibility

The "Common Differentiated Responsibility" concept has given a new meaning to a long-standing practice. Certain countries must contribute more than others to provide global public goods. The policy calls for more aggressive actions to restore global environmental damage. It has also been pushed to be recognized as a traditional principle of international law. The notion of humankind's shared legacy has been distinguished from the principle of broad concern (Opschoor & Hans 1989).

The policy relates to the concept of the general responsibility of the state. However, this obligation is again distinct in light of historical variances, varied social and economic advancement dimensions, and similar concerns based on different sources. The concept of "Common Concern of Humankind," on the other hand, is based on a treaty. "Change in the earth's climate and its detrimental repercussions are a common concern of humankind," the United Nations Framework Convention on Climate Change (UNFCCC) stated in 1992. Furthermore, the 1992 Biodiversity Convention said that "biodiversity conservation is a common concern of humanity."

"Principles of common but different responsibilities" have been formulated in international environmental materials. But all countries are more or less responsible for global environmental damage. Developed and developed countries must actively prevent and reduce global pollution and take responsibility. In addition, developing countries need to help protect the environment. The CBDR policy has been formulated to contain a "soft" international legal policy. It became an important element of international law in the Framework Convention on Climate Change of the Rio Declaration on Environment and Development (1992).

Principle of Cooperation

Principle 7 of the 1992 Rio Declaration, mentions that "States shall cooperate in a spirit of global partnership to conserve, protect and restore the health and integrity of the

Earth's ecosystem. In view of the different contributions to global environmental degradation, States have common but differentiated responsibilities. The developed countries acknowledge their responsibility in the international pursuit of sustainable development because of the pressures their societies place on the global environment and the technologies and financial resources they command."

The "good neighbor policy" states that the responsibility for ensuring that a state does not harm the environment of a neighboring state is vested in the state. The policy of international cooperation is considered to be their duty to restrict the activities of other states within the territory of a particular state. This policy applies to most "*sic utere tuo, et alienum non laedas*" (use your property so that it does not harm others).

The Sustainable Development Principle

Sustainable development refers to two main objectives. These are environmental protection and economic development. Regarding sustainable development, economic development can also be termed a means of alleviating poverty (Kiss & Shelton 2004). In the case of economic development, besides development, the needs of the people of a country should be given importance. Especially those who are in or below the poverty line. However, the present generation constantly struggles for economic development and poverty alleviation. As a result of that development for poverty alleviation, it will not harm the environment. Although economic development is recognized as a means of sustainable development in poverty alleviation, it limits such development based on environmental protection for present and future generations. This policy refers to the balance between environmental protection and economic development. According to this policy, first recognized in the Stockholm Declaration, the state must continue economic development with environmental protection to provide maximum benefits to the people.

According to the policy, states have a sovereign right to use their natural resources. Still, they must ensure that those resources do not adversely affect the environment of neighboring states. The "World Charter for Nature" is an important document in environmental protection in economic development, which has been created to guide development. It emphasizes economic development as well as specific policies for environmental protection. Subsequently, the Rio Declaration emphasizes the principles of the Stockholm Declaration. It says states must exercise caution in balancing economic development and environmental protection. In 1985, the policy of sustainable development of nature and conservation of natural resources was widely discussed

and gained importance in the ASEAN Treaty. The main purpose of this policy is to preserve wild plants, animals, and renewable resources. At the same time, they were protecting ecosystems, habitats, and endangered species and ensuring sustainable harvesting use.

The preamble to the treaty provides guidelines for establishing interrelationships between conservation and socio-economic development. In this case, conservation is important to ensure the sustainability of development. And socio-economic development is needed for that conservation. The agreement contains 8 chapters, including 35 articles, which assure the parties to identify the interdependence of natural resources to achieve a balanced ecosystem. According to this policy, contractual parties must implement the sustainable development policy. Under this policy, the contracting parties will be responsible for any damage to the environment. They will also focus on environmental planning measures, establishing scientific research, and public participation and cooperation among members. But the unfortunate thing is that even though this agreement was considered ahead of its time, it has not been implemented so far. It has ratified only 3 of the 6 signatory countries. The main reason for the non-implementation of this agreement is that none of the signatory members has formulated this agreement. Another organization drafted the treaty, which made ASEAN member states reluctant to ratify the convention.

In the case of Malaysia, the Sustainable Development Policy and the Environmental Quality Control Act 1974 are followed. According to this policy, any scheduled activities such as a large development project, logging, excavation, mining, and other works must be approved by completing an "Environmental Impact Assessment (EIA)" before commencement. The report will contain detailed information on the proposed project's environmental impact, such as identification, forecasting, evaluation, and communication, and details of mitigation measures before project approval and implementation. Although the EIA report is mandatory, the application and environmental impact of this policy in the Malaysian context are still questionable because, in violation of this policy, uncontrolled and destructive bauxite mining activities are taking place in Pahang, where there are rare earth plants. Yet these two events created discussions where the environmental impact was evident. Except for the two cases mentioned so far, there are no major/serious problems with other projects and development in Malaysia.

United Nations Conference on Sustainable Development (UNCSD), Rio 2012. This is the third international conference on sustainable development aimed at reconciling the economic and environmental goals of the global

community (Shelton 2000). The United Nations Department of Economic and Social Affairs organized the conference with the participation of 192 member states, including 57 heads of state and 31 heads of government (Shelton 2000). Besides that, representatives from private sector companies, NGOs, and other groups also joined the conference. It was a high-level conference where heads of state, government, or other representatives came together to create a political document to formulate a global environmental policy. As a result of this conference, the heads of 192 countries stressed the need for sustainable development in a non-binding declaration.

In conclusion, the importance of sustainable development policy in environmental law is undeniable and immeasurable. This policy is the most important in the current era of technology development, resources, and limited resources. People's desire for power never ends, but a clear understanding is needed that development without sustainability will lead to our destruction.

CONCLUSION

It is now universally acknowledged that the world's challenges can be addressed through cooperation. Acid rain, ozone depletion, toxic waste poisoning, and biodiversity loss are among the world's daily difficulties. It is important to address these challenges. Neighboring states can also be affected by the polluting activities of a state. And it is in such a situation that the need for various international policies arises, through which the current problems can be managed, and the incidence of such pollution can be reduced in the future.

However, crafting human rules to protect human activities is critical while maintaining a healthy connection with nature's universal laws. The international community has implemented several environmental policies under various international laws to address and prevent environmental concerns. These measures have considerably impacted the regulatory framework that governs the environment. These policies are made up of a variety of laws or sources at the international or national level.

So it is often difficult to identify the parameters of this policy. So while these may apply to a specific area or region, they may not be suitable for another area. As a result, there isn't a single policy that everyone agrees on. However, most of these policies have changed and evolved, and most are almost the same in the country's legal system. The general principles of these agreements are similar. Decisions and conventions, declarations, or statements of multilateral environmental agreements often result in the creation of many international laws. For example, the precautionary and polluter pays principles were established due to the Rio

Declaration of 1992. Different international law principles have been incorporated into the national laws of different countries in terms of necessity.

Nevertheless, regular checks are required to amend existing laws to ensure environmental justice. It is very important that the world now recognizes the biggest and most real danger of environmental catastrophe. This danger is imminent if the necessary steps are not already taken to protect the environment. Let's look at the past world and consider the importance of material importance. We seem to go through a more difficult path to get universal recognition of these environmental protection policies. For example, we can mention that disasters like big floods are due to the greenhouse effect. Everything is already too late. World leaders, NGOs, and other concerned stakeholders must firmly work hard from now on. They need to analyze in detail that while some conventions effectively protect the environment, many others are not. They have to take steps to make the policies more effective.

REFERENCES

Alam, S. and Hossain, B.M.J. 2013. Handbook of International Environmental Law. Routledge, London.

Bodansky, D., Brunnee, J.B. and Hey, E. 2007. The Oxford Handbook of International Environmental Law. Oxford University Press, Oxford.

Brine, P. and Boyle, A. 2002. International Law and the Environment. Oxford University Press, Oxford.

Bullard, R.D. and Jonson, G.S. 2000. Environmental justice: Grassroots activism and its impacts on public policy discussion making. J. Social Iss., 56(3): 555-578.

Caldwell, L.K. 1990. International Environmental Policy. Duke University Press, North Carolina.

David, A. 1990. Regulating the international hazardous waste trade: A proposed global solution. J. Transnatl., 1(1): 801-845.

Faruque, A.A. 2017. Environmental Law: Global and Bangladesh Context. New Warsi Book Corporation, Dhaka.

Gillespie, A. 1997. International Environmental Law, Policy and Ethics. Oxford University Press, Oxford.

Jardins, J.R.D. 2001. Environmental Ethics. An Introduction to Environmental Philosophy. Fifth Edition. Cengage, Belmont, CA .

Joyner, C.C. 1986. Legal implications of the concept of the common heritage of mankind. Int. Comp. Law Quat., 35(1): 192-95.

Kiss, W. and Shelton, D. 2004. A Guide to International Environmental Law. Third Edition. Transnational Publications, NY.

Mitsuo, M., Thomas, S.J. and Petors, C.M. 2006. The World Trade Organization: Law, Practice, and Policy. Oxford University Press, Oxford.

Nanda, V.P. and Pring, G. 2003. International Environmental Law Policy for the 21st Century. Transnational Publishers, New York.

Opschoor, J.B. and Hans, B.V. 1989. Economic Instruments for Environmental Protection. OECD, Paris.

Reid, C.T. 1997. Environmental Law in Scotland. Sweet and Maxwell, Edinburgh.

Rio Declaration on Environment and Development. 1992. Report of the United Nations Conference On Environment and Development. https://www.un.org/en/development/desa/population/migration/generalassembly/docs/globalcom pact/A_CONF.151_26_Vol.I_Declaration.pdf (Accessed 11 October 2021).

Rolston, H. 1988. Environmental Ethics. Temple University Press, Philadelphia.

Sadleer, A.N.D. 2002. Environmental Principles: From Political Slogans to Legal Rules. Oxford University Press, Oxford.

Sands, P. 1995. Liability for Environmental Damage. In Sun, L. and Kurukulasuriya, L. (eds), UNEP's New Way Forward: Environmental Law and Sustainable Development, UNEP, Nairobi, pp. 73-95.

Shelton, D. 2000 Environmental Rights. Oxford University Press, Oxford.

Thornton, J. and Beckwith, G. 2004. Environmental Law. London: Sweet & Maxwell.

Wolf, S. and Neil, S. 2003. Environmental Law. Cavendish Publishing Limited, London.

Environmental Sustainability: Can Artificial Intelligence be an Enabler for SDGs?

Gyandeep Chaudhary† iD

School of Law, Bennett University, Greater Noida, Uttar Pradesh, India

†Corresponding author: Gyandeep Chaudhary: gyan.2889@gmail.com

ABSTRACT

Environmental issues have continued to spur discussions, debates, public outrages, and awareness campaigns, inciting interest in emerging technologies such as Artificial Intelligence. Its usage is spread across many environmental industries, including wildlife protection, natural resource conservation, clean energy, agriculture, energy management, pollution control, and waste management. In 2017, at the United Nations Artificial Intelligence Summit in Geneva, the UN acknowledged that AI could be an enabler in the sustainable development process towards peace, prosperity, and dignified life for humankind and proposed to refocus on the application of AI in assisting global efforts on sustainable development to eradicate poverty, hunger and to protect the environment as well as to conserve natural resources.
It is vital to address environmental sustainability concerns; however, with the advent of AI, most common environmental issues are now solvable by prioritizing human interests. Sustainability encompasses the interrelated areas of the environment, society, and economy. According to the United Nations' "Our Common Future," also known as the "Brundtland Report," it is defined as "development that satisfies current needs without compromising the ability of future generations to meet their own needs." Unfortunately, the Earth is currently facing serious consequences from global warming and climate change, and immediate action is required to encourage the use of environmentally friendly and sustainable products to address these issues. Environmental degradation and climate change are numerous environmental concerns requiring novel and intelligent artificial intelligence solutions. The literature on AI and environmental sustainability encompasses various domains. Notably, AI is being used to address the bulk of regional and global environmental concerns, including energy, water, biodiversity, and transportation, even though many of these sectors have permeated and evolved. However, there is a need to combine current literature on the application of AI, particularly in relation to environmental sustainability in areas such as energy, water, biodiversity, and transportation. There is a significant lack of research on how AI can promote environmental sustainability. This research aims to explore how AI can be applied to address environmental issues in various sectors to achieve the Sustainable Development Goals (SDGs).

INTRODUCTION

Environmental issues, debates, and programs have recently ignited awareness and public concern, sparking interest in new technologies like Artificial Intelligence (AI). As we grapple with the environmental challenges of the 21st century, AI has emerged as a crucial and distinct area of study for resolving a multitude of sustainability issues.

AI refers to the engineering and science behind the evolution of intelligent machines. It is the discipline of computer science, and its capabilities are based on the learning experience that helps increase the chances of

success in solving environmental problems. According to Poole (1998), the intelligence of sophisticated machines, demonstrated by the innate intelligence of animals and humans, could be AI, scientific and technical information that allows devices to be as intelligent as humans (Wang & Srinivasan 2017). Researchers have also found that AI systems can learn from experience to create artificial services and adapt inputs to changing environmental issues (Nishant et al. 2020).

Artificial Intelligence has pushed the boundaries of human intellect in the modern era, creating a new reality in which intelligent machines with artificial brains communicate with human brains (Duan et al. 2019). As we face new environmental challenges, AI has become an

ORCID details of the authors:

Gyandeep Chaudhary: https://orcid.org/0000-0002-6831-1142

essential tool for developing sustainable solutions that will help us preserve our planet for future generations.

Managing environmental sustainability is a complex and challenging task. However, with the integration of AI, many of these problems can be efficiently solved by utilizing human resources. The economy, the environment, and society are interconnected when it comes to sustainability. Sustainability is defined as sustainable development in the United Nations paper *Sharing Our Future*, also known as the Brundtland report, as "a program that meets the needs of the current generation without compromising the ability of future generations to meet their own needs." To ensure that human interests do not compromise the health of ecosystems, sustainability can also be defined as a strategy for supplying future generations with the goods and services they will require. (Morelli 2011).

AI is a powerful instrument that can assist us in our quest for environmental sustainability. It grants us the ability to delve into vast amounts of data, uncover patterns and make predictions. Artificial intelligence can help us learn more about how our actions affect the natural environment and come up with long-term fixes to protect Earth for future generations. Managing environmental sustainability and ensuring we fulfill the needs of now and tomorrow require AI, which has become increasingly important in the face of new and pressing environmental concerns.

With the Earth in peril from the effects of global warming and climate change, developing eco-friendly and long-lasting products is crucial. Climate change is one of the most complex environmental issues, and recent advancements in AI are providing innovative solutions to address this problem. With the urgent need to address environmental degradation, AI is becoming crucial in finding sustainable solutions.

AI and environmental sustainability can be divided into four primary areas: sustainable agriculture, ecological resource protection, waste and pollution management, pollution control, and pollution removal. Consequently, the sustainable application of AI has been vital for advancing and implementing AI over the past fifty years.

AI research for environmental sustainability encompasses a diverse array of disciplines. Most regional and global environmental problems need to be addressed, and artificial intelligence is used in the energy, transportation, biodiversity, and water sectors. However, these areas are constantly evolving and permeating all aspects of society. In some developed countries, the practical application of AI in biodiversity and transportation has already begun, for example, e-waste collection with a sophisticated routing strategy, protecting the ocean from pollution through

AI-driven automatic garbage trucks, and increasing biodiversity through species protection. Nevertheless, the existing research on the application of AI in the transport and biodiversity sectors needs to be consolidated. It is important to note that there is a lack of studies examining how artificial intelligence might be used to improve environmental sustainability in fields including water, energy, transportation, and biodiversity.

AI APPLICATION

Many companies, including Tesla, Google, and Microsoft, driving innovation barriers, have made substantial advances in "Earth-friendly" AI systems. In Google, for example, DeepMind personal AI has helped the company reduce energy use in its data centers by 40%, making it more efficient and reducing overall GHG emissions. Data centers account for 3% of all global energy Advances in these AIs improve energy efficiency and help communities in remote areas provide access to energy by establishing microgrids and integrated green energy sources.

Unlike traditional power grids, which may be inefficient owing to a lack of power distribution planning, urban smart grids can employ AI technologies to control and regulate elements of the power grid in the neighborhood to provide exactly the amount of energy sought or necessary from its dependents.

As AI-driven autonomous vehicles wait to enter the automotive market, strategies such as eco-driving algorithms, route optimization, and ride-sharing service would reduce the carbon footprint and the number of cars on the road.

In an environment of accessible scale, intelligent buildings and innovative urban development can benefit from integrated sensors that use energy more efficiently and buildings and roads with materials that work more efficiently. Inspired by natural patterns, researchers, architects, and builders have created new materials from natural resources (Zafar 2021), including bricks made with bacteria and concrete, which capture carbon dioxide and build a solar system dependent on wind and sun. Solar energy (Zafar 2022) is increasingly used in cities and abroad to power large urban areas. These are the first steps to supporting an infrastructure that reduces costs while increasing our awareness of the environment (Miguel 2021).

Industrial emissions control and waste management is another problem that can be solved through advanced machine learning and captive grids that detect leaks, hazards, and deviations from industrial usage standards and regulations. For example, IoT technology (Giarratana 2022) has been integrated into various industrial businesses, including thermostats, refrigerators, and retailers.

Microsoft's AI for Earth is a $50 million project launched in 2017 to address climate change, agriculture, water scarcity, and biodiversity loss (Smith 2017). Due to a shortage of algorithms that can translate the data they collect into needed solutions, scientists are currently in a mad dash to foresee climate change and other environmental hurdles or bottlenecks.

Similar AI Earth-based applications infused with AI include *INaturalist* and the *eBirds*, which collect information from its large group of experts on species it encounters, which will aid in keeping an eye on their population, their favorable ecological systems, and patterns of migration. They also play an indispensable role in accurately identifying and protecting marine and freshwater ecosystems.

Many organizations, NGOs, and start-ups provide innovative agricultural solutions by applying artificial fuzzy neural networks. Apart from using bio-sensor-driven and artificial intelligence-based algorithms to monitor soil health and yield of crops and yield comprehensively, some methods can develop predictive analytic models that track and forecast different variables and elements that could impact yields in the near future.

The Berlin-based agricultural tech start-up *PEAT* has created a deep-learning application named *Plantix,* which apparently can detect prospective deficiencies and inadequacies in the soil. An analysis is performed using software algorithms that compare particular foliage patterns to problems with soil, pests, and diseases.

AWhere and *FarmShots,* both United States-based companies, use satellite machine-learning algorithms to forecast the weather, evaluate farms' sustainability, and analyze them without disease and pests. Farmers are paying close attention to the adaptive irrigation system because of its significant role in water management. This system automatically irrigates the land based on data collected from the soil by sensors powered by artificial intelligence technology.

AI APPLICATIONS IN BIODIVERSITY

To model the ecosystem's services, rules-based models like ARIES are one of the most popular and well-known systems (Death 2015). The program incorporates other machine learning models that specifically assist researchers in understanding the different relationships through analysis software (Death 2015). In addition, numerous AI (artificial intelligence) examples show how AI is utilized to enhance the observation of biodiversity and conservation (Kwok,2019). Important to emphasize the significance of preventing excessive use of resources, which may cause

environmental issues, and the understanding of the access to artificial intelligence-related information depends on the ecosystem and its diverse biodiversity has developed effective methods (Nishant et al. 2020) that offer estimates or estimates of the services provided by land. Similar to the use of machine training (ML) (also known as natural processing of language (NLP), most of the research on biodiversity that utilizes Artificial Intelligence can predict ecosystem services (Toivonen et al. 2019). Artificial Intelligence is a novel method to tackle biodiversity issues across space and time. Research into Artificial Intelligence to sustain sustainability through Genetic Algorithms focuses on particular Artificial Intelligence applications that use Genetic Algorithms, the well-liked machine-learning model for biodiversity and artificial neural networks, and one of the well-known modeling networks in ecosystems, known as Bayesian networks (Nishant et al. 2020).

AI APPLICATIONS IN ENERGY

Artificial Intelligence is thought (Wang & Srinivasan 2017) to have helped reduce the use of natural resource consumption and the energy requirements from human-related actions. The main research areas are pattern recognition, expert systems, neural networks, and fuzzy logic (Nishant et al. 2020), which are relevant to energy research (Tyralis et al. 2019). This includes the distribution and production of energy and maintenance and operations, which are the major research areas in energy (González Ordiano et al. 2017). Computer-aided learning is employed to forecast (Olowu et al. 2018), and NC algorithms can also be used in solving complex problems (Li et al. 2018). Most of the algorithms used by scientists are implemented in fuzzy logic systems that aid in making decisions based on forecasts (Wang & Srinivasan 2017). Furthermore, using multiple models, such as the area neural network, produces better results and broad combinations.

AI APPLICATIONS IN TRANSPORTATION

Research into artificial intelligence (AI) applications is available for sustainable transportation. Most articles published can be about the machine learning process (Abduljabbar et al. 2019). Applications of artificial intelligence research are also important for sustainable transportation. Learning through the machine has been the main focus of most published papers (Liyanage et al. 2019). Additionally, the use of computer vision to assist in making decisions was observed in safety and traffic management, urban mobility, and public transportation (Liyanage et al. 2019). The AI applications in transportation include machine learning and other time series and statistical models used to

manage and manage traffic (Nishant et al. 2020). Computer vision methods were primarily employed for road marking.

AI APPLICATIONS IN WATER MANAGEMENT

Since 2015, significant research emphasis has been focused on artificial intelligence (AI) applications to improve water management in water protection. Artificial neural networks, especially neuro-fuzzy adaptive sequence systems, support vector machines (SVMs) for machine learning (ML). In this area, models such as decision trees (mainly random forest) and multiple regression, autoregressive displacement models (ARMS), regression splines, and adaptive neuro-fuzzy inference are used (Salcedo-Sanz et al. 2016), with the genetic algorithm being the best by far a known method. Additionally, popular machine learning models include the most popular regional networks (ANNs) (including ANFIS) and genetic algorithms (Rodríguez-Soto et al. 2017). For example, we could use machine training (ML) algorithms to determine river flow and evaluate water quality parameters (Demirci et al. 2019).

HOW CAN AI HELP COMBAT CLIMATE CHANGE?

The technology is used in Japan's top natural disasters to monitor deforestation in the Amazon and design more sustainable and intelligent urban areas in China. Artificial intelligence applications can also create more efficient buildings, improve electricity storage, and improve and renovate wind and solar energy in the grid when needed. In a small way, this can help households reduce energy consumption when they turn on lights automatically, when not in use, or even control the network requirements of electric vehicles to meet expectations.

A recent research study conducted by the well-known accounting firm PricewaterhouseCoopers in partnership with Microsoft, a company that specializes in developing machine learning solutions for the climate change sector, has uncovered some intriguing findings. The study found that by 2030, implementing AI technology could potentially significantly reduce global greenhouse gas emissions, specifically by 4%. This is a noteworthy finding as it highlights the potential of AI in addressing one of the most pressing concerns of our time, climate change.

The proficiencies of AI, specifically its ability to process enormous amounts of unstructured data such as images, graphs, and maps, are pushing the boundaries of climate modeling and providing unparalleled opportunities to better understand the dynamics of sea-level rise and ice caps. This exemplifies the enormous potential of AI in facilitating a better comprehension of the effects of human activity on the Earth and informing the creation of sustainable solutions.

Artificial intelligence allows us to better grasp the consequences of our actions on the world and create long-term alternatives to the current climate crisis. AI has the ability to significantly contribute to combating climate change and lowering GHG emissions. The partnership between Microsoft and PwC illustrates the significance of the private sector and researchers working together to find solutions. We must continue to invest in research and development of AI technology to address the pressing issue of environmental sustainability and ensure a sustainable future for our planet.

USERS OF TECHNOLOGY AND AI

The costly nature of AI computing power has led to a significant portion of research in this field being undertaken by the private sector. One shining example is Climavision, a state-of-the-art super-resolution radar network that harnesses the power of satellite data and high-altitude weather balloons to fill in the "hundreds of holes" in existing weather forecast networks (Nelsen 2021). This technology allows transportation and energy companies, businesses, and military personnel to real-time weather elements, updating every second. As the world moves towards low-carbon energy, the market for AI-powered applications that predict market behavior, balance transactions in real-time, and maximize energy efficiency from networks to intelligent devices is set to flourish. Investing in research to fully realize the potential of AI in addressing environmental issues and supporting the achievement of Sustainable Development Goals is of paramount importance. It is an investment in our planet's future and the future of generations to come.

CHALLENGES OF USING AI TO ACHIEVE ENVIRONMENTAL SUSTAINABILITY

Artificial Intelligence has been shown to address environmental issues effectively, yet, in contrast, they face challenges because they rely on the historical data used for machine learning. This is because machine-learning models find it challenging to account for AI's unpredictable nature and constantly changing characteristics of human behavior. Thus, before any significant human activity, data from the past can be used to reflect people's ages and climate cycles, so it is challenging to predict the likelihood of climate change. Also, it isn't easy to deal with variance when including historical data in models because most computer scientists pay close attention to it. The data added to the models can be generalized, which can be the basis for

erroneous predictions of future scenarios, and this is called *variance bias shift* (Nishant et al. 2020).

Additionally, increasing cybersecurity risk is a challenge when implementing AI for resilience. The management of cybersecurity risks is essential for incorporating data into AI applications. However, the growing number of cybersecurity threats due to hackers poses a significant challenge when addressing environmental sustainability issues. Third parties have access to vital data, and disparate methods are less effective in mitigating security risks. Another obstacle to using AI for environmental sustainability is the lack of adequate performance indicators and the unreliable human behavioral responses (Nishant et al. 2020) to various AI-based interventions. To increase environmental sustainability, tracking and evaluating the results of actions is essential. The measurement method is complicated and often unsuccessful, so combining analytical and technical aspects into one standard metric is crucial for AI to achieve environmental sustainability. AI software is as sophisticated as human decision-making; However, their approach differs from human reactions to decisions. However, being aware of behavioral responses is crucial to avoid the common problem associated with technological advances due to feedback traps (Nishant et al. 2020). The rebound effect is a common problem that arises from technology.

THE DOWNSIDE OF THE TECHNOLOGY: AI CAN HAVE A SUBSTANTIAL CARBON FOOTPRINT

The computational demands of AI-based systems are incredibly high and require large amounts of data to be processed and analyzed. This leads to an increase in the number of servers and energy needed to cool data centers and causes a significant spike in energy consumption. According to a study, the energy required to process and store data to develop a complex algorithm alone can produce as much carbon dioxide as driving a car for five times its lifetime or taking 300 round trips between New York and San Francisco (Hao 2020). Data centers that process and store information from online activities such as streaming videos and sending emails are accountable for a substantial portion of the world's energy use estimated to be around 1% (IEA 2022). Predictions suggest that by 2030, computing could make up as much as 8% of the world's overall energy demand (Bacchi 2020), raising concerns about the increased use of fossil fuels.

This case of CO_2 emissions generated by artificial intelligence is shocking and disturbing. This is a wake-up call for all of us. Nevertheless, we must see the bigger picture before focusing too much on these findings. This is the only study for a specific type of AI that is not common. The most representative training tasks generate relatively small amounts of carbon. Just because the most commonly used AI techniques today are not massive carbon emissions do not mean they will not significantly contribute in the foreseeable future. Only a few studies are currently available that can help companies assess the carbon footprint of AI.

In the fight against climate change, AI can be both an enabler and a disabler. The need for rare earth materials to build the hardware could have a negative impact, and the AI is not magical and can make mistakes while computing or generating output. The possibility of logging individuals' energy usage raises privacy concerns regarding the capability to track back data that belongs to people (Nelsen 2021). Climate change must "primarily affect the people who contribute most to emissions and significantly change our lives." It is not enough to rely on technology in the near future to solve the problem and thus save one's conscience in the short and medium term (Nelsen 2021).

AI FOR SUSTAINABILITY

Given the interconnectedness inherent in all SDGs and the spectrum of sustainable development and its actors, it makes no sense to separate the third section, which will then provide a more detailed overview of the current use of AI in the context of actors of sustainable development, by evaluating the views of AI experts in the field of application conducted for research purposes give perspectives on particular situations.

On that note, we are attempting to determine how AI is being used by various businesses to engage, identify, and ultimately lead to sustainable development. The potential unpredictability of potential causes as well as other characteristics, such as actors, industries, non-governmental organizations, the scientific and technological community, and local actors, producers are to be made clear to the proposed hypothesis, i.e., best classified political actors, will not only have a higher impact on progress toward the SDGs. However, they will also be the channels through which AI will have an ideal positive impact on sustainable development, and the SDGs will be able to reach that point. Of course, this should be the main effect of the pyramid, which is then created, in which actors can influence or endow other ranks in better positions and more appropriate acting modes than other actors descending into the dynamic. AI can promote social cooperation among actors, in this case sustaining an extensive level of sustainable development.

Each of the SDGs has the potential to benefit from the use of AI. This is demonstrated by a McKinsey Global Institute study, which found up to 135 AI use cases supporting the

SDGs by November 2018. These examples demonstrate definite, partial, or hypothetical opportunities for AI applications.

Various use cases will have different domains, capabilities, restrictions, and risk profiles- AI is applied in various ways. We'll look at a few scenarios that could serve as examples of how AI might be used for overall good and sustainable development. These are just a few examples, but they show a variety of potential applications, skills, and effects. Many textbook cases dealing with various examples of deep learning applications in medical imaging have flourished. An overview that would illustrate the aforementioned trend. In fact, since 2015, an intense and rich economic activity has arisen around this medical imaging and diagnosis field. Reportedly, as many as a third of healthcare AI start-ups that raised funds after January 2015 were working on imaging and diagnostics (Varadharajan & Lee 2020). Additionally, researchers at International Business Machines Corporation, one of the first multinational corporations in the computing industry, predict that by 2026, medical images will account for at least 90% of all medical data. Its enormous amount would make it the most significant source of healthcare data.

When we comprehend the relationship between AI and data, especially in large amounts, as we saw earlier with the rise of big data, deep learning has already been applied in this field for tumor development tracking, quantification, and visualization of blood flow, medical interpretation, and treating diabetic retinopathies. In each of the examples, the use of AI is discussed in relation to a business, including a start-up, but more specifically, three global leaders in technology: IBM, Google, and the Samsung group. An additional well-known name in the technology industry contacted was brought to mind by looking at these scenarios: Argus, a global SAP Labs China project. A team there developed the "Argus" solution, which uses machine learning to detect signs of lung cancer on CT scans. Argus then enables testing more patients in less time while enhancing detection precision. Again, we see the same components as before: artificial intelligence, the contribution to the Sustainable Development Goals for "Nutrition, Health, and Well-Being," but most notably by actors in the "Trade and Industry" sector, as defined by the United Nations. The SAP company is a real-world illustration of how a business can employ AI sensibly for potential effects on sustainable development.

DOCUMENTED CONNECTIONS BETWEEN AI AND THE SDGS

Evidence shows that AI can help achieve 134 (79%) of all SDGs, often through technological improvements to overcome known limitations. However, 59 goals (35% of all SDGs included) can be negatively (UN 2019) impacted by AI development (Stockholm Resilience Centre 2017).

AI AND ENVIRONMENTAL OUTCOMES

The final category of sustainability goals is concerned with the environment; when examined, three of the sustainability goals in this group are concerned with climate measurements, life underwater, and life on land (SDG 13, 14, and 15). For environmental organizations, 25 goals (93%) could be identified where AI can act as an enabler (PwC & Stanford Woods Institute for the Environment 2018). The benefits of artificial intelligence may lie in the ability to analyze massively interconnected databases for collaborative curatorial work. When we look at SDG 13 on climate change, we can see that advances in artificial intelligence are helping to understand climate change and model its potential effects. AI also has the potential to aid in developing low-carbon energy systems, which are essential in the fight against climate change as they use renewable resources and improve energy efficiency. Ecosystem health can also be improved with artificial intelligence. Using AI-based automated oil spill detection algorithms, we can achieve our goal 14.1 of preventing and significantly reducing marine pollution (Keramitsoglou et al. 2006).

15.3 is another example that asks for combatting desertification and rehabilitating degraded lands and soils. Artificial neural networks and particular methodologies can improve the classification of land cover types from satellite photos, potentially processing a considerable number of images quickly (Mohamadi et al. 2015). These artificial intelligence (AI) tools can help spot large-scale patterns of desertification and provide helpful information for decision-making, planning, and environmental supervision, preventing more desertification or reversing trends by identifying root causes. However, as previously indicated, attempts to accomplish SDG 13 on climate change may be impeded by AI applications' high energy requirements, mainly when using carbon-free energy sources.

Moreover, it is anticipated that with more access to information about Artificial Intelligence (AI) related to the environment, there will be an increased likelihood of resource overexploitation, despite the growing number of examples showing how AI is being utilized to aid in biodiversity conservation and monitoring (Kwok 2019). Although these abuses of AI have not yet been extensively documented, they will be examined in more detail later, where the current deficiencies in AI research will be considered.

RESEARCH GAPS IN ARTIFICIAL INTELLIGENCE'S ROLE IN SUSTAINABLE DEVELOPMENT

As Artificial Intelligence (AI) applications are increasingly being utilized to advance Sustainable Development Goals, such as self-driving vehicles, AI-based smart grids (IEA 2017), and healthcare (De Fauw et al. 2018), these systems must become more resilient and valuable to minimize any disruptions. With the increasing use of AI in various industries, investments in AI security research will become even more critical to prevent mishandling or damage.

An important area of research in AI security integration is understanding the potential disasters and system failures that can occur in AI technologies. For instance, a recent World Economic Forum (WEF 2018) study has raised similar concerns about using AI in the banking industry. In a world that is increasingly dependent on this technology, it is vital to raise awareness about the hazards of AI system failures and invest in research addressing these concerns. By doing so, we can ensure that AI is developed and implemented in a way that promotes safety, efficiency, and sustainability. As society continues to evolve and adapt to the impact of AI and non-AI technological advancements, the demands on AI also change, creating a dynamic interplay between society and technology. This ongoing interaction forms a chain of communication where society shapes the development and use of AI, and in turn, AI shapes society.

Furthermore, while we have been able to find some studies that show that AI has the potential to contribute to many SDG goals and calculations, most of this research has limited data. It cannot be performed in a controlled or laboratory setting by using prototypes (Gandhi et al. 2017). Therefore, it is often difficult to extrapolate this information to assess the impact in the real world. This is predominantly true when examining the effects of AI on larger temporal and geographical dimensions. We understand that by performing controlled experiments to assess the impact of AI in the real world, it is possible to describe how well AI tools adapt to a specific environment.

As society evolves and adapts to the impact of non-AI technological advancements, the demands on AI also change, creating a dynamic interplay between society and technology. This ongoing interaction forms a chain of communication where society shapes the development and use of AI, and in turn, AI shapes society.

However, an alarming aspect of current research is society's resistance to change brought about by AI. To ensure that the effect of new technologies is evaluated in terms of efficiency, ethics, and sustainability, there is a need for new methodologies to be implemented before the widespread adoption of A.I., Given the significant risks associated with errors in AI systems. It is essential that research is conducted to understand the causes of these errors and to develop integrated human-machine analysis tools. This will pave the way for the responsible development and use of AI technology (Nushi et al. 2018).

Although we discovered more published evidence suggesting AI would aid rather than impede the fulfillment of the SDGs, there are at least two important considerations to remember. First, vested interests motivate the AI research community and industry to report favorable findings. Second, long-term research may be necessary to discover AI inadequacies, and as stated before, there are a limited number of accessible assessment methodologies. The tendency to report positive results was particularly strong for sustainable development goals corresponding to the environmental group. Coastal and marine protection objective 14.5 is an excellent example of this bias (Beyer et al. 2016). Machine learning algorithms provide the best solution because many parameters are involved in the optimal selection of safety nets. More research is needed to evaluate the long-term ramifications of such algorithms on fairness and justice, even if the output is theoretically optimum (within the provided parameter range).

The second point highlighted above brings to attention a crucial issue in AI – the tendency for funding to be directed toward projects with the highest potential for profit maximization. This can lead to a disproportionate focus on AI applications driven by economic and commercial interests, resulting in greater inequality. As pointed out by researchers in 2018 (Whittaker et al. 2018).

It is imperative to remember that the potential for economic gain should not be the sole determinant in prioritizing AI-based solutions for achieving Sustainable Development Goals (SDGs). Rather, we should also consider emerging AI technology's social, ethical, legal, and environmental effects. It is crucial that funding is allocated to projects that evaluate and address these important factors, in addition to those that hold commercial promise. Doing so will help guarantee that AI advances are made in a way that benefits everyone and helps all communities thrive.

One way to utilize the capabilities of AI technologies in accomplishing the SDGs is through extensive research and application of machine learning algorithms and data mining techniques on the growing amount of data that has been collected over time, from analyzing past weather events to making predictions about future occurrences (Vinuesa et al. 2020). The requirement for this research study is to permit the prep work and feedback for an extensive range of events

ahead if anything comes up unexpectedly without knowing when it will occur. The gap in real-world applications of AI systems is a significant concern for governments seeking ways to effectively incorporate these technologies into their decision-making processes (Chen et al. 2020). Institutions have several barriers that must first be overcome before they can successfully implement such an approach, including setting up cybersecurity measures and protecting citizen's privacy across all aspects related to surveillance issues, as well as tracking what data might potentially leak or become compromised within the institution's operation; this also includes automating specific processes without rigorous ethical standards put forth by law which would target any possible bias present- however small it may seem at times –with using artificial intelligent machines (Courtland 2018).

There is a narrow application for AI technologies at the moment, with many projects addressing problems that only developed countries face. For instance, automated harvesting or optimizing its timing can be done more effectively by systems that operate within these countries because they have access to tools like robust electricity networks and high-end computing power needed for such operations where less developed areas may not always contain everything needed at once – making their AI technology less useful there than if it was designed from scratch using components available locally without any need whatsoever for international trade agreements which often burden low-income economies most heavily as well.

While promising, recent developments in Artificial Intelligence (AI) technology also raise concerns about exacerbating inequality within and between nations. This inequality could potentially hinder progress toward the achievement of Global Goals. Therefore, researchers and funders must focus on designing solutions tailored to the specific needs of less developed nations or regions where adopting AI may be more challenging (Bird et al. 2020).

These solutions must consider the unique cultural and societal dynamics of these regions rather than simply importing solutions from more technologically advanced economies. Every project must be custom fit to the traditions and needs of the region in which it is implemented. By taking a localized approach, we can ensure that AI technology is used to promote equality and contribute to the betterment of all communities.

CONCLUSION

The realm of artificial intelligence is a vast and ever-expanding frontier with the potential to revolutionize industries and sectors across the board. The potential for this technology to be used to protect the world's natural resources is particularly exciting. The environment, though not an industry, is the foundation upon which human life thrives. As such, it has become a top priority for governments worldwide to safeguard it for future generations. The notion that technology could be harnessed for the betterment of our planet was once considered a fanciful dream, yet with the advent of AI. It has become a tangible reality.

As we march towards a more sustainable future, the role of AI in environmental conservation is becoming increasingly apparent. AI technologies and algorithms are constantly evolving to monitor pollution levels, reduce energy use, and increase comprehension of climate change's complex consequences.

Governments at all levels, from local to national governments, recognize AI's potential to protect our planet and incorporate it into their program and policy roadmaps for environmental protection. With its ability to quickly collect and analyze large amounts of data, as well as its ability to learn and adapt to new situations, artificial intelligence can be a powerful tool in the battle against pollution and climate change.

Moreover, integrating AI with IoT (Internet of Things), technology can improve environmental sustainability in new and innovative ways. By connecting various devices, sensors, and machines to the internet, we can gather a wealth of data that can be analyzed and acted upon in real time. By combining AI's power with IoT's connectivity, we can significantly reduce carbon emissions, improve air and water quality, and preserve natural habitats.

This article delves into the many ways in which AI is helping to increase environmental sustainability. From understanding the AI carbon footprint and its impact on the environment to exploring the various applications of AI in environmental conservation, we will gain a deeper understanding of AI's role in preserving our planet for future generations. As the world becomes increasingly dependent on technology, it is vital that we harness its power for the benefit of our planet and all its inhabitants.

REFERENCES

Abduljabbar, R., Dia, H., Liyanage, S. and Bagloee, S.A. 2019. Applications of artificial intelligence in transport: An overview. Sustainability, 11(1): 189. https://doi.org/10.3390/su11010189

Bacchi, U. 2020. How Cat Videos Could Cause A 'Climate Change Nightmare.' Retrieved from https://www.reuters.com/article/us-georgia-tech-climatechange-feature-tr-idUSKBN20C1A7 (Accessed January 12, 2023)

Beyer, H.L., Dujardin, Y., Watts, M.E. and Possingham, H.P. 2016. Solving conservation planning problems with integer linear programming. Ecol. Model., 328: 14-22. https://doi.org/10.1016/j.ecolmodel.2016.02.005

Bird, E., Skelly, J.F., Jenner, N.J., Larbey, R., Weitkamp, E. and Winfield, A. 2020. The Ethics of Artificial Intelligence: Issues and Initiatives.

Retrieved from https://www.europarl.europa.eu/stoa/en/document/EPRS_STU(2020)634452 (Accessed on January 2, 2023)

Chen, X., Xie, H., Zou, D. and Hwang, G.J. 2020. Application and theory gaps during the rise of artificial intelligence in education. Comp. Edu. Artificial Intellig., 1: 100002. https://doi.org/10.1016/j.caeai.2020.100002

Courtland, R. 2018. Bias detectives: The researchers striving to make algorithms fair. Nature, 558(7710): 357-360. https://doi.org/10.1038/d41586-018-05469-3

De Fauw, J., Ledsam, J.R., Romera-Paredes, B., Nikolov, S., Tomasev, N., Blackwell, S., Askham, H., Glorot, X., O'Donoghue, B., Visentin, D., van den Driessche, G., Lakshminarayanan, B., Meyer, C., Mackinder, F., Bouton, S., Ayoub, K., Chopra, R., King, D., Karthikesalingam, A. and Ronneberger, O. 2018. Clinically applicable deep learning for diagnosis and referral in retinal disease. Nature Med., 24(9): 1342-1350. https://doi.org/10.1038/s41591-018-0107-6

Death, RG 2015. An environmental crisis: Science has failed; let us send in the machines. Water, 2(6): 591-600. https://doi.org/10.1002/wat2.1102

Demirci, M., Üneş, F. and Körlü, S. 2019. Modeling groundwater level using artificial intelligence techniques: A case study of Reyhanli region in Turkey. Appl. Ecol. Environ. Res., 17(2): 2651-2663. https://doi.org/10.15666/aeer/1702_26512663

Duan, Y., Edwards, J.S. and Dwivedi, YK 2019. Artificial intelligence for decision-making in the era of big data. Evolution, challenges, and research agenda. Int. J. Inform. Manag., 48: 63-71. https://doi.org/10.1016/j.ijinfomgt.2019.01.021

Gandhi, N., Armstrong, L.J. and Nandawadekar, M. 2017. Application of data mining techniques for predicting rice crop yield in the semi-arid climatic zone of India. Technol. Innov. ICT Agric. Rural Develop., 11: 115-120. https://doi.org/10.1109/tiar.2017.8273697

Giarratana, C. 2022. IoT Technology Making Inroads in Construction Industry. Retrieved from https://www.cleantechloops.com/iot-technology/ (Accessed January 9, 2023)

González Ordiano, J.Á., Waczowicz, S., Hagenmeyer, V. and Mikut, R. 2017. Energy forecasting tools and services. WIREs Data Mining Knowl. Dis., 8(2). https://doi.org/10.1002/widm.1235

Hao, K. 2020. Training a Single AI Model Can Emit as Much Carbon as Five Cars in Their Lifetimes. Retrieved from https://www.technologyreview.com/2019/06/06/239031/training-a-single-ai-model-can-emit-as-much-carbon-as-five-cars-in-their-lifetimes/ (Accessed on January 12, 2023)

IEA. 2022. Data Centers and Data Transmission Networks, Retrieved from https://www.iea.org/reports/data-centres-and-data-transmission-networks (Accessed January 12, 2023).

IEA. 2017. Digitalization and Energy: Analysis. Retrieved from https://www.iea.org/reports/icontion-and-energy (Accessed on January 12, 2023).

Keramitsoglou, I., Cartalis, C. and Kiranoudis, C.T. 2006. Automatic identification of oil spills on satellite images. Environ. Model. Software, 21(5): 640-652. https://doi.org/10.1016/j.envsoft.2004.11.010

Kwok, R. 2019. AI empowers conservation biology. Nature, 567(7746): 133-134. https://doi.org/10.1038/d41586-019-00746-1

Li, G., Jin, Y., Akram, M.W., Chen, X. and Ji, J. 2018. Application of bio-inspired algorithms in maximum power point tracking for PV systems under partial shading conditions – a review. Renew. Sustain, Energy Rev., 81: 840-873. https://doi.org/10.1016/j.rser.2017.08.034

Liyanage, S., Dia, H., Abduljabbar, R. and Bagloee, S. 2019. Flexible mobility-on-demand: An environmental scan. Sustainability, 11(5): 1262. https://doi.org/10.3390/su11051262

Miguel, M. 2021. Looking For Love While Environmentally Conscious? Here's How. Retrieved from https://www.ecomena.org/looking-for-love-while-environmentally-conscious/ (Accessed January 8, 2023).

Mohamadi, A., Heidarizadi, Z. and Nourollahi, H. 2015. Assessing the desertification trend using neural network classification and object-oriented techniques: Case study: Changouleh watershed – Ilam

province of Iran. İstanbul Üniv. Orman Fakült. Derg., 66(2): https://doi.org/10.17099/jffiu.75819

Morelli, J. 2011. Environmental sustainability: a definition for environmental professionals. J. Environ. Sustain., 1(1): 1-10. https://doi.org/10.14448/jes.01.0002

United Nations. (UN). 2019. Sustainable Development. Retrieved from https://www.un.org/ecosoc/en/sustainable-development (Accessed April 21, 2022)

Nelsen, A. 2021. Here's How AI Can Help Fight Climate Change. Retrieved from https://www.weforum.org/agenda/2021/08/how-ai-can-fight-climate-change/ (Accessed January 12, 2023).

Nishant, R., Kennedy, M. and Corbett, J. 2020. Artificial intelligence for sustainability: Challenges, opportunities, and a research agenda. Int. J. Inform. Manag., 53: 102104. https://doi.org/10.1016/j.ijinfomgt.2020.102104

Nushi, B., Kamar, E. and Horvitz, E. 2018. Towards accountable AI: Hybrid human-machine analyses for characterizing system failure. Proceed. AAAI Conf. Human Comp. Crowdsourc., 6: 126-135. https://doi.org/10.1609/hcomp.v6i1.13337

Olowu, T., Sundararajan, A., Moghaddami, M. and Sarwat, A. 2018. Future challenges and mitigation methods for high photovoltaic penetration: A survey. Energies, 11(7): 1782. https://doi.org/10.3390/en11071782

Poole, D.L., Mackworth, AK and Goebel, R.G. 1998. Computational Intelligence: A Logical Approach. Oxford University Press, Oxford.

PwC & Stanford Woods Institute for the Environment. 2018. Harnessing Artificial Intelligence for the Earth. Retrieved from https://www3.weforum.org/docs/Harnessing_Artificial_Intelligence_for_the_Earth_report_2018.pdf (Accessed March 1, 2022)

Rodríguez-Soto, C., Velazquez, A., Monroy-Vilchis, O., Lemes, P. and Loyola, R. 2017. Joint Ecological, geographical, and cultural approach to identify territories of opportunity for large vertebrate conservation in Mexico. Biodiv. Conserv., 26(8): 1899-1918. https://doi.org/10.1007/s10531-017-1335-7

Salcedo-Sanz, S., Cuadra, L. and Vermeij, M. J. A. 2016. A review of computational intelligence techniques in coral reef-related applications. Ecological Informatics, 32, 107-123. https://doi.org/10.1016/j.ecoinf.2016.01.008

Smith, B. 2017. AI for Earth Can Be a Game-Changer for Our Planet. Retrieved from https://blogs.microsoft.com/on-the-issues/2017/12/11/ai-for-earth-can-be-a-game-changer-for-our-planet/ (Accessed September 12, 2022)

Stockholm Resilience Centre. 2017. Stockholm Resilience Centre's (SRC) Contribution to the 2016 Swedish 2030 Agenda HLPF Report. Retrieved from https://www.stockholmresilience.org/download/18.2561f5bf15a1a341a523695/1488272270868/SRCs+2016+Swedish+2030+Agenda+HLPF+report+Final.pdfn (Accessed July 28, 2022)

Toivonen, T., Heikinheimo, V., Fink, C., Hausmann, A., Hiippala, T., Järv, O., Tenkanen, H. and Di Minin, E. 2019. Social media data for conservation science: A methodological overview. Biol. Conserv., 233: 298-315. https://doi.org/10.1016/j.biocon.2019.01.023

Tyralis, H., Papacharalampous, G. and Langousis, A. 2019. A brief review of random forests for water scientists and practitioners and their recent history. Water Resour. Water, 11(5): 910. https://doi.org/10.3390/w11050910

Varadharajan, D. and Lee, J. 2020. Ai in Healthcare: The Future of the Clinical Trial. Research. Retrieved from https://www.cbinsights.com/research/briefing/ai-in-healthcare-future-clinical-trial/ (Accessed May 12, 2022).

Vinuesa, R., Azizpour, H., Leite, I., Balaam, M., Dignum, V., Domisch, S., Felländer, A., Langhans, S. D., Tegmark, M. and Fuso Nerini, F. (2020). The role of artificial intelligence in achieving the sustainable development goals. Nature Commun., 11(1): 1-11. https://doi.org/10.1038/s41467-019-14108-y

Wang, Z. and Srinivasan, R.S. 2017. A review of artificial intelligence based building energy use prediction: contrasting the capabilities of single and ensemble prediction models. Renewable and Sustainable Energy Reviews, 75, 796-808. https://doi.org/10.1016/j.rser.2016.10.079

Whittaker, M., Crawford, K., Dobbe, R., Fired, G., Kaziunas, E., Mathur, V., West, S.M., Richardson, R., Schultz, J. and Schwartz, O. 2018. AI Now Report 2018. Retrieved from https://ainowinstitute.org/AI_Now_2018_Report.pdf (Accessed December 12, 2022)

World Economic Forum (WEF). 2018. The New Physics of Financial Services: How Artificial Intelligence Is Transforming the Financial Ecosystem. Retrieved from https://www.weforum.org/reports/the-new-physics-of-financial-services-how-artificial-intelligence-is-transforming-the-financial-ecosystem (Accessed January 12, 2022).

Zafar, S. 2021. What You Need to Know About the Top Green Building Trends. Retrieved from https://www.ecomena.org/top-green-building-trends/ (Accessed October 20, 2022).

Zafar, S. 2022. What is a Solar Power Bank? Retrieved from https://www.ecomena.org/what-is-a-solar-power-bank/ (Accessed August 18, 2022).

Variance-Based Fusion of VCI and TCI for Efficient Classification of Agriculture Drought Using Landsat Data in the High Atlas (Morocco, North Africa)

Fathallah Fatima Ezzahra† iD **, Algouti Ahmed and Algouti Abdellah**

The Laboratory of Geosciences, Geotourism, Natural Hazards and Remote Sensing, Cadi Ayyad University, Faculty of Sciences, Semlalia, BP 2390, 40000 Marrakech, Morocco

†Corresponding author: Fathallah Fatima-Ezzahra; fathallah.fatimaezzahra01@gmail.com

ABSTRACT

Drought assessment using drought indices has been widely carried out for drought monitoring. Remote sensing-based indices use remotely sensed data to map drought conditions in a particular area or region. Therefore, the objective of the present study is to make a study on drought risk based on the calculation of an indicator from biophysical parameters extracted from NOAA/AVHRR satellite data, namely TCI and VCI, to obtain a better understanding of the differentiation between each index, and their application for drought monitoring in the High Atlas of Marrakech on the Chchaoua Morocco watershed during 1980-2020. Landsat oli7 and8 data were used to construct the indices. The result showed that each index proved to be a useful, fast, sufficient, and inexpensive tool for drought monitoring. However, each index has its differences. The TCI was found to be drought sensitive during the dry season or in months when high temperatures occurred. While VCI detected drought more sensitively in the rainy season as well (December-January-February to May) than TCI and VCI. Meanwhile, VCI, including the improved TCI, combined two indicators to better understand drought occurrence. These indices were calculated using GIS, QGis, ArcGis satellite imagery scenes, and Landsat. After a comparative study of these years, from 1984 to 2020, the evolution of the VCI and TCI was highlighted.

INTRODUCTION

Drought is a natural threat that tends to worsen in the context of climate change, with major socio-economic consequences (Keyantash & Dracup 2002, Wilhite 2007), particularly in vegetation, the sector most vulnerable to this climatic hazard. Several definitions of this severe form of water deficit (Heim 2002, Boken et al. 2005). They are either conceptual or operational (Ndmc 2006). The conceptual definitions, which are rather general, are frequently recycled to set up water management policies (e.g., temperature increase, precipitation deficit, and yield loss). Thus, climate change may have major consequences on the evolution of droughts in several regions of the world.

In Morocco, an agricultural country with an arid to semi-arid climate, surface water resources are becoming increasingly limited and difficult to exploit, as most agricultural areas are strongly linked to the climate, precisely the temperature during the summer period. Due to the lack

of planning, these resources would be threatened in case of probable climate change or variability of the average temperature (Augier & Blanc 2009).

To develop an adaptation strategy to a possible scarcity of water resources, it is necessary to know the drought and its evolution. To do so, it is important to have tools and means adapted to provide data on drought intensity. Several means already exist to measure the drought episodes that characterize a given environment. These are indicators based on climatic data from meteorological stations, such as the TCI temperature index (Hayes et al. 1999).

Unfortunately, this type of approach has limitations in Morocco. Indeed, data remain difficult to access (Shaban & Houhou 2015). This shortage of climatological data and the non-centralized nature of water resources data management are major obstacles to drought monitoring. In this sense, finding a method that ensures the monitoring and communication of spatio-temporal drought information for the whole territory is important. Indicators from satellite images can offer this possibility. The main objective of this study is, in a first step, to monitor the evolution of drought intensity in the Chichaoua catchment area for the period

ORCID details of the authors:

Fathallah Fatima Ezzahra: https://orcid.org/0000-0002-8618-7579

1982-2021, using satellite data from the NOAA-AVHRR sensor. The second objective is to understand the variations in drought intensity over the last few years using another drought indicator, the average TCI.

MATERIALS AND METHODS

The Study Area

The province of Chichaoua was created in 1991 and is part of the Wilaya of Marrakech. Its administrative boundaries are:

- In the North, the province of Safi
- In the South, the province of Taroudant
- In the West, the province of Essaouira
- To the east are the Marrakech Menara prefecture and Al Haouz province.

Its privileged geographical position constitutes an obligatory passage towards the South of the Kingdom and the West towards Essaouira and Safi. The perimeter of Chichaoua upstream is part of the physiographic unit of high-Atlasic Piedmont, with an altitude of about 339 m. It consists of the low terraces along the Chichaoua Wadi and its tributaries.

With a surface area of 2690 km², the Chichaoua basin is part of the Oued Tensift hydraulic system, comprising ten sub-basins of varying importance. Among these, the

Chichaoua basin is located the furthest west in the Haouz Mejjat basin (Fig.1). It is bounded to the east by the Assif Elmal watershed, to the south by the High Atlas Mountains, to the north by Tensift and to the west by the Oulad Bousbaa Plain.

Our watershed (Fig. 1), by its geographical position in relation to a framing mountain range, is characterized by an arid semi-arid climate that evolves towards a significant alteration of rainfall, plant cover, and soils. It is characterized by a rainy season that extends from October to March. In the summer, the influence of subtropical high pressure prevents any rising air and causes an absolute drought from June to September. The climatic conditions play a negative role on the water resources and, consequently, on the vegetation. In this context, it is important to monitor the drought intensity in this region of the Chichaoua watershed to provide local and national decision-makers with reliable information and results to facilitate the implementation of reasonable and efficient management of natural resources, focused on reducing drought-related risks.

Drought Indices

Over the past few decades, several drought indices have been established to monitor and assess drought and to provide early warning. Typically, a drought index is a key variable for assessing the effect of drought and defining various drought parameters, which include intensity, duration, severity, and spatial extent. It should be noted that a drought variable should be able to quantify drought for different time scales for which a long time series is essential. The most commonly used time scale for drought analysis is the year. It can also
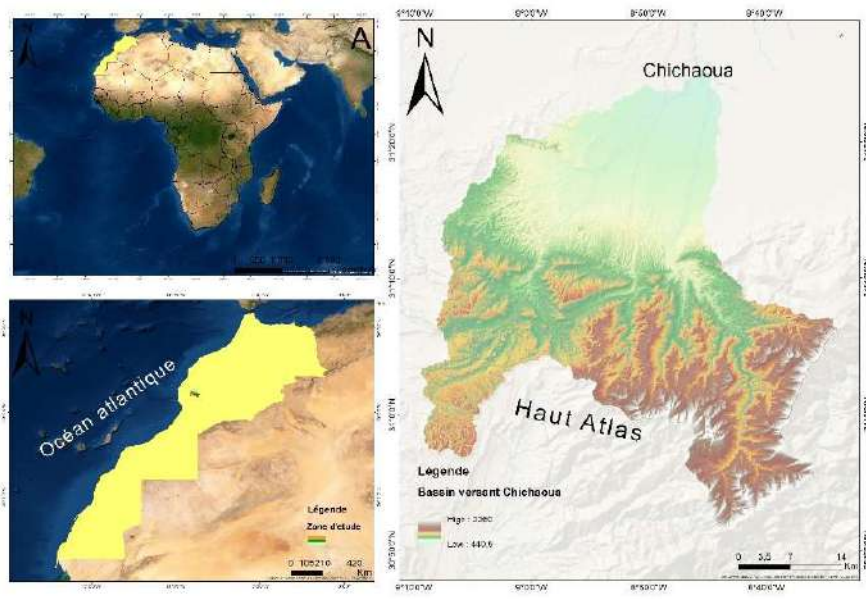

Fig. 1: Geographical location of the Chichaoua watershed.

be used to extract information on the regional behavior of droughts. The annual time scale seems more appropriate for monitoring the effects of a drought in situations related to agriculture, water supply, and groundwater withdrawals (Ramesh et al. 2003).

A time series of drought indices provides a framework for assessing the drought parameters of interest. Several indices have been developed to quantify a drought, each with its strengths and weaknesses. However, in our study, the selection of indices will focus on the following criteria:

- Data availability;
- Their simplicity of calculation;
- Their ability to represent specific rainfall conditions in the study area;
- Their ability to differentiate, to a reasonable degree, between the different intensity levels of different types of drought.

The following section will discuss the index we will use in our study and Fig. 2 shows the summary of the methodology used.

Normalized Difference Vegetation Index (NDVI)

The Normalized Difference Vegetation Index (NDVI), first proposed by Rouse et al. in 1973, is one of the well-known and widely used vegetation indices.

Like other vegetation indices, NDVI is sensitive to the presence of green vegetation. It is an effective tool for crop monitoring (Vogt 1995) and monitoring rainfall and drought (Kogan 1990, Unganai & Kogan 1998, Viau 2000, McVicar & Bierwirth 2001, Boyd et al. 2002).

$$NDVI = \frac{PIR - Rouge}{PIR + Rouge}$$

Where:
- PIR: Reflectance of the near-infrared spectral region.
- Red: Reflectance of the red spectral region.

As this index is normalized, the effects of the illumination and viewing angles are reduced. Normalization also reduces the effect of sensor calibration degradation and minimizes the effect of topography. The NDVI calculated from Landsat satellite image data depends on the satellite's characteristics.

This index remains sensitive to the viewing and illumination geometry, especially in areas with low vegetation density and soil presence.

NDVI also suffers from rapid saturation in dense vegetation, and the contribution of soil in areas of low vegetation density makes its interpretation questionable. Its interpretation may, therefore, be biased in arid or drought-prone areas (Vogt 1992).

Nevertheless, NDVI remains an effective index for identifying areas of water stress, especially in homogeneous environments such as agriculture. Its interpretation becomes more difficult in heterogeneous regions where resources vary greatly over short distances (Kogan 1990).

The Vegetation Condition Index (VCI)

The Vegetation Condition Index (VCI) is another index that measures the degree of green vegetation. Using the minimum, maximum, and current NDVI values from several years as inputs, the VCI transforms the NDVI.

$$VCI(i) = \frac{NDVI(i) - NDVImin}{NDVI\,max - NDVI\,min} \times 100$$

Where:
- NDVI: NDVI of the period studied
- NDVImin: NDVI minimum of the period studied
- NDVImax: Maximum NDVI of the period studied

The VCI attempts to separate the short-term climate signal from the long-term ecological signal (Kogan & Sullivan 1993). It, therefore, reflects the climatic distribution and not the differences in vegetation due to different ecosystems. In this sense, it is a better indicator of rainfall distribution than NDVI (Kogan 1990). It also allows a comparison of the effect of climate on different study areas.

The VCI thus improves the analysis of vegetation conditions for non-homogeneous areas (Kogan 1990). Initially created to monitor drought conditions, the VCI has been used on several continents to detect large-scale drought situations but also excessive moisture conditions (Kogan 1997, Singh et al. 2003, Kogan et al. 2003).

For example, several teams have used the VCI to monitor drought conditions in South Africa and India (Singh et al. 2003). The VCI, like other satellite vegetation indices, has the same limitations associated with the data acquisition method. Moreover, the application of the VCI is strongly linked to the number of images available and the quality of these images. Since this indicator uses composite images, it is important to consider the days of acquisition associated with each pixel since the viewing angle and illumination angle can vary greatly from one pixel to another. In addition, the VCI assumes that the difference between the maximum NDVI and minimum NDVI represents the maximum possible variation for a given period of time and that all NDVI values within this difference have the same frequency.

Temperature Condition Index (TCI) (Kogan & Sullivan 1993)

This indicator is based on the brightness temperature. This indicator is calculated from NOAA AVHRR sensor images based on surface temperature. As with the vegetation indices, it is applicable on a regional or continental scale, instantaneously or for periods ranging from one day to one year.

It is applicable on a regional or continental scale, instantaneously, or for up to one year. The TCI also provides useful information on vegetation stress due to soil water saturation (Kogan 1997, Kogan et al. 2004).

The formula given by Kogan is:

$$TCI = \frac{100(\text{Tmax} - \text{T})}{(\text{Tmax} - \text{Tmin})} \times 100$$

- Tmax is the maximum temperature
- Tmin at a minimum temperature
- T at the temperature of the period under study

Vegetation Health System: Background and Explanation

The Global Satellite System is designed to monitor, diagnose and predict long and short-term terrestrial environmental conditions and climate-dependent socio-economic activities. The system is based on satellite observations of the Earth, the biophysical theory of vegetation response to the environment, and a set of algorithms for satellite data processing, interpretation, product development, validation, calibration, and applications.

Satellite observations are mainly represented by the Advanced Very High-Resolution Radiometer (AVHRR) operated by NOAA polar-orbiting satellites. The data are global, with a resolution of 4 km and a 7-day composite. The system contains vegetation health indices and Drought products.

Satellite Data Processing

Our methodology is based on the joint use of remote sensing and geographic information system to measure drought intensity. For this purpose, we used the VCI and the TCI obtained from satellite images.

Processed on the Arc GIS ESRI platform, it was possible to map them to follow the dynamics and the state of vegetation during the agricultural season in the face of
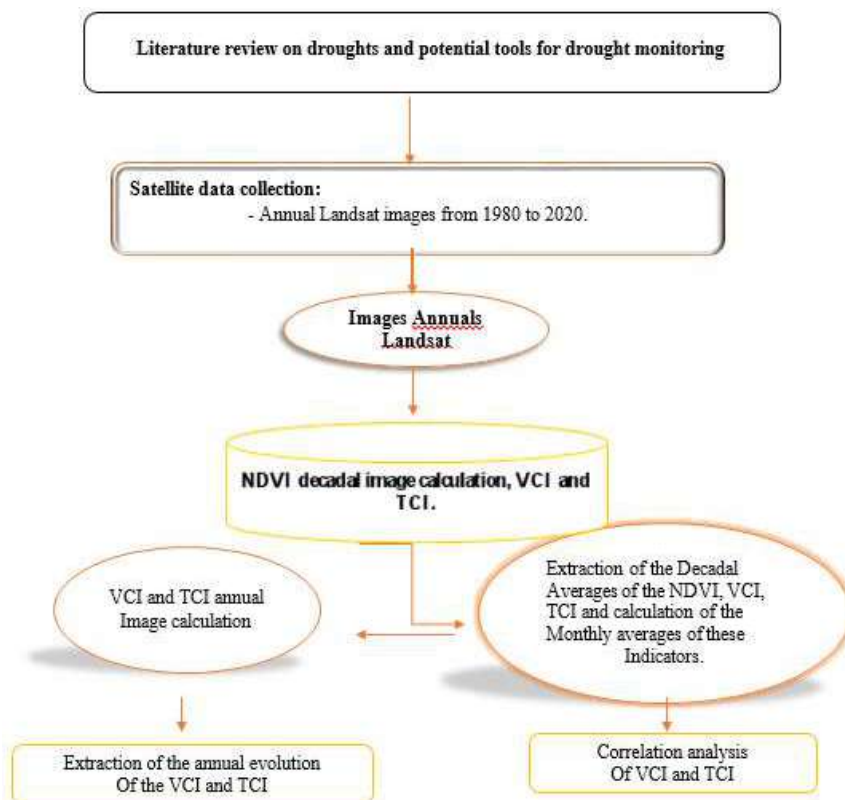

Fig. 2: Summary of the methodology used.

drought. In the Chichaoua watershed, the agricultural season extends from March (budburst) to April-May (entry into the senescence phase). Therefore, satellite images covering this period were selected and downloaded from the VOAA-AVHRR website.

Thus, we imported these data in TIFF (GEOTIFF) format using ARCGIS software. The images were projected in the standard UTM projection using the 29N zone. They were then classified on the ARCGIS-ESRI platform into five VCI and TCI classes ranging from 0 to 100 (Kogan 1997, Kogan 1995). Drought conditions are met when the indices are below 40. To perform this VCI and TCI classification and calculate the average drought-damaged area, we followed the following steps in GIS:

The "Split Layer Feature" is particularly useful for creating a new feature class, also called a study area or area of interest, containing a geographic subset. The "Mask extraction" is used to visualize only the area concerned by our study. Indeed, this treatment allows the extraction of the cells of a raster which correspond to the areas defined by a mask. The "Raster Calculator" tool allows to create and execute a spatial algebra expression that generates a raster output. In our case, it allowed us to select areas according to the range of drought intensity according to the Kogan classification. Each feature represents a VCI and TCI value in pixels, allowing us to estimate the drought intensity. This allowed us to calculate the average drought. Several factors can influence and limit the scope of the results. Indeed, the TCI and VCI index depends largely on the values of other
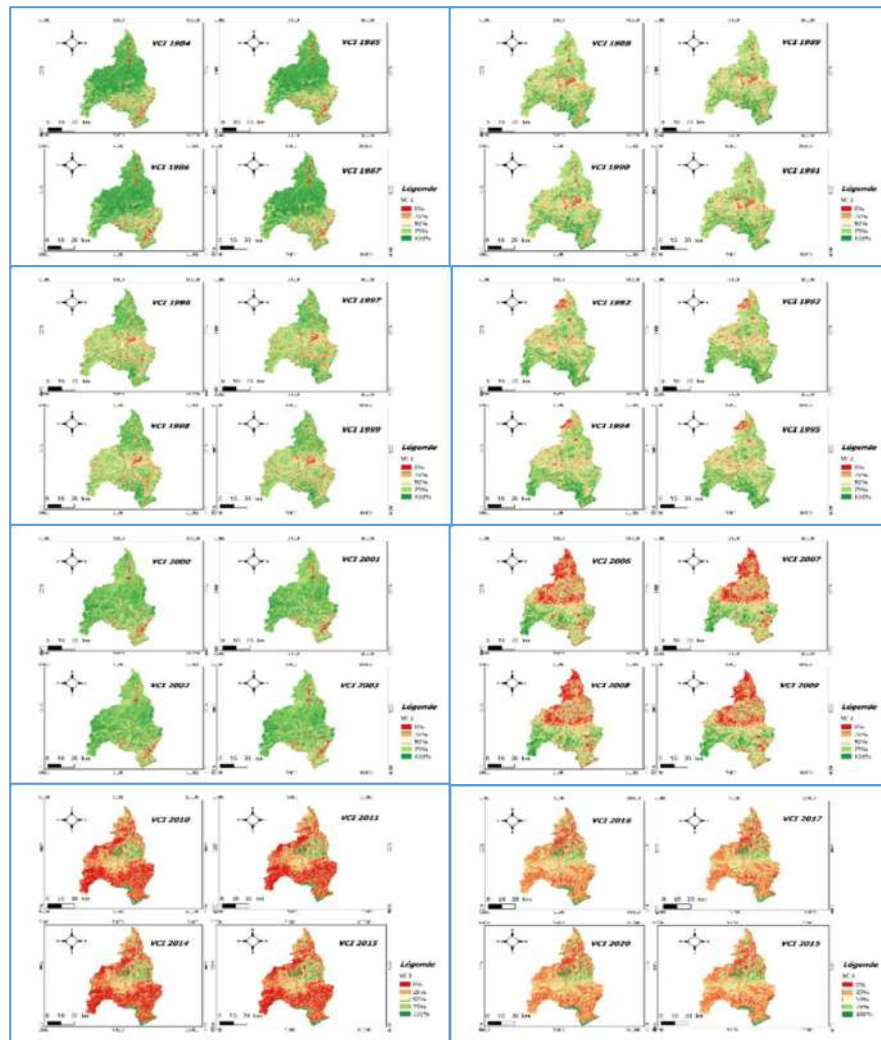

Fig. 3: Distribution of drought intensity estimated by the VCI in the Chichaoua watershed for the agricultural period 1982-2021.

indices, such as temperatures. However, we processed all the raster images obtained by the NOAA-AVHRR remote sensing center. Thus, the possible problem of value, in absolute terms, does not call into question the significance of the results since it is a question of examining the relative variations from one year to another.

RESULTS AND DISCUSSION

Evolution of the VCI and the TCI from 1982 to 2021:

To carry out this work, the study area used in our region was delimited and selected on the ARCGIS software platform using the Chichaoua watershed polygon.

Fig. 3 and Fig. 4 show the spatial distribution of the change in the VCI and TCI from 1982-2021. It shows significant variability in drought intensity in an area characterized by little change in vegetation during the study period between 1982-2021. The color gradient of each pixel represents the drought level. Green corresponds to the lowest value, and red to the most intense.

Table 1 shows the average value of the VCI and the TCI for each year from 1982-2021. The lower the value, the more the vegetation cover condition deteriorated, which could mean a higher drought intensity. The average of 28 reflects almost permanent drought conditions between 2001 and 2015. The VCI and TCI varied between 10 (2008) and 70 from 2001 to 2015, with a maximum of 80 in 1994. Drought impacted Some years more than others, such as 2001, 2008, 2010, and 2015.

From these results, we sought to assess the spatial distribution of different drought levels relative to the mean.
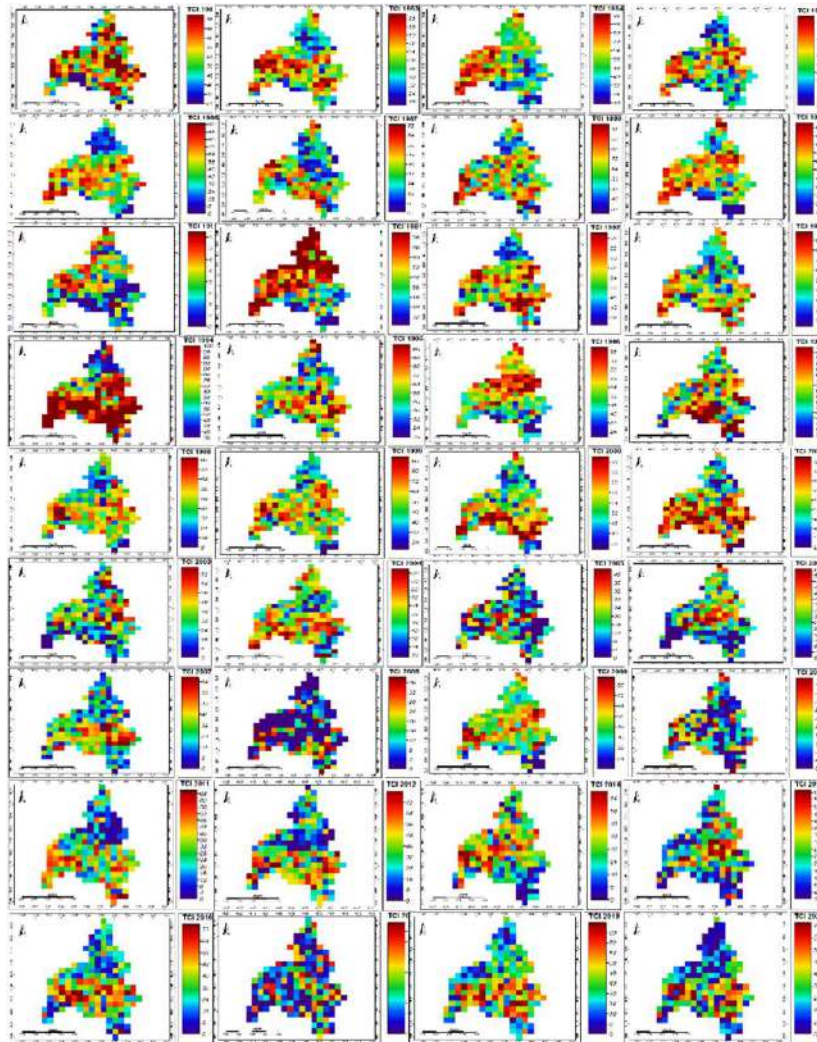

Fig. 4: Distribution of drought intensity estimated by the TCI in the Chichaoua watershed for the agricultural period 1982-2021.

Table 1: Average TCI and VCI value during the period 1982-2021:

Year	Average TCI	Average VCI
1982	70,32	19,59
1983	58,31	16,8
1984	55,86	26,97
1985	40,26	4,5
1986	48,34	27,77
1987	32,96	29,5
1988	64,72	42,36
1989	59,09	49,53
1990	28,52	37,3
1991	75,03	23,12
1992	66,34	43,42
1993	56,42	24,19
1994	80,92	49,12
1995	58,46	68,12
1996	62,55	51,26
1997	71,89	60,02
1998	44,72	8,57
1999	54,81	11,28
2000	66,66	35,54
2002	70,15	43,45
2003	31,99	35,5
2004	59,26	33,98
2005	15,81	51,25
2006	23,84	52,16
2007	30,25	53,71
2008	10,69	42,5
2009	50,92	14,76
2010	15,28	24,49
2011	28,84	15,81
2012	34,03	16,06
2014	31,3	19,44
2015	24,14	13,43
2016	33,54	19,59
2017	14,07	16,8
2018	58,24	26,97
2019	39,97	4,5
2020	26,65	27,77

To better interpret the 1982-2021 TCI results, we clustered TCI intervals to quantify the degree of drought. It allows us to distinguish three types: areas affected by high-intensity drought (TCI< 20), areas affected by low-intensity drought (between 20 and 40), and areas not affected by drought (TCI > 40).

71% to 90.5% of the study area is pretentious by low-intensity drought (Fig. 5). High-intensity drought does not exceed 30% of the vegetation, with the exception of 2008, when there was a significant peak of 10%. This drought could be problematic for agricultural activity, where most crops are irrigated, as farmers' practices are not adapted.

Fig. 5, which shows the spatial distribution of the average VCI and TCI for the period 1982-2021, shows that the mountainous part of the region is the most affected. It is characterized by a higher topography than the rest of the region and a predominance of crops.

87.4 percent of the vegetation cover is affected by drought, of which 51 percent is of the moderate type. On the other hand, the high-intensity drought affected 7.9% of the vegetation. It is noted that the extreme type of drought represents only 10% of the region's total area (Table 1).

The relationship between temperature, vegetation, and climate is essential for studying drought in a vegetative context. Drought, as a climatic hazard, can become a risk by disrupting the balance between the needs of society and the potential resources provided by a given environment (Charre 1977). Drought is a physical phenomenon determined by a rainfall deficit, temperature increase, and a water deficit in the soil. Thus, economic damage to crops can be expected after three successive months of rainfall deficit below 50% of the average (NDMC 2006).

The calculation of the VCI and the TCI made it possible to monitor the water stress of vegetation in the Chichaoua watershed, reflected in the increase in temperature that could affect the plant. The analysis and monitoring of this index thus allow us to identify the vegetation's temperature dynamics and estimate the impacts on the crops in place. There is a risk of a more intense drought during the agricultural season.

Our results for the period studied show that the vegetation of our basin was affected by a weak to moderate drought. We can relate these results to the study of Charre (1977). He distinguished two types of drought: the usual drought and the occasional drought. The usual drought is considered "normal" or "not dangerous" in traditionally dry regions, such as the Chichaoua watershed because the agricultural practices in place are adapted to cope with this type of drought.

We can draw several elements of reflection from this study. From a geographical point of view, we note that our area, located in the High Atlas Mountains, with an arid and semi-arid climate, is more affected than others. Indeed, in the plain, the water tables, the main source of irrigated ion water, are fed mainly by winter rainfall. A succession of
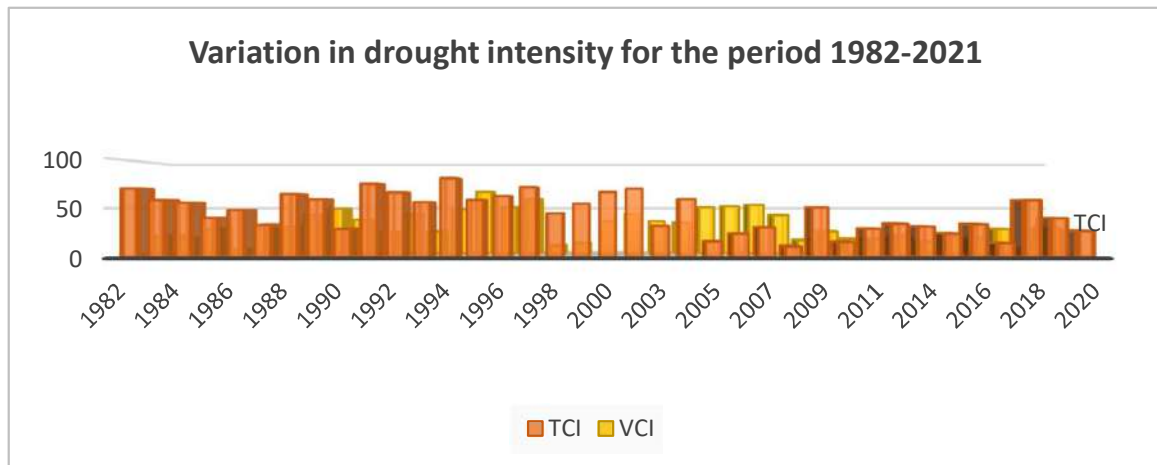
Fig. 5: Variation in drought intensity for the period 1982-2021.

months with insufficient rainfall can have a negative impact on the level of the groundwater and cause a groundwater drought. The consequences will quickly be felt: loss of yield in field crops. Other factors, such as a succession of periods of low rainfall, can influence the state of the vegetation. Strong periods of sunshine or wind influence the surface temperatures that constitute the TCI (Viau & Paquette 1997).

However, there are limitations to our study that must be taken into account when interpreting the results. Using satellite images over a longer time series (36 years) would be more appropriate for calculating the average TCI. Finally, drought is a complex phenomenon that combines climatic and human factors. Nevertheless, the TCI remains an indirect indicator of this major problem for vegetation.

CONCLUSION

The Chichaoua catchment area has experienced a permanent low to moderate-intensity drought over the last 36 years, with a peak of high-intensity drought considered "dangerous. "

Possible climate changes in the coming years predict an intensification of dry episodes, such as those observed in 2008. Climate change, combined with an increase in the number of refugees, is putting increased pressure on environmental resources, particularly water resources, which are becoming increasingly vulnerable. Today, drought monitoring has become a necessity in view of its consequences on the socio-economic activities of the territory. Despite the limits of the proposed indicators, they can constitute a relative and operational monitoring means.

However, in light of the results obtained, it appears that the climatic hazard is aggravated by anthropic pressure.

This drought index has been used in various applications since the advent of remote sensing from space. Its use for quantitative estimates raises several issues that can seriously limit its usefulness if improperly interpreted. They depend on many parameters (solar illumination, viewing angles, etc.) and are affected by several factors (sensitivity to atmospheric effects, soil types, and moisture content).

ACKNOWLEDGEMENT

Data and Codes Availability Statement

The data and codes that support the findings of this study are available on request from https://earthexplorer.usgs.gov/ site and graphs from the NOAA AVHRR site https://www.star.nesdis.noaa.gov/star/index.php and processed exclusively, with Saga Gis and ArcGis. The data are not publicly available because they contain information that could compromise the privacy of research participants.

REFERENCES

Augier, P. and Blanc, P. 2009. Fourth Inter-Lebanese Forum on «Agriculture» CIHEAM, Rue Newton, Paris.

Boken, V.K., Cracknell, A.P. and Heathcote R.L. 2005. Monitoring and Predicting Agricultural Drought. Oxford University Press, Oxford.

Boyd, D.S., Phipps, P.C., Foody, G.M. and Walsh R.P.D. 2002. Exploring the utility of NOAA AVHRR middle infrared reflectance to monitor the impacts of ENSO-induced drought stress on the Sabah rainforest. Int. J. Remote Sens., 23: 5141-5147.

Charre, J. 1977. About drought. Lyon Geogr. Rev., 52(2): 215-226.

Hayes, S. Strosahl. K. and Wilson, K. 1999. Acceptance and Commitment Therapy: An experiential approach to behavior change. Guilford Press, New York.

Heim, R.R. 2002. A review of twentieth-century drought indices used in the United States. Bull. Am. Meteorol. Soc., 83: 1149-1166.

Keyantash, J. and Dracup, J.A. 2002. The quantification of drought: An evaluation of drought indices. Bull. Am. Meteorol. Soc., 83(8): 1167-1175.

Kogan F.N. 1995. Droughts of the late 1980s in the United States as derived from NOAA polar-orbiting satellite data. Bull. Am. Meteorol. Soc., 712: 655-668.

Kogan, F. and Sullivan, J. 1993. Development of a global drought-watch system using NOAA/AVHRR data. Adv. Space Res., 13-5: 219-222.

Kogan, F., Gitelson, A., Zakarin, E., Spivak, L. and Lebed, L. 2003. AVHRR-based spectral vegetation index for quantitative assessment of vegetation state and productivity: Calibr. Valid. Photogramm. Eng. Remote Sens., 69(8): 899-906.

Kogan, F., Stark, R., Gitelson, A., Jargalsaikhan, L., Dugrajav, C. and Tsooj, S. 2004. Derivation of pasture biomass in Mongolia from AVHRR-based vegetation health indices. Int. J. Remote Sens., 25(14): 2889-2896.

Kogan, F.N. 1990. Remote sensing of weather impacts on vegetation in non-homogenous areas. Int. J. Remote Sens., 11(8): 1405-1419.

Kogan, F.N. 1997. Global drought watch from space. Bull. Am. Meteorol. Soc., 78(4): 621-636.

McVicar, T.R. and Bierwirth, P.N. 2001. Rapidly assessing the 1997 drought in Papua New Guinea using composite AVHRR imagery. Int. J. Remote Sens., 22(11): 2109-2128.

National Drought Mitigation Center (NDMC). 2006. Farmers' perception and knowledge on climate change and their coping strategies to the related hazards: A case study from Adiha, Central Tigray, Ethiopia. Agric. Sci., 2: 138-145.

Shaban, M. and Houhou, L. 2015. Drought or humidity oscillations? The case of the coastal zone of Lebanon. J. Hydrol., 529: 1768-1775.

Singh, R., Sudipa, R. and Kogan, F. 2003. Vegetation and temperature condition indices from NOAA AVHRR data for drought monitoring over India. Int. J. Remote Sens., 24(22): 4393-4402

Unganai, L.S. and Kogan, F.N. 1998. Southern Africa's recent drought from space. Adv. Space Res., 21: 507-511.

Viau, A. 2000. Drought monitoring from space. Adv. Natural Technol. Hazards Res., 11: 167-183.

Viau, A. and Paquette, M. 1997. Affective, behavioral and cognitive engagement of primary school students in a pedagogical context of ICT integration: A multi-case study in disadvantaged areas, digital learning research. Int. J. Remote Sens., 16: 564-578.

Vogt, J.V. 1992. Characterizing the Spatio-temporal Variability of Surface Parameters from NOAA AVHRR Data: A Case Study for Southern Mali. Commission of the European Communities. Joint Research Centre, EUR Publication no. 14637 EN, Brussels/Luxembourg, p. 263.

Vogt, J.V. 1995. The Use of Low-Resolution Satellite Data for Crop State Monitoring: Possibilities and Limitations. In Dallemand, J.F. and Vossen, P. (eds.), Agrometeorological Models: Theory and Applications in the MARS Project, (EUR 16008 EN) Luxembourg, pp. 223-240.

Wilhite, A. 2007 Understanding the complex impacts of drought: A key to enhancing drought mitigation and preparedness. Water Resour. Manag., 21: 763-774.

Systemic Economic Viability of Informal Sectors: E-Waste Management

Dharna Tiwari*†, Gautam Mehra** and Nidhi Gauba Dhawan***

*Amaltas Enviro Industrial Consultant LLP, Gurugram, Haryana, India
**Director of Strategos Advisory, Delhi, India
***Modern Delhi Public School, Sector 88, Faridabad 121002, Haryana, India
†Corresponding author: Dharna Tiwari; dharnatiwari@gmail.com

ABSTRACT

The informal sector has been at India's core of recycling WEEE for the last few decades. They do not have the scientific knowledge of processing e-waste and use acid baths and heat treatment to extract precious metals. The existing processes used by informal actors lead to a serious impact on their health as well as the environment. The introduction of advanced recycling technology for mitigating the hazardous effects on the environment and human health is as important as the development of technology for new-age electronic products. The social, economic, and environmental benefits to the informal sector can ensure formalized livelihoods in e-waste recycling by ensuring access to technology. The paper highlights how setting up a recycling facility and capacity building of the informal sector solves the problem of informality and its associated social, economic, and environmental evils, which will benefit the sector as a whole.

INTRODUCTION

E-Waste Management

The e-waste management structure worldwide is a complex system with different stakeholders. However, even in the most advanced countries, there are leakages into the informal sector. Laws in most countries now make it mandatory for producers to manage e-waste environmentally soundly under Extended Producers Responsibility (EPR) (Baldé et al. 2015).

The United Nations (UN), in the World Economic Forum on January 24, 2019, stated that in India, approximately 95 percent of e-waste is handled by the informal sector. The UN also mentioned that e-waste generated was 48.5 MT in 2018 and is likely to increase at 30 percent CAGR annually. The UN report specifies that only 20 percent of global e-waste is recycled. The report indicates that due to poor extraction techniques, the recovery rate of cobalt is just 30% (Lahiry 2019).

E-waste is hazardous; it requires proper segregation, collection, transportation and handling, treatment and recovery, and final disposal. The entire electronics cycle, from manufacturing to final disposal, requires the management of e-waste (UNEP 2007).

Recent data from 2017 states that national e-waste management laws cover 66% of the world's population; it's a rise from 44% that had framed a law in 2014. The large increase was mainly credited to India, where the legislation was revised in 2016. In Asia, most countries have e-waste rules, although, in Africa, very few have legislated e-waste-specific policies and regulations. Though, it is also noticed that even after national e-waste management laws, not all countries have been able to enforce the same. Many countries do not follow the collection and recycling mechanisms mentioned in their policies (Baldé et al. 2017).

Across the world, e-waste is mostly managed by the informal sector. The work of the informal sector is particularly hazardous for women and children as dioxins and furans are emitted on the burning of some components of e-waste. Formalizing the informal sector is the need of the hour, and systemic changes need to be brought in to ensure their integration. The formalization will have a positive impact on their health. It'll also ensure that they have sustainable livelihoods as the e-waste regulation becomes stringent through implementation over a period of time. (Chaturvedi et al. 2010).

Current Scenarios of E-Waste Management in India

- Extended Producer Responsibility (EPR) prolongs the duty of producers across the life cycle of their products, especially during the post-consumer period when products reach the end of life and are ready to be

disposed of, thereby categorizing them as e-waste. EPR is presumed to enhance waste collection, recycling, and treatment. The most important part of EPR is developing a closed loop of responsibility which comprises the product's entire life cycle, enabling waste materials to be used as raw materials in producing new products. By extending producer responsibility to the post-consumer stage, EPR creates a link between the end-of-life of products and product design, considering the Restriction of Hazardous Substances (RoHS) (Hemkhaus et al. 2018).

- EPR, introduced in the e-waste management and handling rules in 2012, proposed that it would be the producers' responsibility to complete the life cycle of an electronic product in an environmentally sound manner. Though stakeholders made no significant achievements regarding the collection of e-waste via EPR, some companies tried to set up collection mechanisms in the Indian context. In 2016 the revised e-waste management rules introduced target-based extended producers' responsibility (EPR) which keeps increasing over a period of time to close the loop. Rules also suggested financial mechanisms, including Deposit Refund Scheme, Advance recycling fee, etc., to implement EPR (MoEF & CC 2016).

- If producers have to meet their EPR targets, they must collect e-waste. The producers are completing their targets by getting associated with not one but multiple PROs. The PROs are very well aware that e-waste is mainly accessible from the informal sector. Hence, the PROs try to collect e-waste from the informal sector by working directly with different collectives of waste pickers or indirectly via collection agencies, aggregators, and recyclers. PROs can motivate or support the informal sector to increase its capacities through formalization. PROs can provide incentives like identity cards, social benefits, educational services, advocacy of workers' rights, etc. PROs can provide awareness-raising activities focusing on sound collection practices, inventorisation, following health and environmental practices, and dismantling and recycling e-waste using scientific means and technologies. Through proper implementation of EPR, recyclers can now access higher amounts of e-waste as producers focus on completing their EPR targets. The availability of more materials will motivate recyclers to adopt advanced technologies to recycle all materials of e-waste within the country, which will lead to social, economic, and environmental benefits. Research work has been done, and information was collected from the

producers. A crosstab analysis has been done to find the connection between at least two variables which is given below in the observation.

- The new rules of e-waste 2016 have now provided guidelines on implementing EPR for producers. This has been linked to a certain set of targets that need to be fulfilled by producers, which would help them meet their EPR compliance within the ambit of the rules. Furthermore, these targets are mandatory and linked to producers' business goals.

Context of the Research Paper

India has a severe waste crisis on hand which is impacted further because of the lack of capacities of stakeholders. The huge population of the country and the rural-urban divide present waste management as the ideal livelihood opportunity with no investments and a sustainable income. This makes the informal sector a key player in waste, as the informal sector is where unregistered businesses work, avoiding paying taxes. Different material wastes create different flows and value chains, creating a multitude of stakeholders in the informal sector. Informal actors accumulate aggregate, dismantle and recycle e-waste. Few of the activities involved in dismantling present little or no hazards to human health and the environment. Though informal sector recycling practice is dangerous due to the material composition of e-waste, which has lead, chromium, cadmium, and mercury, the utilization of which is presently covered under RoHS guidelines of the e-waste management rules, 2016. Informal actors recycle e-waste either at home or in open spaces without using appropriate recycling technology, leading to pollution of the environment around them.

In India, the informal sector has a widespread network, making accessing materials easier. The material collection takes place through door-to-door collection, auctions, etc. Moreover, the low cost of the collection increases the value of waste, which is a deterrent for waste flow in the formal sector (Henzler et al. 2018). This paper is in the background of the resistance to formalization, as the informal sector operates on huge profits compared to the formal recyclers, as associated operational costs are minimal. Furthermore, no technology investments reduce capital costs, making them competitive in the face of expensive recycling technologies that formal players put up. Key steps which can lead to the formalization of the informal sector are the provision of advanced technology, Capacity building, and access to finance, which will lead to safe e-waste disposal. These steps will reduce system failures in this sector and allow different stakeholders to co-exist, ensure sustainability, and enhance resource efficiency, leading to a circular economy.

MATERIALS AND METHODS

In India, approximately 95% of total e-waste management is handled by informal/ unorganized sector. Different methods were used to collect primary and secondary information, including key informant interviews, questionnaires, e-mail communication, direct observation, and a site visit to collection centers, recycling plants, and Informal sectors.

Information was collected from 21 informal sector e-waste recyclers in Shastri Park, Mustafabad, Mandoli, Old Seelampur, Jamalu Ka Bag, Mayapuri Industrial Area, and Seelampur. This study has been carried out to assess the e-waste generated and the quantity handled in the informal sector.

20 producers were also questioned about all the necessary rules & regulations mentioned in the 2016 Notification. The interviews were held using a questionnaire prepared for Producers. A thorough discussion of the manufacturing and e-waste rules was done to understand the perception of producers regarding e-waste. Documentary proofs were also collected during the meetings. They were examined regarding the way of the take-back system, RoHS Certificate, collection of e-waste, Awareness program, information to customers regarding hazardous constituents, Recycling facility, Green Products, etc. Data was gathered from questionnaires, site visits, and interactions with people channeling e-waste.

OBSERVATIONS

Producers are institutions selling electrical and electronic equipment, their components or consumables, or parts or spares under their own brand. The regulatory framework is based on Extended Producer Responsibility (EPR), where the producer or manufacturer manages the products' end-of-life. The information was sought from 20 producers, which are private enterprises located in different states which cover the length and breadth of India. The cross tab was carried out for analysis along with the relevant questions mentioned in the questionnaires prepared for stakeholders, which are given below.

Crosstab of Internal E-waste Disposal Versus EPR

1. Are you aware of the e-waste (Management & Handling) Rules, 2011? (e-waste rules)?

2. Do you have an internal e-waste disposal/management policy for the organization?
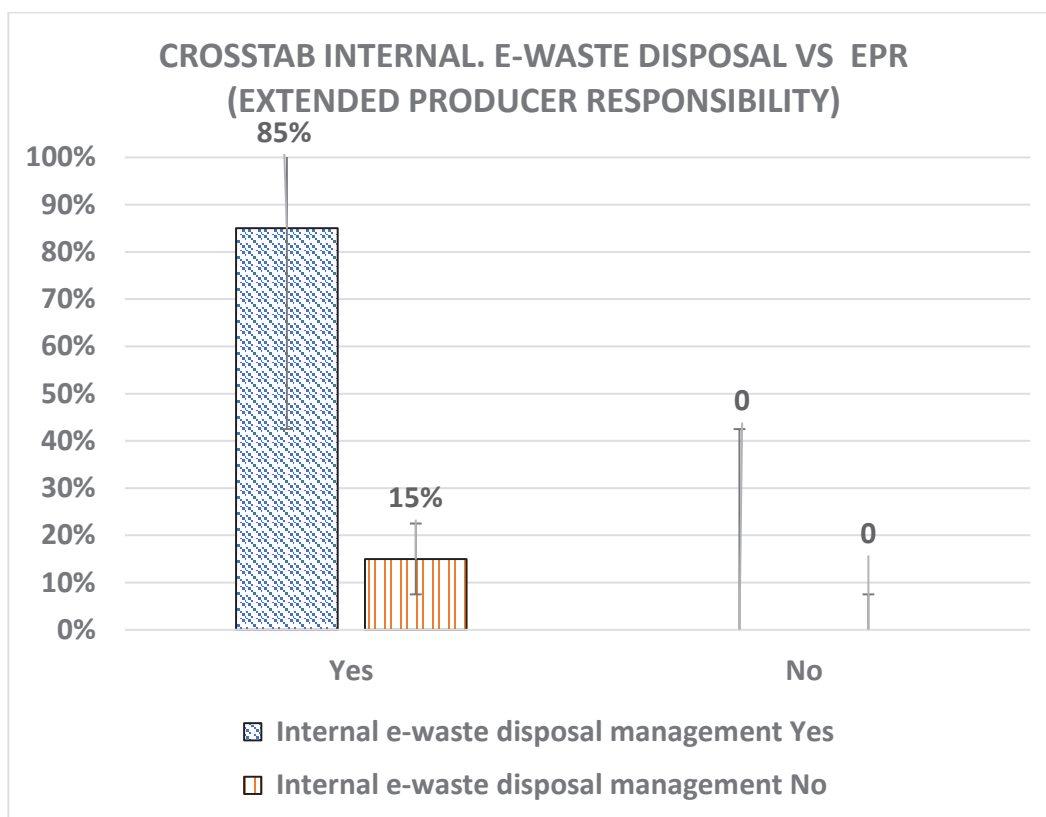

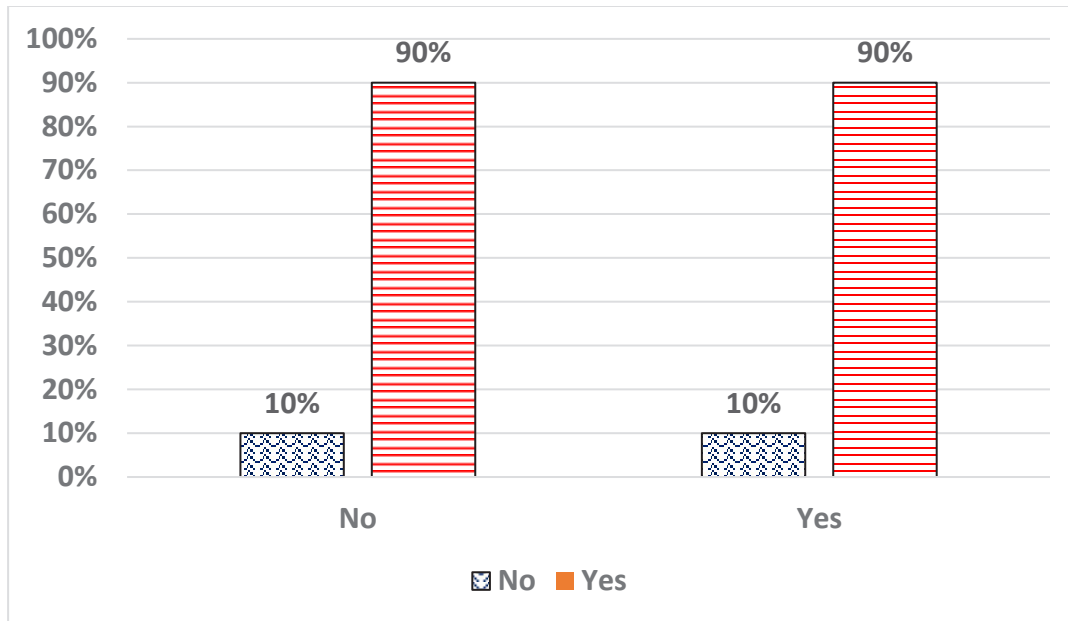Fig. 1: Internal E-waste disposal versus EPR (Extended Producer Responsibility).

Fig. 2: Authorized Collection Centre versus EPR.

Producers mandated to seek authorization under EPR were asked if they also have an internal policy on e-waste. Fig. 1 shows 85 percent stated that they had an internal policy on e-waste, while the remaining 15 percent did not.

The Crosstab of Authorized Collection Centre Versus EPR

1. Are you in compliance with 'Extended Producer Responsibility (EPR) of electrical or electronic equipment to ensure that such e-waste is channelized to a registered dismantler or recycler?

2. Do you have an authorized collection center?

Producers were asked if they had fulfilled the EPR obligations and established collection centers. Fig. 2 shows 90 percent of the producers who have fulfilled the EPR authorization have chosen the PRO model to establish collection centers. There is a significant push towards collective producers' responsibility rather than individual producers' responsibility.

A Crosstab of the Service Center To Refurbish Products Versus EPR

1. Are you complying with the 'Extended Producer Responsibility (EPR) of electrical or electronic equipment to ensure that such e-waste is channeled to a registered dismantler or recycler?

2. Is your service center facilitating the refurbishment of the used product?

Fig. 3 shows only 10 percent of the producers who have EPR (Extended Producer Responsibility) authorization have asked for permission to develop refurbishment facilities so that they can channel their products into the repair market, thereby enhancing the life of the product. Not only does this encourage resource efficiency, but it also allows for reduced e-waste generation and is good for the environment.

The Crosstab of Information Regarding Hazards of Improper Handling, Accidental Breakage, Damage, or Improper Recycling of E-Waste Products Versus EPR

1. Are you complying with the 'Extended Producer Responsibility (EPR) of electrical or electronic equipment to ensure that such e-waste is channeled to a registered dismantler or recycler?

2. Are you informed of the hazards of improper handling, accidental breakage, Damage, or improper recycling of e-waste?

The new e-waste management rules, of 2016 have also helped to change the behavior of the producers in ensuring that proper precaution is taken while handling e-waste and transporting it across to registered recyclers and dismantlers. Fig. 4 shows 94 percent of producers now have the means to inform stakeholders on how to handle material that has hazardous content so that the same does not cause damage to human health or the environment.

The Crosstab of Enlisting the Hazardous Constituents Present in the Equipment Versus EPR
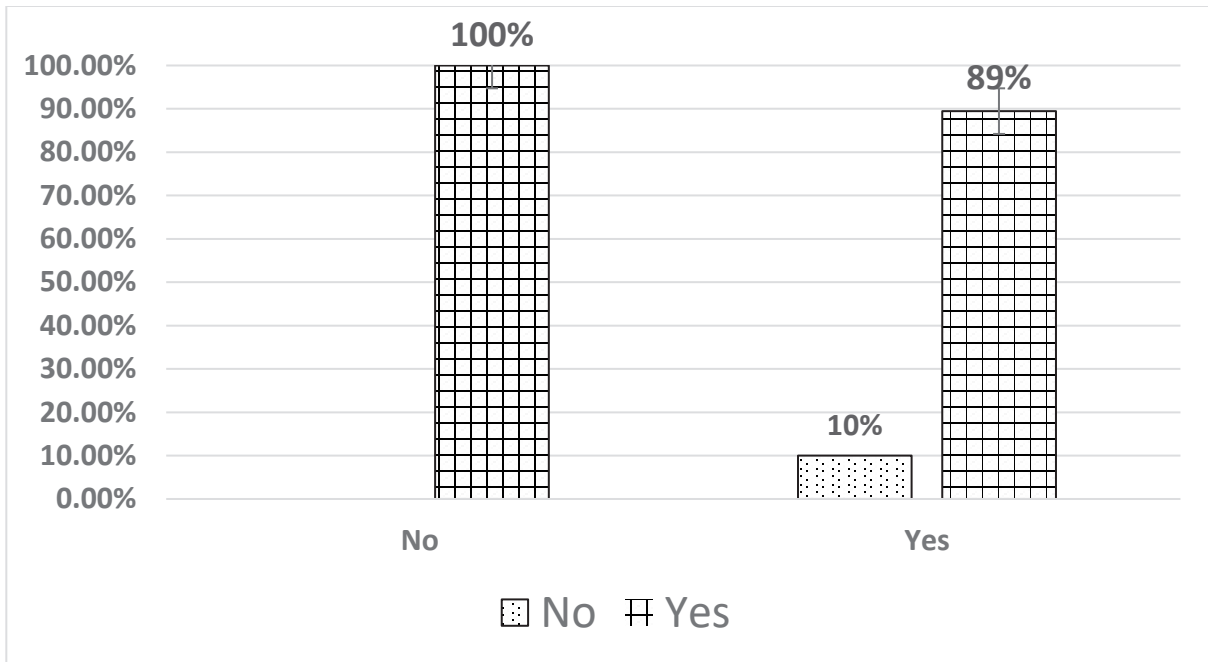
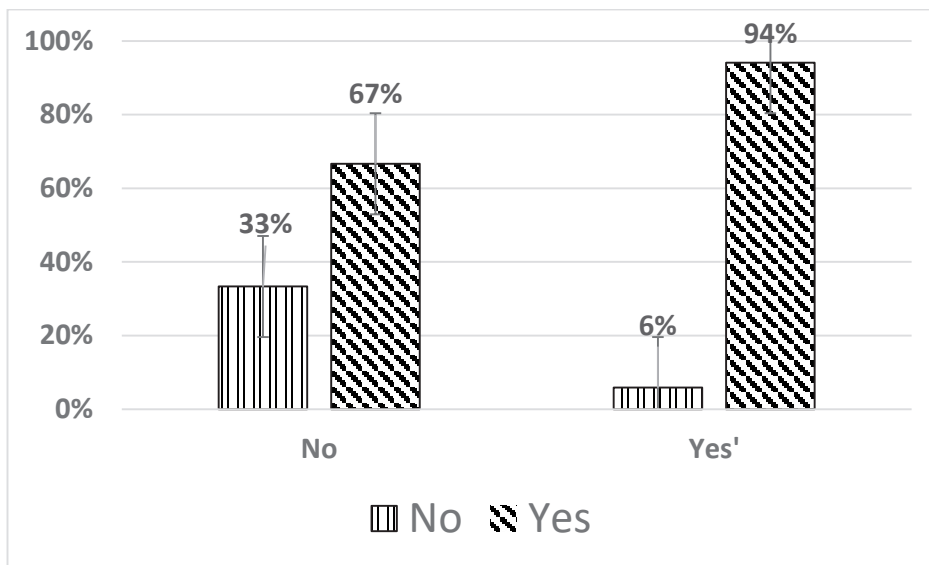Fig. 3: Service center to refurbish products versus EPR.

Fig. 4: Improper handling of e-waste products versus EPR.

1. Do you comply with 'Extended Producer Responsibility (EPR) of electrical or electronic equipment to ensure that such e-waste is channelized to a registered dismantler or recycler?

2. Are you enlisting the hazardous constituents present in the equipment?

The RoHS guidelines have allowed producers to publish hazardous content in the equipment sold.

Fig. 5 shows 93 percent of the producers now publish such content on the packaging of their products sold, which complies with the e-waste management rules of 2016.

Key System Failures in Producers

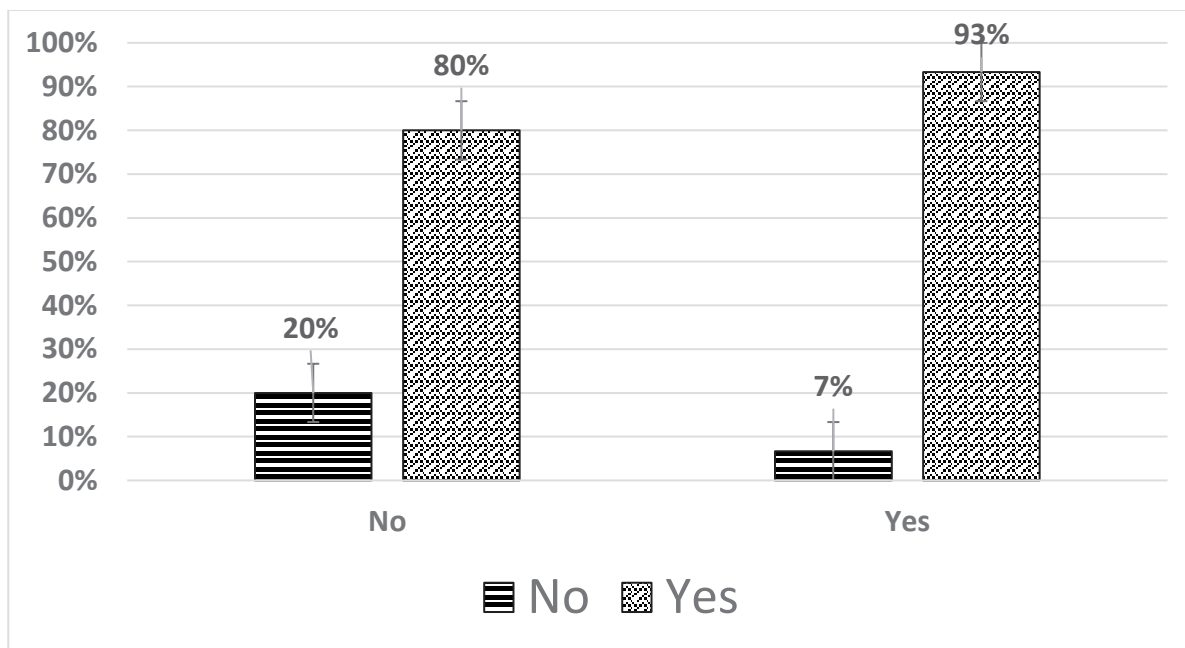- All producers need to be part of the EPR system by seeking authorization.

Fig. 5: Hazardous Constituents Present in the Equipment versus EPR.

- All producers need to set up collection systems and stop paper trading.
- All producers need to help channel materials to authorized recyclers and dismantlers.
- The law has helped to address a lot of concerns in the management of e-waste. However, compliance must be enhanced to ensure producers follow the law in its application and practice.

Informal Sector

In India, approximately 95% of total e-waste management is handled by informal/ unorganized sector. Information was collected from the informal e-waste recyclers in Shastri Park, Mustafabad, Mandoli, Old Seelampur, Jamalu Ka Bag, Mayapuri Industrial Area, and Seelampur. This study has been carried out to assess the e-waste generated and the quantity handled in the informal sector. The collected information for the same is given below.

The activity involves dismantling and recycling e-waste. The dismantled parts are recycled to obtain precious and other valuable metals. During dismantling, informal recyclers are exposed to acid fumes and chemical solvents as they do not use personal protection equipments. High and prolonged exposure to such chemicals/ pollutants emitted during e-waste recycling may lead to health consequences causing irreversible damage.

Dismantling Activities by the Informal Sector

All the steps are necessary for dismantling activities. We can extract valuable resources while dismantling electronic waste. We can properly segregate the parts by using hand tools to recycle devices. After segregation, we can properly treat the recovered parts for reuse and recycling. Data given in **Fig. 6** shows that 38% informal sector transfers electronic waste for further processing, and 19% dismantle their devices using hand tools to recycle devices or parts.

Ways of Recycling Operation by Informal Sector

The informal sector recycling involves a huge concern about human and environmental risks. It contributes to emissions of dioxins, heavy metals such as lead, cadmium, mercury, etc., in the environment, and the workers are exposed to these metals, potentially threatening human life. In addition, the laborers in the informal sector also face problems due to physical injuries, respiratory disorders, asthma, malnutrition, skin diseases, eye irritations, etc. Informal recyclers have expertise in extracting precious metals from PCB by an acid bath. The survey in Fig. 7 shows that 52% is operating manually, followed by 29% semi-manual.

Crosstab of Monthly Income Vs. Different Activities of the Informal Sector

- The income of the informal sector depends upon the kind of activity which it pursues.
- Dismantling and recycling in the informal sector require that a small infrastructure be set up so that they can
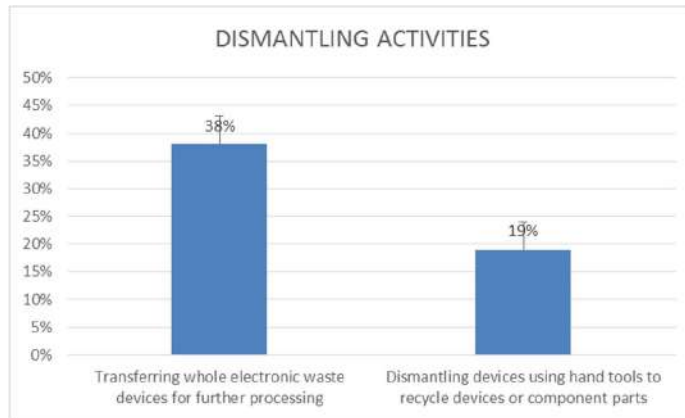
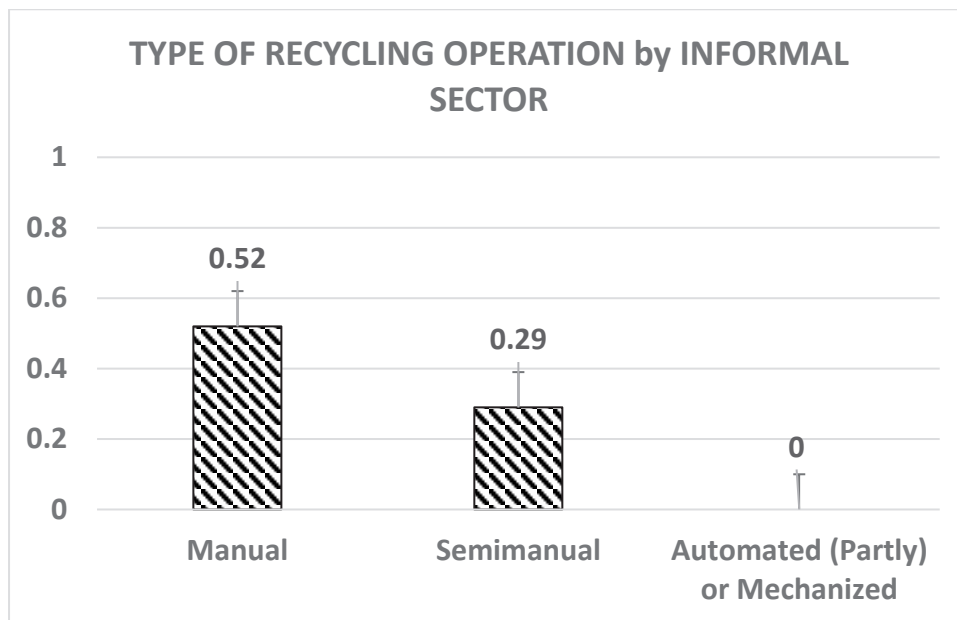Fig. 6: Dismantling activities by informal sector.

Fig. 7: Type of recycling operation.

handle a sufficient quantity of material to justify the input cost.

- Fig. 8 shows that overall, in Haryana, the income indicated is higher than the other areas because Gurgaon, Manesar, and other areas of Delhi NCR are one of the largest generators of e-waste in India and access to the same at a very low logistics cost leading to higher profits for them.

- Traders in the informal sector have a high monthly income compared to the costs they incur. Traders are not liable for expenses such as rent and legitimate wages; do not invest in modern technology; follow unscientific processes for recycling and extraction; and are not bound by any laws and regulations.

Available Space of Informal Sector Vs. Collected Waste

The collected data in Fig. 9 shows that all the traders have less space to be permitted to continue their operations.

Dismantling and Recycling Process by Informal Sector

The survey shows in Fig. 10 that 38% of the informal sector transfers electronic waste for further processing, and 19% dismantle their devices using hand tools to recycle devices or parts.

Survey shown in Fig. 11 shows that (52 %) is operating manually, followed by 29% semi-manual.
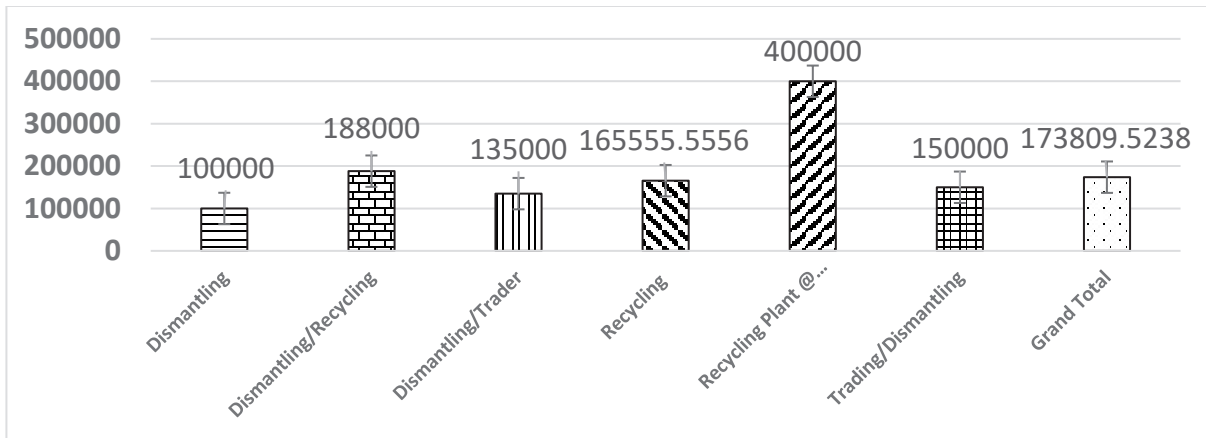
System Failure for Informal Sector
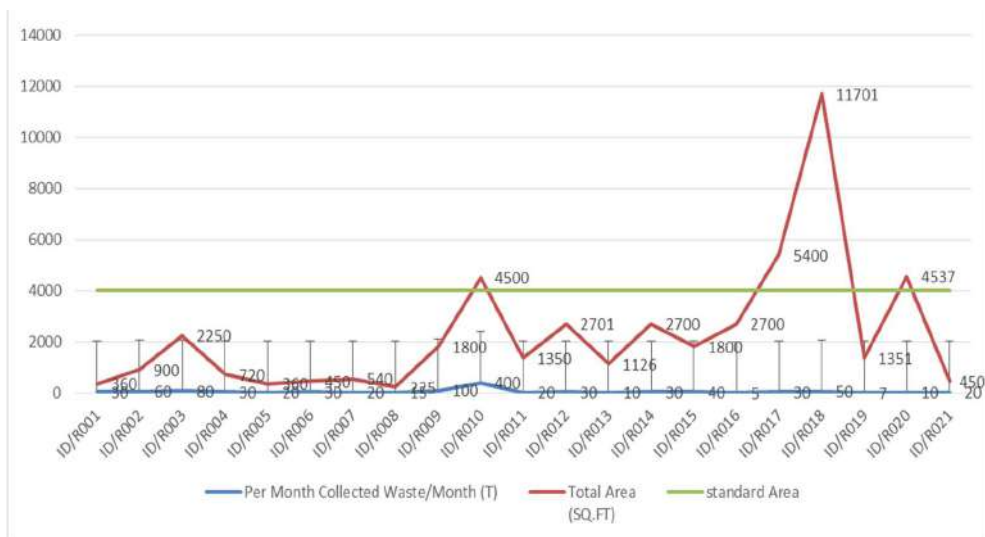
Fig. 8: Activities by informal sector.

Fig. 9: Available Space of Informal Sector.

- Access to material without any authority under the e-waste management rules, 2016.

- Dismantling and recycling without authorization.

- No capacity for understanding the environmental and health hazards of managing e-waste improperly.

- No access to technology and other resources despite having access to finance.

Valuable Materials in E-Waste

The electrical and electronic products which have reached their end of life are considered electronic waste or e-waste. According to the site survey and reports, e-waste contains more than 1000 substances categorized as "hazardous" and "non-hazardous." It comprises ferrous and non-ferrous metals, plastics, glass, wood and plywood, printed circuit boards, concrete, ceramics, rubber, and other items (Rajya Sabha Secretariat Research Unit 2011).

It has been estimated that about 50% of the e-waste is made up of Iron and steel constituents, followed by plastics (21%), non-ferrous metals (13%), and others (16%). Non-ferrous metals comprise copper, aluminum, and precious metals such as silver, gold, platinum, palladium, etc. The presence of elements like lead, mercury, arsenic, cadmium, selenium, hexavalent chromium, and flame retardants beyond threshold quantities in e-waste renders it hazardous waste (Rajya Sabha Secretariat Research Unit 2011).

As stated above, the data collected during the survey of the informal recyclers shared about the recycling of materials from the printers and CPU, which is mentioned below in Table 1. The objective behind collecting the data is to look
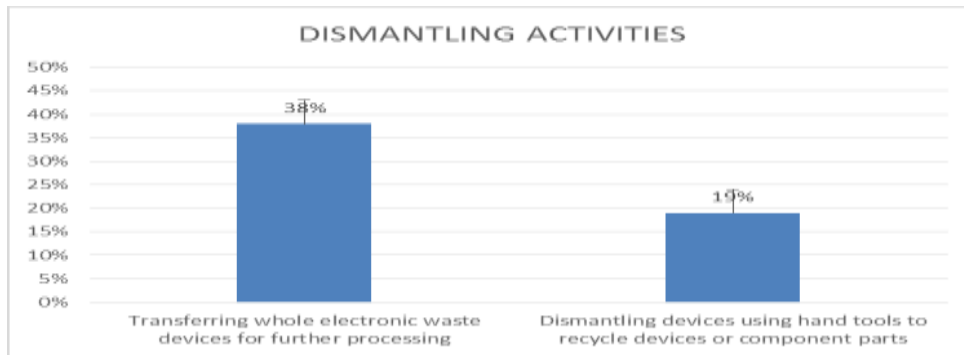
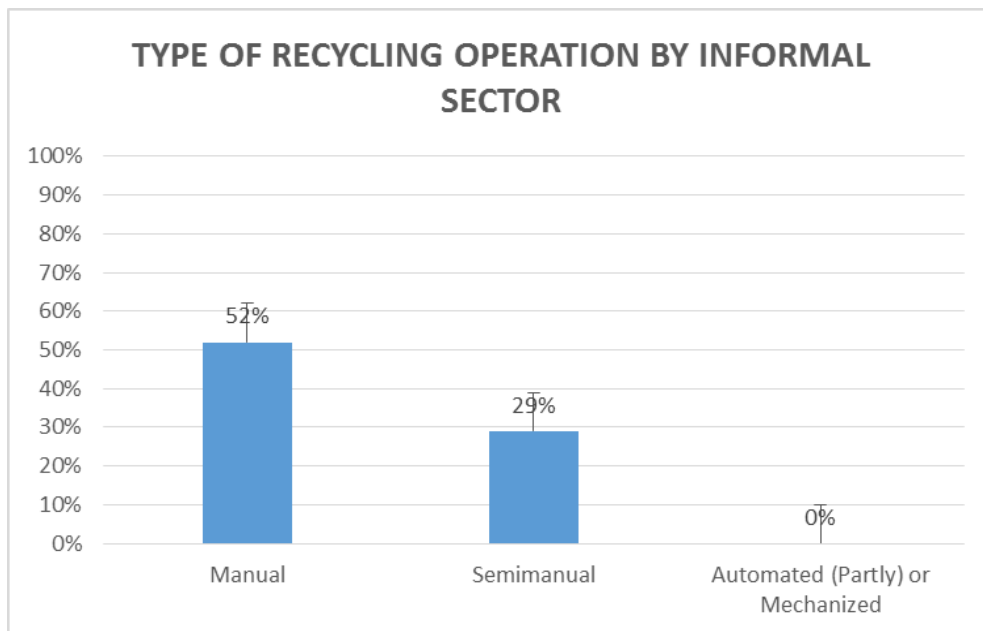Fig. 10: Dismantling process by informal sector.

Fig. 11: Recycling process by informal sector.

at the operation and systemic changes that can be brought about through government and private sector mediation, which will lead to environmentally sound management of e-waste. This will enhance resource security and also lead to the success of key Government of India missions like Make in India, Skill India, Digital India, and Clean India (Swacch Bharat) (Niti Aayog 2018).

The informal recyclers share that from 100 kg mother board efficiency of recovery of materials is a minimum of 30%. We asked to recover materials from the PC motherboard and scrap mobile phones. The data shared by the informal recyclers are described below:

Gold recovery from PC motherboard: IC chips are the main source of gold in the motherboard of scrap computers. The informal recyclers use the hot air gun to separate the IC

chips from the motherboard of scrap computers. Approx. 15-20 IC chips remain available on the main board of computers. As per the informal recyclers, they use the chemicals like sulphuric acid 4 times the IC chips temperature of 80-100^0C to dissolve the components. Use of nitric acid and others. Finally, they extract Gold wire and chips, and at least one mainboard generates approximately-rox—0.0123 g of gold. The recovered material details are given in Table 2.

Gold recovery from scrap cellphones: In mobile phones, gold remains embedded in many places like PCB, circuit boards, CCD cameras, and connectors. Gold wires remain attached to electrical circuit connections and other semiconductor devices. They separate all the gold-plated parts with the help of a hot air gun like a PCB board, CCD

Table 1: Quantity of Extracted Materials from Printers/CPU.

Name of Extracted Material	Quantity
iron,	5 kg
Plastic in printer/CPU	1.5- 2.5 kg
motor	0.5-1kg
useless plastic	0.5 kg
motherboard	1kg
glass	8kg from a total of 14 kg CPU
plastic	2.5 kg in computer
copper	0.5kg

Source: Site Survey by Author

Table 2: Recovery of materials from PC mother board.

Name of Extracted Material	Quantity
Gold	0.0123 gm from One Main Board from the CPU

Source: Site Survey by Author

camera, IC chips, Gold plated pins. They shared the amount of gold-plated parts mentioned in Table 3.

They also shared the chemicals used while extracting the gold from scrap mobile phones, like sulphuric acid @ temp 80-90^{0}C. Use nitric acid, cyanide, gold stripping chemical, Potassium hydroxide, zinc powder, hydrochloric acid, and nitric acid: Aqua regia, sodium meta bisulfate to make gold precipitate, and Borax.

Extracted from CRT monitor: The materials extracted from the CRT monitor, e.g., in 14 inches CRT monitor, the quantity of extracted materials are glass, plastic, copper, lead, PCB, etc. The name and quantity of materials extracted from LCD are also mentioned below in Tables 4 and 5.

Comparison Between Formal and Informal Recyclers

During the survey, queries were raised to formal and informal recyclers to understand the competitiveness in price available for the informal sector vis-à-vis the formal sectors. Based on responses from questionnaires, the information was gathered

Table 3: Recovery of materials from scrap cell phone.

Gold Plated Parts	Amount of Precious Metal
Accelerated Graphics Port (AGP) slot	482 g
RAM slot	209 g
IDE slot pins	689 g
VGA/COM Ports	318 g
Total gold extracted from the motherboard	3082 g
700 gm of mobile phones circuit boards	1.1 g of gold

Source: Site Survey by Author

Table 4: Recovered materials and quantity from CRT monitor

Recovered Materials	Quantity
Glass	4k g
Plastics	900 g
Copper	50-60 g copper in (Degaussing wire & yoke only)
Rest PCB	-

Source: Site Survey by Author

Table 5: Recovered materials and quantity from LCD (Liquid Crystal Display)/TFT (Thin Film Transistor) (17 ″).

Recovered Materials	Quantity
Plastic	700-800 g
LCD/Picture tube	1-2 kg
2Cart (SMPL, circuit)	10-20 g

Source: Site Survey by Author

from formal and informal recyclers. The sample collected during the survey is a computer, laptop, and Mobile PCB. The data in Table 6 shows the serious drawbacks formal actors face regarding the high acquisition cost of e-waste in India.

As per the information collected from the formal recyclers while doing the survey, they shared the Recovered metals per 1,000 kg of PCBs. The details of recovered metals from PCBs are also given in Table 7, and the recovered metals from the Informal Sector are also given in Table 8

Data collected from the survey indicates that the informal sector can pay a higher price for e-waste from different sources than formal recyclers. Formal recycling allows for better extraction of precious metals embedded in PCB's upto the extent of 90-95%, while informal recycling extracts only a few precious metals like Gold, Silver, Copper, and Platinum up to 20-30%. Methods adopted by informal recyclers adversely impact their health and reduce income potential because of the low efficiency of extracting valuable materials from e-waste.

Key Issues in the Regulation of the Informal Sector

The main challenges with the Informal sector in India are mentioned below:

1. The informal sector needs to improve the living conditions and proper disposal methods used for waste. Outreach and advocacy with waste disposers can be improved by building capacities and ensuring awareness programs representing hazards of improper disposal to human health and the environment.

2. As per the survey conducted during research, it was found that informal sectors have developed abundant knowledge of handling and managing e-waste;

Table 6: Informal and formal recyclers activities.

Activities	Informal Recyclers	Formal Recyclers
Computer/Laptop PCB Price	400 INR/kg Double chip (Original) 150-250 INR/kg single chip (pirated)	Computer and laptop PCB -200-250 INR/kg Depending on the grade of the PCB; For low-grade INR 30 /kg, medium-grade INR 80/kg, and high-grade INR 250/kg.
Mobile PCB Price	4000 INR/kg for brands like Sony, Samsung Branded manual keyboard mobile = 1600 INR/kg Non-branded Mobile = 400-800 INR/kg	Mobile PCB 1800 INR/kg
Amount of Extracted Precious Metals (PM)		High-grade PCB will have gold and silver as precious metal Medium grade has more copper, zinc, and traces or plating of gold. Additionally, nickel, chromium, cadmium, and lead are also found. Gold from high-grade PCB is in the range of 0.2 % Mobile PCB tops in grade, followed by laptop and computer RAM and processor have the highest gold quantity. Overall, iron is 60 %, plastic 30-35 %, and the rest other PM It is from a whole product like PC or laptop etc. About 90% of precious metals are extracted from what e-waste contains
What to do with extracted plastic from PCB	Sent to Plastic recycler.	Plastic, upon segregation, can be recycled or sent to a plastic recycler
Materials recovered from e-waste	Mainly gold, silver, copper	All precious metals
The efficiency of recovery of materials	20-30 %	90-95%
Capital costs involved	5-8 Lakh for chemicals, other supporting machines	25-50 Crore
Operational costs	-	20 INR/kg, including transportation and operational cost.

Source: Site Survey by Author

Table 7: Recovered metals per 1,000 kg of PCBs (from the formal sector)

S. No.	Recovered metal	Weight	Market Value	The value of Metal recovered
1.	Gold	279.93 g	36,000/10 g	Rs. 10,07,748
2.	Precious metals (Pt, Pd, In)	93.31 g	40,000/10 g	Rs.3,73,240
3.	Copper	190.512 kg	0.4/g	Rs.76,205
4.	Aluminium	145.152 kg	0.12/g	Rs.17,418
5.	Lead and tin (Pb/Sn)	30.844 kg	0.15/g	Rs.4,627
6.	Silver	450 g	400/10g	Rs.18,000

Source: (Chatterjee & Kumar 2009)

Table 8: Recovered metals per 1 Ton/1000 kg PCBs (From the Informal Sector)

S. No.	Recovered metal	Weight	Market Value	The value of Metal recovered
1.	Gold (1 Ton PCB)	10-100 g (Depends on PCB Grade)	36,000/10 g	Rs. 3,60,000

(Source: Site Survey by Author)

however, they are adopting either obsolete or inefficient technology. It was found that they are considered small-scale units, including easily available labor from their family members, small space, and no rules and regulations (Tiwari et al. 2019).

3. The survey says that Informal sector competencies can be improved by the availability of land, access to technology, and finances, which can change their lifestyle to be more resource efficient and environmentally sound. The work clusters can be made

away from residential areas so that people, especially children, are not exposed to environmental hazards (Hemkhaus et al. 2018).

RESULTS AND DISCUSSION

Capacity building and advocacy with the informal sector are serious bottlenecks encountered in the path toward formalization. The benefits of formalization, which can be accessed through a combination of multiple strategies and policy mix to deliver desired results:

1. Using advanced technology in India will increase opportunities in the recycling sector and its development. It will enhance the livelihood. Access to such technology for the informal sector will set the tone for formalization.

2. The introduction of advanced technology can improve living conditions and proper disposal methods for waste. This will ensure better health and the environment in places where the informal sector is working presently.

3. Capacity building of the informal sector will allow for efficiencies in their livelihoods, leading to higher income. It also allowed for compliance monitoring from the end of the SPCBs.

4. Formalization of the informal sector will result in the successful implementation of key Government of India missions like Make in India, Skill India, and Clean India. It also allowed multiple livelihood opportunities for skilled labour in the country (Niti Aayog 2018).

5. Safe e-waste disposal in an environmentally friendly manner will provide a fillip to the Swacch Bharat Mission.

- It is also important to understand that in a large number of cases, the request for formalization is coming from the informal sector. This is primarily because of 2 reasons:

1. The informal sector understands that the work that they are doing is not conducive to their health as well as the environment, which is why they want access to technology and other inter-alia items

2. The informal sector has been able to continue because of corruption since its margins were high. Higher levels of corruption have reduced their margins to levels where they now believe that it is better to formalize than stay informal because, in both cases, income will not differ much.

The informal sector may still stay in really small pockets, but a major chunk of materials will start to move into the formal domain.

In India, material fractions for which technology is not available for recycling are exported. Many formal recyclers have not invested in such technologies, either due to a lack of resources or access to materials because of the presence of the informal sector. The new rules, which promote Extended Producers' Responsibility, aim to ensure the producers are responsible for collecting e-waste such that the same can be channelized to formal recyclers.

To make the system effective, activity plans must be recognized alongside all the related players who will guarantee time-bound usage of techniques with distinguished stakeholders. As mentioned, the proposed pathways to formalize the informal sector are diagrammatically introduced in Fig. 12 (Tiwari et al. 2019).

For a positive implementation of the above-mentioned strategy, it's essential to involve all the stakeholders together as well as to understand their actual requirements or need to motivate them to get formalized. The proposed flow is given above in Fig. 12. For the last few decades. Many players are engaged in managing e-waste where producers are answerable for confirming the collection of end-of-life material, and the informal players are the one who collects and handle the e-waste through their network. Proper registration of the informal units is required so that the disposers of e-waste, both individuals and bulk consumers, can also reach out to these informal players. To make the strategy successful, it's required that action agendas be identified along with all the associated players who will ensure time-bound implementation of strategies with identified stakeholders.

The informal sector has been India's overall core of recycling WEEE for the last two decades. This sector doesn't have the chemistry knowledge in depth besides the simple knowledge about acid baths and heat treatment to extract precious metals. The existing technology used by the informal sector creates a serious impact on their health as well as the environment. Introducing advanced recycling technology for mitigating hazardous environmental and human health effects is as important as developing new electronic products. All these social and environmental benefits to the informal sector can ensure formalized livelihoods in e-waste recycling by using technology (Tiwari et al. 2019).

The informal sector players are responsible for reusing e-waste or are the backbone of waste collection and resource recovery. As referenced above, the absence of infrastructure and accessibility of advanced technology brings about low creation of sources yet the production of progressively waste. As per our research, we tried to find out the cost estimation details for setting up a material recycling facility, described below.
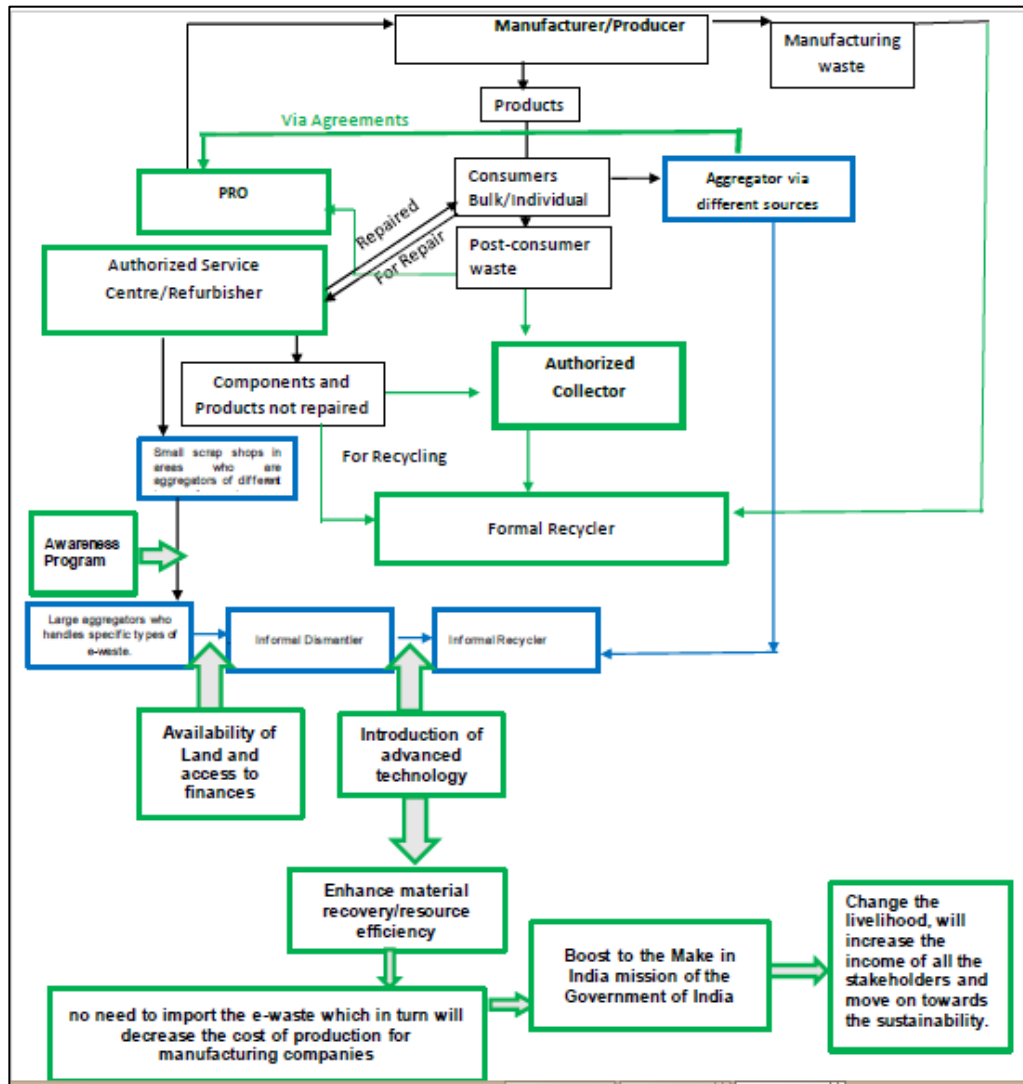
Fig. 12:   Process reengineering for formalizing informal sector.

Cost Estimation for Setting up of Material Dismantling/Recycling Facility

Setting up a recycling facility close to areas that are bulk generators of e-waste has been considered an option to minimize the logistics cost of transportation of e-waste. This has been done based on the assumption that the PROs collecting on behalf of the producers would like to minimize costs so that they can churn out a profit for themselves from the activities they are pursuing. The same is given in Table 9.

In the case of an investment by the informal sector, the scale of operations becomes large, which could be difficult in case little finance is available.

In the case of a dismantling facility, the scale is smaller and more profitable, which allows for higher profits at low capital expenditure.

Centralized facilities for recycling and decentralized facilities for dismantling by formalizing the informal sector are the way forward to avoid system failures in the e-waste management system.

The financial mechanism, which is developed as an output of the business numbers which have been shared, goes on to depict that just formalizing and providing technology is not the solution. Capacity building, advocacy and outreach, and training are important, along with finance, land, and technology, so these actors and other stakeholders

Table 9: Setting up of a dismantling/recycling facility.

S. No.	Description	Cost
1.	Land for setting up of dismantling/recycling facility	30,00,000 for purchase/lease or INR 1,00,000 as rent for the facility.
2.	Set-up costs	5, 00,000 for ensuring proper insulation is completed within the shed so that dust does not go out.
3.	Dismantling tables	2, 50,000 for 5 dismantling tables with a capacity to process 1.5 tonnes a day.
4.	Storage bins and other inventorization infrastructure	1 00,000 for bins for different metals and materials and racks for inventorization.
5.	Rolling stock	20,00,000 per month for 3 months to be able to buy and sell and maintain cash flow
6.	Dust collection and other infrastructure	10,00,000
7.	Authorization and other costs	2,00,000
Operations cost		
1.	Human resource	3,00,000 per month
2.	Logistics cost	1,50,000 per month
3.	Electricity cost	1,00,000 per month
4.	Storage and other costs	50,000 per month
5.	Miscellaneous	50,000 per month

can be aligned as per the rules, which will benefit both the environment and human health.

Capacity building of the informal sector can allow them to uptake technology, leading to enhanced capacities in the country. It will also solve the problem of formalization of the informal sector, which will benefit human health and the environment.

CONCLUSION

The informal sector is a part of the system failure that the Indian e-waste sector has been experiencing for the past several years. The informal sector has access to materials because of the network created due to socio-economic issues faced by a section of the society in India. Large-scale urban migration leads to serious job crunch for unskilled workers. Waste collection is the easiest livelihood since there are no barriers to entry. This has led to networks channeling materials away from proper recycling. It has also created issues with recognizing these actors in the rules since it is difficult to identify them. They are neither part of the tax net nor are their businesses registered with the relevant authorities.

Analysis across the informal sector helps to understand that the socio-economic divide that has pushed a generation into waste picking and informal recycling has given way to aspirations for educating their children. This thought propels them to organize and formalize so they can move to work within the ambit of the law.

Analysis across these stakeholders allows us to understand the key issues which lead to system failure in the e-waste sector. Certain key reasons for the same are:

1. Lack of outreach and advocacy on the e-waste rules has not helped develop and understand the responsibilities across different stakeholders.

2. Lack of forums for the informal sector to speak for themselves and express their key issues has prohibited them from formalization.

3. Lack of recycling infrastructure in the country in the formal domain has not allowed all the material to flow into the formal sector.

4. Lack of compliance with regulation enforcement by authorities has led to slackness in implementing the rules.

Interviews with informal actors and other key actors helped shed light on these actors' key asks. These include the following:

1. Access to land: This will allow them to formalize and practice their livelihood, which they have pursued for the past few years. Furthermore, it will help build capacity within the formal domain so that more material can be recycled in an environmentally sound manner

2. Access to technology: This will allow them to ensure that the work that they do involves scientific processes so that it is environmentally sound and poses no hazards to human health

3. Access to finance: These actors who now formalize must be able to access finance at lower interest rates. This will allow them to invest in technology and land, which is part of the key steps to formalization.

Any system which acts in silos is likely to create unintended consequences. This happens because the cause and effect of the system are studied in tandem and not together. A study of the system, including all stakeholders, their actions, and their behavioral patterns, helps understand how one stakeholder will react to certain actions that could have unintended consequences. Guarding against unintended consequences helps build a stronger systemIt is important to note that certain key points from this study had nothing to do with the approaches taken by various stakeholders to solve the problems relating to effective e-waste management. Analysis of some of the programs which PROs have managed leads one to the following conclusions:

1. Awareness activities conducted by PROs have created a demand for formalization in the informal sector.

2. Over the last 3 years, informal actors have formalized to take the count of recyclers/dismantlers in India from 148 in 2016 to 312 in 2019.

3. Material flow to these formal actors has now helped producers to meet the target of 30 percent as provided for in the e-waste management rules, 2016 (revised guidelines of 2018).

4. PROs assist in formalizing informal actors into collection centers so that e-waste can be channelized for environmentally sound management.

The high-handed approach of compliance and regulatory authorities will likely lead to increasing illegal processes or livelihoods being waned away from the e-waste sector. On the other hand, an approach that looked to not attack the problem directly but indirectly led to demand for formalization within the system with consequences that favor properly implementing the e-waste management rules, 2016.

REFERENCES

Baldé, C.P., Forti, V., Gray, V., Kuehr, R. and Stegmann, P. 2017. The Global E-waste Monitor–2017. United Nations University (UNU), International Telecommunication Union (ITU) & International Solid Waste Association (ISWA), Bonn, Geneva, Vienna. pp. 1-109.

Baldé, C.P., Wang, F., Kuehr, R. and Huisman, J. 2015. The Global E-Waste Monitor 2014. Technical Report, United Nations University and Institute for Advanced Study of Sustainability, pp. 1-116.

Chatterjee, S. and Kumar, K. 2009. Effective electronic waste management and recycling process involving formal and non-formal sectors. Int. J. Phys. Sci., 4(13): 893-905.

Chaturvedi, A., Arora, R. and Ahmed, S. 2010. Mainstreaming the Informal Sector in E-Waste Management. In National Conference on Urban, Industrial and Hospital Waste Management, Ahmedabad, pp. 1-5.

Henzler, M., Eisinger, F. and Hemkhaus, M. 2018. Creating Successful Formal-informal Partnerships in the Indian E-waste Sector. Deutsche Gesellschaft für Internationale Zusammenarbeit (GIZ) GmbH, Bonn, Germany, pp. 1-20.

Lahiry, S. 2019. Recycling of E-waste in India and its Potential. Retrieved from https://www.downtoearth.org.in/blog/waste/recycling-of-e-waste-in-india-and-its potential 64034 (Accessed September 25, 2019)

Ministry of Environment & Forest & Climate Change (MoEF & CC). 2016. Notification to be published in the Gazette of India, Extraordinary Part-II, Section-3, Sub-Section (i)]. MoEF, Dehi, pp. 1-42.

National Institution for Transforming India (NITI) Aayog. 2018. Strategy for Secondary Materials Management for Promoting Resource Efficiency (RE) and Circular Economy (CE) in Electrical and Electronic Equipment Sector. Department of Electronics and IT Ministry of Communications & Information Technology Government of India, New Delhi, pp. 1-50.

Rajya Sabha Secretariat Research Unit. 2011. E-Waste in India. India Research Unit (Larrdis), Rajya Sabha Secretariat, New Delhi.

Tiwari, D., Raghupathy, L., Sardar Khan A. and Gauba Dhawan, N. 2019. A study on the e-waste collection systems in some Asian countries with special reference to India. Nature Environ. Pollut. Technol., 18(1): 149-156.

UNEP. E-waste - Volume I. 2007. Inventory Assessment Manual, United Nations Environment Programme, Retrieved from http://www.unep.or.jp/ietc/Publications/spc/EWasteManual_Vol1.pdf (Accessed June 26, 2009).

Determination of the Dynamics of Thunderstorms Through the Dry Adiabatic Lapse Rate and Environmental Lapse Rate

Shiemaa A. Hashim*, Jasim H. Kadhum*, Zainab M. Abbood*, Osama T. Al-Taai*† iD and Wedyan G. Nassif*

*Department of Atmospheric Science, College of Science, Mustansiriyah University, Baghdad, Iraq
†Corresponding author: Osama T. Al-Taai; osamaaltaai77@uomustansiriyah.edu.iq

ABSTRACT

This research aims to determine the types of thunderstorms formed in the thickness of the cloud (determine the Dry adiabatic lapse rate (DALR) and Environmental lapse rate (ELR)) in the case of precipitation during the day. Data were taken by Temperature, Dew point, Atmospheric Pressure, and Height from re-analysis by the (ECMWF) for the heights (0-18000) m, the levels of pressure (1000-100) mbar, low cloud cover data, and the characteristic days ((18, 24, 27) February, 28 April, and 25 November) of the year 2018 for Baghdad station were chosen to obtain the largest possible number of clouds and their diversity to use them in calculating the cloud cover and weather stability in terms of calculating the daily change, temperature, dew point in addition to calculating the low cloud cover with altitude and atmospheric instability. The Sigma Plot program was used in this research to determine the base of clouds and thunderstorms. The change in temperature, Dew point, clouds base, and altitude was determined, then the cloud thickness, types, and classification were calculated. The clouds found are strong thunderstorm clouds characterized by thickness and height, such as the clouds of Nimbostratus (Ns) and Cumulonimbus (Cb).

INTRODUCTION

A thunderstorm is a turbulence in the atmosphere. It is a single or multiple electric discharge that reveals itself with a flash of light and a Sharpe or bruising sound like thunder. Thunderstorms accompany clouds of load and are often accompanied by precipitation from those that reach the Earth through showers of rain, snow, snowballs, or cold (Tompkins 2003). Strong winds usually accompany them and produce heavy rain and sometimes snow, sleet, or hail, but some thunderstorms produce little precipitation or no precipitation (Abbood & Al-Tai 2018a, 2018b, 2020). As the warm, moist air moves upward, it cools, condenses, and forms a cumulonimbus cloud reaching over 20 kilometers (Al-Taai & Abbood 2020a). As the rising air reaches its dew point temperature, water vapor condenses into water droplets or ice, reducing pressure locally within the thunderstorm cell. Any precipitation falls a long distance through the clouds toward the Earth's surface. As the droplets fall, they collide with other droplets and become larger (Al-Taai & Abbood 2020b, Sun et al. 2000).

ORCID details of the authors:

Osama T. Al-Taai: https://orcid.org/0000-0002-4747-214X

Cloud Formation

The process of forming clouds, or condensation in the air, is very delicate and subject to several physical laws. This difference is responsible for the formation of different types of clouds, such as stratified and cumulative clouds, and it is also responsible for the difference in the height of the rules of the clouds and the difference in thickness (Tompkins 2003, Al-Taai et al. 2021a). Accordingly, the decrease in air temperature decreases in three forms. The first form is called the normal laps rate, which varies according to the times of the day, seasons, and locations, but in general, it is 6.3 percent per 1000 meters. The second, this decrease is at a percentage of 9.8 per 1,000 meters up, and the third is called the Moist Adiabatic Lapse Rate, which equals 6.4 percent per 1,000 meters upwards (Yamashita et al. 2004, Nassif et al. 2021a). The decrease in air temperature by elevation depends on Poisson's law (Which states that a mass of air rising vertically upwards gradually loses part of its temperature).

On this basis, the decrease in air temperature first is subject to Poisson's law until it reaches a certain height and its temperature decreases below the dew point. At this temperature, condensation occurs as clouds form. (Eastman et al. 2011, Al-Taai et al. 2021b).

MATERIALS AND METHODS

The Atmospheric Stability

Clouds are formed when the air contains as much water vapor (gas) as possible. This is called the saturation point (Hartmann 2013, Tierney et al. 2001). The lifting condensation level (LCL) is formed when the temperature reaches the dew point. It is the level at which condensation can occur through uplift. At the lifting condensation level, the base of the cloud is formed. Then the air is saturated (the air retains the largest amount of water vapor at a certain temperature), and the relative humidity is 100% (Cooper et al. 2003, Bryan & Fritsch 2000). When determining the high base of the cloud at the intersection point between the temperature of the antenna ejection temperature curve and the temperature of the dew point temperature curve symbolized by the symbol zb and determining the temperature of the upper cloud at the point of divergence of the temperature curve of the dew point temperature curve symbolized by the symbol zt, a thickness of the cloud (Δzc) can be determined using the following equation (Hartmann et al. 2013 & Nassif et al. 2022):

$$\Delta zc = zt - zb \qquad \text{...(1)}$$

The Δzt can be calculated using the Hypsometric equation (Sun et al. 2000 & Nassif et al. 2021b):

$$\Delta zt = Rd \ \frac{Tv}{g} \ \ln \frac{P_1}{P_2} \qquad \text{...(2)}$$

Where:

Δzt: The thickness of the cloud in km.

Rd: specific gas constant for dry air (287.1 J.kg^{-1}. k^{-1}).

Tv: Virtual temperature of the cloud in ⊡k.

g: ground acceleration (9.8 m.sec^{-2}).

P_1: The pressure at the base of the cloud in mbar.

P_2: Pressure at the top of the cloud in mbar.

The air moves up or down within the atmosphere. It is affected by this process (Sun et al. 2000). The air parcels that do not contain clouds (are not saturated) cool at the dry adiabatic lapse rate (DALR) as they rise through the atmosphere (Sun et al. 2000). The DALR not only applies to absolutely dry air parcels but also parcels containing water vapor, so long as the relative humidity (RH) < 100%.

The parcel of non-saturated air will rise at a rate of cooling given by the dry adiabatic lapse rate where Cp is 1007 J.kg^{-1}. K and Γd are 9.8 °C.km^{-1} (Hartmann 2013, Al-Taai & Wedyan 2020) as the following equation:

$$\Gamma d = \frac{g}{C_p} \qquad \text{...(3)}$$

Where Γd is the dry adiabatic lapse rate, g is the Earth's gravity = 9.8 m.sec^{-2}, and the Cp is the specific heat capacity. The atmosphere is highly variable in air temperature distribution. For dry air, it ranges as shown in Fig. 1 and Table 1 (Abbood et al. 2021, Mahdi et al. 2021).
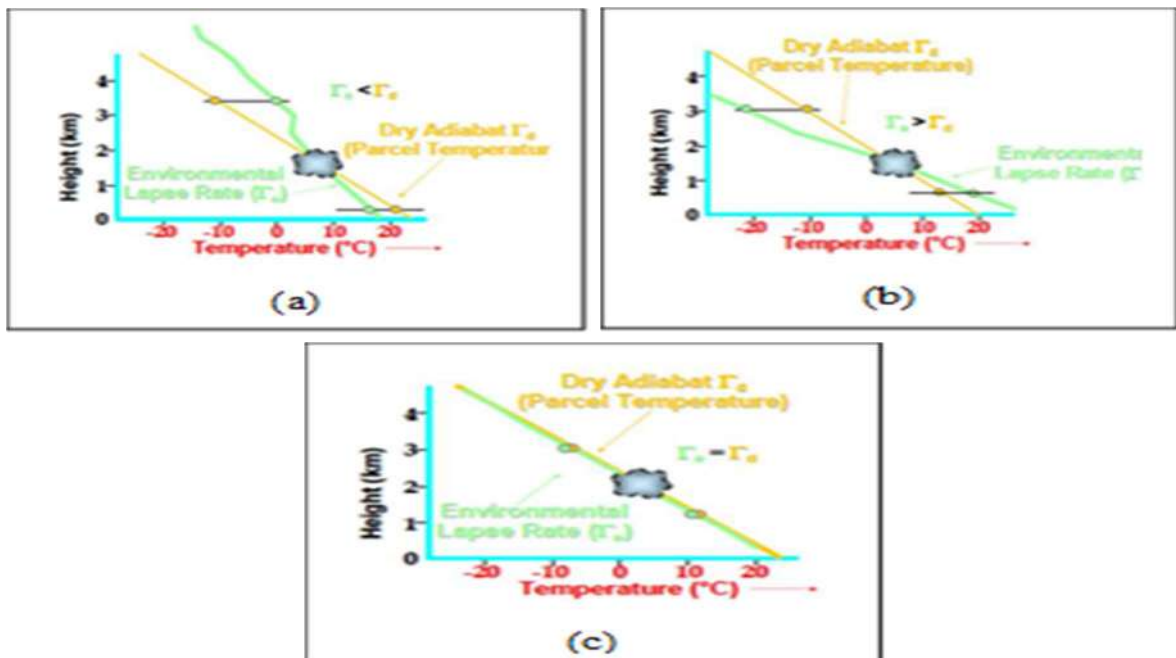

Fig. 1: The formation of clouds, in this case, is a) Stable, b) Unstable, and c) Neutral (Tierney et al. 2001, Buell 1943).

Table 1: The characteristics of ten cloud types (Nassif et al. 2021c).

Cloud Type	Symbol	High cloud base (km)	Temperature cloud base °C	Thickness (km)	Case of water in the clouds	rising airspeed (m.sec^{-1})
Cirrus	Ci	10-5	70-,30-	2-0.5	Ice	0.3-0.1
Cirrostratus	Cs	10-5	40-,25-	2-1	Ice	0.3-0.1
Cirrocumulus	Cc	12-5	40-,25-	0.3-0.1	Liquid or mixed	1-0.3
Altostratus	As	8-3	30-,10-	3-1	Ice or mixed	0.3-0.1
Altocumulus	Ac	8-2	30-,10-	1-0.1	Liquid or mixed	1-0.3
Nimbostratus	Ns	2-0.5	20-,10-	10-2	Ice or mixed	1-0.3
Stratus	St	2-0	20-,10-	0.5-0.1	Liquid	0.3-0
Stratocumulus	Sc	2-0	20-,10-	2-0.1	Liquid or mixed	1-0.1
Cumulus	Cu	4-1	5,25-	4-0.5	Liquid	3-0.3
Cumulonimbus	Cb	4-1	5,25-	20-2	Mixed	30-3

Data Source

The work was carried out using the average hourly values of temperature and dew point temperature for selected days of the year 2018. Dataset values were obtained from the European Center for Medium-Range Weather Forecasts (ECMWF), https://www.ecmwf.int/en/forecasts/datasets (Berrisford 2009, Nassif et al. 2021d), for Baghdad city, located at ….33.375°N latitude, 44.375°E longitude, and 34.0m altitude in the center of Iraq. The determination of thunderstorms depends on weather factors such as temperatures, relative humidity, and dew point temperature over Baghdad City (Nassif et al. 2021a).

RESULTS AND DISCUSSION

The Temperature Changed with the Height

The behavior and temperature change at each pressure altitude how it changes with the height over Baghdad city for the year ( ) 2018. For the daily change in temperatures, it occurs in temperatures during the Day and night, and this is due to the rotation of the Earth around itself and this change in temperature due to latitude; the temperature decreases as we move from the equator towards the poles due to the decrease in solar radiation. Also, as the temperature changes with the height in the first layer of the troposphere, the layer in which different weather phenomena occur. The higher the temperature, the air expands and rises to the top, its density decreases, and its pressure decreases. If the temperature drops, the air shrinks, and the density increase, then the drop to the bottom increases the air pressure. The range of pressure that you adopted in your study ((100-1000) mbar) of the daily temperature changes over Baghdad city during 2018 (Fig. 2).

Dew Point Temperature Change with the Height

The Dew point varies depending on the amount of water vapor in the air, with more humid air resulting in a higher dew point than dry air. Furthermore, the higher the relative humidity, the closer the dew point to the current air temperature, with 100% relative humidity meaning that the dew point is equivalent to the current temperature. When the air pressure increases, the dew point will increase. This means that if the pressure increases, the mass of water vapor in the air must be reduced to maintain the same dew point. The relationship between pressure and the dew point is direct; the higher the atmospheric pressure, the greater the dew point score, and vice versa. The range of pressure that you adopted in your study ((100-1000) mbar) of the daily temperature changes over Baghdad city during 2018 (Fig. 3.)

Calculations of the Daily Changes

The daily report of February 2018 for Baghdad station provides data on the thickness, height, type, and classification of the clouds and the weather stability of the cloud base and under the cloud base. Fig. 4 and Table 2 present the data of Baghdad station for 18th Feb. 2018. The state of instability of the daily cloud cover is determined at the Baghdad station, and it found that the clouds at low altitudes are unstable and clouds at high altitudes of 750 mbar were below or at ELR level, the cloud base being at 750 mbar pressure, either above or at the DALR level. The temperature at the base of the cloud in this form at the ELR level is 275 K, while the temperature at the highest level of DALR is 202 K. As for dew point temperature at the cloud base and the ELR level, it reached 274 K, as for the DALR height, it is 208 K, and we notice that the clouds were of a kind (Cb) and its classification is due to the vertical development clouds.
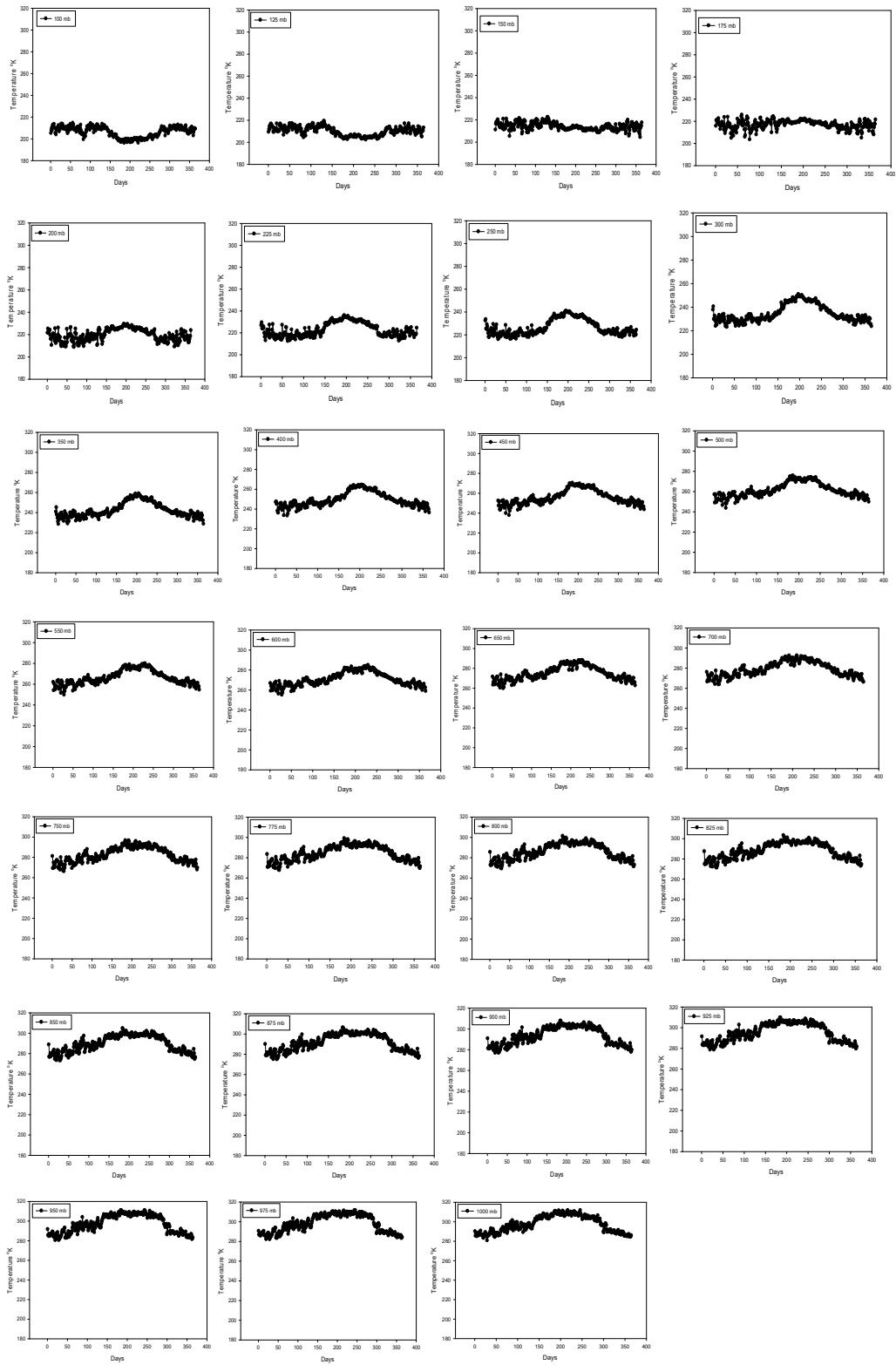
Fig. 2: The daily change of temperature at pressure from (100-1000) mbar for the year 2018 of Baghdad city.
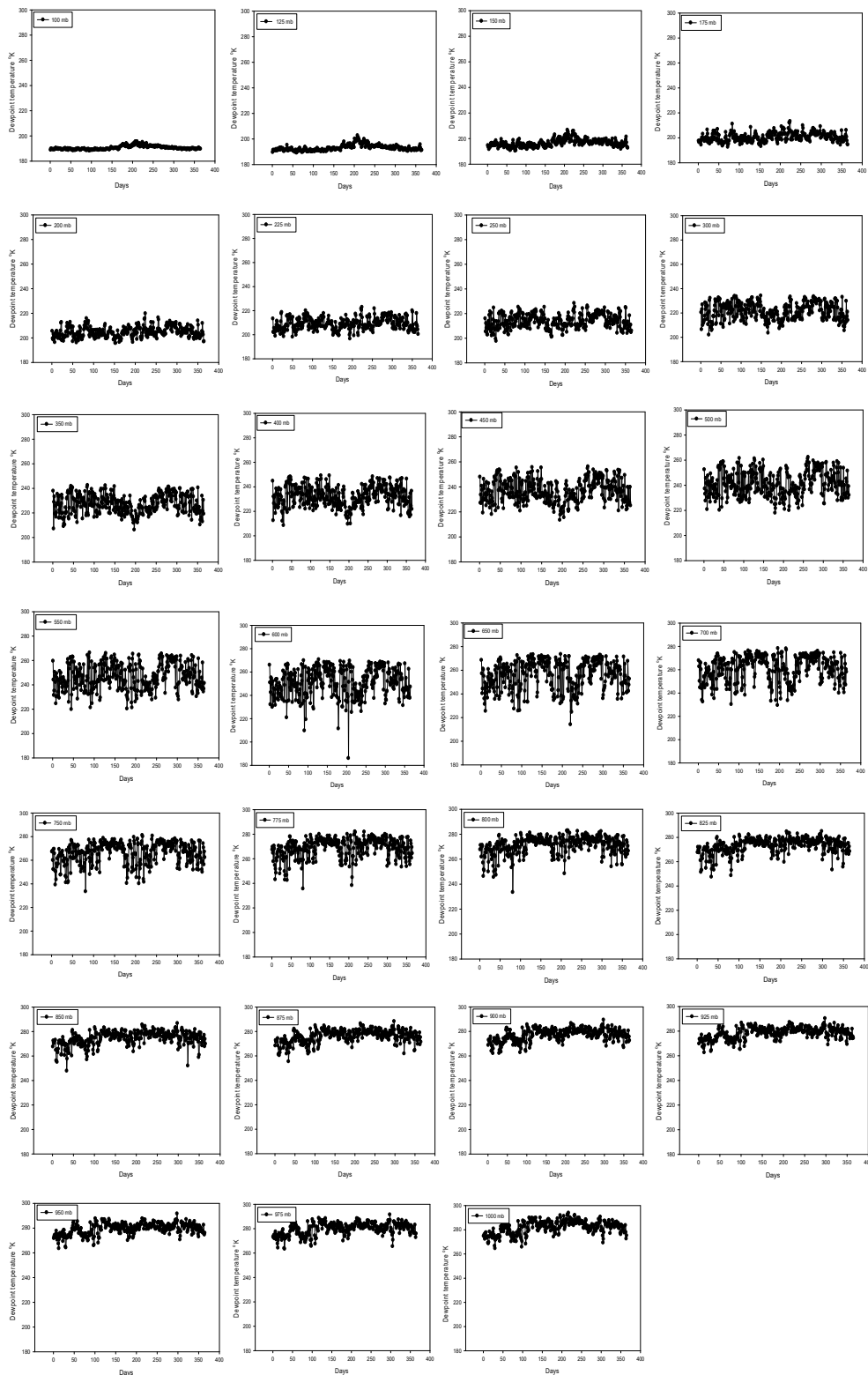
Fig. 3: The daily change of dew point temperature at pressure from (100-1000) mbar for the year 2018 of Baghdad city.
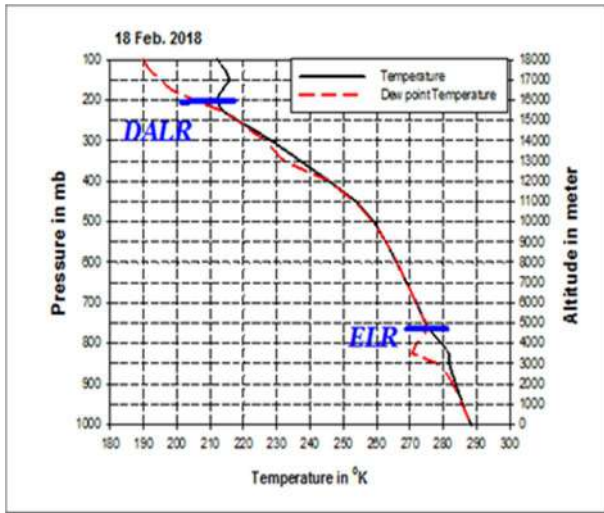
Fig. 4: Determine thunderstorms from the DALR and ELR levels for the
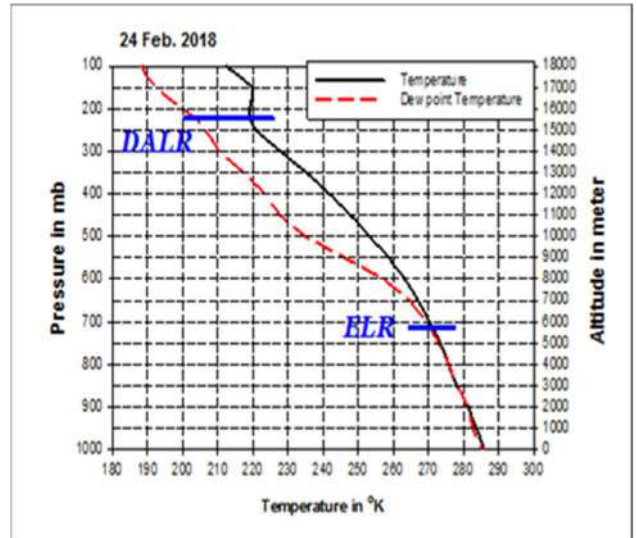day (18 Feb. 2018) in Baghdad city.

Table 2: Information on the weather (18 Feb. 2018).

Baghdad station data	18 Feb. 2018
Pressure base [mbar]	760 mbar
High base [m]	4900 m
The temperatures of the base [ºK]	275 K
Dewpoint the base [ºK]	274 K
Pressure top [mbar]	200 mbar
High-top [m]	16000 m
The temperatures of the top [ºK]	212 K
Dew point the top [ºK]	208 K
Thickness [m]	12000 m
Cloud type	Cb
Cloud classification	Low Clouds
Stability state	Instability
Pressure under the base [mbar]	750 mbar

Fig. 5 and Table 3 present the data of Baghdad station for (24 Feb. 2018). The state of instability of the daily cloud cover was determined at the Baghdad station, the environment laps rate gradual fall, and the decrease of an atmospheric variable with height where below or at ELR level is the cloud base being at 700 mbar pressure, either above or at the DALR level the cloud beings to fade at latitude 15800 m and with your thickness 6000. The temperature at the base of the cloud in this form at the ELR level is 270 K, while the temperature at the highest level of DALR is 219 K. As for the dew point temperature at the cloud base and the ELR level, it reaches 269 K, as for the DALR height, it is 204 K, and we notice that the clouds were of a kind (Ns) and its classification is due to the low clouds.

Fig. 5: Determine thunderstorms from the DALR and ELR levels for the
day (24 Feb. 2018) in Baghdad city.

Table 3: Information on the weather (24 Feb. 2018).

Baghdad station data (hpa)	24 Feb. 2018
Pressure base [mbar]	710 mbar
High base [m]	5900 m
The temperatures of the base [ºK]	270 K
Dewpoint the base [ºK]	269 K
Pressure top [mbar]	220 mbar
High-top [m]	15800 m
The temperatures of the top [ºK]	219 K
Dew point the top [ºK]	204 K
Thickness [m]	10000 m
Cloud type	Ns
Cloud classification	Vertical Clouds
Stability state	Instability
Pressure under the base [mbar]	700 mbar

Fig. 6 and Table 4 present the Baghdad station data (27 Feb. 2018). The instability of the daily cloud cover is determined at the Baghdad station, which shows the daily behavior of the low cloud cover in Baghdad station. In this case, the convective condensation level (CCL) occurs, which leads to a significant increase in the rate of thermal decrease in the lowest layer of air.

Hence, this is the level at which the cumulus cloud rules exist. To confirm the atmospheric instability of the cloud where below or at ELR level is the cloud base being at 940 mbar pressure, either above or at the DALR level, the cloud beings to fade at an altitude of 14000 m and with your thickness of 1800. The temperature at the base of the cloud
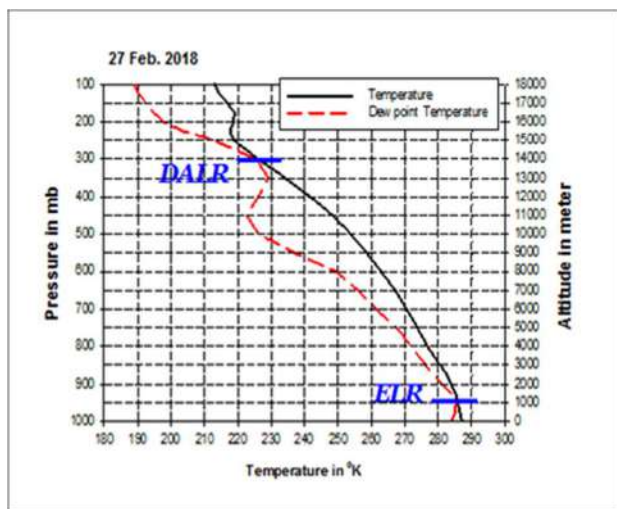
Fig. 6: Determine thunderstorms from the DALR and ELR levels for the day (27 Feb. 2018) in Baghdad city.

Table 4: Information on the weather (27 Feb. 2018).

Baghdad station data	27 Feb. 2018
Pressure base [mbar]	950 mbar
High base [m]	1000 m
The temperatures of the base [°K]	286 K
Dewpoint the base [°K]	284 K
Pressure top [mbar]	300 mbar
High-top [m]	14000 m
The temperatures of the top [°K]	227 K
Dew point the top [°K]	125 K
Thickness [m]	14000 m
Cloud type	Cb
Cloud classification	Low Clouds
Stability state	Instability
Pressure under the base [mbar]	940 mbar

in this form at the ELR level is 286 k, while the temperature at the highest level of DALR is 227 K. As for dew point temperature at the cloud base and the ELR level, it reached 284 K, whereas for the DALR height, it is 125 K, and we note that the clouds were of type (Cb), and its classification is due to the vertical development clouds.

Fig. 7 and Table 5 present the Baghdad station data (28 April 2018). The state of instability of the daily cloud cover is determined at the Baghdad station. When drawing pressure levels in this Fig., the dew point temperature change with height, and for each pressure level and the pressure level at the base of the cloud is about 950 mbar at the height of 1000 m, either above or at the DALR level the cloud at altitude 14000 m and with your thickness 1000.

The temperature at the base of the cloud in this form at the ELR level is 289 K, while the temperature at the highest level of DALR is 228 K. As for the dew point temperature at the cloud base and the ELR level, it reaches 288 k, whereas for the DALR height, the temperature was 223 K, and we notice that the clouds were of a kind (Cb) and its classification is due to the vertical development clouds.

Fig. 8 and Table 6 present the Baghdad station data (25 Nov. 2018). The state of instability of the daily cloud cover is determined at the Baghdad station. Where we notice a severe thunderstorm, starting at the pressure level at the base of the cloud, about 860 mbar at the height of 2700 m, and with a thickness of 3000, then it began to decay at the DALR level at the height of 14000 m and a pressure of 300 mbar. The temperature at the base of the cloud in this form at
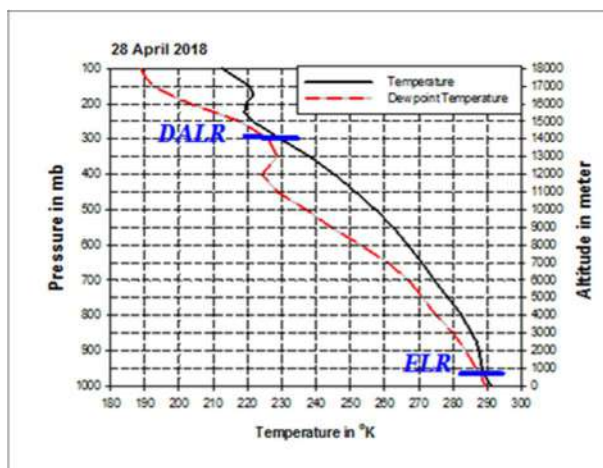

Fig. 7: Determine thunderstorms from the DALR and ELR levels for the day (28 April 2018) in Baghdad city.

Table 5: Information on the weather (20 April 2018).

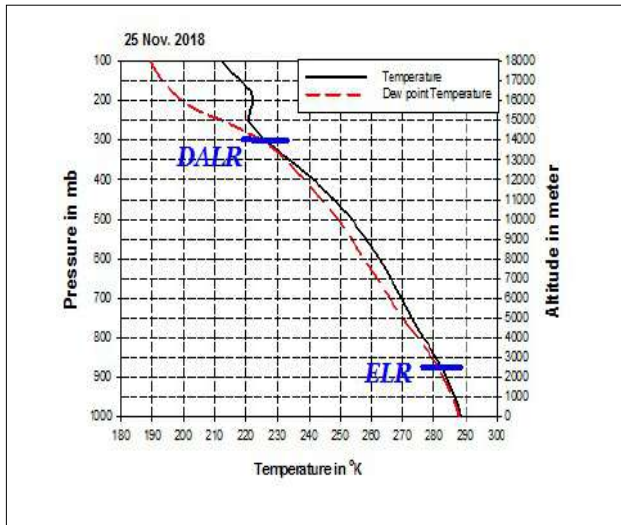| Baghdad station data	20 April 2018
Pressure base [mbar]	960 mbar
High base [m]	900 m
The temperature of the base [°K]	289 K
Dew point the base [°K]	288 K
Pressure top (mbar)	300 mbar
High top [m]	14000 m
The temperature of the top [°K]	228 K
Dew point the top [°K]	223 K
Thickness [m]	14000 m
Cloud type	Cb
Cloud classification	Low Clouds
Stability state	Instability
Pressure under the base [mbar]	950 mbar

Fig. 8: Determine thunderstorms from the DALR and ELR levels for the day (25 Nov. 2018) in Baghdad city.

Table 6. Information weather on the day (25 Nov. 2018).

Baghdad station data	25 Nov. 2018
Pressure base [mbar]	870 mbar
High base [m]	2700 m
The temperatures of the base [°K]	283 k
Dewpoint the base [°K]	282 k
Pressure top [mbar]	300 mbar
High-top [m]	14000 m
The temperatures of the top [°K]	226 k
Dew point the top [°K]	125 k
Thickness [m]	12000 m
Cloud type	Cb
Cloud classification	Low Clouds
Stability state	Instability
Pressure under the base [mbar]	860 mbar

the ELR level is 283 K, while the temperature at the highest level of DALR is 226 K. As for the dew point temperature at the cloud base and the ELR level, it reached 282 K, as for the DALR height, it is 125 K, and we notice that the clouds were of a kind (Cb) and its classification is due to the vertical development clouds.

CONCLUSIONS

The change in the daily average temperature with an altitude in the troposphere at the pressure levels 1000 mbar and 950 mbar. The average daily temperature changes with altitude, as the temperature increases with the increase in altitude above ground level until it reaches its lowest possible level

at the pressure levels of 150 mbar and 100 mbar. The daily average dew point temperature is similar and consistent with the behavior of changing the daily average temperature. That is, the form of the relationship between dew point temperature and temperature is a positive correlation. The thickness of the low clouds was determined for the selected days with the highest daily rains. Depending on these determinations, it had found that there were clouds of Nimbostratus (Ns) and Cumulonimbus (Cb) types.

Determine the clouds of Nimbostratus (Ns) and the Cumulonimbus (Cb) by setting the height of the Dry Adiabatic Lapse Rate (DALR) and the height of the Environmental Lapse Rate (ELR). The amount of precipitation in the (Nimbostratus (Ns) and Cumulonimbus (Cb) clouds was so high. The clouds found were strong thunderstorm clouds characterized by thickness and height, such as those of Nimbostratus (Ns) and Cumulonimbus (Cb).

REFERENCES

Abbood, Z.M. and Al-Taai, O.T. 2018a. Calculation of absorption and emission of thermal radiation by clouds cover. ARPN J. Eng. Appl. Sci., 13(24): 9446-9456.

Abbood, Z.M. and Al-Taai, O.T. 2020. Data Analysis for cloud cover and rainfall over Baghdad City, Iraq. Plant Arch., 20(1): 822-826.

Abbood, Z.M., Al-Taai, O.T. and Nassif, W.G. 2021. Impact of wind speed and direction on low cloud cover over Baghdad city. Curr. Appl. Sci. Technol., 21(3): 590-600.

Abood, Z. and Al-Taai, O.T. 2018b. Study of absorbance and emissivity solar radiation by clouds, aerosols, and some atmospheric gases. J. Appl. Adv., 3(5): 128-134.

Al-Taai, O.T. and Abbood, Z.M. 2020a. Analysis of convective available potential energy by convective and total precipitation over Iraq. Indian J. Ecol., 47: 263-269.

Al-Taai, O.T. and Abbood, Z.M. 2020b. Analysis of the convective potential energy by precipitation over Iraq using ECMWF data for 1989-2018. Sci. Rev. Eng. Environ. Sci., 29(2): 196-211.

Al-Taai, O.T. and Wedyan, G.N. 2020. Impact rainfall on the aerosol optical thickness over selected stations in Iraq. IOP Conf. Ser. Mater. Sci. Eng., 928(7): 072053.

Al-Taai, O.T., Abbood, Z.M. and Kadhum, J.H. 2021a. Determination stability potential energy of thunderstorms for some severe weather forecasting cases in Baghdad city. J. Green Eng., 11(1): 779-794.

Al-Taai, O.T., Hashim, S.A., Nassif, W.G. and Abbood, Z.M. 2021b. Interference between total solar radiation and cloud cover over Baghdad City. J. Phys. Conf. Ser., 2114(1): 012070.

Berrisford, P. 2009. The ERA-interim archive. ERA Rep. Ser., 1: 1-16.

Bryan, G.H. and Fritsch, J.M. 2000. Moist absolute instability: The sixth static stability state. Bull. Am. Meteorol. Soc., 81(6): 1207-1230.

Buell, C. 1943. The determination of vertical velocities in thunderstorms. Bull. Am. Meteorol. Soc., 24(3): 94-95.

Cooper, C.S., Sudarsky, D., Milsom, J.A., Lunine, J.I. and Burrows, A. 2003. Modeling the formation of clouds in brown dwarf atmospheres. The Astrophysical Journal, 586(2), 1320.

Eastman, R., Warren, S.G. and Hahn, C.J. 2011. Variations in cloud cover and cloud types over the ocean from surface observations, 1954–2008. J. Clim., 24(22): 5914-5934.

Hartmann, D.L. 2013. Observations Atmosphere and Surface, Climate Change 2013: The Physical Science Basis. Working Group I Contribution To The Fifth Assessment Report of the Intergovernmental Panel on Climate Change. Cambridge University Press, Cambridge, MA, pp159-254.

Mahdi, Z.S., Abbood, Z.M. and Al-Taai, O.T. 2021. Thunderstorm dynamic analysis based on total precipitation over Iraq. J. Eng. Sci. Technol., 16: 62–70.

Nassif, W.G., Al-Ramahy, Z.A. and Al-Taai, O.T. 2021a. Impact of rainfall and temperature on the frequency of dust storms for the period (1985-2018). AIP Conf. Proceed., 2372: 030005.

Nassif, W.G., Al-Taai, O.T., Mohammed, A.J. and Al-Shamarti, H.K.A. 2021b. Estimate probability distribution of monthly maximum daily rainfall of Iraq. J.Phys. Conf. Ser., 1804(1): 012078.

Nassif, W.G., Jaber, S.H., Naif, S.S. and Al-Taai, O.T. 2021c. Estimate of the dynamical change of air temperature, relative humidity, and dew point temperature for some selected station in Iraq. IOP Conf. Ser. Earth Environ. Sci., 910(1): 012010.

Nassif, W.G., Jasim, F.H. and Al-Taai, O.T. 2021d. Analysis of air temperature, relative humidity, and evaporation over Iraq using ECMWF reanalysis. Indian J. Ecol., 48(2): 446-452.

Nassif, W.G., Lagenean, F.H.S. and Al-Taai, O.T. 2022. Impact of vegetation cover on climate change for different regions in Iraq. J. Agrometeorol., 24(2): 138-145.

Sun, B., Groisman, P.Y., Bradley, R.S. and Keimig, F.T. 2000. Temporal changes in the observed relationship between cloud cover and surface air temperature. J. Clim., 13(24): 4341-4357.

Tierney, H.E., Jacobson, A.R., Beasley, W.H. and Argo, P.E. 2001. Determination of source thunderstorms for VHF emissions observed by the FORTE satellite. Radio Sci., 36(1): 79-96.

Tompkins, A. 2003. Impact of temperature and humidity variability on cloud cover assessed using aircraft data. Quart. J. Royal Meteorol. Sco., 129(592): 2151-2170.

Yamashita, M., Yoshimura, M. and Nakashizuka, T. 2004. Cloud cover estimation using multitemporal hemisphere imageries. International Archives of Photogrammetry Remote Sens. Spat. Inform. Sci., 35(7): 826-829.

Identification of Surface and Groundwater Interaction by Isotopic Hydrological Study - A Critical Review for Kelambakkam Region, Chennai, India

Surendar Natarajan† ⬥

Department of Civil Engineering, SSN College of Engineering, Kalavakkam-603110, Tamil Nadu, India
†Corresponding author: Surendar Natarajan; surendarn@ssn.edu.in

ABSTRACT

Due to the increase in population and urbanization, the availability of freshwater with standard quality to the human population is of great challenge. Recently there has been a demand for fresh water in surface and groundwater, so it is necessary to go for advanced isotopic techniques for identifying surface and groundwater resources. Isotopes are atoms of elements having the same atomic and different mass numbers. The isotopes found their wider application in water resources-related problems. The isotopes in water resources proved to be an effective tool in solving many critical hydrologic problems where conventional methods cannot be used due to their limitations. This research article discusses isotope application in water resources and focuses on different types of stable and unstable isotopes and their applications at Global and National levels. The methodology and research steps are proposed based on research gaps identified through various literature studies. The study will be conducted in the Kelambakkam zone, south of Chennai sub-urban. This research paper will discuss the sequential steps in identifying recharge and discharge mechanisms in study zones through stable isotopic techniques. The hydro-chemical analysis will also be done by measuring water quality in the Kelambakkam zone. The electrical resistivity survey for aquifer mapping will also be developed to identify the groundwater recharge zones. The proposed study will give complete information about recharge and discharge in the study area and recommend suitable groundwater harvesting structures.

INTRODUCTION

The isotopes in catchment hydrology were introduced around 1960 as an alternative tool to conventional hydrologic methods for identifying the water sources, origin, distribution, and the travel time taken for water to reach from one place to another place (Dansgaard 1964, Klauss & McDonnell 2013). In recent decades, isotopes have been used extensively in research on hydrology and water resources.

The stable oxygen and hydrogen isotopes are conservative tracers in hydrological studies (Hu et al. 2009). The stable and unstable isotopes detect the origin, flow patterns, and mixing of surface and groundwaters in hydrological studies (Zhang et al. 2005). The stable isotopes can be used up to 0.01 to 100 sq. km watersheds (Duarte Carlos 2017). The isotopes also renovate continental paleoclimatology and paleohydrology (Aaron et al. 2017). The travel time from surface to groundwater for present and future scenarios can be identified using isotopic techniques. Stable isotopes are

commonly used in field investigations and research projects to better understand hydrological processes (Elliott Arnold et al. 2018). Isotopes of oxygen and hydrogen also extend their application to vapor sources, atmospheric circulation, and paleoclimatic investigations (Westerhold et al. 2018). Recently in hydrological investigations, isotopes were used in phase transitions in the transport paths of water.

The stable δ^{18}O and δD in precipitation are controlled by atmospheric parameters such as temperature, relative humidity, evaporation, and moisture sources. The effects of geographic factors such as altitude and latitude are seen in meteoric water. The Tritium isotopes in hydrology differentiate groundwater's age and residence time. Meteoric water in various places will have various stable hydrogen and oxygen compositions. When meteoric water infiltrates the ground to form groundwater, the differences in isotopic compositions can be seen and used as a base for identifying groundwater resources. The isotopic fractionation also occurs when there is evaporation from seawater to inland precipitation, as it causes changes in the composition of hydrogen and oxygen in meteoric water (Gibson et al. 2016).

The linear relationship of meteoric water was developed by (Craig 1961), which is used as a reference line and a standard tool in isotopic hydrology research. The temperature, quantity of precipitation, height, sampling distance, and location from the sea are the influence parameters in isotopic characteristics at a particular location. The depletion and enrichment of isotopic characteristics are observed in higher and lower altitudes, known as the altitude effect.

Merits of Isotopic Techniques Over Other Tracer Techniques

Isotopes are the advanced tracer methods used for detecting water resources in the field of hydrology. Precipitation is input to surface and groundwater, so the isotopic composition of precipitation gives some knowledge on surface and groundwater interaction. The World Meteorological Organization (WMO), International Atomic Energy Agency (IAEA), and Global Network of Isotopes in Precipitation (GNIP) recognized isotopes as perfect tracers in hydrological studies. The limitations in isotopic studies are fractionation and evaporation, as it affects isotopic composition and characteristics, and their impact is seen in accurate water resources detection.

The aim of this paper is to discuss various isotopes used in hydrological studies. It also discusses isotope applications in precipitation, surface and groundwater interaction, recharge, and discharge in water sources. Based on the previous studies,

suitable stable isotopic techniques in the Kelambakkam zone are adopted for identifying surface and groundwater interactions. The study also deals with developing Local Meteoric Water Lines (LMWL) and spatial isotopic maps for various seasons, which has not been attempted in this study area so far. The electrical resistivity survey will be conducted to determine the aquifer thickness for proper groundwater modeling and management. The study also elaborates on the present situations of isotopic hydrology across the National and Global level, and the objectives are framed accordingly.

Objectives of the Study

- To study the isotopic signatures in precipitation of the Kelambakkam zone.
- To identify the surface, groundwater interaction, and groundwater resources of the study area
- To identify the origin and recharge of surface and groundwater in the Kelambakkam zone.

Need for the Study

The Kelambakkam zone comprises residential, IT, small-scale industries, education sectors, and agricultural fields (Fig. 1 & Fig. 2). The residential and industrial areas near Kelambakkam and Kalavakkam mainly depend upon lakes and nearby wells to supply fresh water for drinking and commercial purposes. So, it necessitates identifying the
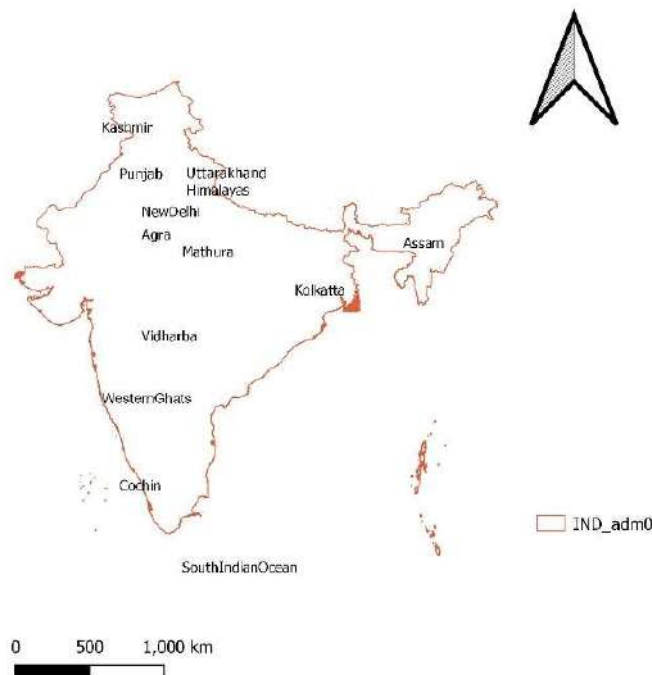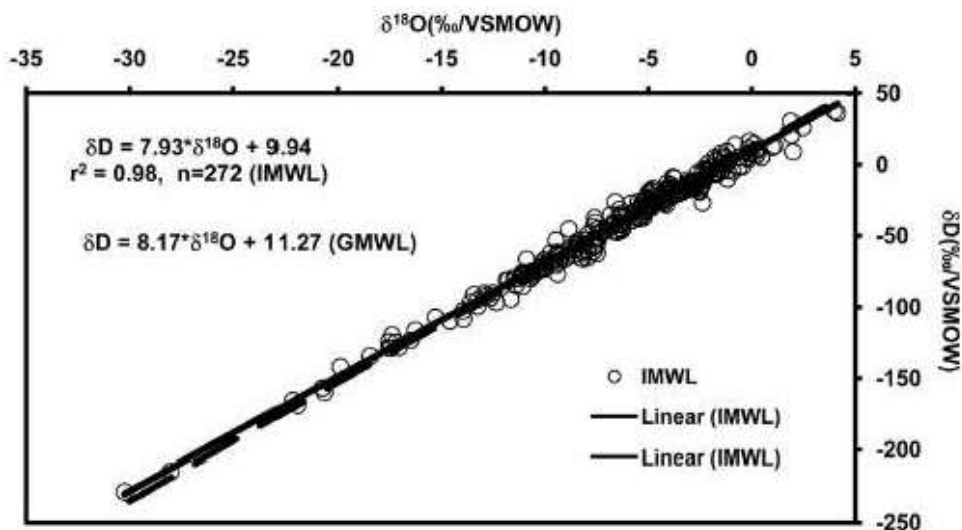

Fig. 1: Isotopic studies in India.

Fig. 2: Handbook for stable isotope data interpretation in India 2020.

water sources, occurrences, origin, recharge, and discharge in the Kelambakkam zone. The stable isotopes of oxygen and hydrogen will be used in the study area for identifying the surface and groundwater interaction.

The following research gaps have been noted from a detailed literature review, and it is to be sought for the present study:

- The study on isotopes in water sources is the first study conducted in the Kelamabakkam zone.

- To date, no studies in the Kelambakkam zone have been done using isotopic techniques to identify the surface and groundwater interaction.

- The spatial isotopic mapping and updated aquifer groundwater modeling will be done for the study area.

LIST OF STABLE AND UNSTABLE ISOTOPES USED IN WATER RESOURCES

Tritium

Tritium (T) or ^{3}H is a radioactive isotope of hydrogen (two neutrons and one proton) with a half-life of 12.32 ± 0.02 years. The Tritium concentration is measured by tritium units (TU). 1 TU is due to the presence of one tritium in 1018 atoms of hydrogen. Secondary neutron cosmic rays generate the natural atmospheric tritium by bombarding nitrogen (Zhou et al. 2016). The Tritium atom combines with oxygen, forms water, and then falls as precipitation. The nuclear tests carried out by various countries during the early 1960s also contributed to Tritium in the atmosphere. During the 1960s, Tritium content in the atmosphere was 2- 8 TU; in recent years, a drop in Tritium content has been seen

in the atmosphere (Duvert et al. 2016). Most of the tritium in the atmosphere is observed in surface water, and later its infiltration is seen on the groundwater table (Beyer et al. 2018). In isotopic hydrology, tritium is used to identify the groundwater recharge, movement, and mixing of water in the groundwater table. The Tritium concentration can also determine groundwater age (Jing et al. 2022).

Chlorine-36

Cl-36 is a cosmogenic isotope produced in the atmosphere by the spallation of 36 argon during interaction with cosmic ray protons. In a system of water resources, it enters groundwater through a wet deposition along with much more abundant stable Cl isotopes of (^{35}Cl and ^{37}Cl) from marine aerosols. Nucleogenic reactions in the sub-surface produce 36 Cl. The ^{36}Cl isotopes are used in measurements of dating very old groundwaters. The ^{36}Cl is also used to identify groundwater recharge and the distances of the recharge areas (Ram et al. 2021).

Ra Isotopes

The Radium has an element number of 88 in the periodic table, which belongs to Group IIA. The four naturally occurring radium isotopes are (^{224}Ra, ^{223}Ra, ^{228}Ra, and ^{226}Ra) continuously produced from the decay of their Th-isotopes parents of the U and TH decay series ^{228}Th, ^{227}Th, ^{232}Th, and ^{230}Th, respectively. The most abundant isotopes are ^{226}Ra from the ^{238}U with a half-life of 1600 y and ^{228}Ra from the ^{232}Th with a half-life of 5.8 y (Marc et al. 2017). The natural form of radium isotopes (^{223}Ra, ^{224}Ra, ^{226}Ra, and ^{228}Ra) are mostly used as geochemical tracers in marine environments. Initially, Ra isotopes were applied to study

open ocean processes, and their common application is in the marine environment. Ra isotopes are used to identify and quantify the Surface Ground Discharge. In addition, it also finds its application in groundwater and submarine studies. In marine environment studies, Ra isotopes act as a geochemical tracer. Traditionally, they used to trace land-ocean interaction processes. It also finds its application in assessing transit times in coastal aquifers, sediment–water interface, and the age of coastal surface waters.

Oxygen and Hydrogen

Oxygen-18 and Hydrogen (^{2}H) are stable isotopes present in water in abundance nature. These stable isotopes are used to trace water sources' origin, occurrence, and movement from the surface and groundwater (Bowen et al. 2012). The stable isotopic composition in water can also measure and modeled on a large scale. The change in the isotopic ratio of ^{2}H/^{1}H and oxygen ^{18}O/^{16}O in water gives an idea of the water source and its quality. The physical process like evaporation can change the δ values of isotopes from the original precipitation sources, which occurs over a surface. The change in δ values will be used for identifying the origin of rainwater, recharging from groundwater, and evaporation from the ponds. The change in δ values will be expressed as fractional deviation from a standard procedure called SMOW (Standard Mean Ocean Water). The change in δ value expression is given as $[(R_s/R_r) - 1] \times 1000 (‰)$, where R_s and R_r are the ratios of the abundances of the heavier isotope to the lighter isotope for the sample and reference standard, respectively. The common isotopes that can be used in water resources are listed in Table 1.

Table 1: Other common isotopes adopted in water resources.

Isotopes	Application
^{15}N, ^{11}B, ^{37}Cl, ^{87}Sr, ^{13}C, ^{34}S,	Pollution and contaminant sources identification
^{2}H, ^{18}O	Estimation of paleo-waters
^{2}H, ^{18}O	Estimating seepages and leakages from the dam
^{37}Cl	To identify the mechanism of salinization in water resources
^{87}Sr, ^{88}Sr, ^{34}S	Rock and water interactions
^{13}C, ^{223}Ra, ^{224}Ra, ^{226}Ra, ^{3}H, ^{87}Sr	In the identification of Sub-marine Groundwater Discharge
^{13}C, ^{3}H	Determining leachate from landfills
^{13}C, Ne, Ar, Kr, Xe	Groundwater monitoring and study in the permafrost regions
^{3}H	Hydrograph separation
^{85}Kr, CFC, ^{81}Kr, ^{35}S, ^{7}Be, Ne, He, ^{3}H, ^{13}C,^{39}Ar	For dating groundwater age

PROCEDURE INVOLVED IN CALIBRATION AND VALIDATION OF ISOTOPIC SIGNATURES

The International Atomic Energy Agency (IAEA) of Vienna, Austria, in collaboration with the World Meteorological Organization (WMO), established the Global Network of Isotopes in Precipitation (GNIP). The global precipitation samples were collected to monitor the isotopic composition of (δ^2H, δ^{18}O). The data produced by IAEA is an important asset to isotope hydrology (http://isohis.iaea.org). The δ^2H and δ^{18}O isotopic values are generally measured with standard references from Standard Mean Ocean Water (SMOW). The lower and high δ values represent the depletion and enrichment of isotopes. The other factors in the hydrological cycle, such as evaporation and condensation, also affect isotopic composition in water resources. The recharge and discharge processes also affect isotopic signatures due to different hydrogeological conditions.

The Global Meteoric Water Line (GMWL) shown in Equation (1) is developed from δ^2H and δ^{18}O. The deviation of the Local Meteoric Water Line (LMWL) from the GMWL gives information about recharge, discharge, evaporation, and geographical conditions.

$$\delta^2H = 8.17(\pm0.07)X\delta^{18}o + 11.27(\pm0.65) \quad …(1)$$

For Indian conditions, the Indian MWL is developed for the Northern, Southern, Western, and Eastern Himalayas. These lines are different for each region in India. The differences between the South Indian meteoric water line and the Northern Indian meteoric water line are their slope and d excess values as shown from equations (2-4). The variations in slope and d excess are mainly due to temperature, evaporation, and geographical conditions.

$$\delta^2H = 7.38(\pm0.21)\delta^{18}o + 8.03(\pm1.05)(n = 81,$$
$$r^2 = 0.94) \quad …(2)$$
$$\delta^2H = 7.98(\pm0.078)\delta^{18}o + 9.29(\pm0.679)(n = 134,$$
$$r^2 = 0.99) \quad …(3)$$
$$\delta^2H = 7.81(\pm0.17)\delta^{18}o + 11.14(\pm1.18)(n = 63,$$
$$r^2 = 0.97) \quad …(4)$$

In most cases in IMWL, there are not many differences in slope and intercepts since 70% of rainfall in India is during the monsoon season. The IMWL, when compared with GMWL, shows a difference in slope and intercept. These differences are mainly due to vapor sources during the Northeast and Southwest monsoons originating from the Bay of Bengal and the Arabian Sea. Altitude effects will also affect the isotopic signatures, mostly noted in western Himalayan regions. The lighter and heavier isotopes are

observed in rainfall at high and low altitude areas. The $\delta^{18}O$ and δ^2H will show positive in lower air temperatures and negative values in colder regions. The continental effect also influences the isotopic compositions.

International Status

The methodology and inferences globally regarding the isotopic studies are discussed in detail in Table 2

Table 2: International Status of Isotopic Hydrological Study.

In Globally	Methodology & Isotopic tools	Inference from the Study
South Africa- Soutpansberg, Limpopo Province (Olatunde et al. 2019)	$\delta^{18}O$ and δ^2H	Geochemical processes were studied from geothermal springs.
China- Heihe River Basin (HRB) (Zhao 2018)	($\delta^{18}O$, D, ^3H and ^{14}C)	The current and former relationships between precipitation, surface runoff, recharge in groundwater, and climate change was studied with the help of stable isotopic tools.
Lower Changjiang, Yangtze River (Li 2020)	Stable hydrogen and oxygen isotopes	The $\delta^{18}O$ shows much seasonal variation during the dry season and low during the flood season. The seasonal variation of $\delta^{18}O$ in the precipitation of the Changjiang basin is calculated based on long-term meteorological and hydrological data availability.
Rhone catchment area (France) (Jean-Baptiste et al. 2020)	Isotope geochemistry, water stable isotopes	The hydrological survey is conducted, and the isotopic signatures are identified in the flowing Rhone River.
Vosges Mountains North-eastern France (Viville et al. 2006)	^{18}O and lumped-parameter model	The water transit times are calculated by applying exponential piston and dispersion models to flow the PC program to isotopic input and output datasets.
Berlin, Germany (Kuhlemann et al. 2020)	Hydro-geochemistry	Sampling isotopes in precipitation, surface water, and groundwater are done for Berlin city on a spatial scale to detect the urban water cycle.
Vienna, Austria (Kern et al. 2020)	tracers, environmental isotopes, radioactive isotopes, deuterium, oxygen-18, tritium, radiocarbon	The groundwater origin, age, recharge, and flow direction between aquifers and characteristics were studied.
Wimbachtal, Germany (Paul et al. 2007)	Tritium and ^{18}O	Tritium and ^{18}O concentrations in precipitation and runoff were studied to identify groundwater recharge in Wimbachtal Valley.
Central, USA (Chao et al. 2018)	δ^2H, $\delta^{18}O$ and $\delta^{17}O$	The stable isotopes of oxygen and hydrogen were used as a natural tracers to understand hydrological and meteorological processes in the USA. The stable isotopic study shows that meteorological factors do not affect the 17O excess in rainfall and snowfall. The study also concludes that ^{17}O-excess also be used as tracers during evaporative conditions.
Budapest, Hungary (Polona & Zoltán 2020)	Stable (^{16}O, ^{17}O, ^{18}O, ^1H, ^2H) and radioactive isotopes (^3H).	The use of stable isotopes in the hydrological process is discussed on regional or local scales related to precipitation. The study also discusses surface and groundwater interactions, soil and xylem water, and geochemical process.
Northern Italy, Lake Frassino (Carlo et al. 2016)	Stable isotopes	The stable isotopic composition was studied in Lake Frassino (Northern Italy). The study analyzes palaeo-hydrological, lithological, malacological, and delineation of freshwater shells using stable isotopic signatures.
Central Italy (Tazioli 2017)	Tritium, stable isotopes	In their study, they discussed monitoring groundwater resources and water flow properties by using isotopic techniques. The study also concludes by identifying recharge areas in the Central part of Italy.
Central Srilanka (Edirisinghe 2014)	Stable isotopic compositions	The stable isotopes were used as effective tracers in detecting surface and groundwater interaction in Central Sri Lanka.
Kilauea Volcano area, Hawaii (Scholl et al. 1995)	Stable isotopes and Tritium	This study discusses the tracer methods and their application in determining Hawaii's Kilauea volcano's flow paths, recharge areas, and groundwater age.
British Isles (Darling & Talbot 2003)	Stable isotopes	The study identifies that the stable isotopic compositions are poorly characterized in the British Isles. It is one of the first studies of a major British river with monthly isotopic records.

Table Cont....

In Globally	Methodology & Isotopic tools	Inference from the Study
Siksik Creek in the Western Canadian Arctic (Doerthe 2017)	Arctic headwaters, isotopes	The data fusion modeling approach is adopted to determine the quantity and isotopic characteristics of the snowpack and its melted water. The soil moisture dynamics and active soil profile layer were also adopted in their study.
Wetlands, North Florida (Glynnis et al. 2020)	oxygen and hydrogen tracers	The stable water isotopes were used to identify the sensitivity and resolution in wetlands in North Florida. From the analysis, notable differences were observed in stable isotopic signatures of precipitation, surface, and groundwater in the forested wetlands of North Florida.
UAE (Ahmed 2009)	Deuterium excess	The stable isotopes and deuterium excess were used to identify groundwater recharge mechanisms in the Northwestern part of the Gulf of Oman and the Southeastern part of the Arabian Gulf. The origin of moisture from the Mediterranean Sea is also studied.
Canada, Mildred Lake Mine (Baer et al. 2016)	^{2}H and ^{18}O	Stable isotopes ^{2}H and ^{18}O are applied in mining water. The LMWL is developed to identify the precipitation characteristics at the mining site. The developed LMWL from this study can be used as a reference line for similar mines waters.

National Status

The isotopic studies regarding surface and groundwater in India are discussed in Table 3. The isotopic application in hydrological studies in India is shown in Fig. 1

MATERIALS AND METHODS

The methodology planned for the present study is shown in Fig. 3. The sequential steps in the study area selection, data collection, analysis, and calibration are discussed below.

Table 3: National level isotopic hydrological study.

National level	Isotopic tools	Inference from study
Western Ghats Mountain range, India (Kushank et al. 2019)	Deuterium excess, ^{2}H, ^{18}O	The hydrogeological nature of the western Ghats shows many influences in isotopic signatures. The derived local evaporation line also indicates that water resources are cascaded and depleted isotopic compositions are seen in the precipitation of Western Ghats, as shown in Fig. 2 The water resources were traced in the Western Ghats from the derived evaporation line and depleted isotopes.
Himalaya, Uttarakhand, India (Rai et al. 2017)	Environmental isotopes, tracers, stable isotopes, radioisotope	The 57 water samples were collected from 19 sites, and isotopic analysis was done using δ^{18}O, δ^2H, and ^{3}H isotopes. The isotopic analysis identified the new water seepage downstream of Lake Nainital in the Himalayan region. A Dual Inlet Isotope Ratio Mass Spectrometer (DIIRMS) and an Ultra-Low-Level Liquid Scintillation Counter (ULLSC) were used in measurements of stable isotopes (δ^2H and δ^{18}O) and a radioisotope (^{3}H) respectively.
Kolkata and New Delhi (Deshpande & Gupta 2012)	Stable isotopes	The isotopic signatures in the water resources of Kolkata and New Delhi were compared. The depletion in isotopic signatures observed in Delhi is due to the altitude effect of the Himalayas.
Agra and Mathura Cities Uttar Pradesh (Purushothaman et al. 2014)	Isotopes, Electrical conductivity	The surface water of river Yamuna and its influence on groundwater level were studied. The study concludes that Yamuna River water has a strong influence on Agra and Mathura's groundwater resources.
Western Himalayas (Kashmir) and Eastern Himalayas (Assam) (Ghulam & Deshpande 2017)	δ^{18}O and δ^2H	The precipitation samples were collected from the Western (Kashmir) and Eastern Himalayas (Assam) to study weather system disturbances and Indian summer monsoon characteristics in isotopic signatures. The isotopic analysis indicates a variation in isotopic signatures in the western and eastern Himalayas.

Table Cont....

| National level	Isotopic tools	Inference from study
Greater Cochin, Ernakulam district, Kerala (Aneesh et al. 2019)	δ D and δ^{18}O	The precipitation samples of Cochin were collected, and isotopic analyses were done to identify the isotopic variation in precipitation sources.
Vidarbha, Maharashtra (Noble & Ansari 2019)	Environmental isotopes	The stable isotope and electrical resistivity tools were used to identify the water resources in drought-prone areas of the Vidarbha region. The monsoon characteristics, groundwater recharge, and evaporation were also studied using environmental isotopes.
Western Himalayas, (Rai et al. 2016)	Stable isotopes	The stable isotopic studies in snow melt water and glaciers were studied in the cryosphere waters of Ladakh and Kashmir regions in the Western Himalayas.
Southern Indian Ocean (Rahul et al. 2017)	δ^{18}O and δ D	The stable isotopic composition in the seawater surface, water vapor, and rainwater were studied from the Indian Ocean to the South Ocean regions.
India to Antarctica (Tiwari et al. 2013)	δ^{18}O and δD	The discrete water mass from the Indian and Southern oceans was studied using stable oxygen isotopes. The study addresses the relationships between oxygen and hydrogen isotope and sea surface salinity.
Southwest (SW) Region of Punjab, India (Krishan et al. 2022)	Stable isotopes, electrical conductivity	The groundwater samples were collected from 142 piezometers at 40 sites for stable isotopic analysis in three regions of Punjab to find the root cause of salinity in the groundwater resources.
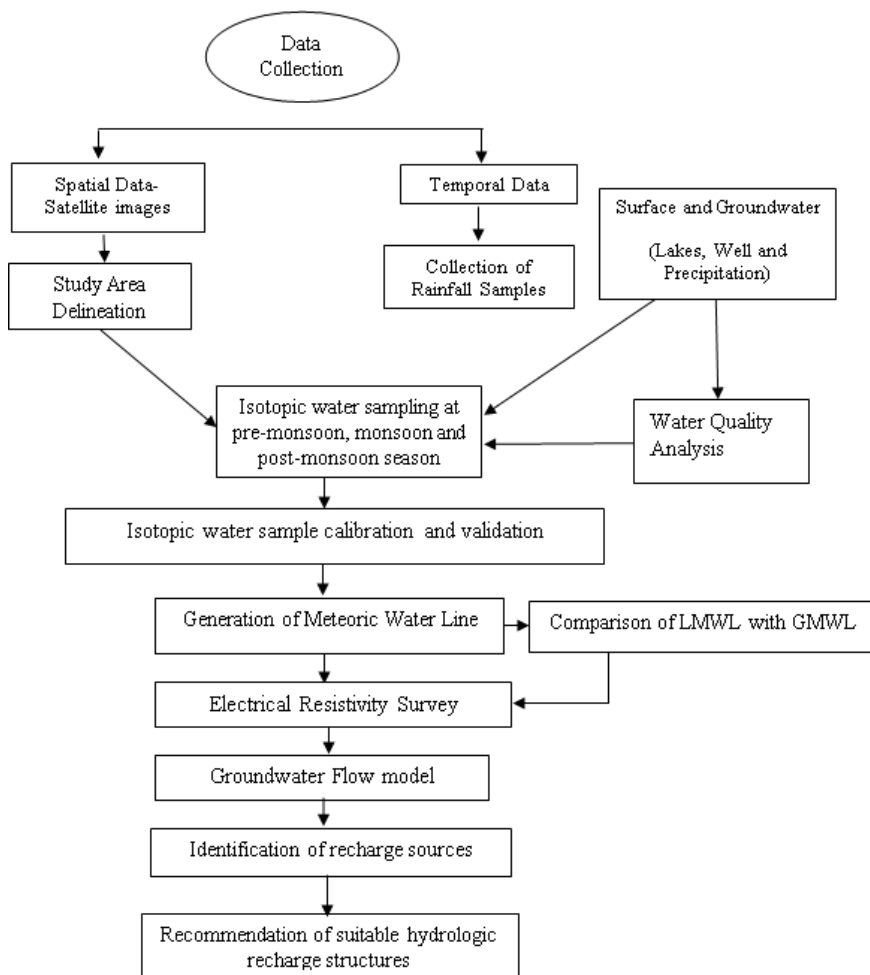
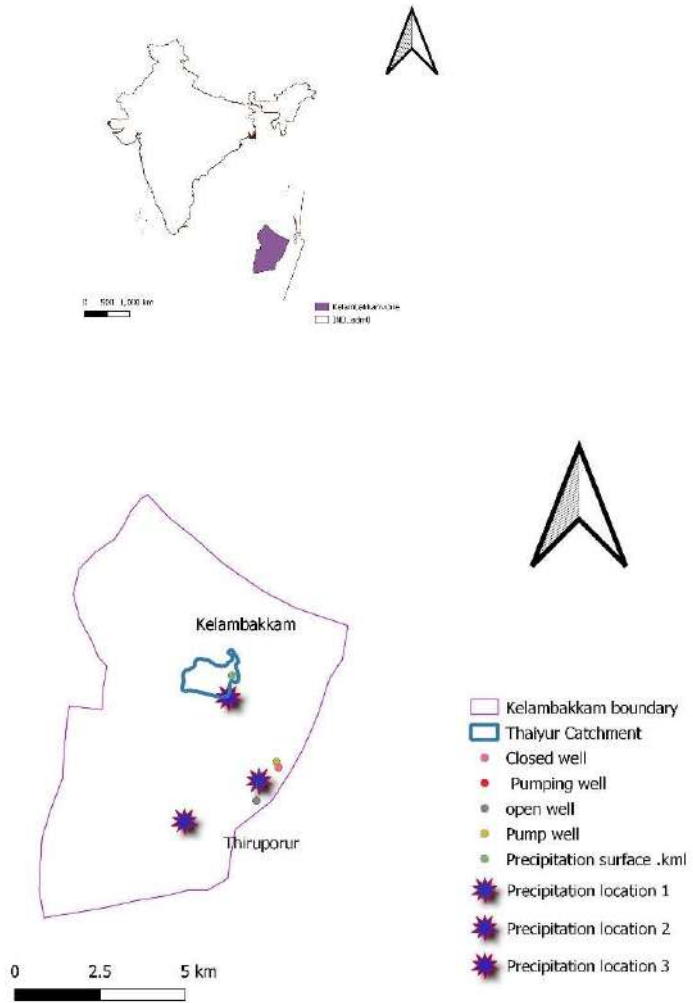Fig. 3: Methodology adopted for the proposed study.

Fig. 4: Location of the study area.

Fig. 5: Isotope ratio mass spectrometer (Isoprime, Micro mass, UK) (George & Gerogios 2020).

Fig. 6: Ultra-Low-Level Liquid Scintillation Counter (ULLSC) (Wolfango & Lauri 2004).

Study Area Geographic Details

Kelambakkam region is a sub-urban of Chennai city, as shown in Fig. 4. It is in the South-Eastern portion of Chennai along Old Mahabalipuram Road (OMR). It extends from a latitude and longitude of 12.48º N to 80.13º E. The Kelambakkam region covers an area of 11.44 sq.km with a surrounding coastline of 57 km. The population in the Kelambakkam region is 4 lakhs as of the 2011 census, and it is expected to be doubled by 2030. The average annual rainfall of Kelambakkam is 1007 mm. The maximum and minimum temperatures during summer and winter range

from 36.6ºC to 28.7ºC. Since Kelambakkam is located near the coastal parts, it receives copious rains based on seasonal patterns. The Southwest and Northeast monsoons are the major contributors of rainfall in the range of 36 % to 54%. The study area is underlain by formation dykes predominantly observed in Thiruporur and the East of Chengalpattu district. The notable hard rock aquifer with alluvial formation is observed in the Kelambakkam region with a good yield of 45-220 pm. The average Transmissivity (T) is 2 m.day^{-1} with permeability (k) of 0.5- 2.5 m.day^{-1}.

The depth of the groundwater level in this region is from 5 m to 12.5 m.

RESULTS AND DISCUSSION

Sequential Steps Involved in the Present Research Study

The steps involved in carrying out an isotopic hydrological study for the Kelambakkam zone are discussed in detail from step 1 to step 10.

Step 1	Source
Data Collection Spatial & Temporal	Satellite 1. Cartosat image of 2 m resolution to be procured from NRSC Hyderabad for generating spatial isotopic maps. 2. Meteorological data like temperature, humidity, and rainfall will be collected from the India Meteorological Department (IMD) portal.
Step 2 Water Sampling	Rainwater samples will be collected from selected Kelambakkam, Thaiyur, and SSN Campus locations for pre-monsoon, monsoon, and post-monsoon seasons. The surface water samples will be collected for pre-monsoon, post-monsoon, and monsoon seasons from Thaiyur Lake and its region. Groundwater samples were also collected from selected wells in the study area for pre-monsoon, monsoon, and post-monsoon seasons. The samples will be collected using 60 ml of high-density polyethylene bottles.
Step 3 Sampling Analysis	The collected samples will be analyzed for isotopic $\delta 18O$ and δ^2H signatures at the Isotopic Hydrologic lab in the Centre for Water Resources Development and Management at Calicut. The Dual Inlet Isotope Ratio Mass Spectrometer (DIIRMS), as shown in Fig. 5, will be used for δ^2H measurements. The Continuous Flow Isotope Ratio Mass Spectrometer (CFIRMS), as shown in Fig. 6, is used to measure $\delta^{18}O$ in water samples. The accuracy and precision measurement for $\delta^{18}O$ and δ^2H should be maintained around ±0.2% to ±0.06% respectively.
Step 4 Calibration	The samples' stable isotopic compositions of hydrogen and oxygen will be expressed using conventional delta notation relative to the Vienna Standard Mean Oceanic Water (VSMOW) in part per thousand. The VSMOW equation (5) is expressed as $$\delta(\%) = \frac{(R_{sample} - R_{standard})}{R_{standard}} * 1000 \qquad \dots(5)$$ R represents either $^{18}O/^{16}O$ or the D/H ratio
Step 5 Validation	The LMWL will be developed for the study area. The developed LMWL will be compared with the VSMOW line. The deviation of LMWL from the VSMOW line will identify the study area's evaporation, recharge, and discharge process.
Step 6 Spatial Maps	The isotopic spatial pattern maps for stable hydrogen and oxygen in the study area will be generated. The generated maps will identify the spatial patterns of isotopes in the Kelambakkam region.
Step 7 Identification of recharge sources	The study area's surface and groundwater interaction, recharge, and discharge locations will be spotted.
Step 8 Quality Analysis	The groundwater quality with respect to pre-monsoon, monsoon, and post-monsoon was also to be analyzed.
Step 9 Electrical Resistivity Surveying	The aquifer mapping and groundwater monitoring will be done through an electrical resistivity survey.
Step 10 Water Harvesting Structures	Suitable groundwater harvesting structures will be recommended in the places of surface and groundwater interactions in the study area.

CONCLUSION

Isotopes in hydrology emerged as a multidisciplinary field as they found their wider application in the hydrological cycle and water resources engineering. The advanced technologies in isotopic measurements have made it easy to measure isotopic signatures with improved accuracy. In present days' geospatial techniques with modeling methods were also used in the spatial prediction of isotopic signatures in water resources. The isotopes in hydrology are useful for identifying water sources, their origin, movement, distribution, and recharge mechanisms. Isotopes are not only used for quantitative measures but are also helpful in tracing groundwater contaminants in terms of quality measurements. The age and residence time of surface and groundwater can also be identified using isotopes.

This study proposes using environmental isotopes to identify precipitation characteristics, surface and groundwater resources, and their interactions. The study will discuss isotopic signatures in groundwater and identify the source of groundwater recharge in the study area. The hydro-chemical analysis will be done to check the seasonal patterns' influence on the water quality parameters. The electrical resistivity survey will be conducted to delineate the potential groundwater zones in the Kelambakkam region.

The study's outcomes will be the spatial pattern of isotopic signatures of surface and groundwater sources in the Kelambakkam region. The study of stable isotopic signatures in the study area will help identify water movement, distribution, and recharge sources. The aquifer mapping of the study area will give a clear insight into recharge and discharge mechanisms in the study region. From a clear understanding of groundwater dynamics in the study area, a suitable water-harnessing hydraulic structure will be recommended. The study will be useful to farmers and town planners for managing the groundwater resources in developing regions of the Kelambakkam zone. The proposed study can also be adopted in places of similar hydrological conditions.

ACKNOWLEDGMENT

REFERENCES

Aaron, F., Diefendorf, M. and Freimuth, E.J. 2017 Extracting the most from terrestrial plant-derived n-alkyl lipids and their carbon isotopes from the sedimentary record: A review. Organic Geochem.,103: 1-21. https://doi.org/10.1016/j.orggeochem.2016.10.016.

Ahmed, M. 2010. Evolution of isotopic compositions in groundwater of the area between the Gulf of Oman and the Arabian Gulf. Chin. J. Geochem., 29: 152-156. doi 10.1007/s11631-010-0152-4.

Aneesh, T.D., Reji, S., Ajit, T.S, Resmi, T.R., Archana, M.N. and Redkar, B.L. 2019. Stable water isotope signatures of dual monsoon precipitation: A case study of Greater Cochin region, south-west coast of India. J. Earth Syst. Sci., 128: 210. https://doi.org/10.1007/s12040-019-1234-2

Baer, T., Barbour, S.L. and Gibson, J.J. 2016. The stable isotopes of site-wide waters at an oil sand mine in northern Alberta, Canada. J. Hydrol., 541: 1155-1164. https://doi.org/10.1016/j.jhydrol.2016.08.017.

Beyer, M., Hamutoko, J.T, Wanke, H, Gaj, M. and Koeniger, P. 2018. Examination of deep root water uptake using anomalies of soil water stable isotopes, depth-controlled isotopic labeling, and mixing models. J. Hydrol., 566: 122-136, https://doi.org/10.1016/j.jhydrol.2018.08.060.

Bowen, G.J., Kennedy, C.D., Henne, P.D., and Zhang, T. 2012. The footprint of recycled water subsidies downwind of Lake Michigan. Ecosphere, 3(6): 53.

Chao, T., Lixin, W., Kudzai, F.K. and Broxton, W.B. 2018. Stable isotope compositions (δ2H, δ18O, and δ17O) of rainfall and snowfall in the central United States. Sci. Rep., 8: 6712, doi:10.1038/s41598-018-25102-7

Craig, H. 1961. Isotopic variations in meteoric waters. Science, 133: 1702-1703

Dansgaard, W. 1964. Stable isotopes in precipitation. Tellus, 16: 436-468.

Darling, W.G. and Talbot, J.C. 2003. The O & H stable isotopic composition of fresh waters in the British Isles. 1. Rainfall. Hydrol. Earth Sys. Sci.,7: 2. doi:10.5194/hess-7-163-2003

Deshpande, R.D. and Gupta, S.K. 2012. Oxygen and hydrogen isotopes in hydrological cycle: New data from IWIN national program. Proc. Indian Natn. Sci. Acad., 78(3): 321-331.

Doerthe, T. 2018. Using stable isotopes to estimate travel times in a data-sparse Arctic catchment: Challenges and possible solutions. Hydrol. Process., 32: 1936-1952.

Duarte Carlos, M. 2018. Stable Isotope (δ13C, δ15N, δ18O, δD) Composition and Nutrient Concentration of Red Sea Primary Producers. Frontiers in Marine Science., 5: 15-26. doi 10.3389/fmars.2018.00298

Duvert, C., Stewart, M.K., Cendón, D.I. and Raiber, M. 2016. Time series of tritium, stable isotopes, and chloride reveal short-term variations in groundwater contribution to a stream. Hydrol. Earth Syst. Sci., 20: 257-277. https://doi.org/10.5194/hess-20-257-2016

Edirisinghea, E. 2017. Spatial and temporal variation in the stable isotope composition (δ18O and δ2H) of rain across the tropical island of Sri Lanka. Isotopes Environ. Health Stud., http://dx.doi.org/10.1080/10256016.2017.1304936

Elliott Arnold, T., Aaron, F., Diefendorf, M., Katherine, H.F. and Allison, A.B. 2018. Climate response of the Florida Peninsula to Heinrich events in the North Atlantic, Quat. Sci. Rev., 194: 1-11. https://doi.org/10.1016/j.quascirev.2018.06.012.

George, K. and Georgios, T. 2020. Chemical Analysis of Food. Second Edition. Springer, Cham.

Ghulam, J. and Deshpande, R.D. 2017. Isotope fingerprinting of precipitation associated with western disturbances and Indian summer monsoons across the Himalayas. J. Earth Syst. Sci., 126: 108. https://doi.org/10.1007/s12040-017-0894-z

Gibson, J., Birks, S. and Yi, Y. 2016. Stable isotope mass balance of lakes: a contemporary perspective. Quat. Sci. Rev., 131: 316-328.

Glynnis, C.B., Johnny, M.G. and Yuch-Ping, H. 2020. Sensitivity of using stable water isotopic tracers to study the hydrology of isolated wetlands in North Florida. J. Hydrol., 580(124): 321, https://doi.org/10.1016/j.jhydrol.2019.124321.

Hu, H.Y., Wei-min, B., Tao, W. and Si-min, Q. 2009. Experimental study on stable isotopic fractionation of evaporating water under varying temperatures. Water Sci. Eng., 2: 11-18. https://doi.org/10.3882/j.issn.1674-2370.2009.02.002.

Jean-Baptiste, J., Corinne, L., Gal La, S. and Patrick, V. 2020. Water stable isotopes and volumetric discharge rates to monitor the Rhone water's seasonal origin. Heliyon, 6, https://doi.org/10.1016/j.heliyon.2020.e04376

Jing, M., Chunhui, L., Falk, H. and Rohini, K. 2022. A novel analytical model for the transit time distributions in urban groundwater systems. J. Hydrol., 10: 127379. 10.1016/j.jhydrol.2021.127379, 605, 127379.

Kern, Z., Hatvani, I.G., Czuppon, G., Fórizs, I., Erdélyi, D., Kanduˇc ,T., Palcsu, L. and Vreˇca, P.2020. Isotopic 'Altitude' and 'Continental' Effects in Modern Precipitation across the Adriatic–Pannonian Region. Water., 12: 1797.

Klaus, J.J. and McDonnell, M. 2013. Hydrograph separation using stable isotopes: Review and evaluation. J. Hydrol., 505: 47-64.

Krishan, G., Rao, M.S., Chaudhary, R., Singh, A. and Kumar, J.A. 2022. Isotopic assessment of groundwater salinity: A case study of the Southwest (SW) Region of Punjab, India. Water, 14: 133. https://doi.org/10.3390/w14010133

Kuhlemann L-M, Doerthe, Te, Chris, S. 2020. Urban water systems under climate stress: An isotopic perspective from Berlin, Germany. Hydrological Processes, 34: 3758-3776.

Kushank, B., Renie, T., Ankita, Y., Amey, D. and Supriyo, C. 2019. Hydrological linkages between different water resources from two contrasting ecosystems of western peninsular India: a stable isotope perspective. Isotopes Environ. Health Stud., 121: 16666. doi 10.1080/10256016.2019.1666121

Li. X. 2020. Seasonal variability of stable isotopes in the Changjiang (Yangtze) river water and its implications for natural climate and anthropogenic impacts. Environ. Sci. Eur., 32: 84. https://doi.org/10.1186/s12302-020-00359-w

Marc, C., Valentí, R., Albert, F. and Jordi, G. 2017. Constraining the temporal variations of Ra isotopes and Rn in the groundwater endmember: Implications for derived SGD estimates. Sci. Total Environ., 595: 849-857, https://doi.org/10.1016/j.scitotenv.2017.03.005.

Noble, J. and Ansari, M.A. 2019. Isotope hydrology and geophysical techniques for reviving a part of the drought-prone areas of Vidarbha, Maharashtra, India. J. Hydrol., 570: 495-507.

Olatunde, S.D, Mike, B., Ekosse, G.E. and Odiyo, J.O. 2019. Hydrochemical Processes and Isotopic Study of Geothermal Springs within Soutpansberg, Limpopo Province, South Africa. Appl. Sci., 9: 1688. doi:10.3390/app9081688

Paul, D., Skrzypek, G. and Fórizs, I. 2007. Normalization of measured stable isotopic compositions to isotope reference scales –a review. Rapid Commun. Mass Spectr., 21: 3006-3014.

Polona, V. and Zoltán, K .2020. Use of water isotopes in hydrological processes. Water, 12: 2227. doi:10.3390/w12082227

Purushothaman, P., Someshwar, R. and Rawat, M.Y.S 2014. Evaluation of hydrogeochemistry and water quality in Bist-Doab region, Punjab, India. Environ. Earth Sci., 72: 693-706. https://doi.org/10.1007/s12665-013-2992-9

Rahul, P., Prasanna, K., Prosenjit, G., Anilkumar, N. and Kei, Y. 2017. Stable isotopes in water vapor and rainwater over the Indian sector of the Southern Ocean and estimation of the fraction of recycled moisture. Sci. Rep., 8: 7552 doi:10.1038/s41598-018-25522-5

Rai, S.P., Renoj, J., Thayyen, P., Purushothaman, B. and Kumar, M. 2016. Isotopic characteristics of cryospheric waters in parts of Western Himalayas, India. Environ. Earth Sci., 75: 600. doi.10.1007/s12665-016-5417-8

Rai, S.P., Singh, D., Ashwani, K.R. and Bhishm, K. 2017. Application of environmental isotopes and hydrochemistry in the identification of the source of seepage and likely connection with lake water in Lesser Himalaya, Uttarakhand, India. J. Earth Syst. Sci., 126: 118. https://doi.org/10.1007/s12040-017-0889-9

Ram, R., Burg, A. and Eilon, M.A. 2021.The Nubian sandstone aquifer in the Sinai Peninsula and the Negev Desert: The many facets of Israel. Hydrogeology, 30: 115-141.

Scholl, M.A., Ingebritsen, S.E., Janik, C.J. and Kauahikaua, J.P. 1995. An isotope hydrology study of the Kilauea volcano area, Hawaii. Water Resour. Invest. Rep., 95: 4213

Tazioli, A. 2017. Does the recharge area of a spring vary from year to year? Information from the water isotopes. Ital. J. Eng. Geol. Environ., 2: 16-25.

Tiwari, M., Siddhesh, S.N., Thammisetti, K., Drishya, G., Parvathy, R.K. and Sivaramakrishnan, R. 2013. Oxygen isotope–salinity relationships of discrete oceanic regions from India to Antarctica vis-à-vis surface hydrological processes. J. Marine Syst., 113-114: 88-93.

Viville, D., Ladouche, B. and Bariac, T. 2006. Isotope hydrological study of mean transit time in the granitic Strengbach catchment (Vosges massif, France): application of the Flow PC model with the modified input function. Hydrol. Process., 20: 1737-1751.

Westerhold, T., Röhl, U., Wilkens, R.H., Gingerich, P.D., Clyde, W.C. and Wing, S.L. 2018. Synchronizing early Eocene deep-sea and continental records—Cyclostratigraphic age models for the Bighorn Basin Coring Project drill cores. Clim. Past., 14(3): 303-319. https://doi.org/10.5194/cp-14-303-2018

Wolfango, P. and Lauri, K. 2004. Surface and underground Ultra Low-Level Liquid Scintillation Spectrometry. Radiocarbon, 46(1): 97-104.

Zhang, X.P., Tian, L.D. and Liu, J.M. 2005. Fractionation mechanism of stable isotope in the evaporating water body. J. Geogr. Sci., 15(3): 375-384. doi:10.1360/gs050312

Zhao, L. 2018. Origin and residence time of groundwater based on stable and radioactive isotopes in the Heihe River Basin, north-western China. J. Hydrol. Region. Stud., 18: 31-49.

Zhou, J., Zhang, Y., Zhou, A., Cunfu Liu, H. and Yunde, L. 2016. Application of hydrochemistry and stable isotopes (δ34S, δ18O, and δ37Cl) to trace natural and anthropogenic influences on the quality of groundwater in the Piedmont region, Shijiazhuang, China. Appl. Geochem., 71: 63-72. https://doi.org/10.1016/j.apgeochem.2016.05.018.

A Master Plan Realization for an Integrated and Sustainable Management System for Household and Similar Wastes in Morocco's Landfills by Sizing a Methanation and Composting Unit

Akram Farhat*†, Ayoub Aziz*, Kaoutar Lagliti* and Mohammed Fekhaoui*

*Mohammed V University, GEOPAC research center, Scientific Institute Av. Ibn Batouta, B.P 703, 10106 Rabat, Morocco

†Corresponding author: Akram Farhat; akram.frht@gmail.com

ABSTRACT

This work is a decision support contribution in Morocco's household and similar waste management. This management based on total waste landfilling leads to several environmental impacts, such as the use of large land areas, also the gaseous pollutants released, such as methane. Our first action was to collect reference data on the composition of this waste through a physicochemical characterization in the landfill in the city of Mohammadia. We sorted the waste generated by four types of populations with different living standards. A quantity of 500 to 2315 kg was treated, which allowed us to classify the household waste studied into nine main components. The sorting results are (organic matter 54.94%, plastic 15,18%, paper and cardboard 9,72%, textiles 7,46%, sanitary textiles 5,82%, metals 2,20%, glass 1, 89%, Wood 1,82% and Other 1,28%). Thus, these results revealed organic matter dominance and an increase in the plastic rate, which did not exceed 8% in the past. Added to this, the physicochemical parameters results are (volatile matter 60,26%, Humidity rate 59,05%, a total organic carbon (TOC) 33,47%, and a lower heating value (LHV) 1840,3 kcal.kg^{-1}). From these data, we can easily deduce that installing a sorting platform with a methanation and composting unit is the most suitable choice for recovering our waste. Therefore, we have chosen the methanation technology that meets the results obtained (dry batch and mesophilic) and sized this unit to assess its electricity production capacity that can be produced in our landfills. We carried out a scenario with a load factor of 0,9 and an electrical efficiency of 39%. The study results are 9 digesters to be built, 6.700 MW.y^{-1} of electrical energy produced, 14.523 tons.y^{-1} of refined compost, and 2.128.680 m^3.y^{-1} of biomethane produced. By offering our own integrated and sustainable management system for household and similar waste, we have connected the landfill bins and the digesters to the same motor to avoid biogas leaks from the bins to the atmosphere and increase electrical efficiency by controlling the gas flow.

INTRODUCTION

The demographic growth that we are experiencing today requires urban expansion and industrial and socio-economic development at extraordinary rates. This impacts our lifestyles and makes us always push towards more consumption. Therefore, more waste is generated, particularly household and similar waste (HSW). According to the World Bank, in 2012, we generated 1,2 kg of waste per person per day, reaching 1,42 kg per person in 2025 (Hoornweg & Bhada-Tata 2012). Thereby, managing this waste represents a real challenge for all societies on Earth.

The planet is going through a critical stage with global warming conditions strongly linked to greenhouse gas (GHG) emissions. Despite the compromises adopted in 2015 at the Paris Climate Conference to limit the rise in temperature below 2°C, scientific evidence indicates that average temperatures are already reaching more than a one-degree increase in pre-industrial level (CLIMAT.BE 2018). The main cause of this phenomenon is the carbon dioxide emission. But there are also other gases, such as methane, which remain part of this major problem. With its warming power exceeding that of carbon dioxide by more than 20 times (EPA 2018), it is necessary to know that waste management is ranked among the four most important sources of its emission (Pierini & Ratto 2015).

HSW management requires many economic means and scientific and technological know-how, which developing countries (DCs) unfortunately do not have. Consequently, the environmental and economic impact of this lack of

management results in life quality and public health deterioration. This has prompted these countries to take this problem very seriously by copying solutions that seem most suited to the nature of their waste. Despite this, these efforts did not lead to satisfactory results. Nevertheless, they proved the importance of focusing on the local context to create and adapt management systems and models.

In Morocco, controlled landfills are the national household waste program (NHWP) axis. This Program consists of ensuring the collection and cleaning of household waste to achieve a collection rate of 100% in 2022, carrying out controlled landfills for all urban centers, rehabilitating all existing wild dumps, developing the "sorting-recycling-recovery" sector to reach a recycling rate of 30% in 2030, generalize the master plans for all the provinces of Kingdom and train and sensitize all concerned actors. However, the targeted recycling and recovery rate will not reduce the severity of environmental impacts. The direct burial of our waste, which is very humid and organic, leads to methane emissions and too much leachate. Above all, we must change the landfill every 25 or 30 years. For this, Morocco must engage in a more innovative and daring approach to achieve the objectives of the NHWP.

This work falls within this perspective. The approach that motivates its development is realizing a system characterized by energy and financial autonomy in integrated and sustainable management (ISM). The term sustainability implies three dimensions: social, economic, and environmental. Its objective is to respond effectively to the many questions raised by implementing an ISM of HSW adapted to the specificities of our country.

Based on the physicochemical characterization of HSW, sizing of a methanation and composting unit, and based on some enlightening international experiences, this work provides four main elements of framing:

- The need to comply with the principles governing a desired integrated and sustainable waste management. In this sense, landfilling, however, controlled, is relegated to the status of an ultimate solution.

- The comparison between the different sectors and technologies must be multi-criteria and be based on all the aspects related to them. Without being limited to simple investment and operating costs, it must consider all the components: landfill lifetime, environmental risks, socio-economic impacts, etc.

- With more than 50% organic matter and 60% humidity in our household waste, we think directly of methanation, biogas, and composting as key elements for integrated and sustainable household waste management. In this sense, the sizing of a dry mesophilic anaerobic digestion and composting unit has been carried out.

- Dealing with the waste problem must rely on several treatment or disposal channels and ensure complementarity between these techniques (Yemadje 2013). In this sense, a management master plan with a technical feasibility study is carried out.
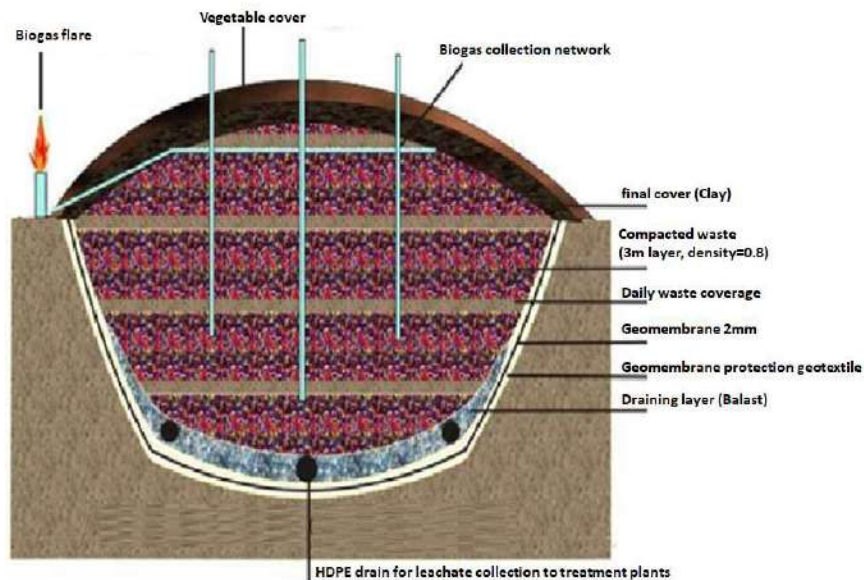

Fig. 1: Biogas Extraction directly from burial bins in controlled landfills.

THE GENERAL CONTEXT ANALYSIS AND BASIC DATA

The controlled landfill solution alone does not fit in efficiency or sustainability; it is considered an ISM system for HSW. We end up with large quantities of biogas seeking to spread into the atmosphere causing significant damage (Wellinger et al. 2013).

To solve this problem, decision-makers in my country have chosen to install duct systems and pipe networks to recover this biogas (Fig. 1).

The recovered biogas is sent to flares (wasteful), in the best of cases, as at the landfill of the city of Oujda, a combustion engine is installed to produce electricity.

This last solution has shown real potential for efficiency and profitability. However, we are faced with two major problems:

- Failure to control the amount of biogas produced.
- The fluctuation during the day of the biomethane rate composing this biogas.

As a result, we realized that we could never improve these two conditions by remaining dependent on landfill bins. Thereby, the addition of digesters becomes obvious to guarantee control over the necessary quantities of biogas and to eliminate the fluctuations of biomethane during the day if we want to maximize the performance of the cogeneration unit.

Today the HSW are directly buried after a mechanical treatment limited to compaction during the burial.

Subsequently, the biogas is sucked by a pump to power a cogeneration engine to consume the biomethane that accumulates in the landfill compartments (Fig. 2).

As shown in Fig. 2, in a system of direct burial and biogas recovery from landfill bins, we are always:

- Limited quantity and quality of the CH4 used caps our electricity production and forces us to stabilize the engine on a moderately low output. Of course, this increases the production rate of other harmful gases.
- Depending on the seasons and the nature of the buried waste, which negatively impacts the triggering of the microbiological movement responsible for methanation.
- Limited if we want to optimize and improve the technical and financial performance of the unit. We cannot hope for an extension of the existing installation.
- Subjected to the production of excessive quantities of leachate for which we have neither the budget nor the technology to treat it.

To better understand the impact of these limitations and dependencies, an analysis was carried out on a cogeneration engine in a landfill that had 850 kWh of power and 39% efficiency. Table 1 shows the difference between what should be (simulation of normal operation) and what is produced in the landfill (actual production):

The difference between our calculations and reality is only the stability of our biogas source and the biomethane rate containing this gas. In the landfill, they are forced to lower the power and reduce the yield to not exhaust the
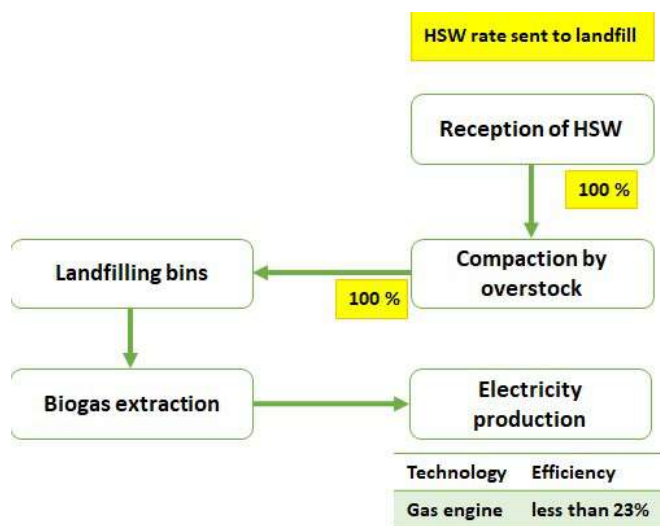

Fig. 2: Direct burial and biogas extraction from the landfill bins at the TLC in Oujda city.

Table 1: Engine output (reality) and output capacity (simulation) differences.

		Reality	Simulation
Electric power	KWh	500	850
Energy production per day	MWh	7,5	13,6
Yield achieved	%	23	39
Working hours	Day	15	16
Lower calorific value of Biomethane	kWh.m^{-3}	4,98	5,98
The biomethane amount per day	m^3.day^{-1}	6.548	5.802

Table 2: Average Rates of each recyclable fraction (Farhat et al. 2021).

Physical component	Average rates [%]
Fermentable waste	54,94
Plastics and rubber	15,18
Paper and cardboard	9,72
Textiles	7,46
Glasses	1,89
Metals	2,20
Wood	1,82

Table 3: Results of the physicochemical characterization of HSW (Farhat et al. 2021).

Chemical parameters	Value
pH	6,5
Density in the TLC [T.m^{-3}]	0,82
Humidity level [%]	59,05
TOC [%]	33,47
Volatile matter %]	60,26
Ashes [%]	39,74
LHV [kcal.kg^{-1}]	1840,3

landfill compartments and to produce all year round, even at 23% yield.

Based on the results of this analysis, we can easily deduce and frame the points for improvement and the objectives to be achieved by setting up our biogas recovery unit at the heart of landfills. This boils down to:

- Improving the efficiency and operating time of the cogeneration engine by controlling the quantity and quality of biogas produced.

- Improving the recycling rate of non-organic matter to reduce the landfilling rate of waste in the TLC and extend the lifetime of our landfills.

- The choice of the methanation process that best adapts to the nature of our waste to improve the biogas production and reduce the landfilling rate.

- Using a composting process for digestate recovery after methanation and diversifying the income sources for our TLC.

Basic Data

To develop an integrated and sustainable management system for household waste, the first thing to know is the physicochemical composition of this waste. The sampling operation must be representative and the sorting very selective to know the paths to follow while developing the sorting and recycling unit for non-organic matter (Sidi 2006).

The rate of organic matter, humidity, and pH will help us decide on the efficiency of methanation and the technology to use (Mata-Alvarez 2003). The lower calorific value will allow us to decide the incineration efficiency.

Tables 2 and 3 give us the rate of the physical components and the chemical parameters we need to carry out our plan.

From the results in Table 2, it is clear that organic matter is dominant. Thus, our plan should focus on recovering this organic part which exceeds 54% of all waste. But it should also be noted that plastic and cardboard represent more than 24% in a total of 38% of recyclable and non-organic matter.

Selecting a wet system is excluded from the analysis because this technology only accepts biomass with a maximum dry matter content of 15%. In comparison, the dry matter content of household organic waste is usually between 20 and 31%. The dominant organic matter, the pH and humidity, respectively at 6,5 and 59%, give us the certainty of the effectiveness of a dry and mesophilic discontinuous anaerobic digestion plan (Mata-Alvarez 2003).

The lower calorific value is average and insufficient to discuss an incineration block in our ISM system (Harzevili & Hiligsmann 2017). This value far exceeds the average of developing countries and is positioned in the range of industrial countries (1500-2700 kcal.kg^{-1}) (Yemadje 2013). This high LHV is due to a relatively high rate of plastic (15.18%).

MASTER PLAN FOR AN ISM SYSTEM FOR HSW AT LANDFILLS IN MOROCCO

After the physicochemical characterization and methanation process choice, we can present our ISM system, which has the following objectives: the extension of the landfills lifetime, the use of the stored biogas in the bins landfilling to avoid its spread in the atmosphere, making the landfill income-generating, as well as total energy autonomy. As shown in Fig. 3, our ISM system is based on inorganic matter
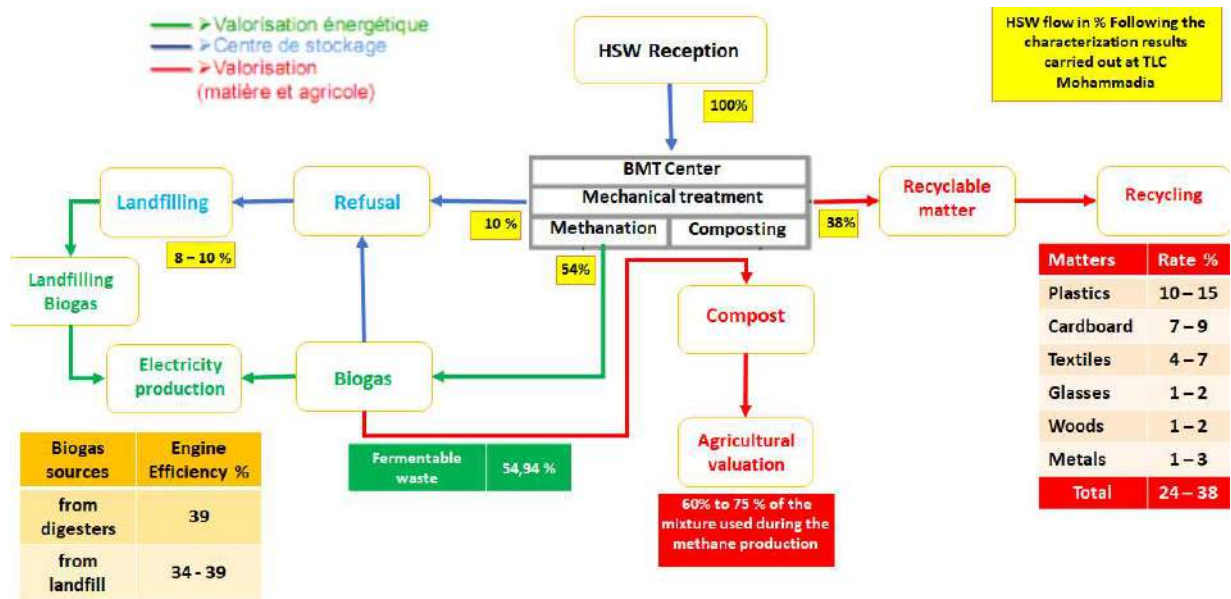
Fig. 3: ISM system with inorganic matter recycling, biogas recovery into electricity, and digestate transformation.

recycling, the methanation of organic fraction of household waste (OFHW), and the digestate composting generated after methanation.

The above system is a set of an ISM's most efficient municipal waste management processes. It focuses on reducing the rate of waste sent to landfill, starting with manual sorting of inorganic materials from HSW, allowing a recycling rate between 24 and 38%. Electricity production is ensured by transforming the biogas produced in our digesters and the landfilling bins (Fig. 4). Thus, OFHW is consumed in its entirety by our methanation and composting processes to further reduce the landfill rate.
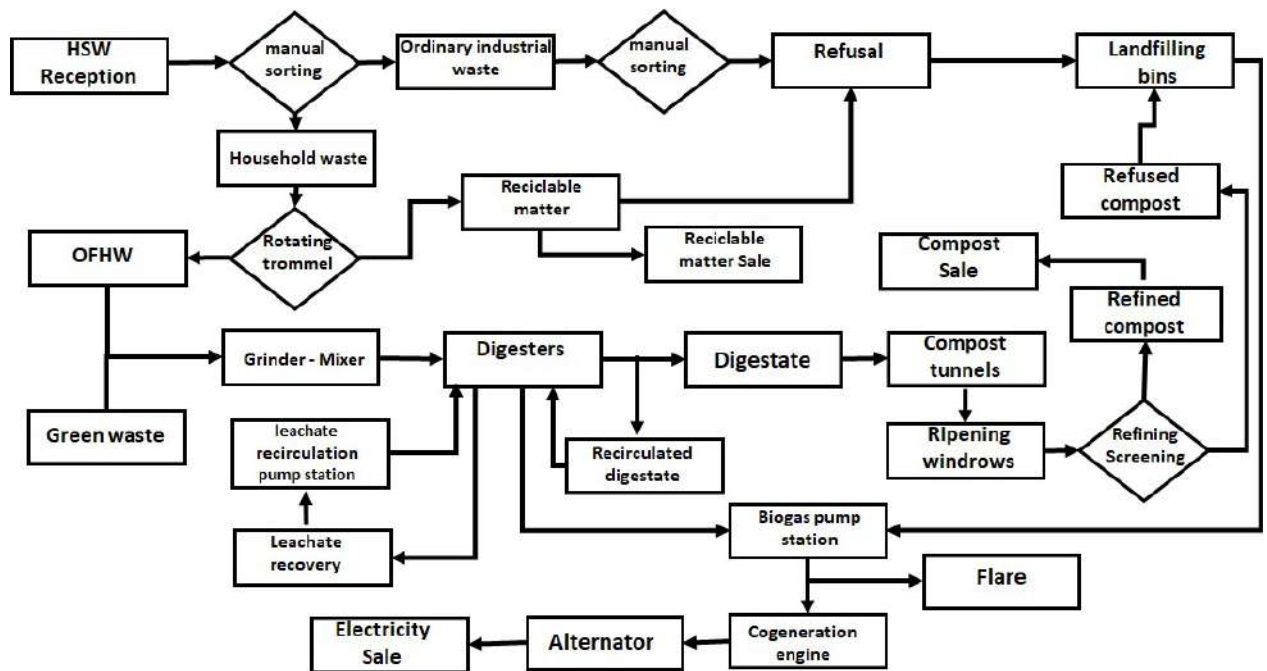

Fig. 4: Block diagram of the HSW recovery and recycling unit to be installed in our TLC.

This system gives us the possibility of recovering the shortcomings present in the management of our landfills and allows us to:

- Extending our landfill's lifetime by limiting the landfilling rate to 20% (maximum) of the waste quantities sent to burial.

- Improving biogas quality produced and increasing CH_4 quantity compared to harmful gases such as H_2S.

- Extracting and recovering the biogas accumulated in the landfill bins to prevent it from spreading into the atmosphere.

- Maximizing energy efficiency, and therefore improving our electricity and thermal production.

- Free our municipalities from the costs of processing and burying HSW through our ISM system's total energy and financial autonomy.

- Limiting the leachate quantities sent to recovery ponds.

HSW Sorting and Conditioning Unit

After receiving the HSW at the TLC, the sorting operation begins with manual sorting to collect all that is visible, large, and reachable, with the help of a loader-turner which turns all of this waste a few times. To reveal what remains buried at the bottom of the heap. After this initial sorting, non-hazardous industrial waste goes directly to landfill. Household waste is sent to the work-bag machine, then to the rotating trommel to continue the sorting operation (Fig. 5).

After the plastic bag shredding operation, the sorting team removes the rest of the large materials to pass the household waste through the rotating trommel. A second manual sorting team is positioned around the conveyor to scoop up what escaped the first team before the waste arrives at the trommel. The rotating screen with different meshes separates the waste according to its size. Waste with a diameter greater than the mesh constitutes rejects or a large organic fraction which will need additional grinding to make it homogeneous.

Smaller diameter waste will continue to a second manual sorting platform provided by another sorting team to recover all of the recyclable material and let the OFHW pass. this FODM at the end of the sorting operation is sent to a mixer. A percentage of green waste is added to this fraction, then mixed and transported to the digesters.

Methanation Unit

This process implements dry anaerobic fermentation through a concrete garage system with a steel overhead door. The number of tunnels can be adjusted according to the deposit. To obtain
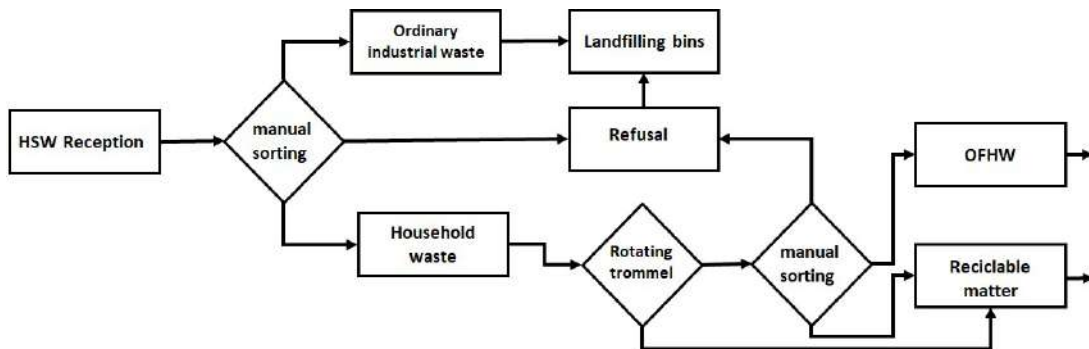

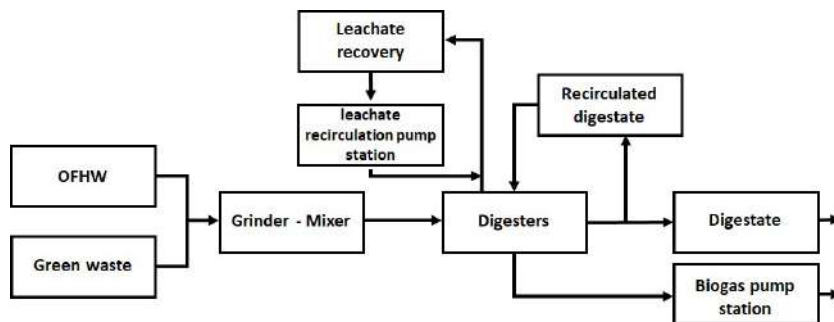Fig. 5: Block diagram of the waste recycling unit received at the TLC.

Fig. 6: Block diagram of the methanation unit of OFHW mixed with green waste.

Table 4: Calculation of the gross energy upstream of the engine and its quantity of substrate required from landfilling bins and the methanation digesters.

Energy balance		Landfill	Digesters
Electricity produced	KWh	850	850
Electrical efficiency	%	39	39
Operational hours	h	8	16
Energy produced per day	KW.day^{-1}	6.800	13.600
The engine's upstream energy	KW.day^{-1}	17.435	34.871
Organic fraction required to produce this energy			
Average biomethane content in biogas	%	50	60
LCV of biomethane	KWh.m^{-3}	4,98	5,98
The biomethane amount per day	m^3.day^{-1}	3.501	5.831
The biogas amount per day	m^3.day^{-1}	7.002	9.718
The biogas amount per ton of HSW	m^3.ton^{-1}	100	90
The substrate amount needed per day	ton.day^{-1}	70	108
The substrate amount needed per year	ton.y^{-1}	25.550	39.420

fresh matter, 15% of green waste is added to the total quantity of organic waste. To speed up the methanation process, 40% of the garage is filled with digestate, and the rest with fresh waste to be methanized (Fig. 6). The process is carried out under mesophilic conditions at 37°C for approximately four weeks. The percolate recirculation carries out a watering of the matter during the process recovered and heated to 37°C.

Sizing of the Biogas Unit

The dimensioning of our basic unit and the calculation of the number of digesters to be used are conditioned by the maximum power of our cogeneration engine.

To ensure the engine's functioning with its maximum efficiency using the biogas from the landfill, the quantity required upstream of the engine must be calculated (Table 4).

The results in Table 4 confirm the possibility of running the engine at full speed for 8 h.day^{-1} all year round with the biogas extracted from the landfill. Also, the table gives us the quantity of substrate necessary with which we can start our anaerobic digestion unit sizing and calculate the number of digesters to be built. Table 5 gives us the quantities needed to start our methanation process:

To calculate the number of digesters needed, we must

Table 5: Matter quantity needed to start the methanation process.

Used matters		Quantity
Organic fraction	ton.y^{-1}	33.507
15% Additional green waste	ton.y^{-1}	5.913
Total fresh matter	ton.y^{-1}	39.420
40% Recirculated digestate	ton.y^{-1}	26.280
Substrate	ton.y^{-1}	65.700

know the filling time and the number of cycles per year for each digester. The filling rate is 80%, and the substrate minimum density is 0,67 ton.m^{-3}. Tables 6 and 7 show the calculations made:

To calculate the cycle number carried out by a single digester during a year, we must first know the duration of a single cycle.

The number of digesters required is obtained by dividing the total volume of the substrate by the useful volume of a digester and the number of cycles at the same period (Table 8).

Composting Unit

The digestate obtained from the methanation of organic waste

Table 6: The volume of substrate for the methanation process.

		Data
The digester volume	m^3	980
the substrate amount	ton.an^{-1}	65.700
Density	ton.m^{-3}	0.67
Substrate volume per year	m^3.y^{-1}	98.060
Substrate volume per day	m^3.day^{-1}	269
filling time of digester per day	day	4

Table 7: Number of cycles per year carried out for a single digester.

	Data
Filling time (days)	4
Residence time (days)	28
Emptying time (days)	1
Digestion cycle time (days)	33
Cycles number of a single digester	11

Table 8: The digesters number calculation for 1 year of substrate.

		Data
Volume of substrate	$m^3.y^{-1}$	98.060
The digester volume	m^3	980
Cycles number per digester		11
Digesters Number		9

should undergo an aerobic process, such as composting, to improve its characteristics and efficiency during use. Green waste is added and mixed with the digestate before being introduced into composting tunnels (Fig. 7). The added green waste corresponds to 40% of the digestate volume (BEKON 2018b).

The process begins by mixing the digestate from the methanizers and the added green waste. Then the mixture is deposited in composting tunnels. We leave it in these tunnels for 10 days. Then, they are transported and deposited as windrows for 60 days for the maturation of the compost. During this period, the windrows are turned using a windrow turner to ensure oxygenation and inactivation of microorganisms still present in the compost before the last screening. The finished compost goes through a refining stage which consists of grinding the large particles to ensure the homogeneity of all the compost produced (Moletta 2009).

To calculate the tunnel number, the same methodology is applied as that carried out previously for calculating the digesters' number. Thus, the starting data is shown in Table 9.

The composting tunnel dimensions also depend on the BEKON (2017) process. We consider a filling rate of 40%, a residence time of 10 days, and an emptying time of 1 day (BEKON 2018b). The results presented in Table 10 relate to the operation of a BEKON composting tunnel:

In this way, the number of tunnels needed for the composting process is 8 tunnels, as shown in the Table 11.

Table 9: Input matter for the composting process.

		Data
Digestate after methanation	$ton.y^{-1}$	31.680
Digestate density	$ton.m^{-3}$	0,8
Digestate volume	$m^3.y^{-1}$	39.600
additional green waste rate	%	40
Additional green waste	$m^3.y^{-1}$	15.840
composting process mixture per year	$m^3.y^{-1}$	55.440
Composting process mixture per day	$m^3.day^{-1}$	152

Table 10: Composting tunnel dimensions and their operation based on the BEKON process.

The composting tunnel dimensions		Data
Long	m	20
Length	m	5,9
Height	m	5
Volume	m^3	590
Filling rate	%	40
Useful volume	m^3	236
The composting tunnel operation		
Filling time	day	2
Residence time	day	10
Drain time	day	1
Time for 1 composting cycle	day	13
Cycles number	$Cycle.y^{-1}$	28
Volume of mix processed	$m^3.y^{-1}*tunnel$	6.608

Maturation

After the stay in the tunnels, the compost is deposited in windrows to follow the maturation stage. A windrow should not exceed 3 meters in height, and its usual dimensions for width and length are 8 and 18 meters, respectively, giving a
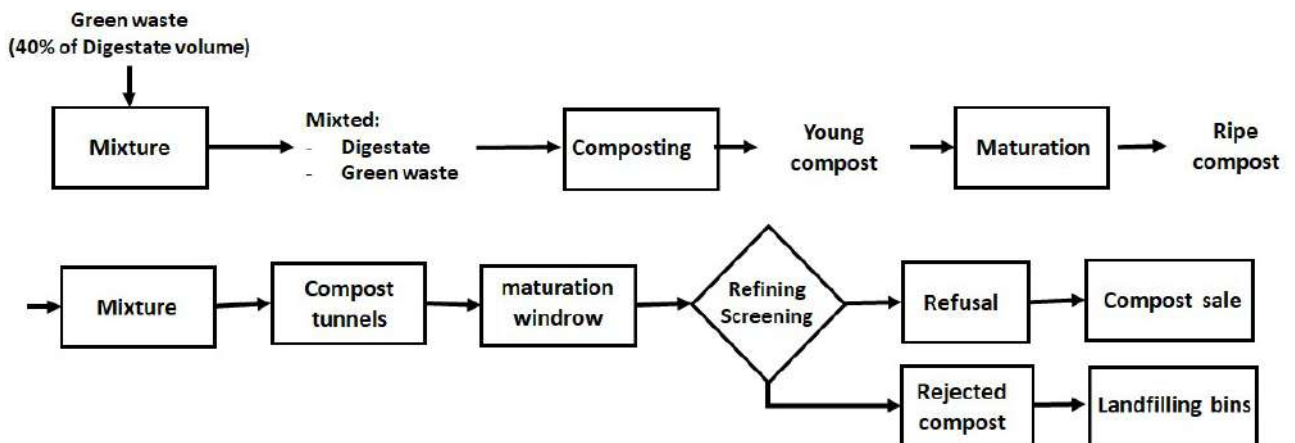

Fig. 7: The different stages of the composting process after anaerobic digestion.

Table 11: Calculation of the number of composting tunnels.

		Data
Volume of the mixture for 1 year	$m^3.y^{-1}$	55.440
Volume of mixture treated for 1 year	$m^3.y^{-1}$*tunnel	6.608
Tunnels number	tunnels	8

Table 12: Dimensions of a maturation windrow and its residence time.

Windrow dimensions		
Long	m	18
Length	m	8
High	m	3
Volume	m^3	432
Operation of a windrow		
Filling time	day	4
Residence time	day	60
Drain time	day	1
Time for 1 maturation cycle	day	65
No. of Cycles	cycle.y^{-1}	6
Volume that can be treated	$m^3.y^{-1}$*windrow	2.592

Table 13: Calculation of the necessary maturation windrows number.

Volume of young compost for 1 year	m^3y^{-1}	44.824
The volume of young compost treated per windrow	$m^3.y^{-1}$*windrow	2.592
Windrows number	Windrow	17

volume of 432 m^3. The values used for the maturation process are shown in Table 12.

In this way, the calculated number of windrows necessary for the compost maturation coming out of the tunnels is 17 windrows, as indicated in the Table 13.

The surface required calculation is based on the same principle as that carried out previously for the digesters and the composting tunnels. Thus, the calculated surface is 2.448 m^2, but taking 20% of the necessary space for circulation, we obtain a total surface of 2.938 m^2.

Refining

Since the pretreatment in discontinuous systems is not

Table 14: Refining the resulting compost.

		Data
Ripe compost	ton.y^{-1}	29.046
Refined compost	ton.y^{-1}	14.523
Refused compost	ton.y^{-1}	14.523

Table 15: Biogas and biomethane estimated production by anaerobic digestion.

		Data
Fresh matter	Ton.y^{-1}	39.420
Biogas production yield	$m^3.ton^{-1}$	90
Biogas produced	$m^3.y^{-1}$	3.547.800
Biomethane content	%	60
Biomethane produced	$m^3.y^{-1}$	2.128.680

demanding, the compost particles obtained will have heterogeneous sizes, which requires a refining process that separates the large particles with a sieve.

Based on experience in similar processes, it is estimated that after the refining stage, 50% of the compost is rejected, and 50% is considered valid for its use (Table 14).

The fresh organic matter used at the start of the methanation process may contain contaminants such as heavy metals or inorganic matter due to poor sorting at the source, which reduces the quality of the compost and may limit its use.

Energy Production

The average biogas yield value is 90 m^3 per ton of substrate. To calculate the amount of biogas produced, we base ourselves on the amount of substrate used in the digesters (Table 15) (BEKON 2018a).

To remain realistic, we will not work 100% of the year. Our load factor is 0,9. This means that 10% of our products will be burned in a torch, as shown in Fig. 8:

Considering the lower calorific value of biomethane at 5,98 $KWhm^{-3}$ (Engineering ToolBox 2003). The amount of energy that can be obtained by cogeneration is shown in Table 16.
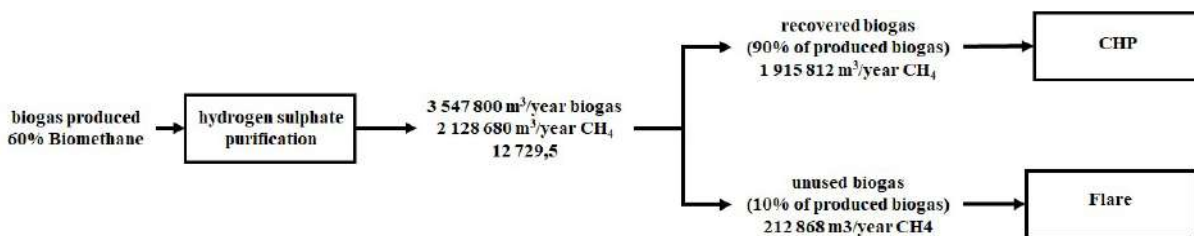

Fig. 8: The biogas recovery unit energy balance for one year of production.

Table 16: Energy contained in biogas available from digesters.

Energy contained in biogas		
Biomethane available	$m^3.y^{-1}$	2.128.680
Biomethane LHV	$KWh.m^{-3}$	5,98
Energy contained in biogas	$MWh.y^{-1}$	12.729
Valorization by cogeneration		
CHP electrical yield	%	39,2
Electric energy	$MWh.y^{-1}$	4.990

Table 17: Total electrical energy produced by the cogeneration engine.

Electrical energy from digesters		
Electricity produced	kWh	850
Electrical efficiency	%	39,2
Operating hours number	H	5.256
Energy produced by the motor	$MW.y^{-1}$	4.467
Electrical energy from bins landfilling		
Electricity produced	KWh	850
Electrical efficiency	%	39,2
Operating hours number	H	2.628
Energy produced by the motor	$MW.y^{-1}$	2.233
Operating hours total	H	7.884
The total electrical energy produced by the motor	$MW.y^{-1}$	6.700

To calculate the cogeneration unit power, we use the biogas energy, the electrical engine efficiency, and the operational hours according to our load factor (Table 17).

The Electrical Fraction Energy Balance

It is expected that a fraction of the electrical energy obtained from the cogeneration unit will be used to meet the energy needs of the digesters. A balance sheet of the energy fraction tells us the net quantity of energy that can be obtained from this biogas plant (Table 21).

Electricity consumption is mainly included in these three stages: (1) pretreatment from the arrival and preparation of waste (Table 18), (2) methanation, and (3) post-treatment (Table 19), including the green waste digestate mixer.

For the pretreatment step, we use the operating capacity of the equipment in this step and their electrical power (bag opener, trommel screen, feed, and dosing hopper with decompactor (FDHD)).

For the methanation step with the BEKON process, the electricity consumption of the digesters is 10% of the electricity produced by the cogeneration unit.

The equipment used in the post-treatment stage is the green waste digestate mixer, the rotary screen after maturation, and the windrow turner during the compost

Table 18: Power consumption of pretreatment equipment.

		bag opener	trommel screen	FDHD
Pretreatment process				
Powerful	kW	52	30	33
Operating capacity	$Ton.h^{-1}$	40	25	7
organic waste quantity	$ton.y^{-1}$	33.507	33.507	39.420
Operating hours	$h.y^{-1}$	838	1.340	5.631
Electrical consumption	$MWh.y^{-1}$	43	40	186
Total electricity consumption	$MWh.y^{-1}$	269		

maturation stage. This equipment is not all electric. We chose to use gas-powered mobile equipment during the composting stages to save on the movements of the loaders and to work where the windows are installed. Therefore, the only electrical equipment is the green waste digestate mixer.

Table 20 presents the electricity consumption of the entire installation:

The cogeneration unit operates with a load factor of 0,9. Consequently, during the engine stoppages hours, it will be necessary to buy electricity from the network to ensure the operation of the rest of the equipment. The quantity of this auxiliary electricity is equal to

Table 19: Power consumption of post-processing equipment.

		Mixer
Post-processing process		
Powerful	kW	102
Operating capacity	$m^3.h^{-1}$	108
organic waste quantity	$m^3.y^{-1}$	55.440
Operating hours	$h.y^{-1}$	514
Electrical consumption	$MWh.y^{-1}$	52

Table 20: The biogas unit's electricity consumption.

		Data
Pretreatment process	$MWh.y^{-1}$	269
Methanation process	$MWh.y^{-1}$	670
Post-processing process	$MWh.y^{-1}$	52
Total electricity consumption	$MWh.y^{-1}$	991

Table 21: Electrical balance of the biogas plant.

		Data
Total electricity consumption	MWh/year	991
Auxiliary electricity	%	10
Auxiliary electricity	$MWh.y^{-1}$	99
CHP electricity	$MWh.y^{-1}$	6.700
Total electricity consumption	$MWh.y^{-1}$	- 991
Net electrical energy	$MWh.y^{-1}$	5.808

10% of the total electricity consumption of the biogas plant.

The net electricity is injected into the national electricity grid, which will improve the number of renewable energies produced in Morocco, ensuring an annual and stable income to cover the expenses.

CONCLUSION

To achieve the NHWP (national household waste program) objectives set by 2030, Morocco must develop an HSW management model adapted to its deposits and problems. For this purpose, dry methanation appears to be an adequate technological solution. However, this approach is underdeveloped and only represents methanizers processing agricultural products. To obtain a Moroccan anaerobic digestion model, it is necessary to identify and study the scientific and technological obstacles relating to the dry process.

The work presented in this article has endeavored to provide a reference database with which the choice of the process becomes obvious. Batch and mesophilic dry methanation is the solution for Morocco to develop its own model of integrated and sustainable management of household and similar waste.

Based on the sorting results, the waste studied is characterized by the dominance of fermentable matter, which presents a significant fraction of the deposit's overall mass. It varies between 42,75% and 64,20% (averaging 54,94%). This reflects the priority of establishing a recovery method for this type of waste.

Therefore, the choice of dry and mesophilic anaerobic digestion is the one that uses the simplest technology with the most stable parameters. Added to this is the investment amount. We should create a system for municipalities that do not have large budgets, so discontinuity seemed to be the exact answer. With a discontinuous and mesophilic dry methanation process, we can make our landfills capable of self-financing by producing energy and compost. The technological level of the solution is acceptable, and the digesters number can increase according to our investment budget.

This plan fills all the gaps in a strategy based essentially on total landfilling: Extend the landfills lifetime, eliminate methane leaks into the atmosphere, increase the operating time of the biogas processing unit, ensure acceptable sorting, and improve the working environment for scavengers, remove the ceiling on the quantity produced of biogas and electricity.

This master plan connects biogas extraction from the landfills to our network of digesters to operate 24 hours a day all year round. We avoid sending the digestate to a landfill by adding a composting process. So, we built a unit that can even be installed in our transfer centers and save the daily trips between these centers and our controlled landfills.

REFERENCES

BEKON. 2017. The BEKON Process: Innovative Methanation Plants for the Energy Recovery of Organic Waste and Other Biomass. Retrieved from https://www.bekon.eu/wpcontent/ uloads/2017/12/BEKON_Broschuere_FR_web.pdf.

BEKON. 2018a. The BEKON Process Innovative Biogas Plants for Energy Production from Organic Waste. Retrieved from https://www.bekon.eu/wpcontent/ uploads/2015/11/BEKON_Brosch%C3%BCre_EN_Web.pdf.

BEKON. 2018b. World Leading Provider of Dry Biogas Plants + Composting Technology. Retrieved from https://www.ccc.org.co/bion/wp-content/uploads/pdf/27 abril-2018/IgnacioBenitezBekon.pdf.

CLIMAT.BE. 2018. The IPCC Publishes Its Special Report on Global Warming of 1.5°C. Retrieved from https://www.climat.be/fr-be/changements-climatiques/les-rapports-du-giec/2018-rapport-special/.

Engineering ToolBox. (2003b). Gases – Density [online] Available at: https://www.engineeringtoolbox.com/gas-density-d_158.html [Accessed 10 December. 2018].

EPA. 2018. Overview of Greenhouse Gases. Retrieved from https://www.epa.gov/ghgemissions/overviewgreenhouse-gases#methane.

Farhat, A., Lagliti, K., Fekhaoui, M. and Zahboune, H. 2021. Physicochemical Characterization of Household and Similar Waste, for Efficient and Income-Generating Waste Management in Morocco, City of Mohammadia. In Hajji, B., Mellit, A., Marco Tina, G., Rabhi, A., Launay, J. and Naimi, S. (eds), Lecture Notes in Electrical Engineering, vol 681, Springer, Singapore, pp. 44-63. https://doi.org/10.1007/978-981-15-6259-4_63.

Harzevili, F.D. and Hiligsmann, I.S. 2017. Microbial Fuels: Technologies and Applications. CRC Press, Boca Raton, Florida.

Hoornweg, D. and Bhada-Tata, P. 2012. What a Waste: A Global Review of Solid Waste Management. Urban Development Series Knowledge Papers No. 15., World Bank, Washington.

Mata-Alvarez, J. 2003. Biomethanization of the Organic Fraction of Municipal Solid Wastes. IWA Publishing, London, UK.

Moletta, R. 2009. Waste Treatment. Elsevier, The Netherlands, p.309

Pierini, V.I. and Ratto, S. 2015. Yard trimming's life cycle: Composting vs. landfilling. Environ. Protect., 3(3): 43-51.

Sidi, O.A. 2006. Methodology of Characterization of Household Waste in Nouakchott: Contribution to Waste Management and Decision-Making Tools. Springer, Berlin. p. 120.

Wellinger, A., Murphy, J.D. and Baxter, D. 2013. The Biogas Handbook: Science, Production, and Applications. Elsevier, The Netherlands.

Yemadje, A. 2013. Characterization of the household solid waste of the municipality of Abomey-Calavi in Benin. J. Environ. Res. Manag., 4(11): 0368-0378.

Artificial Neural Network Modeling for Adsorption Efficiency of Cr(VI) Ion from Aqueous Solution Using Waste Tire Activated Carbon

Gaurav Meena† and Nekram Rawal

Department of Civil Engineering, Motilal Nehru National Institute of Technology, Allahabad, Prayagraj, India

†Corresponding author: Gaurav Meena; gaurav.jpid@gmail.com

ABSTRACT

In this study, waste tires were used to develop activated carbon for the adsorption of Cr(VI) from aqueous solutions, and an artificial neural network (ANN) model was applied to predict the adsorption efficiency of waste-tire activated carbon (WTAC). SEM and FTIR were used to characterize the developed WTAC. A three-layer ANN with different training algorithms and hidden layers with different numbers of neurons was developed using 79 data sets gathered from batch adsorption experiments with different initial Cr(VI) ion concentrations, contact periods, temperatures, and doses. Conjugate gradient backpropagation of Powell-Beale restarts (traincgb) was found to be the best training algorithm among all the training algorithms, with an RMSE of 5.894 and an R^2 of 0.985. The ANN topology had 4, 8, and 4 neurons in the input, hidden, and output layers. The correlation coefficient of the ANN models of Cr(VI) ion adsorption efficiency is 0.977.

INTRODUCTION

Heavy metal water contamination is a major issue everywhere in the world (Dodbiba et al. 2015, Veglio & Beolchini 1997). Chromium is also significant in water contamination because tons of chromite ore is generated annually worldwide. Ferro chromite is created through the direct decrease of the ore, whereas Cr metal is created through the aluminothermic process, chrome alum solutions, or electrolysis of CrO_3. The production of chromate, electroplating, leather tanning, metal polishing, and chromate preparation are only a few industries that make substantial use of chromium and its derivatives (Kowalski 1994). Chromium predominantly appears in two oxidation states in aqueous solutions: trivalent chromium and hexavalent chromium. The hexavalent form of chromium is hazardous, can cause cancer, and can also mutate DNA. For instance, lung cancer has been associated with $Cr_2O_7^{2-}$ (El-Sikaily et al. 2007, Li 2008).

One of the main factors contributing to the importance of chromium (III) and chromium (VI) to the environment is their stability in their native habitats. Due to its high water solubility, mobility, and simplicity of reduction, Cr(VI) is 100 times more dangerous than Cr (III) (Gómez & Callao 2006). The fundamental causes of Cr(VI) toxicological effects are its oxidizing capabilities and the subsequent formation of free radicals during its intracellular reduction to

Cr (III) (Das 2004). The World Health Organization (WHO 2020) recommends a chromium (VI) wastewater toxicity limit of 0.05 mg.L^{-1} with a combined maximum permitted discharge of 2.0 mg.L^{-1} (WHO 2020).

Chromium may be removed from wastewater produced in various industrial settings using several methods. Here are a few instances that exist. Some examples of these processes are reduction followed by chemical precipitation (Zhou 1993), ion exchange (Tiravanti et al. 1997), reduction; electrochemical precipitation (Kongsricharoern & Polprasert 1996); solvent extraction (Meegoda 2000); membrane separation (Chakravarti et al. 2000); evaporation (Aksu 1996); and foam separation (Jiao & Ding 2009). At low quantities, conventional approaches to chromium removal, such as those outlined above, are either prohibitively expensive or ineffective due to the element's solubility in water. In light of this, adsorption ought to be considered a workable alternative. As an adsorbent, commercial activated carbon, also known as CAC, is utilized to remove Cr (Selomulya et al. 1999), Cd (Kannan & Rengasamy 2005), Cu, Zn (Monser & Adhoum 2002) and Ni (Basso et al. 2002) from wastewater. However, commercial activated carbon intended exclusively for eliminating heavy metals can be fairly expensive. In the search for adsorbents that are both effective and economical, a great number of investigations have been carried out. In this research, a wide variety of

absorbents, such as starch xanthate (Religa et al. 2011), chitosan (Ngah et al. 2005), sawdust from *Pinus sylvestris* (Taty-Costodes et al. 2003), bagasse sugar (Gupta 2003), bentonite (Bereket et al. 1997), and old car tires (Rowley et al. 1984) were investigated.

The adsorption mechanism is very complicated, which makes it hard to model and simulate with traditional mathematical models. This is because a wider range of sorption process factors interacts, leading to nonlinear relationships. To ensure that every control measure is managed in the most effective manner possible, it is required to build a suitable model to achieve effective operation and design. A high-quality representative model may be of considerable assistance in optimizing the input parameters. ANNs have been applied to the fields of wastewater treatment (Chen & Kim 2006, Gontarski et al. 2000, Pai 2007, Qiao et al. 2020, Sahoo & Ray 2006), membrane processes (Fagundes-Klen 2007, Guadix et al. 2010, Libotean 2009, Prakash et al. 2008), and biosorption (Sadrzadeh et al. 2009, Yetilmezsoy & Demirel 2008) for prediction and simulation because of their reliability, robustness, and prominent features in picking up the non-linearity relation of variables in intricate systems. Heavy metal adsorption efficiency from water can be predicted using ANNs. However, the available data is scant (Kashaninejad et al. 2009). Therefore, this research aimed to find the best ANN structure and associated parameters for predicting the removal efficiency of activated carbon from waste tires of Cr(VI) ions in an aqueous solution.

MATERIALS AND METHODS

Materials

Analytical grade reagents were used in the study and purchased from Uma Scientific, Prayagraj. Stock Solutions
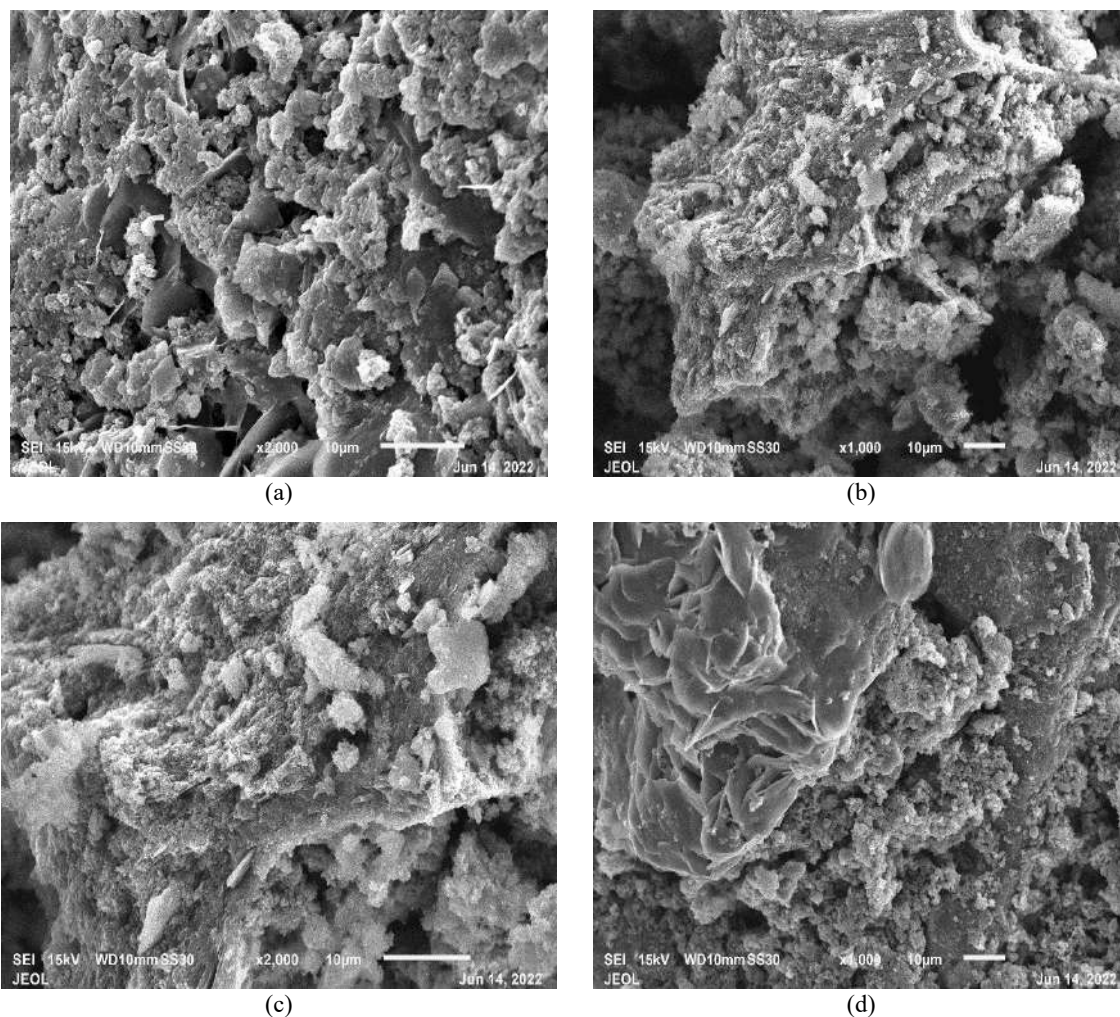

Fig. 1: SEM micrograph (a, b) before adsorption; (c, d) after adsorption.

and other solutions were prepared using a double-distillation unit. A stock solution of Cr(VI) was prepared using 144 mg Potassium dichromate ($K_2Cr_2O_7$) dissolved in 100 mL distilled water which gives 500 mg.L^{-1} Cr(VI). The artificial wastewater with the required Cr(VI) concentration used in the tests was made from a stock solution. Waste tires used during the study were sourced from a near tire repair shop. Fetched tires were cut into 10-12 mm pieces, and the dirt was cleaned by shocking in diluted HCl for 24 h, followed by two to three rinses with distilled water, and drying in a hot air oven at 100°C for 4 h. After cleaning and drying, waste tires were carbonized at 400°C for 4 h. Chemical and heat treatments of carbonized waste tires prepared the activated carbon. A weight ratio of 1:2 of carbonized tires to H_2SO_4 was initially poured into a 250 mL crucible to perform the chemical treatments. The mixture was then left to react for 4 h while being stirred intermittently throughout the reaction duration. After that, the items. After that, the mixture was heated at 400°C for one hour, and then, once the mixture had cooled, it was stored in a glass container.

Adsorbent Media Characterization

Scanning electron microscopy (SEM) was used to investigate the difference in surface morphology between the WTAC before and after the adsorption of the Cr(VI) ions. Fig. 1 (a-b) show the results of SEM imaging before adsorption at a different level of magnification, and Fig. 2 (c-d) shows the results after adsorption at different magnification. The irregular surface and presence of pores before adsorption could be assumed to be active sites for chromium uptake.

The sample's Fourier transform infrared (FTIR) was collected over a wide spectral range between 4000 and 400 cm^{-1} to collect high-resolution information. The critical features of FTIR spectra of the sample are shown in Fig. 2. The 3415.02 cm^{-1} peaks denoted the presence of a hydroxyl group, which might be carbon black surface groups or groups generated from the hydroxylation of oxides (Manchón-Vizuete 2005) chemical and combined (thermal and chemical or vice versa.

Batch Adsorption Experiments

Adsorption batch tests were conducted in a conical flask on a temperature-controlled orbital shaker. Aliquots of treated samples were filtered using grade 1 Whatman filter paper (pore size 11 μ) after adsorption. Colorimetric analysis using a spectrophotometer (LABINDIA UV 30000+) was used to determine chromium levels in the samples. The batch adsorption was done at different contact periods and with different chromium concentrations, times, and temperatures, as indicated by the statistics for the factor mentioned in Table 2. The following equation was used to calculate the adsorption capacities.

$$q_e = \frac{(C_0 - C_t)V}{m} \qquad \ldots(1)$$

Where qe represents the adsorption capacity in mg.g^{-1}, Co represents the initial Cr concentration, Ct represents the Cr concentration at time t, V represents the volume of the solution in L, and m represents the mass of the adsorbent (g).

Artificial Neural Networks

Artificial neural networks (ANNs) have significant computational modeling power. Because of their adaptive structure, they can recognize complicated nonlinear relationships. This is especially true when the evident
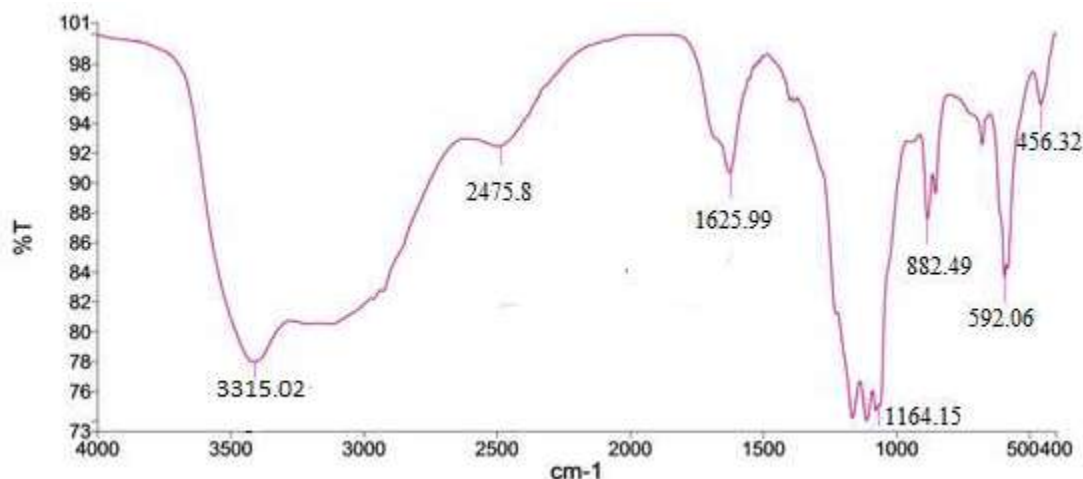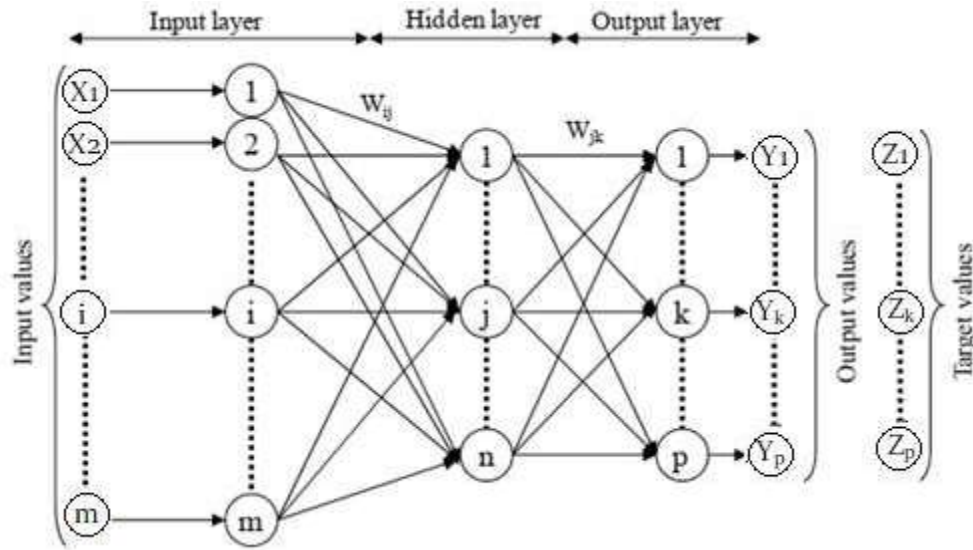

Fig. 2: FTIR spectra of activated carbon.

Fig. 3: ANN fundamental structure.

structure of the variable-variable relationship is ambiguous. The basic purpose of an ANN model is to solve any problem that cannot be solved using more traditional mathematical or statistical methodologies. Fig. 3 depicts an ANN's fundamental structure, consisting of three layers: an input layer with dependent variables, a hidden layer, and an output layer with dependent variables.

As shown in Fig. 3, each layer of a typical ANN consists of many strongly connected processing components called "neurons" or "nodes." In addition, all neurons except the output layer are linked to the sub-layer neurons by the connection strength (w value). The neurons in each layer get information from various sources, including the input layer's original data, the hidden layer's output from other nodes in the previous layer, and the output layer's original data. A line, which conveys information from one node to the following, represents the connectivity between neurons. Data is introduced into the network in the input layer, and the input is calculated in the hidden layer and output layer by weighing the total output obtained in the previous layer. This mechanism is driven by the "weights," or the degree of connectivity between two neurons. However, the inputs are transferred to the hidden and output layers using activation functions, which then compute the outputs of those layers. An activation function is a mathematical term for a nonlinear transfer function. Transfer functions that are among the most
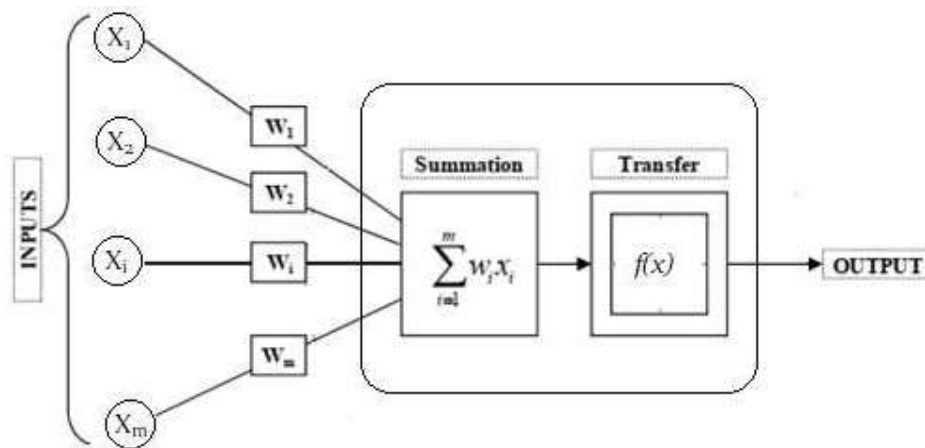

Fig. 4: Illustration of operation within a neuron.

common include the tangent sigmoid (tansig), logarithmic sigmoid (logsig), and linear (purelin). The mathematical descriptions of the logsig and tansig transfer functions are provided by equations (2) and (4), respectively, while equation (3) explains the purelin transfer function. The tansig transfer function provides the most accurate predictions compared to the other transfer functions.

$$f(x) = \frac{e^x - e^{-x}}{e^x + e^{-x}} \qquad \ldots(2)$$

$$f(x) = \frac{1}{1 + e^{-x}} \qquad \ldots(3)$$

$$f(x) = x \qquad \ldots(4)$$

Fig. 4 illustrates a flow that depicts the flow of information within a neuron. When the input is multiplied by its weight, the sum function applies to all inputs of the previous layer, as applied to the previous layer (w value). Then the neuron's output is determined by passing this unique value through the transfer function.

Collecting, analyzing, and processing data is the first step in the development of the ANN model, followed by training the network, testing the training network, selecting the model (determining the optimal structure of the ANN, training functions, training algorithms, and network parameters), and simulating and predicting using the training network. All ANN models developed in this study followed these steps.

In ANN, the training algorithm is a process for adjusting the parameters of a network until they are optimal for a given input-output transformation problem. No universally superior algorithm exists because performance varies greatly among problems of varying sizes, complexities, and data availability. Thus, 11 training algorithms from 6 different categories were compared and evaluated. Table 1 summarizes all the training algorithms and their functions.

Table 1: ANN training algorithms.

Training algorithm	function
Levenberg-Marquardt (LM)	trainlm
Gradient descent(GD) with a variable learning rate	traingdm
	traingda
	traingdx
Resilient backpropagation(RP)	trainrp
Conjugated gradient descent(CG)	traincgb
	traincgp
	trainscg
Quasi-Newton algorithm	trainoss
	trainbfg
Bayesian regularization	trainbr

Performance Assessment Criteria of the ANN Model

The reliability of the created ANN models was evaluated in four different methods: mean absolute error (MAE), root mean square error (RMSE), coefficient of determination (R^2)

The root-mean-squared error (RMSE) was used as a measure of the accuracy of the model, and it may be computed as follows:

$$RMSE = \sqrt{\frac{\sum_{i=1}^{n}(Y_{pre,i} - Y_{obs,i})}{n}} \qquad \ldots(5)$$

$Y_{pre,i}$ stands for the mode prediction, $Y_{obs,i}$ for the associated observed data set, and n for the number of non-missing data points associated with the mode prediction.

The coefficient of determination (R^2) indicates the proportion of variance that the model can explain. It can be determined as follows:

$$R^2 = \left[\frac{n\sum_{i=1}^{n}Y_{obs,i}Y_{pre,i} - (\sum_{i=1}^{n}Y_{obs,i})(\sum_{i=1}^{n}Y_{pre,i})}{\sqrt{\left[n\sum_{i=1}^{n}Y^2_{obs,i} - (\sum_{i=1}^{n}Y_{obs,i})^2\right] \times \left[\sum_{i=1}^{n}Y^2_{pre,i} - (\sum_{i=1}^{n}Y_{pre,i})^2\right]}}\right]^2$$

$$\ldots(6)$$

The statistical performance evaluation criteria, such as RMSE and R^2, are global statistics that do not provide any insight into the error distribution. As a result, other performance evaluation criteria, such as mean absolute error (MAE), were applied to measure the accuracy of the ANN models constructed for this investigation. The MAE not only illustrates the distribution of the errors made in the forecast, but it also demonstrates the performance index in predicting removal efficiency. This is because the MAE gives both of these things. The following equation can be used to determine MAE:

$$MAE = \frac{1}{n}\sum_{i=1}^{n}|Y_{obs,i} - Y_{pre,i}| \qquad \ldots(7)$$

RESULTS AND DISCUSSION

Pre-Processing of Data

Seventy nine data sets in this investigation were gathered through batch experiments with varying adsorbent dosages, contact times, and initial Cr(VI) ion concentrations. Experimental data points were randomly split into training, validation, and testing subsets to create an ANN model for forecasting the percentage of Cr(VI) ions removed by WTAC from aqueous solutions. About 70% of the data went to the training set. The remaining 15% and 15% went to the validation and testing sets, which got 55, 12, and 12 data points, respectively.

Table 2: The basic statistics of the ANN model variable.

Input Parameter	Unit	Min.	Max.	Avg.	Std.
Doges	g	0.2	0.8	0.50	0.21
Concentration	mg.L^{-1}	10	100	58.86	31.21
Time	Min	10	360	175.31	96.99
Temp.	^{o}C	30	50	36.83	7.43

The neural network can recognize patterns present in the data by using the training data, which is the largest set, to adjust the network weights. The testing data is employed to assess the network's quality. The trained network's performance and generalizability are checked one last time using validation data. Table 2 presents the essential statistical information regarding the variables used in the investigation.

Before training the network, input and output variables were normalized to fall between 0.1 and 0.9 to avoid numerical overflows caused by extreme weight values. Here is the equation for normalization:

$$X_i = \frac{(x - x_{min})}{(x_{max} - x_{min})} + 0.1 \qquad \dots(8)$$

Where x_{max} and x_{min} represent the maximum and minimum possible values in the database, respectively, and Xi represents the value of x after it has been normalized.

ANN Architecture Design

The architecture of the AAN considerably affects the overall performance of ANN models. To develop the most effective architecture for an ANN model, the network architecture design must consider two essential characteristics: layering and transfer function. With these parameters, the best training algorithm and number of neurons to use in the hidden layer can be chosen.

Table 3: List of different training algorithms of ANN.

ANN Algorithms	EPOCH	RMSE	R^2
TRINLN	128	8.597	0.967
TRAINBGF	10	6.039	0.984
TRAINCGB	56	5.894	0.985
TRAINCGF	132	6.566	0.981
TRAINCGP	1	6.364	0.982
TRAINGDA	12	6.757	0.980
TRAINGDX	104	8.341	0.969
TRAINLM	8	6.214	0.983
TRAINOSS	39	7.518	0.975
TRAINSCG	62	6.110	0.983

The most effective training algorithm can be identified by analyzing and comparing several different training algorithms. The training algorithms used a three-layer ANN with a linear transfer function (purelin) in the output layer, a tangent sigmoid function (tansig) in the hidden layer, and 10 neurons in each layer. Table 3 displays the results of ANN model evaluations using each available training algorithm. As shown in Table 3, the RMSE values obtained by the traincgb were the lowest, and the R^2 values were the highest, coming in at 5.894 and 0.9885, respectively. Because of this, it was selected as the most effective algorithm for training. This algorithm was followed by the training and traincg functions, which had RMSE of 6.039 and 6.110, respectively. When utilized as a training algorithm, alternative algorithms like trainln, traincgf, and traingda produced more errors than the traincgb.

After figuring out the best training algorithm for the ANN model, the next step is optimal design, which involves
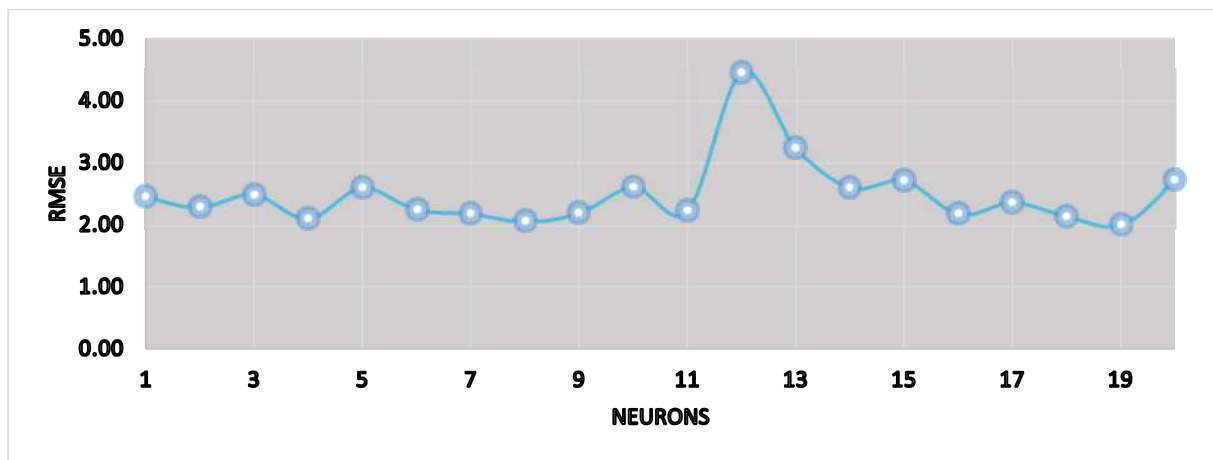

Fig. 5: Variation of RMSE with neurons.

choosing the right number of neurons to use in the hidden layer for further analysis. It can be done by varying the neurons in the hidden layer. Initially, the hidden layer only used two neurons for the guessing process. However, as shown in Fig. 5, the number of neurons in the hidden layer gradually increased from two to twenty.

Fig. 5 shows that the network output a wide range of RMSE and local minimum/maximum values as the number of neurons is enhanced. The lowest RMSE value for the eight hidden neurons was attained in every trial. The smallest RMSE value for a neural network architecture with 8 hidden neurons was 2.06. As a result, the optimal number of neurons was established to be 8 in hidden layers.

Final Selected ANN Model Results

The optimal ANN topology for forecasting Cr(VI) ion adsorption efficiency by WTAC was determined to be 4-8-1 during network architecture design. Table 4 shows the performance of the artificial neural network (ANN) model and the best ANN parameter combination for this structure.

In summary, Fig. 6 illustrates the optimal three-layer ANN topology, comprising a four-neuron input layer, an eight-neuron hidden layer with a tangent sigmoid (tansig) transfer function, and a single-neuron output layer.

A linear relationship between the observed and predicted outputs of the final selected ANN model can be seen in training, validation, and testing over the full dataset. As shown in Fig. 7, the regression plot was obtained for the best ANN model 4-8-1. The good accuracy and fitting abilities of the ANN model are demonstrated by the large R-value of 0.977 for the entire data set. The lower R-value of 0.91014 shown in the testing data may be due to the limited sample size used in this investigation. Expected values based on the best ANN model 4-8-1 are displayed in Table 4.

An evaluation of the ANN model's efficacy was conducted by contrasting the error function with respect to the validation data. The training procedure ends once the validation error has decreased to a certain level. The outcome is predicted, and ANN validates the experimental data. The MSE for the optimized ANN model is shown against the epoch number in Fig. 8. Overfitting was avoided, and the least-error weights and biases were recovered by stopping training after 61 epochs, as shown in Fig. 8. Specifically, the little circle at epoch 61 on the graph represents the highest validation performance.

Table 4: Artificial Neural network (ANN) model's performance.

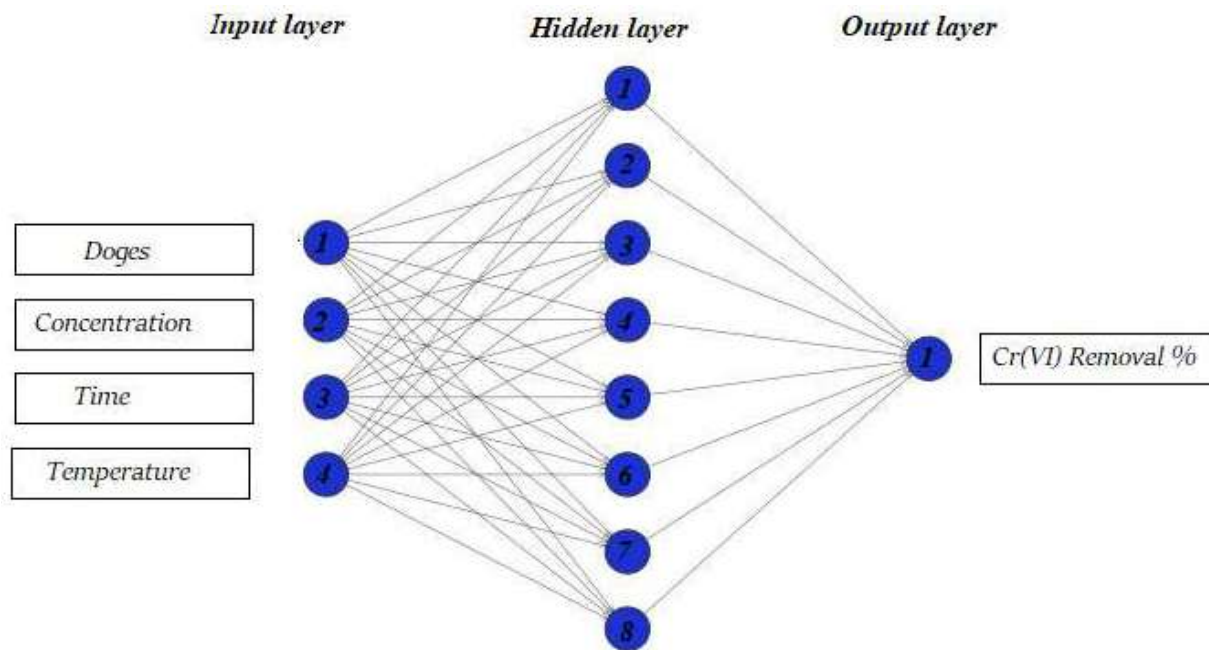| ANN Structure	Algorithm	Transfer function		Assessment Criteria		
		Hidden Layer	Output layer	RMSE	MAE	R^2
4-8-1	Treincbg	tansing	purelin	2.384	1.630	0.977

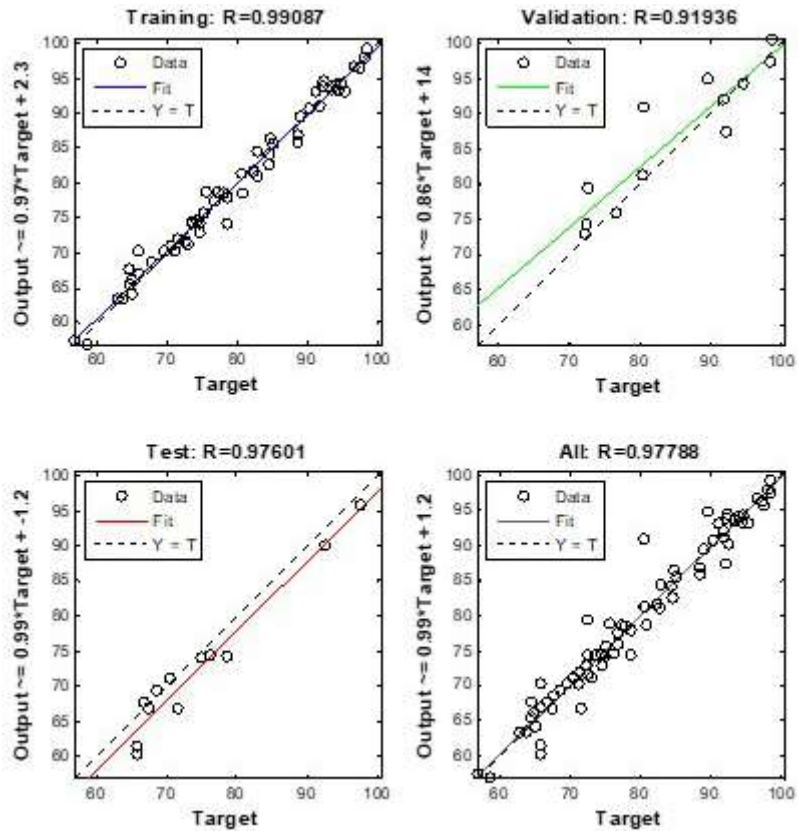Fig. 6: ANN topology (4-8-1) for Cr(VI) adsorption efficiency.

Fig. 7: Regression plots of ANN model for Cr(VI) adsorption efficiency.
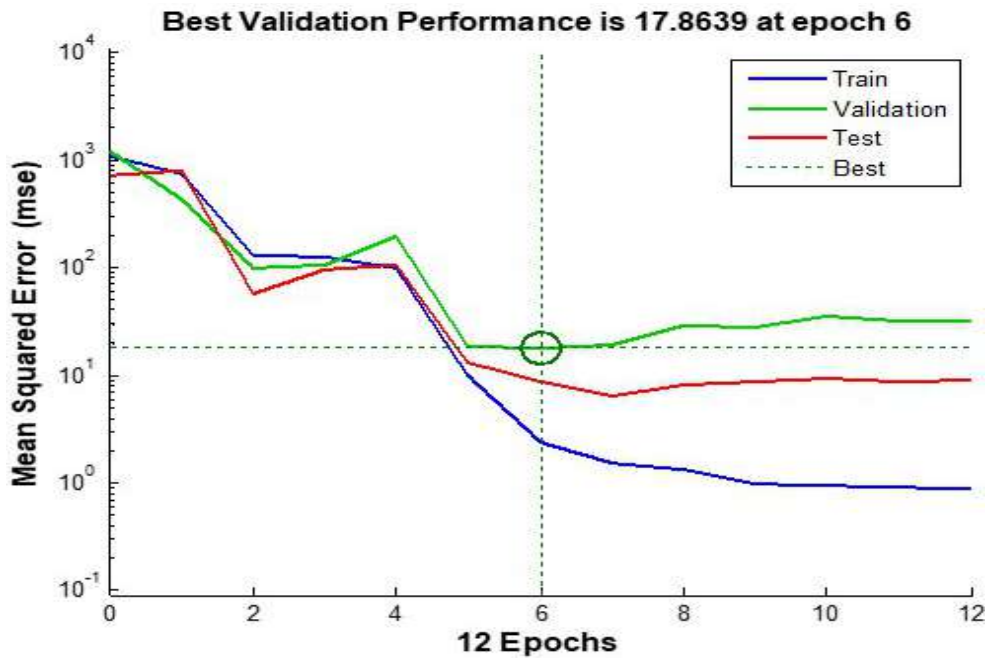

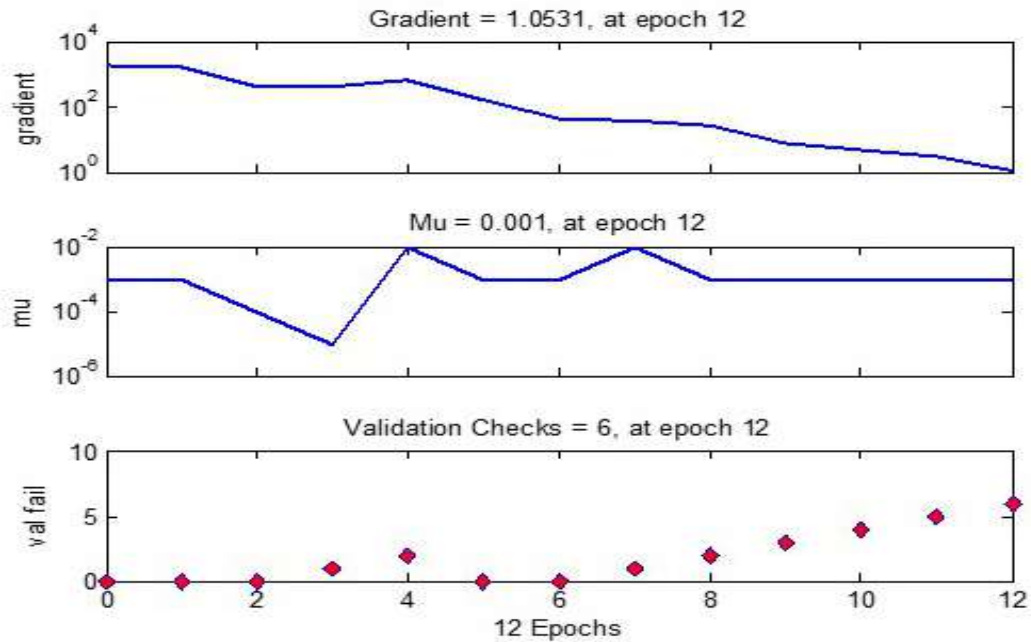Fig. 8: MSE plot of ANN performance for train, validation, and test data.

Fig. 9: ANN Training State (Gradient, mu, and validation check profiles).
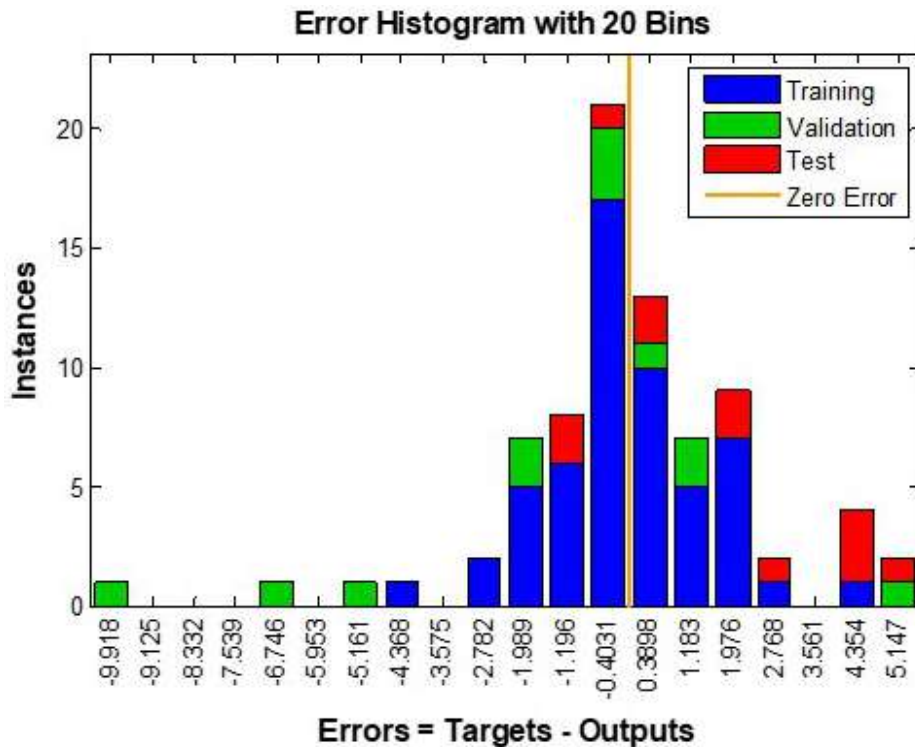

Fig. 10: Histogram of error.

The validation check, also known as Mu, and the gradient profile of the ANN model are depicted in Fig. 9. When the gradient value reached 1.0531. The training was terminated. As shown in Fig. 9, the mu value for the seventh period was 0.001. Additionally, the varying validation checks show no need to evaluate the validity of the data set used in the current investigation.

After projecting the errors for each data point, a 20-bin error histogram is generated and displayed in Fig. 10. Fig. 10 shows that the largest error possible was 10.31, and the smallest error possible was 0.003. The fact that 4 of the observations had zero or tiny errors and the deviations are concentrated closer to the zero error line demonstrates the correctness and reliability of the ANN model developed. However, the limited dataset used means that the amount of errors that significantly depart from the mean is still manageable.

CONCLUSION

The primary aim of this research was to develop an ANN model for the Cr(VI) ion adsorption efficiency of WTAC in batch adsorption tests with four different process parameters (adsorbent dosage, initial concentration of Cr(VI) ions, contact time, and temperature). WTAC was developed using the carbonization of waste tires at 400 °C, which was subsequently activated using a thermal and chemical method. WTAC's FTIR peak at 3415.02 cm indicates the presence of a hydroxyl group.

A three-layer ANN with different training algorithms and hidden layers with different numbers of neurons was developed to predict the adsorption efficiency of the Cr(VI) ion. All algorithms were evaluated at 10 neurons in a hidden layer. The best training algorithm was determined to be CGB of Powell-Beale restarts (traincgb), with RMSE of 5.894 and R^2 of 0.985. It was determined that 8 neurons in the hidden layer are the optimal number for traincgb, with RMSE 2.06. The ANN model's correlation coefficient is 0.977, indicating that it accurately predicted experimental data and could make a reliable prediction on the adsorption efficiency of the Cr(VI) ion.

REFERENCES

Aksu, Z. 1996. Investigation of biosorption of chromium(vi) on cladophora crispata in a two-staged batch reactor. Environ. Technol., 7(2): 215-20.

Basso, M.C., Cerrella, E.G. and Cukierman, A.L. 2002. Activated carbons developed from a rapidly renewable biosource for the removal of cadmium(II) and nickel(II) ions from dilute aqueous solutions. Ind. Eng. Chem. Res., 41(2): 180-89.

Bereket, G., Ayşe, Z., Aroğuz, R. and Mustafa, Z.O. 1997. Removal of Pb(II), Cd(II), Cu(II), and Zn(II) from aqueous solutions by adsorption on bentonite. J. Coll. Interf. Sci.,187(2): 338-43.

Chakravarti, A.K., Chowdhury, S.B. and Mukherjee, D.C. 2000. Liquid membrane multiple emulsion process of separation of copper(II) from wastewaters. Coll. Surf. A Physicochem. Eng. Aspects, 166(1-3): 7-25.

Chen, H. and Kim, A.S. 2006. Prediction of permeate flux decline in crossflow membrane filtration of colloidal suspension: A radial basis function neural network approach. Desalination, 192(1-3): 415-28.

Das, A.K. 2004. Micellar effect on the kinetics and mechanism of chromium(VI) oxidation of organic substrates. Coord. Chem. Rev., 248(1-2): 81-99.

Dodbiba, G., Josiane, P. and Toyohisa, F. 2015. Biosorption of heavy metals. Microbiol. Minerals Metals Mater. Environ., 409-26.

El-Sikaily, A., Ahmed El, N., Azza, K. and Ola, A. 2007. Removal of toxic chromium from wastewater using green alga *Ulva lactuca* and its activated carbon. J. Hazard. Mater., 148(1-2): 216–228.

Fagundes-Klen, M.R. 2007. Equilibrium study of the binary mixture of cadmium-zinc ions biosorption by the *Sargassum filipendula* species using adsorption isotherms models and neural network. Biochem. Eng. J., 34(2): 136-146.

Gómez, V. and Callao, M.P. 2006. Chromium determination and speciation since 2000. TrAC - Trends Anal. Chem., 25(10): 1006-1015.

Gontarski, C.A., Rodrigues, P.R., Mori, M. and Prenem, L.F. 2000. Simulation of an industrial wastewater treatment plant using artificial neural networks. Comp. Chem. Eng., 24(2-7): 1719-1723.

Guadix, A., Jose, E.Z., Carmen Almecija, M. and Guadix, E.M. 2010. Predicting the flux decline in milk crossflow ceramic ultrafiltration by artificial neural networks. Desalination, 250(3): 1118-1120.

Gupta, V.K. 2003. Removal of cadmium and nickel from wastewater using bagasse fly ash - a sugar industry waste. Water Res., 37(16): 4038-44.

Jiao, C. and Ding, Y. 2009. "Foam Separation of Chromium (VI) from Aqueous Solution. Journal of Shanghai University, 13(3): 263-66.

Kannan, N. and Rengasamy, G. 2005. Comparison of cadmium ion adsorption on various activated carbons. Water Air Soil Pollut., 163(1-4): 185-201.

Kashaninejad, M., Dehghani, A.A. and Kashiri, M. 2009. Modeling of wheat soaking using two artificial neural networks (MLP and RBF). J. Food Eng., 91(4): 602-607. http://dx.doi.org/10.1016/j.jfoodeng.2008.10.012.

Kongsricharoern, N. and Polprasert, C. 1996. Chromium removal by a bipolar electrochemical precipitation process. Water Sci. Technology, 34(9): 109-16. http://dx.doi.org/10.1016/S0273-1223(96)00793-7.

Kowalski, Z. 1994. Treatment of chromic tannery wastes. J. Hazard. Mater., 37(1): 137-41.

Li, H. 2008. A novel technology for biosorption and recovery of hexavalent chromium in wastewater by bio-functional magnetic beads. Bioresour. Technol., 99(14): 6271-79.

Libotean, D. 2009. Neural network approach for modeling the performance of reverse osmosis membrane desalting. J. Membr. Sci., 326(2): 408-419.

Manchón-Vizuete, E. 2005. Adsorption of mercury by carbonaceous adsorbents prepared from rubber of tire wastes. J. Hazard. Mater., 119(1-3): 231-38.

Meegoda, J.N. 2000. Emediation of chromium contaminated oils: Practice periodical of hazardous, toxic. Radioact. Waste Manag., 4(1): 7-15.

Monser, L. and Adhoum, N. 2002. Modified activated carbon for the removal of copper, zinc, chromium, and cyanide from wastewater. Sep. Purif. Technol., 26(2-3): 137-146.

Ngah, W.S.,Wan, S., Ghani, A.B. and Kamari, A. 2005. Adsorption behavior of Fe(II) and Fe(III) ions in aqueous solution on chitosan and cross-linked chitosan beads. Bioresour. Technol., 96(4): 443-450.

World Health Organization (WHO). 2020. Chromium in Drinking Water: A Background Document for Development of World Health Organisation Guidelines for Drinking Water. WHO, Geneva, pp. 1-30.

Pai, T.Y. 2007. Grey and neural network prediction of suspended solids and chemical oxygen demand in hospital wastewater treatment plant effluent. Comp. Chem. Eng., 31(10): 1272-1281.

Prakash, N., Manikandan, S.A., Govindarajan, L. and Vijayagopal, V. 2008. Prediction of biosorption efficiency for the removal of c opper(II) using artificial neural networks. J. Hazard. Mater., 152(3): 1268-1275.

Qiao, J.F., Xin, G. and Wen, J.L. 2020. An online self-organizing algorithm for feedforward neural network. Neural Comp. Appl., 32(23): 17505-17518. https://doi.org/10.1007/s00521-020-04907-6.

Religa, P., Kowalik, A. and Gierycz, P. 2011. Application of nanofiltration for chromium concentration in the tannery wastewater. J. Hazard. Mater., 186(1): 288-292. http://dx.doi.org/10.1016/j.jhazmat.2010.10.112.

Rowley, A.G., Husband, F.M. and Cunningham, A.B. 1984. Mechanisms of metal adsorption from aqueous solutions by waste tyre rubber. Water Res., 18(8): 981-984.

Sadrzadeh, M., Toraj, M., Javad, I. and Norollah, K. 2009. Neural network modeling of Pb^{2+} removal from wastewater using electrodialysis" Chem. Eng. Process. Intensif., 48(8): 1371–1381.

Sahoo, G.B. and Ray, C. 2006. Predicting flux decline in crossflow membranes using artificial neural networks and genetic algorithms. J. Membr. Sci., 283(1-2): 147-157.

Selomulya, C., Meeyoo, V. and Amal, R. 1999. Mechanisms of Cr(VI) removal from water by various types of activated carbons. J. Chem. Technol. Biotechnol., 74(2): 111-22.

Taty-Costodes, V. Christian, H.F., Catherine, P. and Alain, D. 2003. Removal of Cd(II) and Pb(II) ions, from aqueous solutions, by adsorption onto sawdust of *Pinus sylvestris*. J. Hazard. Mater., 105(1-3): 121-142.

Tiravanti, G., Petruzzelli, D. and Passino, R. 1997. Pretreatment of tannery wastewaters by an ion exchange process for Cr(III) removal and recovery. Water Sci. Technol., 36(2-3): 197-207. http://dx.doi.org/10.1016/S0273-1223(97)00388-0.

Veglio, F. and Beolchini, F. 1997. Removal of Metals by Biosorption: A Review. Hydrometallurgy, 44(3): 301-316.

Yetilmezsoy, K. and Demirel, S. 2008. Artificial neural network (ANN) approach for modeling Pb(II) adsorption from aqueous solution by Antep Pistachio (Pistacia Vera L.) Shells." Journal of Hazardous Materials, 153(3): 1288-1300.

Zhou, X. 1993. A process monitoring/controlling system for the treatment of wastewater containing chromium(VI).Water Res., 27(6): 1049-1054.

Effectiveness of the River Chief System in China: A Study Based on Grassroots River Chief's Behavior

Wenjie Yao*† and Ming Cheng

*College of Economics & Management, Zhejiang University of Water Resources and Electric Power, Hangzhou, 310018, China
**College of International Education, Zhejiang University of Water Resources and Electric Power, Hangzhou, 310018, China
†Corresponding author: Wenjie Yao; rantom_821024@163.com

ABSTRACT

The River Chief System is an administrative model of water environment governance currently adopted in China. Under this system, the chief CPC and government leaders at various levels serve as "river chiefs" and are responsible for organizing and directing the management and protection of the rivers and lakes within their remit. This paper tries to reveal the actual effectiveness of the River Chief System based on the behaviors of grassroots river chiefs (GRCs). First-hand data about GRCs is obtained through a questionnaire survey. Whether the water environment governance target is achieved and the water quality change of the river sections in the charge of GRCs is quantitatively assessed It has been found that, except for implementing "one policy for one river" and making river patrols, the behaviors of GRCs have no positive effect on river pollution prevention and control, implying the ineffectiveness of the River Chief System. The framework design of the River Chief System should be optimized, and a system with professionals to support GRCs in performing their duties should be established. Moreover, the tendency to use environmental regulation as a mandatory policy tool should be weakened. These measures are of great practical significance to the implementation of the green development concept and the furthering of the River Chief System overall.

INTRODUCTION

As an innovative administrative model of water environment governance in the face of severe water pollution, the River Chief System in China requires chief CPC and government leaders at various levels to serve as "river chiefs" and be responsible for organizing and directing the management and protection of the rivers and lakes within their remit. Essentially, this system is implemented to enhance the overall coordination, authority and accountability of existing river management systems. Since the issuance of the *Opinions on Full Implementation of the River Chief System* by the General Office of the Communist Party of China (CPC) Central Committee and the General Office of the State Council of China in 2016, the River Chief System has shifted from a "bottom-up" self-exploration to a unified "top-down" will (Shen 2018). Taking into consideration both river/lake distribution and administrative divisions, this system puts the decentralized authority of river management into the hands of CPC and government leaders at various levels. Through a stressful interaction mechanism between leadership and

responsibility where all authority is put into one hand and one chief leader is held accountable, it solves the problem of dysfunction caused by overlapping authority between water administration departments to a certain extent.

Grassroots river chiefs (GRCs) are undoubtedly the principal actors in implementing the River Chief System. For example, in Zhejiang Province, it is stipulated that the river chiefs at the county level and above should take the lead in the development of a water environment governance program with one policy for one river and that river chief at town and village levels should be responsible for the daily patrols of the river sections in their charge, with an aim to find and solve problems in a timely manner and assisting the higher-level river chiefs in their work. The term "GRCs' behaviors" refers to GRCs' performance of their daily management responsibilities for the river sections in their charge and their execution of tasks related to overall river pollution prevention and control. As a special form of environmental control, whether the River Chief System is effective in river pollution prevention and control depends directly on GRCs'

behaviors. Theoretically, GRC as a single individual is both a public interest realizer and a rational value selector. GRCs' behaviors are a process where a system uses all available information and takes action. Variables such as gender, age, occupation, and personality indirectly influence behavioral intentions through behavioral attitudes and subjective norms (Ajzen & Madden 1986). From the organizational behavior perspective, concerning an individual's psychological state, there are not only positive factors such as realizing public values and performing duties but also negative factors such as hesitation when facing multiple choices, hesitation to perform job responsibilities, and doubts as to mitigating risk pressure (Sheng & Chen 2019). It is the interaction among these positive and negative factors that provides a direct value judgment on GRCs' behaviors. In general, GRCs' behaviors tend to realize a range of outcomes, including social, organizational, and individual values. In objective reality, the realization of social and organizational values is subject to some uncontrollable factors. The realization of social value can be influenced by factors such as economic and social transformation and external organizational development, and the realization of organizational values can be impacted by heavy administrative duties at the grassroots level and the strong accountability required by higher-level governments. As a result, GRCs can directly devote themselves to the realization of individual values. Especially since the implementation of the River Chief System, GRCs, under stressful assessments and inefficient incentives, can easily develop fears of taking responsibility and dare not take action. Instead, they may be eager to achieve goals or accomplish tasks that are easy, with only controllable risk and a smaller level of accountability. The original property of responsibility is ignored consequently. In terms of the external environment, the River Chief System, which runs based on a principle of local management and a mechanism for river chiefs at all levels to be held accountable, actually transfers the main responsibility for river pollution prevention and control and related great pressure to the grassroots in a top-down way. The whole framework of the River Chief System, comprising various rules regarding meetings, patrol, information reporting, work supervision, assessment, accountability, and other aspects, is often overwhelming for GRCs and can easily bring out formalism, reducing the effectiveness of the system objectively. It has been shown that, although the River Chief System has achieved initial outcomes for water pollution control, it has not significantly reduced the pollutants deep in the water, which may reveal a whitewash of local governments addressing the symptoms but not the root cause (Shen & Jin 2018). In terms of internal requirements, river pollution prevention, and control is a complex, systematic project whose principal implementers must have solid professional knowledge, a positive attitude

at work, excellent comprehensive abilities, and an open mind. These requirements are unachievable for most GRCs, thus subjectively limiting the effectiveness of the River Chief System.

These facts have been shown in existing studies. Scholars have argued that, although it is possible to improve the results of river pollution prevention and control by strengthening the vertical mechanism (Zhou & Xiong 2017, Xiong 2017), the "last mile" of water environment governance is not always smooth due to the capability and action dilemmas for individuals and agencies implementing policy caused by over-reliance on authority (Gao 2019) and role overload caused by information asymmetry in the principal-agent relationship and dual roles (Wang & Cai 2011, Yan & Wang 2019). As very few quantitative analyses have been conducted on the effectiveness of the River Chief system, there is a need to obtain first-hand data about GRCs through questionnaire surveys and quantitatively assess whether the water environment governance target is achieved and water quality changes in the river sections under the charge of GRCs, thus revealing the actual effectiveness of the River Chief System based on GRCs' behaviors. This paper tries to provide some empirical support and a decision-making basis for structuring the positive incentive mechanism for GRCs' behaviors in the reconstruction of the River Chief System and thereby has great practical significance to the implementation of the green development concept and the furthering of the River Chief System overall.

STUDY DESIGN

Sample Selection

Generally speaking, grassroots river chiefs (GRCs) refer to village- and town-level river chiefs. But as stipulated in many regions, it is county-level river chiefs who are responsible for developing and implementing a water environment governance program with one policy for one river, which is the fundamental basis for the assessment and accountability of river chiefs at the county level and below. Due to this fact, county-level river chiefs are also deemed GRCs in our study. In 2022, we conducted a questionnaire survey to assess the duty performance of GRCs in 2021. The survey participants were 683 GRCs attending the professional training on the River Chief System organized by the College of Zhejiang River Chief at Zhejiang University of Water Resources and Electric Power, which is the first college of river chiefs in China. A total of 683 questionnaires were handed out, and 97.66% of them (667) were collected as valid questionnaires based on information screening and reliability assessment. Among the 667 GRCs, 628 river chiefs were from counties within prefecture-level cities Jinhua, Quzhou, and Wenzhou

of Zhejiang Province, and the remaining 39 river chiefs were from Kongdong District (County), Pingliang City, Gansu Province. In terms of administrative level, there were 445 village-level river chiefs (66.72%), 136 town-level river chiefs (20.39%), and 86 county-level river chiefs (12.89%).

Variables

Explained Variables

To examine the effectiveness of the River Chief System, two explained variables were set, namely, whether the water environment governance target is met (OV1) and water quality change (OV2). OV1 is a binary variable with only two possible values: 0 (Yes) or 1 (No). Water quality has been divided into six grades: VI (poorest quality), V, IV, III, II and I (best quality). Grades VI, V, IV, III, II and I are assigned a value of 0, 1, 2, 3, 4 and 5, respectively. And OV2 is the water quality difference over time.

Explanatory Variables

Our core explanatory variables are a set of variables describing GRCs' behavioral characteristics. Nine behavioral variables

were summarized and identified according to GRCs' duties under the River Chief System: (1) whether one policy for one river is implemented; (2) the annual number of river patrols; (3) whether records of river patrols are kept; (4) the annual number of regular work meetings; (5) communication with the public; (6) whether work training is attended; (7) whether annual tasks are disclosed; (8) whether the annual work plan is accomplished on schedule; and (9) overtime work. These nine variables are generally considered to have an effect on river pollution prevention and control. In other words, if one policy for one river is implemented, records of river patrols are kept, annual tasks are disclosed, the annual work plan is accomplished on schedule and there are more river patrols, regular work meetings, communication with the public and overtime work during a period, the River Chief System is likely to be more effective.

Control Variables

Our control variables are a set of variables describing social characteristics. The control variables are included in the study due to the fact that whether the water environment

Table 1: Definitions of variables.

Variables		Definitions
Whether the water environment governance target is met		No = 0, Yes = 1
Previous water quality		Grade VI (poorest) = 0, Grade V = 1, Grade IV = 2, Grade III = 3, Grade II = 4, Grade I (best) = 5
Current water quality		Grade VI (poorest) = 0, Grade V = 1, Grade IV = 2, Grade III = 3, Grade II = 4, Grade I (best) = 5
Change in water quality		Current water quality - previous water quality
Behavioral Characteristics	Whether one policy for one river is implemented	No = 0, Yes = 1
	Annual number of river patrols	The annual number of river patrols
	Whether records of river patrols are kept	No = 0, Yes = 1
	Annual number of regular work meetings	0 meeting = 1; 1 meeting = 2; 2 meetings = 3; 3 meetings = 4; 4 or more meetings = 5
	Communication with the public	Zero = 1; Little = 2; Frequent = 3; Much = 4; Very much = 5
	Whether work training is attended	No = 0, Yes = 1
	Whether annual tasks are disclosed	No = 0, Yes = 1
	Whether the annual work plan is accomplished on schedule	No = 0, Yes = 1
	Overtime work	Never = 1; Little = 2; Occasional = 3; Frequent = 4; Always = 5
Social characteristics	Whether the public report the problems	No = 0, Yes = 1
	Support for work from the public	None = 1; Little = 2; Some = 3; Much = 4; Very Much = 5
	Number of sewage outfalls	Number of sewage outfalls
	Number of rainwater outfalls	Number of rainwater outfalls
	Number of industrial enterprises in catchment areas	Number of industrial enterprises in catchment areas
	Number of livestock and poultry farms in catchment areas	Number of livestock and poultry farms in catchment areas

governance target is met and water quality change is affected by some objective conditions such as the status of the public, infrastructure, industry, etc. Generally speaking, if the public can report problems or support water environment governance or if there are many rainwater outfalls, it will be easier to achieve water environment governance targets and improve water quality. On the contrary, if there are many sewage outfalls, industrial enterprises and livestock and poultry farms, the realization of the above-mentioned outcomes will be adversely affected to some extent. Definitions of the variables are shown in Table 1.

Model Setting

Most behaviors of GRCs have a significant positive effect on the achieving of water environment governance targets and water quality improvement, indicating the effectiveness of the River Chief System. Given the qualitative or quantitative characteristics of the explained variables, two regression models, a binary logistic model and an OLS model, were constructed to reveal the real effectiveness of the River Chief System.

The constructed binary logistic regression model is as follows:

$$\log it(T = 1) = \alpha_0 + \sum_{i=1}^{9}(\alpha_{1i}B_i) + \sum_{j=1}^{6}(\alpha_{2j}S_j) + \theta + \varepsilon$$

…(1)

And the constructed OLS regression model is as follows:

$$\Delta Q = Q_1 - Q_0 = \beta_0 + \sum_{i=1}^{9}(\beta_{1i}B_i) + \sum_{j=1}^{6}(\beta_{2j}S_j) + \eta$$

…(2)

Where, T denotes the probability of having met the water environment governance target; ΔQ denotes the change in water quality; Q_0 and Q_1 denote the previous and current water quality respectively; B_i denotes the core explanatory variables, a set of variables describing behavioral characteristics; S_j denotes the control variables, a set of social characteristics variables; α_0, α_{1i}, α_{2j}, β_0, β_{1i} and β_{2j} are the corresponding regression coefficients; θ is county's fixed effect; ε and η represent random errors. A significantly positive α_{1i} or β_{1i} obtained by regression indicates that the corresponding behavior of GRCs can have a positive effect on river pollution prevention and control. Otherwise, the behavior would be a vain attempt at water environment governance.

EMPIRICAL ANALYSIS

Descriptive Statistics

The descriptive statistics for all variables are shown in

Table 2. As indicated by the survey, a total of 585 GRCs (87.71%) achieved their water environment governance target. In addition, the mean previous and current water quality were 2.2969 and 3.2264, respectively, resulting in a mean water quality change of 0.9295, which suggests that the implementation of the River Chief System has led to a general improvement in water quality from Grade IV to Grade III.

For the behavioral characteristics of GRCs, 624 GRCs (93.55%) implemented one policy for one river; 602 GRCs (90.25%) made river patrol records; 511 GRCs (76.61%) attended work training; 589 GRCs (88.31%) disclosed their annual work tasks; and 488 GRCs (73.16%) accomplished their annual work plan on schedule. In addition, in the year 2021, GRCs made 3.7901 river patrols and attended 4.1244 work meetings on average. At the same time, the mean value of their communication with the public and overtime work are 3.6387 and 2.8426, respectively. It can be seen that, although GRCs made relatively few river patrols in the year, they performed their duties actively in general.

For social characteristics faced by GRCs, 250 GRCs (37.48%) received problems reported by the public and had public support for their work (3.9415); on average, there were 1.7376 outfalls (SD: 8.1862), 3.8441 rainwater outfalls (SD: 25.5761), and 4.2804 industrial enterprises (SD: 51.6797) and 0.5067 livestock and poultry farms in catchment areas (SD: 5.1209). It can be seen that not many GRCs receive reports on problems from the public, and the public is supportive of their work. As indicated by the geographic origins of questionnaire survey respondents, geographic factors such as the number of sewage outfalls, rainwater outfalls, industrial enterprises and livestock and poultry farms in rain catchment areas vary greatly.

Analysis of the River Chief System's Effectiveness

The regression results based on equations (1) and (2) are presented in Table 3 and Table 4, respectively. Column (1) are the results without including any control variables; column (2) are the results when only control variables related to the public (i.e., two social characteristics: whether there are problems reported by the public and public support for the work) are included; column (3) are the results when only control variables related to infrastructure (i.e., two social characteristics: the number of sewage outfalls and the number of rainwater outfalls) are included; column (4) are the results when only control variables related industries (i.e., two social characteristics: the number of industrial enterprises and the number of livestock and poultry farms in catchment areas) are included; and column (5) are the results when all control variables describing social characteristics are included.

Table 2: Descriptive statistics for variables.

Variables		Sample size	Max.	Min.	Mean	Standard Variance
Whether the water environment governance target is met		667	1	0	0.8771	0.3286
Previous water quality		667	5	0	2.2969	1.2777
Current water quality		667	5	0	3.2264	1.2098
Change in water quality		667	5	-4	0.9295	0.9426
Behavioral Characteristics	Whether one policy for one river is implemented	667	1	0	0.9355	0.2458
	Annual number of river patrols	667	30	0	3.7901	4.3171
	Whether records of river patrols are kept	667	1	0	0.9025	0.2968
	Annual number of regular work meetings	667	5	1	4.1244	1.2319
	Communication with the public	667	5	1	3.6387	1.1055
	Whether work training is attended	667	1	0	0.7661	0.4236
	Whether annual tasks are disclosed	667	1	0	0.8831	0.3216
	Whether the annual work plan is accomplished on schedule	667	1	0	0.7316	0.4434
	Overtime work	667	5	1	2.8426	0.9745
Social characteristics	Whether the public reports problems	667	1	0	0.3748	0.4844
	Support for work from the public	667	5	1	3.9415	0.9027
	Number of sewage outfalls	667	164	0	1.7376	8.1862
	Number of rainwater outfalls	667	440	0	3.8441	25.5761
	Number of industrial enterprises in catchment areas	667	1224	0	4.2804	51.6797
	Number of livestock and poultry farms in catchment areas	667	125	0	0.5067	5.1209

For results shown in all columns of Table 3, the county is controlled as a fixed effect.

The results of the two regressions demonstrate that, among the behavioral characteristics, two factors, whether one policy for one river is implemented and the annual number of river patrols, have a significant positive effect on the achievement of water environment governance targets and water quality change, which is robust. In column (5) of Table 3, the average marginal effects of whether one policy for one river is implemented and the annual number of river patrols are estimated to be 0.1662 (SE: 0.0381) and 0.0224 (SE: 0.0060), respectively, both significant at 1% level; their odds ratios are 11.7682 (SE: 6.2846) and 1.3949 (SE: 0.1165), respectively, both significant at 1% level. This indicates that the probability of achieving the water environment governance target will increase by 0.1662 units or 0.0224 units for each unit increase in the extent of implementing one policy for one river or the annual number of river patrols, and the odds ratio will increase by 10.7682 units or 0.3949 units accordingly. Whether one policy for one river is implemented has a larger effect on the achieving of the water environment governance target than the annual number of river patrols. Similarly, the regression coefficients in column (5) of Table 4 shows that the effect of whether one policy for one river is implemented on water quality

change is greater than that of the annual number of river patrols. It is worth noting that overtime work has a significant negative effect on water quality change, which is robust. This may be due to the fact that the work of river chiefs is usually backlogged and can only be finished during overtime hours and that environmental controls are not effectively implemented during normal working hours, resulting in some illegal pollution emissions not being stopped in time. Consequently, the higher the frequency of overtime work, the more serious the deterioration of water quality. Yan & Wang (2019) also illustrated that workload had a significant negative effect on the policy implementation of GRCs. On the contrary, overtime has no significant effect on whether the water environment governance target is met. In addition, although slightly less robust, the annual number of regular work meetings has a significant positive effect on water quality change. Among control variables describing social characteristics, whether the public reports problems have a significant negative effect on water quality change, probably due to the situation where problems reported by the public cannot be resolved in a timely manner.

To ensure the robustness of the regression results, more analyses were conducted under the following settings: first, the Probit model was used for equation (1) for re-estimation; second, as the river sections in the charge of river chiefs

Table 3: Binary logistical regression results for the effectiveness of the River Chief System.

Whether the water environment governance target is met	(1) Logit	(2) Logit	(3) Logit	(4) Logit	(5) Logit
Whether one policy for one river is implemented	2.4661*** (0.5098)	2.4464*** (0.4581)	2.4864*** (0.5027)	2.4660*** (0.5087)	2.4654*** (0.4551)
Annual number of river patrols	0.3482*** (0.1181)	0.3339*** (0.1205)	0.3465*** (0.1159)	0.3485*** (0.1181)	0.3328*** (0.1190)
Whether records of river patrols are kept	0.5616 (0.5264)	0.5246 (0.5552)	0.5352 (0.5303)	0.5631 (0.5250)	0.5016 (0.5687)
Annual number of regular work meetings	0.3692 (0.2789)	0.3839 (0.2770)	0.3871 (0.2770)	0.3700 (0.2780)	0.4060 (0.2715)
Communication with the public	0.0226 (0.2134)	0.0047 (0.1514)	0.0229 (0.2170)	0.0214 (0.2133)	-0.0026 (0.1597)
Whether work training is attended	-0.2994 (0.7952)	-0.3430 (0.8212)	-0.2978 (0.7122)	-0.3094 (0.7737)	-0.3434 (0.7339)
Whether annual tasks are disclosed	0.0232 (0.3091)	0.0383 (0.2789)	0.0016 (0.3273)	0.0258 (0.3051)	-0.0054 (0.2826)
Whether the annual work plan is accomplished on schedule	-0.0077 (0.4121)	-0.0772 (0.3901)	0.0158 (0.4041)	-0.0062 (0.4118)	-0.0444 (0.3799)
Overtime work	0.3498 (0.2460)	0.3516 (0.2290)	0.3439 (0.2464)	0.3512 (0.2466)	0.3485 (0.2318)
Whether the public reports problems	—	-0.5331 (0.4074)	—	—	-0.5245 (0.4015)
Support for work from the public	—	0.2108 (0.2411)	—	—	0.2212 (0.2381)
Number of sewage outfalls	—	—	-0.0407* (0.0236)	—	-0.0366 (0.0251)
Number of rainwater outfalls	—	—	0.0317 (0.0254)	—	0.0338 (0.0241)
Number of industrial enterprises in catchment areas	—	—	—	0.0004 (0.0020)	-0.0012 (0.0009)
Number of livestock and poultry farms in catchment areas	—	—	—	-0.0060 (0.0108)	-0.0062 (0.0070)
Constant terms	-3.8108*** (1.0961)	-4.2500*** (0.9180)	-3.8601*** (1.0932)	-3.8097*** (1.0965)	-4.3335*** (0.9291)
The county as a fixed effect	Yes	Yes	Yes	Yes	Yes
Sample size	667	667	667	667	667
Pseudo R^2	0.3330	0.3409	0.3376	0.3331	0.3456
Likelihood	-165.8267	-163.8557	-164.6932	-165.7952	-162.6894
Correctly (%)	91.90	92.65	91.90	91.90	92.35

Note: *, ** and *** indicate significance at 10%, 5%, and 1% levels, respectively; standard errors are in parentheses; "-" is the default item.

at lower administrative levels in the same region may be part of the river sections in the charge of river chiefs at higher administrative levels, 136 town-level river chiefs and 86 county-level river chiefs were excluded from the overall sample, and only the 445 village-level river chiefs were analyzed using equations (1) and (2); and third, given provincial differences, 39 GRCs from Gansu Province were excluded from the overall sample, and only the 628 GRCs from Zhejiang Province were analyzed using equations (1) and (2).

The results of robustness tests are presented in Table 5. It is shown that, among the behavioral characteristics, two factors, whether one policy for one river is implemented and the annual number of river patrols, have a significant positive effect on the achievement of water environment governance targets and water quality change. When only 445 village-level river chiefs or 628 GRCs from Zhejiang Province are included in the overall sample, the regression results show that: the annual number of work meetings has a significant positive effect on the achieving of the water environment

Table 4: OLS regression results for the effectiveness of the River Chief System.

Change in water quality	(1)	(2)	(3)	(4)	(5)
Whether one policy for one river is implemented	0.6017*** (0.1658)	0.6194*** (0.1716)	0.5544*** (0.1527)	0.5991*** (0.1622)	0.6215*** (0.1686)
Annual number of river patrols	0.0100* (0.0054)	0.0128*** (0.0038)	0.0123** (0.0048)	0.0097* (0.0053)	0.0121*** (0.0039)
Whether records of river patrols are kept	0.1113 (0.1285)	0.1160 (0.1223)	0.1573 (0.1324)	0.1154 (0.1282)	0.1065 (0.1214)
Annual number of regular work meetings	0.0920** (0.0403)	0.0609 (0.0399)	0.0864** (0.0399)	0.0781** (0.0395)	0.0670* (0.0403)
Communication with the public	-0.0292 (0.0355)	-0.0440 (0.0358)	-0.0403 (0.0355)	-0.0403 (0.0353)	-0.0365 (0.0361)
Whether work training is attended	0.0922 (0.1065)	-0.0524 (0.1015)	0.0811 (0.1050)	0.1023 (0.1094)	-0.0445 (0.1062)
Whether annual tasks are disclosed	-0.0081 (0.1245)	0.0276 (0.1142)	0.0131 (0.1295)	0.0349 (0.1229)	0.0308 (0.1153)
Whether the annual work plan is accomplished on schedule	-0.0903 (0.0748)	-0.0470 (0.0766)	-0.0764 (0.0753)	-0.0579 (0.0740)	-0.0655 (0.0765)
Overtime work	-0.0900** (0.0369)	-0.1143*** (0.0362)	-0.0970*** (0.0367)	-0.0894** (0.0369)	-0.1024*** (0.0364)
Whether the public reports problems	—	-0.1354** (0.0668)	—	—	-0.1347** (0.0676)
Support for work from the public	—	0.0805* (0.0455)	—	—	0.0703 (0.0461)
Number of sewage outfalls	—	—	-0.0079 (0.0091)	—	-0.0100 (0.0073)
Number of rainwater outfalls	—	—	0.0011 (0.0019)	—	0.0012 (0.0017)
Number of industrial enterprises in catchment areas	—	—	—	0.0015 (0.0013)	0.0018 (0.0013)
Number of livestock and poultry farms in catchment areas	—	—	—	0.0001 (0.0041)	0.0006 (0.0056)
Constant terms	0.2050 (0.1999)	0.2313 (0.2153)	0.2696 (0.1869)	0.2334 (0.1913)	0.2003 (0.2175)
Sample size	667	667	667	667	667
Adj R^2	0.5699	0.6239	0.5738	0.5692	0.6175
F statistic	89.37***	93.20***	75.83***	74.43***	68.31***

Note: *, ** and *** indicate significance at 10%, 5%, and 1% levels, respectively; standard errors are in parentheses; "-" is the default item

governance target in columns (2) and (3), and has a significant positive effect on water quality change in column (5); disclosure of annual work tasks has a significant positive effect on water quality change in column (4); and overtime work has a significant negative effect on water quality change in columns (4) and (5). There are two points worth noting. First, attendance in work training has a significant negative effect on the achieving of governance targets in columns (2) and (3), and has a significant negative effect on change in water quality in columns (4) and (5). A possible explanation is that the content of the training received by the river chief provides wrong guidance on work to some extent. As a result, the attendance of village-level river chiefs or GRCs from Zhejiang Province in work training leads to water quality deterioration and more difficulty in achieving water environment governance targets. Second, whether the annual work plan is accomplished on schedule has a significant negative effect on the achieving of the governance target in column (3), and has a significant negative effect on water quality change in column (4). A possible explanation is that the setting of annual tasks does not give full consideration to contingent factors. As a result, the accomplishment of annual tasks on schedule makes it harder for GRCs from Zhejiang Province to achieve the water environment governance target

Table 5: Robustness test results.

Whether the water environment governance target is met	(1) Probit	(2) Logit	(3) Logit	Change in water quality	(4) OLS	(5) OLS
Whether one policy for one river is implemented	1.4904*** (0.2736)	2.9539*** (0.5606)	3.0266*** (0.5021)	Whether one policy for one river is implemented	0.7570*** (0.2188)	0.7616*** (0.1709)
Annual number of river patrols	0.1565*** (0.0507)	0.3515*** (0.0845)	0.4003*** (0.0999)	Annual number of river patrols	0.0215*** (0.0037)	0.0141*** (0.0043)
Whether records of river patrols are kept	0.2796 (0.3035)	-0.4960 (0.6978)	-0.3287 (0.5167)	Whether records of river patrols are kept	-0.0598 (0.1632)	-0.1400 (0.1237)
Annual number of regular work meetings	0.2098 (0.1389)	0.6675** (0.2737)	0.6833*** (0.2210)	Annual number of regular work meetings	0.0503 (0.0503)	0.1141*** (0.0405)
Communication with the public	0.0101 (0.0774)	0.1601 (0.1497)	0.1173 (0.1978)	Communication with the public	-0.0457 (0.0394)	-0.0418 (0.0371)
Whether work training is attended	-0.1538 (0.3816)	-1.3638** (0.5878)	-1.3900*** (0.5198)	Whether work training is attended	-0.7592*** (0.1164)	-0.2032** (0.0976)
Whether annual tasks are disclosed	-0.0206 (0.1608)	-0.4195 (0.3738)	-0.1668 (0.2411)	Whether annual tasks are disclosed	0.3842** (0.1543)	0.1513 (0.1161)
Whether the annual work plan is accomplished on schedule	-0.0423 (0.1966)	-0.3472 (0.3855)	-0.5845* (0.3281)	Whether the annual work plan is accomplished on schedule	-0.2479** (0.1024)	-0.1055 (0.0745)
Overtime work	0.1662 (0.1137)	0.1811 (0.1965)	0.1288 (0.2537)	Overtime work	-0.2300*** (0.0385)	-0.1294*** (0.0364)
Control variables	Yes	Yes	Yes	Control variables	Yes	Yes
Constant terms	-2.3374*** (0.5317)	-3.8665** (1.7633)	-4.0704*** (1.0339)	Constant terms	0.9519*** (0.2746)	0.2656 (0.1967)
County as a fixed effect	Yes	Yes	Yes	Sample size	445	628
Sample size	667	445	628	Adj R^2	0.8801	0.6266
Pseudo R^2	0.3408	0.3576	0.4394	F statistic	205.14***	66.86***
Likelihood	-163.8849	-95.0371	-113.4661			
Correctly (%)	91.60	93.93	94.90			

Note: *, ** and *** indicate significance at 10%, 5%, and 1% levels, respectively; standard errors are in parentheses; "-" is the default item

and causes water quality deterioration at the village level. Overall, GRCs' behaviors have no positive effect on river pollution prevention and control, and the River Chief System is not as effective as it should be.

CONCLUSIONS AND POLICY IMPLICATIONS

Except for implementing "one policy for one river" and the annual number of river patrols, the behaviors of grassroots river chiefs (GRCs) have no positive effect on river pollution prevention and control, implying the ineffectiveness of the River Chief System. Therefore, it is imperative to re-construct the River Chief System. Combining the questionnaire survey and interview results, we believe that the most pressing priority in re-construction is to structure a positive incentive mechanism for the behaviors of GRCs. The specific measures are as follows. First, the framework design of the River Chief System should be optimized. On

the basis of continuing to strengthen the implementation of one policy for one river and formalize the patrol system, the government should simplify the rules regarding the meeting, information reporting, and work supervision, and establish a reasonable and effective reward and punishment system based on the achieving of water environment governance targets and water quality improvement for the river sections in the charge of river chiefs. In particular, there should be a focus on enhancing the guidance on and delivery of benefits to mobilize the enthusiasm of GRCs to perform their duties and induce the endogenous driving force for river pollution prevention and control. For example, the government can link the work performance of river chiefs with salary and promotion; elect "excellent river chiefs" according to the assessment results and set up special funds to reward them; and improve the financial system to reimburse or subsidize expenses related to the work of river chiefs. Second, a system with professionals to support GRCs in performing their

duties should be established. Technicians can be recruited by long-term recruitment from the market or temporary transfer from functional departments to enrich the talent pool for GRCs, make up for GRCs' lack of professional capabilities and effectively improve their efficiency in performing duties. Third, the tendency of environmental regulation as a mandatory policy tool should be weakened. Environmental taxes and subsidies and emissions trading can be introduced to optimize the structure of policy tools. And non-governmental forces such as enterprises, the public, NGOs and the media can be absorbed in river pollution prevention and control to effectively alleviate the risk and pressure brought by the "responsibility contracting system" to GRCs.

FUNDING

REFERENCES

Ajzen, I. and Madden, T. 1986. Prediction of goal-directed behavior: Attitudes, intentions, and perceived behavioral control. Journal of Experimental Social Psychology, 22(5): 453-474.

Gao, J. J. 2019. On the path to sustainable development of river chief system: a perspective of Smith's model of policy implementation process. Humanities & Social Sciences Journal of Hainan University, 37(3): 39-48.

Shen, K. R. and Jin, G. 2018. The policy effects of local governments' environmental governance in China - a study based on the evolution of the "river-director" system. Social Sciences in China, (5): 92-115.

Shen, M. H. 2018. Analysis on the river chief system from the view of institutional economics. J. China Population, Resources and Environment, 28(1): 134-139.

Sheng, M. K. and Chen, T. D. 2019. An exploration into the logic, harm, and governance of grass-roots officials' avoidance of responsibility. Journal of Jishou University (Social Sciences Edition), 40(5): 39-47.

Wang, S. M. and Cai, M. M. 2011. Critique of the system of river-leader based on the perspective of new institutional economics. China Population, Resources and Environment, 21(9): 8-13.

Xiong, Y. 2017. On cross-domain environmental governance - take "river-chief system" as a sample. Social Science of Beijing, (5): 108-116.

Yan, H. N. and Wang, S. N. 2019. The implementation capability of the grass-roots river chiefs - an empirical analysis of "the last mile of the policy". Journal of Guangxi Normal University (Philosophy and Social Sciences Edition), 55(6): 36-53.

Zhou, J. G. and Xiong, Y. 2017. "The river chief system": how is continuous innovation possible? A two-dimension analysis on the basis of both policy text and reform practice. Jiangsu Social Sciences, 4: 38-47.

Original Research Paper

doi https://doi.org/10.46488/NEPT.2023.v22i03.035

Open Access Journal

Perception Versus Actual Value of Quality of Drinking Water: A Case Study of Iron and Steel Industry in West Bengal, India

Rahul Rajak* iD**, Arup Jana*, Aparajita Chattopadhyay*, Sushmita Singh*** iD **and Jitender Prasad****†** iD
*Institute of Development Studies, Kolkata, West Bengal, India
**Centre of Social Medicine and Community Health, Jawaharlal Nehru University, New Delhi, India
***Department of Family & Generations, International Institute for Population Sciences, Mumbai, India
†Corresponding author: Jitender Prasad; jitenderprasad18@gmail.com

ABSTRACT

The study aims to understand employees' knowledge, awareness, and overall perception of drinking water quality in the Iron and Steel Industry in Burnpur, India. Further, this study evaluated drinking water's physicochemical and bacteriological properties collected from different company sites. This study uses a mixed-method approach with individual interviews of selected employees (n=342) and the laboratory test of eight selected drinking water sites. The results show that most employees considered drinking water acceptable to be excellent. However, only 30% of employees in Site 1 (Coke Oven By-Product department) have reported organoleptic properties of water under the excellent category. The result explained that other physicochemical and bacteriological properties are in good status in all sites except for a colony count, expressing their suitability for drinking purposes. In summary, employees' perception of water quality aligns with their drinking water's physicochemical and bacteriological properties.

INTRODUCTION

Water, the elixir of organisms, is a precious natural resource for human life. Clean and adequate quantities of drinking water are recognized as fundamental to human dignity (United Nations High Commissioner for Human Rights 2019). However, industrial pollution contributes to deteriorating drinking water quality within and outside the industry (Dogaru et al. 2009, Singh et al. 2018). Different forms of industrial pollutants affect drinking water quality, and it's responsible for many morbidities and mortalities due to water-borne diseases (Rehman et al. 2018. Rakhecha 2020). According to the World Health Organization (2019), nearly 2 billion people use the source of drinkable water contaminated with feces. However, India ranks 120th out of 122 countries on the water quality index, and about 70% of India's water supply is likely contaminated. (NITI Aayog 2018). Therefore, it is essential to monitor the drinking water quality, specifically in the industrial sector in India.

In the Iron and Steel Industry, primarily polluted operations are the preparation of raw materials, manufacturing of coke in coke ovens, sintering, and drilling operations, steel-making furnaces, recovery of chemicals from benzol and tar products, and wind erosion from overburden (OB) dumps, etc. (Nurul et al. 2016, Tiwari et al. 2016). These all-industrial operations, directly and indirectly, damage the physicochemical and bacteriological properties of the quality of drinking water. In India, several studies examined drinking water's physicochemical and bacteriological quality. Many found that water sources nearby the industry were contaminated with pollution indicators such as fecal and total coliforms and unfit for drinking purposes (Srinivas et al. 2013, Sukumaran et al. 2015, Dhawde et al. 2018, Singh et al. 2018). However, a laboratory test of the water is a scientific process to assess the drinking water quality. However, people's perceptions and experience with water quality (i.e., taste, smell, color, appearance, and satisfaction level) are also crucial to identifying water quality (Doria et al. 2009, Eck et al. 2020, Grupper et al. 2021). Whereas chemical contamination in the drinking water may cause numerous health problems among people (Nikaeen et al. 2016). Furthermore, flavor is considered the most relevant variable and more adequately explains consumption than perceived water quality (Doria et al. 2009).

ORCID details of the authors:

Rahul Rajak: https://orcid.org/0000-0002-6009-581X
Sushmita Singh: https://orcid.org/0000-0003-3886-2135
Jitender Prasad: https://orcid.org/0000-0002-2865-6111

Also, changes in perception are related to individual decisions influenced by various socio-demographic, economic, and other factors (Abedin et al. 2014, Eck et al. 2020). In this context, Khalid et al. (2018) found in their study that young respondents (10-30 age group) were more concerned about their drinking water quality as compared with older (51-70 age group) people.

However, the nature and virtue of drinking water standards may vary across countries and regions (WHO, 2017). No single approach is universally applicable to measure the quality of drinking water. It is possible to assess drinking water quality using different physical, chemical, and bacteriological parameters (Nikaeen et al. 2016 & Dhawde et al. 2018). These parameters are; pH value, Total Solids (TS), Total Dissolved Solids (TDS), Total Suspended Solids (TSS), and chemical parameters like total alkalinity, dissolved oxygen (DO), total hardness, calcium (Ca), magnesium (Mg), chlorinate, salinity and bacterial parameters like standard plate count (SPC), total coliform count (TCC), fecal coliform count (FCC) and fecal streptococcal count (FSC) (Krishnan et al. 2007). For this reason, it is important to find out ' 'employees' perceptions and drinking water quality in the Iron and Steel Industry in Burnpur, West Bengal.

The present study briefly overviews drinking water quality in selected sites of the Indian Iron and Steel Industry, Burnpur, India. Previously, many studies have assessed water quality in the nearby industry; however, as per the author's knowledge, no such studies examined the drinking water quality of different sites within the Iron and Steel Industry. Also, this is the first-ever study that matched the employee's perception of drinking water quality with the actual quality by laboratory test. The objective of this research was twofold; first, we assess the employee's knowledge, awareness, and overall perception regarding the water quality in the selected site in the Iron and Steel Industry. Secondly, we evaluated the physicochemical and bacteriological properties of water by laboratory test results of selected sites in the industry. Based on these two objectives, we formulated our research questions: i.e. are there any differences between people's perception of drinking water quality and the actual tested value of the same water?

MATERIALS AND METHODS

Study Area

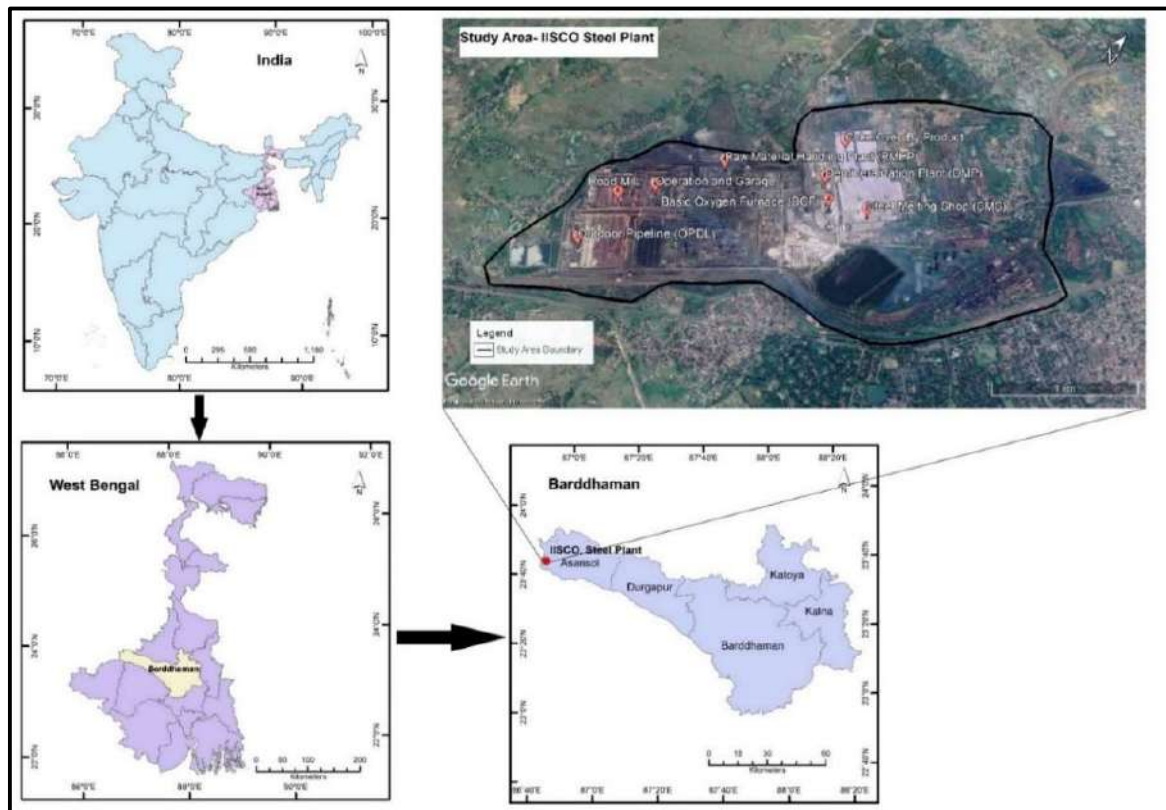A cross-section study was conducted from November

Fig. 1: Study area map.

2019 to March 2020 in the Indian Iron and Steel Industry, Burnpur (District, North Bardhaman, West Bengal), India (Fig. 1). This industry is one of the large-scale public-sector plants managed by the Steel Authority of India Limited (SAIL), under the Government of India. It is the oldest unit established in 1918 for manufacturing pig iron and iron casting in India.

Research Design

This study is based on a mixed-method approach with individual interviews of selected employees and the laboratory test (physicochemical and bacteriological parameters) of eight selected drinking water sites.

Questionnaire-Based Individual Survey

An individual survey and sampling campaigns were conducted from November 2019 to March 2020. The survey was conducted on (n=342) Iron and Steel Industry employees. The individual survey was designed to elicit peoples' perceptions of drinking water quality at the selected industry sites. Study participants were selected from eight different departments in the industry. Subsequently, we selected water samples from the same departments. The selected participants were proportionally allocated to selected departments and employees using a systematic random sampling method.

Scale Development Process

The overall perception of the drinking water quality scale was developed to determine the water quality awareness level among the employees who participated in the research. In the development of this scale, the following phases were included: (a) the formation of scale items, (b) the content validity study, (c) the construct validity study, (e) and the ' 'Cronbach's alpha internal consistency reliability.

Reliability of Data

The scale's reliability was 0.9313 ' 'Cronbach's alpha, which indicates the reliability of consistency of the questionnaire data in the study. Our questions were based on the organoleptic properties of water, such as clarity, color, smell, taste, and healthiness. Many previous studies also used a similar scale to identify the water quality (Abdi-Soojeede & Kullane 2019, Grupper et al. 2021).

Laboratory Analysis

Water sample collection: A total of eight water samples were collected from the selected sites (n=8) of the Iron and Steel Industry, Burnpur. Out of that, six samples are tap water (Site 1 to Site 6), and the other two samples are tank water (Site 7) and reverse osmosis (R.O.) water (Site 8). All these waters were used only for drinking purposes. Water samples from each sampling site were aseptically collected in sterile glass bottles (500 ml) and plastic containers (1 liter). These bottles were rinsed with deionized water, followed by washing (thrice) before filling them. Further, water samples were labeled with the department name and number and transported to the laboratory in the icebox for the physicochemical and bacteriological tests. The water samples were tested with a holding time of 6-8 hours with the selected parameters using the Bureau of Indian Standards (Bureau of Indian Standards 2012).

Selection of sampling points: The primary survey found that water sources are the same in the industry. However, the level of pollution changes by the different departments. Based on these observations, we identified eight major highly polluted departments and collected the water from the same sites. The details of the sample and water selection points are mentioned in (Fig. 2).

Physicochemical and bacteriological analysis: Standard procedures were followed to analyze the physicochemical and bacteriological parameters (APHA 1998, BIS 2012). The parameters such as turbidity, total dissolved solids (TDS), pH-value, total residual chlorine, ammoniacal nitrogen, chloride, total hardness, and total alkalinity were measured in the physicochemical. Whereas bacteriological parameters such as; total colony count, number of coli-aerogenes organisms, fecal bacilli, and odor parameters were analyzed for the study.

Data Analysis

The study area map was prepared using ArcGIS 10.3.1 and Google Earth Pro (Desktop version). The mean value and standard deviation (SD) were calculated for all physicochemical parameters to determine the significant difference between the water sample sites. All statistical analysis was carried out using STATA-Version 14 software.

Ethical Clearance

Ethical authorization was obtained from the student research ethics committee of the International Institute for Population Sciences, Mumbai, India. Employees who agreed to participate and consented to the same were included in the study.

RESULTS

Socio-demographic and Behavioral Characteristics of the Respondents

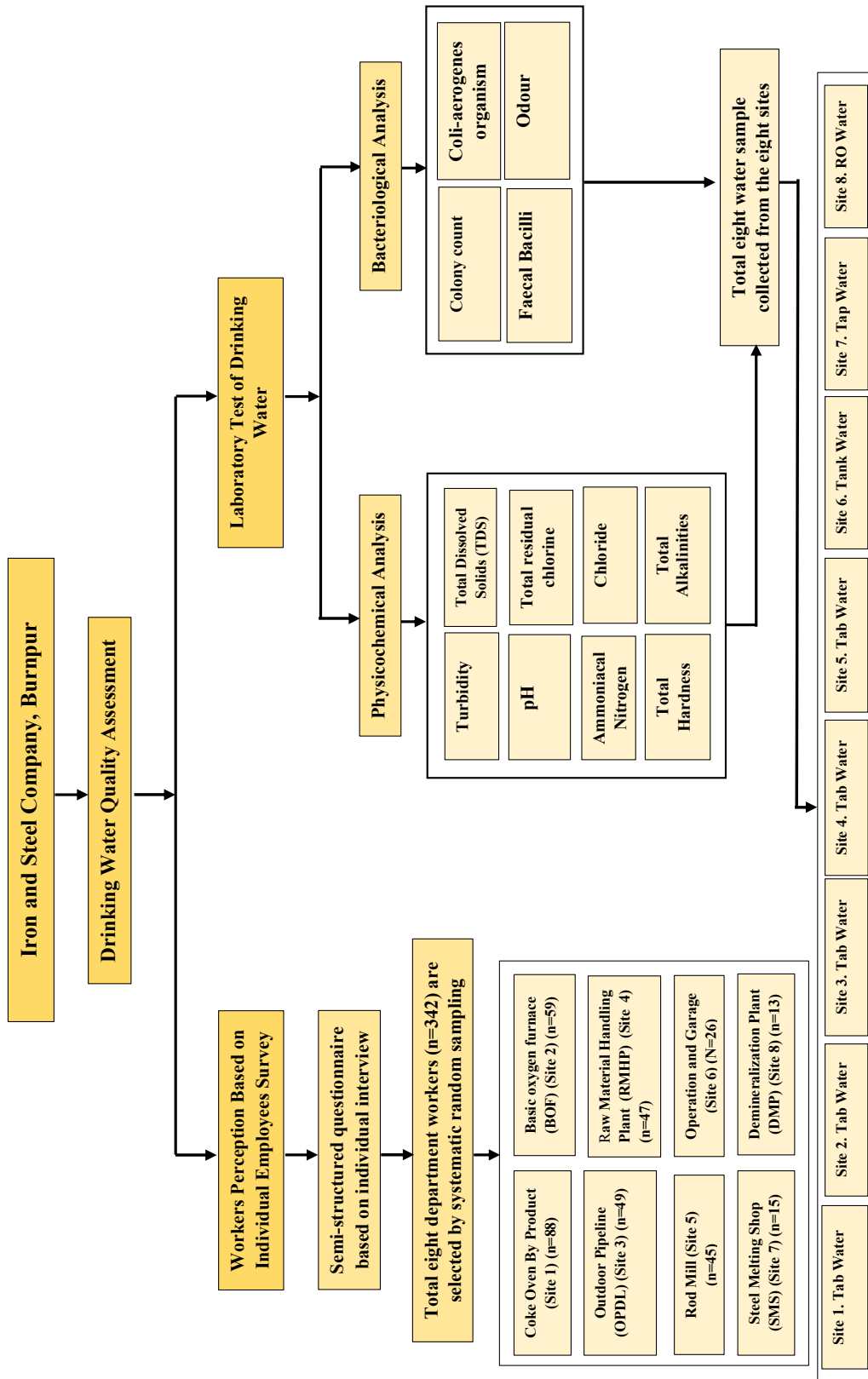All the selected participants agreed to respond to the survey;

Fig. 2: Survey and water sample structure of the study.

Table 1: Socio-demographic and behavioral characteristics of respondents (n = 342).

Characteristics	N	Percentage (%)
Age		
18-30	87	25.44
31-40	160	46.78
More than 40	95	27.78
Mean (S.D)	**36.75 (8.72)**	
Educational Level		
No Schooling	17	4.97
Primary level (1-7)	79	23.10
Secondary and higher secondary (8-12)	116	33.92
Graduation/Technical	130	38.01
Marital Status		
Currently married	301	88.01
Unmarried	44	11.99
Religion		
Hindu	301	88.01
Non-Hindu	41	11.99
Caste		
SC/ST	101	29.53
OBC	66	19.30
Others	175	51.17
Job Category		
Permanent	131	38.30
Contractual	211	61.70
Exposure Category		
Intermittently exposed employee	133	38.89
Exposed employee	209	61.11
Work Experience		
1-5 Years	91	26.61
6-10 years	142	41.52
More than 10 years	109	31.87
Monthly income ('₹' in Indian rupees)		
5000-10000	175	51.17
10000-15000	32	9.36
15000 and above	135	39.47
Mean (S.D)	**20202.92 (15104.65)**	
Department		
Coke Oven By Product	88	25.73
Basic oxygen furnace (BOF)	59	17.25
Outdoor Pipeline (OPDL)	49	14.33
Raw Material Handling Plant (RMHP)	47	13.74
Rod Mill	45	13.16
Operation and Garage	26	7.60
Steel Melting Shop (SMS)	15	4.39
Demineralization Plant (DMP)	13	3.80
Designation		
OCT/ACT	101	29.53
Laborer	85	24.85
Cutters/Solderer	57	16.67
Repair Employees	47	13.74
Foreman/Clerk	31	9.06
Manager/Supervisor	21	6.14

Note: SC/ST: Scheduled Caste/ Scheduled Tribe; OBC: Other Backward Class; OCT/ACT: Operator-cum-Technician/Attended-cum-Technical

therefore, the response rate was 100 percent. In total, 342 employees from the Iron and Steel Industry, Burnpur, were included in this study. The mean age of the employees was 36.75 years. Regarding educational background, 4.97%
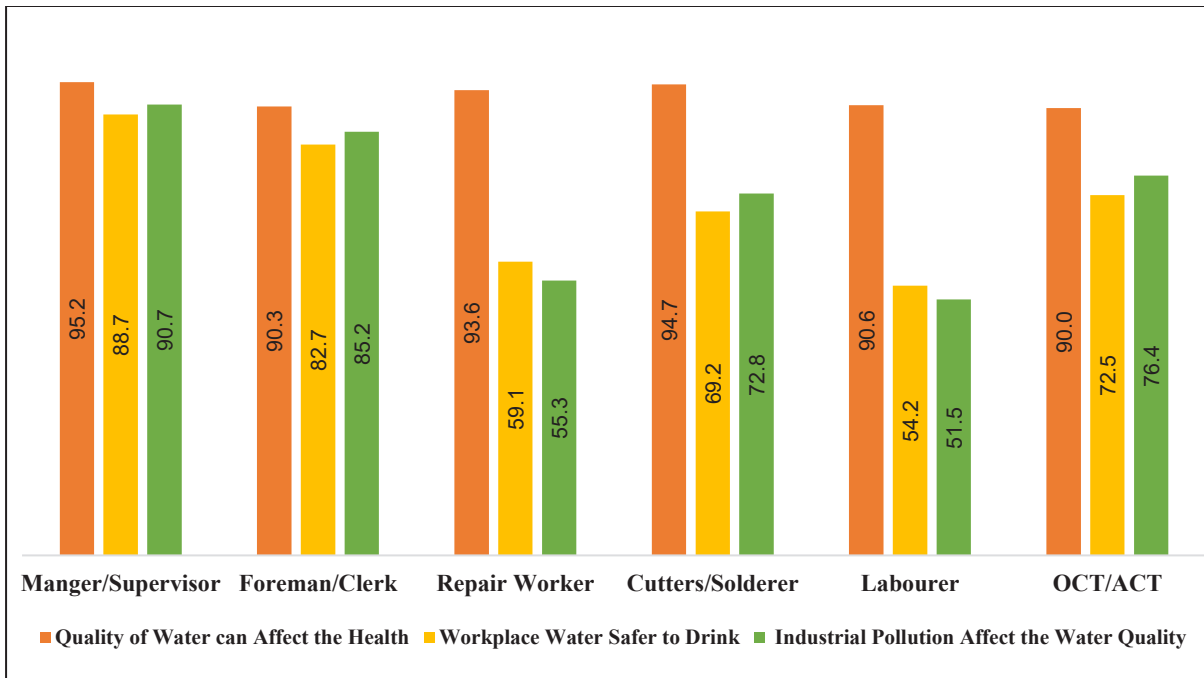
Note: OCT/ACT: Operator-cum-Technician/Attended-cum-Technician

Fig. 3: Knowledge and awareness regarding water quality based on employees' designation.

of employees had no schooling, 23.10% had completed primary schooling, and 38% had graduation or technical education degrees. The mean monthly salary of employees was 19389.31(₹). Among the respondents, 27.13% of the study participants had <5 years of work experience, while 31.87% of employees had more than >10 years. Moreover, the proportion of exposed group employees is about two-thirds (63.17%) of the total employees, and the remaining is intermittently exposed. As per the designation of employees, 29.53 % came under the operator cum technician or attended cum technician, and 24.85% of employees belong to the labor category (Table 1).

Respondent's knowledge and awareness about drinking water quality at the workplace are explained in (Fig. 3). More than 90% of employees from each level believed that poor water quality affects health. Similarly, in questions about water safety, 88.7% of employees under the manager/supervisor skills responded that workplace water is safer to drink. On the contrary, more than 40% of employees from laborers (45.7%) and repair employees (40.9%) responded that workplace water is unsafe to drink. Results regarding employees' perception showed that 90.7% of the manager/supervisor group perceived that industrial pollution affects the drinking water quality at the workplace. However,

Table 2: The overall perception of drinking water quality scale by selected departments.

Department	Poor		Acceptable		Excellent	
	N	%	N	%	N	%
Coke Oven By Product	34	38.64	14	15.91	40	45.45
Basic oxygen furnace (BOF)	9	15.25	8	13.56	42	71.19
Outdoor Pipeline (OPDL)	6	12.24	8	16.33	35	71.43
Raw Material Handling Plant (RMHP)	6	12.77	8	17.02	33	70.21
Rod Mill	2	4.44	6	13.33	37	82.22
Operation and Garage	3	11.54	7	26.92	16	61.54
Steel Melting Shop (SMS)	2	13.33	1	6.67	12	80.00
Demineralization Plant (DMP)	1	7.69	1	7.69	11	84.62
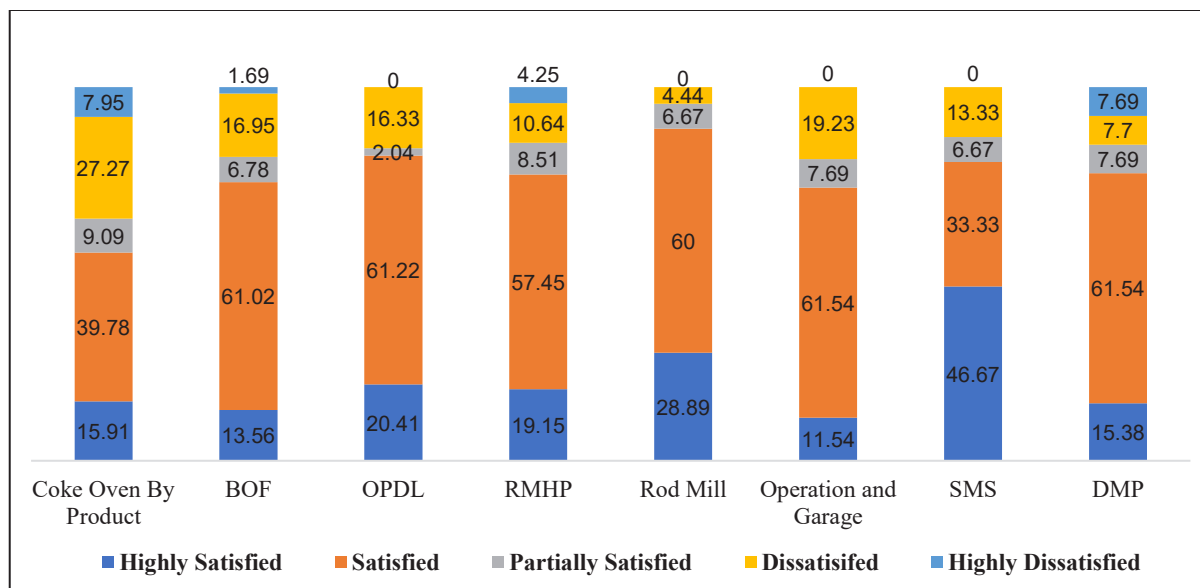
Fig. 4: Level of drinking water quality satisfaction by the selected departments.

more than 51.5% of laborer employees and 55.3% of repair employees perceived that industrial pollution couldn't affect water quality (Fig. 3).

Based on the five organoleptic properties of water, we made the overall quality of the drinking water scale. The ' 'Cronbach's Alpha coefficient of 0.93 in the reliability analysis is perceived as proof of scale reliability. The overall perception of drinking water quality access on a 3-point scale; excellent, acceptable, and poor. More than 80% of employees from Rod mill (82.22), SMS (80.00), and DMP (84.62) considered water under the excellent category. In contrast, 38.64% of Coke Oven by Product department employees believed that water is poor quality and not fit for a drink. Out of the total employees, only 18.42% are considered the water under the poor category (Table 2).

Further questions were asked about the level of satisfaction with drinking water. The result shows that about 35% of employees from coke ovens by the product department expressed dissatisfaction with drinking water quality. By contrast, 46.67% of employees from SMS are highly satisfied with water quality. More than 50% of employees from each department expressed high satisfaction/ satisfaction with the quality aspect (Fig. 4).

Actual Value of Drinking Water Quality by Laboratory Test Analysis

Physicochemical Parameters

The results show that the value of total dissolved solids (TDS) in all sampling sites did not exceed an acceptable level (500 mg.L^{-1}) prescribed by the BIS (2012). The mean concentration of TDS was in the range of 264-312 mg.L^{-1}, with the lowest record from site 1 and site 5 (264 mg.L^{-1}, each), and the highest value was recorded from site 6 (312 mg.L^{-1}), respectively. In the industrial site, the level of pH value varies between 6.72 and 7.64, which is highest at site 7 (7.64 mg.L^{-1}). In terms of total residual chlorine, we found Site 4 has the highest (0.7 mg/l) concentration, which is above BIS (2012) recommended (0.2 mg.L^{-1}), whereas the lowest value was found at Site 6 (0.01 mg/l). Similarly, the mean value and SD of ammoniacal nitrogen, chloride, and total hardness in all sites were (0.05, 0.02 mg.L^{-1}), (33.5, 3.0 mg.L^{-1}), and (118.0, 8.8 mg/l), respectively. The total alkalinity values of all the drinking water samples are below the maximum limit (200 mg.L^{-1}). Similarly, we found that turbidity (0.30) was very low at each site of selected drinking water. Overall physicochemical parameters result indicating water quality at all the selected sites was good and satisfactory (Table 3).

Bacteriological Parameters

The coliform group of bacteria is the key indicator of the fitness of water for drinking purposes. In an ideal situation, all the samples taken from the sample site should be free from coliform organisms. However, the colony count (CFU/ml) ranged between 12 CFU/ml to 20 CFU/ml, showing the presence of bacteria unsuitable for drinking. However, coli-aerogenes organisms and fecal bacilli were present only at Site 6, indicating that other remaining sites are free from the coli-aerogenes organism and fecal bacilli. Furthermore,

Table 3: Physicochemical analysis of selected sites of drinking water.

Characteristics	Max Acceptance Limit (BIS 2012)	Site 1	Site 2	Site 3	Site 4	Site 5	Site 6	Site 7	Site 8	Mean	SD
pH Value	6.5-8.5	6.72	6.95	7.32	6.54	6.86	7.27	7.64	7.38	7.09	.37
Total Dissolved Solids (TDS) [mg.L^{-1}]	500	264	280	276	268	264	312	296	284	280.50	16.76
Turbidity	5	0.3	0.4	0.1	0.1	0.4	0.1	1.0	0.0	0.30	0.32
Total Hardness (as CaCO3) [mg.L^{-1}]	200	112	128	108	124	112	132	116	112	118.00	8.82
Total Alkalinities (CaCO3) [mg.L^{-1}]	200	76	88	72	68	80	100	80	84	81.00	9.97
The total residual chlorine [mg.L^{-1}] Min.	0.2	0.6	0.1	0.09	0.7	0.3	0.01	0.07	0.05	0.24	0.27
Chloride (as Cu) [mg.L^{-1}]	250	36	28	36	36	32	32	32	36	33.50	2.98
Ammoniacal Nitrogen (as N) [mg.L^{-1}]	0.5	0.05	0.08	0.02	0.03	0.07	0.06	0.04	0.02	0.05	0.02

Table 4: Bacteriological analysis of selected sites of drinking water.

Sr. No.	Characteristics	Max Acceptance Limit	Site 1	Site 2	Site 3	Site 4	Site 5	Site 6	Site 7	Site 8
1.	Colony count in agar at 37 degrees after 48 hrs. per ML of original water (CFU.mL^{-1})	100CFU/ml	15	15	13	12	14	20	15	15
2.	Probable number of coli-aerogenes organisms per 100 ML of Original water	Not Traceable (0)	0	0	0	0	0	23	0	0
3.	Faecal Bacilli	Absent	Absent	Absent	Absent	Absent	Absent	Present	Absent	Absent
4.	Odor	Agreeable	1	1	2	1	1	2	2	2

Note: 1: Smell of chlorine, **2:** Unobjectionable

the smell of chlorine (odor) was found at sites 1, 2, 4, and 5, respectively. This indicates that it is not a good indicator of drinkable water in ideal condition; it should be agreeable or unobjectionable in the drinkable water (Table 4).

DISCUSSION

The current study highlights the water quality of selected sites in the Indian Iron and Steel Industry, Burnpur, in West Bengal, India. In the first section of the study, we assess the employee's knowledge, awareness, and overall perception of drinking water quality. In the second section, we evaluated the physicochemical and bacteriological quality of the drinking water.

Based on the analytical results, we found that most employees are more aware of drinking water quality, pollution, and their effects on health. Regarding the job category, most employees (88%) from manager/supervisor roles perceived that industrial pollution could affect water quality. However, almost 45% of employees under the laborer's category reported that industrial pollution does not affect drinking water quality. The possible reason could be that managers/supervisors are educationally qualified and more aware of industrial pollution than other employees. We found that the work designation and location influenced the employees' perception. We found a similar result in Mumbi and Watanabe's (2020) study to validate this context. The current study also highlights the employee's perception of water quality based on organoleptic properties such as clarity, color, smell, taste, and healthiness. Previous studies have revealed that organoleptic evaluations are important and primary determinants of an individual's judgment of the quality of drinking water (Benneyworth et al. 2016, Abdi-Soojeede & Kullane 2019)**.** Our study also found that most of the employees considered all the organoleptic properties of the water under the acceptable to excellent category.

However, only 30% of the employees of site 1 (Coke Oven By Product) have reported organoleptic properties of water under the excellent category. The possible explanation could be that the coke oven plants produce more pollutants than other departments, frequently contaminating drinking water quality. This reason was validated by Mishra et al. (2018) study, where they examined the physio-chemical test of the coke oven water and found that concentrations of BOD (73.13 $mg.L^{-1}$), COD (540.25 $mg.L^{-1}$), and cyanide (27.9 $mg.L^{-1}$) exceeded the tolerance limit of the sample water.

On the contrary, a maximum number of employees (84.62 %) from site 8 (Demineralization Plant) perceived that the organoleptic properties of water are under the excellent category. The summary of the first section reveals that most of the employees from each department are satisfied with water quality, except Coke Oven By-Product department employees are not completely trusted with the drinking water quality. Therefore, our result reflects that employees are satisfied and trust the drinking water quality. However, it is important to note that perception, awareness, knowledge, and satisfaction are subjective and complex interactions that vary.

In the second section, we analyzed the eight physicochemical and four bacteriological parameters using BIS (2012) and WHO (1997, 2008) guidelines for drinking water quality. Our result indicates that most physicochemical properties were within the permissible limit of the quality of drinking water standards. Regarding bacteriological properties, the colony count concentration was higher than the permissible levels for safe drinking water set by the WHO (1997) guidelines. Moreover, only Site 6 reported that most bacteriological properties are above the permissible limit. The possible reason can be irregularity in the cleaning of the water storage tank of Site 6, which was observed during the field visit, and the statement made by the employee during the interview. However, further investigation can bring the actual reason behind the containment of the water in site 6. Overall, our study results are matched with a previous study conducted in Bhilai Steel Plant (BSP) in India; in that study, they found that physicochemical and bacteriological parameters of the water were under the permissible limits except for alkalinities (Vinod et al. 2013). Overall, this study clearly stated a minor difference in tab water, tank water, and RO water in all sites in the industry. In summary, employees' perception of water quality aligns with water's actual physicochemical and bacteriological properties. The overwhelming majority of the employees in each department believed that their water drinking water within the industry was of acceptable to excellent quality, and almost similar results we found after the analyzed laboratory result of the water.

LIMITATIONS

This study may have some potential limitations. 1) The first section of the study was purely based on knowledge and perception, which may vary by various factors; therefore, we cannot generalize our results for other Iron and Steel Industries. 2) This study used a limited number of organoleptic terms. This study did not include other important properties like trust, risk perception, and contextual indicators. 3) Water quality index is the best tool to describe water quality. However, we could not conduct a water quality index due to the limited number of physicochemical properties.

CONCLUSION

The study results indicate that perception and actual water quality are complex interactions, and diverse factors are associated with these two groups. A large number of employees have trusted industrial drinking water. However, we found dissimilarities in perception based on the designation of employees. The result explained that other physicochemical and bacteriological properties are in good status in all sites except for a colony count, expressing their suitability for drinking purposes. However, it is important to note that the presence of colony count in each site's drinking water provokes immediate investigation and corrective action by the Iron and Steel Industry, Burnpur. Also, the steel industry should promote an awareness program about drinking water quality and develop a holistic understanding of industrial pollution and water quality among employees. Additionally, the industry should test water's physicochemical and bacteriological quality at regular intervals to identify those departments where water quality is poor and make the best possible solution for the particular department.

ACKNOWLEDGMENTS

REFERENCES

Abdi-Soojeede, M.I. and Kullane, M.A. 2019. Study of Community Perception on Drinking Water Quality in Mogadishu, Somalia. Open J. Appl. Sci., 9(5): 361-371.

Abedin, M.A., Habiba, U. and Shaw, R. 2014. Community perception and adaptation to safe drinking water scarcity: salinity, arsenic, and drought risks in coastal Bangladesh. Int. J. Dis. Risk Sci., 5(2): 110-124.

American Public Health Association (AHA). 1998. Standard Methods for the Examination of Water and Wastewater. Twentieth Edition. American Public Health Association, American Water Works Association, and Water Environmental Federation, Washington D.C., p. 1213

Benneyworth, L., Gilligan, J., Ayers, J.C., Goodbred, S., George, G., Carrico, A., Karim, M.R., Akter, F., Fry, D., Donato, K. and Piya, B. 2016. Drinking water insecurity: water quality and access in coastal south-western Bangladesh. Int. J. Environ. Health Res., 26(5-6): 508-524.

Bureau of Indian Standard 2012. Indian standard drinking water specification (second revision). Bureau of Indian Standards (BIS) 10500:2012, New Delhi

Dhawde, R., Surve, N., Macaden, R., Wennberg, A.C., Seifert-Dähnn, I., Ghadge, A. and Birdi, T. 2018. Physicochemical and bacteriological analysis of water quality in drought-prone areas of Pune and Satara districts of Maharashtra, India. Environments, 5(5): 61.

Dogaru, D., Zobrist, J., Balteanu, D., Popescu, C., Sima, M., Amini, M. and Yang, H. 2009. Community perception of water quality in a mining-affected area: A case study for the Certej catchment in the Apuseni mountains in Romania. Environ. Manag., 43(6):, 1131-1145.

Doria, M.D.F., Pidgeon N. and Hunter, P.R. 2009. Perceptions of drinking water quality and risk and its effect on behavior: a cross-national study. Sci Total Environ., 407(21): 5455–5464. https://doi.org/10.1016/j.scitotenv.2009.06.031

Eck, C.J., Wagner, K.L., Chapagain, B. and Joshi, O. 2019. A survey of perceptions and attitudes about water issues in Oklahoma: A comparative study. J. Comtemp., 168(1): 66-77.

Grupper, M. A., Schreiber, M. E. and Sorice, M. G. 2021. How Perceptions of Trust, Risk, Tap Water Quality, and Salience Characterize Drinking Water Choices. Hydrology, 8(1): 49.

Khalid, S., Murtaza, B., Shaheen, I., Ahmad, I., Ullah, M.I., Abbas, T., Rehman, F., Ashraf, M.R., Khalid, S., Abbas, S. and Imran, M. 2018. Assessment and public perception of drinking water quality and safety in district Vehari, Punjab, Pakistan. J. Clean. Prod., 181: 224-234. https://doi.org/10.1016/j.jclepro.2018.01.178

Krishnan, R.R., Dharmaraj, K. and Kumari, B.R. 2007. A comparative study on the physicochemical and bacterial analysis of drinking, borewell, and sewage water in the three different places of   S i v a k a s i .   J. Environ. Biol., 28(1): 105-108.

Mishra, L., Paul, K.K. and Jena, S. 2018. Characterization of coke oven wastewater. IOP Conf. Ser. Eart. Environ. Sci., 167: 012011.

Mumbi, A.W. and Watanabe, T. 2020. Differences in risk perception of water quality and its influencing factors between lay people and factory employees for water management in River Sosiani, Eldoret Municipality Kenya. Water, 12(8): 2248.

Nikaeen, M., Shahryari, A., Hajiannejad, M., Saffari, H., Kachuei, Z.M. and Hassanzadeh, A. 2016. Assessment of the physicochemical quality of drinking water resources in the central part of Iran. J. Environ. Health, 78a(6): 40-45.

NITI Aayog 2018. Composite Water Management Index. Available at: https://www.niti.gov.in/sites/default/files/2019-08/CWMI-2.0-latest.pdf

Nurul, A.H., Shamsul, B.M.T. and Noor Hassim, I. 2016. Assessment of dust exposure in a steel plant on the eastern coast of peninsular Malaysia. Work, 55(3): 655-662.

Rakhecha, P.R. 2020. Water environment pollution with its impact on human diseases in India. Int. J. Hydrol., 16: 152-158.

Rehman, K., Fatima, F., Waheed, I. and Akash, M.S.H. 2018. Prevalence of exposure to heavy metals and their impact on health consequences. J. Cell. Biochem., 119(1): 157-184.

Singh, U., Singh, S., Tiwari, R.K. and Pandey, R.S. 2018. Water pollution due to the discharge of industrial effluents with special reference to Uttar Pradesh, India–a review. Int. Arch. Appl. Sci. Technol., 9(4): 111-121.

Srinivas, J., Purushotham, A.V. and Murali Krishna, K.V.S.G. 2013. Determination of water quality index in industrial areas of Kakinada, Andhra Pradesh, India. Int. Res. J. Environ. Sci., 2(5): 37-45.

Sukumaran, D., Sengupta, C., Saha, R. and Saxena, R.C. 2015. Groundwater quality index of Howrah, the Heritage City of West Bengal, India. Sci. Edu., 3(1): 5-10.

Tiwari, M.K., Bajpai, S. and Dewangan, U.K. 2016. Air and leaching pollution scenario by iron and steel plants in central India. Elixir Pollut., 101: 43495.

United Nations High Commissioner for Human Rights 2019. World's Water in the Era of the SDGs". United Nations University, Tokyo. Available from: https://www.ohchr.org/en/statements/2019/03/world-water-day-2019-symposium

Vinod, J., Satish, D. and Sapana, G. 2013. Assessment of water quality index of industrial area surface water samples. Int. J. Chem.Tech. Res., 5(1): 278-283.

World Health Organization (WHO) 1997. Guidelines for Drinking Water Quality. World Health Organization, Geneva. Available from: https://apps.who.int/iris/handle/10665/42002

World Health Organization (WHO) 2008. Guidelines for Drinking Water Quality. World Health Organization, Geneva. Available from: https://www.who.int/water_sanitation_health/dwq/fulltext.pdf

World Health Organization (WHO) 2017. Guidelines for Drinking-Water Quality. World Health Organization, Geneva. Available at: https://www.who.int/publications/i/item/9789241549950

World Health Organization (WHO) 2019. Drinking Water, Factsheet. Available from: https://www.who.int/news-room/fact-sheets/detail/drinking-water

Synthesis and Characterization of Cellulose Acetate Membrane from Cassava Peel for Microfiltration

A. Ma'ruf†, E. Puspawiningtiyas, D. N. Afifah and E. Diaz

Chemical Engineering Department, Universitas Muhammadiyah, Purwokerto Jl., K. H. Ahmad Dahlan, Dukuh Waluh, Kembaran, Purwokerto 53182, Indonesia

†Corresponding author: A. Ma'ruf; anwarump@yahoo.com

ABSTRACT

Cassava peel is a waste product from cassava starch or modified cassava flour (mocaf) production. It is currently not utilized optimally. Cassava peel is a lignocellulosic material that can be used as a source of cellulose. Acetylation of cassava peel cellulose was successfully done using acetic anhydride with glacial acetic acid and sulfuric acid as catalysts. The content of acetyl is 49.54%, and the degree of substitution (DS) is 3.69. The percentage of acetyl of more than 43% and the DS of 3.69 show that the cellulose acetate obtained is categorized as cellulose triacetate. The CA–PEG membrane has a pore range of 1- 4 μm depending on the molecular weight of PEG. The coefficients of rejection of the CA-PEG membrane range from 95.99% to 98.88%. The CA-PEG membrane is effective as a microfiltration membrane.

INTRODUCTION

Cassava peel, a byproduct of cassava starch or modified cassava flour (mocaf) production, is currently underutilized. Cassava peel contains lignin, cellulose, and hemicellulose. The percentages of lignin, cellulose, and hemicellulose are 10.88%, 14.17%, and 23.40%, respectively (Pondja et al. 2018). The content of cellulose and hemicellulose in cassava peel has great potential as a raw material for making cellulose acetate (Rosa et al. 2020, Maryana et al. 2020). Furthermore, cellulose acetate can be used as a raw material for the synthesis of cellulose acetate membranes.

Membrane technology is a technology that has bright prospects. Membrane technology is currently widely used in various processes such as filtration, waste treatment, desalination, and chemical reactions (Roy & Ragunath 2018). Cellulose acetate membranes can be used in various fields of application. Cellulose acetate membranes have the potential to be developed due to the abundant and renewable availability of raw materials. Perera et al. (2014) produced thin film composite (TFC) reverse osmosis membranes from cellulose acetate onto an ultrafiltration membrane support. Cellulose acetate used was commercial acetate (CA, 30 kDa molecular weight, and 39.8 wt% acetyl content). Serbanescu et al. (2020) modified the commercial cellulose acetate membrane for Gd (III) separation. The modification

of commercial CA membranes used aminopropyl triethoxy silane (APTES) immobilization and glutaraldehyde (GA) linkages to the amino groups of APTES, followed by the immobilization of calmagite. Djayanti et al. (2019) synthesized cellulose acetate membrane from cotton spinning waste. The acetylation of cotton spinning waste cellulose used acetic acid for activation and sulfuric acid as a catalyst.

The utilization of cellulose from cassava peel as the material of a cellulose acetate membrane is still rare. This research aims to produce and characterize the cellulose acetate membrane from cassava peel. The production of cellulose acetate membrane involves several stages: delignification of cassava peel, acetylation of cellulose, and cellulose acetate membrane production. The performance of the cellulose acetate membrane produced was evaluated for the microfiltration process.

MATERIALS AND METHODS

Materials

Cassava peel was obtained from PT. Rumah Mocaf Indonesia, Banjarnegara district, Indonesia. Hydrogen peroxide, sodium hydroxide, sulfuric acid, glacial acetic acid, acetic anhydride, polyvinyl alcohol (PVA), and polyethylene glycol (PEG) were obtained from Merck. Demineralized water was produced by Elva-Veolia Technology. Synthetic

limewater as wastewater was obtained from the Chemical Engineering Department Laboratory.

Preparation of Cassava Peel

The cassava peel was separated from the outer skin, then cut and washed using clean water. The cut cassava peel was dried in the sun for 1 day and then dried in an oven at 80°C for 2 hours. The dry cassava skin was then mashed and sieved using a 60-80 mesh. The sifted cassava peel fiber was dried again using an oven until it reached a constant weight at 80°C.

Delignification

Delignification of cassava peel was conducted by alkaline hydrogen peroxide (Ma'ruf et al. 2017). The weight of 20 grams of cassava peel fiber was delignified using a 1.5% alkaline hydrogen peroxide solution with a ratio of 1:9 b/v at 100°C for 3 hours. The delignification process was carried out at a pH of 11.5, and the reaction pH was adjusted using a sodium hydroxide solution.

Bleaching

The delignified cassava fiber was then added to 180 mL of a 3% hydrogen peroxide solution, heated using a hot plate, and stirred using a magnetic stirrer for 2 hours. The cassava fiber was then filtered, washed until it reached a neutral pH, and dried in an oven at 80°C.

Acetylation

The acetylation of cassava peel cellulose uses glacial acetic acid and sulfuric acid as catalysts. The volume of 97 mL of glacial acetic acid was mixed with 1.6 mL of 95% sulfuric acid in a beaker glass and stirred until homogeneous. Prepare as much as 5 g of cassava cellulose (after the bleaching process), then add a mixture of the acetic acid glacial and sulfuric acid solution, stir, and heat in a water bath at a temperature of 55°C for 1 hour. After that, add the mixture to the acetic anhydride solution in a weight-to-acetic-anhydride ratio of 1:2 (w/v) and stir at 55°C for 2 hours. The mixture was then put into a certain amount of water to form a precipitate. The precipitate obtained was then washed until neutral and dried at 70°C in an incubator oven for 24 hours. The cellulose acetate obtained was then analyzed to determine the acetyl content and degree of substitution (DS) to determine the type of cellulose acetate produced.

Cellulose Acetate Membrane Production

PVA solution preparation: Polyvinyl alcohol (PVA) was weighed at 10 g and then dissolved in 10 mL of 1 M nitric acid and 190 mL of distilled water using an Erlenmeyer glass. The mixture was stirred using a magnetic stirrer for 2 hours at 80°C. PVA was used as an adhesive agent between cellulose acetate powders to form a dense cellulose acetate membrane.

CA-PEG solution preparation: The CA–PEG solution was made from cellulose acetate (CA) and polyethylene glycol (PEG) with acetone as solvent. The amounts of 1 g of CA and 1 g of PEG (with various variations of PEG molecular weight: PEG 400, PEG 600, and PEG 4000) were weighed and then dissolved in 8.5 mL of acetone solution in the Erlenmeyer glass. The mixed solution was then stirred using a magnetic stirrer for 8 hours until all of the cellulose acetate dissolved in the acetone. After a homogeneous solution, the Erlenmeyer was opened for 3 hours so that the acetone evaporated.

Membrane synthesis: The CA-PEG solution was then added to 15 mL of PVA solution and stirred for 24 hours using a magnetic stirrer. The homogeneous dope solution was then cast using a Petri dish glass. Then, the dope solution was dried for 8 hours at 80°C in the oven.

Characterization of Cellulose Acetate Membrane

The characteristics of the cellulose acetate membrane were determined using the Fourier transform infrared (FTIR) spectrophotometer to analyze the functional groups and a scanning electron microscope (SEM) to analyze the morphology of the membrane.

Performance Test of Cellulose Acetate Membrane

Permeability test: The permeability test of the membrane was conducted by passing pure water through it. The pure water was flowed using a pump to the surface of the membrane at constant pressure. the volume. The volume of water that passed through the membrane was weighed. The permeability of the membrane can be calculated using Equation (1).

$$L_P = \frac{V}{A.t.\Delta P} \qquad \ldots(1)$$

Where L_P is permeability (L.m^{-2}.h^{-1}.bar^{-1}), V is the volume (L), A is the surface area of the membrane (m^2), and ΔP is transmembrane pressure (bar).

Ultrafiltration test: The microfiltration test can be explained in Fig. 1. The limewater, as synthetic wastewater, was inserted into the feed tank (1). The laundry wastewater was then pumped to the surface of the membrane (3) using a pump (2). The pressure was set by the valve (4). The pressure can be measured by the pressure gauge (5). The permeate was collected in the Erlenmeyer (6) and weighed using a balance (7). The flux of the membrane was calculated by Equation (2).

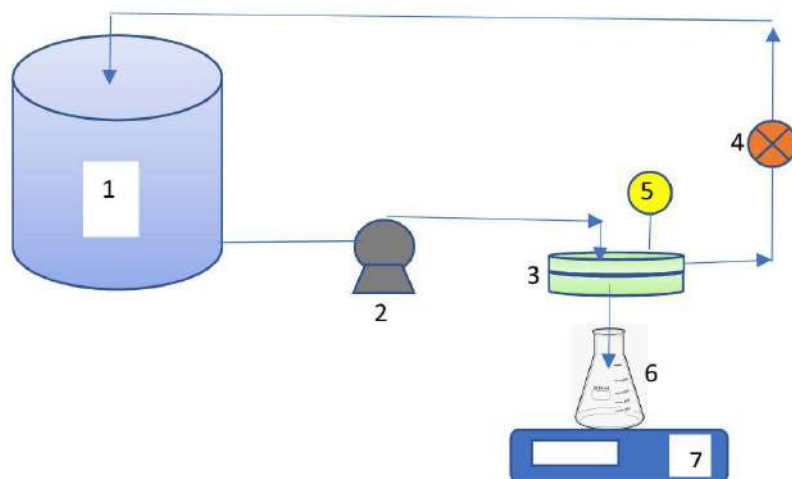$$J = \frac{V}{A.t.} \qquad \ldots(2)$$
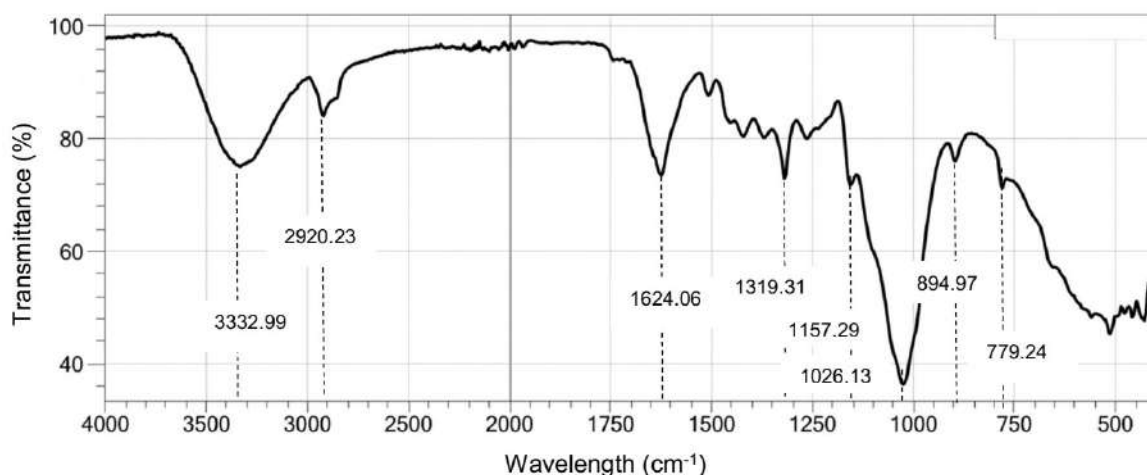
Fig. 1: Equipment set for microfiltration.

Fig. 2: FTIR spectra of cassava peel cellulose.

RESULTS AND DISCUSSION

The Characteristics of Cellulose and Cellulose Acetate from Cassava Peel

Cassava peel is a lignocellulosic material. The three main components are cellulose, hemicellulose, and lignin. The proximate analysis of cassava peel was done using the Chesson-Data method (Ma'ruf et al. 2017). Table 1 shows the approximate analysis of cassava peel. To use the cellulose from cassava peel, delignification of the peel must be conducted. Delignification of cassava peel was done by alkaline hydrogen peroxide. Delignification of cassava peel using alkaline hydrogen peroxide effectively removes the lignin. The analysis shows that almost 89.5% of the lignin was removed.

The FTIR spectra of cassava peel cellulose are shown in Fig. 2. The wave number range of 3660-2900 cm^{-1} is characteristic of the stretching vibration of O-H and C-H bonds in polysaccharides (Hospodarova et al. 2018). The special characteristics of lignin, the guaiacyl (G) unit (at 1269 cm^{-1}) are not found in this FTIR spectra, and the syringyl (S) unit (at 1326 cm^{-1}) is found but has a low intensity. The peak of 1624 cm^{-1} corresponds to the vibration of water

Table 1: The proximate analysis of cassava peel.

Component	Weight percentage
Cellulose	33.33
Hemicellulose	18.57
Lignin	19.00
Water	29.10

molecules absorbed in cellulose. The peaks at 1369.46, 1319.31, 1026.13, and 894.97 cm^{-1} belong to stretching and bending vibrations of -CH$_2$ and -CH, -OH, and C-O bonds in cellulose, respectively.

Acetylation of cassava peel cellulose was done using acetic acid glacial activation and acetic anhydride acetylation with sulfuric acid as a catalyst. The acetylation process requires a cellulose/acetic anhydride ratio of 1:2 (w/v), a temperature of 40 °C, and a reaction time of 3 hours. The analysis of acetyl in cellulose acetate obtained shows that the content of acetyl is 49.54%. While the degree of substitution (DS) is 3.69. The percentage of acetyl of more than 43% and DS of 3.69 show that the cellulose acetate obtained is categorized as cellulose triacetate (Djuned et al. 2014). Fig. 3 shows the reaction of cellulose with acetic anhydride.

The Characteristics of Cellulose Acetate Membrane

The CA-PEG membrane was synthesized using acetone as a solvent. The method of membrane synthesis is phase inversion. The ratio of CA to PEG is 1:1 (w/w). Fig. 4b shows the membrane obtained from cellulose acetate obtained from cassava peel. Fig. 5 shows the FTIR spectra of the cellulose acetate and CA-PEG membranes. There are two main peaks in the difference between cellulose acetate and CA-PEG membranes, indicating the existence of PEG. The peak of

948.98 cm^{-1} shows stretching of C–O and 840.96 cm^{-1} shows rocking vibration of the -CH$_2$- groups in the PEG (Chirea et al. 2011).

The Morphology of Cellulose Acetate Membrane

Fig. 6 shows the morphology of the CA-PEG membrane, (a) using PEG 600 as an additive and (b) using PEG 4000 as an additive. The pores of the membrane are not symmetric, with a range of pores between 2–4 μm and 1–2 μm for PEG 600 and PEG 4000, respectively. It can be seen that the higher weight membrane obtained was more compact. The pores of the membrane are still larger compared with commercial polymeric membranes for microfiltration (polyvinylidene fluoride (PVDF) membrane, 0.22 μm) (Nourbakhsh et al. 2014).

Performance of CA-PEG Membrane

Permeability test: Table 2 shows the permeability of the CA–PEG membrane obtained. At a higher molecular weight of PEG, the permeability of the membrane will decrease, while the membrane resistance will increase. The permeability of the CA–PEG membrane was found to be higher than the permeability of the polyether imide membrane (100 kDa) (Pertile et al. 2018).

Microfiltration performance: The performance test of CA
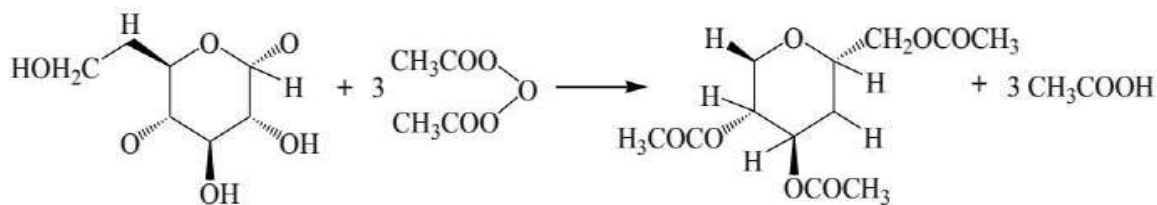
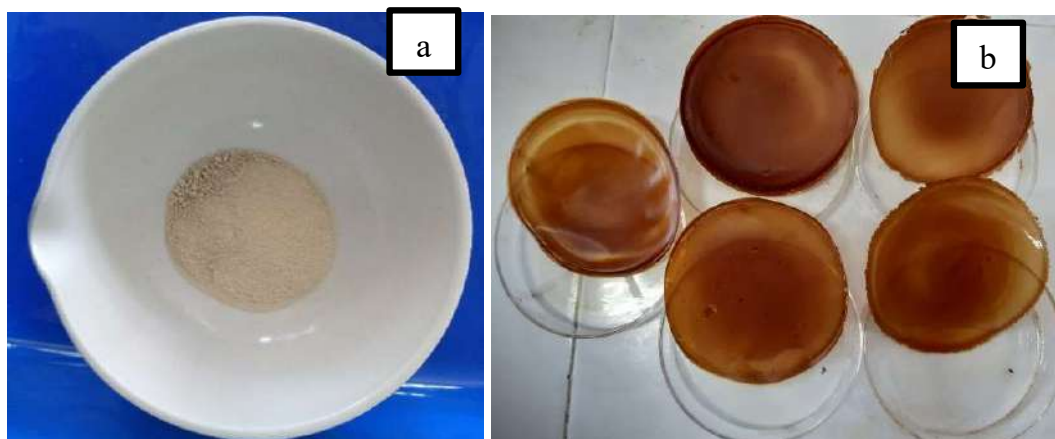Fig. 3: The reaction of acetylation of cellulose.

Fig. 4: (a) Cellulose acetate obtained from cassava peel cellulose; (b) CA-PEG membrane.
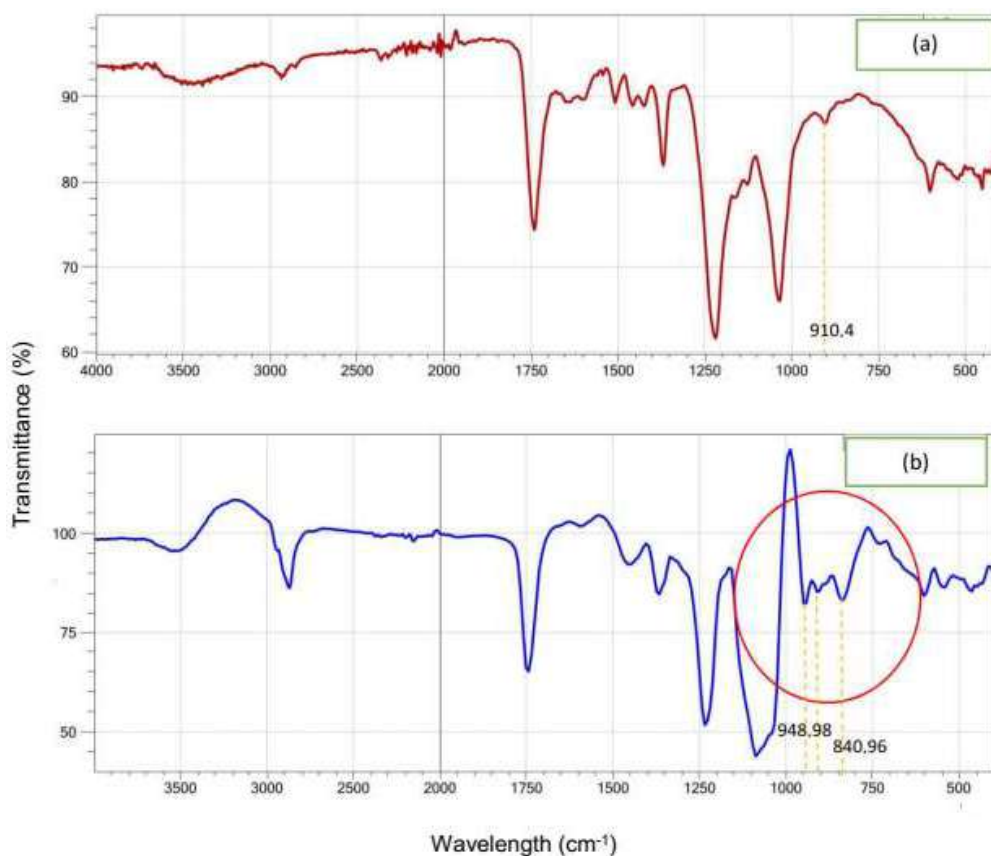
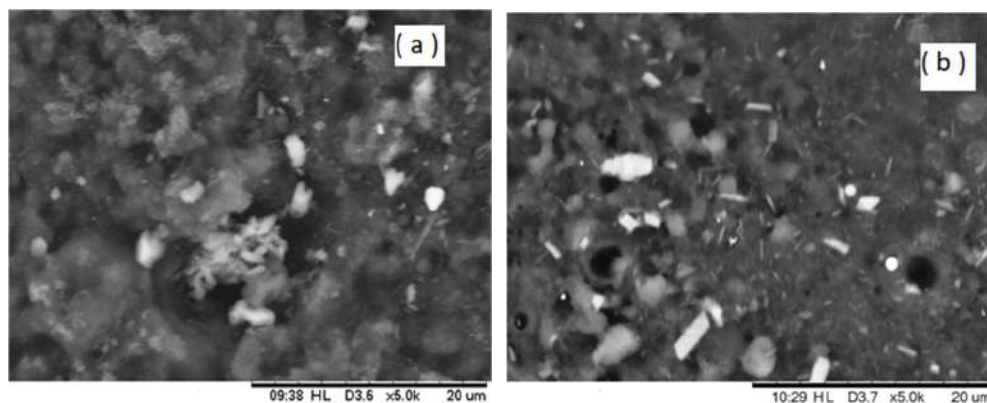Fig. 5: FTIR spectra: (a) cellulose acetate; (b) CA-PEG membrane.

Fig. 6: Morphology of the CA-PEG membrane: (a) PEG 600; (B) PEG 4000.

Table 2: Permeability and membrane resistance of CA-PEG membrane.

Membrane	Permeability ($L.m^{-2}.h^{-1}.bar^{-1}$)	Membrane Resistance ($m.kg^{-1}$)
CA-PEG 400	1.83×10^3	19.688×10^6
CA-PEG 600	1.29×10^3	27.891×10^6
CA-PEG 4000	1.06×10^3	34.066×10^6

membranes was conducted for the microfiltration of synthetic wastewater of limewater. The initial turbidity of limewater is 672 NTU. Fig. 7 shows the flux of the membrane during the microfiltration process. Table 3 shows the rejection coefficient of the membrane. The range of rejection coefficient of 95.99% - 98.99% indicates that the membrane is effective as a microfiltration membrane.
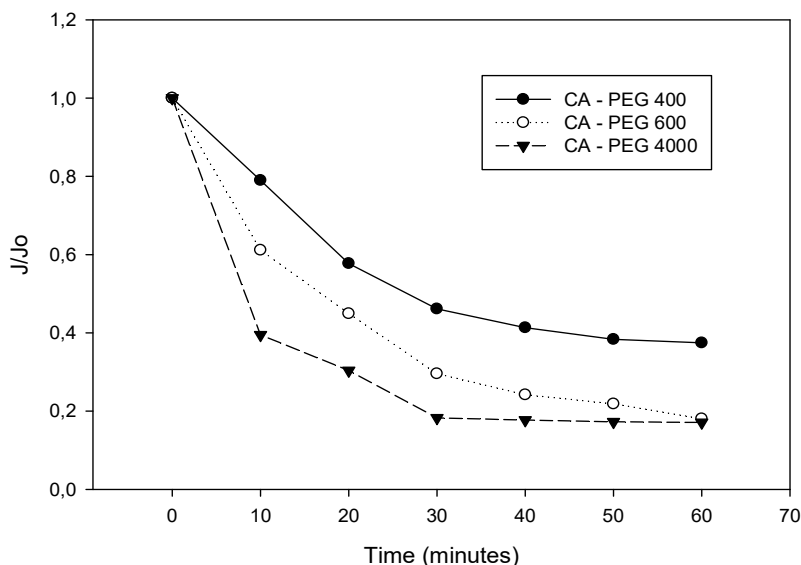
Fig. 7: Flux of the membrane during microfiltration.

Table 3: Rejection coefficient of microfiltration.

PEG	Rejection Coefficient (%)
PEG 400	95.99
PEG 600	98.38
PEG 4000	98.88

CONCLUSION

Cassava peel is a lignocellulosic material that can be used as a source of cellulose. Acetylation of cassava peel cellulose was successfully done using acetic anhydride with glacial acetic acid and sulfuric acid as catalysts. The content of acetyl is 49.54%, and the degree of substitution (DS) is 3.69. The percentage of acetyl of more than 43% and DS of 3.69 show that the cellulose acetate obtained is categorized as cellulose triacetate. The CA–PEG membrane has a pore range of 1-4 μm depending on the molecular weight of PEG. The coefficients of rejection of the CA-PEG membrane range from 95.99% to 98.88%. The CA-PEG membrane is effective as a microfiltration membrane.

ACKNOWLEDGMENT

REFERENCES

Chirea, M., Freitas, A., Vasile, B. S., Ghitulica, C., Pereira, C. M. and Silva, F. 2011. Gold nanowire networks: Synthesis, characterization, and catalytic activity. Langmuir, 27: 3906-3913.

Djayanti, S., Kusumastuti, S.A., Fatkhurrahman, J., Purwanto, A. and Budi-arto, A. 2019. Synthesis and characterization of cellulose acetate membrane from cotton spinning waste. Makara J. of Sci., 25(3): 155-161.

Djuned, F.M., Asad, M., Ibrahim, M.N.M. and Daud, W.R.W. 2014. Synthesis and characterization of cellulose acetate from TCF oil palm empty fruit bunch pulp. Bioresources, 9(3): 4710-4721.

Hospodarova, V., Singovszka, E. and Stevulova, N. 2018. Characterization of cellulosic fibers by FTIR spectroscopy for their further implementation to building materials. American J. of Analytical Chem., 9: 303-310.

Ma'ruf, A., Pramudono, B., and Aryanti, N. 2017. Lignin isolation process from rice husk by alkaline hydrogen peroxide: Lignin and silica extracted. AIP Conference Proceedings 1823, 020013.

Maryana, R., Anwar, M., Suwanto, A., Hasanah, S.U. and Fitriana, E. 2020. Comparison study of various cellulose acetylation methods from its IR spectra and morphological pattern of cellulose acetate as a biomass valorization. Nat. Environ. and Poll. Tech., 19(2): 669-675.

Nourbakhsh, H., Alemi, A., Emam-Djomeh, Z. and Mirsaeedghazi, H. 2014. Effect of processing parameters on fouling resistances during microfiltration of red plum and watermelon juices: A comparative study. J. Food Sci. Tech., 51(1):168-172.

Perera, D.H.N., Nataraj, S.K., Thomson, N.M., Sepe, A., Hüttner, S., Steiner, U., Qiblawey, H. and Sivaniah, E. 2014. Room-temperature development of thin film composite reverse osmosis membranes from cellulose acetate with antibacterial properties. J. of Membrane Sci., 453: 212-220.

Pertile, C., Zanini, M., Baldasso, M., Andrade, M.Z. and Tessaro, I.C. 2018. Evaluation of membrane microfiltration fouling in landfill leachate treatment. Revista Materia., 23(1).

Pondja, E.A.Jr., Persson, K.M. and Matsinhe, N.P. 2018. The potential use of cassava peel for treatment of mine water in Mozambique. J. of Environ. Protection, 8: 277-289.

Rosa, T.S.D., Trianoski, R., Michaud, F., Belloncle, C. and Iwakiri, S. 2020. Efficiency of different acetylation methods applied to cellulose fibers waste from pulp and paper mill sludge. J. of Natural Fibers, 19(1): 185-198.

Roy, S. and Ragunath, S. 2018. Emerging membrane technologies for water and energy sustainability: Future prospects, constraints and challenges. Energies, 11: 2997.

Serbanescu, O.S., Pandele, A.M., Miculescu, F. and Voicu, S.I. 2020. Synthesis and characterization of cellulose acetate membranes with self-indicating properties by changing the membrane surface color for separation of Gd(III). Coatings, 10: 486.

Extended Producer Responsibility and Enforcement of Single-Use Plastic Ban in Pune City of India

M.Z.M. Nomani*† iD **, Md. Mostak Alfarhad**, Faizan Mustafa*** and Merwais Niazy******

*Faculty of Law, Aligarh Muslim University, Aligarh-202001, India
**Centre for Science & Environment, New Delhi, 110062, India
***NALSAR University, Justice City, Hyderabad, Telangana 500101, India
****Department of Law, Kandahar University, Kandahar, Afghanistan
†Corresponding author: M.Z.M. Nomani; zafarnomani@rediffmail.com

ABSTRACT

India has experienced tremendous production, use, and discarding of plastic waste. The municipal and solid wastes proliferation of municipal waste, especially plastic waste, paved the way for the regulatory framework to implement the plastic ban in 18 states and Union Territories of India. In contrast, they have implemented a partial ban on plastic bags respectively. It addressed the phasing out of multi-layered plastics (MLP) and incorporated Extended Producer Responsibility (EPR) within the circular economy of plastic waste generation and recycling. It is generally believed that the plastic ban in India has feeble administrative support and effective implementation. Therefore, the government has passed the Draft Plastic Rules, 2009; Plastic Waste (Management and Handling) Rules, 2011; Plastic Waste Management Rules, 2016 and Draft Plastic Waste Management Rules, 2021. It made vital changes in recycled plastic manufacture and usage at national and state levels. Since the net outcome of the failure is environmental degradation beyond reparable limits, the most vociferous articulation of the banning of the single-use came through the Notification on Plastic and Thermocol Products, 2018, by the Government of Maharashtra. Although the new legal framework carried high deterrent value, the implementation has been heavily flawed. The paper deals with the plastic laws and performance in the context of EPR in Pune city of India. It suggests viable recommendations and strategies from a multi-stakeholder perspective.

INTRODUCTION

Plastic products have internalized into the daily domestic needs but resulted in their adverse impacts on the realization of the human right to environment and health cannot be overlooked (Nomani 2000). Plastic waste's negative consequences and effects are now widely known and have been the subject of much recent media coverage (Gui et al. 2013), both at national and global levels (Thompson & Moore 2009). The use of polymers and plastic materials has had rapid growth since the 1970s. It is growing at a rate of 2.5 times that of the GDP growth in India. The raw plastic material doubled from 3.3 Million Metric tons to 6.8 Million Metric Tons in 2010 (Rafey & Siddiqui 2021). Rapid urbanization can be a significant reason for the spread of consumer goods, retail outlets, and plastics-based wrapping, from nutritional items,

cereal, pulses, meat, and vegetable products to cosmetics and drugs. However, the more substantial hurdle is the alarming proportion of polythene flawed with actual implementation on the ground level (Aryan et al. 2019). Thus, the topic of the performance of the banning notification of the single-use plastic ban in Pune City of India, in the context of EPR and circular economy, assumes an interest to work on the multi-stakeholding of the implementation status of the plastic ban. The countries like Rwanda, Morocco, China, Malaysia, and Israel have already imposed fines for using plastic bags (Adeyanju et al. 2018). Indian government following the suit heralded a slew of legislative support in the shape of the Draft Plastic (Manufacture, Usage, and Waste Management) Rules, 2009, Plastic Waste (Management and Handling) Rules, 2011, Plastic Waste Management Rules, 2016 and Draft Plastic Waste Management Rules, 2021. It is followed by the Plastic and Thermocol Products Notification, 2018, by the government of Maharashtra. The proposed ban is not the first time the world has seen a ban on certain plastics.

ORCID details of the authors:

M.Z.M. Nomani: https://orcid.org/0000-0003-3886-6590

Still, its real-world implementation is ganged by choosing Pune's market are at an in-depth explanation of multi-layered plastics (MLP) phasing out of the rampant use for packaging by consumer goods companies.

MATERIALS AND METHODS

The material and method of the study center around the principles of extended producer responsibility and circular economy applied in numerous jurisdictions of the world for recycling plastic waste. It generally contains plastic pollution and combats its proliferation to foster environmental sustainability (Nomani & Praveen 2021). Applying the principle in the European Union is considered a novel management and waste hierarchy. Such an impetus comes through the policy instruments implementation mechanism of the European waste hierarchy. Its implementation reduces plastic pressures and recycling of waste streams (Leal Filho et al. 2019). The EPR, as an enviro-legal policy, has excellent potential in plastic treatment methods and brand designing essentials under the circular economy of the waste product laws (Wagne 2017). The 'circular economy approach is applied legally for recycling waste streams to achieve economic prosperity and environmental protection in a multi-stakeholding approach and legal remedy (Steenmans 2019). India replicated notions of the EPR and circular economy of plastic waste as a promising alternative to traditional waste management policy without hindering employment avenues (Bhadra & Mishra 2021). The multi-stakeholder approach to the plastic ban is undertaken in the light of the national and state laws and policies and their implementation to carve out the prognostic solution. It is empirically examined by the total sample of 798 people between September 2018 to January 2019 in eight different markets across Pune city (Bhattacherjee 2012), out of which 66% Vendor was (n= 532) and 32% Consumer (n=260) on random stratified method along with the expert qualitative opinions (Brace 2018).

RESULTS AND DISCUSSION

The Plastic Waste Management Rules, 2016, is a basic framework of law dealing with the concept of EPR and circular economy for managing plastics waste in India (Nomani & Rauf 2019). Although it is in an evolutionary phase in terms of the accountability of the producers and enforcement mechanism, it is still a good step in the positive earnest (Liang et al. 2021). It is considered the extension of the polluter pays principles contained under Section 9 of the Environment (Protection) Act, 1986. The draft EPR policy for plastic waste management, 2021, formalized the EPR and circular economy with varying degrees of success in India (Pani & Pathak 2021). The reason behind bringing out the policy is to prevent the excessive amount of plastic that is littered from clogging the pore of the drains, maintenance holes, and sewer system and the threat of choking of fauna. Maharashtra estimated that around 2000 tons of waste was generated per day in Pune. It turned out to be around 350-750 gm per capita daily. Of these, plastic waste generation was about 200-250 tons per day. Against this backdrop, Maharashtra issued the Maharashtra Plastic and Thermocol Products Notification, 2018.

Plastic Waste Generation in Pune

As a case study, the paper empirically studies Pune city and its urban sprawl and metropolitan development in Maharashtra state. Pune city is located between $18°19'$ to $18°45'$ north of the equator and $73°35'$ to $74°12'$ east of Greenwich, encompassing an area of 1643 square km (Fig. 1). It is the second-most populous state in Maharashtra after Mumbai. The study was conducted in the market zones of Pune city during the study. The interviewees were randomly selected. The interviewees were divided into vendors, consumers, and producers.

The interviewees from vendor groups represent groceries, vegetables, non-vegetables, medicines, textiles, and jewelry
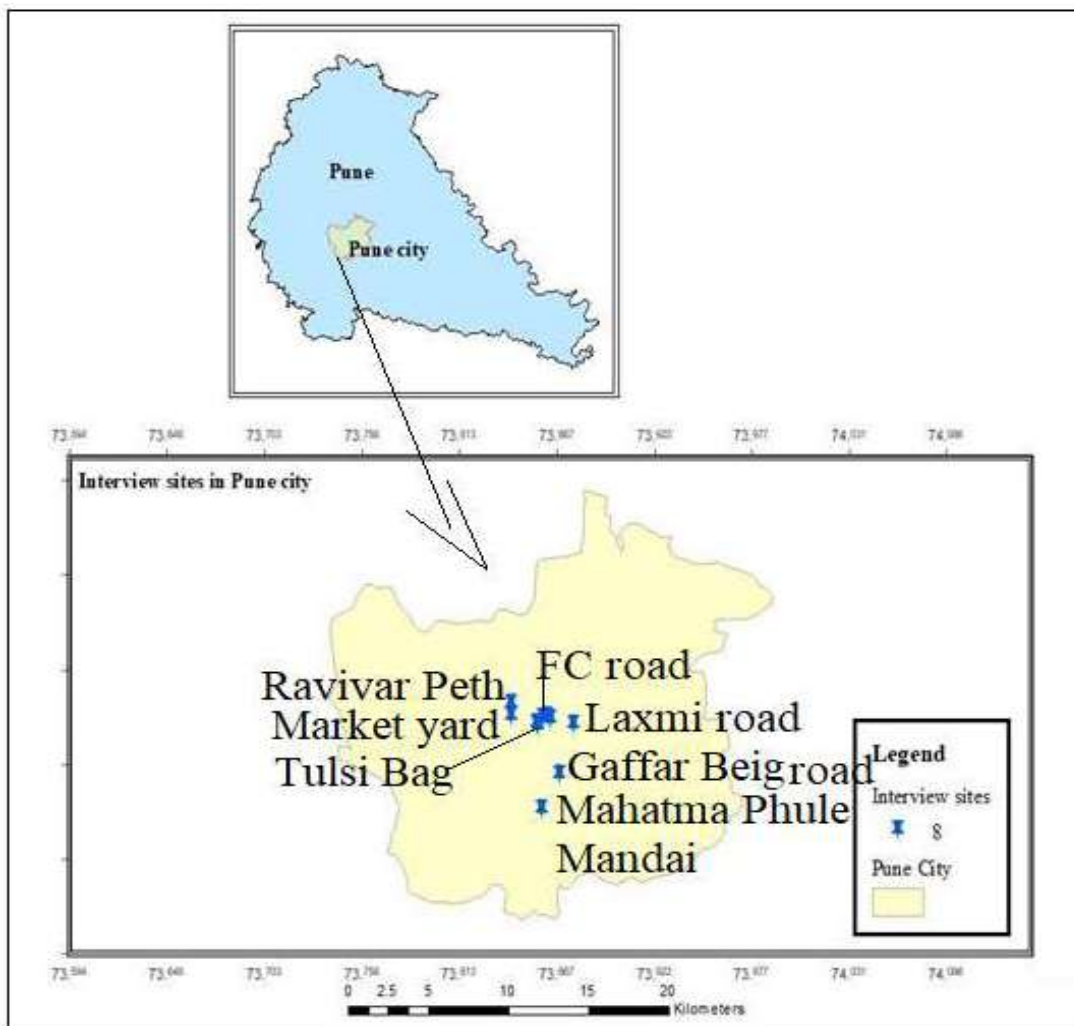

Fig. 1: Study Area and Map.

Fig. 2: Field Study and Market Locations.

in retail and wholesale markets. The number of people interviewed was based on the fact that the markets were located nearby and the markets were the whole seller and biggest markets of Pune city. The survey was conducted in areas like Laxmi Road, Ravivar Peth, Market Yard, FC Road, Tulsi Bag, Gaffar Beig Road, Mahatma Phule Mandai, and Deccan Gymkhana to represent the different spectrum of the population of Pune city (Fig. 2).

The vegetable and flower markets were in the Mahatma Phulemandai, while the hanging stalls were in the Tulsi Baug. The meat markets were found in the Gaffar Beig Road, while the grocery markets were in Market Yard. The markets in the Laxmi roads were mostly jewelry markets, textile manufacturing, and wholesale markets. The expert interview of sweet shops was conducted in Deccan Gymkhana. For the plastic manufacturer, it was conducted in Moti Chowk due

to the conglomeration of middle and upper-class consumers and retailers, and wholesalers.

Features of Plastic Ban Regulations

The slew of legislative support in the shape of the Draft PlasticRules, 2009, Plastic Waste Rules, 2011, Plastic Waste Management Rules, 2016, and Draft Plastic Waste Management Rules, 2021, the legal and institutional mechanism started phasing out of MLP, used for packaging by the consumer goods companies. The Plastic Waste Management Rules, 2016, inserted the notion of EPR to manage plastic waste in India (Nomani et al. 2020). While the Indian EPR is at an experimental phase, its work in the last five years has not realized the policy goals in implementing machinery due to the producers' liability deficit and enforcement from the authorities in the circular
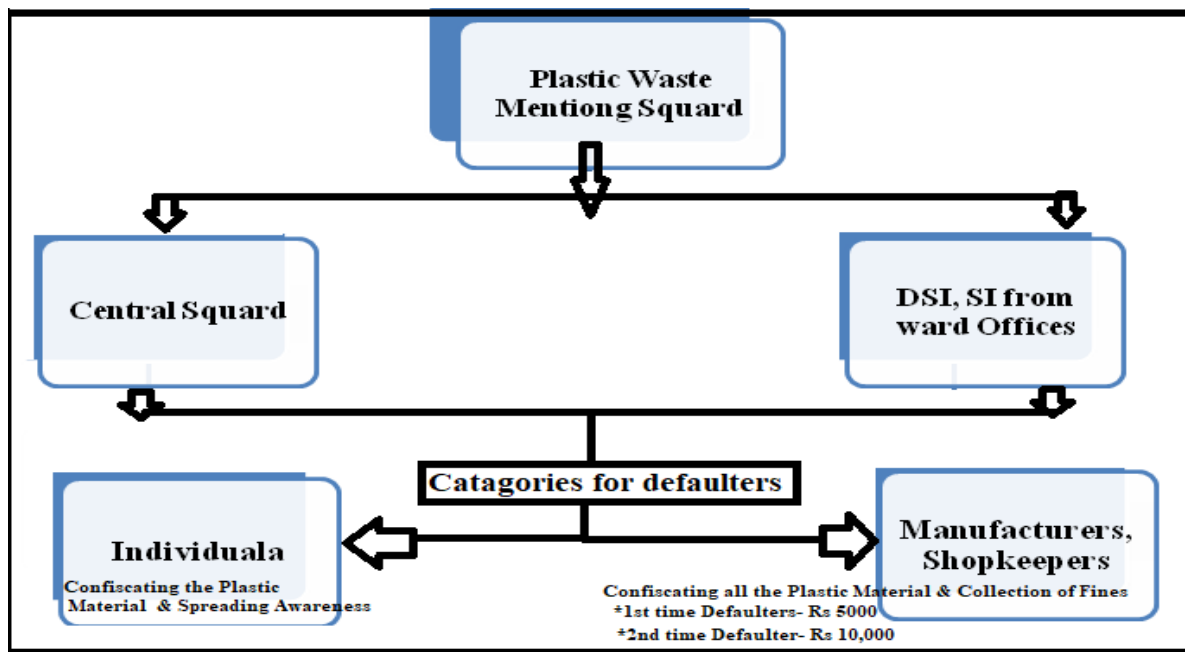
Fig. 3: Features of plastic ban regulations.

economy of plastic thrives by no leaps and bounds. The Indian Ministry of Environment Change released a uniform framework for EPR policy for managing plastic waste in collaboration with the Centre for Science and Environment (CSE), New Delhi (Fig. 3).

The government of Maharashtra has not banned the use of plastics entirely, but certain kinds of plastic, including plastic bags of less than 50 microns, remain in use. However, the use of plastic bags above 50 microns was promulgated by government notification. There have been clear instructions on the type of plastic that can still be used, including the weight and size of the government mentioned in the new notification. GOM announced the penalties as the first-time offender was fined 5000 Rupees, the second-time offender with 10000 rupees, and the third-time offender fined 25000 rupees along with a jail sentence of up to 3 months.

Maharashtra Plastic Ban Notification, 2018

The Maharashtra Plastic and Thermocol Products Notification, 2018, was passed to give effect to the national legislation on the Plastic Waste Rules, 2011, and Plastic Waste Management Rules, 2016. It banned plastic and sensitized people regarding the use and recycling along with the switching to alternative methods amongst the multi-stakeholders in Maharashtra. It resulted in reducing and using alternatives for plastics (Nomani & Hussain 2020). It also generated awareness about the types of plastics exempted

from the ban and the adoption of viable alternative usages (Fig. 4).

The plastic ban is effective for all the people of Maharashtra, including individuals and NGOs, commercials, marriage halls, cinema halls, hotels, pilgrims' places, caterers, hawkers, traders, manufacturers, wholesalers, retailers, stockiest, people in business, public places, tourist places, beaches (Fig. 5). The banning of plastic went along with awareness programs by the government and the NGO on Single-use plastic.

It paved the way for the segregation of Plastic from waste and its ultimate disposal at designated points. The evidence is prominent in the 'Plastic Free Pune' and Changing to an environmentally friendly lifestyle. The fraction of usage suggests designing alternatives for plastic products by reducing the use of low-level plastics and encouraging the use of recycled products. It was structured based on the 4Rs, awareness generation among citizens, provision and exchange of information, and implementation of the law on the *Maharashtra Plastic and Thermocol Products* Notification, 2018. The task is to understand the effects on the stakeholders that are directly and indirectly affected by the ban. The idea and perspective discerned new usage and treatment (Fig. 6).

Since the ban was implemented to curb plastic pollution, it is vital to understand the stakeholding of the ERP and circular economy from a holistic perspective. It also augurs
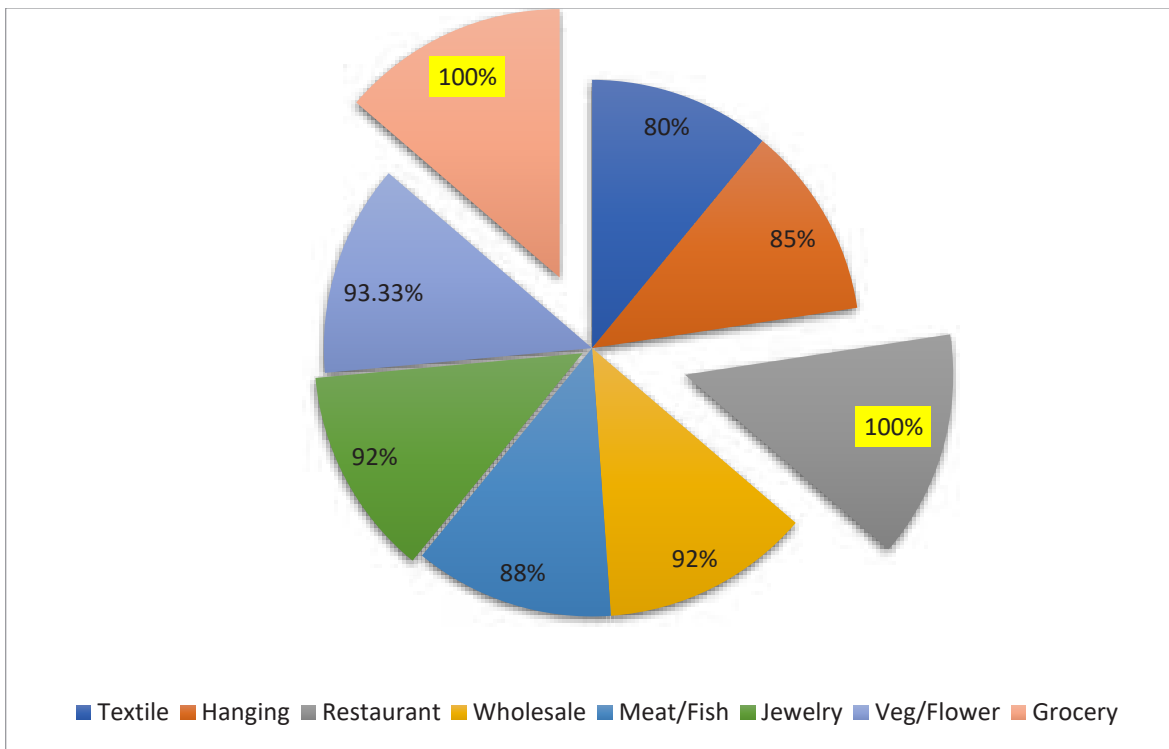
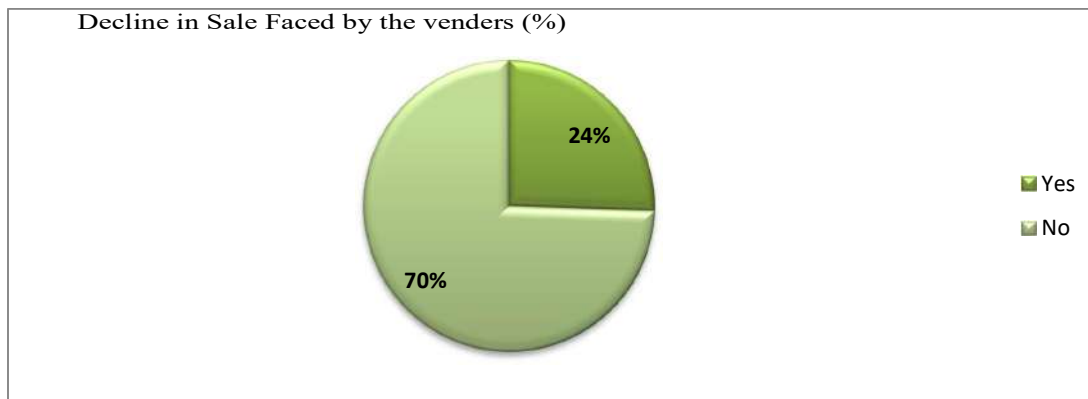Fig. 4: Awareness of plastic ban among vendors.

Fig. 5: Impact of banning notification on vendors.

for the alternatives and prognostic solutions in the urban sprawl of Pune city. The Maharashtra Plastic and Thermocol Products Notification, 2018, aimed to address 2000 tons of plastic waste generated in Pune. The household plastic generation was estimated to be 350-750 gm per capita daily.

Application of Extended Producers Responsibility

The regulatory regime of plastic waste incorporated the concept of EPR under the Maharashtra Plastic and Thermocol Products Notification, 2018. The highest responsibility was

that of the brand owners, followed by the packers and fillers. The onus for EPR primarily vested cast for the plastic carry bag above 50 microns to be exchanged for 15 rupees per kg of the clean and reusable plastic carry bag among the local stakeholders. The highest sense of responsibility is cast on the brand owners, followed by the packers and the fillers. The shrinking of the responsibility is structured on the tower of the two modules and methodological applications (Fig. 7).

The survey in grocery market yards reveals that 76% of the vendors knew of the notion of EPR set into the Maharashtra
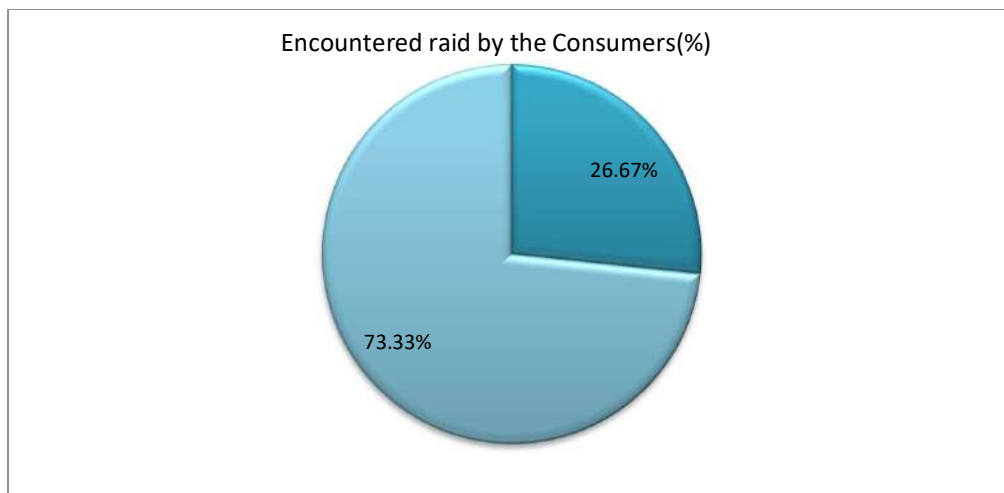
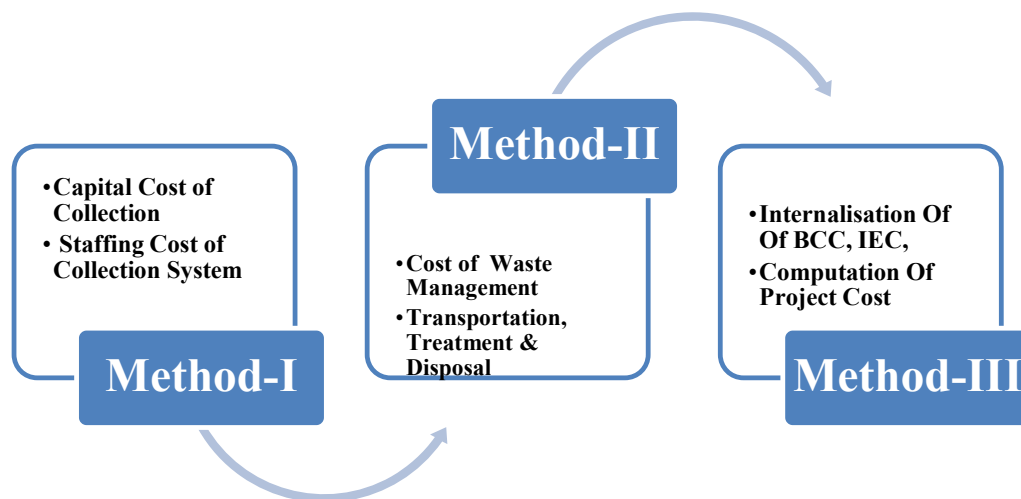Fig. 6: Impact of banning notification on consumers.

Fig. 7: Methodological application of EPR.

Plastic and Thermocol Products Notification, 2018. The legal literacy among general business owners figures out to be 32%. 68% of people need to learn about the concept of EPR and the penal consequences of the plastic ban. However, 92% of the vendor in Sunday weekly and wholesale markets were aware of the nature and content of the law (Fig. 8).

On the other hand, the survey also revealed that 66% of the vendors faced problems due to the plastic ban. It was noticed that 58% of the vendors were aware of the EPR (Fig. 9). Most of the time, the plastics were either burnt on-site or given to the rag pickers. It was also seen that vendors needed help in giving articles in small packets. They preferred to avoid getting a hike in the product prices because they had to

stay in the market competition. The leftover banned plastic is either unused or slowly scraped (Nomani & Parveen 2020). Most big shop owners knew of EPR but felt the regulatory mechanism needed to be more time-consuming and non-cooperation of the consumers.

The cost of collecting and staffing to buy plastic would be chargeable to producers under EPR. The management collection, transportation, treatment, and disposal of plastic waste would be considered a project cost. It enhances the financial contribution toward the collection of plastic waste. It is based on incentives of the EPR credit system and generally scaled on the extent of the contribution by the producers. To this end, it is based on the five years contract with Producers towards meeting their EPR obligations.
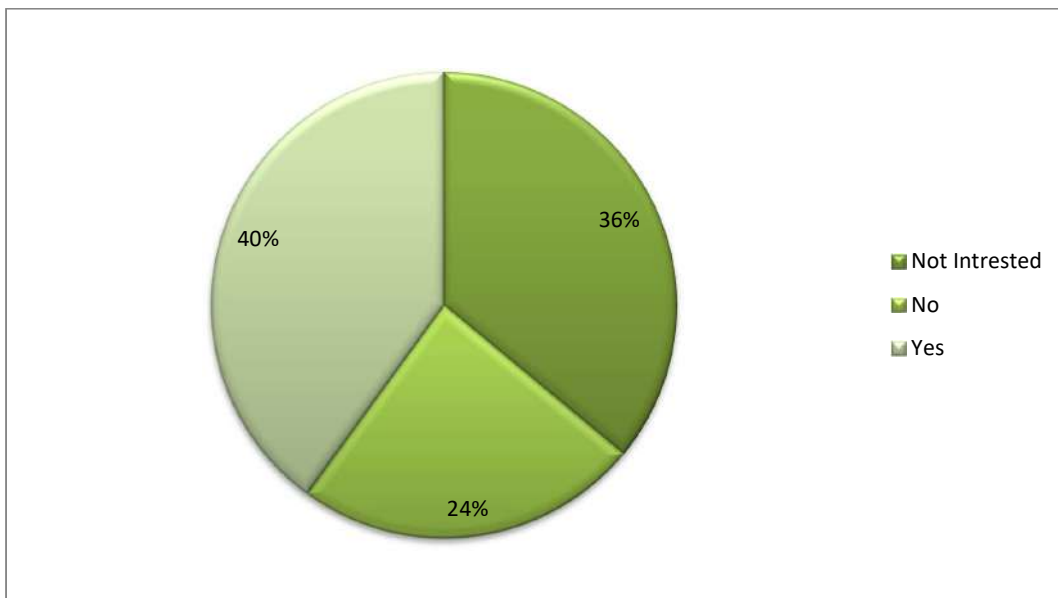
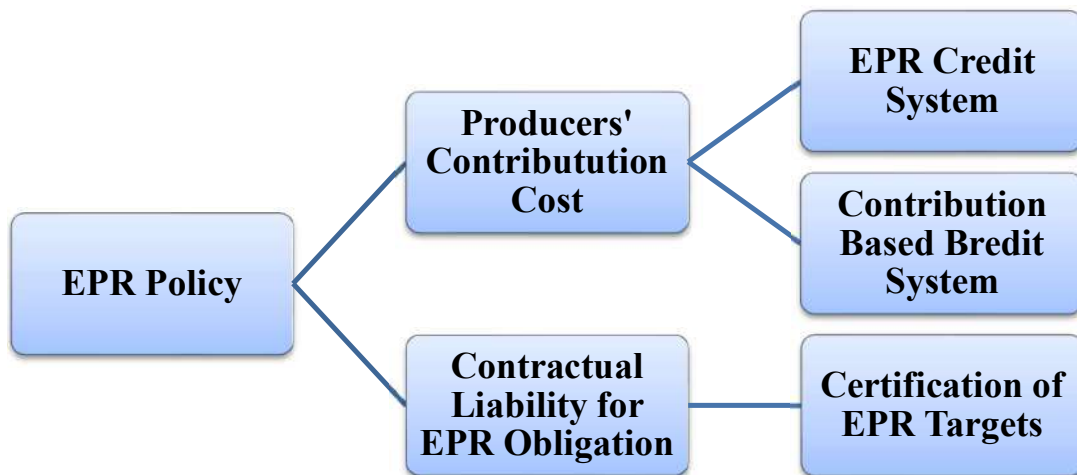Fig. 8: Awareness of the EPR among consumers.

Fig. 9: Features of EPR Policy.

Circular Economy of Plastic Ban

The circular economy of the plastic ban has played a pivotal role in the legal and institutional mechanism of the plastic ban in Pune City. It ordains the take-make-dispose (Steenmans et al. 2017) and strengthens eco-friendly design and waste management. The life-cycle assessment takes a holistic perspective of the resource, substance, product, and waste (Nomani & Salahuddin 2020). It establishes legally binding standards, resource recovery laws, and policies. On the other hand, the life-cycle perspective constitutes the waste hierarchy emphasizing quantity and recycling quality. The nature of

environmental liability under EPR resembles the polluter pays principles in the spectrum of the EPR. The salient features of the EPR are the producer's contribution to the cost of recycling.

The circular economy of the plastic ban revolves around the producers, vendors, and consumers in physical and informative responsibilities (Fig. 10). The survey showed that although 36% of consumers were aware of the plastic ban, only 56% supported it. It also noted that consumers faced problems carrying food in parcels because of the oil or liquid in the food, which might spill and stain. 80% of the consumers wanted a complete ban on plastic or some
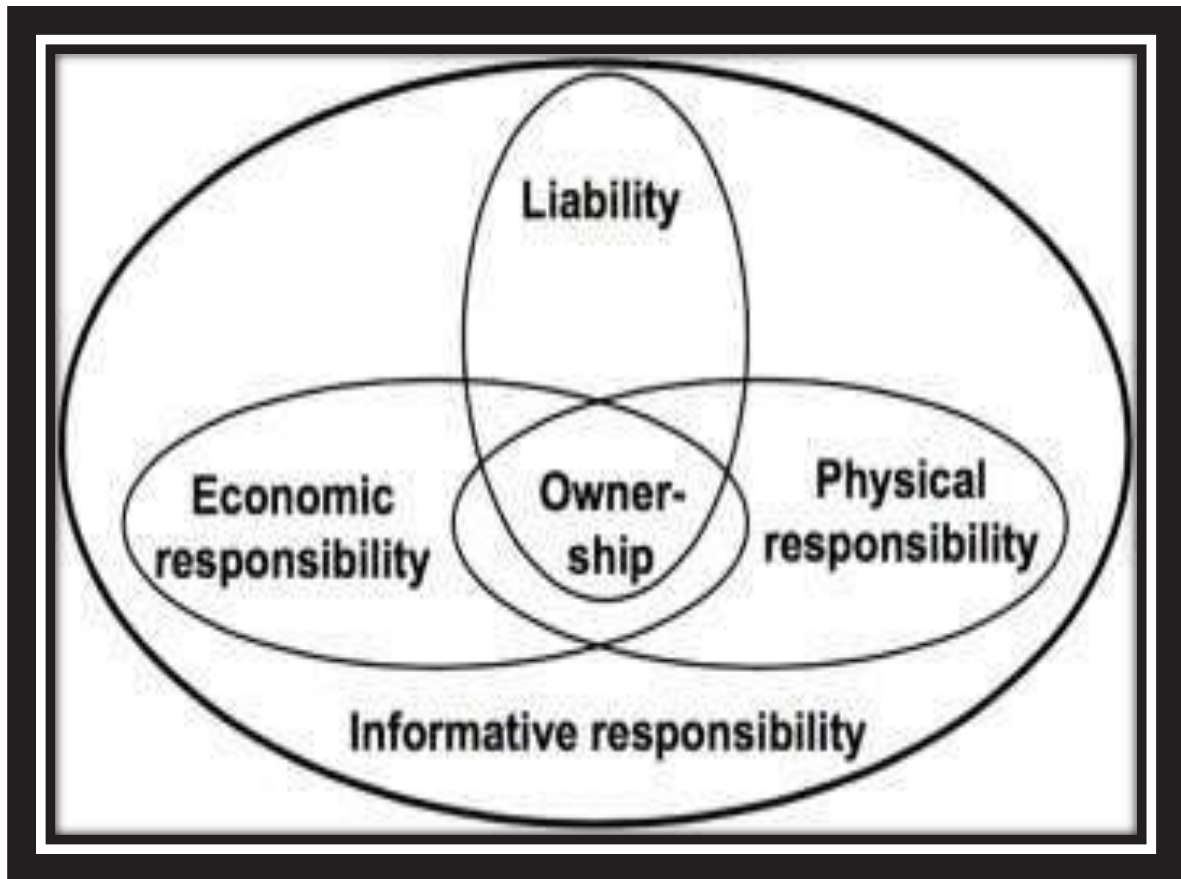
Fig. 10: Circular economy of the plastic ban.

biodegradable alternative to plastic. They understood the alternatives and solutions different stakeholders have switched to were necessary. It finally leads to the annual certificate on waste collected by Producers towards meeting the EPR target by PMC. Other cities must also adopt this system to become effective.

CONCLUSION

Implementing the plastic ban under the Maharashtra Plastic and Thermocol Products Notification, 2018 witnessed changing perceptions towards the use of plastic consumption in daily life. However, it remained in the primitive stage of deviance and compliance. The multi-stakeholder interaction and interview amongst shopkeepers, consumers, environmentalists, and representatives of NGOs tallied a total of 798 people were interviewed to draw a realistic portrayal of the use of disposal and treatment system. The limitation of the study envisages its results and discussions during the span of five months during the year 2018-2019. The conclusions and recommendations reached during the

initial two years of implementing the Maharashtra Plastic and Thermocol Products Notification, 2018, in implementing the plastic ban in Pune City. The trickle-down effect of the law carried out the environmental effect of the plastic ban regarding the Police cognizance, seizure, and fines under the overall supervision of the PMC officials. The salutary impact gauged from the maximum fine collected from police search and seizure amounts to 25,600 rupees in December 2018. The gradual ban on plastic resulted in stratified compliance, as evidenced by the fine collection in January 2019 came to only 8000. Thus, the police action and fine collection by Pune Municipal Corporation under the Maharashtra Plastic and Thermocol Products Notification, 2018, in tandem, discern the level of compliance to the higher side. The study demonstrated partial success in percolating EPR and circular economy, consequential ban implementation, and environmental compliances. The legal and institutional framework needs further impetus to thrash out the menace of the plastic ban effectively. Implementation officers needed to learn about the EPR and the Plastic rules found

out while talking to the vendors in the survey. It resulted in even confiscating and imposing penalties on vendors who did not come under the plastic ban rules.

REFERENCES

Adeyanju, G.C., Augustine, T.M., and Volkmann,S., Oyebamiji, A.U., Ran, S., Oluyomi A. Osobajo O.A. and Otitoju. A. 2018. Effectiveness of intervention on behavior change against the use of non-biodegradable plastic bags: A systematic review. Discover Sustain., 2(1): 13.https://doi.org/10.1007/s43621-021-00015-0

Aryan, Y., Yadav, P. and Samadder, S.R. 2019. Life cycle assessment of India's existing and proposed plastic waste management options: A case study. J. Clean. Prod., 211: 1268-1283.

Bhadra, U. and Mishra, P.P. 2021. Extended producer responsibility in India: Evidence from Recykal, Hyderabad. J. Urban Manag., 10: 430-439.

Bhattacherjee, A. 2012. Social Science Research: Principles, Methods, and Practices. Textbooks Collection, NY, p. 3.

Brace, M. 2018. Questionnaire Design: How to Plan, Structure, and Write Survey Material for Effective Market Research. Kogan Page Publishers, London

Gui, L., Atasu, A., Ergun, Ö. and Toktay, L.B. 2013. Implementing extended producer responsibility legislation: A multi-stakeholder case analysis. J. Ind. Ecol., 17(2): 262-276.https://doi.org/10.1111/j.1530-9290.2012.00574.x

Leal Filho, W., Saari, U., Fedoruk, M., Lital, A., Moora, H., Kloga, M. and Voronova, V. 2019. An overview of the problems posed by plastic products and the role of extended producer responsibility in Europe. J. Clean. Prod., 214: 550-558. https://doi.org/10.1016/j.jclepro.2018.12.256

Liang, Y., Tan, Q., Song, Q. and Li, J. 2021. An analysis of the plastic waste trade and management in Asia. Waste Manage., 119: 242-253.

Nomani, M.Z.M. 2000. The human right to environment in India: Legal precepts and judicial doctrines in critical perspective. Asia Pac. J. Environ. Law, 5: 113-34

Nomani, M.Z.M. and Hussain, Z. 2020. Ecological nuisance and common law environmentalism: Relevance and revival in combating environmental pollution in India. J. Adv. Res. Dyn. Contr. Sys., 12: 1197-1204. https://doi.org/ 10.5373/JARDCS/V12SP5/20201874

Nomani, M.Z.M. and Parveen, R. 2020. Prevention of chronic diseases in climate change scenario in India. Environ. Justice, 13: 97-100. https://doi.org/10.1089/env.2019.0032

Nomani, M.Z.M. and Parveen, R. 2021. Legal connotations of biological resources and its ripple effect on conservation researches in India & abroad. Int. J. Conserv. Sci., 12(2): 571-576.

Nomani, M.Z.M. and Rauf, M. 2019. Legal policy for bio prospecting of natural resources in India. Indian J. Environ. Protect., 39(11): 1009-1015.

Nomani, M.Z.M. and Slalhuddin, G. 2020. River health assessment of Ganga basin in India: a comparative perspective. Pollut. Res., 39S: 266-271.

Nomani, M.Z.M., Rahman, F., Ahmed, Z., Faiyaz, T., Khan, S.A. and Jasim, A.H. 2020. Prevention of transnational environmental crime under the convention on the protection of the environment through criminal law: Agenda and implementation. Int. J. Adv. Sci. Technol., 29: 606-612.

Pani, S.K. and Pathak, A.A. 2021. Managing plastic packaging waste in emerging economies: The case of EPR in India. J. Environ. Manag., 288: 112405.

Rafey, A. and Siddiqui, F.Z. 2021. A review of plastic waste management in India–challenges and opportunities. Int. J. Environ. Anal. Chem., 16: 1-17.

Steenmans, K. 2019. Extended producer responsibility: An assessment of recent amendments to the European Union Waste Frameworks directive. Law Environ. Develop. J., 15: 20-108.

Steenmans, K., Malcolm, R. and Marriott, J. 2017. Commoditization of waste: legal and theoretical approaches to industrial symbiosis as part of a circular economy. The University of Oslo, Faculty of Law Research Paper No. 2017-26, Oslo, Norway.

Thompson, R.C., Moore, C.J., VomSaal, F.S. and Swan, S.H. 2009. Plastics, the environment, and human health: current consensus and future trends. Phil. Trans, Roy. Soc. B Biol. Sci., 364(1526): 2153-2166.

Assessment of the Environmental Impact of Discharges from Fishmeal Factories Located in Levrier Bay, Nouadhibou-Mauritania

M. E. Moulay Ely*(**)† iD **, M. Sakho*** iD **, S. Santana-Viera**** iD **, J. J. Santana-Rodríguez**** iD **, B. Elemine*** iD **, M. Zamel**** iD **, M. V. Deida*** iD **, D. Froelich****** iD ** and I. Babah*** iD

*Unité de Chimie Moléculaire et Environnement, Département de chimie, Faculté des Sciences et Techniques, Université de Nouakchott-Nouakchott, Mauritanie
**Instituto Universitario de Estudios Ambientales y Recursos Naturales (i-UNAT), Universidad de Las Palmas de Gran Canaria, 35017 Las Palmas de Gran Canaria, Spain
***Département Chimie Microbiologie et Suivi du Milieu Aquatique (DCM-SMA), Office National d'inspection Sanitaire des Produits de la Pêche et de l'Aquaculture (ONISPA), 1416, Nouadhibou-Mauritania
****Ecole des Arts Et Métiers ParisTECH-Institut De Chambéry, France
†Corresponding author: Moulay El Mehdi Moulay Ely; moulayely2017@gmail.com

ABSTRACT

Levrier Bay, located in the western part of Mauritanian Cost, has a strategic position in Mauritania's fish economy and reproduction environment. Recently, fishmeal factories have multiplied in the bay. This study was carried out in Levrier Bay. It is the first one in this area which is interested in assessing the environmental impact of fishmeal factory discharges by measuring several parameters such as suspended matter, chemical oxygen demand (COD), biological oxygen demand (BOD), conductivity, turbidity, and salinity. A total of 27 samples were collected at 9 sites distributed on the link between effluents from factories and the Atlantic Ocean (discharge site). Results show that some parameters are over permissible values, like suspended matter content (SS), which reached 2020 mg. L.$^{-1}$ level. The turbidity measure shows excessively high values (50 to 961 mg.L.$^{-1}$); impacted by effluents at the reject point, the seawater conductivity and salinity are particularly low (4.53 to 188.2 and 13 to 56.4, respectively). The total organic carbon (TOC) values ranged from 200 to 780 mg/L, whereas the highest measured level of chemical oxygen demand was 4010 mg.L.$^{-1}$ Biochemical oxygen demand content ranged from 685 to 961 mg/L. The biodegradability index (COD/BOD) shows that these effluents are not easily biodegradable because the index > 3.

INTRODUCTION

The Mauritanian coastline, recognized as one of the most productive in the world, particularly illustrates the fragility of the coastal ecosystems. Their productivity and functionality are closely linked to the quality of the water that composes them. The Levrier Bay, located in the western part of Mauritanian Cost, has a strategic position in Mauritania's fish economy and reproduction environment. Recently, fishmeal

factories have multiplied in the bay. They have an important economic role, but they reject effluents directly into Ocean without treatment, so Levrier Bay suffers from the discharge of untreated wastewater from fishmeal factories (Cheick et al. 2020). Water volume discharged. However, Fishmeal wastewater contains 140 g COD.L$^{-1,}$ which consists of 60% oil and grease, 27% protein, and 13% mixture of soluble organic and suspended solids (Putra et al. 2020). The fish processing industry uses large amounts of water to wash the raw product and manufacture by-products. These factories are generally located in areas with high water content, and they consume more water than needed for seafood processing processes (Ben et al. 2017)

On the other hand, effluents from fishmeal factories may lead to serious pollution problems, especially if they are not treated enough. They contain an important amount of nitrogen and organic load, which conduce, in aquatic,

to the eutrophication phenomenon. This phenomenon is a severe problem caused by industry discharge (Bhuyar et al. 2021a, 2021b).

The most significant anthropogenic pollution is defined by the introduction through the activities of substances or energy in the marine environment that can cause harmful effects. The impact of wastewater discharges in the marine environment has long been minimized due to the significant dilution phenomena of these discharges when they contact the oceanic marine environment (Bezama et al. 2012, Ferraciolli et al. 2018, Vallejos et al. 2020).

In addition, ship-unloading operations are often carried out using pumps that transport the fish from the hold to the land. Besides seawater, pump water contains considerable amounts of fish residue and can have a wide variety of oil and fat residue. Direct discharges of industrial wastewater affect the water quality and coastal marine ecosystems (Holmer et al. 2003, Moncada et al. 2019, Quimpo et al. 2020). Changes induce a variation in physicochemical characteristics such as the salinity of the water, but also the decrease in oxygen required by marine species, the modification of nutrient concentrations, etc. (Gebauer 2004, Anh et al. 2010, Venugopal & Sasidharan 2020).

The studies that have been carried out on the levels of trace metals in fish and sediment in Levrier Bay (Legraa et al. 2019, Cheikh et al. 2020) lack information about the impact of discharges from fish processing, especially when fishmeal manufacturing is involved.

This study aims to determine some wastewater indicators, such as turbidity, conductivity, salinity, suspended solids, Chemical oxygen demand (COD), and biological oxygen demand at the reject point, to evaluate the environmental impact of discharges from fishmeal factories. It is the first one in this area that is interested in this question; Its outcomes will contribute to the global Levrier Bay environmental investigation and give wide information about the resources of environmental pollution.

MATERIALS AND METHODS

Description and Location of the Study Area

The study area is focused on the Bountiya sector located on Levrier Bay in the extreme northwest of Mauritania (Fig.1). It is characterized by strong industrial activity represented by all the factories manufacturing fishmeal and fish oil. Nine sites around fishmeal factories represent the link between the affluent and Ocean.

The samples were collected in accordance with the guidelines of international organizations (WHO 2004) and the recommendations of some literature (Rodier 2010). Briefly, the samples were collected at low tide in aseptically sterile uncolored 500 mL plastic bottles and washed
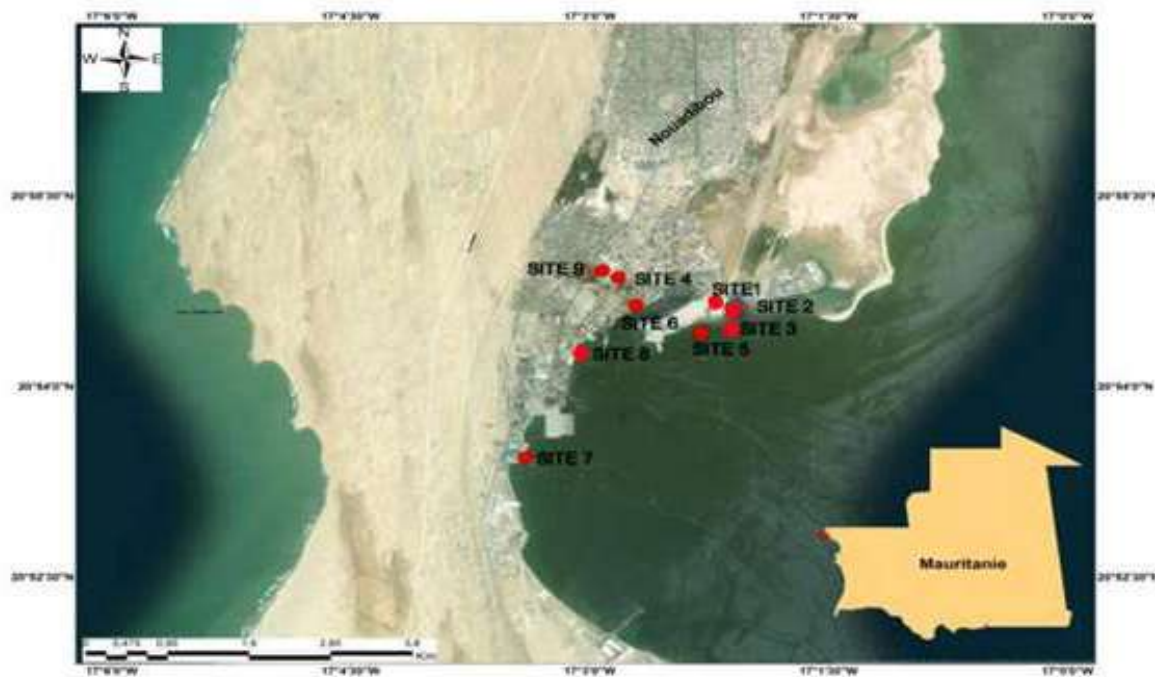

Fig. 1: Sampling sites.

Table 1: Parameters studied.

Parameters	Methods
Turbidity	NF ISO 7027-1: Water quality - Determination of turbidity - Part 1: quantitative methods
Salinity	NF 8502-9: In situ method for the determination of water-soluble salts by conductimetry
Suspended matter	NF EN 872: Water quality - Dosage of suspended solids - Method by filtration on glass fiber filter
Conductivity at 25°C	NF EN 27888: Water quality - Determination of electrical conductivity
Chemical Oxygen Demand (COD)	NF T 90 101: Water quality - Determination of chemical oxygen demand (COD)
Biological Oxygen Demand (BOD) for 5 days	NF T 5815-1: Water quality - Determination of the biochemical oxygen demand after n days (BODn) - Part 1: method by dilution and inoculation with the addition of allylthiourea
Total Organic Carbon (TOC)	MA. 415 –COT 1.0: Determination of organic carbon in effluents: oxidation by persulfate and UV rays – dosage by infrared spectrophotometry

beforehand with 10% acid baths (HCl). Then, the bottles were rinsed with distilled water and sent to the laboratory for further physico-chemical analysis. The samples were stored at a temperature below 4°C and in uncolored bottles for the shortest possible time.

Sampling deep was between 30 and 50 cm to characterize the various effluents discharged by the factories. Three samples per factory were taken. They were 30 meters from each other near the spill point (the first sample is located just at the discharge point, and others are distributed over a radius of approximately 100 m from the discharge point). The analysis was carried out by the ONISPA laboratory in Nouadhibou (Mauritania) according to the methods listed in Table 1.

RESULTS AND DISCUSSION

Effluents from fishmeal factories are discharged into the ocean without treatment. So they may pose a serious problem for the Levrier Bay environment, especially the biodiversity of aquatic ecosystems. This study assessed the concentration of certain parameters indicatives of the pollution of industrial effluents generated by the activity of fishmeal factories. The results obtained from the examination of 27 samples of seawater from 9 reject points are presented in the five figures below (from Fig. 2 to Fig. 6).

Conductivity and Salinity

The conductivity values were low and ranged from 4.53 to 188 $\mu S.cm^{-1}$ at sites 2 and 3, respectively (Fig. 2). Most sites have a conductivity value of around 50 $\mu S.cm^{-1}$. The low conductivity value in this study means that the effluents were sampled before enough time to be well mineralized or the fishmeal factories use urban water in the cleaning process.

Sea water at the ejected point has a salinity between 13 and 56.4 $mg.L^{-1}$. Only three sites have salinity very low (13, 23, and 23.4 at sites 9, 1, and 2, respectively; Fig. 3). In normal cases, sea water salinity is 36 $mg.kg^{-1}$.
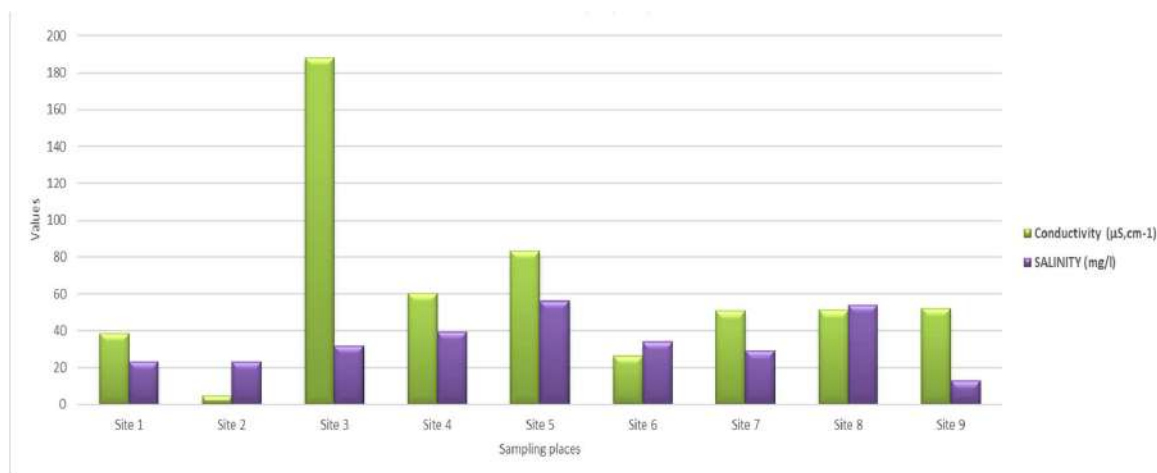

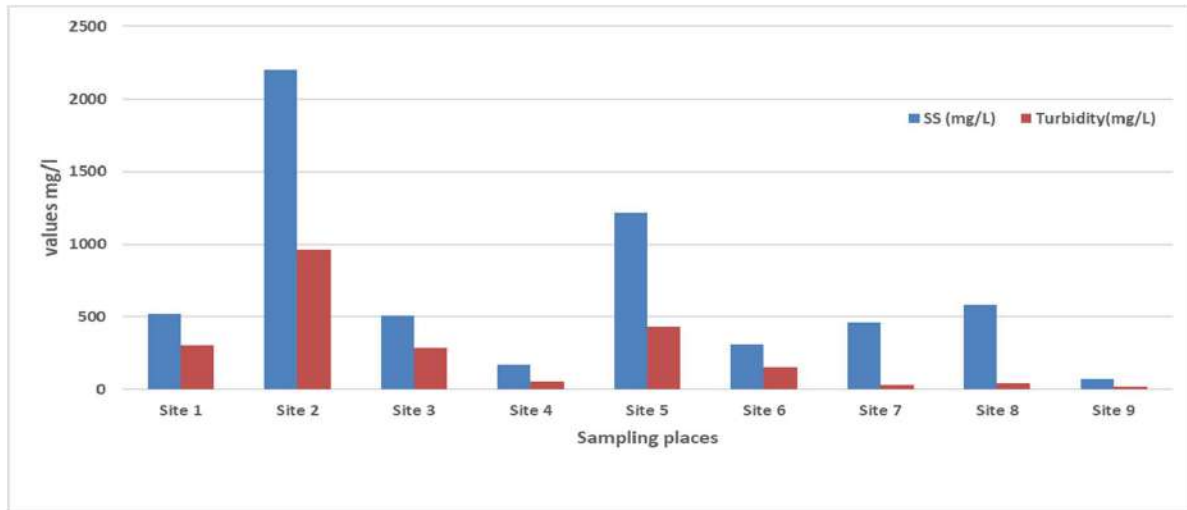Fig. 2: Conductivity and salinity values.

Fig. 3: SS and turbidity values.

Turbidity and Suspended Solids

The mean values of turbidity show a disparity variation between different plants. This difference is variable from 20 to 961 mg.L^{-1} (Fig. 3). The highest value is found at site number 2, and the lowest is at site 9. The difference could be caused by activities period which is different from one to other.

Suspended solids concentration in the effluents of the fish processing plants measured in this study varies between 73 mg.L^{-1} and 2200 mg.L^{-1} (Fig. 3). Like turbidity, the difference between factory effluent SS content is linked to work period.

There is a perfect proportionality between turbidity and SS (Fig. 3). This result was found by a previous study that demonstrated a relationship of proportionality between suspended matter and turbidity. Remili & Kerfouf (2013)

studied how to use turbidity to continuously estimate the concentration of suspended matter. Thus, we observe a high content of turbidity and SS at the level of Site2, which is attributed to suspended solids (SS) constituting the main vector of pollutants transported in rainy weather in the sewers. The importance of pollution from urban discharges during rainy weather and the negative impact of this pollution on receiving environments is a phenomenon highlighted in the literature as early as 1970. However, low turbidity and SS content are recorded for the sampling points least exposed to rainwater, such as Site 4.

Total Organic Carbon

The lowest total organic carbon (TOC) content (200 mg.L^{-1}) is found at site number 6, and the highest one (780 mg.L^{-1})
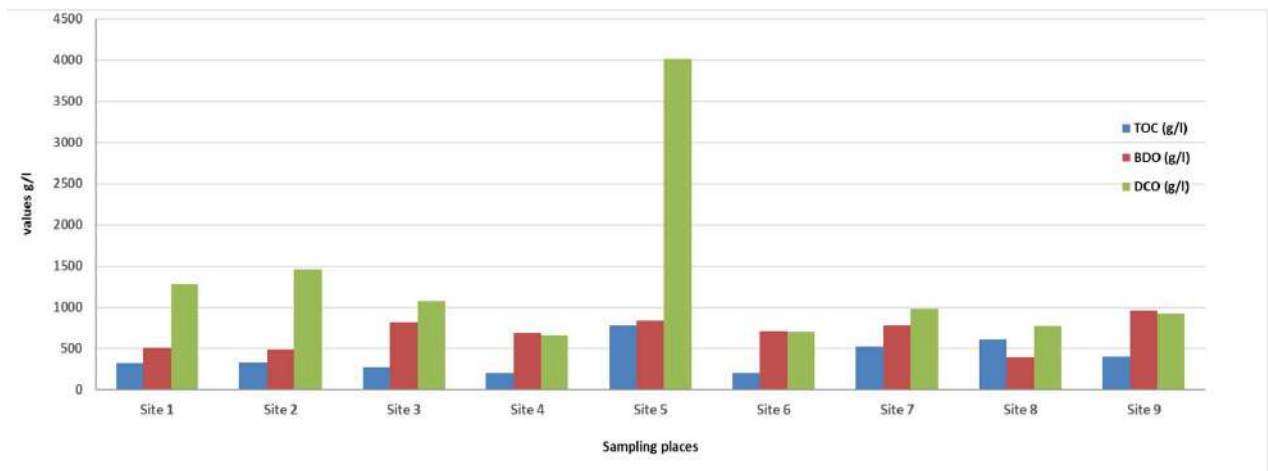

Fig. 4: TOC, BOD$_5$, and COD values.

is detected at site number 5 (Fig. 4). The majority of sites have COT content comprised between 317 and 609 mg.L^{-1}. It reveals an additional clue showing the presence of organic matter. The wastewater from these fishmeal and oil factories contains high levels of protein and oils, so their recovery is a financially viable operation. This is partly explained by an excessive discharge of organic matter and, more particularly, in the case of site 5.

Biochemical Oxygen Demand (BOD5)

The DBO$_5$ values show an inequality variation between different plants. This difference is variable from 396 to 961 mg.L^{-1} at sites number 8 and 9, respectively (Fig. 4). The difference could be linked to the activities period, which differs from one to another.

Chemical Oxygen Demand (COD)

COD values recorded during this study ranged from 655 to 4010 mg.L^{-1}. The highest value was found at site number 5 and the lowest at site 4 (Fig. 4). Most sites have COT content comprising between 774 and 1465 mg.L^{-1}. The chemical oxygen demand (COD) indicates the organic load in the water. It is an important parameter for water quality characterization (Mathurin & Kisto 2021).

Biodegradability Index COD/BOD

All effluents from fish processing plants points have a COD/BOD$_5$ biodegradability index low or equal to 3 except point 5, which has an index of 4.79 (Fig. 5). So, those effluent (that has an index low than 3) are biodegradable. However, a high value of this ratio (higher than 3) indicates that a large part of the organic matter is not biodegradable. In this case, it is better to consider the water treatment by physicochemical methods (Johan & Mizier 2004).
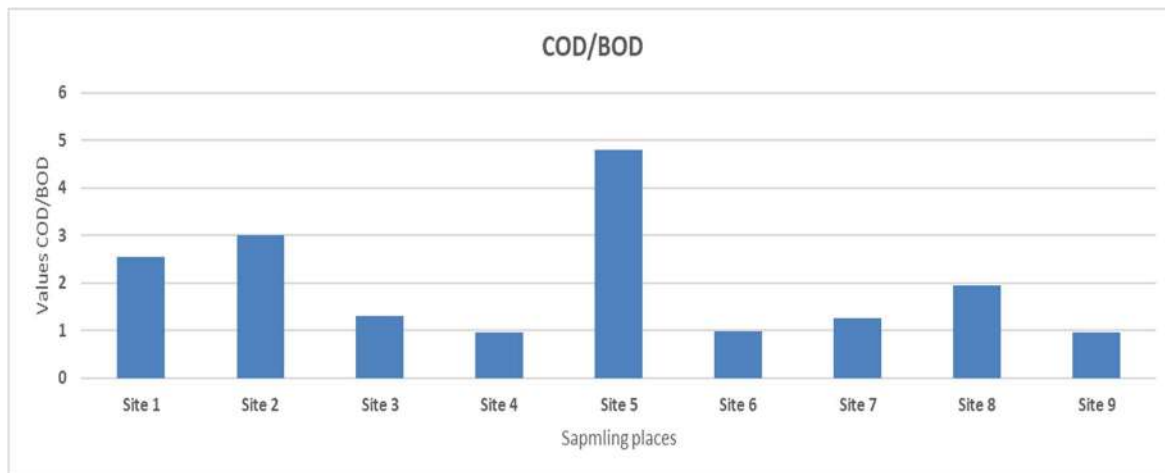

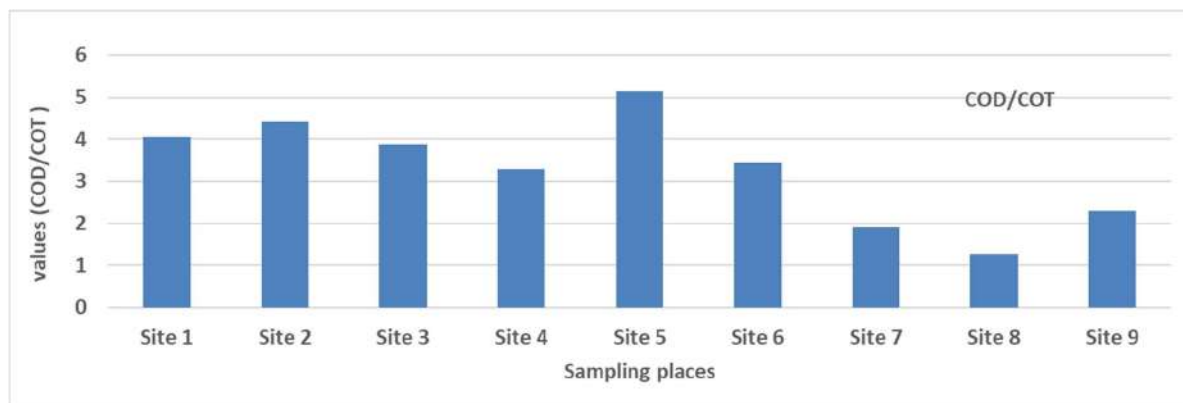Fig. 5: COD/BOD ratio biodegradability index.

Fig. 6: COD/TOC ratio.

COD/TOC Ratio

Determining this ratio for wastewater allows the assessment of nutriment doses in treatment plants. These ratios comprise between 3.28 and 5.14 mg.L^{-1} (Fig. 6), which is extended to the ratio frequently found for urban and industrial wastewater.

As this work is the first in Mauritania interested in fishmeal factories discharged into the environment, the results will be compared with similar ones conducted in other counties (near or far from Mauritania). Table 2 summarizes the study finding.

Conductivity reflects the degree of global mineralization. It is one of the simplest and most important for wastewater quality control (Chikh et al. 2018). The low conductivity values of seawater at reject points are related to the use of pure water by Fishmeal factories. Pure water has a low conductivity, and a huge amount rejected by the factory dilutes the conductivity at the discharge place.

Turbidity and suspended solids have particularly the same meaning because they reflect the water load of insoluble substances. They give important and direct information on water quality variation (Merbouh et al. 2020). Turbidity results in this study show that effluent rejected in the environment is non-treated. Bay et al. (2017) findings show that the content of suspended solids can reach 13,980 mg/L in wastewater from fish processing. Our results are twice lower as those found by John and Mizier (2004) along wastewater discharged from fish processing plants.

Biochemical oxygen demand (BOD) indicates the amount required for oxidizing the organic matter and inorganic oxidizable contained in the sample (Chikh et al. 2018).

The BOD$_5$ results show a similarity in the biodegradable organic matter content of the loads for the different effluents analyzed. This could be explained by the fact that all these factories use the same procedure for processing fishery products. We note that these waters have very high inputs of biodegradable organic matter. The highest levels of BOD$_5$ can be attributed to the concentrations of oils and fats measured in the wastewater from the butchering process. At the same time, the remaining proportion is generated during fish processing operations (Ben et al. 2007).

Other investigations on the effluents from a fish canning factory reveal levels five times higher than ours (Colic et al. 2007). Effluents from Tunna processing contain 6600 g.L^{-1} of BOD$_5$ (Venugopal et al. 2020), which is very high compared with effluents of fishmeal in this study. BOD values reported by Putra et al. from Japon fishmeal are very low than the literature. The difference between the value is related to the factory recycling system. Some factory reuse effluent to collect protein residues that reduce BOD.

Beannassi et al. (2004) reported that the COD content could reach 190000 mg.L^{-1} for industrial extractions of fish oils. Fishmeal effluent has 50000 g.L^{-1} as COD load (Colic et al. 2007). This load in processing plant effluents comprises total suspended solids, fats, oils, and grease. COD in effluent from Tunna processing is 11100 g.L^{-1} (Venugopal et al. 2020); however, effluents from the seafood processing plan contain 1717 g.L^{-1} (Jamieson et al. 2017). This value is comparable with ours.

COD/BOD$_5$ ratio results are comparable with the results of investigations by John and Mizier (2004) in an earlier study concerning the characterization of leachate from a landfill. John and Mizier (2004) showed that this ratio could

Table 2: Comparative analysis with similar studies.

Matrix	SS (g.L^{-1})	COD (g.L^{-1})	BOD$_5$ (g.L^{-1})	COD/BOD	Reference
Effluent from Fishmeal	173 to 2200	655 to 4000	467 to 990	0.96 to 4.79	This study
Fishmeal	30,000	50,000	30,000	0.60	Colic et al. (2007)
Effluent from tuna processing	1570	11100	6600	-	Venugopal et al. (2020)
Fish processing	-	13,180	3,250	0.25	Dhanke et al. (2019)
Effluents from seafood processing plant	27.2 to 1201	458 to 1717	179 to 276	-	Jamieson et al. 2017
Fishmeal wastewater	35 to 37	131 to 140	21 to 23	-	Putra et al. (2020)

Table 3: comparing regional and international standards (PNUE/PAM 2004).

Parameter	This study	Regional standard			International standards				
		Morocco	Algeria	Tunisia	France	Turkey	Italy	Egypt	Malta
COD mg.L^{-1}	655 to 4000	500	120	90	125	180	160	100	600
BOD mg.L^{-1}	467 to 990	100	40	30	25	50	40	60	350
TSS mg.L^{-1}	173 to 2200	50	30	30	35	60	80	60	500

be around 7 for leachate. Other high values were detected in wastewater of a fish canning plant (Ben et al. 2017); However, effluents from Fish and fishmeal processing had a ratio of less than 1 (Colic et al. 2007, Dhanke et al. 2019).

In general, all analyzed parameters have values more important than other types of non-treated effluent. This can be related to many factors, such as the type of production and the factory recycling system. In the case of fishmeal, it is normal that COD and BOD_5 levels to be very important, but this level should be reduced by treatment before it is realized in the environment. Putre et al. (2020) reported that fishmeal wastewater treatment reduces more than 94% of COD and BOD amounts.

Assessment of the Impact

The impact associated with the disposal of fish wastes into the ocean environment (seawaters) includes reduced oxygen levels in the seawaters at the ocean bottom, burial or smothering of living organisms, and introduction of disease or non-native and invasive species to the ecosystem of the sea floor. The high level of COD and BOD leads to an imbalance of phosphorus and nitrogen, which produces a proliferation of algae. Some cases were recorded in Levrier Bay at the beginning of the operation of the fishmeal factories.

We will compare the results found by regional and international standards to show the environmental situation of the discharge points of the effluents of the fishmeal factories.

Comparing Obtained Results with Regional or International Standards for Wastewater Quality

All critical parameters (COD, BOD, and SS) of effluent from fishmeal exude regional and international standards for wastewater (Table 3). These effluents will pose a serious problem for Levrier Bay if we do not act and pay for rigorous treatment of these discharges.

CONCLUSIONS

This work is the first in this area interested in the environmental impact of discharge from fishmeal factories in Levrier Bay. It concluded that the discharge had affected some seawater parameters like suspended matter content (SS) which reached a level of 2200 mg.L^{-1}; moreover, the turbidity shows excessively high values (50 to 961 mg.L^{-1}). The water conductivity and salinity are particularly low. Chemical oxygen demand (COD) and biological oxygen demand (BOD) values are very high that they are permissible, and the biodegradability index (COD / BOD) varies from 0.96 to 4.79. These effluents are not easily biodegradable (index> 3). In general, all analyzed parameters have values

that exceed the international standards for wastewater, especially COD, BOD, and SS.

These results show that it is urgent to take some actions like treatment of the effluent before it is rejected into Ocean. The factories must apply serious environmental politics to protect us and our fish resources.

The outcomes of this study can be used as a reference for upcoming research and decision on fishmeal factoring, especially regarding the environmental control of this activity.

ACKNOWLEDGEMENTS

REFERENCES

Anh, P.T., Kroeze, C., Bush, S.R. and Mol, A.P.J. 2010. Water pollution by Pangasius production in the Mekong Delta, Vietnam: causes and options for control. Aquac. Res., 42: 108-128. https://doi.org/10.1111/j.1365-2109.2010.02578.x.

Bay, L., Ammar, Y., Zouhir, F. and Aitichou, I. 2017. Evaluation of the quality of canneries fish industries wastewater for a good water resource. Am. J. Innov. Res. Appl. Sci., 4(3): 74-84. www.american-jiras.com.

Ben, Y.M., Naji, S. and Belghyti, D. 2007. Caractérisation des rejets liquides d'une conserverie de poissons. Bull. Soc. Pharm. Bordeaux, 146: 225-234. https://www.academia .edu/

Bezama, A.,Valeria, H., Correa, M. and Szarka, N. 2012. Evaluation of the environmental impacts of a cleaner production agreement by frozen fish facilities in the Biobío Region. Chile. J. Clean. Prod., 26, 95-100. https://doi.org/10.1016/j.jclepro.2011.12.029.

Bhuyar, P., Farez, F., Rahim, M.H., Maniam, G.P. and Govindan, M. 2021b. Removal of nitrogen and phosphorus from agro-industrial wastewater by using microalgae collected from the coastal region of peninsular Malaysia. Afr. J. Biol. Sci., 3(1): 58-66. https://doi.org/10.33472/AFJBS.3.1.2021.58-66

Bhuyar, P., Trejo, M., Dussadee, N., Unpaprom, Y., Ramaraj, P. and Whangchai, K. 2021a. Microalgae cultivation in wastewater effluent from tilapia culture pond for enhanced bioethanol production. Water Sci. Technol., 84: 10-11. doi: https://doi.org/10.2166/wst.2021.194

Cheikh, M.A.S., Hamed, M.S.H., Amadou, D., Tounkara, H., Legraa, M.H., Ramdani, M. and Sidoumou, Z. 2020. Assessment of the impact of industrial development at the coast of Lévrier Bay through the spatio-temporal study of metallic contaminants (cd, pb, cu, zn, and hg) in surface sediments. Geographia Technica., 15(2): 127 - 137. DOI: 10.21163/GT_2020.152.13

Chikh, H.A., Kateb, Z., Bessaklia, H. and Habi, M. 2018) Performance

and suitability study of wastewater reuse for irrigation using intensive follow-up of Tlemcen rejects. Sci. Tech. Rev., 16: 56-67.

Colic, M., Morse, W., Hicks, J., Lechter, A. and Miller, J.D. 2007. Case study: Fish processing plant wastewater treatment. Proc. Water Environ. Fed., 11: 1-27. https://doi.org/10.2175/193864707787781557

Dhanke, P., Wagh, S. and Patil, A. 2019. Treatment of fish processing industry wastewater using a hydrodynamic cavitational reactor with biodegradability improvement. Water Sci. Technol., 80: 2310-2319. https://doi.org/10.2166/wst.2020.049.

Ferraciolli, L.M.D.V., Luiz, D.B., Rodrigues, V., dos Santos, V. and Naval, L.P. 2018. Reduction in water consumption and liquid effluent generation at a fish processing plant. J. Clean. Prod., 197: 948-956. https://doi.org/10.1016/j.jclepro.2018.06.088.

Gebauer, R. 2004. Mesophilic anaerobic treatment of sludge from saline fish farm effluents with biogas production, Bioresour. Technol., 93(2): 155-167. https://doi.org/10.1016/j.biortec h.2003.10.024.

Holmer, M., Duarte, C.M., Heilskov, A., Olesen, B. and Terrados, J. 2003. Biogeochemical conditions in sediments enriched by organic matter from net-pen fish farms in the Bolinao area, Philippines. Mar. Pollut. Bull., 46: 1470-1479. https://doi.org/10.1016/S0025-326.

Jamieson, B.L., Gagnon, G.A. and Gonçalves, A.A. 2017. Physicochemical characterization of Atlantic Canadian seafood processing plant effluent, Mar. Pollut. Bull., 116: 137-142. https://doi.org/10.1016/j.marpolbul.2016.12.071

Johan, V. and Mizier, M.O. 2004. Traitement des eaux industrielles. Effluents d'abattoirs : une pollution biodégradable. Eau, Industrie, Nuisances. 269: 33-43.

Legraa, M.H., Erraoui, H. and Dartige, A.Y. 2019. Assessment of metallic contamination of the northern Atlantic coast of Mauritania (Coastal fringe "Lévrier Bay"), using Pernaperna. International J. Civ. Eng. Technol., 10: 782-795.

Mathurin, Z.G. and Kisito, T.P. 2021. Risk Assessment of Chemical Pollution of Industrial Effluents from A Soap Production Plant Located in Bafoussam (Western Region of Cameroon). DOI : https://doi.org/10.21203/rs.3.rs-877488/v1

Merbouh, C., Belhsaien, K., Zouahri, A. and Lounes, N. 2020. Evaluation of the physico-chemical quality of groundwater in the vicinity of the Mohammedia-Benslimane controlled landfill. Europ. Sci. J., 6(6): 455. http://dx.doi.org/10.19044/esj.2020.v16n6p455

Moncada, C., Hassenruck, C., Gardes, A. and Conaco, C. 2019. Microbial community composition of sediments influenced by intensive mariculture activity. FEMS Microbiol. Ecol., 95(2): 1-12. https://doi.org/10.1093/femsec/fiz006.

PNUE/PAM. 2004. Guidelines on coastal litter management for the Mediterranean region. No.: 153 of the MAP Technical Report Series. UNEP, Athens

Putra, A.A., Watari, T., Shinya Maki, S., Hatamoto, M. and Yamaguchi, T. 2020. Anaerobic baffled reactor to treat fishmeal wastewater with high organic content. Environ. Technol. Innov., 17: 100586. DOI: https://doi.org/10.1016/j.eti.2019.100586

Quimpo, T. J.R., Ligson, C.A., Manogan, D.P., Requilme, J.N.C., Albelda, R.L., Conaco, C. and Cabaitan, P.C., 2020. Fish farm effluents alter reef benthic assemblages and reduce coral settlement. Marine Pollut. Bull., 153: 111025. https://doi.org/10.1016/j

Remili, S. and Kerfouf, A. 2013. Evaluation of the physico-chemical quality and the level of metal contamination (Cd, Pb, Zn) of wastewater discharges from Oran and Mostaganem (Western Algerian coast). Physic. Geogr. Environ., 7: 165-182. https://doi.org/10.4000/physio-geo.3258.

Rodier, R. 2010. Going up the streams on Aubrac and Margeride. Get Away, France.

Vallejos, M.B., Marcos, M.S., Barrionuevo, C. and Olivera, N.L. 2020. Fish-processing effluent discharges influenced physicochemical properties and prokaryotic community structure in arid soils from Patagonia. Sci. Tot. Environ., 714: 136882. https://doi.org/10.1016/j.scitotenv.2020.136882

Venugopal, V. and Sasidharan, A. 2020. Seafood industry effluents: environmental hazards, treatment, and resource recovery. J. Environ. Chem. Eng., 10: 758.

Whangchai, K., Souvannasouk, V., Bhuyar, P., Ramaraj R. and Unpaprom, Y. 2021. Biomass generation and biodiesel production from macroalgae grown in the irrigation canal wastewater. Water Sci. Technol., 84: 10-11. doi: http://doi.org/10.2166/wst.2021.195

World Health Organization (WHO) 2004. Report: Water Quality Determination of Suspended Solids by Filtration through Glass Fiber. Who.int/whr/004/en/Waterquality-Determination-of-suspended-solids-Method by filtration through glass fibre. (Accessed 8 June 2005).

Original Research Paper   **Open Access Journal**

Katowice Climate Package: Analysis, Assessment and Outlook

Aditi Nidhi

Gujarat National Law University, Gandhinagar, Gujarat, India

†Corresponding author: Aditi Nidhi; aditinidhirmlnlu@gmail.com

ABSTRACT

Climate change is a widely debated topic in the 21st century, with various perspectives and opinions on its causes and potential remedies. Climate change risks have perplexed authorities and made protecting human life and health difficult. The elements that cause climate change, such as the combustion of fossil fuels, air pollutants, short-lived climatic pollutants, etc., have affected both the climate and human health. The Paris Agreement established several commitment periods that each nation was obligated to follow in accordance with their own individual capacities. This will assist in achieving greater human health and environmental benefits. To develop a robust climate change framework, WHO and other UN organizations have moved up to resolve these challenges. From the first international conference in 1988 to the current Conference of Parties, it has been concluded that "humanity is conducting an unintended, uncontrolled, globally pervasive experiment, the ultimate consequences of which could be second only to a global nuclear war." The recent Katowice Agreement and the climate change package that was put in place demonstrate the seriousness required to resolve the issues of finance, loss and damage, and differentiation mechanisms, which were thoroughly discussed. The paper will focus on the existing legal solutions for providing climate justice to nations. The study will also look at the effectiveness of COP24 in executing adaptation and mitigation plans and adhering to the Paris Agreement in both text and spirit.

INTRODUCTION

Climate change is one of the biggest dangers to human health and puts our entire species at risk. It is also one of the greatest threats to the environment. The severity of climate change's effects on human health is becoming progressively obvious, and each alternative day that passes without action will make the risks even greater (McKeever 2021). Despite fifty years of concerted, targeted effort by policymakers and the health community, climate change threatens to undo those gains. This situation contradicts the government's promises to advance the realization of the human right to health for all individuals (OCHR 2008).

In recent years, the public health community has rapidly increased its involvement with climate change and health, advancing knowledge of the connections between the two, bringing attention to the serious health risks, proposing solutions to mitigate the worst effects, and evaluating the health benefits of climate action, including the extent to which these will outweigh the costs of mitigation (Klenert et al. 2020). To fulfill the commitments made by governments during the UNFCCC climate change negotiations and international negotiations at the World Health Assembly, a large community of organizations, including United Nations agencies, academia, all levels of government, and nongovernmental organizations, are now working together (OHCHR 2019). The conclusions of high-level political gatherings and joint statements by health professional associations and broader civil society reflect how their work generally aligns with a common action agenda. Numerous agendas were discussed in the report, such as the climate change risks, Paris Agreement's central role in promoting good health, and opportunities for improving health provided by addressing climate change (MoHFW 2018). It further discusses how the health sector and civil society are involved, how to measure national climate change progress, and how to ensure financial support for health and climate change action. In addition to these subjects, the report discusses engagement by the health community and civil society, the evaluation of national climate change action progress, and the means of ensuring economic support for health and climate change action (Kruk 2018).

KATOWICE AGREEMENT

Goal and Vision

The agreement took place in December in Katowice, Poland (Glasgow Climate Change Conference 1995). The conference

aims to facilitate the goals of the Paris Agreement in its entirety. The conference organized by the Intergovernmental Panel on Climate Change (IPCC) in Katowice, Poland, marked a small but meaningful progression in the global effort to combat climate change. Though it did not bring about a significant breakthrough, the conference made strides in addressing this important issue. Despite not being a breakthrough, the conference made some progress in the climate change battle. For the treaty to be implemented successfully, the participants were requested to create a set of guidelines that could be used to further the efforts made under the treaty. It is regarded as the greatest achievement in which all governments can take pride. It bolsters the Paris Agreement and paves the way for climate action to be taken on a global scale.

The "Paris Agreement Work Programme" was the focus of the two-week meeting, which was convened to implement a series of decisions to achieve this objective (COP24 2020). Parties voted to accept the Katowice Climate Package as the conference ended (COP24 2019a). This package addresses virtually all of the concerns raised in the PAWP. Even though parties emphasized the need for a comprehensive and balanced rulebook at the outset of the conference, there was still skepticism regarding delivery, given that a wide range of issues needed to be discussed and decided upon briefly (Low 2019).

The most significant achievement at COP24 was the countries' ability to reach a consensus on the regulations that would oversee the execution of the Paris Agreement starting in 2015. The Katowice Climate Change Package, to give the rule book its official title, outlines the procedures that nations should follow to monitor and report their greenhouse gas emissions (Murray 2022), as well as the actions they are taking to reduce those emissions. To put the rule into action in a more orderly fashion, there are a lot of questions that need to be considered. A skeptical person will argue that there is no enforcement mechanism in relation to such goals, what

happens if the countries breach their emissions target, and so on (Maizland 2022).

A cynic would argue that there is no enforcement mechanism. In contrast, in recent years, tremendous work has been achieved to increase energy efficiency and shift away from fossil fuels. Without any worldwide enforcement mechanisms, the energy required to create an additional percentage of the world's gross domestic product (GDP) has fallen by an average of 32% since 1990. It has dropped even more in emerging economies than in advanced economies. This serves as a reminder that change is possible and that the real challenge is not related to developing the appropriate technology or mechanisms but ensuring that all countries are treated fairly.

Analysis

COP 24 in Katowice, Poland, marked a small but meaningful advancement in the worldwide campaign to combat climate change. Though it was not a breakthrough, the conference did make some progress in addressing this important issue. The meeting failed to agree on key issues, including raising national contributions, integrating human rights into the Paris Agreement, and providing equal support for developing nations while adopting a climate package of Paris Rulebook documents. While steps were taken to improve areas like the rights of indigenous people, gender equality, finance, etc., the provisions for carbon trading were left out of the package. Thus, COP 24 failed to adequately address the most crucial matters that are necessary for effectively tackling the difficulties caused by global warming and its effects on communities that are at risk.

The "Intergovernmental Panel on Climate Change (IPCC)" is a respected UN group that aims to access the scientific aspects of climate change regularly (IPCC 2022). On the 8th of October, IPCC issued a report specifically examining the
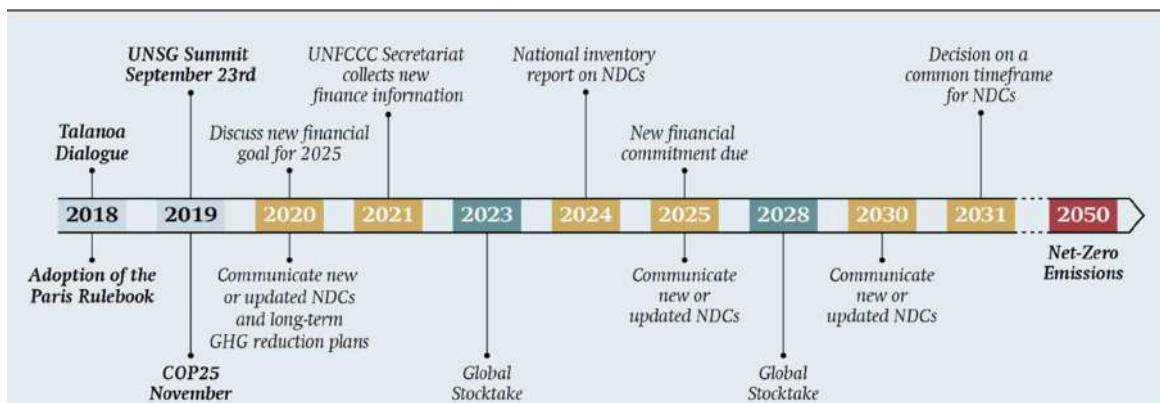

Fig. 1: Source-Stiftung Wissenschaft und Politik (SWP) (Dröge & Rattani 2019).

effects of global warming at 1.5 degrees Celsius. This report is a stark reminder of the imperative need for immediate action to preserve our planet (IPCC 2018). The report's key findings are straightforward: to limit the increase in temperature to 1.5 degrees Celsius by 2030 and reach a state of "net zero" by 2050 (Fig. 1). This is the sole means of achieving this objective. To achieve such a huge reduction in emissions, significant modifications will need to be made to the global energy and transportation networks, in addition to preserving and restoring natural ecosystems. The figure presented also depicts the significance of the "Global Stocktake" within the decentralized framework of the Paris Agreement. It functions as the principal hierarchical element of the accord. The Global Stocktake serves the objective of conducting a thorough worldwide evaluation of the climate policy commitments, referred to as Nationally Determined Contributions (NDCs), made by participating parties at five-year intervals.

What Occurred During Cop 24?

During the first week of the summit meeting, there was no indication of any progress being made on any aspect of the 2015 agreement (Kizzier 2019). Industrialized and emerging nations maintained long-held attitudes and interpreted the Paris Agreement differently (Paris Agreement 2015). These positions have been a source of contention for several years and have centered around scope, differentiation, and financing issues (Tanwar 2013). A discussion about the document's intended audience focused on whether the guidance for Nationally Determined Contributions (NDCs) (Pauw 2019) should only address mitigation or cover all potential NDC components, such as means of implementation and adaptation (Crumpler et al. 2020).

After that, the accord focused on discussing the guiding mechanism that will be followed by both developed and developing countries and how it may differ for each (UN 2015). Also, developing countries asked developed countries for promises to be open and honest about providing complete and accurate information on public finances (Our Common Future, From One Earth to One World 1985) both before and after the information was given. This was done to make things more predictable and accountable. This request was made within the context of the topic of finance (Stéphane & Kevin 2003).

Micha Kurtyka, the president of COP 24, and António Guterres (World Meteorological Organization 2018), the secretary-general of the UN, led closed-door meetings with groups of ministers from developed and emerging nations to agree on each Rulebook issue (Sethi 2018). People were afraid that the negotiations would fail, just like they did at COP 15 in Copenhagen in 2009 because they didn't have enough information and there were rumors of chaos.

As the Conference continued, the problematic situation became more imminent. The issue centered on "Article 6 of the Paris Agreement" (Kizzier 2019), which outlined how nations can voluntarily cooperate in implementing their "nationally determined contributions" to carbon markets. In a global carbon trading system (Burniaux 2009), a nation, a company that produces fossil fuels, or an airline can "offset" excessive emissions by transferring them to a nation with lower emissions. Article 6 refers to "international transfers of mitigation results" rather than "markets," and a "Sustainable Development Mechanism" (United Nations 2007) will substitute the Kyoto Protocol's (UNCTD 2003) "Clean Development Mechanism," which has been heavily condemned for neglecting to offer extra reduction (Benites-Lazaro & Andrade 2019). There is also a plan for making non-market-based strategies for the future (Soutar 2021).

Brazil did not want to make any concessions on this issue, which is referred to as "double counting" (Schneider 2019), so it resisted rules that would apply "corresponding adjustments" (Climate Focus 2022) to transfer credits. Brazil, in particular, had been pushing for looser accounting rules for carbon credits for most of the year. This may allow governments to count other countries' carbon reductions toward their objectives, even if they had previously claimed them. Brazil refused compromises and resisted rules that would apply "corresponding adjustments." Both parties and observers generally regard double counting as cheating.

As a result of the discussions during the first and second weeks, it became abundantly clear that a consensus would not be reached regarding Article 6, and Brazil would not make any concessions (COP25 2019). Nonetheless, a one-page document was documented in which a request was made to the subsidiary body to continue debating the topic at the upcoming June meeting. At the end of the meeting, the President (Marcu & Duggal 2019) presented each participant with a compilation of the Paris Rulebook documents (Huang 2019). However, these documents did not include any rules for carbon trading (COP24b 2018) because the major impasse and potential breakdown in the negotiations had been resolved. One of the noteworthy outcomes of COP 24 was the adoption of the Rulebook known as the Katowice Climate Package.

KATOWICE CLIMATE CHANGE PACKAGE: HOPE FOR ALL (LOW ET AL. 2019)

Guidance on Nationally Determined Contributions (NDC)

NDC, often known as climate commitments, are mandated by "Article 4 of the Paris Agreement" (Paris Agreement

2019), specifying standards for their substance to make it easier to compare and aggregate pledges at the global level.

The decision mandates that all nations follow the IPCC's most recent emissions accounting guidance, which was last updated in 2006 and is scheduled to be amended again next year (IPCC 2008). According to Dr. Robbie Andrew, a senior researcher at the Norwegian research institute (CICERO), the primary change between the 2006 advice and prior versions is that methane's "global warming potential" has increased (Peters 2012). According to his colleague Dr. Glen Peters (Peters 2012), it would be "brilliant" for researchers if all nations adopted the same accounting standards. A climate change lecturer at the Grantham Institute of Imperial College London (Rogelj 2016) named Dr. Joeri Rogelj asserts that certain aspects of NDCs create questions regarding the environmental integrity of the commitments made by countries (climate pledges). He emphasizes the flexibility in the choice of accounting standards by stating, "The Paris Agreement calls for regular comparisons, summations, and evaluations of emissions and projected emissions reductions to determine their adequacy in limiting the temperature increase to well below 2C and 1.5C (Paris Agreement 2022). This calls for standardized regulations on the reporting of emissions. However, the final text agreed upon in Katowice now permits countries to adhere to "nationally appropriate methodologies" rather than requiring them to adhere to scientifically sound methods (Sharma 2020). Likely, this guidance will primarily be utilized for strategic reporting, potentially leading to the presentation of certain countries' emissions in a more favorable manner than they truly are. The land-use sector regularly faces this difficulty (Hill & Hill 2018).

In addition, the countries agreed that their commitments would be documented in a public registry modeled after the present interim website. Despite efforts to get it removed, this will still have a search bar. Pledges were also agreed upon to cover a "shared timeframe" beginning in 2031 (Mathiesen 2018), with the precise duration to be determined later. Some of the present pledges cover five years, while others cover ten years.

Global Stocktake

The Global Stocktake is a procedure established by the Paris Agreement (UNFCCC 2021) to examine the collective progress that Parties have made to accomplish the aim of the agreement and its long-term goals. It is also known as the "Five-Year Review." The next Stocktake, in 2023, will be held during COP 24, occurring every five years after that. The Global Stocktake will allow Parties to assess their advance toward the Paris Agreement's long-term goal and inform their additional nationally decided commitments (Climate Analytics 2018).

The Global Stocktake, a process that will evaluate the Parties' collective progress in achieving the goals of the Paris Agreement, will consider both the short-term and long-term objectives outlined in the agreement. In addition, it will adhere to the principles of transparency, equity, and fairness while considering the most up-to-date and accurate scientific information currently available. This will include the most recent findings of the IPCC (Rajamani et al. 2022).

The Global Stocktake is an evaluation process where the Parties will evaluate their success in reaching the ultimate objective of the Paris Agreement, which is to keep the global average temperature well below 2 degrees Celsius above pre-industrial levels and strive to decrease it to 1.5 degrees Celsius. The Parties will also deliberate on the multiple methods to minimize emissions and adapt to the impacts of climate change (Centre for Science and Environment 2021).

Transparency Framework

The Katowice negotiations sought to standardize reporting timelines and formats for national climate policies (Dal Maso & Antonio Canu 2022). The most susceptible nations will not be required to make quantifiable climate pledges or provide ongoing transparency reports due to the new rules, which provide for some degree of latitude for these nations (COP24 2019b). The conference focused on submitting a climate action report every two years (COP24 2018a) starting in 2024 by every nation.

Climate Finance

Establishing a new climate finance goal was becoming an increasingly sensitive issue for developing countries (ECOSOC Development Cooperation 2016). This should be established by the year 2025 in accordance with the Paris Agreement, and it should be higher than the "floor" sum of one hundred billion dollars per year pledged to developing nations by 2020. (Pauw 2022) The parties agreed to discuss this new target at the COP26 session in November 2021. At COP26, scheduled for November 2021, the parties said they would discuss this new objective.

In the meantime, the contributions from rich countries have not yet reached the target of $100 billion for 2020 (Sirur 2021). However, a number of announcements made during the COP showed that there would be at least some increase in funding.

Germany has announced it will contribute €70 million to the Adaptation Fund. Other countries and organizations, such as Italy, Sweden, the EU, and France, have also made smaller contributions, bringing the total to $129 million. This is the fund's highest-ever annual fundraising total.

Germany was the first nation to declare a specific amount it would donate to the Green Climate Fund's renewal cycle (GCF). The country pledged €1.5 billion, double the amount it had previously contributed in 2014. The Global Climate Fund (GCF) was given a contribution of 516 million dollars by Norway, and Japan stated that it would consider making a larger donation once the renewal process began in 2019. In February, Japan proposed the name of Ambassador Kenichi Suganuma for consideration to head the Global Climate Fund (Skene 2022).

Due to the United States' failure to fulfill a portion of its $3 billion commitment and fluctuations in the exchange rate between the currencies of donor countries and US dollars, the Global Climate Fund (GCF) has only received $7 billion of the $10 billion that was pledged to it in 2014 (Waslander 2019).

Human Rights

Human rights protection can be considered one of the most significant achievements of the Paris Agreement. This is the one victory highlighted in the agreement's Preamble, barring no other articles discussing such a feature. Many civil society organizations and a few national champions argued at COP 24 that including the UDHR and the Preamble's reference to human rights would aid in the agreement's operationalization.

On the 70th anniversary of the UDHR, which coincided with UNFCCC (COP 24), civil society groups and a few countries pushed to integrate human rights references in the Paris Agreement's Rulebook's Preamble. These references, referred to as the "Great Eight," include ecosystem integrity, intergenerational justice, decent work, just transition for workers, food security, women's empowerment, gender equality, public participation, rights of Indigenous Peoples, and poverty alleviation. However, despite these efforts, the coalition ultimately failed to operationalize these references into the Paris Rulebook.

WHAT ELSE HAPPENED AT COP24?

Finance Pledges in Katowice

At COP 24, held in Katowice, Poland, in 2018, countries made no formal pledges for financial support specifically for harm and loss. However, industrialized nations did make some commitments to provide financial support for climate action more generally (Kachi & Day 2020). For example, The UNFCCC's Green Climate Fund (GCF) recently declared that it had secured extra funds from developed countries (Levaï 2021) to aid developing nations in adjusting to and reducing the influence of climate change.

To further aid developing nations in their fight against climate change (Garschagen & Doshi 2022), rich nations renewed their pledge to raise $100 billion annually by 2020. However, it should be noted that this commitment was first made in 2009, and it is still not being met. Developing countries, particularly small island states, argued that this funding was insufficient to address the issue of loss and damage and that more ambitious financial commitments were needed (COP24 2019a, 2019b) It's also important to mention that the Paris Agreement includes a "loss and damage" article. Still, it's not legally binding, doesn't provide a mechanism to compensate countries for loss and damage, and doesn't establish any clear financing mechanism to support countries facing loss and damage (Kuh & Rivkin 2021).

Talanoa Dialogue

To successfully implement the goal of the Talanoa Dialogue and the Paris Agreement, the outcome of COP24 must include a clear statement emphasizing the need for increased ambition (Stockholm Environment Institute 2019). Holding a conversation in a welcoming and accepting environment is referred to as "talanoa" in the Fijian language. It is a tried-and-true approach to conflict resolution in the Pacific region.

The goal of the Talanoa Dialogue (Lesniewska & Siegele 2018) is to find a way to break the impasse regarding climate change by bringing participants together by sharing their personal experiences with the phenomenon. It has been requested that governments, civil society, non-governmental organizations (NGOs), businesses, cities, and other entities share their experiences in response to the following three questions: Where do we stand right now? How do we want to go? What is the best way to get there? Hundreds of countries, organizations, and people have contributed to this cause.

To aid with and improve the enactment of the Paris Agreement, the UNFCCC established the Talanoa Dialogue as part of the UNFCCC. The process takes its name from the traditional Fijian idea of Talanoa, which refers to a method of discourse that is open to involvement from all members and is conducted transparently (Waskow 2018a, 2018b). The Talanoa Dialogue aims to foster cooperation and mutual understanding among Parties to the UNFCCC and enhance ambition in mitigation, adaptation, and support. It is designed to be inclusive and participatory, providing opportunities for all Parties to the UNFCCC to share their experiences, challenges, and best practices and to explore opportunities for cooperation. The Dialogue also serves as a forum for participation by non-Party stakeholders, such as municipalities, NGOs, and businesses. An ongoing effort, the Talanoa Dialogue seeks to aid UNFCCC Parties in raising their ambition in support, adaptation, mitigation, and carrying out the Paris Agreement (Recio & Hestad 2022).

Damage and Loss

The discussions on damage and loss during the COP 24 were focused on the "Warsaw International Mechanism for Loss and Damage Associated with Climate Change Impacts" (WIM), which was formed in 2013. Developing countries, particularly least developing nations, have urged strengthening the World Insurance Mechanism (WIM) and developed countries to give financial help for loss and damage. Since small islands are more susceptible to climate change's negative effects, including rising sea levels, eroding coastlines, and bleaching coral reefs, they have made it clear that resolving the issue of loss and damage is crucial to their very survival. COP 24 served as a platform for the Parties to the Paris Agreement and the subordinate organization for implementation to convene and hold high-level sessions and discussions on loss and damage. Despite the efforts made by developing countries and small island nations, the COP 24 did not result in any official promises to provide financial assistance for damage and loss

It is essential to note that loss and damage are complex issues encompassing various impacts and challenges, with different views on addressing them. Developed nations have argued that adaptation methods, not compensation or financial aid, are the best way to deal with loss and damage. Some poor nations have argued that loss and damage should be handled in a way distinct from adaptation under the UNFCCC framework. COP 24 failed to reach a consensus on how to address loss and damage, and the issue remains a contentious point of discussion in international climate negotiations.

Gender and Climate Change

An additional focal point of the conference was the intersection between gender and climate change. This emphasis recognized that climate change disproportionately affects women and other marginalized groups and that their participation and leadership are essential for effective climate action. The COP24 decisions included a call for climate policies and actions that take gender into account. In addition, they emphasized the need for a gender perspective to be incorporated into all facets of the enactment of the Paris Agreement. The resolutions also advocated advancing gender equality in the climate and energy sectors and including women in climate change decision-making processes (IMF 2021).

In general, including a gender and climate change focus at COP24 underscores the importance of understanding the unique implications of climate change on women and other marginalized groups and the necessity of their participation and leadership in solving this global crisis (UN 2021).

The Katowice Ministerial Declaration on Forests for the Climate

During the United Nations Climate Change Conference in 2018, this Declaration was adopted in Katowice to highlight forests' importance in climate change. The Declaration includes several commitments and actions that countries can take to protect and manage forests sustainably. The Declaration highlights the importance of "Reducing Emissions from Deforestation and Forest Degradation" (REDD+) as a key tool for mitigating climate change and encourages countries to enhance the implementation of REDD+ activities (PIB 2018). Additionally, the declaration acknowledges the significance of promoting sustainable forest management, afforestation, and reforestation as effective ways to increase carbon sequestration. It also advocates for advancing forest governance and protecting the rights of communities and indigenous peoples that depend on forests.

The Declaration also encourages countries to consider the application of market-based mechanisms and other incentives to support the protection and sustainable management of forests. The Declaration is a non-binding agreement, but it serves as a political statement and a call to action for countries to protect and manage forests sustainably and recognize the importance of forests in addressing climate change.

Furthermore, the Declaration highlights the need for data and information on forests and calls for strengthening forest monitoring, assessment, and reporting. This is important to track progress and to identify areas where additional action is needed. It also encourages Parties to include forest protection in their respective Nationally Determined Contributions (NDCs).

Henceforth, this Declaration calls for various actions and commitments, including using market-based mechanisms, strengthening forest governance, enhancement of afforestation and reforestation, reduction of emissions from forest degradation, deforestation, and other incentives to aid in the protection and sustainable management of forests.

COP 24 AND INDIA PRIORITIES

The conference aimed to negotiate the Paris Agreement's implementation plan, which was adopted at COP 21 in 2015 and went into effect in 2016. (IPCC 2018b) India, as a party to the UNFCCC, participated in COP 24. India's priorities at the conference included (Sinha 2018):

a) Making arrangements in such a way that the industrialized nations provide technological and financial support to the emerging nations and help them adjust to the changing pattern of climate change.

b) Maintaining the idea of "common but differentiated responsibilities" which recognizes that industrialized countries have a higher historical responsibility for climate change and should shoulder a bigger burden in addressing it. (Sengupta 2019)

c) Protecting the rights and livelihoods of local communities and vulnerable populations

d) Encouraging the adoption of energy-efficient practices and the use of renewable energy sources.

e) India proposes that the concentration of greenhouse gases in the atmosphere be stabilized below two degrees Celsius.

f) Lowering the susceptibility of agricultural systems, water infrastructure, and coastal communities to the effects that are being caused by climate change.

g) Promoting land management methods less destructive to the environment, such as agroforestry and agroecological farming.

h) Promoting the participation of local communities, women, and other marginalized groups in decision-making and policy-making related to climate change.

i) Encouraging cooperation among countries to share knowledge, technology, and best practices for addressing climate change.

j) In addition, India emphasized the importance of developed nations living up to the financial promises they made about climate change in the Paris Agreement.

India's aims at COP 24 were consistent with its broader approach to climate change, emphasizing the need for developed countries to assume greater responsibility for solving the problem while assisting developing countries' attempts to adapt to and mitigate its consequences. (Nandi 2018).

Additional Secretary AK Mehta spoke on behalf of Environment Minister Harsh Vardhan to explain India's stance and efforts in the battle against climate change. (PTI 2018) It's a chance for nations to discuss what they're doing to combat climate change, from lowering their carbon footprint to preparing for its effects. (Gopalakrishnan 2014) The conference is also an opportunity for countries to engage in negotiations and obtain common answers to the challenges triggered by climate change.

CONCLUSION

The Katowice Agreement includes several important provisions that will help countries implement the Paris Agreement, such as guidelines for disclosing and monitoring greenhouse gas emissions and improvements in adapting to the effects of climate change. These guidelines are intended to increase transparency and accountability and to ensure that countries are on track to meet their emissions reduction goals. To help vulnerable nations deal with climate change impacts that cannot be prevented through mitigation and adaptation measures, the accord also includes a resolution on executing the "loss and damage" mechanism established in 2015.

Thus, the importance of this conference can be seen from varied angles, i.e., to establish a "facilitative dialogue" process, which will be held in 2023 to assess progress in implementing the Paris Agreement and inform countries' emissions reduction efforts in the future. The agreement also includes a decision to establish the "Article 6" negotiations, which will establish a framework for cooperation on emissions reductions between countries. The negotiations will address carbon markets, carbon credits, and carbon offsetting.

Overall, the Katowice Agreement is an important step forward in implementing the Paris Agreement and addressing climate change. However, some criticized it for not going far enough in some areas, such as loss and damage, and for not funding climate change adaptation in developing nations.

REFERENCES

Benites-Lazaro, L.L. and Andrade, C. 2019. Clean development mechanism: key lessons and challenges in mitigating climate change and achieving sustainable development. Reference Module in Earth Systems and Environmental Sciences. https://doi.org/10.1016/b978-0-12-409548-9.11863-9

Burniaux, J. 2009. The economics of climate change mitigation. OECD Economics Department Working Papers. https://doi.org/10.1787/224074334782

Centre for Science and Environment 2021. Addressing global stocktake under the Paris Agreement (an equity-based approach). https://unfccc.int/sites/default/files/890.pdf

Climate Analytics 2018. Taking stock of the global stocktake. https://climateanalytics.org/blog/2018/taking-stock-of-the-global-stocktake/

Climate Focus. 2022. Article 6 Corresponding Adjustments. Climate Focus. https://climatefocus.com/publications/article-6-corresponding-adjustments/

COP 24 2020. Baker McKenzie InsightPlus. https://insightplus.bakermckenzie.com/bm/environment-climate-change_1/international-cop-24

COP24 2018a. Special report: health and climate change. https://apps.who.int/iris/handle/10665/276405

COP24 2018b. Carbon market talks go downhill. https://www.downtoearth.org.in/news/climate-change/cop24-carbon-market-talks-go-downhill-62505

COP24 2019. UN climate change conference, what's at stake and what you need to know. UN News. https://news.un.org/en/story/2018/11/1026851

COP24 2019a. Great expectations, low execution: the Katowice climate change conference COP 24. https://eu.boell.org/en/2019/01/08/great-expectations-low-execution-katowice-climate-change-conference-cop-24

COP25 2019. The lack of consensus for international carbon market rules should not distract from domestic decarbonisation. https://newclimate.org/news/cop-25-the-lack-of-consensus-for-international-carbon-market-rules-should-not-distract-from

Crumpler, K., Dasgupta, S., Federici, S., Meybeck, A., Bloise, M., Slivinska, V., Damen, B., Von Loeben, S., Wolf, J. and Bernoux, M. 2020. Regional analysis of the nationally determined contributions in Asia: gaps and opportunities in the agriculture and land use sectors. Environment and Natural Resources Management. Working Paper (FAO) Eng No. 78.

Dal Maso, M. and Antonio Canu, F. 2022. Unfolding the reporting requirements for developing countries under the Paris Agreement's enhanced transparency framework, Vol. 1. https://climateactiontransparency.org/wp-content/uploads/2019/11/ICAT-MPGs-publication-final.pdf

Dröge, S. and Rattani, V. 2019. After the Katowice climate summit: building blocks for the EU climate agenda. Earth Negotiations Bulletin (ENB), 12(747): 7. https://doi.org/10.18449/2019c09

ECOSOC Development Cooperation. Making development cooperation on climate change sensitive to the needs of the most vulnerable countries. 2016. ECOSOC Development Cooperation Forum Policy Briefs, 14: 1-7. https://www.un.org/ecosoc/sites/www.un.org.ecosoc/files/publication/dcf-policy-brief-14.pdf

Garschagen, M. and Doshi, D. 2022. Does funds-based adaptation finance reach the most vulnerable countries? Glob. Environ. Change, 73: 102450. https://doi.org/10.1016/j.gloenvcha.2021.102450

Glasgow Climate Change Conference 1995. IISD Earth Negotiations Bulletin. https://enb.iisd.org/glasgow-climate-change-conference-cop26

Gopalakrishnan, T. 2014. COP24: A principled debate on adaptation communications. https://www.downtoearth.org.in/blog/climate-change/cop24-a-principled-debate-on-adaptation-communications-62410

Hill, C. and Hill, C. 2018. GeoPolicy: COP24 – key outcomes and what it's like to attend. https://blogs.egu.eu/geolog/2018/12/28/geopolicy-cop24-key-outcomes-and-what-its-like-to-attend/

Huang, J. 2019. A brief guide to the Paris agreement and 'rulebook. https://www.c2es.org/wp-content/uploads/2019/06/paris-agreement-and-rulebook-guide.pdf

IMF 2021. Advancing gender equality through climate action. https://www.imf.org/en/Publications/fandd/issues/2021/09/advancing-gender-equality-through-climate-action-COP26-trevelyan

IPCC 2008. Climate Change 2007 - Impacts, adaptation, and vulnerability: working group II contribution to the fourth assessment report of the IPCC (1st ed.). Cambridge University Press, UK.

IPCC 2018a. IPCC says limiting global warming to 1.5 °C will require drastic action. https://www.nature.com/articles/

IPCC 2018b. Summary for policymakers of IPCC special report on global warming of 1.5°C approved by governments. https://www.ipcc.ch/2018/10/08/summary-for-policymakers-of-ipcc-special-report-on-global-warming-of-1-5c-approved-by-governments/

IPCC 2022. Climate change: mitigation of climate change. https://www.ipcc.ch/report/ar6/wg3/

Kachi, A. and Day, T. 2020. Results-based finance in the Paris era considerations to maximise impact. NewClimate Institute, 1-20. https://newclimate.org/sites/default/files/2020/12/NewClimate_Results_-based_finance_in_the-Paris_era_Dec20.pdf

Kizzier, K. 2019. What you need to know about Article 6 of the Paris Agreement. https://www.wri.org/insights/what-you-need-know-about-article-6-paris-agreement

Klenert, D. 2020. Five lessons from COVID-19 for advancing climate change mitigation. Environmental and Resource Economics, 76(4): 751-778. https://doi.org/10.1007/s10640-020-00453-w

Kruk, M.E. 2018. High-quality health systems in the sustainable development goals era: time for a revolution. Lancet Glob. Health, 6(11): e1196–e1252. https://doi.org/10.1016/s2214-109x(18)30386-3

Kuh, K. and Rivkin, D. 2021. Legal aspects of climate change adaptation. https://www.ibanet.org/document?id=Climate-Change-Adaptation-Report-2021.

Lesniewska, F. and Siegele, L. 2018. The Talanoa dialogue: A crucible to spur ambitious global climate action to stay within the 1.5°C limit. Carbon Clim. Law Rev., 2(1): 41-49. https://www.jstor.org/stable/26478085

Levaï, D. 2021. Replenishment of the green climate fund: a missed opportunity. https://ideas4development.org/en/replenishment-of-the-green-climate-fund-a-missed-opportunity/

Low, M. 2019. Katowice climate package: operationalising the climate change regime in the Paris agreement. Energy Studies Institute (ESI) Policy Brief, 27: 1-4. https://esi.nus.edu.sg/docs/default-source/esi-policy-briefs/katowice-climate-package.pdf?sfvrsn=2

Low, M., Bea, E. and Lu, S. 2019. Katowice climate package: operationalizing the climate change regime in the Paris agreement. Energy Studies Institute Policy Brief, 27: 1-4. https://esi.nus.edu.sg/docs/default-source/esi-policy-briefs/katowice-climate-package.pdf?sfvrsn=2

Maizland, L. 2022. Global climate agreements: successes and failures. council on foreign relations. https://www.cfr.org/backgrounder/paris-global-climate-change-agreements

Marcu, A. and Duggal, V.K., 2019. Negotiations on Article 6 of the Paris Agreement–Road to Madrid. https://think-asia.org/handle/11540/11644

Mathiesen, K.M. 2018. Countries breathe life into the Paris climate agreement. https://www.climatechangenews.com/2018/12/15/countries-breathe-life-paris-climate-agreement/

McKeever, A. 2021. Why climate change is still the greatest threat to human health. Science. https://www.nationalgeographic.com/science/article/why-climate-change-is-still-the-greatest-threat-to-human-health

MoHFW 2018. National action plan for climate change & human health. https://ncdc.gov.in/WriteReadData/l892s/27505481411548674558.pdf

Murray, L.S. 2022. Practical implications of the Katowice climate package for developing country parties and land sector reporting. The Nature Conservancy. https://www.nature.org/content/dam/tnc/nature/en/documents/TNC_Transparency_LandUseReport.pdf

Nandi, J. 2018. High stakes for India as 'make or break' climate meet begins in Poland. https://www.hindustantimes.com/india-news/high-stakes-for-india-as-make-or-break-climate-meet-begins-in-poland/story-vctMcG88CZ6fNSwNoKMx7H.html

OCHR 2008. The right to health. https://www.ohchr.org/sites/default/files/Documents/Publications/Factsheet31.pdf

OHCHR 2019. Understanding human rights and climate change. https://www.ohchr.org/sites/default/files/Documents/Issues/ClimateChange/COP21.pdf

Paris Agreement 2015. Paris Agreement. https://unfccc.int/files/meetings/paris_nov_2015/application/pdf/paris_agreement_english_.pdf

Paris Agreement 2019. Key aspects of the Paris Agreement. https://unfccc.int/most-requested/key-aspects-of-the-paris-agreement

Paris Agreement 2022. Climate action. https://climate.ec.europa.eu/eu-action/international-action-climate-change/climate-negotiations/paris-agreement_en

Pauw, W.P. 2019. Conditional nationally determined contributions in the Paris Agreement: foothold for equity or Achilles heel? Clim. Policy, 20(4): 468-484. https://doi.org/10.1080/14693062.2019.1635874

Pauw, W.P. 2022. Post-2025 climate finance target: how much more and how much better? Clim. Policy, 22(9-10): 1241-1251. https://doi.org/10.1080/14693062.2022.2114985

Peters, G.P. 2012. The challenge to keep global warming below 2 °C. Nature Clim. Change, 3(1): 4–6. https://doi.org/10.1038/nclimate1783

PIB 2018. Cooperation of society in implementation of Redd+ strategy is crucial 2018. https://pib.gov.in/newsite/PrintRelease.aspx?relid=183155

PTI 2018. The outcome of UN climate summit should be balanced, inclusive: Harsh Vardhan. https://www.businesstoday.in/pti-feed/story/outcome-of-un-climate-summit-should-be-balanced-inclusive-harsh-vardhan-120405-2018-12-01

Rajamani, L., Oberthür, S. and Guilanpour, K. 2022. Designing a meaningful global stocktake. center for climate and energy solutions. https://unfccc.int/sites/default/files/resource/202202281808_C2ES_Designing_A_Meaningful_Global_Stocktake_Under_the_Paris_Agreement.pdf

Recio, E. and Hestad, D. 2022. Indigenous peoples: defending an environment for all. https://www.iisd.org/articles/deep-dive/indigenous-peoples-defending-environment-all

Rogelj, J. 2016. Paris Agreement climate proposals need a boost to keep warming well below 2°C. Nature, 534(7609): 631-639. https://doi.org/10.1038/nature18307

Schneider, L. 2019. Double counting and the Paris Agreement rulebook. Science, 366(6462): 180–183. https://doi.org/10.1126/science.aay8750

Sengupta, S. 2019. India's engagement in global climate negotiations from Rio to Paris. India in a warming world, 114-141. https://doi.org/10.1093/oso/9780199498734.003.0007

Sethi, N. 2018. Climate change report is a "wake-up" call on 1.5°C global warming. Climate Change: World Meteorological Organisation. https://www.business-standard.com/article/current-affairs/countries-state-their-true-positions-behind-closed-doors-115120701372_1.html

Sharma, A. 2020. Guide to the Paris Agreement. Oxford Climate Policy. https://ecbi.org/sites/default/files/Guide%20to%20Paris%20Agreement.pdf

Sinha, A. 2018. COP24: Will achieve all our climate targets ahead of deadlines, India tells environment meet. The Indian Express. https://indianexpress.com/article/india/climate-change-summit-cop24-katowice-india-5477197/

Sirur, S. 2021. What is COP26? Why it is important and India's role at the climate change conference. https://theprint.in/theprint-essential/what-is-cop26-why-it-is-important-indias-role-at-the-climate-change-conference/757909/

Skene, J. 2022. Forward progress at COP27 in Egypt and the path ahead. https://www.nrdc.org/experts/jake-schmidt/forward-progress-cop27-egypt-and-path-ahead

Soutar, R. 2021. Carbon market grows in Brazil ahead of expected regulation in Glasgow. https://dialogochino.net/en/climate-energy/41641-carbon-market-grows-in-brazil-ahead-of-expected-regulation-in-glasgow/

Stéphane, W. and Kevin, B. 2003. Institutional Capacity and Climate Actions. https://www.oecd.org/env/cc/21018790.pdf

Stockholm Environment Institute 2019. The Talanoa Dialogue: An Explainer. https://www.sei.org/featured/talanoa-dialogue-an-explainer/

Tanwar, R. 2013. Porter's generic competitive strategies. IOSR J. Bus. Manag., 15(1): 11-17. https://doi.org/10.9790/487x-1511117

UN 1985. Our common future, from one earth to one world: An overview by the world commission on environment and development. https://sustainabledevelopment.un.org/content/documents/5987our-common-future.pdf

UN 2015. Principles for responsible contracts: integrating the management of human rights risks into state-investor contract negotiations-guidance for negotiators. https://www.ohchr.org/sites/default/files/Documents/Publications/Principles_ResponsibleContracts_HR_PUB_15_1_EN.pdf

UN 2021. Women Watch: Women, gender equality and climate change. United Nations. https://www.un.org/womenwatch/feature/climate_change/

UNCTD 2003. An implementation guide to the clean development mechanism. (2003). In Geneva. https://unctad.org/system/files/official-document/ditcted20031_en.pdf

UNFCCC 2021. Preparing for the first global stocktake revised non-paper by the chairs of the SBSTA and SBI. https://unfccc.int/sites/default/files/resource/REV_Non-paper_on_Preparing_for_GST1_forSBs_15Sept.pdf

United Nations. 2007. Sustainable development within the climate context. https://www.un.org/en/chronicle/article/sustainable-development-within-climate-contextsouthsouthnorth-and-clean-development-mechanism

Waskow, D. 2018a. COP24 climate change package brings Paris Agreement to life. World Resources Institute. https://www.wri.org/insights/cop24-climate-change-package-brings-paris-agreement-life

Waskow, D. 2018b. Talanoa dialogue: jump-starting climate action in 2018. World Resources Institute. https://www.wri.org/insights/talanoa-dialogue-jump-starting-climate-action-2018

Waslander, J. 2019. How much should countries contribute to the green climate fund's replenishment? World Resources Institute. https://www.wri.org/insights/how-much-should-countries-contribute-green-climate-funds-replenishment

World Meteorological Organization. 2018 Climate change report is a "wake-up" call on 1.5°C global warming. https://public.wmo.int/en/media/press-release/climate-change-report

Study on the Experimental Conditions of Adsorption of Lanthanum (III) on Boron Nitride Nanosheets

C. Fu*, Y. He*, C. Yang*, J. He*, L. Sun*, G. Sheng*, X. Zhang**, L. Wang*†, L. Li* and W. Linghu*

*School of Chemistry and Chemical Engineering, Department of Zhejiang Engineering Research Center of Fat-soluble Vitamin, Shaoxing University, Zhejiang 312000, P. R. China

**Department of International Education, Beijing University of Chemical Technology, Beijing 100029, P. R. China

†Corresponding authors: Linxia Wang; wlxsyx@163.com

ABSTRACT

This paper investigated the adsorption properties of boron nitride materials for La(III), and the possible action mechanism was put forward based on experiments. Then the boron nitride materials were characterized by SEM, TEM, XRD, and FT-IR before and after adsorption. In addition, the effects of pH, the amount of adsorbent, the concentration of La(III) solution, and adsorption time on the adsorption efficiency were also investigated. It is found that under a certain amount of adsorbent when the pH is 7.0 and the concentration of La(III) is 40 mg.L^{-1}, the adsorption ability of La(III) is the best. The maximum adsorption capacity is 201.45 mg.g^{-1}. The adsorption kinetic data are in good agreement with the pseudo-second-order and intra-particle diffusion models. These results show that boron nitride has a good application prospect for removing and recovering La(III) in water and has a certain practical application value.

INTRODUCTION

Due to their excellent properties, rare earth elements are widely used in metallurgy, petrochemicals, glass, ceramics, aerospace, and other fields. Therefore, rare earth elements are also known as "industrial vitamins." In recent years, with the continuous development of science and technology, the demand for rare earth elements keeps rising. Lanthanum, one of the most common rare earth elements (Wu et al. 2011), is usually used in synthesizing superalloys and preparing catalysts (Sert et al. 2008). As one of the most used rare earth elements, lanthanum also causes some pollution to the ecological environment. For example, manufacturing various industrial materials and using agricultural rare earth fertilizers will lead to soil pollution (Shen et al. 2014).

Moreover, studies have shown that rare earth minerals will produce various kinds of pollution during processing, such as harmful nitrogen and chloride produced by hydrometallurgy and harmful gases such as chloroform VOCs produced by high temperatures of pyrometallurgy. Rare earth elements will induce cardiovascular diseases in the human respiratory and nervous systems (Shin et al. 2019). Lanthanum is also very harmful to the human body. Studies have shown that lanthanum may cause nervous system disorders and accumulate in bones, kidneys, spleen, and other organs (Zarros et al. 2013, Chen & Zhu 2008, Wu et al. 2005, Liu et al. 2010) and has potential effects on the immune system (Cheng et al. 2014).

To reduce the pollution caused by lanthanum and other heavy metal elements to the environment, scientific researchers have used various treatment methods. Common treatment methods include biological methods, physical-chemical methods, and so on. For example, Du et al. (2020) concluded that planting water hyacinth can effectively enrich heavy metal elements through experiments. In this case, heavy metal ions are fixed in plant roots through the water absorption of plant roots, thus playing a role of enrichment. Physical chemistry mainly includes the chemical adsorption method. At present, the chemical method is the most commonly used chemical fixation method, such as the Zhen study group, through the use of inorganic amine hydrazine hydrate and sulfur dioxide synthesis of a new collector, produced a better removal effect on metal ions (Zhen et al. 2012). In recent years, more and more researchers have explored the recovery effect of different adsorbents on lanthanum due to the high recovery rate and low cost of the adsorption method. For example, Kusrini et al. (2018) used pectin in durian peel to study the adsorption of lanthanum, and the adsorption amount was 41.2 mg.g^{-1}. In recent years, boron nitride has been widely used in hydrogen storage (Lale

et al. 2018), electrical breakdown (Zhi et al. 2010), and other fields because of its special properties. In addition to the above applications, some researchers have used boron nitride in adsorption. For example, Liu et al. (2018) carried out adsorption research on Cu^{2+}, Pb^{2+}, Zn^{2+}, and Cr^{3+} and found that they all had good adsorption effects, and the adsorption kinetics were all in line with the pseudo-second-order model.

Based on the above facts and analysis, this paper will study the following three aspects: First, the two-step synthesis method is used to prepare boron nitride, and the prepared material is characterized by SEM-EDS, TEM, and XRD analysis; Secondly, the adsorbent of boron nitride was used to explore the adsorption performance of boron nitride on La(III), and the reaction conditions were optimized to explore the adsorption mechanism.

MATERIALS AND METHODS

Experimental Reagents and Materials

Lanthanum nitrate, hydrochloric acid, and sodium hydroxide were provided by Shanghai Lingfeng Chemical Reagent Co., Ltd. Sulfamic acid, hydroxylamine hydrochloride, arsine azo III, citric acid, disodium hydrogen phosphate, melamine, and boric acid were provided by Shanghai Aladdin Biochemical Science and Education Co., Ltd. The purity of the reagents was all analytical grade, and the deionized water was self-made. The components of the prepared reducing agent are hydroxylamine hydrochloride and sulfamic acid, and the components of the buffer solution are citric acid and disodium hydrogen phosphate.

Experimental Equipment

The ultrasonic cleaning machine (KQ5200DA) was produced by Kunshan Ultrasonic Instrument Co., Ltd., the UV-Vis Spectrophotometer (SP-756P) was produced by Shanghai Spectrum Instrument Co., Ltd., and the vacuum drying oven (DZF-6020) was produced by Shanghai Jinghong Experimental Equipment Co., Ltd., pH meter (Five Easy plus) and electronic balance (AL204) are produced by METTLER TOLEDO (Shanghai) Co., Ltd., using the muffle furnace (KSL-1700) produced by Hefei Kejing Material Technology Co., Ltd. The pipette (7010101017) was produced by Dalong Xingchuang Experimental Instrument (Beijing) Co., Ltd., and the desktop low-temperature constant temperature shaking shaker was the IKA KS4000i control shaker produced in Germany.

Preparation of Boron Nitride Adsorbent

The research teams (Li et al. 2013, Li et al. 2020a) have detailedly explored the preparation method of boron nitride (BN). Based on this team, this experiment adopted a two-step synthesis method to prepare BN. The specific steps were: Melamine and boric acid were evenly mixed uniformly in a molar ratio of 1:2, then roasted in a tubular furnace and heated to 1100 at a certain speed, held for 1h, and then cooled to room temperature naturally to prepare BN material.

Static Adsorption Experiment

The analytical balance was used to measure 2.3392 g La$(NO_3)_3$ dissolved in deionized water and transferred to a 1000 mL volumetric bottle. Water was added for constant volume to obtain 1000 ppm La(III) solution. Several 150 mL reaction bottles were selected, and La(III) was quantitatively removed by pipetting gun. The solution was put into the reaction bottle, and deionized water was added to adjust the total volume of the solution to 100 mL. Before the adsorption experiment, 0.1 $mol·L^{-1}$ HCl and 0.1 $mol.L^{-1}$ NaOH were used, respectively, to adjust the initial pH value of the solution. In the static adsorption experiment, 100 mL of La(III) with different initial concentrations was adjusted to explore the influence of La(III) solution with different concentrations on the adsorption performance of BN. The initial pH of the solution was 6.0. After the quantitative BN was added, the reaction bottle was placed in the ultrasonic cleaning machine for 30min ultrasonic treatments. After the ultrasound, the reaction bottle was transferred to the bench low-temperature constant temperature oscillating shaking bed for 24h to ensure the adsorption balance. To explore the influence of different amounts of adsorbent on adsorption properties, the La(III) solution was set at 50 $mg·L^{-1}$, and the BN adsorbent dosage was set at 10, 15, 20, 25, 30, and 35 mg. Experimental studies were carried out for adsorption kinetics using 20 mg BN and La(III) solutions of 30 and 40 $mg·L^{-1}$ at an initial pH of 7.0. The equilibrium solution was filtered through a 0.22-μm polyether sulfone membrane filter, and the solid and aqueous solutions were separated for 1 mL. The clear liquid was placed in the colorimetric tube, and 1mL reducing agent, 5 mL buffer solution, and 1 mL color developing agent were added. The absorbance was measured by SP-756P UV-visible spectrophotometer at constant volume.

Data Processing of Adsorption Experiments

The adsorption capacity of BN can be expressed by the adsorption capacity (q_e). The adsorption capacity is the amount of La(III) adsorbed per unit weight of BN. The relevant parameters are calculated by the formula (1-2):

$$q_t = \frac{c_0 - c_t}{m} V \qquad \qquad \ldots(1)$$

$$q_e = \frac{c_0 - c_e}{m} V \qquad \qquad \ldots(2)$$

The adsorption capacity at equilibrium and at any time t is expressed as q_e and q_t (mg·g^{-1}). C_0 is the initial concentration of La(III) solution before adsorption (mg·L^{-1}); C_e is the concentration of La(III) solution after adsorption equilibrium, V is the volume of the solution, and m is the mass of the adsorbent.

In this study, the pseudo-first-order model, pseudo-second-order model (Wang et al. 2021), Elovich model (Wu et al. 2009), and intra-particle diffusion model (Li et al. 2020b) were used to fit the kinetic data. The calculation formulas of the relevant parameters are as follows.

Pseudo-first-order model:

$$ln\,(q_e - q_t) = lnq_e - k_1 t \qquad \ldots(3)$$

pseudo-second-order model:

$$\frac{t}{q_t} = \frac{1}{k_2 q_e^2} + \frac{t}{q_e} \qquad \ldots(4)$$

Elovich model:

$$q_t = \frac{1}{\beta} \cdot ln\alpha\beta + \frac{1}{\beta} \cdot lnt \qquad \ldots(5)$$

intra-particle diffusion model:

$$q_t = K_d \times t^{1/2} + I \qquad \ldots(6)$$

k_1(min^{-1}) is the pseudo-first-order kinetic adsorption rate constant. The pseudo-second-order kinetic adsorption rate constant is k_2 (g·mg^{-1} min^{-1}), α(mg·g^{-1} min) and β(g·mg^{-1}) represent the initial adsorption rate constant and desorption rate constant, respectively, K_d (g·mg^{-1}min$^{-1/2}$) is the rate constant of intraparticle diffusion, and I is a parameter related to the thickness of the boundary layer.

To further analyze the adsorption mechanism of BN, Freundlich and Langmuir fit the thermodynamic data. The

linearization formulas of the two fits are as follows:

Freundlich model:

$$lnq_e = lnK_F + nlnC_e \qquad \ldots(7)$$

Langmuir model:

$$\frac{1}{q_e} = \frac{1}{q_m} + \frac{1}{K_L \times q_m} \cdot \frac{1}{C_e} \qquad \ldots(8)$$

Characterization Methods

In this study, the JEM-1011 transmission electron microscope of Japan Electronics Company was used for TEM characterization to analyze the fine internal structure of materials, and the scanning electron microscope (SEM) of Japan Electronics (JEOL) and JSM-6360LV was used to analyze the surface topography of materials. This team used the Fourier infrared spectrometer (NICOLET6700) of the United States Thermoelectric Technology Company to determine BN samples' molecular structure and chemical composition, ranging from 400 to 4000 cm-1. The resolution is better than 4 cm$^{-1.}$ At the same time, an X-ray energy spectrometer (XRD), manufactured in Panalytical, Netherlands, model Empyrean, uses a *Cu* target as the radiation source. XRD is mainly used in this paper to determine the crystal shape of BN material.

RESULTS AND DISCUSSION

Adsorption Results

pH has a significant effect on the adsorption of La(III) by BN, and it can be seen from Fig. 1(A) that the adsorption effect of BN on La(III) increases significantly with the increase of pH. However, it can be found from Fig. 1(B) that after the pH value exceeds 6.0, the residual concentration of
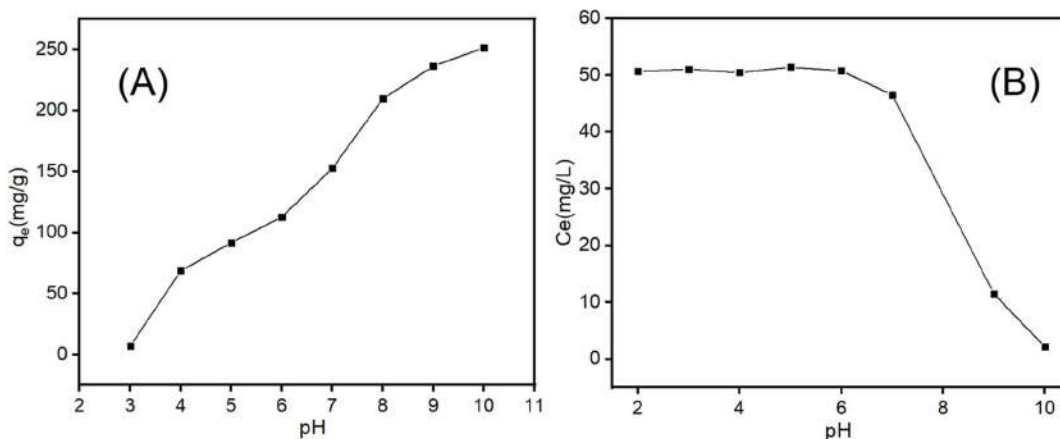

Fig. 1: (A) Effect of Initial pH on La(III) Adsorption by BN (q_e), (B) Under different pH conditions, the residual concentration of La(III) solution after sufficient reaction (C_e). Experimental conditions, C = 50 mg·L^{-1}, m = 20 mg, V = 100 mL

La(III) solution will gradually decrease even if no adsorbent is added. This is because La(III) will precipitate at a higher pH, thus affecting the experimental results. Therefore, considering both, pH 6.0 or 7.0 is selected for the subsequent experiments.

To explore the influence of the amount of adsorbent on the adsorption performance, different qualities of adsorbent

were added into the lanthanum solution of 100 mL and 50 mg·L^{-1}, showing that the amount of adsorbent is closely related to the adsorption performance. Increasing the amount of adsorbent will lead to a gradual decrease in the adsorption amount of adsorbent, but the removal rate of La(III) will gradually increase.

As can be seen from Fig. 3 (A), the concentration also significantly impacts the performance of the adsorbent. With
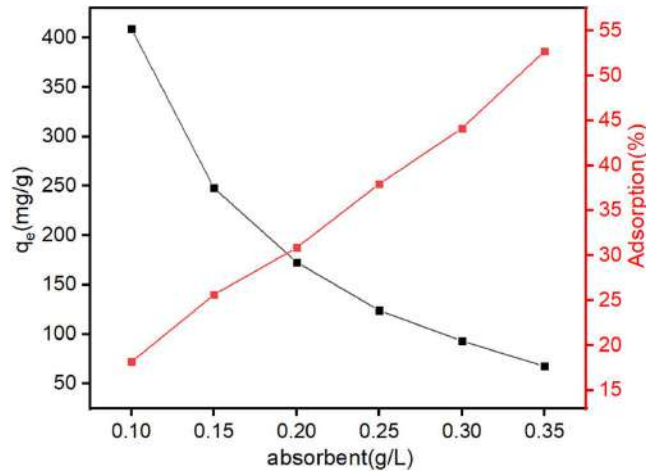

Fig. 2: Effects of different adsorbent concentrations on BN adsorption capacity (q_e) and removal rate.
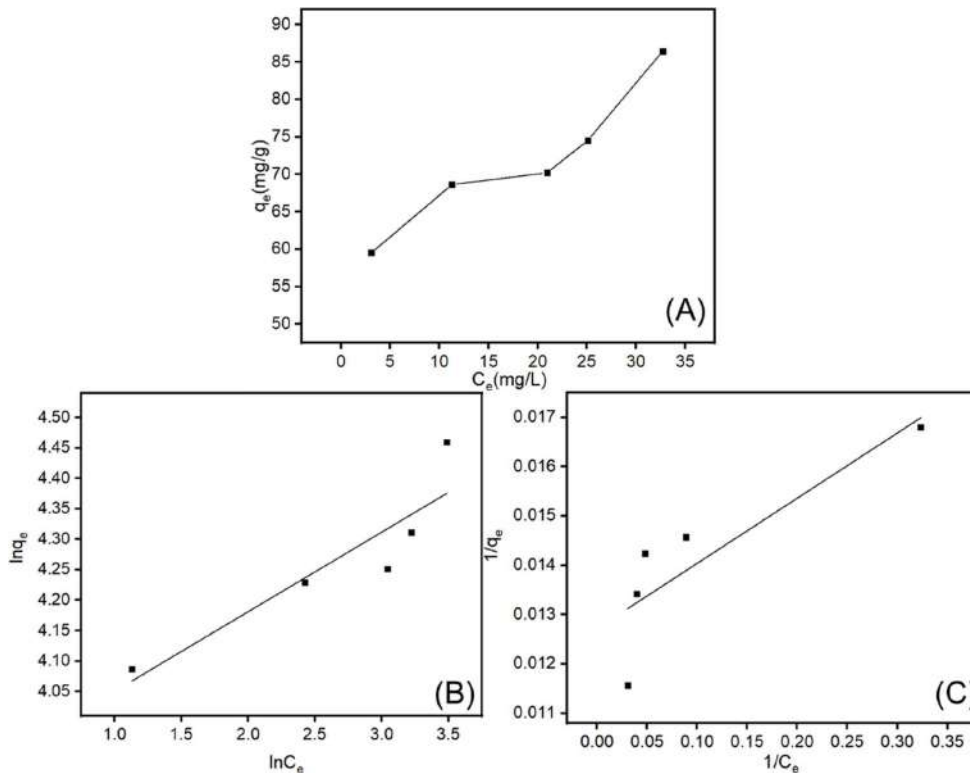

Fig. 3: (A) Isotherm of La(III) Adsorption on BN, (B) Freundlich model, (C) Langmuir model.
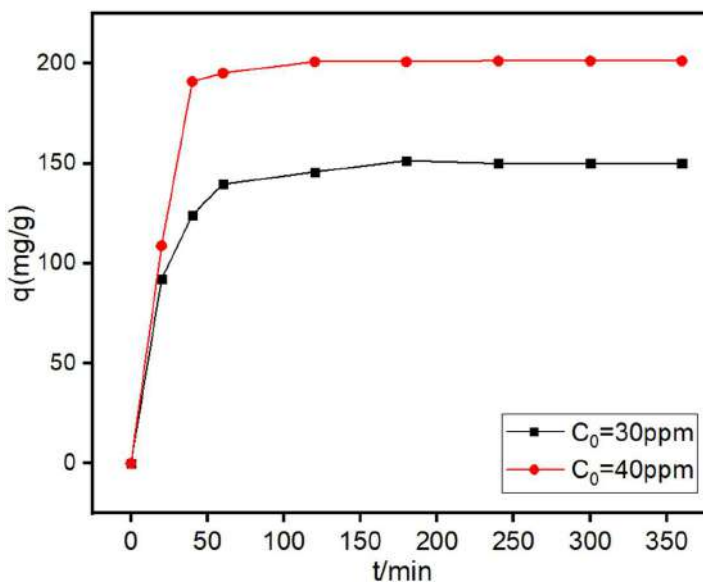
Fig. 4: The adsorption time curve of BN to 30 mg·L^{-1} and 40 mg·L^{-1} La(III) Experimental solution conditions, V = 100 mL, m = 20 mg, pH = 7.0

the increase of the concentration, the adsorption capacity of the adsorbent also increases. To explore its adsorption mechanism, we performed Freundlich and Langmuir fitting on the curve. The results in Fig. 3 (B-C) show that the experimental data are not in line with the Langmuir fitting model and the Freundlich fitting model, indicating that the adsorption mechanism is relatively complex, with both single-layer adsorption and multi-layer adsorption.

Next, the kinetic curve of BN adsorption of La(III) solution is discussed. Fig. 4 shows that no matter La(III), the initial concentration of solution is 30.0 mg·L^{-1} or 40.0 mg·L^{-1}, the growth trend of BN adsorption capacity is roughly similar. With the increase of time, the adsorption capacity increases gradually. The adsorption capacity increased rapidly, the growth was relatively slow in 60~180 min, and the adsorption equilibrium was reached around 180 min. When the initial concentration of La(III) solution is 30.0 mg·L^{-1}, the maximum adsorption capacity of BN on La(III) is 150.05 mg·g^{-1}. When the concentration is 40.0 mg·L^{-1}, the maximum adsorption capacity reaches 201.46 mg·g^{-1}. The results are consistent with the previous results of the effect of concentration on the adsorbent, indicating that the experimental results have good reproducibility.

Fig. 5 (A) is a pseudo-first-order model fitting of the kinetic curve of BN adsorption La(III) solution, Fig. 5 (B) is a pseudo-second-order fitting model, and Fig. 5 (C) is an Elovich model fitting combined. After fitting and analysis, it is found that the kinetic curve of BN to La(III) solution is more in line with the pseudo-second-order fitting model, indicating that the adsorption process is mainly chemical

adsorption (Li et al. 2020a). Although the adsorption of BN can be obtained by fitting the pseudo-first-order and pseudo-second-order models, the adsorption mechanism cannot be further speculated. Therefore, using the particle internal diffusion model, as shown in Fig. 5 (D), the adsorption process is divided into two stages. The first stage La(III), diffuses to the surface of the material to complete the adsorption, and the second stage adsorption reaches the adsorption equilibrium (Shan et al. 2020).

Characterization Results

SEM and TEM characterize the BN material to analyze its surface morphology and internal structure. The results are shown in Fig. 6. According to SEM images (A), (B), and TEM images (C), BN material presents a circular or elliptical sheet structure with an average diameter ranging from one micron to several microns. The sheet structure can increase the contact area and increase adsorption efficiency.

The material's microstructure will have a greater impact on the macro performance, and the functional group will significantly impact the adsorption process. Therefore, we conducted the infrared spectroscopic measurement and characterization of the prepared BN material. It can be seen from Fig. 7 (A) that there are two characteristic absorption peaks at ~1380cm^{-1} and ~810cm^{-1}, which are caused by the bending vibration of B-N-B and B-N combined by the sp^2 bond. In contrast, a wide peak appeared at ~3420cm^{-1}, which was attributed to the fact that BN material may contain more -OH groups and have a strong vibration peak here (Zhang et al. 2021, Hou et al. 2019). The absorption peak at ~1592
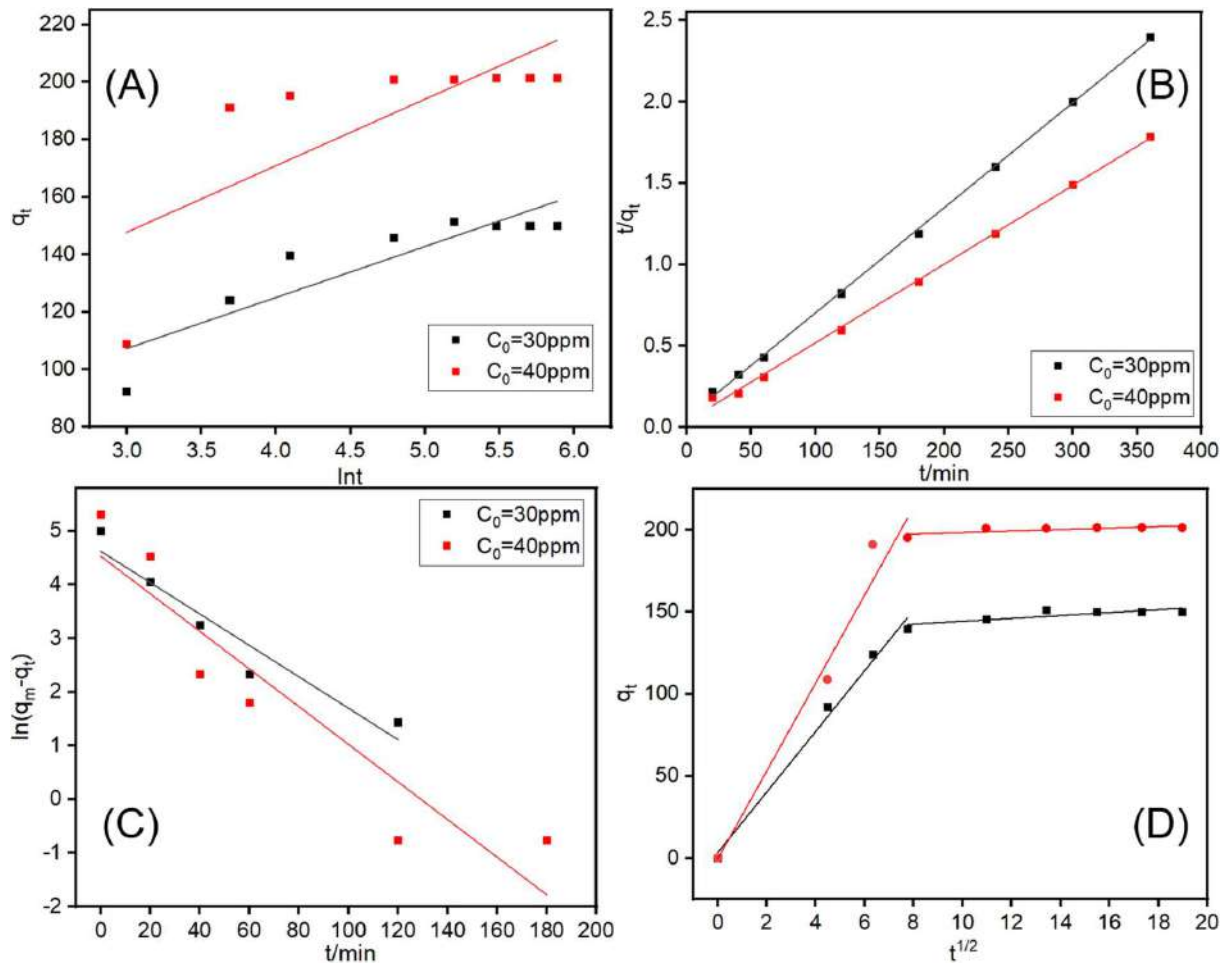
Fig. 5: (A) pseudo-first-order model; (B) pseudo-second-order model; (C) Elovich model; (D) intra-particle diffusion model.
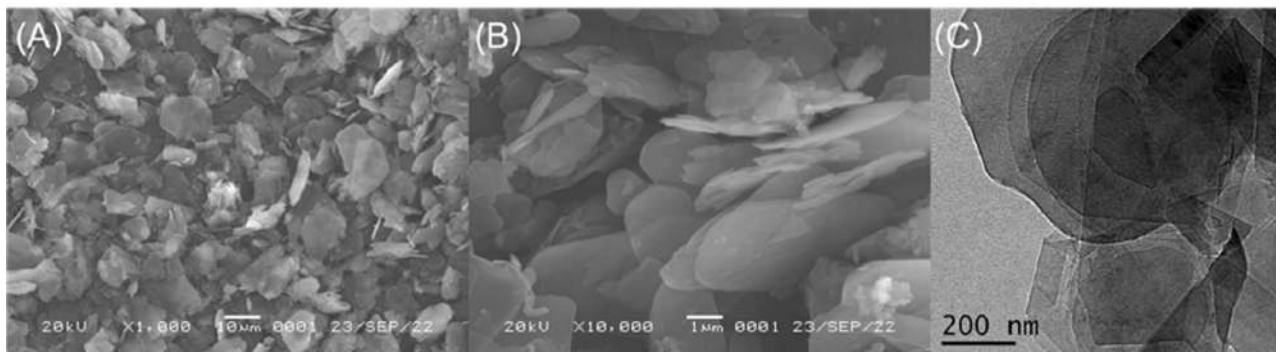

Fig. 6: (A, B) SEM image of the BN, (C) a TEM image of the BN.

cm^{-1} can be attributed to the uneven surface of BN material, which changes the position of the acromion of the B-N bond (Tang et al. 2008).

To determine the crystal plane of the material, we conducted XRD characterization of the material. Fig. 7

(B) is the XRD characterization image of BN. The front appearing at 26.7°, 41.5°, and 55° corresponds to the crystal planes (002), (100), and (004) of BN, respectively, which is similar to the results of Li et al. (2015) and Fu et al. (2023).
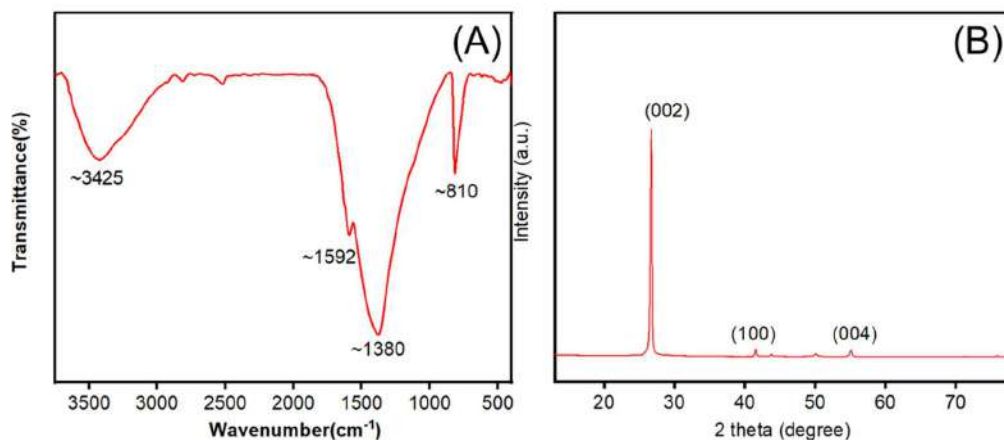
Fig. 7: (A) FT-IR spectrum of BN (B) XRD pattern of BN.

CONCLUSION

Based on the above experiments and analysis, this paper describes a preparation method of BN material and explores the adsorption performance and mechanism of BN for La(III) solution. The results show that BN has a good adsorption effect on La(III) in water, and the adsorption property of the material is closely related to the concentration of a solution with the amount of adsorbent, pH value, and contact time.

Under 303K and pH = 7.0, the maximum adsorption capacity of BN can reach 201.45mg·g^{-1}. The results show that the kinetic fitting of the adsorption experiment conforms to the pseudo-second-order model fitting, indicating that the adsorption experiment is chemical adsorption. The in-particle diffusion model shows that the adsorption process is mainly divided into two stages: La(III) diffusion to BN surface stage, and the adsorption reaches the adsorption equilibrium stage.

Through SEM, TEM, FT-IR, and XRD characterization, it is found that the BN prepared by this method is very similar to the common BN materials in the structure, which proves that the preparation of BN by this method is feasible. The preparation method has a low cost, simple process, and good adsorption effect on La(III), which has a good application prospect in water pollution control.

ACKNOWLEDGEMENT

REFERENCES

Chen, Z.Y. and Zhu, X. D. 2008. Accumulation of rare earth elements in bone and its toxicity and potential hazard to health. J. Ecol. Rural. Environ., 24: 88-91.

Cheng, J., Cheng, Z., Hu, R., Cui, Y., Cai, J., Li, N. and Hong, F. 2014. Immune dysfunction and liver damage of mice following exposure to lanthanoids. Environ. Toxicol., 29(1): 64-73.

Du, Y., Wu, Q., Kong, D., Shi, Y., Huang, X., Luo, D. and Leung, J.Y. 2020. Accumulation and translocation of heavy metals in water hyacinth: Maximising green resources to remediate sites impacted by e-waste recycling activities. Ecol. Indic., 115: 106384.

Fu, C.K., He, Y.C., Yang, C.Y., He, J.Y. and Wang, L.X. 2023. Investigation of Adsorption of Nd (III) on Boron Nitride Nanosheets in Water. Nat. Environ. Pollut. Technol., 16: 225-233

Hou, Y., Yang, W., Zhong, C., Wu, S., Wu, Y., Liu, F. and Wen, G. 2019. Thermostable SiCO@ BN sheets with enhanced electromagnetic wave absorption. Chem. Eng. J., 378: 122239.

Kusrini, E., Wicaksono, W., Gunawan, C., Daud, N. Z. A. and Usman, A. 2018. Kinetics, mechanism, and thermodynamics of lanthanum adsorption on pectin extracted from durian rind. J. Environ. Chem. Eng., 6(5): 6580-6588.

Lale, A., Bernard, S. and Demirci, U. B. 2018. Boron nitride for hydrogen storage. ChemPlusChem, 83(10): 893-903.

Li, J., Huang, Y., Liu, Z., Zhang, J., Liu, X., Luo, H. and Tang, C. 2015. Chemical activation of boron nitride fibers for improved cationic dye removal performance. J. Mater. Chem. A, 3(15): 8185-8193.

Li, J., Xiao, X., Xu, X., Lin, J., Huang, Y., Xue, Y. and Tang, C. 2013. Activated boron nitride is an effective adsorbent for metal ions and organic pollutants. Sci. Rep., 3(1): 1-7.

Li, L., Chang, K., Fang, P., Du, K., Chen, C., Zhou, S. and Guo, X. 2020b. Highly efficient scavenging of Ni (II) by porous hexagonal boron nitride: kinetics, thermodynamics, and mechanism aspects. Appl. Surf. Sci., 521: 146373.

Li, L., Guo, X., Jin, Y., Chen, C., Abdullah M.A., Marwani, H.M. and Sheng, G. 2020a. Distinguished Cd (II) capture with rapid and superior ability using porous hexagonal boron nitride: Kinetic and thermodynamic aspects. Inorg. Mater., 35(3): 461-475.

Liu, F., Li, S., Yu, D., Su, Y., Shao, N. and Zhang, Z. 2018. Template-free synthesis of oxygen-doped bundlelike porous boron nitride for highly efficient removal of heavy metals from wastewater. ACS Sustain. Chem. Eng., 6(12): 16011-16020.

Liu, J., Li, N., Ma, L., Duan, Y., Wang, J., Zhao, X. and Hong, F. 2010. Oxidative injury in the mouse spleen caused by lanthanides. J. Alloys Compd., 489(2): 708-713.

Sert, Ş., Kütahyali, C., İnan, S., Talip, Z., Çetinkaya, B. and Eral, M. 2008. Biosorption of lanthanum and cerium from aqueous solutions by Platanus orientalis leaf powder. Hydrometallurgy, 90(1): 13-18.

Shan, R., Shi, Y., Gu, J., Bi, J., Yuan, H., Luo, B. and Chen, Y. 2020. Aqueous Cr (VI) removal by biochar derived from waste mangosteen shells: Role of pyrolysis and modification on its absorption process. J. Environ. Chem. Eng., 8(4): 103885.

Shen, Y., Zhang, S., Li, S., Xu, X., Jia, Y. and Gong, G. 2014. Eucalyptus tolerance mechanisms to lanthanum and cerium: subcellular distribution, antioxidant system, and thiol pools. Chemosphere, 117: 567-574.

Shin, S.H., Kim, H.O. and Rim, K. 2019. Worker safety in the rare earth elements recycling process from the review of toxicity and issues. Saf. Health Work, 10(4): 409-419.

Tang, C., Bando, Y., Huang, Y., Zhi, C. and Golberg, D. 2008. Synthetic routes and formation mechanisms of spherical boron nitride nanoparticles. Adv. Funct. Mater., 18(22): 3653-3661.

Wang, D., Luo, W., Zhu, J., Wang, T., Gong, Z. and Fan, M. 2021. Potential of removing Pb, Cd, and Cu from aqueous solutions using a novel modified ginkgo leaves biochar by simply one-step pyrolysis. Biomass Convers. Biorefin., 2: 1-10.

Wu, D., Zhang, L., Wang, L., Zhu, B. and Fan, L. 2011. Adsorption of lanthanum by magnetic alginate‐chitosan gel beads. J. Chem. Technol. Biotechnol., 86(3): 345-352.

Wu, F.C., Tseng, R.L. and Juang, R.S. 2009. Characteristics of Elovich equation used to analyze adsorption kinetics in dye-chitosan systems. Chem. Eng. J., 150(2-3): 366-373.

Wu, H., Zhang, X., Li, X., Wu, Y. and Pei, F. 2005. Acute biochemical effects of La (NO$_3$)$_3$ on liver and kidney tissues by magic-angle spinning 1H nuclear magnetic resonance spectroscopy and pattern recognition. Anal. Biochem., 339(2): 242-248.

Zarros, A., Byrne, A.M., Boomkamp, S.D., Tsakiris, S. and Baillie, G.S. 2013. Lanthanum-induced neurotoxicity: solving the riddle of its involvement in cognitive impairment. Arch. Toxicol., 87: 2031-2035.

Zhang, Y., Si, H., Liu, S., Jiang, Z., Zhang, J. and Gong, C. 2021. Facile synthesis of BN/Ni nanocomposites for effective regulation of microwave absorption performance. J. Alloys Compd., 850: 156680.

Zhen, H.B., Xu, Q., Hu, Y.Y. and Cheng, J.H. 2012. Characteristics of heavy metals capturing agent dithiocarbamate (DTC) for treatment of ethylene diamine tetraacetic acid–Cu (EDTA–Cu) contaminated wastewater. Chem. Eng. J., 209: 547-557.

Zhi, C., Bando, Y., Tang, C. and Golberg, D. 2010. Boron nitride nanotubes. Mater. Sci. Eng. R Rep., 70(3-6): 92-111.

Influence of Vermicomposted Coal Fly Ash on Morphological and Cytological Attributes of *Ricinus communis* L.

R. U. Raval*† iD **, D. B. Kapdi*, N. H. Bhavsar*, V. V. Surati*, J. D. Solanki*, S. R. Panjabi*, P. M. Patel*, Y. H. Vaidya*, D. N. Verma** and K. P. Patel*****

*Department of Microbiology, Shri Alpesh N Patel PG Institution of Science and Research, Anand, Gujarat, India
**Department of Biochemistry, Shri Alpesh N Patel PG Institution Science and Research, Anand, Gujarat, India
***Department of Biosciences, Veer Narmad South Gujarat University, Surat, Gujarat, India
†Corresponding author: R. U. Raval; ravalrucha92@gmail.com

ABSTRACT

In view of the environmental problems generated by the large-scale production of fly ash, increasing attention is now being paid to the recycling of fly ash as a good source of nutrients. To reduce the cost of fly ash disposal and best utilization, it aimed to convert the fly ash into valuable vermicompost. Stated throughout the experiment, we opted for a soil sample and fly ash and pressed with different concentrations (control, 20%, 50%, 80% and 100%). Subsequently, all the mixtures were vermicomposted for 60 days by adding 100 Earthworms (*Eisenia foetida*) in each pile. The X-ray fluorescence spectroscopy measured the composition of the metal in fly ash as well as the nutritional content in the soil. This is followed by examining the morphological characteristics and cytogenetic study of *Ricinus communis* L. The present study indicated that *E. foetida* mitigates the toxicity of fly ash and is hence used as valuable vermicompost.

INTRODUCTION

To being with, due to this modernization came along with industrialization in metropolitan cities, electricity demand deliberately increased in day-to-day life (Mistry & Jadav 2018) (Raval et al. 2018) whereas in developing countries, depending upon the major source of fuel as coal; despite coal near to soil surface makes it easily minable and thus is relatively less expensive than hydro or nuclear power-based generations of electricity. In India, major power plants are using coal as fuel though alternatives have been searched for more than the last 10 years. Still, no feasible replacement for coal is available in India (Sharma & Akhai 2019). Lignite, bituminous, and anthracite are classified into organic maturity coal, which (proportion may differ) contains magnesium, calcium, and sulfate. Coal-based thermal plants contribute to major electricity production in India. From all these thermal power plants, dry fly ash has been collected through Electrostatic Precipitator (ESP) in dry conditions, and pond ash from ash ponds in semi-wet

conditions (Ahmad 2015). Fly ash composes of fine glass, which has a spherical shape and ranges from approximately ~0.5 to 100µm. There has been seen that mainly two types were found (Mupambwa et al. 2015). Fly ash is used in the industry for manufacturing cement. Around 2.45 million tons of fly ash were used in 1998-1999. Whereas the disposal of fly ash is either dry state or wet state, even though the process of leaching the heavy metals, Wet state disposal facilitates in biomagnification of toxic components. The coal ash by-product has been classified as a Green List waste under the Organization for Economic Cooperation and Development (OECD) (Khan et al. 2013).

Fly Ash contains nutrients such as S, B, Ca, Mg, Fe, Cu, Zn, Mn, and P that benefit plants. It also contains toxic metals, including Cr, Pb, Hg, Ni, V, As, and Ba. Adding Fly Ash increases the availability of Na, K, Ca, Mg, B, and other nutrients except for N (Sharma & Kalra 2006). Thus, it was found that this material could be used as an additive/amendment material in agriculture applications. Some experience was gained in the country and abroad regarding the effect of fly ash utilization in agriculture & related applications (Swamy et al. 2010). In addition, Fly Ash significantly influences soil physical properties

such as water-holding capacity and aggregation (Daniels et al. 2002).

MATERIALS AND METHODS

Sample Collection of Fly Ash

Fly Ash was collected in a clean bag directly from the Electrostatic Precipitator (ESP) of the Thermal Power Plant, Ukai Dam, on the Tapi River in the Tapi district of Gujarat, India.

Soil Sample Collection

The soil sample was collected from an agricultural field in the Bardoli region of Surat, Gujarat, India. Plants were grown in the same soil sample throughout the research period.

Pressmud Collection

Pressmud is a solid waste generated from Sugarcane in Sugar factories. Pressmud is a rich source of organic compounds. It was collected from Shree Khedut Sahakari Khand Udhyog Mandali Ltd., Sugar Factory, Madhi, Surat, Gujarat, India.

Seeds Collection

Seeds of *Ricinus communis* L. were purchased from Agriculture Produce Market Committee, Surat. Seeds were surface sterilized with H_2O_2.

Analysis of Fly Ash

X-Ray Fluorescence Spectroscopy detected metal in Fly Ash samples at SVNIT, Surat. Fe, Zn, Cu, Mn, and S were checked at Soil Testing Laboratory, Bardoli. Other physicochemical parameters such as pH, Electrical Conductivity, Organic Carbon (%), Available Potash (%), and Available Phosphate (%) were also checked at Soil Testing Laboratory, Bardoli.

Analysis of Soil

X-Ray Fluorescence Spectroscopy did Metal Detection in Soil samples at SVNIT, Surat. Virgin Soil (Control Soil) and different vermicomposted mixtures of Fly Ash, Pressmud, and Soil were tested for the same. Ca, Mg, and Na were checked in the control soil at Pollucon Laboratories, Surat. Other physicochemical parameters such as pH, Electrical Conductivity, Organic Carbon (%), Available Potash (%), and Available Phosphate (%) were also checked in Control Soil at Soil Testing Laboratory, Bardoli.

Vermicomposting of Mixtures

Different mixtures of Fly Ash, Pressmud, and Soil were prepared in different concentrations (Control, 20%, 50%, 80%, and 100%). All the mixtures were vermicomposted for 60 days by adding 100 Earthworms *(Eisenia foetida)* in each pile. The effect of Fly Ash on Earthworms was also checked in each concentration for 60 days at 15 days, in which numbers of live adult earthworms and numbers of Juveniles were counted. Ca, Mg, and Na were checked in these vermicomposted mixtures at Pollucon laboratories in Surat. Nitrogen, phosphorus, and potassium content were also checked in the vermicomposted mixtures at Soil Testing Laboratories, Bardoli.

Pot Experiment

Initially, the experiment was carried out with three controls, i.e., Control Soil, Soil and Vermicompost, and Soil and Pressmud. For the test, the mixtures of Soil, Vermicompost, Pressmud, and different concentrations of Fly Ash were taken, and 10 seeds were planted in each pot. The result was improved in the soil, vermicompost, pressmud, and fly ash mixtures. And so these mixtures with different concentrations of Fly Ash were further taken for the next set of experiments. The final experiment was carried out in black polyethylene bags and plastic pots varying in size. 5 kg of the prepared vermicomposted mixture was taken, and 10 seeds were added to each pot. Vermicomposted mixtures taken for the experiment were (Control, 20%, 50%, 80%, and 100%.). Tap water was used for the irrigation. The study was carried out in two phases. Initially, the plants were grown for 30 days and studied for 10 days. Later, plants were grown and studied up to maturation.

The parameters included in the plant study are as follows:

Seed Germination

Ricinus communis L. seeds were procured from Agricultural Produce Market Committee (APMC), Surat. The germination was carried out in pots. Seeds were surface sterilized with H_2O_2 to prevent surface fungal/bacterial contamination. Different concentrations of vermicomposted Fly Ash, viz. 20%, 50%, 80%, and 100%, were prepared, and tap water was used as a control for the study. Ten seeds were sown in the pots.

Cytogenetic Study

Slide preparation: Root tips were taken from seeds grown in different concentrations of Fly Ash, stained by the Darlington & La Cour (1976) method (Chakraborty et al. 2009). The root tips of different plants were collected at a particular time. The root tips were fixed in 3:1 Methanol: Acetic Acid for 12 hours, followed by hydrolysis in 5 N HC1 for 30 minutes. The root tips were washed 3 times with distilled water and stained in 1:1 Acetoorcein: Acetocarmine for 30 minutes.

Slides were observed under Carl-Zeiss Axioscope after the mitotic squash preparations. Various stages of mitosis, such as Prophase, Metaphase, Anaphase, and Telophase, were observed. Mitotic Index and Percentage Chromosomal Aberrations were counted. Mitotic squash preparations were made, and scoring was done to determine the mitotic index and the percentage of chromosomal aberration.

Calculation of the percentage of the mitotic index and percentage of aberrant cells: Mitotic index and aberrant cells were scored per hundred cells from the slides prepared from treated and control plants. Various stages of mitosis viz. prophase, metaphase, anaphase, and telophase were counted. The percentage of the mitotic index and percentage of aberrant cells was calculated using the following formulas.

$$\text{Mitotic index} = \frac{No. of\ dividing\ cells}{Total\ No. of\ cells\ studied} \times 100$$

$$\text{Aberrant cell} = \frac{No. of\ aberrant\ cells}{No. of\ dividing\ cells} \times 100$$

RESULTS AND DISCUSSIONS

Analysis of Soil

X-ray fluorescence spectrometry of fly ash: In the present study, X-Ray Fluorescence Spectrometry was performed for metal detection in Fly Ash. XRF was done at SVNIT, Surat. Table 1 illustrates the Fly Ash composition used throughout the experiment. Firstly, Silica was found to be the main content with 52.07%. Other than it, Iron and Calcium were present in higher amounts, 12.0853%, and 10.1632%, respectively. Secondly, Magnesium was present in moderate amounts, which was 3.7293%, Potassium was 3.1954% present, and 3.0246% Phosphorus was present in Fly Ash, while 3.41% Aluminium was also detected. Sulfur was 1.4832%, and Titanium was 1.7473% present in Fly Ash. Lastly, 0.184% Nickel, 0.3215% Chlorine, 0.3178% Manganese, 0.4212% Rhodium, and 0.4778% Palladium were also detected in Fly Ash. At the same time, a very less amount of Copper (0.0371%), Strontium (0.0569%), and Zirconium (0.0536%) was detected in Fly Ash by X-Ray Fluorescence Spectrometry. The analysis of soil shows that the soil contains all the necessary elements required for healthy plant growth. The control soil sample was checked for the following parameters in Table 2, indicating that physical-chemical parameters of soil such as pH (5.76), EC millimhos/cm (0.40), Organic carbon (0.69), Available potash % (5.53), and Available phosphate % (0.418) were present in a requisite level of germination of seeds. Table 3 lucid that nutritional content was present in the soil, a mixture of fly ash, Pressmud, and Farm Soil. In this method, elements presented in soil are detected, namely calcium, magnesium, sodium, nitrogen, phosphorus, and potassium. Moreover, we opted for different concertation such as 20%,

50%, 80%, and control. 20% concertation was optimistic among the all. Around 0.13 % calcium, 0.031% magnesium, 3.71% nitrogen, and around 536 ppm sodium were present. In addition, the mixture contained 24 and 156 (kg.hectare^{-1}) of phosphorus and potassium. Mineralogically, fly ash is similar to the soil but rich in macro and micronutrients. The major attribute which makes fly ash suitable for agriculture is its texture and the fact that it contains almost all the essential plant nutrients except organic carbon and nitrogen (Kumar et al. 2005).

Germination

After plantation, the seed germination in control and 20% Fly Ash concentration was observed within 2 to 3 days in *Ricinus communis* L., while it was observed within 3 to 4 days in other concentrations. Overall, in the plant, seed germination was delayed with the increased Fly Ash concentration.

Table 1: XRF analysis of fly ash.

Elements	Amount present %
MgO	3.7293
Al$_2$O$_3$	3.41
SiO2	52.0781
P$_2$O$_5$	3.0246
SO3	1.4832
Cl	0.3215
K$_2$O	3.1954
CaO	10.1632
TiO$_2$	1.7473
MnO	0.3178
Fe2O$_3$	12.0853
CuO	0.0371
SrO	0.0569
ZrO$_2$	0.0536
Rh$_2$O$_3$	0.4212
PdO	0.4778
NiO	0.184
CaO	10.1632
TiO$_2$	1.7473

Table 2: Physicochemical properties of soil.

Parameters	Results
pH	5.76
EC [milimohs.cm^{-1}]	0.40
Organic Carbon %	0.69
Available Potash %	5.53
Available Phosphate %	0.418

Table 3: Soil Nutritional Content.

Elements	Control	20%	50%	80%
Ca (%)	0.04	0.13	0.13	0.22
Mg (%]	0.007	0.031	0.031	0.06
Na [ppm]	460	536	1115	1133
N [%]	3.62	3.71	3.89	2.85
P [kg.hectare^{-1}]	21	24	29	24
K [kg.hectare^{-1}]	130	156	134	132

Morphological Characteristics

The Shoot Length, Root Length, Number of Leaves, Fresh Weight, and Dry weight were noted on the germination's 10th (Fig. 1), 20th (Fig. 2), and 30th (Fig. 3) days. The parameters were noted as highest in control on the 10th day and highest at 20% on the 20th and 30th days. Shoot, Root Length, and Fresh Weight of Pods were also checked in mature plants (Fig. 4). All the parameters were noted the best in 20% of the Fly Ash concentrated mixture. A comparison was made between control soil and vermicomposted fly ash. Initially, the Morphology of the plant was observed. In 2005, Sharma and his co-worker (Jaroli & Sharma 2005) reported that since fly ash comprises useful nutrients, it enhances the availability of the micro and macro elements for plants. Observations noted after 10 days depicted that the root length initially increased when the concentration increased to 20% (Fig. 1). The length was 12.86 cm as opposed to 9.43cm for control. With the increase in concentration to 50 %, the length decreased to 10.36 cm (Fig. 3).

Further Increase in concentration ultimately resulted in a decrease in the root length. Thus, vermicomposted fly ash suitably favors root length growth at optimal concentration, but the effects are reversed with increased concentrations. Studies by (Emamverdian et al. 2015) have

Fig. 1: Growth of *Ricinus communis* L. on the 10th Day.

Fig. 2:   Growth of *Ricinus communis* L. on the 20th Day.
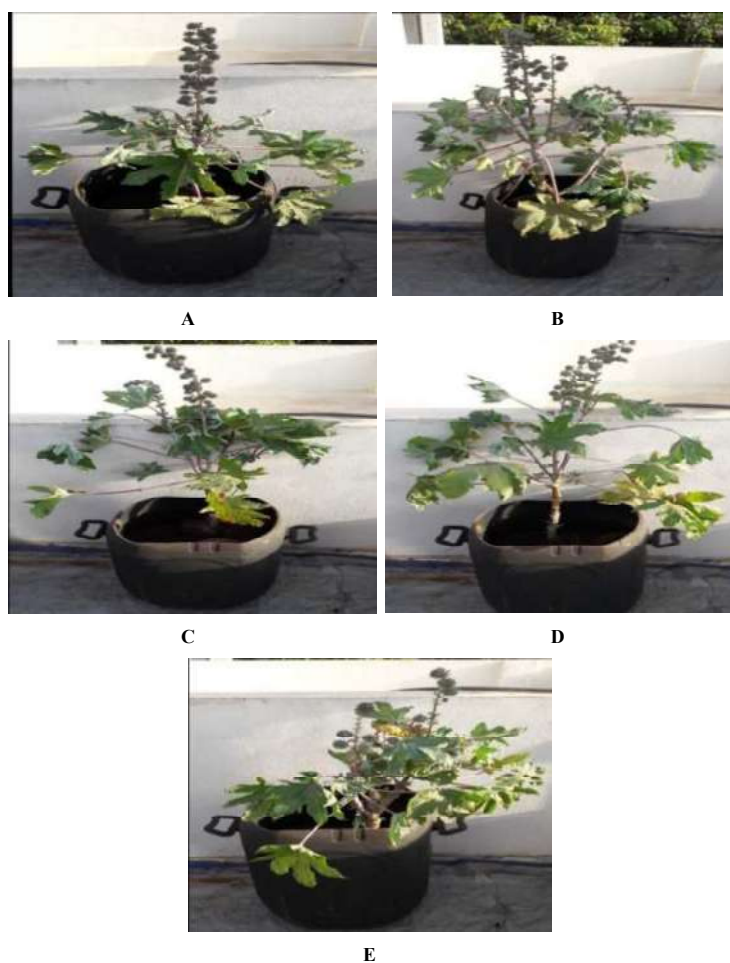
Fig. 3: Growth of *Ricinus communis* L. on the 30th Day.

Fig. 4: Mature plants of *Ricinus communis* L. in different concentrations of Fly ash.
A. Plant is grown in Control.
B. Plant is grown in 20% fly ash.
C. Plant is grown in 50% fly ash.
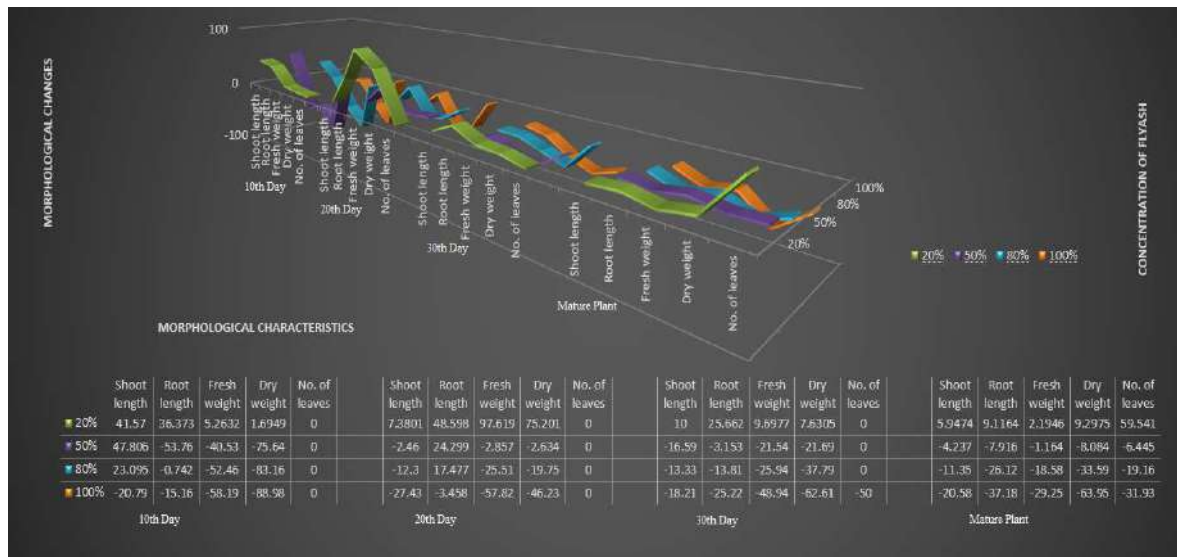D. Plant is grown in 80% fly ash.
E. Plant is grown in 100% fly ash.

Fig. 5: Graphical representation of morphological changes occurred in *Ricinus communis* L.

	Shoot length	Root length	Fresh weight	Dry weight	No. of leaves		Shoot length	Root length	Fresh weight	Dry weight	No. of leaves		Shoot length	Root length	Fresh weight	Dry weight	No. of leaves		Shoot length	Root length	Fresh weight	Dry weight	No. of leaves
20%	41.57	36.373	5.2632	1.6949	0		7.3801	48.598	97.619	75.201	0		10	25.662	9.6977	7.6305	0		5.9474	9.1164	2.1946	9.2975	59.541
50%	47.806	-53.76	-40.53	-75.64	0		-2.46	24.299	-2.857	-2.634	0		-16.59	-3.153	-21.54	-21.69	0		-4.237	-7.916	-1.164	-8.084	-6.445
80%	23.095	-0.742	-52.46	-83.16	0		-12.3	17.477	-25.51	-19.75	0		-13.33	-13.81	-25.94	-37.79	0		-11.35	-26.12	-18.58	-33.59	-19.16
100%	-20.79	-15.16	-58.19	-88.98	0		-27.43	-3.458	-57.82	-46.23	0		-18.21	-25.22	-48.94	-62.61	-50		-20.58	-37.18	-29.25	-63.95	-31.93
	10th Day						20th Day						30th Day						Mature Plant				

highlighted that fly ash benefits plants up to some optimum concentration.

The given histogram (Fig. 5) illustrates the morphological changes that occurred in *Ricinus communis* L. during the addition of fly ash with different concentrations of 20%, 50%, 80%, and 100%. The primary changes transpire in the shoot length, root length, number of leaves, measured fresh weight, and dry weight in different time intervals such as the 10th day, 20th day, 30th day, and after the plant's maturation. A cursory glance shows that the leaves emerged after the plant's maturation in a 20% fly ash concentration. Approximately 60 leaves were observed.

To start with, among all the concentrations of fly ash, 20% was optimized and gave a pleasant outcome. In the shoot length, the concentration of fly ash 20% and 50% give around 42% and 48% growth, respectively (all these percentages are compared with control), which was maximum on the 10th-day incubation. Speculating more, after the 20th and 30th days of incubation, shoot lengths reach up to 8% and 10%, respectively, greater than the control. After the plant's maturation, around 6% of the shoot length was greater than the control plant. In contrast, oddly, 50%, 80%, and 100% concentrations of fly ash give a negative outcome (except on 10th-day incubation in 80%), showing the inhibitory effect on plant growth, indicating that it would be catastrophic.

Moreover, in root length among all the incubation with fly ash on the 10th day, 20% was decent for the growth around 37%, and if we talk about 50%, 80%, and 100% provide negative aftermath after the 20th-day incubation gives better growth in 20%, 50% and 80% around 49%, 24%,

and 18% respectively, somehow in 100% obtained negative stimulation. On the 30th day, 20% fly ash concentration gives 26%; after the plant's maturation, it gets 10% higher than the control plant. It also indicated that fly ash was also responsible for the development of roots.

With germination, plants gain some weight for their physical stability. Here we scaled two types of weights, first fresh weight, and second dry weight. It has been seen in the graph overall, only 20% could be the best. More precisely, on the 10th day of incubation, fresh weight increased by around 5.3%. On the 20th day, it reached up to 98%, and on the 30th day, around 10% increment was noted, whereas at the maturation, around 2.1% weight was increased in the control plant. However, 50%, 80%, and 100% had given negative stimulation for the plant weight. This elucidation indicated that the huge concertation of fly ash inhibited plant growth. Besides, the same outcome was obtained on the 10th day of incubation; somehow, dry weight in 20% fly ash concentration increased by 1.7%. On the 20th day, it increased to around 75%. On the 30th day, it was around 8%, and finally, at the maturation, approximately a 9.3% increment from the control plant was noted. Also, 50%, 80%, and 100% did not satisfy results, were observed. This indicated that higher fly ash concentration shows detrimental consequences for their stimulation.

Cytogenetic Study

The chromosome number in *Ricinus communis* L. is 2n=20. Cytological effects of vermicomposted fly ash with different concentrations were checked in *Ricinus communis* L. root

Table 4: Effect of different concentrations of vermicomposted fly ash on root tip cells of *Ricinus communis L.*

Concentration (%)	Control	20	50	80	100
Mitotic Index (%)	95.51±1.300	96.45±0.930	86.04±0.772	67.99±1.798	52.22±0.831
Aberrant Cells(%)	0.000±0.000	0.023±0.023	1.420±0.381	6.95±0.504	13.26±0.381

A

B

C

D

E
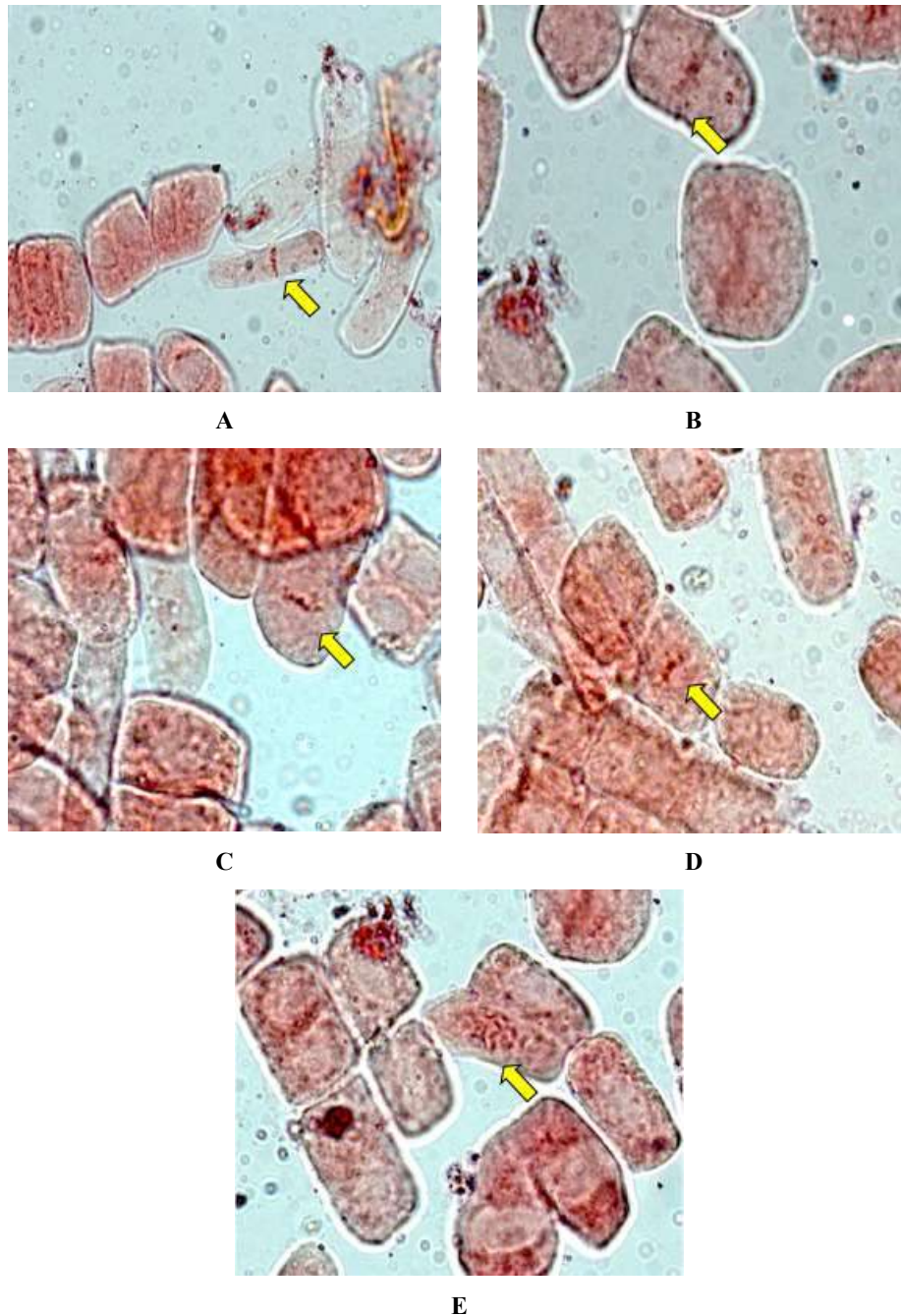
Fig. 6: Chromosomes of *Ricinus communis* L.A. Anaphase in control.
B. Metaphase in 20% fly ash.
C. Disturbed Metaphase in 50% fly ash.
D. Disturbed Metaphase in 80% fly ash.
E. Scattered chromosome in 100% fly ash.

tip cells. The study revealed that mitotic division increased in the presence of fly ash and created some abnormalities at higher concentrations. The percentage of the mitotic index decreased, and the percentage of aberrant cells increased with the higher fly ash concentration. The percentage of aberrant cells in control was negligible (Table 4). This indicates the presence of a certain cytotoxic or genotoxic substance in fly ash. The reduction in the mitotic index could be due to the inhibition of DNA synthesis or blocking in the G2 phase of the cell cycle, preventing the cell from entering mitosis (Sudha et al. 2018). No abnormalities were noted in Control and 20% fly ash concentration. While some abnormalities, like Disturbed metaphase and Scattered Chromosomes, were observed in the rest of the concentrations (Fig. 6). Disturbed metaphase was observed in 50% and 80% fly ash concentrations. Whereas, scattered chromosome was observed in 100% fly ash concentration. Disturbance during metaphase arises because of the effect of the treatment on the spindle that, leads to failure of the spindle mechanism. Chromosome scattering results from a prolonged metaphase arrest and is characterized by an uncoordinated loss of chromatid cohesion (Ananthakrishnasamy et al. 2009).

CONCLUSION

The present investigation indicates that the lower concentration of Fly Ash, i.e., 20% works as the enhancer for plant growth when mixed with pressmud, and the mixture is vermicomposted. The higher amount of Fly Ash can be toxic at the chromosome level, and hence it influences the overall growth of the plant.

REFERENCES

Ahmad, S. 2015. Impact of coal-based thermal power plant on environment and its mitigation measure. Coal Manag., 1: 60-64.

Ananthakrishnasamy, S., Sarojini, S., Gunasekaran, G. and Manimegala, G. 2009. Flyash - A lignite waste management through vermicomposting by indigenous earthworms *Lampito mauritii*. J. Agric. Environ. Sci., 5(6): 720-724.

Chakraborty, S., Solanki, R., Dave, J., Rana, S., Kumar, R.N. and Bhattacharya, T. 2009. Effect of airborne fly ash deposition on morphology and biochemical parameters of *Medicago sativa* L . and *Brassica juncea*. Res. Environ. Life Sci., 2(1): 13-16.

Daniels, W., Stewart, B., Haering, K. and Zipper, C. 2002. The potential for beneficial reuse of coal fly ash in southwest Virginia mining environments. Coal Manag., 15: 36

Emamverdian, A., Ding, Y., Mokhberdoran, F. and Xie, Y. 2015. Plant defense response. Sci. World J., 16: 7-9.

Jaroli, D.P. and Sharma, B.L. 2005. Effect of organophosphate insecticide on the organic constituents in liver of *Channa punctatus*. Asian J. Exp. Biol. Sci., 19(1): 121-129.

Khan, A., Javid, S., Muhmood, A., Majeed, T., Niaz, A., Majeed, A., Eddleman, K., Chinwendu, S., Emmanuel, E., Ifeanyi, N., Micheal, C., State, A., Aba, P., Polytechnic, A. S., Polytechnic, A. S., Polytechnic, A. S., Chemicals, P. O., Lakes, G., Safe, E. and Kartal, S. 2013. What is bioaccumulation ? What are persistent chemicals ? Acad. J., 3(1): 1-4.

Kumar, V., Singh, G. & Rai, R. 2005. Fly ash : A material for another green revolution. fly ash India, 12, 1-16.

Mistry Brijal, Jadav Rajendra, P. K. 2018. Soil irrigation effect of thermal power plant effluent on biochemical changes of *Pisum sativum* L. Int. J. Sci. Res., 4(2): 839-844.

Mupambwa, H.A., Dube, E. and Mnkeni, P.N.S. 2015. Fly ash composting to improve fertiliser value: A review. S. Afr. J. Sci., 111(7-8): 1-6.

Raval, R.U., Patel Kailash, P.J. R. and R. M. N. 2018. Effects of vermicomposted fly ash on morphological and biochemical attributes including antioxidant enzymes of *Allium cepa* L. Biosci. Disc., 9(1): 166-170.

Sharma, V. and Akhai, S. 2019. Trends in utilization of coal fly ash in India: A review. J. Eng. Desg. Anal., 2(1): 12-16.

Sharma, S.K. and Kalra, N. 2006. Effect of fly ash incorporation on soil properties and productivity of crops: A review. JSIR, 65(5): 383-390.

Sudha, M.R., Jayanthi, N., Aasin, M., Dhanashri, R.D. and Anirudh, T. 2018. Efficacy of *Bacillus coagulans* unique IS2 in treatment of irritable bowel syndrome in children: A double-blind, randomized placebo-controlled study. Benef. Microbes, 9(4): 563-572. https://doi.org/10.3920/BM2017.0129

Swamy, T.N., Dash, N., Nahak, G., Deo, B. and Sahu, R.K. 2010. Effect of coal fly ash on growth, biochemistry, cytology, and heavy metal content of *Allium cepa*. Science, 3(5): 10-16.

Study on the Adsorption Properties of Cr(VI) by Biochar with Different Treatments

X. Zhang*†

*Department of International Education, Beijing University of Chemical Technology, Beijing 100029, P. R. China
†Corresponding authors: Xinyu Zhang; 1691748468@qq.com

ABSTRACT

The paper investigated the adsorption of Cr(VI) on biochar in simulated wastewater by static adsorption method, Fourier Transform Infrared spectra (FTIR), Raman, X-ray photoelectron spectroscopy (XPS), scanning electron microscope (SEM), and transmission electron microscope (TEM) characterization analysis. The results show that biochar can effectively remove Cr(VI) in wastewater, and the adsorption equilibrium can be quickly reached within 100 min. The kinetic analysis shows that the quasi-second-order kinetic model can better fit the kinetic process of Cr(VI) adsorption by biochar, which shows that the main mechanism of the adsorption is the chemical bonding cooperation between Cr(VI) and the functional groups on the surface of biochar. Fit analysis of the isotherm at different temperatures shows that temperature increase promotes the adsorption of Cr(VI) on biochar, and thermodynamic analysis reveals that the adsorption of Cr(VI) on biochar is a spontaneous endothermic process. The Freundlich model effectively fits the adsorption isotherm of Cr(VI), indicating that the surface of biochar is uneven and Cr(VI) has undergone multilayer adsorption. The adsorption isotherm of Cr(VI) under the influence of HA and FA can be effectively fitted by the Freundlich model, and the adsorption efficiency is the highest when FA is added. The national analysis of Fourier Transform Infrared spectra (FTIR), Raman, X-ray photoelectron spectroscopy (XPS), scanning electron microscope (SEM), and transmission electron microscope (TEM) further reveals the bond cooperation between Cr(VI) and the surface functional groups of biochar. The results show that biochar has potential application value in treating chrome-containing wastewater.

INTRODUCTION

With the rapid development of industry and commerce, a large amount of chromium-containing wastewater is produced in industrial production processes such as metal smelting, electroplating, tanning, printing, and dyeing, which is discharged into natural water bodies, seriously polluting the soil and groundwater environment (Zou et al. 2021). In nature, the main valence states of chromium (Cr) are trivalent and hexavalent, among which the compounds of chrome (Cr(VI)) are usually highly water-soluble and usually present in the form of CrO_4^{2-} and $Cr_2O_7^{2-}$ in the wastewater. With high toxicity, carcinogenicity, mutagenicity, and teratogenicity, Cr(VI) is hundreds of times more toxic than Cr(III), which may cause many serious health problems (Chen et al. 2018). Therefore, efficient and environmentally friendly methods are urgently needed to restore Cr(VI) in the environment.

Nowadays, the treatment of chrome-containing wastewater is mainly about physical and chemical methods, including chemical precipitation, ion exchange, flocculation, membrane treatment, adsorption, and so on. Adsorption is an efficient treatment method to remove heavy metal pollutants in water, usually using carbon adsorbents, clay mineral adsorbents, and adsorption resins (Wang et al. 2022). As a pore-rich carbon material formed under high temperatures and the conditions of hypoxia or no oxygen, biochar has the characteristics of high specific surface area, abundant surface active functional groups, and strong ion exchangeability, showing great development potential in the field of heavy metal pollution remediation (Mian & Liu 2018). Lyu et al. (2017, 2018) studied the removal of hexavalent chromium from aqueous solutions and in contaminated soils by a novel biochar-supported nanoscale iron sulfide composite. Herein, this paper selects biochar as the adsorbent of Cr(VI) in simulated wastewater and studies the effects of initial Cr(VI) concentration, reaction temperature, humic acid (HA), fulvic acid (FA), and other factors on the adsorption of Cr(VI) by biochar, conduct adsorption kinetics, adsorption isotherm, and material characterization analysis, and explore the mechanism of Cr(VI) adsorption by biochar and its potential application value in the treatment of chrome-containing wastewater.

MATERIALS AND METHODS

Experimental Materials and Instruments

The chemicals used in the experiment, such as potassium dichromate, diphenylcarbazide, sulfuric acid, hydrochloric acid, ethanol, sodium hydroxide, etc., are all commercially available analytical reagents. No purification treatment was done before use, and all solutions were prepared with deionized water. Some of the instruments used are as follows: pH meter (Five Easy plus, Mettler-Tollidor Instrument (Shanghai) Co., LTD.), Table type Low-temperature Constant Temperature Oscillating Shaker (PSE-T150A, Stoker Instrument Equipment (Shanghai) Co., LTD.), Electronic balance (AL204, Mettler-Tollidor Instrument (Shanghai) Co., LTD.), Uv-visible spectrophotometer (SP-756-P(scanning type), Shanghai spectrometer Co., LTD.), drum heating constant temperature drying oven (DHG-9053A, Shanghai sanfa scientific instrument Co., LTD.), automatic micro confocal Raman spectrometer (XploRA PLUS, Horiba France SAS Co., LTD.) France), Fourier Transform Infrared spectrometer (NICOLET6700, Thermo Scientific).

Adsorption Experiments

Adsorption of Cr(VI) by biochar: Under different reaction conditions (reaction time, HA, FA, temperature), static adsorption experiments on Cr(VI) are carried out. In each group of experiments, a certain amount of chromium standard solution is taken into glass bottles, diluted to a suitable concentration with deionized water, adjust pH with HCl (1.0 mol.L^{-1}) and NaOH (1.0 mol.L^{-1}). Finally, biochar is added, and the reaction temperature and time are controlled. After ultrasound for 30 min, the reaction is carried out in a constant temperature shaker. After the reaction, a pinhead filter filters part of the solution, and the concentration of Cr(VI) in the filtrate is determined by photometry.

Analysis of the Cr(VI) content in the liquid phase: Transfer the filtered solution shaken well into a glass bottle with a pipette, add 0.5 mL sulfuric acid solution and 0.5 mL 1+1 phosphoric acid solution, and shake up. Add 2 mL color developing agent (I) and shake up. After a period of time, use a 10 mm colorimetric dish to measure the absorbance of the sample at the wavelength of 540 nm. After deducting the absorbance of the blank experiment, the content of Cr(VI) can be obtained from the calibration curve. Calculate the Cr(VI) content in the liquid phase according to the calibration curve.

RESULTS AND DISCUSSION

Sorption Kinetics

Fig. 1 shows the adsorption kinetics of Cr(VI) by biochar under different initial Cr(VI) concentrations, and the overall trend is similar. According to Fig. 1(A), the adsorption of Cr(VI) by biochar increases with time. Due to the many adsorption sites on the biochar surface, the adsorption of Cr(VI) by biochar increases rapidly in the first 20 min. As the adsorption reaction proceeds, the point sites on the biochar surface tend to be saturated. The adsorption rate mainly
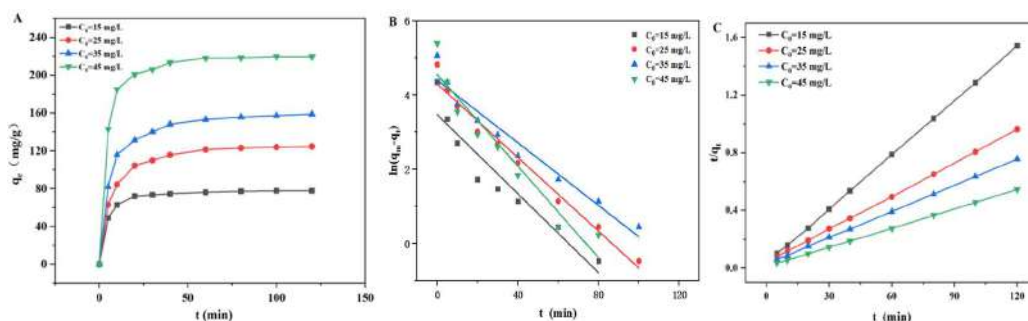

Fig. 1: Results of the dynamic adsorption experiment under different concentration conditions: Results of adsorption amount of biochar on Cr(VI) at different concentrations (A), Results of the first-order dynamic fitting curve (B), Results of the second-order dynamic fitting curve (C).

Table 1: Results of experimental adsorption kinetics at different concentrations.

Conditions	Pseudo-first-order model			Pseudo-second-order model		
	q_e [mg.g^{-1}]	K_1 [h^{-1}]	R^2	q_e [mg.g^{-1}]	K_2 [mg·mg^{-1}.h^{-1}]	R^2
C_0=15 mg.L^{-1}	32.254	0.05322	0.90497	79.6178	4.750	0.99995
C_0=25 mg.L^{-1}	74.135	0.04963	0.97972	130.3781	1.474	0.99991
C_0=35 mg.L^{-1}	82.122	0.04225	0.9542	165.0165	1.247	0.99993
C_0=45 mg.L^{-1}	95.238	0.06175	0.9286	224.7191	1.866	0.99993

depends on the speed of Cr(VI) entering the internal point sites, and the adsorption rate decreases gradually (Chen et al. 2017). After 100 min, the adsorption amount is unchanged with time, and the reaction reaches adsorption equilibrium. The maximum adsorption amount of biochar on 15, 25, 35, and 45 mg.L^{-1} Cr(VI) are 77.726, 124.515, 158.783, and 219.657 mg.g^{-1}. Due to the short time required to reach equilibrium, the adsorption of Cr(VI) by biochar is mainly a chemical reaction (Chawla et al. 2016). In the follow-up experiment, the contact time is at least 100 min to achieve a complete adsorption balance.

To obtain more information on the adsorption mechanism of Cr(VI), two models (equations (1) and (2)), the quasi-first-order kinetic model and the quasi-second-order kinetic equation, are used to study the kinetic adsorption process of Cr(VI):

$$\ln (q_m - q_t) = \ln q_e - k_1 t \qquad \ldots(1)$$

$$\frac{t}{q_t} = \frac{1}{k_2 q_e^2} + \frac{t}{q_e} \qquad \ldots(2)$$

q_t (mg.g^{-1}) represents the adsorption capacity of Cr(VI) by biochar at adsorption equilibrium, and q_e (mg.g^{-1}) represents the adsorption capacity of Cr(VI) by biochar at adsorption time t. k_1 (h^{-1}) and k_2 (mg·mg^{-1}·h^{-1}) are the rate constants of the quasi-first-order and quasi-second-order kinetic equations. The experimental data of different initial concentrations of Cr(VI) are fitted and analyzed, and the results are shown in Fig. 1 B and C, respectively. The fitting parameters of adsorption kinetics are listed in Table 1. According to Table 1, when fitting the experimental data with the quasi-second-order kinetic model, the correlation coefficient (R^2) reached 0.99995, much higher than the fitting data of the quasi-first-order kinetic model. Therefore, the adsorption characteristics of Cr(VI) by biochar are more consistent with the quasi-second-order kinetic model, which indicates that the adsorption of Cr(VI) by biochar is mainly based on the chemisorption of ion exchange and chelation reaction between surface compounds and activated functional groups on biochar (Herath et al. 2021).

Adsorption Isotherms at Different Temperatures

Fig. 2 shows the thermodynamic curves of biochar adsorption of Cr(VI) at different temperatures. According to Fig. 2(A), the adsorption capacity of Cr(VI) on biochar gradually increases with the increase of system temperature, indicating that high temperature is conducive to the adsorption of Cr(VI) and biochar adsorption of Cr(VI) is a spontaneous endothermic process. To further obtain the influence of biochar surface on adsorption, Langmuir and Freundlich models (equations 3 and 4) are used for the fitting analysis

of isotherms, respectively:

$$\frac{c_e}{q_e} = \frac{c_e}{q_{max}} + \frac{1}{k_l q_{max}} \qquad \ldots(3)$$

$$\lg q_e = \lg k_f + \frac{1}{n} \lg c_e \qquad \ldots(4)$$

Herein, q_e (mg.g^{-1}) is the adsorption amount of Cr(VI) by biochar when the adsorption reaction reaches equilibrium, and c_e (mg.L^{-1}) is the concentration of Cr(VI) in the solution after the adsorption reaches the equilibrium. $1/n$ is the Freundlich constant, k_f is the equilibrium constant of the Freundlich adsorption isothermal model, and k_l is the Langmuir adsorption isothermal model (Fan et al. 2009). The results of isotherm fitting analysis at different temperatures are shown in Fig. 2, and the fitting parameters are listed in Table 2. According to Fig. 2 and Table 2, the Freundlich adsorption isotherm model can better describe the adsorption of Cr(VI) by biochar at different temperatures, indicating that the adsorption process of Cr(VI) by biochar is not only single-molecular layer adsorption but multi-layer adsorption from outer layer to the inner layer (Ho & Mckay 2000). A comparison of adsorption amounts of Cr(VI) on biochar with other common adsorbents such as diatomite (108.56 mg.g^{-1}), activated carbon (257.64 mg.g^{-1}), zeolite (206.37 mg.g^{-1}), activated alumina (164.59 mg.g^{-1}), revealed that biochar exhibited much higher adsorption than other common adsorbents did. These results demonstrated that the biochar investigated herein could be a promising adsorbent to effectively decontaminate toxic Cr(VI) in wastewater.

Adsorption Isotherms under the Influence of HA and FA

Fig. 3 shows the isothermal adsorption of Cr(VI) of biochar under the influence of HA and FA. According to Fig. 3, the biochar with FA has the largest adsorption of Cr(VI), followed by biochar with HA, and the adsorption amount of Cr(VI) is the lowest without HA or FA addition. The adsorption amount of Cr(VI) of biochar with FA is significantly higher than that of HA, indicating that FA can improve biochar's adsorption performance on Cr(VI). To further obtain the influence of biochar surface on adsorption, the paper fits the isotherms with Langmuir and Freundlich models (equations 3 and 4). The results of the isotherm fitting under the influence of HA and FA are shown in Fig. 3, and the fitting parameters are listed in Table 3. According to Fig. 3 and Table 3, the Freundlich adsorption isotherm model can better describes the adsorption of biochar to Cr(VI) under the influence of different HA and FA, indicating that the adsorption process of Cr(VI) under the influence of HA and FA is not only single-molecular layer adsorption but multi-layer adsorption from outer layer to the inner layer.
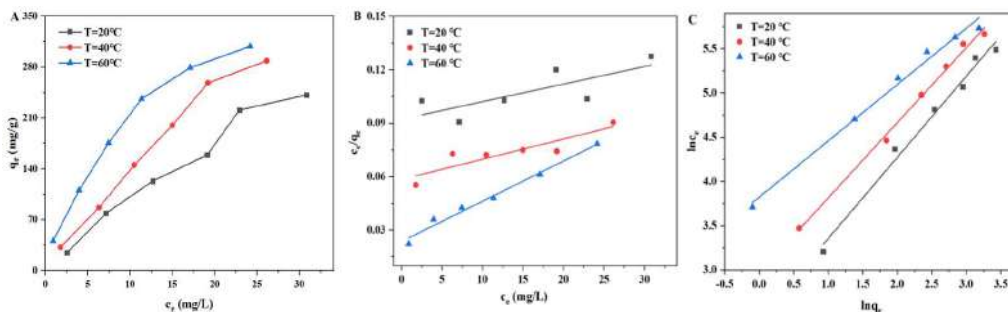
Fig. 2: Adsorption isotherms at different temperatures (A), Langmuir Model fitting result (B), Freundlich Model fitting result (C).

Table 2: Adsorption isotherm fitting results at different temperatures.

Experiment Condition	Langmuir model			Freundlich model		
	q_m [mg.g^{-1}]	K_L [h^{-1}]	R^2	n	K_L [g·mg^{-1}.h^{-1}]	R^2
T=20°C	1014.3572	0.0107	0.59205	1.0898	11.453	0.99047
T=40°C	884.9558	0.0193	0.80384	1.1772	19.417	0.98452
T=60°C	442.4779	0.0959	0.98405	1.5712	45.756	0.99563

Moreover, FA can improve biochar's adsorption performance to Cr(VI) (Deng et al. 2021).

DISCUSSION

FTIR Analysis

Surface properties of the biochar before and after the adsorption of Cr(VI) are characterized and analyzed by FTIR and Raman spectra. The biochar's infrared spectrum (FTIR) is shown in Fig. 4(A). According to Fig. 4(A), the

biochar after Cr(VI) adsorption mainly has five characteristic absorption peaks. The peak at ~450 cm^{-1} can be attributed to the complexation between the metal and oxygen, indicating that Cr(VI) successfully adsorption onto the biochar surface. According to the Raman spectra of the biochar before and after the adsorption of Cr(VI), the peak located at ~1350 cm is attributed to the D segment of the defective structural biochar, indicating the disorder and defect degree of the biochar. The peak located at ~1580 cm is attributed to the G segment of the biochar with the sp^2 characteristic structure,
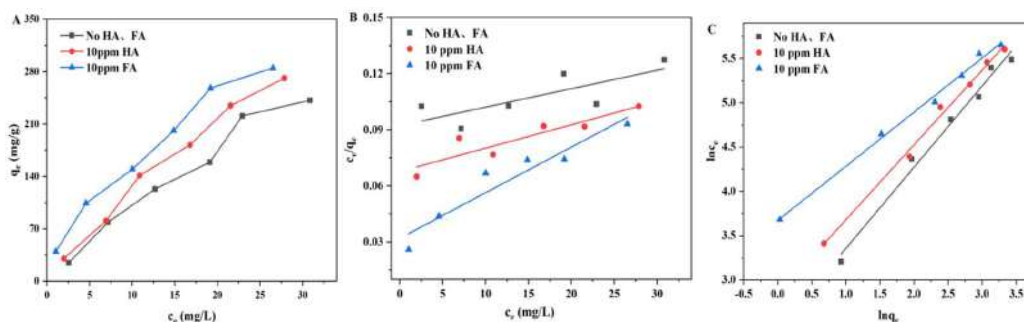

Fig. 3: Adsorption isotherms under the influence of HA and FA (A), Langmuir Model fitting results (B), Freundlich Model fitting results (C).

Table 3: Results of the adsorption isotherms fitting under the influence of HA and FA.

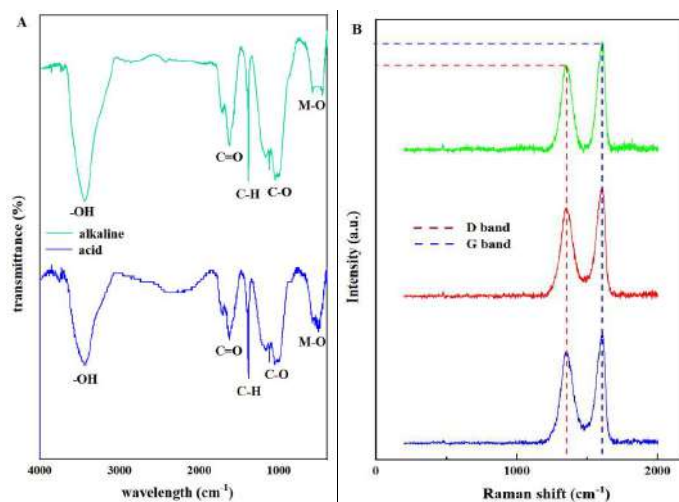| Experiment Condition	Langmuir model			Freundlich model		
	q_m[mg.g^{-1}]	K_L[h^{-1}]	R^2	n	K_L[g·mg.h^{-1}]	R^2
No HA, FA	79.6178	0.3782	0.59205	1.0898	11.453	0.98694
10 mg/L HA	130.3781	0.1922	0.82703	1.1828	17.022	0.99435
10 mg/L FA	165.0165	0.2057	0.91533	1.6348	39.319	0.99484

Fig. 4: Infrared spectrogram of Cr(VI) under acid and alkaline conditions (A). Raman spectra before and after Cr(VI) adsorption under acid and alkaline conditions (B).
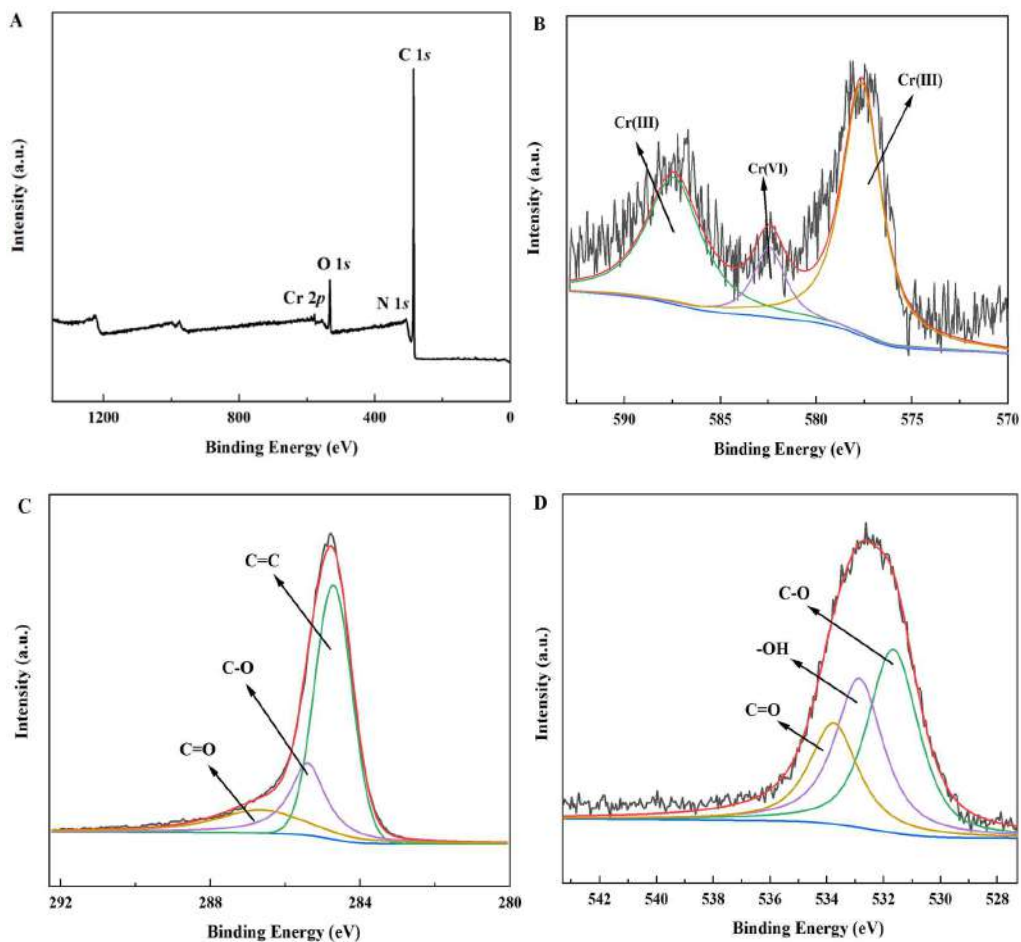

Fig. 5: Full spectrum of biochar after Cr(VI) adsorption (A). Cr 2p XPS Spectrum map (B). C 1s XPS spectra of biochar after Cr(VI) adsorption (C). O 1s XPS spectra of biochar after Cr(VI) adsorption (D).
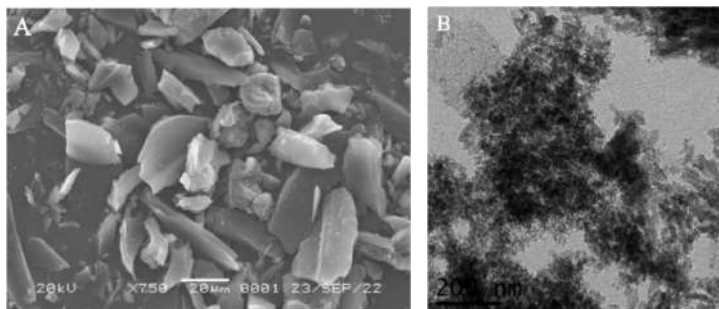
Fig. 6: SEM diagram of the biochar after adsorption of Cr(VI) (A). TEM biochar diagram after Cr(VI) (B) adsorption.

indicating the symmetry and crystallinity of the biochar (Wang et al. 2015). According to Fig. 4(B), the intensity ratio of D and G peaks on Raman spectra differs before and after biochar adsorption. This indicates that the defects and C hybrid structures on the biochar surface have changed after absorbing Cr(VI).

XPS Analysis

The XPS full spectrum of biochar after Cr(VI) adsorption is shown in Fig. 5(A). After adsorption, a new Cr 2p characteristic peak appears, indicating that Cr ions are successfully adsorbed on the surface of biochar (Hou et al. 2020). According to Cr 2p monoelement spectrum (Fig. 5(B)), after the adsorption of Cr(VI), the three peaks produced are two Cr(VI) peaks and one Cr(VI) peak, indicating that biochar reduces part of Cr(VI) to Cr(VI). According to the single element spectrum of C 1s (Fig. 5(C)), there are three types of C, and the peaks at 284.71 eV, 285.40 eV, and 286.65 eV correspond to C=C, C-O, and C=O (Yang et al. 2016). According to the single element spectrum of O 1s (Fig. 5(D)), there are three types of O, and the peaks at 531.67 eV, 532.86 eV, and 533.77 eV correspond to C-O, -OH, and C=O (Wilson & Langell 2014).

SEM and TEM Analysis

Employing scanning electron microscope (SEM) and transmission electron microscope (TEM) to gain the morphology and structure of biochar after the adsorption of Cr(VI), and the results are shown in Fig. 6. According to Fig. 6(A), biochar is composed of many irregular blocks, which are about 10-50 µm long. According to Fig. 6(B), after Cr(VI) adsorption, there are a large number of network materials on the surface of biochar, indicating that Cr(VI) is adsorbed on the biochar surface, and some new reticular substances are formed.

CONCLUSION

Selecting biochar as the adsorbent material, the paper studies the removal performance, influencing factors, and adsorption

mechanism of Cr(VI) by static and characterization methods. The results are as follows:

(1) Biochar has a strong adsorption capacity for Cr(VI), and the adsorption reaches a dynamic equilibrium at ~100 min. Moreover, the quasi-second-order kinetic model can better describe the dynamics of Cr(VI), indicating that the adsorption of Cr(VI) by biochar is mainly the chemisorption of ion exchange and chelation reactions between activated functional groups.

(2) Isotherm analysis shows that the adsorption of Cr(VI) is a spontaneous heat absorption process and more in line with the Freundlich equation, indicating that the adsorption process is mainly multilayer adsorption from the outer layer to the inner layer. The adsorption amount of Cr(VI) of biochar with FA is significantly higher than that of HA, indicating that FA can improve biochar's adsorption performance to Cr(VI).

(3) The characterization analysis shows that after the adsorption of Cr(VI), the biochar surface's defect structure and C atomic hybrid structure are changed. Biochar reduces part of Cr(VI) into Cr(III). After the adsorption of Cr(VI) on the surface of biochar, some new substances similar to the network are formed.

REFERENCES

Chawla, A., Prasad, M., Goswami, R., Ranshore, S., Kulshreshtha, A. and Kumar S.A.S. 2016. Kinetic model for sorption of divalent heavy metal ions on low-cost minerals. Korean. J. Chem. Eng., 33(2): 649-656.

Chen, L., Zhou, S.L., Shi, Y.X., Wang, C.H., Li, B.J., Li, Y. and Wu, S.H. 2018. Heavy metals in food crops, soil, and water in the Lihe River watershed of the Taihu Region and their potential health risks when ingested. Sci. Total Environ., 615:141-149.

Chen, N., Kang, M.M., Jiang, X., Wang, H.S., Jia, X.F. and Ji, Y.X. 2017. Study on adsorption mechanism of Cr(VI) from aqueous solutions on biochar produced from coconut shell. Environ. Sci. Manag., 42(12): 66-69.

Deng, C.Y., Lü, J.W. and Chen Z.Y. 2021. Adsorption kinetics and thermodynamics analysis of U(VI) by microbial putrefaction. J. Univ. South China, 35(3): 56.

Fan, Q.H., Shao, D.D., Lu, Y., Wu, W.S. and Wang, X.K. 2009. Effect of

pH, ionic strength, temperature, and humic substances on Ni(II) sorption to Na- attapulgite. Chem. Eng. J., 150(1): 188-195.

Herath, A., Laynea, C., Perezb, F., Hassanc, E.B., Pittmana, C.U. and Mlsnaa, T. 2021. KOH-activated high surface area Douglas fir biochar for adsorbing aqueous Cr(VI). Chemosphere, 269: 128409.

Ho, Y.S. and Mckay, G. 2000. The kinetics of sorption of divalent metal ions onto sphagnum moss flat. Water Res., 34(3): 735-742.

Hou, S.Z., Tian, H.R., Huang, C., Wang, P., Zeng, Q.J., Peng, H.L., Liu, S.L. and Li, A. 2020. Removal of Cr(VI) from aqueous solution by amino-modified biochar supported nano zero-valent iron. Acta Sci. Circum., 40(11): 3931-3938.

Lyu, H., Tang, J., Huang, Y., Gai, L., Zeng, E.Y., Liber, K. and Gong, Y. 2017. Remove hexavalent chromium from aqueous solutions by a novel biochar-supported nanoscale iron sulfide composite. Chem. Eng. J., 322: 516-524.

Lyu, H., Zhao, J., Tang, Y., Gong, Y., Huang, Q., Wu, B. and Gao, G. 2018. Immobilization of hexavalent chromium in contaminated soils using biochar-supported nanoscale iron sulfide composite. Chemosphere, 194: 360-369.

Mian, M.M. and Liu, G.J. 2018. Recent progress in biochar-supported

photocatalysts: synthesis, the role of biochar, and applications. RSC Adv., 8(26): 14237-14248.

Wang, F.F., Wang, F., Gao, G.D. and Chen, W. 2015. Transformation of graphene oxide by ferrous iron: environmental implications. Environ. Toxicol. Chem., 34(9): 1975-1982.

Wang, K.X., Tang, X.H., Liu, L., Yao, S.S., Pu, Y., Zhao, F. and Chen, Q.Y. 2022. Adsorption of Cr(VI) from water by modified tea residue biochar. Shandong Chem. Ind., 51(21): 5-10.

Wilson, D. and Langell, M.A. 2014. XPS analysis of oleylamine/oleic acid capped Fe_3O_4 nanoparticles as a function of temperature. Appl. Surf. Sci., 303: 6-13.

Yang, J.P., Zhao, Y.C., Ma, S.M., Zhu, B.B., Zhang, J.Y. and Zheng, C.G. 2016. Mercury removal by magnetic biochar derived from simultaneous activation and magnetization of sawdust. Environ. Sci. Technol., 50(21): 12040-12047.

Zou, H.W., Zhao, J.W., He, F., Zhong, Z., Huang, J.S., Zheng, Y.L., Zhang, Y., Yang, Y.C., Yu, F., Bashir, M.A. and Gao, B. 2021. Ball milling biochar iron oxide composites for the removal of chromium (Cr(VI)) from water: Performance and mechanisms. J. Hazard. Mater., 413: 125252.

Integrated Method of Ozonation and Anaerobic Process for Treatment of Atrazine bearing Wastewater

Saba Khurshid*, Abdur Rahman Quaff*† and Ramakar Jha*

*Department of Civil Engineering, National Institute of Technology, Patna-800005, Bihar, India

†Corresponding author: Abdur Rahman Quaff; arquaff@nitp.ac.in

ABSTRACT

The paper presents the treatment of atrazine-contaminated wastewater by ozonation followed by an anaerobic process using Upflow Anaerobic Sludge Blanket (UASB) reactor. The experiment was performed with 100 ppb synthetic solutions of atrazine prepared in ultra-pure water. The corresponding initial Chemical Oxygen Demand (COD) is 226 mg.L^{-1}. The initial pH was adjusted to 9.5. The atrazine-bearing synthetic wastewater was ozonated with an ozone dose of 9.4mg/l for 40 minutes of optimum ozonation time, resulting in a 35% reduction in the initial concentration of atrazine. Along with atrazine reduction, there was a COD removal of 54.42%. Further, it was degraded with an anaerobic process, resulting in the final reduction in atrazine concentration of 81% and the corresponding removal in COD of 86.7%. The process of ozonation led to the mineralization of atrazine and enhancement in the biodegradability of the wastewater. Using ion chromatography, the ozonated wastewater sample was analyzed for ionic by-products before and after ozonation. The ion chromatography results showed the breaking of the atrazine compound and the formation of Cl$^-$, NO$_3^-$, SO$_4^{2-}$, and F$^-$ as intermediate products. Further, the BOD$_5$/COD ratio increased, reflecting the increased biodegradability. This ozonated wastewater was treated in a UASB reactor where the pesticide was degraded to 19 ppb, and COs degraded to 30 mg.L^{-1}. The overall removal of atrazine pesticide and COD were 81% and 86.7%, respectively, in the integrated system of ozonation followed by anaerobic degradation.

INTRODUCTION

The disposal from agrochemical industries contains many toxic substances of great environmental and health concern. This industry produces large amounts of organic wastewater with a significantly high COD. It has been found that pesticides are among the priority substances polluting water propagating to surface and groundwater (Philip & Ghosh 2006). In a monitoring program, pesticides have been widely noticed in European countries ranging from surface water to streams, rivers, lakes, reservoirs, and ditches (Oller et al. 2011). Some of these pesticides are recalcitrant, resistant to biological decay, and noxious for aquatic species. Among a wide range of recalcitrant chemicals released from this industry, atrazine is frequently found in water bodies worldwide (Philip & Ghosh 2006). It has been addressed as an emerging contaminant as it disrupts the endocrine system and is carcinogenic. The term "Emerging Contaminants" (ECs) has been defined in various ways. Still, fundamentally, it refers to any naturally occurring or artificial compounds that disrupt the endocrine system resulting in abnormal reactions. (Oller et al. 2011). Atrazine is among a series of an

s-triazine group of herbicides mainly used to control annual grass and broad-leafed weeds in maize, sorghum, pineapple, sugarcane, macadamia nuts, and many other crops (Philip & Ghosh 2006). It is also used on roadway grasses, golf course turf, and residential lawns. Due to its widespread use and solubility in water, it is found in surface and groundwater, exceeding its maximum contaminant level of 3 µg.L^{-1} (Ghosh et al. 2005). The World Health Organization has established a limit of 2 µg.L^{-1} for drinking water. (Ghosh et al. 2005). The European Union banned using atrazine as its degradation products remain in the soil even after 6 months (USEPA 2007). This reveals that it has a very high persistence in the environment. Atrazine is a pesticide commonly used as a model compound in research because it is a potential endocrine disruptor and is carcinogenic (USEPA 2007). Also, it remains hard to degrade due to its triazine ring, as shown in Fig. 1. (Mohammed & Mustafa 2017).

Atrazine is difficult to degrade with conventional coagulation, filtration, precipitation, reverse osmosis, etc., due to its high chemical stability and minimal biodegradability (Pathak 2011). Although biological
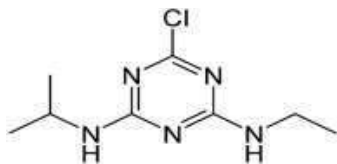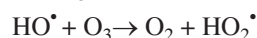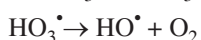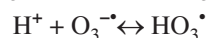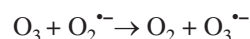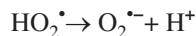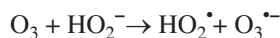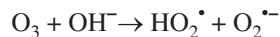
Fig. 1: Structure of atrazine.

processes are popular for treating such organic pollutants, many operational difficulties exist. Biological methods usually fail because of such toxic compounds as these compounds inactivate waste-degrading microorganisms. The low biodegradability of such compounds is another reason for low efficiency (Philip & Ghosh 2006). Removal of atrazine by adsorption is also considered a good technology. Still, the demerit is that the atrazine-contaminated wastewater from industries contains not only atrazine but also a large amount of dissolved organic matter, which decreases the adsorptive capacity of the adsorbent (Ghosh et al. 2005). There are studies on removing atrazine by aerobic and anaerobic processes, but they are neither efficient nor practicable because of operational difficulty (Ghosh et al. 2005). So the new idea is to partially pre-treat such toxic substances by Advanced Oxidation Processes (AOPs), forming more readily biodegradable intermediates (Covinich et al. 2014). Nowadays, ozone technology plays an important role in the degradation of refractory organic pollutants in an eco-friendly way (Hulsey et al. 2008). AOPs are chemical processes that are environmentally safe and prevent contaminants from moving from one phase to another. Rather, it degrades contaminants into harmless products in a short reaction time (Saleh et al. 2020). They can eliminate inorganic contaminants like cyanides, sulfides, nitrites, and dissolved organic contaminants, including halogenated hydrocarbons, volatile organic compounds, aromatic compounds, and nitrophenols, detergents, pesticides (Covinich et al. 2014). It can completely oxidize organic pollutants to CO_2, water, and salts. AOPs are generally categorized as ozone-based treatment, electrochemical AOP (eAOP), ultraviolet (UV)-based treatment, catalytic AOP (cAOP), and photo AOP (AOP). The effluents from pulp and paper mills and those from the chemical, petrochemical, textile, and other sectors can be treated using AOPs (Oller et al. 2011). The ozonation-based process of AOPs plays an important role in water treatment and can degrade refractory organic pollutants in an environmentally friendly way (Saleh et al. 2020). Ozone, an oxidizing gas, interacts directly or indirectly with inorganic and organic substances by producing hydroxyl radicals. Ozonation's best performance occurs at alkaline pH (Wang 2020). At alkaline pH the molecular ozone and the oxygen radicals, including the hydroxyl radical are present which

reacts with almost all organic and inorganic compounds (Oller et al. 2011). The breakdown of ozone produces free radicals ($HO_2^•$ and $HO^•$), which interact with various contaminants (Venkatesh et al. 2014). The mechanism of ozone decomposition at alkaline pH in aqueous solution is shown in the following equations.

$$O_3 + OH^- \rightarrow HO_2^• + O_2^{•-}$$
$$O_3 + HO_2^- \rightarrow HO_2^• + O_3^{•-}$$
$$HO_2^• \rightarrow O_2^{•-} + H^+$$
$$O_3 + O_2^{•-} \rightarrow O_2 + O_3^{•-}$$
$$H^+ + O_3^{-•} \leftrightarrow HO_3^•$$
$$HO_3^• \rightarrow HO^• + O_2$$
$$HO^• + O_3 \rightarrow O_2 + HO_2^•$$

The main factors affecting the ozonation process are pH, ozone dose, contact time, the type and amount of oxidizable organic compounds, the presence of ozone scavengers, and the ozone mass transfer (Oller et al. 2011). Numerous studies have looked at the use of ozone for the decomposition of pesticides and are well-reputed (Oller et al. 2011). Meijers et al. (1995) conducted a study on 23 pesticides using ozonation. Among them, six pesticides were removed efficiently: dimethoate, chlortoluron, diuron, isoproturon, motoneuron, and vinclozolin (Saleh et al. 2020). In another study, ozonation was used to degrade 40 pesticides (Ormad et al. 2010). Maldonado et al. (2006) conducted a study to observe the effect of ozone on five pesticides. In a study, when nano-ZnO (nZnO) was added to the ozonation process to remove atrazine from contaminated water, it was observed that the removal efficiency was higher than with the ozonation alone. The nZnO catalytic ozonation method successfully removed atrazine with an initial concentration between 0.5 and 5 mg.L^{-1}. When the initial loading concentration was raised to 5 mg.L^{-1}, the removal rate dropped to 90.2% (Pérez-Lucas et al. 2020). When ozonation was combined with UV light, it increased the removal of fluroxypyr to 92% (Saleh et al. 2020). Ozone helps to decompose detergents, chlorinate hydrocarbons, phenols, pesticides, and aromatic hydrocarbons (Derco et al. 2021). This literature shows that AOPs are powerful and efficient treatment methods for degrading recalcitrant materials or mineralizing stable, inhibitory, or toxic contaminants (Legrini et al. 1993, Venkatesh et al. 2015). At the first stage of degradation, AOP alters the compound's structure, making it more biodegradable. Further, it degrades the compound and reduces its toxicity. In the last step, it leads to the mineralization of organic compounds. Hence, AOPs can transform recalcitrant compounds into inorganic substances (CO_2 and H_2O_2) and lead to total and partial mineralization,

transforming them into more biodegradable substances. It has been reported that chemical oxidation for complete mineralization is usually expensive. Its combination with a biological treatment is widely reported to reduce operating costs (Covinich et al. 2014). Once these substances became biodegradable, it is treated through the biological process. The anaerobic process is more economical than the aerobic process. Among the anaerobic process, the UASB reactor has been extensively used to treat various wastewaters (Lettinga & Hulshoff Pol 1991, Ghosh et al. 2005). A number of aerobic and anaerobic treatment methods have been studied for the degradation of atrazine (Pathak 2011). But the bacterial culture in actual field is a difficult and is not feasible at all. Reports show that the anaerobic method is better than the aerobic method for aliphatic and aromatic compounds (Mandelbaum et al. 1993). Atrazine degrades more rapidly under anaerobic conditions than in aerobic environments (Kearney et al. 1965, Ghosh et al. 2005). Atrazine may completely degrade and mineralize through the economically viable method of biodegradation, which also yields simple chemicals like carbon dioxide, water, nitrogen, and organic materials (Baghapour et al. 2013). Biodegradation is the best method for eliminating atrazine and other herbicides from the environment. A study examined atrazine removal by two Pseudomonas bacteria (fluorescence and aeruginosa) and found that atrazine was significantly degraded by Pseudomonas bacteria (Baghapour et al. 2013). Combining biological and chemical processes may produce a more practical way to improve the treatability of refractory effluents by increasing the BOD_5/COD ratio (Oller et al. 2011).

MATERIALS AND METHODS

The herbicide 'atrazine' used in the experiment was of analytical grade from Sigma- Aldrich with a purity of 99.8%. All the chemicals used were of HPLC grade. Acetonitrile (99.9%) and methanol (99.7%) used were of HPLC grade of Merck company purchased from Angel Scientific. NaOH and H_2SO_4 were used for adjusting pH. Ultrapure water was prepared using a Milli-Q system. Sucrose ($C_{12}H_{22}O_{11}$), ammonium chloride (NH_4Cl), and potassium dihydrogen orthophosphate (KH_2PO_4) were used in the experiment and were of analytical grade.

Synthetic Water Preparation

An aqueous solution of atrazine was prepared by dissolving atrazine in Milli Q filtered water. This was to minimize the interferences and effects of any ozone-consuming impurities. The observed characteristics of the prepared synthetic wastewater are shown in Table 1. For ozonation, the pH was increased to 9.5 using NaOH.

Table 1: Characteristics of synthetic wastewater.

S.No.	Parameters	Observed values
1.	COD ($mg.L^{-1}$)	226
2.	TDS ($mg.L^{-1}$)	6.7
3.	pH	6.3
4.	Alkalinity ($mg.L^{-1}$ as $CaCO_3$)	40
5.	Conductivity ($\mu S.m^{-1}$)	9.4
6.	Atrazine (ppb)	100

Analysis of Atrazine

The atrazine concentration was measured by Thermo Fischer SCIENTIFIC Ultimate 3000 HPLC (High-Performance Liquid Chromatography) using a reversed-phase C18 column of 250x4.6 mm with a particle size of 5 μm at a wavelength of 220nm. The mobile phase was acetonitrile: water (70:30 v/v) with a flow rate of 1mL.min^{-1}. The injection volume was 20 μL. The column temperature was set at 25°C. All the analytes were filtered through a 0.45 μm syringe filter.

Extraction of Atrazine

The extraction of atrazine was done by liquid-liquid extraction technique (Aslam et al. 2013). Samples were extracted using the QuEChERS method. 10 mL of sample was taken in a polypropylene 50 mL centrifuge tube. Then 10 mL of dichloromethane was added and vortexed for 45 seconds. Further, 3g of $MgSO_4$ was added to it and vortexed for 45 seconds. Then it was centrifuged at 4000 rpm for 10 min. After that, the supernatant was taken in a cleanup tube, vortexed for 45 sec, and then centrifuged at 4000 rpm for 10 min. Again, the supernatant thus obtained was evaporated to dryness at a temperature of 45°C. It was then redissolved in methanol for HPLC analysis (Dong et al. 2016).

Analysis of Intermediate Products after Ozonation

Ion Chromatography analyzed the sample for ionic components before and after ozonation. Analysis of sulfate, nitrate, chloride, and fluoride was performed using Ion Chromatography Model 882, Compact IC plus, Metrohm, Ltd. with Anion Dual 2 column Metrosep, 6.1006.530. The instrument was operated in suppressed conductivity detection mode using 50 mM H_2SO_4. The eluent was a mixture of sodium bicarbonate ($NaHCO_3$) and sodium carbonate (Na_2CO_3). The flow rate was 0.7 mL.min^{-1}. Each sample run was for 35 min and started with the injection of 20 μL of the sample. Before injection, the samples were filtered through a 0.22μm pore size syringe filter.

Ozonation Procedure

Ozone was generated from the air by an ozone generator

Table 2: Operating parameters of ozonation.

Parameters	Value
Gas flow rate (liters per minute)	1.5
Ozone concentration (mg.L^{-1})	9.4
The volume of the sample (mL)	500
Ozone output (g.h^{-1})	0.42

and an oxygen concentrator from Eltech company. Oxygen was supplied to the ozone generator through the oxygen concentrator, producing 93%±3% pure oxygen. The maximum ozone production capacity of the ozone generator was 10 gm.h^{-1}. The gas flow rate was fixed at 1.5 L.min^{-1}, and an ozone dose of 9.4 mg.L^{-1} was supplied. The volume of the sample ozonated at a time was 500 mL.

The ozone output (P) was calculated using the formula shown in equation (1). The values are tabulated in Table 2.

$$P = (R*C*60)/1000 \qquad …(1)$$

where,

P = Ozone output (gm.h^{-1})

R = Flow rate of feed gas (m^3.h^{-1}) or (LPM)

C = Ozone conc. (mg.L^{-1})

The KI starch method was used to measure the amount of ozone in the feed gas (Baird et al. 2017). An ozone destructor destructed the residual ozone in the off-gas.

Anaerobic Degradation

A laboratory-scale UASB reactor made of transparent plexi glass of vertical cylindrical shape tube of 5 cm diameter with a total volume of 2.08 L was used for biological analysis. The UASB reactor has an effective working volume of 1.68 liters. The remaining 0.4 liters were kept for gas liquid solid (GLS) separation arrangement. The overall height of the UASB reactor was 1.06 meters, and the effective height was kept at 0.86 m. The biomass in the UASB reactor was conditioned sludge prepared using fresh sludge fed with sucrose as a carbon source at 300 mg.L^{-1}. The details of conditioned sludge are given in the next heading.

Seed Sludge

Fresh sludge collected from the UASB reactor from Barauni Dairy Plant, Bihar, India, was used as the seed sludge for this study. The sludge was fed with the synthetic wastewater from the start-up to the steady state condition containing sucrose, ammonium chloride, potassium di hydrogen orthophosphate (KH$_2$PO$_4$) in the ratio 300:10:1. The sludge was then acclimatized to the changed environment for 17 days as it was never exposed to atrazine earlier. The system was used for further experiments once the sludge got stabilized

Analyses

The line diagram for the integrated system is shown in Fig. 2. Standard methods were used to analyze the sample (Baird et al. 2017). The COD was measured by the closed reflux method, and pH was measured with a pH meter (PCS Tester 35). Atrazine concentration was analyzed through HPLC. The liquid-liquid extraction method was used for the extraction of atrazine. Every time 500 mL of prepared synthetic wastewater was taken for treatment. All the parameters and the atrazine concentration were analyzed for all the samples. The KI starch titration method measured the amount of ozone in the feed gas (Baird et al. 2017). Alkalinity and VFA were determined by the method suggested by DiLallo & Albertsonn (1961). Liquid displacement method adopted for collection of biogas in the anaerobic process.

RESULTS AND DISCUSSION

Reduction in COD

The oxidation of atrazine by ozonation led to the decline in the COD of the wastewater sample. As the ozonation time increases, the reduction in COD also increases. After a certain time, it was observed that COD removal was almost constant, as shown in the Fig. 3. From this result, it is observed that the COD reduction of 54.4% was observed after 40 min of ozonation. The COD of synthetic wastewater declined with certain ozonation times, whereas additional ozonation proved ineffective in reducing COD. Although in literature, it has been reported that COD content was found to increase with increased ozonation time due to the formation of tiny organic molecules such as aldehyde, ketones acetic acid, which are not completely mineralized (Venkatesh et al. 2015). Reduction in
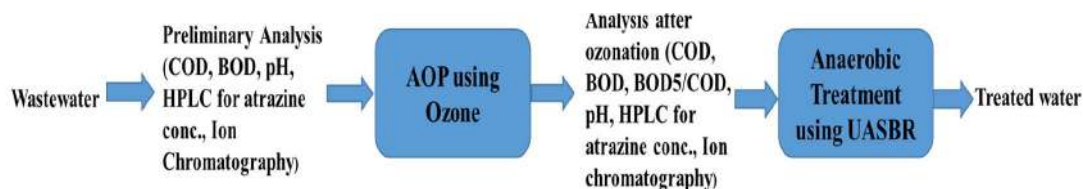

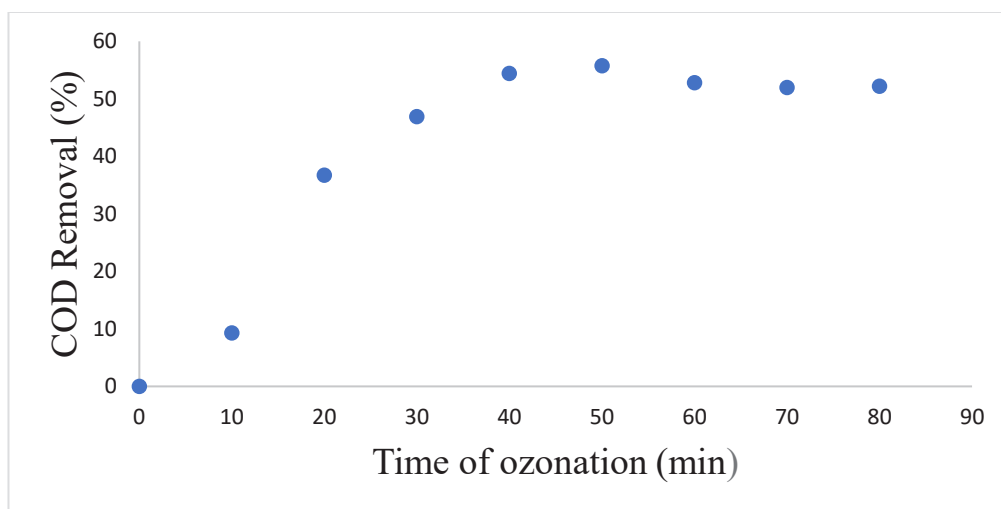Fig. 2: Line diagram for an integrated system.

Fig. 3: COD removal Vs. Time of ozonation.

COD value led to partial oxidation but not full mineralization. The results reveal that ozone contact time had a notable effect on COD removal. The ozonated wastewater was treated with a UASB reactor for further reduction of COD.

The COD removal achieved after the anaerobic degradation was 86.7%, as represented in Fig. 7.

Enhancement of Biodegradability

The atrazine-containing wastewater inhibit the anaerobic biodegradation process in the UASB reactor. The ozonation process enhances these types of wastewater by increasing biodegradability. The enhancement of biodegradability can be checked by the increasing value of the BOD_5/COD ratio. The BOD_5/COD ratio of wastewater increased with ozonation resulting in enhanced biodegradability of ozonation by-product. Ozone treatment breaks long-chain compounds making them biodegradable (Oller et al. 2011). After 40 min of ozonation, the biodegradability ratio increased from zero to 0.27. An increase in the ratio of BOD_5/COD indicates an improved biodegradability of recalcitrant substrates. This indicates that ozonation changes the functional groups in herbicide to produce more biodegradable by-products, which are easily eliminated by biological treatment.

Mineralization of Atrazine

The removal of COD represents the mineralization of organic contents of atrazine. The untreated wastewater, as well as ozonated wastewater samples, were analyzed through Ion Chromatography (IC) for ionic components like fluoride, nitrate, chloride, and sulfate. The chromatogram obtained from IC is shown in Fig. 4 and Fig. 5. Ozonation resulted in the release of nitrogen atoms connected with triazine bonds of atrazine molecules. Sulfate, chloride, and fluoride were found in unozonated and ozonated water samples. These anions show the presence of other chemicals in the unozonated water sample. Similar observation on the presence of anions in real wastewater has been reported by other researchers (Liang et al. 2009). F-, Cl-, SO_4^{2-} concentrations before ozonation were 0.015 mg.L^{-1}, 0.166 mg.L^{-1}, and 0.618 mg.L^{-1} respectively. The concentration after the treatment was 0.062 mg.L^{-1} F$^-$, 0.335 mg.L^{-1} Cl$^-$, 0.143 mg.L^{-1} NO_3^- and 22.205 mg.L^{-1} SO_4^{2-} respectively. The formation of nitrate and increased concentration of other ions signify the degradation of atrazine into other compounds.

Ozone treatment is paired with a biological process to entirely remove the organic content of specific wastewater because treatment is typically not considered complete until compound mineralization is almost complete. In this regard, several research projects have also been conducted recently (Covinich et al. 2014).

Degradation of Atrazine

The concentration of atrazine pesticide decreased with the ozonation time. The rate of ozonation applied for this experiment is mentioned in the previous section, including materials and methods. The decrease in the concentration of pesticide was analyzed through HPLC. The retention time obtained for atrazine was 1.537 minutes. The identification and concentration of atrazine in the aqueous solution were based on the retention times and area of the chromatogram of the samples tested. The maximum atrazine removal was observed at 40 min of ozonation.

Further, ozonation has a very mild or no effect in removing atrazine. So, the optimum time of ozonation
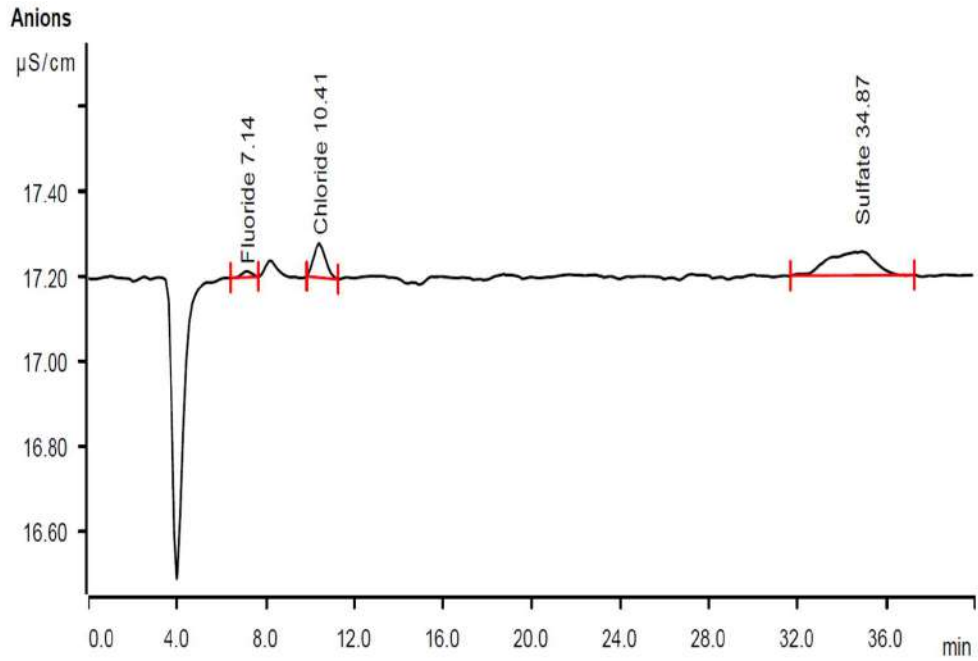
Fig. 4: Ions present in the synthetic wastewater before ozonation.
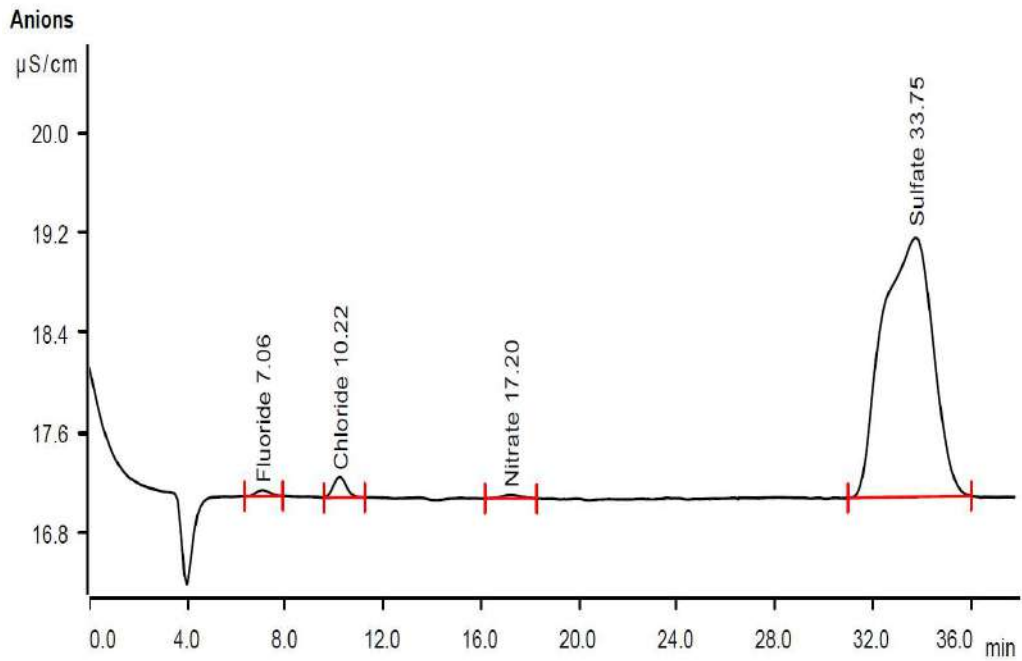

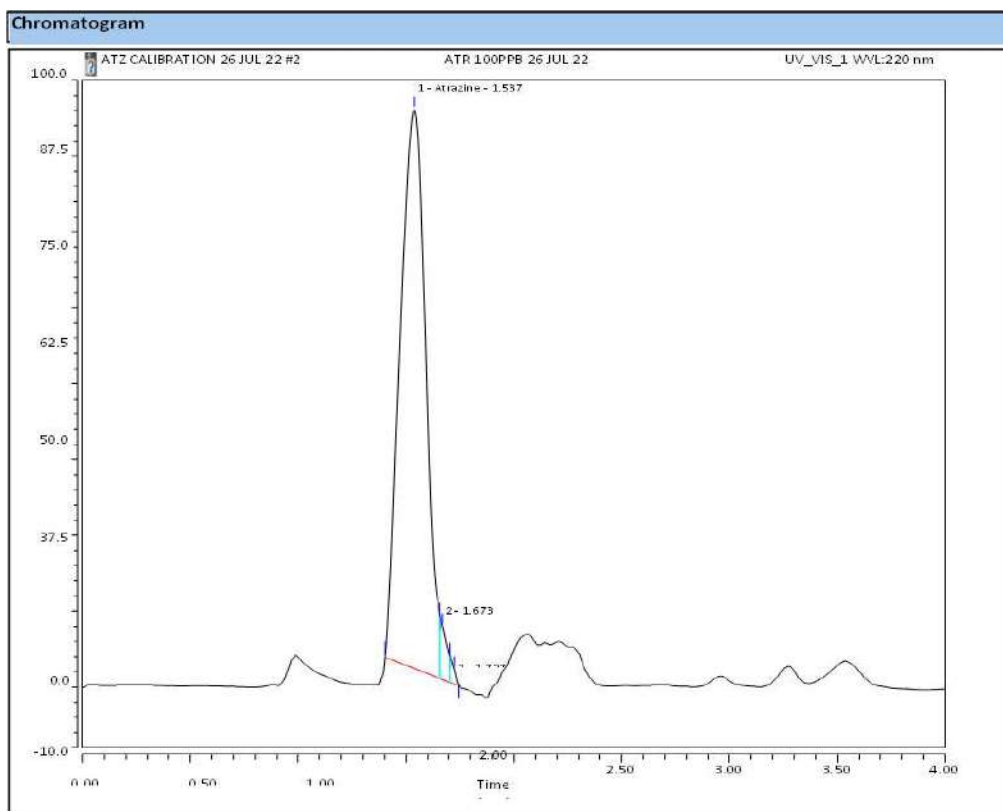Fig. 5: Ionic product present in the sample after 40 minutes of ozonation.

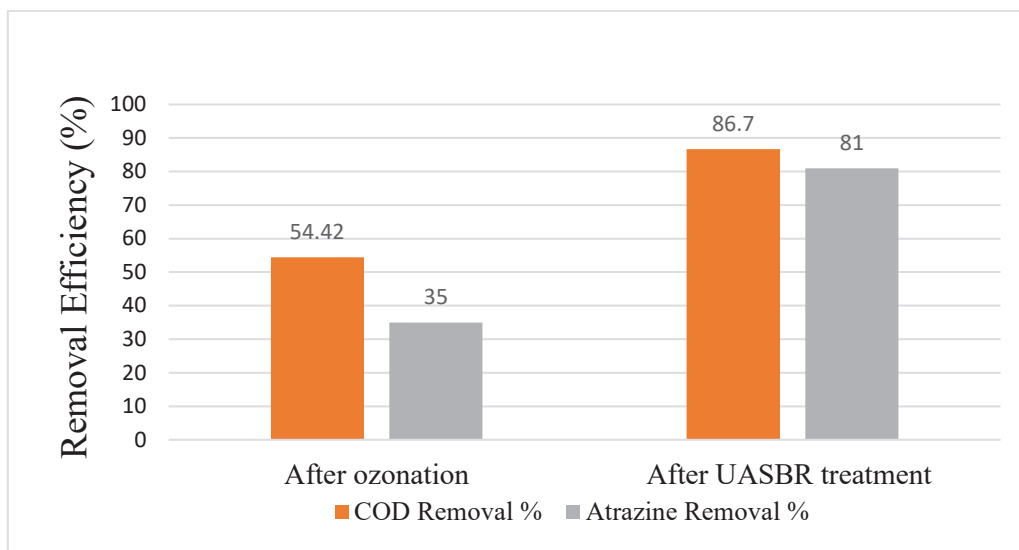Fig. 6: A typical HPLC chromatogram (Area vs. Time).

Fig. 7: Graph of removal efficiency of atrazine and COD.

adopted was 40 minutes. The HPLC chromatogram is also shown in Fig. 6.

The removal of atrazine concentration after ozonation was 35%. After the anaerobic treatment using UASBR, the removal of atrazine increases to 81%. The removal efficiency graph for COD and atrazine is shown in Fig. 7.

Observation for Removal Efficiency

Reactor Performance treating Atrazine-bearing Wastewater

The UASB reactor was maintained at a steady state condition. The Hydraulic Retention Time (HRT) was maintained at 16 hours. Initial COD removal was less at this operating condition, but the reactor could achieve more than 85% removal in almost 10 days of operation. After 17 days of operation, there was a COD removal of 86.7% and the corresponding atrazine removal of 81%.

Stability Parameters (pH, volatile fatty acids, and alkalinity)

The reactor's pH and VFA stayed well under the allowed limit. The pH was monitored daily and remained at 6.9-8.2. The VFA/Alkalinity ratio remained in the range of 0.19-0.27. The total biogas production was near about 130 mL.day^{-1}.

The alkalinity was measured daily, and VFA was measured intermittently. The results clearly showed that an integrated chemical and biological method is an effective way to reduce COD. Ozonation helped in the degradation of atrazine into biodegradable components. Hence, ozonation as a pretreatment is a potential process.

CONCLUSION

The results showed that the integrated process of ozonation and anaerobic degradation emerged as a boon for the removal of COD as well as atrazine concentration. The experiment results showed that the atrazine concentration decreased from 100 ppb to 19 ppb, and the corresponding COD value decreased from 226 mg.L^{-1} to 30 mg.L^{-1} after the combined treatment. Studies show that atrazine has been degraded efficiently through ozonation, but it was not economical. A new combination developed is economical, eco-friendly, and an efficient idea for the degradation of total organics. It can surely be considered for pesticide removal at the industrial level to treat agro-industry wastewater.

ACKNOWLEDGEMENT

REFERENCES

Aslam, M., Alam, M. and Rais, S. 2013. Detection of atrazine and simazine in groundwater of Delhi using high-performance liquid chromatography with an ultraviolet detector. Curr. World Environ. J., 8(2): 323-329.

Baghapour, M.A., Nasseri, S. and Derakhshan, Z. 2013. Atrazine removal from aqueous solutions using submerged biological aerated filter. J. Environ. Health Sci. Eng., 11(6): 456.

Baird, R.B., Eaton, A.D. and Federation, W.E. 2017. Standard Methods for the Examination of Water and Wastewater., 23rd Edition. CRC Press, Boca Raton, Florida.

Covinich, L.G., Bengoechea, D.I., Fenoglio, R. J. and Area, M.C. 2014. Advanced oxidation processes for wastewater treatment in the pulp and paper Industry : A review. Am. J. Environ. Eng., 4(3): 56-70.

Derco, J., Gotvajn, A.Ž., Čižmárová, O., Dudáš, J., Sumegová, L. and Šimovičová, K. 2021. Removal of micropollutants by ozone-based processes. Processes, 9(6): 1013.

DiLallo, R. and Albertson, O.E. 1961. Volatile acids by direct titration. J. Water Pollut. Control Fed., 33: 356-356.

Dong, X., Liang, S. and Sun, H. 2016. Analysis of herbicide atrazine and its degradation products in agricultural soil by ultra-performance liquid chromatography – Mass spectrometry. Int. J. Environ. Agric, Res., 2(5): 29-35.

Ghosh, P.K., Philip, L. and Bandyopadhyay, M. 2005. Management of atrazine-bearing wastewater using an upflow anaerobic sludge blanket reactor – Adsorption system. ASCE, 9(2): 112-121.

Hulsey, R.A., Long, B.W., Randtke, S.J. and Adams, C.D. 2008. Atrazine removal using ozone and GAC : A pilot plant study. J. Int. Ozone Assoc., 11: 37-41.

Kearney, P.C., Kaufman, D.D. and Sheets T.J. 1965. Metabolites of simazine by aspergillus fumigatus. J. Agric. Food Chem., 13(4): 369-372.

Lettinga, G. and Hulshoff Pol, L.W. 1991. UASB-process design for various types of wastewaters. Water Sci Technol; 24(8):87–107.

Li, S.F., Liang, Y., Zhang, R.Q. and Ye, F. 2009. Efficiency of atrazine degradation by O$_3$/H$_2$O$_2$. Huan Jing ke Xue., 30(5):1425-1429.

Legrini., E, Oliveros, O. and Braun, A.M. 1993. Photochemical processes for water treatment. Chem. Rev., 93(2): 671-698.

Maldonado, M.I., Malato, S., Perez-Estrada, L. A., Gernjak., W., Oller, I., Domenech, X. and Peral, J. 2006. Partial degradation of five pesticides and an industrial pollutant by ozonation in a pilot-plant scale reactor. J. Hazard. Mater., 138(2): 363-369.

Mandelbaum, R.T., Wackett, L.P. and Allan, D. L. 1993. Mineralization of the s-triazine ring of atrazine by stable bacterial mixed cultures. Appl. Environ. Microbiol., 59(6): 1695-1701.

Meijers, R.T., Oderwald-Muller., E.J., Nuhn, P. A.N.M. and Kruithof, J.C., 1995. Degradation of pesticides by ozonation and advanced oxidation. Ozone Sci. Eng., 17 (6): 673-686.

Mohammed, S.J. and Mustafa, Y.A. 2017. Removing of atrazine from water using advanced oxidation processes. J. Assoc. Arab Univ. Basic Appl. Sci., 24: 654.

Oller, I., Malato, S. and Sánchez-pérez, J. A. 2011. Combination of Advanced Oxidation Processes and biological treatments for wastewater decontamination — A Review. Science of the Total Environment journal., 409: 4141-4166.

Ormad, M.P., Miguel, N., Lanao, M., Mosteo, R. and Ovelleiro, J.L. 2010. Effect of application of ozone and ozone combined with hydrogen peroxide and titanium dioxide in removing pesticides from water. Ozone Sci. Eng., 32(1): 25-32.

Pathak, R.K. 2011. Various techniques for atrazine removal. IPCBEE., vol.3: 19-22.

Pérez-Lucas, G., Aliste, M., Vela, N., Garrido, I., Fenoll, J. and Navarro, S. 2020. Decline of fluroxypyr and triclopyr residues from pure, drinking, and leaching water by photo-assisted peroxonation. Process. Saf. Environ. Prot., 137: 358-365.

Philip, L. and Ghosh, P.K. 2006. Environmental significance of atrazine in aqueous systems and its removal by biological process: An overview. Glob. Nest J., 8(2): 159-178

Saleh, I.A., Zouari, N. and Al-ghouti, M.A. 2020. Removal of pesticides from water and wastewater: Chemical, physical and biological treatment approaches. Environ. Technol. Innov., 19: 14-21.

Venkatesh, S., Quaff, A.R., Pandey, N.D. and Venkatesh, K. 2014. Decolorization and mineralization of C. I. direct red 28 azo dye by ozonation. Desal. Water Treat., 16: 37-41.

USEPA. 2007. US EPA: Atrazine Summary. TEACH Chemical Summary. USEPA, US, pp.1-12.

Venkatesh, S., Quaff, A.R. and Pandey, N.D. 2015. Treatment and degradation of synthetic azo dye solution containing acid red 14 by ozone. J. Innov. Res. Sol., 1(1): 16

Wang, S. 2020. Enhanced degradation of atrazine by microbubble ozonation. The J. Roy. Soc. Chem., 5: 45-63.

Original Research Paper   **Open Access Journal**

Locating the Contours of Sustainability and Environmental Protection Within Competition Law in India: Swinging in Tandem or Isolation?

Pallavi Mishra*(**)†

*Symbiosis Law School, Noida, Symbiosis International (Deemed University), Pune, India
**National Law Institute University, Bhopal, India
†Corresponding author: Pallavi Mishra; pallavi@symlaw.edu.in

ABSTRACT

Environmental policy plays a major role in integrating environmental protection goals into economic policy areas. Environmental deterioration will proceed rapidly until this intersection is successfully achieved. The paper uses European Green Deal as a reference for fostering sustainable development goals through competition laws. This paper discusses sustainability in the context of the competition laws of various jurisdictions such as the European Union (EU), the United States (US), the United Kingdom (UK), and India. While highlighting conflicts around the intersection of competition law and environmental policies, this paper also provides their solution for making competition law environment-friendly. It suggests implementing such laws to promote sustainability and progress toward climate neutrality.

INTRODUCTION

A recent 'Hindu article titled "Climate change fueling the rise in extreme weather events" discussed the repercussions faced by forecasting agencies to make predictions accurately. The gist of the article revolved around how climate change has increased the instability in the atmosphere. One can assess that if the right actions, whether at an individual or global level, are not taken, it can further lead to tragic consequences. Environmental policy plays a major role in integrating environmental protection goals into economic policy areas. Environmental deterioration will proceed rapidly until this intersection is successfully achieved. Various efforts are being made, and initiatives are being taken to prioritize environmental protection through various laws, regulations, and schemes. The efforts of such nature are focused on one thing: Sustainable Development (World Commission on Environment and Development 1987). According to eminent economist Sir Nicholas Stern, "Climate change is a result of the greatest market failure the world has seen." He opined that the market price does not include the "climate and environment cost" caused by greenhouse gas emissions and pollution, implying that the price of a product does not accurately reflect its true cost. Such "negative externalities" are not reflected in the price and are borne by society. The consumers and others pay these costs later, however, not in

monetary terms but as a "tragedy of the commons" in the form of natural calamities, diseases, and health concerns caused by pollution, debilitated resources, or even societal instability. One can say that the market has a direct impact on our environment. The need of the hour is to bring both under the same regime (Stern 2007).

Governments have become more conscious of the market behavior in determining the goals they set to combat climate change, and their prime focus is to ensure that their efforts help them achieve the same. Competition law, therefore, plays a significant role in determining the nature of interactions in the market between competitors. From a legal and economic standpoint, there has been a concern about how economic and non-economic impacts on the environment are included in the competitive assessment. It is for policymakers to comprehend the application of competition law in a way that fosters sustainable development goals (Boushey & Knudsen 2017).

Until recently, sustainability discussions in the context of competition law did not attract much attention. The European Green Deal has sparked debates on making the competition law environment-friendly and how to implement such law to promote sustainability and progress toward climate neutrality. The deal was introduced in 2019. By 2050, the European Green Deal intends to make Europe

the first continent to be climate-neutral. The deal strongly emphasizes promoting sustainable economic growth with the hindsight of environmental and social policy. It intends to decarbonize electricity, infrastructure, transportation, industry, and agriculture. (Ismail & Tebbe 2021). The competition law framework has more than a 'supportive' role in green policy objectives. One may say that competition law indirectly supports sustainable development by continuously improving economic governance. To achieve sustainability, companies constantly strive for innovation, seeking a better version and improving their product to sustain themselves in the competition. To appease consumers' environmental and social expectations, companies may seek to create new product lines or enhance existing ones. However, the theoretical and actual consumer behavior varies, especially in India, where meeting necessities daily is a priority. (Malinauskaite 2022) Therefore, our country should encourage greater equity facilitating economic growth while helping to eradicate poverty. Environmental considerations must play a part in assessing a company's behavior in the market. Environmental Impact Assessment (EIA) can be introduced in the competition law regime to evaluate the consequences. From a broader perspective, EIA is also part of ESG (environmental and social governance). ESG is a form of analysis considering non-financial factors to identify risks and growth opportunities.

Further, applying provisions for anti-competitive agreements, abuse of dominance, merger, and combination in terms of environmental policy only strengthens the goal of sustainability. The tendency to consider environmental arguments with prime importance in evaluating the impact of companies on the environment may become the new normal in the near future. The dilemma lies in maintaining an efficient environmental policy, competing with others in the market, and striving to be in consumer demand. (Qaqaya & Lipimile 2012) Efficient techniques may also lead to anti-competitive effects such as cartelization, which we will further analyze in the article.

BRIDGING THE GAP BETWEEN COMPETITION LAW AND ENVIRONMENTAL PROTECTION

While analyzing whether the relationship between the two is acrimonious or complementary, there is a greater need to understand that this determination is based on the nature of agreements. In agreements leading to synchronized availability of sustainable and non-sustainable products, as opposed to such agreements leading to withdrawals due to quality standards, it may be considered pro-competition. In contrast, the latter must undergo a cost-benefit analysis (Watson et al. 2022). From the other side of the pond,

competition laws might not allow for the pursuance of agreements promoting sustainability, in which case, the environmental perspective would deem it anti-sustainability. While the thin line in between may be tough to walk, the growing concern for sustainability while promoting ethical market practices necessitates that the middle ground becomes a norm. A cost-benefit analysis is an equally complex process for two reasons: firstly, sustainability is tough to calibrate and quantify in absolute terms; and secondly, the nature of cost and benefit may be vastly different, prompting certain levels of conversion (Watson et al. 2022).

The Organization for Economic Co-operation and Development (OECD) promotes this idea of attaining sustainability with its constant effort to determine how the regulatory authorities can facilitate sustainable and pro-competitive business practices (OECD 2021). ESG and CSR (Corporate Social Responsibility) are important economic and social welfare concepts. While many areas of law have already adapted to these phenomena, competition law is yet to find its place in the "sustainability movement" (Arvidsson 1999).

CARTELS, GREENWASHING AND CLIMATE CHANGE

Collaborative efforts for sustainability stand to be tested beneath the ever-looming sword of cartels. In this space of collusion versus cooperation, many defend the pillars of antitrust on the ground that competition has a greater scope of incentivizing investment in green technology than cooperation (Nuys & Huerkamp 2021).

The perspective of competition runs the risk of assuming that consumers are willing to pay more for green technology. On the other hand, cooperative efforts risk getting slashed due to a bar on cartelization. However, certain reports asseverate that a competition policy may be the best way to improve the environment. This also warrants protecting products against greenwashing on the pretense of sustainability to bury investigations into what cartels are. In one such case concerning the Consumer-Detergents Cartel of the European Union, an environment-centric effort was a front for a cartel to synchronize price increases. Thus, the relationship between green efforts and competition is increasingly complicated due to this essential factor (European Commission 2005).

- When companies are working towards positive societal benefits, a big challenge lies ahead of them regarding the execution of the projects in such a way that does not result in cartelization by increasing prices or signing agreements horizontally or vertically, etc. This is where EIA or/and ESG come into play, requiring the

companies to evaluate the pros and cons to ensure the project's positive impact. There are no predefined parameters for this category. The assessment shall be based on jurisdiction and facts. However, there are certain criteria a regulating authority can adhere to reduce risks (Malinauskaite 2022):

- Ensure that the required authorities are keeping an eye on the antitrust organization to prevent future issues.

- Ensure that adequate training and awareness are provided to such organizations regarding sustainable development goals.

- Ensure that the competition among the players is sustained.

- Analyze a project or proposal's environmental considerations, benefits, and impact.

- Ensure a compliance program is formulated to safeguard the consumers and society and avoid unforeseen risks.

UNDERSTANDING REGULATORY FRAMEWORKS

Any cooperation or collaboration agreement must be carefully analyzed to avoid violating the Competition Law. When assessing risk in the context of sustainability cooperation, factors to be taken into account are as follows:

- Which Government authorities are responsible for enforcing competition law?

- How often do regulatory authorities enforce sustainability agreements?

- What factors are the regulating authorities considering to investigate sustainability cooperation cases?

- What factors do regulatory authorities consider to determine whether the company's conduct violates the competition law?

- Does the regulating authority publish any additional notifications or guidelines?

- What is the standard of regulating authorities in resolving cases involving sustainability agreements?

The answers provided for these questions vary significantly among competition authorities across the jurisdictions (Herbert Smith Freehills 2022a).

One must note that certain environmental considerations may entail potentially anti-competitive behavior. However, it can lead to significant benefits to sustainability. Authorities have resorted to some criteria (stated above) that help to assess the status of the company's conduct. The environmental considerations can be perceived in a way that promotes sustainable development goals. Analyzing the factors provides us with the pros and cons, where the former benefits the individual and the society at large, and the latter is anti-competitive in its totality (OECD 2021).

ENVIRONMENTAL CONSIDERATIONS IN ANTI-COMPETITIVE AGREEMENTS

This category can be further categorized into cooperation agreements, Abuse of Dominance, and Mergers & Acquisitions. Co-operation Agreements can be of two types: Horizontal and Vertical.

A coordinated effort to phase out an environmentally damaging product, a shared environmental norm binding on the participants, or the sharing of resources to advance sustainability goals is among the examples of horizontal agreements. The European Commission has considered efficiency factors when dealing with such anti-competitive but sustainable conduct. It has permitted such agreements where certain criteria were met, as was evident from the Philips-Osram case. Philips and Osram formed a joint venture to manufacture and market lead glass tubing for incandescent and fluorescent lamps in this case. Unless expensive and efficient filters are installed, using lead glass causes environmental damage. The agreement intended "a lower total energy usage and a better prospect of realizing energy reduction and waste emission programs" (OECD 2021). Undoubtedly, this reduces the "negative externalities" on the environment.

ENVIRONMENTAL CONSIDERATIONS IN CASES OF ABUSE OF DOMINANCE

When a company holds a strong position due to its market share, it might exploit that position to boost profits or drive out competitors, which are clear examples of abuse of dominance. However, the company can also use its market dominance to achieve environmental goals. For example, the dominant company may refuse to deal with trade partners who do not meet its defined sustainability criteria or tie or bundle its products with green goods to increase the sales of those latter products (OCED 2021). In such cases, it is at the authorities' discretion to determine whether the dominant position is being abused in its totality or benefits the environment and society.

ENVIRONMENTAL CONSIDERATIONS IN MERGER CONTROL

The approach to merger control and acquisitions needs to adapt to changes in sustainability. The concept of combination regulation intends to analyze the 'structural changes' in the market due to the merger or acquisition. The aim is to avoid anti-competitive practices in disguise. The

competition authorities can rely on certain factors to ensure that the merger is not intended with objectives that may result in environmental damages. Continuous technological advancements and stimulation of innovation are required to 'green' the competition law and achieve sustainable development goals. Attaining the same with positive outcomes would take a long period (OECD 2021). Therefore, when companies merge with one of their objectives to promote sustainability, analyzing the impact of the same on the environment can be a complex process. However, relying on certain parameters, setting up a compliance program, and keeping a tab on the mergers can help to strengthen the environmental goals.

PAINTING THE GLOBAL PICTURE

The international community and governments worldwide have acknowledged that immediate action is required to prevent the catastrophic effects of climate change. Since the Stockholm Conference of the United Nations (UN) in 1972, the debate on climate change has revolved around the influence of human activity and development proposals on the deterioration of the environment. Such debates have led to establishing a relationship between economic growth and pollution and providing efficient alternatives and mitigation strategies. The importance of private actors is repeatedly emphasized because of their significant social impact and ability to support public and government investments in environmental protection.

The 2030 Agenda for Sustainable Development, adopted by the UN General Assembly in 2015, intends a "plan of action for people, planet, and prosperity to guide all countries" toward sustainable development. The Paris Agreement seeks to strengthen the worldwide action plan toward climate change "through appropriate financial flows, a new technology framework, and an enhanced capacity building framework." The EU unveiled the European Green Deal in response to these international commitments, establishing it as an "integral part of the Commission's strategy to implement the United Nations' 2030 Agenda".

Both domestic and international analyses of various jurisdictions hint at two things: firstly, there are mostly general antitrust laws and not specific sui generis provisions designed to address environmental protection within competition law; secondly, there is a growing concern to incorporate sustainability and so, laws are now being interpreted to achieve the same.

Article 81 of the European Commission (EC) Treaty forbids agreements between businesses, decisions by groups of businesses, and collaborative practices which involve anti-competitive conduct such as prevention, restriction,

or distorting of competition within the market. Clause (3) provides that certain agreements may be exempted from the prohibition. Article 81 employs tools of economic analysis to assess any agreement. The tools evaluate the impact of an agreement in terms of positive or negative impact. The article seems to allow for an exemption only if the agreement is advantageous economically.

Article 101(1) of the Treaty on the Functioning of the European Union (TEFU) has provisions on collusions and cartels, an example of which can be seen in the case of German carmakers case whereunder they were levied with heavy fines for collusions on technical development. While this may seem preventive, the EU and the Commission are taking promising steps, such as revising Horizontal Guidelines with a dedicated chapter on sustainability agreements. The EU Green Deal and certain private efforts to guide sustainability can also be seen in Europe. Even in the UK, while sustainability agreements are read into the general antitrust laws, they have come up with Guidelines to help this complexity further. Similar is the position in US and Australia. Austria has a dedicated Cartel Act, amended to incorporate sustainability-related exemptions in 2021. Even the Netherlands Authority for Consumers and Markets (ACM) has issued guidelines on placing sustainability within competition law. While this isn't an exhaustive list of European countries, efforts also come from Asia, such as China, which actively reads sustainability into its competition law. Cambodia and Malaysia's laws specifically address agreements with substantial and evident social welfare benefits. In its plan for 2021-25, the Malaysian Competition Commission stated that it would research and work towards greening its competition policy and how it can support the ESG agenda (OECD 2021). The Competition Commission of Singapore has spotlighted sustainability for the year 2022. The Business Roundtable pledged to "protect the environment by embracing sustainable practices across our businesses" in its 2019 "Statement on the Purpose of a Corporation" (ICC 2020). Rightfully, the various examples demonstrate that more countries are jumping onto the wagon to initiate a discussion domestically and take concrete steps accordingly.

CORRELATION BETWEEN ENVIRONMENTAL LAW AND COMPETITION ACT IN THE EUROPEAN UNION, THE UNITED STATES, AND THE UNITED KINGDOM

The European Union (EU)

When the European Union was first established, social considerations were not considered. However, with the surge in pollution and climate change, the debate on sustainability

became the need of the hour. It led to discussions where strong initiatives for the execution and implementation of environmental policies were emphasized. The seriousness of the matter has led to the normalization of environmental agreements between the market players. In such agreements, the companies cooperate or collaborate to harmonize sustainable development goals in their businesses. These agreements can potentially jeopardize the environment at the risk of being anti-competitive under Article 101 of the Treaty on the Functioning of the European Union (TFEU).

Article 3 of TFEU highlights the objectives of the EU. According to clause (3), the internal market must be built on a social market economy with high levels of competition and environmental protection. The shift of the EU from a rigid economic project to considering social welfare factors is evident under Article 191. Clause (1) lists several environmental objectives such as "preserving, protecting and improving the quality of the environment, prudent and rational utilization of natural resources, promoting measures at international level to deal with regional or worldwide environmental problems, and in particular combating climate change." All these objectives are crucial in attaining sustainable development goals. It is Article 11 that consolidates environmental protection and the EU's activities and policies to promote sustainability. It states, "Environmental protection requirements must be integrated into the definition and interpretation of the Union policies and activities, particularly to promote sustainable development." The inclusion of environmental protection into Union policies is emphasized even in Article 37 of the Charter of Fundamental Rights of the EU (Krause 2020). Article 101 of the Treaty prohibits agreements that limit competition between two or more independent market operators. This provision covers both horizontal agreements and vertical agreements. Only limited exceptions are permissible.

The factors to be considered in this article are:

- Whether the agreement intends to promote sustainability or, in disguise, aims to cover up price fixing, cartels, etc.
- If the agreement promotes sustainability, is it causing appreciable effects?

If four conditions are met, sustainability agreements restricting competition may be exempted under Article 101(3) TFEU. The article provides for 'Block Exemption Regulation.' It allows certain agreements to be exempted from the prohibition of restrictive agreements laid in Article 101(1).

The four conditions are as follows:

- Improving the production/distribution of goods or promoting technical or economic progress
- Consumers receive a fair share of benefits
- Indispensability
- No elimination of competition

The United Kingdom (UK)

In the UK, the Competition Act of 1998 (CA 1998) and the Enterprise Act 2002 are among the sources of competition law. Chapter I of the CA, 1998 provides for the assessment of the sustainability agreements. These agreements are subject to the same exemptions as laid under Treaty on the Functioning of the European Union (TFEU) under Section 9 of CA, 1998. It can exempt agreements that "contribute to improving the production or distribution … or to promoting technical progress while allowing consumers the fair share of the resulting benefit," provided they do not eliminate competition and do not impose any limitations that are not necessary for achieving the objectives laid. Thus, if an agreement is prohibited under Article 101(1) TFEU, it can still be held as permissible through the exemption provided by Article 101(3), provided it entails environmental protection objectives. In its Competition Policy Report 2016, the commission noted that 'competition law also intends to drive companies to make maximum use of scarce resources and thus includes an environmental protection perspective.'

The European Commission also relies on certain guidelines and rules such as Climate, Energy, and Environmental State Aid Guidelines (CEEAG), General Block Exemption Regulation (GBER), and Important Projects of Common European Interest (IPCEI) (CMS Law 2021).

The CEEAG includes facets such as 'Environmental Protection Costs,' 'Stricter Conditions for non-green infrastructure projects, etc. In 2021, GBER shifted to the green and digital economy, enabling its Member States to provide aid under certain conditions without prior notification. The rules on aid on Important Projects of Common European Interests govern cross-border initiatives that require joint investments from several EU Member States. The development of innovative technologies and industrial methods that advance the goals of the Green Deal will be aided by the updated IPCEI regulations. All these guidelines are employed to promote the objectives of the European Green Deal.

In 1999, the Commission in Conseil Européen de la Construction d'Appareils Domestiques (CECED) case considered broader environmental benefits. This case involved a deal between domestic washing machine manufacturers to stop making and importing the least

energy-efficient models. Not only did this deal directly assist customers by lowering energy bills, but it also positively impacted the environment by reducing CO_2 emissions. The Commission determined that the agreement could be exempted under Article 101(3) of the TFEU despite the limitation on competition. The commission weighed the economic efficiency and environmental benefits on an equal footing. (European Commission 1999)

The United States (US)

Antitrust scholars consider non-economic policy objectives as falling outside the scope antitrust law regime. Many antitrust scholars argue that considering non-economic policy goals is against the very objective of antitrust laws. Some scholars have argued that antitrust analysis should include non-economic factors that affect consumers. Time and again, it is contended that antitrust laws must address social issues like climate change (Khan 2021).

Post the United Nations General Assembly of 2015, the emphasis has been on the sustainable development agenda. The main antitrust laws in the US are The Sherman Antitrust Act of 1890, the Federal Trade Commission Act of 1914 (The FTC Act), and the Clayton Antitrust Act of 1914. The Sherman Act provides for free competition in trade or commerce. The FTC Act established the Federal Trade Commission. It vests the commission with the power to "prevent unfair methods of competition and unfair or deceptive acts or practices in or affecting commerce." The Clayton Act aims to prevent anti-competitive conduct. It strengthens the antitrust regime in the US. The act forbids predatory and discriminatory pricing, anti-competitive mergers, and other unethical practices. Section 1 of the Sherman Act, which prohibits "contracts, combinations, or conspiracies in restraint of trade or commerce, " and Section 5 of the FTC Act, which prohibits "unfair methods of competition," may apply to agreements between companies on sustainability issues.

The antitrust agencies in the US are the US Department of Justice and the Federal Trade Commission (Herbert Smith Freehills 2022). By assisting legislators and policymakers in understanding the competitive impacts of laws and warning them of potential unintended consequences of regulation, the agencies contribute significantly to the environmental regulation process. This enables legislators to weigh potentially conflicting policy concerns. Thereby, evaluating the legality of future collaborations or cooperation concerning sustainability agreements should consider the antitrust laws and guidelines. The antitrust agencies acknowledge that "competitive forces are driving firms toward complex collaborations to achieve goals such

as expanding into foreign markets, funding expensive innovation efforts, and lowering production and other costs" and that these collaborations "often are not only benign but pro-competitive." Collaborations that embrace the potential of the latest technological advancements to promote sustainability by establishing industry standards may be permissible under antitrust laws.

In 2021, US President Joseph R. Biden issued an Executive Order on "Promoting Competition in the American Economy." The Order broadly reaffirmed the Administration's position that it would pursue US antitrust laws by "combatting excessive concentration in the industry, abuses of market power, and the harmful effects of monopoly." However, the Order did not outline any specific policy to promote sustainability or address how US antitrust laws would affect sustainability collaborations (Herbert Smith Freehills 2022b). It is important to note that preserving the environment and sustaining a competitive economy can go hand in hand.

The joint ventures among the competitors are assessed through the rule of reason. Rule of Reason analysis is applied as the scrutiny procedure for the agreements under the US antitrust law. The purported pro-competitive benefits of an agreement are weighed against its anti-competitive conduct in a fact-intensive, burden-shifting evaluation. If an agreement is per se unlawful, the courts, irrespective of its pro-competitive nature, will not inquire into it. However, if under Rule of Reason analysis, an agreement is shown to have specific pro-competitive effects, such as "higher output, lower costs, reduction in the effects of market failure, or promotion of the competitive process," it shall render an agreement permissible. In light of this, if a competitor's collaboration benefits the competition, it is not considered a violation of antitrust law. Another scrutiny standard applied in the US is the 'reasonableness of the restraint.' Market power and market impact are analyzed under this step (Herbert Smith Freehills 2022b).

In the *United States v. Automobile Mfrs. Ass'n,* 643 F.2d 1028 (9th Cir. 1981). The US sued to 'prohibit an agreement between the manufacturers to stifle the advancement of ecologically friendly technology.' The Department of Justice sued major automobile manufacturers for conspiring to eliminate competition in the design, development, and production of air pollution control technology. Such conduct was held in violation of the antitrust laws. The action was settled through a consent decree that forbade the defendants from participating in the allegedly illegal conduct.

Since the US does not have specific laws or guidelines dedicated to sustainable development goals, balancing the public policy goals of competitive markets and preservation

of the environment depends on the interlinking of these areas and interpreting the law in a way that considers societal factors as well. The agreements relating to environmental objectives are treated the same as other agreements for purposes of antitrust analysis. (Hylton 2008)

India

The courts, tribunals, and policy-makers actively note India's obligations to promote sustainable development goals, especially since the Apex Court declared the right to a healthy environment a fundamental right under Article 21. However, the Competition Commission of India (CCI) hasn't yet incorporated, negatively or positively, into this discussion surrounding the interplay. No specific prohibition would only apply to company collaboration agreements on sustainability issues. EU and other regimes serve as a great example for India to realize and actuate the path it must take in the future and improve.

According to a report submitted to the CCI, the integration of environmental concerns into competition law in India is a complex issue due to the non-economic nature of environmental effects in the short term (Siddiqui 2022). However, the report concludes that the CCI's goal of preserving consumer welfare aligns well with the promotion of sustainable development, and consolidating exemptions related to public interest or India's treaty obligations under Section 54 of the Indian Competition Act, 2002 could be a potential solution. This approach would allow for a gradual incorporation of environmental concerns into competition law without the need for an immediate overhaul of the competition regime. India has the opportunity to take a leading role in promoting sustainable development through competition practices, and could also serve as an example for other developing countries. While economic practices differ between developed and developing countries, each jurisdiction has lessons to offer India, provided that it takes the necessary steps.

A common concern across the countries has regarded the formation of cartels to hold anti-competitive practices in disguise for promoting sustainability.

According to the Indian Competition Act 2002, there are three ways by which healthy competition and consumer welfare can be promoted:

- By prohibiting anti-competitive agreements and practices that cause appreciable adverse effect on competition in India (AAEC);
- By preventing abuse of dominant position in the market;
- By regulating mergers and acquisitions.

Governments and corporations are working towards including environment-friendly trade and manufacturing practices in their regular business practices supporting sustainable development. In light of the threat posed by climate change, the scope of consumer welfare can be broadened to encompass environmental sustainability goals in addition to consumer surplus.

In India, competition assessment can place greater emphasis on sustainability by utilizing section 54 of the Competition Act (the Act). This section empowers the Central Government to exempt the application of the Act or any of its provisions for a specified period. Given the importance of environmental protection and sustainability in policymaking, the government can use Section 54(a) to exempt certain provisions of the Act if the project's impact on the environment is thoroughly analyzed and evaluated and if the measures adopted by the company benefit society at large. Section 54(b) further enables the government to fulfill its commitment made at the Paris Summit 2015 by exempting the Act's provisions to fulfill any obligation assumed by India under a treaty, agreement, or convention with other countries (Bhatia 2017).

Therefore, the Competition Act of 2002 can be a valuable tool in addressing larger environmental concerns in India. Rather than amending the provisions, we should interpret the Act in a way that excludes climate change and promotes sustainability. The proposed framework can be applied when companies make efforts to improve quality, avoid pollution, stimulate innovation, and benefit society. After a thorough analysis of various jurisdictions, including India's, it can be concluded that companies may be eligible for an exemption from general prohibitions if their agreements or conduct promote sustainable development goals. However, it is crucial to interpret existing laws in a way that aligns with environmental policy and promotes consumer welfare.

To prevent anti-competitive practices under the guise of sustainability, authorities must ensure that guidelines are in place. For instance, the EU's dedicated chapter on sustainability agreements offers well-formed guidelines that facilitate better implementation and demonstrate the importance of environmental considerations. Implementing such guidelines in India would provide clarity and improve the effectiveness of competition assessments in promoting sustainability.

CONCLUSION

Several conflicts arise at the intersection of competition law and environmental policies. Some market players argue that competition law impedes sustainability collaboration, while regulators claim that they have not received any concrete proposals for sustainability collaboration from the industry. This emphasizes the need to focus on consumer behavior.

There is also a debate about whether easing competition rules would lead to eco-friendly proposals or whether promoting a competitive market while adhering to existing policies would be more effective in achieving greener results in practice.

Furthermore, quantifying "effectiveness" in complying with competition law principles is a complex process, creating challenges for cost-benefit analysis. Agreements that provide social benefits that cannot be measured in monetary terms can be problematic if they restrict competition. However, if the restriction is proportionate to its environmental benefits, such agreements may be permissible.

It is necessary to strike a balance between competition law and environmental policies by considering the specific circumstances of each case and evaluating the trade-offs between the benefits of competition and environmental protection. The solution to these conflicts is that the Competition Law regime incorporates sustainability, or the law is interpreted to supplement environmental goals. The former option can lead to a difficult balance between consumer welfare, environmental goals, and the aim of market players (which cannot be based on the factor of environmental betterment only). The former may lead to anti-competitive practices (Siddiqui 2022). That said, it does not mean the possible solutions aren't effective. It is on the government and regulatory authorities to adopt thorough guidelines and ensure that the difficulties mentioned above are eliminated.

In order to integrate environmental considerations in competitive assessment, several questions need to be addressed, including:

- To what extent can environmental factors be included when there are no direct consequences on competition in the market?
- At what stage should the impact of the project or proposal be assessed in relation to environmental factors?
- Can a common ground be reached between environmental factors and other factors in competitive assessment?

These questions are important to consider as competition law and environmental policies intersect and finding a balance between the two is necessary to achieve sustainable development goals.

Integrating environmental considerations in competitive assessment raises complex questions that lack straightforward solutions. Determining the scope of environmental consequences is difficult since they are non-economic in nature. To address this, practices like incorporating the cost of "negative externalities" can be adopted to ensure that products reflect their true cost. Regulators can also categorize the effects in economic terms, either positively or negatively, depending on the transaction or company conduct.

Formal quantification measures, such as the OECD guidelines for "cost-benefit analysis" of environmental initiatives, can also be used. These guidelines use shadow pricing and consider long-term environmental effects for future generations. The competition authorities of Greece and the Netherlands have already adopted this approach (Siddiqui 2022).

Sustainability discussions are inevitable in light of the European Green Deal and international commitments toward environmental goals. We cannot shield ourselves from discussions surrounding environmental protection within competition law. Further, the market is going to dictate a lot of what the repercussions of its actions will be on our climate. From a bird's eye view, Competition Law safeguards the effects of anti-competitive agreements, abuse of dominance, etc., on the consumer in the relevant market. However, sustainability benefits are more likely to translate into a combination of some direct benefit to the individual consumer, with other benefits being enjoyed by the wider society at large or even by the future wider society. The exigent nature of the problem demands that jurisdictions expressly read sustainability within the competition law's design and make any necessary modifications and amendments. While maintaining a pro-competition spirit, environmental exemptions can be accommodated in certain situations after a fact-based cost-benefit analysis (EIA; ESG), especially in complexities arising from collaborative agreements.

Apart from all the legal and economic regimes that must be followed to ensure sustainability, consumer awareness and sensitivity towards sustainable goals is of prime importance. It is their behavior that impacts the market. The preference for green products can act as a drive for competition between the market players/suppliers. A good environmental image can be an important marketing instrument for market players.

REFERENCES

Arvidsson, M. 1999. Integrating environmental concerns into competition policy. Journal of Environmental Law, 11(2): 165-176. doi: 10.1093/jel/11.2.165

Bhatia, K. 2017. The competition act, 2002 and sustainable development in India. Journal of South Asian Studies, 5(1): 63-78.

Boushey, H. and Knudsen, H. 2001. The importance of competition for the American economy. The Center for American Progress. https://www.americanprogress.org/wp-content/uploads/issues/2001/10/pdf/competition.pdf

Brundtland, G. H. 1987. Our Common Future: The World Commission on Environment and Development. Oxford University Press.

CMS Law. 2021. EU competition law and sustainability. Retrieved from https://cms.law/en/int/expert-guides/cms-expert-guide-to-

eu-competition-law-and-sustainability/eu-competition-law-and-sustainability.

European Commission 2005. Commission Decision of 8 June 2005 relating to a proceeding pursuant to Article 81 of the EC Treaty and Article 53 of the EEA Agreement against Henkel KGaA and others (Case COMP/38.121 — Consumer-Detergents Cartel). Official Journal of the European Union, L177/32-L177/53.

Herbert Smith Freehills 2022a. Sustainability Cooperation and Competition Law: A Global Perspective. Retrieved from https://www.herbertsmithfreehills.com/latest-thinking/sustainability-cooperation-and-competition-law-a-global-perspective

Herbert Smith Freehills 2022b. Sustainable cooperation and competition law: a global guide. Retrieved from https://www.herbertsmithfreehills.com/ content/dam/herbert-smith-freehills/pdf/practices/antitrust-competition-law/sustainable-cooperation-and-competition-law-a-global-guide.pdf

Hylton, K. N. 2008. Antitrust Law: Economic Theory and Common Law Evolution. Cambridge University Press.

ICC 2020. ICC Commission on Environment and Energy Policy Report 2020. International Chamber of Commerce. Retrieved from https://iccwbo.org/publication/icc-commission-on-environment-and-energy-policy-report-2020/

Ismail, M. and Tebbe, A. 2021. The intersection of competition law and sustainability: The case of the European Green Deal. Energy Research & Social Science, 70, 101912. https://doi.org/10.1016/j.erss.2020.101912

Krause, T. 2020. EU Competition law and environmental protection are environmental benefits considered in the assessment of Article 101 TFEU? Orebro Universitet, 17: 1-29. https://www.diva-portal.org/smash/get/diva2:1476448/FULLTEXT01.pdf

Khan, L. M. 2021. The antitrust case for regulation on non-economic policy objectives. Harvard Law Review, 134(4): 961-1012.

Koga, D. C. 2020. Teamwork or collusion? changing antitrust law to permit corporate action on climate change. Washington Law Review, 95(4): 1989-2026.

Lenz, M. 2000. The interplay between the environment and competition law in the EU. European University Institute. https://cadmus.eui.eu/bitstream/handle/1814/5459/Lenz_2000.pdf?sequence=1

Malinauskaite, J. 2022. Competition law and sustainability: EU and national perspectives. Journal of European Competition Law & Practice, 13(5): 336-348. https://doi.org/10.1093/jeclap/lpac003

Nuys, B. V. and Huerkamp, C. 2021. Antitrust enforcement and sustainability: why antitrust law and sustainability should collaborate. Journal of European Competition Law & Practice, 12(4): 267-274. doi: 10.1093/jeclap/lpaa051.

OECD 2021. Corporate Sustainability: A Role for Competition Authorities? OECD Policy Responses to Coronavirus (COVID-19). OECD Publishing. https://doi.org/10.1787/43b8b551-en

Office of Public Sector Information. (1998). Competition Act 1998. http://www.legislation.gov.uk/ukpga/1998/41/contents

Qaqaya, H. and Lipimile, G. 2012. The effects of anti-competitive business practices on developing countries and their development prospects. Journal of International Competition Law and Economics, 8(4), 1031-1065. doi:10.1093/joclec/nhs045

Siddiqui, S. A. 2022. Integrating environmental concerns in competition law: An analysis of the Indian regulatory framework. Journal of Cleaner Production, 324, 129044.

Stern, N. 2006. The Economics of Climate Change: The Stern Review. Cabinet Office, HM Treasury.

Watson, B., Ivanova, M. and Zhang, Y. 2022. Greening competition law: the environmental benefits of antitrust. Harvard Environmental Law Review, 46(1): 1-39.

Watson, N., Pereiras, S. and Palomino, F. 2022. Q&A: Competition law and Sustainability. Financier Worldwide. Retrieved August 6, 2022, from https://www.financierworldwide.com/qa-competition-law-and-sustainability#.Yu6DIC8RodV

Original Research Paper

Open Access Journal

Postnatal Exposure to A Low Dose of Imidacloprid: Oxidative Stress in Brain Without Affecting Learning and Behavior in Swiss Albino Mice

A. Sharma*† iD, S. Gupta* and M. Kaur*

*Department of Zoology, IIS (Deemed to be University), Jaipur 302020, India
†Corresponding author: A. Sharma; dranju1110@gmail.com

ABSTRACT

The neurotoxic effects of exposure to low levels of the pesticide imidacloprid (IMI) and the effect of curcumin are of current interest when exposure occurs during early development. Male weanlings of Swiss albino mice (21 days old) were given 1 mg.kg^{-1} body weight (1/130 of LD50 and 2 mg.kg^{-1} body weight (1/65 of LD50) of imidacloprid and Curcumin (100 mg/kg body wt.) by oral gavage from postnatal day 21 to postnatal day 60. Young adult offspring were studied for behavioral parameters and learning ability using open field and Morris water maze. After completing the behavioral test, brains were processed for acetylcholine esterase activity and antioxidant enzyme estimation. The level of lipid peroxidation and activity of catalase, superoxide dismutase, and glutathione were assayed. In the present study, parameters such as locomotor activities and cognitive skills were not affected compared to lower doses of imidacloprid in the open field and Morris water test. However, activities and levels of antioxidant enzymes such as catalase and lipid peroxidation were found to be altered. In contrast, superoxide dismutase, acetylcholine esterase activity, and glutathione remained unchanged compared to the control. This suggests that subchronic exposure to low doses of IMI can lead to significant alterations in the enzymes of antioxidant protective systems such as catalase and lipid peroxidation. Co-treatment with curcumin was able to restore the activities of the affected enzymes in comparison with the control.

INTRODUCTION

Imidacloprid (neonicotinoid insecticide) is widely used to control sucking pests on a diverse range of major crops, including vegetables, rice, cotton, potato, and others (Fossen, 2006, Jeschke et al. 2011, Simon-Delso et al. 2015). Thus, non-target populations, such as mammals, especially humans, get exposed to xenobiotics via food and contaminated drinking water (US EPA 2020). Long-term acute and chronic exposure to imidacloprid and other neonicotinoids causes various health deficits in mammals (Lonare et al. 2014, Cimino et al. 2017, Katic et al. 2020).

Recent studies have also shown that imidacloprid exposure leads to biochemical changes in the central nervous system, thereby affecting the behavior of organisms. It can bind to the nicotinic cholinergic receptors in the nervous system (Tomizawa & Casida, 2002, 2003). Chronic imidacloprid exposure and adverse development can be correlated, and this has been further strengthened and confirmed by human exposure studies (Yang et al. 2014, Carmichael et al. 2014)

According to the guidelines laid down by the European Food Safety Authority (EFSA), the acceptable daily intake (ADI) and acceptable operator exposure level (AOEL) of imidacloprid for humans have been set to 0.06 mg.kg^{-1} bw.day^{-1} and 0.08 mg.kg^{-1} bw.day^{-1} respectively (EFSA 2008). A change in the previously set reference values was suggested by the EFSA 2013, lowering the AOEL to the same level as ADI to avoid developmental neurotoxicity in humans (EFSA 2014).

The most available literature on the toxicity of such chemicals is based on high doses and the adult population (Toor et al. 2013, Bagri et al. 2013, Vohra & Khera 2015, Sharma et al. 2019, 2021). Though the current limit of concern regarding imidacloprid for mice, no observed adverse effect level (NOAEL) has been found at 5 and 10 mg.kg^{-1} per day (Arfat et al. 2014). However, sub-chronic low-level exposure and its effect on young and developing populations have not yet been well investigated (Katic et al. 2020).

Younger populations, such as neonates and kids, can be indirectly/directly exposed to these toxic agents.

ORCID details of the authors:

A Sharma: https://orcid.org/0000-0003-2719-6878

Even low-dose exposure during such vulnerable and sensitive development periods may cause disruption and malfunctioning of adults' brains and nervous systems, thereby affecting their behavior (Gawade et al. 2013, Burke et al. 2018).

Furthermore, during the development phase, the brain is highly susceptible to neurotoxic insults as the developing blood-brain barrier (BBB) is less resistant to these toxicants than the mature adult brain, thus allowing the toxicant to reach the blood supply and brain. Therefore, exposure during the developing period is of significant interest. It has been reported by various studies that preschool children are being exposed to higher levels of pesticides than the recommended ADI. Such a high consumption rate of these pesticides indicates a possible fetal neurotoxic risk and may impair children's cognitive skills, behavior, and motor and sensory functions. Suggesting that the effect of such xenobiotics on vulnerable populations such as children and young adults should be thoroughly researched (Van Wendel de Joode et al. 2016).

Curcumin (Cur), an important ingredient of turmeric, is a potent inhibitor of free radical formation and reactive oxygen species (ROS) generation in conditions such as lung injury induced due to paraquat exposure (Venkatesan 2000), propanil-induced hepatotoxicity (Otuechere et al. 2014), malathion induced testicular toxicity and oxidative damage in male mice (Ali & Ibrahim 2018). Curcumin is protective against free radical damage. Its role in improving cognitive function has recently been identified and studied thoroughly, especially in neurodegenerative diseases such as Alzheimer's and Down syndrome (Pan et al. 2015, Rueda et al. 2020).

Thus, the present study has been planned to evaluate the effects of 40-day oral exposure to two (1 mg.kg^{-1} bw and 2 mg.kg^{-1} bw) low doses of imidacloprid on young male Swiss albino mice. The effect of curcumin after low-dose exposure to imidacloprid with emphasis on learning behavior and biochemical endpoints was also investigated.

MATERIALS AND METHODS

Chemicals

A commercial formulation of imidacloprid (Victor Imidacloprid) 17.8%SL from the division of Insecticides India Ltd. (Delhi, India) was used to treat mice. In mice, the LD 50 value (oral) of imidacloprid was 131 mg.kg^{-1}.bw^{-1} (WHO 2008). In the present study, the mice were given imidacloprid at 1 mg.kg^{-1}.bw^{-1} (1/130 of LD 50) and 2 mg.kg^{-1}.bw^{-1} (1/65 of LD 50). Food-grade curcumin was used.

Animals were divided into four groups (6 each) and treated daily by oral gavage from postnatal day 21 to postnatal day 60. The chosen imidacloprid doses were lesser than the documented non-observable level in mice (5-10mg. kg^{-1}bw.day^{-1}) (Arfat et al. 2014)

Test Animals and Treatment

Adult Swiss albino mice were obtained from the Indian Veterinary Research Institute, Izetnagar Bareli UP. The animals were housed in a well-ventilated vivarium at around 29 ± 20 C (relative humidity 33-40%) with natural light and dark cycles. The animals were housed in polypropylene cages with wood shavings spread on the floor evenly. They were maintained on standard mice feed obtained from Hindustan Level Ltd Delhi, India, and drinking water ad libitum. The Institutional Animals Ethical Committee approved the study, and all the experiments were carried out according to the guidelines of the CPCSEA (Committee for Control and Supervision of Experiments on Animals) Government of India, New Delhi.

The colony was maintained, and pregnant females were checked for parturition. The day of birth of the offspring of healthy females was noted as postnatal day 0. Healthy male weanlings (21 days old pups) weighing 93 g were selected for the study. Animals were divided into four groups (n=6 each) and treated daily via oral gavage from postnatal day 21 to postnatal day 60.

Group I served as the control and received only vehicle (Distilled Water).

Group II was exposed to imidacloprid at the dose of 1 mg.kg^{-1}.bw^{-1}

Group III was exposed to imidacloprid at the dose of 2 mg.kg^{-1}.bw^{-1}

Group IV was exposed to 2 mg.kg^{-1} bw^{-1} imidacloprid and 100 mg.kg^{-1}.bw^{-1} curcumin in combination

Animals were observed regularly for clinical signs of toxicity; food and water consumption were also recorded. Young animals were subjected to behavioral tests at the end of the exposure periods.

Behavioral Tests

The open-field test (locomotor activity and anxiety) (Seibenhener & Wooten 2015): The locomotor activity and anxiety behavior were assessed using an open field (Seibenhener & Wooten 2015) with slight modifications. The open field behavior was assessed using a square wooden box measuring 50 x 50cm (side x side) and a height of 38 cm. The box was divided into 10 x10cm blocks with black lines painted into 25 similar spaces. For observations, each mouse was placed in the center arena and left free to explore for the next 5 minutes. Further, it was scored on the following

parameter: Exploration time (total time duration animals were in a mobile state), Number of blocks crossed (number of floor units crossed with four paws), and freezing duration.

The Morris water maze (learning and memory) (Vorhees & Williams 2006): Morris water maze (MWM) was used to assess spatial learning and memory in young mice following the procedure by Vorhees et al. (2006). The apparatus contained a circular tank (150cm in diameter and 50 cm in height) filled with water maintained at 29 ± 2° C and was placed in a room with extra cues around the apparatus. The tank was divided into four equal quadrants, North-West (NW), South-East (SE), South-East (SE), and North-East (NE), with extra maze cues. A hidden platform (10 cm^2) was located in one of the quadrants. This experiment was performed during postnatal days 56-60. A video system was used to record the movement of each mouse within the maze. Mice were given four training sessions. For each trial, mice were placed in each quadrant, and the time taken to reach the platform was noted. The animals use the extra cues for reference to reach the platform. After training sessions, the platform was completely submerged in the test session. Each mouse was placed in the test paradigm in all the quadrants, and latency to reach the platform was noted.

On postnatal day 60, all the animals were weighed and euthanized by cervical dislocation. The brain was removed and stored in cold isotonic saline after being weighed. They were further homogenized in the appropriate buffer for biochemical estimation.

Biochemical Estimation

Acetylcholine esterase (Ellman et al. 1961): The acetylcholinesterase enzyme activity (AchE) was estimated in brain tissue according to the method described by Ellman et al. (1961) using acetylcholine iodide as a substrate and 5,5 dithibis-2 nitrobenzoic acid (DTNB) as the coloring agent. The degradation of acetylcholine iodide was measured at 412 nm.

Lipid peroxidation (Ohkawa et al. 1979): Malonaldehyde (MDA) was measured according to the standard method. The level was determined by thiobarbituric acid (TBA) reactive substance (TBARS) in brain tissue, based on the reaction between MDA and TBA. The absorbance of the organic layer (upper layer) was read by the UV-Vis spectrophotometer at 532 nm against blank using distilled water. TBA was allowed to react with MDA and formed a colored complex [MDA-(TBA)2 complex], which was measured by the spectrophotometer (Systronics UV-Vis Double Beam Spectrophotometer 2201)

Catalase activity (Luck et al. 1965): Catalase is an enzyme that scavenges hydrogen peroxide converting it to water and oxygen molecule. The activity of this enzyme depends on the ultraviolet absorption of the hydrogen peroxide solution, which can be measured at 240 nm (Luck et al. 1965. The activity of catalase is expressed as a unit/mg protein.

Superoxide dismutase (Marklund & Marklund 1974): It catalyzes the dismutation of superoxide radicals. Measurement of superoxide dismutase activity was based on the inhibition of pyrogallol autoxidation caused by superoxide dismutase as described by (Marklund & Marklund 1974).

Glutathione (Moron et al. 1979): Reduced GSH as a non-enzymatic antioxidant was measured according to the method described. GSH is determined based on the reaction 5,5- dithiobis-2-nitrobenzoic acid (DTNB) with GSH, which is yellow colored chromophore with maximum absorbance at 412 nm. The amount of reduced glutathione in brain tissue was calculated at $l g.g^{-1}$ tissue.

STATISTICAL ANALYSIS

GraphPad Prism 8 was used to analyze the data. One-way analysis of variance (ANOVA) and post hoc test (Tukey's multiple comparisons test) were applied to the data set. The data are represented as mean SEM, and differences were considered significant when $p<0.05$ and highly significant $p<0.01$.

RESULTS

No adverse signs of clinical toxicity were observed in control and treated animals. The gain in the body weight of mice has exhibited significant change ($p < 0.05$) at both the dose levels $1mg.kg^{-1}$ and $2mg.kg^{-1}.bw^{-1}$ as compared to the control (Table 1). At the same time, co-treatment with curcumin resulted in a decrease in body weight gain compared to the control (Table 1). A similarly highly significant decrease was observed in the neurosomatic index of treated animals at 1mg/kg bw (1.74 ± 0.053, $p < 0.01$) and 2mg/kg bw (1.465 ± 0.078, $p < 0.01$) dose levels as compared to control (2.207 ± 0.036). Co-treatment with curcumin resulted in a nonsignificant increase in the neurosomatic index compared to the treated group (Table 1).

Parameters

Open Field Exploration Test: The effects of imidacloprid in the open field behavior are summarized in Table 2

The locomotor activity of animals was assessed by the number of squares crossed during 300 seconds. The animals in the control group could cross an average of 267 ± 22.36 squares. While the average number of squares crossed by $1mg.kg^{-1}.bw^{-1}$ IMI and 2 $mg.kg.bw^{-1}$ IMI group animals

Table 1: Effect of IMI and Cur exposure in Swiss albino mice on Body Weight Gain and Percent neurosomatic index following exposure to IMI, Cur, and their combination in young male weanlings. IMI: Imidacloprid; Cur: Curcumin.

Parameter	Group I Control	Group II 1mg.kg.bw^{-1} IMI	Group III 2mg.kg.bw^{-1} IMI	Group IV 2mg.kg.bw^{-1} IMI + 100mg.kg.bw^{-1} Cur
Weight Gain (gm) (Mean ±SEM)	9.2 ± 0.2	13.37 ± 0.23*	15.25 ± 1.26**	13.25 ± 0.42*
Brain Weight	0.465 ± 0.0078	0.440 ± 0.0176	0.451 ± 0.0034	0.487 ± 0.0145
% Neurosomatic Index	2.207 ± 0.036	1.74 ± 0.053**	1.465 ± 0.078**	1.802 ± 0.054*

Values represent Mean ± SEM bearing different superscripts in the same rows differ significantly * indicates (p<0.05) and ** indicates (p<0.01). One-way analysis of variance followed by Tukey's multiple comparison test.

Table 2: Effect of IMI and Cur exposure in Swiss albino mice on Exploration percent time, Number of Blocks Crossed, and Freezing percent time in Open Field Test following exposure to IMI, Cur, and their combination in young male weanlings. IMI: Imidacloprid; Cur: Curcumin

Parameters	Group I Control	Group II 1mg.kg.bw^{-1} IMI	Group III 2mg.kg.bw^{-1} IMI	Group IV 2mg.kg.bw^{-1} IMI + 100mg.kg.bw^{-1} Cur
Number of Blocks Crossed	267 ± 22.36	239.33 ± 34.49	194.75 ± 32.28	207.33 ± 63.63
Exploration % time	86.13 ± 1.78	87.19 ± 4.44	74.86 ± 4.96	89.88 ± 0.80
Freezing % time	4.518 ± 1.82	5.93 ± 2.49	11.7767 ± 4.91	4.7733 ± 0.98

Values represent Mean ± SEM bearing different superscripts in the same rows differ significantly (p<0.05). One-way analysis of variance followed by Tukey's multiple comparison test.

were recorded to be 239.33 ± 34.49 and 194.75 ± 32.28, respectively. The number is less in comparison to the control. However, not significant. Similarly, a non-significant decrease in the percent exploration time of 74.86 ± 4.96 was noted in animals exposed to 2 mg.kg^{-1}.bw^{-1} IMI. At the same time, no change was observed in the 1 mg.kg^{-1}.bw^{-1} (87.19 ± 4.44) animals compared to the control (86.13 ± 1.78). Further, a non-significant increase in the freezing percent time (11.7767 ± 4.914) was observed in animals exposed to 2 mg.kg^{-1}.bw^{-1} of IMI, while no change was observed at the 1 mg.kg^{-1}.bw^{-1} (5.93 ± 2.49) dose level compared to the control (4.518 ± 1.82). Curcumin co-treatment resulted in a non-significant increase in the number of blocks crossed (207.33 ± 63.63) and exploration percent time (89.88 ± 0.80) while freezing percent time (4.7733 ± 0.98) was found to be reduced in the group exposed to 2 mg.kg^{-1}.bw^{-1} IMI + 100 mg.kg^{-1}.bw^{-1} Cur in comparison to the group exposed with 2 mg.kg^{-1}.bw^{-1} IMI.

Morris Water Maze test: The effects of imidacloprid in the Morris water maze test are summarized in Table 3. It is one of the most widely used behavioral tests for studying spatial learning and memory. In the target quadrant, latency to locate the platform in percent time was increased in the animals exposed to 1mg.kg^{-1}.bw^{-1} (27.66 ± 7.21) and 2 mg.kw^{-1}.bw^{-1}

(12.33 ± 5.56) IMI compared to the control (11.998 ± 1.334). However, it is not significant. Further, curcumin co-treatment resulted in an even more reduction in the latency period to locate the platform (6.32 ± 1.22) compared to the control.

Acetylcholine Esterase Activity (Table 4): Developmental exposure to IMI has resulted in a non-significant decrease in AchE activity in both 1 mg.kg^{-1}.bw^{-1} (0.003146 ± 0.0005) and 2 mg.kg^{-1}.bw^{-1} (0.003659 ± 0.0008) IMI-exposed animals compared to control (0.004857 ± 0.0012). However, no change in the acetylcholine esterase activity was observed in the curcumin co-treated group (0.003360 ± 0.0007) compared to the 2 mg.kg^{-1}.bw^{-1} group.

Lipid Peroxidation (Table 4): LPO estimated in the brain tissue at the end of the exposure period was significantly (p<0.05) higher in 2 mg.kg^{-1}.bw^{-1} (0.11735 ± 0.0134*) IMI exposed animals. No change was seen in the 1 mg.kg^{-1}.bw^{-1} (0.042075 ± 0.0048) compared to the control (0.046325 ± 0.0072). However, it was found to be lowered significantly (p<0.05) by curcumin in the co-treated (0.047575 ± 0.0206) group compared to the 2 mg.kg^{-1}.bw^{-1} group.

Catalase (Table 4): IMI treatment resulted in a decrease in brain catalase levels at 1 mg.kg^{-1}.bw^{-1} (17.69 ± 4.38**) dose level when compared to the control (41.325 ± 3.65)

Table 3: Effect of IMI and Cur exposure in Swiss albino mice on Latency to Reach Platform. IMI: imidacloprid; Cur: curcumin.

Parameters	Group I Control	Group II 1mg/kg bw IMI	Group III 2mg/kg bw IMI	Group IV 2mg/kg bw IMI + 100mg/kg bw Cur
Latency in finding a platform	11.998 ± 1.334	27.66 ± 7.21	12.33 ± 5.56	6.32 ± 1.22

Values represent Mean ± SEM bearing different superscripts in the same rows differ significantly (p<0.05). One-way analysis of variance followed by Tukey's multiple comparison test.

Table 4: Effect of IMI and Cur exposure in Swiss albino mice on Acetylcholinesterase (AchE) Activity, Lipid Peroxidation, Catalase Activity, Superoxide Dismutase Activity IMI: imidacloprid; Cur: curcumin.

Test	Group I Control	Group II 1mg/kg bw IMI	Group III 2mg/kg bw IMI	Group IV 2mg/kg bw IMI + 100mg/kg bw Cur
Catalase (µmole H2O2 decomposed/min//mg protein)	41.325 ± 3.65	17.69 ± 4.38**	42.47 ± 4.96	19.72 ± 3.49*
Superoxide Dismutase (Units/mg protein)	558.33 ± 121.66	509.41 ± 56.52	439.58 ± 76.63	521.58 ± 105.18
Lipid Peroxidation (n moles /mg protein)	0.046325 ± 0.0072	0.042075 ± 0.0048	0.11735 ± 0.0134*	0.047575 ± 0.0206
Acetylcholine (µM acetylthiocholine hydrolysed/min/mL)	0.004857 ± 0.0012	0.003146 ± 0.0005	0.003659 ± 0.0008	0.003360 ± 0.0007

Values represent Mean ± SEM bearing different superscripts in the same rows differ significantly * indicates ($p < 0.05$) and ** indicates ($p < 0.01$). One-way analysis of variance followed by Tukey's multiple comparison test

($p < 0.05$). However, catalase activity was significantly ($p < 0.05$) increased in 2 mg.kg^{-1}.bw^{-1} (42.47 ± 4.96*) exposed animals compared to the low dose (1mg/kg bw) group, reaching almost control values. Treatment with curcumin has shown a significant ($p < 0.05$) decrease (19.72 ± 3.49*) in comparison to the control.

Superoxide Dismutase (Table 4): Superoxide dismutase activity was not affected by IMI exposure across all the treatment and co-treatment groups compared to the control.

DISCUSSION

The growing evidence of the toxic effects of various pesticides, including imidacloprid in animals and humans, as non-target organisms, calls for assessing the adverse health effects it could exert. The most available literature on the toxicity of such chemicals is based on high doses and the adult population. While the effects of acute and sub-chronic low-level exposure, especially in young and developing population, has not been well investigated. The effects of such xenobiotics ought to be well studied among the most vulnerable population, i.e., neonates and young offspring. The developing brain goes through various changes and is far more susceptible to these harmful toxins than the adult brain. Thus, to better understand the toxicity of imidacloprid, the present study was designed to evaluate whether a consecutive 40 days of exposure to imidacloprid at doses (1 mg.kg^{-1}.bw^{-1} and 2 mg.kg^{-1}.bw^{-1}) lower than what most past studies have been based on (El-Gendy et al. 2009, Badgujar et al. 2013, Lonare et al. 2014). These are environmentally relevant with respect to mammals and humans and produce neurobehavioral effects and oxidative stress in young male mice weanlings (Kara et al. 2015, Khalil et al. 2017, Burke et al. 2018). The present doses were selected based on several toxicological reference values (acceptable daily intake, no-observed effect level dose, and acute oral LD50). They were applied orally to 21 days old male Swiss albino weanlings.

Results have indicated that imidacloprid treatment of male mice weanlings has increased body weight gain in treated animals compared to the control group at the end of 40 days of exposure. This increase in body weight in the treated animals can be attributed to the fact that male Swiss albino weanlings were in their growing age during the exposure period. Further, imidacloprid has been reported to impair glucose and lipid metabolism, leading to insulin resistance and weight gain, consistent with the present finding (Kim et al. 2013, Sun et al. 2016).

In the open field test, locomotory behavior indicates locomotor and exploratory activities, whereas freezing can positively correlate with fear and emotionality (Khalil et al.2017). In the current study, IMI exposure led to a non-significant decrease in exploratory behavior. This suggests that exposure to low doses of IMI during the development phase does not affect the locomotor and exploratory activity of young Swiss albino mice. Similar results have been reported by Terçariol & Godinho (2011), where open-field behavior was not affected significantly at the low dose level of fipronil with respect to the other dose levels used in the study.

In the Morris water maze (MWM), performance was used to assess spatial learning and memory in young mice. In the present study, a non-significant increase in latency to reach the platform in the target quadrant was observed at both the dose levels compared to the control. Indicating that cognitive skills are not affected due to sub-chronic low-dose exposure to IMI in developing Swiss albino male mice. The present finding is consistent with Koslowski et al. 2020 where long-term low-dose exposure to another neonicotinoid fipronil did not affect memory and cognitive skills.

Acetylcholinesterase (AchE) is a cholinergic enzyme at postsynaptic nerve endings. It breaks down the naturally occurring neurotransmitter acetylcholine. Results from the

present study have indicated a non-significant decrease in the levels of acetylcholinesterase activities at both the dose levels compared to the control. Similar results have been reported by Tariba Lovaković et al. (2020) at 0.06 and 0.8 mg.kg^{-1}.bw^{-1} IMI dose levels.

Antioxidant enzymes such as catalase, superoxide dismutase, and lipid peroxidation protect the cellular components from reactive oxygen species by deactivating the free radicals (Kurutas 2016).

Peroxidation of the membrane lipids affects the structure, functions, and activity of various membrane-bound enzymes and transport mechanisms. In the present study, imidacloprid exposure to mice at 2 mg.kg^{-1}.bw^{-1} has significantly increased brain LPO levels. The present finding is consistent with results obtained by (El-Gendy et al. 2009, Duzguner & Erdogan 2009, Lonare et al. 2014). These studies were carried out on doses much higher than those selected in the present study. Present findings further strengthen the hypothesis suggesting that oxidative stress is one of the central pathways by which such pesticides exert their cytotoxic effects (Mahaboob Khan & Kour 2007, El-Gendy et al. 2009).

After an initial decrease at the 1mg/kg bw dose level, a significant increase in the activity of the antioxidant enzyme catalase was observed at the 2 mg.kg^{-1}.bw^{-1} dose level compared to the 1 mg.kg^{-1}.bw^{-1}. It acts as the first line of defense against the oxy-free radicals generated due to the toxicity of imidacloprid. This has been attributed to the fact that these defense mechanisms against oxidative stress are in the process of attempted cellular repair. The present finding is consistent with the results obtained in studies where catalase activity was found to increase when male Swiss albino mice were exposed to 1/10th of LD50 of IMI and in another study where animals exposed to IMI intravenously (El-Gendy et al. 2009) but in much higher dose levels compared to those selected in the present study.

Plant-based drugs help alleviate oxidative stress induced by various environmental neurotoxicants. Evidence has shown that consuming naturally occurring antioxidants can decrease oxidative stress markers (Vouldoukis et al. 2004, Lonare et al. 2014). Curcumin has been known Scavenge free radicals and induce detoxification of enzymes protecting against degenerative disease and cancer (Kim et al. 2014, Duan et al. 2014). The antioxidant mechanism of Cur has been attributed to its unique conjugated structure, uses an intramolecular Diels-Alder reaction, and uses linoleate as oxidizable poly-unsaturated lipid (Masuda et al. 2001, Guo et al. 2011, Lonare et al. 2014).

Co-treatment with curcumin resulted in a decrease in body weight gain and an increase in the neurosomatic index, indicating that curcumin could partially reverse the toxic effects of IMI. However, no effect was seen in the open field and Morris water behavior after curcumin co-treatment.

While results from the present study have indicated that the animal group co-treated with curcumin and imidacloprid has shown significant improvement in the antioxidant parameters such as catalase activity and lipid peroxidation, at the same time, no effect was seen in the activity of superoxide dismutase and acetylcholine esterase.

Adolescent brains undergo several anatomical, physiological, and biochemical changes during puberty. Such maturational modifications can influence the pharmacokinetics of these xenobiotics (Blakemore et al. 2010; Kaur et al. 2023). Further, it may also be due to the lower absorption of active insecticide metabolites from the digestive system of young male mice weanlings following oral administration, which results in lesser bioavailability of IMI to tissues (Kim et al. 2007). It has been reported that the major enzymes responsible for the metabolization of IMI P450 (CYP450), especially CYP2C19 and flavin monooxygenase (FMO), have age-dependent functional changes and have been reported to display comparatively greater catalytic effectivity in adolescent liver samples compared to adult samples (Schulz-Jander & Casida 2002, Basaran & Can-Eke 2017). Thus, it can be said that the consequences of IMI metabolism may differ in young and adults. Thus, adolescent mice could detoxify IMI more effectively (Zane et al. 2018; Zhang et al. 2015). It has also been reported that adolescent renal and hepatic clearance capability surpasses the adult capability to do the same. Hence, they metabolize pesticides more easily than adults (Bruckner 2000; Kirti 2023).

CONCLUSION

Our data show that low doses of pesticides like imidacloprid can disrupt the biochemical profile, leading to the generation of oxidative stress in the brains of the developing population; however, behavior and cognitive skills appear unaffected. The young developing population can metabolize and detoxify the pesticides more effectively than adults.

Further, staying on top of oxidative stress is essential in the increasingly toxic world. Results from the present study have indicated that curcumin, a naturally occurring antioxidant, can restore the antioxidant enzyme profile effectively. Thus, dietary intake of such naturally occurring substances by individuals who come in direct and regular contact with pesticides is beneficial in combating the deleterious effects of imidacloprid.

ACKNOWLEDGEMENT

REFERENCES

Arfat, Y., Mahmood, N. and Tahir, M.U. 2014. Effect of imidacloprid on hepatotoxicity and nephrotoxicity in male albino mice. Toxicol. Rep., 1: 554-561.

Badgujar, P.C., Jain, S.K, Singh, A., Punia, J.S., Gupta, R.P. and Chandratre, G.A., 2013. Immunotoxic effects of imidacloprid following 28 days of oral exposure in BALB/c mice. Environ. Toxicol. Pharmacol., 35(3): 408-18.

Bagri, P., Kumar, V. and Sikka, A.K. 2016. Assessment of imidacloprid-induced mutagenic effects in somatic cells of Swiss albino male mice. Drug Chem. Toxicol., 39: 412-417.

Basaran, R. and Can-Eke, B. 2017. Flavin contains monooxygenases and the metabolism of xenobiotics. Turk. J. Pharm. Sci., 14:90-94.

Blakemore, S.J., Burnett, S. and Dahl, R.E. 2010. The role of puberty in the developing adolescent brain. Hum. Brain Mapp., 31: 926-933.

Bruckner, J.V. 2000. Differences in sensitivity of children and adults to chemical toxicity: The NAS Panel Report. Regul. Toxicol. Pharmacol., 31: 280-285.

Burke, A.P., Niibori, Y. and Terayama, H. 2018. Mammalian susceptibility to a neonicotinoid insecticide after fetal and early postnatal exposure. Sci. Rep., 8: 16-32.

Carmichael, S.L., Yang, W. and Roberts, E. 2014. Residential, agricultural pesticide exposures and risk of selected congenital heart defects among offspring in the san joaquin valley of California. Environ. Res., 135: 133-138.

Cimino, A.M., Boyles, A.L. and Thayer, K.A. 2017. Effects of neonicotinoid pesticide exposure on human health: A systematic review. Environ. Health Perspect. 125: 155-162.

Duan, W., Guo, Y. and Xiao, J. 2013. Neuroprotection by aminocarbonyl dimethoxy curcumin C: Ameliorating the toxicity of mutant TDP-43 via HO-1 Mol. Neurobiol. 49: 368-379

Duzguner, V. and Erdogan, S. 2010. Acute oxidant and inflammatory effects of imidacloprid on rats' mammalian central nervous system and liver. Pestic. Biochem. Phys., 97: 13-18.

EFSA (European Food Safety Authority) Scientific Report 2008. Conclusion on the peer review of imidacloprid. 148: 1-120.

EFSA Journal 2014. Conclusion on the peer review of the pesticide risk assessment of confirmatory data submitted for the active substance imidacloprid. EFSA Journal, 12(7): 3741.

EL-Gendy, K.S., Aly, N.M. and Mahmoud, F.H. 2010. The role of vitamin C as an antioxidant in the protection of oxidative stress induced by imidacloprid. Food Chem. Toxicol., 48: 215-221.

Ellman, G.L., Courtney, K.D. and Andres, V. 1961. A new and rapid colorimetric determination of acetylcholinesterase activity. Biochem. Pharmacol., 7: 88-95.

Gawade, L., Dadarkar, S.S. and Husain, R. 2013. A detailed study of developmental immunotoxicity of imidacloprid in wistar rats. Food Chem. Toxicol., 51: 61-70.

Guo, H., Xu, Y. and Fu, Q. 2015. Curcumin inhibits the growth of prostate carcinoma via mir-208-mediated CDKN1A activation. Tumor Biol., 36: 8511-8517.

Jeschke, P., Nauen, R. and Schindler, M. 2011. Overview of the status and global strategy for neonicotinoids. J. Agric. Food Chem., 59: 2897-2908.

Katic, A., Kašuba, V. and Kopjar, N. 2021. Effects of low-level imidacloprid oral exposure on cholinesterase activity, oxidative stress responses, and direct DNA damage in the blood and brain of male wistar rats. Chem. Biol. Interact., 338: 109287.

Kaur M, and Sharma A. The potential neurobehavioral effects of an anti-asthmatic drug (Montelukast): A Review. Bull. Env. Pharmacol. Life Sci., 10(7): 01-10.

Khalil, S.R., Awad, A. and Mohammed, H.H. 2017. Imidacloprid insecticide exposure induces stress and disrupts glucose homeostasis in male rats. Environ. Toxicol. Pharmacol., 55: 165-174.

Kim, J., Park, Y. and Yoon, K.S. 2013. Imidacloprid, a neonicotinoid insecticide, induces insulin resistance. J. Toxicol. Sci., 38: 655-660.

Kim, K.B., Anand, S.S. and Kim, HJ. 2007. Toxicokinetics and tissue distribution of Deltamethrin in adult Sprague-Dawley rats. Toxicol. Sci., 101: 197-205.

Kim, K.T., Kim, M.J. and Cho, D.C. 2014. The neuroprotective effect of treatment with curcumin in acute spinal cord injury: Laboratory investigation. Neurol. Med. Chir., 54: 387-394.

Kirti Sharma, A. Bhatnagar, P., 2023. Comparative reproductive toxicity of phthalate on male and female reproductive potential of rodent when exposure occurs during developmental period, Materials Today: Proceedings, ISSN 2214-7853, https://doi.org/10.1016/j.matpr.2023.04.013.

Koslowski, S., Latapy, C. and Auvray, P. 2020. Long-term fipronil treatment induces hyperactivity in female mice. Int. J. Environ. Res., 17: 1579.

Kurutas, E.B. 2015. The importance of antioxidants which play a role in cellular response against oxidative/nitrosative stress: Current State. Nutr. J., 15: 447.

Lonare, M., Kumar, M. and Raut, S. 2014. Evaluation of imidacloprid-induced neurotoxicity in male rats: A protective effect of curcumin. Neurochem. Int., 78: 122-129.

Luck, H. 1965. Catalase. In: Bergmeyer, H.U., Ed., Method of Enzymatic Analysis, Academic Press, New York and London, 885-894. http://dx.doi.org/10.1016/B978-0-12-395630-9.50158-4

Mahaboob Khan, S. and Kour, G. 2007. Subacute oral toxicity of chlorpyriphos and protective effect of green tea extract. Pesticide Biochem. Phys., 89: 118-123.

Marklund, S. and Marklund, G. 1974. Involvement of the superoxide anion radical in the antioxidation of pyrogallol and a convenient assay for superoxide dismutase. Eur. J. Biochem., 47: 469-474

Masuda, T., Maekawa, T. and Hidaka, K. 2001. Chemical studies on antioxidant mechanism of curcumin: analysis of oxidative coupling products from curcumin and linoleate. J. Agric. Food Chem., 49: 2539-2547.

Moron, M., Depierre, J. and Mannervik, B. 1979. Levels of glutathione, glutathione reductase, and glutathione S-transferase activities in rat lung and liver. Biochim. Biophys. Acta, 582: 67-68

Ohkawa, H., Ohishi, N. and Yagi, K.1979. Assay for lipid peroxides in animal tissue by the thiobarbituric acid reaction. Anal. Biochem., 95: 351-358

Otuechere, C.A., Abarikwu, S.O. and Olateju, V.I. 2014. Protective effect of curcumin against the liver toxicity caused by propanil in rats. Int. Sch. Res. Notices, 16: 1-8.

Pan, R., Qiu, S. and Xiang, L.U. 2008. E-learning and memory ability and its neuroprotective mechanism in mice. Chin. Med. J., 121: 832-839.

Rueda, N., Vidal, V. and García-Cerro, S. 2020. Prenatal, but not postnatal, curcumin administration rescues Neuromorphological and cognitive alterations in ts65dn Down syndrome mice. J. Nutr., 150:2478-2489.

Schulz-Jander, D.A. and Casida, J.E. 2002. Imidacloprid insecticide metabolism: Human cytochrome P450 isozymes differ in selectivity for imidazolidine oxidation versus nitroimine reduction. Toxicol. Lett., 132: 65-70.

Seibenhener, M.L. and Wooten, M.C. 2015. Use the open field maze to measure locomotor and anxiety-like behavior in mice. J. Vis. Exp., 96.

Sharma, A., John, P. and Bhatnagar, P. 2021. Fluoride and endosulfan potentiate cytogenetic effects in Swiss albino mice bone marrow cells. Toxicol. Ind. Health, 37: 68-76.

Sharma, A., John, P.J. and Bhatnagar, P. 2019. Combination of fluoride and endosulfan induced teratogenicity and developmental toxicity in Swiss albino mice exposed during organogenesis. Toxicol. Ind. Health, 35: 604-613.

Simon-Delso, N., Amaral-Rogers, V. and Belzunces, L.P. 2014. Systemic insecticides (neonicotinoids and Fipronil): Trends, uses, mode of action and metabolites. Environ. Sci. Pollut. Res., 22: 5-34.

Sun, Q., Xiao, X. and Kim, Y. 2016. Imidacloprid promotes high-fat diet-induced adiposity and insulin resistance in male C57BL/6J mice. J. Agric. Food Chem., 64: 9293-9306.

Tariba Lovaković, B., Kašuba, V. and Katić, A. 2020. Evaluation of oxidative stress responses and direct DNA damage in blood and brain of rats exposed to low levels of tembotrione. Chemosphere, 253: 126643.

Terçariol, P.R. and Godinho, AF. 2011. Behavioral effects of acute exposure to the insecticide fipronil. Pestic. Biochem. Phys., 99: 221-225.

Tomizawa, M. and Casida, J.E. 2002. Desnitro-imidacloprid activates the extracellular signal-regulated kinase cascade via the nicotinic receptor and intracellular calcium mobilization in N1E-115 cells. Toxicol. Appl. Pharmacol., 184: 180-186.

Tomizawa, M. and Casida, J.E. 2003. The selective toxicity of neonicotinoids is attributable to the specificity of insect and mammalian nicotinic receptors. Annu. Rev. Entomol., 48: 339-364.

Toor, H.K., Sangha, G.K. and Khera, K.S. 2013. Imidacloprid induced histological and biochemical alterations in the liver of female albino rats. Pestic. Biochem. Phys., 105: 1-4.

Van Wendel de Joode, B., Mora, A.M. and Lindh, C.H. 2016. Pesticide exposure and neurodevelopment in children aged 6-9 years from Talamanca, Costa Rica. Cortex, 85: 137-150.

Venkatesan, N. 1999. Pulmonary protective effects of curcumin against paraquat toxicity. Life Sci., 66: 1145.

Vohra, P. and Khera, K.S. 2015. A three-generation study with the effect of imidacloprid in rats: Biochemical and histopathological investigation. Toxicol. Int., 22: 119.

Vorhees, C.V. and Williams, M.T. 2006. Morris water maze: Procedures for assessing spatial and related forms of learning and memory. Nat. Protoc., 1: 848-858.

Vouldoukis, I., Lacan, D. and Kamate, C. 2004. Antioxidant and anti-inflammatory properties of a *Cucumis melo* LC. Extract rich in superoxide dismutase activity. J. Ethnopharmacol., 94: 67-75.

Yang, W., Carmichael, S.L. and Roberts, E.M. 2014. Residential, agricultural pesticide exposures and risk of neural tube defects and orofacial clefts among offspring in the san joaquin valley of California. Am. J. Epidemiol., 179: 740-748.

Zane, N.R., Chen, Y. and Wang, M.Z. 2017. Cytochrome P450 and flavin-containing monooxygenase families: Age-dependent differences in expression and functional activity. Pediatr. Res., 83: 527-535.

Zhang, L., Fang, Y. and Xu, Y. 2015. Curcumin improves amyloid β-peptide (1-42) induced spatial memory deficits through the BDNF-Erk Signaling pathway. PLoS One, 10: 11-17.

Original Research Paper

https://doi.org/10.46488/NEPT.2023.v22i03.046

Open Access Journal

Screening and Isolation of Polypropylene Degrading Fungi from Waste Dumping Site, Kolhapur, India

A.A. Parit (iD)**, A. S. Jadhav** (iD) **and P. D. Raut†** (iD)

Department of Environmental Science, Shivaji University, Kolhapur, Maharashtra, India
†Corresponding author: P. D. Raut; drpdraut@yahoo.co.in

ABSTRACT

Polypropylene (PP) and other plastic wastes are found to accumulate in the environment, creating significant ecological issues. They are determined to be considered non-biodegradable, It has been established that once it enters the environment, it stays there permanently. The present investigation aims to biodegrade PP without physical treatment and exposing it to UV light and sunlight exposed to potential fungi isolated from the soil of solid waste dumping site based on 18SrRNA analysis and the isolated strains were identified as 98.54% similar to *Cladosporium* sp. The fungal strain was submitted with Gene Bank accession number ON024632 and registered as a *Cladosporium halotolerans* strain SUK PRAKASH. The degradation was performed for 8 months of incubation in the aqueous medium. The biodegradation of polypropylene FTIR spectroscopy was performed to further examine the sheets, and the results indicated that perhaps the bonds between the sheets were weakening and breaking. The biodegraded samples of without treated PP sheets, UV-exposed PP sheets, and sunlight-exposed PP sheets exhibit weight loss of 4.2%, 6.1%, and 8.6% respectively.

INTRODUCTION

Polymers made of monomers bound by chemical bonds are called plastics (Vignesh et al. 2016). In the previous several years, plastic output on a global scale has surpassed 330 million tonnes. Polypropylene (PP) is the material most in demand by the plastic converter sector out of all polymers. Because of its excellent processing capabilities and adaptability, PP is one of the most widely used and consumed polymers globally (Samper et al. 2018). It is used for numerous applications like commodities, medical applications, automotive, packaging plastics and packaging products, etc. (Samper et al. 2018). Nowadays, plastic is the major constituent of domestic solid waste and it is approximately 30-40% of the total volume of solid waste. When this polymeric substance is discarded, it is exposed to microorganisms for biodegradation, which leaves a deposit in the soil and landfills. Polymeric discard is a serious issue (Matos & Schalch, 2007). Plastics are strong, long-lasting, moisture-resistant carbon polymers with hydrogen, nitrogen, sulfur, and other organic and inorganic components produced

from fossil fuel, a non-renewable resource. They are also lightweight, robust, and non-biodegradable (Kamble 2015), (Kumari et al. 2013).

Plastics have limitations since they don't biodegrade easily, which causes pollution and adverse effects on the environment. These resistive polymers strengthen and adsorb, which promotes the spread of unwanted and unwanted organisms (Ghosh et al. 2019). Furthermore, the harmful consequences involve swallowing by animals due to mistaken food which leads to entanglement (Yoshida et al. 2016). Therefore, there have been multiple attempts to minimize plastic waste. Plastic can take several centuries for natural degradation in the environment. There are several methods for addressing both physical and chemical degradation, including UV therapy, physical stress, oxidant methanolysis, hydrolysis, etc.

Microorganisms break down plastic by enzymatic activities that convert polymers into monomers and oligomers, followed by metabolic activity by microbial cells (Starnecker & Menner 1996). Microbes like bacteria, fungi, and actinomycetes deteriorate both synthetic and natural plastics (Ghosh et al. 2013). Using microbial enzymes, oxidation or hydrolysis of plastic resulted in chain cleavage of large compound polymers into small molecular monomers,

---

ORCID details of the authors:

A. A. Parit - https://orcid.org/0000-0001-7947-0600

A. S. Jadhav- https://orcid.org/0000-0002-7738-2727

P. D. Raut- https://orcid.org/0000-0002-1916-8343

which is the metabolic process that causes microbial degradation of plastic (Hugenholtz et al. 1998).

The purpose of the current study should be to identify and describe the high potential Polypropylene degraders using isolating microorganisms from soil and screening them. Through the serial dilution technique, soil samples from several areas where waste has been placed are used to accomplish the isolation. To find prospective PP degraders, the Clear Zone technique, an In-Vitro Biodegradation assay, and the calculation of the weight of PP were all utilized sequentially. The isolated strain was identified as the *Cladosporium halotolerans* strain based on an 18S rRNA study. PP deterioration was observed during an 8-month incubation period in an aqueous medium. Changes in PP weight and FTIR spectroscopy provided proof of the degradation.

MATERIALS AND METHODS

Soil Sampling: Soil samples were collected from solid waste dumping sites. The soil layer was dug up to 1 foot and collected soil samples in sample containers using a spatula. These sites are rich with microorganisms that can degrade plastic. Two sites were selected for soil collection, viz. Kasba Bawda and Jayanti Nala from Kolhapur City, Maharashtra, India.

Polypropylene: Polypropylene is a synthetic polymer synthesized from a hydrocarbon source and is synthesized by the polymerization of propylene. Among the various types of polypropylene Isotactic polypropylene was selected for the biodegradation study as these are used on a large scale in day-to-day life. PP sheets which have a thickness of 1 mm. and a size of 500×500 mm. were purchased from Sigma-Aldrich.

Preparation of enrichment culture: 1 g of soil from each site was put into a 500 mL conical flask containing 100 mL of synthetic medium (SM) that was sterilized. The preparation of the enrichment medium involved adding 0.1g of PP powder to it as the sole source of carbon. The prepared sets of flasks were incubated for a further week at room temperature on the shaker at 120 rpm.

Serial dilution method: One mL of enrichment culture was placed into a conical flask that contains 99 mL of saline. The mixture was serially diluted after shaking.

Isolation of PP degrading microorganisms: PP powder served as the primary source of carbon during the initial isolation of microorganisms using solid media (synthetic minimum medium-agar). Plating out on culture media and serial dilution (1:2, 1:5, 1:10) were performed to final enrichment cultures (FECs) (Esmaeili et al. 2013) for grams per liter was: NH_4NO_3 - 1g/L, $MgSO_4.7H_2O$ - 0.2g/L,

K_2HPO_4 - 1 g/L, $CaCl_2.2H_2O$ - 0.1 g/L, KCl - 0.15 g/L, Yeast extract - 0.1 g/L and agar 8.0 g/L. Culture media was autoclaved at 121ºC for 15 minutes. After sterilization, the media was cool and then poured into a sterilized Petri plate. 0.2 mL of each dilution's suspension was streaked out on culture media. These plates were kept for 10 days at 37°C for incubation. After 10 days, the isolated colony, the number of colonies, and the characteristics of the colonies were observed (Burd 2008).

Purification of microbial strain: Colony was picked up by wire loop, re-suspended in 0.2 mL of 0.85% NaCl and streaked onto the same culture under sterile conditions. This suspension was streaked onto potato dextrose agar (PDA) for fungi and nutrient agar (NA) for bacteria to separate the bacterial and fungal strains. Plates were incubated for 36 hours and growth was observed. The subculturing was carried out to get a single isolated colony. As a result, a single colony was found and then suspended again on culture media with PP as the only supply of carbon (Burd, 2008).

The isolates were purified by streaking a pure culture on solid media, depending on the variations in morphology/ colony characteristics. These isolated strains were preserved on PDA slants at 4ºC for further identification and biodegradation study.

Identification of isolate 1: DNA was extracted and its purity was assessed on the 1.0 % agarose Gel, A single band of DNA with such a high molecular weight was shown. Fragments of the Internal Transcribed Spacer (ITS) region were amplified by PCR. When the PCR amplicon was resolved on agarose gel, only a single discrete band, approximately 700 bp, was observed. To remove contaminants, the PCR amplicon undergoes purification (Mandragutti et al. 2021). ITS1 and ITS4 primers using a BDT v3.1 Cycle sequencing kit on ABI 3730xl Genetic Analyzer performed forward and reverse DNA sequencing reaction of PCR amplicon (Gudikandula et al. 2017). From the forward and reverse sequencing data, aligner software was used to create the consensus sequence of the PCR amplicon (Majeed et al. 2019). The ITS region sequence was used to perform BLAST with the database of NCBI Gene Bank. The first ten sequences were selected and aligned using Clustal W's multiple alignment software based on the maximum identity score (https://www. barcodebiosciences.com/genomics -services/microbial-identification/). Using MEGA 7, the distance matrix was generated, and the phylogenetic tree was constructed (Nanda, 2020).

***In-vitro* biodegradation assay:** The biodegradation of PP was investigated by exposing polypropylene sheets to a submerged cultivation process. In conical flasks, degradation using microorganisms was performed on shaker conditions.

There was 100 mL of the synthetic medium and PP sheets in each flask. Aliquots (100 mL) of synthetic media were added into a 500 mL conical flask and sanitized in an autoclave for 20 minutes at 121°C. After sanitizing aliquots (100 mL) of the synthetic medium in an autoclave for 20 minutes at 121°C. although it cooled, the medium was inoculated with 5 mL of fungal spore suspension made by suspending spores from the SM-agar plate in 20 mL sterile water. On a rotary shaker rotating at 110 rpm, the fermentation broth was kept for incubation. Sets were incubated for 8 months to evaluate PP degradation. The sole carbon in the medium originated from PP sheets.

Without inoculating any microbial strain, the control was preserved. The two sets were maintained in 3 groups sunlight-exposed PP sheets, UV-exposed PP Sheets, and PP sheets without treatment.

Determination of weight loss of polypropylene: To facilitate accurate measurement of weightless PP, biofilms were washed off the PP surface with ethanol.

$$Weight\ loss = Wi - Wf$$

$$Weight\ loss\ \% = \frac{Wi}{Wf} \times 100$$

Where, Wi - Initial weight

Wf - Final Weight

Characterization of identified isolate: Isolated pure fungal strains were sent to Eurofins Genomics India Private Limited, Banglore for identification of microbial strains by 18S rRNA technique. FTIR spectroscopy was used to investigate whether PP was degrading biologically. The data were recorded in the spectral range 4000-500 cm^{-1}.

RESULTS

Identification of Isolate-1: At Eurofins Genomics India Private Limited, Bangalore Isolate-1 was identified using

Table 1: Weight loss (%) of PP sheets, UV exposed PP sheets, Sunlight exposed PP sheets incubated with *Cladosporium halotolerans* strain SUK PRAKASH.
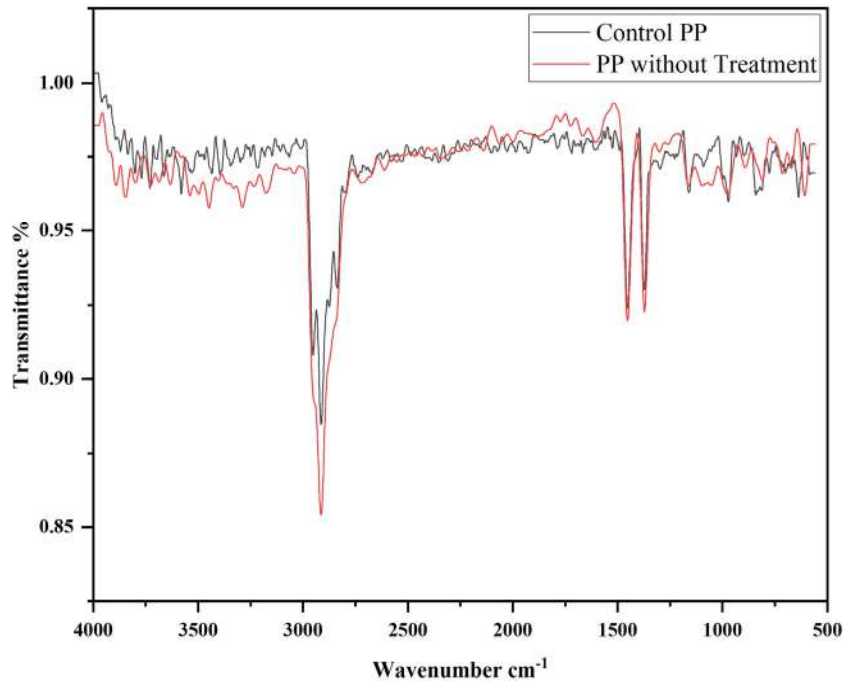
Sr. No.	Time (Month)	Weight Loss (%) on treated with Isolate-1		
		PP sheets	UV-exposed PP sheets	Sunlight-exposed PP sheets
1	0	0	0	0
2	2	2.0	3.1	3.3
3	4	2.6	4.0	4.1
4	6	3.3	5.3	6.0
5	8	4.2	6.1	8.6
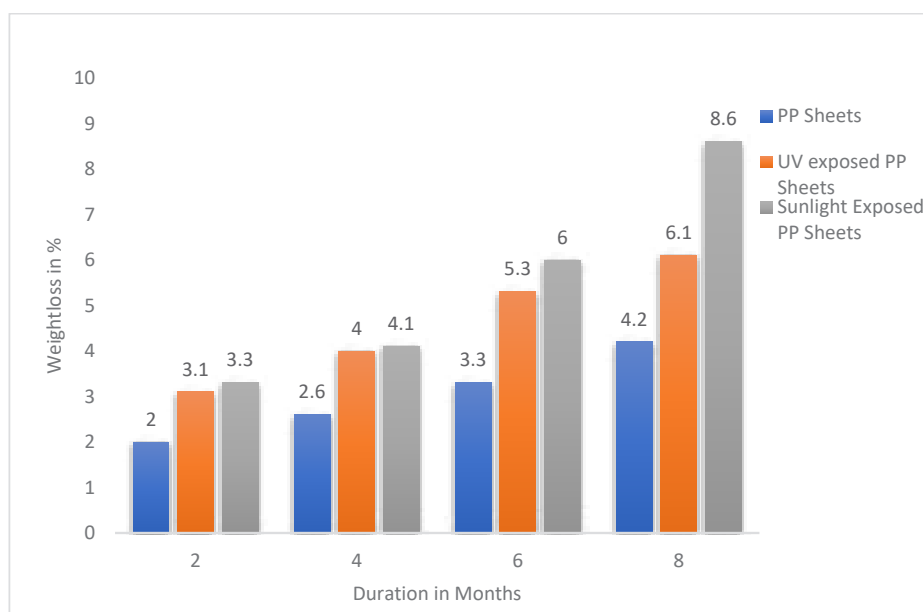
Graph 1: Weight loss (%) of PP sheets, UV exposed PP sheets, Sunlight exposed PP sheets incubated with *Cladosporium halotolerans* strain SUK PRAKASH.

Fig. 1: FTIR spectrum of control PP Vs PP without treatment for the range 4000-550 cm⁻¹.

18SrRNA gene sequencing. With a maximum identification of 98.54% in the *Cladosporium sp.* phylogenetic tree, the identification report of Isolate-1 by 18SrRNA gene sequencing approach indicates the closest phylogenetic affiliation to *Cladosporium halotolerans* 18S ribosomal RNA gene partial sequence. The fungal strain, designated as *Cladosporium halotolerans* strain SUK PRAKASH, was deposited with Gene Bank accession number ON024632.
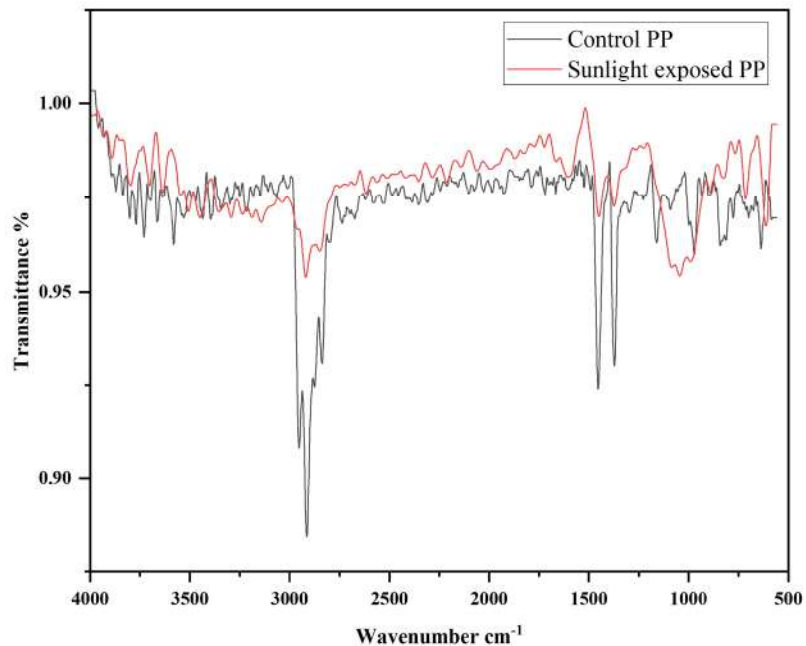
Fig. 2: FTIR spectrum of control PP Vs sunlight-exposed PP for the range 4000-550 cm⁻¹.
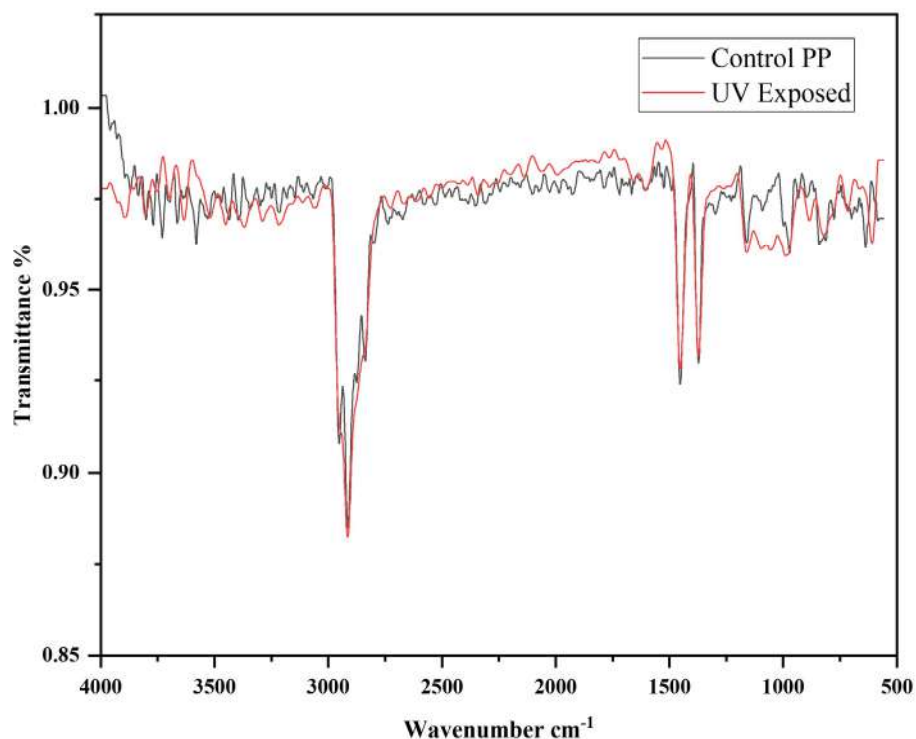
Fig. 3: FTIR spectrum of control PP Vs UV-exposed PP for the range 4000-550 cm⁻¹.

Evaluation of weight loss: The polypropylene sheets were treated with *Cladosporium halotolerans* strain SUK PRAKASH and showed weight loss after 8 months. The highest weight loss is in sunlight-exposed PP sheets i.e. 8.6%, UV-exposed PP sheets, and without treated PP sheets showed weight loss of 6.1%, and 4.2% respectively (Table 1, Graph 1)).

FTIR analysis: Many biodegradation studies employ FTIR spectroscopy as an analytical technique. It is a useful instrument to examine the development of new functional groups and the disintegration of existing functional groups (Das 2015). The presence of additives like antioxidants, as well as degradation products, chemical moieties attached to polymer molecules like branches, co-monomers, and unsaturation, may all be detected using this approach. When the test materials were incubated with microorganisms, such as untreated PP sheets, UV-exposed PP sheets, and sunlight-exposed PP sheets, there was a variance in the intensity of bands in the different locations. For the control spectrum, the specific absorption bands were allocated at 2951cm⁻¹, 2837 cm⁻¹ (C-H stretch), 1491cm⁻¹ (phenol ring), 1371 cm⁻¹ (O-H bend), 1159 cm⁻¹ (alkyl amine) and 971 cm⁻¹, 897 cm⁻¹ (C-H bend mono) (Fig. 1, Fig. 2, Fig. 3).

DISCUSSION

Weight loss is a simple and rapid approach to assess the biodegradation of polymers. Since biodegradation often begins at the polymer's surface, an increase in weight caused by growing microorganisms within the polymer is related to accumulation, whereas a loss is proportional to the surface area. The pretreatment technique typically consists of physicochemical oxidation with a time-consuming, intricate UV exposure process (Jeon et al. 2021). The highest weight loss is in sunlight-exposed PP sheets i.e. 8.6%, UV-exposed PP sheets, and without treated PP sheets showed weight loss of 6.1%, and 4.2% respectively. The pre-treated PP with UV and sunlight has increased biodegradation by facilitating microbial growth than without treated PP. The constraints of the plastic biodegradation process might therefore be addressed by using microorganisms or enzymes that have inadequate biodegradation activity without pretreatment (Jeon et al. 2021). Ahmed & Swrgiary (2021) isolated *Enterococcus cloacae* as a PE degrader for 30 days of incubation weight loss was recorded at 59.02%. As the sample was untreated the microbial colonization requires time to initiate the consuming LDPE (Sudhakar et al. 2008). In biological systems, large molecules are broken down through oxidation and hydrolysis. It is essential that there

are hydrolyzable and oxidizable functional groups along the polymer chain for biodegradation. For the degradation of polyethylene, findings of *Cladosporium, Fusarium, Aspergillus, Penicillium*, and *Phanerochaete* have been highlighted (Munuru et al. 2022). *Pseudomonas* are among the most sought-after bioremediation agents for hydrophobic polymers, according to Wilkes & Aristilde (2017) review of the genus. This is because of their distinctive cell-surface attachment, numerous catalytic enzymes, and extensive metabolic pathways customized for plastic polymers (Habib et al. 2020). *Pseudomonas* and *Vibrio* bacteria as well as the fungus *Aspergillus niger* have been identified to degrade PP (Cacciari et al. 1993 & Mohanan et al. 2020). Mukherjee & Chatterjee (2014) have observed 32% weight loss by *Bacillus weihenstephanensis* for the degradation of thick plastics after six months of incubation. Chonde et al. (2012) noticed comparable weight loss patterns of Nylon 6 sheets on fungus *Phanerochaete chrysosporium* NCIM 1073 incubation and observed the weight loss of Nylon 6 sheets reduced from 0.013 gm to 0.006 gm after 75 days. Ingavale et al. (2018) observed similar results with LDPE and HDPE biodegradation with *Bacillus weihenstephanensis* for 6 months of incubation and recorded weight loss was 7.02% and 7.08% respectively. Pretreated PP has been used in most of the research. The preliminary treatments involved UV-irradiation (Kaczmarek et al. 2005), -irradiation (Iwamoto & Tokiwa 1994), or thermal treatment (Ramis et al. 2004) and have been shown to reduce the polymer's hydrophobicity or add groups like C=O or -OH, which are more susceptible to degradation (Mohanan et al. 2020). During the biodegradation process, new groups (carboxyl and hydroxyl) are formed as well as a decrease in viscosity (Iwamoto & Tokiwa 1994, Sameh et al. 2006). Significant and similar changes were found in all incubated samples the peaks at 2951 cm^{-1}, 2837 cm^{-1} correspond to C-H stretch, 1491 cm^{-1} corresponds to phenol ring and 1371 cm^{-1} corresponds to O-H bond was slightly weakened in PP without treatment but in the sunlight exposed PP and UV exposed PP observed peak were close to disappearing. After incubation for 8 months, some peaks disappeared and a few new peaks are formed which indicates depolymerization occur or starts in the polymer. Peaks at 1720-1730 cm^{-1} and 1640 cm^{-1} areas might be caused by carboxylic ester, aldehyde, ketone, or even double bond groups (Mahlberg et al. 1998). According to Arkatkar et al. (2010), the oxidation of the polymer is indicated by the development of keto carbonyl and ester carbonyl groups. The biodegradation process is initiated by the microorganisms submerged in the landfill using sample oxidation (1723 cm^{-1}) to form carbonyl groups.

CONCLUSION

PP degradation by oxidation or microbial enzymes' principal method of hydrolysis activity for the biodegradation of high molecular weight polymers to produce functional groups that can significantly enhance their hydrophilicity. The FTIR technique estimates the change in transmittance of the native bonds found in PP, which serves as an indication of biodegradation. For the economically and environmentally favorable degradation of PP, many more effective laboratory studies with PP-degrading microbes are needed to explore. Biodegradation of PP without any pretreatment or addition of chemicals to tackle the problem of commercially available plastic.

ABBREVIATIONS

Polypropylene (PP), Fourier transform spectroscopy (FTIR), Final enrichment culture (FEC), Internal Transcribed Spacer (ITS)

ACKNOWLEDGMENT

REFERENCES

Ahmed R. S. and Swargiary M. D. 2021. Plastic and Petroleum Hydrocarbon Degrading Potentials of Single and Mixed Bacterial Cultures Isolated from Garbage Areas of Darrang, Assam. Nature Environment and Pollution Technology, 20(1): 275-280.

Arkatkar, A., Juwarkar, A. A., Bhaduri, S., Uppara, P. V. and Doble, M. 2010. Growth of Pseudomonas and Bacillus biofilms on pretreated polypropylene surface. International Biodeterioration & Biodegradation, 64(6): 530-536.

Burd, D. 2008. Plastic not fantastic. Project Reports of the Canada Wide Science Fair, 1-5.

Cacciari, I., Quatrini, P., Zirletta, G., Mincione, E., Vinciguerra, V., Lupattelli, P. and Giovannozzi Sermanni, G. 1993. Isotactic polypropylene biodegradation by a microbial community: physicochemical characterization of metabolites produced. Applied and Environmental Microbiology, 59(11): 3695-3700.

Chonde S.G., Chonde S.G., Bhosale P.R. and Raut P. D. 2012. Studies on Degradation of Synthetic polymer Nylon 6 by ligninolytic fungus *Phanerochaete chryosporium* NCIM 1073, Journal of Environmental Research and Development, 6(3A): 709-714.

Das, M. P. and Kumar, S. 2015. An approach to low-density polyethylene biodegradation by *Bacillus amyloliquefaciens*. 3 Biotech, 5(1): 81-86.

Esmaeili, A., Pourbabaee, A. A., Alikhani, H.A., Shabani, F. and Esmaeili, E. 2013. Biodegradation of low-density polyethylene (LDPE) by mixed culture of *Lysinibacillus xylanilyticus* and *Aspergillus niger* in soil. PLoS One, 8: e71720.

Ghosh, S. K., Pal, S. and Ray, S. 2013. Study of microbes having potentiality for biodegradation of plastics. Environmental Science and Pollution Research, 20(7): 4339-4355.

Ghosh, S., Qureshi, A. and Purohit, H. J. 2019. Microbial degradation of plastics: Biofilms and degradation pathways. Contaminants in

Agriculture and Environment: Health Risks and Remediation, 1: 184-199.

Gudikandula K., Vadapally P. and Singara Charya M. 2017. Biogenic synthesis of silver nanoparticles from white rot fungi: Their characterization and antibacterial studies. OpenNano, 2, 64-78. https://doi.org/10.1016/j.onano.2017.07.002.

Habib, S., Iruthayam, A., Abd Shukor, M. Y., Alias, S. A., Smykla, J. and Yasid, N. A. 2020. Biodeterioration of untreated polypropylene microplastic particles by antarctic bacteria. Polymers, 12(11): 2616.

Hugenholtz, P., Goebel, B. M. and Pace, N. R. 1998. Impact of culture-independent studies on the emerging phylogenetic view of bacterial diversity. Journal of Bacteriology, 180(18): 4765-4774.

Ingavale, Rachana and Raut, Prakash 2018. Comparative biodegradation studies of LDPE and HDPE using *Bacillus weihenstephanensis* isolated from garbage soil. Nature Environment and Pollution Technology, 17: 649-655.

Iwamoto, A. and Tokiwa, Y. 1994. Enzymatic degradation of plastics containing polycaprolactone. Polymer Degradation and Stability, 45(2): 205-213.

Jong-Min Jeon, J. Jeon, So-Jin Park, S. Park, Tae-Rim Choi, T. Choi, Jeong-Hoon Park, J. Park, Yung-Hun Yang, Y. Yang, and Jeong-Jun Yoon, J. Yoon. 2021. Biodegradation of polyethylene and polypropylene by *Lysinibacillus* species JJY0216 isolated from soil grove. Polymer Degradation and Stability, 191: 109662.

Kaczmarek, H., Ołdak, D., Malanowski, P. and Chaberska, H. 2005. Effect of short wavelength UV-irradiation on ageing of polypropylene/cellulose compositions. Polymer Degradation and Stability, 88(2): 189-198.

Kamble, A., Shubhamsingh, T. and Tejashree, S. 2015. Isolation of plastic degrading micro-organisms from soil samples collected at various locations in Mumbai, India. International Research Journal of Environmental Science, 4(3): 77-85.

Kumari, N. A., Kumari, P. and Murthy, N. S. 2013. A novel mathematical approach for optimization of plastic degradation. Int. J. Engg. Trends and Tech., 4(8): 3539-3542.

Mahlberg, R., Niemi HEM, Denes F. and Rowell, R.M. 1998. Effect of oxygen and hexamethyledisiloxane plasmaon morphology, wettability and adhesion properties of polypropylene and lignocellulosics. International Journal Adhesion and Adhesives, 18: 283-297.

Matos TFL and Schalch V. 2007. Composition of post consumer polymers waste generated in the city of Sao Carlos, SP. Polymers, 17(4): 346-351.

Mohanan, N., Montazer, Z., Sharma, P. K. and Levin, D. B. 2020. Microbial and Enzymatic Degradation of Synthetic Plastics. Frontiers in Microbiology, 11: 580709.

Mukherjee S. and Chatterjee S. 2014. A comparative study of commercially available plastic carry bag biodegradation by microorganisms isolated from hydrocarbon effluent enriched soil. International Journal of Current Microbiology and Applied Sciences, 3(5): 318-325.

Munuru, S., Sandeep, T.S.R.S. and Sucharitha, K. 2022. Biodegradation of plastic polymers by fungi: A brief review. Bioresources and Bioprocessing, 9: 42.

Nanda, T. and Sharma, D. 2020. First report of isolation of *Aeromonas taiwanensis* from India. New Microbes and New Infections, 36: 100721.

Ramis, X., Cadenato, A., Salla, J. M., Morancho, J. M., Valles, A., Contat, L. and Ribes, A. 2004. Thermal degradation of polypropylene/starch-based materials with enhanced biodegradability. Polymer Degradation and Stability, 86(3): 483-491.

Sameh Alariqi, A. Pratheep Kumar, Rao B. S. M. Raj Pal Singh. 2006. Biodegradation of ɣ-sterilized biomedical polyolefins under composting and fungal culture environments. Polymer Degradation Stability, 91(5): 1105-1116.

Samper, M. D., Bertomeu, D., Arrieta, M. P., Ferri, J. M. and López-Martínez, J. 2018. Interference of biodegradable plastics in the polypropylene recycling process. Materials, 10)11): 1886.

Starnecker, A. and Menner, M. 1996. Assessment of biodegradability of plastics under simulated composting conditions in a laboratory test system. International Biodeterioration and Biodegradation, 37(1-2): 85-92.

Sudhakar M., Dobel M., Shriyutha Murthy and Venkatesan R. 2008. Marine microbe-mediated biodegradation of low and high-density polyethylenes. Polymer Degradation Stability, 61: 203-213.

Vignesh, R., Deepika, R. C., Manigandan, P. and Janani, R. 2016. Screening of plastic degrading microbes from various dumped soil samples. Int. Res. J. Eng. Tech., 3(4): 2493-2498.

Wilkes, R. A. and Aristilde, L. 2017. Degradation and metabolism of synthetic plastics and associated products by *Pseudomonas* sp.: Capabilities and challenges. Journal of Applied Microbiology, 123(3): 582-593.

Yoshida, S., Hiraga, K., Takehana, T., Taniguchi, I., Yamaji, H., Maeda, Y. and Oda, K. 2016. A bacterium that degrades and assimilates poly (ethylene terephthalate). Science, 351(6278): 1196-1199.

https://www.barcodebiosciences.com/genomics -services/microbial-identification/

An Approach for Biodiesel Production from Blends of *Azadirachta indica* and *Simarouba glauca* Triglycerides by Graphene-Doped Calcium Oxide Catalyst and Its Comparative Studies

S. G. Chethan†*, M. H. Moinuddin Khan* and L. K. Sreepathi**

*Department of Chemistry, Jawaharlal Nehru New College of Engineering, Shimoga-577204, Karnataka, India
**Department of Mechanical Engineering, Jawaharlal Nehru New College of Engineering, Shimoga-577204, Karnataka, India
†Corresponding author: S.G. Chethan; chethansgs@jnnce.ac.in

ABSTRACT

Over the past several decades, people from many nations have adopted and supported using biodiesel energy sources due to their accessibility and advantages in reducing CO_2 and H.C. emissions to the environment. Today, biodiesel is recognized as a sustainable alternative energy source. Commercially, biodiesel was produced by converting homogenous oil treated with a catalyst like NaOH or KOH in Alcohol. These homogeneous catalysts are hazardous to the environment and cannot be recycled. As an alternative, this research article focuses on biodiesel production from a 1:1 blend of *Simarubha glauca* (Laxmitharu in Kannada) and *Azadirachta indica* (Neem) triglyceride via acid-base catalyzed transesterification reaction. The heterogeneous-based graphene-doped CaO was used as a catalyst obtained through the calcination method by doping it with graphene oxide by the hummers' method. SEM, FTIR, and XRD were used to characterize the GaO-CaO catalyst. The results predict that the prepared catalyst yielded a high percentage of ASFAME (94.0%) and meets the quality as per ASTM standards 6751D.

INTRODUCTION

Energy increases are in demand because of rapid population growth and automation worldwide. The increase in energy demand in the last few years, because of the fast population growth and mechanization all over the country, has made humans much more dependent on non-renewable energy fuel resources. These fuel resources are rapidly depleting, resulting in price instability, decreased global security, stockpile ambiguity to consuming nations, more significant expenses on crude oil fuel imports, and vulnerable economic conditions (Verhoef et al. 2018). Nations depend on non-renewable energy fuel resources, which has led to price fluctuations, decreased energy security, uncertainty in fuel supply to consuming countries, high costs associated with fuel imports of crude oils, and vulnerable economic conditions affected (Jiménez-Xamán et al. 2019). Additionally, these depletable energy sources cause environmental pollution by releasing toxic emissions (Jacobson 2009). The substantial addition of GHG and SOx to the atmosphere results in global warming and acid rain. Because of these problems, it is necessary to search for other environmentally friendly

energy resources that fulfill the energy demands (Boldrin et al. 2009). As per the survey, a sustainable renewable resource for replacing conventional fuels in the future, especially in the transport sector, is biodiesel can be considered as an alternative. Both biodiesel and diesel exhibit similar physicochemical properties. They can be used commercially by blending with diesel fuel or biodiesel (B100) in existing CI engines without moderation (Shelke et al. 2016). As plants produce these resources as a source and can absorb CO_2 emitted into the atmosphere, utilizing biodiesel has the benefit of producing zero carbon dioxide emissions. Therefore, biodiesel fuel sources are known to be CO_2-neutral (Živković et al. 2017).

The feedstock for biodiesel production is from tree-borne oil seeds in India; these non-edible oils are obtained from tree-borne oil species (TBO), some of which are still traditionally used as a fuel source in rural areas (Cheng et al. 2016). Tree Borne Oilseeds (TBOs) are cultivated in distributed forest and non-forest areas and wasteland/deserts/hilly areas concerning agro-climatic conditions (Gomiero 2015). In India, the essential TBOs for biodiesel resources are

as follows Neem (*Azadirachta indica*), Karanja (*Pongamia pinnata*), Mahua (*Madhuca indica*), Jatropha (*Jatropha curcas*), Kusum (*Schleichera*), Simarubha glauca, Pilu (*Salvadora oleoides*), Bhikal (*Prince piautilis*), Surahonnae (*Calophyllum inophyllum*), etc., The oil content found in these seeds varies between 21 to 60%. Pongamia pinnata, Neem (Azadirachta indica), and Simarubha glauca (Laxmitharu in Kannada) are among the several tree-borne oilseeds (TBOs) available for biodiesel production. These tree-borne seeds are seasonal varieties only accessible for 2-3 months annually. The seeds of neem and simarubha contain a high percentage of oil (40-50 %), while the seed pulp provides a significant source of protein. Furthermore, the resources of the neem and simarubha plants are employed in cancer therapy and bacterial infection. Cultivating TBOs and implementing blended seed oil resources for biodiesel production overcome the problem of raw material scarcity. The consumption of total available non-edible oil resources will reduce the Indian crude oil imports from other countries and also improves the Indian economy (Dhyani et al. 2015). In traditional techniques, biodiesel was synthesized with a homogenous catalyst; however, these homogenous catalysts are allied with problems such as soluble, non-recycling, high percentage of soaps and glycerol during transesterification reaction, resulting in a low yield fatty acid methyl ester (Biodiesel). Therefore, to overcome limitations nowadays, heterogeneous catalysts are used as a catalyst in transesterification reactions. The GaO-CaO catalyst exploited in this research was a heterogeneous catalyst derived from waste eggshells calcinated and doped with graphene oxide. The prepared catalyst is environment-friendly and used in biodiesel production. Furthermore, the crude biodiesel was refined from the novel reefing technique in the presence of areca husk resin(ARH). The biodiesel quality was evaluated according to ASTM Standard 6751 D and compared with conventional methods.

MATERIALS AND METHODS

Materials

Azadirachta indica and *Simarouba glauca* oil were received from the Biofuel Research Information and Demonstration Centre, JNNCE, Shimoga, Karnataka. The areca husk was obtained from a farmer in the Shivamogg villages, and further, the chemicals utilized in this research were procured from S.D. fine chemicals, Mumbai, India.

Preparation of GO-CaO Catalyst

The modified Hummer process was followed to synthesize graphene oxide (GO). Graphite powder (1.0 g) with 20 mL of concentrated sulfuric acid in a clean 250 mL R.B. flask was stirred in the ice bath. The above mixture is treated with $NaNO_3$ and $KMnO_4$ at the maintained temperature of 5°C. Further, water was added, and the suspension was heated to 98°C. Finally, the obtained graphene mixture was treated with H_2O_2 (30%). The product was filtered, washed with distilled water, and dried. The dried powder was refluxed with derived CaO from waste eggshell at 300°C for 2 h to yield a catalyst. The GO-CaO catalyst was allowed to cool before being stored in an airtight container for future use in biodiesel synthesis.

Synthesis of *Azadirachta Indica-Simarouba Glauca* Fatty Acid Methyl Ester (ASFAME)

Transesterification, or fatty acid methyl ester (FAME), was synthesized from mixed triglyceride with an alcohol-containing dissolved catalyst. In recent years, transesterification has been the most accepted for biodiesel synthesis (FAME). The general reaction of the transesterification is shown in Scheme 1 (Fadhil & Saeed 2016)

The biodiesel was produced using acid-catalyzed or base-catalyzed processes, depending on the fatty acid concentration of the feedstock. Acid-catalyzed transesterification processes occur in the presence of acids, the most frequent of which is sulfuric acid(Agarwal 2007). The acid-catalyzed process is the first step before the base-catalyzed transesterification operations; the resulting ASO oil is evaluated for free fatty acid content (FFA). Based on the presence of FFA in ASO oil, the ASO oil is first treated with sulphuric acid for the esterification process, as seen
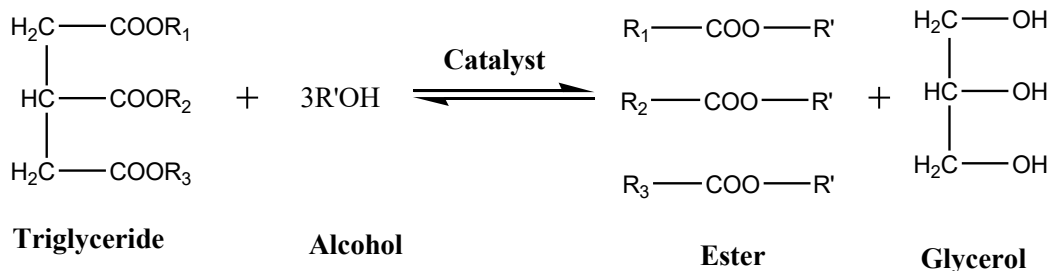
Scheme.1. Trans-esterification reaction *Azadirachta indica-Simarouba glauca* fatty acid methyl ester.
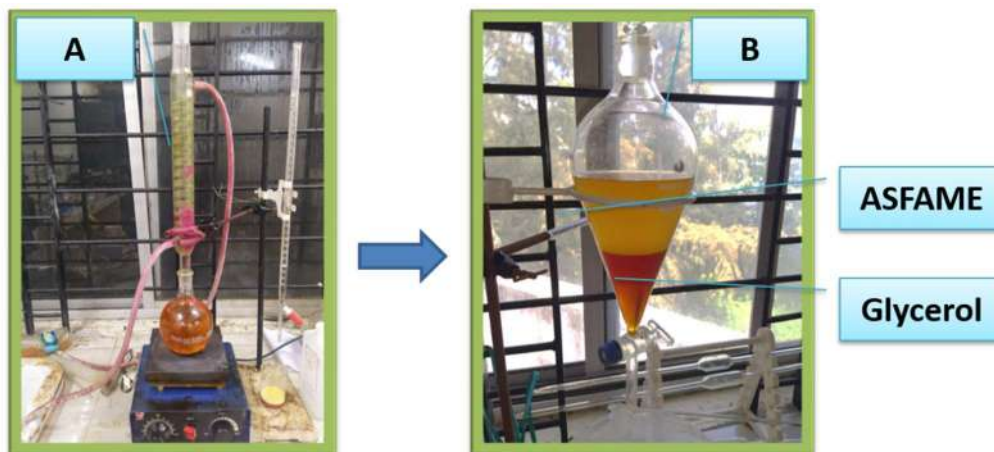
Fig. 1: Transesterification setup (a), Illustration of *Simarouba glauca* and neem fatty acid methyl ester on the top and the glycerol separation (b).

in Fig. 1. The reaction mixture was heated at 60-65°C for around 90 minutes on a hot pallet magnetic stirrer with 900 RPM until the reaction was completed. After 90 minutes, the reaction mixture was transferred to a separating funnel to separate the acid impurities at the top(Yatish et al. 2018); the reduced FFA content of oil was exposed to base-catalyzed transesterification.

Base Catalyzed Trans-Esterification

The recovered ASO oil layer (2.2.1) is transferred in a clean, dry R.B. flask. Again, FFA content was tested for ASO. The catalyst concentration was tuned by combining 0.25, 0.5, 0.75, 1.0, and 1.25 g of produced GO-CaO with a constant amount of methanol. The reaction was set up similarly to an acid-catalyzed reaction, and the reaction mixture was refluxed for roughly 1 h at 60°C. The mixture was allowed to cool to yield Azadirichita-Simaruba fatty acid methyl ester (ASFAME) and crude glycerol at the bottom. The obtained biodiesel was tested for various physicochemical quality parameters such as kinematic viscosity, fire point, Fourier transform infrared spectroscopy (FTIR), relative density, gas chromatography (G.C.), and flash point. Further, the ASFAME yield was optimized.

Bioresin Treatment for Refining Crude ASFAME

The ion exchange column 30 cm⁻¹ in height and 1 cm⁻¹ in diameter was pre-filled with Areca husk resin (ARH) with crude ASFAME passed over bio-resin. The eluted refined ASFAME from the ion exchange column with a 30 drops/minute flow rate, according to Chethan et al. (2023),was collected and stored separately for further study. The physicochemical parameters of refined ASFAME from the ion exchange process and ASFAME refined from the

conventional approach were compared using the ASTM 6751 D standard.

Characterization of GO-CaO and ASFAME

Thermo Nicolet iS50 FTIR spectrophotometer was used to investigate ASO oil and ASFAME liquid samples. The Thermo Nicolet iS50 FTIR spectrophotometer with 0.2 cm⁻¹ resolution was used for the FTIR spectral examination in the spectral range between 400 and 4000 cm⁻¹. The morphological aspects of GO-CaO and AHR were investigated using the JOEL JSM-IT500. For GO-CaO catalysts with known crystalline characteristics, X-ray diffraction experiments were performed.

RESULTS AND DISCUSSION

SEM Characteristics of Graphene-CaO Catalyst

Fig. 2(a-d) are the Scanning Electron Microscope (SEM) images of the Graphene coated CaO respectively. SEM provides high-resolution pictures of a sample surface, exposing features as low as 1 nm. GaO – CaO catalyst magnification was observed in SEM at 500X, 1,500X, 3,500X, 7,000X, and 10,000X, respectively (Musharraf et al. 2012a).

X-ray powder diffraction (XRD) analysis confirms the phase identification of a crystalline material and can provide information on unit cell dimensions as per the hkl values. The D/MAX 2200PC diffractometer (Rigaku Corporation, Japan) with copper Kα irradiation was used, operating at 40 kV and 30 mA with a scanning rate of 0.2° min⁻¹ in the 2θ range of 0–80° Fig. 3 shows that the GO concentration in Calcium Oxide significantly influenced the variation in characteristic peak intensity and crystal grain size, which
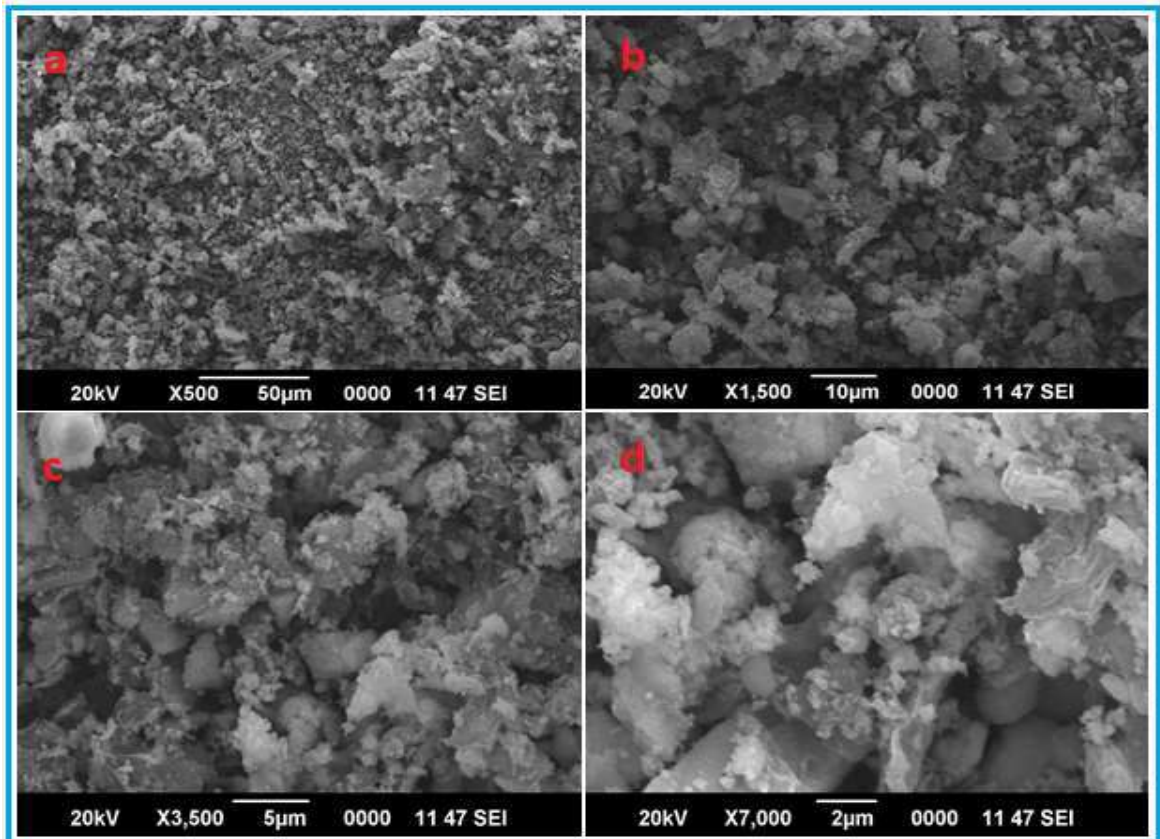
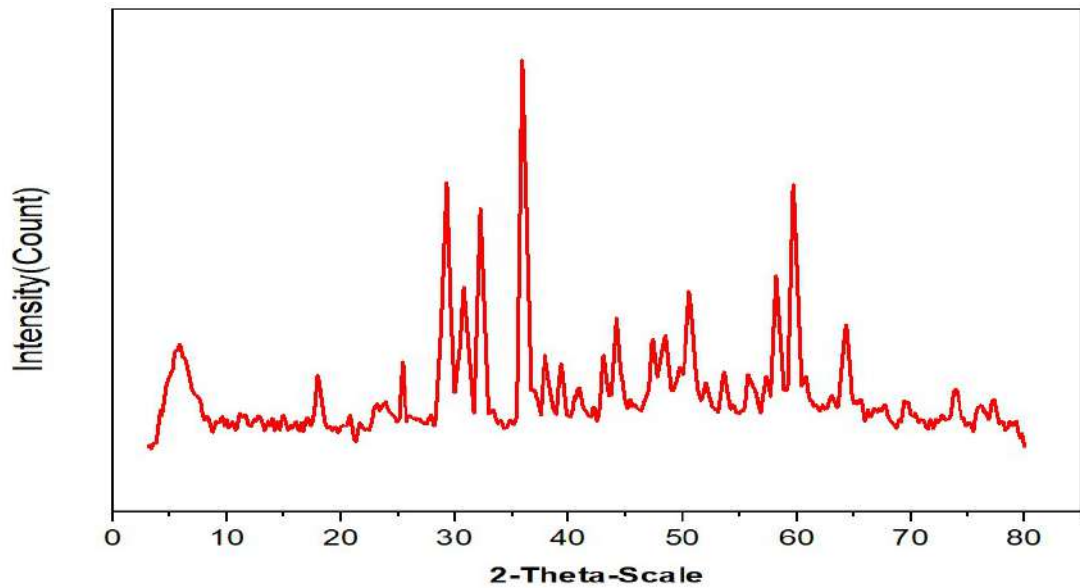Fig. 2: Scanning electron microscope images of the graphene-coated CaO XRD characteristic of graphene-CaO catalyst.

Fig. 3: PXRD of graphene coated calcium oxide.

Table 1: Optimization of GO-CaO and ASO Oil.

Sl.No	Samples	GO-CaO in [w/v]	Yield [%]
1.	ASO-1	0.25	61.10
2.	ASO-2	0.5	94.69
3.	ASO-3	0.75	53.40
4.	ASO-4	1	50.50
5.	ASO-5	1.25	44.64

displayed a characteristic pattern as GO (Sharma et al. 2021) agriculture, forestry, and other land-use practices account for 24% of global greenhouse gas (GHG. The XRD details of GaO-CaO show that CaO is cubic in structure and was confirmed by SEM morphology.

Optimization of Catalyst and ASO Oil for Biodiesel Synthesis

ASO oil was pretreated with methanol (0.60 w/w) containing 1% w/w H_2SO_4 catalyst was refluxed for 1 h at 60°C. in the second step of the reaction, the product from the first step was used for transesterification with GO- CaO catalyst using specified optimization conditions designed (Table 1). The optimization conditions for the second step catalyst concentration with an increase in 0.25 g of catalyst, reaction time for 65 min, and methanol/oil molar ratio were carried out as per Graboski and McCormick (1998). Table 1 results show that as the concentration of the catalyst increases up to 0.5g of Go-CaO results in a high percentage of ASFAME (biodiesel) due to the high reactivity of catalyst with large surface area results in proper separation of ester and glycerol layers (Colombo et al. 2017). Moreover, it is observed that biodiesel yield decreased as an increase above 0.5 g of the catalyst.

Physicochemical Properties of the ASFAME

The physicochemical properties of ASO oil, ASFAME, conventional biodiesel method, and diesel were analyzed

as per ASTM standard 6751D. Table 2 results show that the physicochemical of ASO oil were reduced after the transesterification reaction (Alptekin & Canakci 2008). The biodiesel obtained after optimization catalyst at 0.5g of GO-CaO catalyst and methanol, ASO ratio of 0.20:1 ratio yields 94% of ASFAME. Further, it is observed that the percentage yield of ASFAME filtered from AHR resins resulted in a high yield of biodiesel, compared to the percentage yield of ASFAME from the conventional biodiesel refining method (86%). Moreover, table -2 shows that ASFAME refined from novel refining AHR resins are of superior quality, and purity was found to be similar to conventional diesel quality within the limits of ASTM standards 6751D. Hence, the synthesized biodiesel from the newly proposed method is safer and eco-friendly to adopt as a fuel source in present IC engines

FTIR Characterization of 1:1 ASO oil and ASFAME

The I.R. spectra show the stretching and bending vibrations of *Azadirachta indica* and *Simarouba glauca* oil (1:1) blend and ASFAME (Fig. 4). A narrow peak at 2876 cm^{-1} corresponds to –C.H. stretching, showing the oil's presence. The intense peak at 986 cm^{-1} is due to the presence of ester groups which was expected for C–O–C stretching. The vibration peaks at 1789 cm^{-1} are due to the C=O stretching of the triglyceride ester and the peaks at 1464 cm^{-1}. Vibration for C–H bending further observed that the peak at 876 cm^{-1} is due to methylene rocking vibration in the ASFAME. The peak of C=O for neem seed oil appeared at 1674 cm^{-1} bending, and its intensity corresponds to 3387 cm^{-1}. A broad light peak at cm^{-1} corresponds to -C.H. stretching. This confirms the presence of the alkane group. A sharp peak at 3855.1 cm^{-1} corresponds to -C.H. stretching. This confirms the presence of the alkene group (Silverstein and Webster 1988). A broad light peak at 148.3 cm^{-1} corresponds to the -C-O stretching of the carboxylic ester group (Kim et al. 2007). This confirms the presence of the ester group. A broad

Table 2: Physicochemical properties of ASO oil, ASFAME, and conventional diesel.

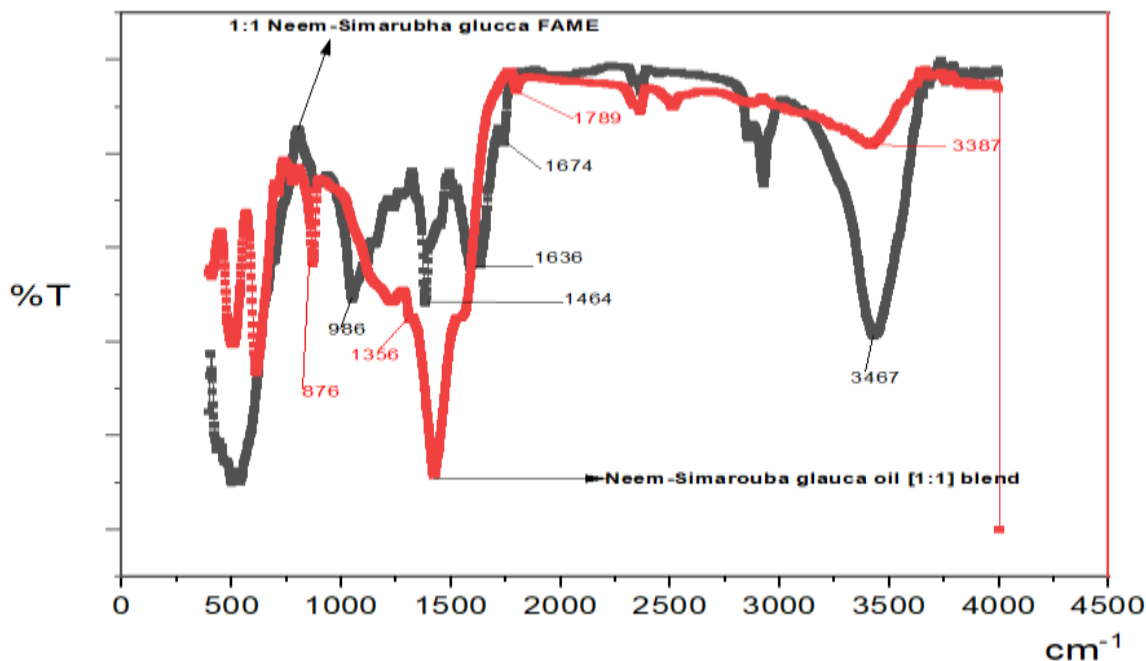| Sl. No.	Name Of The Analysis	ASO Oil	Conventional Biodiesel refining	ASFAME By ARH Refining	Diesel	Test Method ASTM 6751D
1.	Density (kg.m^{-3})	1.58	0.990	0.864	0.79	D-287
2.	Kinematic Viscosity at 40°C (Cst)	61.87	6.09	5.62	5.20	ASTM D 445
3.	Flashpoint (°C)	219	185	175	74	D93
4.	Fire point (°C)	230	188	180	78	D93
5.	Copper corrosion test at 50°C for 2 h	Complies	Complies	Complies	Complies	D 130
6.	Moisture (%)	0.5	0.05	0.01	0.01	----
7.	Calorific value kJ.kg^{-1}	41.0	39.0	40.0	43.0	---
8.	The yield of ASFAME (%)	----	86.0	94.0	----	---

Fig. 4: FTIR spectrum of ASO and ASFAME (biodiesel).

light peak at 1743 cm^{-1} corresponds to -C=O stretching. This confirms the presence of the carboxylic ester group. A broad light peak at 1246 cm^{-1} corresponds to -C.O. stretching, and its intensity corresponds to 3347 cm^{-1} (Sorichetti et al. 2014). This confirms the presence of the carboxylic ester group. A broad light peak at 1435 cm^{-1} corresponds to -CH$_3$ bending. This confirms the presence of the alkane group. The shifts in I.R. peaks confirm the formation of ASO oil into ASFAME.

Gas Chromatography Analysis of *Azadirachta indica* and *Simarouba glauca* Oil

Fig. 5 illustrates a G.C. chromatogram of triglycerides from ASO oil blends. Fig. 6 displays G.C. data from ASFAME, revealing that the separated peaks are free of glycerin, mono, di, and triglycerides (Musharraf et al. 2012b), showing that the triglycerides were transformed into short-chain fatty acid methyl ester. The graph clearly shows that; the produced biodiesel is free from glycerin by comparing the data of standard G.C. of biodiesel.

Heat of Combustion

ASFAME (biodiesel) blended with diesel has been discovered to have similar conventional diesel qualities and lower SOx and H.C. emissions during combustion in IC engines. The heat of combustion, also known as calorific value, is the heat created by the fuel within the engine that allows it to accomplish work. According to Freedman and Bagby, calorific values rose with chain length, and ASO oil, Biodiesel, and diesel were 41.325, 39.345, and 43783 kJ/kg, respectively (1989). Because of the separation of glycerol and other components in the ASO backbone, the calorific value of ASO oil is roughly 8% less than that of diesel; esterification of ASO oil into biodiesel lowers the calorific value of diesel.

Wash Water Demand Calculations

The traditional biodiesel refining process uses water. For one liter of crude ASFAME, refining takes roughly 10 to 11 liters of warm water (40°C). It generates an equal amount of contaminated biodiesel-washed water. The Na$^+$ ion and glycerol in crude ASFAME-washed water were analyzed using Dunstan's and the phenolphthalein test. In the usual approach, the ASFAME yield was roughly 86.0%. With decreased processing time, crude ASFAME refining via developed AHR resins yields 94.0% without warm water (40°C) and fulfills ASTM standard 6751D (Table 2). As a result, the devised technique of refining crude ASFAME in the presence of an ion exchange column packed with AHR resin consumes less water (Sorichetti et al. 2014).

CONCLUSION

This research aims to study the synthesis of ASFAME using blends of *Azadirachta Indica* and *Simarouba*
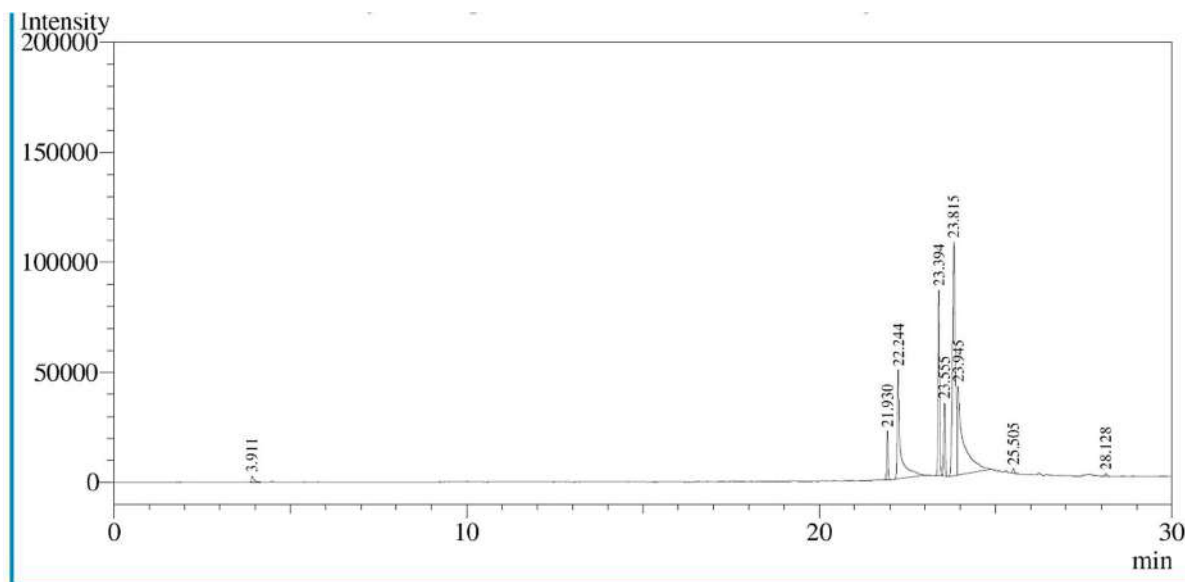
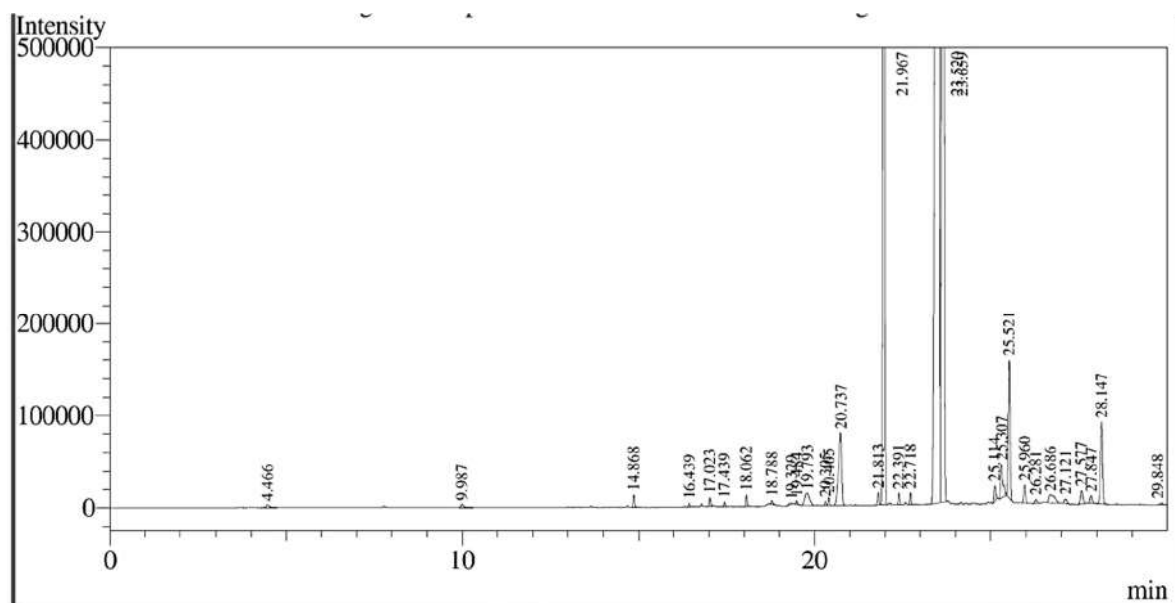Fig. 5: Gas chromatogram analysis of ASO oil.

Fig. 6: Gas chromatogram analysis of ASFAME (Biodiesel).

glauca oils (ASO) in the presence of a heterogeneous catalyst, GO-CaO, made from a waste eggshell. The ASFAME yield was optimized using various catalyst concentrations, and it was found that 0.5 g of GO-CaO yielded 94.69% ASFAME (biodiesel). Furthermore, the physicochemical parameters of ASFAME were evaluated and compared with conventional diesel, resulting in high-quality biodiesel that meets ASTM Standards 6751D.

This study helps to meet fuel demand by employing the ecologically friendly heterogeneous catalyst GO-CaO, which can be recovered and reused as a catalytic material. This article helps small-scale biodiesel manufacturers get catalysts at a lower cost and use various residual wastes in synthesizing catalysts. The proposed work helps decrease disposal challenges and ensure sustainability by blending different oils for biodiesel

REFERENCES

Agarwal, A.K. 2007. Biofuels (alcohols and biodiesel) applications as fuels for internal combustion engines. Prog. Energy Comb. Sci., 33(3): 233-71. https://doi.org/10.1016/j.pecs.2006.08.003.

Alptekin, E. and Canakci, M. 2008. Determination of the density and the viscosities of biodiesel–diesel fuel blends. Renew. Energy, 33(12): 2623-30. https://doi.org/10.1016/j.renene.2008.02.020.

Boldrin, A., Jacob, K., Andersen, J.M., Thomas, H.C. and Enzo, F. 2009. Composting and compost utilization: accounting of greenhouse gases and global warming contributions. Waste Manag. Res. J. Sustain Circular Econ., 27(8): 800-812. https://doi.org/10.1177/0734242X09345275.

Cheng, Y.L., Lee, Y.L., Huang, C., Buckner, R.M., Lafrenie, J.A. and Dénommée, J.M. 2016. Advanced Biometric Tecnologies, InTEchOpen. Scientishttps://www.intechopen.com/books/advanced-biometric-technologies/liveness-detection-in-biometrics.

Chethan, S.G., Moinuddin, K. and Sreepathi, L.K. 2023. Development of areca husk resin for purification of crude Millettia Pinnata fatty acid methyl ester (biodiesel) and its comparative studies. Emerg. Mater., 1: 452. https://doi.org/10.1007/s42247-023-00452-9.

Colombo, K., Laercio, E. and António André Chivanga Barros. 2017. The study of biodiesel production using CaO as a heterogeneous catalytic reaction. Egypt. J. Petrol., 26(2): 341-49. https://doi.org/10.1016/J.EJPE.2016.05.006.

Dhyani, S.K., Vimala Devi, S. and Handa, A.K. 2015. Tree Borne Oilseeds for Oil and Biofuel. Technical Bulletin 2/2015. ICAR-CAFRI, p. 5.

Fadhil, A.B. and Saeed, L.I. 2016. Sulfonated tea waste: A low-cost adsorbent for purification of biodiesel. Int. J. Green Energy, 13(1): 110-18. https://doi.org/10.1080/15435075.2014.896801.

Gomiero, T. 2015. Are biofuels an effective and viable energy strategy for industrialized societies? A reasoned overview of potentials and limits. Sustainability, 7(7): 8491-8521. https://doi.org/10.3390/su7078491.

Graboski, M.S. and McCormick, R.L. 1998. Combustion of fat and vegetable oil derived fuels in diesel engines. Prog. Energy Comb. Sci., 24(2): 125-64. https://doi.org/10.1016/S0360-1285(97)00034-8.

Jacobson, M.Z. 2009. Review of solutions to global warming, air pollution, and energy security. Energy Environ. Sci., 2(2): 148-73. https://doi.org/10.1039/B809990C.

Jiménez-Xamán, C., Xamán, J., Nelson, O., Moraga, I., Hernández-Pérez, I., Zavala-Guillén, J. and Jiménez, M.J. 2019. Solar chimneys with a phase change material for buildings: An overview using CFD and global energy balance. Energy Build., 186: 384-404. https://doi.org/10.1016/j.enbuild.2019.01.014.

Kim, H., Michael, G., Hudgens, J.M., Dreyfuss, D.J., Westreich, J. and Christopher, D.P. 2007. Comparison of group testing algorithms for case identification in the presence of test error. Biometrics, 63(4): 1152-63. https://doi.org/10.1111/j.1541-0420.2007.00817.x.

Musharraf, S., Ghulam, M. Arif, A., Noureen, Z., Nurul Kabir, M., Iqbal, C. and Atta-ur, R. 2012. Biodiesel production from microalgal isolates of southern Pakistan and quantification of FAMEs by GC-MS/MS analysis. Chem. Central J., 6(1): 149. https://doi.org/10.1186/1752-153X-6-149.

Sharma, M., Rajesh, K., Prashant, K. and Seeram, R. 2021. Carbon farming: Prospects and challenges. Sustainability, 13(19): 11122. https://doi.org/10.3390/su131911122.

Shelke, M., Pankaj, S., Nitin, M.S. and Subhash, Lahane. 2016. Investigation of combustion characteristics of a cottonseed biodiesel fuelled diesel engine. Proced. Technol., 25: 1049-1055. https://doi.org/10.1016/j.protcy.2016.08.205.

Silverstein, R.M. and Webster, M. 1988. Spectrometric Identification of Organic Compounds. Sixth edition. Wiley, NY.

Sorichetti, P., Silvia, D.R. and Patricio, A.S. 2014. Water consumption in biodiesel production: optimization through measurement of electrical properties development of ultrasonic sensors for optoacoustic systems. Environ. Res. J., 6: 425. https://www.researchgate.net/publication/284061425.

Verhoef, L., Bart, W., Budde, A., Cindhuja, C., Brais. G.N. and Van Wijk, J.D.M. 2018. The effect of additive manufacturing on global energy demand: An assessment using a bottom-up approach. Energy Policy, 112: 349-60. https://doi.org/10.1016/j.enpol.2017.10.034.

Yatish, K.V., Lalithamba, H.S., Suresh, R. and Harsha, H.R. 2018. Optimization of Bauhinia variegata biodiesel production and its performance: Combustion and emission study on a diesel engine. Renew. Energy, 122: 561-75. https://doi.org/10.1016/j.renene.2018.01.124.

Živković, S., Milan, V., Veljković, I.B., Banković-Ilić, M., Krstić, S. and Konstantinović, S., Social, human health risk, toxicological and policy considerations of biodiesel production and use. Renew. Sustain Energy Rev., 79: 222-47. https://doi.org/10.1016/j.rser.2017.05.048.

Environmental Protection Measures for Unplanned Land Use and Land Cover Changes in a Subbasin of the Ganga River System

Zeenat Ara†, Ramakar Jha and A. R. Quaff

Department of Civil Engineering, National Institute of Technology, Patna 800005, Bihar, India

†Corresponding author: Zeenat Ara; zeenata.phd19.ce@nitp.ac.in

ABSTRACT

In the Ganga river system, unplanned land use land cover (LULC) changes have serious threat to the environment. Protective measures are essential at local, regional, and global scales to save human life and the environment. In the present work, the land use and land cover (LULC) changes have been studied from 2002 to 2021 in a basin area between river Gandak and river Burhi Gandak in India. For the analysis, Landsat 5, 7, and 8 satellite data have been used to analyze the changes in vegetation, urban land, open land, water body, and wet soil in the last two decades. The result shows that from 2002 to 2021 the agricultural area and open land have decreased by 16.12% (158,676 ha) and 11.85% (116794.8 ha), respectively. The urban and the waterlogged area have increased by 24.32% (240,070 ha) and 4.75% (46937.3 ha), respectively. The environmental protection measures, namely conjunctive use, multiple cropping practices, land reclamation, and decentralized urban development to reduce floating population, have been studied and recommended in the study region for better land use/land cover.

INTRODUCTION

Using satellite remote sensed data provides excellent results over the land surface in temporal and spatial domains (Jovanović et al. 2015). It is cost-effective to map LULC and detect changes using remote sensing and GIS tools. Different satellite data are being used for different purposes based on spatial resolution, electromagnetic spectrum, energy source, imaging medium, and several bands. The high-resolution satellite data will attain a better degree of classification accuracy. In the past, numerous LULC estimation methods have been used to assess the shifting cultivation, landscape changes, and benefit from change detection (Anitha 2021, Jamali et al. 2015, Lu et al. 2004, Usman et al. 2015, Gaurav & Singh 2022, Jensen 1996, Bajirao et al. 2018, Mas 1999, Olokeoguna et al. 2014). Land use is influenced by environmental factors like soil characteristics, climate, topography, and vegetation (Baboo & Devi 2010).

Urbanization, industrialization, the influx of point and non-point source pollution, and the floating population are the main causes of LULC changes. Scientists and researchers have used different methods to assess the causes of changes in LULC and the repercussions of those changes owing to human activity (Cardille & Foley 2003). In water resource engineering, land use classification is crucial in determining a catchment area's runoff response (Ara 2021). Using remote sensing and geographic information systems, the ecological system uses and land cover changes have reached their optimum limits (Sultana et al. 2023).

The floating population in urban areas is very high due to the influx of people from nearby areas, villages, or towns. This creates environmental pollution regarding water pollution, sewage, and wastewater. Moreover, some environmental protection measures are essential for effective water resource management. In the present work, all such important aspects have been discussed.

MATERIALS AND METHODS

Study Area

The study area is in between Gandak to Burhi Gandak rivers system, and the total area is 9859.25 km^2 (Fig. 1). The Gandak river originates at an altitude of 7620 m above MSL in the north of Dhaulagiri in Tibet near the Nepal border at Latitude 29°18' N and Longitude 83°58' E. It flows through west Champaran, East Champaran, Muzaffarpur, Gopalganj, Siwan, Saren, and Vaishali districts of Bihar and joins Ganga at Hazipur. Burhi Gandak River is one of the tributaries of the Ganga River, which originates from Chautarwa Chaur near Bisambharpur in the district of West Champaran in Bihar at 84°12' E longitudes and 27°05' N latitude and is
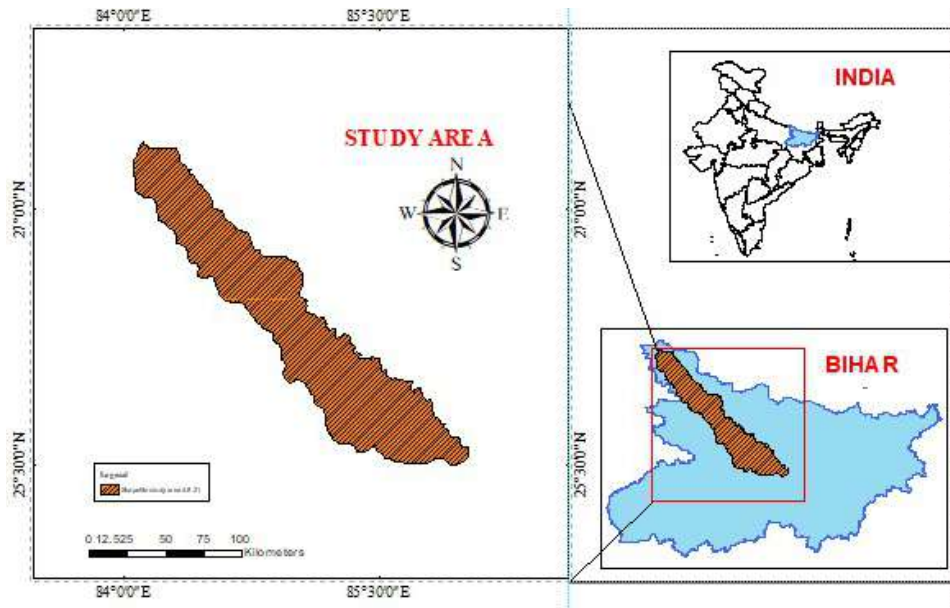
Fig. 1: Location map of the study area.

known as the Sikrahana in its upper reaches (Zakwan et al. 2018, Zakwan & Ahmad 2021). The study area is bounded by latitude 25°29'0" to 27°22'0" ` and longitude 84°13'0" to 86°0'0". Fig 1 provides a location map of the study area.

In the study area, there are canals that are the tail end of the Tirhut canal or Eastern Gandak canal, and important canals are Tirhut main canal (TMC), Jaitpur branch canal, Mallikpur branch canal, Vaishali branch canal (VBC), Birpur distributary, Pipara distributary, and Hajipur distributary, etc.

Data Acquisition

The Survey of India Topographical map on the 1: 100,000 scale for 2002 was used for the study. To identify the areas of vegetation, open land, barren land, water body, and changes in the wet soil using the satellite data of Landsat 5, 7, and 8 of path/row 140/42, 141/41, 141/42 and 142/41 for 20 years (between 2002 to 2021) of post-monsoon (October to December) were selected for downloading from https://earthexplorer.usgs.gov (Table 1). Four spectral bands, which

Table 1: Satellite data used in the present work.

Satellite/Sensor	Bands used	Wavelength ranges (µm)				Acquisition date	Path/Row no
		Green	Red	NIR	MIR/SWIR-1		
Landsat-5 TM	2,3,4,5	0.52-0.60	0.63-0.69	0.77-0.90	1.55-1.75	2009/12/02	140/42
						2009/11/07	141/41
						2009/10/22	141/42
						2009/10/29	142/41
Landsat-7 ETM+	2,3,4,5	0.52-0.60	0.63-0.69	0.77-0.90	1.55-1.75	2002/12/07	140/42
						2009/11/28	141/41
						2009/10/27	141/42
						2009/11/03	142/41
Landsat-8 OLI	2,3,4,5,6	0.53-0.59	0.64-0.67	0.85-0.88	1.57-1.65	2016/11/03, 2021/11/01	140/42
						2016/11/10, 2021/11/10	141/41
						2016/10/10, 2021/11/08	141/42
						2016/11/01, 2021/10/14	142/41

correspond to the green (G), red (R), near-infrared (NIR), and short-wave infrared (SWIR) bands, were taken from Landsat data. The cloud-free data that could be downloaded was chosen with care.

Methodology

Land Use and Land Cover (LULC) Mapping

To prepare the LULC map, a layer stack of 2, 3, 4, and 5 bands and mosaic the images. After mosaicking all the layers, the study area shape file was prepared using the software ERDAS. The Supervised image classification "Maximum Likely hood" technique was used to classify land use maps (Patel et al. 2019). The current study primarily examines five types of land use: vegetation, urban land, open land water body, and wet soil. Here is a methodology flow chart cover. A flow chart of the methodology used is given in Fig 2.

Normalized Difference Vegetation Index

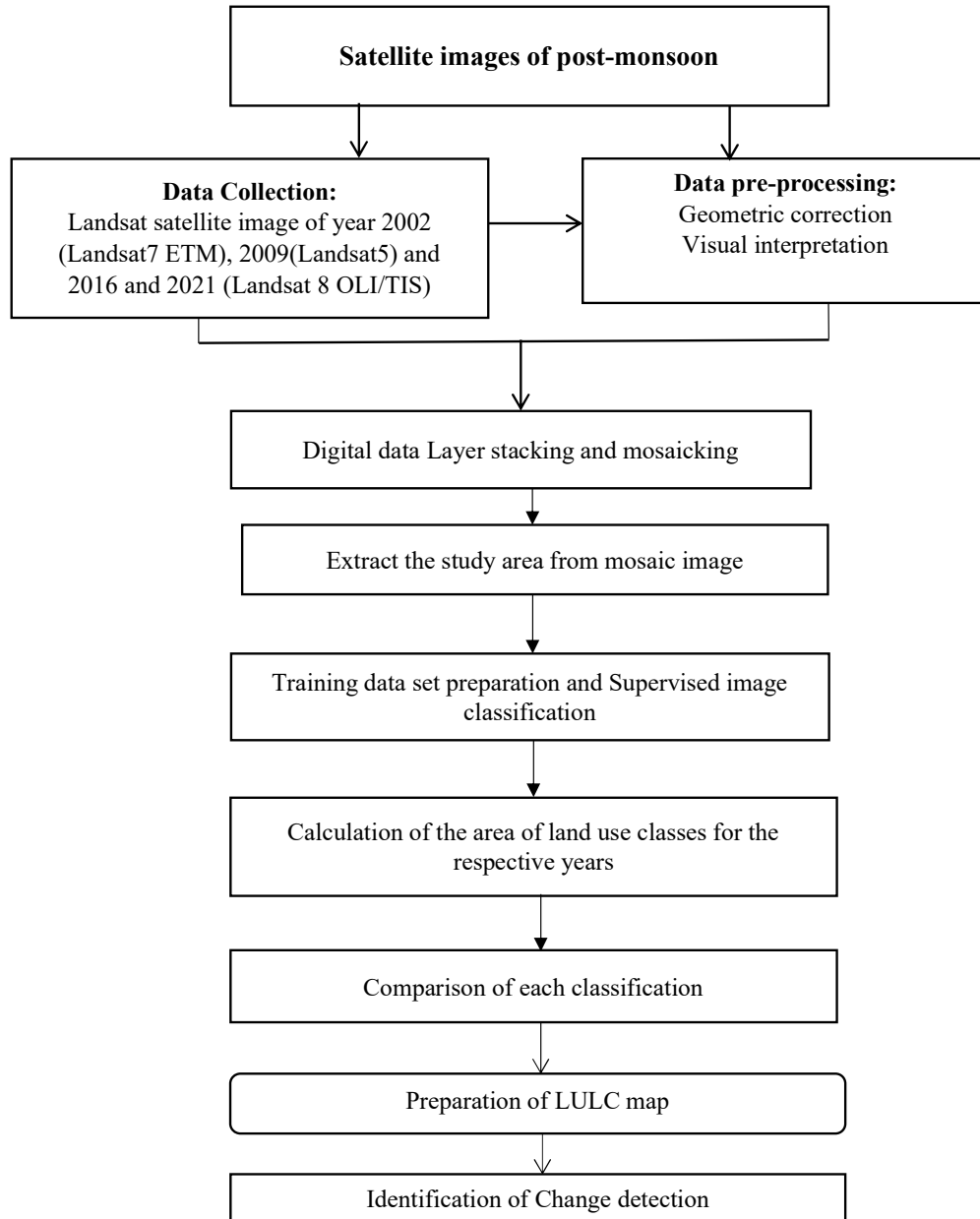The Normalized Difference Vegetation Index (NDVI)

Fig. 2: Land-use/Land-cover mapping flow chart.

measures the greenness of the vegetation and helps determine vegetation density and evaluate changes in plant health. The Normalized Difference Vegetation Index is useful for interpreting land resources (Gandhi et al. 2015). The normalized difference vegetation index between the red and near-infrared bands from an image is used to calculate NDVI on a per-pixel basis. (Equation 1)

$$NDVI = \frac{NIR - R}{NIR + R}. \qquad \ldots(1)$$

The range of the NDVI is from -1 to 1. Higher NDVI values indicate high Near Infrared (NIR) reflection, which indicates heavy greenery. In general, NDVI values between -1 and 0 reflect water bodies, between -0.1 and 0.1 indicate barren rocks, sand, or snow, 0.2 and 0.5 indicate shrubs and grasslands, and 0.6 and 1.0 indicate thick vegetation or tropical rainforest.

Normalized Difference Water Index

Normalize Difference Water Index (NDWI) is used for water bodies exploration. The index makes use of remote-sensing images of green and near-infrared wavelengths. NDWI can be calculated using Equation 2.

$$NDWI = \frac{Green - NIR}{Green + NIR} \qquad \ldots(2)$$

The values of NDWI range between 0 and $\pm$ 1, and vegetation is represented by negative values or values near 0. In contrast, positive values or values close to 1 represent surface and deep water bodies.

Conjunctive Use

Combining surface and groundwater resources is called conjunctive use. It also discusses the hydrological cycle, water balance components, interactions between surface water and groundwater, and groundwater recharge. In general, the conjunctive is a function of (a) rainfall characteristics, (b) types of soil and soil moisture, (c) types of crop, (d) crop water requirement, and (e) groundwater table being used in the study area (equation 3).

$$C_u = (a*C_{WR} + b*G_{WT} + c*S_{MC} + d*R_I + e*C_T) \qquad \ldots(3)$$

Where C_u = Conjunctive Use, C_{WR} = Crop water requirement, G_{WT} = Ground Water Table, S_{MC} = Soil Moisture Content, R_I = Rainfall intensity, C_T = Types of Crop, and a, b, c, and d = Constant

Multiple Cropping Practices

Two or more crops are typically grown in the same field yearly. Cropping is intensified in both the temporal and spatial dimensions during multiple cropping. With the minimal deterioration of soil health, multiple cropping aims to produce the most crops per unit of land area. Multiple cropping can improve agricultural efficiency and reduce crop production's sometimes negative environmental impact.

Land Reclamation Using "Cut and Fill" Approach

In the study area, extensive waterlogging was observed. For the land use/land cover analysis, it is essential to adopt the 'cut-fill' analysis and 'raised bed' concept to develop the agriculture area and reduce the waterlogging area, as shown in Fig 3.

Decentralization of Urban Area Development

The land uses Land cover analysis shows that urban areas like west Champaran, East Champaran, Muzaffarpur, Gopalganj, and Hajipur Vaishali have centralized development, and it causes significant water scarcity and water pollution. Decentralized development is the need of the day for
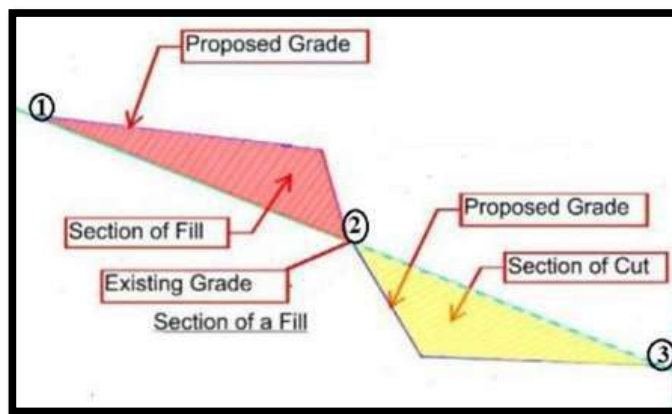

Fig. 3: Method for raised bed and cut-fill analysis.

environmental protection work in the urban and peri-urban areas of the study region.

The floating population in urban areas is very high due to the influx of people from nearby areas, villages, or towns for work and various activities. This creates environmental pollution in terms of water pollution, sewage, and wastewater generation after consuming good food and freshwater.

RESULTS AND DISCUSSION

Land Use and Land Cover (LULC) Mapping

The LULC maps were prepared for the years 2002 to 2021. Fig 4 shows the results of LULC classification for 2002, 2009, 2016, and 2021 as representative results. All these images were classified using the maximum likelihood
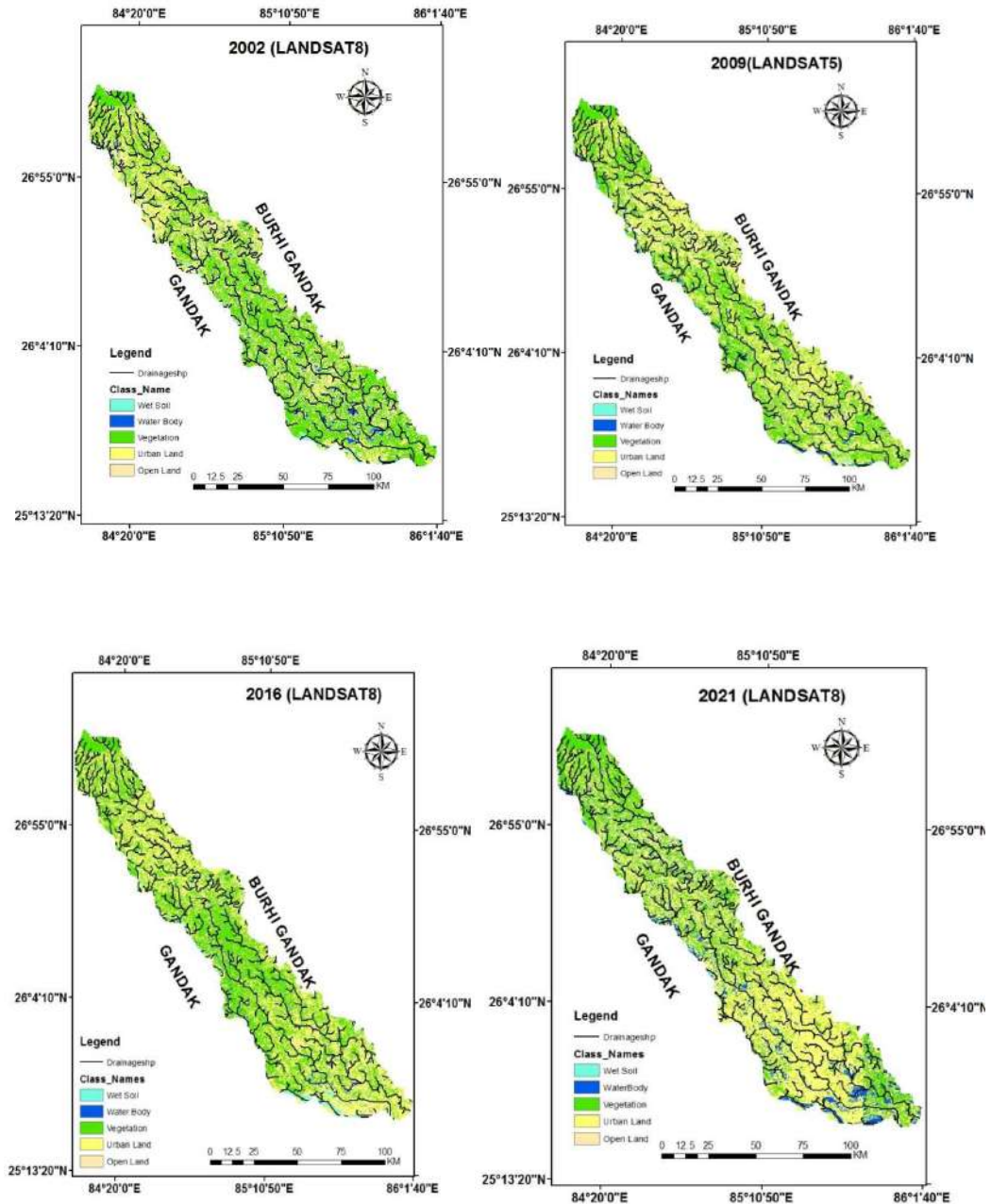

Fig. 4: Land use changes in the years 2002, 2009, 2016, and 2021 (post-monsoon).
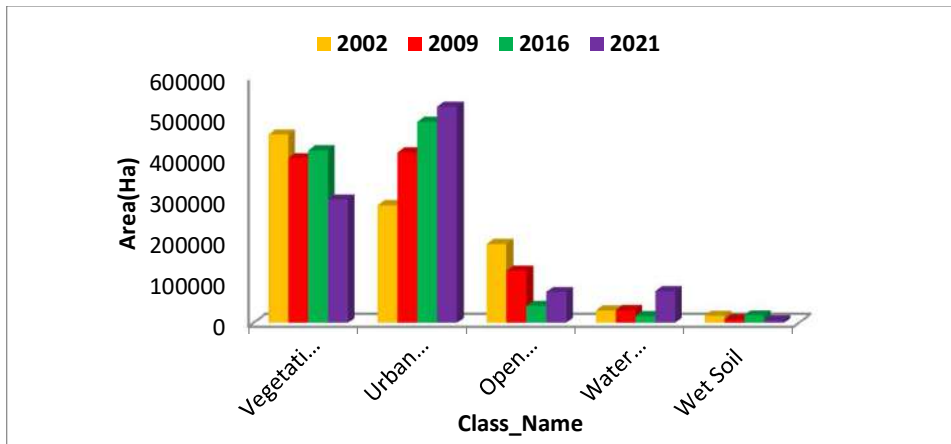
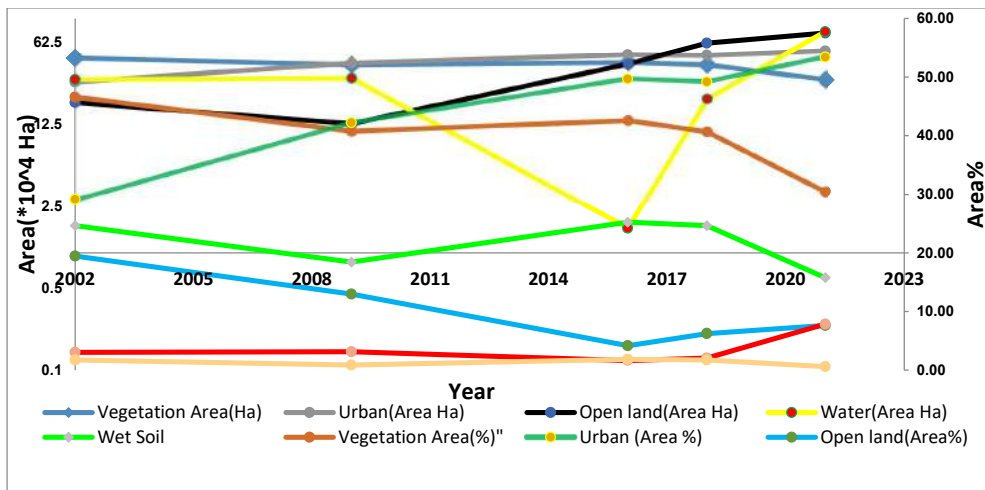Fig. 5: Bar chart of LULC change from 2002 to 20021.

Fig. 6: Post-monsoon Land use/Land cover change from 2002 to 20021.
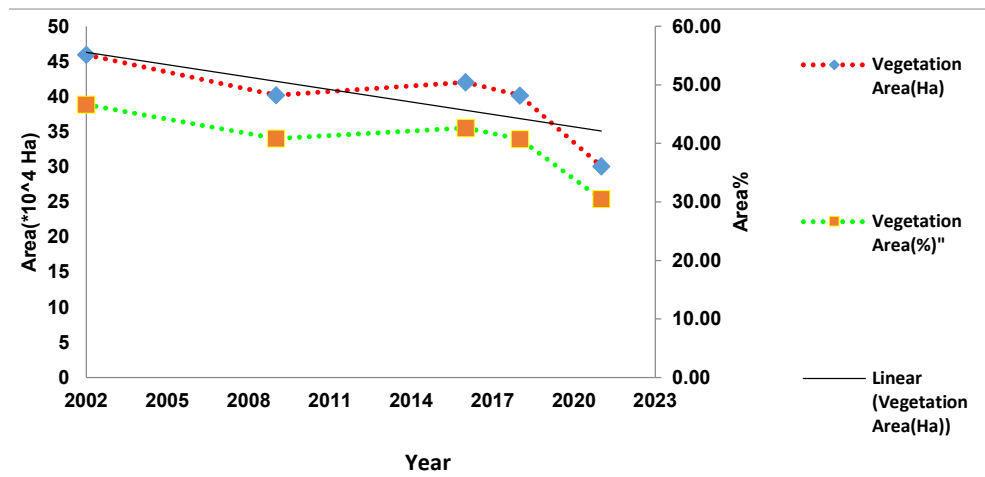

Fig. 7: Extent of vegetation during post-monsoon and the trend.

supervised classification technique using the combination of near-infrared (NIR), red (R), and green (G) bands of satellite images in ERDAS-Imagine software.

The results indicate that in the past 20 years, i.e., from 2002 until 2021, vegetation area and open land decreased to 158,676 ha (16.12%) and 116794.8 ha (11.85%), respectively. However, the urban land and waterbodies increased to 240,070 ha (24.32%) and 46937.3 ha (4.75%), respectively, during this period (Fig. 5). The vegetation values found to decrease due to centralized urbanization and migration of the population in urban fringes. LULC changes in the study area are mostly influenced by population growth.

Fig 6 indicates both are area and percentage of the total area under each land use category. Fig 7 indicates the changes in vegetation using the supervised classification "maximum likely hood method."

Normalized Difference Vegetation Index (NDVI) and Normalized Difference Water Index (NDWI)

There has been a change in vegetation cover over the past two decades. The area covered under vegetation by NDVI is found to increase from 36.08% to 70.25% from 2002 to 2021 (Fig. 8). It was observed that NDWI values over zero are seen in water bodies. In contrast, negative values are
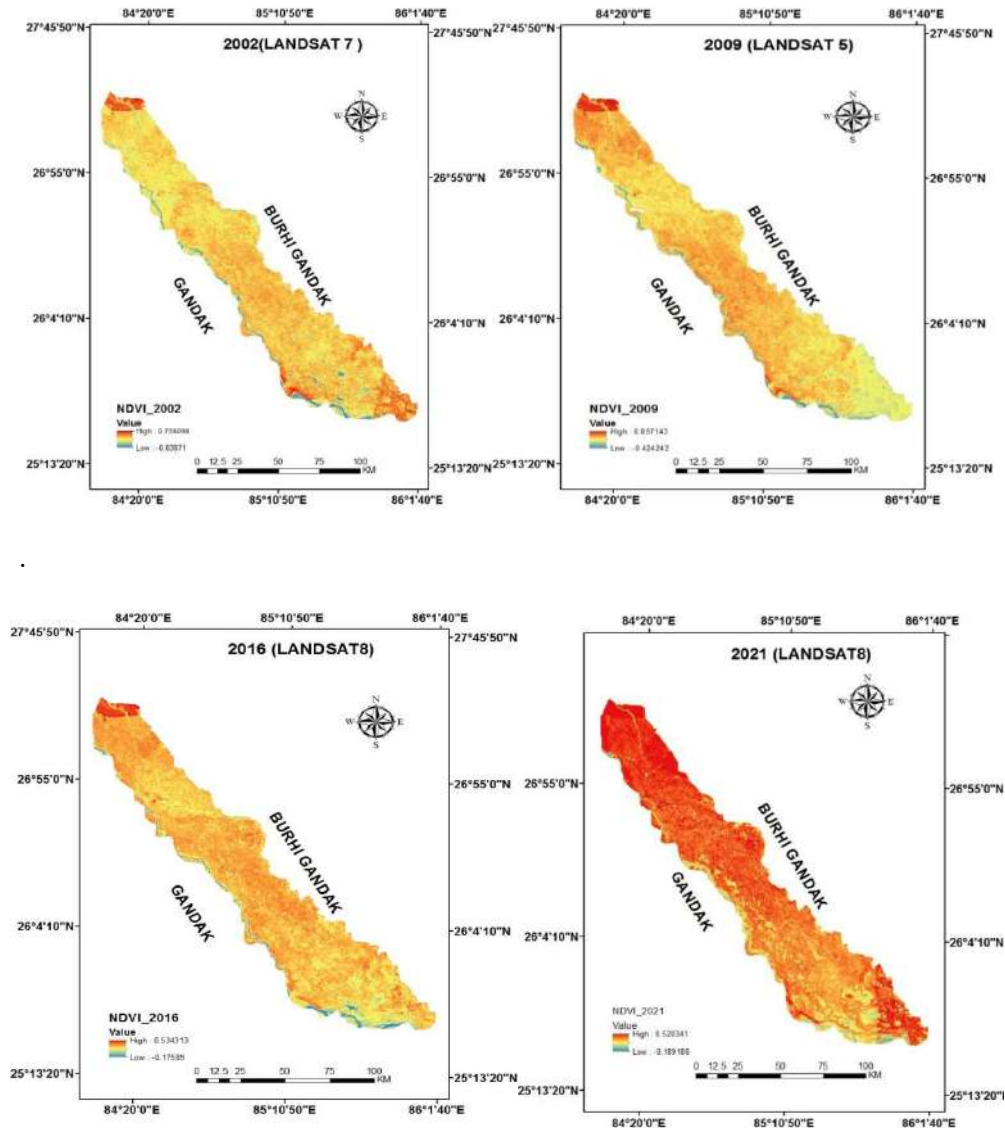

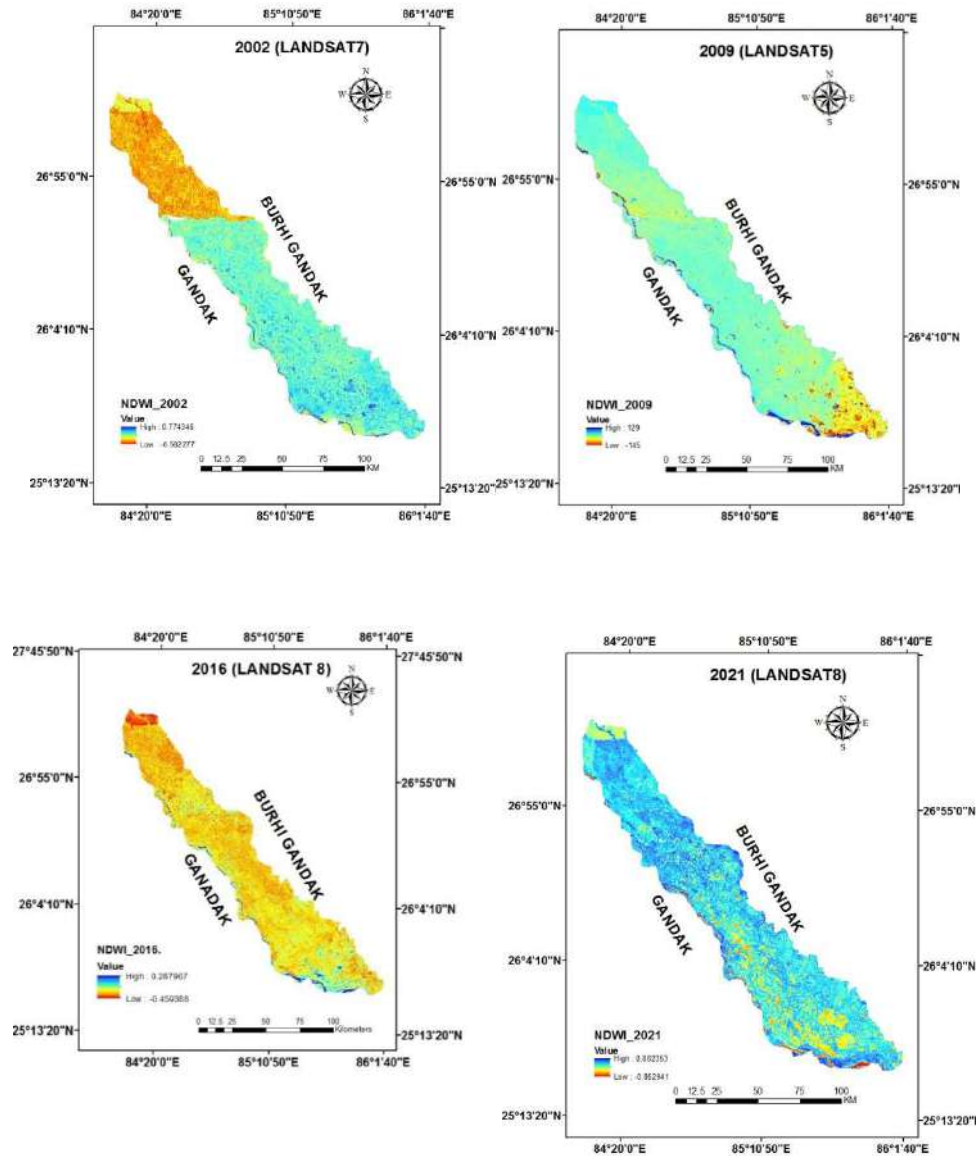Fig. 8: Images of NDVI calculated for the years 2002, 2009, 2016 and 2021.

Fig. 9: Images of NDWI calculated for the years 2002, 2009, 2016 and 2021.

observed in urban areas and vegetative land. The NDWI indices are shown in Fig 9 for the study area from 2002 - 2021. A comparison of all the methods is shown in Fig 10, with the best results as supervised classification.

Conjunctive Use

Conjunctive use is a function of (a) rainfall characteristics, (b) types of soil, (c) types of crop, (d) crop water requirement, and (e) groundwater table. Based on the net irrigation requirement (NIR) and available water resources from rainfall, groundwater, and water available in the soil, the

irrigation schedule is prepared for different crops in different study area locations.

Fig 11 indicates the rainfall map of the study area. The rainfall has been varying between 600 mm to 1200 mm, except for heavy rainfall in 2007. It is also observed that the rainfall trend is similar in all four stations, namely East Champaran, Muzaffarpur, Vaishali, and Samastipur. The rainfall trend provides a guideline for using surface water and groundwater in the study area. The Kharif crops can use the rainfall by rainwater harvesting at agricultural lands. Also, the same rainwater can be used to store water,
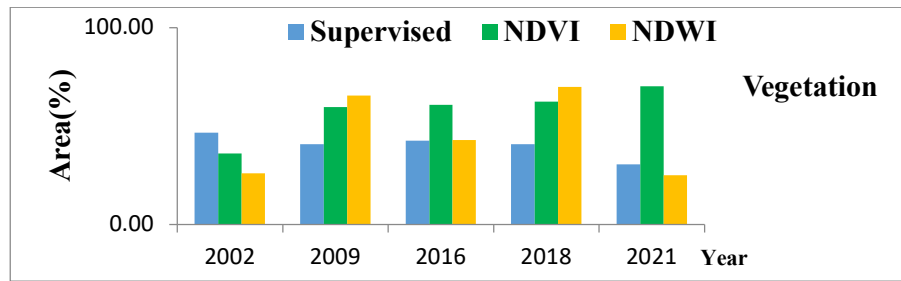
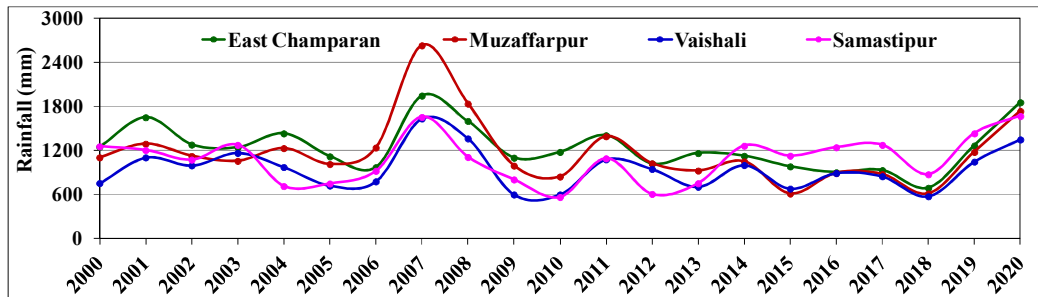Fig. 10: Comparison of the Vegetation computed by different methods.

Fig. 11: Rainfall map of different rain gauge stations in the study area.

reduce waterlogging, and use it for irrigation during the Kharif period by the "Cut and Fill" approach, as discussed above.

For conjunctive use analysis, it is important to study the soil types. Different samples at 30 and 60 cm depths were collected and analyzed in the laboratory. It is found that the Clay contents are 10-15%. The top layer root zone depth up to 2 m is predominantly silt and finds sand, i. e. silt load. The percentage of sand varied between 32-45%, whereas the silt varied between 38-68% at 30 to 60 cm depths.

The cropping pattern of the study area is predominantly a paddy growing area. Maize and Wheat are other important cereal crops. Arhar, Gram, Moong, and Masoor are the principal pulses grown in the area. Rapeseed and Mustard are major oil seed crops. Sugarcane, Chilly, and Tobacco are the main cash crops.

As in most parts of North Bihar, there are three distinct crop seasons: Garam or Summer (March to June), Kharif (July to October), and Rabi (November to February). The most common Kharif crops are paddy and maize, and during Rabi, wheat, winter maize, gram, mustard, and tobacco are taken. In Garam, lands are kept, or certain summer crops like maize and vegetables are grown. In addition to these crops, perennial crops like sugarcane are also grown. Apart from these crops grown in various seasons, mixed cropping, i.e., growing more than one crop in a given crop season is also practiced.

The crop water requirement (CWR) is estimated using a particular crop's evapotranspiration (ETcrop). It depends on the crop coefficient (K_c) and is given by the equation.

$$ET_{crop} = ET_0 \times K_c \qquad \dots(4)$$

Several factors influence the crop coefficient, including the type of crop, its rate of growth, as well as the harvesting season, and the prevailing weather conditions. The Value of Kc has been used from FAO-33. Net irrigation requirements (NIR) are the depths of irrigation required to meet evapotranspiration (ETcrop) minus the contributions from precipitation, groundwater, and stored soil water, excluding operational losses and leaching requirements. Therefore,

NIR = $ET_0 \times K_c$ + special need if any − effective rainfall- groundwater- stored soil water   …(5)

Using equation (5), the NIR for each crop is estimated for each region and crop, as shown in Table 2 below.

Multiple Cropping Practices

As shown in Table 2, two or more crops are typically grown on the same field in a single year, and the cropping is intensified in both the temporal and spatial dimensions during multiple cropping. The present practices must be enhanced for three crops, oils, fruits, and vegetables, in one annual cycle with minimal deterioration of soil health to produce the most crops per unit of land area.

Table 2: NIR for different crops in different seasons.

Hot Season			Kharif Season		
S.No.	Crop	NIR (mm)	S.No.	Crop	NIR (mm)
1	Vegetables	555.00	1	Paddy	424.00
2	Maize	547.00	2	Maize	97.00
Rabi Season					
1	Wheat	523.00	4	Mustard	487.00
2	Maize	315.00	5	Tobacco	415.00
3	Potato	414.00	6	Gram	432.00

Land Reclamation Using "Cut and Fill" Approach

In the study area, extensive waterlogging was observed in the agricultural land due to the influx of rainfall, river flood water, and leakage in the Tirhut Canal. The area-elevation and elevation capacity curves were derived for all major waterlogged areas and are shown in Fig 12.

Using equations of area elevation and elevation capacity to understand their utility, a typical water body is considered for the study, and the calculation for a 5% reduction/reclamation of the areal extent is done, as shown in Fig 13.

Decentralization of Urban Area Development

Fig 14 illustrates the urban area population growth at West Champaran, East Champaran, Muzaffarpur, Gopalganj, Hajipur, and Vaishali, causing significant water scarcity and water pollution. With the development of peri-urban areas near the above towns, a significant improvement can be observed at par with developed townships elsewhere.

Decentralized development is the need of the day for environmental protection work in the urban and peri-urban areas of the study region. The floating population in urban areas is also very high due to various offices, colleges, and

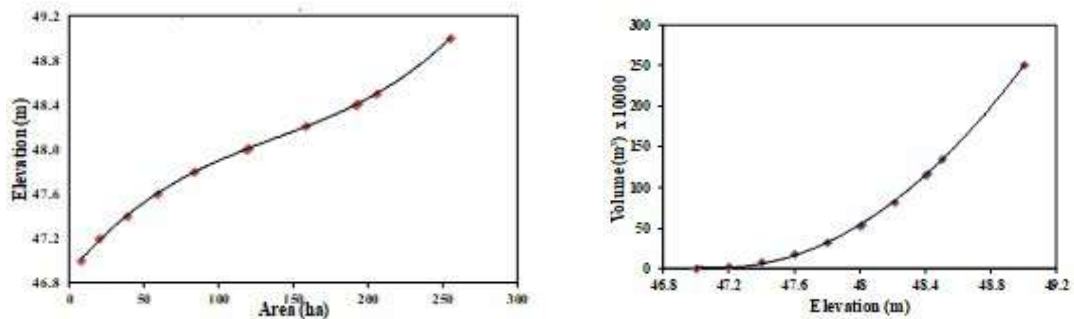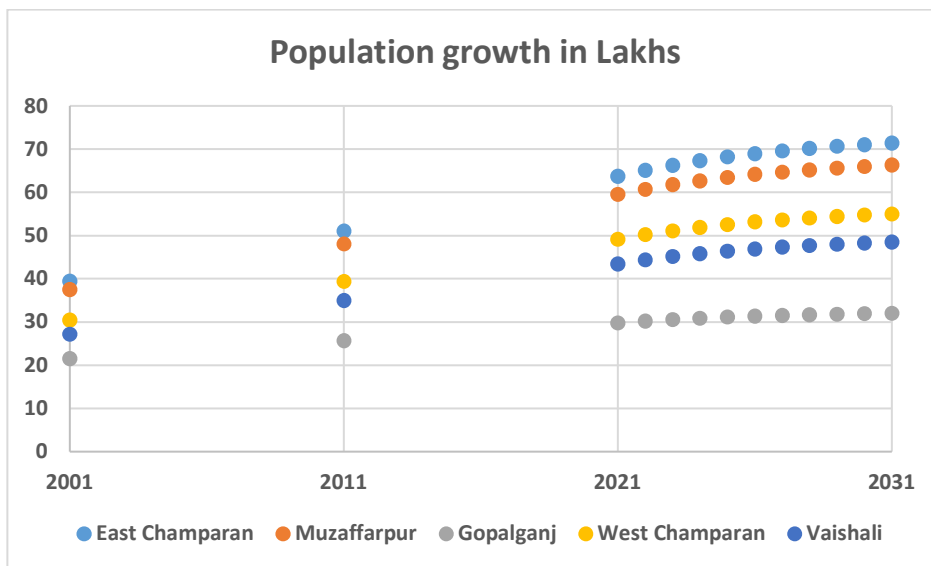
Fig. 12: Area-elevation, elevation-capacity curve.
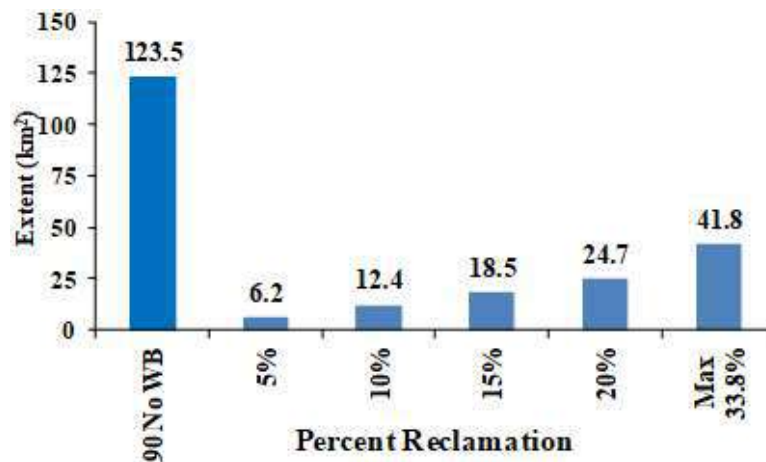
Fig. 13: Waterlogged area reclamation using the "Cut and Fill" approach.

Fig. 14: Population growth in urban areas of the study region.

Institutes. This needs to be changed as it generates sewage and wastewater pollution.

CONCLUSIONS

In the present work, the LULC changes have been studied from 2002 to 2021 in a basin area between river Gandak and river Burhi Gandak in India and precisely detect changes in LULC. It has been determined that the vegetation is decreasing at the expense of the uncertain expansion settlements. The agricultural area and open land have decreased by 16.12% and 11.85% respectively whereas the urban and the waterlogged areas have increased by 24.32% and 4.75% respectively.

The conjunctive use based on net irrigation requirement (NIR), available rainfall, groundwater, river flow, and soil moisture is very useful in the study area. The cropping pattern being utilized and the use of multiple cropping would help to improve the land use of the study area.

Land reclamation using the "Cut and fill" approach is useful for increasing agricultural land and preserve for future uses. It is also important to develop peri-urban areas to protect the environment from sewage, solid waste, and wastewater.

The study is very useful for effective environmental protection and land use management in India's study area and other river systems.

REFERENCES

Anitha, S.D. 2021. Land use and land cover change detection using GIS and remote sensing of Coimbatore District, Tamilnadu. Turkish J. Comp. Math. Edu., 11)12): 1660-1665.

Ara, Z. 2021. Land use classification using remotely sensed images: A case study of eastern sone canal Bihar. Water Manag. Water Govern., 47: 60.

Bajirao, T.S., Kumar, P. and Kumar, A. 2018. Spatio-temporal variability of land use/land cover within Koyna River Basin. Int. J. Curr. Microbiol. App. Sci., 7(9): 944-953.

Baboo, S.S. and Devi, M.R. 2010. Integrations of remote sensing and GIS to land use and land cover change detection of Coimbatore district. Int. J. Comput. Sci. Eng., 2: 3085-3088

Cardille, J.A. and Foley, J.A. 2003. Agricultural land-use change in Brazilian Amazonia between 1980 and 1995: Evidence from integrated satellite and census data. Remote Sens. Environ., 87(4): 551-562.

Gandhi, G.M., Parthiban, S., Thummalu, N. and Christy, A. 2015. NDVI: Vegetation change detection using remote sensing and GIS–A case study of Vellore District. Proceed. Comp. Sci., 57: 1199-1210.

Gaurav, N. and Singh, G. 2022. Delineation of groundwater, drought and flood potential zone using weighted index overlay analysis and GIS for district Patna, Bihar, India. Nat. Env. Poll. Tech., 21(2): 813-828.

Jamali, S., Jönsson, P., Eklundh, L., Ardö, J. and Seaquist, J. 2015. Detecting changes in vegetation trends using time series segmentation. Remote Sens. Environ., 156: 182-195.

Jensen, J.R. 1996. Introductory Digital Image Processing: A Remote Sensing Perspective. Second Edition. Prentice-Hall Inc., NJ.

Jovanović, D., Govedarica, M., Sabo, F., Bugarinović, Ž., Novović, O., Beker, T. and Lauter, M. 2015. Land cover change detection by using remote sensing: A case study of Zlatibor (Serbia). Geogr. Pannonica, 19(4): 162-173.

Lu, D., Mausel, P., Brondizio, E. and Moran, E. 2004. Change detection techniques. Int. J. Remote Sens., 12)25): 2365-2401.

Mas, J.F. 1999. Monitoring land-cover changes: A comparison of change detection techniques. Int. J. Remote Sens., 1)20): 139-152.

Olokeoguna, O.S., Iyiolab, O.F. and Iyiolac, K. 2014. Application of remote sensing and GIS in land use/land cover mapping and change detection in Shasha forest reserve, Nigeria. Int. Arch. Photogramm. Remote Sens. Spat. Inf. Sci., 40: 613-616.

Patel, R., Vadher, B.M., Waikhom, S. and Yadav, V.G. 2019. Change detection of land use/land cover (LULC) using remote sensing and GIS in Surat City. Glob. Res. Dev. J. Eng., 24: 573.

Sultana, Q., Sultana, A. and Ara, Z. 2023. Assessment of the land use and land cover changes using remote sensing and GIS techniques. Water

Land Forest Suscep. Sustain., 11: 267-297.

Usman, M., Liedl, R., Shahid, M.A. and Abbas, A. 2015. Land use/land cover classification and its change detection using multi-temporal MODIS NDVI data. J. Geogr. Sci., 25(12): 1479-1506.

Zakwan, M. and Ahmad, Z. 2021. Trend analysis of hydrological parameters of Ganga River. Arab. J. Geosci., 14(3):1-15.

Zakwan, M., Ahmad, Z. and Sharief, S.M.V. 2018. Magnitude-frequency analysis for suspended sediment transport in the Ganga River. J. Hydrol. Eng., 55: 671 https://doi.org/10.1061/(ASCE)HE.1943-5584.0001671

Synthesis of *Persea Americana* Bio-Oil and Its Spectroscopic Characterization Studies

V. Hariram*†, Pavan Kumar Reddy*, B. Gajalakshmi**, S. K. Siraj Basha*, A. Saravanan***, S. K. Khamruddin* and B. Ravikumar Reddy*

*Department of Mechanical Engineering, Hindustan Institute of Technology and Science, Padur, Chennai-603103, Tamil Nadu, India
**Department of Chemistry, Hindustan Institute of Technology and Science, Padur, Chennai-603103, Tamil Nadu, India
***Department of Chemical Engineering, Hindustan Institute of Technology and Science, Padur, Chennai-603103, Tamil Nadu, India
†Corresponding author: V. Hariram; connect2hariram@gmail.com

ABSTRACT

The present investigation aims to evaluate the feasibility of using *Persea americana* (Avocado) biodiesel in compression ignition engines. *Persea americana* bio-oil was extracted through a soxhlet extraction process using *n*-hexane solvent after careful pre-processing of the feedstocks. Since the Free Fatty Acid content was 1.78% estimated through titration, single stage base-catalyzed transesterification technique was adopted using methanol and sodium hydroxide as catalysts in the molar ratio of 1:6. Gas Chromatography-Mass Spectrometry analysis revealed the presence of Oleic acid in major proportions. The Fourier transform Infra-Red analysis confirmed the presence of carbonyl group ester ions between 722.19 cm^{-1} and 1460 cm^{-1}. The ^{13}C NMR and ^{1}H NMR studies supported the successful transformation of triglycerides into Fatty Acid Methyl Esters with distinct peaks at 3.369 ppm and 48.147 ppm, respectively.

INTRODUCTION

The continuously rising human population and limited fossil fuel availability create an everlasting demand for energy supply. Depletion of petroleum reserves and upsurging transportation and Industrial pollution unveiled the need for renewable energy resources. Agricultural-based non-edible liquid fuel was one of the important alternatives to encounter the diminishing "Petro" products and the global environment and economic concerns. In European and American nations, the dependency on fossil fuel was greatly reduced by substituting it as the fuel source for animal fat and vegetable oil. Bio-diesel, a fuel source encompassing renewability, biodegradability, and non-toxicity, proved an eco-friendly substitute for "petrodiesel."

Literature report that bio-diesel-based fuel in compression ignition engine produces lesser and unborn hydrocarbons, carbon monoxide, and particulate matter comparatively. Few researchers reported higher levels of carbon dioxide emission. Still, its effects are minimized by the floral photosynthetic reactions at the ground levels. Thereby its effect on greenhouse gas is curtailed. The avocado fruit

(*Persea americana*) is a native of Central America, found abundantly in Indonesia. It belongs to the order of Laurales, Lauraceae family, and the genes of *Persea*. The flesh of this fruit is highly nutritious and possesses a pleasant smell and flavor. The pulpy flesh of this fruit contains minerals and nutrients of human absorbable nature, which controls the blood's cholesterol level, thereby preventing cardio-vascular malfunctioning. The seeds of *Persea americana* is considered to be agriculturally based, which were found to have promising lipids and can be extracted by approximate methods. The processing of *Persea americana* seeds involves almost care, and suitable lipid extraction procedures like ultrasonication, enzymatic extraction, or solvent extraction method can be applied.

The transformation of *Persea americana* bio-oil into its biodiesel can be accomplished by many proven methods, including thermal cracking, catalytic and non-catalytic transesterification, biochemical fermentation, and others for converting the mono alkyl tri-glycerides into its fatty acid methyl esters (Macro et al. 2014). The standardization and quantification of the derived bio-diesel from non-edible feedstocks can be achieved by a series of spectroscopic

studies like Gas Chromatography-Mass Spectrometry (GCMS), Fourier Transform Infrared Spectroscopy (FT-IR) and Nuclear Magnetic Resonance (NMR) studies. The literature reported numerous studies on the extraction and characterization of vegetable-based bio-oil, but fewer studies were reported on its standardization, quality, and authenticity.

Biodiesel from *Persea grastissima* was produced through a single-stage-based catalyzed transesterification process. Sodium Hydroxide was used as a catalyst at a major ratio of 1:6, with the reaction temperature and reaction time being 60°C and 60 min, respectively. The transesterification efficiency was 84.56% (Rachimoellah et al. 2009). A comparative study in the transesterification process of Avocado and sesame seed oil and standardized them using Gas Chromatography and Mass Spectrometry. It was noticed that *Persea americana* seed oil contains a major proportional mono-unsaturated fatty acid in prominent quantity (Marwa et al. 2017). A hybrid methodology (Gas Chromatography Mass Spectrometry/ modified QuEcHERS) mass spectrometric analysis was employed on various edible and non-edible oils to identify the presence of prominent fatty acid methyl esters (Xiao et al. 2022, Hariram et al. 2017).

A non-invasive Fourier Transform Infrared Spectroscopy on Avocado fruit, including seeds, was performed practically. Lipid water and carbohydrates were estimated on the entire dry mass percentage of the *Persea americana* (Wedding et al. 2013). Estimating the presence of trans-fat and lipid profiles using FTIR and GC-FID studies with nitrogen-inert gas was performed. It was noticed that the cooking oil consisted relatively higher percentage of lipids than *Persea americana* seeds and other non-edible vegetable feedstocks (Sherazi et al. 2009). Detection and quantifying the presence of corn and soybean oil trends in *Persea americana* seed oil employing the multivariate calibration of Fourier Transform mid Infrared spectroscopic analysis with the root means the square value of soyabean oil and corn oil as 0.52% (V/V) and 0.2% (V/V) in the raw oil of *Persea americana* was estimated and was found to be accurate and deformation of authenticity (Fajar et al. 2015). A comparative Chemometric NMR analysis of *Persea americana* bio-oil with kennel, safflower, and olive oils was conducted to identify lipids, hydrolysis products, oxidation products, and steer oils. They have applied a novel NaOH super sequencing methodology in the traditional two-dimensional Nuclear Magnetic Resonance studies (Fenfen et al. 2021). A Chemometric analysis combined with compact, low field Nuclear Magnetic Resonance spectroscopy on *Persea americana*, grape seed, sesame, walnut, corn, linseed, and soybean bio-oils was conducted. The fatty acid methyl esters are estimated and compared with each other. The multivariate approach to understand analytical and statistical parameters on NMR outcomes with each other (Diego et al. 2021).

Most literature has concentrated on the chemometric analysis of *Persea americana* bio-oil. The objective of the present investigation is to evaluate the potential of *Persea americana* bio-oil and its bio-diesel to be used as the fuel for compression Ignition engines. Further, spectroscopic studies like Fourier Transform Infrared spectroscopy, Nuclear Magnetic Resonance Spectroscopy, and Gas Chromatography-Mass Spectroscopy leverage it's suitable to be used along with need diesel in the blended form without making any modification in the Compression Ignition engine.

Persea Americana Bio-Diesel Extraction

The raw *Persea americana* fruits were procured locally in Padur, Chennai, and Tamil Nadu, and seeds were removed from the flesh. The seeds were sundried for 72 hours, and the outer covers were carefully removed. The remaining seats were kept in a hot oven at 70 °C for four hours and later shuddered into small pieces, as shown in Fig. 1. For further process, the shuddered seed was powder in an automated motor and piston arrangement to make it into a powder form. Solvent bio-oil extraction techniques using Soxhlet apparatus as shown in Fig. 1. Fifty grams of dry *Persea americana* seed powder was filled in a suitable arrangement of the Soxhlet apparatus 200mL of n-hexane solvent was placed in the boiling flask as the extraction solvent upon heating the round bottom flask of the Soxhlet apparatus to 90 degrees Celsius the *n-hexane* solvent is vaporized. It occupies the upper condensation chamber of the Soxhlet apparatus, where the n-hexene solvent condenses and drops down into the extraction chamber and reacts with the thimble containing *Persea americana* seed powder.

At an elevated temperature above 45 to 50 degrees Celsius, the *n-hexane* solvent reacts with the cell wall membrane of the powder seeds. Thus, the remaining lipid content from the Persea americana seeds further drops into the solvent along with *n-hexane*. Currently, the boiling flask contains a magnet inducement of *n-hexane* and *Persea americana* seed oil. Further and contained heating, the boiling flask of the Soxhlet apparatus vaporizes the n-hexane solvent alone due to its lower boiling point, and the entire cycle is repeated thereafter. By employing the extraction methodology, 475mL *Persea americana* bio-oil was obtained for 27 batch cycles at a % extraction efficiency of 37.75%.

Persea americana Bio-Oil Transesterification

The free fatty acid content of *Persea americana* bio-oil was estimated by the titration process with potassium hydroxide and phenylethylene indicator, which was found to be 1.78%.
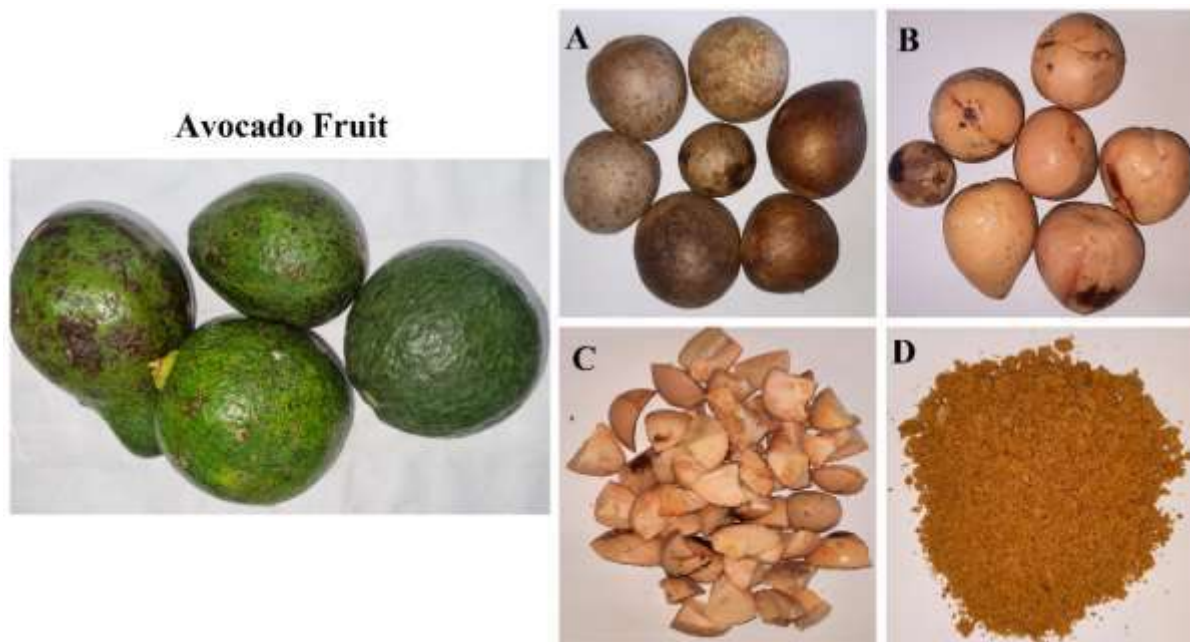
Fig. 1: *Persea americana* Fruit, Seeds (A), Ripening (B) and feedstock processing (C and D).

Hence the FFI contains a loss of less than 2%. The single state base catalyzes justification was a proven method per the literature. 240 mL of methanol was taken in a flat bottom conical flask to esterify 450 mL of *Persea americana* bio-oil at a molar ratio of 1:6. 1.72 grams of sodium hydroxide was thoroughly minimum with the methanol in the flat bottom conical flask at 60 degrees Celsius and 400 rpm of agitating speed for 45 minutes, eventually forming sodium methoxide solution.

Further, 450mL of *Persea americana* bio-oil was transferred into the flat bottom conical flask containing sodium net solution. The reaction temperature was elevated

Fig. 2: *Persea americana* (Avocado) bio-oil (A), Transesterification (B) and Biodiesel (C).

to 70 degrees Celsius for 120 minutes at 450 rpm agitation speed. After the reaction period, the entire content of the flat bottom conical flask was transferred into an inverted separating funnel under a cooling period of 4 hours. It was allowed to initiate the transesterification reaction process for converting tri Glyceride into glycerol and fatty acid methyl esters from Fig. 2. It was visible that airing formation took place in the separating funnel distinction the two layers of FAME as the upper layer and glycerol as the lower layer upon burning the rotating of carefully, glycerol was allowed to drop down in a beaker thereby crude *Persea americana* biodiesel was obtained. Five percent of hydrochloric acid diluted with double distilled water was used to remove impurities like a residual catalyst, unreacted triglycerides, glycerol, soaps, etc., from the crude biodiesel for washing the obtained crude biodiesel. This transesterification process yielded 375mL of *Persea americana* biodiesel at an efficiency of 83.33%.

Comparison of Physio-Chemical properties of Diesel, and *Persea americana* Bio-oil and Biodiesel

The physicochemical properties of *Persea americana* bio-oil and biodiesel were compared with commercial diesel in Table 1. The transesterification process considerably reduced the kinematic viscosity from 23.089 cSt to 2.789 cSt, thus making it more suitable for CI engine usage. The density of *Persea americana* biodiesel was slightly increased by 0.404% but was found to be within limits. The Gross calorific value showed significant appreciation up to 23.48% and a notable upsurge in oxygen content.

Spectroscopic Analysis

GCMS-Gas Chromatography-Mass Spectroscopic Analysis

Table 1. Physio-chemical properties of *Persea americana* – raw bio-oil, biodiesel, and diesel

Property	Diesel	*Persea americana* biodiesel	*Persea americana* bio-oil
Density [kg.m^{-3}]	842	851	847.56
Molecular formula	$C_{12}H_{22}$	-	C_{14}-C_{25}
Cetane number	48.5	44	37
Sulfur content [% vol]	0.04	0.22	0.31
Gross calorific value [kJ.kg^{-1}]	42700	41256	31568
Kinematic Viscosity (cSt)	2.82	2.798	23.089
Ash content	0	0.524	1.265
Flashpoint [^{o}C]	69	49	262-289
Oxygen content [% wt]	0	9.784	5.569

A single Quadrupole Agilent 8890 GC mass spectrometer was employed to identify various fatty acid methyl esters to estimate *Persea americana* bio-diesel. Agilent spectrometer works at over temperatures between 40°C to °450C. The chromatographic area repeatability and retention type repeatability are less than 0.5% and 0.8%, respectively, with an inlet split ratio of 7500:1. Heated hyperbolic monolithic quadrupole mass filter with chemical ionization with a mass range of 1.6 to 1050 amu was employed. The temperature of the ion source and the quadrupole was maintained between 150-350°C and 106-200°C respectively. Four μL of methanol was used as a pre-injection solvent, after which 10 μL of Avocado bio-diesel was injected into the spectrometer and the distant injection speed was maintained at 6000 μm.m^{-1}.

FTIR-Fourier Transform Infrared Spectrometry

A single reflection Attenuated Portal Interval Reflectance molecule Bruker- Alpha- Platinum- Instrument was employed to understand the transmittance range of *Persea americana* bio-diesel. This FT-IR instrument uses deuterated tri-glyceride sulfate as a detector under the spectrometer from 500cm^{-1} to 400cm^{-1} with a resolution of 2 cm^{-1}. Infrared light radiation will enter the crystal cavity and diffract into internal reflections. The resultant incident angle fall between the crystal and the sample is shown as the transmittance range of *Persea americana* bio-diesel.

NMR-Nuclear Magnetic Resonance

Bruker Avance 3 500 MHz non-invasive nuclear magnetic spectrometer was used to understand the 1H and 13C nuclei NMR spectrometer in the *Persea americana* bio-diesel. The equipment comprises a 5.4 cm long holed standard bore with an 11.7 Tesla shielded superconducting magnet with temperature shins (34 channel) and cryoshims. The RF console of the Bruker Avance 3 spectrometer has low heat dissipation due to its gradient shining with Deuterium solvent. The face resolution and the frequency resolution of the RF console are 0.1° and 0.1Hz, respectively. ^{1}H de-coupling was observed using a 5 mm broadband gradient prob, and the 13C de-coupling was observed using a 5 mm quadruple inverse probed gradient.

RESULTS AND DISCUSSION

Gas Chromatography-Mass Spectrometry

The Gas Chromatography-Mass Spectrometry was carried out to evaluate the presence of fatty acid methyl esters in the presence of *Persea Americana* biodiesel. It was derived through base catalyst transesterification using methanol. In prominent quantities, unsaturated and saturated fatty acids were present in the *Persea americana* biodiesel. It was observed that oleic acid (9112 - Octadecadienoic acid (Z, Z)
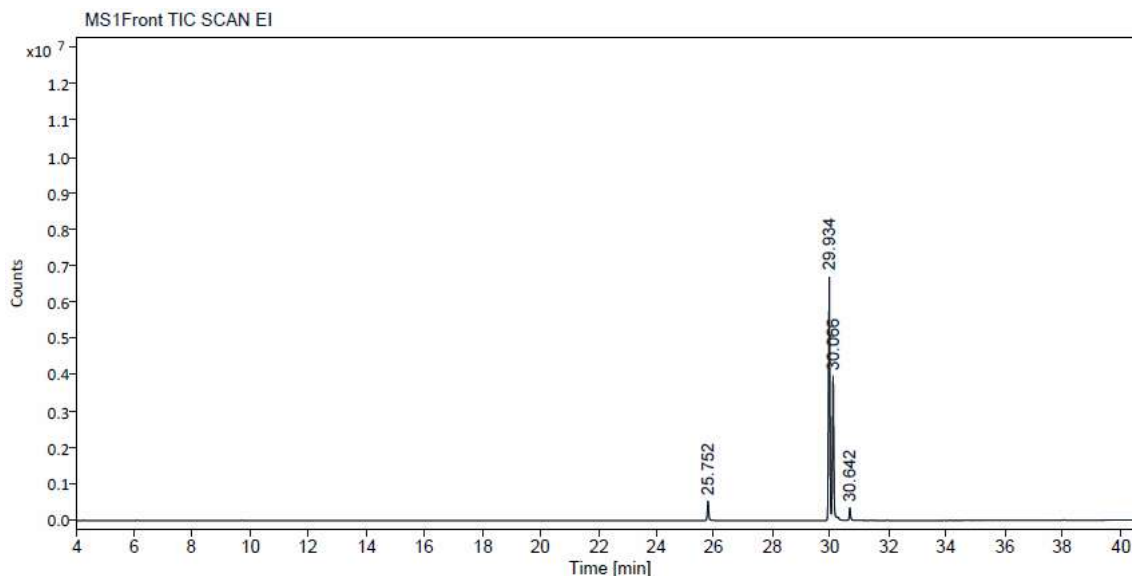
Fig. 3: *Persea americana* (Avocado) – GC MS mass chromatogram.

methyl ester) constituted a significant portion, accounting for up to 43.7% of the total composition of fatty acid methyl esters (FAME). At the retention time of 29.934 min. The other relevant fatty acid methyl ester such as palmitic acid (hexadecanoic acid methyl ester), linoleic acid (trans - 13 - octadecanoic acid methyl ester), and stearic acid (octadecanoic acid methyl ester) in notable proportions (Fig. 3).

Fourier Transform Infrared Spectrometry (FTIR)

The Fourier Transform Infrared spectroscopic analysis on the *Persea americana* biodiesel sample showed the stretching and bending vibration between 524.73 cm^{-1} and 3008.40 cm^{-1} of wave number as the percentage of transmittance. Stretching vibrations between 722.19 cm^{-1} and 1460.81 cm^{-1} confirmed the presence of carbonyl group ions (C = O) (Fig.

Fig. 4. *Persea americana* (Avocado) – FT IR spectrum transmittance.

4). A strong signal at 1714.21 cm⁻¹ indicated the presence of fatty acid methyl esters in *Persea americana* biodiesel. The combination of stretching and bending vibration between 2853.93 cm⁻¹ and 3008.40 cm⁻¹ is also supported as evidence for the presenc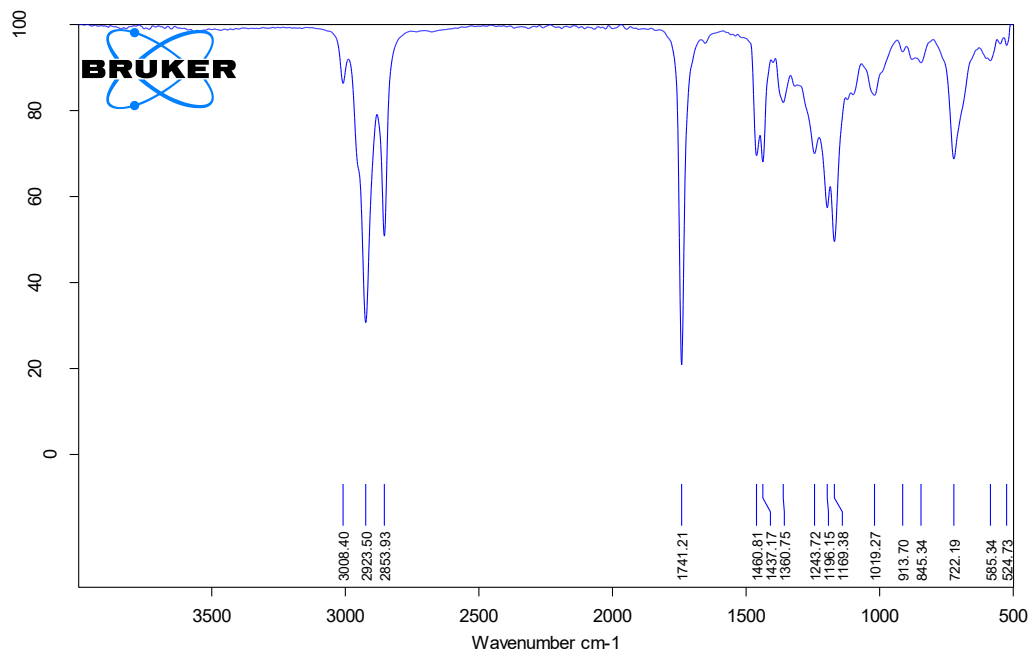e of FAMES in the biodiesel sample. A strong stretching signal at 722.19 cm⁻¹ and 1196.15 cm⁻¹ indicated the presence of a C-H bond in the biodiesel. The absence of signals and vibrations between 1741.21 cm⁻¹ and 2853.93 cm⁻¹ showed that the effectiveness in the transesterification reaction for converting the bio-oil of *Persea americana* feedstock into its biodiesel was more than 80%.

Nuclear Magnetic Resonance (NMR)

The derived *Persea americana* biodiesel was characterized using ¹H NMR (proton NMR) and ¹³C NMR carbon in Bruker Avance 3 500 MHz equipment.

Fig. 5 shows the typical ¹H NMR spectrum of the *Persea americana* biodiesel. A strong characteristic singlet peak was noticed at 3.369 ppm, which is the distinctive feature indicating the presence of methoxy proton. 2 triplet peaks at 5.39 ppm and 2.08 ppm confirmed the presence of fatty acid methyl ester in *Persea americana* biodiesel. The absence of singlet and triplet peaks beyond 5.411 ppm indicated the absence of oleic and aliphatic acid hydrogen in the transesterified *Persea americana* biodiesel. Furthermore, a strong singlet peak at 4.899 ppm indicated the presence of a methanol group in the hydrocarbon chain. Several weak signals (singlet and doublet peaks) at one point (6.24 ppm and 3.333 ppm) were also noted in the 1H NMR spectrum, possibly due to the minimal hydroxy and amine group.

Fig. 6 shows the NMR spectrum at ¹³C (carbon) belonging to the *Persea americana* biodiesel at 48.147 ppm. A characteristic singlet peak was noticed, which indicates the presence of fatty acid methyl esters in *Persea americana* biodiesel. A clustered peak between 26.785 ppm and 33.443 ppm was formed, which may be due to the existence of (-COO) and (C-O) carbonyl groups. A singlet terminal carbon peak was also noticed at once 17 ppm, with may be due to the presence of the methylene group. Multiple singlet peaks were seen between 127.681 ppm and 129.556 ppm, possibly due to the long-chain hydrocarbon formed due to the transesterification process. The formation of a weak signaled singlet peak at 179.40 pm may be due to hydroxy ions in the *Persea americana* biodiesel.
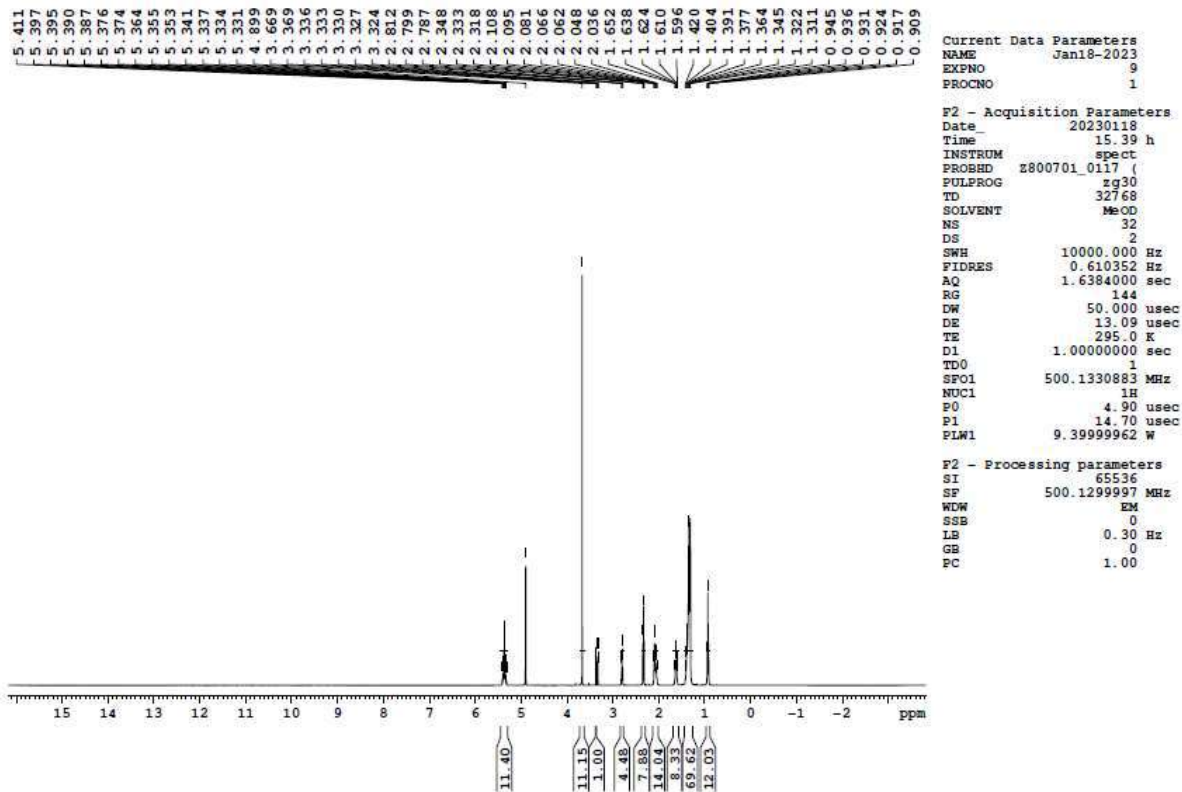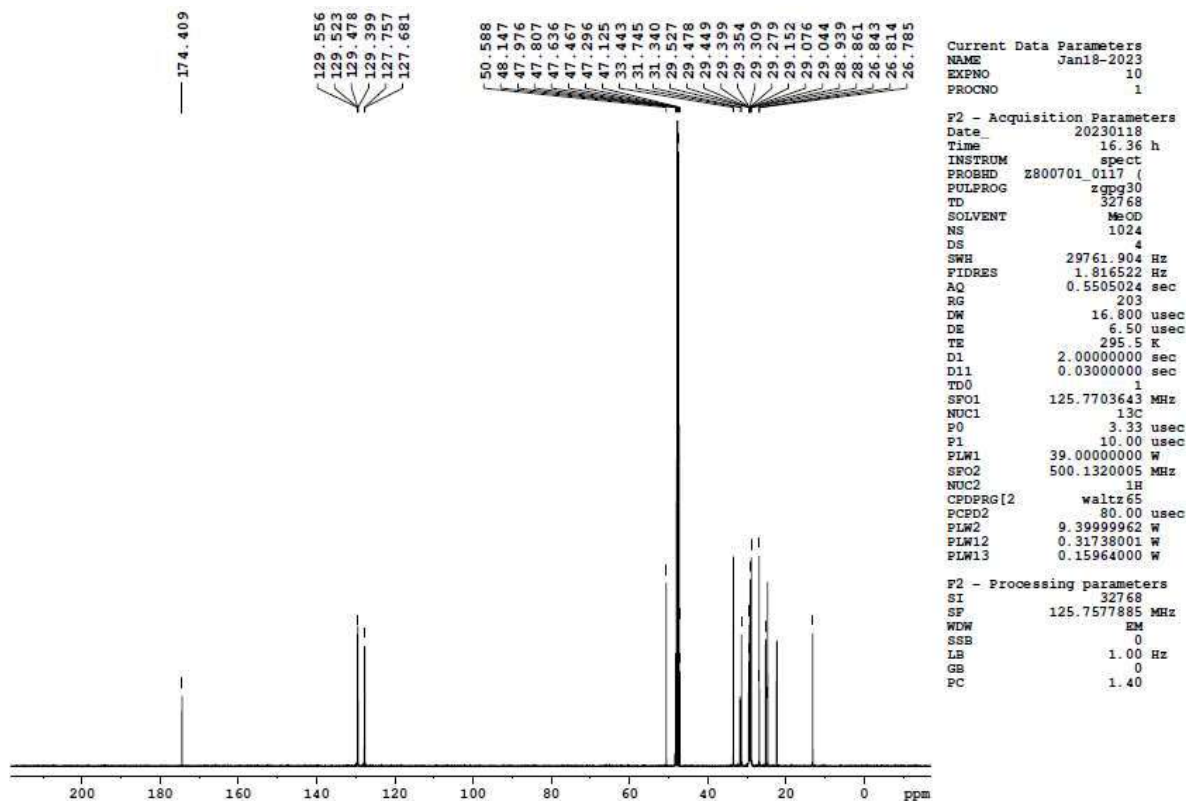

Fig. 5: *Persea americana* (Avocado) – ¹H NMR spectrum.

Fig. 6: *Persea americana* (Avocado) – ^{13}C NMR spectrum.

CONCLUSION

The present investigation evaluates the feasibility of using *Persea americana* biodiesel blends in compression ignition engines. The following conclusions were drawn.

1. The pre-processing of *Persea americana* seeds and a Soxhlet extraction technique with 200 mL of n-hexane in 27 batches isolated 475 mL of *Persea americana* bio-oil at an extraction efficiency of 37.5%.

2. A single-stage base-catalyzed transesterification process with methanol and NaOH at a molar ratio of 1:6 was employed to produce *Persea americana* biodiesel with a reduced FFA content (less than 1.78%). The process yielded 375 mL of biodiesel with an esterification efficiency of 83.33%.

3. Significant reduction in kinematic viscosity, flash point, and ash content was evidenced along with appreciation in density, gross calorific value, and oxygen content of the derived *Persea americana* biodiesel.

4. GC-MS analysis identified the presence of Oleic acid in prominent proportions.

5. FT-IR spectroscopic analysis confirmed the presence of carbonyl ester ions by revealing a stretching vibration between 722.19 cm^{-1} and 1460.81 cm^{-1}. Additionally, a strong signal at 1196.15 cm^{-1} attributed to the above outcomes.

6. A singlet peak at 3.369 ppm in the 1H NMR spectrum and strong cluster peaks between 26.785 ppm and 33.443 ppm in the 13C NMR evidenced the transformation of triglycerides into FAMEs during the transesterification reaction.

Therefore, it can be concluded that the biodiesel derived from *Persea americana* feedstock can be utilized as a substitute fuel for commercial diesel in blended form without making any modifications to the existing compression ignition engine.

ACKNOWLEDGMENT

REFERENCES

Diego, G., Ailey, A., Coelho, T., Federico, C., Ernesto, D., Evandro, B., Mario, H. and Killner, M. 2021. Compact low-field NMR spectroscopy and chemometrics applied to the analysis of edible oils. Food Chem., 365: 130476.

Fajar, A., Lumakso, A.R., Handoy, M., Sugeng, R. and Farahwahida, M.Y. 2015. Detection and quantification of soyabean and corn oils as adulterants in Avocado oil using Fourier Transform Mid Infrared (FT-MIR) spectroscopy aided with multivariate calibration. J. Teknol., 77(1): 251-255.

Fenfen, T., Hilary, S., Green, S., Wang, C. and Emmanuel, H. 2021. Analysis and authentication of avocado oil using high-resolution NMR spectroscopy. Molecules, 26: 310.

Hariram, V., Godwin, J. and Seralathan, S. 2017. Spectrometric analysis of algal biodiesel as a fuel derived through base-catalyzed transesterification. Int. J. Amb. Energy, 40(2): 195-202.

Macro, A.Z, Tationa V.P, Claudi M.P. and Carla R.B. 2014. Profile bioactive compounds in avocado pulp oil: Influence of the drying processes and extraction methods. J. Am. Oil Chem. Soc., 91(1): 19-27.

Marwa, A., Ashraf, N., El-Sayed, H., Amr, N.A.K. and Mohamed, S.K. 2017. GC/MS analyses of avocado and sesame fixed oils. J. Pharm. Phytochem., 6(4): 721-725.

Rachimoellah. H.M, Dyah. A.R., Ali, Z., Dan, I.W.S. 2009. Production of biodiesel transesterification of avocado (*Persea gratissima*) seed oil using base catalyst. J. Tek. Mesin 11(2): 85-90.

Sherazi. S.T J, Aftab, K., Mahesar, S.A., Bhanger, M.I, Younis Talpur, M. and Sarfraz, Arain. 2009. Application of transmission FT-IR spectroscopy for the trans fat determination in industrially processed edible oils. Food Chem., 114(2009): 323-327.

Wedding, B.B, Wright, C., Grauf, S., White, R.D., Tilse, B. and Gadek, P. 2013. Effects of seasonal variability on FT-NIR prediction of dry matter content for whole Hass avocado fruit. Post-harvest Biol. Technol., 75: 9-16.

Xiao, W., Xiaoman, S., Xuefang, W., Xin, Qi, D., Wang, J.J., Jin, M., Fei, M., Li, Y., Liang, Xiao, Z. and Peiwu, Li. 2022. Determination of 15 phthalic acid esters based on GC-MS/MS coupled with modified QuEChERS in edible oil. Food Chem., 16: 100520.

Microplastic Pollution in Seawater: A Review Study

Sheela Upendra†* (iD) **and Jasneet Kaur****

*Department of Mental Health Nursing, Symbiosis College of Nursing, Symbiosis International (Deemed University), Pune, India

**Department of Community Health Nursing, Symbiosis College of Nursing, Symbiosis International (Deemed University), Pune, India

†Corresponding author: Sheela Upendra; sheelaupendra@scon.edu.in

ABSTRACT

Due to its detrimental effects, notably on the well-being and biota of the ocean, microplastic contamination is becoming a bigger concern. Because of this, the issue of microplastics in the marine ecosystem is currently a major concern. The purpose of the study is to objectively evaluate the most recent data supporting the impact of microplastic contamination in seawater. When creating the standards for assessing the literature, P.I.C.O. was taken into account. For this inquiry, databases were selected and used throughout the data-collecting process. We checked PubMed, CINAHL, Google, Hinari, and the Cochrane Library. Boolean operators (AND, OR) and keywords were employed in the search to avoid oversaturating the data. Keywords used as per MeSH: Microplastic, plastics, seawater, ocean, pollution, microplastic exposure. The last five years (Since 2017) worth of studies were incorporated. Boolean search for relevant terms used. This limited my query to 188 records through various database searches. Several things were removed because they were unrelated to the study's subject. Due to its detrimental impact on marine biota, the issue of microplastic contamination in the marine ecosystem is a current concern. Microplastics, which serve as a vector, become stuck with harmful pollutants. It is necessary to implement conservation management strategies and assistance for different educational programs to protect the environment from these hazardous microplastics. Humans are exposed to plastic waste when eating fish tainted with plastic. As a result, there are various outbreaks of chronic diseases, and people suffer the effects. The public's education on the harmful effects of microplastics is a crucial need in this field. As a result, many inventions would be promoted to decrease the use and consumption of plastic and its products.

INTRODUCTION

One of the most significant contaminants in the marine environment is microplastics, which accumulate in sediments worldwide. (Zhao et al. 2018). Marine ecosystems all around the world are contaminated by microplastic litter. Due to the durability of these materials, the impact of microplastic contamination in the marine ecosystem may endure for years to come. Microplastics are a new category of pollutants that might be problematic, and there are currently few established methods for detecting them (Uyarra et al. 2016)

In the marine environment, plastic waste is common and disintegrates into tiny particles known as microplastics. The size of microplastics is limited to those with a diameter of less than 5 mm, and there are two subgroups: big MPs (1–5 mm) and tiny MPs. However, this categorization has no

official name (0.1-1 mm). Microplastics comprise 92.4% of the estimated 5 trillion plastic objects, or 268 940 tonnes, in the world's seas. Bottles, containers, buoys, textile fibers, cosmetic microbeads, and even nanoparticles from industrial discharge are some of the main sources. Based on size, they are separated into macroplastics (2.5 cm to 1 m), mesoplastics (5 mm to 2.5 cm), microplastics, and nanoplastics. Under the effects of environmental weathering, primary plastic debris breaks down and biochemically degrades into secondary Microplastics (Thi Kim Khuyen et al. 2021)

The ocean is currently filled with plastic waste, which almost certainly affects every marine species. A conservative estimate of a recent study indicates that 2,141 different species have been discovered to face plastic pollution in their natural settings (Tekman et al. 2022)

Plastic microparticle buildup in lower trophic levels may have a cascading impact on marine food webs, ultimately harming humans. This emphasizes the significance of plastics

---

ORCID details of the authors:

Sheela Upendra: https://orcid.org/0000-0003-2413-1219

as a growing source of toxins that are dangerous to both the environment and human health (Campanale et al. 2020).

Justification

For the management of pellets and to prevent heavy objects from entering the ocean, specific efforts directed at the primary and secondary sources of microplastic are needed (where they decay). Sadly, if current patterns continue, both humans and animals will continue to be in danger, and mishaps will happen before these objectives are met. Different issues arise when environmental passives are addressed. Microplastic cannot be removed from saltwater or separated from the sand by sieving. It would be ineffective even if one could collect these tiny particles. Microplastic will continue to travel in sluggish, complicated patterns to the ocean's floor, where they will eventually be buried for millennia in sand and muck (Ivar Do Sul & Costa 2014)

According to reports, microplastic can operate as a vector for pollutants by absorbing them and aiding in their bioaccumulation, particularly in marine environments, organisms & consequently, food webs (Amelia et al. 2021)

Experts have long voiced concern about the growing amount of plastic in the environment. The alarm about macroplastics has been raised by iconic images of sea creatures wrapped in soda can rings or straws sticking out of their nostrils. However, microplastics, smaller than 5 mm in diameter and shed from synthetic fabrics or resulting from the breakdown of larger chunks, are even more widespread, and their effects on human health are still unknown.

Corals, planktons, fish, whales, and other marine invertebrates are just a few examples of marine biota that may consume microscopic plastics passed down to the food chain. Due to their large surface-to-volume ratio, microplastics easily absorb hydrophobic contaminants from the aquatic system. Microplastic pollution is a growing problem because of its negative impacts, particularly on the health and biota of the ocean. Because of this, the issue of microplastics in the marine ecosystem is currently a major concern.

However, there has not yet been a comprehensive look at seawater microplastic contamination. This review study focuses on the abundance and features of microplastics in various environmental and biological components to better understand the condition of microplastic contamination in seawater. The background information on microplastics provided by this study might aid in developing successful plastic pollution management policies by the government.

Microplastics can unintentionally introduce various hazardous hydrophobic pollutants into the food chain by absorbing these contaminants from the environment. Further methods must be devised to solve the major problem of marine environment microplastic contamination. It is crucial to cease further production of plastic and swap it out for more environmentally friendly materials to prevent a problem in the future.

The problem of microplastics has been ignored for a long time, and the necessity to study the possible consequences, exposure routes, and toxicity of microplastic towards living organisms of the marine ecosystem and on human health is highlighted by the unavoidable exposure of people to microplastic.

Aim

The study aims to critically review current evidence contributing to the effect of microplastic pollution in seawater.

Objectives

1. To critically analyze current literature on microplastic pollution in seawater
2. To draw findings based on the results of the qualified investigations to facilitate review studies
3. Interpret, contextualize, and provide a summary and conclusion of the selected research results.

Research Question

The research question of this study was how microplastics pollute seawater and what is the impact of these microplastics.

MATERIALS AND METHODS

A comprehensive review of all relevant studies related to Microplastic pollution is included. The research design included published and unpublished studies and summarizing the findings.

Data collection is crucial to systematic reviews since it provides the basis for conclusions. If it turns out that there are better methods to define the populations, treatments, outcomes, or study designs, changes to the protocol should only be approved after the review questions have been developed. We looked at several printed and digital sources. Search engines were also employed to hunt for websites that may be used as references. The preset selection criteria for the research were directly derived from the review questions.

A more detailed examination of the quality of a few studies was carried out using wide critical evaluation principles. A comprehensive technique was used to choose the best research sample for this evaluation (Table 1). When creating the standards for assessing the literature, P.I.C.O.

was taken into account. This demonstrated that the suggested study had received enough responses.

A question must address the topic at hand specifically and be phrased in a way that makes it simpler to locate an answer. PICO makes this procedure simpler. It provides an example of the essential elements of a suitable query.

Criteria for PICO

Data Collection Strategies

Databases were chosen and utilized throughout the data collection method for this investigation. PubMed, CINAHL, Google Scholar, Hinari, and the Cochrane Library were consulted. Boolean operators (AND, OR) and keywords were employed in the search to avoid oversaturating the data. This shows that intentional or unintentional bias may be found depending on how a search is done. Therefore, it is crucial to demonstrate that a comprehensive, extended, and wide search was carried out.

The scientific literature search was first carried out in Pubmed using the keywords: Microplastic AND Pollution OR Seawater OR Ocean OR Plastics within the article title, abstract, and keywords. Subsequently, a second, advanced search was carried out in CINAHL, Google Scholar, and Hinari using the keyword combinations ("microplastic," "pollution"), ("seawater," "microplastics"), ("seawater," "pollution,") and ("microplastic," "ocean,") within article titles. Further, the scientific literature was carried out in The Cochrane Database of Systematic Reviews (Cochrane Reviews)

Keywords Used as Per MeSH

Microplastic, plastics, seawater, ocean, pollution, microplastic exposure. The principal investigator and abstracts did initial searches, screening of tiles, and study reviews were conducted by co-authors. Any differences of opinion were discussed, and a consensus was reached; Coauthors extracted the data independently and compared the results. The following data was extracted from each study, published year of study, Author name, location, additional factors, and key findings

Inclusion/Exclusion Criteria

The last five years (Since 2017) of studies were incorporated. Articles not originally published in English were disqualified

Table 1: Criteria for PICO.

Participants	Studies related to microplastic pollution in seawater
Intervention	Microplastic pollution in seawater
Comparison/Control	Role of microplastic in seawater
Outcome	Impact of microplastic pollution

due to the possibility of language bias due to the writers' limited experience and the possibility of an inaccurate translation. After doing a boolean search for them, the study utilized several filters to choose appropriate phrases based on my inclusion criteria (Table 2). This restricted the search using different databases to 188 records.

A PRISMA flow diagram was framed (Fig. 1). Many articles were removed because they were unrelated to the study's subjects. After removing the duplicates, the abstracts of each publication were reviewed. Once further studies that did not meet the requirements were excluded, eight papers that satisfied the inclusion criteria were included.

17 relevant studies that fulfilled the inclusion criteria were identified as potentially useful but eventually disregarded, along with the justifications for each.

RESULTS

Eight studies were analyzed (Table 3).

The discovery that marine life and all ocean ecosystems include tiny particles made from plastic garbage is no longer news. Microplastic contamination seems to be one of the largest environmental challenges facing the planet right now. 240 samples of sixteen species of fish, squid, and shrimp that are all suitable for human consumption were collected. In water samples and marine life, microplastic debris was found. The most common size range for microplastic particles was 150 to 500 m. One of the first studies to concurrently measure the amount of microplastic particles and how they affect marine life in this area (Alfaro-Núñez et al. 2021).

The quantity of marine plastics in seawater is a useful indicator of marine plastic pollution since it shows the current level of pollution and the levels of waterborne exposure that marine organisms are exposed to. Two microplastic monitoring techniques are suggested for use in regional and global assessments of pollution status through time and space, assessments of ecological risk, and a description of their key characteristics. Despite the strong connection

Table 2: Inclusion and Exclusion Criteria.

Inclusion Criteria	Exclusion Criteria
Studies related to microplastic pollution in seawater	Studies related to rivers/ ponds/streams
Studies related to articles written in English	Articles in pre-printed literature
Articles Free to access	Case Reports
Peer-reviewed articles	
Studies Published in the year 2017 and afterward	
Non-experimental quantitative studies	

PRISMA

```
┌──────────────────────────────┐
│ 188  records located while   │
│ searching the database       │
└──────────────────────────────┘
              │
              ▼
┌──────────────────────────────┐
│ excluded 140 irrelevant      │
│ records                      │
└──────────────────────────────┘
              │
              ▼
┌──────────────────────────────┐
│ Due to title and duplicate   │
│ articles excluded 14 records │
└──────────────────────────────┘
              │
              ▼
┌──────────────────────────────┐
│ Assessed 17 full text        │
│ articles - eligibility       │
└──────────────────────────────┘
              │           ┌──────────────────────────────┐
              │──────────▶│ excluded 09 full text        │
              │           │ articles excluded rationally │
              ▼           └──────────────────────────────┘
┌──────────────────────────────┐
│ At last 08 full text articles│
│ selected for the study       │
└──────────────────────────────┘
```
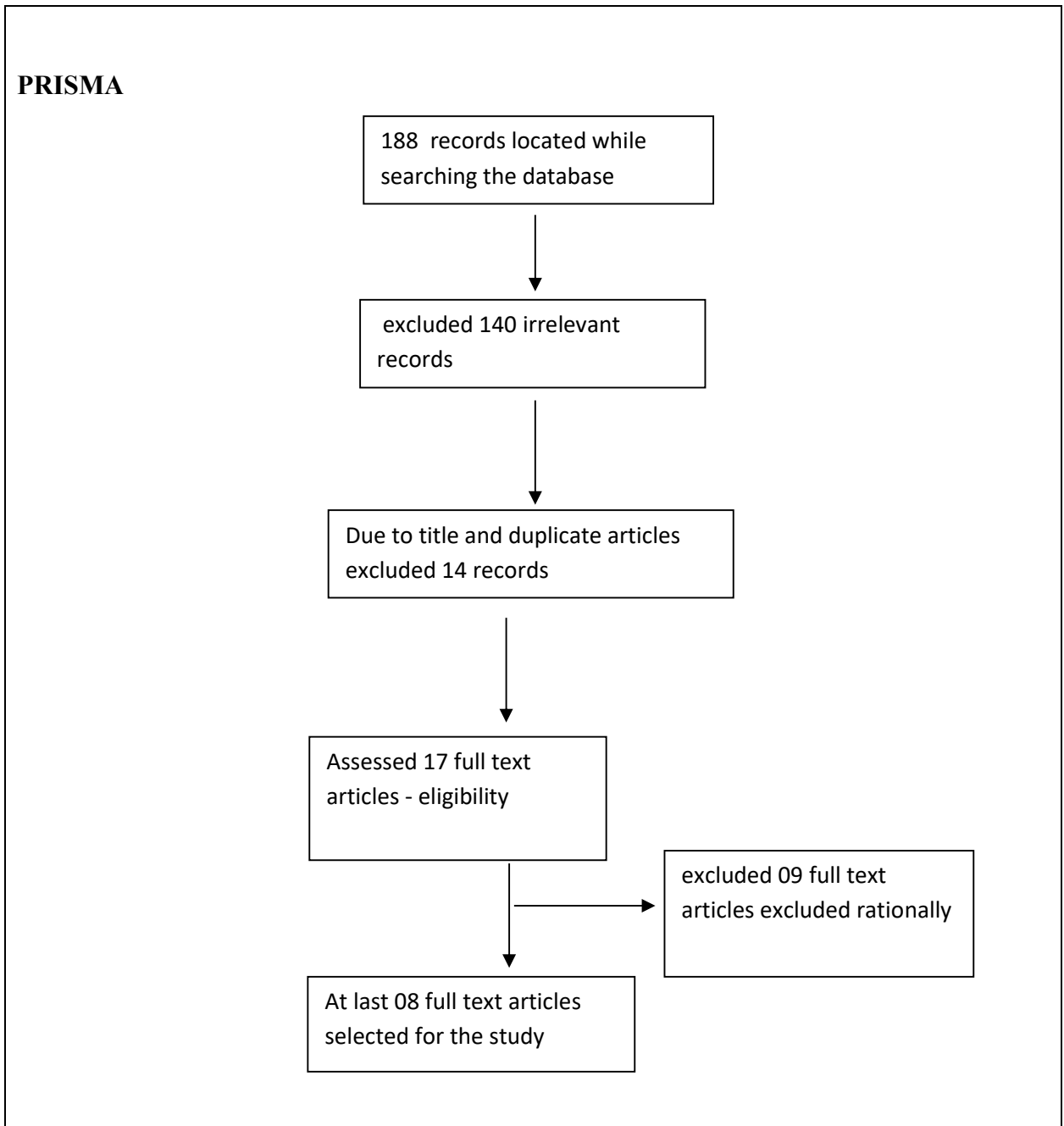
Fig. 1: PRISMA Flow chart.

between macroplastic and microplastic pollution (Shim et al. 2022).

Over time, unreacted monomers, oligomers, and additives from plastics released into the water may leach. Additionally, metals and polychlorinated biphenyls, as well as other organic and inorganic pollutants, are absorbed by plastics from the surrounding saltwater. The research determined the amount of additives found in seven categories of common plastic debris in the waters in 2015. (Bottles, bottle caps, EPP containers, silverware, supermarket bags, meal wrappers, straws, or stirrers) (De Frond et al. 2019).

The polymeric kinds found were high-density polyethylene, polystyrene, polypropylene, and polyethylene terephthalate. This investigation discovered microplastic

Table 3: Characteristics of Included Study.

Author and Year	study design	Location	Additional Factor	Key findings
(Alfaro-Núñez et al. 2021)	Exploratory study design	4000 km-trajectory encompassing 453,000 square kilometers- Tropical Eastern Pacific & the Galápagos archipelago	specimens of the sixteen distinct species- fish, crabs, and mollusks.	The bulk of the particles ranged in size from 150 to 500 m and were microscopic microplastics. Microplastic fragments - sedimentary habitats, shores, pelagic zones 7, 36, deep sea 37, and in living organisms
(Shim et al. 2022)	Review study	Between- North Pacific and the world's other ocean basins.	Two microplastic monitoring techniques: evaluation of ecological risk and pollution status throughout time and space	The North Pacific has seen more extensive microplastic monitoring efforts than other ocean regions. However, these studies were geographically skewed towards marginal waters in the Northwest Pacific region.
(De Frond et al. 2019)	Comparative case studies	Locations - Two coastal (Hong Kong & Hawaii), Two open ocean (North Pacific & South Atlantic gyres)	the volume of certain chemical additives entering the global seas with everyday plastic waste, & the volume of chemicals that have been sorbed	With more PCBs present closer to the source, where plastic is more prevalent /square foot than in the ocean, the mass of chemicals and plastics in a site are connected.
(Mohan et al. 2022)	Microplastic prevalence study	Beaches of Port Blair, ANI: Cove Beach, Quarry Beach, and Wandoor Beach are three coastal stations.	The analyzed locations contained lines, bits, pellets, foams, and microplastic fibers.	Waste from a nearby municipal landfill that contains microplastics. Fourier Transform Infrared Spectroscopy (FTIR) discovered that the beach silt included plasta zinc, a novel sort of polymer that may or may not be a nano plastic. Its presence indicates that the marine environment biologically and enzymatically degraded microplastic.
(Dutta et al. 2022)	Exploratory study	03 beaches viz Aksa, Versova, and Girgaon Chowpatty of Mumbai city	Spatial variation was also observed	Beads were the most common MPs in both the sediments and the saltwater column, whereas fibers contributed the least. Most of the seen particles were in the 0.45 to 500 m range. The number of smaller size fractions has been shown to increase, which raises the likelihood of harm to aquatic life.
(Keerthika et al. 2022)	Exploratory study	Beach sediment - Thoothukudi region, south-east coast of India, Gulf of Mannar region	The presence of inorganic materials on the surface Microplastics may result from environmental factors or plastic additions.	Along the Thoothukudi coast, microplastics (5 mm) are pervasive and pose a major danger to the marine ecosystem and life.
(Jeyasanta et al. 2020)	Exploratory study	08 sandy beaches- shoreline of Tuticorin, TN	fishing activity intensity and macro- and microplastic concentrations	These polymers are frequently found: PET, PS, PE, PP, NY, and PVC. The concentrations of micro- and mesoplastics are highly correlated.
(Sun et al. 2018)	comprehensive study	Yellow Sea, bounded by China and the Korean Peninsula	composition of the polymer type	In 80% (40 of 50) of the sample stations in the Yellow Sea, there were microplastics found in the seawater.

contamination from municipal garbage dumps close to the shore. Transforming Fourier, the beach silt was found to include plasta zinc, a novel sort of polymer that may or may not be a nano plastic, according to infrared spectroscopy. Its presence indicates that the marine environment biologically and enzymatically degraded microplastic. Further research is necessary to identify the variables affecting microplastic

prevalence, its hazardous effects on the marine environment, and the mechanisms of microplastic degradation in the marine ecosystem (Mohan et al. 2022).

Microplastic concentrations averaged 204 by 110 particles per kilogram and 103 by 60 particles per liter in marine sediments, respectively. The most common kinds of microplastic were beads, whereas fibers contributed the

least to the sediments and saltwater column. Most of the seen particles were in the 0.45 to 500 m range. The number of smaller size fractions has been shown to increase, which raises the likelihood of harm to aquatic life (Dutta et al. 2022).

A recent investigation demonstrated that microplastics (<5 mm) are widespread, providing a major hazard to the marine ecosystem and marine species. Energy dispersive X-ray (EDX) spectroscopy spectra revealed that the inorganic elements present at the surface of the microplastic may have come from the environment or as plastic additives (Keerthika et al. 2022).

Plastic trash prevalence differs among the research locations depending on the level of fishing and other activities of human nature. Using the polymers PP, NY, PET, PE, PS, and PVC as their constituents, mean concentrations of microplastics have been determined. PE is the most predominant polymer (Jeyasanta et al. 2020).

Plastic contamination in the ocean is a global issue. Most marine plastic pollution comes from microplastic, which is tiny enough to be consumed and possibly harmful to marine life. Polypropylene and polyethylene account for 88.13% of all main polymer types. Seawater contains a patchy distribution of MPs, with large MP concentrations seen in coastal cities. The polymer type has a varied composition, with 46% of the MPs in zooplankton being fiber-shaped. The taxa and their abundance in the Yellow Sea are factors in the retention of MPs in zooplankton (Sun et al. 2018).

Fish exposed to microplastics experience neurotoxicity, growth slowdown, and aberrant behavior. Microplastic effects on human health are not well understood. Owing to the high concentration of MPs in the environment, exposure might happen by eating, breathing, or skin contact. After exposure to MPs, humans may undergo oxidative stress, cytotoxicity, neurotoxicity, immune system disturbance, and MP translocation to other tissues. There is still much to learn about MPs' harmful effects on fish and humans (Bhuyan 2022).

DISCUSSION

The current study found that bioaccumulation is quite likely to happen with microplastics due to their tiny size. After being eaten by a range of marine species, such as corals, plankton, fish, seabirds, and marine mammals, they migrate up the food chain. Several chemical stabilizers and additives are also included in plastic polymers, which lead them to absorb toxic substances from their environment. Since the amount of pollution in the ocean has risen, there is an apparent and growing threat to human health.

Ocean pollution poses a clear and present danger to human health and well-being, as supported by Landrigan et

al. (2020), who mentioned that Methylmercury and PCBs are the ocean pollutants whose human health effects are best understood. Exposing infants *in utero* to these pollutants through maternal consumption of contaminated seafood can damage developing brains, reduce IQ and increase children's risks for autism, ADHD, and learning disorders (Landrigan et al. 2020).

The quantities of floating plastic in the Mediterranean Sea were investigated to see if this basin might be considered a major plastic waste accumulation location. The Mediterranean exhibited more big plastic items than oceanic gyres, indicating the region was close to pollution sources even if most of the plastic debris was in millimeter-sized bits (Cózar et al. 2015).

It is anticipated that interactions between micro- and nanoplastics and the immune system might result in immunotoxicity and, as a result, detrimental outcomes (such as immunosuppression, immunological activation, and aberrant inflammatory response). The ability of micro- (10 m) and nano-plastics (40-250 nm) to generate lethal effects at the cell level in terms of oxidative stress was recently demonstrated by in vitro investigations using cerebral and epithelial human cells, supporting the scientific hypotheses about the potential impacts on human health (Barboza et al. 2018).

When ingested by humans, the fate and consequences of microplastics are still debatable and poorly understood. If the distribution of particles in secondary tissues, such as the liver, muscles, and brain, is possible, then only microplastics smaller than 20 m can penetrate organs. Those with a size of about 10 m should be able to access all organs, cross cell membranes, cross the blood-brain barrier, and enter the placenta. The effects of microplastics on human health are not entirely understood. However, they might be caused by their physical characteristics (size, shape, and length), chemical characteristics (additives and polymer type), concentration, or microbial biofilm development (Campanale et al. 2020).

CONCLUSION

Microplastic pollution of the marine ecosystem is a contemporary issue due to its negative effects on marine biota. The toxic contaminants attach themselves to the microplastics, which act as vectors. To better comprehend the various variables that affect the occurrence of microplastic in marine ecosystems and its biological effects on marine biota, further research is necessary. Fish may be exposed to toxic compounds and harmful microbes through MPs. People consume fish contaminated with plastic and are exposed to plastic debris. As a result, numerous outbreaks of chronic illnesses happen, and individuals experience the consequences. It is necessary to implement conservation management strategies

and assistance for different educational programs to protect the environment from these hazardous microplastics. The public's education on the harmful effects of microplastics is a crucial need in this field. Many innovations to reduce the usage and consumption of plastic and its products would be encouraged. The collection and reuse of plastic waste is the most important strategy for lowering the quantity of plastic that enters the ecosystem. Find alternatives to plastic things to eliminate future dangers.

REFERENCES

Alfaro-Núñez, A., Astorga, D., Cáceres-Farías, L., Bastidas, L., Soto Villegas, C., Macay, K. and Christensen, J.H. 2021. Microplastic pollution in seawater and marine organisms across the Tropical Eastern Pacific and Galápagos. Sci. Rep., 11: 6424. https://doi.org/10.1038/s41598-021-85939-3

Amelia, T.S.M., Khalik, W.M.A.W.M., Ong, M.C., Shao, Y.T., Pan, H.J. and Bhubalan, K. 2021. Marine microplastics as vectors of major ocean pollutants and their hazards to the marine ecosystem and humans. Prog. Earth Planet. Sci., 8(1): 405. https://doi.org/10.1186/s40645-020-00405-4

Barboza, L.G.A., Dick Vethaak, A., Lavorante, B.R.B.O., Lundebye, A.K. and Guilhermino, L. 2018. Marine microplastic debris: An emerging issue for food security, food safety, and human health. Marine Pollut. Bull., 133: 336-348. https://doi.org/10.1016/J.MARPOLBUL.2018.05.047

Bhuyan, M.S. 2022. Effects of microplastics on fish and in human health. Front. Environ. Sci., 10: 250. https://doi.org/10.3389/FENVS.2022.827289/BIBTEX

Campanale, C., Massarelli, C., Savino, I., Locaputo, V. and Uricchio, V.F. 2020. A detailed review study on the potential effects of microplastics and additives of concern on human health. Int. J. Environ. Res. Pub. Health, 17(4): 212. https://doi.org/10.3390/IJERPH17041212

Cózar, A., Sanz-Martín, M., Martí, E., Ignacio González-Gordillo, J., Ubeda, B., Gálvez, J.Á., Irigoien, X. and Duarte, C.M. 2015. Plastic accumulation in the Mediterranean Sea. Plos One, 1: 62. https://doi.org/10.1371/journal.pone.0121762

De Frond, H.L., van Sebille, E., Parnis, J.M., Diamond, M.L., Mallos, N., Kingsbury, T. and Rochman, C.M. 2019. Estimating the mass of chemicals associated with ocean plastic pollution to inform mitigation efforts. Integr. Environ. Assess. Manag., 15(4): 596-606. https://doi.org/10.1002/IEAM.4147

Dutta, S., Sethulekshmi, S. and Srivastava, A. 2022. Abundance, morphology, and spatio-temporal variation of microplastics at the beaches of Mumbai, India. Reg. Stud. Marine Sci., 56: 102722. https://doi.org/10.1016/J.RSMA.2022.102722

Ivar Do Sul, J.A. and Costa, M.F. 2014. The present and future of microplastic pollution in the marine environment. Environ. Pollut., 185: 352-364. https://doi.org/10.1016/j.envpol.2013.10.036

Jeyasanta, K.I., Sathish, N., Patterson, J. and Edward, J.K.P. 2020. Macro-, meso- and microplastic debris in the beaches of Tuticorin district, Southeast coast of India. Marine Pollut. Bull., 154: 111055. https://doi.org/10.1016/J.MARPOLBUL.2020.111055

Keerthika, K., Padmavathy, P., Rani, V., Jeyashakila, R., Aanand, S. and Kutty, R. 2022. Contamination of microplastics, surface morphology, and risk assessment in beaches along the Thoothukudi coast, Gulf of Mannar region. Environ. Sci. Pollut. Res., 29(50): 75525-75538. https://doi.org/10.1007/S11356-022-21054-8/METRICS

Landrigan, P.J., Stegeman, J.J., Fleming, L.E., Allemand, D., Anderson, D.M., Backer, L.C., Brucker-Davis, F., Chevalier, N., Corra, L., Czerucka, D., Bottein, M.D., Demeneix, B., Depledge, M., Deheyn, D.D., Dorman, C.J., Fénichel, P., Fisher, S., Gaill, F., Galgani, F., Gaze, W.H., Giuliano, L., Grandjean, P., Hahn, M.E., Hamdoun, A., Hess, P., Judson, B., Laborde A, McGlade J, Mu J, Mustapha A, Neira M, Noble RT, Pedrotti ML, Reddy C, Rocklöv, J., Scharler, U.M., Shanmugam, H., Taghian, G., van de Water, J.A.J.M., Vezzulli, L., Weihe, P., Zeka, A., Raps, H., and Rampal, P. 2020. Human health and ocean pollution. Ann. Glob. Health., 86(1): 151. doi: 10.5334/aogh.2831.

Mohan, P.M., Tiwari, S., Karuvelan, M., Malairajan, S., Mageswaran, T. and Sachithanandam, V. 2022. A baseline study of meso and microplastic predominance in pristine beach sediment of the Indian tropical island ecosystem. Marine Pollut. Bull., 181: 113825. https://doi.org/10.1016/J.MARPOLBUL.2022.113825

Shim, W.J., Kim, S.K., Lee, J., Eo, S., Kim, J.S. and Sun, C. 2022. Toward a long-term monitoring program for seawater plastic pollution in the north Pacific Ocean: Review and global comparison. Environ. Pollut., 311: 119911. https://doi.org/10.1016/J.ENVPOL.2022.119911

Sun, X., Liang, J., Zhu, M., Zhao, Y. and Zhang, B. 2018. Microplastics in seawater and zooplankton from the Yellow Sea. Environ. Pollut., 242: 585–595. https://doi.org/10.1016/J.ENVPOL.2018.07.014

Tekman, M.B., Walther, B.A., Peter, C., Gutow, L. and Bergmann, M. 2022. Impacts of plastic pollution in the oceans on marine species, biodiversity, and ecosystems: A summary of a study for WWF. Zenodo, 52: 684. https://doi.org/10.5281/zenodo.5898684

Thi Kim Khuyen, V., Vu, L.D., René Fischer, A., Dornack, T.K., Khuyen, C.V, Fischer, A. R., Dornack, C. and Le, D.V. 2021. Comparison of microplastic pollution in beach sediment and seawater at UNESCO Can Gio mangrove biosphere reserve. Glob. Chall., 5(11): 2100044. https://doi.org/10.1002/GCH2.202100044

Uyarra, M.C., Tecnalia, A., Barletta, M., Aliani, S., Gago, J., Galgani, F., Maes, T. and Thompson, R.C. 2016. Microplastics in seawater: Recommendations from the marine strategy framework directive implementation process. Front. Marine Sci., 3: 219. https://doi.org/10.3389/fmars.2016.00219

Zhao, J., Ran, W., Teng, J., Liu, Y., Liu, H., Yin, X., Cao, R. and Wang, Q. 2018. Microplastic pollution in sediments from the Bohai Sea and the Yellow Sea, China. Sci. Total Environ., 640-641: 637-645. https://doi.org/10.1016/J.SCITOTENV.2018.05.346

Recent Advances and Sustainable Approaches Towards Efficient Wastewater Treatment Using Natural Waste Derived Nanocomposites: A Review

K. Haroon*, J. Kherb*, C. Jeyaseelan* and M. Sen*†

*Department of Chemistry, Amity Institute of Applied Sciences, Amity University, Noida-201301, India

†Corresponding author: M. Sen; msen@amity.edu

ABSTRACT

Pollutants like arsenic, chromium, or other toxic heavy metals have the most dreadful impact on humans or animals and also become a threat worldwide. Introducing these contaminants into the environment is not just due to the chemical industry but also coexists in combined form in underground rocks, contaminating groundwater during breakdown. Epidemics are now largely blamed on toxic pollution in many different nations worldwide. The issue has gotten worse in underdeveloped nations, where metal contamination of the groundwater affects more than a million people. Different techniques are used to remove toxic pollutants from water, but most are expensive and energy intensive. Adsorption is preferable for removing contaminants such as heavy metals or chemical dyes. As nanomaterials have been demonstrated to be more effective as nanocomposites, we used an adsorbent of nanomaterial to use the adsorption approach. These materials have become more well-liked because of their useful applications and improved characteristics. Magnetic synthesized nanocomposites have magnetic properties, which become beneficial for adsorption as it enhances adsorption capacity. The insertion of the plant or aggregate waste material for nanocomposite synthesis inhibits the growth of bacteria or other microorganisms, preventing the material from getting infected if it is in the environment. In this review paper, we have focused on the green synthesis of nanomaterials used for water treatment.

INTRODUCTION

Nanoparticles play an essential role in today's world as they are classified as advanced materials in nanotechnology. They are defined as modifying a matter through physical and chemical techniques to produce a material with specific characteristics that are helpful in many applications (Nazri & Sapawe 2020). Plants, animals, and bacteria have cell walls consisting of cellulose, lipids, and chitin, which are used to form different natural nanomaterials by the electrostatic interaction or hydrogen bonding. These materials are abundant, renewable, biodegradable, and easily prepared (Visakh & Thomas 2010). These cell walls have various functional groups on their surfaces that interact with organic or inorganic nanoparticles to form nano biocomposite materials. Nanoparticles come in the range of 1 to 100 nm, which has a very important contribution to the advancement of nanoscience and nanotechnology which is increasing quickly (Ahmad et al. 2011). Nanotechnology came into the picture after its scientific discovery in the twenty-first century. This developing area started grabbing attention as it includes the creation, handling, and use of those materials scaling in size less than 100 nm, which can become of great

use as applications of nanoparticles are vast (Jadoun et al. 2021). Researchers and scientists have started showing great interest in exceptional features and discovered that these contain individual applications in diverse fields. The green synthesis is a method of producing nanoparticles using eco-friendly and biocompatible precursors, reducing agents, and solvents. This approach can significantly reduce the toxicity of the resulting nanoparticles compared to conventional synthesis methods, which often use hazardous chemicals. Natural precursors, such as plant extracts, can also add advantageous functional groups to the nanoparticles' surfaces, reducing their toxicity and increasing their biocompatibility. Additionally, compared to conventional synthesis techniques, using green synthesis techniques frequently results in nanoparticles with enhanced stability and higher purity, significantly lowering their potential toxicity (Jadoun et al. 2021). With time, green chemistry has become the first choice for many scientists as it is an efficient method for nanoparticle synthesis. Plant extract-based green synthesis is widely used for synthesizing various nanoparticles and has been considerably studied over the last decades (Mondal et al. 2020). Numerous strategies have been used to enhance the recycling of used cartons to safeguard

the environment. Some of these are composting, exploiting biomethane sources, using them as raw materials to make lactic acid and bioplastics, and other techniques. However, there are restrictions because these methods can only partially encourage the recycling of used cartons. Additionally, they have several drawbacks, such as complicated processes, little financial value, and secondary contamination, which restricts the range of applications (Han et al. 2018). Recycling concrete waste addresses the increasing demand for plant, coal, and aggregate wastes. The burden of disposing of the enormous amount of construction and demolition waste also decreases and helps the environment. These usages of concrete recycled plant, coal, and aggregate waste have drawn the interest of researchers and scientists worldwide. They are believed to be a vital step toward the growth of the sustainable development of the construction industry (Yue et al. 2020). There is an immense need to develop better approaches using green nanotechnology to synthesize antiviral, antibacterial, or antimicrobial materials for water treatment (Naikoo et al. 2021). Recent studies revealed that nanoparticles are highly promising for antiviral and antimicrobial properties. A deep insight was provided into these nanoparticles' antibacterial and antimicrobial activities and how these antibacterial materials are used for water treatment (Naikoo et al. 2021). Hence, in this paper, we have discussed the preparation of nanoparticles in four critical domains: plant-based nanomaterials, coal waste nanomaterials, aggregate waste nanomaterials, and microbial waste, and discussed their beneficial applications.

PLANT-BASED NANOCOMPOSITES

Plants have antibacterial, antioxidant, and anti-inflammatory properties, providing great potential for heavy metal accumulation and detoxification (Iravani 2011). According to recent studies, plants and plant waste can be utilized to synthesize nanoparticles. Plant structures and components inside it have drawn researchers' attention to the fabrication of NPs due to the desired properties like minimizing cost, rapid process, eco-friendly, and simplicity in biosynthesis (Nazri & Sapawe 2020). These approaches avoid complicated processes to synthesize and modify nanomaterials for a better purpose and are economical and environmentally benign. Researchers have widely investigated the metal nanoparticles obtained from plant extract that are biocompatible and nontoxic (Naikoo et al. 2021). Many nanoparticles are synthesized using the green approach, such as copper, gold, silver, zinc oxide, and iron (Jadoun et al. 2021). Table 1 demonstrates different plant-based waste materials used for the novel growth of nanoparticles.

Synthesis of Nanocomposites with Plant Waste

Green synthesis of Fe_2O_3-Ag nanocomposite using Plant leaf extract, as represented in Fig. 1. Separate preparations of $AgNO_3$ solution and $Fe(NO_3)_3$ solution were made to synthesize Fe_2O_3Ag/GL nanocomposites. The prepared solutions were continuously stirred to ensure proper mixing. The leaf extract was added dropwise to the solution using a burette after the mixture had been well homogenized, with continual stirring. The solution was left undisturbed once the precipitate had fully formed before being centrifuged. The residue was extensively cleaned with DI water to remove any ionic impurities before being cleaned with acetone to remove any organic impurities. After the precipitate had formed, it was oven-dried before being burned. Following collection, the sample was characterized using a variety of techniques.
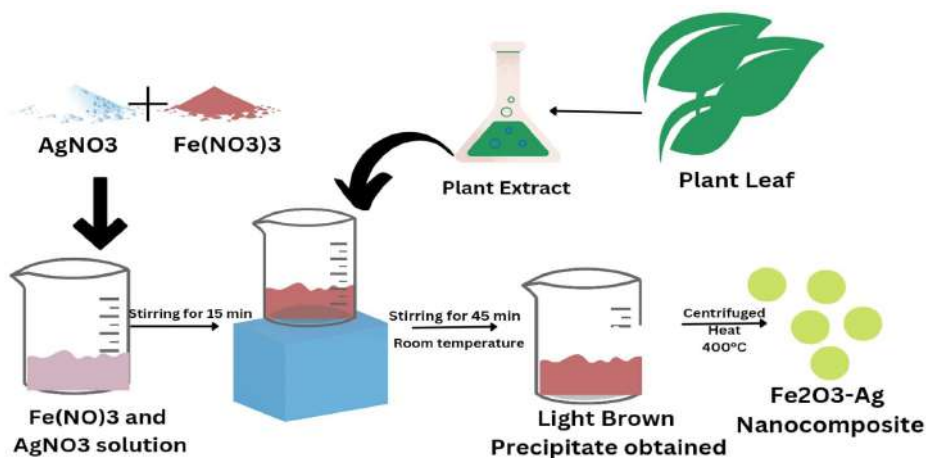

Fig. 1: Green synthesis of Fe_2O_3-Ag nanocomposite using Plant leaf extract.

Table 1: Plants waste used for nanocomposite synthesis and their characteristics.

Plant Origin	Waste	Nanocomposite and technique	Size (nm)	Applications	Reference
Basil (*Ocimum basilicum*)	Leaf	Alginate-gum acacia-Ag0-Basil, Solvent Extraction	20	Antimicrobial Activity	(Kanikireddy et al. 2019)
Neem (*Azadirachta indica*)	Leaf	Chitosan-Neem, Solvent Evaporation	30	Antimicrobial Activity	(Mohammad & Hasobo 2012)
Tulsi (*Ocimum tenuiflorum*)	Leaf	Ag/ZnO-Basil Mediated Ultrasonication	50	Antimicrobial Activity	(Panchal et al. 2020)
Aloe vera (*Aloe barbadensis*)	Leaf	PVA/Cellulose Nanofiber-Aloe vera Ultrasonication	-	Antimicrobial Activity	(Kakroodi et al. 2014)
Jamun (*Syzygium cumini*)	Leaf	ZnO-Jamun Biogenic	11.35	Antimicrobial Activity	(Sadiq et al. 2021)
Guava (*Psidium guajava*)	Leaf	Fe_2O_3-Ag-Guava Biological	50-90	Antimicrobial Activity	(Biswal et al. 2020)
Tea (*Camellia sinensis*)	Leaf	Ag-Tea NPs Biological	50	Antibacterial Activity	(Loo et al. 2012)
Goatsbeard (*Tragopogon collinus*)	Leaf	Ag-Tea NPs Biological	50	Antibacterial Activity	(Seifipour et al. 2020)

COAL ASH-BASED NANOCOMPOSITES

The usage of coal energy production is significant worldwide, despite the concern generated by the government. According to market analysis, the international coal demand for renewable energy production will increase in the coming years. Still, it also leads to the waste of coal, which is a concern for the environment. However, coal combustion generates immense amounts of solid waste, such as fly ash, bottom ash, boiler slag, fluidized bed combustion ash, and other products. Coal fly ash, also known as CFA, is primarily used for the exhibition of blended cement, as a definite addition, in concrete blocks, road construction, etc. (Boycheva et al. 2020). Ash is a highly available waste generated mainly through industrial and agriculture as a by-product. These waste by-product ashes raise environmental concerns about disposal issues and gained much attention for the sustainable utilization of ash as a renewable supporting material in synthesizing nanocomposites.

The prospective uses of coal waste, including coal fly ash, coal husk ash, and volcanic ash, are now being investigated. These waste materials have key features, including high adsorption activity, ion exchange capacity, surface area, and reusability (Lum et al. 2020). The production of CFA increases by about 5% every year. Therefore, Recycling waste is very important. This can be done by altering coal fly ash into reusable materials rather than dumping it into landfills which could be a problem with removal costs and environmentally dangerous circumstances.

Furthermore, fly ash from coal has been determined to be a valuable substance for photocatalysis and adsorption activity, which is further used to remove toxic pollutants from water bodies. These coal waste nanomaterials contain important metal oxides, including Fe_3O_4, SiO_2, TiO_2, and Al_2O_3, and are helpful in photocatalysis and adsorption (Umejuru et al. 2020). In this review paper, Carbon hybrid nanocomposite-coated coal fly ash (CFA/C HNCPs), which was synthesized as the effective removal of pollutants like cadmium ion (Cd^{2+}) from wastewater, and the spent adsorbent (CFA/C– Cd^{2+} HNCPs) was recycled in the photocatalytic degradation of methylene blue (Umejuru et

Table 2: Coal waste and its nanocomposites with the applications.

Coal Waste	Nanocomposite And Techniques	Size (nm)	Applications	Reference
Coal fly ash	CFA-$CuFe_2O_4$ (Coal fly ash-copper ferrite), Hydrothermal	1	Degrade dye (pollutant)	(Nadeem et al. 2021)
Coal fly ash	CFAZ (Coal fly ash-Zeolites), hydrothermally	2-10	Substitution, recovery, and use reduction of CRMs (critical raw materials)	(Boycheva et al. 2020)
Fly ash	CFA/C HNCPs (Coal fly ash/carbon hybrid nanocomposite), hydrothermal	100	Heavy metals can be removed from wastewater.	(Umejuru et al. 2020)
Fly ash	CNT -fly ash (Carbon nanotubes-fly ash polymer nanocomposite), Ball Mining	500	Environmental-friendly construction and building materials.	(Chaturvedi et al. 2021)

al. 2020). Table 2 lists the applications for coal waste and its nanocomposites.

Synthesis of Coal Waste Nanocomposites

For the preparation of CNT supported by fly ash, industrial waste particulates were collected from across India and were prepared through the Ball milling technique, which supports chemical-mechanical grinding, followed by a compressive molding technique underneath an epoxy system at low temperature. The polymer nanocomposite synthesis was also done utilizing a compressive molding apparatus at room temperature. The polymer used was Epoxy, and dimethylformamide or DMF solvent was used to spread the carbon nanotubes in the fly ash waste, as shown in Fig. 2. The prepared synthesized materials were ball milled using a ball milling machine, then rushed into the mold frame and allowed cure at room temperature. Finally, carbon nanotubes having fly ash-based waste polymer nanocomposites were obtained. These nanocomposites have functional groups on the surface, which will be analyzed using FT-IR spectroscopy. These instrumentation techniques were done to analyze the exciting properties of carbon nanotubes and fly ash waste, their interfacial bonding, and the size and structure of the synthesized nanocomposites, which can be used for various applications (Chaturvedi et al. 2021).

AGGREGATE WASTE-BASED NANOCOMPOSITES

Nanotechnology has become the growing field in the research areas for the synthesis of cellulose-based nanocomposites, which are synthesized using not only plants but also from waste agriculture material such as rice husk, bamboo leaves, sugarcane bagasse, groundnut shell, etc. (Vaibhav et al. 2015). The requirement for the formation of these nanocomposites from waste material is to purify water or remove the heavy metals present in the water by the adsorption activity on the toxic pollutants by using agricultural wastes as a composite material, which will prevent long-term risk to the ecosystem and human beings (Younes et al. 2021). Researchers use agricultural waste or natural fillers to synthesize metallic or polymer-based nanocomposites. These materials are used because they have benefits over conventional filler, including low cost, high toughness, excellent specific strength, and improved energy recovery (Bello et al. 2015). Corn cob is one of the most common agricultural wastes, which produces an estimated amount of waste load of thousands of tons yearly. Yet, it is also a good source of xylem, a crucial bioactive polysaccharide (Viana et al. 2020). The core of the maize plant, the corn cob, is disposed of as waste and burned as fuel, raising environmental issues. Corn cob waste can be used to create green nanocomposite materials that are environmentally safe and have the qualities needed to perform the intended function in the water purification process. Corn cob can be chemically processed to produce new end products with added value at low prices, achieving its value in new research areas (Kumar et al. 2010). A growing argument has been made for using magnetic adsorbents to make separating carbonaceous adsorbents easier and increasing the efficiency
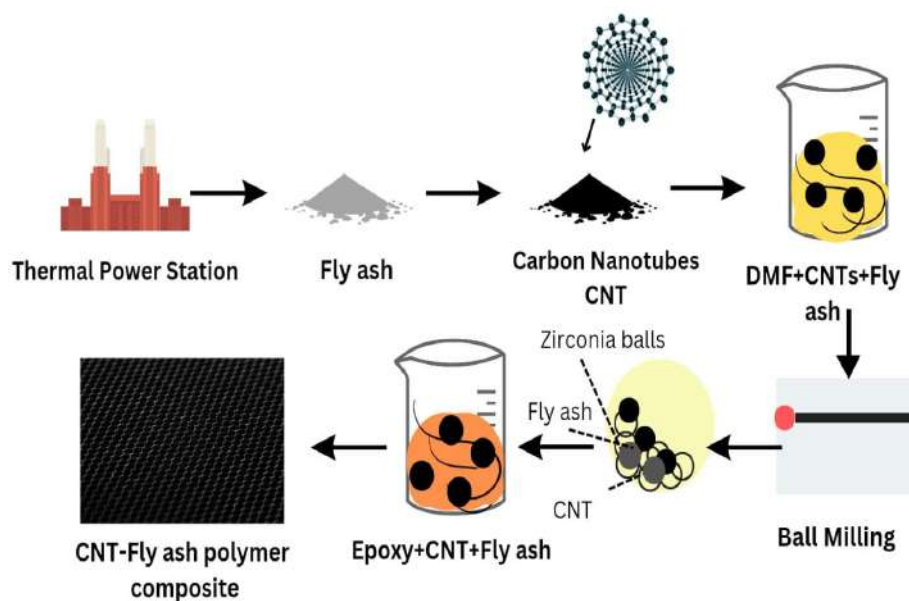

Fig. 2: Representation of preparation of CNT/fly ash.

Table 3: Listed down the origin of Aggregate waste and their nanocomposites with the applications.

Aggregate waste origin	Nanocomposites and Techniques	Size (nm)	Applications	References
Corn cobs	AgNP/CC (xylan extract containing silver nanoparticles), Microwave	100	Reducing and stabilizing agent	(Viana et al. 2020)
Sawdust	MPSB (magnetic pine sawdust biochar), Biogenic	50	Synthesis of magnetic adsorbents for inorganic and organic contaminants	(Reguyal & Sarmah 2018)
Groundnut shell	SnO_2/GNSAC (Tin oxide groundnut shell activated carbon), chemical precipitation	1	Photocatalytic oxidation of MB dye	(Ragupathy& Sathya 2016)
Coconut shell	AgNPs/CS (synthesis of silver nanoparticles containing coconut shell), Photochemical	1.20 - 22.96	Antibacterial activity against *S. aureus* infections	(Sinsinwar et al. 2018)
Bagasse	BAE/AgNPs (Silver nanoparticles with bagasse), Microwave	100	Reducing and stabilizing agents	(Shen et al. 2016)

of the entire adsorption process. The surface of corn cobs has several functional groups that might be used to bind various metal oxides to create nanocomposites, which would remove water contaminants (Younes et al. 2021). Agricultural waste has often been the source of some of the most widely used carbonaceous adsorbents. For various inorganic and organic pollutants, carbonaceous adsorbents such as activated carbon, biochar, charcoal, and char have demonstrated good adsorptive capacity (Reguyal & Sarmah 2018). The origin of aggregate waste and its nanocomposites with the applications is depicted in Table 3.

Synthesis of Silver Nanocomposite with the Aggregate Waste Bagasse

For synthesis, the required quantity of solution of $AgNO_3$ was prepared by dissolving the desired amount in distilled water. After that, a few drops of diluted sodium hydroxide were added to entirely convert the precipitate Ag+ to silver oxide Ag2O. The aqueous ammonia solution was added until all brown silver oxides were completely dissolved. At this stage, the clear mixture contained Ag+ ions in the form of $[Ag(NH_3)_2]OH$. The $[Ag(NH_3)_2]OH$ solution was diluted with pure water and added to a flask with BAE (Fig. 3). The solution was filtered, and the BAE/AgNPs were successfully

synthesized using microwave irradiation. Finally, the BAE/AgNPs nanocomposite was synthesized, followed by the Cysteine for possible applications (Shen et al. 2016).

MICROBES BASED NANOCOMPOSITES

Green nanocomposite synthesis is an environmentally friendly, highly stable, cost-effective method that does not involve harmful chemicals. This technique reduces and stabilizes agents such as aggregate wastes, microbes, plants, and other natural waste resources to produce sustainable nanoparticles. Synthesis of nanoparticles using microbes is an eco-friendly green procedure that utilizes bacteria, fungi, viruses, and their products to produce nano biocomposites. Natural microbes are used as a component in nanoparticle synthesis as they provide templates for well-defined structures for the synthesized nanoparticles. Inorganic/Metallic nanoparticles like gold, silver, copper, zinc, titanium, palladium, and nickel are synthesized. These synthesized nanoparticles can be accepted both extracellularly and intracellularly using microbes. The filtrate was collected using centrifugation in the extracellular synthesis, and metallic aqueous solutions were mixed. The color change of the hybrid solution monitors the synthesis of NPs (Ali et al. 2020). Nanoparticles now play a crucial
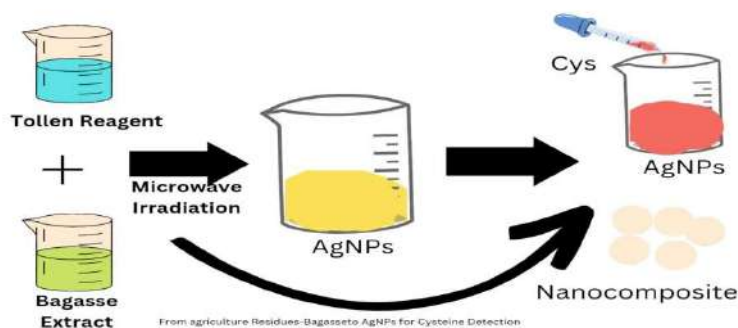

Fig. 3: Green synthesis pathway of silver nanocomposite with the aggregate waste bagasse.

Table 4: List of recently reported nanocomposites derived from microbes.

Microbes	Nanocomposite & Techniques	Size (nm)	Application	Reference
Algae *C. crispus*	AuNPs- *C. crispus* & Biogenic	50	Clean method for nanoparticles production	(Castro et al. 2013)
Algae *H. alcalis*	AgNPs-*H. alcalis* & Biogenic	20	Sensing	(Tomer et al. 2019)
Algae *Chlorella ellipsoidea*	AgNPs- *Chlorella ellipsoidea* & Biological	20	Degradation of Methylene Blue	(Borah et al. 2020)
Cyanobacteria C-phycoerythrin	CdS NPs- C-phycoerythrin & Biological	5	biolabeling	(Mubarakali et al. 2012)
Fungi *R. oryzae*	AuNPs-*R. oryzae* & Biological extracts	20	High-yield and low-cost NPs production	(Das & Marsili 2010)

role in most technologies (Bahrulolum et al. 2021). Algae are polymer-based molecules such as polysaccharides that can gather together heavy metal ions and recondition them into malleable form with the help of a biological reduction process. The typical algal-mediated synthesis of inorganic nanoparticles is silver and gold, the most examined noble metals algae microbes use for making nano biocomposites (Uzair et al. 2020). Table 4 shows a list of recently published microbe-derived nanocomposites.

Synthesis of Microbes-Based Nanocomposites

The synthesis of algae-mediated inorganic nanoparticles can be achieved intracellularly or extracellularly (Sabo-Attwood et al. 2012). In intracellular nanoparticle synthesis protocol,

algae microbes waste is collected and washed multiple times with distilled water to clear all the contaminants. Afterward, the prepared solution of $AgNO_3$ is mixed with algae. The resulting mixture needs to be incubated at a specific temperature and pH conditions for a fixed period of time, as required for the bioreduction method. Contents are finally sonicated and centrifuged to produce a good yield of stable nanoparticles. The extracellular synthesis protocol begins with collecting and washing an Algae sample with plenty of distilled water to remove the impurities. The collected algae are dried for a specific time, and the dried powder is mixed with distilled water. The algae extract is then sonicated for some time, followed by adding a metal precursor solution. Contents are then incubated for 8-16 hours, and the obtained
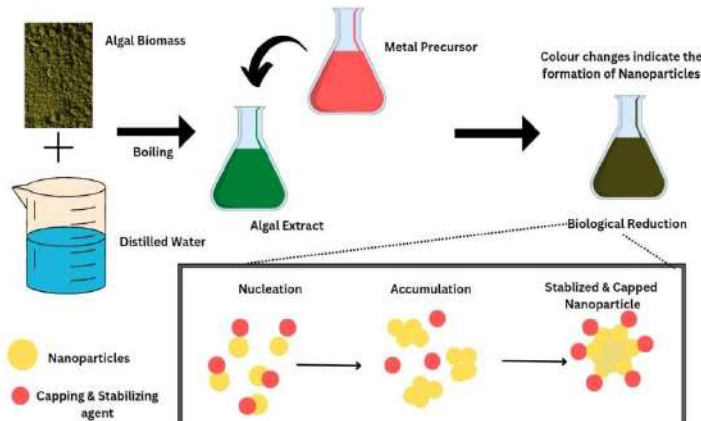

Fig. 4: Mechanism of formation of algae microbe-based nanocomposites.

Table 5: List of some recently reported metal-based nanocomposites and their comparative adsorption capacities.

Adsorbent	Size (nm)	Adsorption Capability mg/g	Application	References
Fe_3O_4-GO	200	59.6	Removal of metals	(Sheng et al. 2012)
Fe_3O_4-chitosan-GO	50	95.16	MB dye adsorption	(Fan et al. 2012)
$MnFe_2O_4$-GO	100	240.4	As(V) adsorption	(Lan Huong et al. 2018)
Ni Fe_2O_4-GO	41	59.52	As(III) adsorption	(Lum et al. 2020)
$MnFe_2O_4$	10	31.5	Fast Removal and Recovery of Cr(VI).	(Hu et al. 2005)
$MnFe_2O_4$/rGO	5	41	Adsorption of Tetracycline	(Bao et al. 2018)

Table 6: Green metal-based nanocomposites and their adsorption capacities.

Adsorbent	Size (nm)	Adsorption Capability (mg/g)	Application	Reference
Fe_3O_4 MNPs	107.5	80	Removing MB dye	(Jabbari et al. 2016)
CFA/C HNCPs	100	77	Heavy metals can be removed from wastewater	(Umejuru et al. 2020)
MnO_2/BC	190-220	185.185	Adsorptive removal of Methylene blue	(Siddiqui et al. 2019)
Fe_2O_3-ZrO_2/BC	200	1.01	Adsorptive removal of arsenic	(Siddiqui & Chaudhry 2019)
Fe_2O_3-ZrO_2/BC	200	38.10	Adsorptive removal of dyes	(Siddiqui & Chaudhry 2019)
FeOx-GO	5	147 and 113	Adsorptive removal of As(III) and As(V)	(Siddiqui & Chaudhry 2017)

Table 7: Green polymer-based nanocomposites and adsorption capacities.

Adsorbent	Size (nm)	Adsorption Capability (mg/g)	Application	Reference
SS/Fe_3O_4	12-15	265.4	Adsorptive removal of Pb(II)	(Ahamad et al. 2020)
SS/Fe_3O_4	12-15	247.2	Adsorptive removal of Cd(II)	(Ahamad et al. 2020)
PPy/ Fe_3O_4/SiO_2	500	361	Removal of Congo red dye (CR)	(Alzahrani et al. 2021)
PPy/ Fe_3O_4/SiO_2	500	298	Removal of hexavalent chromium Cr(VI)	(Alzahrani et al. 2021)
GA-cl-PAM/ZnO	500	766.52	Malachite Green Dye Adsorption	(Mittal et al. 2020)
PAPE/AZO	100	94.46	Removal of malachite green dye.	(Gouthaman et al. 2019)

product is then filtered. A distinct change in solution color during incubation indicates the nanoparticles' successful formation. During the bioreduction process of metal ions, nucleation, and successive condensation processes ensures the formation or growth of stabilized nanoparticles surrounded by capping agents, as schematically highlighted in Fig. 4. Synthesized nano biocomposites can be chemically and morphologically characterized by various spectroscopic and microscopic techniques. List of several recently published metal-based nanocomposites in Table 5 along with a comparison of their adsorption capabilities.

Table 6 lists the adsorption capabilities of green metal-based nanocomposites and Table 7 lists the adsorption capabilities of green polymer-based nanocomposites.

APPLICATIONS OF NANOCOMPOSITES FOR WATER TREATMENT

Severe contamination of soft water resources by organic, inorganic, and biological pollutants is a global environmental crisis causing health and societal problems on a large scale. The biggest culprits among these toxic pollutants are inorganic metal ions and organic dyes commonly released by industries in the environment. These untreated effluents cause tremendous damage not only to the surrounding soil but also to the groundwater and nearby water bodies. Prolonged exposure to such primary pollutants in the aqueous environment, especially heavy metal ions, increases the risk of health problems for plants, humans, and animals (Lingamdinne et al. 2019). Clean water, an essential natural resource, is vital for the healthy coexistence and survival of all living creatures on Earth. Water pollutants endanger the biosphere, so removing toxic pollutants from water resources has become important (Pandey et al. 2017). In this aspect, clean, affordable, and effective solutions are needed to overcome this environmental crisis. Nanomaterials with high separation capacity, good porosity, recyclability, and reusability are attractive for effectively treating polluted water (Dhiman & Sharma 2019). Prodigious progress has happened in the synthesis and properties optimization of nanomaterials with very good control over their size/shape, porosity, hydrophilicity/hydrophobicity, adsorption specificity, and photochemical activity (Pandey et al. 2017). This also makes them more versatile and effective in removing chemically different pollutants from water samples.

Magnetic Functionalization of Graphene Oxide-Based Nanocomposites

Iron oxide-based nanostructures have become widespread among nanomaterials because of their strong magnetic properties. These favorable magnetic features can be utilized for even more effective water treatment. These materials can also be combined with other entities, such as graphene, to further improve their stability and performance. Protective surface coating of hydrophobic graphene or graphene oxide on iron oxide core has been found to provide excellent stability, high surface area, mechanical strength, and porous nature to the composites. Co-precipitation is commonly employed to synthesize several iron oxide composites with graphene or graphene oxides (Siddiqui & Chaudhry 2017). As can be seen in the schematic in Fig. 5,
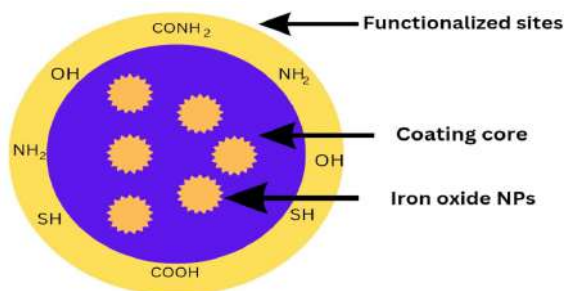
Fig. 5: Functionalized graphene-iron oxide nanocomposites for water treatment.

the graphene layer around the nano iron oxide particles not only provides protection but also enables the attachment of various functional groups such as COOH, NH$_2$, and OH to the material surface, resulting in improved solubilization and enhanced metal ion removal capabilities (Iravani 2011).

Mechanism of Pollutants Removal with Synthesized Nano Biocomposites

Nano-biocomposites can be easily synthesized using hydrothermal, co-precipitation, sol-gel, or ball-milling techniques. Most materials from plant, coal, or aggregate-based wastes have active functional groups like -OH, -COOH on the surface (Gadore & Ahmaruzzaman 2021). For example, black cumin seed has important functional groups like -OH, -COOH, and -NH$_2$ at the surface that attract Mn^{2+} ions from surroundings to form manganese oxide nanoparticles. The formation of MnO$_2$ in the seed carbon framework resulted from the redox reaction between MnCl$_2$ and KMnO$_4$ (Siddiqui & Chaudhry 2017). All such reactions are highly pH dependent as the charge on functional groups will be governed by it. For solutions having a pH value above the pKa of these functional groups, the overall charge on the composite will be negative. This will generate an electrostatic pulling force for cationic inorganic compounds such as Mn^{2+} ions. These ions get trapped in the plant framework primarily through hydrogen bonding. When bases like NaOH are added, the metal ions change into hydroxide form and form Mn(OH)$_2$, which contain more hydroxy groups wherein
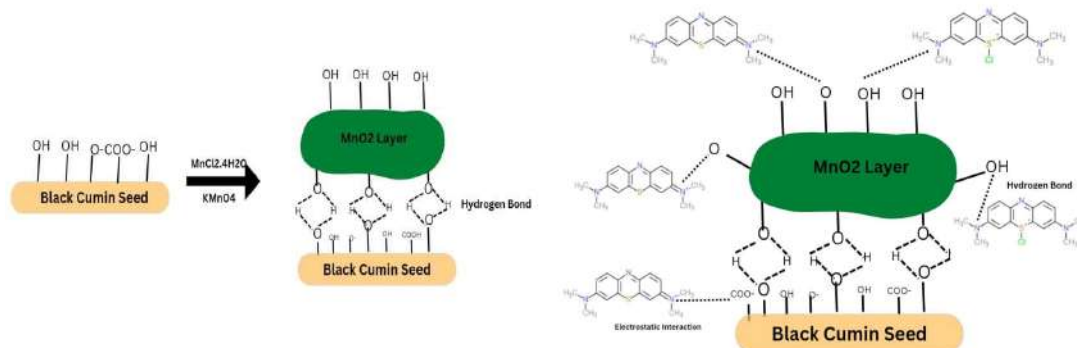

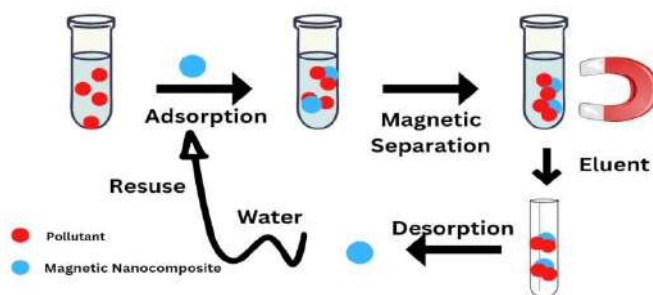Fig. 6: Mechanism of nanocomposite formation and removal of methylene dye by the adsorption activity.

Fig. 7: Schematic representation of removal of pollutants from water.

nucleation and dehydration growth occur. This leads to the development of the MnO_2/BC phase. This process is called Nucleation driven dehydration growth and forms the complex structure of nano-biocomposites as shown in Fig. 6 (Siddiqui et al. 2019).

Further studies have shown that the oxygen-containing functional groups play an essential role in the size of the adsorbent material as it enhances the adsorption capacity resulting in the strong interaction of the solute and adsorbent. Toxic chemical species such as arsenic metal ions or dyes attach themselves to the surface's functional groups via intramolecular hydrogen or electrostatic bonding, forming the complex. Pollutants adsorbed on the surface of nanocomposites have further adsorption activity, which can be utilized to remove even more contaminants from the water.

UTILIZATION AND RECOVERY OF NANOCOMPOSITES FROM WATER SAMPLES

Recovery and recyclability of non-magnetic nanocomposites like Graphene Oxide (GO) are more challenging than magnetized graphene oxide (MGO) containing composites. Moreover, magnetic graphene oxide has a very high adsorption capacity. An external magnet can easily separate the nanocomposite from the water, along with pollutants adsorbed on the surface. Fig. 7 highlights the various important steps in successfully using magnetic GO-based nanocomposites to remove harmful water pollutants and their facile recovery process employing a simple external magnetic field. It is essential to isolate the solute-loaded adsorbents from water for desorption and regeneration (Siddiqui & Chaudhry 2019). Metal ions adsorbed on these magnetic materials can be utilized for other applications. It has been reported that recovered magnetic nanomaterials can be efficiently reused for multiple cycles. This exhausted adsorbent regeneration technique is crucial for creating a cost-effective procedure.

CONCLUSION

Nanocomposites made from waste materials have gained much attention among the scientific community because of their vastly effective properties, ultrahigh surface area, and easy and cost-effective synthesis protocols. The prospect of using these materials is also high, as indicated by their current annual growth rate of nearly 25 %, which is excellent. Most of the current demand for this material is from tissue engineering and water treatment fields. The global drinking water shortage problem is closely connected to the growth of the world population, industrialization, and water pollution. This problem is especially severe in small, developing countries where the resources for water treatment are very

scant. Although many different types of nanoparticles are synthesized using various green processes, biomass-based nanomaterials have received the most significant attention from scientists and researchers. This is because of their outstanding antimicrobial, antibacterial, antifungal, and antiviral properties. Many waste materials, including dead residues from plants, coal ash, and aggregate waste, can be used as a substrate to obtain natural nanoparticles such as iron NPs. The presence of some biomolecular structures is vital to getting highly stable nanomaterials, as revealed by many research studies discussed above. In recent years, the use of nanocomposites for water remediation has increased considerably. Multiple government agencies and pharmaceutical industries worldwide are investing huge efforts and resources toward a facile synthesis of waste-based nanocomposites and their applications in diverse fields.

REFERENCES

Ahamad, T., Naushad, M., Mousa, R.H. and Alshehri, S.M. 2020. Fabrication of starch-salicylaldehyde-based polymer nanocomposite (PNC) for the removal of pollutants from contaminated water. Int. J. Biol. Macromol., 165: 2731-2738. doi: 10.1016/j.ijbiomac.2020.10.170.

Ahmad, M.B., Tay, M.Y., Shameli, K., Hussein, M.Z. and Lim, J.J. 2011. Green synthesis and characterization of silver/chitosan/polyethylene glycol nanocomposites without any reducing agent. Int. J. Mol. Sci., 12(8):4872-4884. doi: 10.3390/ijms12084872.

Ali, M.A., Ahmed, T., Wu, W., Hossain, A., Hafeez, R., Islam Masum, M.M., Wang, Y., An, Q., Sun, G. and Li, B. 2020. Advancements in plant and microbe-based synthesis of metallic nanoparticles and their antimicrobial activity against plant pathogens. Nanomaterials, 10(6): 1-24.

Alzahrani, F.M., Alsaiari, N.S., Katubi, K.M., Amari, A., ben Rebah, F. and Tahoon, M.A. 2021. Synthesis of polymer-based magnetic nanocomposite for multi-pollutants removal from water. Polymers, 13(11): 1-16. doi: 10.3390/polym13111742.

Bahrulolum, H., Nooraei, S., Javanshir, N., Tarrahimofrad, H., Mirbagheri, V.S., Easton, A. J. and Ahmadian, G. 2021. Green synthesis of metal nanoparticles using microorganisms and their application in the agrifood sector. J. Nanobiotechnol., 19(1): 22-32.

Bao, J., Zhu, Yezi, Yuan, Sijia, Wang, F., Tang, H., Bao, Z., Zhou, H. and Chen, Y. 2018. Adsorption of tetracycline with reduced graphene oxide decorated with MnFe2O4 nanoparticles. Nanosc. Res. Lett., 13: 396. doi: 10.1186/s11671-018-2814-9.

Bello, S.A., Agunsoye, J.O. and Hassan, S.B. 2015. Synthesis of coconut shell nanoparticles via a top down approach: Assessment of milling duration on the particle sizes and morphologies of coconut shell nanoparticles. Mater. Lett., 159: 514-519. doi: 10.1016/j.matlet.2015.07.063.

Biswal, S.K., Panigrahi, G.K. and Sahoo, S.K. 2020. Green synthesis of Fe_2O_3-Ag nanocomposite using Psidium guajava Leaf extract: An eco-friendly and recyclable adsorbent for remediation of Cr(VI) from aqueous media. Biophys. Chem., 263: 106392. doi: 10.1016/j.bpc.2020.106392.

Borah, D., Das, N., Das, N., Bhattacharjee, A., Sarmah, P., Ghosh, K., Chandel, M., Rout, J., Pandey, P., Ghosh, N.N. and Bhattacharjee, C.R. 2020. Alga-mediated facile green synthesis of silver nanoparticles: Photophysical, catalytic and antibacterial activity. Appl. Organome. Chem., 34(5): 1-10. doi: 10.1002/aoc.5597.

Boycheva, S., Zgureva, D., Lazarova, H., Lazarova, K., Popov, C., Babeva, T. and Popova, M. 2020. Processing of high-grade zeolite nanocomposites from solid fuel combustion by-products as critical raw materials substitutes. Manufact. Rev., 7: 22. doi: 10.1051/mfreview/2020019.

Castro, L., Blázquez, M.L., Muñoz, J.A., González, F. and Ballester, A. 2013. Biological synthesis of metallic nanoparticles using algae. IET Nanobiotechnol., 7(3): 109-116. doi: 10.1049/iet-nbt.2012.0041.

Chaturvedi, A.K., Gupta, M.K.G. and Pappu, A. 2021. The role of carbon nanotubes on flexural strength and dielectric properties of water sustainable fly ash polymer nanocomposites. Phys. B Cond. Matter, 620: 418232. doi: 10.1016/j.physb.2021.413283.

Das, S.K. and Marsili, E. 2010. A green chemical approach for the synthesis of gold nanoparticles: Characterization and mechanistic aspect. Rev. Environ. Sci. Biotechnol., 9(3): 199-204. doi: 10.1007/s11157-010-9188-5.

Dhiman, N. and Sharma, N. 2019. Batch adsorption studies on the removal of ciprofloxacin hydrochloride from aqueous solution using ZnO nanoparticles and groundnut (Arachis hypogaea) shell powder: A comparison. Indian Chem. Eng., 61(1): 67-76. doi: 10.1080/00194506.2018.1424044.

Fan, L., Luo, Chuannan, Li, X., Lu, F., Qiu, H. and Sun, M. 2012. Fabrication of novel magnetic chitosan grafted with graphene oxide to enhance adsorption properties for methyl blue. J. Hazard. Mater., 215-216: 272-279. doi: 10.1016/j.jhazmat.2012.02.068.

Gadore, V. and Ahmaruzzaman, M. 2021. Fly ash–based nanocomposites: A potential material for effective photocatalytic degradation/elimination of emerging organic pollutants from aqueous stream. Environ. Sci. Pollut. Res., 28(34): 46910-46933.

Gouthaman, A., Auslin Asir J., Gnanaprakasam, V.M., Sivakumar, M., Mohamed, A., Riswan A. and Raja, S.A. 2019. Enhanced dye removal using polymeric nanocomposite through incorporation of ag doped ZnO nanoparticles: Synthesis and characterization. J. Hazard. Mater., 373: 493-503. doi: 10.1016/j.jhazmat.2019.03.105.

Han, J., Zhang, G., Zhou, L., Zhan, F., Cai, D. and Wu, Z. 2018. Waste carton-derived nanocomposites for efficient removal of hexavalent chromium. Langmuir, 34(21): 5955-5963. doi: 10.1021/acs.langmuir.8b00225.

Hu, J., Lo, I.M.C. and Chen, G. 2005. Fast removal and recovery of Cr(VI) using surface-modified jacobsite (MnFe2O4) nanoparticles. Langmuir, 21(24): 11173-11179. doi: 10.1021/la051076h.

Iravani, S. 2011. Green synthesis of metal nanoparticles using plants. Green Chem., 13(10): 2638-2650. doi: 10.1039/c1gc15386b.

Jabbari, V., Veleta, J.M., Zarei-Chaleshtori, M., Gardea-Torresdey, J. and Villagrán, D. 2016. Green synthesis of magnetic MOF@GO and MOF@CNT hybrid nanocomposites with high adsorption capacity towards organic pollutants. Chem. Eng. J., 304: 774-783. doi: 10.1016/j.cej.2016.06.034.

Jadoun, S., Arif, R., Jangid, N. Kumari and Meena, R.K. 2021. Green synthesis of nanoparticles using plant extracts: A review. Environ. Chem. Lett., 19(1): 355-374.

Kakroodi, A.R., Cheng, S., Sain, M. and Asiri, A. 2014. Mechanical, thermal, and morphological properties of nanocomposites based on polyvinyl alcohol and cellulose nanofiber from Aloe vera Rind. J. Nanomater., 20:1-7. doi: 10.1155/2014/903498.

Kanikireddy, V., Kanny, K., Padma, Y., Velchuri, R., Ravi, G., Jagan Mohan Reddy, B. and Vithal, M. 2019. Development of alginate-gum acacia-Ag0 nanocomposites via green process for inactivation of foodborne bacteria and impact on shelf life of black grapes (Vitis vinifera). J. Appl. Polym. Sci., 136(15): 1-9. doi: 10.1002/app.47331.

Kumar, S., Negi, Y.S. and Upadhyaya, J.S. 2010. Studies on characterization of corn cob based nanoparticles. Adv. Mater. Lett., 1(3): 246-253. doi: 10.5185/amlett.2010.9164.

Lan Huong, P.T., Tu, N., Lan, H., Thang, L.H., Van Quy, N., Tuan, P.A., Dinh, N.X., Phan, V.N. and Le, A.T. 2018. Functional manganese ferrite/graphene oxide nanocomposites: Effects of graphene oxide on the adsorption mechanisms of organic MB dye and inorganic As(v) ions from aqueous solution. RSC Adv., 8(22): 12376-12389. doi: 10.1039/c8ra00270c.

Lingamdinne, L.P., Koduru, J.R. and Karri, R.R. 2019. A comprehensive review of applications of magnetic graphene oxide based nanocomposites for sustainable water purification. J. Environ. Manag., 231: 622-634. doi: 10.1016/j.jenvman.2018.10.063.

Loo, Y.Y., Chieng, B.W., Nishibuchi, M. and Radu, S. 2012. Synthesis of silver nanoparticles by using tea leaf extract from Camellia sinensis. Int. J. Nanomed., 7: 4263-4267. doi: 10.2147/IJN.S33344.

Lum, P.T., Foo, K.Y., Zakaria, N.A. and Palaniandy, P. 2020. Ash-based nanocomposites for photocatalytic degradation of textile dye pollutants: A review. Mater. Chem. Phys., 241: 2405. doi: 10.1016/j.matchemphys.2019.122405.

Mittal, H., Morajkar, P.P., Al Alili, A. and Alhassan, S.M. 2020. In-situ synthesis of ZnO nanoparticles using gum Arabic-based hydrogels as a self-template for effective malachite green dye adsorption. J. Polym. Environ., 28(6): 1637-1653. doi: 10.1007/s10924-020-01713-y.

Mohammad, A. and Hasabo A. 2012. Synthesis and characterization of neem chitosan nanocomposites for the development of antimicrobial cotton textiles. J. eng. Fab Fibers, 7: 161.

Mondal, P., Anweshan, A. and Purkait, M.K. 2020. Green synthesis and environmental application of iron-based nanomaterials and nanocomposite: A review. Chemosphere, 259: 127509.

Mubarakali, D., Gopinath, V., Rameshbabu, N. and Thajuddin, N. 2012. Synthesis and characterization of CdS nanoparticles using C-phycoerythrin from the marine Cyanobacteria. Materi. Lett., 74: 8-11. Doi: 10.1016/j.matlet.2012.01.026

Nadeem, N., Abbas, Q., Yaseen, M., Jilani, A., Zahid, M., Iqbal, J., Murtaza, A., Janczarek, M. and Jesionowski, T. 2021. Coal fly ash-based copper ferrite nanocomposites as potential heterogeneous photocatalysts for wastewater remediation. Appl. Surf. Sci., 565: 5421. Doi: 10.1016/j.apsusc.2021.150542

Naikoo, Gowhar A., Mujahid Mustaqeem, Israr U. Hassan, Tasbiha Awan, Fareeha Arshad, Hiba Salim, and Ahsanulhaq Qurashi. 2021. Bioinspired and Green Synthesis of Nanoparticles from Plant Extracts with Antiviral and Antimicrobial Properties: A Critical Review. Journal of Saudi Chemical Society, 25(9): 37-49.

Nazri, M.K.H.M. and Sapawe, N. 2020. A short review on green synthesis of iron metal nanoparticles via plant extracts. Mater. Today Proceed., 31: 48-53. doi: 10.1016/j.matpr.2020.10.968.

Panchal, P., Paul, D. R., Sharma, A., Choudhary, P., Meena, P. and Nehra, S. P. 2020. Biogenic mediated Ag/ZnO nanocomposites for photocatalytic and antibacterial activities towards disinfection of water. J. Coll. Interf. Sci., 563: 370-380. DOI: 10.1016/j.jcis.2019.12.079

Pandey, N., Shukla, S.K. and Singh, N.B. 2017. Water purification by polymer nanocomposites: An overview. Nanocomposites, 3(2): 47-66. doi: 10.1080/20550324.2017.1329983

Ragupathy, S. and Sathya, T. 2016. Synthesis and characterization of SnO2 loaded on groundnut shell activated carbon and photocatalytic activity on MB dye under sunlight radiation. J. Mater. Sci. Electr., 27(6): 5770-5778. doi: 10.1007/s10854-016-4491-8

Reguyal, F. and Sarmah, A.K. 2018. Site energy distribution analysis and influence of Fe3O4 nanoparticles on sulfamethoxazole sorption in aqueous solution by magnetic pine sawdust biochar. Environ. Pollut., 233: 510-519. doi: 10.1016/j.envpol.2017.09.076

Sabo-Attwood, T., Unrine, J.M., Stone, J.W., Murphy, C.J., Ghoshroy, S., Blom, D., Bertsch, P.M. and Newman, L.A. 2012. Uptake, distribution and toxicity of gold nanoparticles in tobacco (nicotiana Xanthi) seedlings. Nanotoxicology, 6(4): 353-360. doi: 10.3109/17435390.2011.579631

Sadiq, H., Sher, F., Sehar, S., Lima, E.C., Zhang, S., Iqbal, H.M.N., Zafar, F. and Nuhanović, M. 2021. Green synthesis of ZnO nanoparticles from Syzygium cumini Leaves extract with robust photocatalysis applications. J. Mol. Liq., 335: 116567. doi: 10.1016/j.molliq.2021.116567

Seifipour, R., Nozari, M. and Pishkar, L. 2020. Green synthesis of silver nanoparticles using Tragopogon collinus Leaf extract and study of their antibacterial effects. J. Inorg. Organomet. Polym. Mater., 30(8): 2926-2936. doi: 10.1007/s10904-020-01441-9

Shen, Z., Han, G., Liu, C., Wang, X. and Sun, R. 2016. Green synthesis of silver nanoparticles with bagasse for colorimetric detection of cysteine in serum samples. J. Alloys Comp., 686: 82-89. DOI: 10.1016/j.jallcom.2016.05.348

Sheng, G., Li, Y., Yang, X., Ren, X., Yang, S., Hu, J. and Wang, X. 2012. Efficient removal of arsenate by versatile magnetic graphene oxide composites. RSC Adv., 2(32): 12400-12407. DOI: 10.1039/c2ra21623j

Siddiqui, S., Ilahi, O.M., Mohd M. and Saif, A.C. 2019. Nigella sativa seed based Nanocomposite-MnO2/BC: An antibacterial material for photocatalytic degradation, and adsorptive removal of methylene blue from water. Environ. Res., 171: 328-340. DOI: 10.1016/j.envres.2018.11.044

Siddiqui, S.I. and Chaudhry, SA. 2017. Iron oxide and its modified forms as an adsorbent for arsenic removal: A comprehensive recent advancement. Process Safety and Environmental Protection, 111: 592-626. DOI: 10.1016/j.psep.2017.08.009

Silva Viana, R.L., Pereira Fidelis, G., Jane Campos Medeiros, M., Antonio Morgano, M., Gabriela Chagas Faustino Alves, M., Domingues Passero, L.F., Lima Pontes, D., Cordeiro Theodoro, R., Domingos Arantes, T., Araujo Sabry, D., Lanzi Sassaki, G., Fagundes Melo-Silveira, R. and Rocha, H.A.O. 2020. Green synthesis of antileishmanial and antifungal silver nanoparticles using corn cob xylan as a reducing and stabilizing agent. Biomolecules, 10(9): 1-21. DOI: 10.3390/biom10091235

Sinsinwar, S., Sarkar, M.K., Suriya, K.R., Nithyanand, P. and Vadivel, V. 2018. Use of agricultural waste (coconut shell) for the synthesis of silver nanoparticles and evaluation of their antibacterial activity against selected human pathogens. Microb. Pathogen., 124: 30-37. DOI: 10.1016/j.micpath.2018.08.025

Tomer, A.K., Rahi, T., Neelam, D.K. and Dadheech, Pawan K. 2019. Cyanobacterial extract-mediated synthesis of silver nanoparticles and their application in ammonia sensing. Int. Microbiol., 22(1): 49-58. DOI: 10.1007/s10123-018-0026-x

Umejuru, E. C., Prabakaran, E. and Pillay, K. (2020). Coal fly ash coated with carbon hybrid nanocomposite for remediation of cadmium (II) and photocatalytic application of the spent adsorbent for reuse. Results in Materials, 7:1-16. DOI: 10.1016/j.rinma.2020.100117

Uzair, B., Liaqat, A., Iqbal, H., Menaa, B., Razzaq, A., Thiripuranathar, G., Fatima Rana, N. F. and Menaa, F. 2020. Green and cost‑effective synthesis of metallic nanoparticles by algae: Safe methods for translational medicine. Bioengineering, 7(4): 1-22. DOI: 10.3390/bioengineering7040129

Vaibhav, V., Vijayalakshmi, U. and Roopan, S.M. 2015. Agricultural waste as a source for the production of silica nanoparticles. Spectrochim. Acta. Part A Mol. Biomol. Spectrosc., 139: 515-520. DOI: 10.1016/j.saa.2014.12.083

Visakh, P.M. and Thomas, S. 2010. Preparation of bionanomaterials and their polymer nanocomposites from waste and biomass. Waste Biomass Valor., 1(1): 121-134. DOI: 10.1007/s12649-010-9009-7

Younes, A.A., Abdulhady, Y.A.M., Shahat, N.S. and El-Din El-Dars, F.M.S. 2021. Removal of cadmium ions from wastewaters using corn cobs supporting nano-zero valent iron. Sep. Sci. Technol., 56(1): 1-13. DOI: 10.1080/01496395.2019.1708109

Yue, Y., Zhou, Y., Xing, F., Gong, G., Hu, B. and Guo, M. 2020. An industrial applicable method to improve the properties of recycled aggregate concrete by incorporating nano-silica and micro-CaCO$_3$. J. Clean. Prod., 259: 1209. DOI: 10.1016/j.jclepro.2020.120920

Analysis of Laboratory Experimental Tests on Mixed Oil Disposal (Bilge) from Ships Based on Marpol Annex I: A Case Study of Port of Tanjung Mas Semarang and Port of Tegal

S. Awel†* and A. R. Fuad*

*Port and Shipping Management Program, Merchane Marine Polytechnic of Semarang, Central Java,
Jl. Singosari No. 2A, Wonodri, Semarang Sel, Semarang City, Central Java 50242, Indonesia
**Engine Department Program, Merchane Marine Polytechnic of Semarang, Central Java, Jl. Singosari No. 2A,
Wonodri, Semarang Sel, Semarang City, Central Java 50242, Indonesia
†Corresponding author: S. Awel; info@pip-semarang.ac.id

ABSTRACT

Management of marine pollution is a difficult condition to realize, especially the pollution of mixed oil disposal (bilge) resulting from the operation of ships. The oil component has different characteristics compared to the essence of other substances; namely, oil can float on the surface of the water because it has an extra weight the type/density of the essence. The parameters tested in this research are oil/fat content parameters and their extraction according to National Certification Institution 6989.59:2008. Bilge water samples were taken from five commercial ships that leaned on the port and then carried out pre-treatment and post-treatment tests with the liquid separation process in the Oil Water Separator (OWS) device on the ship and then tested in the laboratory to determine the infrared spectrum in the absorption of oil content emissions in water samples, which may not exceed the standard threshold for port water quality, i.e., 5 mg.L^{-1}. The sampling tests were carried out for the variables temperature, pH, Total Dissolved Solid (TDS), and oil content obtained values were below the threshold for water quality. To find out the relationship between Group I and Group II, linear regression was used showing the Ho result in reject (0.000<0.05), which means there is a significant relationship between Group I and II.

INTRODUCTION

Indonesia has potential fisheries and transportation resources that are quite promising and can even increase the activities in the port area of fishing vessels and commercial vessels operating at sea. The port is a strategic place for the coastal area, and there are ecological boundaries between the farthest limits from the sea to the land (Puryono et al. 2019). Ports play a crucial role in supporting a country's economic growth, facilitating transportation, and promoting tourism. However, the activities in these waters will undoubtedly have negative impacts. For example, the pollution of the sea, which is interpreted by the presence of waste/dirt from the activities of living things above the waters, was introduced into the marine environment intentionally or unintentionally. These pollutants can change the quality of the water, thus affecting marine ecosystems. Fishing activity with the use of fish traps damages the ecosystem and contributes to the destabilization of maritime climate patterns. Ship collisions pose a risk of oil or cargo spills, which can have devastating consequences for

aquatic ecosystems. The pollution caused by waste disposal from ships and the emissions from auxiliary engines and ship propulsion engines further contributes to the degradation of marine environments (State Minister of the Environment 2010).

Furthermore, contamination from oil and liquid waste resulting from ship engine operations is another pollution source affecting marine ecosystems. These various forms of pollution highlight the negative impacts of port activities on the marine environment. Government Regulation of the Republic of Indonesia No.21 in 2021 concerning Pollution Control and or Maritime Environmental Protection explains that preventing pollution from ships is an effort that the captain and crew must make of the ship as early as possible to avoid or reduce pollution from oil spills, toxic liquid materials, dangerous cargo, sewage, garbage, and exhaust gases from ships into the waters and air.

Oil spills/discharges from ships or disposal of engine room wastewater without proper treatment/procedures is one

of the sources of oil pollution at sea (Kuncorowati 2018). Even though the intensity of the oil content discharged into the sea is not too large, it is carried out continuously by the operator-ship operators so that it impacts maritime environmental pollution, which disrupts the life of marine ecosystems. Regulation of the Minister of Transportation No. 4 in 2004 concerning preventing pollution from ships limits pollution from ships by requiring each vessel to have a procedure for disposing of waste in the form of liquid or solid originating from ships with criteria based on tonnage. For example, ships with a cargo of 100 GT to 339 GT or having the main propulsion of at least 200 PK must have an Oil Water Separator (OWS) (Ministry of Environment Government of the Republic of Indonesia 2021) Tegal. It has a function to treat water mixed with oil (bilge) from liquid waste disposal from ships before being discharged into the sea not exceeding the required content, i.e., 15 ppm.

The bustling port of Semarang, located in Central Java, experiences a high volume of loading and unloading activities. It has witnessed a rapid increase in traffic, with a diverse and substantial number of tugboat ships. As a result, the port of Semarang has become a preferred choice for many individuals seeking reliable and efficient sea transportation services (Hanjani 2004). Table 1 shows the general conditions of Tugboat ships at Port of Tanjung.

The second research focuses on the Port of Tegal, situated in the northern coastal area of Central Java. This region, which includes the areas of Brebes, Slawi, Tegal, and Pemalang (Bergasmalang), is experiencing significant growth. The Port of Tegal serves as a crucial stopover for ships traveling from various parts of the archipelago or abroad en route to the ports of Semarang or Cirebon (State Gazette of the Central Java Provincial Government 2014). The researchers are motivated to explore the bilge water content on board vessels that rely on these ports. They aim to analyze the bilge water content before it undergoes processing using Oil Water Separators (OWS). After OWS treatment, laboratory testing and analytical methods will be employed to assess the oil/fat content in the bilge water.

Table 1: General conditions of Tugboat ships at Port of Tanjung Emas, Semarang.

Description	Tugboat Ship
Gross Weight (DWt)	< 10.000
Total Length (Loa)-(m)	120-142
Width (B)-(m)	20-22.43
Full Draft (m)	7.00-8.00
Length requirements standard	160-187
Container capacity (TEUs)	300

Source: Christino (2019)

The research data will be supported by variables such as pH, salinity, temperature, and other relevant factors. Considering these variables, the research findings will represent the actual conditions in the ports of Semarang and Tegal.

MATERIALS AND METHODS

This research is quantitative with a correlational method using statistical methods to measure the effect of different variables (Creswell 2014). The research was conducted in 2 ports, namely KSOP IV Tegal and Port of Tanjung Mas Semarang, with a total sample of 5 ships, they are the Semar Sebelas 88 ship, Tugboat Irving, Tugboat Roswin, Tugboat Bima 306, and Tugboat Jaya Negara 305 with taking sample on each ship, two treatments before and after processing using OWS, then it will be tested to determine the correlation between the pre-treatment and OWS pre-treatment variables. The sample is adjusted to the Indonesian National Standard SNI 6989.59:2008 concerning water and waste sampling (This study is included in the Laboratory Experimental category because the pre-test and post-test testing of 2 control groups have different treatments (Kuntjojo 2009) with the type of experimental research intact-Group Comparison Design, i.e., the study is divided into two groups, the control group is not given treatment, and the experimental group given the treatment (Setyanto 2005).

Research Stages

The research consisted of the preparatory stage in determining the ship sample according to the provisions of the ship size (tonnage), having an oil-containing water settling tank (bilge), and having a means of protection against oil (OWS). The second stage was to take two bilge samples from each ship before and after entering OWS; the third stage was testing with additional variables, i.e., pH, temperature, and TDS, using a pH and TDS meter. Then the samples were put into an ice box to be preserved naturally and then tested for oil/fat content in the laboratory using an FTIR (Fourier Transform Infrared Spectroscopy) instrument to determine the infrared emission spectrum of a simple substance in water containing oil. Then, the results of the data were analyzed and tested for the hypothesis using the SPSS application with the stages of analyzing descriptive data, validity, and reliability to find out the data was normally distributed. The F test was to see the suitability of the analysis model, and the regression test was to determine the effect between groups.

RESULTS AND DISCUSSION

The variable tests on ship samples are adjusted to research needs which aim to find the pre-post treatment samples

using a means of protection against oil-containing water on board; the variables tested are total dissolved solids (TDS), liquid temperature, water acidity (pH) and oil content. The main function of an OWS (Oil Water Separator) system is to separate two liquids with different viscosities, such as water and oil. These liquids have distinct specific gravities, with oil typically having a specific gravity of 1 mg.L^{-1} and viscosity of 0.89 cst. The difference in specific gravity prevents oil and water from being dissolved or mixed together. In the OWS, the oil will be filtered and separated by the coalescer filter so that the oil sticks to the filter and cleans the water. Before water is discharged into the sea, it goes through an oil content detection sensor connected to a monitor, commonly known as an oily discharge monitoring system. This sensor can detect oil content in the water, ensuring it is below the acceptable limit of 15 ppm. The water mixed with oil whose content is detected to be less than 15 ppm automatically flows and is wasted overboard, while liquids that did not meet the requirements because they were more than 15 ppm are returned to the OWS tank for further separation (Nwokedi 2020). The sampling from commercial vessels at Semarang and Tegal ports met the ship's criteria, particularly as shown in Table 2.

After direct conducting and laboratory testing according to the testing variables, the data were obtained as shown in Table 3.

pH (Degrees of Acidity)

pH is the negative logarithm of the concentration of hydrogen ions released in a liquid and is an indicator of the good and bad of water (Hamuna 2018). Because pH is essential for aquatic ecosystems, the biota can develop well when influenced by a standard pH value so that increased productivity, such as plankton, phytoplankton, and other biotas, because the availability of nutrients in the waters is sufficient (Megawati et al. 2014) based on the Decree of the Minister of the Environment No. 51 in 2004, the normal pH of seawater ranges from 6.5-8.5, so the results of pH measurements both in group I and group II were still within normal limits, at least 7.2°C I, it is the Bima 306 ship and the highest in group II, 7.1°C, it is the Semar Eleven 88, Irving and Jaya Negara 305 ships.

Water Temperature

Water temperature influences aquatic organisms' metabolism in waters and the distribution of water (Nontji 2005); temperature also affects the growth and life of biota and plays a role in controlling ecosystem conditions. On the surface also affects physical, biological, and chemical processes in sea waters (Kusumaningtyas et al. 2014). Nontji (2005) states that waters have average surface temperatures ranging from 28-31°C. The temperature measurements of ship samples in

Table 2: The particulars of sample vessels from Semarang Port and Tegal Port.

Name of Ship	Years of build	Gross Tonnage (GT)	Type OWS	Hours of power	Position of ship's
TB Bima 306	2009	294	PROTO HRS	-	Semarang
Jaya Negara 305	2018	350	PROTO HRS	-	Semarang
TB. Irving	2010	217	CYF-0,25	Mitsubishi 2 x 823 HP	Tegal
Semar Sebelas 88	2006	231	CYF-0,25	Yanmar 2 x 829 HP	Tegal
Roswin	2017	2230	CYF-J1 Electrical Controller	Yanmar 2 x 837 HP	Tegal

Source: Data Analysis in 2021.

Table 3: The Results of measurement and analysis of oil-containing vessel water (Bilge)

Name of Ship	pH water sample		Water temperature sample		TDS water sample		Oil/Fat Content	
	Grp. I	Grp. II	Grp. I	Grp. II	Grp. I	Grp. II	Grp. I	Grp. II
Semar Sebelas 88	7.5	7.1	27	28	32.5	14.5	4.515	25.27
TB Irving	7.8	7.1	27.6	28	48.5	27.3	71.84	52.27
TB Roswin	7.6	7	28	29	48.7	30.0	3.436	46.01
TB Bima 306	7.2	7	26.8	28	36.2	22.6	4.687	41.65
TB Jaya Negara 305	7.4	7.1	27	28	36.7	23.3	7.196	52.00

- According to KM for Environment No. 51 in 2004 concerning quality standards for variable seawater, the maximum oil/fat content is 5 mg.L^{-1}.
- Natural temperature variable
- The pH variable is 6.5-8.5
- TDS is 80
- Group I before being processed by OWS and Group II after being processed by OWS

Table 4: Results of SPSS regression.

Model	Sum of Squares	Df	Mean Square	F	Sig.
1 Regression	1133.393	1	1133.393	65.841	0.000[a]
Residual	309.852	18	17.214		
Total	1443.245	19			

a. Predictors: (Constant), Kelompok_1
b. Dependant Variable: Kelompok_2
Data Analysis: 2021

group I and group II are still within normal limits, at least 27°C in group I, the Semar Eleven 88 and Jaya Negara 305 ships, and the highest in group II, which is 29°C in Roswin ship.

TDS (Total Dissolved Solids)

TDS has dissolved solids in a liquid, showing that the liquid contains salinity/saltwater content because TDS is related to salinity (Nurrohim 2012). From the data, it was found that the highest TDS content was in Group I on the TB Roswin ship, and the lowest TDS content was in Group I on the Semar March 88 ship. In group II, the highest TDS was on TB Roswin. The lowest TDS was on the Sebelas Maret 88 ship. However, it can be concluded that the TDS content in Group I and Group II had significant changes resulting in a decrease after going through the separation process at OWS.

Oil Content

Oil has different characteristics from other liquid contents (Hardian 2014); oil content can form a thin layer and float on the surface of the water. In Marine Pollution 1978 (MARPOL 73/78), in annex I, it is explained that every ship that has a GT of more than 100 GT or has a minimum propulsion power of 200 HP must have a means of protection against oil/fat content because oil pollution from ships is quite dangerous for marine ecosystems. The oil/ fat content in group I and group II experienced significant differences in testing using FTIR/Fourier Transform Infrared Spectroscopy which was tested at the Center for Industrial Pollution Prevention Technology (BBTPPI) Semarang. FTIR is a laboratory testing process to find out the infrared spectrum in absorbing the emission of a substance. Its function is to detect liquid functional group compounds and analyze the mixture in the sample being analyzed, both qualitatively and quantitatively identified, so that the valid value is known in the sample.

Regression Data Analysis

Regression analysis aims to determine whether there is a binding relationship between Group I (before processing at OWS) and Group II (after processing at OWS). Regression test by comparing data on temperature, pH, TDS, and oil content in group I to group II there is an effect.

Significant research data (0.000 <0.05) means Ho is rejected (Table 4). In other words, Group I and Group II have a significant effect. From this data, it was stated that after processing at OWS, there were significant differences in data between Group I and Group II.

Significant research data (0.000 <0.05) means Ho is rejected in both Group I and Group II. The data suggests there were significant differences in data between Group I and Group II after undergoing processing in the OWS system.

CONCLUSION

A sample of water was taken from two out of five vessels for analysis. The first sample was collected before being processed by an Oily Water Separator (OWS), while the second sample was taken after being processed by an OWS, as guided by the Minister of Transportation Regulation No. 4 of 2005. According to this regulation, oil ships ranging from 100 to 149 GT and other non-oil ships between 100 and 339 GT, equipped with a 200 PK or main engine, must have oil protection devices installed. Unfortunately, not all ships in Indonesia are adhering to these regulations properly. Many motorized sailing ships, for instance, do not have OWS installed. Additionally, several commercial ships have OWS, but their crew fails to process bilge liquid according to the required conditions.

The sampling test results showed that the variables Temperature, pH, Total Dissolved Solids (TDS), and oil content obtained values below the threshold for water quality standards set by the Decree of the Minister of Environment No. 51 in 2004, which defines water quality standards. After the hypothesis testing, there was a significant and intertwined relationship between the variables, as the Ho results were rejected because the value reached 0.000.

REFERENCES

Christino, Boyke S.P. 2019. Port And Terminal Planning. Department of Marine Transportation Engineering, Faculty of Marine Technology, Sepuluh Nopember Institute of Technology, Surabaya.

Creswell, J.W. 2014. Qualitative, Quantitative and Mixed Approach. Government Regulation of the Republic of Indonesia no. 21 of 2021, Concerning the Protection of the Maritime Environment. Pustaka Pelajar, Yogyakarta.

Hamuna, B. 2018. Study of seawater quality and pollution index based on physical-chemical parameters in the waters of the Depapre District, Jayapura. J. Environ. Sci., 16(1): 35-43

Hanjani, M. 2004. Analysis of operational performance unloading containers at Tanjung Emas Port, Semarang. J. Transport., 4:1-12.

Hardian, S. 2014. Development of Methods for Analysis of Fat Oil Parameters in Water Samples: Development on Oil and Grease Analysis in Water Sample. BBTPPI, Semarang.

Kuncorowati, S. 2018, The importance of understanding crews regarding annex I Marpol 73/78 and oil pollution prevention exercises on overcoming oil pollution from ships. J. Maritime Sci., 16: 15-46.

Kuntjojo. P. 2009. Research Methodology. Nusantara University PGRI Kediri, Kediri.

Kusumaningtyas, M.A., Bramawanto, R., Daulat, A. and Pranowo, W.S. 2014. Quality of Natuna waters in the transition season. Depik. 3(1): 10-20.

Marine Pollution 1978. International Convention for the Prevention of Pollution from Ships.

Megawati, C., Yusuf, M. and Maslukah, L. 2014. Distribution of water quality in terms of nutrients, dissolved oxygen, and pH in the southern waters of Southern Bali. J. Oceanogr., 3(2): 142-150.

Ministry of Environment Government of the Republic of Indonesia 2021. Concerning prevention of pollution from the sea.

National Certification Institution 2008. Concerning Water and Wastewater: Wastewater Sampling Methods. National Standardization Agency, Jakarta.

Nurrohim, A. 2012. Study of seawater intrusion in the coastal area of Rembang sub-district, Rembang district. Geo-image, Vol. 1: 2012.

Nwokedi, T. C. 2020. Dominant constraints to the effective use of oily-water separator (OWS) in the control of ship-based oil pollution in West African water. Maritime Technol. Res., 4(2): 253937.

Puryono, S., Anggoro, S. and Suryanti, A.I. 2019. Ecosystem-Based Coastal and Ocean Management. Diponegoro University Publishing Agency, Semarang.

Setyanto, A.E. 2005. Reintroducing experimental methods in communication studies. J. Commun. Stud., 3(1): 37-48.

State Gazette of the Central Java Provincial Government 2014. Concerning Increasing the Effectiveness Of Ports In Central Java.

State Minister of the Environment 2010. Regulation of the State Minister of the Environment No. 19 of 2010 concerning Wastewater Quality Standards for Oil and Gas and Geothermal Business and/or Activities. State Secretariat, Jakarta.

Original Research Paper

Open Access Journal

Sustainable Alternative Materials to Concrete Masonry Partition Walls: Light-Weight Wall Panel Using Polymethyl Methacrylate (PMMA) and Shredded Waste Metalized Film Packaging

R. C. G. Prado*† and T. A. Amatosa Jr.**

*Graduate School, Polytechnic University of the Philippines, Sta. Mesa Manila 1016, Philippines
**College of Engineering and Architecture, Northwest Samar State University, Calbayog 6710, Philippines
†Corresponding author: R. C. G. Prado; rcgprado@rtu.edu.ph

ABSTRACT

The amount of plastic waste produced yearly is significantly increasing. Approximately 300-400 million metric tons of plastic waste are produced yearly. One of the dominant plastic wastes is a metalized film, a shiny, non-homogeneous polymer used in packaging that is considered the least recycled. Meanwhile, partition walls in buildings are traditionally made of concrete masonry, one of the most utilized materials in the construction industry globally, consumed yearly by about 11 billion metric tons. Because of the excessive use of concrete, the necessary raw materials are undeniably depleting, therefore demanding some alternatives. Polymethyl methacrylate (PMMA) is one option that can be utilized as an alternative because of its remarkable characteristics better than that of the traditional. This paper proposed the utilization of PMMA in fabricating the hollow panel filled with shredded waste metalized film packaging resulting in the lightweight wall panel being used as an alternative to concrete masonry for constructing partition walls. After the experiment, PMMA produced compressive strength of 75.30-84.30MPa, a tensile strength of 52.00-59.10MPa, a flexural strength of 102.00-107.00MPa, and water absorption of 0.80-0.90%. Also, shredded waste metalized films add aesthetic to the panel and are complemented by the remarkable transparency of PMMA. In conclusion, using this lightweight wall panel instead of traditional concrete masonry partition walls will reduce plastic waste in landfills and the raw materials necessary to produce concrete.

INTRODUCTION

The high demand for better plastic packaging led to the invention of Metallized film, a non-homogeneous plastic with a thin layer of metals (Alyousef et al. 2022), usually aluminum metals that give the packaging a shiny and metallic appearance with a lighter weight and cheaper cost, but with excellent moisture and oxygen barring properties (Flexpack Mag 2020). However, metalized film packaging is considered single-use plastic that contributes to the accumulation of plastic waste in our landfills, resulting in harmful environmental effects (Bhogayata & Arora 2019). Approximately 300-400 million metric tons of plastic waste are produced every year (UNEP 2018, EAPM 2018, Payne et al. 2019, Awoyera & Adesina 2020, Alhazmi et al. 2021, Silva et al. 2021, Lamba et al. 2021). In fact, in 2018, a study conducted by United Nations Environment Programme (UNEP) highlighted that 50% of the total weight of plastic waste on our planet comes from plastic packaging, and 32% of this packaging is expected to enter the environment. Around

8 million tons from this percentage go straight into the ocean (Guillard et al. 2018). Meanwhile, one of the considered significant contributors to the fast-growing economy of one country is the construction industry. According to a recent study, it is estimated to become the third-largest industry in the world by 2025 (Durgalakshmi & Janani 2019). Concrete, for instance, the traditional construction material utilized to build any infrastructure (Goyal & Kumar 2018), particularly in partition walls, requires cement consumed every year of about 4.1 billion metric tons (Garside 2023). Because of the excessive use, the chances for the depletion of the necessary raw materials over time is undeniably inevitable, therefore demanding some alternatives. Polymethyl methacrylate (PMMA) or simply acrylic is one option that can be utilized as an alternative because of its remarkable characteristics better than traditional ones, such as outstanding clarity, glass-like transparency, high scratch resistance (Shen et al. 2020), high mechanical strength (Sivanathan et al. 2020), shatter resistance (Shaari et al. 2021), durability and low

cost (Leão et al. 2019) and is generally available in the form of particles, sheets, pipes, tubes and rods (Lianghua 2021).

This paper has three objectives. The first is to use shredded waste metalized film packaging and PMMA sheets to construct partition walls as alternative materials to concrete masonry. This will reduce the volume of the accumulating plastic wastes in our landfills and will eliminate the painting works in constructing partition walls due to the outstanding clarity of PMMA complemented by the aesthetic appearance of shredded waste metalized film packaging. The second is to determine which, among 3mm, 10mm, and 18mm PMMA sheets, is the best for compressive strength, tensile strength, flexural strength, and water absorption. Thirdly and lastly, eliminate the utilization of any concrete masonry materials in constructing partition walls. This results in conserving raw materials necessary for producing concrete and reducing the carbon dioxide emitted into the atmosphere due to cement production. Unlike the previous research studies, the shredded waste metalized film in this research will not be incorporated into the concrete as an alternative reinforcement to steel bars nor as a partial replacement for cement, sand, or gravel. The shredded waste metalized film, once deposited to the wall panel made of PMMA, will significantly increase the aesthetic appearance of the wall because of the outstanding clarity and illuminance of PMMA that will eliminate the necessary painting works. Also, because of the expected high mechanical properties of PMMA, the wall panel is suitable as an alternative construction material in constructing partition walls.

Research Significance

The result of this study will be of value to the community first because this paper will participate in eliminating some harmful factors risking the community's health by reducing the accumulating plastic waste in landfills and dumpsites. Second, the government will help them to appropriately take action in dealing with the problems brought by the accumulating plastic wastes in landfills and dumpsites, causing detrimental effects on the environment third to the environment, because this study will further promote the protection, conservation, and rehabilitation of the environment towards sustainable development. Lastly, to future researchers, this paper will serve as a guide in conducting further studies to increase understanding of sustainable practices and may be a source of related literature.

MATERIALS AND METHODS

To achieve the desired product, two primary materials are required. First is waste metalized film packaging. This material will be collected from litter, landfills, and dumpsites. First, clean the collected waste metalized film packaging to remove
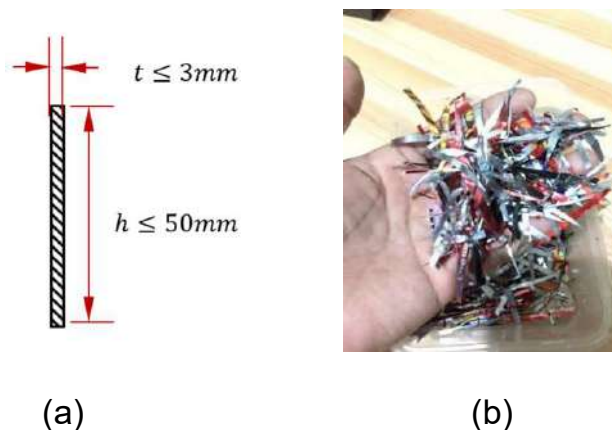

(a) (b)

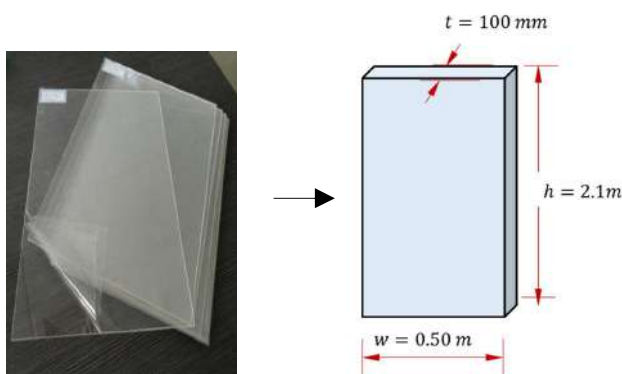Fig. 1: Dimensions for the waste metalized film packaging strips.

Fig. 2: Cut PMMA sheets (left) to hollow parallelepiped-liked wall panel (right).

all foreign materials. Next, dry the waste metalized film packaging and cut it into small and thin strips with thickness and height not exceeding 3mm and 50mm, respectively. Refer to Fig. 1 (a) and (b). The second primary material is 4ft x 8ft PMMA sheets with thicknesses varying from 3mm, 10mm, to 18mm. The good news is that woodworking tools can also be used to cut PMMA sheets (The Plastic People 2021) into panels having the dimensions shown in Fig. 2. Assemble the cut sheets using a screw and solvent to bond one another to create the hollow parallelepiped-like panels.

Research Design

Fig. 3 shows the process followed during the research work. It shows the steps followed starting with bringing the specimen samples to the testing center to developing of PMMA sheets hollow parallelepiped light-weight wall panel.

PMMA Specimen Details

Specimen samples have the following dimensions conforming to ASTM standards. 13mm × 50mm × t for compression test
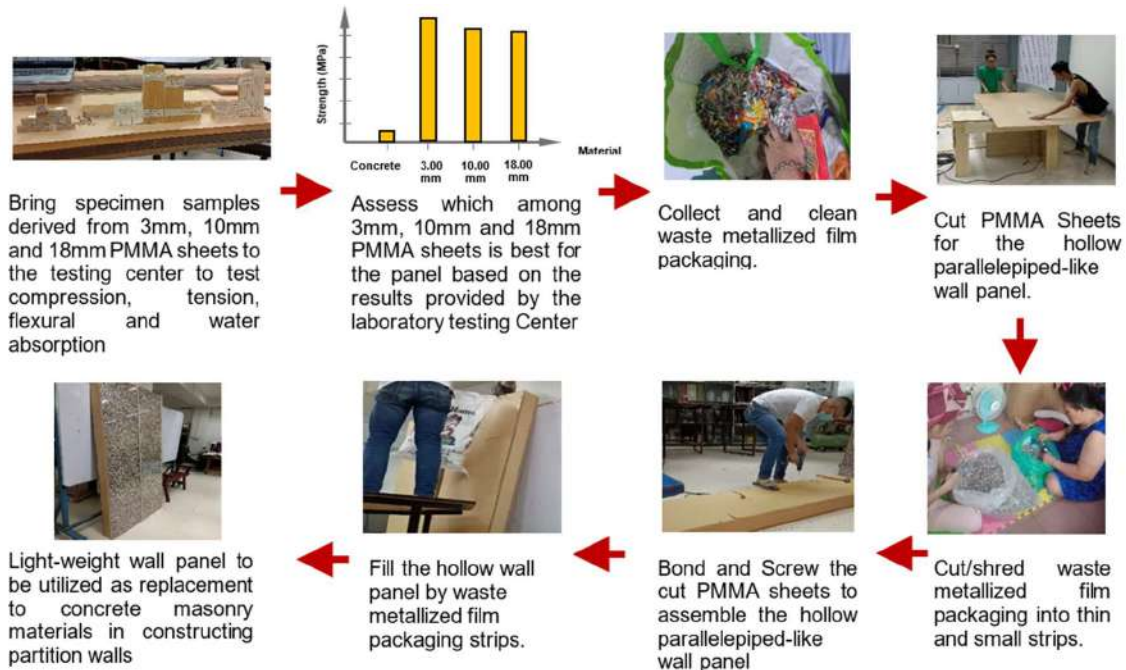
Fig. 3: Distribution flow of PMMA sheets hollow parallelepiped light-weight wall panel.

(ASTM D695) where "t" denotes the thickness of 3 PMMA variables: the 3mm, 10mm, and 18mm. 13mm × 150mm × t for tension test (ASTM D638), 13mm × 125mm × t for flexural strength (ASTM D790), and 25mm × 50mm × t for water absorption test (ASTM D570). All specimen samples are sent to the Standards and Testing Division (STD) under the Department of Science and Technology (DOST) and waited 20 working days for the results.

RESULTS AND DISCUSSION

Compressive Strength Comparison

A typical concrete masonry's compressive strength ranges

from 20 to 50 MPa (Bošnjak et al. 2019, AlQudah & Freewan 2020). Unfortunately, no data was gathered relative to the 3mm PMMA sheet due to its minimal thickness the UTM cannot support, whereas the compressive strength of 10mm and 18mm PMMA is 75.30 MPa and 84.30 MPa, respectively, based on the results provided by the testing center. Note that the higher the compressive strength, the better. Therefore, the two variables' compressive strength is higher than traditional concrete masonry. Refer to the data shown in Table 1.

Tensile Strength Comparison

The tensile strength of a typical concrete masonry ranges

Table 1: Mechanical properties comparison among 3mm, 10mm, 18mm PMMA, and typical concrete masonry.

Materials PMMA		Compressive Strength [MPa]	Tensile Strength [MPa]	Flexural Strength [MPa]	Water Absorption [%]	Observation
Thickness	3mm	-	59.10	107.00	0.205	No discoloration of the deformity was observed in all the tested specimens after the 24h immersion test
	10mm	75.30	53.70	102.00	0.188	No discoloration of the deformity was observed in all the tested specimens after the 24h immersion test.
	18mm	84.30	52.00	102.00	0.090	No discoloration of the deformity was observed in all the tested specimens after the 24h immersion test.
Concrete Masonry		20-50	2-5	2-5	0.80-0.90	Note: Values are obtained based on the study conducted by Bošnjak et al. (2019), AlQudah and Freewan (2020), Onyeka (2019), and the recommendations given by NSCP in 2015.

only from 2 to 5 MPa (AlQudah & Freewan 2020), whereas the tensile strength of 3mm, 10mm, and 18mm PMMA are 59.10 MPa, 53.70 MPa, and 52.00 MPa, respectively, based on the results provided by the testing center. Adapting the principles of Mechanics, note that the higher the tensile strength, the better. Therefore, by analyzing the data, it is noticeable that the tensile strength of PMMA decreases as the thickness increases; however, the values of the three variables are still way higher than that of concrete masonry. Refer to the data shown in Table 1.

Flexural Strength Comparison

Like the tensile strength, the flexural strength of typical concrete masonry ranges from 2 to 5 MPa (AlQudah & Freewan 2020). On the other hand, the flexural strength of 3mm, 10mm, and 18mm PMMA are 107 MPa, 102 MPa, and 102 MPa, respectively, based on the results provided by the testing center. By adopting the principles of Mechanics again, note that the higher the flexural strength, the better. Therefore, by analyzing the data, the flexural strength of PMMA decreases as the thickness increases. However, just like the tensile strength, the values of the three variables are still way higher than that of concrete masonry. Refer to the data shown in Table 1.

Water Absorption Comparison

The water absorption of a typical concrete masonry ranges from 0.80% to 0.90% (Onyeka 2019), whereas that of 3mm, 10mm, and 18mm PMMA are 0.205%, 0.188%, and 0.09%, respectively, based on the results provided by the testing center. Note that the lower the water absorption, the better. Therefore, by analyzing the data, 18mm has the best property in terms of water absorption. Refer to the data shown in Table 1.

CONCLUSION

Based on the presented results, the mechanical properties of all 3 PMMA variables (3.00mm, 10.00mm, and 18.00mm) are far better than that of the concrete masonry. However, considering the bending characteristic, a 3mm PMMA sheet cannot be suggested because of its small thickness resulting in significant sagging. Also, an 18mm PMMA sheet cannot be suggested considering it is the most expensive among the 3 PMMA variables. Therefore, the most recommended is a 10mm PMMA sheet. Since half of the needed materials to manufacture this panel comes from waste metalized film packaging, the volume of waste plastics accumulating in landfills and dumpsites will be reduced. Also, since no cement will be utilized during the entire construction of partition walls, less carbon dioxide will be emitted into the

atmosphere. Painting works for partition walls will also be eliminated because of the aesthetically pleasing appearance of the metalized film strips complemented by the outstanding clarity and illuminance of PMMA. Other miscellaneous concluded benefits of the proposed sustainable construction material are the following; (1) electricity consumption for lighting will be minimized (2) The panel is long-lasting and requires lesser maintenance (3) Because the wall panel is light-weight, dead loads being carried by the beams or floor systems coming from partition walls will be lessened, thus resulting to fewer reinforcements and concrete volume from the supporting elements (4) Since the proposed material is a ready-made light-weight panel, the duration for the construction of partition walls will be faster compared to that when using traditional concrete masonry materials (5) Huge amount of money will be saved from the entire construction cost.

Recommendation for Future Studies

It is evident that using fabricated lightweight wall panels using polymethyl methacrylate as waste metalized film strips receptacle is a sustainable replacement to concrete masonry materials. However, there are some points that the researcher/s figured out, upon executing the experiments, that require improvements which are no anymore entertained due to the lack of time, resources, and budget, thus, included in this part as recommendations to the future researchers. (1) The design width of the panel, which is 500mm, can be increased up to 1 meter since the panel has sufficient compression, tensile and flexural strength. It will also reduce units to be installed during the construction of partition walls, expediting the installation process. (2) The researcher/s also used PMMA material for the edges of the panel, which was later on figured out not advised because the physical attributes of PMMA, such as its outstanding clarity and illuminance, will just get wasted since the edges of the panel are purposely used to bond it to the ceiling, floor, and other panels. Therefore, the researcher recommends using other construction materials, such as metal, aluminum, or other polymers, for the edges of the panel. (3) The waste metalized film strips with the designed dimensions not greater than 3mm and 50mm for thickness and height are not recommended because strips with varying thickness and height compromise the panel's aesthetic. The strips' dimensions must be uniform; thus, the recommended thickness and height of the strips must be strictly equal to 3mm and 50mm, respectively. The values, therefore, that are less (or greater) than the said dimensions are not advised. (4) Because the researcher did not focus on the bonding methodology of the panel to the ceiling or flooring, this particular area can be recommended to future researchers. (5) the researcher recommends that future

researchers study the sagging attributes of PMMA with the thickness varying from 5mm to 9mm for a better alternative to 10mm thick in terms of economical cost.

ACKNOWLEDGEMENT

REFERENCES

Alhazmi, H., Almansour, F.H. and Aldhafeeri, Z. 2021. Plastic waste management: a review of existing life cycle assessment studies. Sustainability, 13(10): 5340. DOI: 10.3390/su13105340

AlQudah, R. and Freewan, A. 2020. Acrylic panels are applications as building materials and daylighting devices. J. Daylight., 7(2): 258-272. DOI: 10.15627/jd.2020.22

Alyousef, R., Mohammadhosseini, H., Ebid, A.A.K., Alabduljabbar, H., Ngian, S.P. and Mohamed, A.M. 2022. Durability enhancement of sustainable concrete composites comprising waste metalized film food packaging fibers and palm oil fuel ash. Sustainability, 14(9): 5253. DOI.org/10.3390/su14095253

Awoyera P.O. and Adesina A. 2020. Plastic wastes to construction products: Status, limitations and future perspective - Case studies in construction materials. Sustainability, 12: 330. DOI.org/10.1016/j.cscm.2020.e00330

Bhogayata, A.C. and Arora, N.K. 2019. Utilization of metalized plastic waste of food packaging articles in geopolymer concrete. J. Mater. Cycl. Waste Manag., 21(1526): 1014-1026. DOI:10.1007/s10163-019-00859-9

Bošnjak, J., Sharma, A. and Grauf, K. 2019. Mechanical properties of concrete with steel and polypropylene fibres at elevated temperatures. Fibers, 7(2): 1-13. DOI: 10.3390/fib7020009

Durgalakshmi, S. and Janani, R. 2019. Energy efficient/green buildings and their related issues: A literature review. J. Architect. Technol., 11(2): 474

Europe Association of Plastics Manufacturers (EAPM). 2018. Plastics: The Facts 2018: An Analysis of European plastics production, demand, and waste data. Retrieved from https://plasticseurope.org/wp-content/uploads/2021/10/2018-Plastics-the-facts.pdf

Flexpack Mag. 2020. Metallized Flexible Plastic Packaging Shows Strength. Retrieved from https://www.flexpackmag.com/articles/90404-metallized-flexible-plastic-packaging-shows-strength

Garside, M. 2023. Cement Production Worldwide from 1995 to 2022. Retrieved from https://www.statista.com/statistics/1087115/global-cement-production-volume/

Goyal, M. and Kumar, H. 2018. Green concrete: a literature review. Int. J. Eng. Res. Technol., 6(11): 1-3.

Guillard, V., Gaucel, S., Fornaciari, C., Angellier-Coussy, H., Buche P. and Gontard, N. 2018. The next generation of sustainable food packaging to preserve our environment in a circular economy context. Front. Nutr., 5: 1-13. DOI: 10.3389/fnut.2018.00121

Lamba, P., Kaur, D.P., Raj, S. and Sorout, J. 2021. Recycling/reuse of plastic waste as construction material for sustainable development: A review. Environ. Sci. Pollut. Res., 8: 1-24. DOI: 10.1007/s11356-021-16980-y

Leão, R.S., Moraes, S.L.D., Gomes, J.M.L., Lemos, C.A.A., Casado, B.G.S., Vasconcelos, B.C.E. and Pellizzer, E.P. 2019. Influence of addition of zirconia on PMMA: A systematic review. Mater. Sci. Eng., 106: 2092. DOI: 10.1016/j.msec.2019.110292

Lianghua, Z. 2021. Acrylic board wall. Retrieved from https://worldwide.espacenet.com/patent/search/family/079162383/publication/CN214995200U?

Onyeka, F.C. 2019. Effect of partial replacement of coarse aggregate by crushed broken glass on properties of concrete. Int. J. Civ. Eng. Technol., 10(10): 356-367.

Payne, J., McKeown, P. and Jones, M. 2019. A circular economy approach to plastic waste. Polym. Degrad. Stab., 165: 170-181. DOI: 10.1016/j.polymdegradstab.2019.05.014

Shaari, H.A.H., Ramli, M.M., Mohtar, M.N., Rahman, N.A. and Ahmad, A. 2021. Synthesis and conductivity studies of poly(methyl methacrylate) (PMMA) by co-polymerization and blending with polyaniline (PANi). Polymers, 13(12): 1-27. DOI: 10.3390/polym13121939

Shen, J., Liang, J., Lin, X., Lin, H. Yu, J. and Yang, Z. 2020. Recent progress in polymer-based building materials. Int. J. Polym. Sci., 6: 1-15. DOI:10.1155/2020/8838160

Silva, T.R., de Azevedo, A.R.G., Cecchin, D., Marvila, M.T., Amran, M., Fediuk, R. and Szelag, M. 2021. Application of plastic wastes in construction materials: A review using the concept of life-cycle assessment in the context of recent research for future perspectives. Materials, 14(13): 3549. DOI.org/10.3390/ma14133549

Sivanathan, A., Dou, Q., Wang, Y., Li, Y., Corker, J., Zhou, Y. and Fan, M. 2020. Phase change materials for building construction: An overview of nano-/micro-encapsulation. Nanotechnol. Rev., 9: 896-921. DOI: 10.1515/ntrev-2020-0067

The Plastic People. 2021. 5 Ways to Cut Acrylic & Perspex Sheets. Retrieved from https://www.theplasticpeople.co.uk/blog/how-to-cut-acrylic-sheets/

United Nations Environment Programme (UNEP). 2018. Single-Use Plastics: A Roadmap for Sustainability. Retrieved from https://www.unep.org/resources/report/single-use-plastics-roadmap-sustainability

... Continued from inner front cover

- The text of the manuscript should run into Abstract, Introduction, Materials & Methods, Results, Discussion, Acknowledgement (if any) and References or other suitable headings in case of reviews and theoretically oriented papers. However, short communication can be submitted in running with Abstract and References. The references should be in full with the title of the paper.

- The figures should preferably be made on a computer with high resolution and should be capable of withstanding a reasonable reduction with the legends provided separately outside the figures. Photographs may be black and white or colour.

- Tables should be typed separately bearing a short title, preferably in vertical form. They should be of a size, which could easily be accommodated in the page of the Journal.

- References in the text should be cited by the authors' surname and year. In case of more than one reference of the same author in the same year, add suffix a,b,c,.... to the year. For example: (Thomas 1969, Mass 1973a, 1973b, Madony et al. 1990, Abasi & Soni 1991).

List of References

The references cited in the text should be arranged alphabetically by authors' surname in the following manner: (Note: The titles of the papers should be in running 'sentence case', while the titles of the books, reports, theses, journals, etc. should be in 'title case' with all words starting with CAPITAL letter.)

Dutta, A. and Chaudhury, M. 1991. Removal of arsenic from groundwater by lime softening with powdered coal additive. J. Water Supply Res. Techno. Aqua., 40(1) : 25-29.

Hammer, D.A. (ed.) 1989. Constructed Wetlands for Wastewater Treatment-Municipal, Industrial and Agricultural. Lewis Publishers Inc., pp. 831.

Haynes, R. J. 1986. Surface mining and wetland reclamation. In: Harper, J. and Plass, B. (eds.) New Horizons for Mined Land Reclamation. Proceedings of a National Meeting of the Ameri can Society for Surface Reclamation, Princeton, W.V.

Submission of Papers

- The paper can be submitted by e-mail as an attachment in a single WORD file at **contact@neptjournal.com**
- The paper can also be submitted online in a single WORD file through the online submission portal of journal's website: **www.neptjournal.com**

Attention

1. Any change in the authors' affiliation may please be notified at the earliest.
2. Please make all the correspondence by e-mail, and authors should always quote the manu script number.

Note: In order to speed up the publication, authors are requested to correct the galley proof immediately after receipt. The galley proof must be checked with utmost care, as publishers owe no responsibility for mistakes. The papers will be put on priority for publication only after receiving the processing and publication charges.

For further details of the Journal, please visit the website. All the papers published on a particular subject/topic or by any particular author in the journal can be searched and accessed by typing a keyword or name of the author in the 'Search' option on the Home page of the website. All the papers containing that keyword or author will be shown on the home page from where they can be directly downloaded.

www.neptjournal.com